OAK RIDGE NATIONAL LABORATORY LIBRARY
3 4456 0002883 2

ornl

NUREG/CR-4183
Volume 2
(ORNL/TM-9567/V2)

OAK RIDGE NATIONAL LABORATORY

MARTIN MARIETTA

Pressurized Thermal Shock Evaluation of the H. B. Robinson Unit 2 Nuclear Power Plant

Prepared for the
Division of Risk Analysis and Operations
Office of Nuclear Regulatory Research
U.S. Nuclear Regulatory Commission
Under DOE Interagency Agreement 40-550-75

OAK RIDGE NATIONAL LABORATORY
CENTRAL RESEARCH LIBRARY
CIRCULATION SECTION
4500N ROOM 175
LIBRARY LOAN COPY
DO NOT TRANSFER TO ANOTHER PERSON
If you wish someone else to see this report, send in name with report and the library will arrange a loan.
UCN-7969 (3 9-77)

OPERATED BY
MARTIN MARIETTA ENERGY SYSTEMS, INC.
FOR THE UNITED STATES
DEPARTMENT OF ENERGY

NOTICE

This report was prepared as an account of work sponsored by an agency of the United States Government. Neither the United States Government nor any agency thereof, or any of their employees, makes any warranty, expressed or implied, or assumes any legal liability or responsibility for any third party's use, or the results of such use, of any information, apparatus product or process disclosed in this report, or represents that its use by such third party would not infringe privately owned rights.

Available from

Superintendent of Documents
U.S. Government Printing Office
Post Office Box 37082
Washington, D.C. 20013-7982

and

National Technical Information Service
Springfield, VA 22161

NUREG/CR-4183
Volume 2
ORNL/TM-9567/V2
Distribution Category RG

Engineering Physics and Mathematics Division

PRESSURIZED THERMAL SHOCK EVALUATION OF THE H. B. ROBINSON UNIT 2 NUCLEAR POWER PLANT

(Appendices A–K)

by

Oak Ridge National Laboratory
PTS Study Group

assisted by

Science Applications International Corporation
Idaho National Engineering Laboratory
Purdue University

Project Manager: D. L. Selby, ORNL
Program Manager: G. F. Flanagan, ORNL
Project Editor: Lorraine Abbott, ORNL
Technical Monitor: Carl Johnson, NRC

Date Published: September 1985

Prepared for the
Division of Risk Analysis and Operations
Office of Nuclear Regulatory Research
U.S. Nuclear Regulatory Commission
Under DOE Interagency Agreement 40-550-75
NRC FIN No. B0468

Prepared by the
Oak Ridge National Laboratory
Oak Ridge, Tennessee 37831
operated by
Martin Marietta Energy Systems, Inc.
for the
U.S. DEPARTMENT OF ENERGY
under Contract No. DE-AC05-840R21400

OAK RIDGE NATIONAL LABORATORY LIBRARY
3 4456 0002883 2

PARTICIPANTS IN THE PTS STUDY FOR H. B. ROBINSON UNIT 2

Principal Author

D. L. Selby
Oak Ridge National Laboratory

Contributing Authors

D. G. Ball G. F. Flanagan
R. D. Cheverton W. T. Hensley
J. D. White
Oak Ridge National Laboratory

P. N. Austin A. F. McBride
D. Bozarth J. W. Minarick
D. E. Korns L. B. LaMonica
C. L. Mason R. Olson
G. L. Zigler
Science Applications International Corporation

C. B. Davis C. D. Fletcher
D. M. Ogden
Idaho National Engineering Laboratory

P. Gherson H. P. Nourbakhsh
K. Iyer T. G. Theofanous
Purdue University

P. Humphreys L. D. Phillips
Decision Analysis Unit
London School of Economics and Political Science

D. Embrey
Human Reliability Associates, Lancashire, England

Report Staff

Lorraine Abbott Katie Ingersoll
Cheryl Buford Jacqueline Lasch
Oak Ridge National Laboratory

LIST OF CHAPTERS AND APPENDICES

Chapters

1. INTRODUCTION
   J. D. White and D. L. Selby, Oak Ridge National Laboratory

2. DESCRIPTION OF THE H. B. ROBINSON UNIT 2 NUCLEAR POWER PLANT
   R. Olson, A. F. McBride, and P. N. Austin, Science Applications International Corporation
   D. L. Selby and W. T. Hensley, Oak Ridge National Laboratory

3. DEVELOPMENT OF POTENTIAL OVERCOOLING SEQUENCES FOR H. B. ROBINSON UNIT 2
   C. L. Mason, A. F. McBride, R. Olson, and P. N. Austin, Science Applications International Corporation
   D. L. Selby, Oak Ridge National Laboratory

4. THERMAL-HYDRAULIC ANALYSES OF POTENTIAL OVERCOOLING TRANSIENTS FOR H. B. ROBINSON UNIT 2
   C. D. Fletcher, C. B. Davis, and D. M. Ogden, Idaho National Engineering Laboratory
   L. B. LaMonica, Science Applications International Corporation
   T. G. Theofanous, Purdue University
   D. L. Selby, Oak Ridge National Laboratory

5. PROBABILISTIC FRACTURE-MECHANICS ANALYSIS OF POTENTIAL OVERCOOLING SEQUENCES FOR H. B. ROBINSON UNIT 2
   R. D. Cheverton and D. G. Ball, Oak Ridge National Laboratory

6. INTEGRATED PTS RISK FOR H. B. ROBINSON UNIT 2 AND POTENTIAL MITIGATION MEASURES
   J. W. Minarick, Science Applications International Corporation
   D. L. Selby, Oak Ridge National Laboratory

7. SENSITIVITY AND UNCERTAINTY ANALYSES OF ESTIMATED THROUGH-THE-WALL CRACK FREQUENCIES FOR H. B. ROBINSON UNIT 2
   D. Bozarth, C. L. Mason, and J. W. Minarick, Science Applications International Corporation

8. CONCLUSIONS AND RECOMMENDATIONS
   D. L. Selby, R. D. Cheverton, and G. F. Flanagan, Oak Ridge National Laboratory
   D. P. Bozarth, Science Applications International Corporation

Appendices

A. SUPPORT SYSTEM INTERACTION ANALYSIS FOR H. B. ROBINSON UNIT 2
P. N. Austin, D. E. Korns, and G. L. Zigler, Science Applications International Corporation

B. PTS INITIATING-EVENT FREQUENCY AND BRANCH PROBABILITY SCREENING ESTIMATES
J. W. Minarick and P. N. Austin, Science Applications International Corporation
D. L. Selby, Oak Ridge National Laboratory

C. A SOCIO-TECHNICAL APPROACH TO ASSESSING HUMAN RELIABILITY (STAHR)
L. D. Phillips and P. Humphreys, London School of Economics and Political Science
D. E. Embrey, Human Reliability Associates, Lancashire, England
D. L. Selby, Oak Ridge National Laboratory

D. QUANTIFICATION OF OPERATOR ACTIONS
D. L. Selby, Oak Ridge National Laboratory
L. D. Phillips, London School of Economics and Political Science
D. E. Embrey, Human Reliability Associates, Lancashire, England

E. BUOYANCY EFFECTS IN OVERCOOLING TRANSIENTS CALCULATED FOR H. B. ROBINSON UNIT 2
T. G. Theofanous, K. Iyer, H. P. Nourbakhsh, and P. Gherson, Purdue University

F. ESTIMATIONS OF PRESSURES, TEMPERATURES, AND HEAT TRANSFER COEFFICIENTS FOR POSTULATED OVERCOOLING SEQUENCES
C. D. Fletcher, Idaho National Engineering Laboratory

G. THE USE OF *RTNDT* AND Δ*RTNDT* AS INDEPENDENT VARIABLES
R. D. Cheverton and D. G. Ball, Oak Ridge National Laboratory

H. IMPORTANCE SAMPLING METHODS IN THE OCA-P PROBABILISTIC FRACTURE-MECHANICS ANALYSIS
R. D. Cheverton and D. G. Ball, Oak Ridge National Laboratory

I. COMPILATION OF RESULTS FOR HBR-HYPO PROBABILISTIC FRACTURE-MECHANICS ANALYSIS
R. D. Cheverton and D. G. Ball, Oak Ridge National Laboratory

J. USEFUL RESULTS FOR THE LOG-NORMAL DISTRIBUTION
D. Bozarth and J. W. Minarick, Science Applications International Corporation

K. RESPONSES TO UTILITY COMMENTS
D. L. Selby, Oak Ridge National Laboratory

TABLE OF CONTENTS

	Page
PARTICIPANTS IN PTS STUDY FOR CALVERT CLIFFS UNIT 1	iii
LIST OF CHAPTERS AND APPENDICES	v
LIST OF ACRONYMS	ix
ABSTRACT	xiii

Chapters 1–8

(Note: See Volume 1 for chapters)

1. INTRODUCTION	1
2. DESCRIPTION OF THE H. B. ROBINSON UNIT 2 NUCLEAR POWER PLANT	7
3. DEVELOPMENT OF POTENTIAL OVERCOOLING SEQUENCES FOR H. B. ROBINSON UNIT 2	57
4. THERMAL-HYDRAULIC ANALYSES OF POTENTIAL OVERCOOLING TRANSIENTS FOR H. B. ROBINSON UNIT 2	157
5. PROBABILISTIC FRACTURE-MECHANICS ANALYSIS OF POTENTIAL OVERCOOLING SEQUENCES FOR H. B. ROBINSON UNIT 2	261
6. INTEGRATED PTS RISK FOR H. B. ROBINSON UNIT 2 AND POTENTIAL MITIGATION MEASURES	307
7. SENSITIVITY AND UNCERTAINTY ANALYSES OF ESTIMATED THROUGH-THE-WALL CRACK FREQUENCIES FOR H. B. ROBINSON UNIT 2	327
8. CONCLUSIONS AND RECOMMENDATIONS	357

Appendices A–K

A. SUPPORT SYSTEM INTERACTION ANALYSIS FOR H. B. ROBINSON UNIT 2	365
B. PTS INITIATING-EVENT FREQUENCY AND BRANCH PROBABILITY SCREENING ESTIMATES	421
C. A SOCIO-TECHNICAL APPROACH TO ASSESSING HUMAN RELIABILITY (STAHR)	449

D. QUANTIFICATION OF OPERATOR ACTIONS 465

E. BUOYANCY EFFECTS IN OVERCOOLING TRANSIENTS CALCULATED FOR H. B. ROBINSON UNIT 2 479

F. ESTIMATIONS OF PRESSURES, TEMPERATURES, AND HEAT TRANSFER COEFFICIENTS FOR POSTULATED OVERCOOLING SEQUENCES 503

G. THE USE OF *RTNDT* AND Δ*RTNDT* AS INDEPENDENT VARIABLES 645

H. IMPORTANCE SAMPLING METHODS IN THE OCA-P PROBABILISTIC FRACTURE-MECHANICS ANALYSIS 653

I. COMPILATION OF RESULTS FOR HBR-HYPO PROBABILISTIC FRACTURE-MECHANICS ANALYSIS 657

J. USEFUL RESULTS FOR THE LOG-NORMAL DISTRIBUTION 961

K. RESPONSES TO UTILITY COMMENTS 967

LIST OF ACRONYMS

AFW	—	Auxiliary Feedwater
ANS	—	American Nuclear Society
ASG	—	Affected Steam Generator
ASME	—	American Society of Mechanical Engineers
ASP	—	Accident Sequence Precursor
BNL	—	Brookhaven National Laboratory
CCD	—	Central Composite Design
CCW	—	Component Cooling Water
CVC	—	Chemical and Volume Control
CVCS	—	Chemical and Volume Control System
DS	—	Designated Shutdown
ECC	—	Emergency Core Cooling
ECCS	—	Emergency Core Cooling System
EFPY	—	Effective Full Power Years
ESFS	—	Engineered Safety Features System
FCV	—	Feedwater Control Valve
FM	—	Fracture-Mechanics
Fr	—	Froude Number
FSAR	—	Final Safety Analysis Report
FW	—	Feedwater
HBR-HYPO	—	Hypothetical HBR Vessel
HBR-2	—	H. B. Robinson Unit 2
HPI	—	High-pressure Injection
HPSI	—	High-pressure Safety Injection
HVAC	—	Heating, Ventilating, and Air Conditioning
HX	—	Heat Exchanger
HZP	—	Hot 0% Power
INEL	—	Idaho National Engineering Laboratory
IPRD	—	In-Plant Reliability Data
LANL	—	Los Alamos National Laboratory
LEFM	—	Linear Elastic Fracture Mechanics
LER	—	Licensee Event Report
LOCA	—	Lost-of-Coolant Accident
LOFW	—	Loss of Feedwater
LPI	—	Low-pressure Injection
MAFW	—	Mechanically Operated Auxiliary Feedwater
MBLOCA	—	Medium-break Lost-of-Coolant Accident
MCC	—	Motor Control Valve
MFBV	—	Main Feedwater Bypass Control Valve
MFCV	—	Main Feedwater Control Valve
MFIV	—	Main Feedwater Isolation Valve

MFW	—	Main Feedwater
MFWP	—	Main Feedwater Pump
MSIV	—	Main Steam Isolation Valve
NRC	—	Nuclear Regulatory Commission
NREP	—	National Reliability Evaluation Program
OA	—	Operation Action
ORNL	—	Oak Ridge National Laboratory
PSV	—	Pressurizer Safety Valve
PTC	—	Plant Trip Control
PORV	—	Pressurizer Power-operated Relief Valve
PTS	—	Pressurized Thermal Shock
PWR	—	Pressurized Water Reactor
PZR	—	Pressurizer
PZR PORV	—	Pressurizer Power-operated Relief Valve
PZR SV	—	Pressurizer Safety Valve
RC	—	Reactor Coolant
RCP	—	Reactor Coolant Pump
RCS	—	Reactor Coolant System
RHR	—	Residual Heat Removal
RMM	—	Regional Mixing Model
RPV	—	Reactor Pressure Vessel
RSM	—	Response Surface Model
RT	—	Reactor Trip
RTNDT	—	Reference Temperature for Nil-ductility Transition
RWST	—	Refueling Water Storage Tank
SAIC	—	Science Applications International Corporation
SBLOCA	—	Small-break Loss-of-coolant Accident
SCFM	—	standard cubic feet/minute
SDV	—	Steam Dump Valve
SG	—	Steam Generator
SI	—	Safety Injection
SIS	—	Safety Injection System
SIAS	—	Safety Injection Actuation Signal
SLB	—	Steam-line Break
SPC	—	Steam Pressure Control
SRV	—	Safety Relief Valve
SSLB	—	Small Steam-line Break
SSV	—	Steam-line Safety Valve
STAHR	—	Socio-technical Assessment of Human Reliability
STM PORV	—	Steam-power-operated Relief Valve
SUT	—	Startup Transformer
SW	—	Service Water
SWS	—	Service Water System

TBV	—	Turbine Bypass Valve
TCV	—	Turbine Control Valve
THERP	—	Technique for Human Error Rate Prediction
TROTS	—	Turbine Redundant Overspeed Trip System
TSV	—	Turbine Stop Valve
TT	—	Turbine Trip
TWC	—	Through-the-wall Crack
UAT	—	Unit Auxiliary Transformer
USG	—	Unaffected Steam Generator
WPS	—	Warm Prestressing
WR	—	Wide Range

ABSTRACT

An evaluation of the risk to the H. B. Robinson Unit 2 nuclear power plant (HBR-2) due to pressurized thermal shock (PTS) has been completed by Oak Ridge National Laboratory (ORNL) with the assistance of several other organizations. This evaluation was part of a Nuclear Regulatory Commission program designed to study the PTS risk to three nuclear plants, the other two plants being Oconee Unit 1 and Calvert Cliffs Unit 1. The specific objectives of the program were to (1) provide a best estimate of the frequency of a through-the-wall crack (TWC) in the pressure vessel at each of the three plants, together with the uncertainty in the estimated frequency and its sensitivity to the variables used in the evaluation; (2) determine the dominant overcooling sequences contributing to the estimated frequency and the associated failures in the plant systems or in operator actions; and (3) evaluate the effectiveness of potential corrective measures. In the study for HBR-2, thousands of hypothetical overcooling events were constructed and quantified using computer-generated event trees and quantified branch points. All scenarios with a frequency greater than 10^{-7} per reactor year were considered explicitly, and those having lower frequencies were assigned to 12 "residual" groups to ensure that their contributions to the TWC frequency were included in the study. Idaho National Engineering Laboratory (INEL) performed thermal-hydraulics analyses for all the identified scenarios, using detailed models for a few of them and simpler models for the remaining ones. The INEL models and results were reviewed by Brookhaven National Laboratory, and, in addition, mixing calculations pertinent to some of the scenarios were performed at Purdue University. Probabilistic fracture-mechanics calculations were performed by ORNL to determine the conditional TWC probability for each scenario, and it was found that, except in extreme cases, the probabilities for the HBR-2 vessel were too low to permit an appropriate illustration of the fracture-mechanics analysis method. Therefore, a hypothetical vessel (designated as HBR-HYPO) which had higher concentrations of the contaminants copper and nickel and a higher initial nil-ductility reference temperature was utilized in the fracture-mechanics analysis. The fracture-mechanics results were then integrated with the sequence frequencies to obtain the TWC frequency. The best estimate for the HBR-HYPO vessel was determined to be approximately 1.3×10^{-8} per year at a nil-ductility temperature of 270°F. An uncertainty analysis indicated that a factor of about 1000 is an appropriate 95% confidence interval, assuming a log-normal uncertainty distribution. Steam-line breaks involving the blowdown of more than one steam generator were found to be the most significant contributors to the PTS risk, and the uncertainty in the flaw density in the pressure vessel was found to be the most important contributor to the overall uncertainty in the risk. The most important operator actions for negating pressurized thermal shock at HBR-2 are the closure of the main steam isolation valves (MSIVs) following a small or medium-sized steam-line break downstream of the MSIVs and the isolation of auxiliary feedwater to low-pressure steam generators following a steam-line break. This study considered some system interactions but no external events such as fires, floods, or seismic events.

Appendix A

SUPPORT SYSTEM INTERACTION ANALYSIS FOR H. B. ROBINSON UNIT 2

P. N. Austin, D. E. Korns, and G. L. Zigler

Science Applications International Corporation

APPENDIX A. SUPPORT SYSTEM INTERACTION ANALYSIS FOR H. B. ROBINSON UNIT 2

A.1. Introduction

This appendix describes the response of key H. B. Robinson Unit 2 (HBR-2) plant systems to failures of required support systems in identified overcooling sequences. Support system failures can be important since single support system failures can result in multiple failures of the systems comprising the pressurized thermal shock (PTS) event sequences.

The electric power, instrument air, component cooling water, and service water systems were identified as the support systems that could most impact the plant systems and associated control instrumentation comprising the HBR-2 PTS event tree sequences. In addition, the necessity of the plant's heating, ventilating and air conditioning (HVAC) systems for continued plant operation was recognized. However, the effect of HVAC failures on equipment performance is expected to be long-term with respect to the effects of failures of the other identified support systems. In general, the effect of HVAC failures and severe equipment operating environments is considered to be beyond the scope of this analysis.

In Section A.2, the methodology used to identify and analyze the response of plant systems and components to support systems failures is described. Section A.3 provides a brief description of the support systems considered in the analysis. Section A.4 details the data base of components considered in the analysis and their failure modes in response to support system failures. The response of the key plant systems and components comprising PTS event sequences to postulated support system failures is provided in Section A.5, and finally the major results of the support system failure are summarized in Section A.6.

The identification of support system failures which could lead to adverse PTS sequences is the first step in evaluating their impact. Although not assessed in this analysis, the frequency of each support system failure and associated events (including the effects of operator intervention) must be calculated and compared to the frequencies of equivalent sequences occurring independently to evaluate the overall impact of support system failures on the PTS sequences. This type of evaluation is presented in Chapter 3.

A.2. Methodology

The objective of this study is to identify common cause failures which result from failures in the electric power, instrument air, component cooling water or service water systems and affect PTS sequence quantification.

The methodology used in this study is outlined below:

1. Identify plant systems and components potentially affecting the PTS event sequences.

2. Identify support system components, including controls, potentially affecting the plant system components.
3. Identify the specific failure modes of individual systems and components in response to electric power, instrument air, component cooling water, and service water system failures.
4. Determine the combined impact on the plant systems and components potentially affecting PTS from postulated failures of the support systems.
5. Identify the failures which could be "PTS adverse" (i.e., make the pressure-temperature response of the reactor coolant system (RCS) more severe from a PTS standpoint).
6. Determine which support system failures (from Step 5) could initiate PTS sequences of concern.

Using the methodology outlined above, the effects of support system failures on PTS sequences can be evaluated. It should be noted that the results are not necessarily applicable to non-PTS accident sequences and that the effects of common-cause initiators, such as operator errors, severe operating environments, severe natural phenomena or sabotage, have not been considered.

A.3. Support System Descriptions

This section provides a brief description of the support systems considered in this study. The plant-level systems and components that impact PTS sequences are described in detail in Chapter 2 and are described in terms of their pertinent failure modes in Section A.5.

A.3.1. Electric Power Distribution System

The HBR-2 ac-dc electric power distribution is shown in a simplified schematic diagram in Figure A.1. The unit generator and the 115KV switchyard are the primary sources of electrical power during on-line operation of the plant. Power from the unit generator is supplied to plant systems through the 22/4.16KV unit auxiliary transformer (UAT). Electric power is supplied from the 115KV switchyard via the 115/4.16KV startup transformer (SUT).

The 4160V buses supply the 480V buses through 4160V/480V station service transformers. In particular, 4160V bus 1 supplies 480V buses 2A and 2B; 4160V bus 2 supplies 480V buses 1 and E1; 4160V bus 3 supplies 480V buses 3, E2, and DS; and 4160V bus 4 supplies 480V bus 4. Tie breakers are provided between 480V buses 1, and 2A, 2B and 3, and E1 and E2. Buses E1 and E2 can also be supplied from emergency diesel generators A and B, respectively. The designated shutdown diesel generator DS can supply power to the 480V bus DS.

The 480V buses supply the 12 motor control centers (MCCs). Figure A.1 details which 480V buses supply the individual MCCs. In addition, MCC-5 has an alternate feed from 480V bus DS.

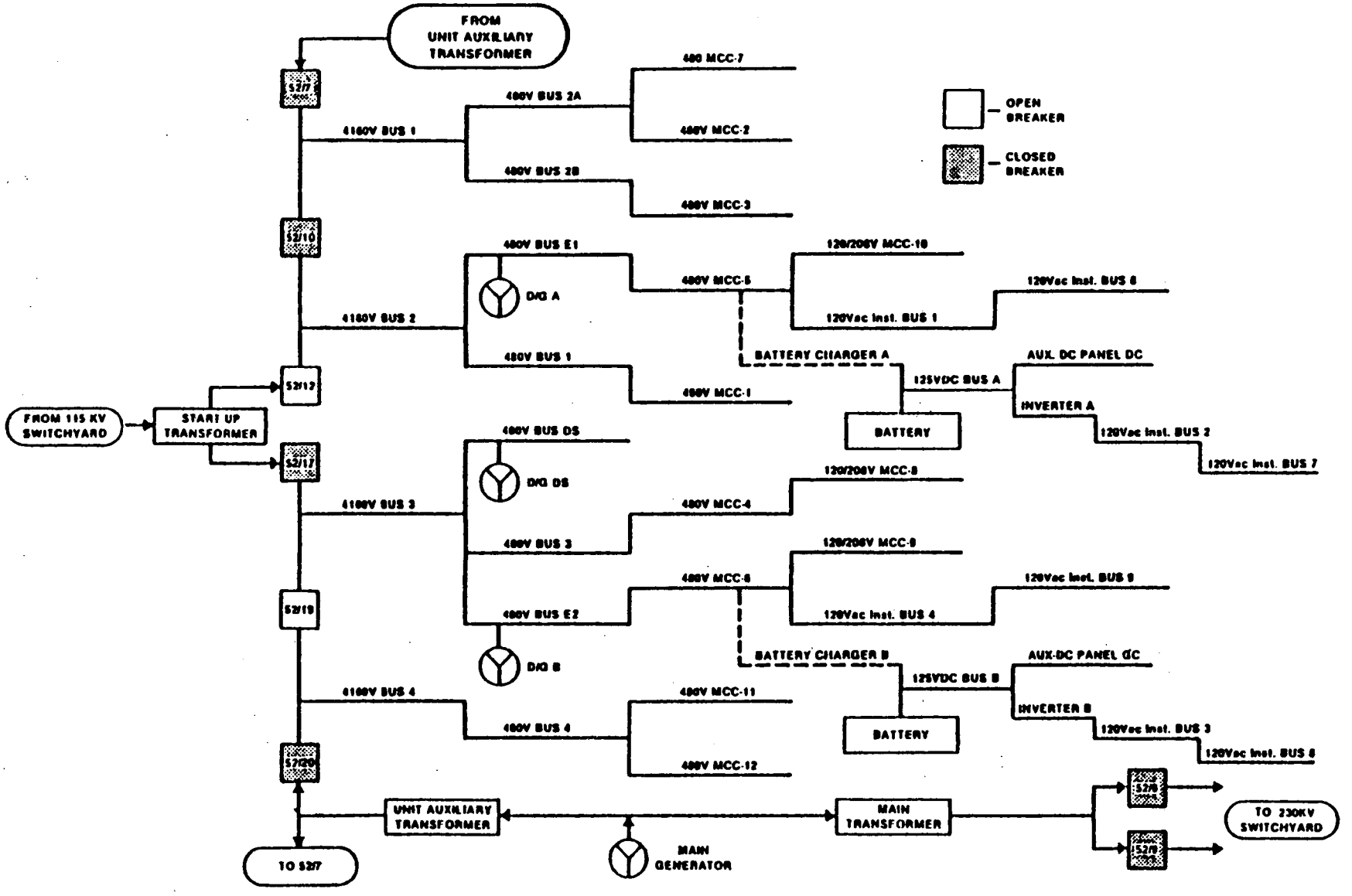

Figure A.1. Simplified schematic of H. B. Robinson Unit 2 ac/dc power distribution.

Plant dc loads are supplied by 125V dc buses A and B. Each dc bus is fed by its associated battery charger. The two 125V dc battery chargers, A and B, are fed by 480V ac MCC-5 and MCC-6, respectively.

The 120V instrument power supply is split into eight buses. Buses 1, 2, 3, and 4 each have a normal and an alternate power supply. Instrument buses 2 and 3 are normally fed from 125V dc bus A and bus B, respectively, via inverters. Instrument buses 1 and 4 are normally fed from 480V MCC-5 and MCC-6, respectively. The alternate power supply for instrument buses 1, 2, 3, and 4 is 120/208V MCC-8. Instrument buses 6, 7, 8, and 9 are fed from instrument buses 1, 2, 3, and 4, respectively.

Instrument buses 1, 2, 3, and 4 supply control power to process instrumentation via the analog instrument racks. Some of this instrumentation includes pressurizer pressure transmitters, turbine overspeed channels (TROTS), steam dump instrumentation, pressurizer level control, charging line flow control, residual heat removal (RHR) flow control, feedwater (FW) flow control, and bistables for safety injection and auxiliary feedwater (AFW) initiation.

A.3.2. Instrument Air System

The HBR-2 instrument air system consists of multiple trains of air compressors, aftercoolers, dryers and air receivers which provide air to the instrument air headers. Instrument air headers are located in the Turbine Building, Reactor Containment Building, Reactor Auxiliary Building, and Corridor and Fuel Handling Area.

Nominal instrument air header conditions are 100 to 110 psig and 85°F. Air flow demands may fluctuate with peak demands between 200 and 400 scfm. A 516-scfm primary air compressor normally supplies the instrument air requirements through the plant. The compressor controller regulates the compressor cylinder load to maintain pressure in its 427-ft^3 air receiver.

Two 200-scfm instrument air compressors, A and B, normally provide intermittent air flow to meet peak air flow demands. These instrument air trains are in parallel and are normally auto-aligned to provide an on-line backup to the primary air train. Aligned in the auto-mode, the compressors automatically start and stop to maintain pressure in a single shared 150-ft^3 air receiver.

In addition, a 400-scfm station air compressor is used as a manual backup instrument air supply when the primary air and instrument air systems are unavailable. This compressor is normally operating on its own header but can be manually valved in when needed. The station air is not of instrument air quality, but it is available if required.

Power to the primary air compressor is supplied from 480V bus 2A; instrument air compressors A and B are supplied from 480V MCC-5 and MCC-6, respectively. The compressors are cooled by the service water system.

Instrument air is required by the following components: the pressurizer power-operated relief valves (PZR PORVs), the main steam isolation valves (MSIVs), steam-side power-operated relief valves (STM PORVs), FW control and bypass valves, the charging pump and AFW pump lube oil cooling valves, the letdown isolation and charging flow control

valves, the charging pump and AFW turbine pump speed control valves, and RHR system valves.

A.3.3. Component Cooling Water System

The component cooling water (CCW) system is a closed loop system with three centrifugal CCW pumps and two CCW heat exchangers cooled by service water. The three CCW pumps discharge into a common header that feeds the heat exchangers. The heat exchangers discharge into another common header and out to the various plant loads. Normally, one pump and one heat exchanger have sufficient capacity to remove the heat loads during full power operation. During normal operation the CCW system provides cooling water to the reactor coolant and charging pumps. Two CCW pumps and heat exchangers are utilized for removing residual heat and pump heat during normal plant shutdown.

Power to CCW pumps A, B, and C is supplied from 480V buses DS, E1, and E2, respectively. CCW pumps B and C are actuated by safety injection (SI) trains A and B, respectively. The pump motor circuit breakers have undervoltage trips which open upon loss of power.

A.4.4. Service Water System

The service water (SW) system is an open loop system taking its suction from Lake Robinson. The SWS is a two-train system, with each train supplying cooling water to one of two or three redundant items of plant equipment.

There are four service water pumps with three pumps normally operating. Complete train separation is possible at the discharge header from the four pumps, which then discharge into the two 30-in. train headers.

The SW system provides heat removal from the following components: main feedwater (MFW) pumps; motor- and steam-driven AFW pumps; CCW heat exchangers; primary, station, and instrument air compressors; isolated phase bus heat exchanger; and the SI pumps.

The service water pumps are supplied motive power from the following 480V buses: pumps A and B from 480V bus E1, and pumps C and D from 480V bus E2.

A.4. Systems and Components Affecting PTS Sequences

In this analysis, a data base associated with the plant components important in determining potential impacts on PTS sequences was developed. The data base identifies the systems and components considered, their interfaces with support systems, and their failure modes in response to failure of required support systems. With this information the effect of postulated support system failures on aspects of the plant state potentially important to PTS sequences could be assessed. That assessment is provided in Section A.5. This section describes the data base developed.

A.4.1. Selection of Systems and Components

Identification of the plant systems and components that could impact PTS sequences is the first step in performing the PTS support system interaction analysis. The specific purpose of performing the support system interaction analysis is to determine whether one or more individual "branch events" of the PTS event sequences may occur owing to a failure of the support systems. The principal sources of information to select the systems and components affecting PTS sequences are the PTS event trees and the branch failure modes.

The systems and components identified from the PTS sequences, and potentially important failure modes, are listed in Table A.1. Each of the key components was evaluated to determine whether a potential failure due to a support system failure was possible.

For those key systems and components that could be impacted by support system failures, additional components that would be required for proper functioning were identified. For example, the additional components for the AFW pumps included specific pump discharge and control valves, the flow controllers for the turbine-driven pump and motor-driven pump trains, the turbine pump steam supply valves, and the steam generator (SG) bistables that can initiate AFW. Support system components required for proper functioning of plant-level or "front-line" components were then similarly identified. Table A.2 provides a complete list of the front-line and support system components selected and subsequently considered in this analysis.

A.4.2. Support System Interfaces

The support system interfaces for the components considered in the analysis were established (see Table A.2 for a listing of these components). A complete summary of the interfaces between these components and the electric power, instrument air, CCW, and SW systems is provided in Table A.3. The table lists all components considered in the study according to which support systems they require.

A.4.3. Description of System and Component Failure Modes in Response to Support System Failures

Once the systems and components that could impact PTS sequences were identified, their failure modes were determined. This was done based on available design documentation and from specific information provided by Carolina Power and Light Company. Failure modes on loss of electric power, instrument air, CCW, and SW were determined for each component requiring these support systems.

Failure modes determined for applicable components on loss of instrument air, CCW, and SW are provided in Table A.4. Component failure modes that would occur on loss of electric power supply are included in Table A.5 for the components requiring motive power and/or control power. Also included in the table is the source of motive and/or control power for the components.

Tables A.4 and A.5 (with Table A.2) complete the data base required to assess the impact of postulated support system failures on aspects of the plant state potentially important to PTS sequences.

Table A.1. Summary of potential support system impact on key PTS event tree systems and components

Key Systems and Components	Failure Modes of Interest	Component Response Impacted by Support System Failures
1. Reactor Coolant System		
a. Pressurizer Relief Valves	Inadvertently open or fail to close on demand	Yes
b. Safety Valves	Fail to close on demand	No
c. Reactor Coolant Pumps	Seal Failure (LOCA)	Yes
d. Piping	Piping Failure (LOCA)	No
e. Steam Generator Tubes	Tube Rupture (LOCA)	No
2. Main Steam System		
a. Turbine Trip Systems	Fail to trip on demand	Yes
b. Steam-Side Power-Operated Relief Valves	Inadvertently open or fail to close on demand	Yes
c. Steam Dump Valves	Inadvertently open or fail to close on demand	Yes
d. Main Steam Isolation Valves	Fail to close on demand	Yes
e. Main Steam Bypass Valves	Inadvertently open or fail to close on demand	Yes
f. Main Safety Valves	Inadvertently open or fail to close on demand	No
g. Piping	Steam line breaks	No
3. Main Feedwater System		
a. Feedwater Pumps	Overfeed or fail to isolate	Yes
b. Feedwater Control Valves	Overfeed or fail to runback	Yes
c. Feedwater Isolation Valves	Fail to isolate	Yes
d. Feedwater Bypass Valves	Inadvertently open or fail to close on demand	Yes
4. Chemical Volume and Control System		
a. Charging Pumps	Overfeed or loss of flow	Yes
b. Letdown Isolation Valves	Fail to isolate on demand	Yes
5. Emergency Core Cooling System		
a. Safeguards Actuation System	Inadvertent actuation or fails to actuate	Yes
b. High Pressure Safety Injection	Inadvertent overfeed or failure	Yes
c. Low Pressure Safety Injection	Fails on demand	Yes
6. Auxiliary Feedwater System		
a. AFW Electric-Motor-Driven Pumps	Inadvertent actuation or failure to actuate	Yes
b. AFW Steam-Driven Pump	Inadvertent actuation, overfeed or failure	Yes
c. AFW valves	Fail to close on demand	Yes
7. Reactor Protection System	Reactor Trip	Yes

Table A.2. Components considered in PTS interaction study by system

Systems	Components
	Front Line Systems
1. Reactor Coolant System	• RCP A • RCP B • RCP C • PZR Control Heaters • PZR Backup Heaters A • PZR Backup Heaters B • PZR Pressure Transmitter PT-445 • PZR Pressure Transmitter PT-444 • PORV RC-456 • PORV RC-455C • PORV Block Valve RC-535 • PORV Block Valve RC-536
2. Turbine Protection System	• Turbine Auto Trip Logic and Solenoid (20-AST) • Turbine Emergency Trip Logic and Solenoid (20-ET) • Governor/Intercept Trip Logic and Solenoids (20-1, 20-2) • Governor Control Cabinet • EH System Logic • EH Oil Pump A • EH Oil Pump B • TROTS Channel 1 • TROTS Channel 2 • TROTS Channel 3
3. Main Steam System	• Steam-Side PORV RV1 • Steam-Side PORV RV2 • Steam-Side PORV RV3 • Steam Dump PORV 1324A-1 • Steam Dump PORV 1324B-1 • Steam Dump PORV 1324B-2 • Steam Dump PORV 1324A-2 • Steam Dump PORV 1324B-3 • Steam Dump Controller T-408 • Steam Dump Pressure Controller P-464 • High T_{avg} Output Logic Steam Dump Loss-Load Pressure Monitor PM-447 • MSIV V1-3A • MSIV V1-3B • MSIV V1-3C • V1-3A Bypass Valve • V1-3B Bypass Valve • V1-3C Bypass Valve
4. Main Feedwater System	• FW Pump A • FW Pump B • MFIV V2-6A • MFIV V2-6B • MFIV V2-6C • FW Control Valve FCV-478 • FW Control Valve FCV-488 • FW Control Valve FCV-498 • FW Bypass Valve FCV-479 • FW Bypass Valve FCV-489 • FW Bypass Valve FCV-499 • FW Valve Controller Loop 1 • FW Valve Controller Loop 2 • FW Valve Controller Loop 3

Table A.2 (Continued)

Systems	Components
	Support Systems (Cont'd)
5. Auxiliary Feedwater System	• Motor-driven AFW Pump A • Motor-driven AFW Pump B • Steam-driven AFW Pump Controller • Pump A Train Controller • Pump B Train Controller • Pump Train A Control Valve, 45 • Pump Train B Control Valve, 46 • MAFW Disch VLV V2-16A • MAFW Disch VLV V2-16B • MAFW Disch VLV V2-16C • SAFW Disch VLV V2-14A • SAFW Disch VLV V2-14B • SAFW Disch VLV V2-14C • SAFW Supply VLV V1-8A • SAFW Supply VLV V1-8B • SAFW Supply VLV V1-8C • SG 1 Level LC-474A String • SG 1 Level LC-475A String • SG 1 Level LC-476A String • SG 2 Level LC-484A String • SG 2 Level LC-485A String • SG 2 Level LC-486A String • SG 3 Level LC-494A String • SG 3 Level LC-495A String • SG 3 Level LC-496A String
6. Chemical and Volume Control System	• Charging Pump A • Charging Pump B • Charging Pump C • PZR Level Controller LC-459F • Charging Pump Suction Valve LCV-115C • Charging Pump Suction Valve LCV-115B • Boric Acid Valve MOV-350 • Loop 1 Cold Leg Inlet Valve CVC-310A • Loop 2 Cold Leg Inlet Valve CVC-310B • Aux Spray Valve CVC-311 • Letdown Stop Valve LCV-460A • Letdown Stop Valve LCV-460B • Letdown Isolation Valve CVC-200A • Letdown Isolation Valve CVC-200B • Letdown Isolation Valve CVC-200C • Letdown Isolation Valve CVC-204A • Letdown Isolation Valve CVC-204B • Charging Line FCV HCV-121
7. Safety Injection System	• SI Pump A • SI Pump B • SI Pump C • ACC Nitrogen Supply SI-855 • ACC Drain Valve SI-852A • ACC Drain Valve SI-852B • ACC Drain Valve SI-852C • ACC Vent Valve SI-853A • ACC Vent Valve SI-853B • ACC Vent Valve SI-853C • ACC Disch Valve SI-865A • ACC Disch Valve SI-865B • ACC Disch Valve SI-865C • Cold Leg Injection VLV SI-870A

Table A.2 (Continued)

Systems	Components
	Front Line Systems (Cont'd)
	• Cold Leg Injection VLV SI-870B • BIT Inlet VLV SI-867A • BIT Inlet VLV SI-867B • Inlet Valve to Loop 3 Hot Leg SI-866A • Inlet Valve to Loop 2 Hot Leg SI-866B • Isolation Valve to Hot Legs SI-869
8. Residual Heat Removal System	• RHR Pump A • RHR Pump B • RHR Suction Valve SI-862A • RHR Suction Valve SI-862B • RHR Disch Valve HCV-758 • RHR Disch Valve FCV-605 • Cold Leg Injection Valve RHR-744A • Cold Leg Injection Valve RHR-744B
9. Safeguards System	• Safeguards Train A Logic • Safeguards Train B Logic • PZR Pressure PC-455E String • PZR Pressure PC-456D String • PZR Pressure PC-457D String
10. Reactor Protection System	• Control Rod Drive MG Set A • Control Rod Drive MG Set B • RCP Undervoltage TRP Relay UV-1 • RCP Undervoltage TRP Relay UV-2 • RCP Undervoltage TRP Relay UV-3 • Reactor Protection Train A Logic • Reactor Protection Train B Logic
	Support Systems
11. Component Cooling Water System	• Component Cooling Pump A • Component Cooling Pump B • Component Cooling Pump C • Component Cooling Heat Exchangers • CCW Disch Valve TCV-659A from Charging Pump • CCW Disch Valve TCV-659B from Charging Pump • CCW Disch Valve TCV-659C from Charging Pump • Header Supply Valve to RCP CC-716A • Header Supply Valve to RCP CC-716B • RCP Motor Oil Cooler Valve CC-730 • RCP Thermal Barrier Cooling Coil Valve FCV-626
12. Service Water System	• Service Water Pump A • Service Water Pump B • Service Water Pump C • Service Water Pump D • SW Disch Valve V6-12B • SW Disch Valve V6-12C • SW Isolation Valve V6-16A • SW Isolation Valve V6-16B • Steam-Driven AFW Pump SW Valve TCV-1902 • Motor-Driven AFW Pump SW Valve TCV-1903A • Motor-Driven AFW Pump SW Valve TCV-1903B • SW Disch Valve TCV-1629A from IA Compressor A • SW Disch Valve TCV-1629B from IA Compressor B

Table A.2 (Continued)

Systems	Components
	Front Line Systems (Cont'd)
13. Instrument Air System	• Primary Air Compressor • Instrument Air Compressor A • Instrument Air Compressor B
14. Electric Power System	• Diesel Generators A, B, and DS • Startup Transformer • Unit Auxiliary Transformer • 125V dc buses • 4160V ac buses • 480V ac buses • 120/208V ac buses

The component failure modes determined are discussed further, by key system and/or component, in Sections A.4.3.1 through A.4.3.15.

A.4.3.1. Reactor Coolant Pumps

The three reactor coolant pumps (RCPs) require 4160V ac motive power and 125V dc breaker control power to operate. Seal injection water is supplied to the RCPs from the charging pumps, and cooling water for the bearing lube oil coolers and thermal barrier cooling coil is supplied from the CCW system.

Loss of dc control power to the RCP breakers will prevent operating pumps from being tripped. Loss of charging flow could lead to RCP seal failure unless the pumps are tripped.

A.4.3.2. Pressurizer Power Operated Relief Valves

The two PZR PORVs are designed to open on high pressurizer pressure to prevent or minimize the lifting of pressurizer code safety valves. They are opened by energizing solenoid valves powered from 125V dc auxiliary panels DC and GC. The solenoids supply opening air to the PZR PORVs. The pressurizer pressure transmitters, PT-445 and 444, which are powered from instrument buses 3 and 4, respectively, open the PZR PORVs on high pressure.

Loss of instrument air, failure of the 125V dc auxiliary panels, or loss of power on the respective instrument buses will result in the PZR PORVs closing or remaining closed.

A.4.3.3. Turbine Protection System

Turbine protection by turbine trip is accomplished by depressurizing the hydraulic fluid system which normally holds the governor, reheat, intercept, and stop valves to the turbine open. Hydraulic pressure release is accomplished by opening any of three solenoid-

Table A.3. Summary of interfaces between components and support systems considered

Systems	Components Requiring Instrument Air	Components Requiring CCW	Components Requiring SWS	Components Requiring Electric Power
		Front Line Systems		
1. Reactor Coolant System	• PORVs RC-456 RC-455C	• RCP (bearings and thermal barrier cooling coil)		• RCPs A, B, and C • PZR Heaters • PZR Pressure Transmitters • PZR PORVs • PORV Block Valves
2. Turbine Protection System				• Turbine Auto Stop Trip System and Solenoid 20-AST • Turbine Emergency Trip System and Solenoid 20-ET • Gov/Intercept Trip System and Solenoids 20-1, 20-2 • Governor Control Cabinet • EH System • EH Oil Pumps • TROTS
3. Main Steam System	• MSIVs • Steam-Side PORVs			• MSIVs • Steam Dump Valves • Steam-Side PORVs • Steam Dump Controllers • Main Steam Bypass Valves
4. Main Feedwater System	• Feedwater Control Valves • Feedwater Bypass Valves		• Feedwater Pumps A and B (oil cooler)	• Feedwater Pumps • Feedwater Control Valves • Feedwater Bypass Valves • Feedwater Isolation Valves • Feedwater Valve Controllers
5. Auxiliary Feedwater System	• Turbine Drive Pump Speed Control		• Motor-Driven and Turbine-Driven AFW Pumps (Bearings)	• Motor-Driven AFW Pumps • Turbine-Driven AFW Pump Controller • Motor-Driven Pump Train Controllers • Motor-Driven AFW Pump Discharge Valves V2-16A, B, and C • Motor-Driven AFW Pump Control Valves 45 and 46 • Turbine-Driven AFW Pump

Table A.3 (Continued)

Systems	Components Requiring Instrument Air	Components Requiring CCW	Components Requiring SWS	Components Requiring Electric Power
		Front Line Systems (Cont'd)		
				Discharge Valves V2-14A, B, and C • Turbine-Driven AFW Steam Supply Valves V1-8A, B, and C • Steam Generator Low-Low Level Instr. Strings SG1 LC-474A, 475A, 476A SG2 LC-484A, 485A, 486A SG3 LC-494A, 495A, 496A
6. Chemical and Volume Control System	• Isolation Valves to RCS: CVC-310A, B CVC-311 • Charging Line FCV • Letdown Isolation Valves • Pump Suction Valve from RWST • Charging Pump Speed Control	• Charging Pumps (Lube Oil Cooling)		• Charging Pumps • Pumps Suction Valves LCV-115C, LCV-115B, MOV-350 • Isolation Valves to RCS CVC-310A and B, CVC-311 • Charging Line FCV, HCV-121 • Letdown Isolation Valves LCV-460A and B • Letdown Orifice Valves CVC-200A, B and C • Letdown Isolation Stops CVC-204A and B • PZR Level Controller, LC-459F
7. Safety Injection System	• N_2 Supply Valve to Accumulators SI-855 • Accumulator Drain and Vent Valves	• SI pumps (seal water heat exchanger)	• SI pumps (thrust bearing cooling)	• SI Pumps • N_2 Supply Valve to Accumulators SI-855 • Accumulator Drain and Vent Valves • Accumulator Discharge Valves • Cold Leg Injection Valves SI-870A and B • Boron Injection Tank Inlet Valves SI-867A and B • RWST Outlet Valves SI-864A and B

Table A.3 (Continued)

Systems	Components Requiring Instrument Air	Components Requiring CCW	Components Requiring SWS	Components Requiring Electric Power
		Front Line Systems (Cont'd)		
				• Hot Leg Injection Valves SI-869, 866A and B • Low PZR Pressure Bistables PC-455E, 456D, 457D
8. Residual Heat Removal System	• Discharge Valves FCV-605 HCV-758	• RHR pump (seal water heat exchanger)		• RHR Pumps • Pump Suction Valves from RWST SI-862A and B • Cold Leg Inlet Valves RHR-744A and B • RHR Discharge Valve FCV-605
9. Safeguards System				• Safeguards Trains A and B • Pressurizer Pressure Instrument Strings PC-455E, 456D and 457D
10. Reactor Protection System				• Control Rod Drive Motor Generator Sets A and B • RCP Under Voltage Relays UV-1, 2, and 3 • Reactor Protection Trains A and B
		Support Systems		
11. Component Cooling Water System	• CCW Discharge Valves from Charging Pumps TCV-659A, B, and C		• CCW heat exchangers A and B	• CCW Pumps • RCP Supply Valves CC-716A and B • RCP Lube Oil Coolers CCW valve CC-730 • RCP Thermal Barrier Cooling Coils CCW Valve FCV-626

Table A.3 (Continued)

Systems	Components Requiring Instrument Air	Components Requiring CCW	Components Requiring SWS	Components Requiring Electric Power
		Support Systems (Cont'd)		
12. Service Water System	• Suction Control Valves to AFW Pumps A, B, and Turbine TCV-1902 TCV-1903A TCV-1903B • Discharge Control Valves from Air Compressors A and B TCV-1629A and B			• SW Pumps • SW Discharge Cross-Tie Valves V6-12B and C • SW Supply Train Isolation Valves V6-16A and B • SW Control Valve to AFW Turbine-Driven Pump TCV-1092 • SW Control Valve to AFW Motor-Driven Pumps TCV-1903A and B
13. Instrument Air System			• Primary Air Compressor • Instrument Air Compressors A and B	• Primary Air Compressor • Instrument Air Compressors A and B
14. Electric Power System			• Diesel generator cooling	• Diesel Generators A and B

Table A.4. Component failure modes on loss of instrument air, component cooling water and service water

Component Requiring Support System	Normal Position/Mode	Failure Mode on Loss of		
		Instrument Air	CCW	SWS
		Front Line Systems		
1. Reactor Coolant System				
RCP A, B, and C	Operating	N/A	Eventual failure due to bearing failure or thermal barrier cooling coil failure, unless tripped. Seal injection degraded by loss of CCW to charging pumps.	N/A
PORV RC-456 RC-455C	Closed	Closed	N/A	N/A
2. Turbine Protection System	Operable	N/A	N/A	N/A
3. Main Steam System				
Steam-Side PORVs RV1 RV2 RV3	Closed	Closed	N/A	N/A
MSIVs	Open	Closed	N/A	N/A
4. Main Feedwater System				
FW Pumps A and B	Operating	N/A	N/A	Eventual failure, unless tripped.
FW Control Valves	Open	Closed	N/A	N/A
FW Bypass Valves	Closed	Closed	N/A	N/A
5. Auxiliary Feedwater System				
Motor-Driven AFW Pumps A and B	Standby	N/A	N/A	Pumps fail (bearing failure).
Steam-Driven AFW Pump	Standby	Full Speed	N/A	Pumps fail (bearing failure).
6. Chemical and Volume Control System				
Charging Pumps	Operating (1 pump on auto-control, 2 on standby)	Full speed	Pumps fail (loss of lube oil cooling).	N/A
Charging Line Isolation Valves CVC-310A	Closed	Open	N/A	N/A
CVC-310B	Open	Open	N/A	N/A
Auxiliary Spray Isolation Valves CVC-311	Closed	Closed	N/A	N/A
Charging Line FCV HCV-121	Open	Open	N/A	N/A
Letdown Stop Valves LCV-460A	Open	Closed	N/A	N/A
LCV-460B	Open	Closed	N/A	N/A
Letdown Orifice Isolation Valves CVC-200A	Closed	Closed	N/A	N/A
CVC-200B	Closed	Closed	N/A	N/A
CVC-200C	Open	Closed	N/A	N/A
Letdown Isolation Stop Valves CVC-204A	Open	Closed	N/A	N/A
CVC-204B	Open	Closed	N/A	N/A
Charging Pump Suction Valve from RWST LVC-115B	Closed	Closed	N/A	N/A
7. Safety Injection System				
SI Pumps A, B, and C	Operable	N/A	Eventual failure of pump seals.	Eventual bearing failure.
N_2 Supply Valve to Accumulators SI-855	Closed	Closed	N/A	N/A
Accumulator Drain Valves SI-852 A, B, and C	Closed	Closed	N/A	N/A
Accumulator Vent Valves SI-853 A, B, and C	Closed	Closed	N/A	N/A

Table A.4 (Continued)

Component Requiring Support System	Normal Position/Mode	Failure Mode on Loss of		
		Instrument Air	CCW	SWS
		Front Line Systems Cont'd		
8. Residual Heat Removal System				
RHR Pumps A and B	Standby	N/A	Eventual pump seal failure.	N/A
RHR Discharge Valves				
FCV-605	Closed	Closed	N/A	N/A
HCV-758	Closed	Closed	N/A	N/A
9. Safeguards Systems	Standby	N/A	N/A	N/A
10. Reactor Protection System	Standby	N/A	N/A	N/A
		Support Systems		
11. Component Cooling Water System				
Charging Pump Discharge Valves TCV-659 A, B, and C	Open	Open	N/A	N/A
CCW Heat Exchangers	Operating	N/A	N/A	Loss of cooling capacity
12. Service Water System				
SWS Control Valves to AFW Pumps A and B and Turbine Pump				
TCV-1902	Closed (open on pump start)	Open	N/A	N/A
TCV-1903A	Closed (open on pump start)	Open	N/A	N/A
TCV-1903B	Closed (open on pump start)	Open	N/A	N/A
SWS Control Valves from Instrument Air Compressors				
TCV-1629 A and B	Open	Open	N/A	N/A
13. Instrument Air system				
Primary Air Compressor	Operating	N/A	N/A	Eventual failure, unless tripped.
Instrument Air Compressor A and B	Intermittent Operation	N/A	N/A	Eventual failure unless tripped.

operated valves (20-ET, 20-1, and 20-2) or by opening the mechanically activated auto-stop trip valve maintained closed by the auto-stop lube oil pressure. A fourth solenoid-operated valve, 20-AST, can also open the mechanical auto-stop trip valve.

All four solenoid-operated valves require electrical power to open (to actuate turbine trip). The nonmechanical auto-stop turbine trip will not occur if the 125V dc bus A is de-energized owing to the lack of power availability to the solenoid of 20-AST. This is also true for the turbine emergency trip (20-ET), except that the power is supplied from 125V dc bus B. Loss of power from dc bus B also fails solenoids 20-1 and 20-2, preventing a governor/intercept trip.

Additional and diverse turbine protection is provided by the turbine redundant overspeed trip system (TROTS) which operates under a two-out-of-three logic scheme. Loss of power to two of the three TROTS control channels powered from 120V ac instrument buses 6, 7 and 8 will initiate turbine trip. Actuation of additional solenoids* is required to implement this turbine trip.

*The power supply to these solenoids has not been determined at this time but is assumed to be from dc bus A and dc bus B to redundant solenoids. Failure of both dc buses would then be required to fail the TROTS turbine trip.

Table A.5. Component power supplies and associated failure modes

Component	Control Power Source	Supply Power Source	Failure Mode
		Front Line Systems	
1. Reactor Coolant System			
RCP A	DC PNL. A, CKT. 2	4160V Bus 1	Pump fails on loss of supply power. Pump fails to trip on loss of control power.
RCP B	DC PNL. B, CKT. 2	4160V Bus 4	Pump fails on loss of supply power. Pump fails to trip on loss of control power.
RCP C	DC PNL. A, CKT. 2	4160V Bus 2	Pump fails on loss of supply power. Pump fails to trip on loss of control power.
PZR Control Heaters	DC PNL. B, CKT. 4	480V Bus 2B (4160 Bus 1)	Heaters fail on loss of supply power. Heaters fail to trip on loss of control power.
PZR Backup Heaters "A"	DC PNL. A, CKT. 4	480V Bus 1 (4160 Bus 2)	Heaters fail on loss of supply power. Heaters fail to trip on loss of control power.
PZR Backup Heaters "B"	DC PNL. A, CKT. 4	480V Bus 2A (4160 Bus 1)	Heaters fail on loss of supply power. Heaters fail to trip on loss of control power.
PZR Pressure Transmitters			
PT-445		Instrument Bus 3 (Inverter B)	PORV-456 fails closed.
PT-444		Instrument Bus 4 (4160V Bus 3)	PORV-455C fails closed.
PORVs			
RC-456	DC Aux. Pnl. DC CKT. 27		Valve fails closed on loss of control power.
RC-455C	DC Aux. Pnl. GC CKT. 23		Valve fails closed on loss of control power.
PORV Shutoff Valves			
RC-535	120V ac from 480V MCC-6	480V MCC-6 (4160V Bus 3)	Valve fails as is (open).
RC-536	120V ac from 480V MCC-6	480V MCC-6 (4160V Bus 3)	Valve fails as is (open).
2. Turbine Protection System			
Turbine Auto Stop Trip Logic and Solenoid (20-AST)	DC PNL. A, CKT. 22		No turbine auto stop trip on loss of control power.
Turbine Emergency Trip Logic and Solenoid (20-ET)	DC PNL. B, CKT. 13		No turbine emergency trip on loss of control power.
Gov./Intercept Trip Logic and Solenoids (20-1, 20-2)	DC PNL. B, CKT. 13		No Gov./Intercept valve trip on loss of control power.

Table A.5 (Continued)

Component	Control Power Source	Supply Power Source	Failure Mode
		Front Line Systems (Cont'd)	
Governor Control Cabinet		PP-21 off MCC-8 (4160V Bus 3)	Turbine trips on loss of power to cabinet.
EH System Logic	120V ac LP27, CKT. 2 (4160V Bus 1)		Turbine trip over long term due to EH depressurization.
EH Oil Pump "A"	PP-21 from MCC 8 (4160V Bus 3)	480V MCC 4 (4160V Bus 3)	Failure of Pumps "A" and "B" will cause turbine trip over long term. Loss of PP-21 will fail both pumps.
EH Oil Pump "B"	PP-21 from MCC 8 (4160V Bus 3)	480V MCC 3 (4160V Bus 1)	Failure of Pumps "A" and "B" will cause turbine trip over long term. Loss of PP-21 will fail both pumps.
Turbine Overspeed Protection (TROTS) Channel 1	Instr. Bus 6, CKT. 23 4160V Bus 3		Turbine trip on loss of power to 2/3 channels.
Turbine Overspeed Protection (TROTS) Channel 2	Instr. Bus 7, CKT. 23 Inverter A		Turbine trip on loss of power to 2/3 channels.
Turbine Overspeed Protection (TROTS) Channel 3	Instr. Bus 8, CKT. 23 Inverter B	DC Panel "A" and "B"	Turbine trip on loss of power to 2/3 channels.
TROTS Logic	DC Panel A and B		No TROTS turbine trip.
3. Main Steam System			
Steam-Side PORVs			
RV1	Aux. Pnl. DC, CKT. 40 for solenoids (PIC-477 controller self contained)		Valve fails closed on loss of control power.
RV2	Aux. Pnl. DC, CKT. 41 for solenoids (PIC-487 controller self contained)		Valve fails closed on loss of control power.
RV3	Aux. Pnl. DC, CKT. 42 for solenoids (PIC-497 controller self contained)		Valve fails closed on loss of control power.
Steam Dump Valves			
PRV 1324 A-1	Aux. DC Pnl. DC, CKT.38		Fails closed on loss of control power.
PRV 1324 B-1	Aux. DC Pnl. DC, CKT. 38		Fails closed on loss of control power.
PRV 1324 B-2	Aux. DC Pnl. DC, CKT. 38		Fails closed on loss of control power.
PRV 1324 A-2	Aux. DC Pnl. GC, CKT. 38		Fails closed on loss of control power.
PRV 1324 B-3	Aux. DC Pnl. GC, CKT. 38		Fails closed on loss of control power.

Table A.5 (Continued)

Component	Control Power Source	Supply Power Source	Failure Mode
		Front Line Systems (Cont'd)	
Steam Dump Control System			
T-408 (Temperature Controller)		Inst. Bus 4 (4160V Bus 3)	Dump valves fail closed and steam side PORVs fail closed if load reject signal from PM-447 exists.
P-464 (Pressure Controller)		Inst. Bus 4 (4160V Bus 3)	Not normal control mode.
High T_{avg} Logic	Instrument Bus 4 (4160V Bus 3)		Dump valves fail closed.
PM-447 (Loss of Load Pressure Monitor)	Instrument Bus 1 (4160V Bus 2)		Dump valves fail closed.
MSIVs			
V1-3A ISO	DC Aux. Pnl. DC, CKT. 1 or DC Aux. Pnl. GC, CKT. 40		Fails closed on loss of power to either redundant 3-way solenoid.
V1-3B ISO	DC Aux. Pnl. GC, CKT. 1 or DC Aux. Pnl. DC, CKT. 43		Fails closed on loss of power to either redundant 3-way solenoid.
V1-3C ISO	DC Aux. Pnl. GC, CKT. 2 or DC Aux. Pnl. DC, CKT. 44		Fails closed on loss of power to either redundant 3-way solenoid.
V1-3A BYP	120V MCC 8	208V MCC-8 (4160V Bus 3)	Fails as is on loss of supply power (closed).
V1-3B BYP	120V MCC 8	208V MCC-8 (4160V Bus 3)	Fails as is on loss of supply power (closed).
V1-3C BYP	120V MCC 8	208V MCC-8 (4160V Bus 3)	Fails as is on loss of supply power (closed).
4. Main Feedwater System			
FW Pump A	Circuit breaker 52/3, DC Pnl. A, CKT. 2	4160V Bus 1	Pump fails on loss of supply power. Pump fails to trip on loss of control power.
FW Pump B	Circuit breaker 52/26, DC Pnl. B, CKT. 2	4160V Bus 4	Pump fails on loss of supply power. Pump fails to trip on loss of control power.
MFW Isolation Valves			
V2-6A	208V MCC 10	208V MCC-10 (4160V Bus 2)	Fail as is on loss of supply power (open).
V2-6B	208V MCC 9	208V MCC-9 (4160V Bus 3)	Fail as is on loss of supply power (open).
V2-6C	208V MCC 9	208V MCC-9 (4160V Bus 3)	Fail as is on loss of supply power (open).
MFW Control Valves			
FCV-478			
Sol. A	DC Aux. Pnl. DC, CKT. 47		Valve closes on loss of power to either solenoid.
Sol. B	DC Aux. Pnl. GC, CKT. 43		
FCV-488			
Sol. A	DC Aux. Pnl. DC, CKT. 47		Valve closes on loss of power to either solenoid.
Sol. B	DC Aux. Pnl. GC, CKT. 43		
FCV-498			
Sol. A	DC Aux. Pnl. DC, CKT. 47		Valve closes on loss of power to either solenoid.
Sol. B	DC Aux. Pnl. GC, CKT. 43		

Table A.5 (Continued)

Component	Control Power Source	Supply Power Source	Failure Mode
	Front Line Systems (Cont'd)		
MFW Bypass Valves			
FCV-479			
Sol. A	DC Aux. Pnl. DC, CKT. 46		Valve closes on loss of power to either solenoid.
Sol. B	DC Aux. Pnl. GC, CKT. 42		
FCV-489			
Sol. A	DC Aux. Pnl. DC, CKT. 46		Valve closes on loss of power to either solenoid.
Sol. B	DC Aux. Pnl. GC, CKT. 42		
FCV-499			
Sol A	DC Aux. Pnl. DC, CKT. 46		Valve closes on loss of power to either solenoid.
Sol B	DC Aux. Pnl. GC, CKT. 42		
FW Valve Controllers			
Loop 1	Inst. Bus #1 (4160V Bus 2)		FW control valves fail closed.
Loop 2	Inst. Bus #2 (Inverter A)		FW control valves fail closed.
Loop 3	Inst. Bus #3 (Inverter B)		FW control valves fail closed.
5. Aux. Feedwater System			
Motor-Driven AFW Pump A	DC PNL. A, CKT. 1	480V Bus E1 (4160V Bus 2)	Pump fails as is (normally off) on loss of control power. Pump fails on loss of supply power.
Motor-Driven AFW Pump B	DC PNL. B, CKT. 1	480V Bus E2 (4160V Bus 3)	Pump fails as is (normally off) on loss of control power. Pump fails on los of supply power.
Steam-Driven AFW Pump Controller	DC PNL. B, CKT. 23 or Aux. Pnl. DC, CKT. 35 for relay "OX"		Pump fails to start on loss of control power.
Motor-Driven AFW Pump Disch. Valves			
V2-16A	208V MCC-10 or 208V MCC-9	NORM: 208V MCC-10 (4160V Bus 2) ALT: 208V MCC-9 (4160V Bus 3)*	Fails as is normally closed) on loss of supply power.
V2-16B	208V MCC-10	208V MCC-10 (4160V Bus 2)	Fails as is (normally closed) on loss of supply power.
V2-16C	208V MCC-9	208V MCC-9 (4160V Bus 3)	Fails as is (normally closed) on loss of supply power.
Steam-Driven AFW Pump Disch. Valves			
V2-14A	208V MCC-10	208V MCC-10 (4160V Bus 2)	Fails as is (closed) on loss of supply power.
V2-14B	208V MCC-9	208V MCC-9 (4160V Bus 3)	Fails as is (closed) on loss of supply power.
V2-14C	208V MCC-10	208V MCC-10 (4160V Bus 2)	Fails as is (closed) on loss of supply power.

Table A.5 (Continued)

Component	Control Power Source	Supply Power Source	Failure Mode
		Front Line Systems (Cont'd)	
Steam-Driven AFW Pump Steam Supply Valves			
V1-8A	120V MCC-5	480V MCC-5 (4160V Bus 2)	Fails as is (closed) on loss of supply power.
V1-8B	120V MCC-6	480V MCC-6 (4160V Bus 3)	Fails as is (closed) on loss of supply power.
V1-8C	120V MCC-6	480V MCC-6 (4160V Bus 3)	Fails as is (closed) on loss of supply power.
SG Low Low Level Instrument Strings			
SG1-LC-474A		Inst. Bus 1 (4160V Bus 2)	AFW actuates if 2/3 channels de-energize.
SG1-LC-475A		Inst. Bus 2 (Inverter A)	AFW actuates if 2/3 channels de-energize.
SG1-LC-476A		Inst. Bus 3 (Inverter B)	AFW actuates if 2/3 channels de-energize.
SG2-LC-484A		Inst. Bus 1 (4160V Bus 2)	AFW actuates if 2/3 channels de-energize.
SG2-LC-485A		Inst. Bus 2 (Inverter A)	AFW actuates if 2/3 channels de-energize.
SG2-LC-486A		Inst. Bus 3 (Inverter B)	AFW actuates if 2/3 channels de-energize.
SG3-LC-494A		Inst. Bus 1 (4160V Bus 2)	AFW actuates if 2/3 channels de-energize.
SG3-LC-495A		Inst. Bus 2 (Inverter A)	AFW actuates if 2/3 channels de-energize.
SG3-LC-496A		Inst. Bus 3 (Inverter B)	AFW actuates if 2/3 channels de-energize.
6. CVC System			
Charging Pumps			
A	120V ac from 480V Bus DS	480V Bus DS (4160V Bus 3)	Pump fails off on loss of 480V Bus DS.
B	DC PNL. A, CKT. 1	480V Bus E1 (4160V Bus 2)	Pump fails as is (off) on loss of control power. Pump fails off on loss of supply power.
C	DC PNL. B, CKT. 1	480V Bus E2 (4160V Bus 3)	Pump fails as is (off) on loss of control power. Pump fails off on loss of supply power.
Charging Pump Suction Valves			
VCT LCV-115C	120V ac from 480V MCC-6	480V MCC-6 (4160V Bus 3)	Fails as is (normally open).
RWST LCV-115B	DC Aux. Pnl. DC, CKT. 31		Fails closed on loss of control power.
Boric Acid Valve MOV-350		480V MCC-5 (4160V Bus 2)	Fails as is on loss of supply power (mormally closed).

Table A.5 (Continued)

Component	Control Power Source	Supply Power Source	Failure Mode
	Front Line Systems (Cont'd)		
Charging Line Valves			
CVC-310A	DC Aux. Pnl. GC, CKT. 15		Fails open on loss of control power (normally closed).
CVC-310B	DC Aux. Pnl. DC, CKT. 22		Fails open on loss of control power (normally open).
Aux. Spray CVC-311	DC Aux. Pnl. DC, CKT. 23		Fails closed on loss of control power (normally closed).
Letdown Stop Valves			
LCV-460A	DC Aux. Pnl., CKT. 13		Fails closed on loss of control power to valve and to PZR level controller LC-459F.
LCV-460B	DC Aux. Pnl., CKT. 13		Fails closed on loss of control power to valve and to PZR level controller LC-459F.
PZR Level Controller LC-459F	Instrument Bus 4 and 9 (4160V Bus 3)		LCV-460 A and B fail closed on loss of controller power and charging pump in "auto" goes to minimum speed.
Letdown Orifice Isolation Valves			
CVC-200A	DC Aux. Pnl. DC, CKT. 18		Fails closed on loss of control power.
CVC-200B	DC Aux. Pnl. GC, CKT. 13		Fails closed on loss of control power.
CVC-200C	DC Aux. Pnl. DC, CKT. 2		Fails closed on loss of control power.
Letdown Isolation Stop Valves			
CVC-204A	DC Aux. Pnl. DC, CKT. 3		Fails closed on loss of control power.
CVC-204B	DC Aux. Pnl. GC, CKT. 3		Fails closed on loss of control power.
Charging Line FCV, HCV-121	Instrument Bus 1 and 6 (4160V Bus 2)		Fails open on loss of control power. Normally open.
7. Safety Injection System			
SI Pumps			
A	DC PNL. A, CKT. 1	480V Bus E1 (4160V Bus 2)	Pump fails to start on loss of control power. Fails off on loss of supply power.
B	DC PNL. B, CKT. 1 and DC PNL. A, CKT. 1	480V Bus E2 (4160V Bus 3)	Pump fails to start on loss of both sources of control power. Fails off on loss of supply power.

Table A.5 (Continued)

Component	Control Power Source	Supply Power Source	Failure Mode
		Front Line Systems (Cont'd)	
C	DC PNL. B, CKT. 1	480V Bus E2 (4160V Bus 3)	Pump fails to start on loss of control power. Fails off on loss of supply power.
Accumulators A, B, C			
Acc. N_2 Supply Valve SI-855	DC Aux. Pnl. DC, CKT. 17		Fails closed on loss of control power (normally closed).
Acc. Drain Valves			
SI-852A	DC Aux. Pnl. DC, CKT. 8		Fails closed on loss of control power.
SI-852B	DC Aux. Pnl. GC, CKT. 8		Fails closed on loss of control power.
SI-852C	DC Aux. Pnl. GC, CKT. 9		Fails closed on loss of control power.
Acc. Vent Valves			
SI-853A	DC Aux. Pnl. DC, CKT. 9		Fails as is on loss of control power (closed).
SI-853B	DC Aux. Pnl. GC, CKT. 10		Fails as is on loss of control power (closed).
SI-853C	DC Aux. Pnl. GC, CKT. 11		Fails as is on loss of control power (closed).
Acc. Discharge Valves			
SI-865A	120V ac from 480V MCC-5	480V MCC-5 (4160V Bus 2)	Fails as is (normally open).
SI-865B	120V ac from 480V MCC-6	480V MCC-6 (4160V Bus 3)	Fails as is (normally open).
SI-865C	120V ac from 480V MCC-5	480V MCC-5 (4160V Bus 2)	Fails as is (normally open).
Cold Leg Injection Valves			
SI-870A	120V ac from 480V MCC-5	480V MCC-5 (4160V Bus 2)	Fails as is on loss of supply power (closed).
SI-870B	120V ac from 480V MCC-6	480V MCC-6 (4160V Bus 3)	Fails as is on loss of supply power (closed).
Boron Inj. Tank Inlet Valves			
SI-867A	120V ac from 480V MCC-5	480V MCC-5 (4160V Bus 2)	Fails as is on loss of supply power (closed).
SI-867B	120V ac from 480V MCC-6	480V MCC-6 (4160V Bus 3)	Fails as is on loss of supply power (closed).
RWST Outlet Valves			
SI-864A	120V ac from 480V MCC-5	480V MCC-5 (4160V Bus 2)	Fails as is on loss of supply power (open).
SI-864B	120V ac from 480V MCC-6	480V MCC-6 (4160V Bus 3)	Fails as is on loss of supply power (open).

Table A.5 (Continued)

Component	Control Power Source	Supply Power Source	Failure Mode
		Front Line Systems (Cont'd)	
SI Valves to Hot Legs			
SI-866A	120V ac from 480V MCC-6	480V MCC-6 (4160V Bus 3)	Fails as is on loss of supply power (closed).
SI-866B	120V ac from 480V MCC-5	480V MCC-5 (4160V Bus 2)	Fails as is on loss of supply power (closed).
SI-869	120V ac from 480V MCC-5	480V MCC-5 (4160V Bus 2)	Fails as is on loss of supply power (open).
Pressurizer Pressure Instrument Strings			
PC-455E		Inst. Bus 1 (4160V Bus 2)	SI signal if 2/3 channels de-energize.
PC-456D		Inst. Bus 2 (Inverter A)	SI signal if 2/3 channels de-energize.
PC-457D		Inst. Bus 3 (Inverter B)	SI signal if 2/3 channels de-energize.
8. RHR System			
RHR Pump A	DC Pnl. A, CKT 1	480V Bus E1 (4160V Bus 2)	Fails on loss of supply power. Fails as is (off) on loss of control power.
RHR Pump B	DC Pnl. B, CKT 1	480V Bus E2 (4160V Bus 3)	Fails on loss of supply power. Fails as is (off) on loss of control power.
Pump Suction Valves from RWST			
SI-862A	120V ac from 480V MCC-5	480V MCC-5 (4160V Bus 2)	Fails as is on loss of supply power (open).
SI-862B	120V ac from 480V MCC-6	480V MCC-6 (4160V Bus 3)	Fail as is on loss of supply power (open).
RHR Pump Disch. Valve FCV-605	Inst. Bus 4 and 9 (4160V Bus 3)		Fails closed on loss of supply power.
Cold Leg Inlet Valves			
RHR-744A	120V ac from 480V MCC-5	480V MCC-5 (4160V Bus 2)	Fails as is on loss of supply power (closed).
RHR-744B	120V ac from 480V MCC-6	480V MCC-6 (4160V Bus 3)	Fails as is on loss of supply power (closed).
9. Safeguards System			
Safeguards Train "A" (DC Logic Rack A)		DC Panel A	Loss of safeguards. Train A.
Safeguards Train "B" (DC Logic Rack B)		DC Panel B	Loss of safeguards. Train B.

Table A.5 (Continued)

Component	Control Power Source	Supply Power Source	Failure Mode
		Front Line Systems (Cont'd)	
10. Reactor Protection System			
Control Rod Drive Motor Generator Set A	DC Pnl. A	480V Bus 2B (4160V Bus 1)	Reactor trips on loss of supply power to both motor generator sets.
Control Rod Drive Motor Generator Set B	DC Pnl. B	480V Bus 3 (4160V Bus 3)	Reactor trips on loss of supply power to both motor generator sets.
RCP Undervoltage Trip Relays			
UV-1		4 KV Bus 1	RT on trip of 2/3 relays.
UV-2		4 KV Bus 2	RT on trip of 2/3 relays.
UV-3		4 KV Bus 4	RT on trip of 2/3 relays.
Reactor Protection Train "A" Logic		DC Panel A	RT on de-energizing of undervoltage trip coils which occurs on loss of power to Logic Rack.
Reactor Protection Train "B" logic		DC Panel B	RT on de-energizing of undervoltage trip coils which occurs on loss of power to Logic Rack.
		Support Systems	
11. Component Cooling Water			
CCW Pump A		480V Bus DS (4160V Bus 3)	Pump fails off on loss of supply power.
CCW Pump B	DC Pnl. A, CKT. 1	480V Bus E1 (4160V Bus 2)	Pump fails as is (normally off) on loss of control power. Pump fails on loss of supply power.
CCW Pump C	DC Pnl. B, CKT. 1	480V Bus E2 (4160V Bus 3)	Pump fails as is (normally off) on loss of control power. Pump fails on loss of supply power.
Header Supply Valves to RCPs			
CC-716A	120V from 480V MCC-5	480V MCC-5 (4160V Bus 2)	Fails as is on loss of supply power (open).
CC-716B	120V from 480V MCC-6	480V MCC-6 (4160V Bus 3)	Fails as is on loss of supply power (open).
CCW Return Valve from RCP Lube Oil Coolers, CC-730	120V from 480V MCC-6	480V MCC-6 (4160V Bus 3)	Fails as is on loss of supply power (open).
CCW Return Valve from RCP Thermal Barrier Cooling Coils, FCV-626	120V from 480V MCC-6	480V MCC-6 (4160V Bus 3)	Fails as is on loss of supply power (open).

Table A.5 (Continued)

Component	Control Power Source	Supply Power Source	Failure Mode
		Support Systems (Cont'd)	
12. Service Water System			
SW Pump A	DC Pnl. A, CKT. 1	480V Bus E1 (4160V Bus 2)	Pump fails as is on loss of control power. Pump fails off on loss of supply power.
SW Pump B	DC Pnl. A, CKT. 1	480V Bus E1 (4160V Bus 2)	Pump fails as is on loss of control power. Pump fails off on loss of supply power.
SW Pump C	DC Pnl. B, CKT. 2	480V Bus E2 (4160V Bus 3)	Pump fails as is on loss of control power. Pump fails off on loss of supply power.
SW Pump D	DC Pnl. B, CKT. 2	480V Bus E2 (4160V Bus 3)	Pump fails as is on loss of control power. Pump fails off on loss of supply power.
SW Disch. Cross-Tie Valves			
V6-12B	120V from 480V MCC-5	480V MCC-5 (4160V Bus 2)	Fails as is on loss of supply power (open).
V6-12C	120 V from 480 V MCC-6	480 V MCC-6 (4160 V Bus 3)	Fails as is on loss of supply power (open).
SW Train Isolation Valves			
V6-16A	208 V MCC-9	208 MCC-9 (4160 V Bus 3)	Fails as is on loss of supply power (open).
V6.16B	208 V MCC-10	208 MCC-10 (4160 V Bus 3)	Fails as is on loss of supply power (open).
SW Suction Control Valve to AFW Turbine Driven Pump			
TCV-1902	120 V PP-21, CKT 15 (4160 V Bus 3)		Fails open on loss of control power.
SW Suction Control Valves from AFW Motor Pump Lube Oil Coolers			
TCV-1903A	120 V PP-21, CKT. 15 (4160 V Bus 3)		Fails open on loss of control power.
TCV-1903B	120 V PP-21, CKT. 15 (4160 V Bus 3)		Fails open on loss of control power.

Table A.5 (Continued)

Component	Control Power Source	Supply Power Source	Failure Mode
		Support Systems (Cont'd)	
13. Instrument Air System			
Primary Air Compressor		480 V Bus 2A (4160 V Bus 1)	Compressor fails on loss of supply power.
Instrument Air Compressors			
A		480 V MCC-5 (4160 V Bus 2)	Compressor fails on loss of supply power.
B		480 V MCC-6 (4160 V Bus 3)	Compressor fails on loss of supply power.
14. Electric Power System			
Diesel Generator A Circuit Breaker (52/17B)	DC PNL. A		D/G A fails to close onto 480 V bus E1.
Diesel Generator B Circuit Breaker (52/27B)	DC PNL. B		D/G B fails to close onto 480 V bus E2.

*Alternate supply was assumed in the study.

A.4.3.4. Steam Dump System

Three STM PORVs and five steam dump valves (SDVs) are provided to relieve steam from the main steam lines to the atmosphere and condenser when required. These valves are pneumatically operated and designed to fail closed upon loss of pneumatic pressure.

The STM PORVs and SDVs open by energizing solenoid valves to open (powered by 125V dc auxiliary panels DC and GC), which results in pressurization of the STM PORVs with air and the SDVs with nitrogen. Additionally, the SDVs require the nitrogen supply to be armed (supply valves open), which requires that an arming signal exist.

The SDVs normally operate under the T_{avg} steam dump control system but can be operated under the steam dump pressure control system for plant cooldown. This analysis assumes the T_{avg} control configuration. Control of the STM PORVs, which is normally from independent pressure controllers, switches to the T_{avg} steam dump control when a sudden loss of load occurs. Loss of power to PM-447, the loss-of-load signal generator, precludes control of the STM PORVs by the T_{avg} control system. The loss-of-load signal from PM-447 also provides the arming signal to the SDVs. When T_{avg} falls below a certain set point, the arming signal is removed. The signals required for automatic opening of the SDVs and STM PORVs under T_{avg} control (high T_{avg} and sudden of loss-of-load signals) require 120V ac power from instrument buses 1 and 4.

A.4.3.5. Main Steam Isolation Valves

Each of the three main steam lines has an air-operated swing disk MSIV. The MSIVs (V1-3A, B, and C) are designed to isolate the containment and limit the release of steam

from the SGs following main steam-line break accidents. The MSIVs are located in the steam lines downstream of the main steam safety relief valves (SRVs) and the STM PORVs and outside the containment.

Each MSIV has two three-way solenoids series, which when energized supply instrument air pressure to the MSIV bottom chamber and hold the MSIV open. These two solenoids are supplied 125V dc power from auxiliary dc panels DC and GC, respectively. Loss of power supply to either solenoid or loss of instrument air to the bottom chamber will cause the valve to close with spring assist. The MSIVs also close on any of the following signals: high steam flow coincident with either low steam-line pressure or low T_{avg}; high-high containment pressure; or manual actuation.

Each steam line has a motor-operated bypass valve to equalize upstream and downstream pressures to permit MSIV reopening after closure. All three bypass valves are normally closed and fail as is on loss of their power supply (120/208V ac MCC-8). The bypass valves must be manually actuated.

A.4.3.5. Main Feedwater Pumps

Safety injection or high SG level signals will trip the MFW pumps. Switchgear for FW pumps A and B is powered from 125V dc buses A and B, respectively. Failure of the 125V dc power supply will prevent tripping of operating pumps. The pumps will trip from undervoltage on their respective motive power supply (4KV buses 1 and 4). In the long term, the pumps will fail if service water cooling to the pump lube oil coolers is lost.

A.4.3.7. Main Feedwater Control Valves

The MFW flow rate to each SG is controlled by a pneumatically operated control valve in response to FW demand signals. Flow to SG 1, 2, and 3 is controlled by control valves FCV-478, 488, and 498, respectively. The FW demand signal for each control valve is developed based on SG steam flow, FW flow rate and SG water level. The normal demand signals are overridden by low T_{avg} coincident with reactor trip, high SG water level, or SI signals, which close all control valves.

The FW control valves are designed to close on loss of instrument air or control power. The instrument air supply to the control valves from the positioners is isolated by solenoid valves upon loss of power to the solenoids or loss of power to the FW loop control instrumentation. The control instrumentation which positions the FW valves is powered through 120V ac instrument buses 1, 2, and 3 for valves FCV-478, 488, and 498, respectively.

Each control valve has two solenoid valves, in series, which supply air to the valve. These solenoids are powered from auxiliary dc panels DC and GC, respectively. Loss of power to either solenoid results in the control valve closing.

A.4.3.8. Main Feedwater Isolation Valves

Main feedwater isolation valves (MFIVs) V2-6A, B, and C are designed to close and isolate FW pump discharge flow to the SGs. The MFIVs automatically close on a SI signal or may be manually closed by the operator.

The valve motors for V2-6A, B and C and associated switchgear are powered from 120/208V ac MCC-10, 9, and 9, respectively. During normal operation the MFIVs are open. Failure of the associated MCC will result in the valves remaining open.

A.4.3.9. Main Feedwater Bypass Valves

Feedwater bypass valves FCV-479, 489, 499 are designed to regulate the FW flow to SGs 1, 2, and 3, respectively, at low power conditions. During power operation the bypass valves are normally closed. At low power conditions, the operator normally will manually position the bypass valves to regulate SG level. The opening of the bypass valves is prevented in the presence of either SI or high SG level signal. As a part of the reactor trip runback sequence, this valve is manually opened to supply necessary feedwater to maintain SG level. The bypass valves can allow a maximum flow rate of about 15% of nominal FW flow.

Each bypass valve has two solenoid valves, in series, which supply opening air to the valve. These solenoids are powered from auxiliary dc panels DC and GC, respectively. Loss of power or instrument air to either solenoid results in the bypass valve remaining closed or closing.

A.4.3.10. Auxiliary Feedwater System

The AFW system is designed to provide FW to the SGs if the MFW system is incapable of maintaining a minimum SG level.

The AFW system consists of two motor-driven pumps, A and B, and one steam-turbine-driven pump. The motor-operated isolation valves on the pump discharge lines to the SG open when their respective pumps are actuated. These valves can be manually closed from the control room to isolate flow to any of the SGs. A low-level signal in any two SGs or a direct signal of loss of power to the MFW pumps will automatically start the steam-driven AFW pump by opening steam admission valves and the AFW discharge valves to individual SGs. The signals for starting the motor-driven AFW pumps and opening the associated discharge valves are both FW pump breakers open, low level in any SG, or a safeguards actuation signal.

Control of AFW flow is based on a constant, predetermined flow rate to each SG and may be manually controlled via the discharge valves to the individual SGs.

On loss of power, the motor-operated isolation valves and turbine pump steam supply valves will fail as is, which is normally in the closed position. The turbine pump speed controller requires instrument air and will fail at full speed on loss of instrument air.

All three AFW pumps require service water to cool their motor bearings. Loss of service water can cause these pumps to fail in the long term.

A.4.3.11. Chemical and Volume Control System

The chemical and volume control system (CVCS) is designed to remove, purify and replace reactor coolant at a controlled flow rate to maintain pressurizer level during reactor operation. The system provides chemicals to the RCS to control reactor coolant chemistry and seal water to the RCP seals. Letdown flow is controlled by the letdown orifices and isolation valves, CVC-200 A, B, and C.

Reactor coolant is delivered to the RCS by one or more of the positive displacement charging pumps. When in automatic control, the pressurizer level controller will automatically vary the speed of the operating charging pumps to control pressurizer level. One pump is normally in use, with the second and third pumps on standby with manual start and optional automatic control.

The CVCS requires instrument air and control power for valve positioning and motive power for charging pumps and motor-operated valves to function. Loss of instrument air results in closure of the letdown stop valves, resulting in letdown isolation. Loss of air to the charging pump speed controllers results in full-speed pump operation.

Loss of power to the pressurizer level controller from 120V ac instrument bus 4 results in letdown isolation and runback of the charging pump speed to a preset minimum speed designed to ensure that sufficient seal water and minimum charging flow requirements are met. Flow can be restored by operating the pumps in the manual rather than the automatic mode.

In addition to electric power, the charging pumps require cooling water from the CCW system for their lube oil coolers. Loss of CCW can lead to eventual pump failure in the long term.

A.4.3.12. Safeguards Actuation System

The safeguards actuation system consists of two trains, A and B. Safeguards trains A and B can be actuated by low pressurizer pressure, high containment pressure, high steam-line differential pressure, or high steam flow coincident with either low steam-line differential pressure or with low T_{avg}. The actuation of both trains causes the two low-pressure injection (RHR) pumps and the three high-pressure injection (SI) pumps to start. In addition, the SI discharge valves open, the reactor trips, the MFW isolates, all SW pumps and CCW pumps are started, and AFW is initiated.

Safeguards trains A and B are powered from 125V dc buses A and B, respectively. If power is lost on dc bus B, train A safeguards system components can still actuate on demand, but train B components cannot (and vice versa).

The three strings of pressurizer pressure instrumentation that are each powered from separate instrument buses produce a low signal on loss of their power supply. Loss of power to any two of these generates the low-pressure signal, which initiates SI. Other instrumentation signals that initiate SI will not do so on loss of their power supplies since these others require a high signal to initiate SI and the power loss results in low signals.

A.4.3.13. Safety Injection System

The SI system is designed to supply borated water to the reactor core in the event of a loss-of-coolant accident (LOCA). The SI system discussed here is the high-pressure injection portion of the system. The system consists of three SI pumps and associated injection valves, as well as three pressurized accumulators that can passively deliver borated water to the RCS at lower RCS pressure. The three SI pumps take suction from the refueling water storage tank (RWST) and feed a common header which supplies the three cold legs through the boron injection tank (BIT) and also feeds two RCS hot legs. Hot leg injection is manually actuated, while cold leg injection is actuated on an SI signal.

The SI electric power supply is divided into two trains, A and B, each providing 480 and 120V ac power. Train A (480V ac bus E1 and 480V ac MCC-5) powers SI pump A, cold leg injection valve SI-870A, and the RCS loop 2 hot leg injection valve. Train B (480V ac bus E2 and 480V ac MCC-6) powers SI pumps B and C, cold leg injection valve SI-870B, and the RCS loop 3 hot leg injection valve. The SI pump circuit breakers require power from 125V dc bus A for train A pumps and 125V dc bus B for train B pumps.

The cold leg injection valves are arranged in parallel, so that either valve can deliver SI flow to the three cold legs. The hot and cold leg injection valves are motor operated and normally closed. These will fail as is upon loss of power.

In addition to electric power, the pumps require cooling water from the CCW and SW systems. Cooling water for the pumps' bearing and seal coolers is provided from the SW and CCW systems, respectively. Loss of cooling water can lead to eventual pump failure.

A.4.3.14. Residual Heat Removal System

The RHR system provides low-pressure injection (LPI), which is actuated on an SI signal, and decay heat removal during shutdown. The system utilizes two pumps which take suction from the RWST during LPI. Flow from these pumps is controlled by two air-operated control valves and passes through two motor-operated isolation valves before discharging into the RCS cold legs.

The system power supply is divided into two trains, A and B, each providing 480 and 120V ac power. RHR pump A and isolation valve RHR-744A are supplied train A power from 480V ac bus E1 and 480V ac MCC-5, respectively. RHR pump B and isolation valve RHR-744B are supplied train B power from bus E2 and MCC-6, respectively. The RHR pump circuit breakers require power from the associated 125V dc bus A for pump A and 125V dc bus B for pump B.

The RHR motor-operated isolation valves are normally closed and will fail as is on loss of power. The air-operated control valves are normally open and will fail closed on loss of air. There is a locked-open bypass valve around one of the control valves that ensures flow to the isolation valves. The isolation valves automatically open on an SI signal.

In addition to electric power, the RHR pumps require CCW for the pump seal water heat exchangers. Loss of cooling water can lead to eventual pump failure in the long term.

A.4.3.15. Reactor Protection System

The reactor protection system consists essentially of control/logic cabinets which cause the control rods to drop into the core on the detection of a variety of unfavorable plant states. Reactor trip (rod drop) will occur on: loss of power to both motor generator sets powered from the 480V buses 2B and 3; or loss of 125V dc power from buses A or B to either reactor protection train or to the reactor trip circuit breakers. Reactor trip will also occur upon under-voltage detection on two-thirds of the 4KV buses 1, 2 or 4. Failure of any one of the 120V ac instrument buses, which power the separate reactor trip channels transmitting process signals, will not directly cause a reactor trip due to the two-out-of-three logic arrangement that prevails in the reactor protection system.

A.5. Impact of Support System Failures

In this section the effects of postulated support system failures on aspects of the plant state potentially important to PTS sequences are assessed. The impact of each support system failure postulated is described in Section 6.1 and the potential impact of the plant responses on PTS sequences is assessed. Section 6.2 summarizes the support system failures that are considered of potential concern to PTS sequences.

A.5.1. Impact of Postulated Failures

In this section the change in plant systems and components in response to postulated support system failures is described. Thirty-six support system failures were postulated, including 33 cases involving failure of electrical buses (loss of voltage on the bus), failure of the instrument air system (loss of instrument air pressure), and failure of the CCW and SW systems (loss of system flow).

Many of the failures postulated are low-probability events. In addition, the operator may be able to take remedial action or manual control to restore operability in many cases.

The initial conditions assumed for the analysis are that the plant is in a normal automatic control mode and the on-site electrical system is configured as shown in Figure A.1. Immediate effects due to support system failures have been noted. In addition, certain failures leading to long-term effects, such as the potential loss of RCP seals due to the unavailability of seal water, have been noted.

A.5.1.1. Electrical Bus Failures

Electric bus failures can occur for a variety of reasons, including isolation or failure of feeder buses, equipment faults not cleared by local breakers, or faults that could occur during maintenance. For purposes of this analysis, single unspecified failures were postulated at various points in the power distribution circuitry. A bus failure was assumed to de-energize the directly affected bus and buses fed from the failed bus. The batteries supplying dc buses A and B were considered to be fully charged and the diesel generators were assumed to be unavailable.

The impact of single bus failures was assessed first. The buses considered included the 4KV buses, the 480V buses, the 480V and 120V/208V MCCs, the 125V dc buses, and dc auxiliary panels DC and GC. In addition, certain double bus failures were postulated. Those considered two failed 4KV buses at a time and failure of both dc buses A and B. Lastly, the existence of maintenance ties was considered by postulating failure of the vital instrument buses tied to MCC-8 on 4KV bus 3. The 125V dc buses have multiple power supplies and have no maintenance ties.

The response of the systems and components to the postulated electric power failures are summarized in Table A.6. The table also includes an assessment of whether or not the plant response is of potential concern to PTS sequences and warrants further consideration. The assessment is based on eliminating those sequences that were clearly not of PTS concern.

Loss of any one of the 4KV buses 1, 2 (and associated bus E1 diesel) or 4 would be expected to have little or no impact from a PTS standpoint, although a reactor and turbine trip would be expected due to loss of RCPs. However, loss of 4KV bus 3 would result in the following simultaneous effects: turbine trip, subsequent reactor trip, letdown isolation, one PZR PORV failed closed, all SDVs failed closed, charging flow (assumed in the auto mode) runback to a minimum level, and only one SI pump available. The pressurizer relief block valves would not be operable if required to close. Loss of 4KV bus 2 would result in isolation of one MFW loop and failure of all five SDVs in the closed position.

Loss of power to the 125V dc buses results in multiple effects. Loss of dc bus A produces a reactor trip signal, which initiates a turbine trip and transfer of the 4KV buses from the UAT to the SUT; however, the transfer cannot be completed without power from dc bus A and, thus, power is also lost on 4KV buses 1 and 2. This sequence does not occur on the loss of dc bus B; or on the simultaneous loss of both dc buses. When power is lost on both dc buses, the 4KV buses are backfed from the 230KV switchyard. With the loss of dc bus A and the consequential loss of 4KV buses 1 and 2, AFW and SI are initiated and the secondary side is isolated. With loss of power on dc bus B, the pressurizer heaters are failed on with both pressurizer relief valves failed closed, and the turbine trips, initiating transfer of 4KV bus 1 to the SUT. This induces a momentary power loss on instrument bus 1, which, coupled with the loss of instrument bus 3 from dc bus B, results in SI actuation on a two-out-of-three low pressurizer pressure channel logic. (See Table A.6 for other components impacted by single 125V dc bus failures.)

With loss of power on both 125V dc buses A and B, a reactor trip is initiated, but at least three-out-of-four turbine trip systems are failed due to loss of power to the trip solenoids. The fourth trip system (TROTS) will also fail if dc buses A and B power its trip solenoids as well.* Also, AFW, SI, and low-pressure safety injection (RHR) are failed on loss of dc buses A and B, and all RCPs and pressurizer heaters are failed on and cannot be tripped.

All combinations of double 4KV bus failures were postulated and analyzed (that is, all double failure combinations of the four buses). The postulated failure of 4KV buses 2 and

*The power supply configuration for the TROTS solenoids has not been determined at this time.

Table A.6. Impact of electric power failures on systems and components important to PTS sequences

Postulated Failures	System/Component Response	Response of Potential Concern to PTS Sequences
	Single Bus Failures	
1. Loss of 4KV Bus 1	• FW Pump A off • RCP A off (reactor trip due to resulting transient)	No
2. Loss of 4KV Bus 2	• FW Loop 1 isolation • STM dump valves fail closed • RCP C off (reactor trip due to resulting transient) • Loss of all but one SI pump	No
3. Loss of 4KV Bus 3 (and associated 480V diesel generator)	• PORV RC-455C stays closed • PORV block valves fail open • STM dump valves fail closed • STM PORVs fail closed if load reject signal PM-447 exists • Turbine trip (and reactor trip by logic) • Letdown isolation • Minimum auto charging pump flow (manual recovery may be required) • Loss of all SI pumps except A • Loss of two of three charging pumps	No
4. Loss of 4KV Bus 4	• FW Pump B off • RCP B off (reactor trip due to resulting transient)	No
5. Loss of 125V dc Panel A (which through logic, also results in loss of 4KV Buses 1 and 2)	• All PZR heaters off • PZR aux-spray valve fails closed • Reactor trip • Turbine trip (from 2/3 TROTS channels) • SI Train B actuated (from 2/3 PZR low pressure) • RCP A and C off • MSIVs close (given spring assist operates) • AFW actuates • PORV RC-456 stays closed • All STM dump valves and STM PORVs fail close • FW isolation • Letdown isolation	Yes

Table A.6 (Continued)

Postulated Failures	System/Component Response	Response of Potential Concern to PTS Sequences
	Single Bus Failures (Cont'd)	
	• Instrument air capacity marginal (compressor B only) • Charging line to Loop 2 cold leg failed open, but no change in charging flow	
6. Loss off 125V dc Panel	• Reactor trip (and TT by logic) • SI Train B actuated (from 2/3 PZR low pressure) • 2 STM dump valves fail closed (A-2 and B-3) • FW isolation • Letdown isolation • Both pressurizer PORVs fail closed • PZR control heaters on • AFW actuates with only MAFW pump A available • MSIVs close (given spring assist operates)	Yes
7. Loss of 125V dc Aux. Panel DC	• PZR aux-spray valve fails closed • PORV RC-456 fails closed • STM PORVs fail closed • 3 STM dump valves fail closed (A-1, B-1, B-2) • MSIVs close (given spring assist operates) • FW isolation (control and bypass valves closed) • Letdown isolated • Charging line to Loop 2 cold leg failed open, but no change in charging flow	Yes
8. Loss of 125V dc Aux. Panel GC	• PORV RC-455C fails closed • 2 STM dump valves closed (A-2, B-3) • MSIVs close (given spring assist operates) • FW isolation • Letdown isolated • Charging line to Loop 1 cold leg failed open, but no change in charging flow	No

Table A.6 (Continued)

Postulated Failures	System/Component Response	Response of Potential Concern to PTS Sequences
	Single Bus Failures (Cont'd)	
9. Loss of 480V Bus 1	• None	No
10. Loss of 480V Bus 2A	• Primary air compressor fail • Delayed turbine trip (due to eventual EH system depressurization)	No
11. Loss of 480V Bus 2B	• None	No
12. Loss of 480V Bus 3	• Delayed turbine trip (eventual EH system depressurization) • Turbine trip (RT by logic)	No
13. Loss of 480V Bus E1	• STM dump valves fail closed • Loop 1 FW isolated	No
14. Loss of 480V Bus E2	• PORV RC-455C fails closed • STM dump valves fail closed • STM PORVs fail closed if load reject signal PM-447 exists • Minimum auto charging pump flow (manual recovery may be required) • Letdown Isolated • 2/3 SI pumps off (B and C)	No
15. Loss of 480V Bus DS	• One charging pump and one CCW pump failed	No
16. Loss of 480V MCC-2	• Delayed TT (due to eventual EH system depressurization)	No
17. Loss of 480V MCC-3	• None	No
18. Loss of 480V MCC-4	• Turbine trip (RT by logic) • Delayed TT (due to eventual EH system depressurization) • MSIV bypass valves fail closed	No
19. Loss of 480V MCC-5	• Loop 1 FW isolated • STM dump valves fail closed	No
20. Loss of 480V MCC-6	• PORV RC-455C fails closed • STM dump valves fail closed • STM PORVs fail closed if load reject signal PM-447 exists • Minimum auto charging flow (manual recovery may be required)	No

Table A.6 (Continued)

Postulated Failures	System/Component Response	Response of Potential Concern to PTS Sequences
	Single Bus Failures (Cont'd)	
21. Loss of 480V MCC-8	• Turbine trip (RT by logic) • Delayed TT (due to eventual EH system depressurization) • MSIV bypass valves fail closed	No
22. Loss of 480V MCC-9	• None	No
23. Loss of 480V MCC-10	• None	No
	Multiple Bus Failures	
1. Loss of 4KV Buses 2 and 3 (and associated 480V diesel generators)	• Turbine trip (RT by logic) • PORV RC-455C fails closed • PORV block valves failed open • RCP C off • STM dump valves fail closed • FW Loop 1 isolation • Charging pumps off • Letdown isolated (loss of PZR level control) • HPI not operable • AFW not operable • RHR not operable • Component cooling pumps lost* • Service water pumps off* (resulting in loss of instrument air) MSIV closure (given spring assist operates) Primary and secondary PORV closure FW isolation	Yes
2. Loss of 4KV Buses 1 and 2 (and associated 480V diesel generator)	• RCPs A and C off (reactor trip due to resulting transient) • PZR heaters off • Delayed TT and immediate TT by logic • Reactor trip • STM dump valves fail closed • Only instrument air compressor B is left • FW Loop 1 isolated • Charging flow can't be throttled by valve (level control on pump speed is operable)	Yes

Table A.6 (Continued)

Postulated Failures	System/Component Response	Response of Potential Concern to PTS Sequences
	Multiple Bus Failures (Cont'd)	
3. Loss of 4KV Buses 1 and 4	• Reactor trip • Turbine trip (by logic) • RCPs A and B off • FW isolation • AFW actuated by logic (turbine pump only)	No
4. Loss of 4KV Buses 1 and 3 (and associated 480V diesel generators)	• PORV RC-455C stays closed • PORV block valves failed open • Delayed TT (eventual EH system depressurization) • RCP A is off • Reactor trip • Instrument air compressor A left only • Minimum auto charging pump flow (manual recovery may be required) • Letdown isolation • STM dump valves fail closed • STM PORVs fail closed if load reject signal PM-447 exists • SI available with Pump A only	No
5. Loss of 4KV Buses 2 and 4 (and associated 480V diesel generator)	• Reactor trip • Turbine trip (by logic) • RCPs B and C off • STM dump valves fail closed • FW isolated to Loop 1 via control valve closure	No
6. Loss of 4KV Buses 3 and 4 (and associated 480V diesel generators)	• PORV RC-455C stays closed • PORV block valves failed open • Delayed TT (eventual EH system depressurization) • Immediate turbine trip from governor control cabinet (RT by logic) • RCP B is off • Minimum auto charging pump flow (manual recovery may be required) • Letdown isolation • STM dump valves fail closed • STM PORVs fail closed if load reject signal PM-447 exists • SI available with pump A only	No

Table A.6 (Continued)

Postulated Failures	System/Component Response	Response of Potential Concern to PTS Sequences
	Multiple Bus Failures (Cont'd)	
7. dc Panels A and B	• Reactor trip • PZR aux-spray valve fails closed • Both primary PORVs closed • TT failure (if TROTS also fails on loss of dc power) • STM dump valves and STM PORVs fail closed • MSIVs closed (given spring assist operates) • FW isolated • Letdown isolated • Charging flow continues to cold legs 1 and 2 from Pump A only; operator can shut off pump A • All RCPs on and cannot be tripped • All PZR heaters on and cannot be tripped • SI not operable • AFW not operable • RHR not operable	Yes
	Bus Failures with Maintenance Ties	
1. Loss of 4KV Bus 3** with Instrument Bus 2 tied to 120/208V MCC-8 (Instrument Bus 1 also incurs a temporary voltage reduction due to the 4KV transfer that is initiated by TT)	• Turbine trip (RT by logic) • PORV RC-455C stays closed • PORV block valves fail open • STM dump valves fail closed • STM PORVs fail closed if load reject signal PM-477 exists • FW Loop 2 isolates • Minimum auto charging flow (manual recovery may be required) • SI actuated (one SI pump available) • AFW actuated • Letdown isolated	Yes
2. Loss of 4KV Bus 3** with Instrument Bus 3 tied to 120/208V, MCC-8 (Instrument Bus 1 also incurs a temporary voltage reduction due to the 4KV transfer that is initiated by TT)	• Turbine trip (RT by logic) • PORVs RC-455C and RC-456 stay closed • STM dump valves fail closed • STM PORVs fail closed if load reject signal PM-447 exists • FW loop 3 isolates • Minimum auto charging flow (manual recovery may be required) • SI actuated (one SI pump available) • AFW actuated • Letdown isolated	Yes

Table A.6 (Continued)

Postulated Failures	System/Component Response	Response of Potential Concern to PTS Sequences
	Bus Failures with Maintenance Ties (Cont'd)	
3. Loss of 4KV Bus 3** with Instrument Buses 2 and 3 tied to 120/208V, MCC-8 (Instrument Bus 1 also incurs a temporary voltage reduction due to the 4KV transfer that is initiated by TT)	• Turbine trip (RT by logic) • PORVs RC-456 and RC-455C stay closed • STM dump valves fail closed • STM PORVs fail closed if load reject signal PM-447 exists • FW loops 2 and 3 isolate • Minimum auto charging flow (manual recovery may be required) • SI actuated (one SI pump available) • AFW actuated • Letdown isolated	Yes

*See Table A.7 for additional effects.

**Also assumes loss of associated 480V diesel generators.

3 (including loss of associated diesel generators on bus E1 and E2) had the greatest impact. The other combinations involving failure of 4KV bus 3 (bus 3 and 1, and 3 and 4) had lesser impacts. These combinations result in all SDVs failing closed and runback of charging pump flow (although flow could be restored manually). With failure of 4KV buses 2 and 3, all SI pumps and charging pumps would be inoperable, as would all AFW, CCW and SW pumps. Loss of seal flow to the RCPs due to the charging pump failure could potentially lead to RCP seal failure. And, in addition, although the lag time would be greater, loss of SW could fail all instrument air compressors, which would eventually cause FW isolation, MSIV closure, and primary- and secondary-side PORV closure.

Failure of 4KV buses 1 and 2, 1 and 4, and 2 and 4 are similar; except the 1 and 4 combination results in actuation of AFW, and the 1 and 2 combination results in the pressurizer heaters failing off and all instrument air compressors except B failing. These failed bus combinations would all result in a reactor trip, turbine trip, two RCPs off, and at least partial FW isolation.

The postulated failure of 4KV bus 3 with maintenance ties to 120V instrument buses 2 or 3 through MCC-8 maintenance tie led to evaluation of three additional failure modes. Failure of 4KV bus 3 will initiate a transfer of the 4KV buses to the SUT. The transfer of 4KV bus 1 to the SUT will induce a momentary power loss on instrument bus 1. This momentary loss, coupled with the loss of either instrument bus 2 or 3 will actuate SI on a two-out-of-three low pressurizer pressure channel logic.

In addition to the conditions that failure of 4KV bus 3 would initiate, loss of instrument bus 2 or instrument bus 3, in combination with the momentary loss of instrument bus 1, will result in SI and AFW actuation, MFW isolation (due to SI), and PORV RC-456 unavailability (instrument bus 3 only).

A.5.1.2. Instrument Air System Failures

Instrument air system failure (low pneumatic supply pressure) can be caused by a passive failure of the instrument air headers or loss of motive or control power to the instrument air compressors. Normal plant instrument air requirements can be satisfied by the primary air compressor or by either instrument air compressor (A or B). Thus, failure of one or two of the compressors will not result in system failure. No single or double bus failures will directly result in loss of all three compressors. Loss of SW to the compressors would lead, ultimately, to failure of the three instrument air compressors, as well as the station air compressor. A double bus failure of 4KV buses 2 and 3 will fail SW. The time required for the compressors to fail following a loss of SW is unknown; however, the operator is expected to trip the compressors rather than allow them to run to failure. Following loss of the compressors, the instrument air system is expected to depressurize over a period of minutes, perhaps longer, depending on the air requirements during the particular transient.

The effects of instrument air failure on the systems and components important to PTS are provided in Table A.7. The primary- and secondary-side PORVs would fail closed, as would the MSIVs, FW control and bypass valves (if open), letdown isolation valves, and RHR supply valves to the RCS. This would isolate FW and letdown flow but would not fail low-pressure injection since a locked-open bypass exists around one of the air-operated RHR valves. The SDVs, which require nitrogen for actuation, are not impacted by loss of instrument air, but fail closed on loss of nitrogen. Loss of air to the speed controllers on the AFW turbine pump and the charging pumps would result in pump operation at full speed. In addition, charging flow supply and control valves would fail open. Thus, charging pumps would have to be manually controlled (turned off and on) to control charging flow.

A.5.1.3. Cooling Water System Failures

Failure of the CCW system and SW system can be caused by loss of power to the respective supply pumps or by mechanical pump failures. Supply valves in the systems are normally open. The air-operated valves normally fail open and the motor-operated valves fail as is.

All three CCW pumps must be inoperable in order to fail CCW. Loss of motive power on the 480V buses DS, E1, and E2 or loss of motive power on the 480V bus DS and control power on dc buses A and B would fail the CCW pumps. If diesel generators were unavailable, faults on 4KV buses 2 and 3 would also fail CCW.

Normally two of the four SW pumps are required for the SW system to be operable during transient conditions. Loss of motive power on both 480V buses E1 and E2 would fail the four SW pumps. Depending on which pumps were operating, loss of control power from either dc Panel (A or B) could prevent standby pumps from being started, if required. In addition, loss of SW to the CCW heat exchangers would result in a slow degradation of the CCW system due to loss of heat removal.

Table A.7. Impact of loss of instrument air, component cooling water, and service water on systems and components important to PTS sequences

Postulated Failures	System/Component Response	Response of Potential Concern to PTS Sequences
Loss of Instrument Air	• Primary PORVs fail closed • STM PORVs fail closed • MSIVs fail closed (given spring assist operates) • FW isolation (control and bypass valves closed) • Auto throttling of charging flow is failed (control valves failed open and charging pump speed control is lost) • Letdown isolated and charging pump speed control is lost, failing pump full speed • AFW turbine pump full speed, if pump is operating (due to failure of speed controller)	Yes
Loss of CCW	• Charging pump failure (due to loss of lube oil cooling) • Potential RCP seal failure (due to loss of RCP thermal barrier coil cooling and seal injection from charging pumps) • SI pump seal failure • RHR pump seal failure	Yes
Loss of SW	• Loss of FW pumps (FW isolation) • Loss of AFW (pumps) • SI (pump) failure • Loss of IA (primary and instrument air compressors) MSIV close (given spring assist operates) PORVs fail closed STM PORVs closed Letdown isolated Auto throttling of charging flow failed Loss of RHR • Slow loss of CCW (loss of heat sink from HX's) • Potential RCP bearing failure	Yes

The effects of cooling water system failures on the systems and components important to PTS are provided in Table A.7, along with the effects of instrument air failures. Loss of CCW could lead to eventual seal degradation or failure of the charging pumps, the SI pumps, and the RHR pumps. Loss of the charging pumps would fail seal water to the RCPs, which could lead to RCP seal failure and a small-break LOCA. However, this would be a very long-term sequence and operator recovery is expected to occur before seal failure occurs. CCW also cools the RCP bearings and the thermal barrier cooling coil.

Loss of SW would result in loss of all three instrument air compressors and subsequent unavailability of the instrument air system. AFW pumps, FW pumps, and SI pumps also require SW. The system level effects of a SW system failure, including the subsequent loss of instrument air, would include: FW and letdown isolation; inoperability of AFW, SI, RHR, and charging flow auto control; and closure of the MSIVs and primary- and secondary-side PORVs.

A.5.2. Support System Failures Considered To Be of Potential Concern to PTS Sequences

Plant responses from 12 of the 36 support system failures postulated were considered to be of potential concern to PTS sequences. These included loss of instrument air, loss of CCW, loss of SW, and nine cases involving electrical bus failures. The plant responses to these support system failures are summarized in Table A.8.

A.5.2.1. Electric System Failures

Three postulated electric system failures would directly result in FW isolation with AFW operable, and so could potentially initiate certain PTS sequences. Three additional failures would initiate SI directly, which would then subsequently isolate MFW. These three also do not impact AFW operability and could initiate certain PTS sequences involving potential AFW overfeed.

Two of the electrical system failures (loss of both dc buses A and B and loss of 4KV buses 2, 3, and their diesel generators) result in a reactor trip, AFW and SI inoperability, and secondary-side isolation. The 4KV bus failure also results in loss of RCP seal water flow. These may not be of direct PTS concern, since overcooling and pressurization do not occur directly, but upon recovery from the bus failures, system responses may be PTS adverse. Subsequent failures on recovery of the buses may also be adverse to PTS sequences but have not been addressed in this study.

Loss of 4KV buses 1 and 2 and their diesel generator result in a reactor trip, with AFW and HPI operable and with the STM PORVs and MSIVs operable. The expected frequency of the failure is lower than that of an unspecified reactor trip, but the failure could still initiate sequences adverse to PTS.

A.5.2.2. Loss of Instrument Air

The loss of instrument air results in secondary-side isolation but potential overfeed of AFW and charging flow if operator recovery does not occur. The FW isolation forced by the failure could initiate PTS sequences of concern.

Table A.8. Selected postulated support system failures and responses considered to be of potential concern to PTS sequences

Postulated Failure	System/Component Response												
	Reactor Trip	Turbine Trip	RC Pumps	Pressurizer and Primary PORVs	STM Dump Valves	Steam Side PORVs	MSIVs	Feedwater Isolation	Feedwater Runback	AFW	Safety[a] Injection	Charging Pump Flow	Letdown Flow
Electrical System Failures													
1. 125V dc Panel A (and associated 4KV Buses 1 and 2)	Reactor Trip	Turbine Trip	RCP A and C off	PZR heaters Off, aux-spray valve closed, RC-456 stays closed	Closed	Closed	Closed	Isolated	N/A	Actuates	Train B actuates	Operable	Isolated
2. 125V dc Panel B	Reactor Trip	Turbine Trip	Operable	PORVs failed closed, control heaters on	A-2 and B-3 closed	Operable	Closed	Isolated	N/A	Actuates (only 1 motor driven pump available)	Train A actuates	Operable	Isolated
3. 125V dc Aux Panel "DC"	Operable	Operable	Operable	RC-456 closed, aux-spray valve closed	A-1, B-1, B-2, closed	Closed	Closed	Isolated	N/A	Operable	Operable	Operable	Isolated
4. dc Buses A and B	Reactor Trip	Immediate turbine trip fails	Cannot be tripped off	PORVs closed, aux spray valve closed, PZR heaters failed on	Closed	Closed	Closed	Isolated	N/A	Not operable	HPI and LPI not operable	Operable	Operable
5. 4KV Buses 2 and 3 (and associated D/G's)	Reactor Trip	Turbine Trip	RCP C off, Potential seal failure	RC-455C closed, block valves failed open, and RC-456 eventually closed[d]	Closed	Eventual[d] closure	Eventual[d] closure	Loop 1 isolated, and eventual isolation of other FW loops[d]	Operable	Not Operable	HPI and LPI not operable	No flow, pumps failed	Isolated
6. 4KV Buses 1 and 2 (and associated D/G's)	Reactor Trip	Turbine Trip	RCP A and C off	PZR heaters off	Closed	Operable	Operable	Loop 1 Isolated	Operable	Operable	Operable	Operable, but discharge throttle valve fails open	Operable
7. 4KV Bus 3 with maintenance tie to instr. bus 2	Reactor Trip	Turbine Trip	Operable	RC-455C closed, block valves failed open	Closed	Closed[b]	Operable	Loop 2 isolated	Operable	Actuated	Actuated (only 1 SI pump available)	Low flow[c]	Isolated
8. 4KV Bus 3 with maintenance tie to instr. bus 3	Reactor Trip	Turbine Trip	Operable	PORVs closed	Closed	Closed[b]	Operable	Loop 3 isolated	Operable	Actuated	Actuated (only 1 SI pump available)	Low flow[c]	Isolated

Table A.8 (Continued)

Postulated Failure	System/Component Response												
	Reactor Trip	Turbine Trip	RC Pumps	Pressurizer and Primary PORVs	STM Dump Valves	Steam Side PORVs	MSIVs	Feedwater Isolation	Feedwater Runback	AFW	Safety[a] Injection	Charging Pump Flow	Letdown Flow
Electrical System Failures (Cont'd)													
9. 4KV Bus 3 with maintenance tie to instr. bus 2 and 3	Reactor Trip	Turbine Trip	Operable	PORVs closed	Closed	Closed[b]	Operable	Loop 2 and 3 isolated	Operable	Actuated	Actuated (only 1 SI pump available)	Low flow[c]	Isolated
Instrument Air Failures													
10. Loss of Instr. Air	Operable	Operable	Operable	PORVs closed	Operable	Closed	Closed	Isolated	N/A	Overfeed if turbine pump is actuated	RHR inoperable	Overfeed (loss of speed control and throttle valve open)	Isolated
Component Cooling Water System Failures													
11. Loss of CCW	Operable	Operable	Potential RCP seal failure	Operable	Operable	Operable	Operable	Operable	Operable	Operable	RHR and SI pump seal failure	Pump seal failure	Operable
Service Water System Failures													
12. Loss of SWS	Operable	Operable	Potential RCP bearing failure	PORVs closed[d]	Operable	Eventual[d] closure	Eventual[d] closure	Isolated	N/A	Inoperable	SI pumps inoperable. RHR operable	Overfeed[d] (loss of speed control and throttle valve open)	Isolated[d]

[a]Accumulator injection remains operable under all failures postulated.

[b]Steam-side PORVs only failed closed if load reject signal from PM-447 exists.

[c]Manual recovery may be required.

[d]Failure results in loss of SWS, which can fail the instrument air compressors.

A.5.2.3. Loss of Component Cooling Water

The loss of CCW could initiate an RCP seal failure LOCA and subsequent PTS sequences of concern due to loss of seal flow to the charging pumps. However, many recovery actions are available to prevent the RCP seal failure, including alternating use of the three charging pumps and tripping of the RCPs.

A.5.2.4. Loss of Service Water

The loss of the SW could fail the instrument air compressors or force them to be tripped. The failure could then initiate some PTS sequences similar to those initiated by loss of instrument air. FW isolation would also be forced by a SW failure, due to pump cooling requirements, and AFW would be similarly failed due to AFW pump cooling requirements.

A.6. Summary of Results

The HBR-2 systems and components identified in the PTS event trees have been analyzed to determine the effects of postulated failures of the electric power, instrument air, CCW, and SW systems. Plant responses from 12 of the 36 support system failures postulated were initially considered to warrant further study to assess their potential concern to PTS sequences. The 12 failures included loss of instrument air, loss of CCW, loss of SW and several electrical bus failures. Plant responses from all failures postulated can be found in Tables A.6 and A.7 and the plant responses to the selected 12 failures are summarized in Table A.8.

The only significant plant responses found that could be of concern from a PTS standpoint were: AFW and charging flow overfeed on loss of instrument air; electric bus failures that would result in isolation of MFW with AFW still operable (and thus subject to potential overfeed); and reactor trip with AFW still operable. The AFW and charging flow overfeed result from loss of pump speed control on the charging pumps and on the steam-driven AFW pump. Charging pump control can be switched to the manual mode and operated in a start-and-stop mode to gain flow control. Loss of SW can fail the instrument air system compressors and over a longer term, similarly lead to the charging flow overfeed. A double bus failure on 4KV buses 2 and 3 (including their diesel generators) will fail all charging pumps and could lead to a potential RCP seal failure.

The SDVs, primary- and secondary-side PORVs, and MSIVs all assume closed positions on support system failures. No MFW overfeed results from support system failures; in all cases investigated FW isolates.

Some electric bus failures would actuate AFW and SI, but this would not impact PTS sequences since AFW is typically demanded anyway in the sequences and the SI pumps could not deliver flow to the reactor coolant system (RCS) unless RCS pressure were reduced. These failures include the three bus failures that involve vital instrument buses tied to 4KV bus 3 for maintenance, failure of dc bus A, and failure of dc bus B. However, the coincident FW isolation with AFW still operable is a potential initiator in sequences involving AFW overfeed.

Loss of CCW results in loss of oil cooler in the charging pumps. This could lead to a RCP seal failure over a long period of time due to eventual loss of the charging pump if no remedial action is taken. However, many recovery actions are available to prevent the RCP seal failure, including alternating use of the three charging pumps and tripping the RCPs.

Electric bus failures involving the loss of the 480V ac bus E2 would result in charging flow runback due to loss of signal from the pressurizer level controller. However, the charging pumps are each equipped with a variable control stop which will not permit pump flow lower than a minimum specified to ensure that RCP seal water and minimum charging flow requirements are met. It has been assumed in this analysis that this minimum flow stop is set to ensure adequate seal flow.

Other electrical bus failures involving 4KV bus 3 fail the PZR PORV block valves open while at least one of the PORVs is operable. Thus, the likelihood of small-break LOCA isolation may be impacted for certain PTS sequences involving PORV failures.

Loss of power or both dc buses A and B will fail circuit breakers on the pressurizer heaters and the RCP pumps so that these components cannot be tripped off. Loss of both dc buses would also cause failure of three-out-of-four turbine trip systems. If loss of dc power also fails the solenoid trip valves associated with the fourth turbine trip system, the TROTS,* the turbine can only be tripped manually or by mechanical overspeed actuation of the auto-stop trip system. However, the dc power failure also results in the MSIVs closing and other equipment responses that would preclude excessive heat removal from the secondary side.

The support system failures postulated are typically low-probability events. The frequency of each potentially significant support system failure and subsequent possible sequences is developed in Chapter 3.

Addendum: Computerized Data Base Sorts for Postulated Electric Bus Failures

The data base for the selected components (see Section A.4.1 and Table A.2) requiring electric power was computerized to facilitate the analysis of numerous postulated electric bus failures.

The computerized data base includes components, power supplies, component failure modes, and the normal component operating modes. The components were sorted by their power supplies for each power supply failure combination postulated. The sorts included components directly powered from the failed bus(es), components powered from buses fed by the failed bus(es), and components that could be fed by diesel generators associated with the failed bus(es).

*The power supply configuration for the TROTS solenoids has not been determined at this time.

Examples of a few of the sorts done are provided below.

COMPONENT RESPONSE TO 4160V BUS 1 FAILURE

COMPONENT	FAILURE MODE	NORMAL POSITION
RCP A	OFF	ON
PZR CONTROL HEATERS	OFF	ON
PZR BACKUP HEATERS B	OFF	AUTO
EH SYSTEM	SLOW TT PMP A&B FAIL	
EH OIL PUMP B	SLOW TT ON PUMPS A&B	
FW PUMP A	OFF	ON
PRIMARY AIR COMPRESSOR	OFF	ON
CNTRL ROD DRIVE MG SET A	RT ON MG A&B FAILURE	
RCP UNDERVOLTAGE TRP UV-1	RT ON 2/3 TRIP RELAY	

COMPONENT RESPONSE TO 4160V BUS 2 FAILURE

COMPONENT	FAILURE MODE	NORMAL POSITION
RCP C	OFF	ON
PZR BACKUP HEATERS A	OFF	AUTO
C-TROTS CHANNEL 1	TT ON 2/3 CHANNELS	
STM DMP LOSS-LOAD PM-447	DMP VLVS FAIL CLOSED	
MFIV V2-6A	AS IS	OPEN
FW VALVE CONTROL LOOP 1	CONTROL VALVE CLOSED	CONTROL VALVE OPEN
CHARGING PUMP B	OFF	OFF
BORIC ACID VLV MOV-350	AS IS	CLOSED
CHG LINE FCV HCV-121	OPEN	THROTTLED
SI PUMP A	OFF	OFF
ACC DISCH VLV SI-865A	AS IS	OPEN
ACC DISCH VLV SI-865C	AS IS	OPEN
COLD LEG INJ SI-870A	AS IS	CLOSED
BIT INLET SI-867A	AS IS	CLOSED
RWST OUTLET SI-864A	AS IS	OPEN
TO HOT LEGS SI-866B	AS IS	CLOSED
TO HOT LEGS SI-869	AS IS	OPEN
MOTOR AFW PUMP A	OFF	OFF
MAFW DISCH V2-16B	AS IS	CLOSED
SAFW DISCH V2-14A	AS IS	CLOSED
SAFW DISCH V2-14C	AS IS	CLOSED
SAFW SUPPLY V1-8A	AS IS	CLOSED
RHR PUMP A	OFF	OFF
RHR SUCTION SI-862A	AS IS	OPEN
COLD LEG IN RHR-744A	AS IS	CLOSED
COMP COOLING PUMP B	OFF	OFF
HEADER TO RCP CC-716A	AS IS	OPEN
SERV WATER PUMP A	OFF	ON
SERV WATER PUMP B	OFF	ON
SW DISCH VLV V6-12B	AS IS	OPEN
SW ISO VLV V6-16B	AS IS	OPEN
INST AIR COMPRESSOR A	OFF	AUTO
PZR PRESSURE PC-455E	LOW SIGNAL, 2/3 SI	
S/G 1 LEVEL LC-474A	LOW SIGNAL, 2/3 AFW	
S/G 2 LEVEL LC-484A	LOW SIGNAL, 2/3 AFW	
S/G 3 LEVEL LC-494A	LOW SIGNAL, 2/3 AFW	
RCP UNDERVOLTAGE TRP UV-2	RT ON 2/3 TRIP RELAY	

COMPONENT RESPONSE TO 4160V BUS 3 FAILURE

COMPONENT	FAILURE MODE	NORMAL POSITION
PZR PRES TRAN PT-444	PORV455C STAYS CLOSE	
PORV SHUTOFF RC-535	AS IS	OPEN
PORV SHUTOFF RC-536	AS IS	OPEN
GOVERNOR CONTROL CABINENT	TURBINE TRIP	

EH OIL PUMP A	SLOW TT ON PUMPS A&B	
STEAM DUMP CONTROL T-408	DMP VLVS FAIL CLOSED	
STEAM DUMP CONTROL T-408	PORV FC IF LR EXISTS	
STM DUMP PRESS CTL P-464	NOT NORMAL CNTL MODE	
HIGH Tavg	DMP VLVS FAIL CLOSED	
V1-3A BYPASS	AS IS	CLOSED
V1-3B BYPASS	AS IS	CLOSED
V1-3C BYPASS	AS IS	CLOSED
MFIV V2-6B	AS IS	OPEN
MFIV V2-6C	AS IS	OPEN
CHARGING PUMP A	OFF	ON
CHARGING PUMP C	OFF	OFF
PZR LEVEL CONTROL LC-459F	MINIMUM CH PMP SPEED	AUTO-CONTROL
CHG PMP SUC LCV-115C	AS IS	OPEN
SI PUMP B	OFF	OFF
SI PUMP C	OFF	OFF
ACC DISCH VLV SI-865B	AS IS	OPEN
COLD LEG INJ SI-870B	AS IS	CLOSED
BIT INLET SI-867B	AS IS	CLOSED
RWST OUTLET SI-864B	AS IS	OPEN
TO HOT LEGS SI-866A	AS IS	CLOSED
MOTOR AFW PUMP B	OFF	OFF
MAFW DISCH V2-16A	AS IS	CLOSED
MAFW DISCH V2-16C	AS IS	CLOSED
SAFW DISCH V2-14B	AS IS	CLOSED
SAFW SUPPLY V1-8B	AS IS	CLOSED
SAFW SUPPLY V1-8C	AS IS	CLOSED
RHR PUMP B	OFF	OFF
RHR SUCTION SI-862B	AS IS	OPEN
RHR DISCH FCV-605	CLOSED	CLOSED
COLD LEG IN RHR-744B	AS IS	CLOSED
COMP COOLING PUMP A	OFF	ON
COMP COOLING PUMP C	OFF	OFF
HEADER TO RCP CC-716B	AS IS	OPEN
RCP OIL COOLER CC-730	AS IS	OPEN
RCP COOLING COIL FCV-626	AS IS	OPEN
SERV WATER PUMP C	OFF	OFF
SERV WATER PUMP D	OFF	OFF
SW DISCH VLV V6-12C	AS IS	OPEN
SDAFW PMP SW VLV TCV-1902	OPEN	CLOSED
MAFW PMP SW VLV TCV-1903A	OPEN	CLOSED
MAFW PMP SW VLV TCV-1903B	OPEN	CLOSED
SW ISO VLV V6-16A	AS IS	OPEN
INST AIR COMPRESSOR B	OFF	AUTO
CNTRL ROD DRIVE MG SET B	RT ON MG A&B FAILURE	

COMPONENT RESPONSE TO 4160V BUS 4 FAILURE

COMPONENT	FAILURE MODE	NORMAL POSITION
RCP B	OFF	ON
FW PUMP B	OFF	ON
RCP UNDERVOLTAGE TRP UV-3	RT ON 2/3 TRIP RELAY	

COMPONENT RESPONSE TO 125VDC BUS A & B FAILURE

COMPONENT	FAILURE MODE	NORMAL POSITION
PZR PRES TRAN PT-445	PORV456 STAYS CLOSED	
PORV RC-456	CLOSED	CLOSED
PORV RC-455C	CLOSED	CLOSED
TURBINE AUTO TRIP 20-AST	NO TURBINE AUTO TRIP	
TURB EMERGENCY TRIP 20-ET	NO TURB EMERG TRIP	
GOV/INTCPT TRIP 20-1,20-2	NO GOV/INTCPT TRIP	
TROTS LOGIC TRAIN A	NO TROTS TT W/O DC B	
TROTS LOGIC TRAIN B	NO TROTS TT W/O DC A	
C-TROTS CHANNEL 2 *	TT ON 2/3 CHANNELS	

C-TROTS CHANNEL 3 *	TT ON 2/3 CHANNELS	
STEAM SIDE PORV RV1	CLOSED	CLOSED
STEAM SIDE PORV RV2	CLOSED	CLOSED
STEAM SIDE PORV RV3	CLOSED	CLOSED
STM DUMP PRV 1324A-1	CLOSED	CLOSED
STM DUMP PRV 1324B-1	CLOSED	CLOSED
STM DUMP PRV 1324B-2	CLOSED	CLOSED
STM DUMP PRV 1324A-2	CLOSED	CLOSED
STM DUMP PRV 1324B-3	CLOSED	CLOSED
MSIV V1-3A ISO	CLOSED	OPEN
MSIV V1-3A ISO	CLOSED	OPEN
MSIV V1-3B ISO	CLOSED	OPEN
MSIV V1-3B ISO	CLOSED	OPEN
MSIV V1-3C ISO	CLOSED	OPEN
MSIV V1-3C ISO	CLOSED	OPEN
FW CTRL VLV FCV-478 SOL-A	CLOSED	OPEN
FW CTRL VLV FCV-478 SOL-B	CLOSED	OPEN
FW CTRL VLV FCV-488 SOL-A	CLOSED	OPEN
FW CTRL VLV FCV-488 SOL-B	CLOSED	OPEN
FW CTRL VLV FCV-498 SOL-A	CLOSED	OPEN
FW CTRL VLV FCV-498 SOL-B	CLOSED	OPEN
FW BYP FCV-479 SOL-A	CLOSED	CLOSED
FW BYP FCV-479 SOL-B	CLOSED	CLOSED
FW BYP FCV-489 SOL-A	CLOSED	CLOSED
FW BYP FCV-489 SOL-B	CLOSED	CLOSED
FW BYP FCV-499 SOL-A	CLOSED	CLOSED
FW BYP FCV-499 SOL-B	CLOSED	CLOSED
FW VALVE CONTROL LOOP 2	CONTROL VALVE CLOSED	CONTROL VALVE OPEN
FW VALVE CONTROL LOOP 3	CONTROL VALVE CLOSED	CONTROL VALVE OPEN
C-FW PUMP A *	ON-FWP TRIP FAILS	ON
C-FW PUMP B *	ON-FWP TRIP FAILS	ON
CHG PMP SUC LCV-115B	CLOSED	CLOSED
CH ISO CVC-310A LOOP1 C L	OPEN	CLOSED
CH ISO CVC-310B LOOP2 C L	OPEN	OPEN
AUX SPRAY CVC-311	CLOSED	CLOSED
LETDOWN VLV LCV-460A	CLOSED	OPEN
LETDOWN VLV LCV-460B	CLOSED	OPEN
LETDOWN ISO CVC-200A	CLOSED	CLOSED
LETDOWN ISO CVC-200B	CLOSED	CLOSED
LETDOWN ISO CVC-200C	CLOSED	OPEN
LETDOWN ISO CVC-204A	CLOSED	OPEN

* "C-" indicates circuit breaker or control for components.

COMPONENT RESPONSE TO 125VDC BUS A & B FAILURE

COMPONENT	FAILURE MODE	NORMAL POSITION
LETDOWN ISO CVC-204B	CLOSED	OPEN
ACC NITRGEN SUPPLY SI-855	CLOSED	CLOSED
ACC DRN VLV SI-852A	CLOSED	CLOSED
ACC DRN VLV SI-852B	CLOSED	CLOSED
ACC DRN VLV SI-852C	CLOSED	CLOSED
ACC VENT VLV SI-853A	AS IS	CLOSED
ACC VENT VLV SI-853B	AS IS	CLOSED
ACC VENT VLV SI-853C	AS IS	CLOSED
STEAM AFW PUMP CNTRL	OFF	OFF
C-RCP A	RCP TRIP FAIL	RCP ON
C-RCP B	RCP TRIP FAIL	RCP ON

C-RCP C	RCP TRIP FAIL	RCP ON
C-PZR CNTL HEATERS	ON	AUTO
C-PZR B-UP HEATERS A	OFF	AUTO
C-PZR B-UP HEATERS B	OFF	AUTO
C-CHARGING PUMP B	AS IS	OFF
C-CHARGING PUMP C	AS IS	OFF
C-SI PUMP A	AS IS	OFF
C-SI PUMP B	AS IS	OFF
C-SI PUMP C	AS IS	OFF
C-MAFW PUMP A	AS IS	OFF
C-MAFW PUMP B	AS IS	OFF
C-RHR PUMP A	AS IS	OFF
C-RHR PUMP B	AS IS	OFF
C-COMP COOL PUMP B	AS IS	OFF
C-COMP COOL PUMP C	AS IS	OFF
C-SW PUMP A	AS IS	ON
C-SW PUMP B	AS IS	ON
C-SW PUMP C	AS IS	OFF
C-SW PUMP D	AS IS	OFF
PZR PRESSURE PC-456D	LOW SIGNAL, 2/3 SI	
PZR PRESSURE PC-457D	LOW SIGNAL, 2/3 SI	
S/G 1 LEVEL LC-475A	LOW SIGNAL, 2/3 AFW	
S/G 1 LEVEL LC-476A	LOW SIGNAL, 2/3 AFW	
S/G 2 LEVEL LC-485A	LOW SIGNAL, 2/3 AFW	
S/G 2 LEVEL LC-486A	LOW SIGNAL, 2/3 AFW	
S/G 3 LEVEL LC-495A	LOW SIGNAL, 2/3 AFW	
S/G 3 LEVEL LC-496A	LOW SIGNAL, 2/3 AFW	
SAFEGUARDS TRAIN A LOGIC	NO SI ON TRAIN A	
SAFEGUARDS TRAIN B LOGIC	NO SI ON TRAIN B	
DIESEL GENERATOR A	FAILS TO ENERGIZE E1	OFF
DIESEL GENERATOR B	FAILS TO ENERGIZE E2	OFF
C-CTRL ROD DRIVE MG SET A	RT ON MG A&B FAILURE	
C-CTRL ROD DRIVE MG SET B	RT ON MG A&B FAILURE	
REACTOR PROTECT. TRAIN A	REACTOR TRIP	
REACTOR PROTECT. TRAIN B	REACTOR TRIP	

COMPONENT RESPONSE TO DC BUS "A" AND 4KV BUS 1 & 2 FAILURE

COMPONENT	FAILURE MODE	NORMAL POSITION
RCP A	OFF	ON
RCP C	OFF	ON
PZR CONTROL HEATERS	OFF	ON
PZR BACKUP HEATERS A	OFF	AUTO
PZR BACKUP HEATERS B	OFF	AUTO
PORV RC-456	CLOSED	CLOSED
TURBINE AUTO TRIP 20-AST	NO TURBINE AUTO TRIP	
EH SYSTEM	SLOW TT PMP A&B FAIL	
EH OIL PUMP B	SLOW TT ON PUMPS A&B	
TROTS LOGIC TRAIN A	NO TROTS TT W/O DC B	
C-TROTS CHANNEL 1	TT ON 2/3 CHANNELS	
C-TROTS CHANNEL 2	TT ON 2/3 CHANNELS	
STEAM SIDE PORV RV1	CLOSED	CLOSED
STEAM SIDE PORV RV2	CLOSED	CLOSED
STEAM SIDE PORV RV3	CLOSED	CLOSED
STM DUMP PRV 1324A-1	CLOSED	CLOSED
STM DUMP PRV 1324B-1	CLOSED	CLOSED
STM DUMP PRV 1324B-2	CLOSED	CLOSED
STM DMP LOSS-LOAD PM-447	DMP VLVS FAIL CLOSED	
MSIV V1-3A ISO	CLOSED	OPEN
MSIV V1-3B ISO	CLOSED	OPEN
MSIV V1-3C ISO	CLOSED	OPEN
FW PUMP A	OFF	ON
MFIV V2-6A	AS IS	OPEN
FW CTRL VLV FCV-478 SOL-A	CLOSED	OPEN
FW CTRL VLV FCV-488 SOL-A	CLOSED	OPEN
FW CTRL VLV FCV-498 SOL-A	CLOSED	OPEN
FW BYP FCV-479 SOL-A	CLOSED	CLOSED

FW BYP FCV-489 SOL-A	CLOSED	CLOSED
FW BYP FCV-499 SOL-A	CLOSED	CLOSED
FW VALVE CONTROL LOOP 1	CONTROL VALVE CLOSED	CONTROL VALVE OPEN
FW VALVE CONTROL LOOP 2	CONTROL VALVE CLOSED	CONTROL VALVE OPEN
C-FW PUMP A	ON-FWP TRIP FAILS	ON
CHARGING PUMP B	OFF	OFF
CHG PMP SUC LCV-115B	CLOSED	CLOSED
BORIC ACID VLV MOV-350	AS IS	CLOSED
CH ISO CVC-310B LOOP2 C L	OPEN	OPEN
AUX SPRAY CVC-311	CLOSED	CLOSED
LETDOWN VLV LCV-460A	CLOSED	OPEN
LETDOWN VLV LCV-460B	CLOSED	OPEN
LETDOWN ISO CVC-200A	CLOSED	CLOSED
LETDOWN ISO CVC-200C	CLOSED	OPEN
LETDOWN ISO CVC-204A	CLOSED	OPEN
CHG LINE FCV HCV-121	OPEN	THROTTLED
SI PUMP A	OFF	OFF
ACC NITRGEN SUPPLY SI-855	CLOSED	CLOSED
ACC DRN VLV SI-852A	CLOSED	CLOSED
ACC VENT VLV SI-853A	AS IS	CLOSED
ACC DISCH VLV SI-865A	AS IS	OPEN
ACC DISCH VLV SI-865C	AS IS	OPEN

COMPONENT RESPONSE TO DC BUS "A" AND 4KV BUS 1 & 2 FAILURE

COMPONENT	FAILURE MODE	NORMAL POSITION
COLD LEG INJ SI-870A	AS IS	CLOSED
BIT INLET SI-867A	AS IS	CLOSED
RWST OUTLET SI-864A	AS IS	OPEN
TO HOT LEGS SI-866B	AS IS	CLOSED
TO HOT LEGS SI-869	AS IS	OPEN
MOTOR AFW PUMP A	OFF	OFF
MAFW DISCH V2-16B	AS IS	CLOSED
SAFW DISCH V2-14A	AS IS	CLOSED
SAFW DISCH V2-14C	AS IS	CLOSED
SAFW SUPPLY V1-8A	AS IS	CLOSED
RHR PUMP A	OFF	OFF
RHR SUCTION SI-862A	AS IS	OPEN
COLD LEG IN RHR-744A	AS IS	CLOSED
COMP COOLING PUMP B	OFF	OFF
HEADER TO RCP CC-716A	AS IS	OPEN
SERV WATER PUMP A	OFF	ON
SERV WATER PUMP B	OFF	ON
SW DISCH VLV V6-12B	AS IS	OPEN
SW ISO VLV V6-16B	AS IS	OPEN
PRIMARY AIR COMPRESSOR	OFF	ON
INST AIR COMPRESSOR A	OFF	AUTO
C-RCP A	RCP TRIP FAIL	RCP ON
C-RCP C	RCP TRIP FAIL	RCP ON
C-PZR B-UP HEATERS A	OFF	AUTO
C-PZR B-UP HEATERS B	OFF	AUTO
C-CHARGING PUMP B	AS IS	OFF
C-SI PUMP A	AS IS	OFF
C-MAFW PUMP A	AS IS	OFF
C-RHR PUMP A	AS IS	OFF
C-COMP COOL PUMP B	AS IS	OFF
C-SW PUMP A	AS IS	ON
C-SW PUMP B	AS IS	ON
PZR PRESSURE PC-455E	LOW SIGNAL, 2/3 SI	
PZR PRESSURE PC-456D	LOW SIGNAL, 2/3 SI	
S/G 1 LEVEL LC-474A	LOW SIGNAL, 2/3 AFW	
S/G 1 LEVEL LC-475A	LOW SIGNAL, 2/3 AFW	
S/G 2 LEVEL LC-484A	LOW SIGNAL, 2/3 AFW	
S/G 2 LEVEL LC-485A	LOW SIGNAL, 2/3 AFW	
S/G 3 LEVEL LC-494A	LOW SIGNAL, 2/3 AFW	
S/G 3 LEVEL LC-495A	LOW SIGNAL, 2/3 AFW	
SAFEGUARDS TRAIN A LOGIC	NO SI ON TRAIN A	

DIESEL GENERATOR A	FAILS TO ENERGIZE E1	OFF
CNTRL ROD DRIVE MG SET A	RT ON MG A&B FAILURE	
C-CTRL ROD DRIVE MG SET A	RT ON MG A&B FAILURE	
RCP UNDERVOLTAGE TRP UV-1	RT ON 2/3 TRIP RELAY	
RCP UNDERVOLTAGE TRP UV-2	RT ON 2/3 TRIP RELAY	
REACTOR PROTECT. TRAIN A	REACTOR TRIP	

COMPONENT RESPONSE TO 480V BUS 3 FAILURE

COMPONENT	FAILURE MODE	NORMAL POSITION
GOVERNOR CONTROL CABINENT	TURBINE TRIP	
EH OIL PUMP A	SLOW TT ON PUMPS A&B	
V1-3A BYPASS	AS IS	CLOSED
V1-3B BYPASS	AS IS	CLOSED
V1-3C BYPASS	AS IS	CLOSED
SDAFW PMP SW VLV TCV-1902	OPEN	CLOSED
MAFW PMP SW VLV TCV-1903A	OPEN	CLOSED
MAFW PMP SW VLV TCV-1903B	OPEN	CLOSED
CNTRL ROD DRIVE MG SET B	RT ON MG A&B FAILURE	

COMPONENT RESPONSE TO 480V MCC 4 FAILURE

COMPONENT	FAILURE MODE	NORMAL POSITION
GOVERNOR CONTROL CABINENT	TURBINE TRIP	
EH OIL PUMP A	SLOW TT ON PUMPS A&B	
V1-3A BYPASS	AS IS	CLOSED
V1-3B BYPASS	AS IS	CLOSED
V1-3C BYPASS	AS IS	CLOSED
SDAFW PMP SW VLV TCV-1902	OPEN	CLOSED
MAFW PMP SW VLV TCV-1903A	OPEN	CLOSED
MAFW PMP SW VLV TCV-1903B	OPEN	CLOSED

COMPONENT RESPONSE TO INSTRUMENT BUS 1 FAILURE

COMPONENT	FAILURE MODE	NORMAL POSITION
C-TROTS CHANNEL 1	TT ON 2/3 CHANNELS	
STM DMP LOSS-LOAD PM-447	DMP VLVS FAIL CLOSED	
FW VALVE CONTROL LOOP 1	CONTROL VALVE CLOSED	CONTROL VALVE OPEN
CHG LINE FCV HCV-121	OPEN	THROTTLED
PZR PRESSURE PC-455E	LOW SIGNAL, 2/3 SI	
S/G 1 LEVEL LC-474A	LOW SIGNAL, 2/3 AFW	
S/G 2 LEVEL LC-484A	LOW SIGNAL, 2/3 AFW	
S/G 3 LEVEL LC-494A	LOW SIGNAL, 2/3 AFW	

Appendix B

PTS INITIATING-EVENT FREQUENCY AND BRANCH PROBABILITY SCREENING ESTIMATES

J. W. Minarick and P. N. Austin

Science Applications International Corporation

D. L. Selby

Oak Ridge National Laboratory

APPENDIX B. PTS INITIATING-EVENT FREQUENCY AND BRANCH PROBABILITY SCREENING ESTIMATES

B.1. Introduction

Initiating-event frequency and event-tree branch probability estimates have been developed for use in quantifying event sequences in the H. B. Robinson Unit 2 pressurized thermal shock (PTS) evaluation. These estimates have been developed for initiators and system/component failures specified by ORNL.

The complete LER data base for H. B. Robinson Unit 2 was reviewed for initiating-event occurrences and system failures, as well as for a general overview of the performance of plant systems of interest. However, in lieu of relying solely on the plant information, Westinghouse-specific and PWR-specific operational information was employed when it was available and when it was felt that the plant operational experience did not provide an adequate data base. Additional information was obtained from the NREP Generic Data Base[1] and from the Nuclear Power Plant Operating Experience Summaries,[2-5] as well as from other sources. With the constraints imposed by programmatic needs and the availability of operational data, only simplified approaches to frequency and probability estimation were permitted. However, the estimates are considered to be acceptable for use as screening estimates. Table B.1 includes the estimates developed, the rationale used, relevant information, and information sources.

As stated above, a number of the estimates included in Table B.1 have been developed from generic sources. This is necessary, since many of the failures of interest are sufficiently infrequent that they will be seen only over a large operating period, if at all. The estimates may not be representative of H. B. Robinson Unit 2 failure probabilities if the plant systems and components differ significantly from systems and components used throughout the industry, although potential differences have been considered in developing the estimates in Table B.1.

A number of initiating transients have been found to be of significance from previous PTS analyses. In general, these include three initiator classes: (1) reactor trip, (2) steam-line break (SLB), and (3) loss-of-coolant accident (LOCA), including steam generator tube ruptures. Several LOCA and SLB situations are of interest — whether a break is small or large, whether it is isolable or nonisolable, and whether the plant is at full power or at hot standby. Although separate event trees may be appropriate to describe all these situations, many of the plant responses of interest are expected to be common among the trees. Also, considering the amount of data available, the frequency estimate developed for one of the initiating events is sometimes an appropriate estimate for others.

B.2. Initiating-Event Frequency Estimates

Initiating-event frequencies have been developed based on the number of observed events within selected periods of operation. The calculational method is consistent with that developed in Ref. 6 and utilized the χ^2 distribution to estimate a conservative lower

bound on mean time between failures, and hence a conservative upper bound on frequency. This frequency estimate is $\chi^2_{1-\alpha}(2r + 2)/2T$, where $1 - \alpha$ is the confidence level, r is the number of observed failures, and T is the total observation time. A 50% confidence level was employed.

For some initiators, it may be necessary to estimate the frequency of events in a particular operating mode. The 1980, 1981 and 1982 operating experience of H. B. Robinson Unit 2 identified in Refs. 4 and 5 was reviewed to estimate the fraction of time the units were at power and in hot shutdown and cold shutdown modes. The fractions of time in these three states were: power operation, 61.3%; hot shutdown, 1.2%; and cold shutdown, 37.5%.

For medium and large steam-line breaks and medium-break LOCAs, no data exist as to the relative incidence of these initiators at power and at hot shutdown; therefore, fractions based on the amount of time at hot shutdown and at power were used. These fractions were: power operation, 98.1%; and hot shutdown, 1.9%.

Historic small steam-line breaks and small LOCAs identified in Refs. 7 and 8 were reviewed to estimate the fraction of these initiators occurring at hot shutdown and at power. For small steam-line breaks, 25% occurred at hot shutdown and 75% occurred at power. For small-break LOCAs, 9% occurred at hot shutdown and 91% occurred at power.

B.3. Branch Failure Probability Estimates

Branch failure probability estimates on a per-demand basis were developed using the effective number of failures observed within a period of time and estimating the number of demands expected within that same period.* If no failures on demand were observed, and no other information was available with which to estimate a failure-on-demand probability, then a Poisson approximation of a binomial process (the number of demands was always large) was assumed to be applicable and the probability was estimated by assuming there was a 50% probability of observing the zero failures actually observed. In such a case,

$$P(r = 0) = e^{-m}(m)^0/0!,$$

where r is the number of failures and m the expected number of failures. The expected number of failures m is equal to the probability of failure (p) multiplied by the number of demands (D). If the probability of zero observations is 0.5, then $P(r = 0) = 0.5 = e^{-m} = e^{-pD}$. If an estimate of D is available, $p \sim 0.7/D$. (It is interesting to note that the initiating-event frequency estimate reduces to $\sim 0.7/T$ for zero-observed events.)

---

* Failure-per-demand probability estimates developed primarily from test demands may overestimate the actual failure probability up to a factor of two if the actual failures are time dependent and the test demands are spaced at regular intervals. However, based on events documented in the Accident Sequence Precursor (ASP) program (Refs. 7 and 8), there appears to exist in many cases a greater likelihood of failure on demand following an actual initiating event than that determined based on testing. These two effects tend to offset one another; the per-demand estimates developed herein are considered to be acceptable for screening purposes.

In estimating the likelihood of multiple valve failures, conditional probabilities of subsequent component failure given failure of the first component were developed based on the multiple failure rates identified in Ref. 9. These estimates are:

- For air-operated valves in a system of three valves — 0.094 for a specific second valve failing given the first is failed; and 0.081 for both remaining valves failing given the first is failed.
- For motor-operated valves in a system of three valves — 0.020 for a specific second valve failing given the first is failed; and 0.012 for both remaining valves failing given the first is failed.

As with all event trees, the probability associated with a particular branch is conditional on the prior branches in the sequence. Although event-tree development was not in the scope of this phase of the work, certain conditionalities were accounted for when appropriate. Questions of conditionality and potential system interaction effects (which are being considered separately) must be carefully considered prior to the use of Table B.1 estimates with a particular event tree. In addition, quantification of human error was not in the scope of the study, and many of the estimates included in Table B.1 do not consider plant-specific potential operator recovery actions.

It should also be noted that, for traceability, numerical values included in Table B.1 have been developed to two significant figures. This is not to imply a lack of error bands on the estimates. The error bands associated with many of the estimates are expected to be large — at least an order of magnitude in either direction considering the generic nature of much of the data base and the small amount of information on particular initiators and multiple component failures available.

Table B.1. Event-tree frequencies and branch probabilities for screening purposes

Function	Discussion	Screening Estimate
	Initiators	
1. Reactor trip	During 1980, 1981, and 1982, HBR-2 experienced 26 manual and auto scrams from power (Refs. 4 and 5). This results in a reactor trip estimate of 26/3 years = 8.7 per reactor year (RY).	8.7/RY
2. Steam-line break		
(a) Large break	Two early events of potential importance to steam-line break frequency have been recorded in the LER data: (1) Turkey Point safety valve header failure, (2) HBR-2 safety valve header failure. Both of these events occurred before criticality and in view of the fact that no large breaks have been observed in the 577 combined BWR and PWR years of post-critical operation, an alternate estimate of main steam-line break frequency has been developed. Using the χ^2 distribution and zero observations with a 50% confidence level, this estimate is 1.2×10^{-3}/RY. This estimate applies for breaks greater in area than typical valve-dominated small breaks and for both isolable and nonisolable breaks.	1.2×10^{-3}/RY
(b) Small break	One event at HBR-2 was observed involving failure of steam-side relief valves to close (NSIC 76461). In addition, four small SLB occurrences were observed in the Accident Sequence Precursor (ASP) program (Refs. 7 and 8) over a 288-year observation period. This screening estimate has been developed using the χ^2 distribution with five occurrences in 288 reactor years. This estimate, 2×10^{-2}/RY, does not include the potential for recovery. Small steam-line break occurrences observed in the ASP program were considered 40% non-recoverable. However, the steam-side PORVs at HBR-2 are not isolable using a series isolation valve, and therefore small SLBs associated with these PORVs will be less recoverable than in the industry in general, unless the valve failures are dominated by valve operator failures and the valve operators are accessible.	2.0×10^{-2}/RY

Table B.1 (Continued)

Function	Discussion	Screening Estimate
3. Loss-of-coolant accident (LOCA)		
(a) Due to failed-open safety valve	No major events involving stuck-open safety valves have been observed. However, a safety valve apparently did open below set-point pressure at St. Lucie 1 and depressurized the RCS from 2410 to 1670 psig in late 1981. Because of a lack of detailed information concerning this event, it has not been used in developing a frequency estimate. Using the χ^2 distribution with zero observations and an observation period from 1969 through July 1983 (406 PWR reactor years), a value of 1.7×10^{-3} is estimated.	1.7×10^{-3}/RY
(b) Due to an open PORV	NUREG-0611 (Ref. 10) reports 50 applicable PORV lifts at Westinghouse plants. Assuming NUREG-0611 covered the period up to September 1979, which includes 164 Westinghouse reactor years of operation, the Westinghouse PORV lift rate is: 50/(164 Westinghouse RY) = 0.30/RY. A value of 0.027 for PORV failure to close, once open, is developed from Ref. 11 (four failures to close in approximately 150 actuations). Utilizing these two values results in an estimate for a LOCA due to an open PORV of 0.30/RY × 2 valves × 0.027, or 1.6×10^{-2}/RY. Consideration of operator response to close the block valve associated with a stuck-open PORV will reduce this estimate.	1.6×10^{-2}/RY
(c) LOCA due to isolable breaks other than PORV occurrences	One minor event involving a leak from the letdown piping, followed by SI, occurred at HBR-2 (NSIC 164149). Because of the minor nature of this event and in light of no other substantial data, the χ^2 distribution with zero occurrences in the total number of PWR reactor years (406 years) has been used to estimate the recommended value of 1.7×10^{-3}/RY.	1.7×10^{-3}/RY
(d) LOCA due to non-isolable breaks	Reactor coolant system leakage is considered a LOCA if it is large enough to initiate SI. One such event was observed at HBR-2: a RCP seal failure (NSIC 103077). A seal failure at Arkansas Nuclear One, Unit 1 also initiated SI. Two events involving tube ruptures followed by SI occurred at Ginna and Prairie Island. (HBR-2 experienced a significantly greater than average number of SG tube leak LERs, but the SG bundles were replaced in 1985 and there is no reason to believe that the new bundles will result in significantly higher than average tube ruptures. The estimates provided here are based on the above events and are as follows:	
	(1) SG tube ruptures — two events in 406 PWR reactor years (1969–July 1983):	6.6×10^{-3}/RY
	(2) Other LOCAs — two events in 406 PWR reactor years:	6.6×10^{-3}/RY

Table B.1 (Continued)

Function	Discussion	Screening Estimate
	These values are considered consistent with the NREP screening values of 10^{-2}/year.	
	No medium-break LOCAs have been observed. A screening value of 1×10^{-3}/RY is recommended, based on Ref. 1.	1×10^{-3}/RY
(e) Overall small-break LOCA not immediately isolated	An overall estimate for a small-break LOCA not immediately isolated (~10-minute time frame) was obtained using the frequency estimates developed in (a), (b), and item (2) of (d) above and assuming a probability of 0.05 of the operator not isolating a blowing-down PORV and a probability of 0.9 that an initially blowing-down safety valve will not reseat. This results in an overall estimate of 8.9×10^{-3}/RY.	8.9×10^{-3}/RY
(f) Overall small-break LOCA isolated in the long term	Assuming that ~40% of all PORV LOCAs not isolated in the short term are eventually isolated and other small-break LOCAs cannot be isolated results in a probability estimate for late isolation of $0.05 \times (1.6 \times 10^{-2})/8.9 \times 10^{-3} = 0.039$.	0.039/RY

NOTE: Several of the operational events used to develop the above estimates were associated with HBR-2. While each of these events was considered a random event across the entire reactor population for the purposes of developing these screening estimates, the number which occurred at HBR-2 may indicate an actual frequency for such events at this plant that is higher than that for the industry as a whole.

Branch Probabilities

1. Turbine fails to trip on demand	PWR LERs were reviewed for turbine trip, turbine stop valve (TSV), etc., failures. While there have been several failures of individual stop valves (single steam line) to close, only one event (NSIC 92449 at Turkey Point 3, 4) identified a total failure of TSVs. Assuming ~12 shutdowns/plant year (Ref. 3) and ~406 PWR years applicable to this review, the number of TSV demands is ~4900. One failure in this number of demands results in a failure estimate of $\sim 2 \times 10^{-4}$. This estimate does not consider use of the turbine control valves (TCVs) in isolating the turbine if the TSVs fail to close. Consideration of the TCVs would reduce this estimate somewhat, perhaps by a factor of up to 10. Assuming a value of 0.2 for the conditional probability of TCV failure, given TSV failure, results in a screening estimate of $(2 \times 10^{-4}) \times 0.2$ or 4×10^{-5}. (Considering zero observed failures of the turbine to isolate on demand over the ~406 year period results in an estimate of $\sim 1.4 \times 10^{-4}$ based on observation alone.)	4×10^{-5}

Table B.1 (Continued)

Function	Discussion	Screening Estimate
2. Steam-side PORVs fail to close on demand	Based on discussion with HBR-2 operators, these valves have been known to open on power runbacks of greater than 70%. (Thus for this analysis, it is assumed that the steam-side PORVs open on every power runback of greater than 70% power.) It should be noted that this assumption has no effect on the results. If the number of openings were less, the failure per demand would be higher and the number of failures/RY would still be the same value. Two failure-to-close occurrences at HBR-2 were reported in the same LER (NSIC 76461). Since the failures did not occur simultaneously, no deductions were made concerning common mode coupling and the events were assumed to be independent. The estimates provided here were based on the two failures and a demand estimate. The number of demands was estimated based on the number of reactor trips at HBR-2 from greater than 70% power in 1978, 1979, and 1980 (15); the number of PORVs (3); and 12.7 RY of operation at HBR-2 from criticality through May 1983:	
	$\frac{15 \text{ demands/valve}}{3 \text{ years}} \times 12.7 \text{ RY} \times 3 \text{ valves} = 190 \text{ demands}$	
	Recognizing that the valves open only on trips above 70% gives the following effective demand probability estimates for a general reactor trip:	
	(1) For a single valve failure $[(2/190 = 1.05 \times 10^{-2}) \times (5/8.7)]$:	6.3×10^{-3}
	(2) For failure of any one of three valves $[3 \times (1.05 \times 10^{-2}) \times (5/8.7)]$:	1.8×10^{-2}
	(3) For failure of any two valves $[3 \times (1.05 \times 10^{-2}) \times 0.094 \times (5/8.7)]$:	1.7×10^{-3}
	(4) For failure of all three valves $[(1.05 \times 10^{-2}) \times 0.081 \times (5/8.7)]$:	4.9×10^{-4}

NOTE: The assumption that the STM PORVs open on every power runback of greater than 70% power has no effect on the results. If the number of openings were less, the failure per demand would be higher and the number of failures/RY would still be the same value.

Table B.1 (Continued)

Function	Discussion	Screening Estimate
3. Steam dump valves (SDVs) fail to close on demand	No failures to close of SDVs at HBR-2 were reported in the LERs. Based on zero observed failures, the failure on demand probability can be estimated using the Poisson approximation to the binomial discussed earlier and an estimate of the number of demands. All five SDVs open when demanded (Ref. 12) and, assuming they are demanded on startup as well as on shutdown, the number of demands at HBR-2 is: 5 valves × 12.7 HBR-2 RYs × (17.3 startups/yr + 17.3 shutdowns/yr)(Refs. 4, 5), or ~2200 demands. The following probability estimates result:	
	(1) For a single valve failure ($0.7/2200 = 3.18 \times 10^{-4}$):	3.2×10^{-4}
	(2) For failure of any one of five valves [${}_5C_1 \times (3.18 \times 10^{-4})$]:	1.6×10^{-3}
	(3) For failure of any two of five valves [${}_5C_2 \times (3.18 \times 10^{-4}) \times 0.094$]:	3.0×10^{-4}
	(4) For failures of any three of five valves [${}_5C_3 \times (3.18 \times 10^{-4}) \times 0.081$]:	1.3×10^{-4}
	(5) For failure of five valves [${}_5C_4 \times (3.18 \times 10^{-4}) \times 0.081$]:	2.6×10^{-5}
	(6) For failure of three or more valves [(d) + (e) + (f)]:	4.2×10^{-4}

NOTE: Reference 9 indicates no substantial differences in failure rates for air-operated valves in systems of greater than three components than those in three-component systems.

4. Main feedwater system (MFWS) fails to correctly run back following non-specific reactor trip (not applicable for other initiators)	Potential MFW end states following a nonspecific reactor trip are developed in Attachment A following this table. Based on the frequency estimates developed in Attachment A, the following end-state conditional probability estimates are developed:	
	(1) Probability of utilizing MFSW and bypass valves following nonspecific reactor trip $\{(\lambda_{RT} - \lambda_{LOFW}[1/RY])/\lambda_{RT}\} = [(8.7 - 1)/8.7] = 0.89\}$:	0.89
	(2) Probability of requiring AFW following RT$\{[(\lambda_{RT} - \lambda_{LOFW}) - P_{op.\,error} + \lambda_{LOFW}]/\lambda_{RT}\} = [(8.7 - 1) - 0.03 + 1]/8.7 = 0.14\}$:	0.14

Table B.1 (Continued)

Function	Discussion	Screening Estimate
	Development of steam generator (SG) overfill probabilities requires development of failure probabilities for MFW control valve closure and main feed pump trip.	
	MFW Control Valves Fail to Close on Demand. The FW control valves on HBR-2 are run back on each shutdown. Failure to run back is usually not reportable, but has occurred at some PWRs. Because of the lack of observational information concerning these valves, the failure probability for an air-operated valve included in Ref. 1 (1×10^{-3}) has been utilized in conjunction with conditional probabilities of multiple valve failures developed from Ref. 9. This results in the following estimates:	
	• For a single valve failure:	1×10^{-3}
	• For failure of any one of three valves, ${}_3C_1 \times (1.0 \times 10^{-3})$:	3×10^{-3}
	• For failure of any two of three valves, ${}_3C_2 \times (1 \times 10^{-3}) \times 0.094$:	2.8×10^{-4}
	• For failure of three valves, ${}_3C_3 \times (1 \times 10^{-3}) \times 0.081$:	8.1×10^{-5}
	MFW Pumps Fail to Trip on Demand. The MFW pumps are tripped on high SG level (2/3 signals in any SG) and by a SI signal. Given the existence of one of these signals, the likelihood of a MFW trip is considered high. The value per pump recommended is:	1×10^{-3}
	Using the failure logic combinations developed in Attachment A, and recognizing that the probability of failing to generate a MFW pump trip signal on high SG level is small compared to the likelihood of failing to trip a MFW pump given the trip signal has been generated, the following probabilities of SG overfeed given a nonspecific reactor trip are estimated:	
	(3) Probability of one SG overfeed following RT $[(\lambda_{RT} - \lambda_{LOFW}) \times P$ (any one feed control valve fails to close) $\times P$ (either MFW pump fails to trip/SG high-level signal or failure to generate SG high-level signal)$/\lambda_{RT} = [(8.7 - 1) \times (3 \times 10^{-3}) \times (2 \times 10^{-3})/8.7]$:	5.3×10^{-6}

Table B.1 (Continued)

Function	Discussion	Screening Estimate
	(4) Probability of two SG overfeeds following RT [(λ_{RT} − λ_{LOFW}) × P (two of three feed control valves fail to close) × P (either MFW pump fails to trip/SG high-level signal or failure to generate SG high-level signal)/λ_{RT} = [(8.7 − 1) × (2.8 × 10^{-4}) × (2 × 10^{-3})/8.7]:	5.0 × 10^{-7}
	(5) Probability of three SG overfeeds following RT [(λ_{RT} − λ_{LOFW}) × P (all three feed control valves fail to close) × P (either MFW pump fails to trip/SG high-level signal or failure to generate SG high-level signal)/λ_{RT} = [(8.7 − 1) × (8.1 × 10^{-5}) × (2 × 10^{-3})/8.7]:	1.4 × 10^{-7}
5. Failure of engineered safety features system (ESFS) to actuate	Failure to actuate ESFS will result in unavailability of trip signals for main steam-line isolation, MFW isolation, and SI initiation, necessitating manual trip of the affected components and manual initiation of AFW and SI. A general multichannel instrumentation failure probability of 3 × 10^{-5} is recommended for screening purposes.	3 × 10^{-5}
6. Failure to isolate MFW following initiators other than nonspecific reactor trip (not applicable for nonspecific reactor trip)	Boolean expressions for the probability of continued MFW flow to one or more SGs are developed in Attachment B following this table. Development of numeric estimates requires estimation of main feed isolation valve (MSIV) failure to close probabilities:	
	MFIVs Fail to Close. A preliminary estimate developed in the IPRDS program (Ref. 13) for the failure of a motor-operated valve to close, based on review of maintenance records at a small number of PWR plants, is 6.4 × 10^{-3}/demand. No failures of these valves have been observed at HBR-2. Since these valves are tested quarterly, a failure estimate of 0.7/(12.7 RY × 3 valves/test × 4 tests/RY) = 4.6 × 10^{-3} can be developed, which is consistent with the IPRDS value. The failure probability estimates for combinations of these valves are:	
	• Any one of three valves fail to close, $_3C_1$ × (4.6 × 10^{-3}):	1.4 × 10^{-2}
	• Any two of three valves fail to close, $_3C_2$ × (4.6 × 10^{-3}) × 0.020:	2.8 × 10^{-4}

Table B.1 (Continued)

Function	Discussion	Screening Estimate
	• Any three valves fail to close, ${}_3C_3 \times (4.6 \times 10^{-3}) \times 0.012$:	5.5×10^{-5}
	Based on this development, other component failure probabilities developed previously, the Attachment B Boolean expressions, and assuming limited failure coupling between MFW control valves and MFIVs (a conditional probability of 0.01 was assumed, to recognize some maintenance coupling), the following estimates can be made:	
	(1) Continued feed flow to any one generator = 6 × (probability of one MFW pump failing to trip) × (probability of a single MFIV failing to close) × (probability of the associated MFCV failing to close) = $6 \times (1 \times 10^{-3}) \times (4.6 \times 10^{-3}) \times 0.01$:	2.8×10^{-7}
	(2) Continued feed flow to any two SGs = 6 × (probability of one MFW pump failing to trip) × (probability of two MFIVs failing to close) × (probability of both associated MFCVs failing to close) = $6 \times (1 \times 10^{-3}) \times (2.8 \times 10^{-4}) \times (0.01 \times 0.094)$:	1.5×10^{-9}
	(3) Continued feed flow to all three SGs = 2 × (probability of one MFW pump failing to trip) × (probability of all three MFIVs failing to close) × (probability of all three MFCVs failing to close) = $2 \times (1 \times 10^{-3}) \times (5.5 \times 10^{-5}) \times (0.01 \times 0.081)$:	1×10^{-10}
	The Attachment B expressions for failure of MFW isolation while in hot shutdown require estimation of the probability of the MFW bypass valves failing to close on demand. These valves are normally closed during power operation but are opened for decay heat removal using the MFWs while in hot shutdown. For this development, failure probability and common-mode coupling values equivalent to those used for the MFCVs have been assumed. Based on these values, the probability estimates for continued MFW flow given SI and while in hot shutdown are:	
	(1) Continued MFW flow to any one SG = 3 × (probability of MFW pump failing to trip) × (probability of single MFBV failing to close) = $(3 \times 10^{-3}) \times (3 \times 10^{-3})$:	9×10^{-6}

Table B.1 (Continued)

Function	Discussion	Screening Estimate
	(2) Continued MFW flow to any two SGs = 3 × (probability of MFW pump failing to trip) × (probability of two MFBVs failing to close) = $(3 \times 10^{-3}) \times (2.8 \times 10^{-4})$:	8.4×10^{-7}
	(3) Continued feed flow to all three SGs = (probability of MFW pump failing to trip) × (probability of three MFBVs failing to close) = $10^{-3} \times (8.1 \times 10^{-5})$:	8.1×10^{-8}

NOTE: The above failure estimates have been developed without considering potential common-cause failure effects, which, for the multiple SG overfeed situations, would be expected to dominate.

7. Failure to isolate MFW on SIAS given failure to run back MFW (non-specific reactor trip only)	Given a failure to run back MFW to any SG, closure of the associated MFIV is required for isolation. Based on the conditional probabilities utilized in (6) above, failure of these valves to close given failure of the associated MFCV to close results in the following probability estimates.	
	If one line fails to run back, and	
	(1) One line fails to isolate:	1×10^{-2}
	If two lines fail to run back, and	
	(1) One line fails to isolate:	2×10^{-2}
	(2) Both lines fail to isolate:	9.4×10^{-4}
	If three lines fail to run back, and	
	(1) One line fails to isolate:	3×10^{-2}
	(2) Two lines fail to isolate:	2.8×10^{-3}
	(3) Three lines fail to siolate:	8.1×10^{-4}

Table B.1 (Continued)

Function	Discussion	Screening Estimate
8. Multiple SGs blow down following steam-line break	Boolean expressions for the probability of multiple SG blowdown given a steam-line break are developed in Attachment C following this table. To develop numeric estimates from these expressions, the probability of multiple MSIV failure must first be estimated.	
	Main Steam Isolation Valves Fail to Close on Demand. One instance potentially involving failure of an MSIV to fully close was reported at HBR-2 (NSIC 146521). Considering this one occurrence, a demand failure probability is estimated for the 12.7 years of operation at HBR-2 as (1)/{(12.7 years) × [12 test demands/year/valve (partial stroke testing)] × 3 valves} = 2.2×10^{-3}. Based on a review of all MSIV LERs, the number of failures to close for single valves is on the same order as for multiple valves failing to close. Thus, it can be concluded that the potential for common-mode coupling among these valves is large. Consistent with these observations, 0.3 was chosen for the conditional probability of a specific second valve failing, given that one has failed; and 0.8 was chosen for the conditional probability of a specific second valve failing, given that one has failed; and 0.8 was chosen for the conditional probability of the third valve failing given that the other two have failed. This results in the following estimates:	
	• For failure of a particular MSIV to close:	2.2×10^{-3}
	• For failure of a particular set of two MSIVs to close, $(2.2 \times 10^{-3}) \times 0.3$:	6.6×10^{-4}
	• For failure of three MSIVs to close, $(2.2 \times 10^{-3}) \times 0.3 \times 0.8$:	5.3×10^{-4}

Table B.1 (Continued)

Function	Discussion	Screening Estimate
	Based on the probability expressions developed in Attachment C and the above valve failure probabilities, the following probabilities of SG blowdown following an arbitrary large steam-line break can be estimated:	
	(1) No SG blows down:	0.5
	(2) One SG blows down:	0.5
	(3) Two SGs blow down, $1.5 \times (6.6 \times 10^{-4})$:	9.9×10^{-4}
	(4) Three SGs blow down, $0.5 \times (3.3 \times 10^{-4})$:	1.7×10^{-4}
	The above estimates are also applicable to small steam-line breaks which result in MSIV closure. For small breaks which do not result in MSIV closure, the following estimates, developed in Attachment C, are applicable:	
	(1) No SG blows down:	0.0
	(2) One SG blows down:	0.5
	(3) Two SGs blow down:	0.0
	(4) Three SGs blow down:	0.5
	Operator action to close the MSIVs would reduce the estimate for three SG blowdowns by the operator action probability.	

Table B.1 (Continued)

Function	Discussion	Screening Estimate
9. HPSI fails to occur on demand	At HBR-2, four failures of SI pumps were reported in LERs in 1979 and subsequent years. Assuming half of the number of HBR-2 years of operation, since all the failures occurred after 1976, yields a demand estimate of 12 demands/year $\times$ 6.4 years $\times$ 3 pumps = 228 demands; and a demand failure probability estimate of 1.7×10^{-2} per pump. With conditional probabilities of 0.1 and 0.3 applied for subsequent failures of a second pump and then the third, respectively, a failure probability for the system of 5.2×10^{-4} is estimated. This is consistent with the estimate available from the ASP data base for Westinghouse plants of 4.8×10^{-4}. (The estimate with potential recovery considered is lower by a factor of 0.34.) The recommended estimate is 4.8×10^{-4}, from the larger data base. Given HPI actuation success, successful HPI injection is dependent on the primary side pressure dropping low enough and check valves in the injection paths opening. There are three check valves in each of three injection paths that are inside containment and are not typically tested during monthly HPI testing. Using the Ref. 1 value of 10^{-4}/demand for a check valve failing to open, the probability of any one of three valves failing in a given path is 3.0×10^{-4}. Using coupling factors developed from Ref. 9 for other check valves failing to open (0.5 for failure of a second specific valve and 0.42 for both remaining valves in a set of three), and assuming that dependent coupling is much more likely for equivalent valves results in an estimate for the probability of 1.3×10^{-4} for not delivering HPI through any path given actuation success. Combining these values for failure to actuate and failure to deliver flow through the injection paths results in an overall estimate of 6.1×10^{-4}.	6.1×10^{-4}

Table B.1 (Continued)

Function	Discussion	Screening Estimate
10. AFW fails to actuate on demand	An estimated AFW system failure probability, suitable for screening purposes, has been developed based on the average PWR operational experience from 1969 through 1981 as evaluated in the ASP program (Refs. 7, 8). This value is 1×10^{-3} without considering potential recovery. Considering potential short-term recovery results in an estimate of 3×10^{-4}. Since these values are based on averaged experience and do not consider potential learning (except as evidenced in the averages), they may not be representative of expected future experience at HBR-2. However, they are considered consistent with the AFW component failure experience observed to date at HBR-2: 7 motor pump failures, 2 steam turbine pump failures, and 13 failures of pump discharge valves to open. No total AFW system failures have been observed at HBR-2.	See discussion

Attachment A to Table B.1: Development of MFW End State Probability Estimates for Nonspecific Reactor Trip Initiator

Following a general reactor trip, the MFW system is run back and an attempt is made (typically successfully) to utilize the MF pumps and the bypass valves for decay-heat removal. Depending on power level and the extent of SG level shrink, AFW can be initiated on RT. Isolation of AFW following such initiation is a normal part of RT recovery, along with manual opening of the bypass valves.

Following a nonspecific RT, the following SG feed situations are possible:

- MFW using bypass valves (normal situation).
- AFW (main MFW not recovered).
- One SG overfeed.
- Two SG overfeeds.
- Three SG overfeeds.

For the overfeed situations, AFW would be expected to be provided to the isolated SGs once low level in one SG is reached. Responses which include partially or totally faulted AFW are possible, but have not been included because they are considered less conservative than the above situations with respect to PTS.

The above states require the following responses:

- MFW using bypass valves for flow control — operator actions to open bypass valves following control valve closure and secure AFW if initiated due to shrink.
- AFW — operator action to open bypass valves and use MFW not effective or RT due to LOFW.
- One SG overfeed — failure of feed control valve in one train to run back and failure of either MFW pump to trip on high SG level.
- Two SG overfeeds — failure of feed control valves in two of three trains to run back and failure of either MFW pump to trip on high SG level.
- Three SG overfeeds — failure of feed control valves in all three trains to run back and failure of either MFW pump to trip on high SG level.

The frequencies associated with the above states can then be written as:

- λ (on bypass valves following RT) $\simeq \lambda_{RT} \times P$ (operator opens bypass valves following runback) $- \lambda_{LOFW}$.

- λ (on AFW following RT) $\simeq (\lambda_{RT} - \lambda_{LOFW}) \times P$ (operator fails to open bypass valves following RT) $+ \lambda_{LOFW}$.
- λ (one SG overfeed) $\simeq (\lambda_{RT} - \lambda_{LOFW}) \times P$ (one feed control valve fails to close) $\times P$ (either MFW pump fails to trip/SG high-level signal or failure to generate SG high-level signal).
- λ (two SG overfeeds) $\simeq (\lambda_{RT} - \lambda_{LOFW}) \times P$ (two feed control valves fail to close) $\times P$ (either MFW pump fails to trip/SG high-level signal in either SG or failure to generate SG high-level signal in either SG).
- λ (three SG overfeeds) $\simeq (\lambda_{RT} - \lambda_{LOFW}) \times P$ (three feed control valves fail to close) $\times$ (either MFW pump fails to trip/SG high-level signal in any SG or failure to generate SG high-level signal in any SG).

MFW isolation in the event of overfeed will occur due to closure of the MFIVs on SI if SI occurs. If SI does not occur, or if the applicable MFIV(s) fail to close on demand, then operator action is required to trip the condensate pumps or close the MFIVs (if SI has not been initiated).

Attachment B to Table B.1:

Development of MFW Isolation Failure Probability Estimates (All Initiators Except Reactor Trip)

The HBR-2 main feedwater system is arranged as follows:

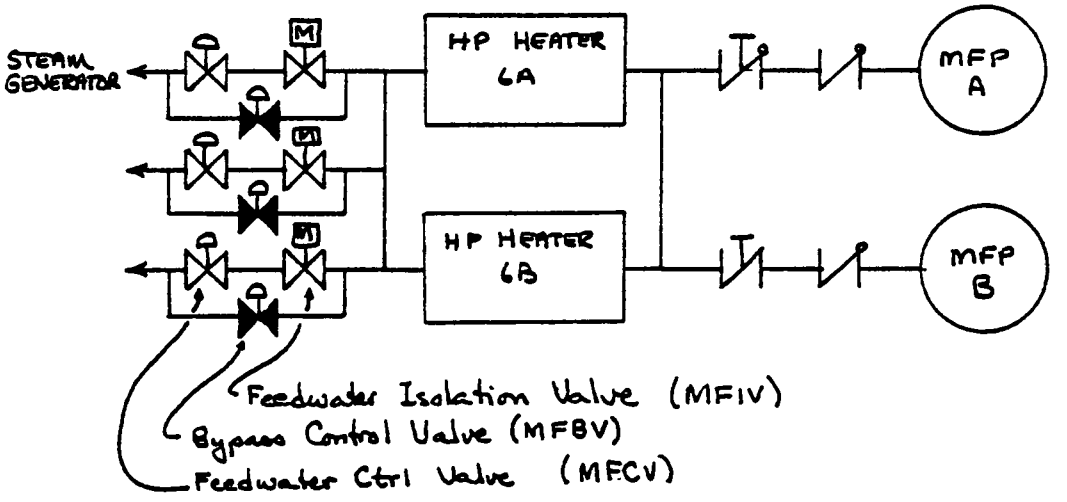

On reactor trip plus safety injection initiation, the MFCVs and MFIVs are commanded shut and the MFW pumps are tripped. Continued feedwater flow to one SG will occur if both of the valves in the associated feed line fail to close and either MFW fails to trip.

Continued feedwater flow to one SG will therefore occur if:

$$(\text{MFP A} \cup \text{MFP B}) \cap (\text{MFIV A} \cap \text{MFCV A} \cap (\overline{\text{MFIV B}} \cup \overline{\text{MFCV B}}) \cap (\text{MFIV C} \cup \overline{\text{MFCV C}}) \cup \text{other feed-line combinations}).$$

Continued feedwater flow to two SGs will occur if two of the three feed lines fail to isolate and either MFW pump fails to trip:

$$(\text{MFP A} \cup \text{MFP B}) \cap (\text{MFIV A} \cap \text{MFCV A} \cap \text{MFIV B} \cap \text{MFCV B}) \cap (\overline{\text{MFIV C}} \cup \overline{\text{MFCV C}}) \cup \text{other feed-line combinations}).$$

For continued flow to all SGs, the following is required:

$$(\text{MFP A} \cup \text{MFP B}) \cap (\text{MFIV A} \cap \text{MFCV A} \cap \text{MFIV B} \cap \text{MFCV B} \cap \text{MFIV C} \cap \text{MFCV C}).$$

To reduce the above equations, it is assumed that system response is symmetric (i.e., the likelihood of pump A failing to trip is equal to the likelihood of pump B failing to trip) and that pump and valve response is loosely coupled.

The probabilities of continued flow to N steam generators are then approximately:

$$P(\text{flow to 1 SG}) \simeq 6 \times P(\text{MFP}) \times P(\text{MFIV}) \times P(\text{MFCV}|\text{MFIV}),$$

$$P(\text{flow to 2 SGs}) \simeq 6 \times P(\text{MFP}) \times P(\text{MFIV1}) \times P(\text{MFIV2}|\text{MFIV1}),$$

$$\times P(\text{MFCV1}|\text{MFIV1,MFIV2})$$

$$\times P(\text{MFCV2}|\text{MFIV1,MFIV2,MFCV1}),$$

$$P(\text{flow to 3 SGs}) \simeq 2 \times P(\text{MFP}) \times P(\text{MFIV1}) \times P(\text{MFIV2}|\text{MFIV1})$$

$$\times P(\text{MFIV3}|\text{MFIV1, MFIV2}) \times P(\text{MFCV1}|\text{MFIV1, ...})$$

$$\times P(\text{MFCV2}|\text{MFIV1, ...}) \times P(\text{MFCV3}|\text{MFIV1, ...}),$$

$$P(\text{flow to 0 SGs}) \simeq 1 - P(\text{flow to 1 SG}) - P(\text{flow to 2 SGs})$$

$$- P(\text{flow to 3 SGs}).$$

In hot shutdown, the bypass valves (MFBVs) are used to control feedwater flow to the SGs. Feed flow is typically provided by one pump. The MFBVs are in parallel with the MFIV-MFCV pairs, and hence the closure or MFP trip is necessary for SG isolation. In hot shutdown, then, the probabilities of continued flow to N steam generators is approximately:

$$P(\text{flow to 1 SG}) \simeq 3 \times P(\text{MFP}) \times P(\text{MFBV}),$$

$$P(\text{flow to 2 SGs}) \simeq 3 \times P(\text{MFP}) \times P(\text{MFBV1}) \times P(\text{MFBV2}|\text{MFBV1}),$$

$$P(\text{flow to 3 SGs}) \simeq 3 \times P(\text{MFP}) \times P(\text{MFBV1}) \times P(\text{MFBV2}|\text{MFBV1})$$

$$\times \text{P(MFBV3|MFBV1, MFBV2)},$$

$$P(\text{flow to 0 SGs}) = 1 - P(\text{flow to 1 SG}) - P(\text{flow to 2 SGs})$$

$$- P(\text{flow to 3 SGs}).$$

Attachment C to Table B.1:

Development of Multiple Steam Generator Blowdown Frequency Estimates

The HBR-2 steam-line arrangement utilizes both MSIVs and check valves for SG isolation:

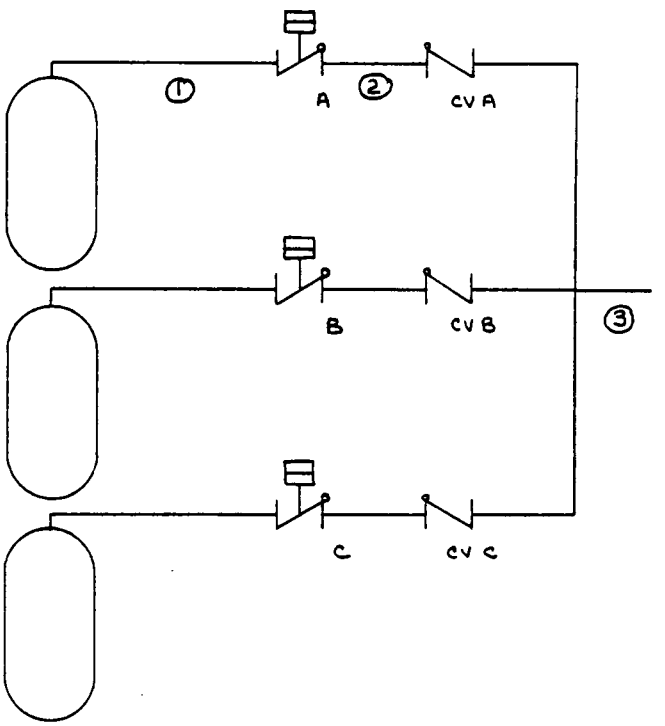

Consider potential breaks at location (1) with frequency λ_1, at location (2) with frequency λ_2, and at location (3) with frequency λ_3. The break locations and valve states for n steam generator blowdowns are as shown in Table B.2. Considering the frequency of breaks in locations (1), (2), and (3), the frequencies of n steam generator blowdowns, $\Lambda(n)$, are

$$\Lambda(0) = \lambda_2 \times P[\overline{A} \cap (\overline{CVA} \cup \overline{B} \cap \overline{C})] + \lambda_3 \times P[\overline{A} \cap \overline{B} \cap \overline{C}],$$

$$\Lambda(1) = \lambda_1 \times P[\overline{A} \cup (\overline{CVA} \cup \overline{B} \cap \overline{C})] + \lambda_2 \times P[A \cap (\overline{CVA} \cup \overline{B} \cap \overline{C}) \cup \overline{A} \cap CVA \cap (B \cap \overline{C} \cup \overline{B} \cap C)] + \lambda_3 \times P[\overline{A} \cap \overline{B} \cap C \cup \overline{A} \cap B \cap \overline{C} \cup A \cap \overline{B} \cap \overline{C}],$$

$$\Lambda(2) = \lambda_1 \times P[A \cap CVA \cap (B \cap \overline{C} \cup \overline{B} \cap C)] + \lambda_2 \times P[A \cap CVA \cap (\overline{B} \cap C \cup B \cap \overline{C})] + \lambda_3 \times P[A \cap B \cap \overline{C} \cup A \cap \overline{B} \cap C \cup \overline{A} \cap B \cap C],$$

$$\Lambda(3) = \lambda_1 \times P[A \cap CVA \cap B \cap C] + \lambda_2 \times P[A \cap CVA \cap B \cap C] + \lambda_3 \times P[A \cap B \cap C].$$

Table B.2. Break locations and valve states for steam generator blowdowns

End State	Break Location (1)	Break Location (2)	Break Location (3)
0 SGs blow down		A closed and (CVA closed or B closed and C closed)	A closed and B closed and C closed
1 SG blows down	A closed or CVA closed or B closed and C closed	A open and (CVA closed or B closed and C closed) or A closed and CVA open and (B open and C closed or B closed and C open)	A open and B closed and C closed or B open and A closed and C closed or C open and A closed and B closed
2 SGs blow down	A open and CVA open and (B open and C closed or B closed and C open)	A open and CVA open and (B open and C closed or B closed and C open)	A open and B open and C closed or A open and C open and B closed or B open and C open and A closed
3 SGs blow down	A open and CVA open and B open and C open	A open and CVA open and B open and C open	A open and B open and C open

The following assumptions have been made in reducing the above equations for an arbitrary large SLB:

(1) Because of the proximity of the MSIVs and check valves, λ_2 is small compared to λ_1 and λ_3.

(2) Even if three MSIVs fail to close, the probability of check valve failure is less than 0.1.

(3) Break locations (1) and (2) are equally applicable to all steam generators. Furthermore, because of the lack of data, breaks in locations (1) (for all three SGs taken together) and (3) are equally likely (i.e., breaks upstream of the MSIVs are as likely as breaks downstream of the MSIVs).

The above equations can then be reduced to

$$\Lambda(0) \simeq 3 \times \lambda_2 + \lambda_3,$$

$$\Lambda(1) \simeq 3 \times \lambda_1 + 3 \times \lambda_2 \times [P(\mathrm{A}) + P(\mathrm{B}) \times P(\mathrm{CVA}|\mathrm{B}) + P(\mathrm{C}) \times P(\mathrm{CVA}|\mathrm{C})] + \lambda_3 \times [P(\mathrm{A}) + P(\mathrm{B}) + P(\mathrm{C})],$$

$$\begin{aligned}\Lambda(2) \simeq\ & 3 \times \lambda_1 \times [P(\mathrm{A}) \times P(\mathrm{A}|\mathrm{B}) \times P(\mathrm{C}|\mathrm{AB}) \times P(\mathrm{CVA}|\mathrm{ABC}) \\ & + P(\mathrm{A}) \times P(\mathrm{C}|\mathrm{A}) \times P(\mathrm{B}|\mathrm{AC}) \times P(\mathrm{CVA}|\mathrm{ABC})] \\ & + 3 \times \lambda_2 \times [P(\mathrm{A}) \times P(\mathrm{B}|\mathrm{A}) \times P(\mathrm{C}|\mathrm{AB}) \times P(\mathrm{CVA}|\mathrm{ABC}) \\ & + P(\mathrm{A}) \times P(\mathrm{C}|\mathrm{A}) \times P(\mathrm{B}|\mathrm{AC}) \times P(\mathrm{CVA}|\mathrm{ABC})] \\ & + \lambda_3 \times [P(\mathrm{A}) \times P(\mathrm{B}|\mathrm{A}) \times P(\mathrm{C}|\mathrm{AB}) + P(\mathrm{A}) \times P(\mathrm{C}|\mathrm{A}) \\ & \times P(\mathrm{B}|\mathrm{AC}) + P(\mathrm{B}) \times P(\mathrm{C}|\mathrm{B}) \times P(\mathrm{A}|\mathrm{BC})],\end{aligned}$$

$$\begin{aligned}\Lambda(3) =\ & 3 \times \lambda_1 \times [P(\mathrm{A}) \times P(\mathrm{B}|\mathrm{A}) \times P(\mathrm{C}|\mathrm{AB}) \times P(\mathrm{CVA}|\mathrm{ABC})] \\ & + 3 \times \lambda_2 \times [P(\mathrm{A}) \times P(\mathrm{B}|\mathrm{A}) \times P(\mathrm{C}|\mathrm{AB}) \times P(\mathrm{CVA}|\mathrm{ABC})] \\ & + \lambda_3 \times [P(\mathrm{A}) \times P(\mathrm{B}|\mathrm{A}) \times P(\mathrm{C}|\mathrm{AB})] .\end{aligned}$$

Assumptions (1) and (2) result in the following further simplification:

$$\Lambda(0) = \lambda_3 ,$$
$$\Lambda(1) = 3 \times \lambda_1 ,^*$$
$$\Lambda(2) = 3 \times \lambda_3 \times P(\mathrm{A}) \times P(\mathrm{B}|\mathrm{A}) \times P(\mathrm{C}|\mathrm{AB}) ,$$
$$\Lambda(3) = \lambda_3 \times P(\mathrm{A}) \times P(\mathrm{B}|\mathrm{A}) \times P(\mathrm{C}|\mathrm{AB}) .$$

Since $3 \times \lambda_1 \simeq \lambda_3$ and $\lambda_2 << \lambda_3, \lambda_1$, an event tree can be constructed representing potential SG blowdown following an arbitrary large steam-line break:

---

* Since $P(\mathrm{A})$, etc. $\simeq 10^{-2}$.

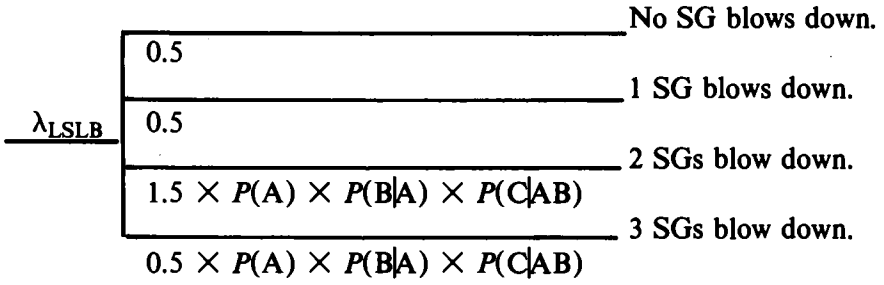

A review of historic small steam-line breaks indicates approximately 50% have been associated with steam-line relief valves located upstream of MSIVs, and the remaining have been associated with condenser dump valves, typically located downstream of MSIVs. Because of these ratios, the above development for large steam-line breaks is also considered applicable to small steam-line breaks, provided the break is sufficiently large to require MSIV closure.

If a small steam-line break is large enough to close the appropriate check valve (if it is located upstream of the check valve) but is not large enough to initiate MSIV closure and operator action is not taken to close the MSIVs, then the frequency of multiple SG blowdowns can be estimated as:

$$\Lambda(0) \simeq 0 \ ,$$

$$\Lambda(1) \simeq \lambda_1 \times P(\mathrm{CVA}) + \lambda_2 \times P(\mathrm{CVA}) \ ,$$

$$\Lambda(2) \simeq 0 \ ,$$

$$\Lambda(3) \simeq \lambda_1 \times P(\mathrm{CVA}) + \lambda_2 \times P(\mathrm{CVA}) + \lambda_3 \ .$$

Small SLBs upstream of the check valves may be associated with any of the SGs. Since the number of breaks related to relief valves is consistent with the number of breaks related to condenser dump valves and the number of small SLBs associated with region (2) is expected to be small compared with valve-related breaks, the following simplifications of the above equations can be made:

$$\Lambda(0) \simeq 0 \ ,$$
$$\Lambda(1) \simeq 3 \times \lambda_{1,\mathrm{SSLB}} \simeq 0.5 \times \lambda_{\mathrm{SSLB}} \ ,$$
$$\Lambda(2) \simeq 0 \ ,$$
$$\Lambda(3) \simeq \lambda_{3,\mathrm{SSLB}} \simeq 0.5 \times \lambda_{\mathrm{SSLB}} \ .$$

Potential SG blowdown, given a small steam-line break which does not initiate MSIV closure, can be represented by the following event tree:

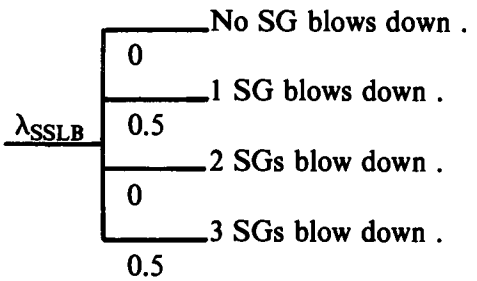

B.2. References

1. *Generic Data Base for Data and Models Chapter of the National Reliability Evaluation Program (NREP),* EGG-EA-5887, June 1982.
2. *Nuclear Power Plant Operating Experience — 1978,* NUREG-0618, December 1979.
3. *Nuclear Power Plant Operating Experience — 1979,* NUREG/CR-1460, May 1981.
4. *Nuclear Power Plant Operating Experience — 1980,* NUREG/CR-2378, October 1982.
5. *Operating Units Status Reports — Licensed Operating Reactors,* NUREG-0020, published monthly.
6. Mann, Schafer, and Singpurwalla, *Methods for Statistical Analysis of Reliability and Life Data,* John Wiley and Sons, New York, 1974.
7. *Precursors to Potential Severe Core Damage Accidents: 1969–1979, A Status Report,* NUREG/CR-2497, June 1982.
8. *Precursors to Potential Severe Core Damage Accidents: 1980–1981, A Status Report,* NUREG/CR-3591, June 1984.
9. *Common Cause Fault Rates for Valves,* NUREG/CR-2770, February 1983.
10. *Generic Evaluation of Feedwater Transients and Small Break Loss-of-Coolant for Accidents in Westinghouse-Designed Operating Plants,* NUREG-0611, January 1980.
11. *In-Plant Reliability Data Base for Nuclear Plant Components: The Valve Component,* NUREG/CR-3154, November 1983.
12. *H. B. Robinson Unit 2 Nuclear Station, Updated Final Safety Analysis Report.*
13. *Staff Report on the Generic Assessment of Feedwater Transients in Pressurized Water Reactors Design by the Babcock & Wilcox Company,* NUREG-0560, May 1979.

Appendix C

A SOCIO-TECHNICAL APPROACH TO ASSESSING HUMAN RELIABILITY (STAHR)

L. D. Phillips and P. Humphreys

London School of Economics and Political Science

D. E. Embrey

Human Reliability Associates, Lancashire, England

D. L. Selby

Oak Ridge National Laboratory

APPENDIX C. A SOCIO-TECHNICAL APPROACH TO ASSESSING HUMAN RELIABILITY (STAHR)

C.1. Introduction

This appendix describes the status, as of June 1983, of a new approach for assessing human reliability in complex technical systems such as nuclear power plants. This approach was utilized in the present PTS study for H. B. Robinson Unit 2, the results of which are described in Appendix D.

The new approach includes both a social component and a technical component. To help keep this in mind and also to provide an easily recognized acronym, we are calling our methodology a "socio-technical assessment of human reliability" — or the STAHR approach.

It is important to emphasize that the approach described here does not provide the definitive technical fix to a problem on which a great deal of effort has already been spent. It does, however, provide regulators and risk assessors with another methodology that has certain advantages and disadvantages compared to existing approaches. How useful it proves to be in practice is yet to be determined, but work to date indicates that additional research on this approach is warranted.

A key feature of the approach is that it draws on two fields of study: decision theory and group processes. Decision theory provides the form of the model that allows the desired error rates to be determined, while group processes provide the input data through the group interaction of experts who are knowledgeable about the factors influencing the event whose error rate is being assessed. The different perspectives of these experts, if managed effectively by the group, can lead to informed, useful inputs to the model. Thus, the validity of any error rates that are produced by the model depends not only on the technical model itself, but also on the social processes that help to generate the model inputs.

The impetus for the socio-technical approach began in 1982 at an Oak Ridge, Tennessee, meeting addressing methods for assessing human reliability in the PTS studies. One of us (Phillips) introduced influence diagram technology[1] as a potentially easier modeling tool than event trees or fault trees. The main advantage of an influence diagram from a technical perspective is that it capitalizes on the independence between events and models only dependencies; that is, the influence diagram organizes the dependencies as a system of conditional probabilities, as explained in Section D.2. By the early spring of 1983, the Decision Analysis Unit at the London School of Economics and Human Reliability Associates, Lancashire, England, together had developed a human reliability assessment technology utilizing influence diagrams to the point that it could be tested in the field. In late May a field test was carried out at Hartford, Connecticut, to address operator actions associated with potential pressurized thermal shock events that could occur at the H. B. Robinson Unit 2 nuclear power station, the results of which are described in Appendix D.

In the paragraphs that follow, a general discussion of influence diagrams is first presented, followed by a description of how group processes work to provide specific diagrams and the input data. Finally, the particularized STAHR approach is described.

C.2. General Description of the STAHR Approach

C.2.1. The Technical Component: The Influence Diagram

As stated above, STAHR consists of both a social component and a technical component. The technical component is the influence diagram. Influence diagrams were developed in the mid-70's by Miller *et al.*[2] at the Stanford Research Institute and then were applied and further developed at Decisions and Designs, Inc.[3] for intelligence analysis, all without a single paper being published in a professional journal. In 1980, Howard and Matheson[1] extended the theory and showed that any event tree can be represented as an influence diagram, but not all influence diagrams can be turned into event trees unless certain allowable logical transformations are performed on the linkages between the influencing events.

The key principles of influence diagram technology are illustrated by the simple diagrams shown in Figure C.1. Diagram (a) shows the simplest kind of influence. Here Event A is influenced by Event B; that is, the probabilities that one would assign to the occurrence or non-occurrence of Event A are conditional on whether or not Event B has occurred. Shown with the influence diagram is an equivalent event tree representation, where Events A and B are assumed to have only two outcomes, A and $\bar{A}$, B and $\bar{B}$. In the event tree the probability of B occurring is given by p_1. The probability of A occurring, given that B has occurred, is shown by p_2, and the probability of A occurring, given that B has not occurred, is given by p_3. The point here is that p_2 is not equal to p_3. If p_2 and p_3 were equal, then the influence diagram would show two circles unconnected by any influencing link.

Diagram (b) shows a slightly more complex influence. Here, Event A is influenced by both Event B and Event C. The comparable event tree consists of three tiers because the probability assigned to A at the extreme right depends upon the previous occurrence or non-occurrence of both B and C. These probabilities for A, conditional on previous events, are shown by p_3 through p_6. Note that p_2 appears in two places, indicating that the probability assigned to B is the same whether or not C occurs.

Finally, diagram (c) shows the same influences on A as diagram (b), but now Event C influences not only Event A but also Event B. Note that the event trees for diagrams (b) and (c) have the same structure, but for diagram (c) the probability assigned to B conditional on C is no longer the same as the probability of B conditional on C. Thus, while there are six different probabilities in the event tree for diagram (b), there are seven different probabilities in the event tree for diagram (c). It is easy to see that the influence diagram representation not only is compact, but also contains more information than the structure of the event trees without any probability assignments.

In practical situations for which an influence diagram has many nodes, it is typical for the actual number of influencing paths to be far fewer than the maximum that could occur if every node were linked to every other node. Any assessment procedure based on the influence diagram will require only the minimum number of probability assignments. For example, an influence diagram procedure for (b) in Figure C.1 would require only six probabilities and would recognize that the same probability is assigned to Event B whether or not Event C occurs. In an event tree representation of the same problem, dependencies between events are not obvious until probabilities have been associated with each branch, and keeping track of independent events within a large tree can be a tedious housekeeping chore.

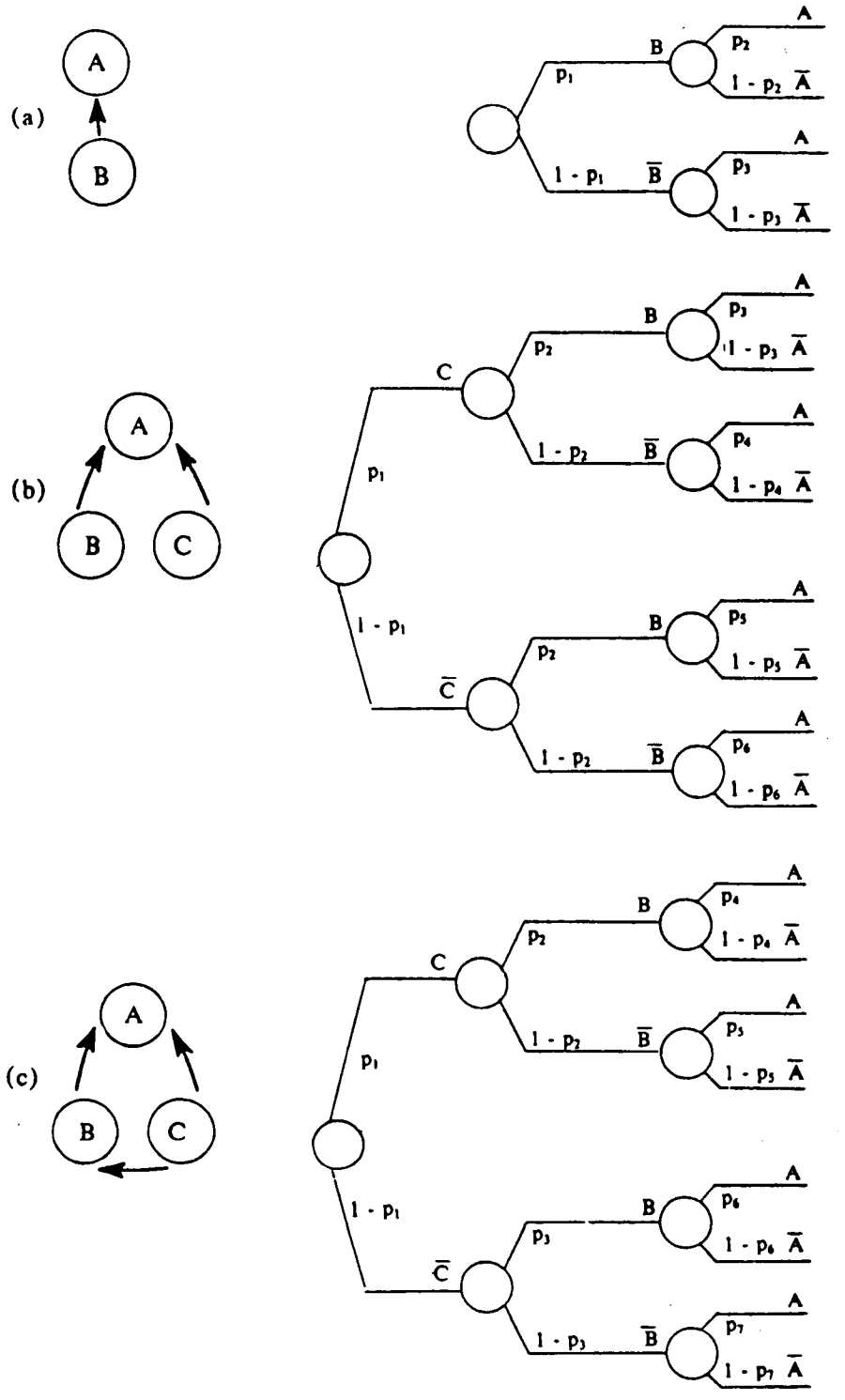

Figure C.1. Influence diagrams and their corresponding event trees. (a) Event A is influenced by Event B; (b) Event A is influenced by Events B and C; and (c) Event A is influenced by Events B and C, and B is influenced by C.

In applying influence diagram technology, Event A is taken as the target event and assessments are made of only the necessary and sufficient conditional probabilities that enable the unconditional probability of the target event outcomes to be calculated. For example, in diagram (a) of Figure C.1, the probability of A is given by calculating the joint probabilities of all paths on which an A occurs and then summing the joint probabilities, i.e., $p_1p_2 + (1 - p_1)p_3$. For more complex influence diagrams, successive application of the addition and multiplication laws of probability are sufficient to enable the unconditional probability of the targeted event to be calculated.

It is, of course, important to recognize that no probability is ever unconditional. All events shown on an influence diagram occur within some context, and it is this context that establishes conditioning events that are not usually shown in the notation on the influence diagram. Thus, in applying this technology, it will be important to establish at the start of every assessment procedure what these common conditioning events are.

C.2.2. The Social Component: Human Judgments

The preceding discussion has illustrated how the influence diagram provides the technical means for organizing the conditional probability assessments that are required for calculating the unconditional probability of the target event. But where does the specific influence diagram needed come from, and how are the conditional probability assessments obtained? The answer is that they are developed mainly through human judgments obtained from experts working in groups, and it is these judgments that comprise the "socio" component of the STAHR approach.

The theory behind the socio component was developed and illustrated with a case study by Phillips.[4,5] The key idea is that groups of experts are brought together to work in an iterative and consultative fashion to create a requisite model of the problem at hand. A judgmental model is considered requisite if it is sufficient in form and content to solve the problem. A requisite model is developed by consulting "problem owners," people who have the information, judgment and experience relevant to the problem.

The process of creating a model is iterative, with current model results being shown to the problem owners who can then compare the current results with their own holistic judgments. Any sense of discrepancy is explored, with two possible results: intuition and judgment may be found lacking or wrong, or the model itself may be inadequate or incorrect. Thus, the process of creating a requisite decision model uses the sense of unease felt by the problem owners about current model results, and this sense of unease is used to develop the model further and to generate new intuitions about the problem. When the sense of unease has gone and no new intuitions emerge, then the model is considered requisite. The aim of requisite modeling is to help problem owners toward a shared understanding of the problem, thus enabling decision makers to act, to create a new reality.

A requisite model usually is neither optimal or normative, is rarely descriptive, and is at best conditionally prescriptive. A requisite model is about a shared social reality, the current understanding by the problem owners. Requisite models are appropriate when there is a substantial judgmental element that must be made explicit in order to solve a problem.

Because judgment, intuition and expertise are important ingredients of requisite models, there can be no external reality that can serve as a criterion against which optimality would be judged. Thus, requisite models are not optimal models. Nor are requisite models normative models in the sense that they describe the behavior of idealized, consistent decision makers; that claim would be too strong. Neither can they be considered as descriptive models in the sense that they describe the behavior of actual people. Requisite models are stronger than that; they serve as guides to action, though they may not themselves model alternative courses of action. A requisite model attempts to overcome limitations on human processing of information due to bounded rationality.

Requisite modeling seems ideally suited for the determination of human error rates in complex technical systems. The human operator in a complex system cannot, for the purpose of determining error rates, be treated as an unreliable machine component. In determining error rates for machines, two fundamental assumptions are made. First, that all machines of a particular type are identical as far as error rates are concerned, and second, that all machines of a particular type will be operating within environmental bounds over which the error rate remains unchanged. Neither of these assumptions is true for the human operator. Each person is different from the next, and not even requiring certain standards of training and competence can ensure that other factors, such as those affecting morale and motivation, will not have over-riding effects on the error rates. Moreover, environmental factors can have a substantial impact on human error rates. The same operator may perform differently at a new plant of the same design, if, for example, teams function differently in the two plants. In short, people are different, and the environments they operate in are different, not only from plant to plant but also, from time to time, within a plant. Human error rates are not, then, unconditional figures that can be assigned to particular events. Rather, they are numbers that are conditional on the individual, and on the social and physical environment in which he is operating.

The effective assessment of error rates should take these conditioning influences into account. Technically, the STAHR approach does this by using the influence diagram to display the conditioning influences, and by using the educated assessments of experts to provide judgments that can take account of the uniqueness of the influences for a particular plant.

As yet, it is not known when the STAHR approach should be used in preference to other approaches. It is not even clear whether the STAHR approach should be considered as a competitor to other methods, for it may well turn out that different methods are called for in different circumstances. Clearly, the STAHR approach focuses on the process of obtaining assessments and in this respect it differs considerably from the handbook approach (the THERP approach) of Swain and Guttman.[6] At this stage of research, it can only be said that the STAHR approach is different from THERP. Our guess is that both STAHR and THERP, and possibly other approaches as well, will each find their own uses, depending on the circumstances. Research is needed to identify those circumstances.

Finally, can experts provide assessments that are valid? Our view is that given the right circumstances people can provide precise, reliable and accurate assessments of probability. This viewpoint is elaborated on by Phillips,[7] but some authorities believe that bias is a pervading element in probability assessment.[8] Unfortunately, virtually none of the research

that leads to the observation of bias in probability assessments has been conducted under circumstances that would facilitate good assessments. Many of these circumstances are explained in Stael von Holstein and Matheson.[9]

Recent research by the Decision Analysis Unit with insurance underwriters suggests that two additional factors contribute to obtaining good probability assessments. One is the structure of the relationships of events whose probabilities are being assessed, and the other is the use of groups in generating good assessments. In the STAHR approach, the influence diagram presents a well-understood structure within which groups of experts generate assessments.

The success of the STAHR approach depends, in part, on the presence of a group facilitator who is acquainted with the literature on probability assessment and who is experienced in using techniques that facilitate good assessments. How crucial this role is we do not yet know, but we are sure that the necessary expertise and skills can be acquired with reasonable effort by potential group facilitators. In any event, there is nothing in the research literature to suggest that people are incapable of making good assessments. In the United States, weathermen do it now. For example, a review of weather predictions showed that when weathermen predicted a 60% chance of rain within 24 hours, 60% of the time it rained within 24 hours. Thus, weather forecasts are said to be "well-calibrated"; the STAHR approach tries to arrange for circumstances that will promote "well-calibrated" probability assessments. However, calibrating the very low probabilities that emerge from the STAHR approach, or indeed any other approach, is technically difficult because of the low error rates implied. There are simply too few opportunities to determine whether the weathermen's low probability of rain in the desert is realistic.

C.3. Design of the STAHR Influence Diagram

After several revisions, the influence diagram as of June 1983 for events that are influenced by operator actions in nuclear power stations is shown in Figure C.2. We do not yet know whether this influence diagram is generic in the sense that it can handle all events in which operators are expected to take actions. Possibly parts of the diagram are generic and others need to be developed to fit the specific situation. The STAHR approach is sufficiently flexible that modifications to the influence diagram can be made to suit the circumstances, or entirely different influence diagrams could be drawn.

The top node in Figure C.2 indicates the target event. For example, if an alarm in the control room signals that some malfunction has occurred and the operator attempts to correct the malfunction by following established procedures, one target event might be that the operator correctly performs a specified step in the procedures. The influence diagram shows three major influences on the target event. One is the quality of information available to the operator, the second is the extent to which the organization of the nuclear power station contributes to getting the work done effectively, and the third is the impact of personal and psychological factors pertaining to the operators themselves. Another way of saying this is that the effective performance of the target event depends on (A) the physical environment, (B) the social environment, and (C) personal factors.

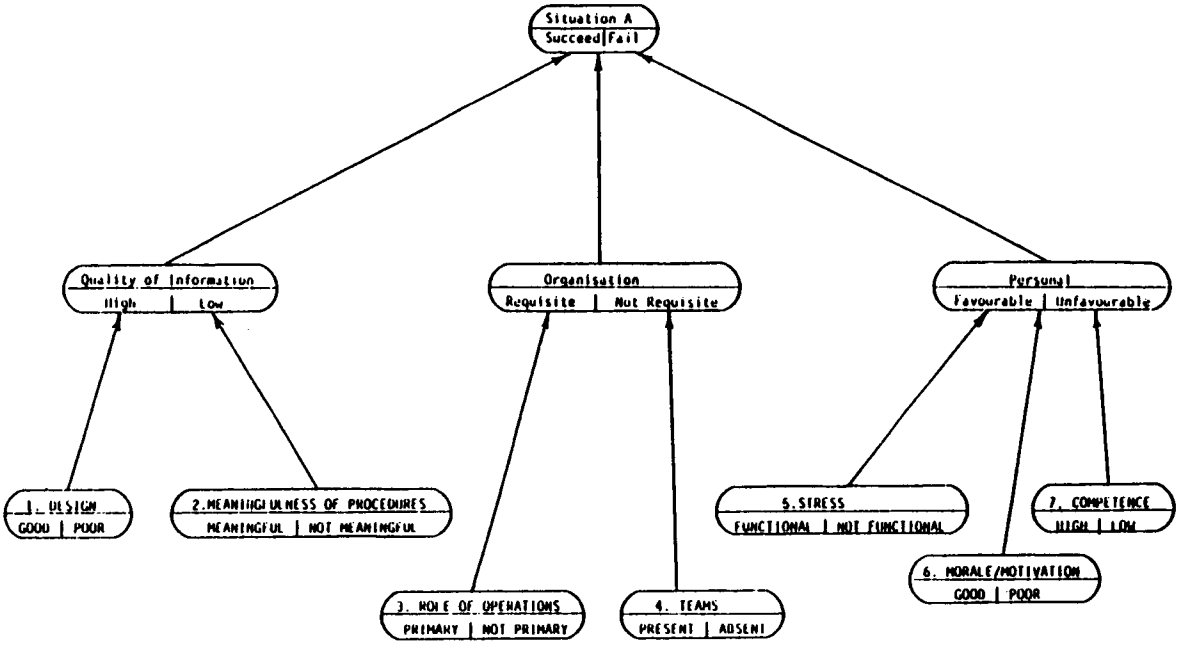

Figure C.2. The STAHR influence diagram (as of June 1983).

Each of these three major factors is itself influenced by other factors. The quality of information available is largely a matter of good design of the control room and of the presence of meaningful procedures. The organization is requisite; i.e., it facilitates getting the required work done effectively if the operations department has a primary role at the power station and if the organization at the power station allows the effective formation of teams. Personal factors will contribute to effective performance of the target event if the level of stress experienced by operators is helpful, if morale and motivation of the operators are good, and if the operators are highly competent. In other words, the following seven "bottom-level" influences actually describe the power station, its organization and its operators:

(A) Physical Environment

- (1) Design of control room (good vs. poor).
- (2) Meaningfulness of procedures (meaningful vs. not meaningful).

(B) Social Environment

- (3) Role of Operations Department (primary vs. not primary).
- (4) Effectiveness of teams (team work present vs. absent).

(C) Personal Factors

- (5) Level of stress (helpful vs. not helpful).
- (6) Level of morale/motivation (good vs. bad).
- (7) Competence of operators (high vs. low).

These seven influences are discussed in more detail in Appendix D with respect to their application during the field testing of the STAHR methodology at H. B. Robinson Unit 2. Suffice it to say here that in considering the impact of these seven influences, most nuclear power stations will be found to have mixtures of "good" vs. "poor," "high vs. low," etc.

C.4. Application of the STAHR Influence Diagram

Using the STAHR influence diagram is a matter of applying the following ten steps:

(1) Describe all relevant conditioning events.

(2) Define the target event.

(3) Choose a middle-level event and assess the weight of evidence for each of the bottom-level influences leading into this middle-level event.

(4) Assess the weight of evidence for this middle-level influence conditional on the bottom-level influences.

(5) Repeat steps 3 and 4 for the remaining middle- and bottom-level influences.

(6) Assess probabilities of the target event conditional on the middle-level influences.

(7) Calculate the unconditional probability of the target event and the unconditional weight of evidence of the middle-level influences.

(8) Compare these results to the holistic judgments of the assessors; revise the assessments as necessary to reduce discrepancies between holistic judgments and model results.

(9) Iterate through the above steps as necessary until the assessors have finished refining their judgments.

(10) Do sensitivity analyses on any remaining group disagreements; report either point estimates if disagreements are of no consequence, or ranges if disagreements are substantial.

In step 1, participants would describe the general setting in which the target event might occur, as well as all conditions leading up to the target event. Assessors are reminded that this description and statement of initial conditions form a context for their subsequent assessments and that these assessments are conditional on this context.

In the second stage, the target event is defined in such a way that its occurrence or non-occurrence is capable, at least theoretically, of confirmation without additional information. Thus, "rain tomorrow" is a poorly defined event, whereas "less than 0.1 mm of precipitation falls in a range gauge located at weather station x" is a well-defined event.

In carrying out step 3, the assessors might begin by focusing attention on the left-most middle node, quality of information, and assess weights of evidence for the two bottom

influences, design and procedures. This is done with reference to the specific definitions of these bottom influences.* For example, with respect to the design influence, the group of assessors must decide whether, on balance, the design of the particular power station is more similar to the good definitions or to the poor definitions (see items A1 and A2 in list of bottom-level influences in Section C.3). The assessors may find it helpful to imagine a continuous dimension between good and poor and then try to determine where on this dimension this particular power station lies with respect to the event in question. In short, the assessors are judging numbers that reflect the relative weight of evidence as between the poles of the design influence. The weight of evidence would also be judged for the next bottom node, meaningfulness of procedures, but here six different factors, from realism to format, must be taken into account in making the judgment.

The weights of evidence placed on the poles of each dimension are assigned as numbers that sum to 1. Thus, by letting w_1 represent the weight of evidence on the design being good and w_2 represent the weight of evidence on the procedures being meaningful, the assessments for these two bottom nodes can be represented as follows:

	Good	Poor
Design	w_1	$1 - w_1$

	Meaningful	Not Meaningful
Procedures	w_2	$1 - w_2$

Step 4 requires the assessment of probabilities for the quality of information, a middle-level influence, conditional on the lower-level influences. The poles of the two bottom-level influences combine to make four different combinations: good design and meaningful procedures; good design and not-meaningful procedures; poor design and meaningful procedures; and poor design and not-meaningful procedures. Each of these four combinations describes a hypothetical power station of the sort under consideration, and these hypothetical stations are kept in mind by the assessors when they determine the weight of evidence for the quality of information. This can be set out as follows:

If DESIGN	& PROCEDURES	then QUALITY OF INFORMATION is HIGH	LOW	JOINT WEIGHTS
Good	Meaningful	w_3	$1 - w_3$	$w_1 w_2$
Good	Not meaningful	w_4	$1 - w_4$	$w_1(1 - w_2)$
Poor	Meaningful	w_5	$1 - w_5$	$(1 - w_1)w_2$
Poor	Not meaningful	w_6	$1 - w_6$	$(1 - w_1)(1 - w_2)$

*For specific definitions, see Table D.2 in Appendix D.

For example, w_3 is the weight of evidence that the quality of information is high, given that design is good and the procedures are meaningful. Here high quality of information does not mean an ideally perfect power station; instead it means a power station in which both the design and the procedures are of a high, yet practically realizable standard. Neither does low quality of information mean some abysmally bad standard, but rather a standard that is minimally licensable. The assessments w_3 through w_6 capture possible interactions between design and procedures. This is a key feature of the influence diagram technology and experience to date suggests that it is an important feature for human reliability assessment. For example, in some power stations good design may compensate to some extent for procedures that are not very meaningful, whereas if the design were poor the additional burden of procedures that were not meaningful could be very serious indeed.

At this point, a brief technical diversion from describing the ten-step procedure is warranted because it is now possible to illustrate the calculations that are involved in using influence diagrams. The weights are assessed in such a way that they are assumed to follow the probability calculus. Thus, the overall weights of evidence that would be assigned to those four hypothetical stations described at step 4 can be obtained by multiplying the two relevant weights of evidence. For example, the weight of evidence assigned to the actual power station under consideration being both good in design and meaningful in procedures is given by the product of w_1 and w_2. These are shown above as joint weights. Note that the product rule for probabilities is applied. The next stage in the calculation is to multiply these four joint weights by the weights w_3 through w_6 and then to add these four products to obtain the overall weight of evidence that quality of information is high for the power station under consideration. That is,

$$w(\text{HIGH}) = w_3 w_1 w_2 + w_4 w_1 (1 - w_2) + w_5 (1 - w_1) w_2 + w_6 (1 - w_1)(1 - w_2) \ .$$

Note that this calculation makes use of both the product and the addition laws of probability. It is the repeated application of these two laws that allows unconditional weights at higher nodes to be determined. The unconditional weights now determined for the quality of information will serve as weights on the rows of the matrix for the next higher level event, and the types of calculations just illustrated are repeated to obtain the unconditional probabilities for the target event.

Returning now to the ten-step procedure, step 5 requires that steps 3 and 4 be repeated for the rest of the middle- and bottom-level influences. Thus, weights of evidence would be assessed for the role of operations and for teams; then a matrix of conditional probabilities would be assessed for the organizational influence conditional on the lower-level influences. The same procedures would then be followed in making the necessary assessments for the personal factors.

Step 6 requires, for the first time, assessments of probabilities. However, these probabilities are for the target event conditional on the middle-level influences. In a sense, what is being assessed is conditional error rates; that is, assessors are giving their judgments about what the error rates would be under the assumption of particular patterns of influences. Since the quality of information can be either high or low, the organization can either be requisite or not, and personal factors can be favorable or unfavorable. There are eight possible combinations of these influences. A separate error rate associated with the target

event is assessed for each of those eight combinations. This is not a particularly easy job for assessors because they must keep in mind three different influences as well as their possible interaction. Favorable personal factors, for example, may well save the day even if the organization is not requisite, and may even compensate to some extent for low quality of information. Insofar as the middle-level influences interact, this stage in the assessment process is important, for it allows assessors to express the effect on error rates of these interactions.

Step 7 is best carried out by a computer which can apply the multiplication and addition laws of probability to determine the unconditional probability of the target event as well as the next-lower influences.

In step 8, the unconditional probabilities and weights of evidence for the middle-level influences are given to the group of assessors who then compare these results to their own holistic judgments. Descrepancies are usually discussed in the group and revisions made as necessary to any assessment.

Step 9 indicates that iteration through the first 8 steps may occur as individual assessors share their perceptions of the problem with each other, develop new intuitions about the problem, and revise their assessment. Eventually, when the sense of unease created by discrepancies between current model results and holistic judgments disappear, and when no new intuitions arise about the problem, model development is at an end, and the model can be considered requisite.

Since individual experts may still disagree about certain assessments, it is worthwhile in step 10 to do sensitivity analyses to determine the extent to which these disagreements influence the unconditional probability of the target event. An easy, but not entirely satisfactory, way to do this is first to put in all those assessments that would lead to the lowest probability for the target event and see what its unconditional value is and then to put in all assessments that would lead to the largest probability, thus determining a range of possible results. The difficulty with this is that no individual in the group is likely to believe all of the most pessimistic or all of the most optimistic assessments, so the range established by this approach to sensitivity analysis is unduly large. It should not be too difficult, however, to develop easy and effective procedures for establishing realistic ranges for the probability of the target event, ranges that accommodate the actual variation of opinion in the group.

This has been only a very brief description of the stages that appear to be necessary for applying the influence diagram technology. As experience is gained in the STAHR approach, these steps no doubt will be modified and elaborated. The steps are certainly not intended as a rigid procedure to be followed without deviation. Instead, they should be thought of as an agenda that will guide the work of the group.

C.5. Group Processes

So far, little has been said about the group processes that form the "socio" component of the STAHR approach. A key assumption here is that many heads are better than one for probability assessments. Particularly for human reliability assessment in complex systems,

there is unlikely to be any single individual with an unbiased perspective on the problem. Although each individual may be biased in his view, the other side of the coin is that each person has something worthwhile to contribute to the overall assessment. It is within the context of the group that different perspectives of the problem can most effectively be revealed and shared with others, so that the group's main function is the generation of assessments that take into account these different perspectives.

To ensure that all perspectives on the problem are fairly represented, it is important that a group climate be established within which information is seen as a neutral commodity to be shared by all regardless of an individual's status or investment in the problem. The role of group consultant can be established to help create this climate. This individual needs to be conversant with the technical aspect of influence diagrams and with probability assessment and to have a working knowledge of group processes. The group consultant should be seen by the group as an impartial facilitator of the work of the group, as someone who is providing structure to help the group think about the problem but is not providing any specific content. Although the group consultant needs some minimal acquaintance with the principles of nuclear power generation and with the key components in the plant itself, it is probably desirable that he not be a specialist in nuclear power; otherwise he might find it more difficult to maintain a neutral, task-oriented climate in the group. Thus, a major role for the group consultant is not to tell people what to think about the problem but how to think about it.

The other major role for the group consultant is to attend to the group processes and intervene to help the group maintain its task orientation. The group can easily become distracted from its main task because viewpoints in the group will often be divergent. The cognitive maps that a design engineer and a reactor operator have of the same system may be quite different, yet each will at times insist on the validity of his particular viewpoint. The group consultant must help the group to legitimize each of these viewpoints and to explore them in generating useful assessments.

To a certain extent, adversarial processes may even operate in these groups. Operators will openly criticize certain aspects of design, and design engineers may well be contemptuous of procedures that they deem to be unnecessary if only people would operate the system properly. Trainers may be somewhat sceptical of the optimistic "can-do" attitude of the operators, while operators may feel that anyone who has not had "hands-on" experience in the real control room rather than just simulator experience is out-of-date at best and simply out of touch at worst. Unless the group consultant manages the group processes effectively, minor squabbles can easily turn into major confrontations that seriously divert the group from its effective work.

This discussion is not meant to imply that the group should be composed so as to reduce adversarial processes. On the contrary, an underlying assumption of the STAHR approach is that diversity of viewpoint is needed if good assessments are to be generated. Differences are to be confronted openly in the group and to be taken seriously regardless of the status of the holder of the viewpoint. Thus, diversity of viewpoint is a key criterion in composing the groups. As yet, we are not certain about the roles that should be represented in the groups but it would appear that at least the following are necessary: group consultant, technical moderator to help direct the discussion on technical issues,

trainer of nuclear power station operators, reliability and systems analyst, thermal-hydraulics engineer, possibly one or two other engineers with specialized knowledge of the power station, and, of course, reactor operators. Further work is needed to establish exactly who the problem owners are for these human reliability assessments.

C.6. Summary Statement

This appendix has described the STAHR approach as it was originally conceived for application to the assessment of the reliability of operator actions at a nuclear power station during potential PTS events. As will be apparent from Appendix D, the first field test of the methodology resulted in some modifications of the detailed definitions of the bottom-level influences, and further revisions are anticipated as the approach is more generally applied.

C.7. References

1. Howard and Matheson, 1980.
2. Miller *et al.*, 1976.
3. Selvidge, 1976.
4. Phillips, 1983.
5. Phillips, 1982.
6. A. D. Swain and H. E. Guttmann, *Handbook of Human Reliability Analysis with Emphasis on Nuclear Power Plant Applications*, NUREG/CR-1278 (October 1980).
7. L. D. Phillips and H. Otway, "Limitations to Human Judgements: Implications for System Modelers," *Energy Systems Analysis*, R. Kavanaun, Ed., 600-620, Dordrecht: Reidel (1981).
8. Fischhoff and MacGregor, 1982.
9. Staël Von Holstein and J. Mathemon, *A Manual for Encoding Probability Distributions*, SRI Project 702B, SRI International (August 1979).

Appendix D

QUANTIFICATION OF OPERATOR ACTIONS

D. L. Selby

Oak Ridge National Laboratory

L. D. Phillips

London School of Economics and Political Science

D. E. Embrey

Human Reliability Associates, Lancashire, England

APPENDIX D. QUANTIFICATION OF OPERATOR ACTIONS

D.1. Introduction

In order to complete the quantification of the event trees, it was necessary to identify success and failure frequencies associated with operator actions. The STAHR methodology described in Appendix C was the primary means by which frequencies of error were assigned to a predetermined set of operator actions associated with potential PTS events at H. B. Robinson Unit 2. A four-day meeting was held at a Carolina Power and Light Company (CP&L) training facility to implement this group evaluation process. Although the composition of the group attending the meeting varied somewhat over the four days, the following roles were represented: group consultant and facilitator, technical moderator, trainer of reactor operators, thermal-hydraulic engineer and procedures specialist, engineer familiar with pressurized thermal shock phenomena, probabilistic risk analyst, reliability and systems analyst, human reliability specialist, and reactor operator.*

At the first session of the meeting, a brief description of the role of human judgment in risk assessments was given, with particular emphasis on the view of probability as an expression of a degree of belief. The conditions under which good calibration of probability assessments could be expected were also described. The group was then charged with the responsibility of applying the STAHR methodology to the preselected target events (operator actions) during the remainder of the meeting. This appendix summarizes the deliberations of the group in sessions in which the STAHR methodology was applied to target events and describes how the results of these sessions were utilized in the quantification of the event trees.

D.2. Practice Session with STAHR Methodology

At the practice session, the group was presented with the list of target events to be considered (see Table D.1). It was recognized that in general all these target events involved determining whether or not an operator would successfully perform some mitigating action. After some discussion the group selected operator action 1b from the table as the target event for the practice session.

The group was then introduced to influence diagrams and their relationship to event trees. The influence diagram described in Appendix C was presented, together with definitions of the bottom-level influences. Considerable discussion of the influences followed, with the result that the definitions of the influences were slightly changed and extended. Table D.2 gives the final definitions as they were used throughout the remainder of the week.

*One of the authors (Phillips) served as the group consultant and another (Embry) served as the human reliability analyst. A member of the PTS study group (Selby of Oak Ridge National Laboratory) acted as the technical moderator.

Table D.1. List of operator actions to be quantified[a]

1. Operator isolates AFW flow to affected SG following:

   a. A large steam-line break from full power upstream of MSIVs.
   b. A large steam-line break from hot 0% power upstream of MSIVs.
   c. A small steam-line break from full power upstream of MSIVs.
   d. A small steam-line break from hot 0% power upstream of MSIVs.

2. Operator controls AFW to maintain SG level in unaffected SGs following:

   a. A large steam-line break from full power upstream of MSIVs.
   b. A large steam-line break from hot 0% power upstream of MSIVs.
   c. A small steam-line break from full power upstream of MSIVs.
   d. A small steam-line break from hot 0% power upstream of MSIVs.
   e. A small-break LOCA from full power.
   f. A small-break LOCA from hot 0% power.

3. Operator isolates PZR PORV that has failed to close owing to:

   a. PZR PORV failure being the initiating event.
   b. PZR PORV failure occurring during repressurization following a separate event.

4. Operator terminates SI within 10 min after subcooling is greater than 40°F, operable heat sink is available, and pressurizer level is greater than 6% following:

   a. A large steam-line break from full power upstream of MSIVs.
   b. A large steam-line break from hot 0% power upstream of MSIVs.
   c. A small steam-line break from full power upstream of MSIVs.
   d. A small steam-line break from hot 0% power upstream of MSIVs.

5. Operator closes the MSIVs following:

   a. The failure of a single SDV to close on demand.
   b. The failure of two SDVs to close on demand.
   c. The failure of more than two SDVs to close on demand.
   d. A small steam-line break downstream of the MSIVs.

6. Operator terminates SI within 25 min following:

   a. A single SG tube rupture occurring at full power.
   b. A single SG tube rupture occurring at hot 0% power.

[a]The acronyms used in this table (in order of their appearance) are: AFW = auxiliary feedwater, SG = steam generator, MSIV = main steam isolation valve, PZR PORV = pressurizer power-operated relief valve, SI = safety injection, and SDV = steam dump valve.

Table D.2. Definitions of lowest-level influences in influence diagram (revision on December 1983)

	Good	Poor
1. Control Room Design		
a. Displays		
	Easy to read and understand and accessible.	Hard to read, difficult to interpret, inaccessible.
	Make sense, directly related to controls.	Confusing, not directly related to controls.
	Alarms discriminable, relevant, coded.	Alarms confusing, irrelevant, not coded.
	Mimic display employed.	Non-representational display.
	Displays regarding event are present, clear, unambiguous.	Displays regarding event are not present, are unclear or ambiguous.
b. Operator involvement		
	Operators have say in design modifications.	Operators have little or no say in design modifications.
	Operator receives prompt confirmation of action.	No confirming information.
c. Automation of routine functions		
	Highly automated.	Low level of automation.
	Operators act as systems managers.	Operators perform many routine functions.
2. Operating Procedures		
	Meaningful	**Not meaningful**
a. Realism		
	Realistic; the way things are done.	Unrealistic; not the way things are done.
b. Location aids		
	Location aids provided.	Few or no location aids provided.
c. Scrutability		
	Procedures keep operators in touch with plant.	Procedures do not keep operators in touch with plant.

Table D.2. (Continued)

2. Operating Procedures (Contd.)	
Meaningful	**Not meaningful**
d. Operator involvement	
Operators involved in developing procedures.	Operators not involved in developing procedures.
e. Diagnostics	
Allow unambiguous determination of event in progress.	Allow inappropriate diagnosis.
f. Format	
Procedures clear, consistent, and in easily read format.	Procedures confusing, difficult to read.
3. Function of Operations Department	
Primary	**Not primary**
a. Accountability	
All other functions report to operations supervisor.	Other functions are ends in themselves.
b. Relationship to maintenance and other functions	
Good relations.	Antagonistic relations.
c. Paperwork	
About right.	Excessive.
d. Operator involvement	
Operators have a say in how the place is run.	Operators have no say in how place is run.
4. Teamwork in Control Room	
Present	**Absent**
a. Shifts	
Allow teams to stay together.	Prohibit team formation.
b. Roles	
Well-defined accountabilities, but with scope for exercising discretion.	Poorly defined accountabilities or rigid job descriptions that leave little scope for exercise of discretion.
c. Training	
Team members train together.	Team members do not train together.

Table D.2. (Continued)

5. Level of Operator Stress	
Level Helpful	**Level Not helpful**
a. Shifts	
No jet lag.	Permanent jet lag.
b. Time available	
Adequate time.	Too little time.
c. Operating objectives	
No conflict.	Conflict.
d. Transient-related stress	
Appropriate.	Understressed or overstressed.
6. Level of Operator Morale/Motivation	
Good	**Poor**
a. Status of operators	
Treated as professionals.	Treated as laborers.
b. Career structure	
Operators can find best level in organization.	Peter Principle operates.
c. Physical/mental well being	
Operators physically and mentally capable of performing job.	Job performance adversely affected by physical and/or mental impairment.
7. Competence of Operators	
High	**Low**
a. Training	
Operators generally well trained in emergency procedures.	Operators poorly trained in emergency procedures.
b. Certification	
Peer review is used.	No peer review is used.
c. Performance feedback	
Operators given periodic feedback on performance.	Operators given no feedback on performance.
d. Experience	
Operators experienced in dealing with target event.	Operators not experienced in dealing with target event.

At this point David Embrey gave a review of the cognitive processes that the group might wish to consider when thinking about possible reasons for the failure of an operator to perform a target event successfully. Next, the operators within the group described the display configurations in the plant with particular emphasis on those displays that would be relevant to the target event. Considerable discussion followed while the group attempted to develop a common understanding of the control room, procedures and the nature of the event being evaluated. The process of eliciting assessments then began with the facilitator giving the group the responsibility of telling the secretary when a point of consensus had been reached. Thus, the group had to make a judgement about when sufficient agreement about technical matters had been reached so that the secretary could be instructed to record the reasons for the assessments given.

The evaluation began with a review of the H. B. Robinson Unit 2 display system with respect to the target event. The initial discussion centered around the miniature control room concept with its relatively small annunciators. The general feeling was that although they could not be read from a distance, one could be right in front of any annunciator by simply taking a few steps. The conclusion was that there are better designs but H. B. Robinson is certainly adequate for dealing with this event. A relative value of 70 was assigned as a weighting factor for display associated with the target event.

Evaluations were performed for the remaining performance shaping factors in a similar manner. The resulting failure probability for failure to isolate AFW within 10 min was determined to be 0.0023/demand. The relatively low failure rate was mostly attributed to the impact of the new symptom-based procedures which were felt to lead to early directions to isolate due to its flow chart structure.

D.3. Application of STAHR and Other Methodologies to Target Events of Table D.1

D.3.1. Isolation of AFW to Affected SG Following a Steam-line Break Event

The first step was to review the results of the practice session and to examine the failure probability with respect to perturbations in the initiating event (operator actions 1a, 1c and 1d). It was determined that the weights used were reasonable and thus it was felt that there was no need to redo the event evaluated as part of the practice session. It was also determined that there would be no difference in probabilities as a result of power level; i.e., operator action 1a should be treated the same as operator action 1b. The operator would go through almost the same sequence of actions regardless of power level. However, it was felt that there might be a difference between a small break and large break owing to the timing of the event; i.e., operator actions 1c and 1d could be different from operator actions 1a and 1b, respectively. The timing could be different since the drop in SG level would be much slower in the case of the small break. It was felt that the best way to quantify operator actions 1c and 1d would be to evaluate them at 20 min rather than at 10 min. Thus the evaluation was repeated for the small break at 20 min. This led to a value of 0.0017/demand for the failure probability. As before, the power level was not considered to have an impact on the potential for failure and thus the same failure value was used for both operator actions (1c and 1d).

D.3.2. Control of AFW to Maintain SG Level Following Steam-line Break or Small-Break LOCA

A STAHR analysis was not performed for any of the operator action perturbations identified under this category. At the time, it was felt that this operator action would have little if any effect on the consequences of the event and that time available for STAHR analysis would be better spent dealing with what were considered to be more important events. For analysis purposes, the quantification was performed using the time reliability curve displayed as Figure D.1 (from Ref. 1). This resulted in a recommended failure probability of 0.01 for this event. With one exception, this was the failure value used in the analysis. The exception was that when there was a failure to isolate AFW to the affected SG following a steam-line break, the failure to control AFW was considered to be a complete dependence; i.e., the failure probability was assumed to be 1.0 given failure to isolate AFW. The values defined by these assumptions were used consistently for all six cases (operator actions 2a-2f). It should be noted that the thermal-hydraulic analysis confirmed that failure to control AFW to maintain level had very little effect on the downcomer temperature. Thus variances in the failure probability would have no effect on the final outcome of the analysis.

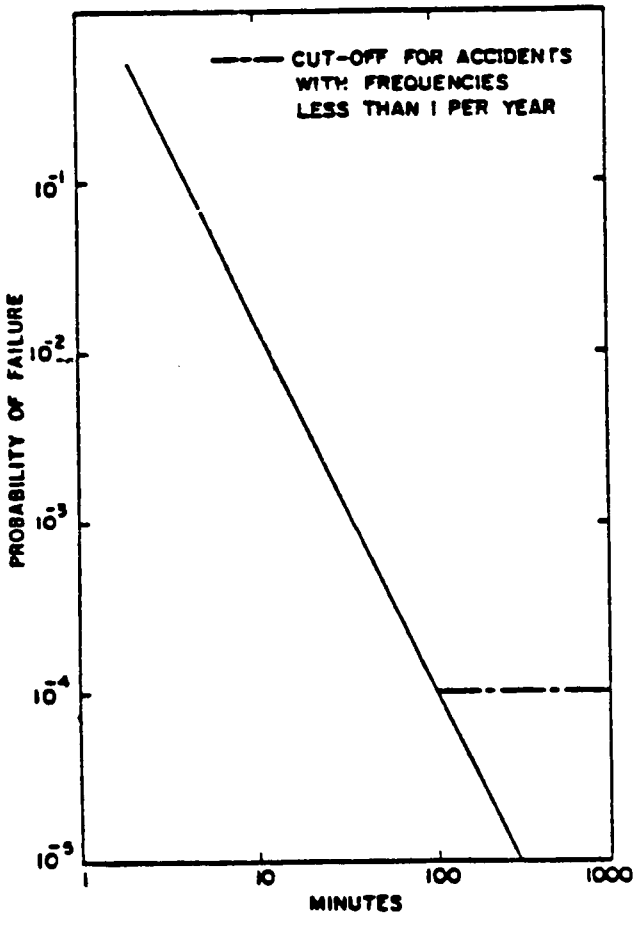

Figure D.1. Failure probability vs. time for operators, original model.

D.3.3. Isolation of a PZR PORV That Has Failed to Close

A general review of this operator action was made in the hope that a consensus could be reached on a final value without a rigorous analysis. The general feeling was that given 10 min the probability of a failure to isolate would be very small and on the order of 0.001. This was the value agreed to by the group at the time of the human factors evaluation sessions. However, after further review by ORNL it was the opinion of the ORNL analysts that this value was probably too low for two reasons. First, one of the principal reasons for the low failure probability was the relative importance assigned to a PZR PORV failure as a result of the accident at Three Mile Island Unit 2. However, since this analysis is required to cover a 30-yr life, it was felt that the relative importance of this event might be reduced. Second, successful isolation of the PZR PORV requires that the PZR PORV block valve close as required. Although as a single failure condition the failure probability assigned to a block valve closing would also be on the order of 0.001/demand, it was perceived that there could be some coupling between a PZR PORV failure and a PZR PORV block valve failure. After consideration of the above information, the ORNL analysts chose to use a value of 0.01/demand for the failure to isolate the PZR PORV following a failure to close. It should be noted that this was the only value coming out of the human factors sessions which was subsequently changed by the ORNL analysts.

The next step was to examine a PZR PORV failure which occurred not as an initiating event but as part of the repressurization process following a separate event. In the analysis for Calvert Cliffs Unit 1 (Ref. 2), the failure probability was higher under these conditions since a separate operator action failure (failure to control repressurization) was necessary to achieve the initial PZR PORV opening. However, in the case of H. B. Robinson Unit 2, the charging system automatically throttles to control level in the pressurizer and thus avoids a PZR PORV lift. As a result, for this plant there would be no couple between the failure and the recovery and it was determined that the same failure value of 0.01/demand would be used under these circumstances.

D.3.4. Termination of SI Within 10 min After Specified Conditions for Termination Are Met Following a Steam-line Break

This operator action was addressed since it was perceived that in the case of a steam-line break the operator might terminate SI early and thus reduce the cooldown. After some discussion, it was determined that the operator would probably terminate SI within 10 min after the following conditions were achieved: (1) subcooling is greater than 40°F, (2) operable heat sink is available, and (3) pressurizer level is greater than 6%. From the thermal-hydraulic information available, it was determined that these criteria would be met between 10 to 15 min into the transient for most steam-line breaks. Thus the operator action of interest would occur at 20 to 25 min into the transient. In the evaluation of the performance shaping factors, some of the discussion centered around the new symptom-based procedures. It was identified that there was a point in the flow chart procedure that would call for the termination of SI. However, it was not clear whether or not the operator would reach this point in the procedures within the allotted 20 to 25 min. After a walk-through of the procedures, it was decided that the operator would more than likely

reach this point in the procedures within the time frame of interest. In fact, it was the opinion of the operators that the entire procedure usually could be completed within 20 min. This was one of the principal factors which led to a low failure rate of 0.0073/demand.

As with previous operator actions, the effects of power level and break size were examined. It was determined that for the 20- to 25-min time frame, neither the power level nor the break size would have much impact on the failure value. Thus, the 0.0073/demand value was used in all instances. It is interesting to note that this value agrees very well with the value which would have been chosen if the time-line reliability curve shown in Figure D.1 had been used.

In the final analysis, this operator action was not included. Subsequent analysis of the steam-line break thermal-hydraulic calculations revealed that the dead-head of the HPI system was reached at about the 20-min time frame for the steam-line breaks examined. Thus there would be no need for the operator to terminate SI.

D.3.5. Closure of the MSIVs Following Failure of SDV(s) or Steam-line Break

For small steam-line break events, the closure of the MSIVs is a very important operator action and unfortunately was not considered as part of the human factors analysis sessions. At the time, it was not anticipated that the MSIVs would not automatically close in the event of a small steam-line break. The operator was perceived as a backup to the automatic system and thus was not considered. However, the thermal-hydraulic calculations revealed that the condition of high steam flow required for automatic closure of the MSIVs would not be reached for the small steam-line break.

An examination of the potential events in which the closure of the MSIVs would be left to the operator revealed four major events as listed in Table D.1. The first event involves the failure of a single SDV. This event leads to a small steam-line break downsteam of the MSIVs. Conversations were held with personnel with operational experience at H. B. Robinson and with CP&L staff. It was concluded that for a single SDV failure there would be reluctance on the part of the operator to isolate the system by closing the MSIVs. It was perceived that the operator would most likely monitor the system and observe the cooldown rate but the need for closure of the MSIVs is not expected to be identified. Thus for analysis purposes, no credit was taken for the closure of the MSIVs in the case of a single SDV failure.

The second event for which MSIV closure by the operator might be required involves the failure of two SDVs to close. This event leads to a somewhat larger break and a slightly different situation. Again, it was felt that there might be some reluctance to close the MSIVs and thus isolate the system, but it was also felt that after some monitoring of the system the operator would eventually close the MSIVs. After careful consideration the ORNL analysts chose a failure value of 0.01/demand for this event.

The third event in question is actually a class of events and involves the failure of three or more SDVs to close. This type of event leads to a relatively rapid blowdown of the secondary system but will not result in the automatic closure of the MSIVs. The first step

taken to understand the operators' response to this event was to examine the timing of the event. A review of the thermal-hydraulics and fracture-mechanics calculations revealed that if the MSIVs were closed within the first 30 min of the event, the consequences would be limited; i.e., the event would not appear as a dominant PTS risk sequence. Thus, the potential for failure was evaluated with respect to the 30-min time frame. The next step was to examine the operator actions which were evaluated during the human factors sessions to determine whether any similar situations existed. It was found that operator action 1c discussed in Section D.3.1 would be a very similar situation; i.e., a reasonably long period of time is available to perform the action and it is the type of action that one would expect to see performed following a diagnosis of a steam-line break. In addition, the time-line reliability curve predicts a similar failure value for the 30-min time frame as that determined for sequence 1c. Thus, for analysis purposes, a failure value of 0.002/demand was used under the above circumstances. In addition, it was felt that there was a heavy dependence between a failure to close the MSIVs and a failure to throttle AFW. Based on the dependency equations developed elsewhere,[1] a coupling factor of 0.5 was assumed when appropriate.

Finally, the closure of the MSIVs by the operator was examined for the case of a small steam-line pipe break. A small steam-line pipe break was considered both upstream and downstream of the MSIVs. In the case of an up-stream break, the closure of the MSIVs has no impact on the event since the steam-line check valve prevents the blowdown of the other two SGs and the closure of the MSIVs will not prevent the blowdown of the affected SG. Thus, for the upstream break, closure of the MSIVs was not considered in the analysis. Since the downstream break was represented by the failure of a single SDV, the argument presented above for the single SDV would also apply to the small steam-line break downstream of the MSIVs. Therefore, closure of the MSIVs by the operator within the 2-hr time frame was also not considered for the small steam-line break downsteam of the MSIVs.

D.3.6. Termination of SI Within 25 min Following SG Tube Rupture

The response to a SG tube rupture involves several operator actions, but the termination of SI was singled out as the action which should be examined during the human factors sessions. Two tube rupture events were considered: (1) a single tube rupture occurring from a full-power condition and (2) a single tube rupture occurring from a low decay heat hot 0% power condition. The decision of the group was to analyze the hot 0% power event (considered by most of the group to be the worst case condition) and to use the results for both cases. Based on thermal-hydraulic data, it appeared that conditions would exist for performing this operator action at approximately 20 min into the transient. Therefore, the action was evaluated for occurrence within 25 min into the transient. The discussion of the effects of the display system on this event centered around the discussion of the radiation-monitoring system. It was determined that better radiation-monitoring systems and displays are available for the diagnosis of a tube rupture and that some improvements could be made in the H. B. Robinson system. However, since the time frame of interest was 25 min into the transient, the present system was considered to be at least adequate with respect to its effect on the target operator action. The new procedures were again identified as an important factor. The old procedures were felt to have enough ambiguity to cause hesitation, which could have allowed complete filling of the SG before SI was terminated.

The final evaluation produced a failure probability of 0.0039/demand for this event. In the actual analysis, however, this value was not used. It was not clear that the conditions examined during the human factors sessions represented the tube rupture conditions covered by the actual analysis. The ORNL analysts chose to use a value of 0.1/demand as a screening value for this operator action failure. As stated in Chapter 3, this is probably an over-estimation of the failure probability, but an early review of the thermal hydraulics of the tube rupture event revealed that a conservative frequency estimation for this sequence would not impact the overall frequency for a through-the-wall crack and the high failure rate would cover all circumstances.

D.4. Summary

This appendix has described how the operator action success and failure probabilities used in the analysis were developed. A summary of the success and failure probabilities developed are presented in Table D.3. It should be noted that it was the consensus of the human factors group that the failure probabilities obtained during the human factors sessions were reasonable and compatible with values which could be obtained using other methodologies.

Table D.3. Summary of operator action success and failure probabilities[a]

Operator Action	Conditions	Probability/Demand For Success	Probability/Demand For Failure
(1) Isolation of AFW to affected SG following:			
a. A large steam-line break from full power or hot 0% power.	Within 10 min.	0.9977	0.0023
b. A small steam-line break from full power or hot 0% power.	Within 20 min.	0.9983	0.0017
(2) Control of AFW to maintain SG level following a steam-line break or small-break LOCA from full power or hot 0% power.	Base case.	0.99	0.01
	Following a failure to isolate AFW to an affected SG.	0.0	1.0
	Following a failure to close the MSIVs.	0.5	0.5
(3) Isolation of a PZR PORV that has failed to close.	Within 10 min.	0.99	0.01
(4) Termination of SI following:			
a. A steam-line break.	Within 25 min.	0.9927	0.0073
b. A SG tube rupture.	Within 25 min.	0.90	0.10
(5) Closure of MSIVs following:			
a. Failure of a single SDV to close or a small steam-line pipe break.	Base case.	0.0	1.0
b. Failure of two SDVs to close.	Within 30 min.	0.99	0.01
c. Failure of three or more SDVs to close.	Within 30 min.	0.998	0.002

[a]The acronyms used in this table (in order of their appearance) are: AFW = auxiliary feedwater, SG = steam generator, MSIV = main steam isolation valve, PZR PORV = pressurizer power-operated relief valve, SI = safety injection, and SDV = steam dump valve.

Appendix E

BUOYANCY EFFECTS IN OVERCOOLING TRANSIENTS CALCULATED FOR H. B. ROBINSON UNIT 2

T. G. Theofanous, K. Iyer,
H. P. Nourbakhsh, and P. Gherson

Purdue University

APPENDIX E. BUOYANCY EFFECTS IN OVERCOOLING TRANSIENTS CALCULATED FOR H. B. ROBINSON UNIT 2

E.1. Introduction

Chapter 4 of this report presents the results of a thermal-hydraulic analysis of potential overcooling transients for H. B. Robinson Unit 2. It was pointed out, however, that the temperatures produced by Idaho National Engineering Laboratory (INEL) for the PTS analysis (Ref. 1) were bulk coolant temperatures that did not account for thermal stratification phenomena that could result from low flow through one or more cold legs. Since these phenomena could cause temperature variations in some regions of the coolant, it was important that their impact on the vessel wall temperatures, particularly in the downcomer region, be determined in separate analyses.

This appendix describes a joint experimental and calculational study performed to investigate the extent of mixing of the coolant during certain postulated transients. The study, performed at Purdue University, utilized a 1/2-scale PTS experimental facility and a Regional Mixing Model (RMM)[2] with its associated computer code REMIX.[3] This appendix documents the experimental and analytical bases and procedures employed in the derivation of the results. The results of this study, discussed in Chapter 4, are presented in Reference 2.

E.2. Buoyancy Forces Under Low Flow Conditions

From a fracture mechanics standpoint, one is interested in the RPV wall cooling that can potentially develop during postulated overcooling transients. Since certain locations are potentially more important than others due to their chemical composition (e.g., pressure vessel welds), this cooling must be estimated as a function of space as well as time. That is, estimates of both fluid temperatures and heat transfer coefficients are needed, on a local basis, over the whole downcomer region and for the duration of the postulated transient.

As long as the flow velocities are high enough, spatial gradients in the downcomer fluid temperature are negligible, forced convection dominates heat transfer from the wall, and the RELAP5 calculation results are directly applicable. At lower velocities, however, thermal stratification and free convection effects become increasingly important.

Thermal stratification arises due to incomplete mixing of the high pressure injection (HPI) fluid with the primary coolant in the cold leg and in the downcomer region. It is a characteristic of this condition that due to the development of buoyancy forces, the velocity and temperature fields become spatially nonuniform and strongly coupled, yielding significant deviations of the thermal-hydraulic response from that expected in a well-mixed system.

In addition to these bulk buoyancy effects, low convective velocities allow the development of buoyancy forces within a very thin fluid layer in immediate contact with the RPV wall. The effect of these forces is to destabilize this boundary layer and thus augment the rate

of heat transfer from the wall. The term "free convection effects" will be used in this report to describe this condition. The resulting combination of free and forced heat transfer is known as the "mixed convection regime" and may be important even in the absence of thermal stratification.

The approach for performing the analysis discussed in this report is based on the assumption that the buoyancy forces in the layer next to the wall are not strongly coupled to the bulk buoyancy processes. That is, thermal stratification is evaluated first and the resulting velocities and temperature at the wall surface are utilized in the prediction of the heat transfer rates. This assumption is consistent with the physical behavior trends delineated in this study.

E.3. The Regional Mixing Model (RMM) and the REMIX Code

It has already been established[2] that even at natural circulation levels (loop flow) the fluid velocities are high enough to ensure good mixing of the coolant. Therefore, stratification effects are relevant to PTS studies only for transients that yield loop stagnation (i.e., interruption of the natural circulation path).

Loop stagnation is the physical situation addressed by the Regional Mixing Model (RMM)[2] and the computer code REMIX.[3] RMM is a model that is based on fundamental thermal hydraulic principles and integrates local plume mixing behavior into an overall system response. Initial testing[4,5] of RMM indicated good agreement with applicable simple plume tests, as well as with tests on the CREARE 1/5-scale system,[6] and more recently with the Configuration-0* experiments[2] at the Purdue 1/2-scale PTS facility (see Section E.4 below). This is convenient for testing the consistency between flow and dilution instrumentation and also for establishing that the response of the distorted lower downcomer/plenum model is appropriate (see Section E.4 and reference 2).

Only a brief description of the RMM conceptual development is included in this appendix, a more detailed discussion of the evolution of RMM being found in references 2-5 and 7. A model of the flow patterns as originally postulated in reference 4 is shown in Figure E.1. A cold stream originates with the HPI plume at the point of injection, continuing towards both ends of the cold leg and decaying away as the resulting plumes fall into the downcomer and pump/loop seal regions. A hot stream flows counter to the cold stream, supplying the flow necessary for mixing (entrainment) at each location. This mixing is most intense in certain mixing regions (MRs). MR1 is the region in which the injected, falling, and highly buoyant axisymmetric plume is mixed. MR3 and MR5 are regions in which mixing occurs due to the transition (jump) from a horizontal layer into a falling plume, and MR4 is the region of final decay of the downcomer (planar) plume.

The cold streams have special significance since they induce a global recirculating flow pattern with flow rates significantly higher (several times) than the net flow throughput (Q_{HPI}). This keeps a major portion of the system volume in a well-mixed condition such that the whole process may be viewed as the quasi-static decay of the cold stream with a slowly varying ambient temperature (indicated as T_M in Figure E.1).

*Configuration-0 represented a truncated cold leg geometry (pump and loop seal absent) to ensure that all HPI flow would be in the direction of the downcomer.

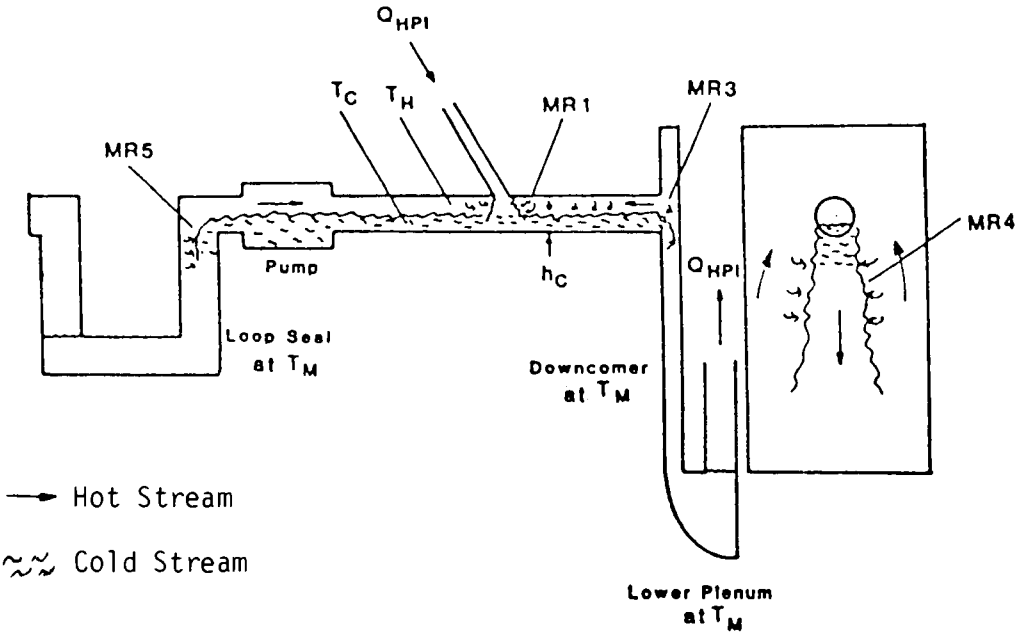

Figure E.1. Conceptual definition of the regional mixing model. (MRi indicates mixing in region i.)

For each time step considered, the calculations are performed as follows:

(a) The whole system is assumed to be well mixed and the ambient temperature is calculated in terms of the cold water injected and the heat released from the walls.

(b) For the portion of the system that is considered to be stratified, the energy associated with the ambient temperature is partitioned into a cold stream [a cold leg layer of height h_c (see Figure E.1)] and a hot stream (the remaining cold leg volume, 25% of the pump volume, plus a horizontal downcomer slice 2.5 cold leg diameters in height).

(c) This partition (energy conservation) is made iteratively such that it is also consistent with mixing rates predicted for MR1 and counter-current flow limitations at the cold leg/downcomer junction.

The mixing in MR1 depends on the injection Froude number (Fr) and the length of the plume that is immersed in the hot stream.[2] In the original formulation[4] we predicted that for Fr << 1 the counter-current flow would extend well into the injection line but there was no basis on which to quantify the resulting additional mixing. From our Configuration-0 experiments[2] we confirmed this expectation and showed that it can be incorporated into the RMM by considering an effective origin for the MR1 plume within the injection line (i.e., more plume travel distance available for mixing). The extra length that was consistent with the observed entrainment rates turned out to be equal to 1/2 of the observed counter-current flow penetration into the injection line. The resulting correlation as shown in Figure E.2 is presently used in REMIX.

The mixing in MR3, also quantified by the Configuration-0 experiments, can be simply expressed by an entrainment rate nearly equal to the cold stream flow rate. Finally, the resulting planar plume (MR4) decays as it falls in the downcomer, and this decay is quantified in terms of its Froude number and the distance traveled.[2,3]

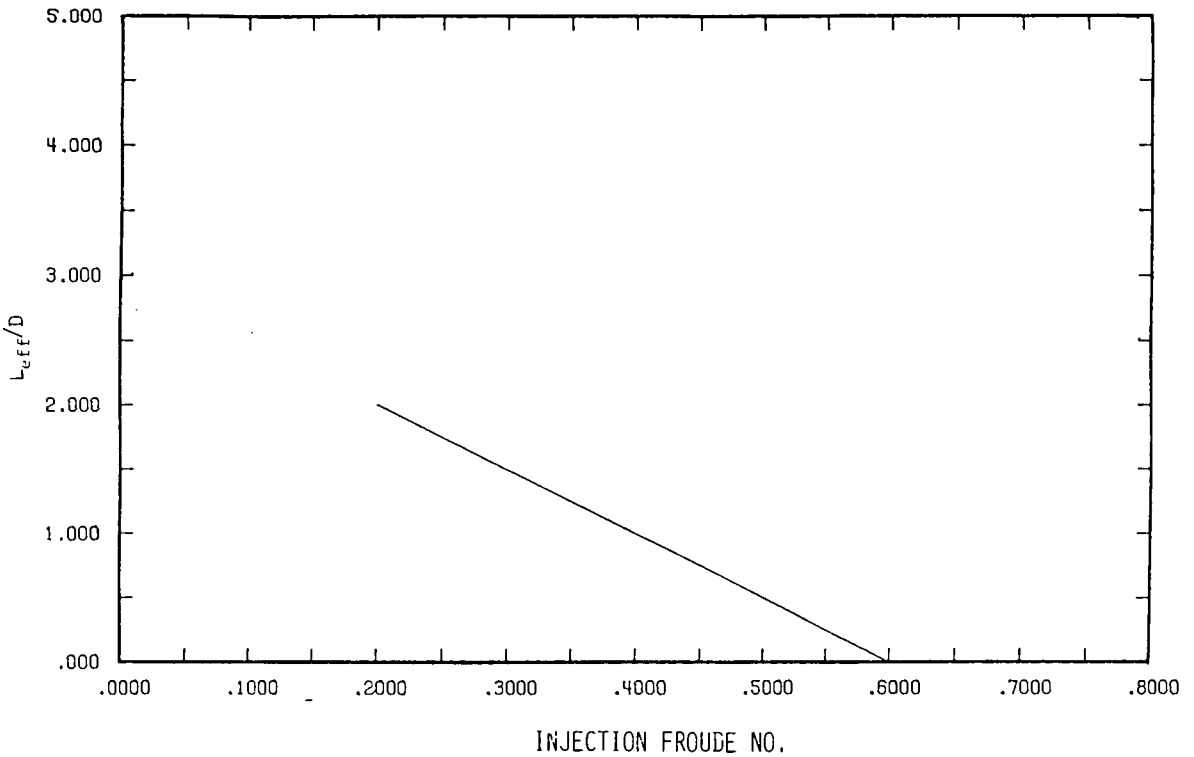

Figure E.2. Correlation of effective plume length (L_{eff}) and injection Froude number. (D = diameter of injection line.)

E.4. Experimental Simulation at 1/2-Scale: Comparison of REMIX Predictions with Measured Results

As indicated above, a 1/2-scale PTS facility is used at Purdue University for testing various cold leg/downcomer configurations. The basic experimental facility (Configuration 0) consists of a transparent (acrylic) 1/2-scale model of a typical PWR cold leg with attached downcomer and lower plenum regions as illustrated in Figure E.3. The lower portion of the downcomer and the lower plenum (corresponding to one of the cold legs) are geometrically distorted to keep the overall height of the facility manageable. Based on this reference configuration, the essential features of any reactor geometry of interest can be assembled by making appropriate attachments to the cold leg.

The 1/2-scale facility was used with the injector attachment (Configuration-W) shown in Figure E.4 to test the configuration for H. B. Robinson Unit 2. The essential features of the experimental geometry are a large diameter HPI line and the availability of fluid volume which is open to gravity flow on either side of the injection point. This causes a gravity-driven (buoyant) plume with the HPI flow mixed in a nearly symmetrical fashion with the fluid on both sides of the injection point. The aim of the Configuration-W experiment was to quantify the rate of global cooldown and the degree of stratification within the cold leg, as well as in the upper portion of the downcomer (the lower portion follows the global cooldown).

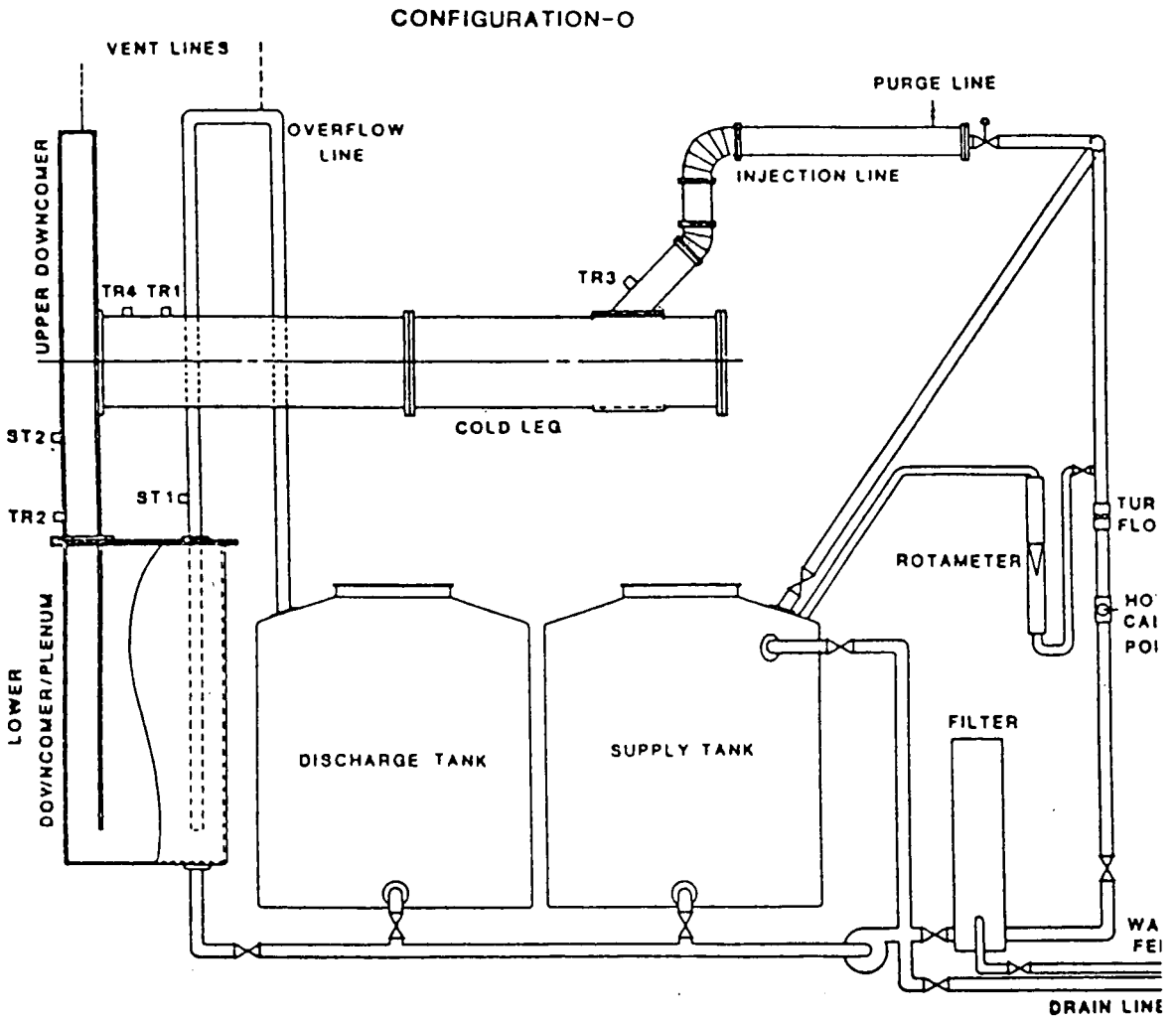

Figure E.3. Schematic of Purdue University's 1/2-scale PTS facility (Configuration 0). Dimensions are given as diameter (D), length (l), width (w), gap (L), and volume (V). For cold leg, D = 0.343 m, $l_{\text{HPI to DC}}$ = 2.11 m, and $l_{\text{HPI to blind flange}}$ = 0.76 m. For injection line, D = 0.108 m, $l_{45°}$ = 0.39 m, l_{vert} = 0.37 m, and l_{horiz} = 1.07 m. For upper downcomer, l = 2.72 m, w = 1.18 m, L = 0.127 m. For lower downcomer/plenum, V = 0.912 m^3. For supply tank, V = 1.05 m^3. For discharge tank, V = 1.05 m^3. For overflow line, D = 0.051 m. Probe locations: TR1, $l_{\text{to DC}}$ = 0.257 m; TR3, $l_{\text{to CL}}$ = 0.127 m; ST2, $l_{\text{to CL lip}}$ = 0.463 m.

The 1/2 scale experiments begin with the model filled with fresh water. The buoyancy effect is then observed by injecting salt solutions (brine) in the model and measuring salt concentrations in the system. In this procedure it is assumed that the heat and mass transport processes are similar, which is well justified for turbulence-controlled processes; that is, concentration changes during the experiment directly reflect the temperature changes that would be expected in a thermal simulation. The advantage of this approach is that

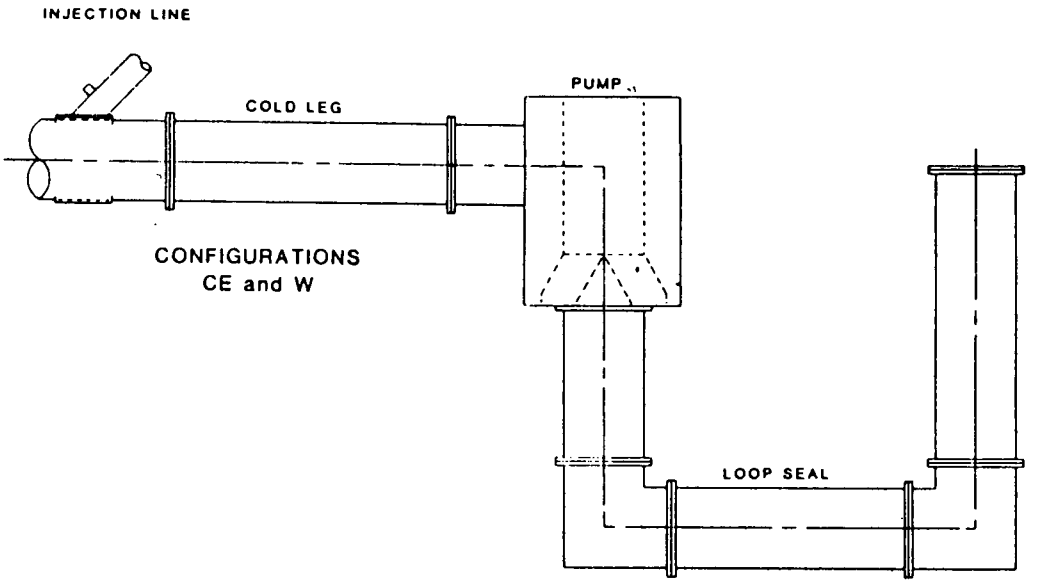

Figure E.4. H. B. Robinson pump and loop seal assembly used in 1/2-scale PTS facility (Configuration W). Dimensions are given as diameter (D), length (l), volume (V). For cold leg, D = 0.343 m. For pump, V = 0.28 m^3. For loop seal, D = 0.343 m, l_{vert} (pump side), = 0.98 m, l_{horiz} = 1.65 m, l_{vert} = 1.59 m.

the phenomena may be studied under near-prototypic density gradients ($\Delta\rho/\rho \sim 18\%$) while avoiding the high pressure associated with the thermal simulations and thus allowing direct visualization.

The significance of achieving near-prototypic density gradients in a selected near-prototypic geometric scale may be appreciated through dynamic similarity considerations as follows. Both the plume (jet) mixing phenomenon and the stratification behavior in the cold leg are governed by the Froude number

$$\mathrm{Fr} = U\left[gD\,\frac{\Delta\rho}{\rho}\right]^{-1/2}, \tag{E.1}$$

where

U = velocity,

g = acceleration of gravity,

D = diameter,

$\Delta\rho/\rho$ = density difference.

This number, therefore, must be preserved between the experimental model and the prototype. That is, for any particular choice of salt concentration, the appropriate value of the Froude number may be obtained by selecting the injection flow rate. With the help of

Equation E.1, the resulting Reynolds number ratio (the prototype Re divided by experimental Re) may be expressed as

$$\mathrm{Re}_R = \frac{\mathrm{Re}_P}{\mathrm{Re}_E} = D_R^{3/2} \nu_R^{-1} \left[\frac{\Delta\rho}{\rho} \right]_R^{1/2} , \tag{E.2}$$

where D_R, ν_R, and $(\Delta\rho/\rho)_R$ are the ratios of the diameters, the kinematic viscosities and the density differences, respectively, of the prototype and the experiment.

At the high prototype temperatures, the kinematic viscosity is low; that is, $\nu_R << 1$. The combination of this low kinematic viscosity with a geometric scale that is too low and/or a density difference that is too low could produce a laminar flow condition (low Re_E), whereas a highly turbulent flow would be expected in the prototype. For our experiments, $D_R = 2$, $\nu_R = 0.13$, and $1 < \Delta\rho/\rho < 2$, yielding $\mathrm{Re}_R \sim 20$ to 30. Typically, the Re_P values in the injector and the cold leg are ~80,000 and ~300,000, respectively, and application of the above ratios indicates an experiment which is well within the turbulent regime. Similar considerations apply to momentum flux effects, which may become important in the plume (jet) impact regions with opposite walls.

During an experimental run the salt solution is filtered, metered and pumped from the supply tank, through the injection line, and into the facility (see Figure E.3). The displaced fluid volume exits through the overflow line and into the discharge tank. With a tank capacity of 1.05 cubic meters (275 gallons), a typical run lasts 10 to 20 min. Salt concentrations are measured by means of probe traverses at positions TR1 and TR2 in Figure E.3. Spatial profiles and temporal variations in concentration are then constructed from these data. The concentration of the exiting stream (called herein the "ambient" region) is also measured continuously. The details of instrumentation and data reduction techniques are documented in a separate report.[2]

The experiment for H. B. Robinson (Configuration-W) was performed using a representative Froude number value of 0.459 and a $\Delta\rho/\rho$ of ~10%. The component volumes of the experiment are compared with those of the actual plant in Table E.1, and the experimental conditions are given in Table E.2. The measured salt concentrations of the ambient region, the cold stream, the hot stream, and the downcomer fluid throughout the run are compared to the RMM-REMIX predictions in Figures E.5, E.6, and E.7. A satisfactory overall performance of the RMM was indicated with slightly conservative predictions for the downcomer region. Thus, the RMM model is adequate for simulating mixing conditions for H. B. Robinson Unit 2.

E.5. Generic Trends of RMM-REMIX Calculations for PWR Systems

Complete system calculations for PWRs revealed that cold leg stratification (stagnation) may occur in two significantly different circumstances. One involves stagnation of all loops and zero net flow through the downcomer, which leads to a transient cooldown along the lines discussed in the previous two sections. The other is characterized by a net flow condition through the downcomer that is due to only partial loop stagnation. That is, some

Table E.1. Geometric configuration of H. B. Robinson injection diameter 21.6 cm

	Cold Leg	Vessel/ Downcomer	Lower Plenum	Pump	Loop Seal	Core Barrel	Thermal Shield
Inner Diameter (cm)	69.8	405.3	–	–	69.8	340.0	362.3
Length (cm)	704.1	662.3	–	–	284.4	662.3	467.0
Base Metal Wall Thickness (cm)	6.7	23.6	15.0	–	6.7	5.2	6.8
Clad Thickness (cm)	0.318	0.6	0.6	–	0.318	–	–
Insulation Thickness (cm)	0.30	0.30	0.30	–	0.30	–	–
Wall Heat Tr.* Area to Water (cm^2) $\times 10^{-5}$	1.54	2.74	0.82	**	0.62	2.43	3.54
Internal Structures:*							
Heat Tr. Area (cm^2)	–	–	–	3.08**	–	–	–
Thickness (cm)	–	–	–	6.35	–	–	–
Fluid Volume* (cm^3) $\times 10^{-6}$	2.69	5.59	4.62	5.44	1.09	–	–

*Per cold leg.

**Pump casing and internal structures have been lumped to 33700 lb equivalent of stainless steel.

Table E.2. Experimental conditions

Parameter	Value
HPI flow $\times\ ^{-3}$ (m^3/s)	1.281
HPI density (kg/m^3)	1096
Loop density (kg/m^3)	1000
Injection Froude No.	0.459

of the loops may be in natural circulation, while the rest are stagnated. Now the downcomer conditions are governed by the imposed system flow, and stratification in the stagnated legs must be considered only to the extent that the resulting plume can survive the downcomer flow conditions. This second condition will be referred to as "cold leg stratification."

The objective of the cold leg stratification calculations is to determine the strength and direction of the resulting plumes. For systems that have vent valves (such as Oconee), the entire cold stream will flow in the direction of the vessel, where it will encounter relatively strong vent valve flow. This flow is typically warmer due to circulation through the core

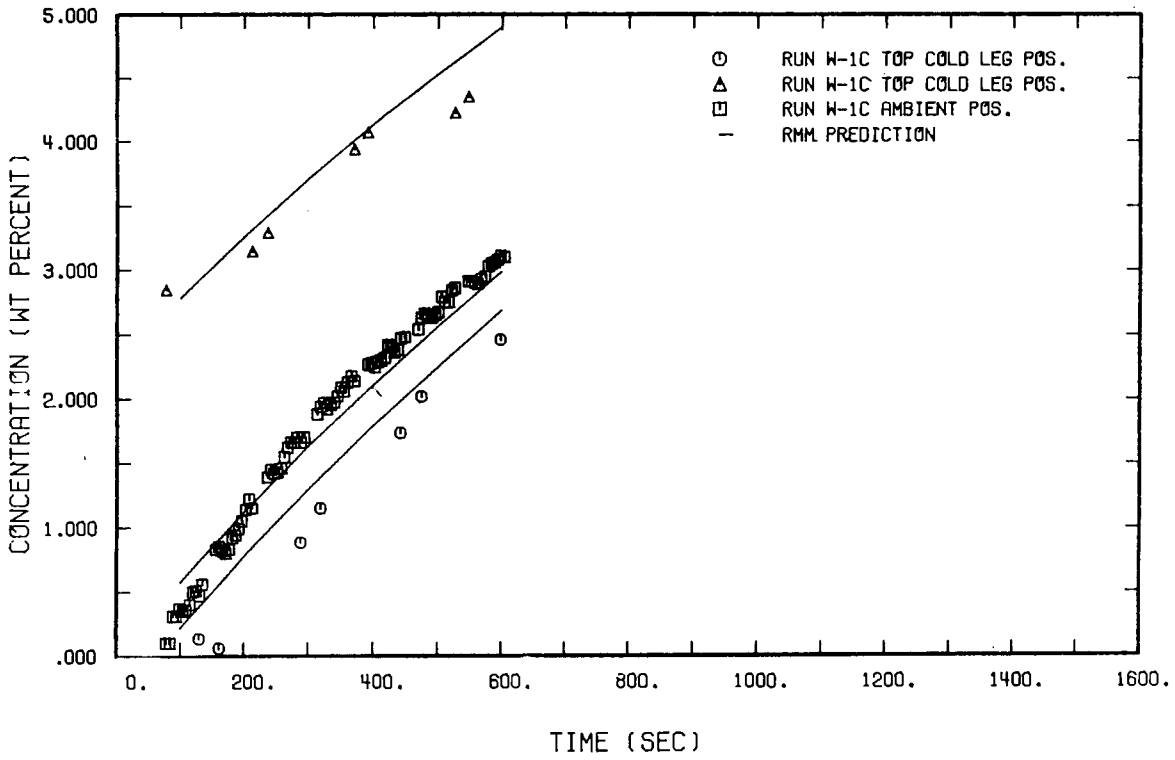

Figure E.5. Comparison of RMM predictions with experimental results in ambient region and at two locations on cold leg.

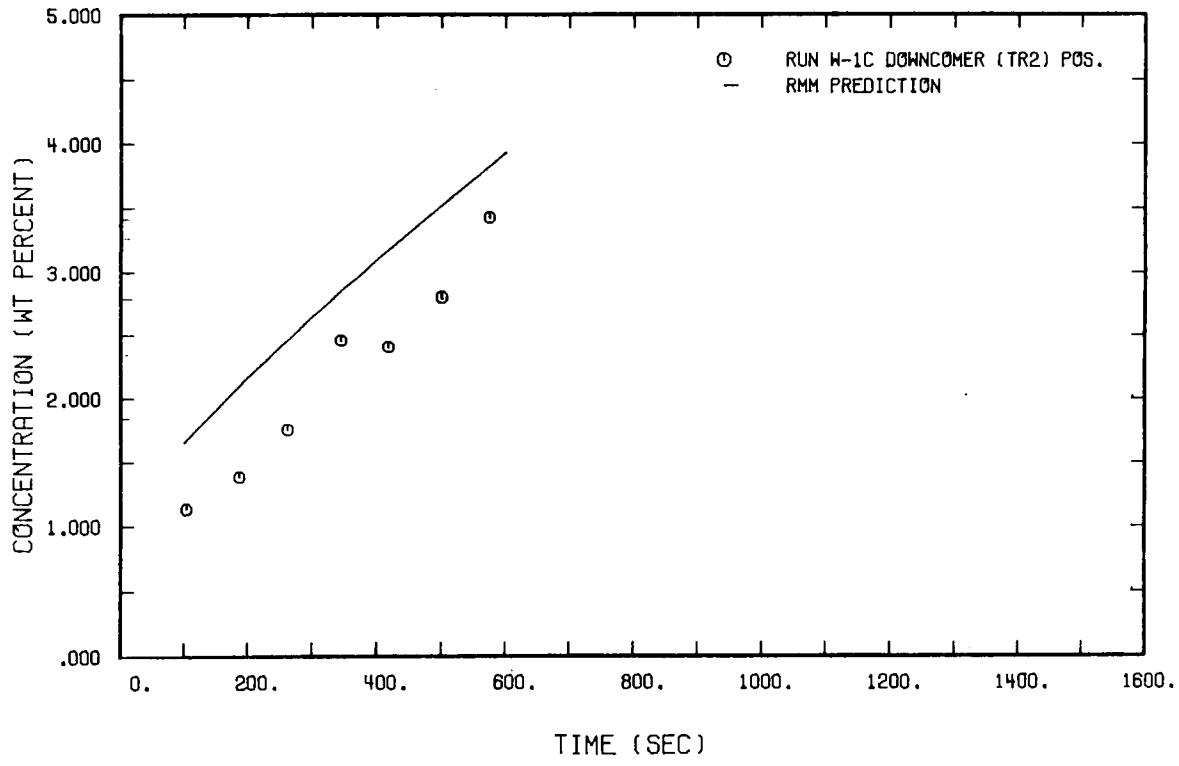

Figure E.6. Comparison of RMM predictions with experimental results in the downcomer region.

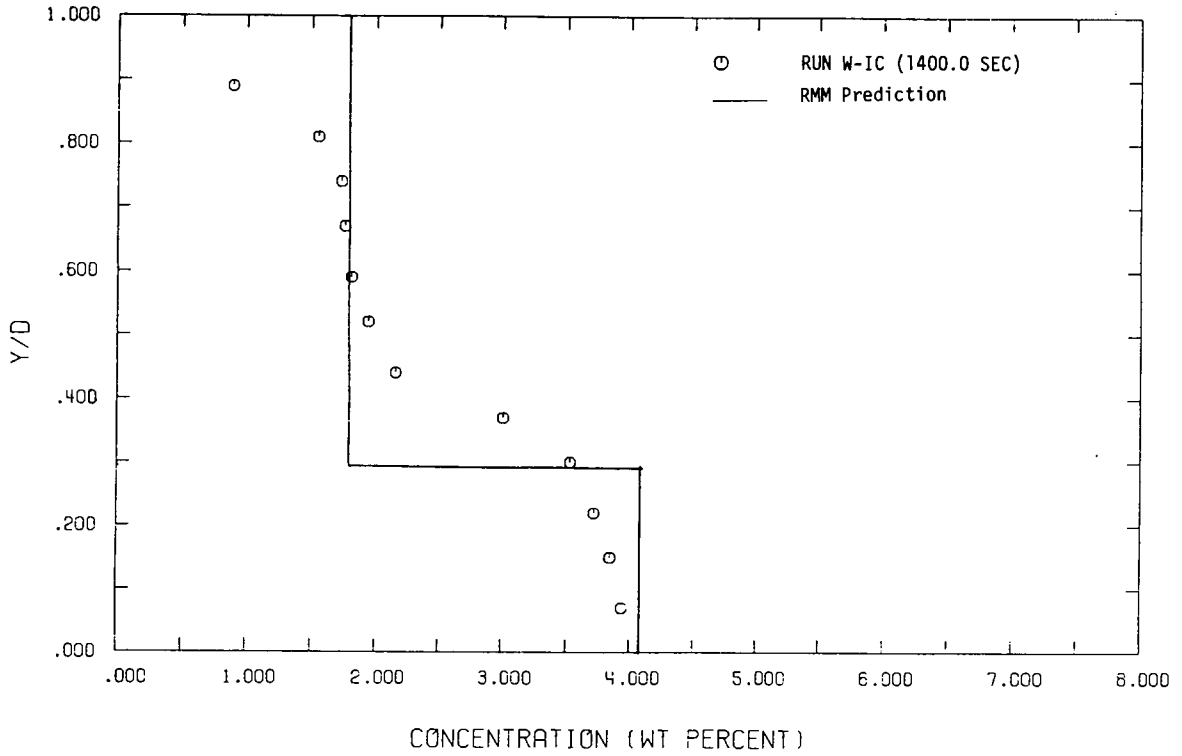

Figure E.7. Comparison of RMM predictions with experimental results for the concentration distribution in the cold leg. *D* is the diameter of the cold leg, and *Y* is the vertical coordinate.

and provides an "ambient" region for the entrainment processes in MR1 and MR3 (see Figure E.1). In such cases the RMM is applied with a prescribed "ambient" temperature. For systems that do not have vent valves (such as H. B. Robinson), the flowing loop cools faster than the stagnated one, and the resulting downcomer temperatures are already cooler than the cold stream in the stagnated leg. In such cases, the cold stream interacts only with the cold leg, pump, and loop seal volumes until the calculated "ambient" temperature in those volumes becomes low enough that the resulting cold stream is cooler than the downcomer. From this point on, the calculation proceeds with all cold stream flow directed towards the downcomer. This provides a prescribed "ambient" region for entrainment in the cold leg.

It was shown that for the several cases examined for H. B. Robinson Unit 2, the cold leg stratification process is incapable of altering the downcomer response with respect either to temperatures or to heat transfer coefficients. Therefore, the stagnated case remains important as far as quantitative details are concerned. A postulated H. B. Robinson Unit 2 stagnated case with a constant HPI flow rate of 13.6 kg/sec was chosen here to illustrate the trends. The results of the RMM applied for a complete stagnation condition with the volumes shown in Table E.1 are summarized in Figures E.8–E.13 for a "non-charging loop" and Figures E.14–E.19 for a "charging loop." The different temperature profiles presented in these figures represent different HPI water temperature and flow rates.

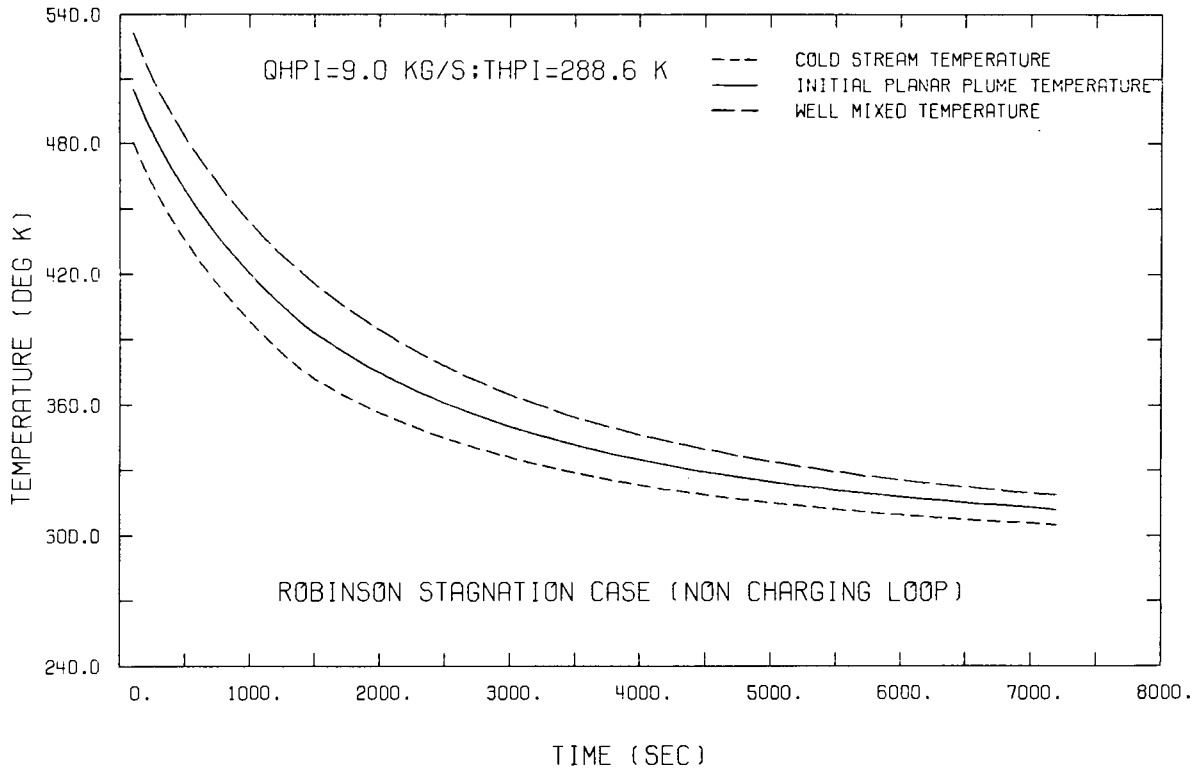

Figure E.8. Temperature traces for a non-charging loop with constant HPI flow of 9.0 kg/s under total stagnation condition at time zero (T_{HPI} = 288.6 K).

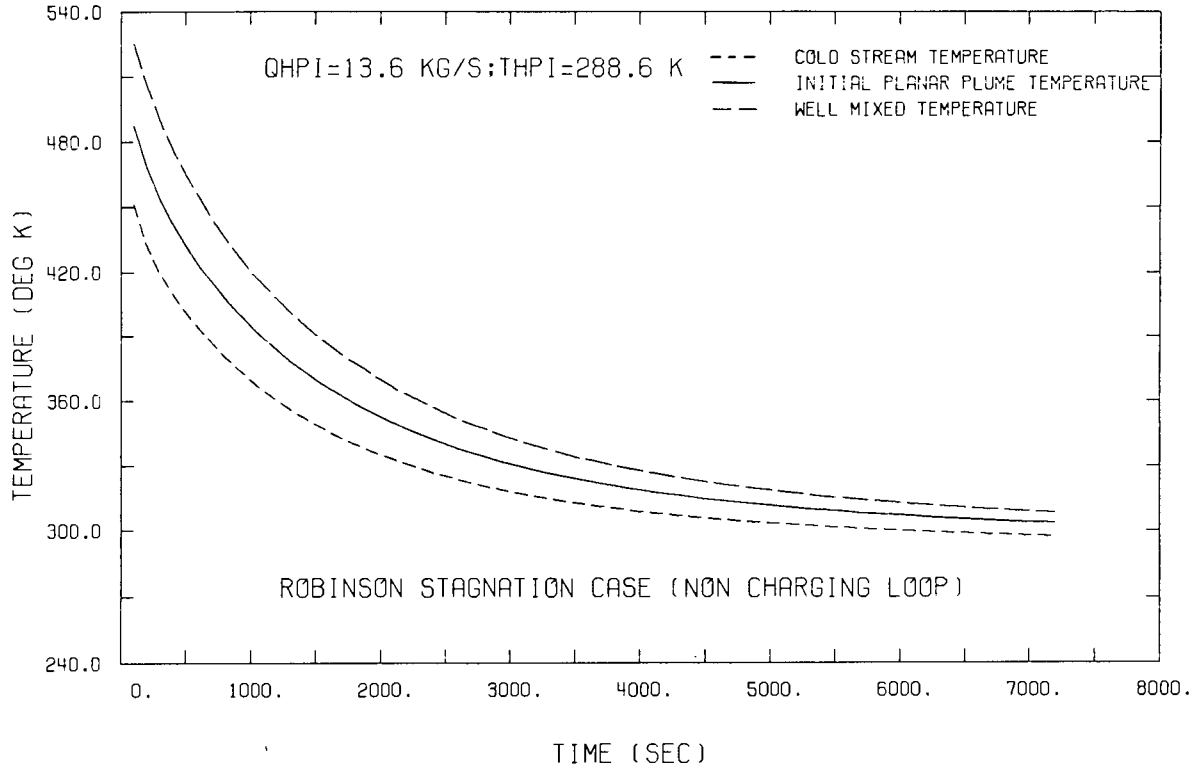

Figure E.9. Temperature traces for a non-charging loop with constant HPI flow of 13.6 kg/s under total stagnation condition at time zero (T_{HPI} = 288.6 K).

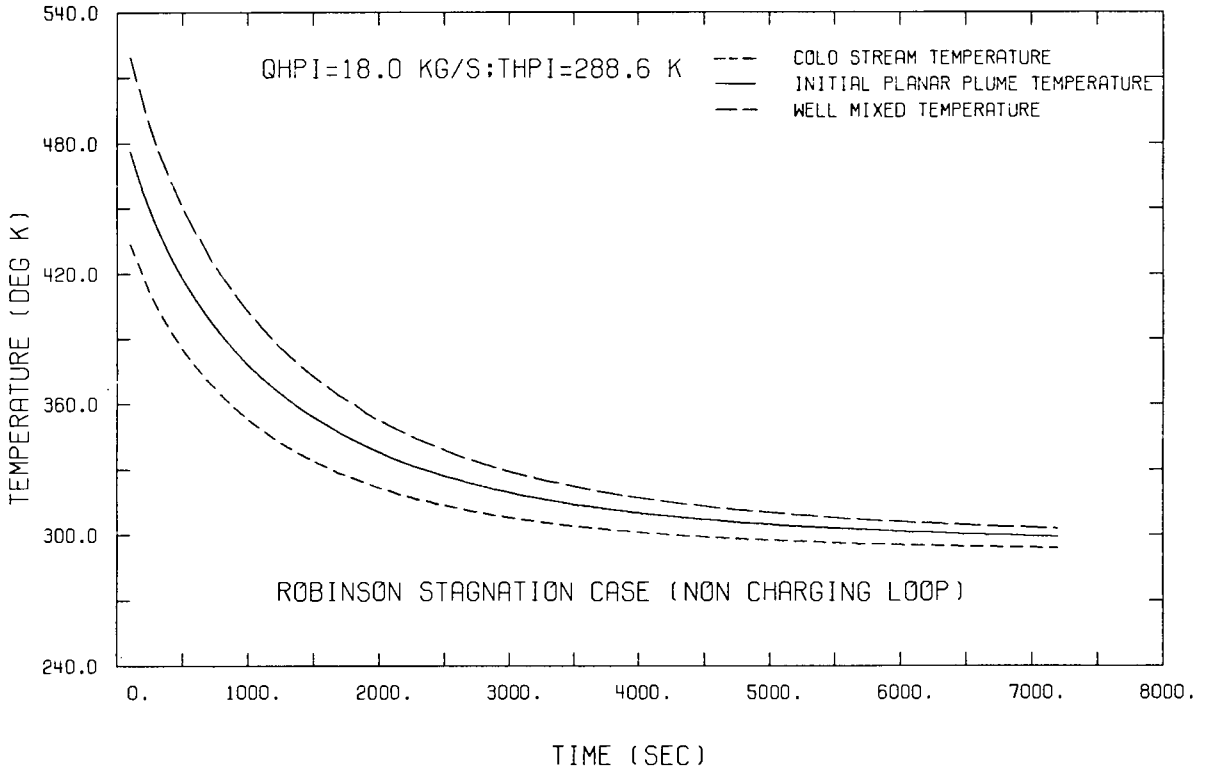

Figure E.10. Temperature traces for a non-charging loop with constant HPI flow of 18.0 kg/s under total stagnation condition at time zero (T_{HPI} = 288.6 K).

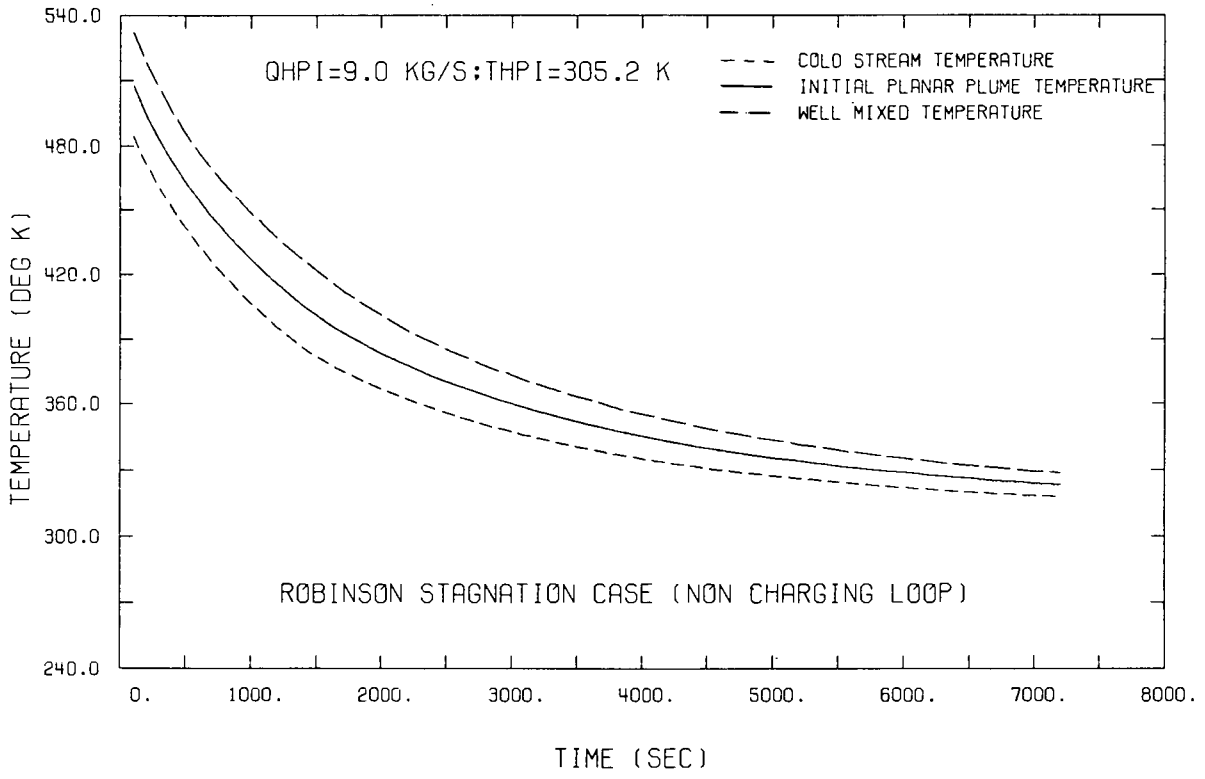

Figure E.11. Temperature traces for a non-charging loop with constant HPI flow of 9.0 kg/s under total stagnation condition at time zero (T_{HPI} = 305.2 K).

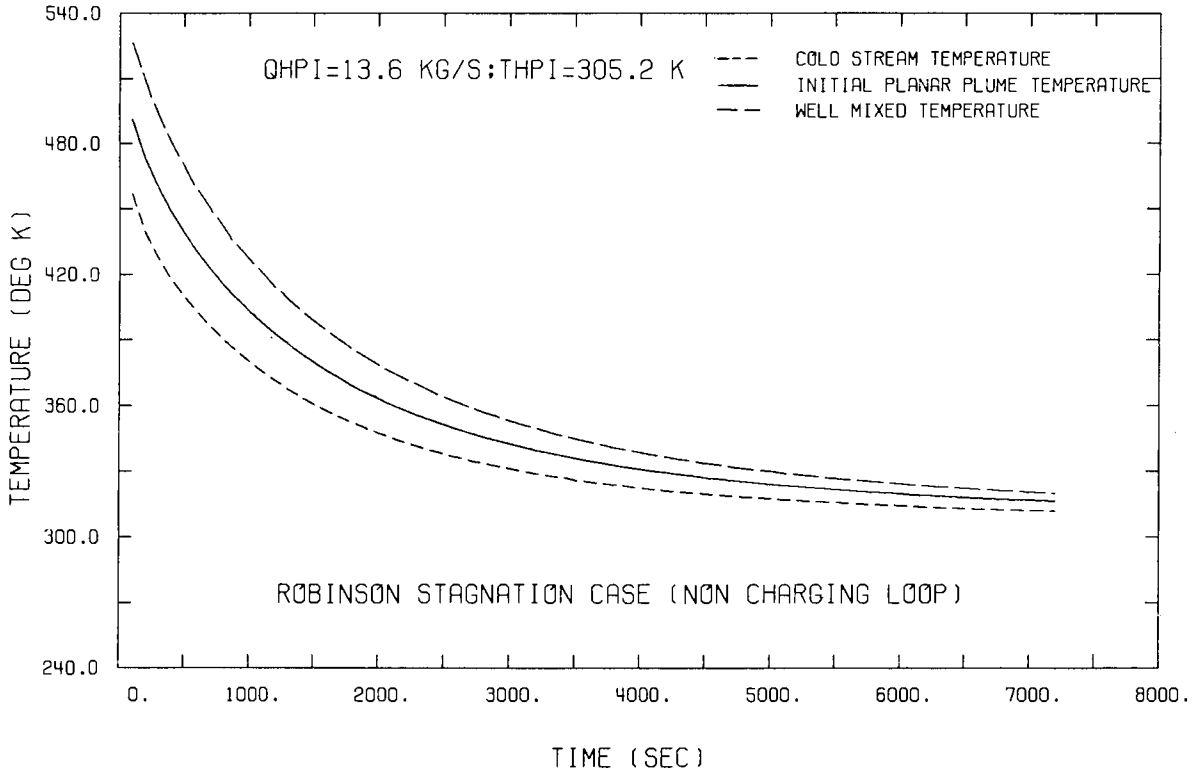

Figure E.12. Temperature traces for a non-charging loop with constant HPI flow of 13.6 kg/s under total stagnation condition at time zero (T_{HPI} = 305.2 K).

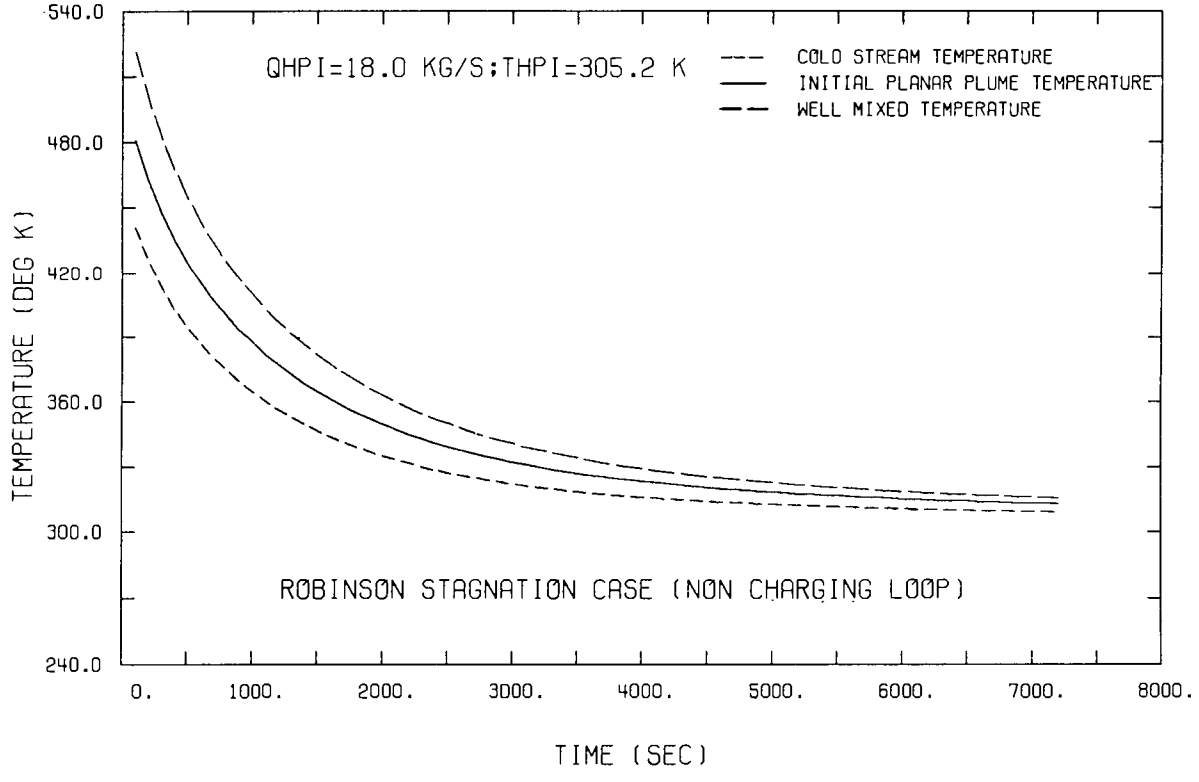

Figure E.13. Temperature traces for a non-charging loop with constant HPI flow of 18.0 kg/s under total stagnation condition at time zero (T_{HPI} = 305.2 K).

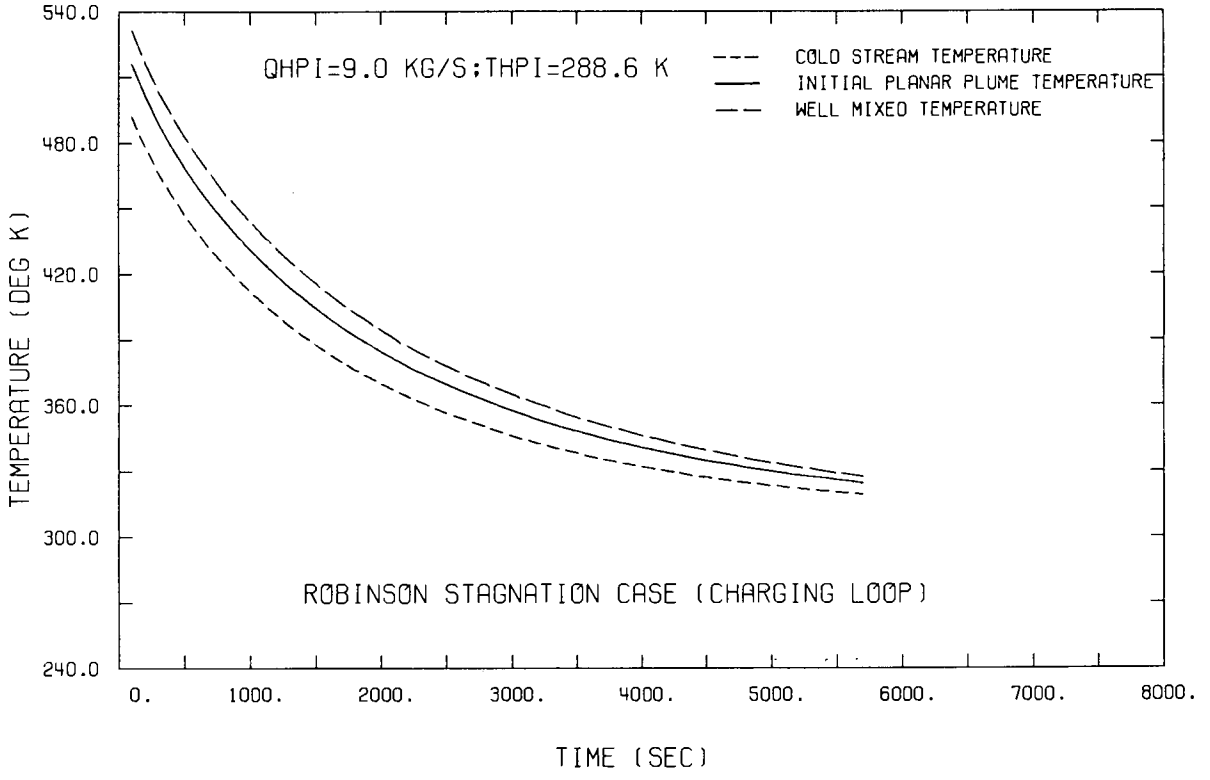

Figure E.14. Temperature traces for a charging loop with constant HPI flow of 9.0 kg/s under total stagnation condition at time zero (T_{HPI} = 288.6 K).

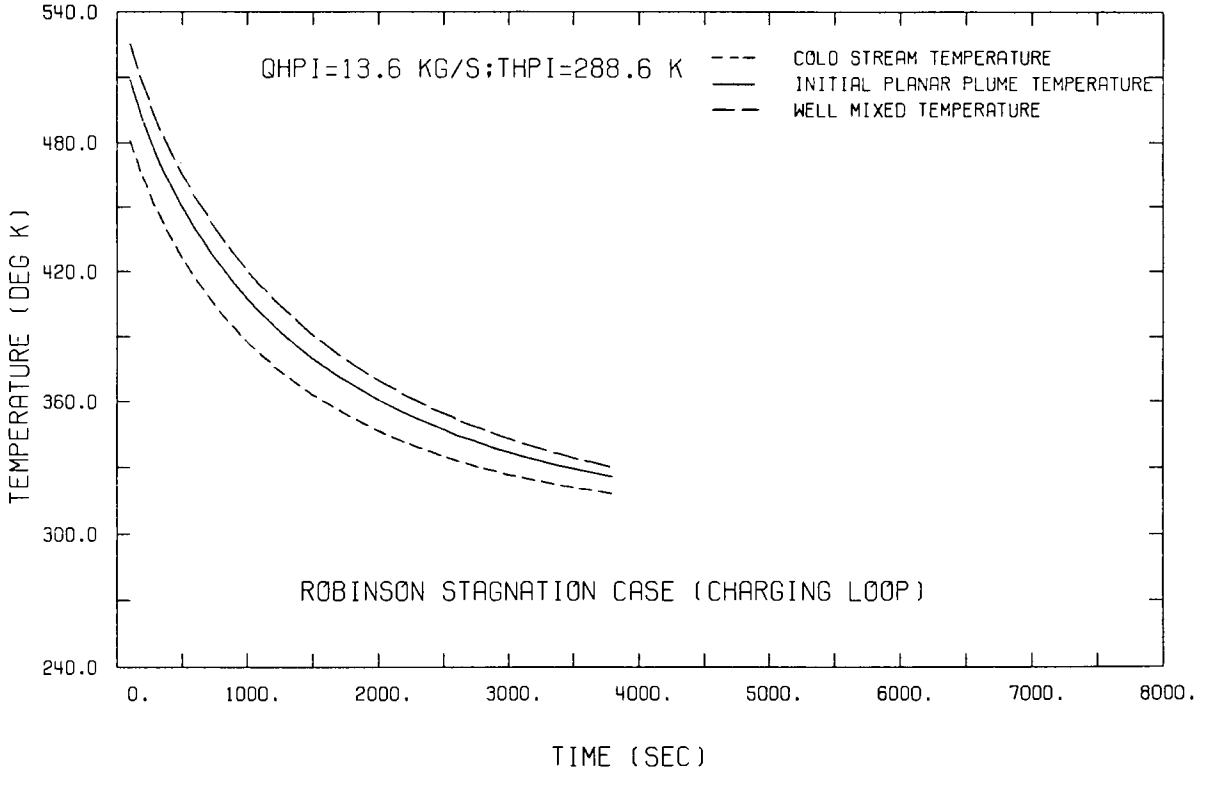

Figure E.15. Temperature traces for a charging loop with constant HPI flow of 13.6 kg/s under total stagnation condition at time zero (T_{HPI} = 288.6 K).

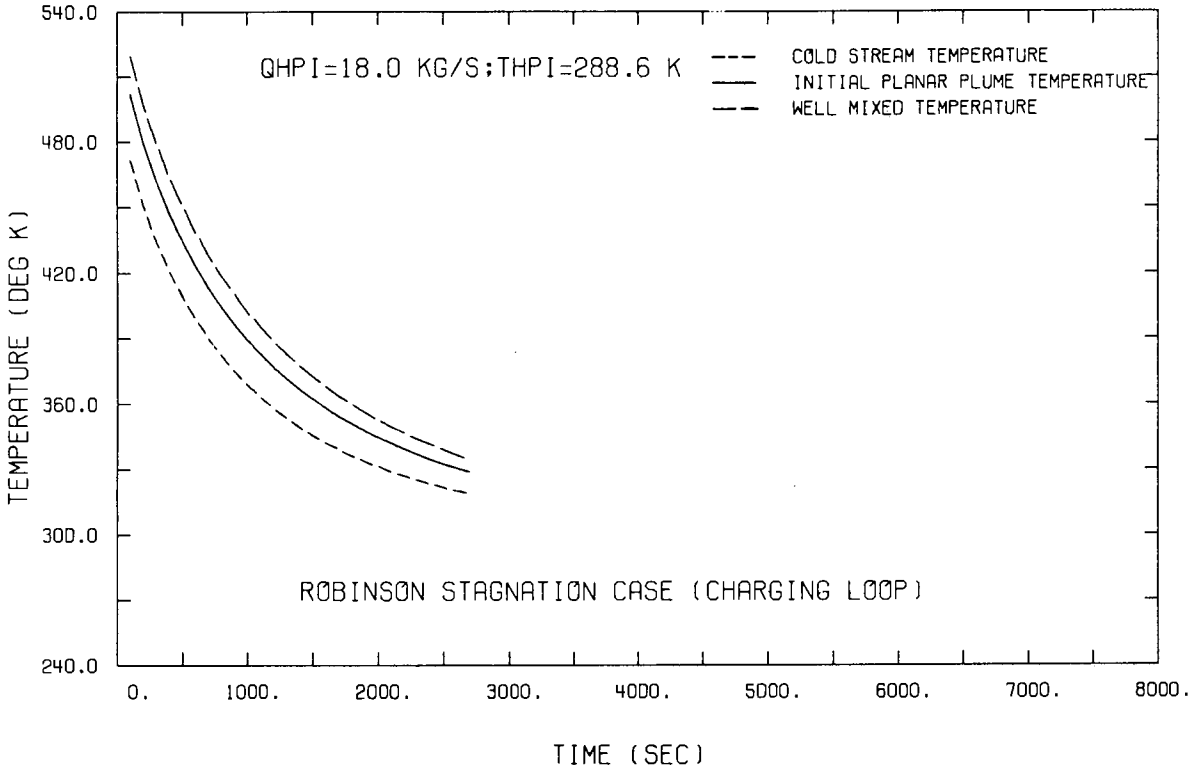

Figure E.16. Temperature traces for a charging loop with constant HPI flow of 18.0 kg/s under total stagnation condition at time zero (T_{HPI} = 288.6 K).

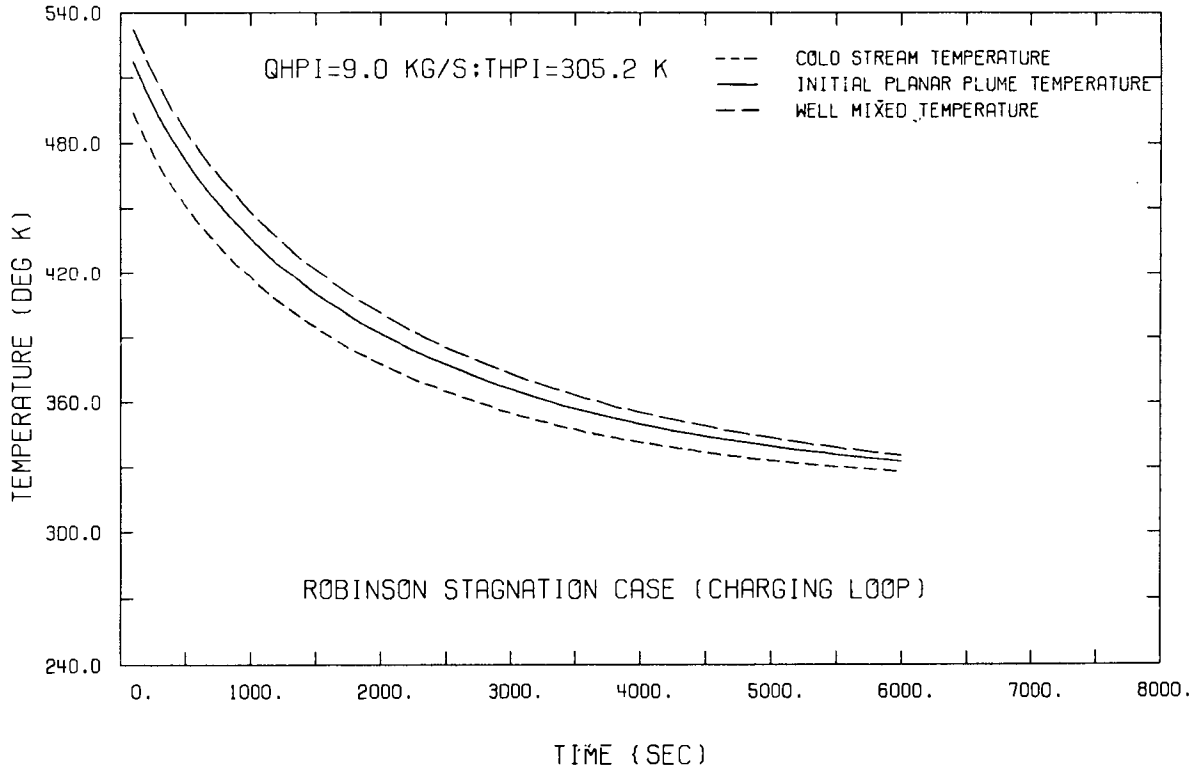

Figure E.17. Temperature traces for a charging loop with constant HPI flow of 9.0 kg/s under total stagnation condition at time zero (T_{HPI} = 305.2 K).

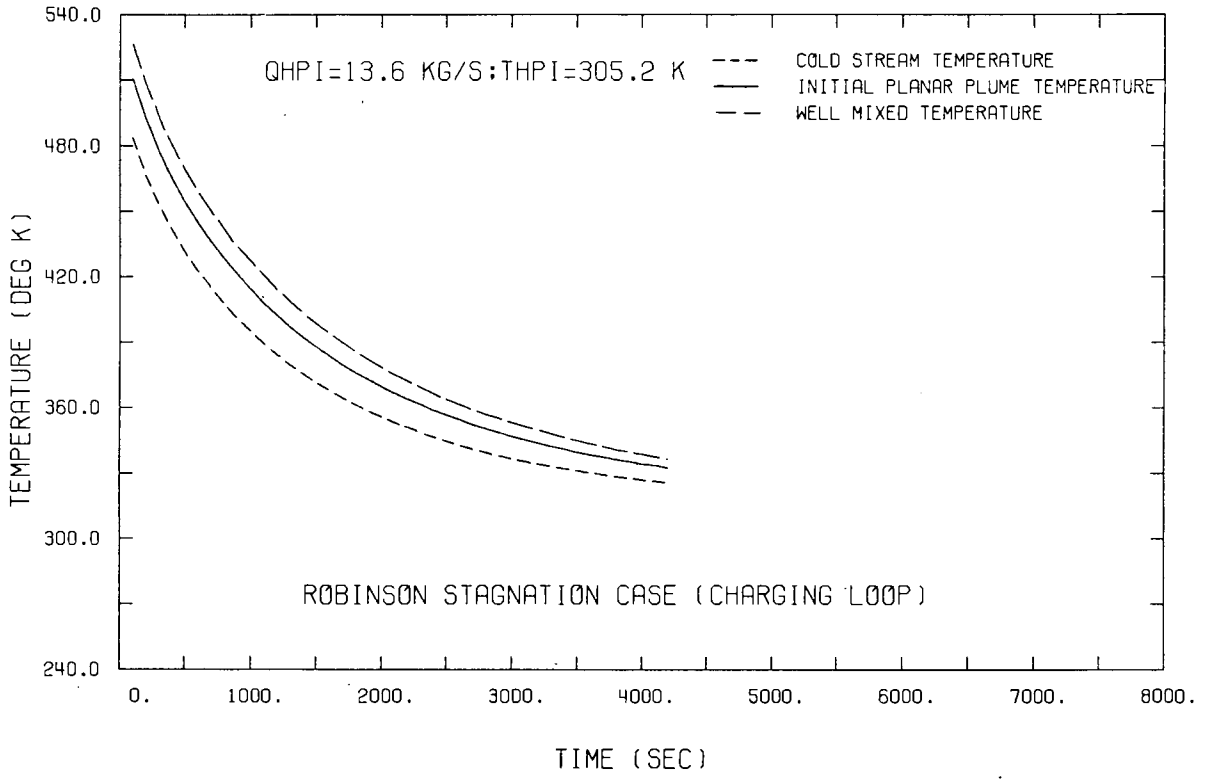

Figure E.18. Temperature traces for a charging loop with constant HPI flow of 13.6 kg/s under total stagnation condition at time zero (T_{HPI} = 305.2 K).

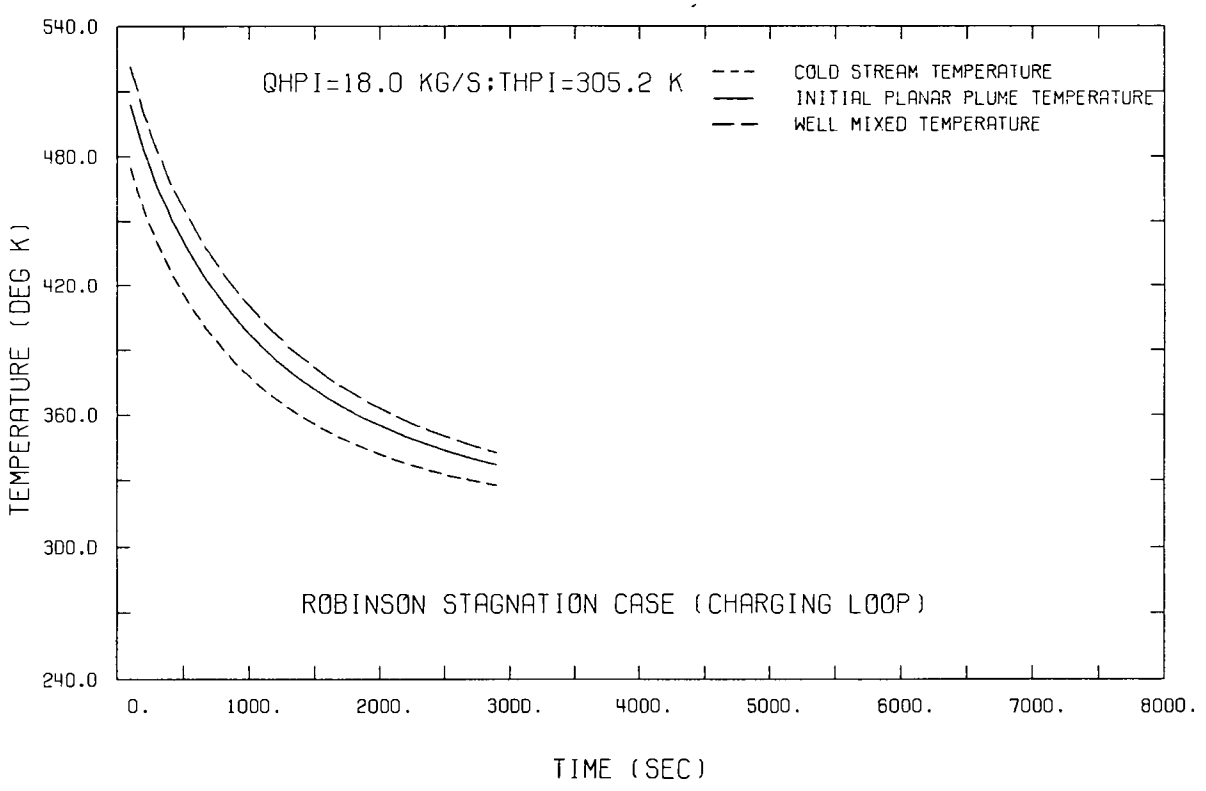

Figure E.19. Temperature traces for a charging loop with constant HPI flow of 18.0 kg/s under total stagnation condition at time zero (T_{HPI} = 305.2 K).

On the basis of the information presented in these figures, it can be concluded that a relatively small degree of stratification (of ~30 K) is adequate to drive the overall recirculation pattern, which forces the whole system to participate in the mixing process. The associated large system volume extends the cooldown, thus allowing time for structural heat release, which diminishes the cooldown rate even further. With reasonable variations of the applied heat transfer coefficient for the release of this wall heat, the results vary by less than 1 to 2 K.

For the purpose of PTS analyses, the indicated initial planar plume temperature is important. This temperature results in the ambient fluid being entrained in the cold stream in MR3, and, as shown in Figures E.8–E.19, the plume temperature tracks the ambient temperature within ~15 K. A decay of the planar plume will occur, as shown in Figure E.20, from the initial temperature to the ambient temperature (this includes accounting for MR3 mixing). Our experiments show that, at most, within 1.5 cold leg diameters below the cold leg/downcomer junction a very nearly uniform temperature distribution along the downcomer gap is already achieved. The minimum plume travel required for such uniformity has not yet been determined. However, the plume decay has been estimated with the help of Figure E.20. With an initial velocity obtained by continuity from the cold stream flow rate and a downcomer plume width assumed to be equal to the width of the cold stream in the cold leg, an initial plume Froude number of ~0.6 is typically estimated. With a Froude number of this size, the decay occurs rapidly along the downcomer length.

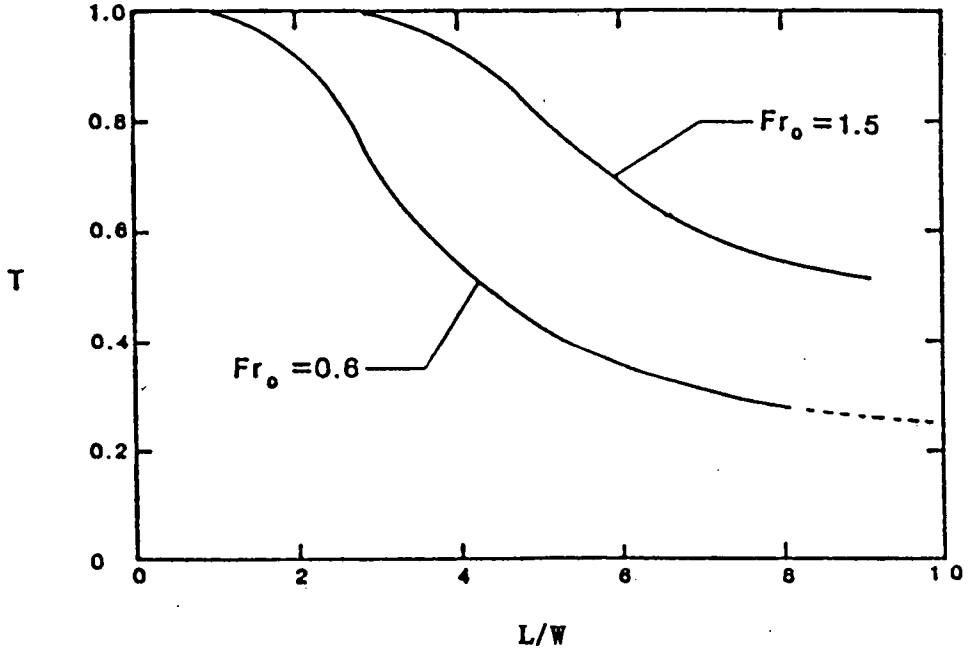

Figure E.20. Prediction of centerline temperature in planar plumes as function of axial position. Fr_0 is based on plume width (W) and velocity at the entrance to downcomer; L = plume length.

E.6. Generic Vessel Wall Cooling Considerations

E.6.1. Mixed Convection Characterization

The criterion commonly used to judge the importance of free convection effects is

$$\mathrm{Gr}/\mathrm{Re}^2 > 1 \ , \tag{E.3}$$

where

Gr = Grashof number

$= 1/2\ \beta(T_w - T_b)\ gD^3/\nu^2$,

T_w = wall temperature,

T_b = coolant bulk temperature.

For a flow direction opposite to buoyancy, the destabilization of the thin thermal boundary layer in contact with the RPV wall leads to an increase in the heat transfer coefficient as compared to that estimated on the basis of forced convection only. This increase was correlated by Fewster and Jackson[8] by the expression

$$\frac{\mathrm{Nu}}{\mathrm{Nu}_0} = \left[1 + 4{,}500\frac{\overline{\mathrm{Gr}}}{\mathrm{Re}^{2.63}}\right]^{0.31} , \tag{E.4}$$

where

Nu = Nusselt number

$= hD/k$,

h = heat transfer coefficient,

k = thermal conductivity.

Fewster and Jackson developed their correlation from data obtained with water in a tube geometry and parameter values or ranges of D = 9.8 cm, $\mathrm{Gr}/\mathrm{Re}^2$ = 0.1 to 10, Gr = 1.0×10^6 to 5×10^8, and $\mathrm{Re} = 5 \times 10^3$ to 6×10^4. These data are complemented by the data of Brdlik *et al.*[9] obtained with air in a flat plate geometry and a rectangular cross-section channel (40 × 50 × 200 cm) with: $\mathrm{Gr}_x/\mathrm{Re}_x^2$ = 0.01 to 100, $\mathrm{Gr}_x = 0.5 \times 10^{10}$ to 6×10^{10}, and $\mathrm{Re}_x = 0.8 \times 10^4$ to 10^6.

These data were correlated as shown in Figure E.21. It is noted that for the region with strong free convection effects, $\mathrm{Gr}_x/\mathrm{Re}_x^2 > 0.8$, the value of $\mathrm{Nu}_x/\mathrm{Gr}_x^{1/3}$ is almost constant (h is independent of x) and does not exceed 0.18; that is,

$$\mathrm{Nu} = 0.18\,\mathrm{Gr}^{1/3} \ . \tag{E.5}$$

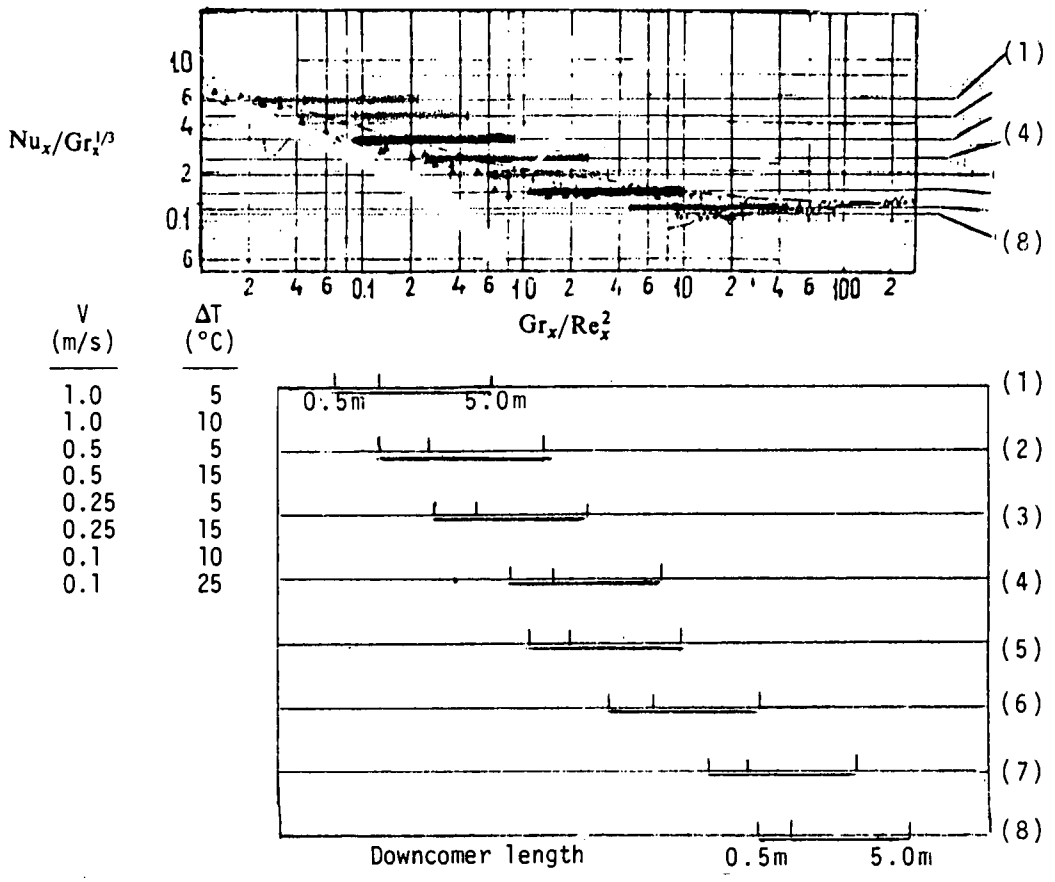

Case	V (m/s)	ΔT (°C)
1	1.0	5
2	1.0	10
3	0.5	5
4	0.5	15
5	0.25	5
6	0.25	15
7	0.1	10
8	0.1	25

Figure E.21. The Brdlik *et al.* data trends and illustration of entrance length for various combinations of velocities and temperature differences (fluid to wall) as deduced by comparison to the Fewster-Jackson correlation results (line by segments). (Note this figure should be interpreted as follows: the bar graphs in the second half of the figure represent the range of GR_x/Re_x^2 over the downcomer length for the case in question. For any particular case the predicted $Nu_x/Gr_x^{1/3}$ can be compared with the actual value used as indicated at right of the top figure by examining the same GR_x/Re_x^2 section in the top half of the figure.

For the conditions of interest, the Prandtl number, Pr, is ~ 1, and thus

$$Nu_0 = 0.023 Re^{0.8} \ . \tag{E.6}$$

By employing the well-known interpolation scheme

$$Nu = \left[Nu_1^3 + Nu_2^3\right]^{1/3} \ , \tag{E.7}$$

Equation E.4 can be derived from Equations E.5 and E.6 as follows:

$$\frac{Nu}{Nu_0} = \left[1 + \frac{0.18^3 Gr}{0.023^3 Re^{2.4}}\right]^{1/3} = \left[1 + 479\,\frac{Gr}{Re^{2.4}}\right]^{1/3} \ . \tag{E.8}$$

And by forcing the Fewster-Jackson form,

$$\frac{\mathrm{Nu}}{\mathrm{Nu}_0} = \left[1 + 479\mathrm{Re}^{0.23}\frac{\mathrm{Gr}}{\mathrm{Re}^{2.63}}\right]^{1/3} . \tag{E.9}$$

This agrees with Equation E.4 for a reasonable range of Re around the value of 17,000, indicating the interpolative nature of the Fewster-Jackson correlation.

Furthermore in order to visualize the extent of the entrance length in the downcomer region as depicted by the data of Brdlik *et al.*, we have shown the Fewster-Jackson correlation results also on Figure E.21. Eight combinations of velocities and temperature differences (wall to fluid) were examined covering the range of forced-to-free heat transfer regimes and also the ranges of conditions of interest in a PWR downcomer. We see that the entrance length is never more than 0.5 m long (i.e., ~ one half of the cold leg diameter), and that the use of Fewster-Jackson correlation is adequate for our purposes.

E.6.2. Convection/Conduction Coupling Effects

From Equation E.4 the augmentation of heat transfer from the wall in the mixed convection regime is seen to increase with the wall surface temperature. For the present application, however, such contributions cannot be correctly appreciated without considering heat transfer limitations within the RPV wall (and its stainless steel cladding). That is, if the wall surface temperature is considerably higher than that of the fluid, the free convection augmentation occurs, increasing the heat transfer coefficient. As the heat flux leaving the wall increases, the wall surface will have to cool such that the wall-internal conduction resistance may be accommodated (i.e., by increasing the driving force). The actual behavior is determined by the direct coupling of these two processes and, given that wall conduction is a transient phenomenon (i.e., resistance increasing with time), this coupling should be studied under realistic cooldown rates.

In order to scope these effects, a series of calculations were performed by numerically coupling, through Equation E.4, a finite difference conduction calculation in the wall with a prescribed fluid cooldown. A 20-cm-thick carbon steel wall with a 0.7-cm-thick stainless steel cladding and an initial temperature of 550 K were considered. The water temperature decay was specified in terms of the final temperature (T_∞) and an exponential time constant (τ). Five combinations of these two parameters (T_∞ = 477, 422, and 343 K; and τ = 0, 250, 500, and 1500 s) were considered.

These sample transients covered the range from instantaneous cooldown, which was considered for illustration purposes, to the very slow cooldown expected in a PWR stagnated-loop case. For each such combination, the heat transfer calculation was performed for six constant water velocities (0.05, 0.1, 0.25, 0.5, 0.75, and 1.0 m/s) specified such as to encompass the strongly free and purely forced convection regimes.

The results of the scoping calculations can be summarized as follows. The forced convection regime, delineated by $\mathrm{Nu}/\mathrm{Nu}_0 \sim 1$, dominates the heat convection for velocities higher than 0.25 m/s. Even at the 0.25-m/s flow, only ~25% of the total heat convection can be attributed to free convection.

As shown in Section E.7, downcomer velocities of 0.25 to 0.5 m/s are common for transients with the loops in a natural circulation mode, indicating the dominance of forced convection. For stagnated-loop cases, plume velocities of ~1 m/s are expected, indicating a purely forced convection heat transfer regime (h ~4,000 W/m^2·K or ~700 Btu/hr·ft^2·°F). Outside of the plume peak, upward downcomer velocities of ~0.25 m/s are predicted, which again indicates a forced convection situation. As the plume decays in the downcomer, the flow pattern becomes increasingly more complicated and lower velocities prevail. The heat transfer coefficients become insensitive to the flow for velocities below 0.25 m/s when the limiting value of ~1,500 W/m^2·K (~260 Btu/hr·ft^2·°F) is approached. Interestingly enough, the trends appear to indicate that even in the presence of free convection, the heat transfer coefficient is essentially independent of time for all gradual cooldown cases (t = 0).

The surface wall temperatures fall within a narrow band 2 to 12 K below the fluid temperature. A sample wall temperature gradient is shown in Figure E.22. Clearly, with a maximum uncertainty of ±5 K, the wall temperatures could be calculated merely by imposing the fluid temperature +6 K directly on the cladding surface (i.e., bypassing the use of a heat transfer coefficient). The reason for this insensitivity may be traced to the relatively high value of the wall conduction resistance compared to that of the film heat transfer. Thanks to this behavior, even significant uncertainties in the heat transfer coefficient and flow velocities shrink to a negligible impact on wall temperatures.

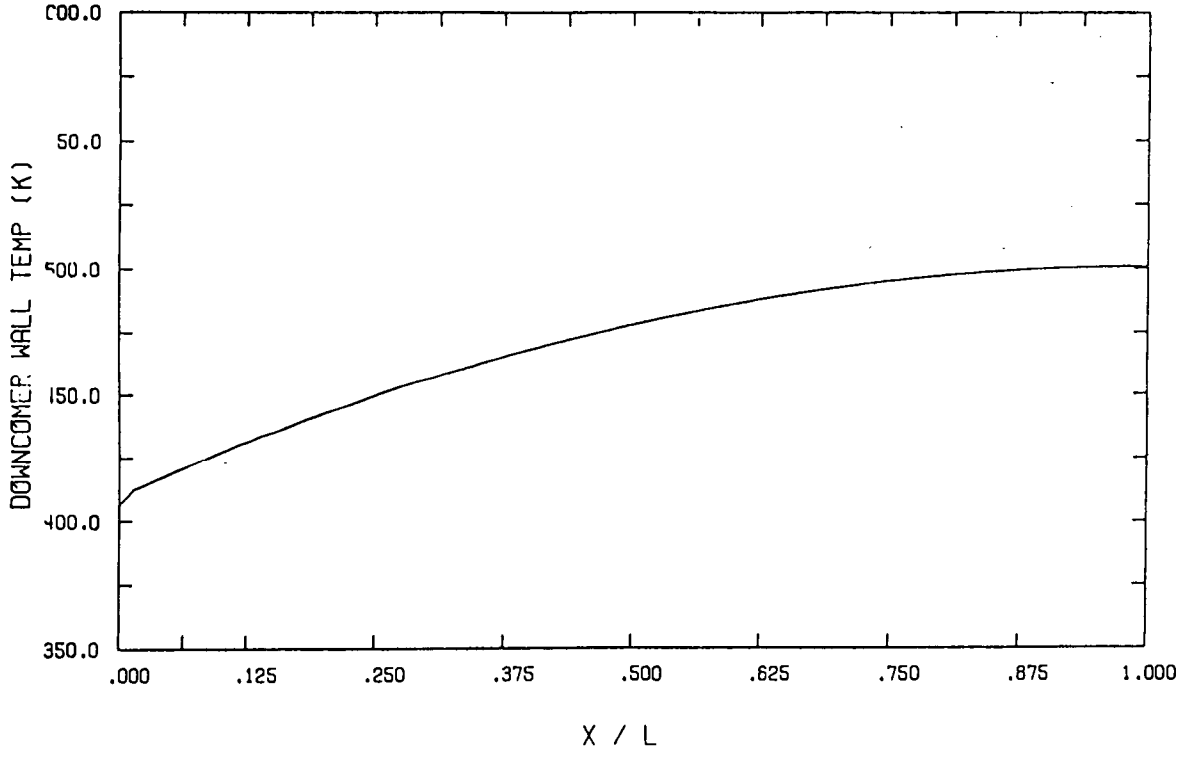

Figure E.22. Sample wall temperature gradient. (X = distance into wall, L = total width of wall.)

E.7. References

1. C. D. Fletcher *et al., RELAP5 Thermal-Hydraulic Analysis of Pressurized Thermal Shock Sequences for the H. B. Robinson Unit 2 Pressurized Water Reactor,* NUREG/CR-3977, September 1984.

2. T. G. Theofanous, P. Gherson, H. P. Nourbakhsh, and K. Iyer, *Decay of Buoyancy Driven Stratified Layers with Applications to PTS,* NUREG/CR-3700, February 1984.

3. H. P. Nourbakhsh and T. G. Theofanous, *REMIX: A Computer Program for Temperature Transients Due to HPI at Stagnated Loop Flow,* NUREG/CR-3701, May 1984.

4. T. G. Theofanous and H. P. Nourbakhsh, "PWR Downcomer Fluid Temperature Transients Due to High Pressure Injection at Stagnated Loop Flow," pp. 583-613 in *Proceedings of Joint NRC/ANS Meeting on Basic Thermal Hydraulic Mechanisms in LWR Analysis,* September 14-15, 1982, Bethesda, MD, NUREG/CP-0043.

5. T. G. Theofanous, H. P. Nourbakhsh, P. Gherson, and K. Iyer, "Decay of Buoyancy Driven Stratified Layers with Application for PTS," *Proceedings of the Eleventh Water Reactor Safety Research Information Meeting,* NUREG/CP-0048, Vol. 2, October 1983.

6. M. W. Fanning and P. H. Rothe, *Transient Cooldown in a Model Cold LRG and Downcomer,* EPRI Report NP-2122-3, May 1983.

7. H. P. Nourbakhsh and T. G. Theofanous, "Decay of Buoyancy Driven Stratified Layers with Applications to PTS Part I: The Regional Mixing MODEL," *Nuclear Engineering Design* (in press).

8. J. D. Jackson and J. Fewster, "Enchantment of Turbulent Heat Transfer Due to Buoyancy for Downward Flow of Water in Vertical Tubes," *Convection* by D. B. Spalding and N. Afgan.

9. P. M. Brdlik *et al.,* "Heat Transfer Investigation for Mixed Free and Forced Turbulent Convection on Vertical Plate," *Second Symposium on Turbulent Shear Flow, 1979.*

Appendix F

ESTIMATIONS OF PRESSURES, TEMPERATURES, AND HEAT TRANSFER COEFFICIENTS FOR POSTULATED OVERCOOLING SEQUENCES

C. D. Fletcher

Idaho National Engineering Laboratory

APPENDIX F. ESTIMATIONS OF PRESSURES, TEMPERATURES, AND HEAT TRANSFER COEFFICIENTS FOR POSTULATED OVERCOOLING SEQUENCES

A pressurized thermal shock analysis of the H. B. Robinson Unit 2 reactor vessel requires that pressure and temperature histories of the reactor vessel downcomer fluid be known over a 2-hr period following the initiating event for each of the potential overcooling sequences identified in Chapter 3. As discussed in Chapter 4, Idaho National Engineering Laboratory (INEL) developed a RELAP5 model of the HBR-2 plant and performed detailed thermal-hydraulics calculations for a limited number of the sequences. However, to carry out such calculations for all the sequences was economically impractical. Instead, pressure and temperature histories for the remaining sequences were generated by INEL through a process combining (1) detailed RELAP5 calculations covering only part of the 2-hr period, (2) calculations with a simplified RELAP5 model for the full 2-hr period, and (3) hand calculations. A full description of the process is given in a separate report[1] and will not be repeated here; however, it was felt that the results of the process should be included. Thus, this appendix presents the pressure and temperature profiles for the 229 sequences identified in Chapter 3 and listed in Table F.1, but with the following three general exceptions:

(a) For sequences that are thermal-hydraulically equivalent, the data are given for only one of the sequences. For all the other sequences, the equivalent sequence is identified in Table F.1 in parentheses labeled with a superscript a.

(b) After the INEL analysis had been completed, some additional transients were identified, and ORNL chose bounding sequences to represent the thermal-hydraulic condition for these transients. These sequences are identified in Table F.1 in parentheses labeled with a superscript b.

(c) A few of the overcooling sequences did not result in an automatic reactor trip in the INEL model calculations, and it is believed that in actuality, in most instances an automatic reactor trip would not occur. However, it was decided that a reactor trip should be assumed for these sequences since the potential for a manual trip was reasonably high. Thus, for these sequences, a bounding sequence was chosen to represent the transient under the assumption that a manual trip had occurred. The bounding sequence is identified in Table F.1 in parentheses labeled with a superscript c.

Heat transfer coefficients were not specifically determined for each sequence. Instead heat transfer coefficients calculated from the full-scale RELAP5 calculations were assigned by INEL to each sequence based on an evaluation of the reactor vessel downcomer flow conditions. The heat transfer coefficients assigned to each sequence are presented in Ref. 1 and are not repeated in this appendix.

Table F.1. Index to HBR-2 thermal-hydraulic plots and summary of minimum temperatures (T_{min}) and maximum pressures (P_{max}) of reactor vessel downcomer fluid

Seq. No.	Page No.	T_{min} (°F)	P_{max} (psia)	Seq. No.	Page No.	T_{min} (°F)	P_{max} (psia)
1.1	509	474	924	5.10	(9.27)[c]		
1.2	510	382	578	5.11	(9.26)[c]		
1.3	511	473	919	5.12	(5.30)[a]		
1.4	512	381	576	5.13	(9.26)[c]		
1.5	513	233	338	5.14	535	311	2371
1.6	514	218	328	5.15	536	309	2371
1.7	515	203	317	5.16	537	311	2371
1.8	516	171	300	5.17	538	277	1553
1.9	517	224	368	5.18	539	303	2371
1.10	518	224	356	5.19	540	286	2371
1.11	519	224	368	5.20	541	244	1618
1.12	520	217	358	5.21	(9.6)[c]		
1.13	(1.1)[a]			5.22	(9.4)[c]		
1.14	(1.2)[a]			5.23	(9.3)[c]		
1.15	(1.3)[a]			5.24	(9.6)[c]		
1.16	(1.5)[a]			5.25	(9.5)[b]		
1.17	(1.1)[a]			5.26	(9.5)[b]		
1.18	(1.1)[a]			5.27	(9.4)[b]		
1.19	(1.8)[b]			5.28	(9.19A)[b]		
1.20	(9.3)[b]			5.29	(6.8)[b]		
1.21	(9.34)[b]			5.30	Residual Group		
1.22	(9.19A)[b]						
2.1	521	100	144	6.1	(6.8)[a]		
2.2	522	100	144	6.2	542	302	2371
2.3	523	100	144	6.3	543	302	2371
2.4	524	100	144	6.4	544	302	2371
2.5	525	210	144	6.5	545	229	1772
2.6	526	198	144	6.6	546	227	2371
2.7	527	185	144	6.7	547	229	1772
2.8	528	160	144	6.8	548	299	2371
2.9	529	190	144	6.9	549	229	1781
2.10	530	190	144	6.10	(9.20B)[b]		
2.11	531	203	144	6.11	(9.20B)[b]		
2.12	(1.8)[b]			6.12	(6.8)[b]		
2.13	(2.1)[b]			6.13	(6.8)[b]		
2.14	Residual Group			6.14	(6.8)[b]		
				6.15	(6.8)[b]		
3.1	532	279	679	6.16	Residual Group		
3.2	533	246	393				
3.3	(3.4)[a]			7.1	550	412	2371
3.4	Residual Group			7.2	551	409	2371
				7.3	552	369	2371
4.1	534	100	144	7.4	553	283	1565
4.2	(4.1)[b]			7.5	554	270	2371
4.3	Residual Group			7.6	555	283	1565
				7.7	556	393	2371
5.1	(7.1)[c]			7.8	557	288	1528
5.2	(9.27)[c]			7.9	558	239	1508
5.3	(9.26)[c]			7.10	559	229	1470
5.4	(9.28)[c]			7.11	560	209	1537
5.5	(5.30)[a]			7.12	561	332	1505
5.6	(5.30)[a]			7.13	(9.3)[b]		
5.7	(9.26)[c]			7.14	(9.4)[b]		
5.8	(9.28)[c]			7.15	(9.5)[b]		
5.9	(9.9A)[c]			7.16	(7.3)[b]		

Table F.1 (Continued)

Seq. No.	Page No.	T_{min} (°F)	P_{max} (psia)	Seq. No.	Page No.	T_{min} (°F)	P_{max} (psia)
7.17	(9.5)[b]			9.41	608	268	1615
7.18	(7.3)[b]			9.42	609	251	1517
7.19	(7.3)[b]			9.43	610	262	2371
7.20	Residual Group			9.44	611	244	2371
				9.45	612	272	1490
8.1	562	284	2371	9.46	613	259	1632
8.2	563	283	2371	9.47	614	265	2371
8.3	564	284	1792	9.48	615	546	2296
8.4	565	204	1947	9.49	616	446	2371
8.5	566	274	2371	9.50	(9.1)[a]		
8.6	567	201	1995	9.51	617	446	2371
8.7	(6.8)[b]			9.52	(9.1)[a]		
8.8	(6.8)[b]			9.53	618	446	2371
8.9	(6.8)[b]			9.54	(9.1)[a]		
8.10	Residual Group			9.55	619	446	2371
				9.56	(9.1)[a]		
9.1	568	546	2296	9.57	620	312	1544
9.2	569	312	1544	9.58	(9.3)[a]		
9.3	570	294	1553	9.59	(9.4)[a]		
9.4	571	305	2371	9.60	(9.5)[a]		
9.5	572	282	2371	9.61	(9.6)[a]		
9.6	573	306	1527	9.62	(9.9B)[a]		
9.7	574	297	1694	9.63	(9.10B)[a]		
9.8	575	308	2371	9.64	(9.11B)[a]		
9.9B	576	264	1611	9.65	621	267	1545
9.10B	577	248	1518	9.66	(9.1)[a]		
9.11B	578	257	2371	9.67	622	446	2371
9.12B	579	241	2371	9.68	(9.50)[a]		
9.13B	580	267	1545	9.69	623	446	2371
9.14B	581	234	1610	9.70	(9.52)[a]		
9.15B	582	226	1613	9.71	624	446	2371
9.16B	583	225	2371	9.72	(9.54)[a]		
9.17B	584	220	2371	9.73	625	446	2371
9.18B	585	258	1754	9.74	(9.56)[a]		
9.19B	586	203	1594	9.75	626	312	1544
9.20B	587	201	1575	9.76	627	294	1533
9.21B	588	199	2371	9.77	628	305	2371
9.22B	589	196	2371	9.78	(9.6)[a]		
9.23B	590	213	1669	9.79	(9.9B)[a]		
9.24	591	203	1594	9.80	629	267	1545
9.25	592	343	1675	9.81	(9.1)[a]		
9.26	593	292	1647	9.82	(9.49)[a]		
9.27	594	333	2371	9.83	(9.50)[a]		
9.28	595	282	2371	9.84	630	446	2371
9.29	596	344	1623	9.85	(9.52)[a]		
9.30	597	293	1602	9.86	631	312	1544
9.31	598	334	2371	9.87	(9.9B)[a]		
9.32	599	283	2371	9.88	(9.10B)[b]		
9.33	600	295	1833	9.89	(9.12B)[b]		
9.34	601	287	1782	9.90	(9.19A)[b]		
9.35	602	285	2371	9.91	(9.22A)[b]		
9.36	603	280	2371	9.92	(6.3)[b]		
9.37	604	298	1823	9.93	(6.2)[b]		
9.38	605	290	1816	9.94	(9.19B)[b]		
9.39	606	289	2371	9.95	(9.19B)[b]		
9.40	607	283	2371	9.96	Residual Group		

Table F.1 (Continued)

Seq. No.	Page No.	T_{min} (°F)	P_{max} (psia)	Seq. No.	Page No.	T_{min} (°F)	P_{max} (psia)
9.97	Residual Group			11.9	(7.11)[b]		
9.98	Residual Group			11.10	Residual Group		
9.99	Residual Group						
10.1	632	386	1080	12.1	640	463	2371
10.2	633	277	1080	12.2	641	463	1942
10.3	634	394	950	12.3	642	356	2371
10.4	635	406	1020	12.4	643	356	1941
10.5	636	406	1401	12.5	Residual Group		
11.1	637	517	2554	13.1	(9.49)[b]		
11.2	638	501	2554	13.2	(9.51)[b]		
11.3	639	516	2554	13.3	(9.52)[b]		
11.4	(11.2)[a]			13.4	(9.53)[b]		
11.5	(11.1)[b]			13.5	(9.54)[b]		
11.6	(11.2)[b]			13.6	(9.55)[b]		
11.7	(7.11)[b]						
11.8	(7.11)[b]			14.1	(9.53)[b]		
				14.2	(9.55)[b]		

[a,b,c]See explanations in accompanying text.

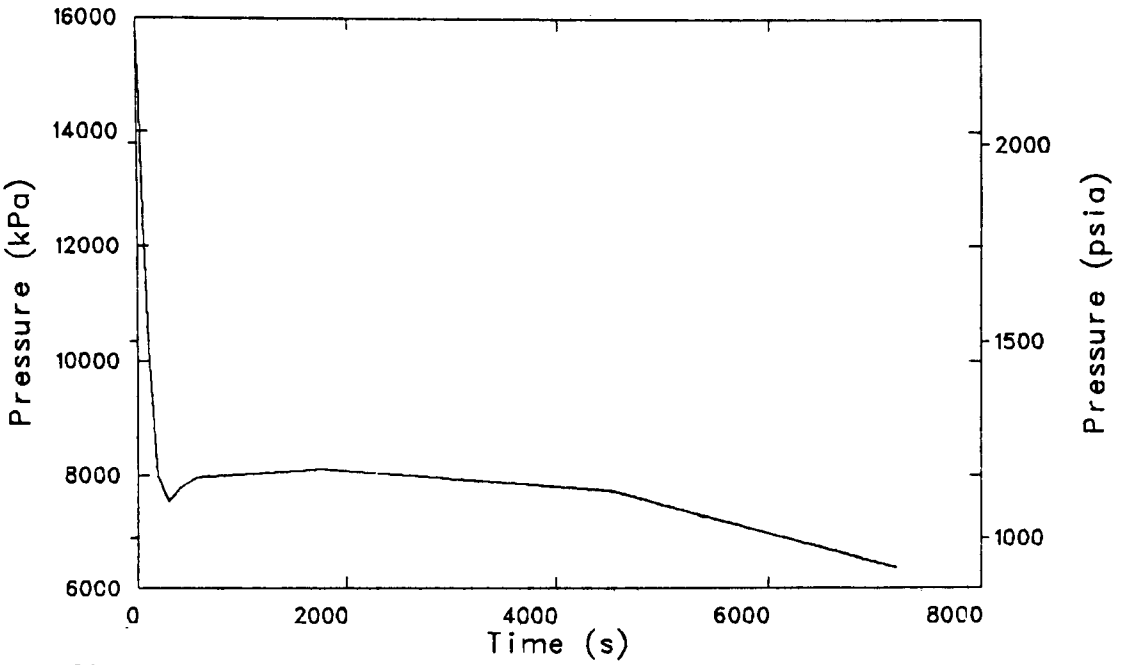

Figure F.1. Sequence 1.1: Reactor vessel downcomer fluid pressure.

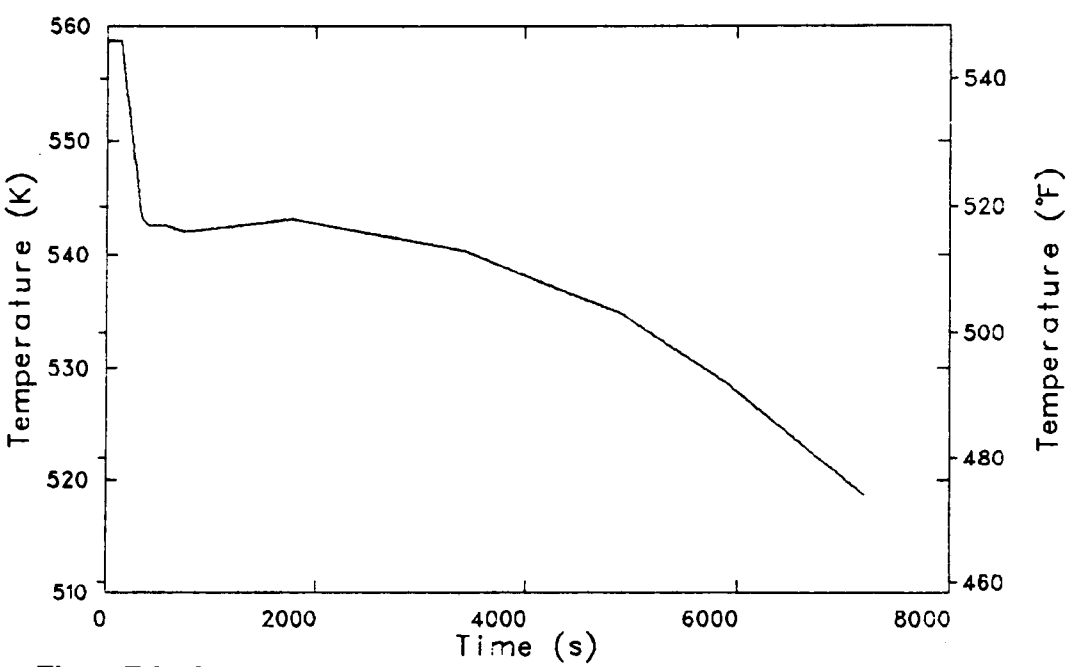

Figure F.2. Sequence 1.1: Reactor vessel downcomer fluid temperatures.

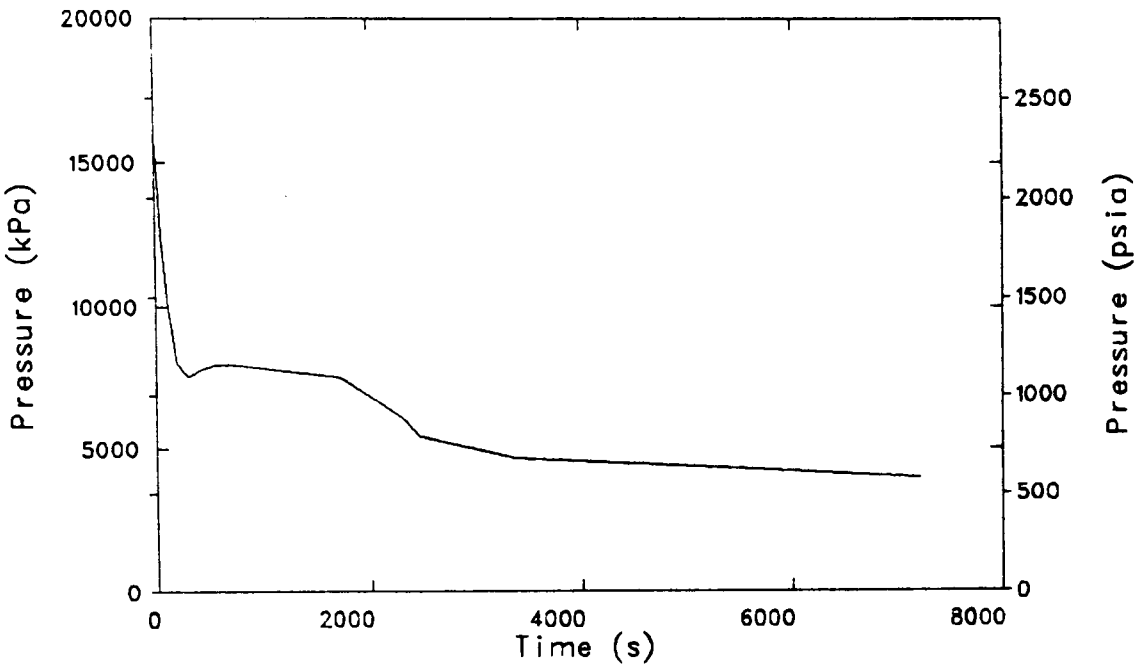

Figure F.3. Sequence 1.2: Reactor vessel downcomer fluid pressure.

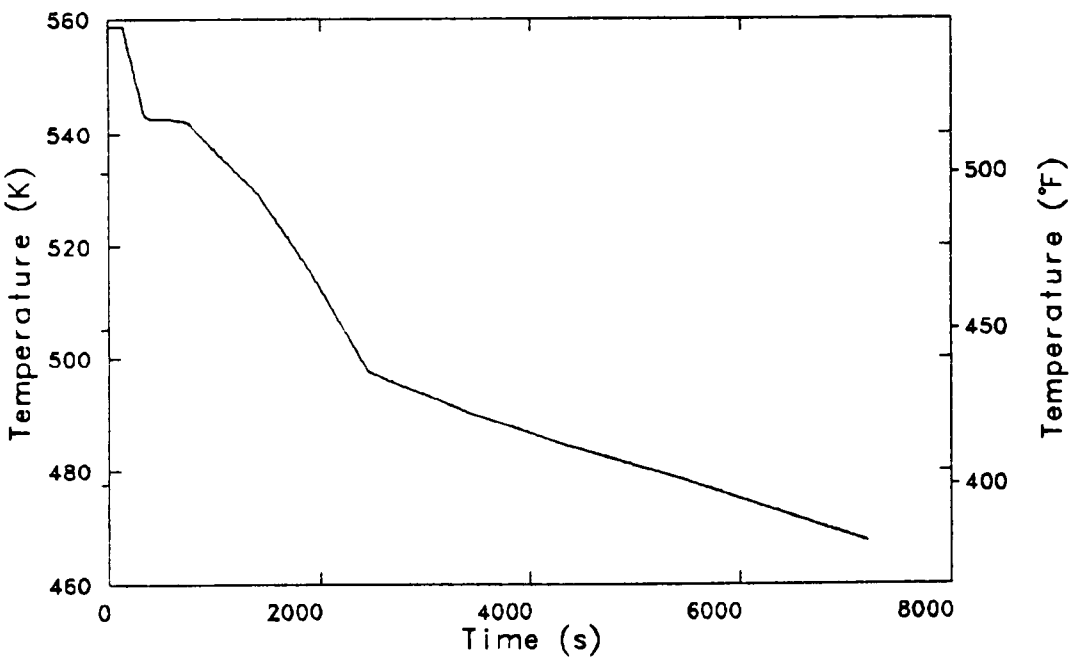

Figure F.4. Sequence 1.2: Reactor vessel downcomer fluid temperatures.

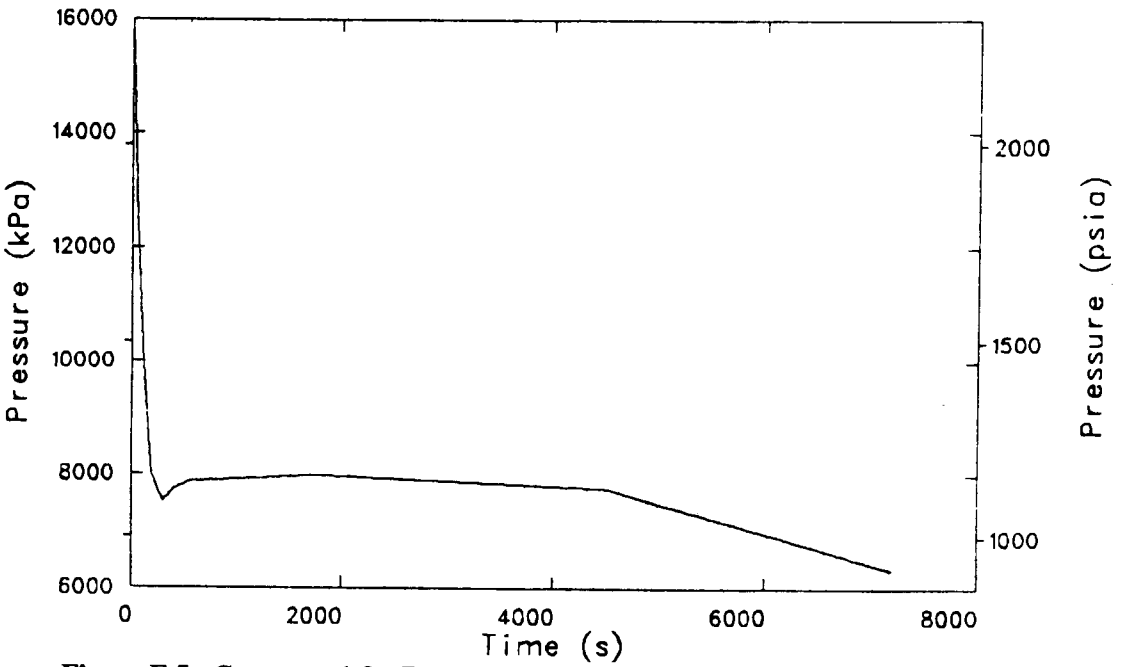

Figure F.5. Sequence 1.3: Reactor vessel downcomer fluid pressure.

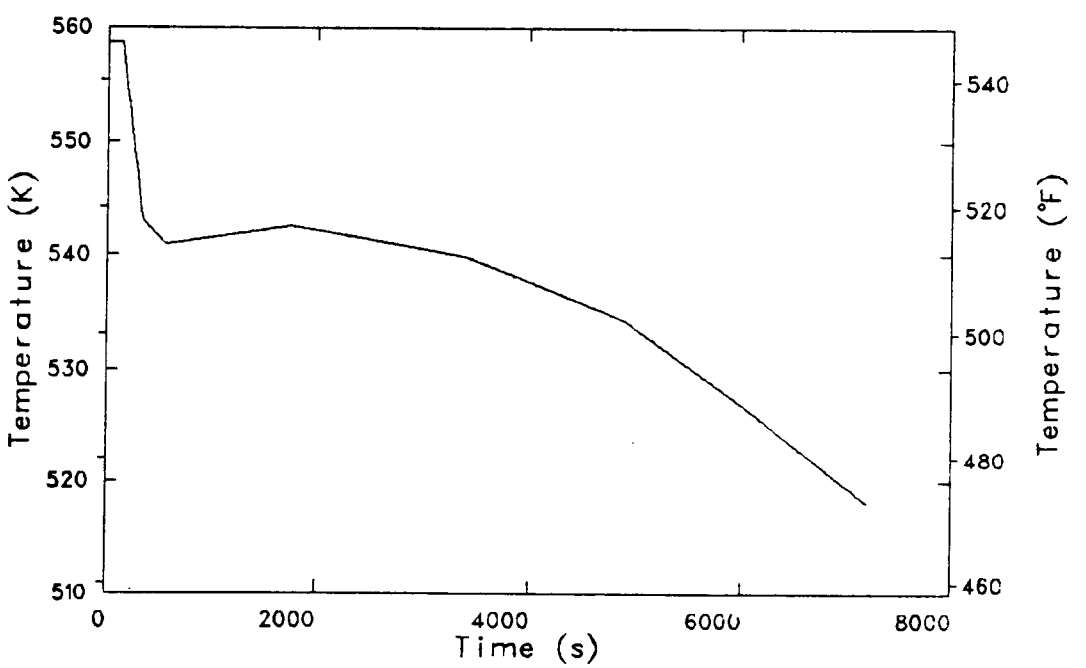

Figure F.6. Sequence 1.3: Reactor vessel downcomer fluid temperatures.

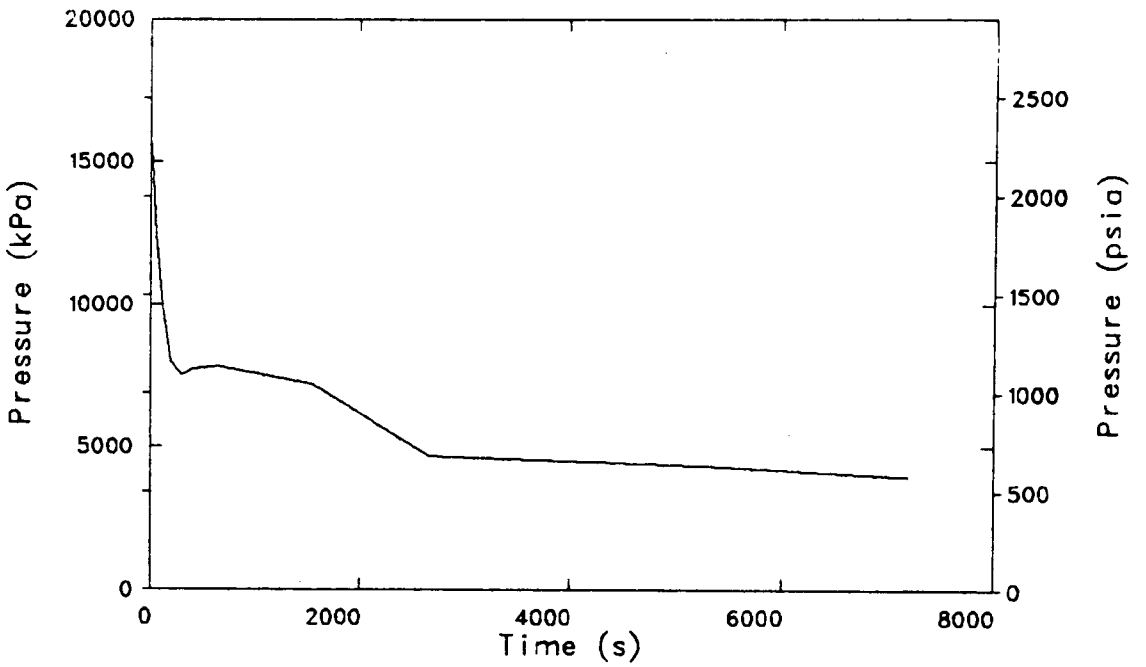

Figure F.7. Sequence 1.4: Reactor vessel downcomer fluid pressure.

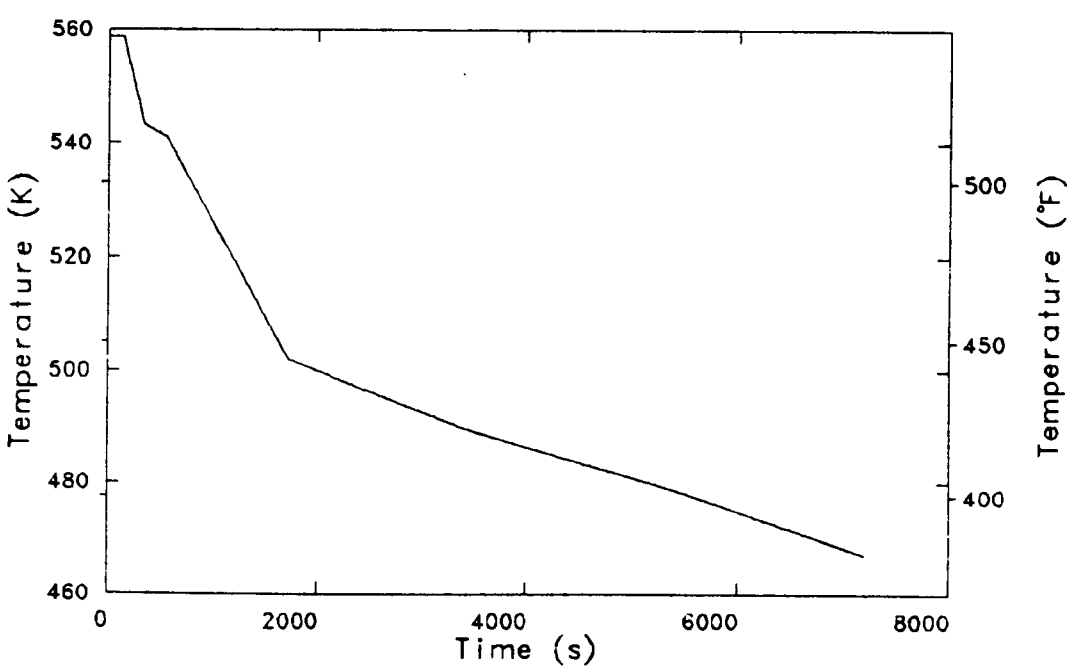

Figure F.8. Sequence 1.4: Reactor vessel downcomer fluid temperatures.

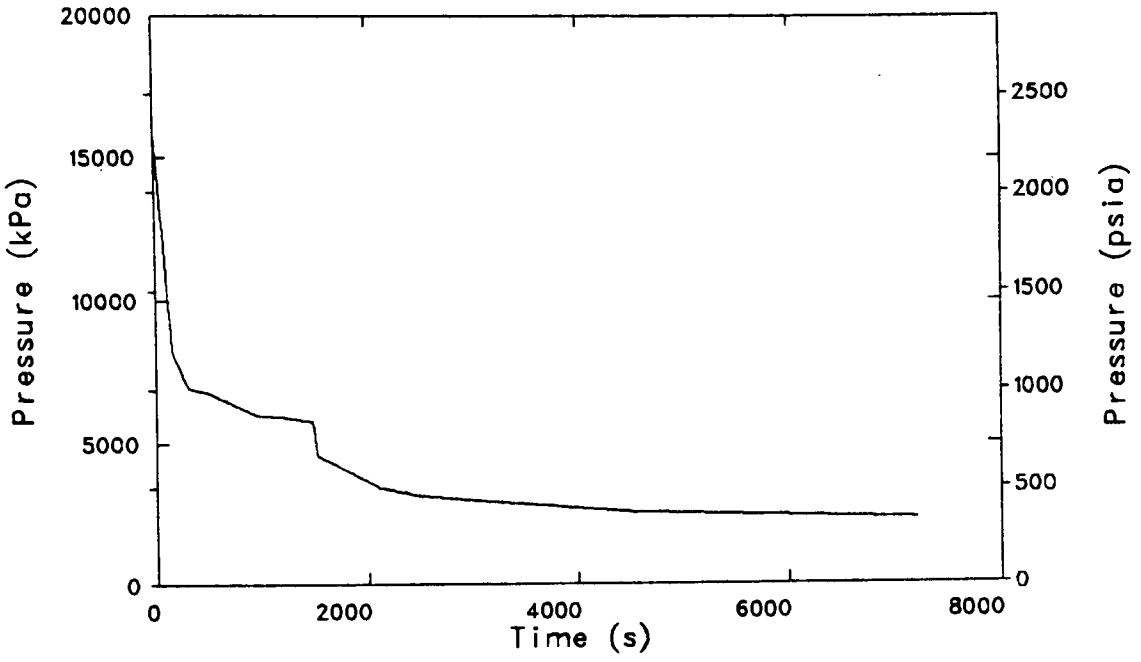

Figure F.9. Sequence 1.5: Reactor vessel downcomer fluid pressure.

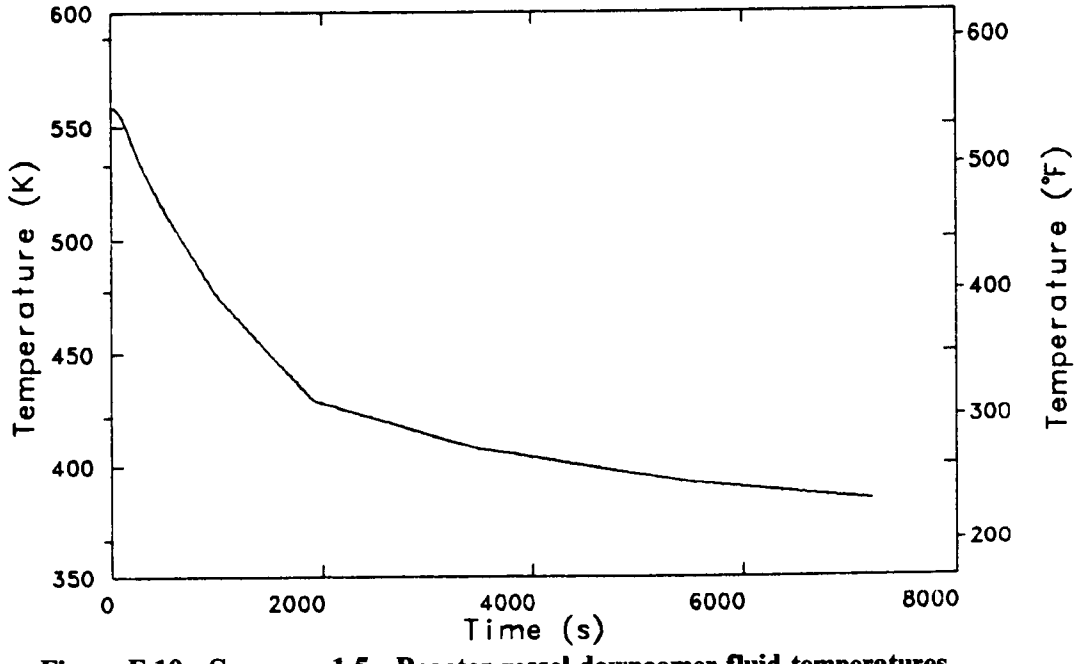

Figure F.10. Sequence 1.5: Reactor vessel downcomer fluid temperatures.

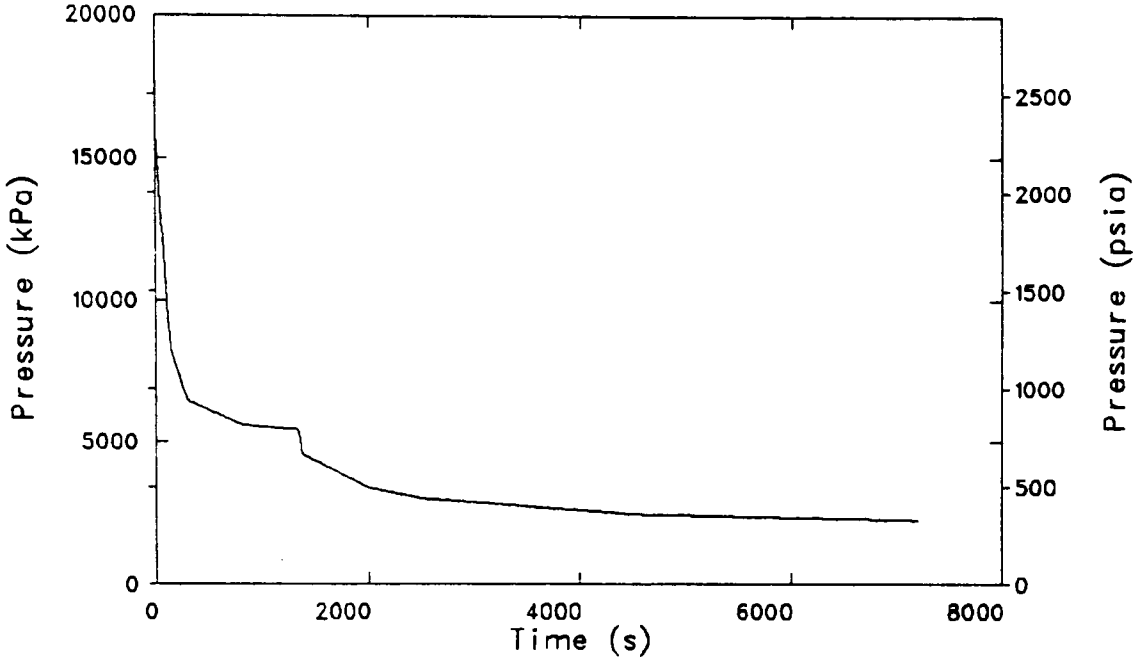

Figure F.11. Sequence 1.6: Reactor vessel downcomer fluid pressure.

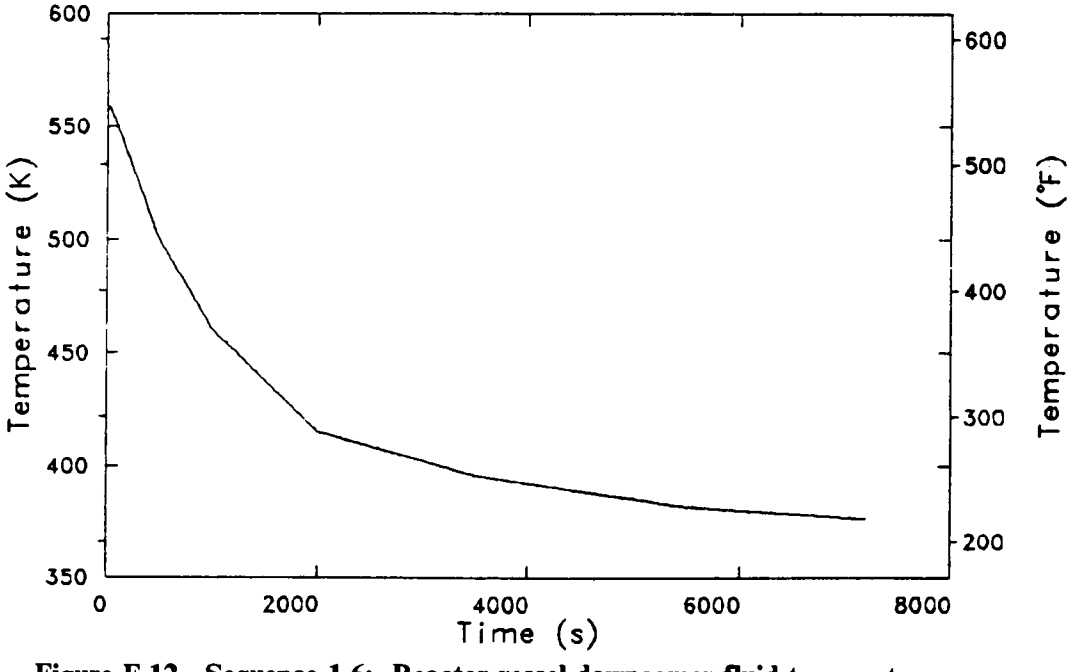

Figure F.12. Sequence 1.6: Reactor vessel downcomer fluid temperatures.

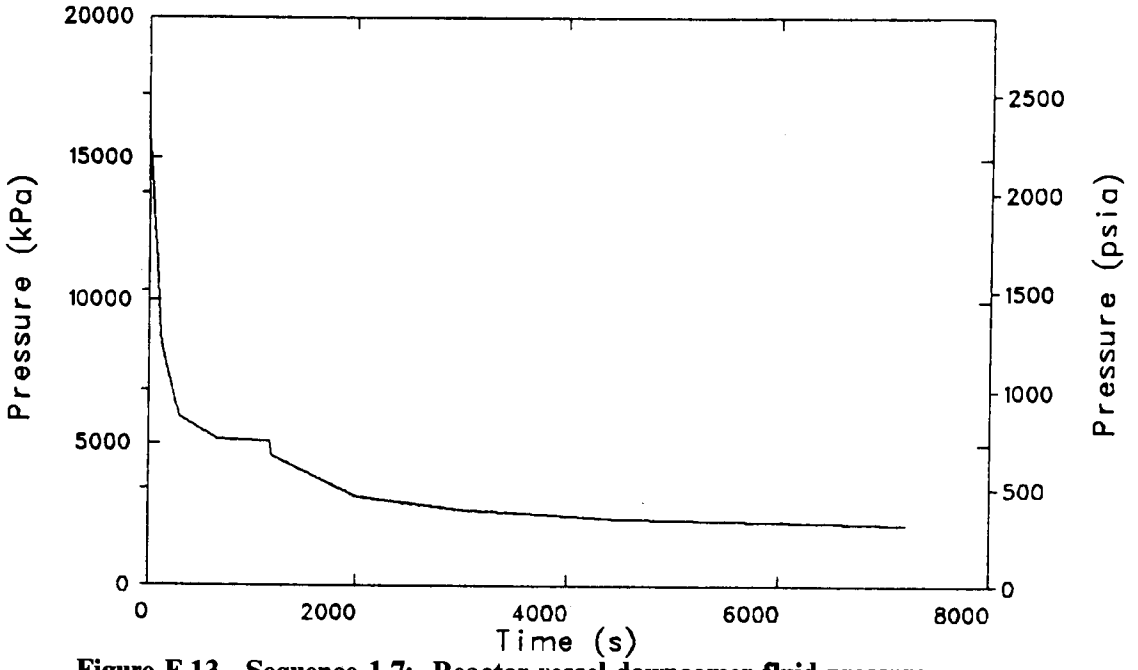

Figure F.13. Sequence 1.7: Reactor vessel downcomer fluid pressure.

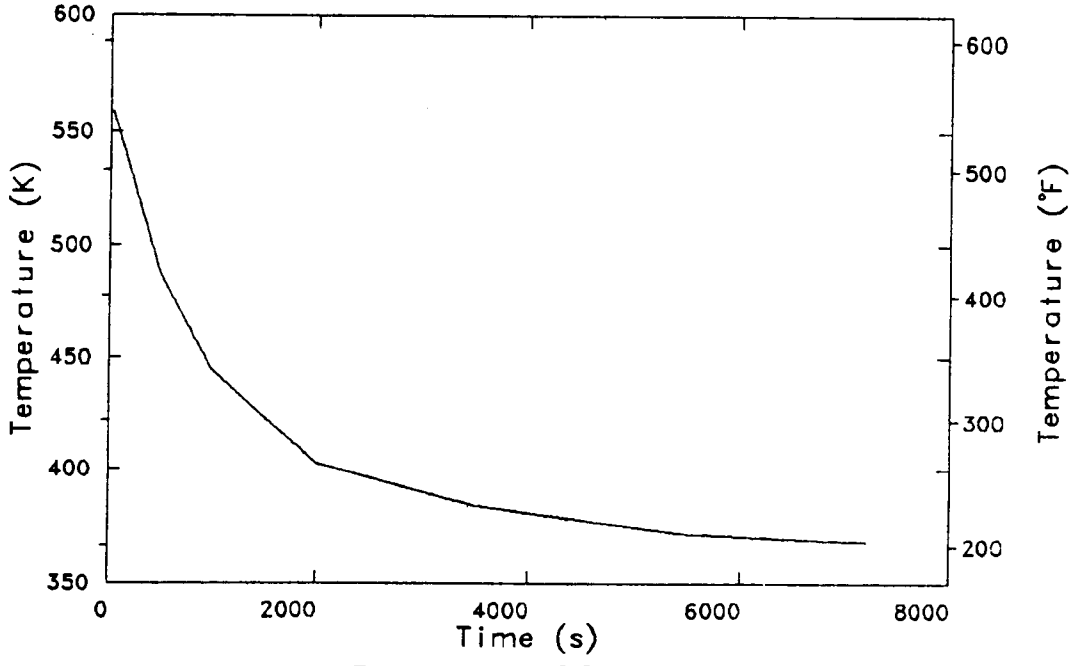

Figure F.14. Sequence 1.7: Reactor vessel downcomer fluid temperatures.

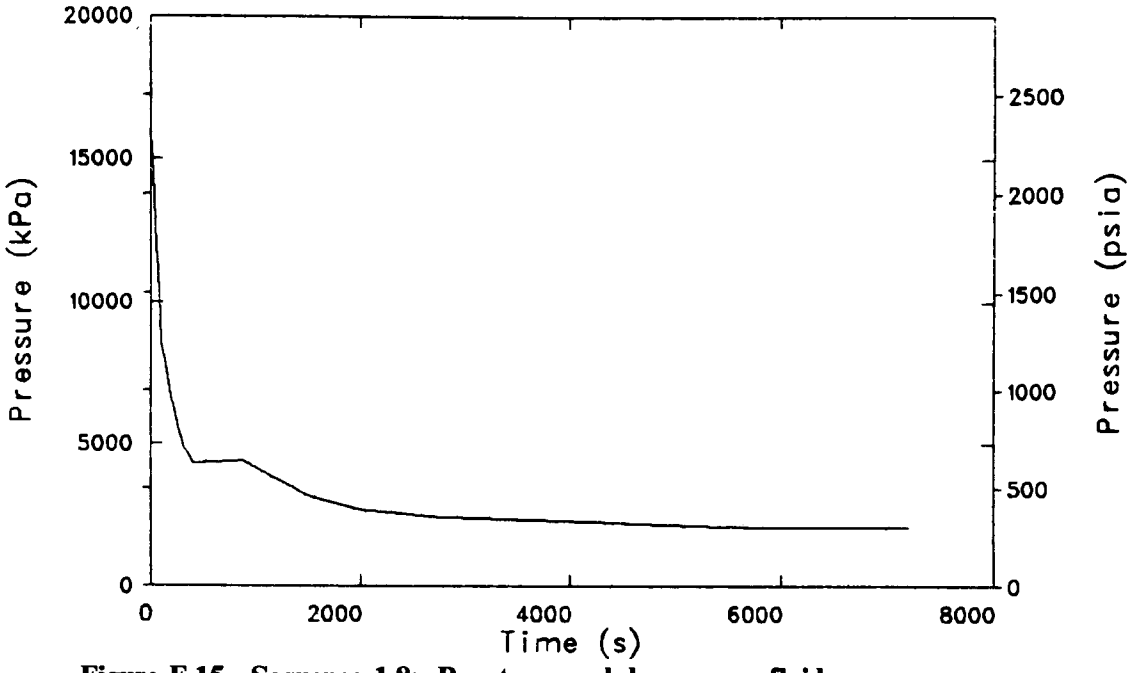

Figure F.15. Sequence 1.8: Reactor vessel downcomer fluid pressure.

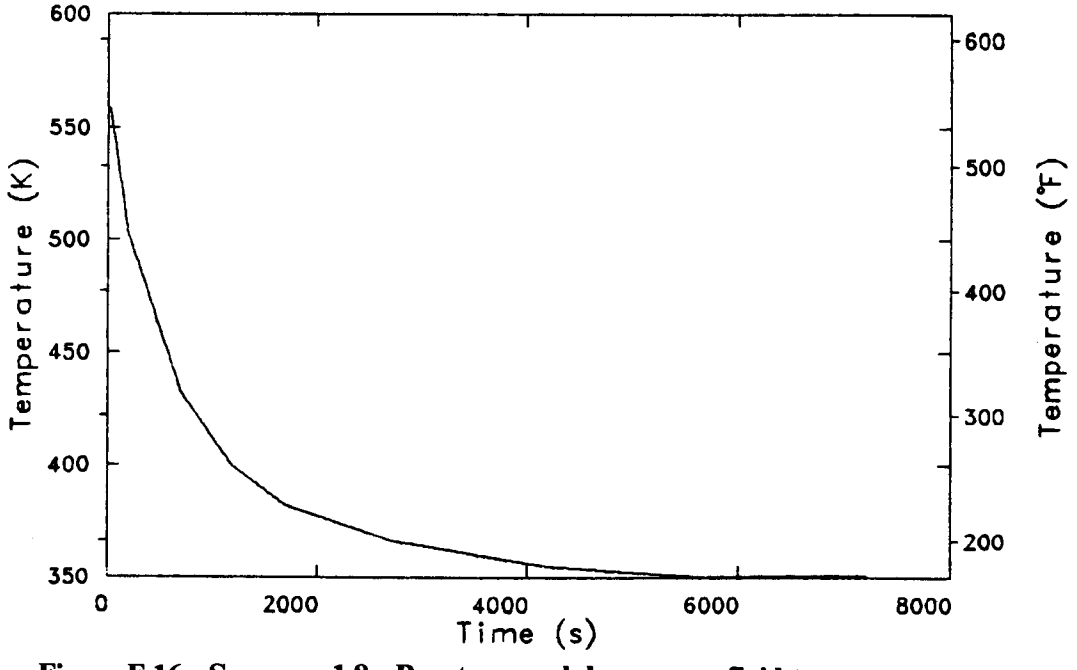

Figure F.16. Sequence 1.8: Reactor vessel downcomer fluid temperatures.

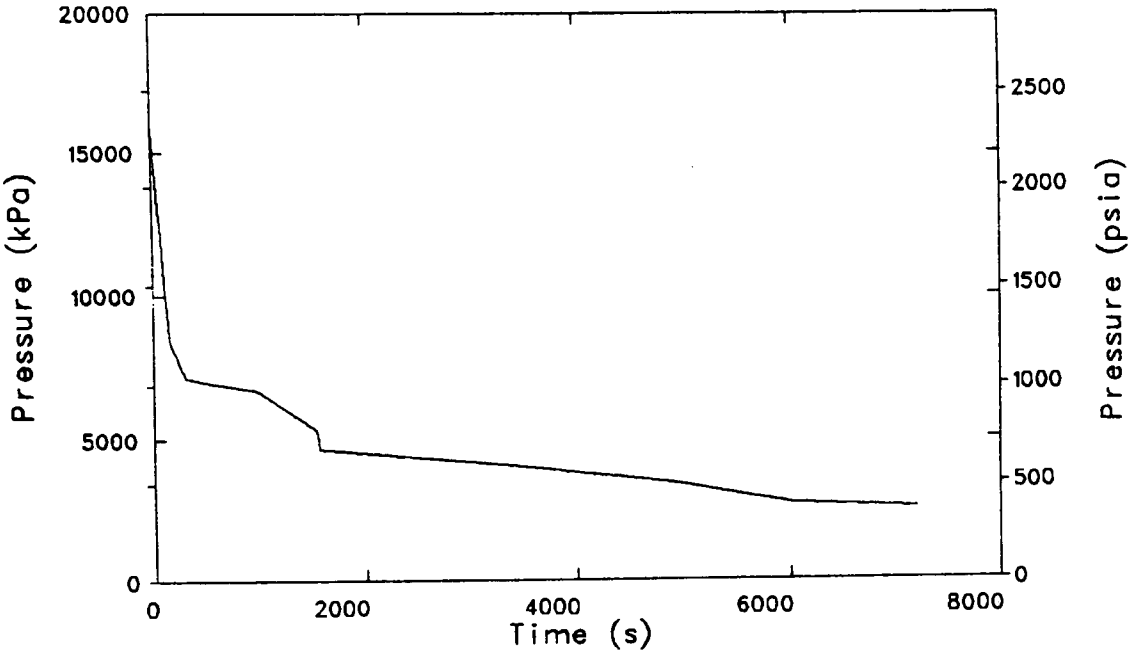

Figure F.17. Sequence 1.9: Reactor vessel downcomer fluid pressure.

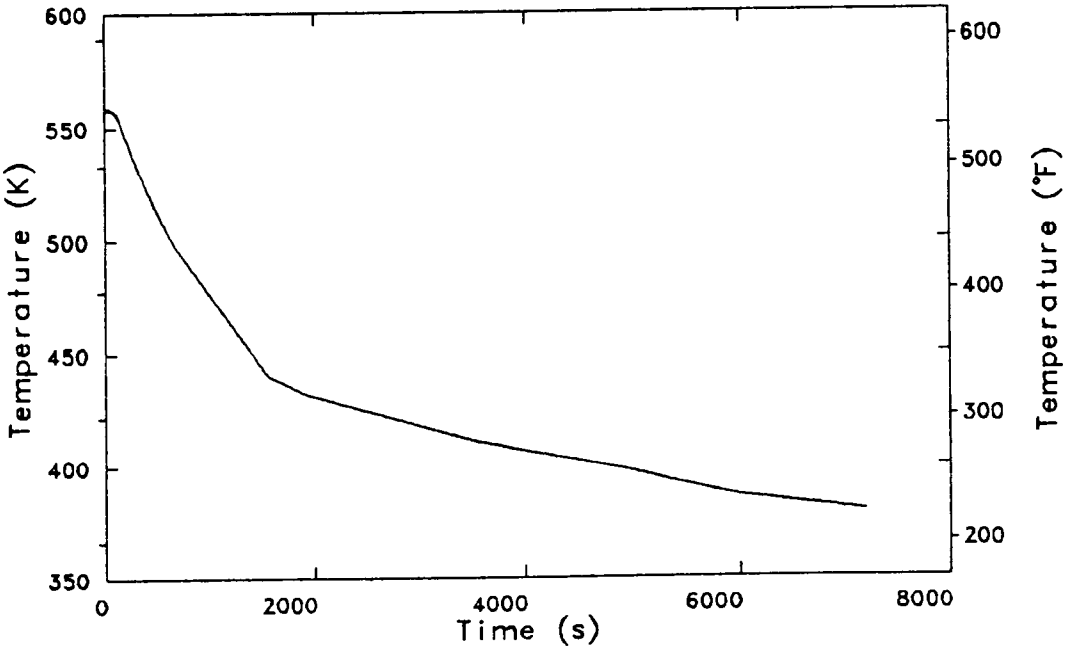

Figure F.18. Sequence 1.9: Reactor vessel downcomer fluid temperatures.

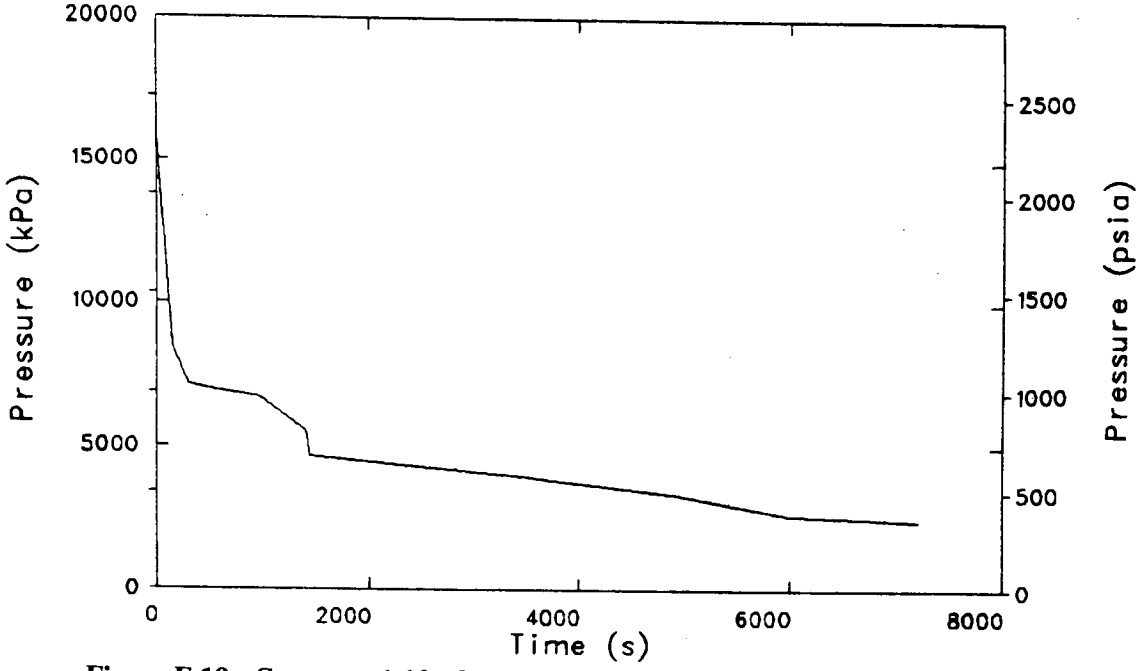

Figure F.19. Sequence 1.10: Reactor vessel downcomer fluid pressure.

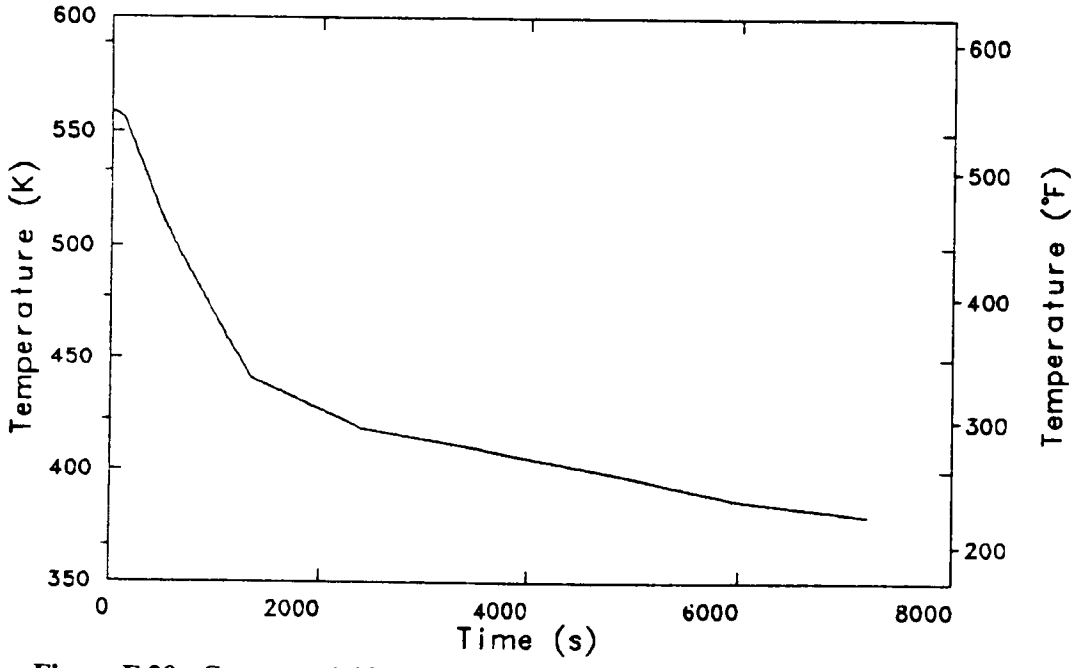

Figure F.20. Sequence 1.10: Reactor vessel downcomer fluid temperatures.

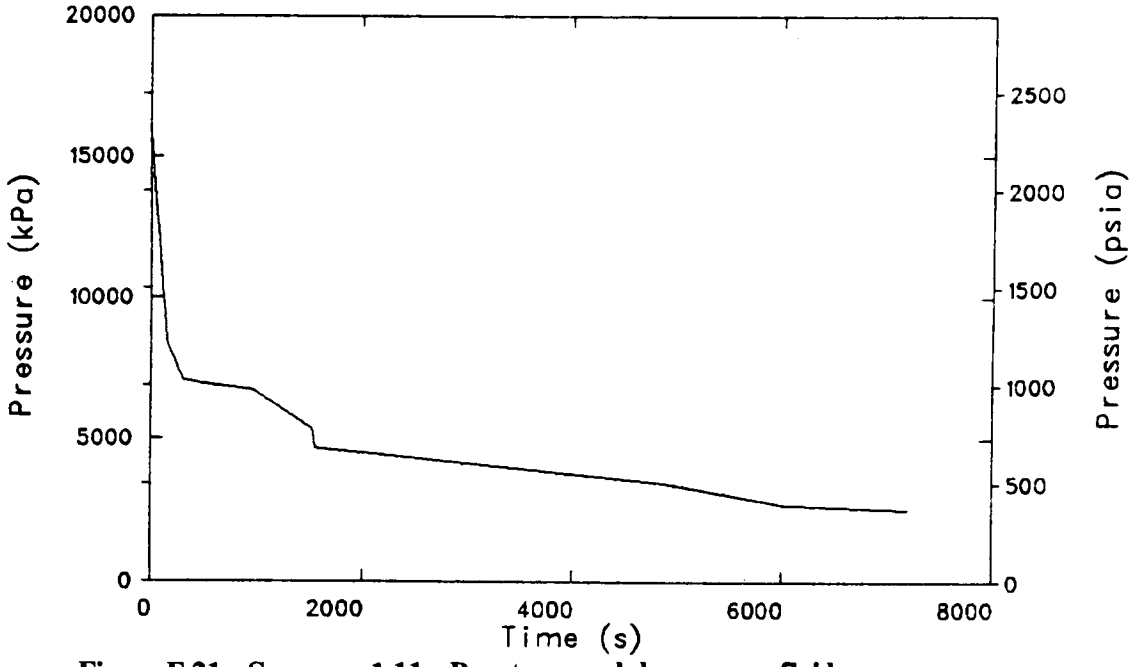

Figure F.21. Sequence 1.11: Reactor vessel downcomer fluid pressure.

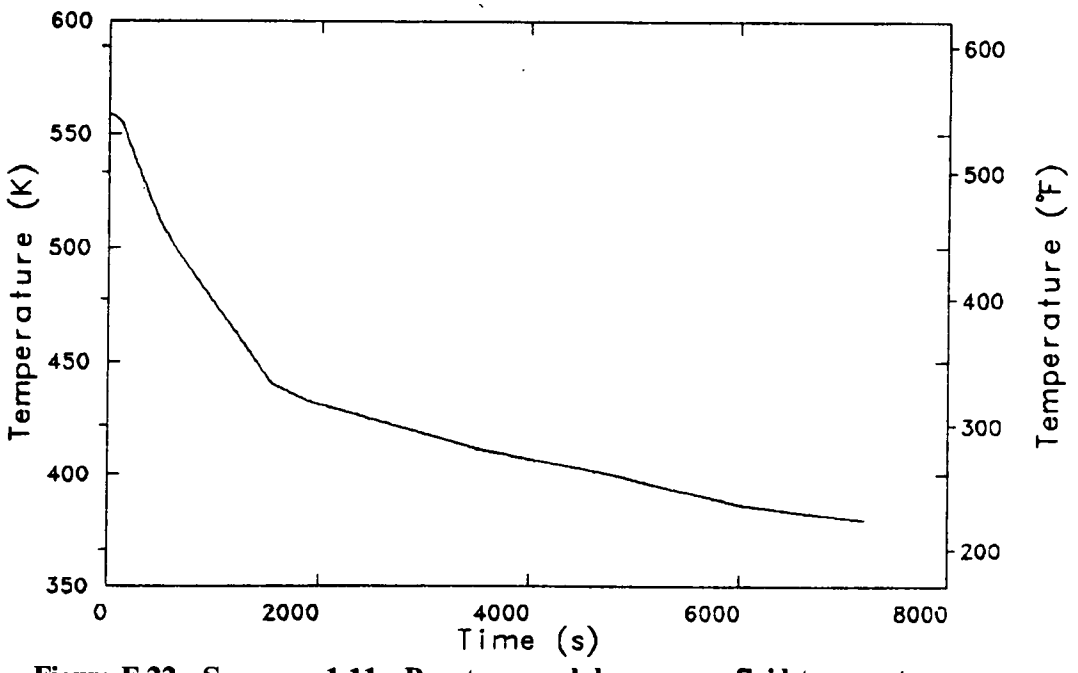

Figure F.22. Sequence 1.11: Reactor vessel downcomer fluid temperatures.

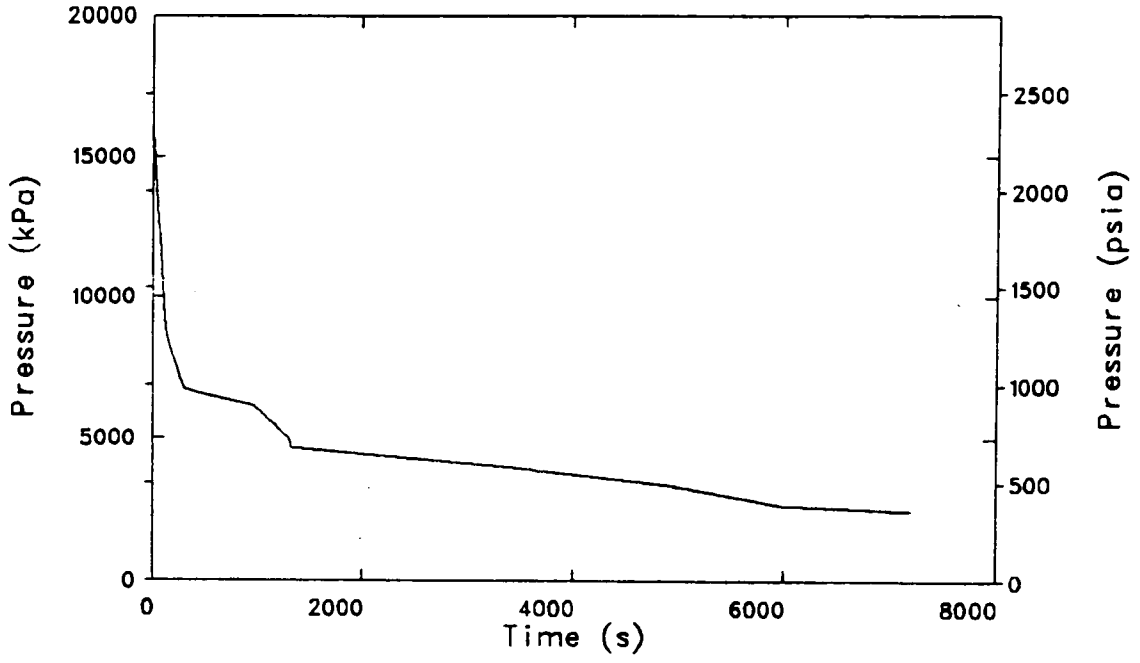

Figure F.23. Sequence 1.12: Reactor vessel downcomer fluid pressure.

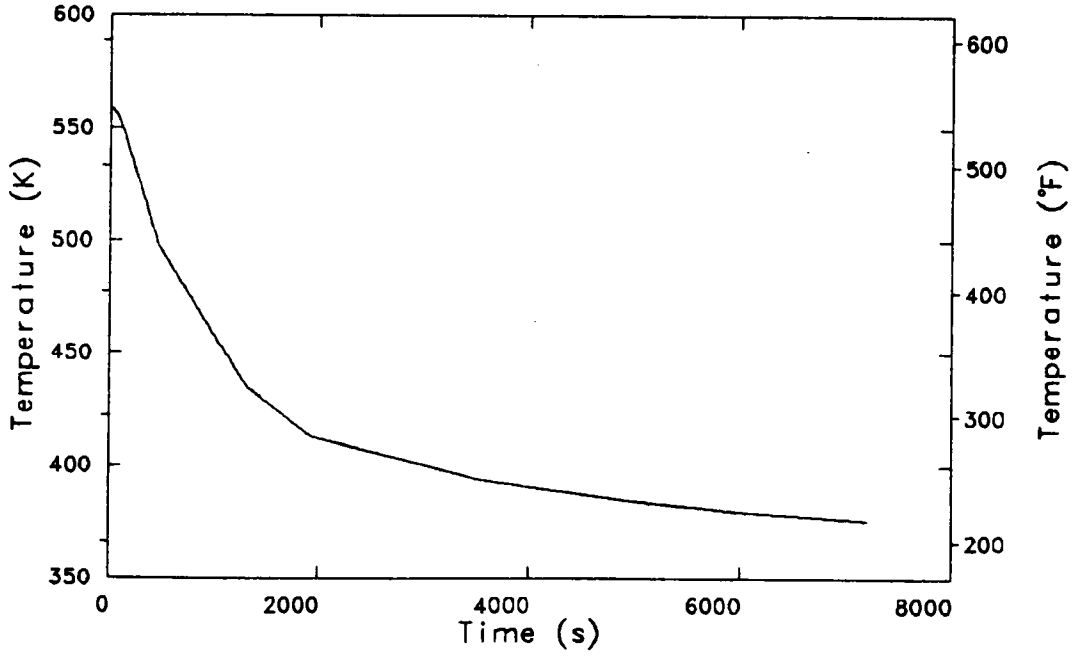

Figure F.24. Sequence 1.12: Reactor vessel downcomer fluid temperatures.

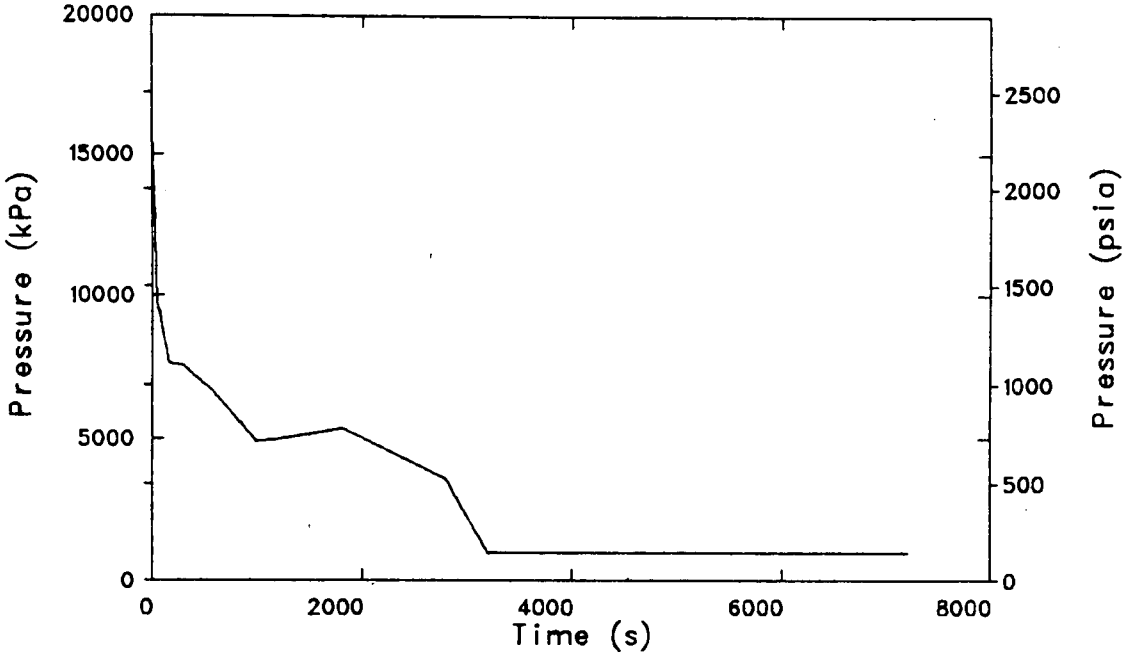

Figure F.25. Sequence 2.1: Reactor vessel downcomer fluid pressure.

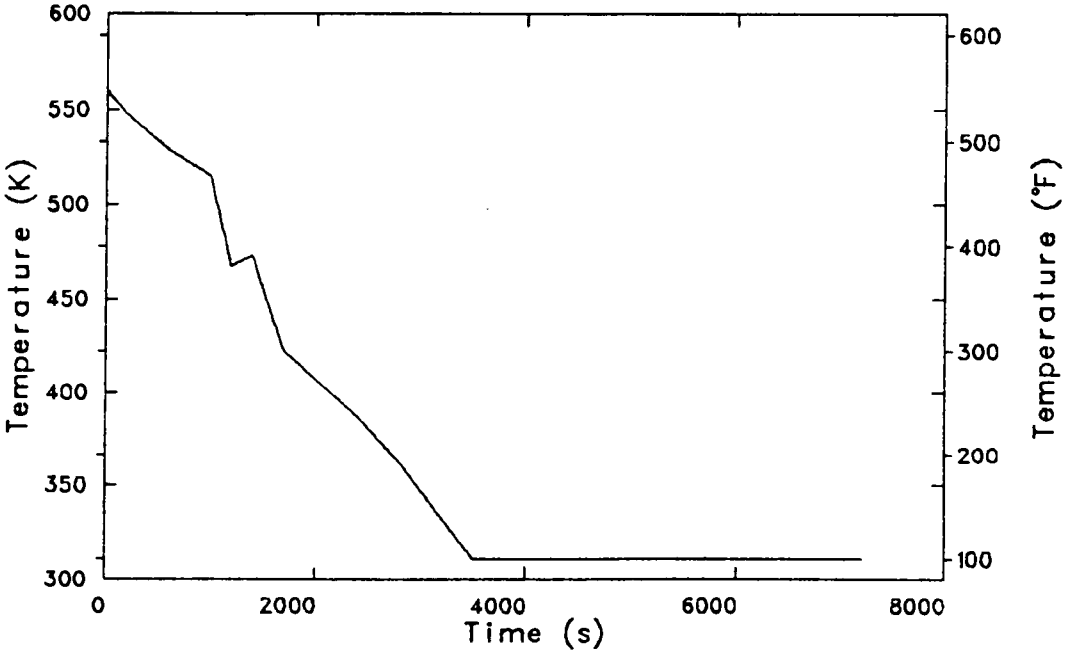

Figure F.26. Sequence 2.1: Reactor vessel downcomer fluid temperatures.

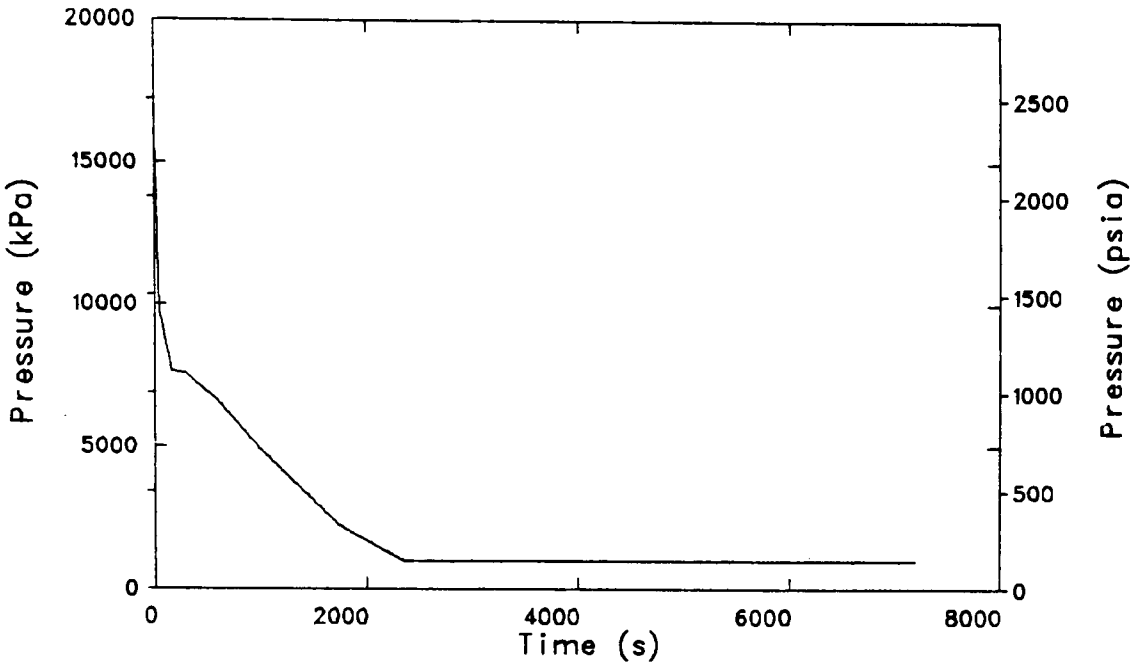

Figure F.27. Sequence 2.2: Reactor vessel downcomer fluid pressure.

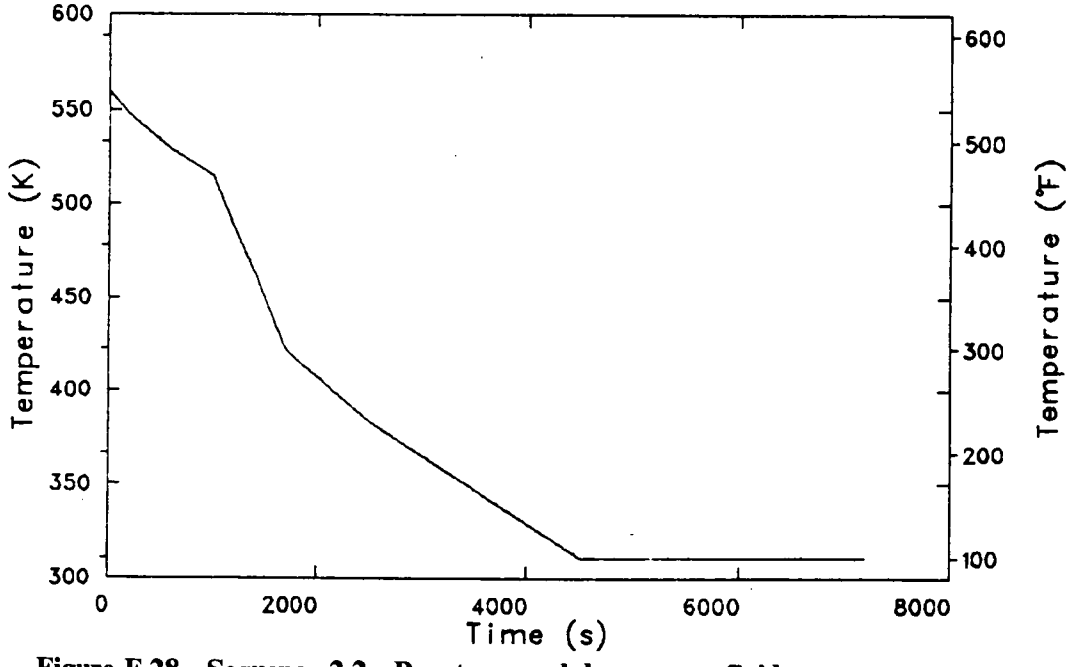

Figure F.28. Sequence 2.2: Reactor vessel downcomer fluid temperatures.

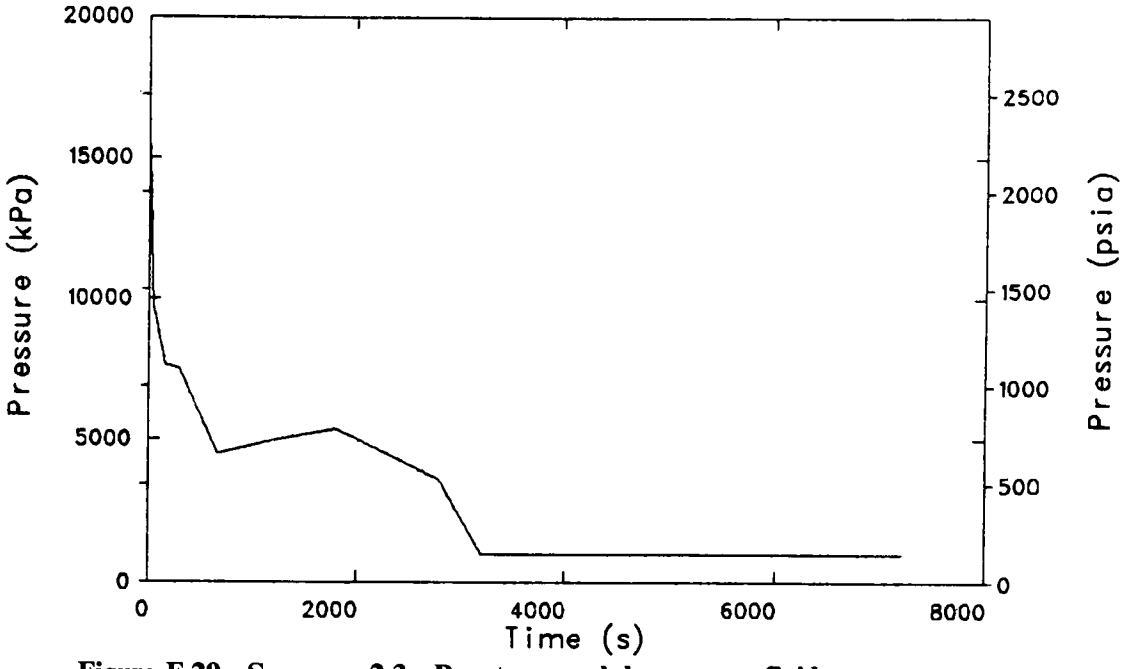

Figure F.29. Sequence 2.3: Reactor vessel downcomer fluid pressure.

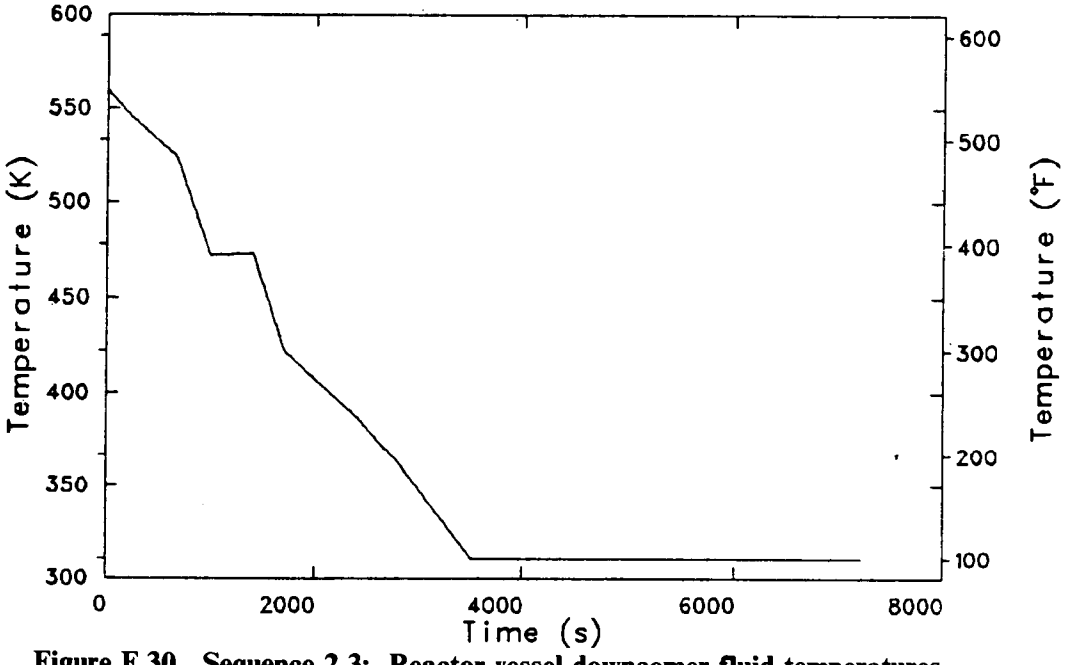

Figure F.30. Sequence 2.3: Reactor vessel downcomer fluid temperatures.

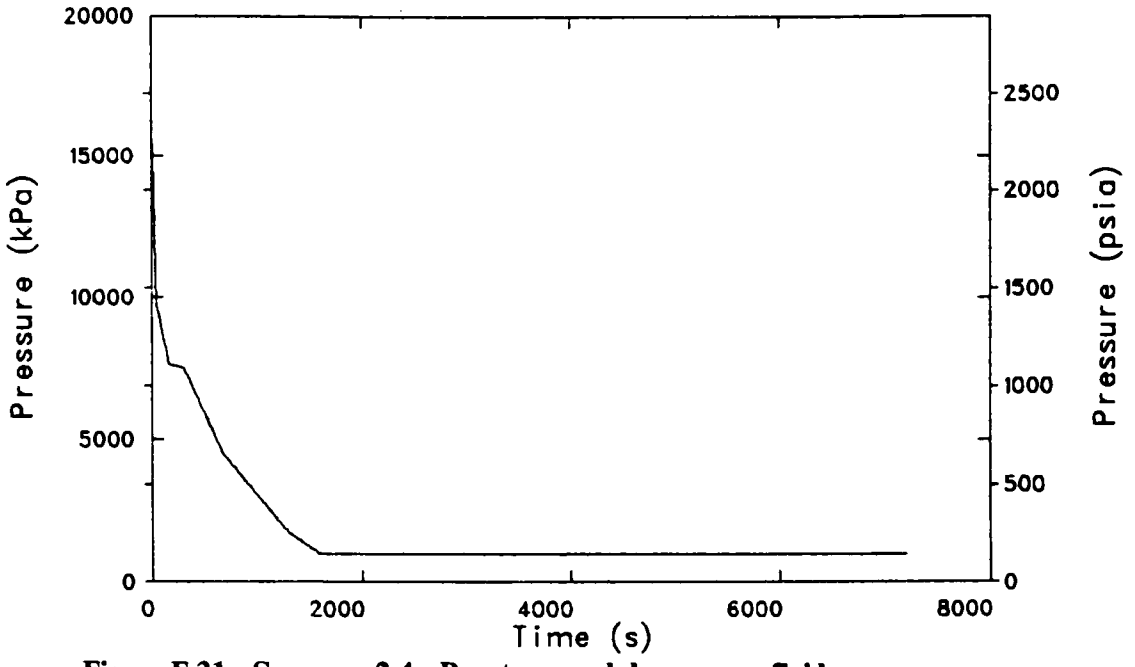

Figure F.31. Sequence 2.4: Reactor vessel downcomer fluid pressure.

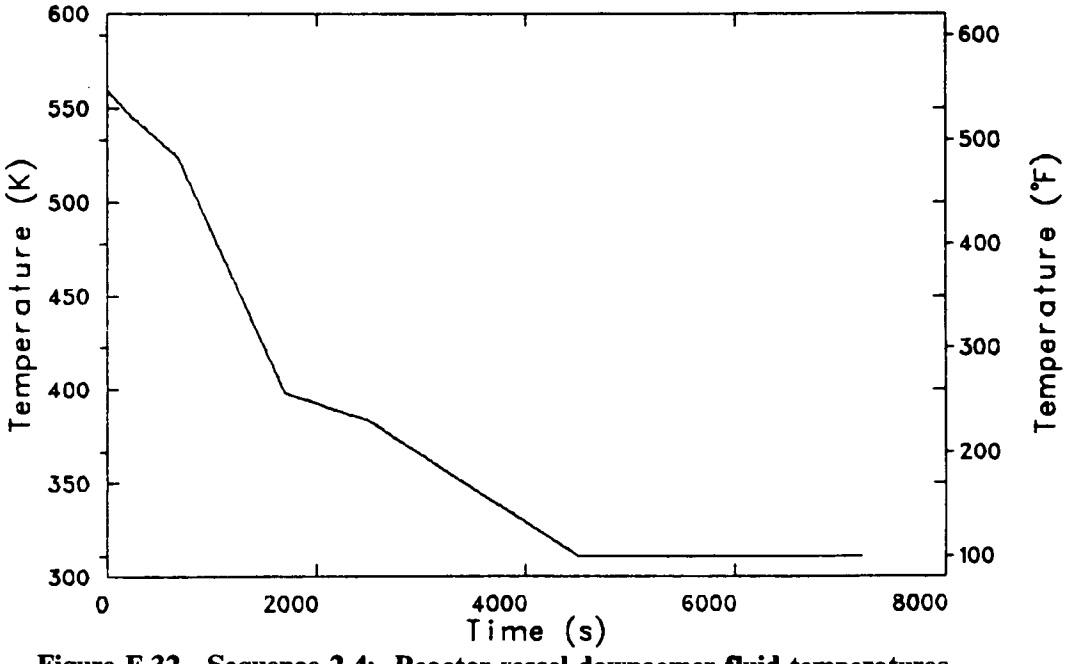

Figure F.32. Sequence 2.4: Reactor vessel downcomer fluid temperatures.

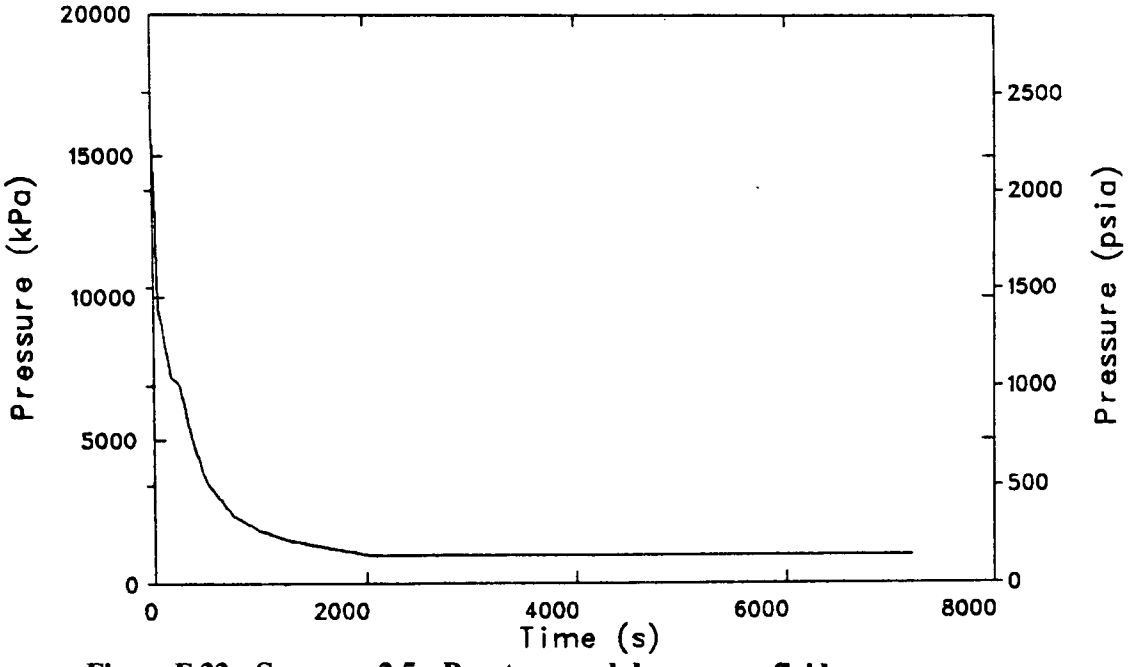

Figure F.33. Sequence 2.5: Reactor vessel downcomer fluid pressure.

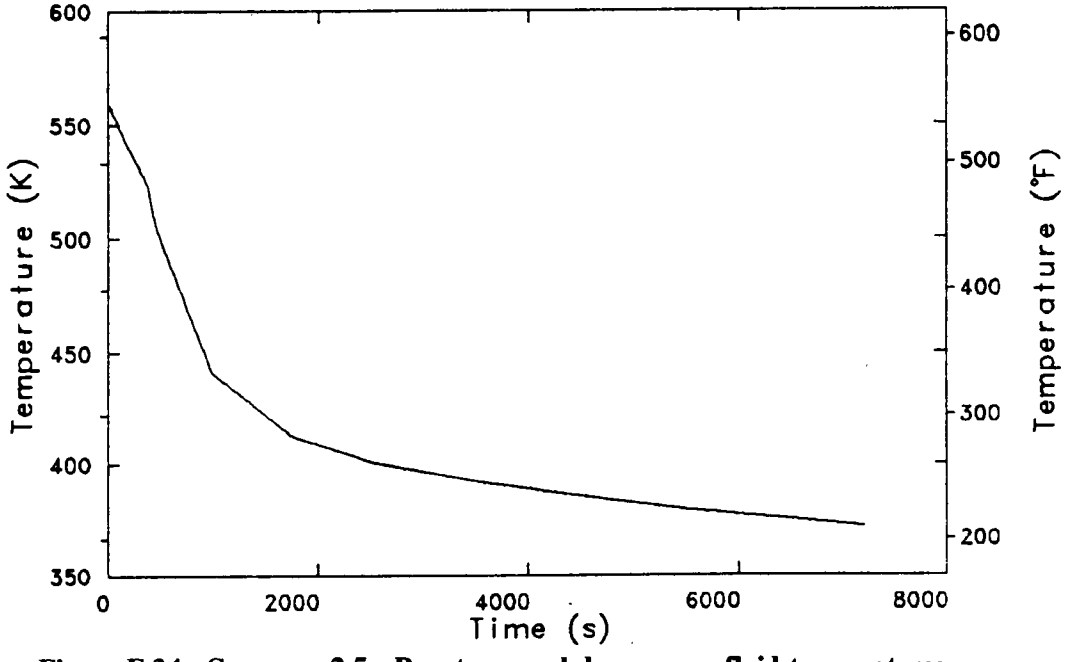

Figure F.34. Sequence 2.5: Reactor vessel downcomer fluid temperatures.

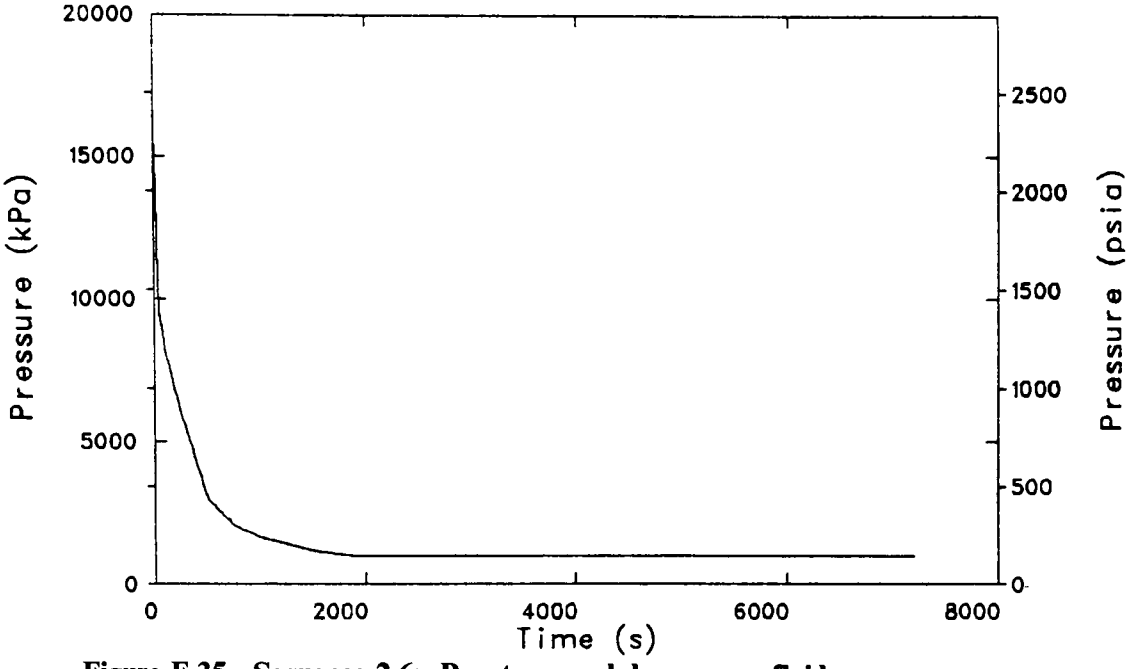

Figure F.35. Sequence 2.6: Reactor vessel downcomer fluid pressure.

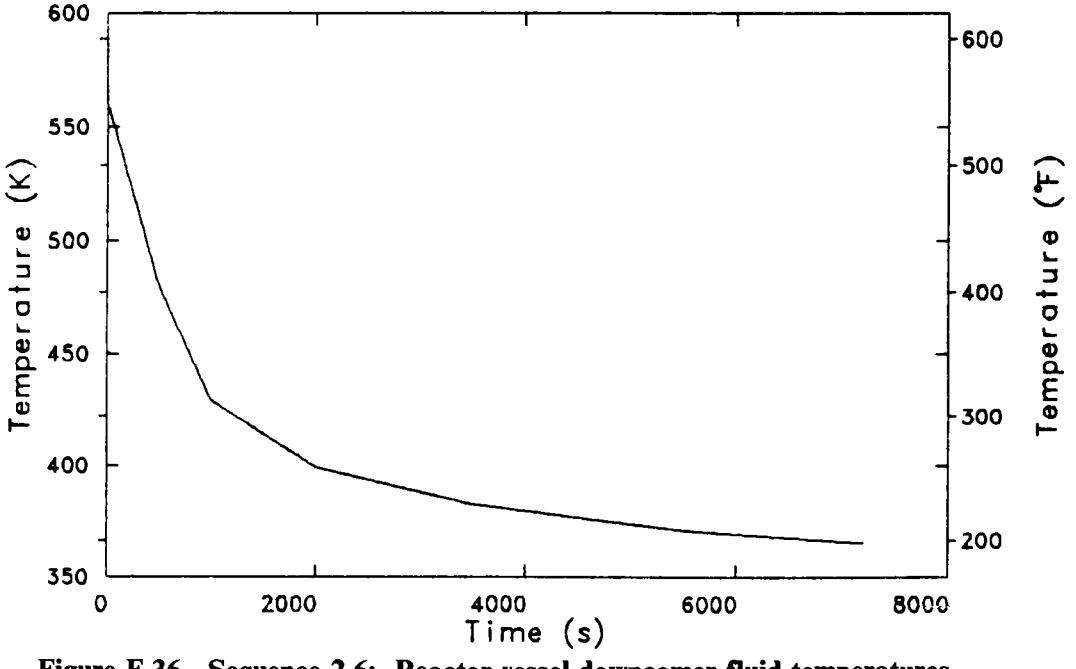

Figure F.36. Sequence 2.6: Reactor vessel downcomer fluid temperatures.

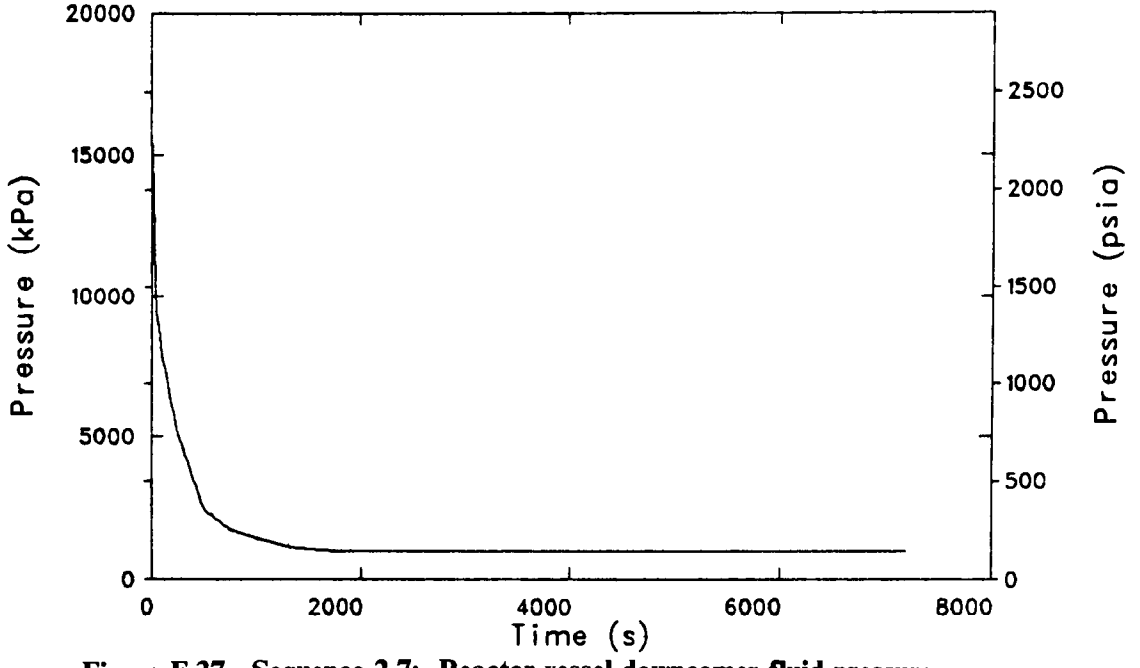

Figure F.37. Sequence 2.7: Reactor vessel downcomer fluid pressure.

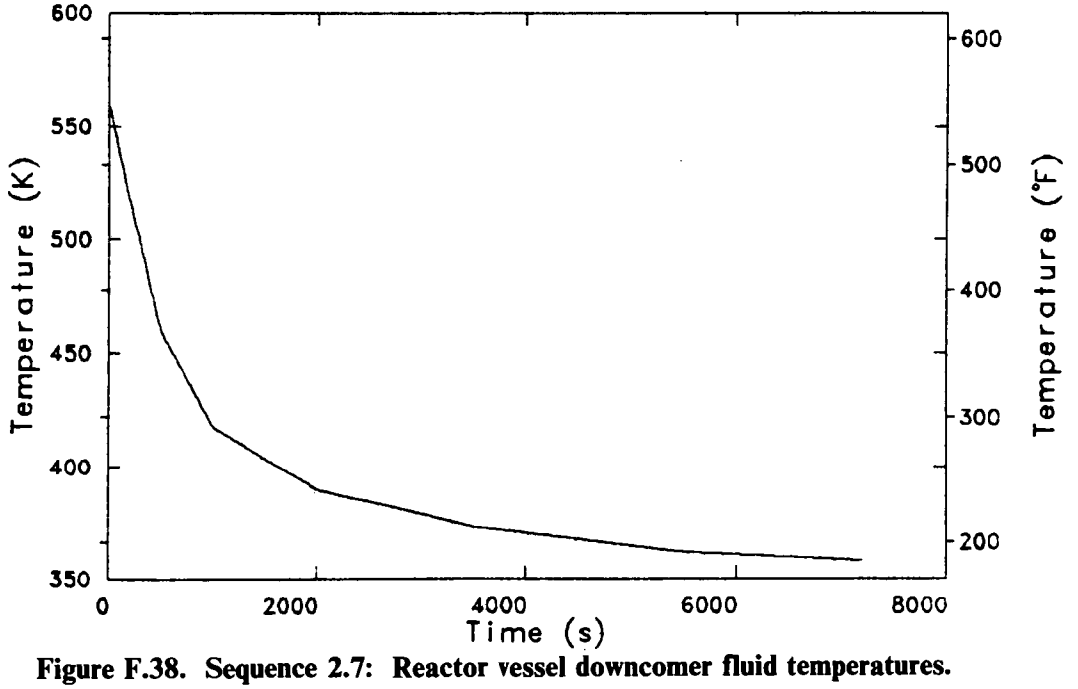

Figure F.38. Sequence 2.7: Reactor vessel downcomer fluid temperatures.

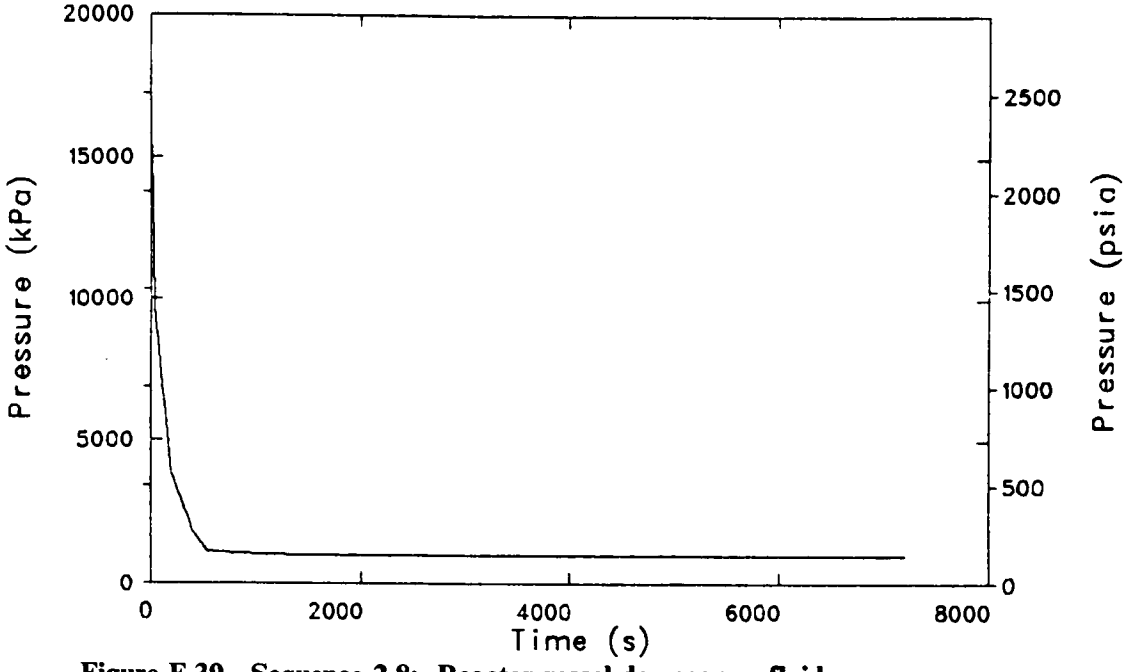

Figure F.39. Sequence 2.8: Reactor vessel downcomer fluid pressure.

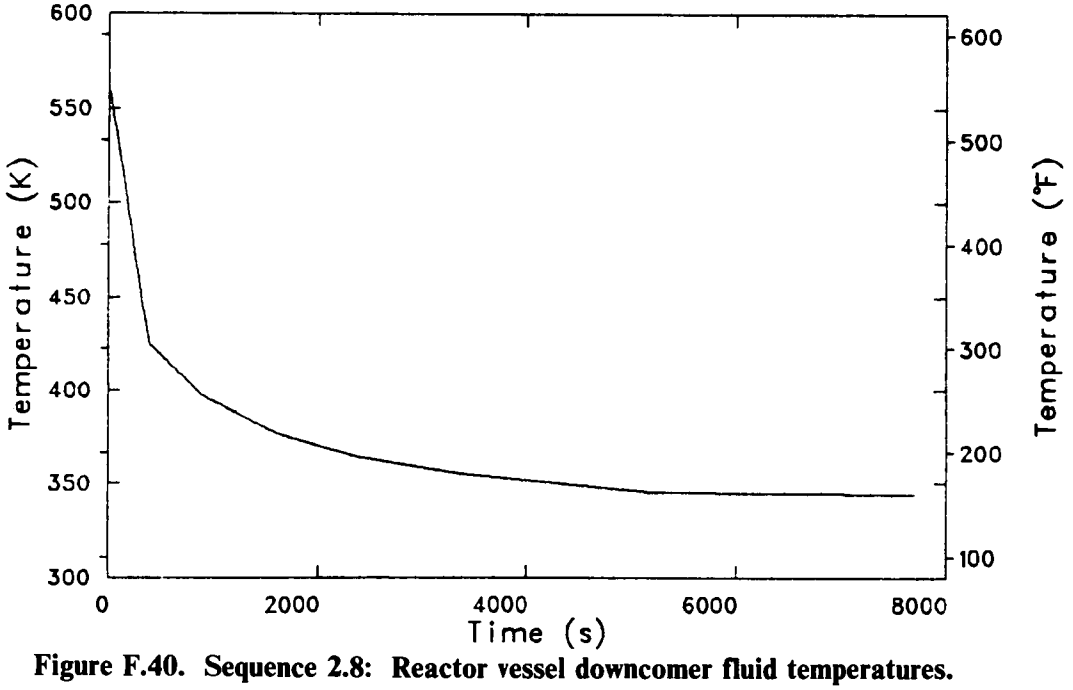

Figure F.40. Sequence 2.8: Reactor vessel downcomer fluid temperatures.

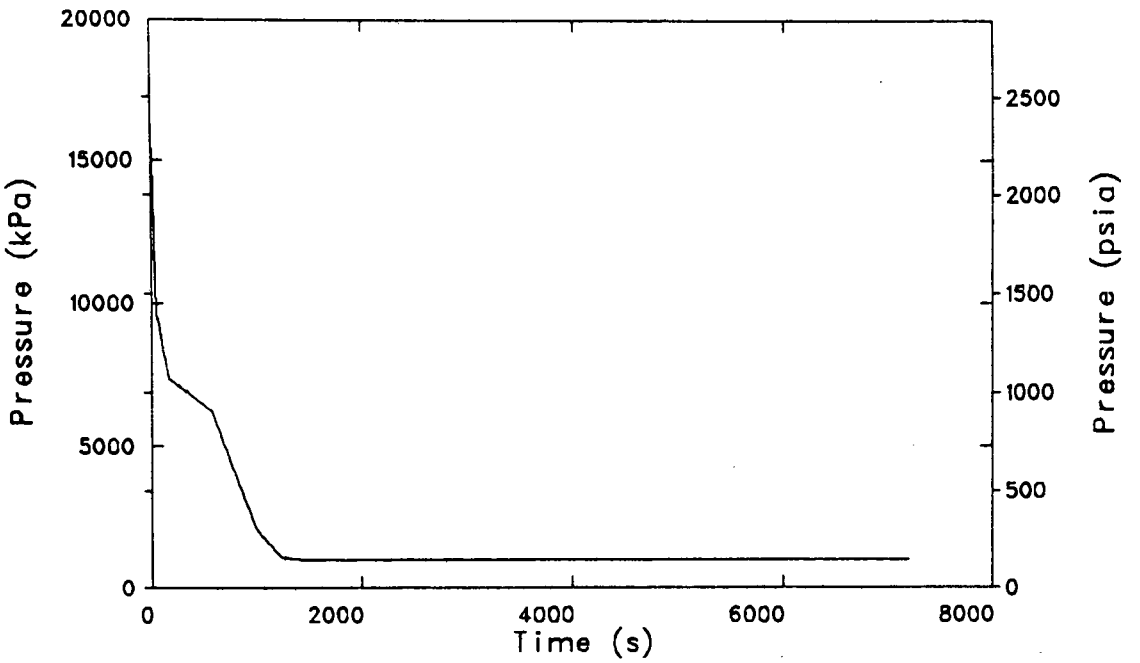

Figure F.41. Sequence 2.9: Reactor vessel downcomer fluid pressure.

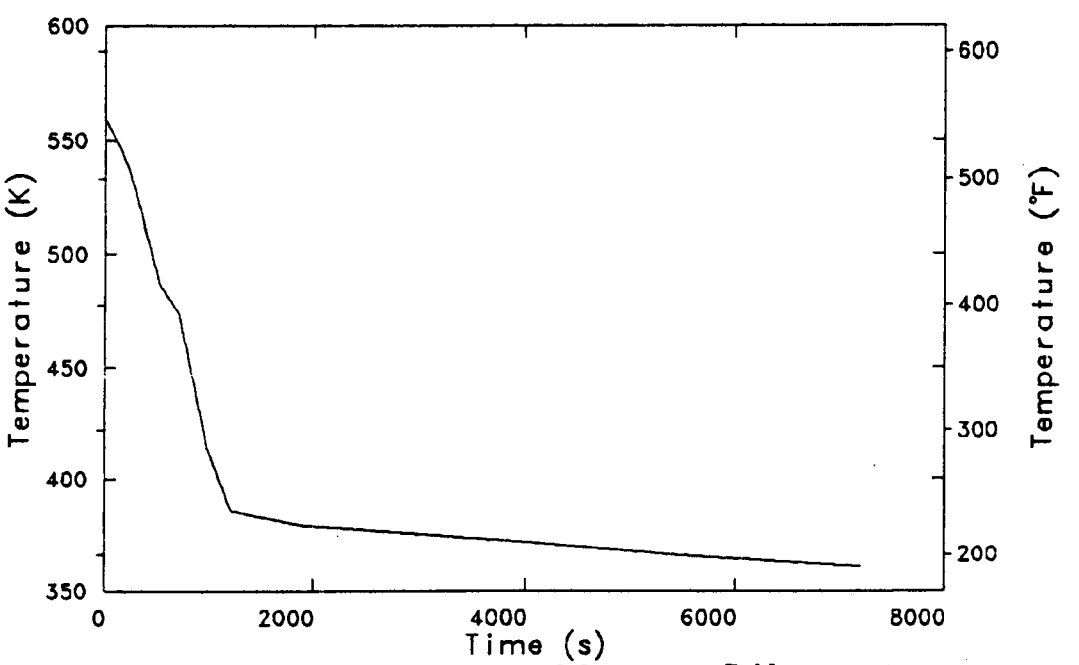

Figure F.42. Sequence 2.9: Reactor vessel downcomer fluid temperatures.

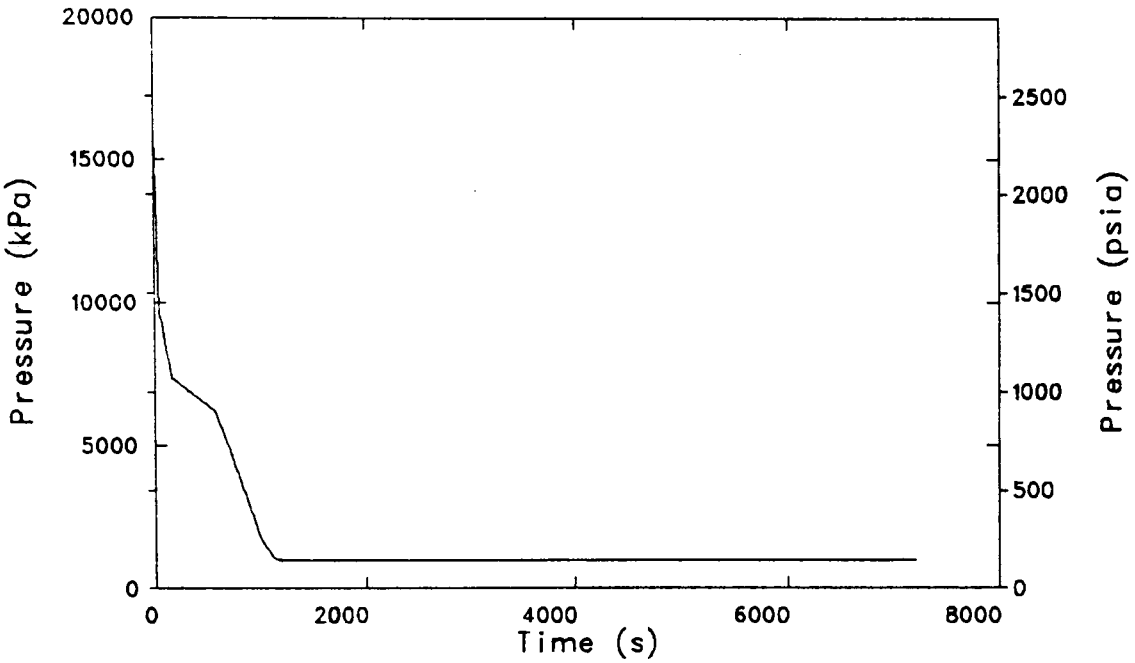

Figure F.43. Sequence 2.10: Reactor vessel downcomer fluid pressure.

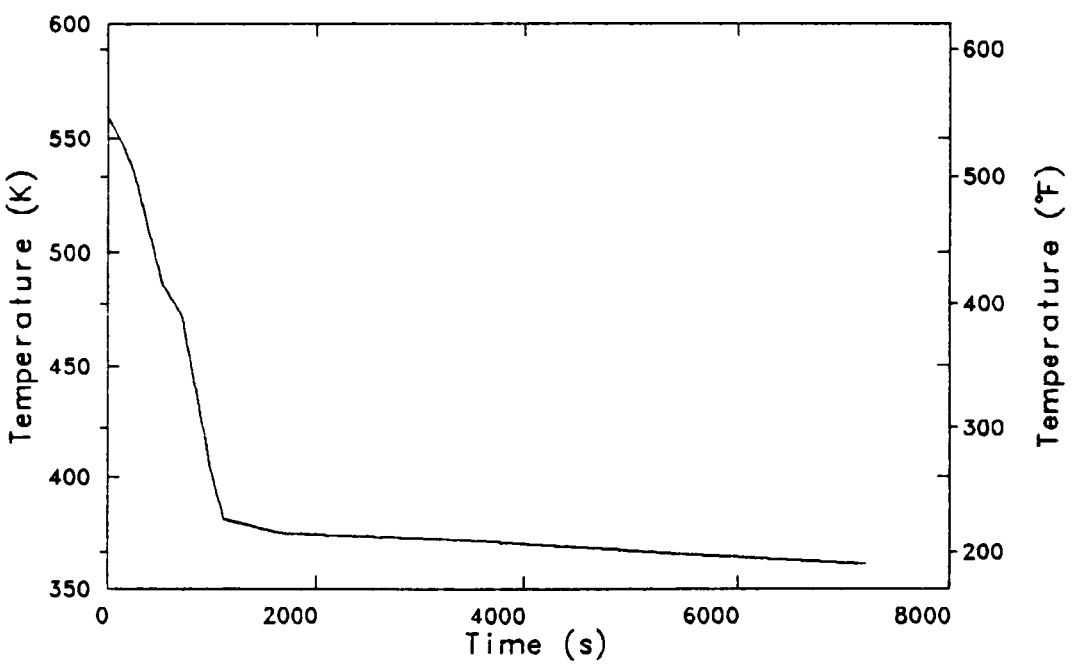

Figure F.44. Sequence 2.10: Reactor vessel downcomer fluid temperatures.

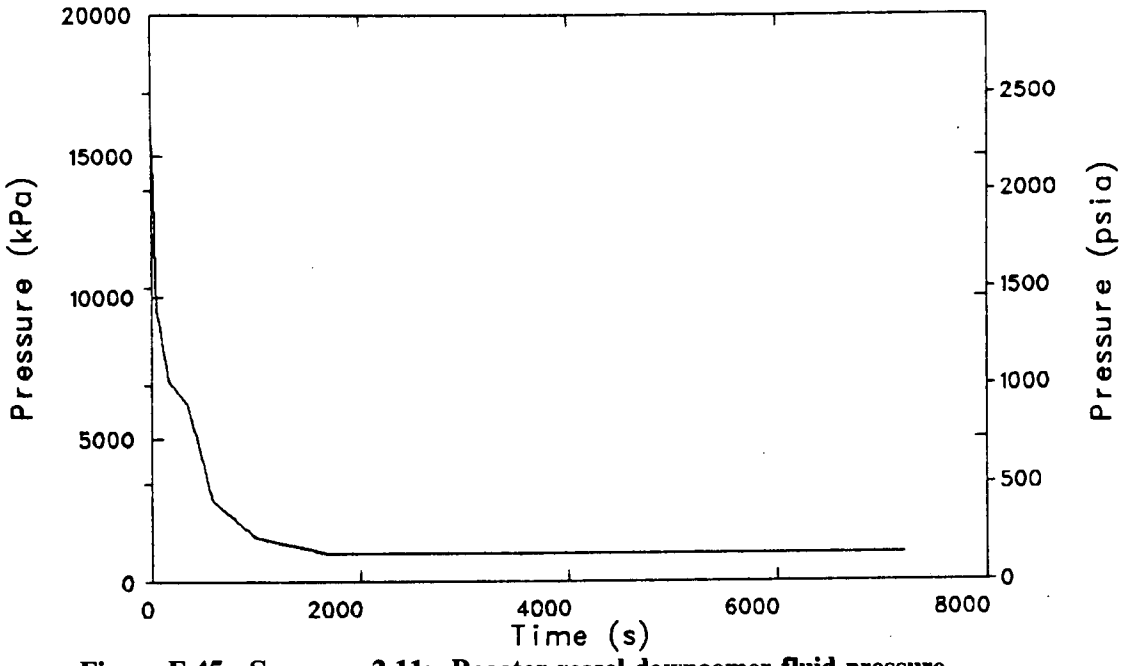

Figure F.45. Sequence 2.11: Reactor vessel downcomer fluid pressure.

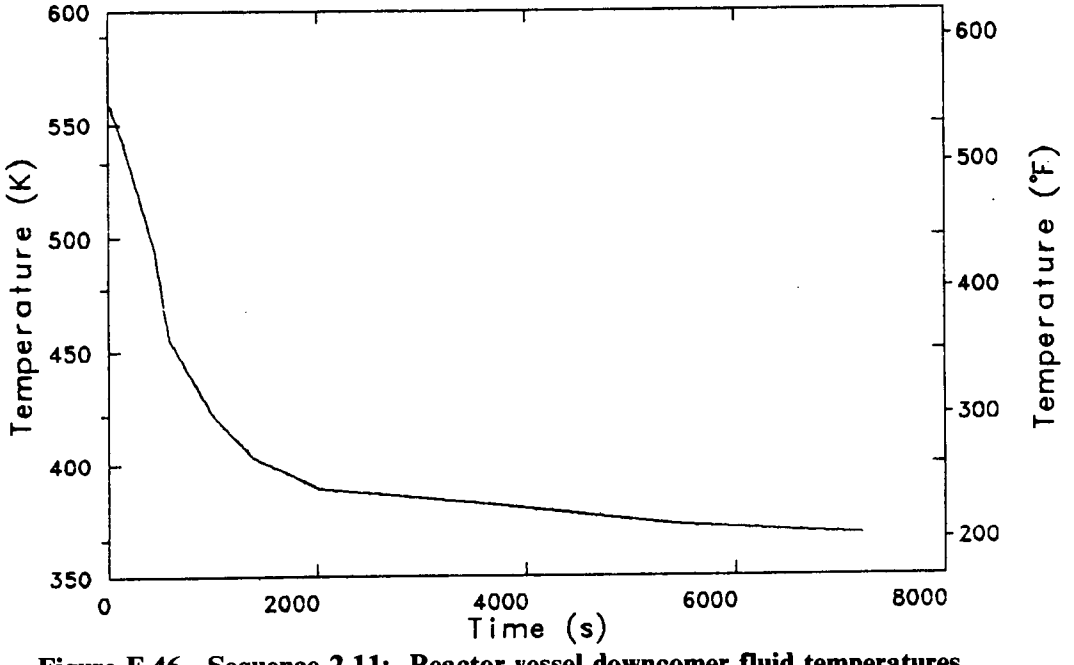

Figure F.46. Sequence 2.11: Reactor vessel downcomer fluid temperatures.

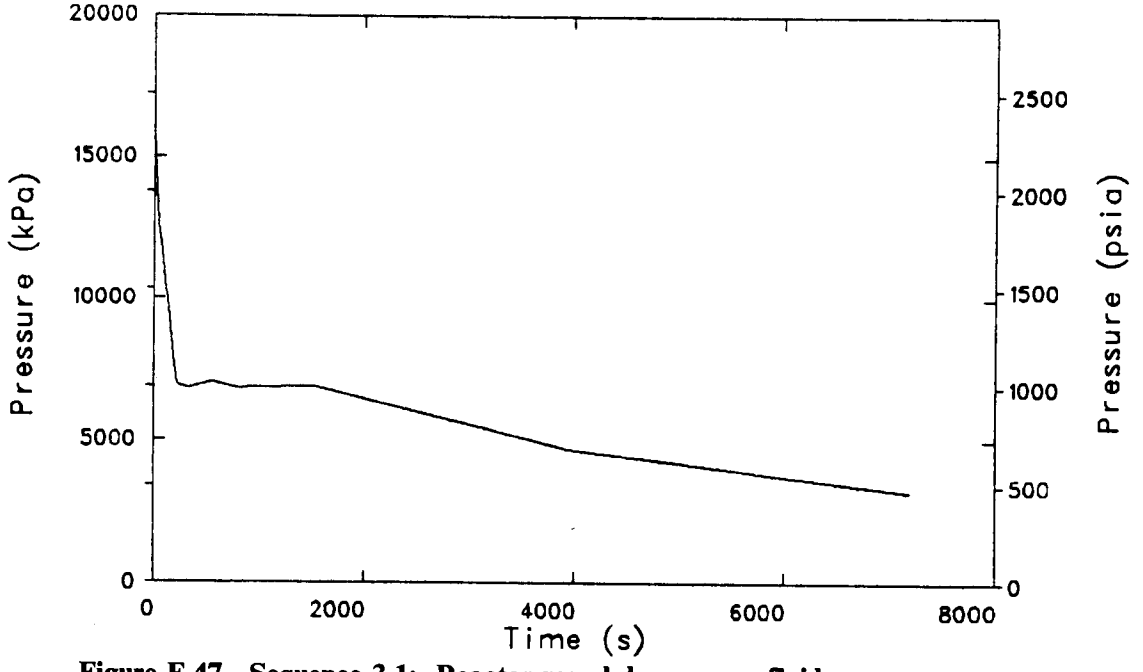

Figure F.47. Sequence 3.1: Reactor vessel downcomer fluid pressure.

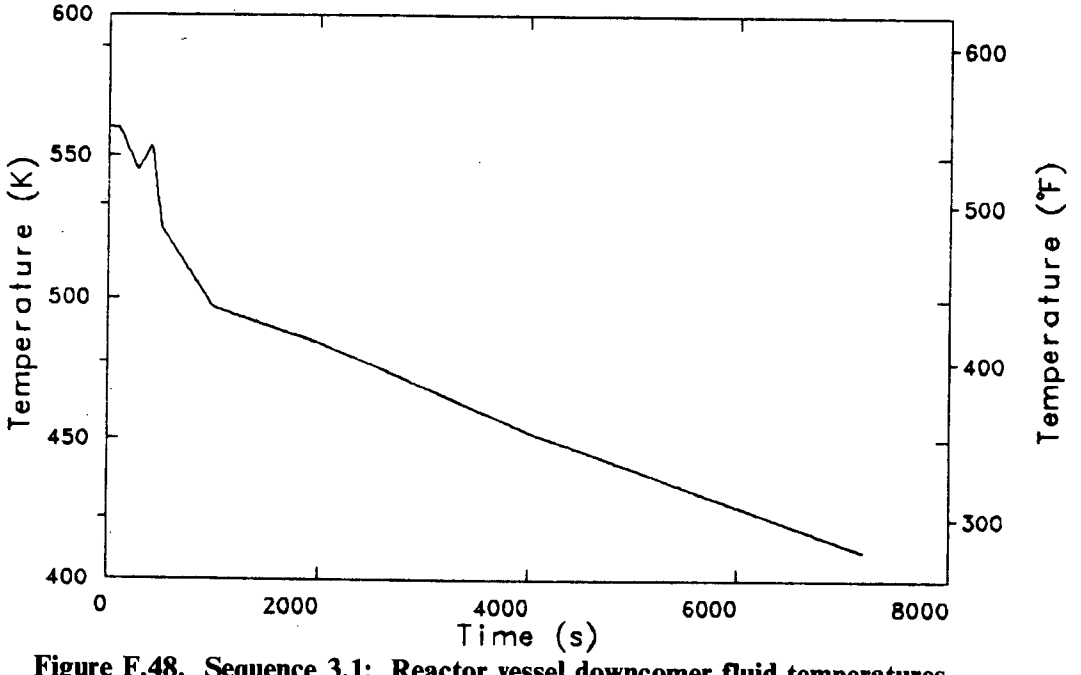

Figure F.48. Sequence 3.1: Reactor vessel downcomer fluid temperatures.

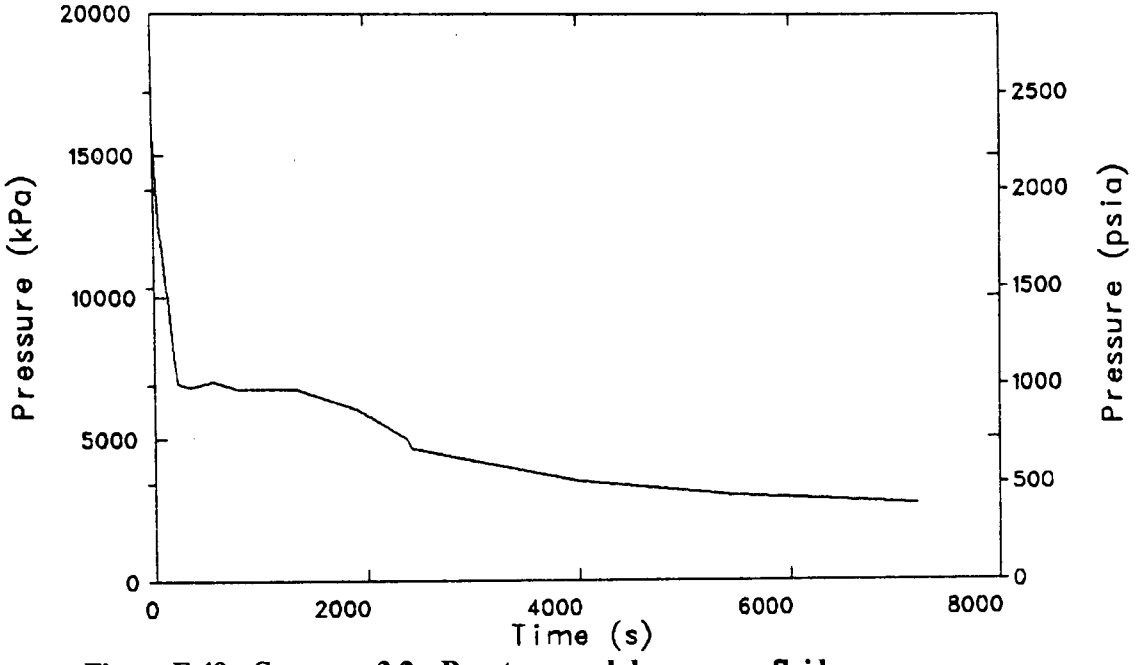

Figure F.49. Sequence 3.2: Reactor vessel downcomer fluid pressure.

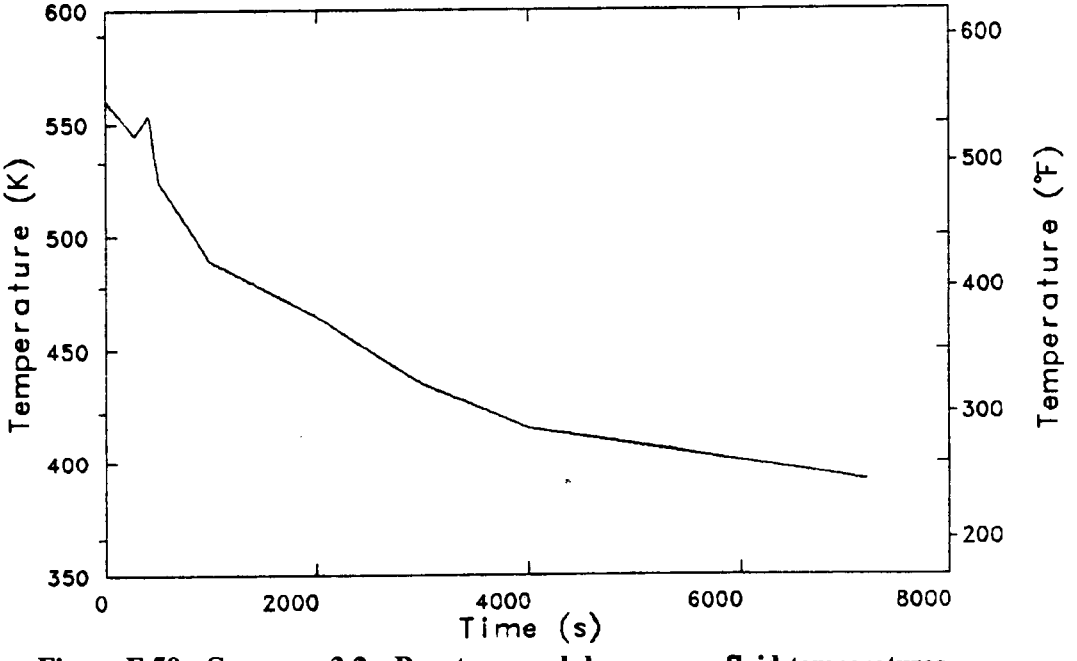

Figure F.50. Sequence 3.2: Reactor vessel downcomer fluid temperatures.

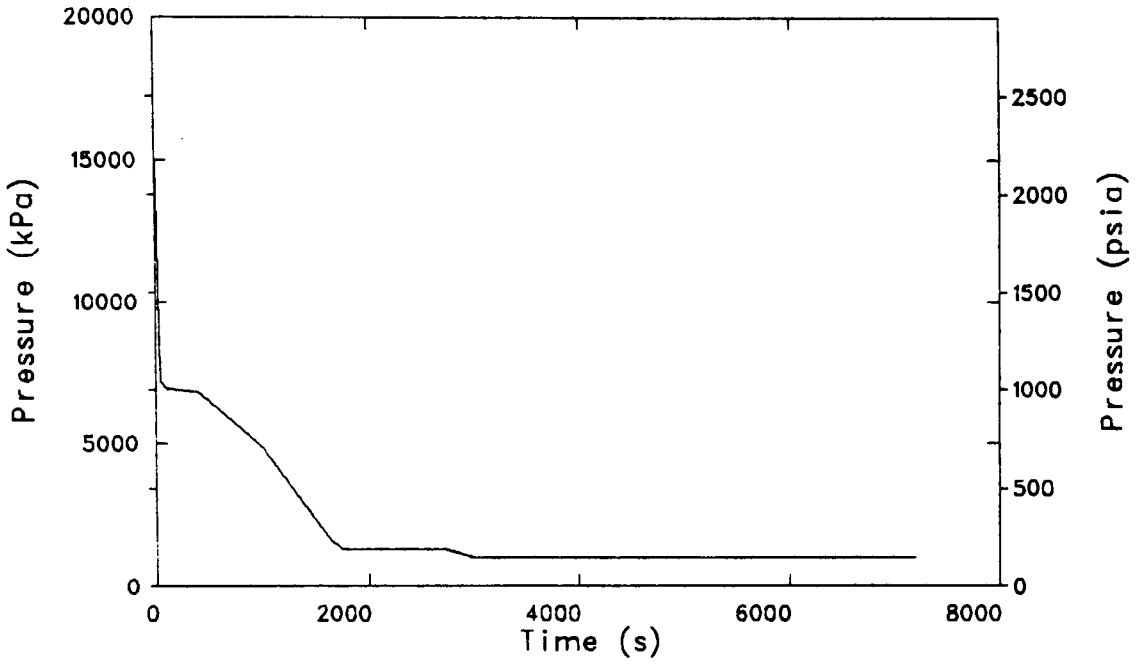

Figure F.51. Sequence 4.1: Reactor vessel downcomer fluid pressure.

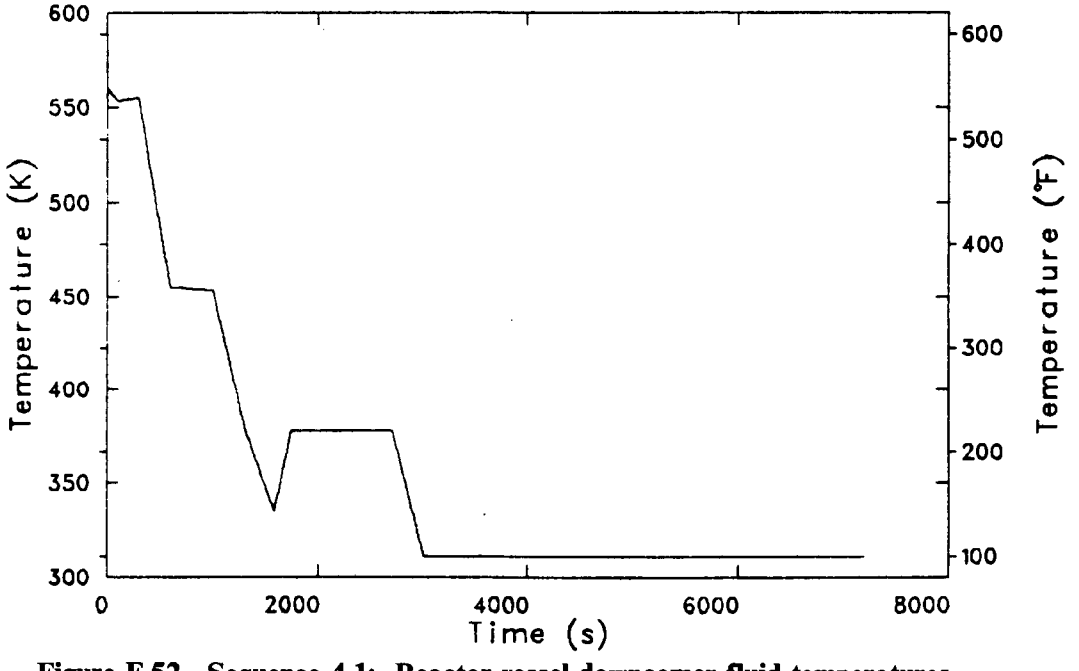

Figure F.52. Sequence 4.1: Reactor vessel downcomer fluid temperatures.

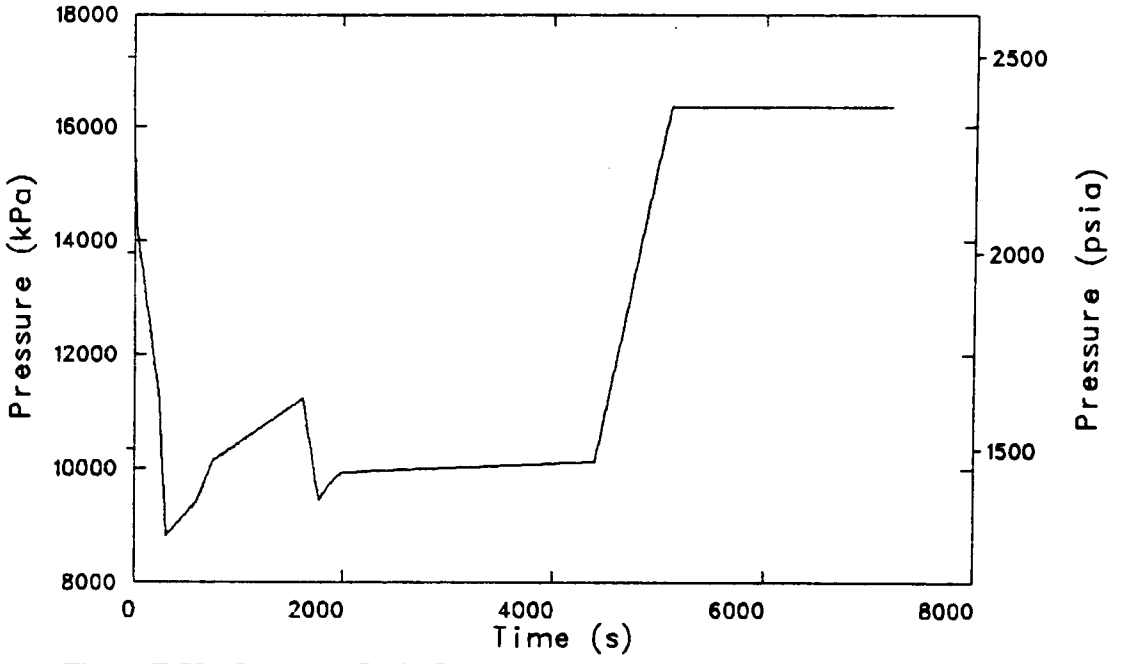

Figure F.53. Sequence 5.14: Reactor vessel downcomer fluid pressure.

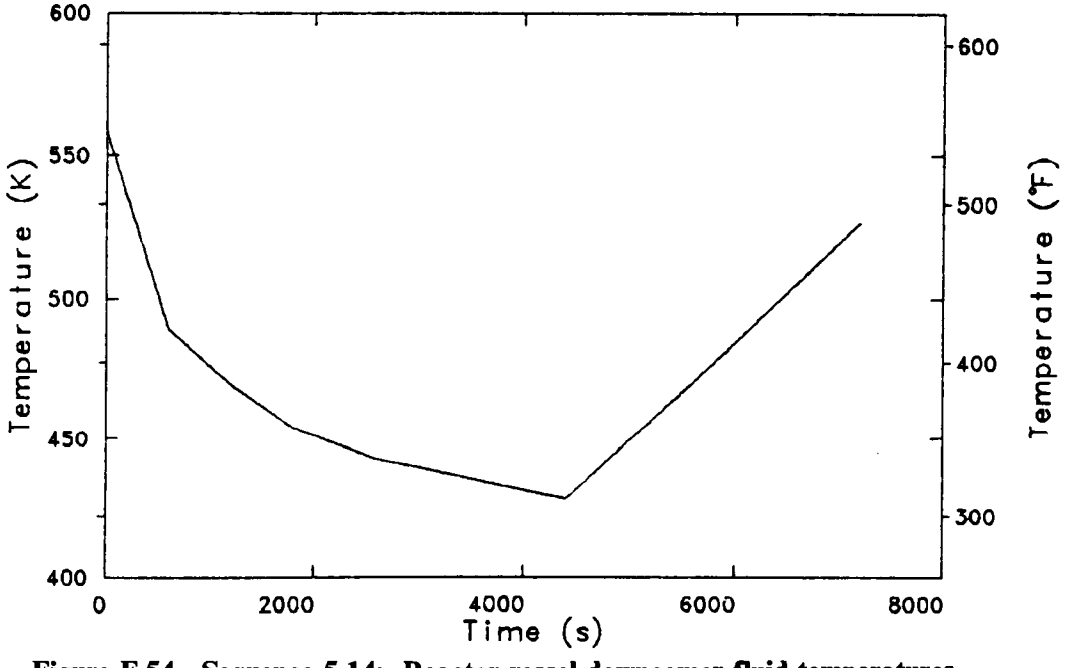

Figure F.54. Sequence 5.14: Reactor vessel downcomer fluid temperatures.

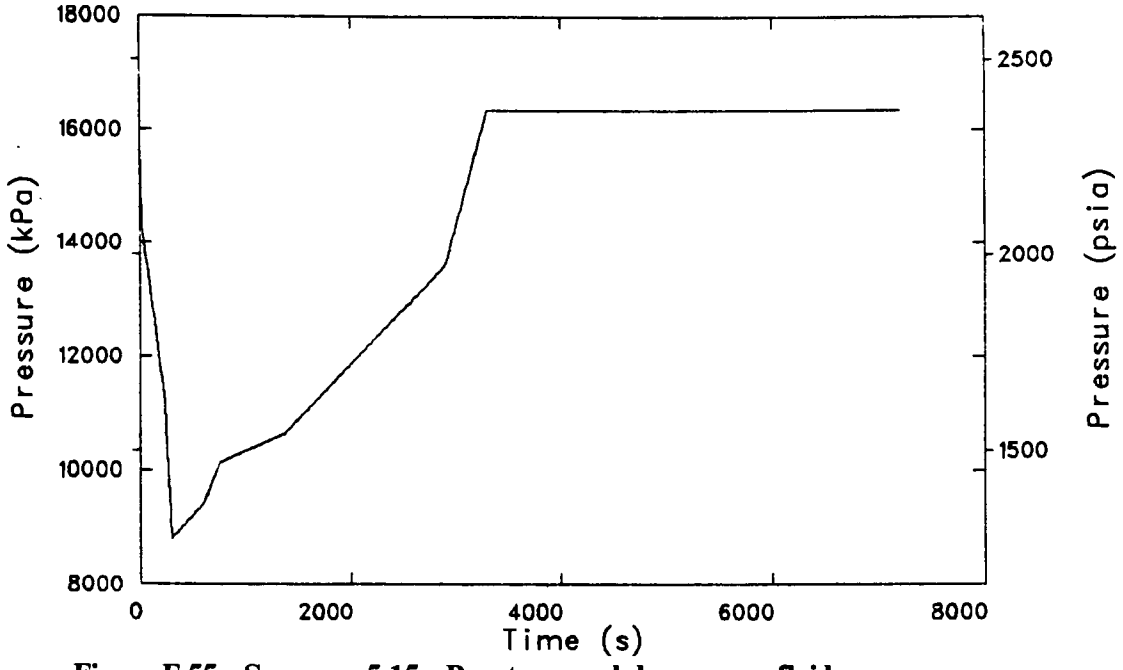

Figure F.55. Sequence 5.15: Reactor vessel downcomer fluid pressure.

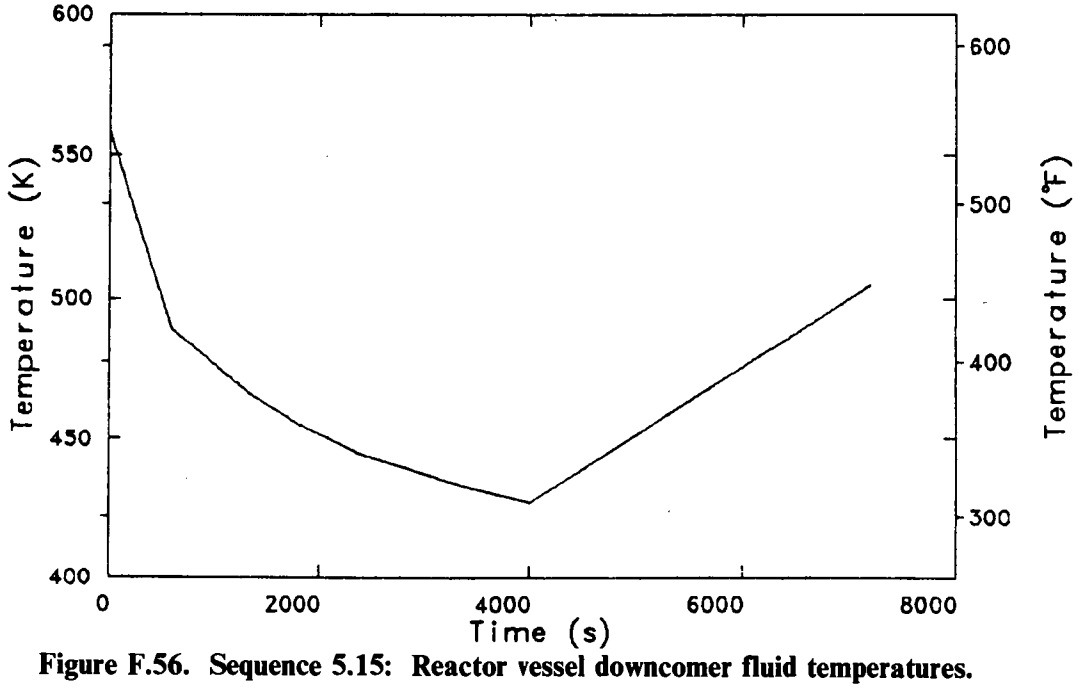

Figure F.56. Sequence 5.15: Reactor vessel downcomer fluid temperatures.

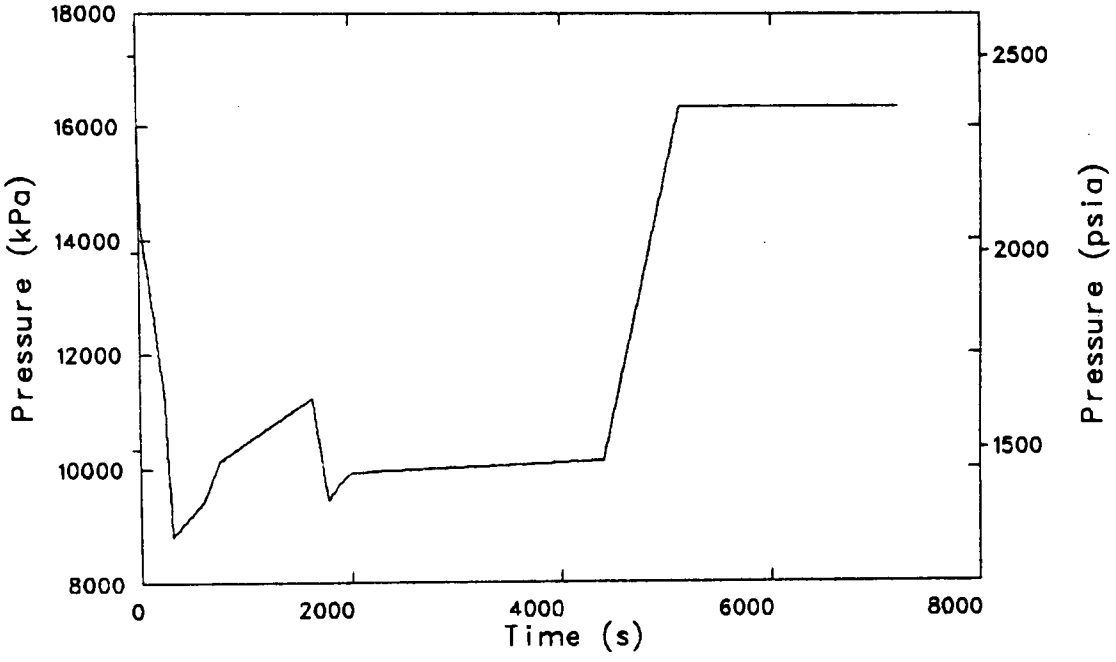

Figure F.57. Sequence 5.16: Reactor vessel downcomer fluid pressure.

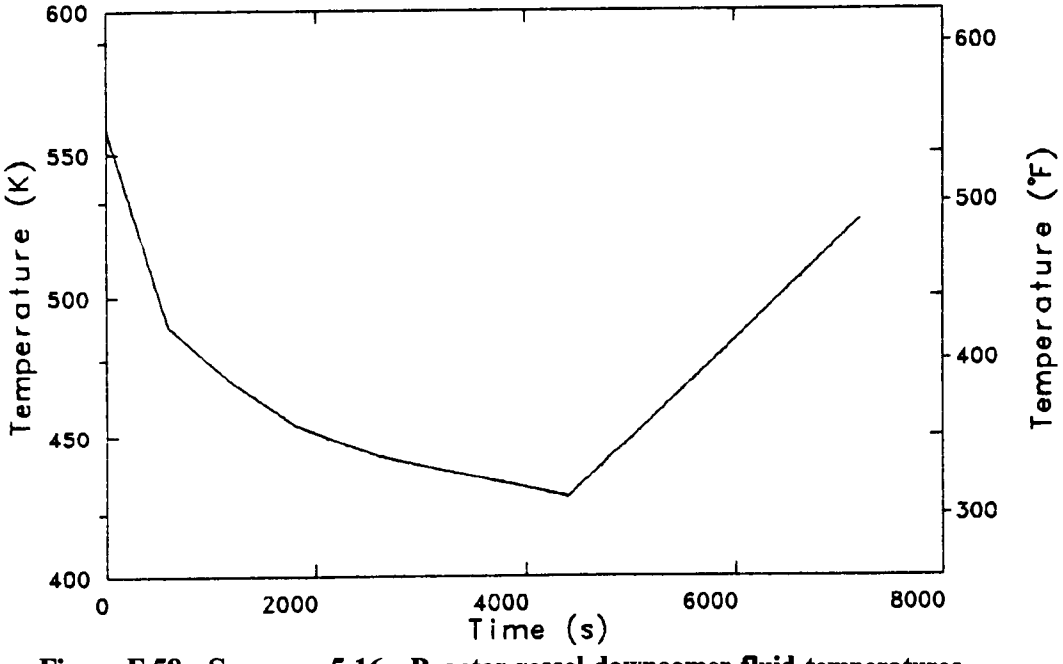

Figure F.58. Sequence 5.16: Reactor vessel downcomer fluid temperatures.

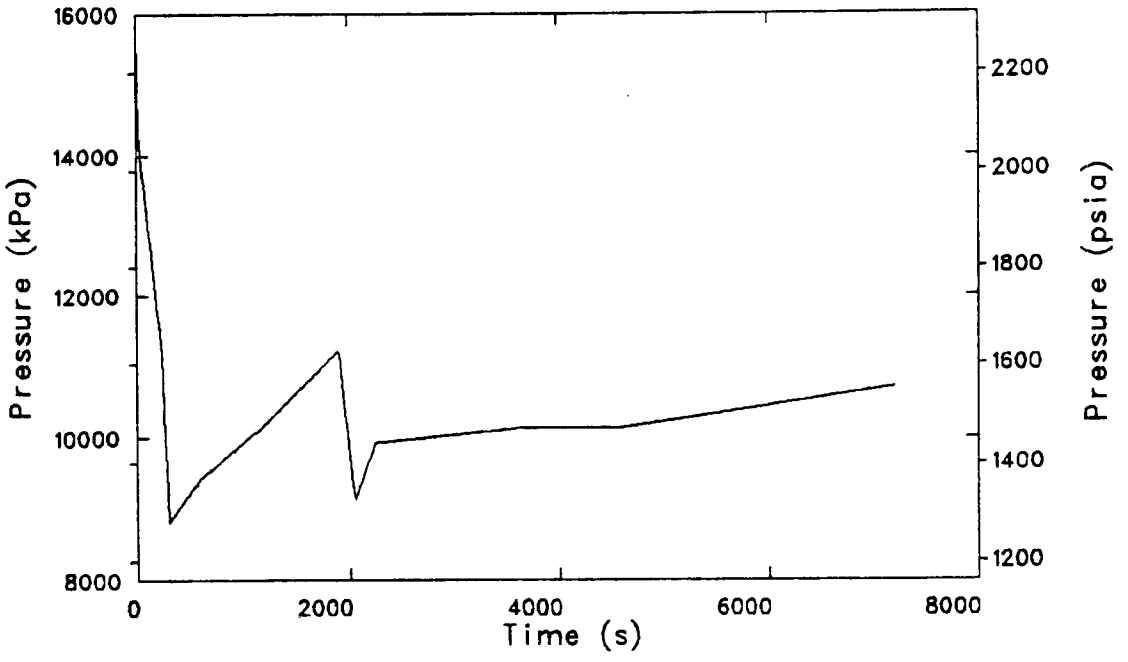

Figure F.59. Sequence 5.17: Reactor vessel downcomer fluid pressure.

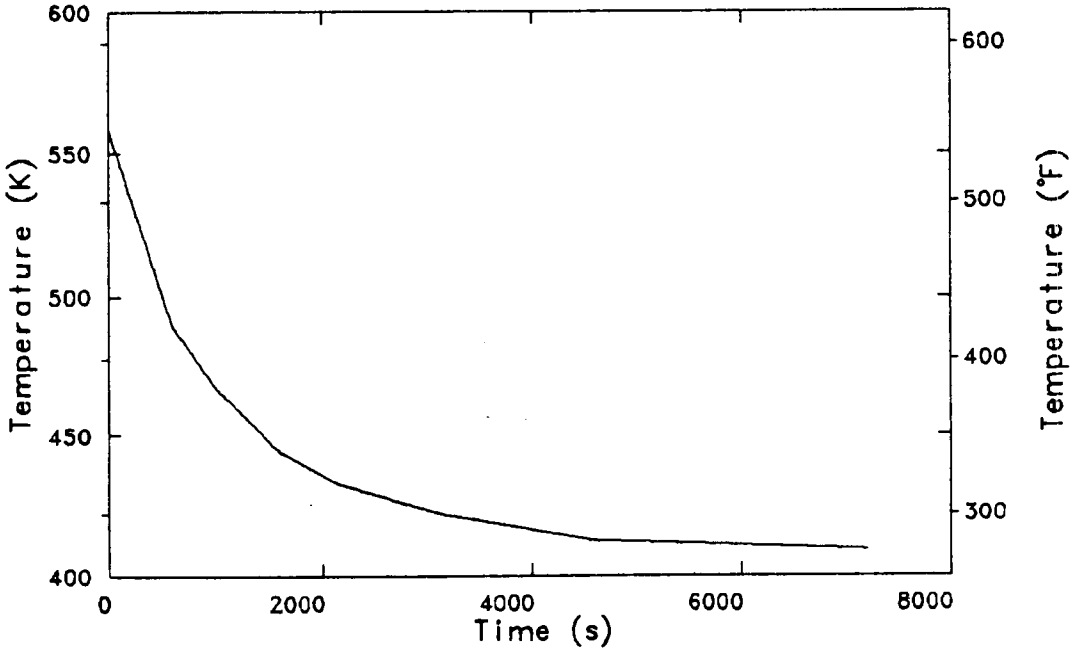

Figure F.60. Sequence 5.17: Reactor vessel downcomer fluid temperatures.

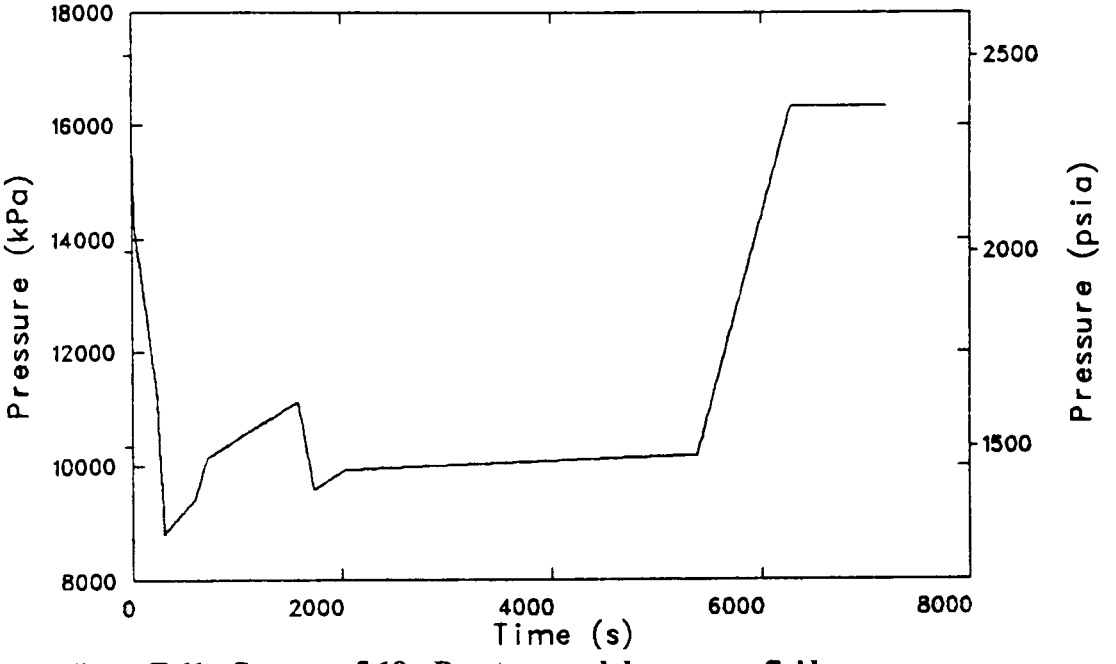

Figure F.61. Sequence 5.18: Reactor vessel downcomer fluid pressure.

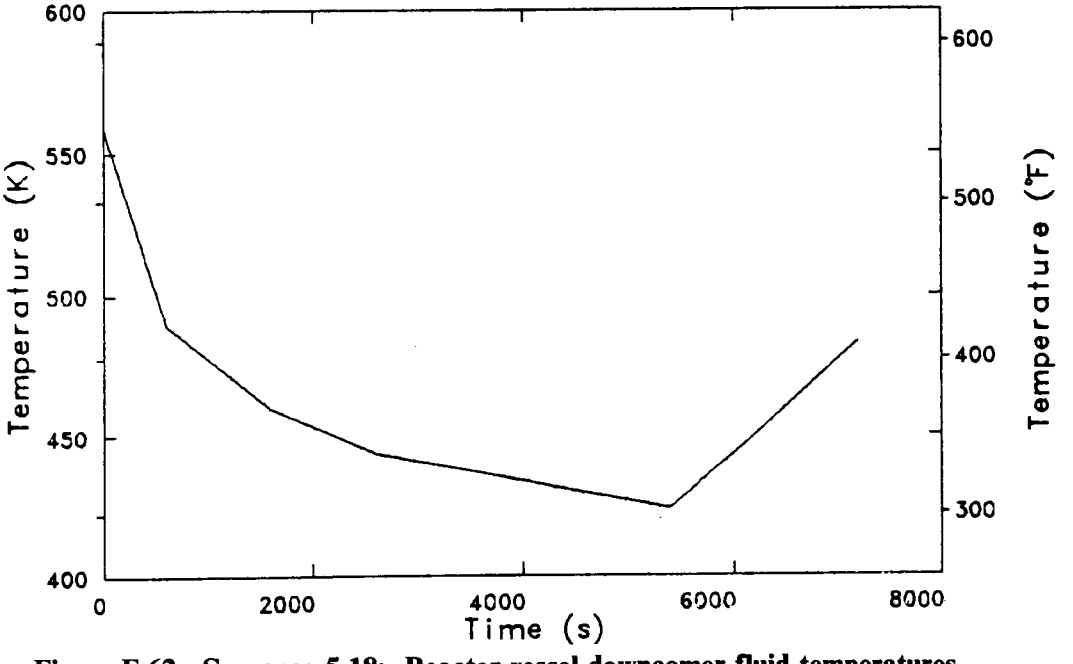

Figure F.62. Sequence 5.18: Reactor vessel downcomer fluid temperatures.

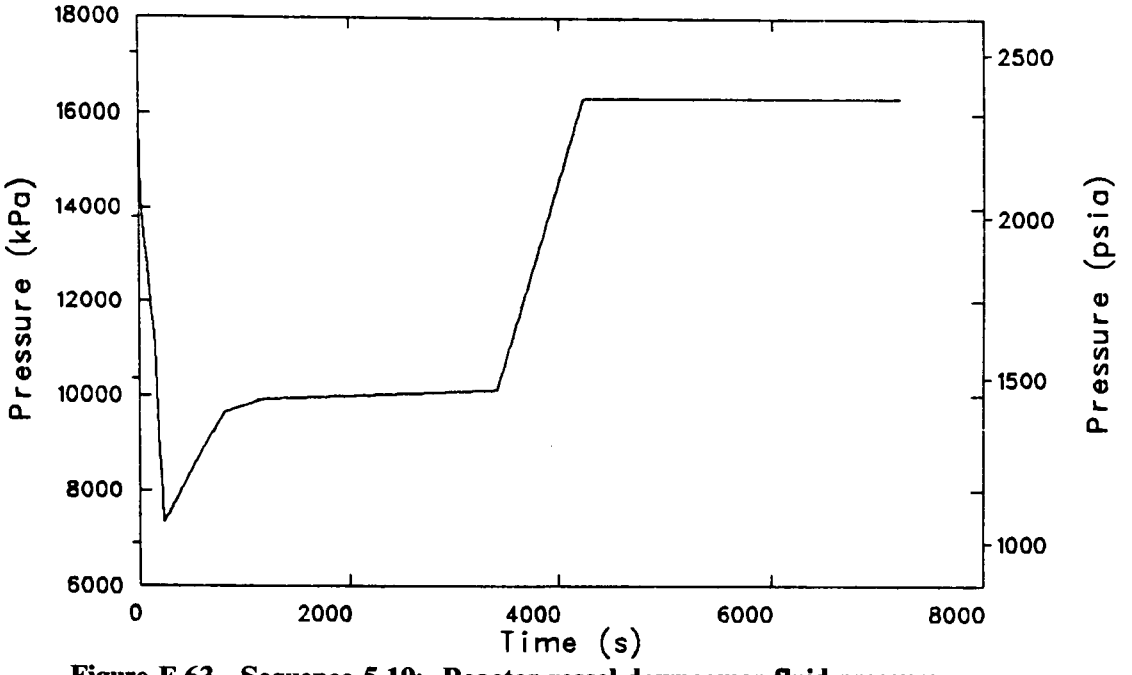

Figure F.63. Sequence 5.19: Reactor vessel downcomer fluid pressure.

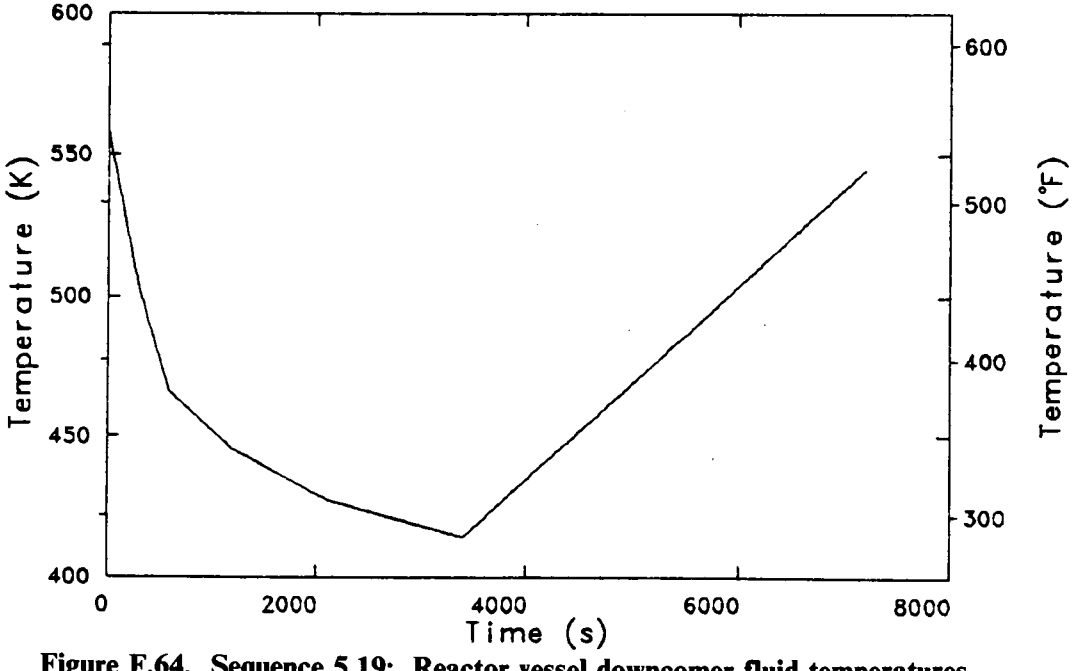

Figure F.64. Sequence 5.19: Reactor vessel downcomer fluid temperatures.

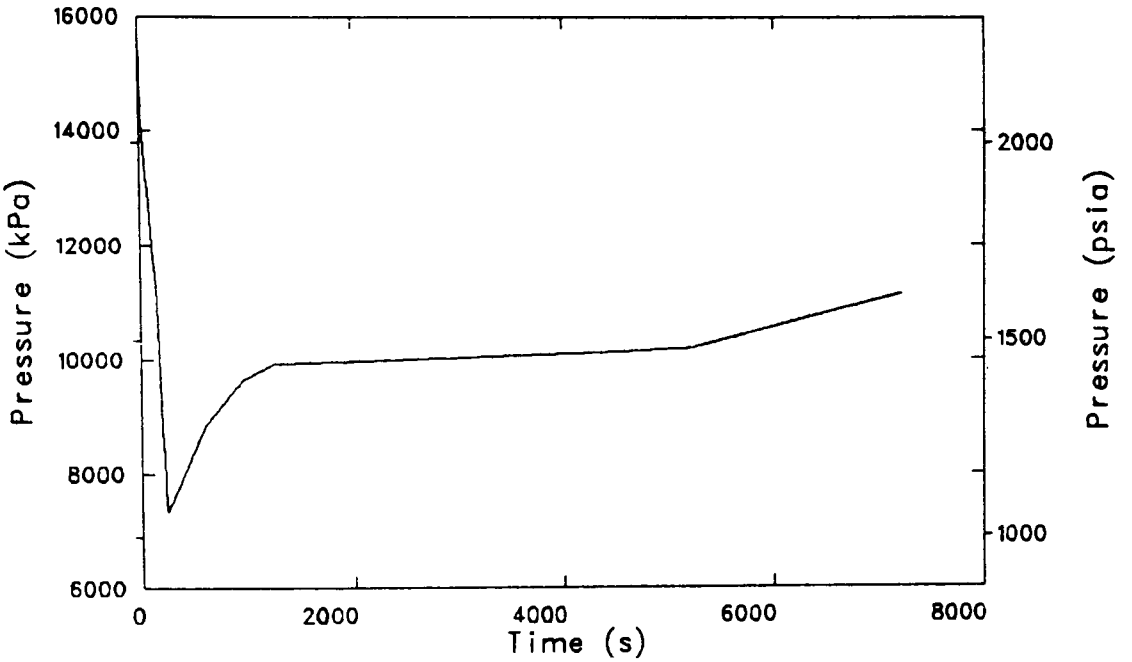

Figure F.65. Sequence 5.20: Reactor vessel downcomer fluid pressure.

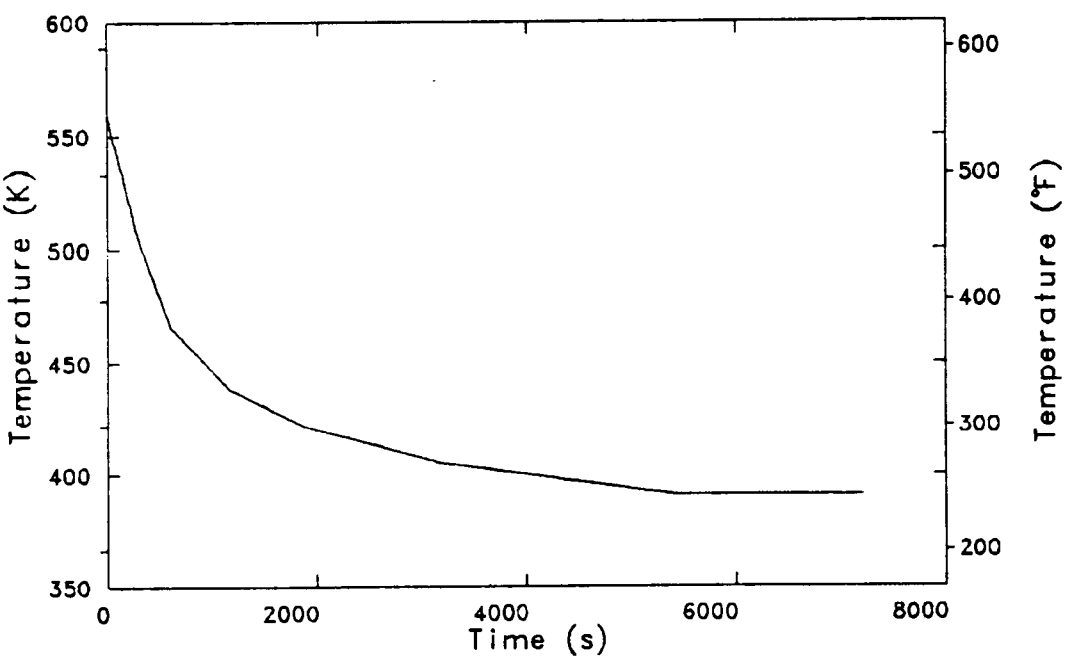

Figure F.66. Sequence 5.20: Reactor vessel downcomer fluid temperatures.

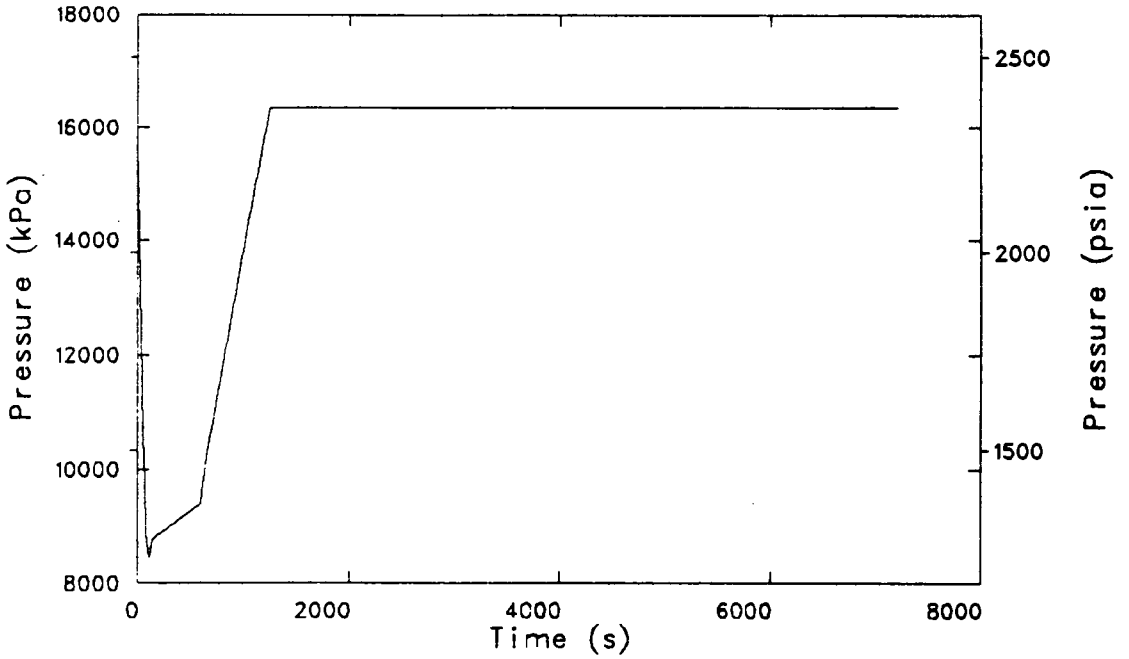

Figure F.67. Sequence 6.2: Reactor vessel downcomer fluid pressure.

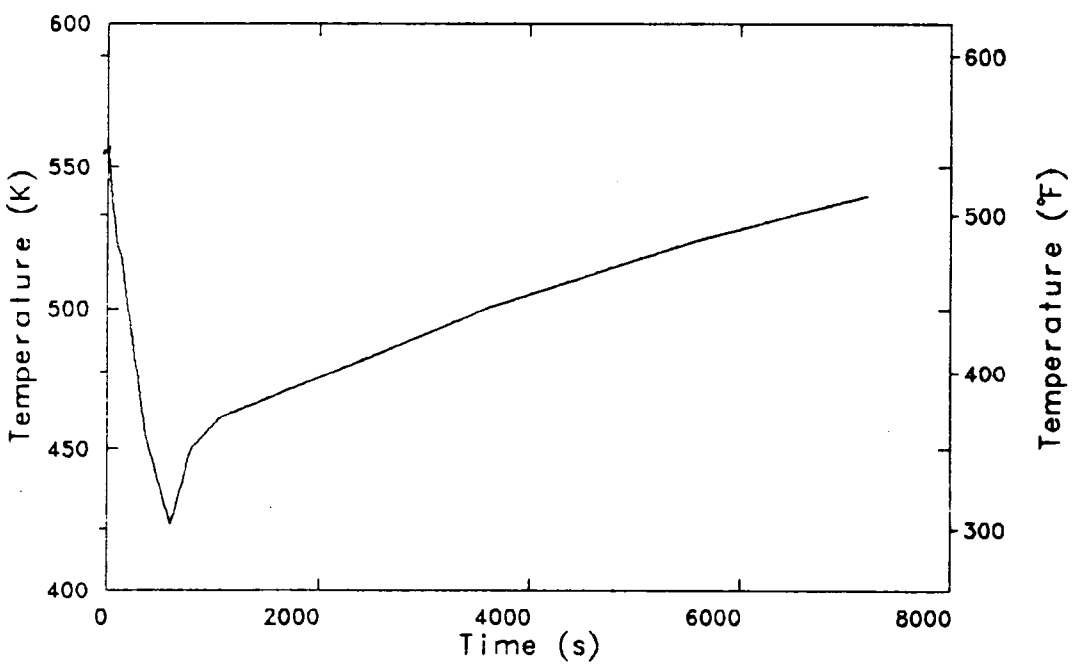

Figure F.68. Sequence 6.2: Reactor vessel downcomer fluid temperatures.

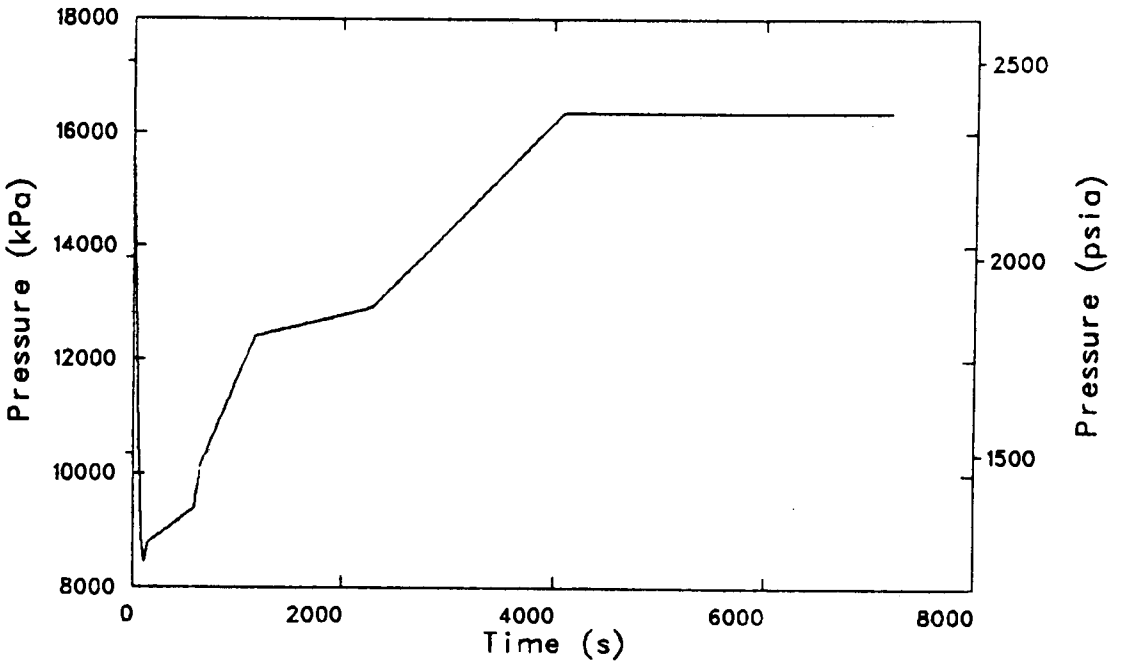

Figure F.69. Sequence 6.3: Reactor vessel downcomer fluid pressure.

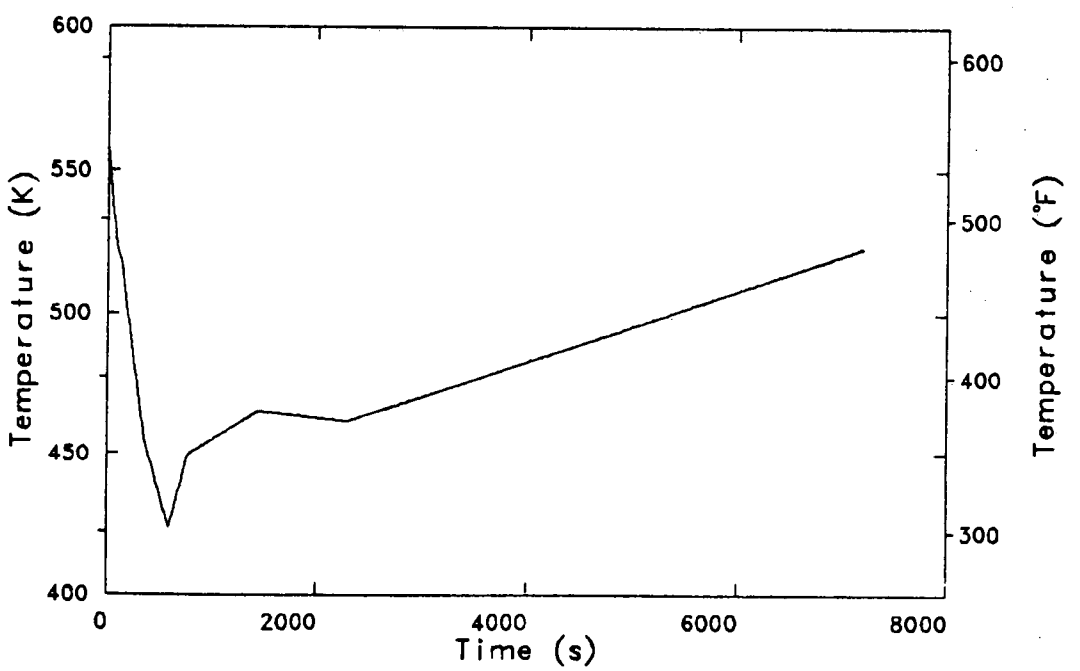

Figure F.70. Sequence 6.3: Reactor vessel downcomer fluid temperatures.

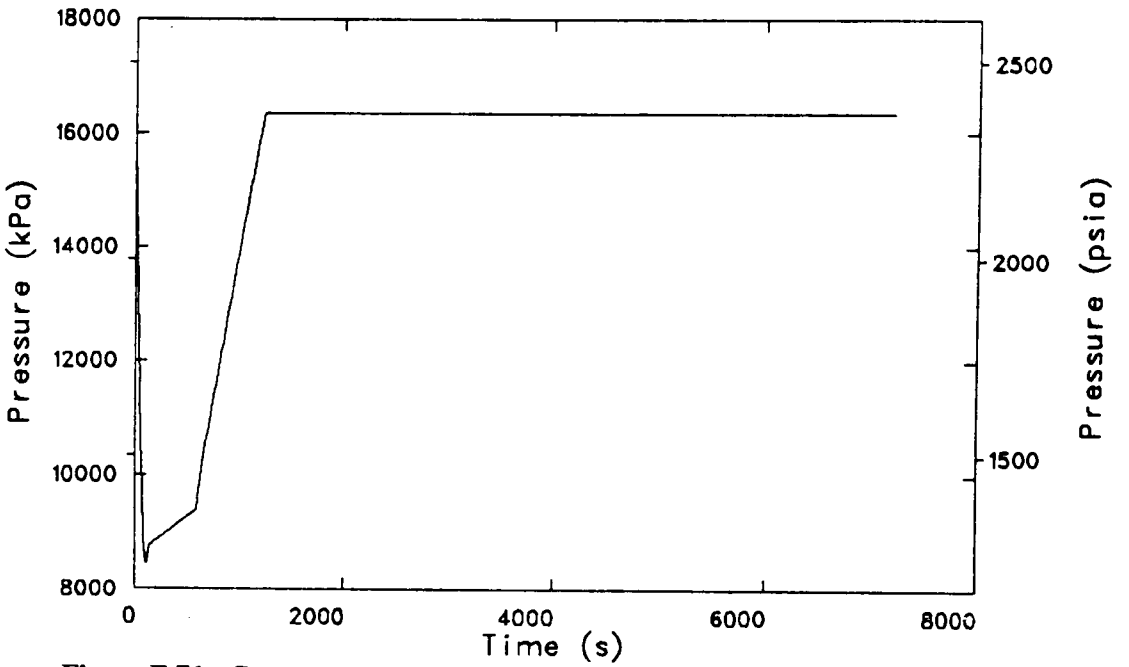

Figure F.71. Sequence 6.4: Reactor vessel downcomer fluid pressure.

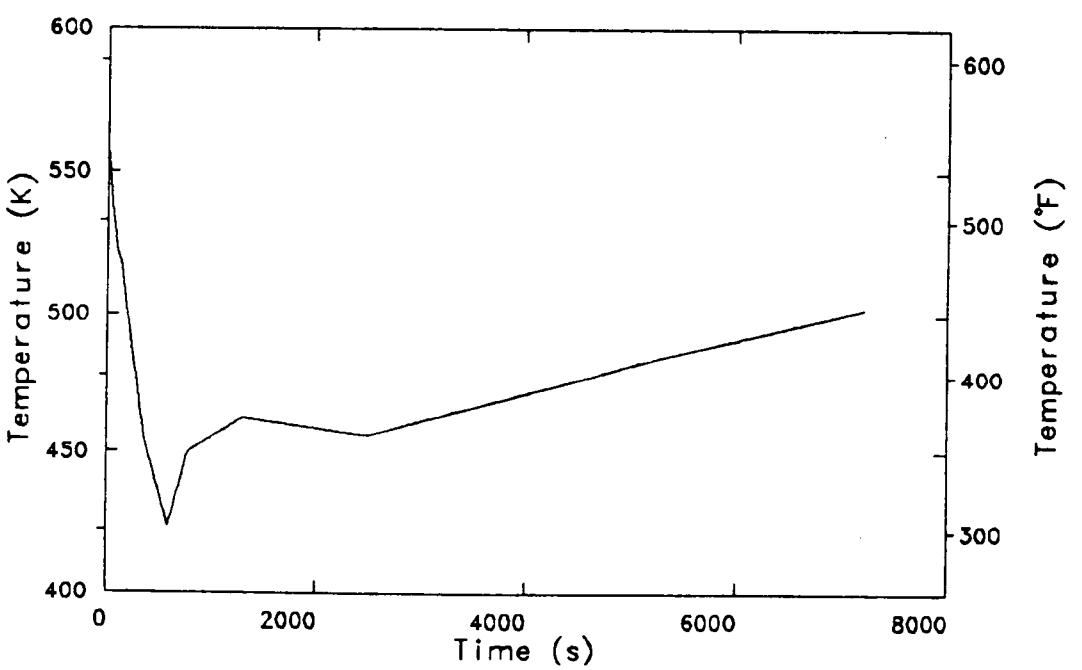

Figure F.72. Sequence 6.4: Reactor vessel downcomer fluid temperatures.

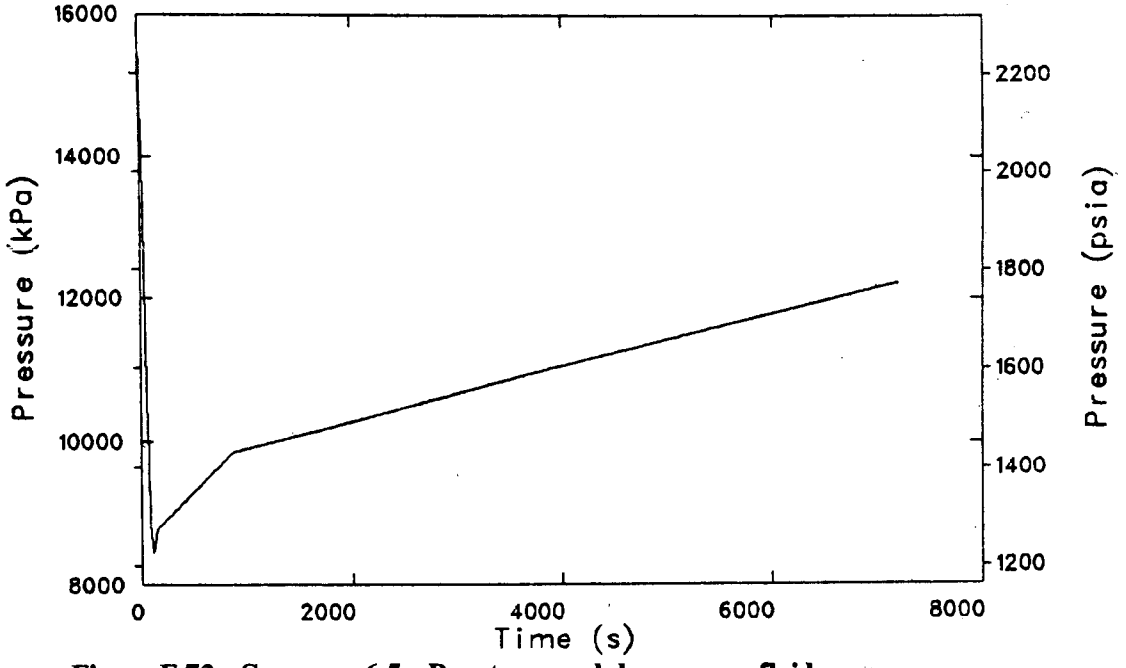

Figure F.73. Sequence 6.5: Reactor vessel downcomer fluid pressure.

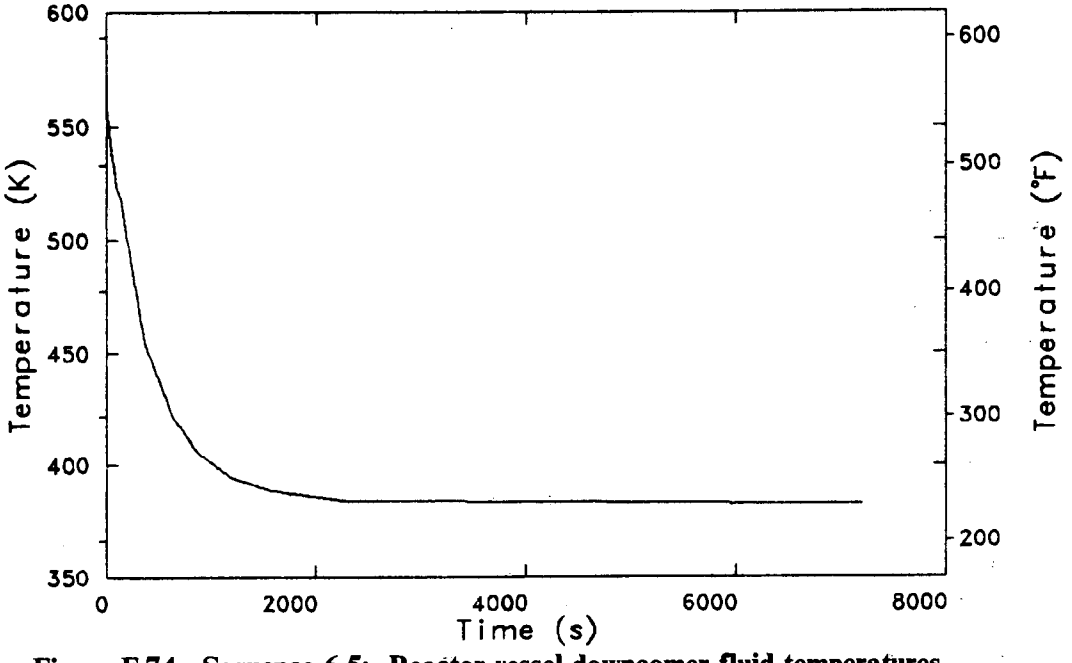

Figure F.74. Sequence 6.5: Reactor vessel downcomer fluid temperatures.

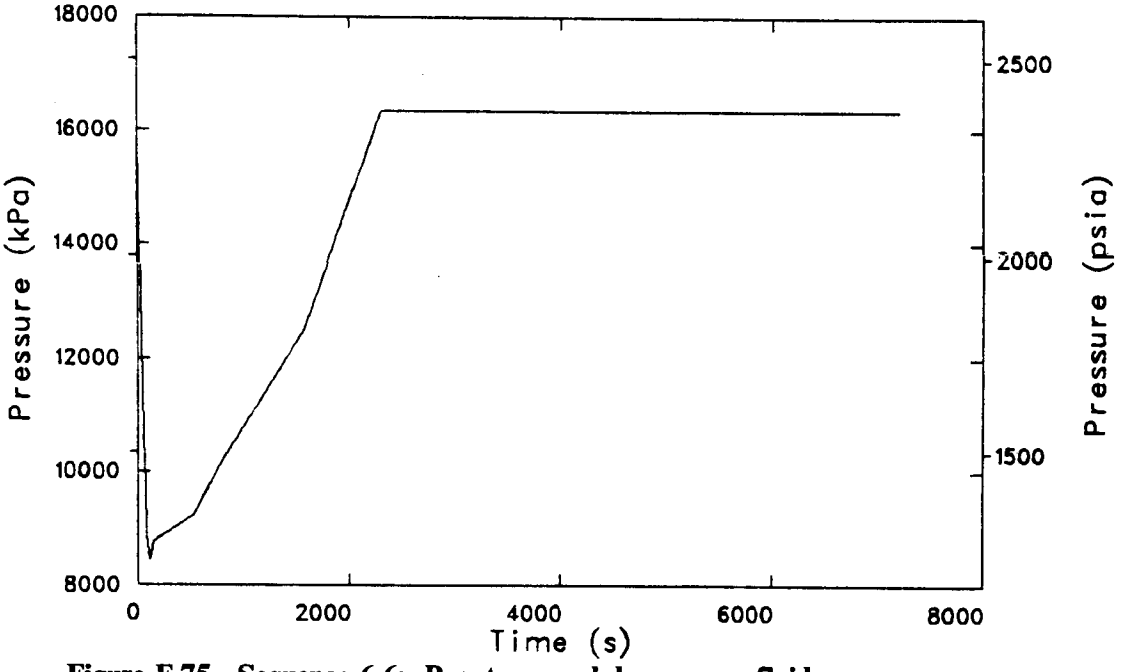

Figure F.75. Sequence 6.6: Reactor vessel downcomer fluid pressure.

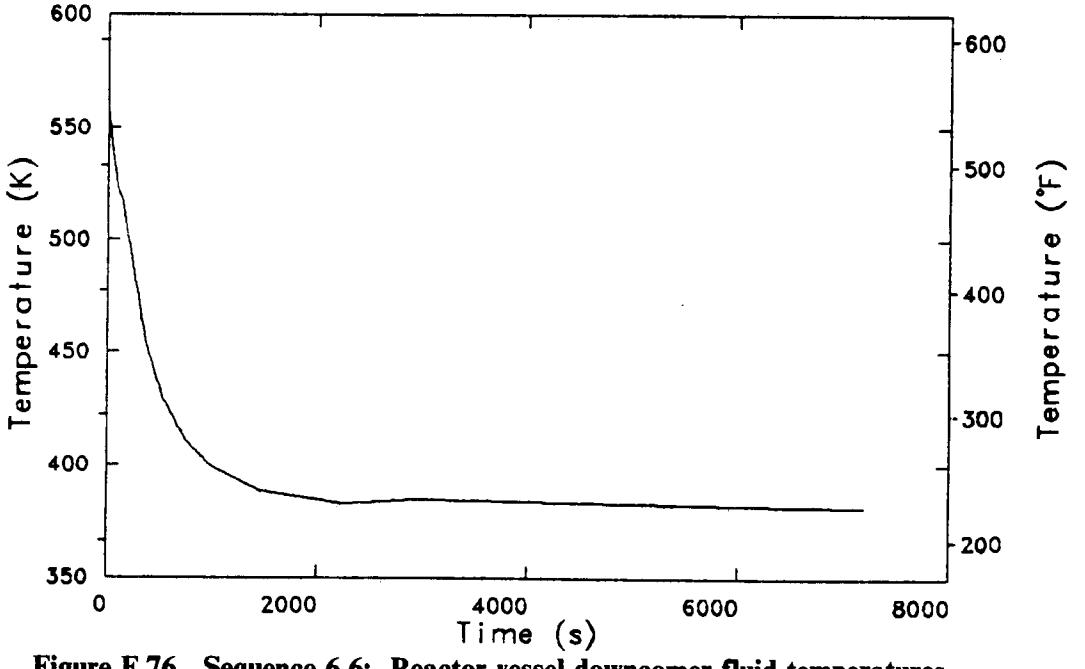

Figure F.76. Sequence 6.6: Reactor vessel downcomer fluid temperatures.

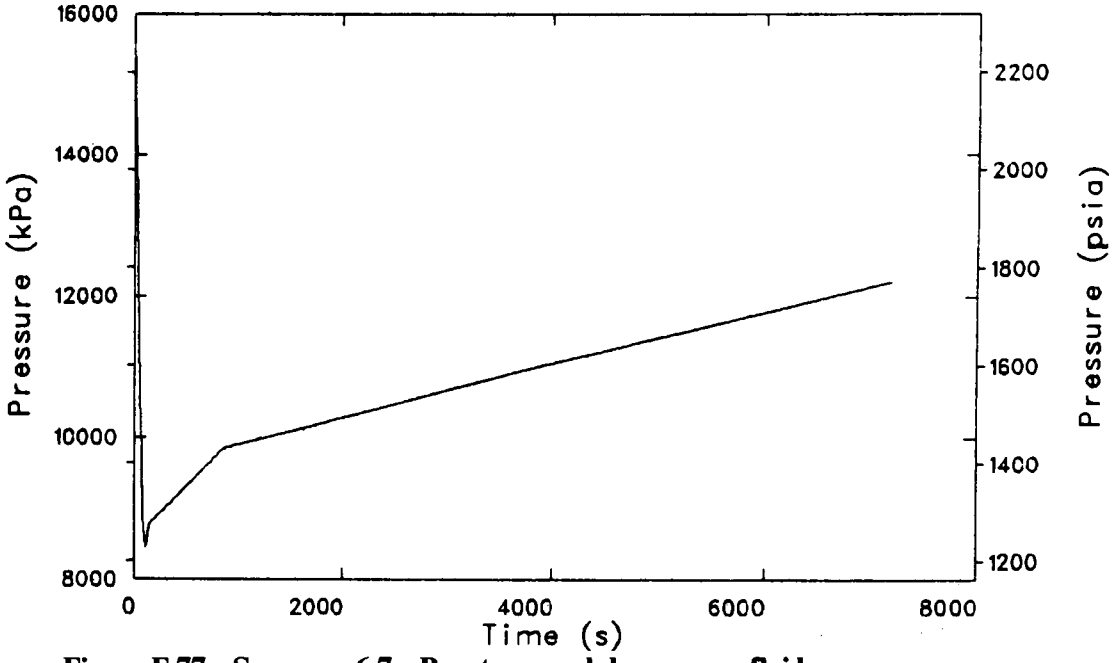

Figure F.77. Sequence 6.7: Reactor vessel downcomer fluid pressure.

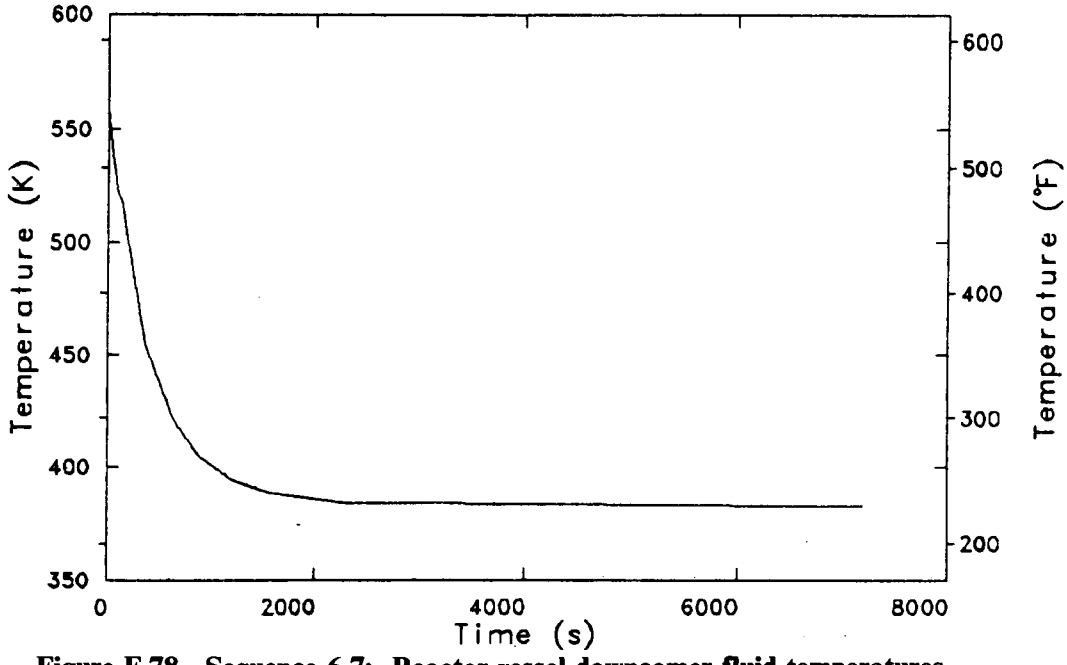

Figure F.78. Sequence 6.7: Reactor vessel downcomer fluid temperatures.

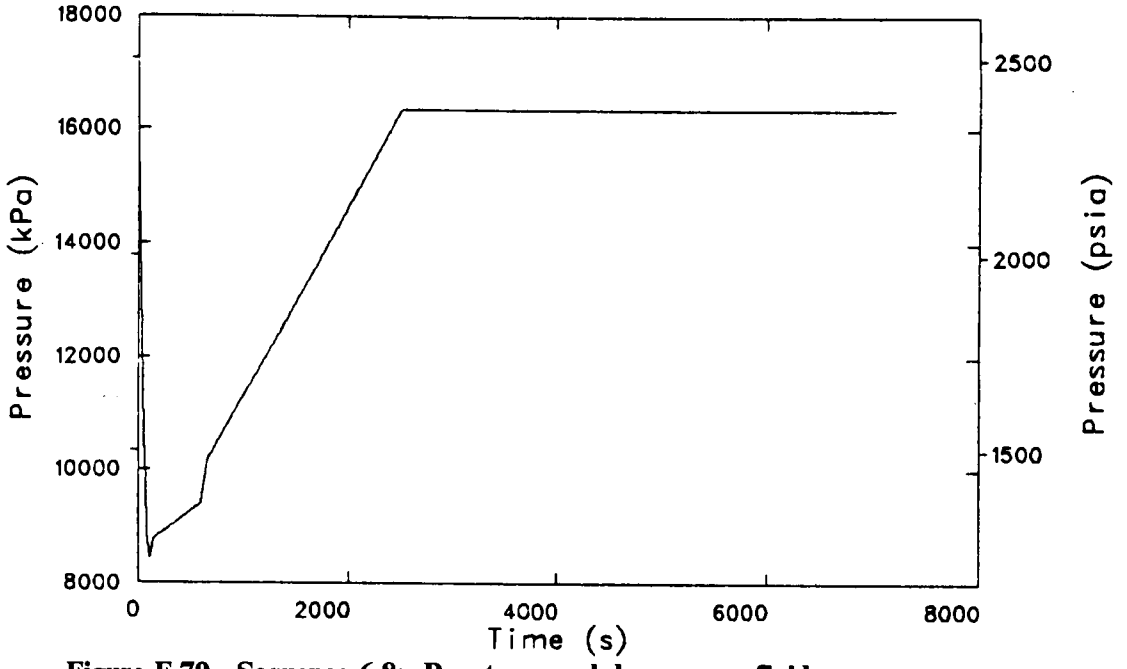

Figure F.79. Sequence 6.8: Reactor vessel downcomer fluid pressure.

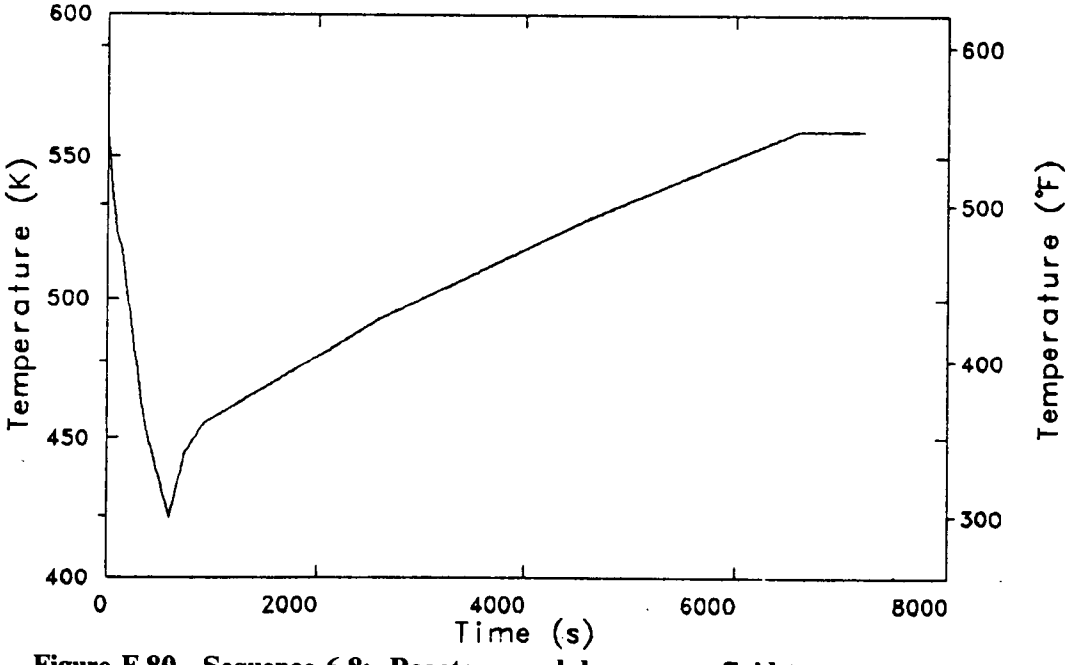

Figure F.80. Sequence 6.8: Reactor vessel downcomer fluid temperatures.

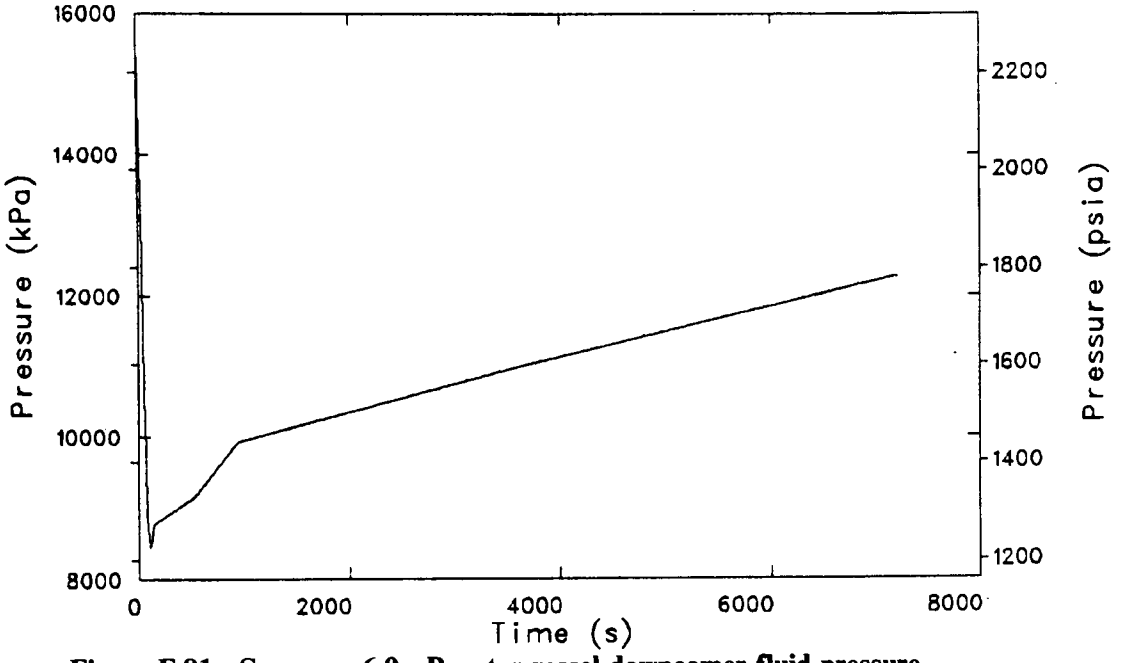

Figure F.81. Sequence 6.9: Reactor vessel downcomer fluid pressure.

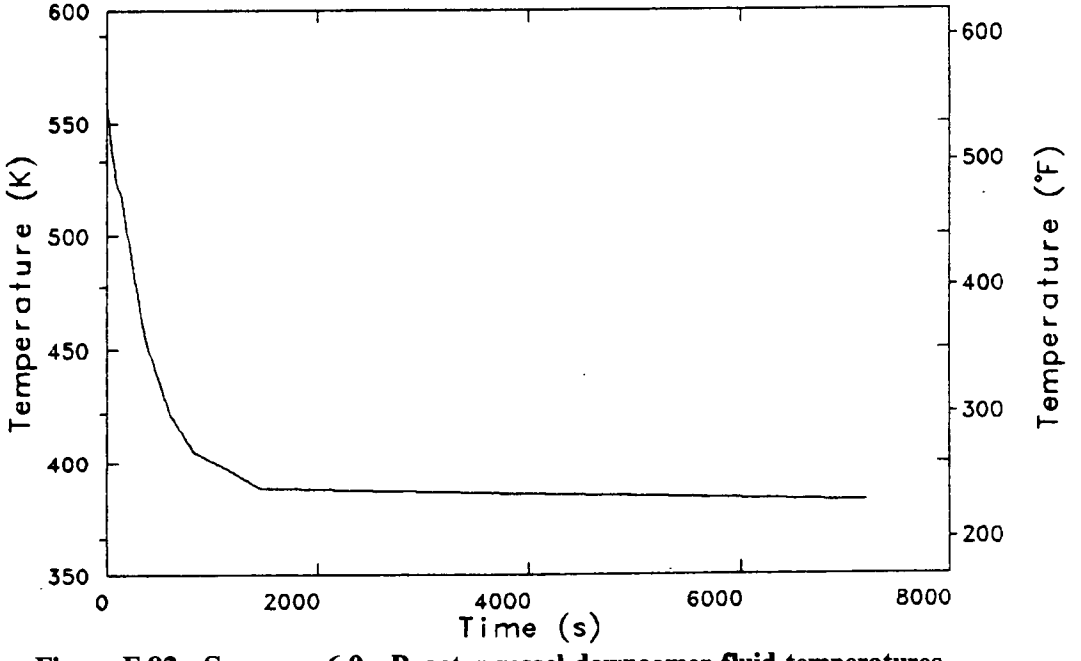

Figure F.82. Sequence 6.9: Reactor vessel downcomer fluid temperatures.

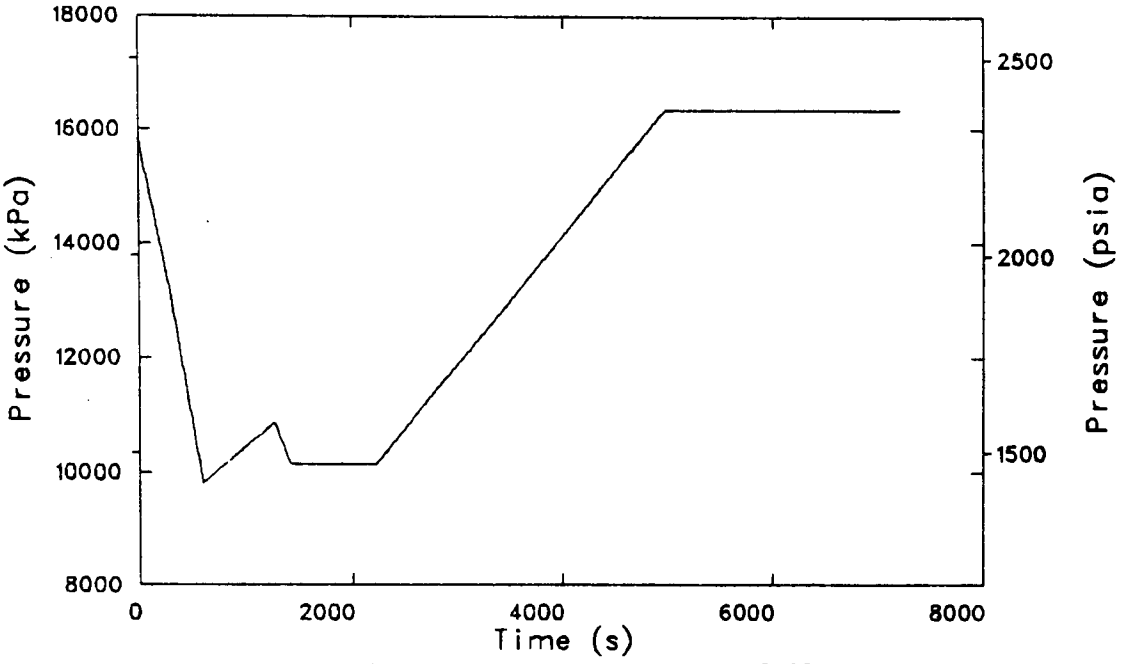

Figure F.83. Sequence 7.1: Reactor vessel downcomer fluid pressure.

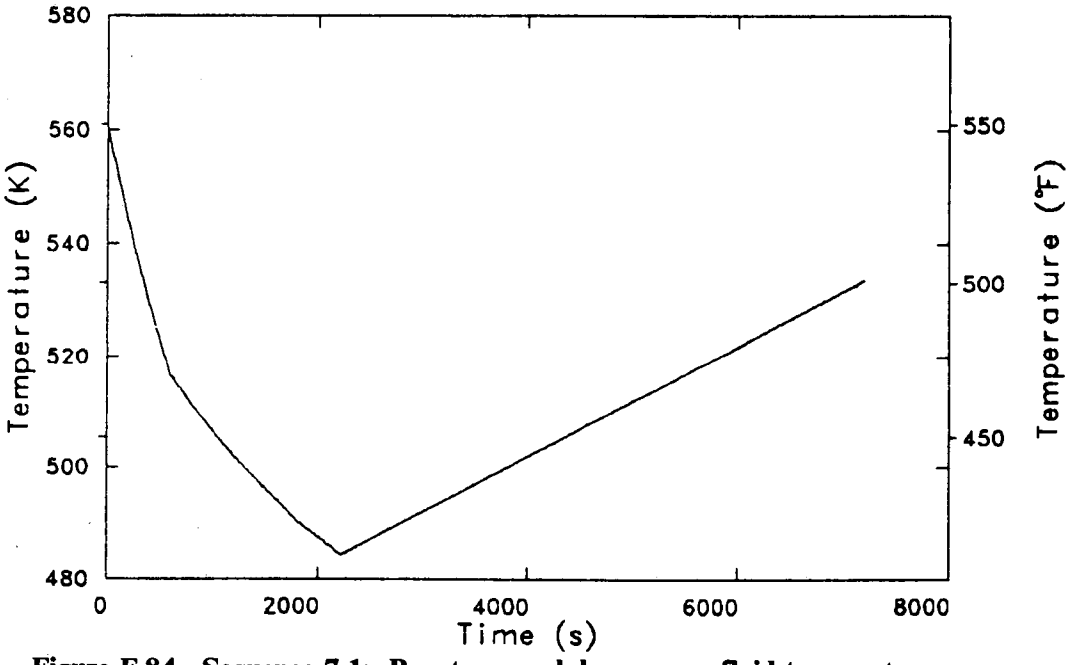

Figure F.84. Sequence 7.1: Reactor vessel downcomer fluid temperatures.

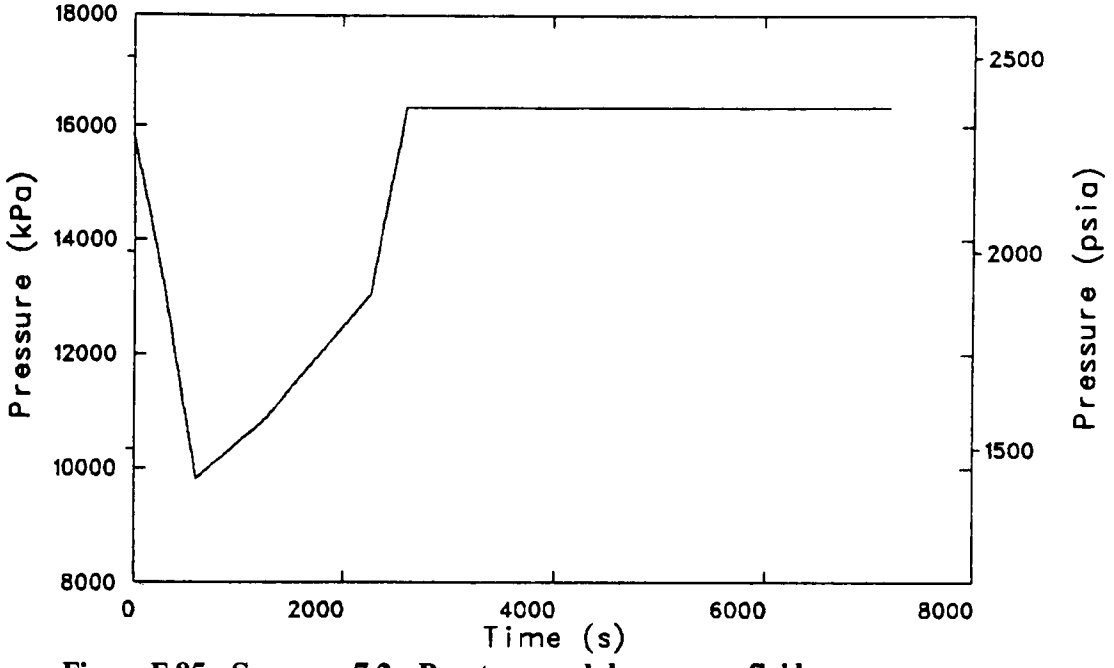

Figure F.85. Sequence 7.2: Reactor vessel downcomer fluid pressure.

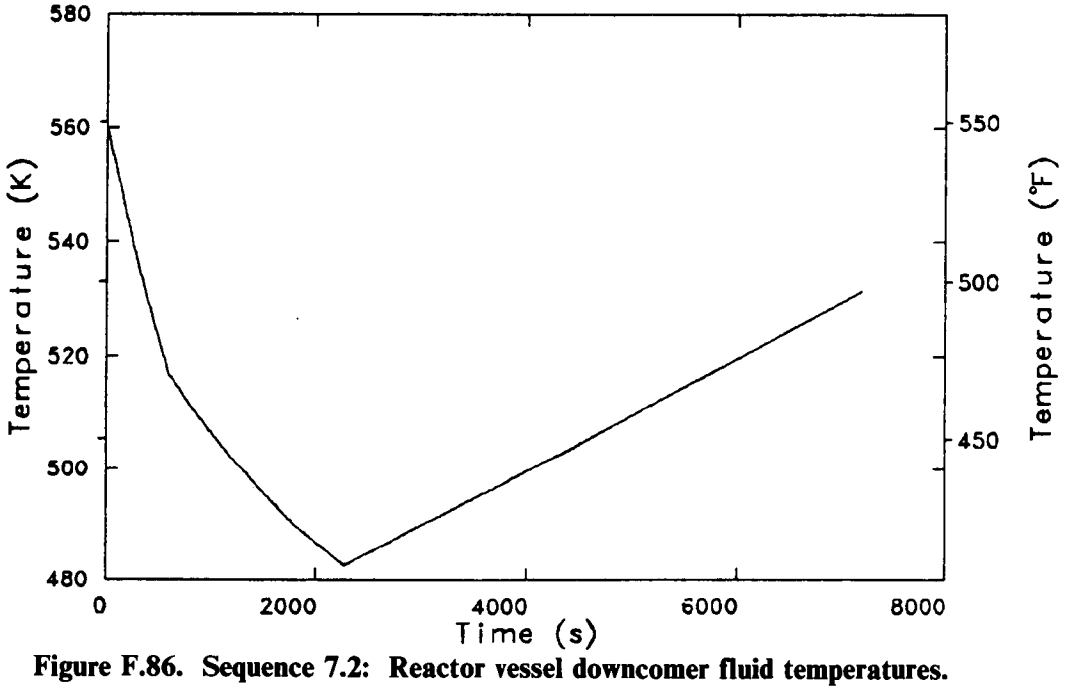

Figure F.86. Sequence 7.2: Reactor vessel downcomer fluid temperatures.

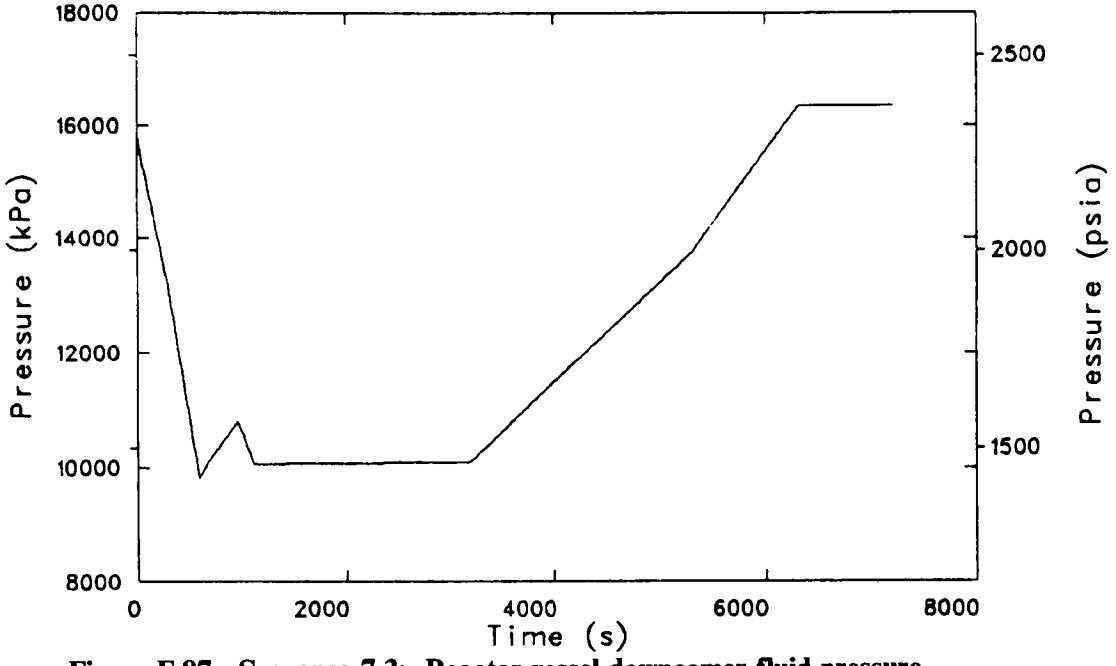

Figure F.87. Sequence 7.3: Reactor vessel downcomer fluid pressure.

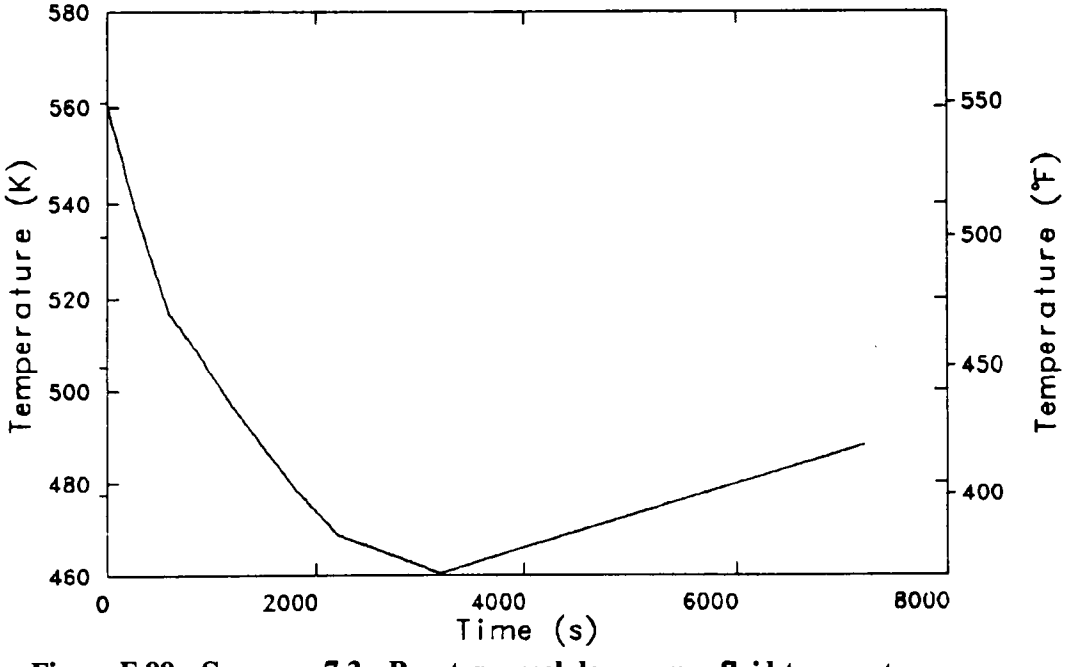

Figure F.88. Sequence 7.3: Reactor vessel downcomer fluid temperatures.

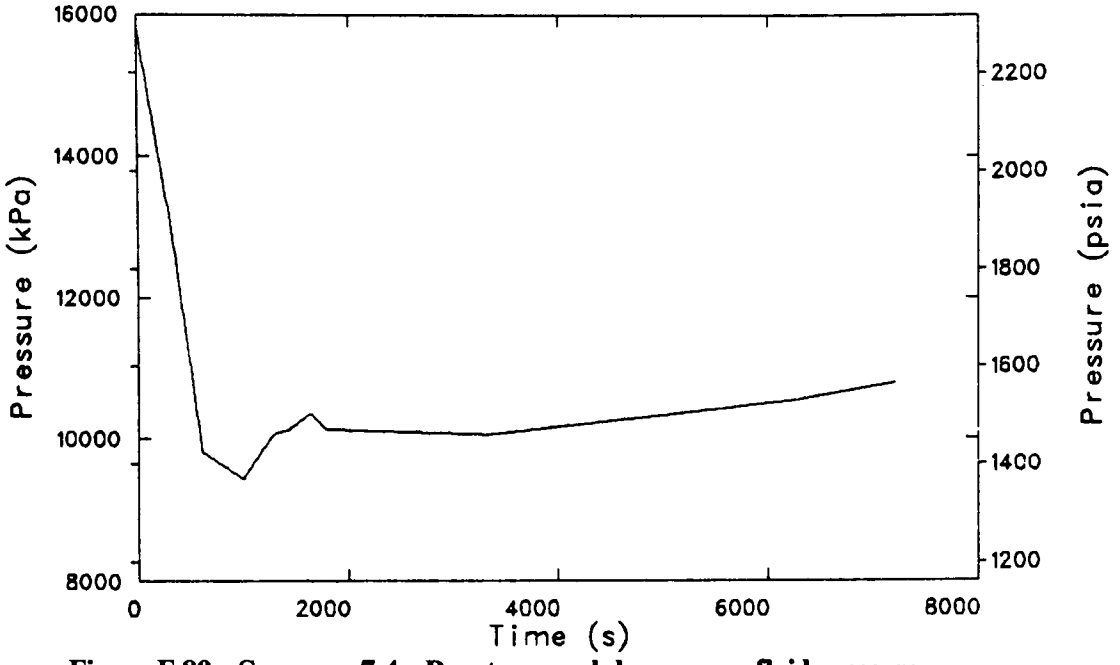

Figure F.89. Sequence 7.4: Reactor vessel downcomer fluid pressure.

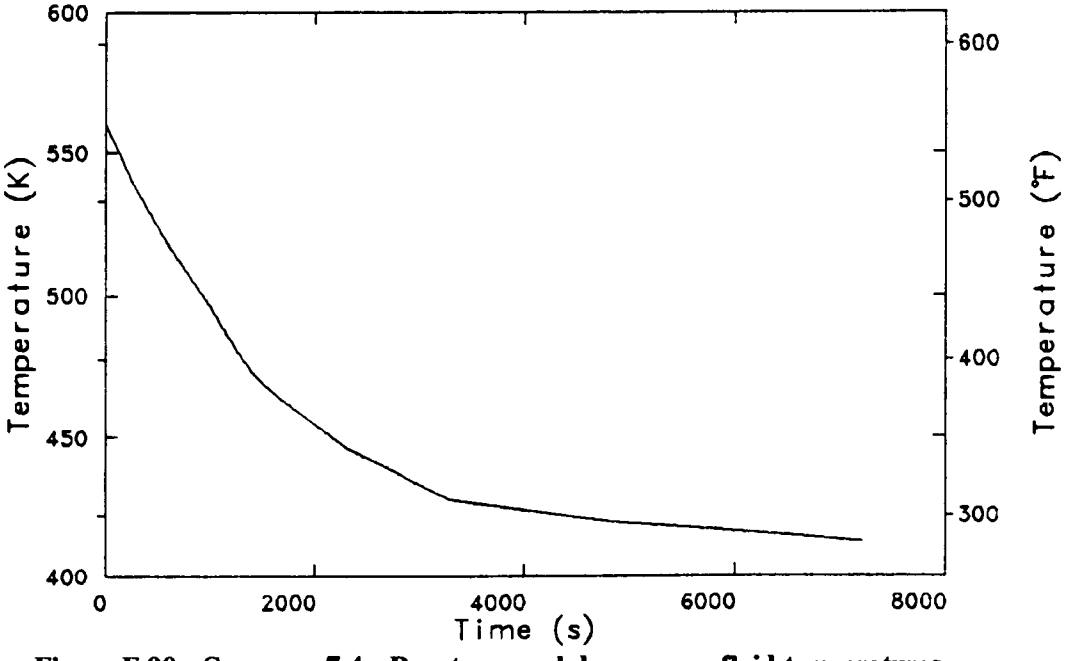

Figure F.90. Sequence 7.4: Reactor vessel downcomer fluid temperatures.

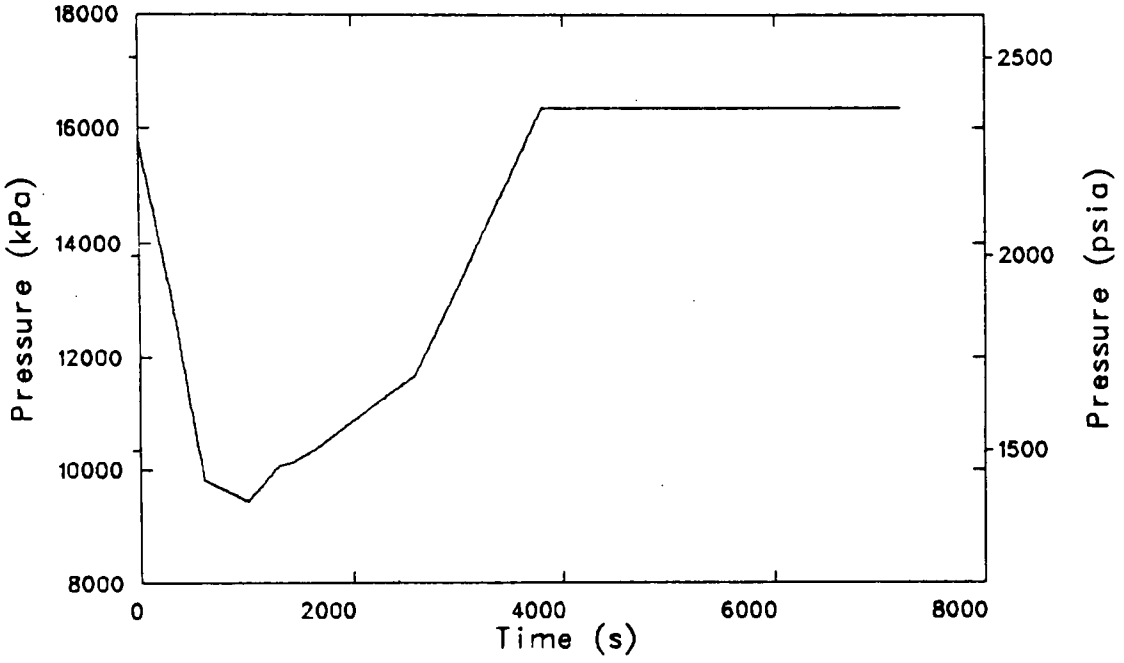

Figure F.91. Sequence 7.5: Reactor vessel downcomer fluid pressure.

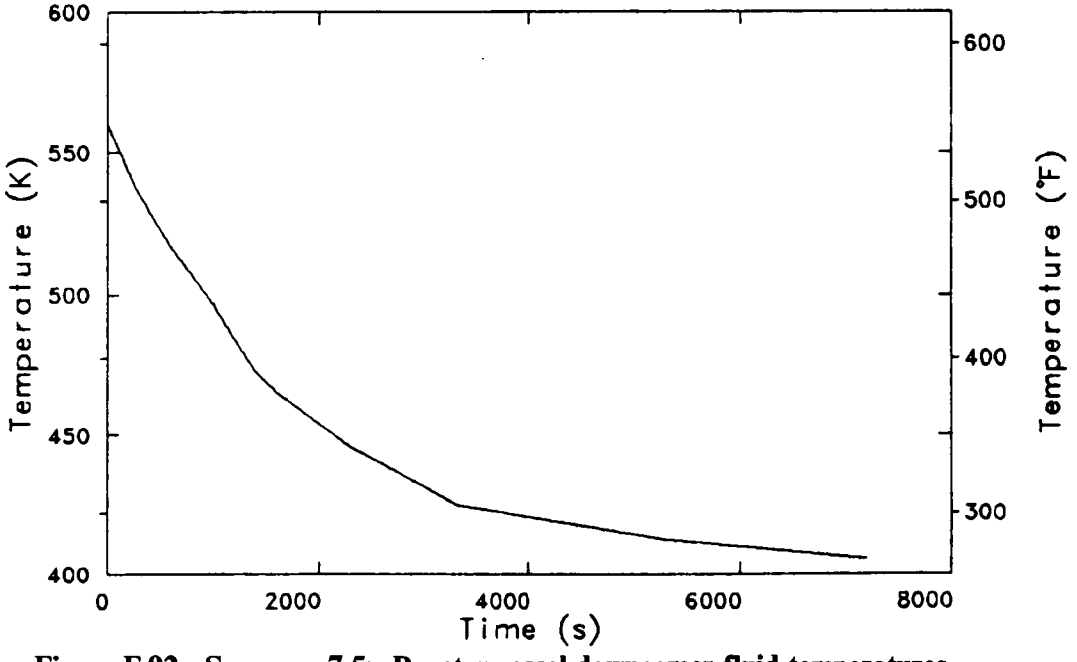

Figure F.92. Sequence 7.5: Reactor vessel downcomer fluid temperatures.

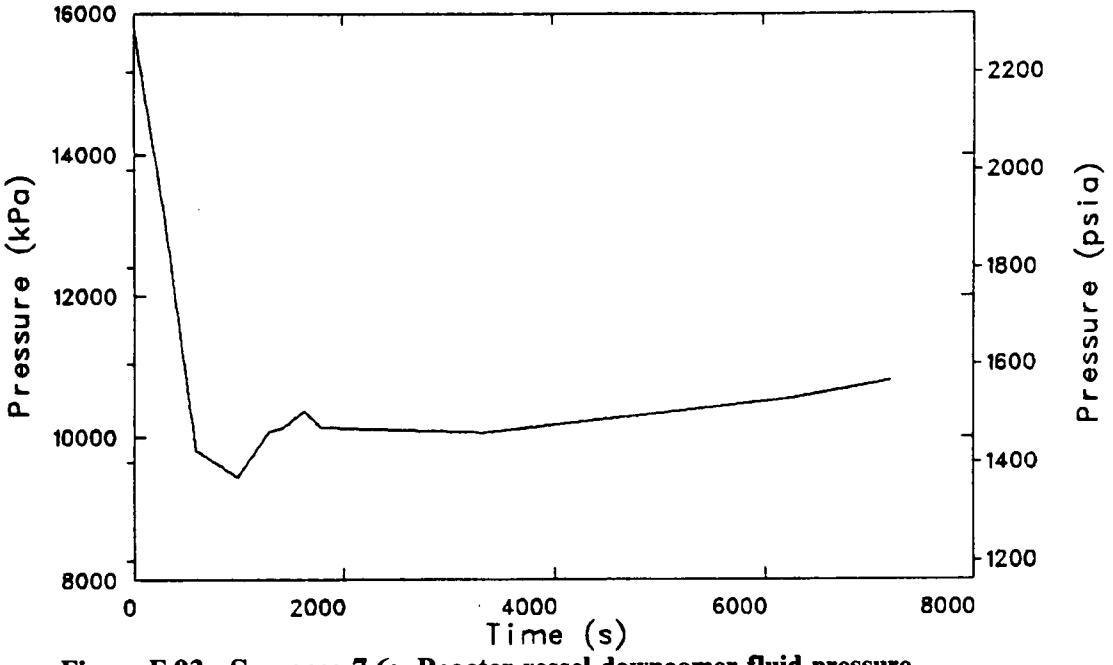

Figure F.93. Sequence 7.6: Reactor vessel downcomer fluid pressure.

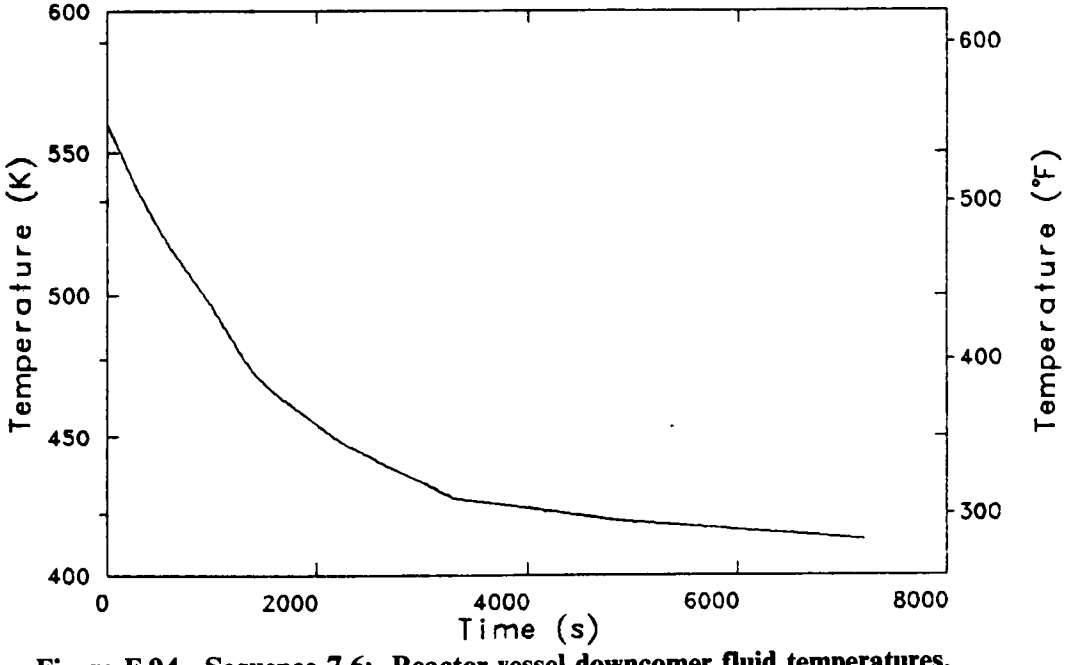

Figure F.94. Sequence 7.6: Reactor vessel downcomer fluid temperatures.

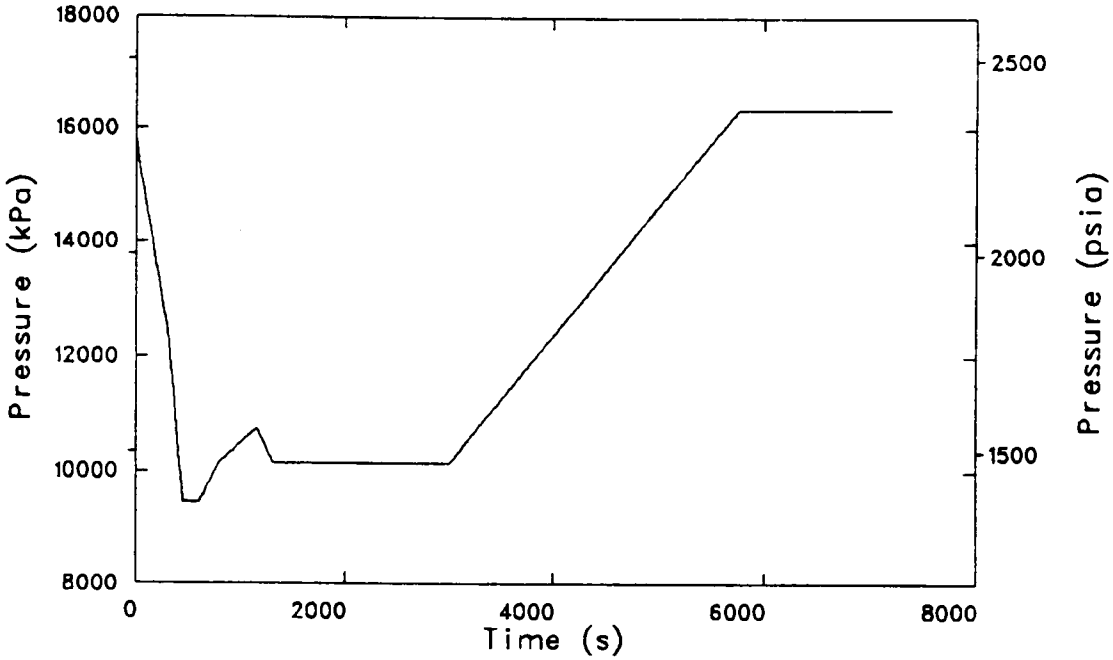

Figure F.95. Sequence 7.7: Reactor vessel downcomer fluid pressure.

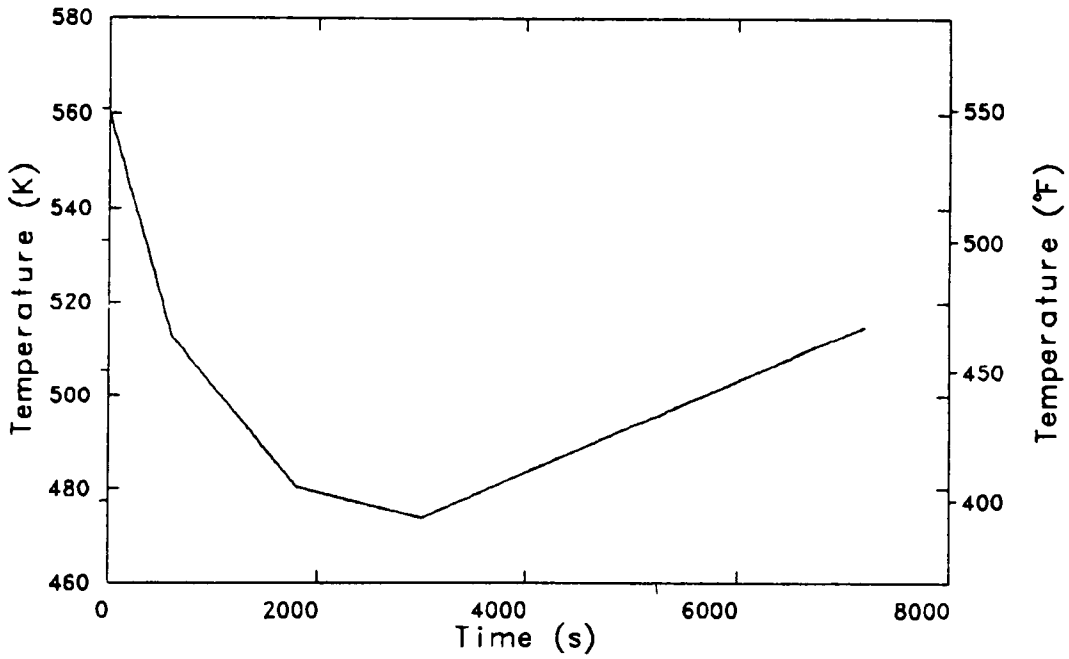

Figure F.96. Sequence 7.7: Reactor vessel downcomer fluid temperatures.

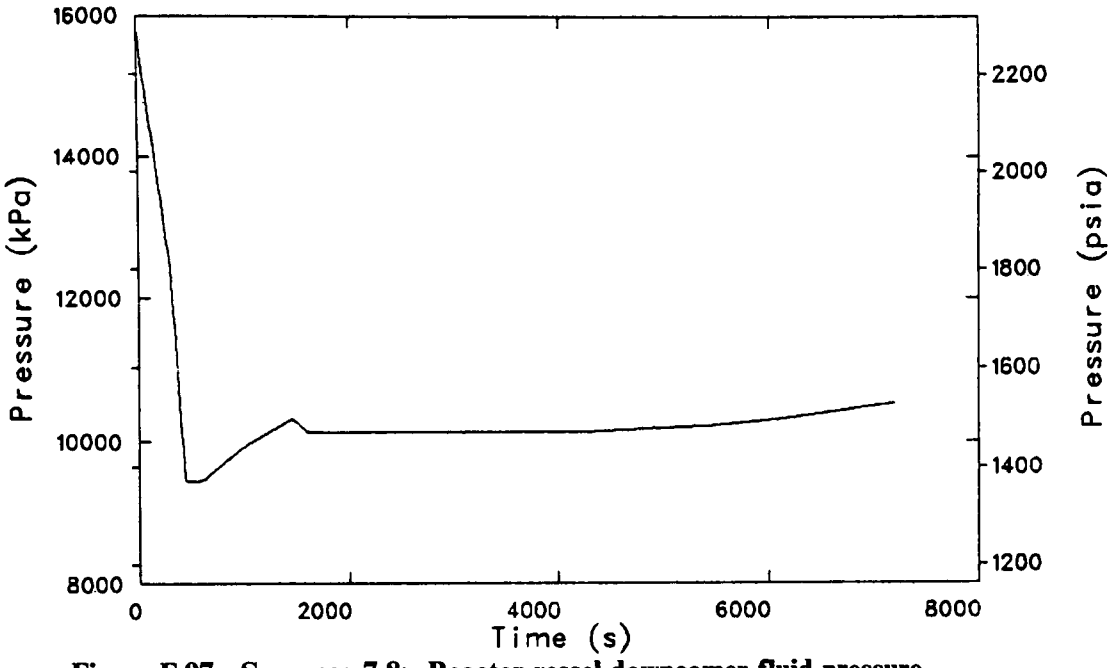

Figure F.97. Sequence 7.8: Reactor vessel downcomer fluid pressure.

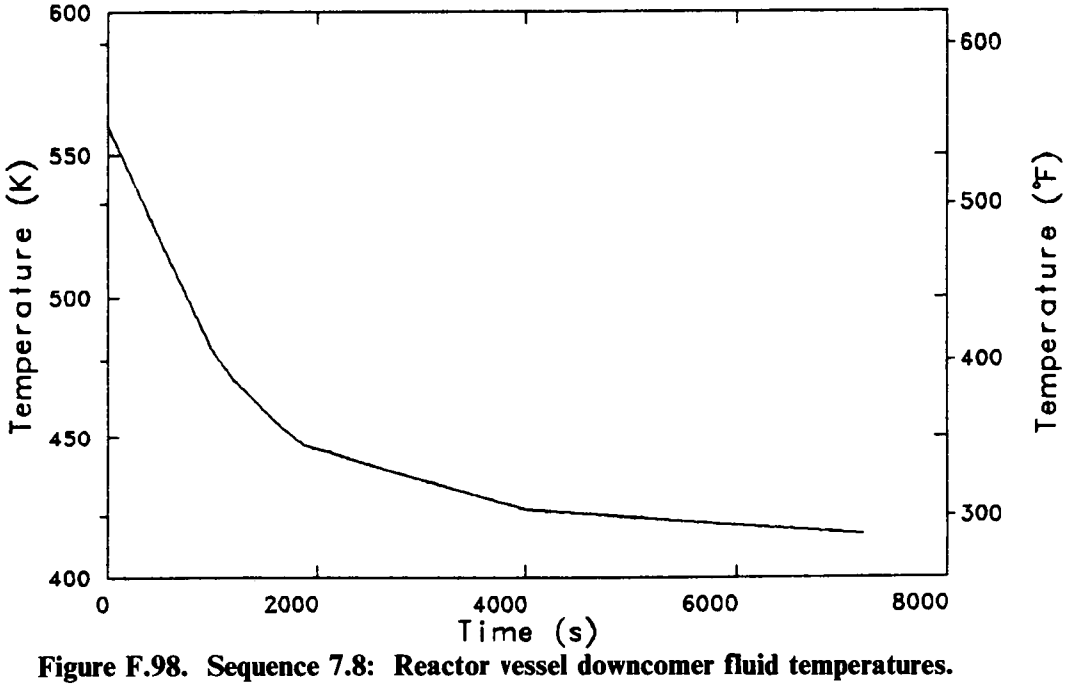

Figure F.98. Sequence 7.8: Reactor vessel downcomer fluid temperatures.

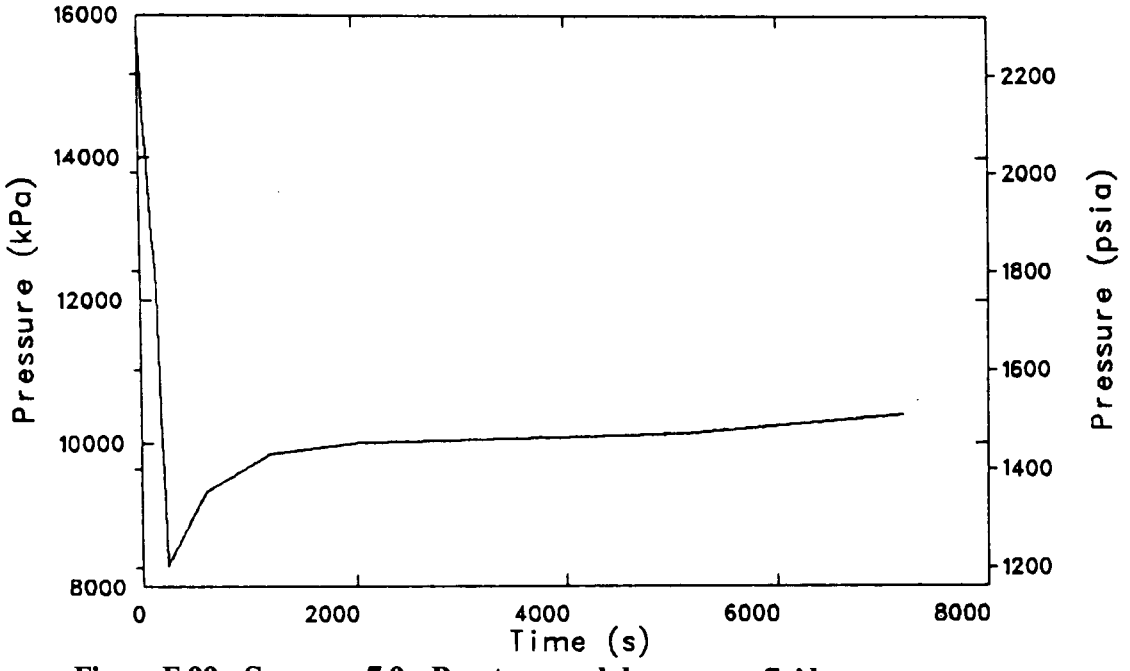

Figure F.99. Sequence 7.9: Reactor vessel downcomer fluid pressure.

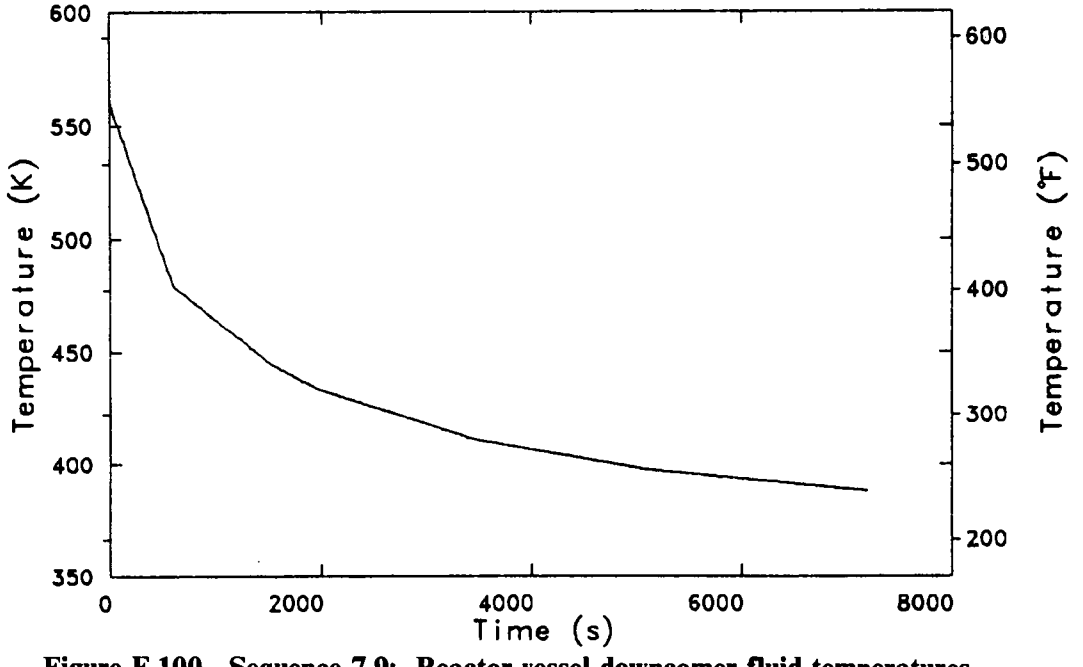

Figure F.100. Sequence 7.9: Reactor vessel downcomer fluid temperatures.

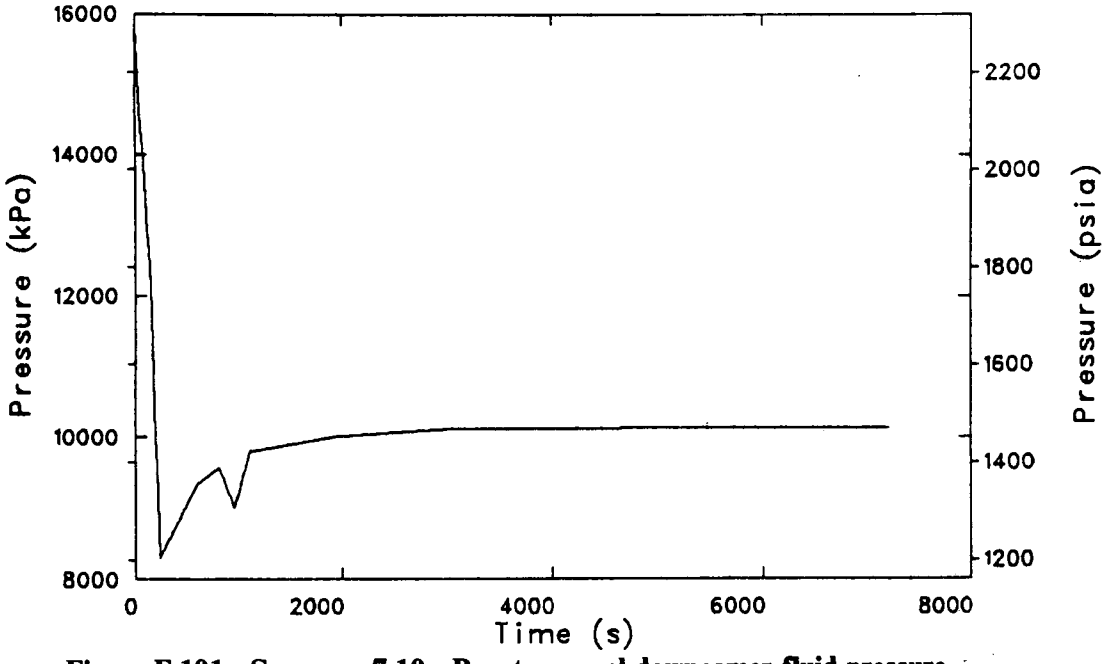

Figure F.101. Sequence 7.10: Reactor vessel downcomer fluid pressure.

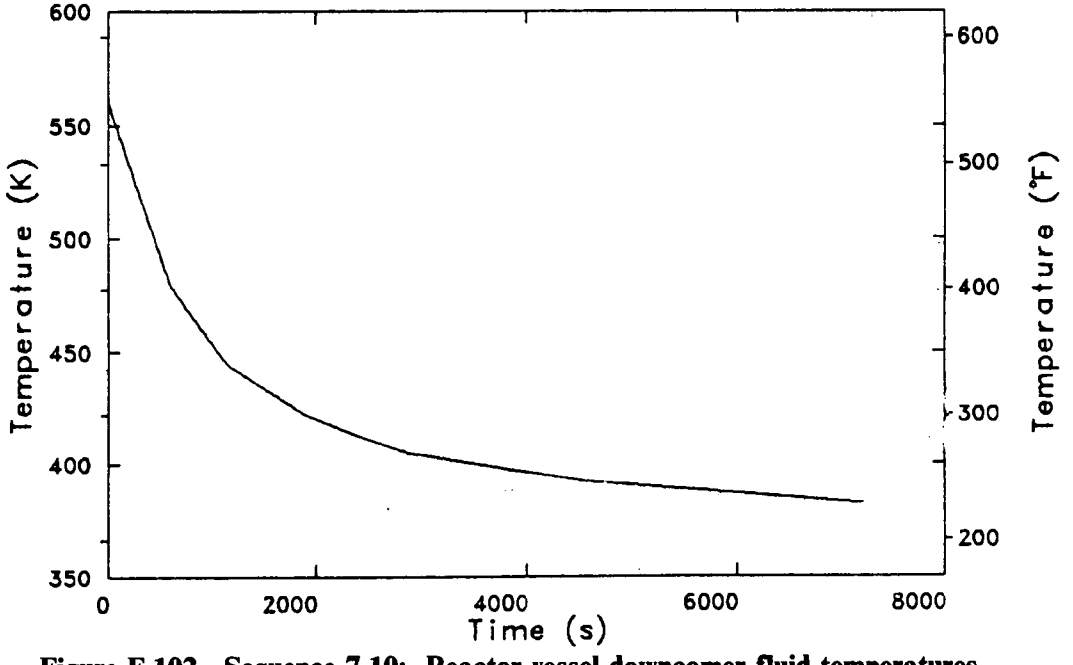

Figure F.102. Sequence 7.10: Reactor vessel downcomer fluid temperatures.

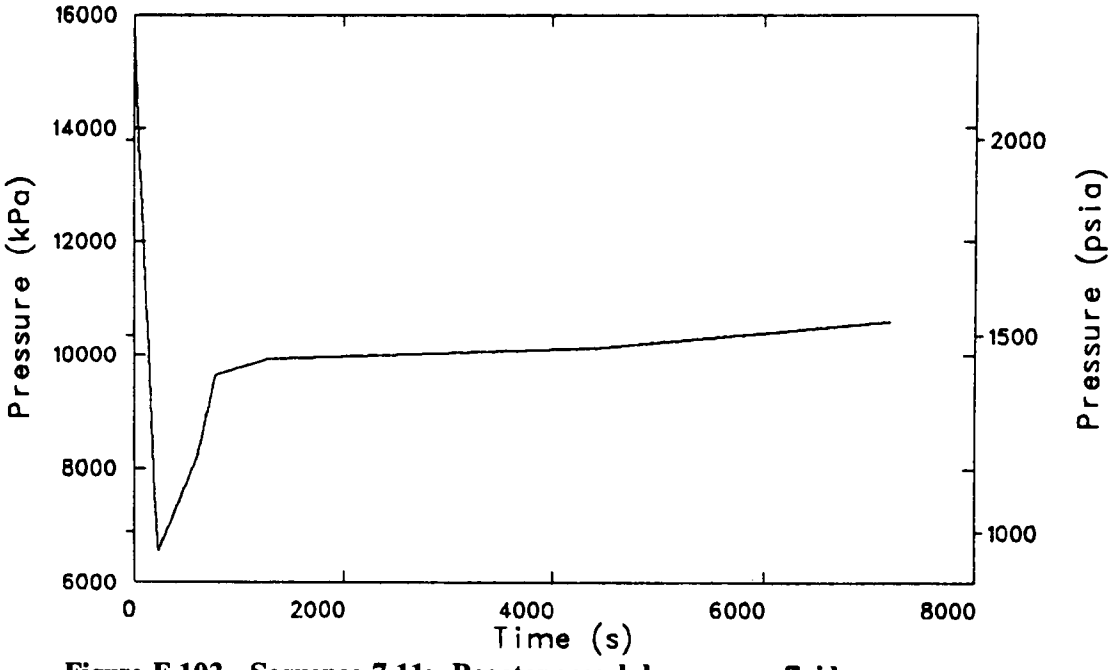

Figure F.103. Sequence 7.11: Reactor vessel downcomer fluid pressure.

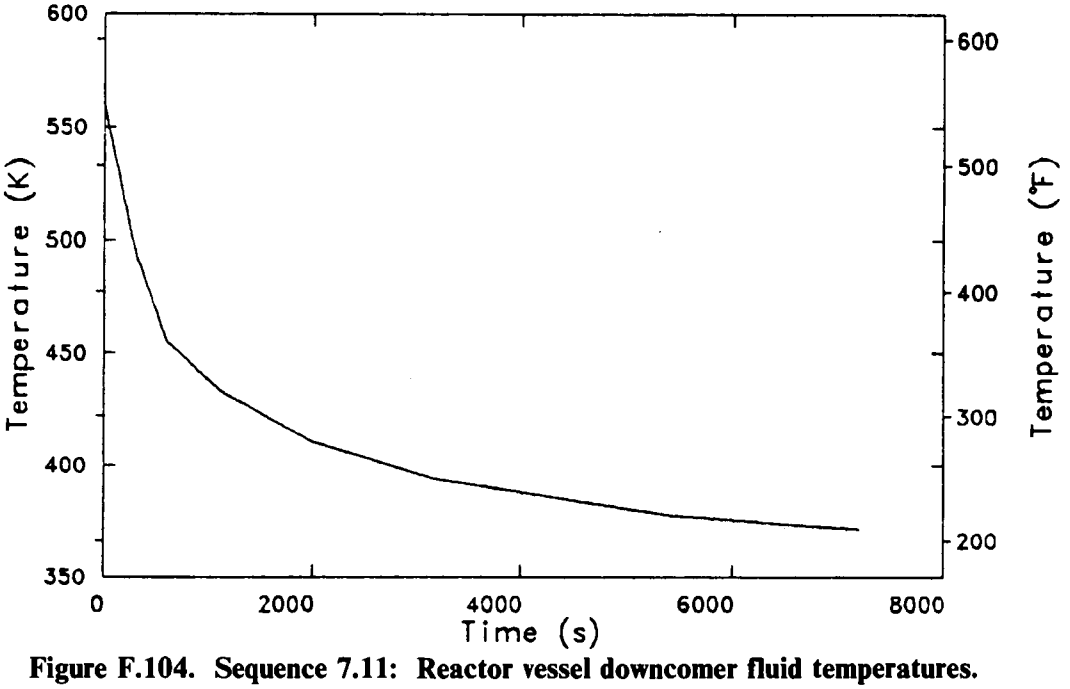

Figure F.104. Sequence 7.11: Reactor vessel downcomer fluid temperatures.

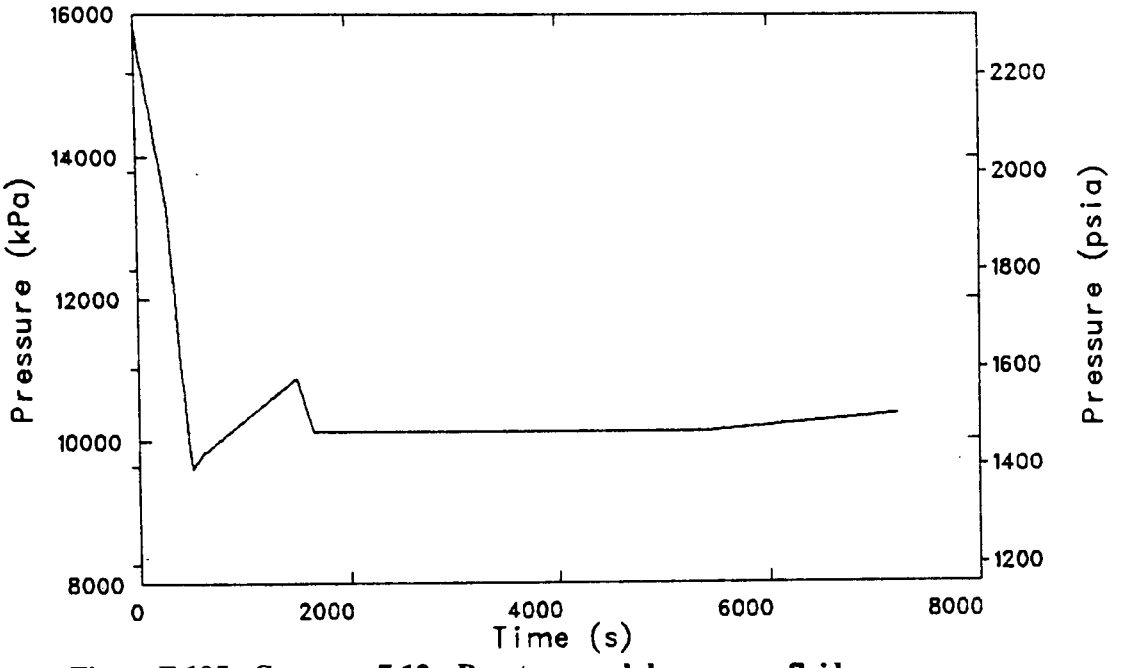

Figure F.105. Sequence 7.12: Reactor vessel downcomer fluid pressure.

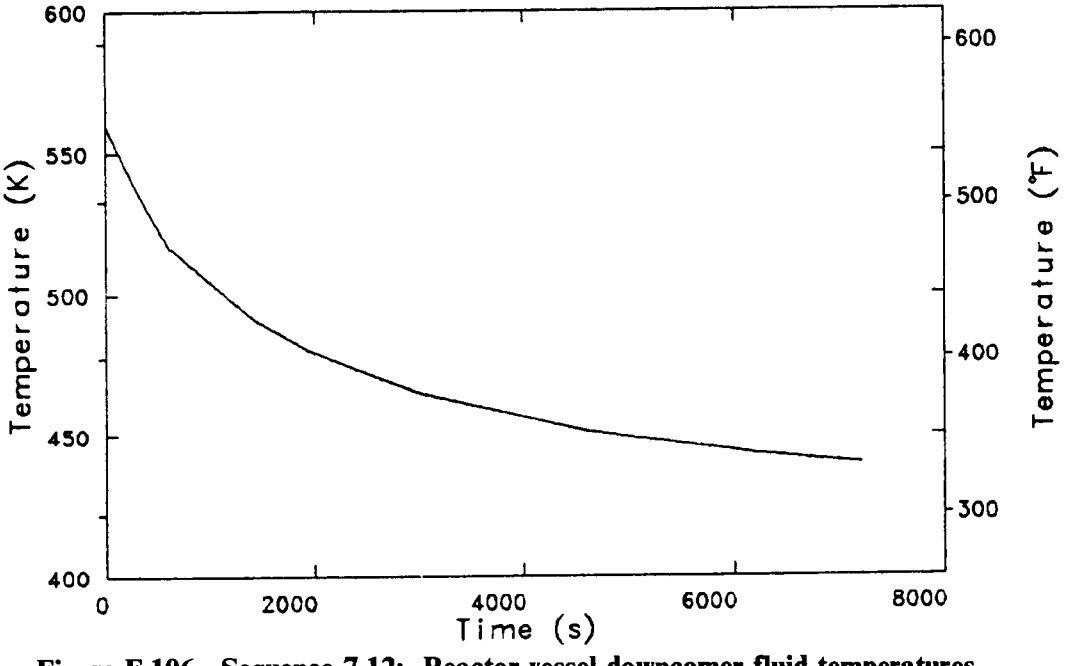

Figure F.106. Sequence 7.12: Reactor vessel downcomer fluid temperatures.

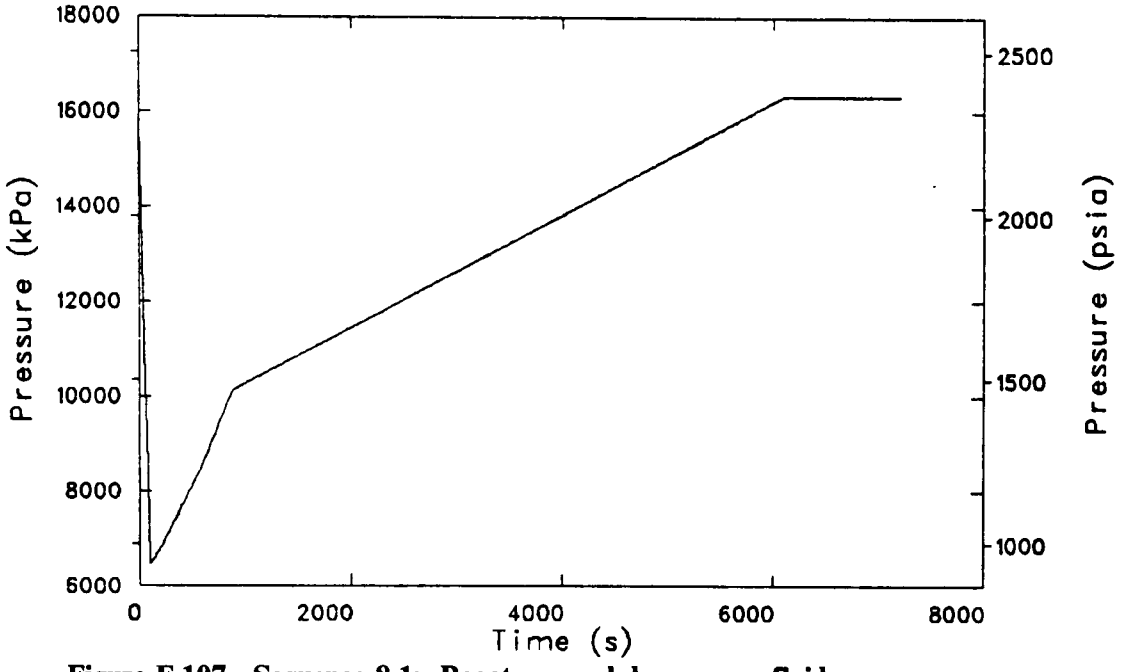

Figure F.107. Sequence 8.1: Reactor vessel downcomer fluid pressure.

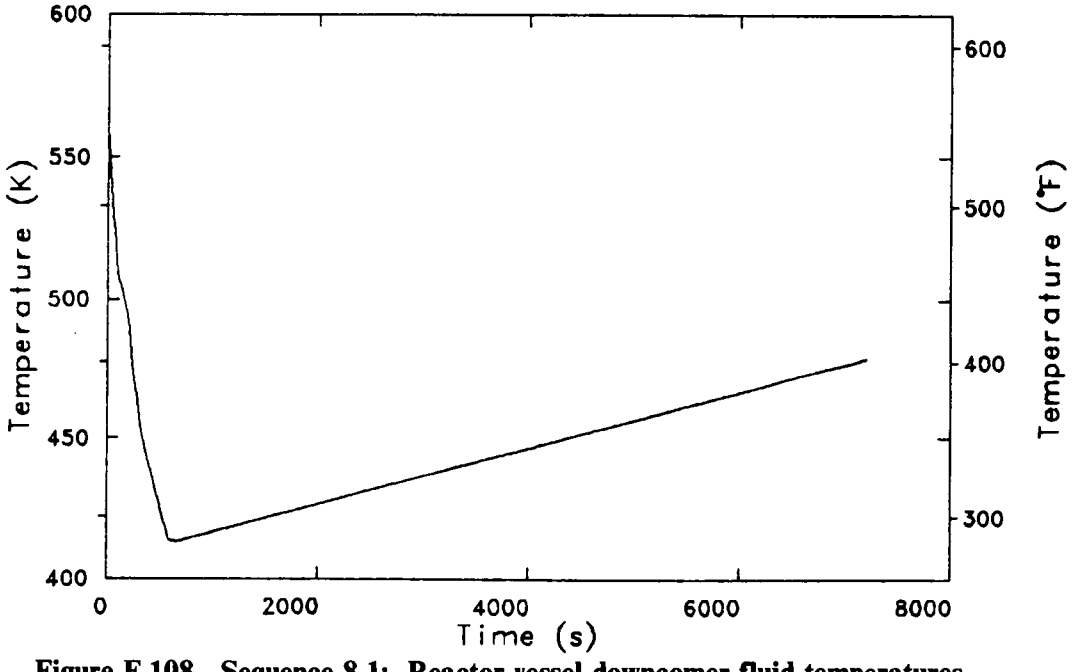

Figure F.108. Sequence 8.1: Reactor vessel downcomer fluid temperatures.

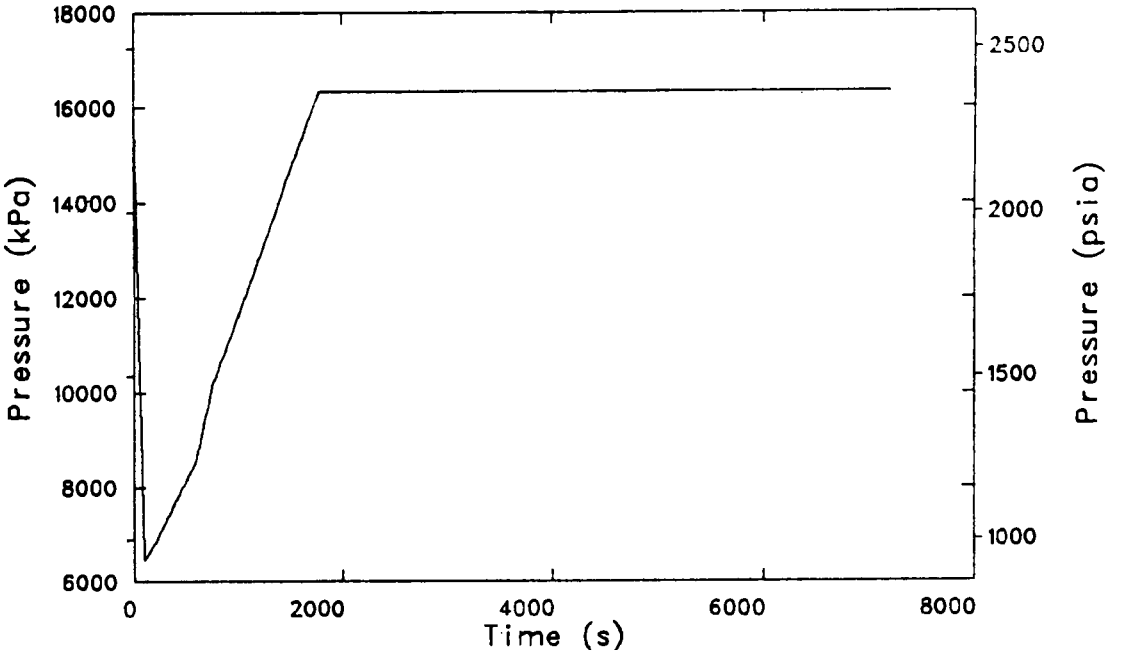

Figure F.109. Sequence 8.2: Reactor vessel downcomer fluid pressure.

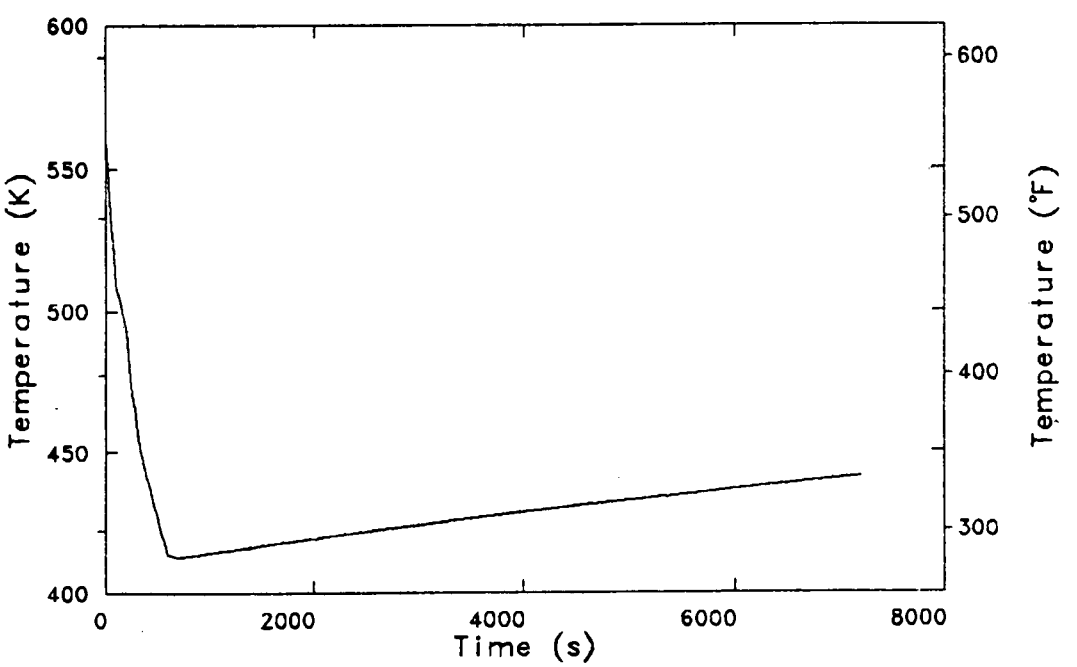

Figure F.110. Sequence 8.2: Reactor vessel downcomer fluid temperatures.

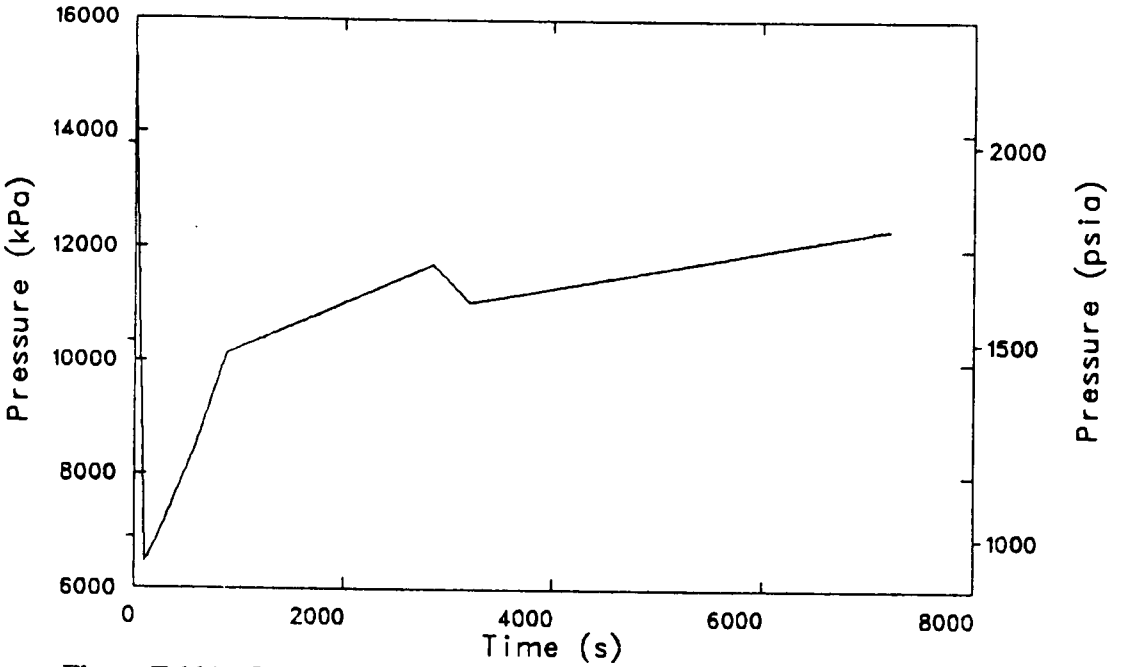

Figure F.111. Sequence 8.3: Reactor vessel downcomer fluid pressure.

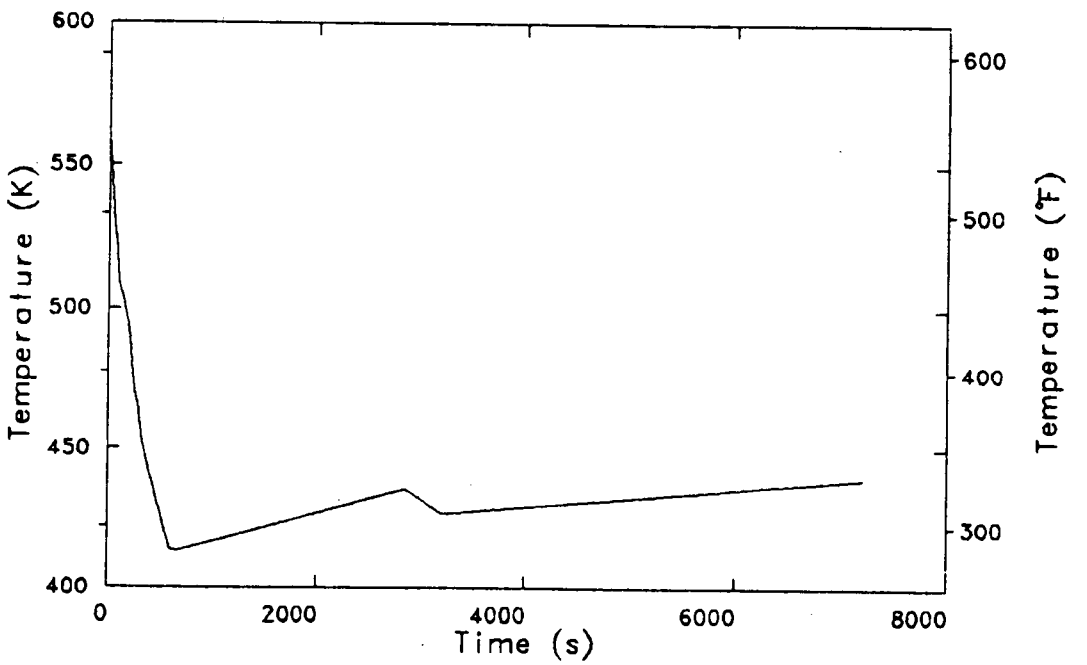

Figure F.112. Sequence 8.3: Reactor vessel downcomer fluid temperatures.

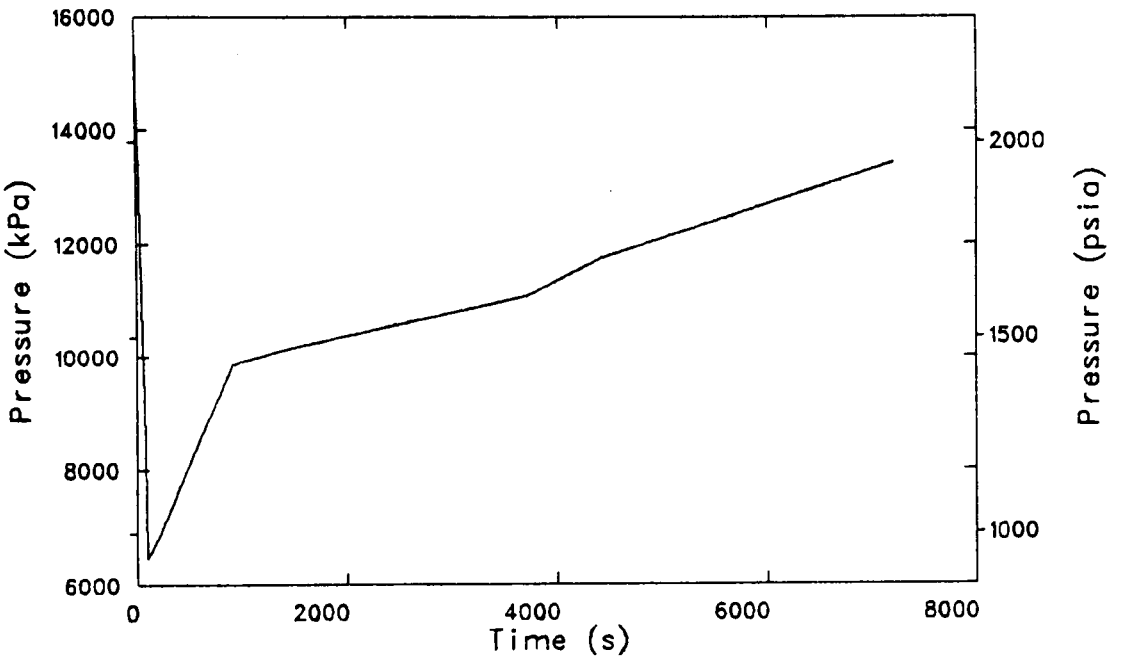

Figure F.113. Sequence 8.4: Reactor vessel downcomer fluid pressure.

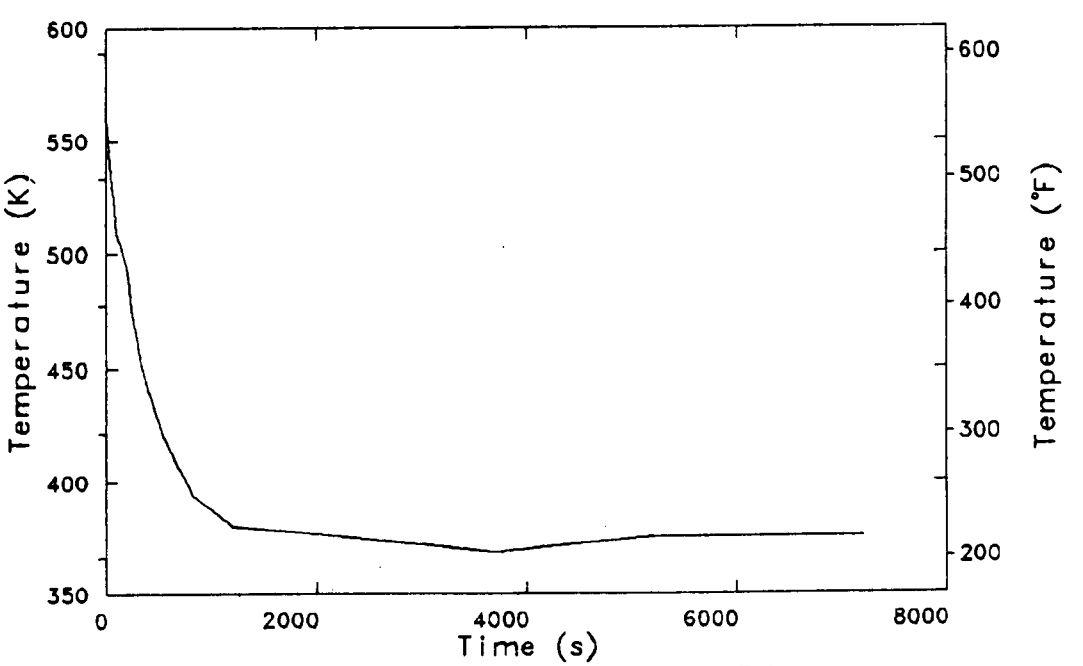

Figure F.114. Sequence 8.4: Reactor vessel downcomer fluid temperatures.

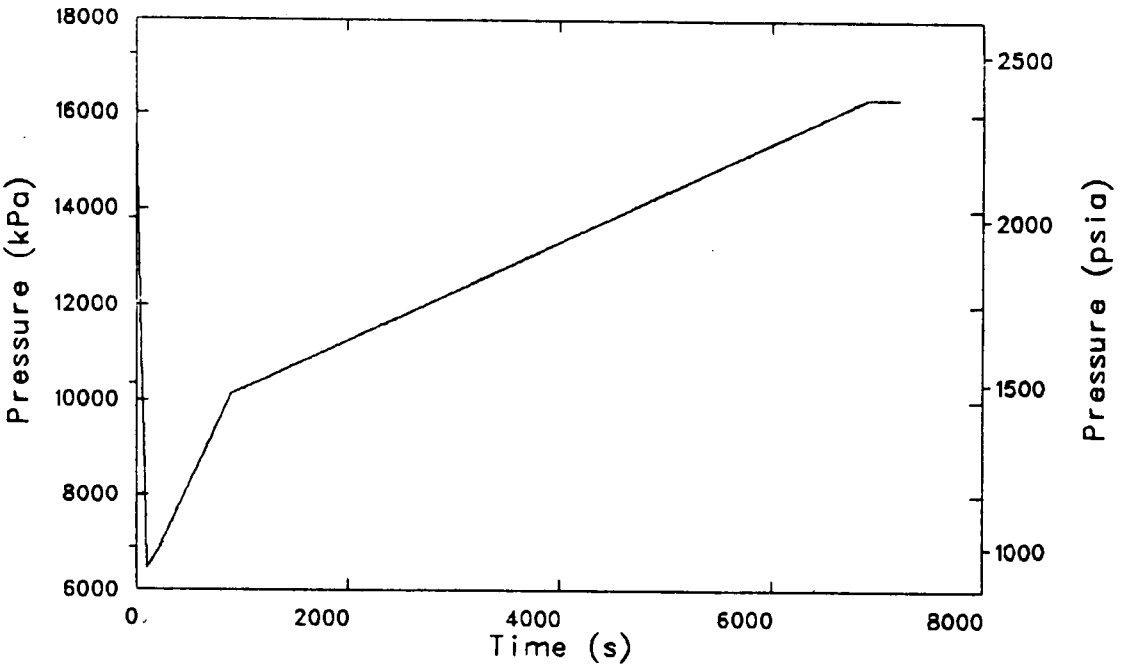

Figure F.115. Sequence 8.5: Reactor vessel downcomer fluid pressure.

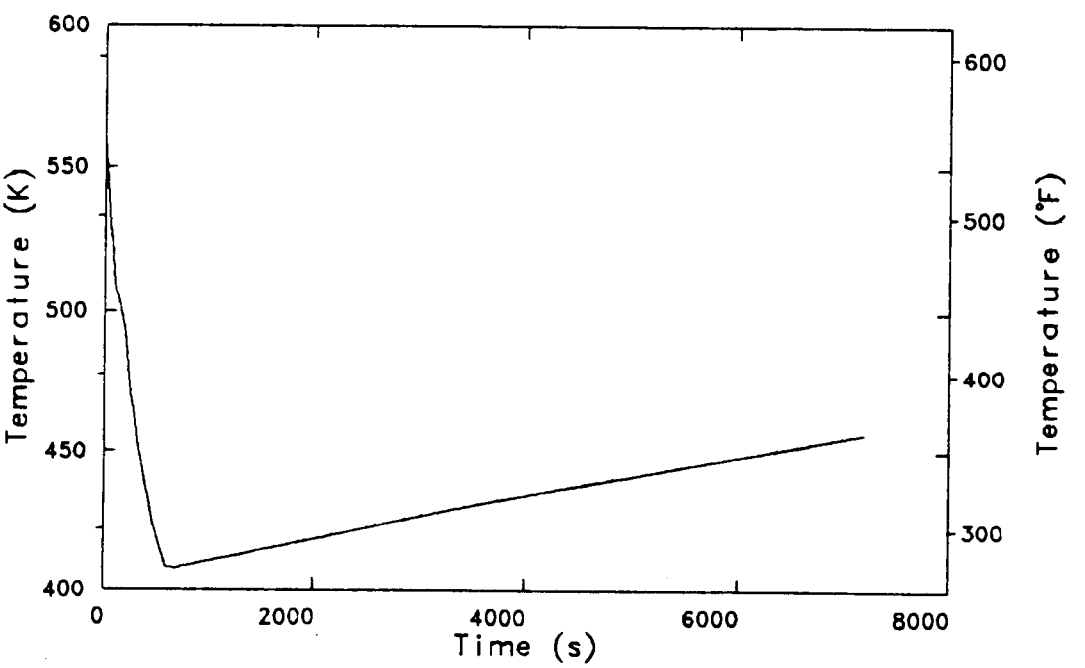

Figure F.116. Sequence 8.5: Reactor vessel downcomer fluid temperatures.

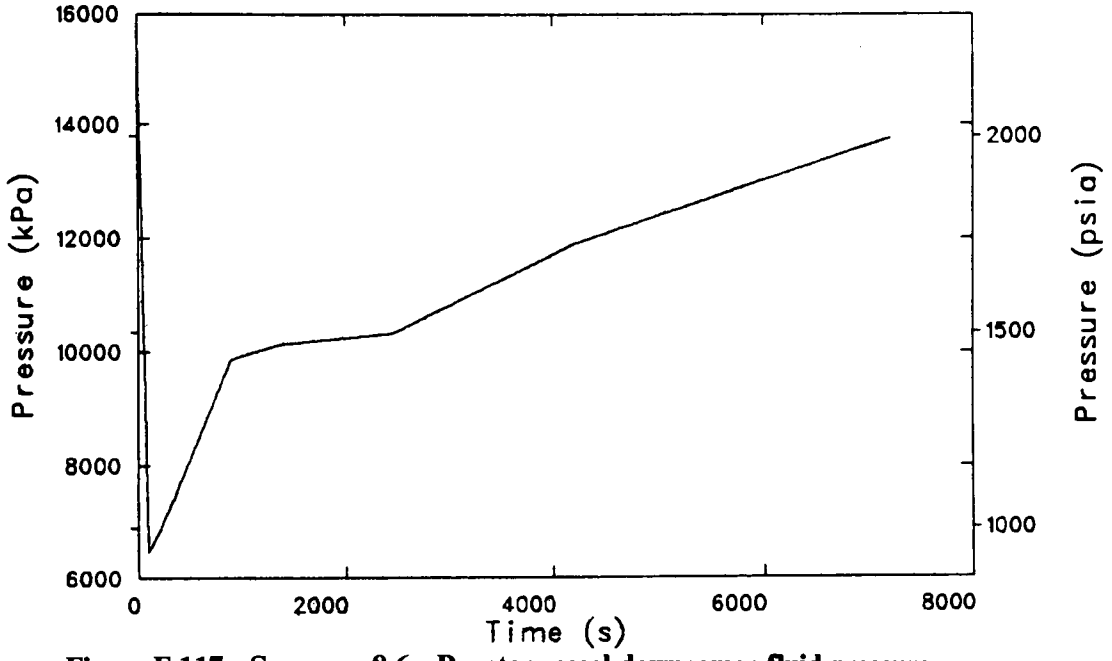

Figure F.117. Sequence 8.6: Reactor vessel downcomer fluid pressure.

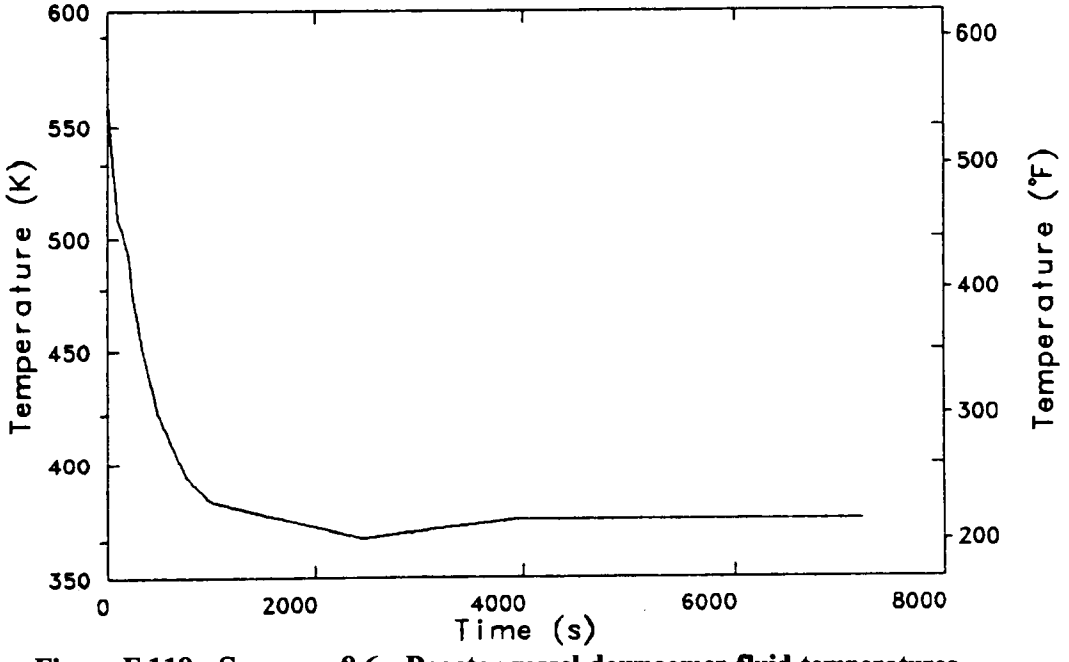

Figure F.118. Sequence 8.6: Reactor vessel downcomer fluid temperatures.

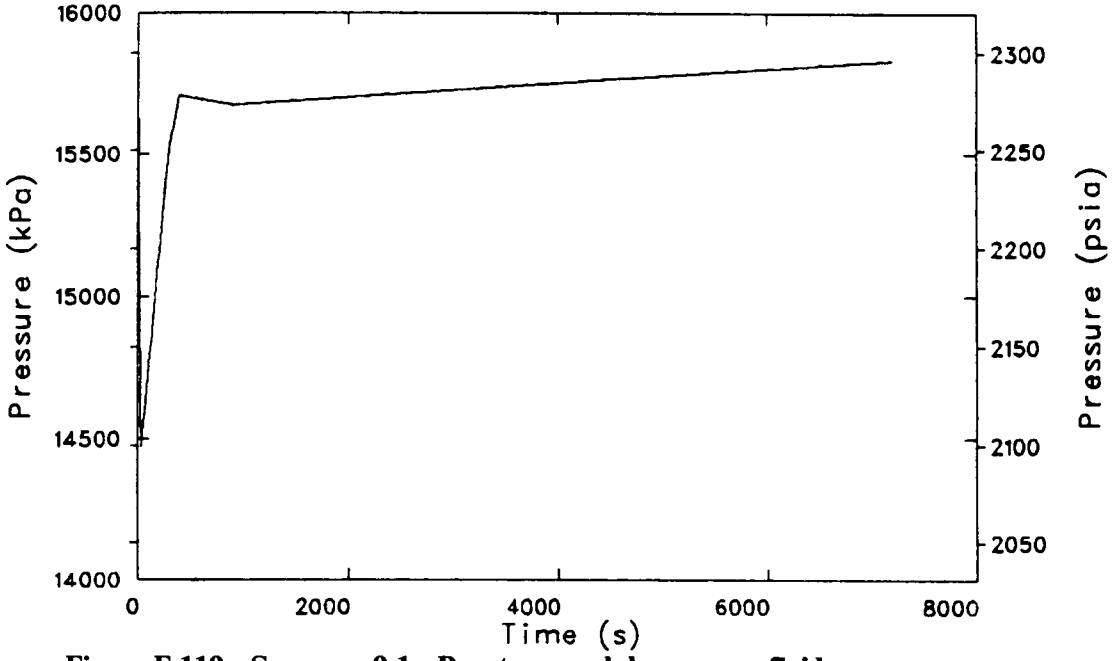

Figure F.119. Sequence 9.1: Reactor vessel downcomer fluid pressure.

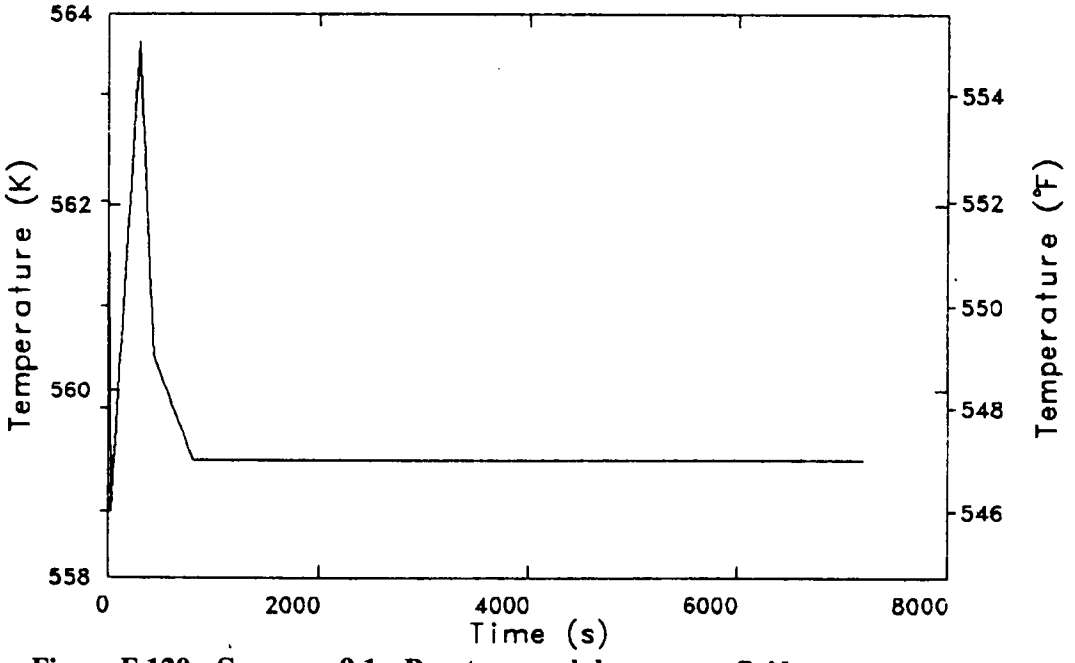

Figure F.120. Sequence 9.1: Reactor vessel downcomer fluid temperatures.

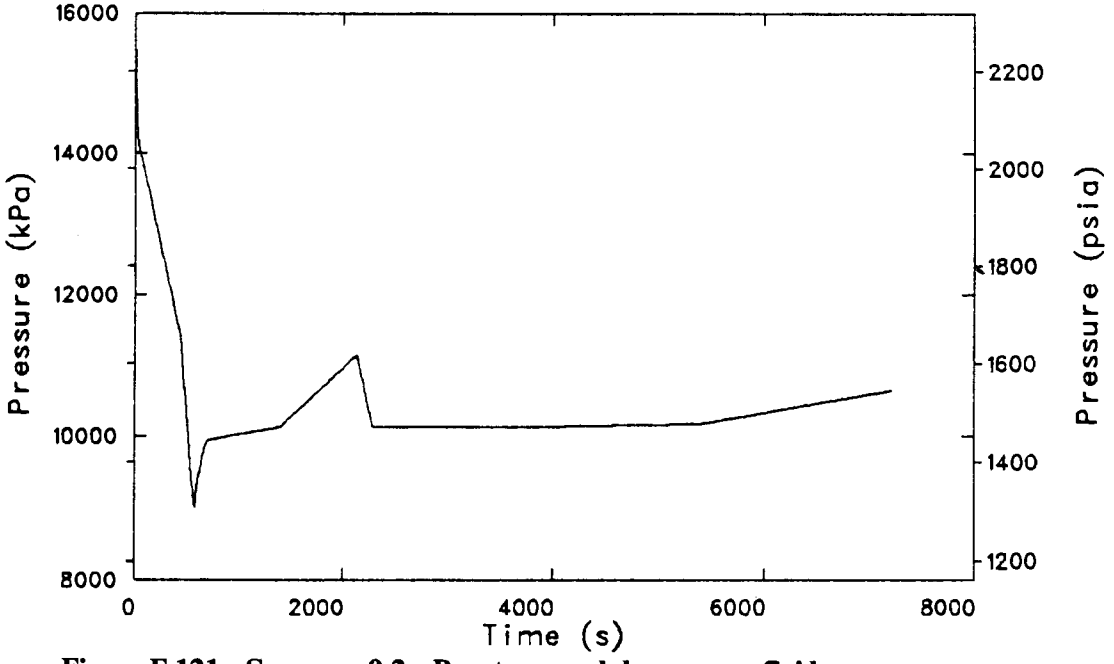

Figure F.121. Sequence 9.2: Reactor vessel downcomer fluid pressure.

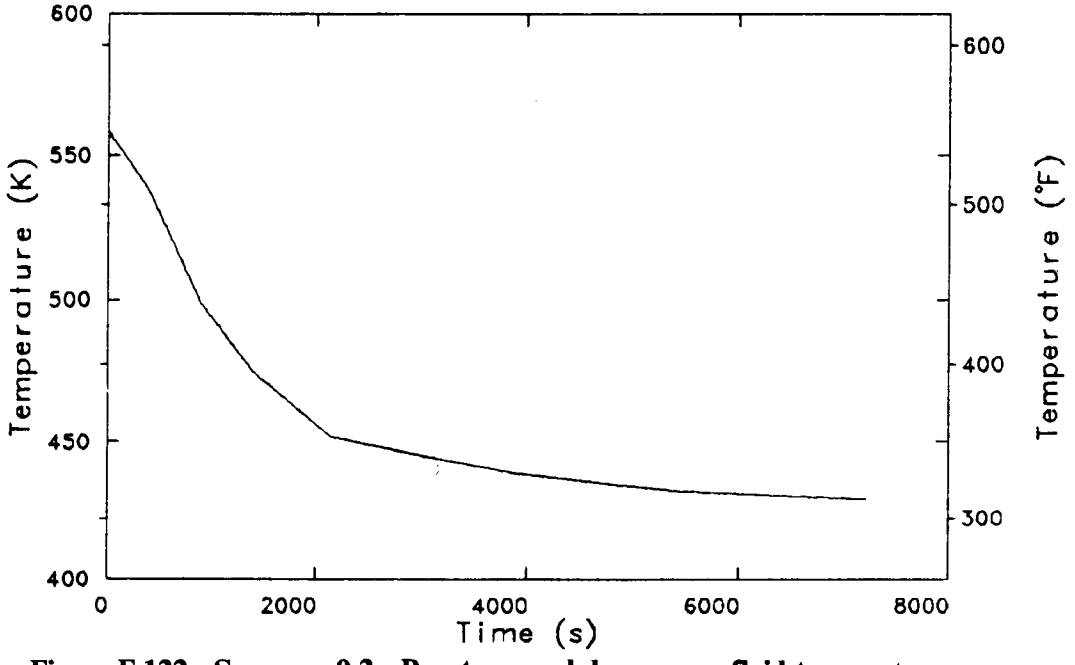

Figure F.122. Sequence 9.2: Reactor vessel downcomer fluid temperatures.

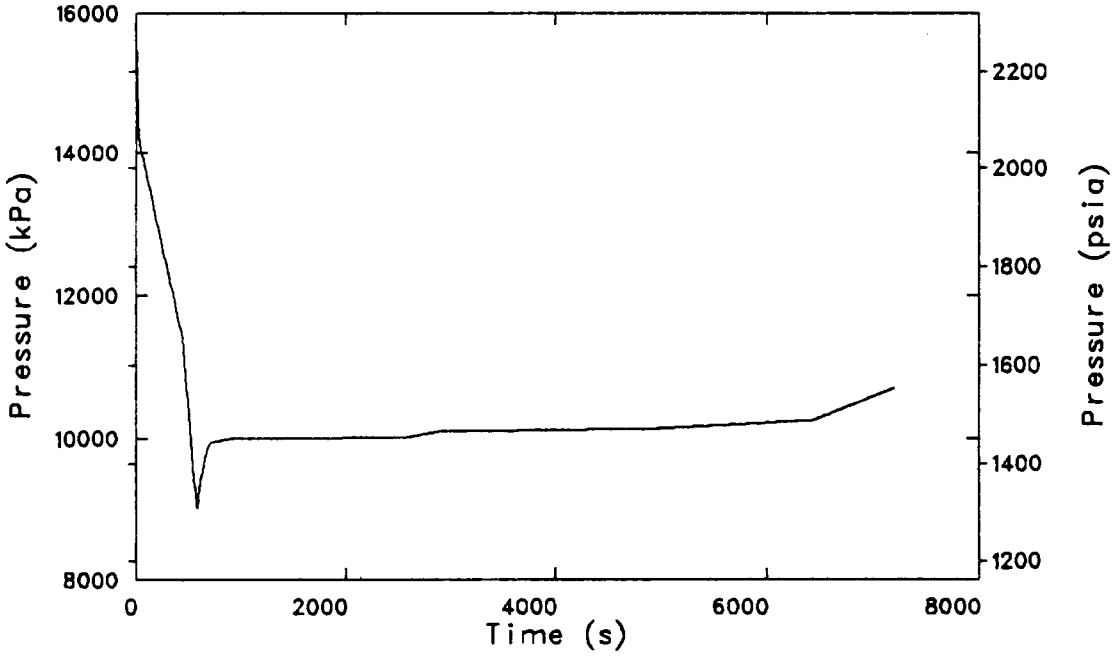

Figure F.123. Sequence 9.3: Reactor vessel downcomer fluid pressure.

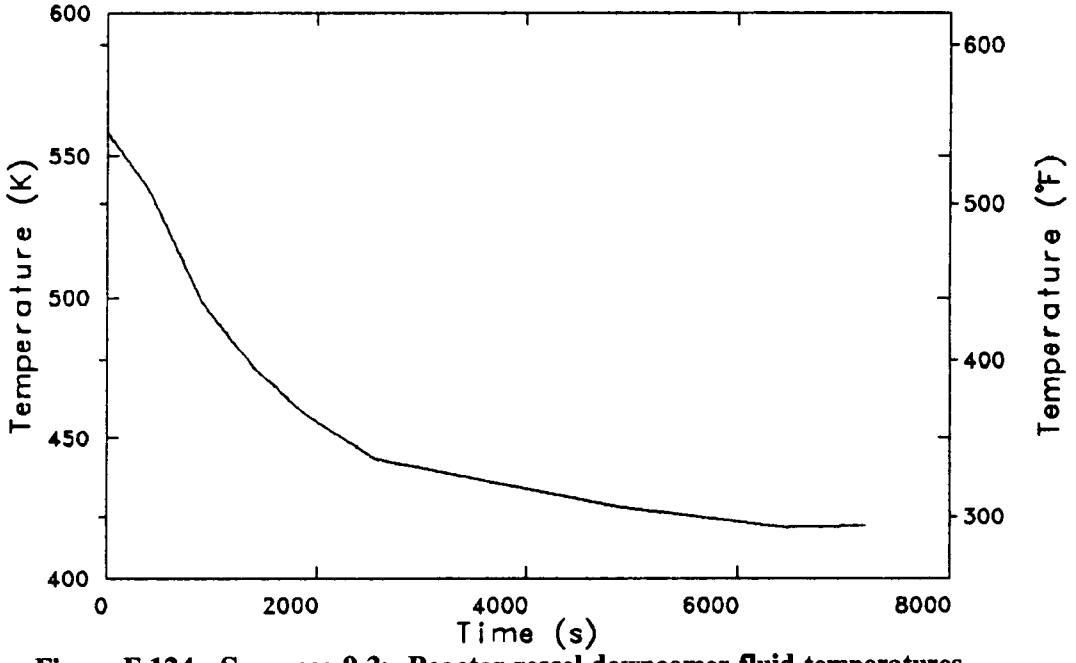

Figure F.124. Sequence 9.3: Reactor vessel downcomer fluid temperatures.

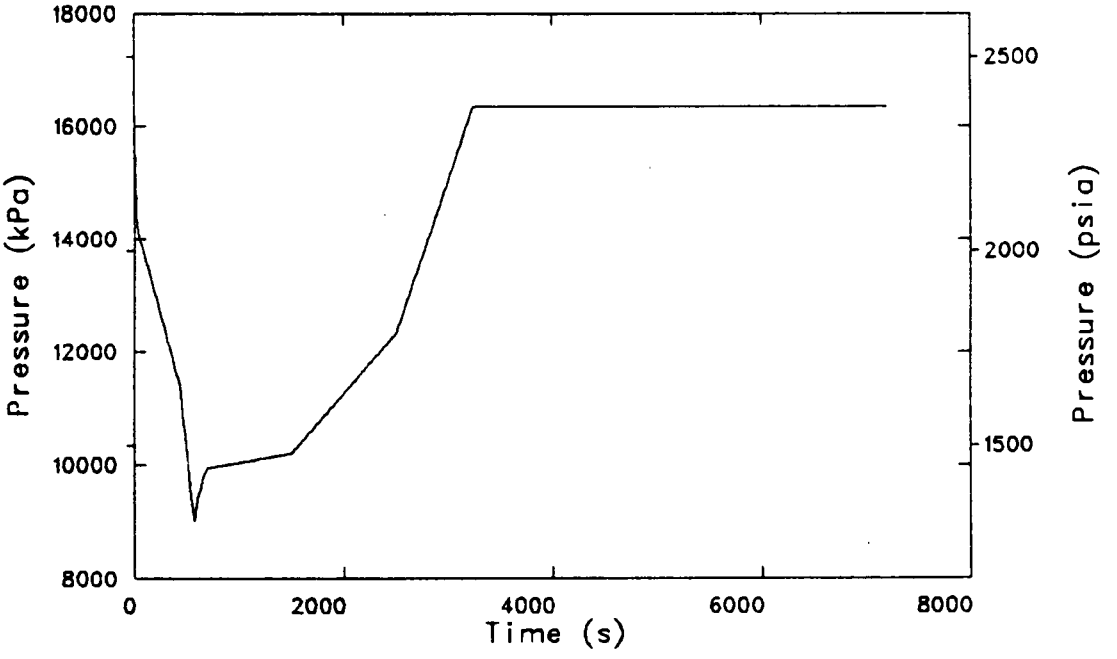

Figure F.125. Sequence 9.4: Reactor vessel downcomer fluid pressure.

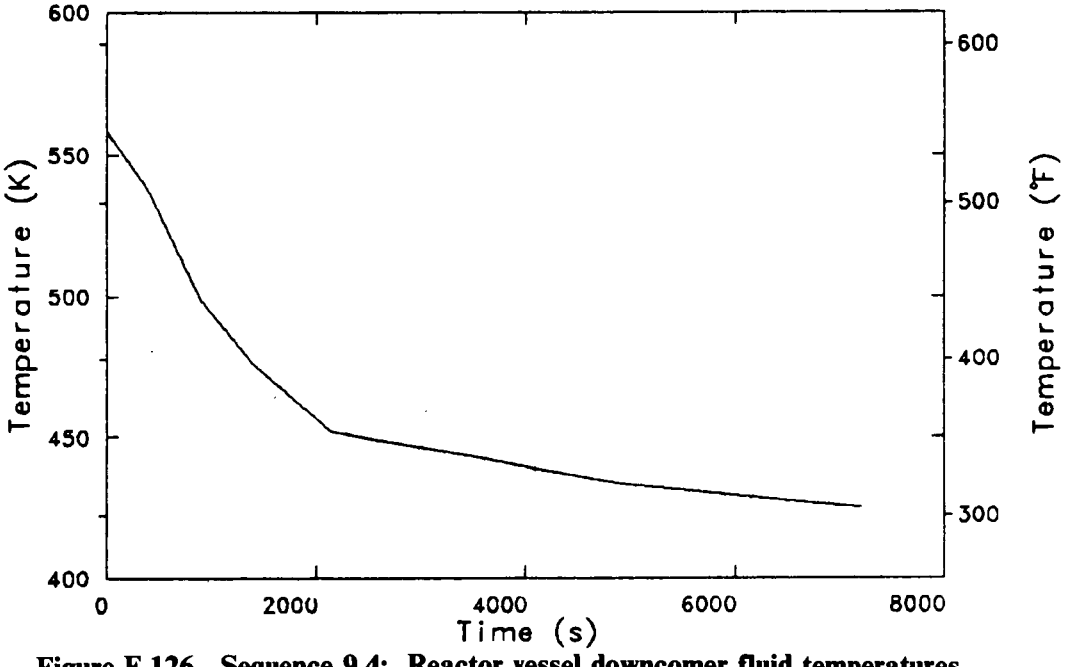

Figure F.126. Sequence 9.4: Reactor vessel downcomer fluid temperatures.

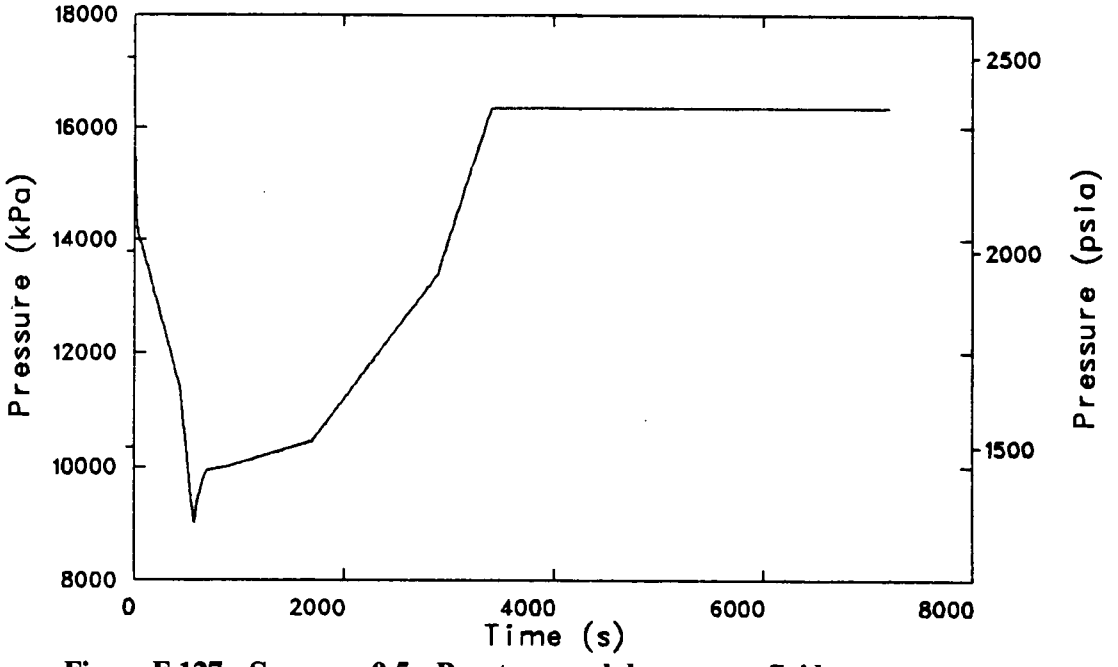

Figure F.127. Sequence 9.5: Reactor vessel downcomer fluid pressure.

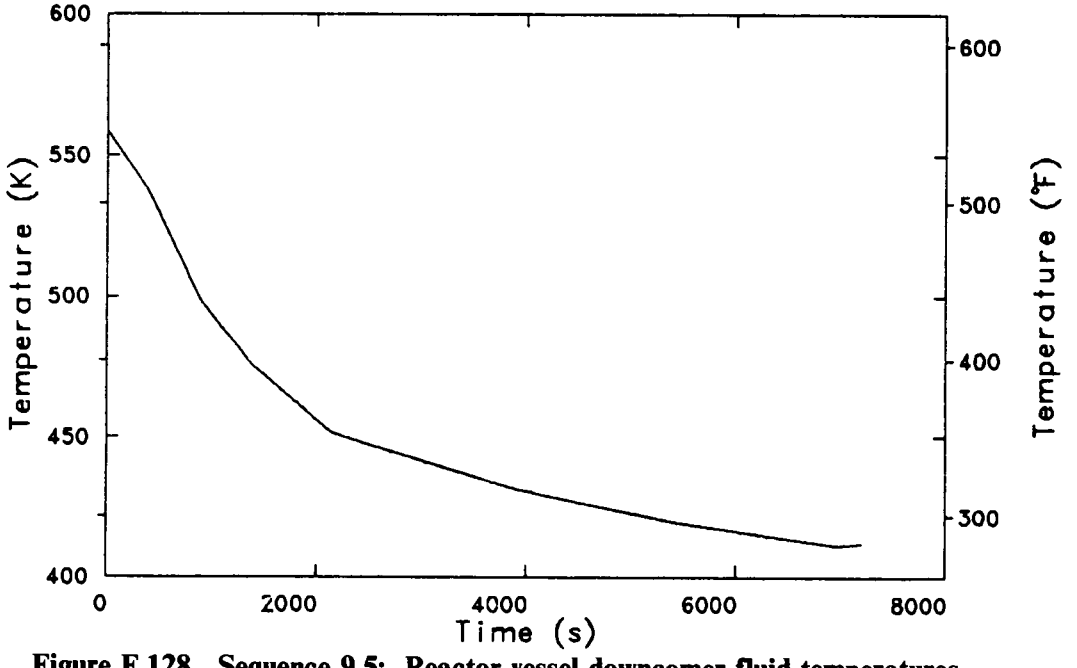

Figure F.128. Sequence 9.5: Reactor vessel downcomer fluid temperatures.

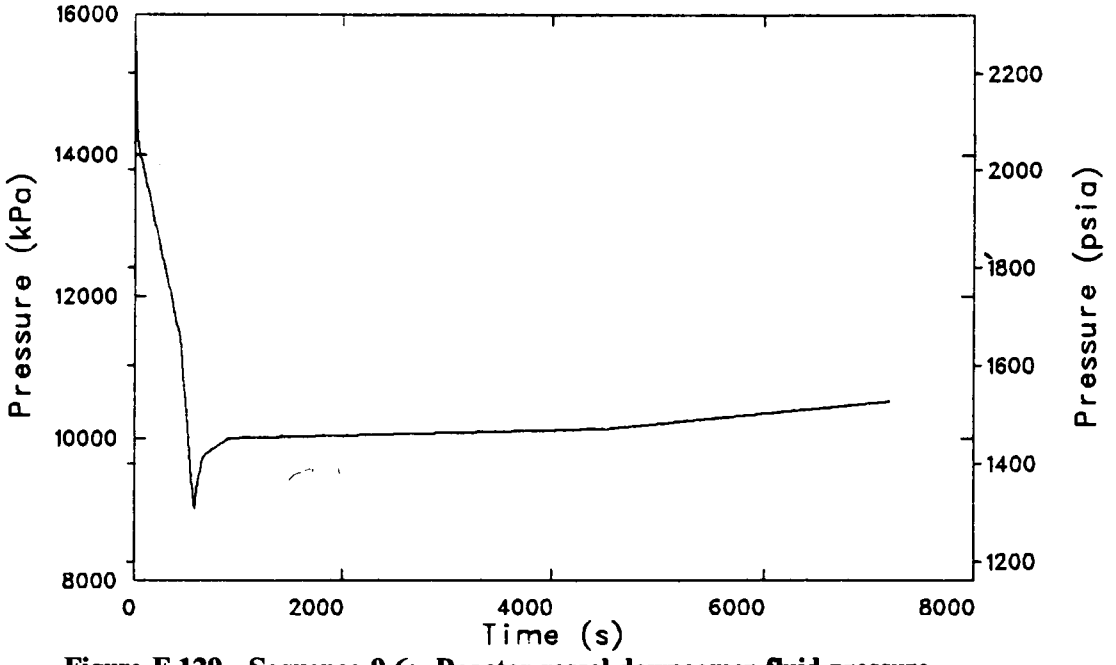

Figure F.129. Sequence 9.6: Reactor vessel downcomer fluid pressure.

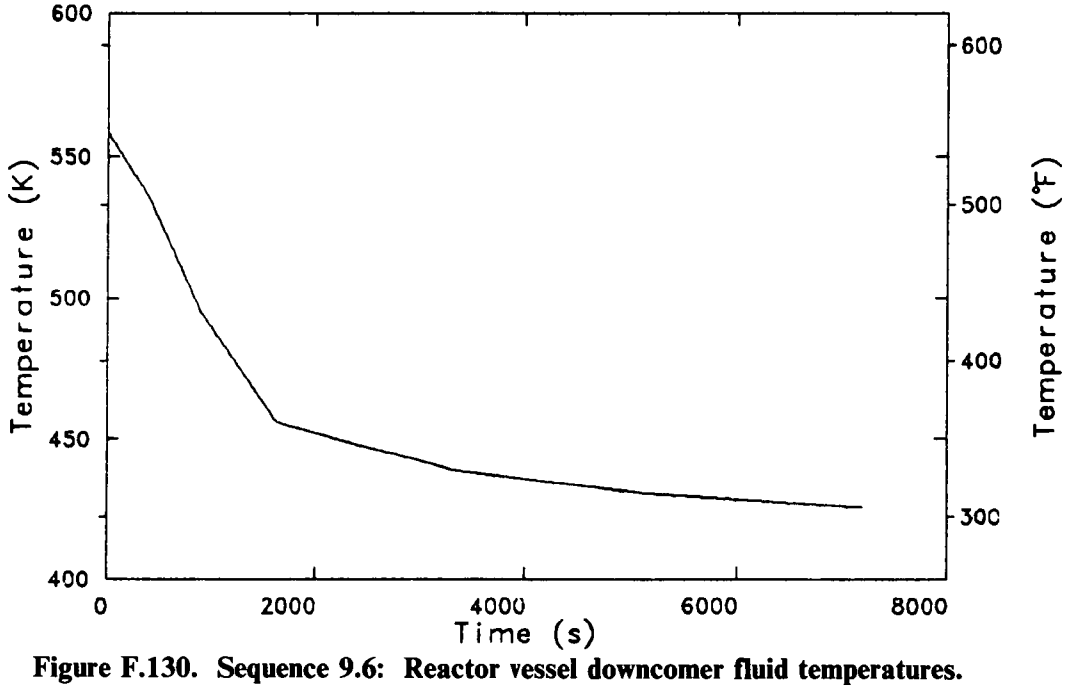

Figure F.130. Sequence 9.6: Reactor vessel downcomer fluid temperatures.

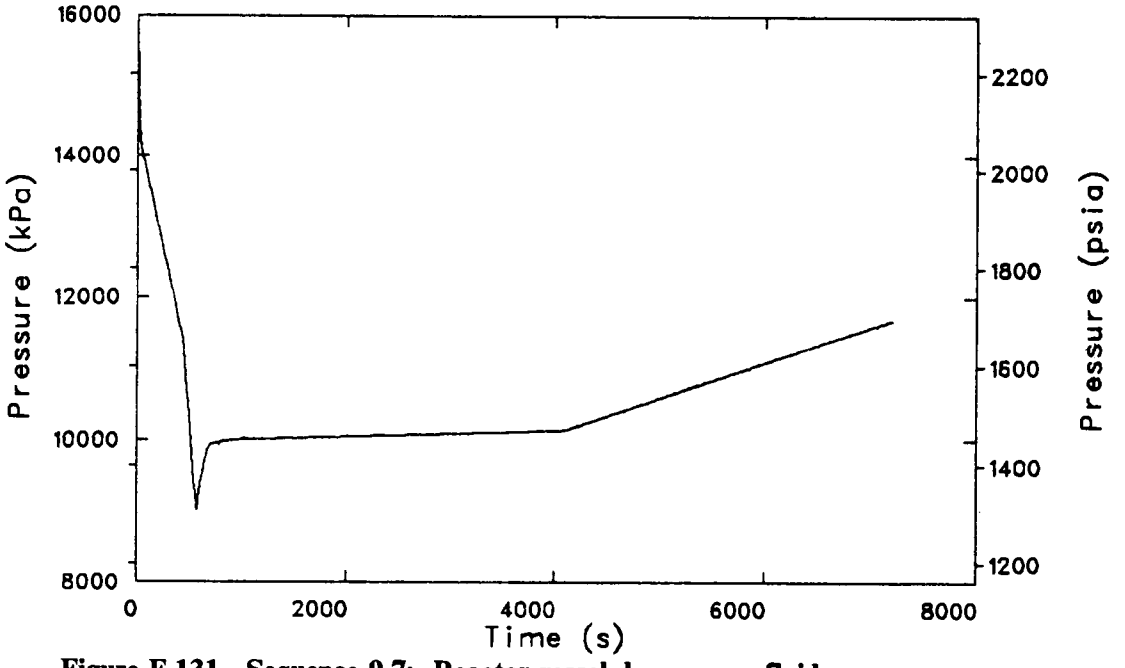

Figure F.131. Sequence 9.7: Reactor vessel downcomer fluid pressure.

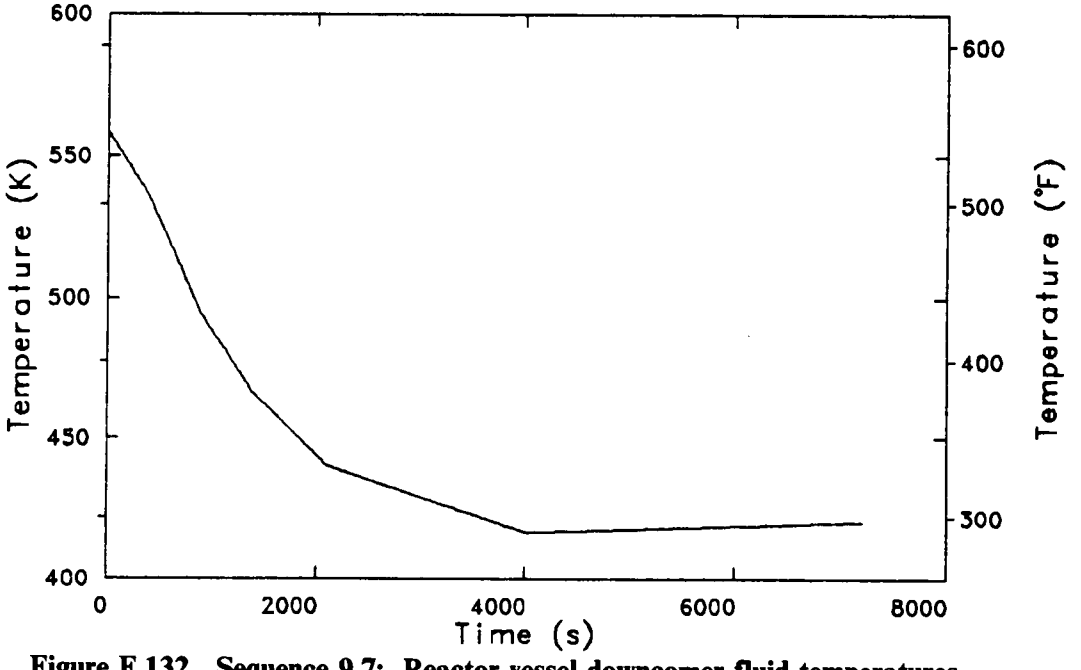

Figure F.132. Sequence 9.7: Reactor vessel downcomer fluid temperatures.

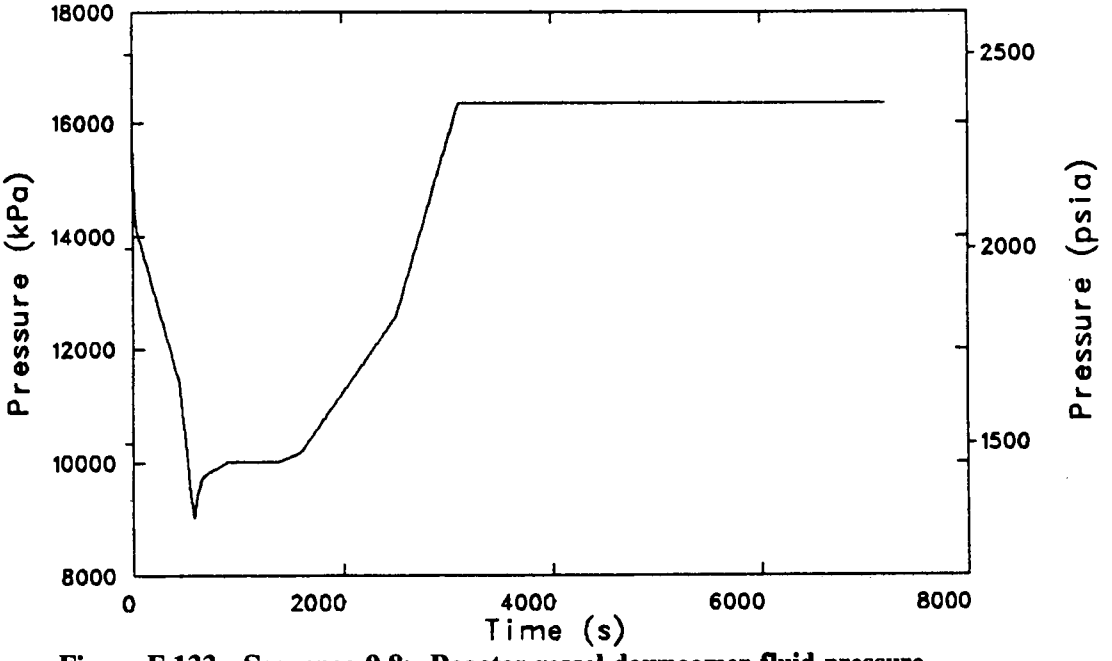

Figure F.133. Sequence 9.8: Reactor vessel downcomer fluid pressure.

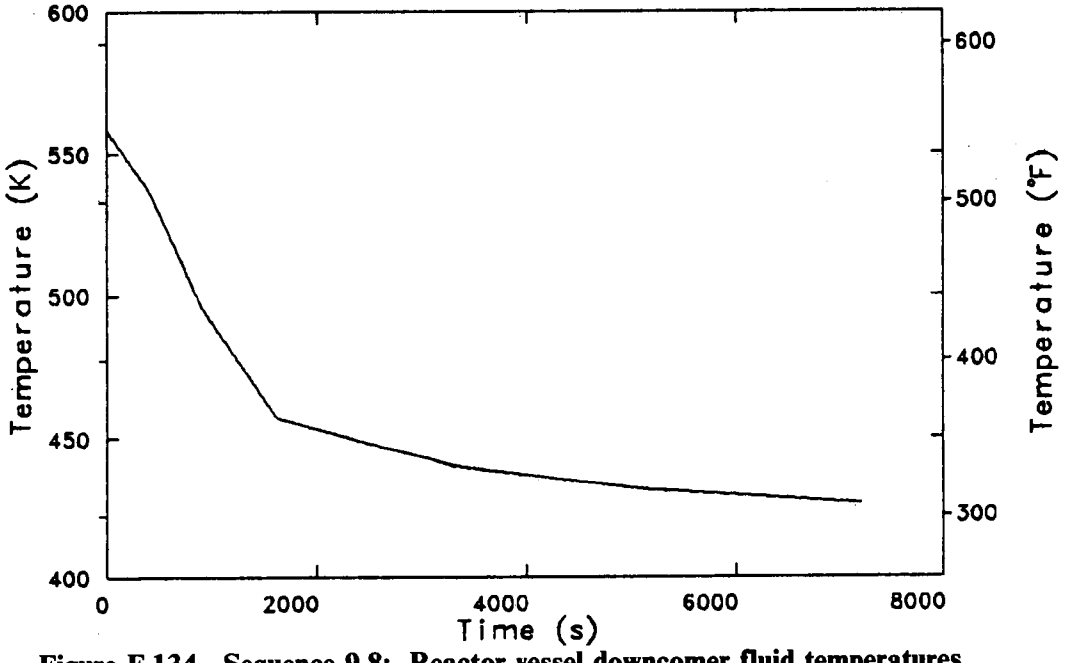

Figure F.134. Sequence 9.8: Reactor vessel downcomer fluid temperatures.

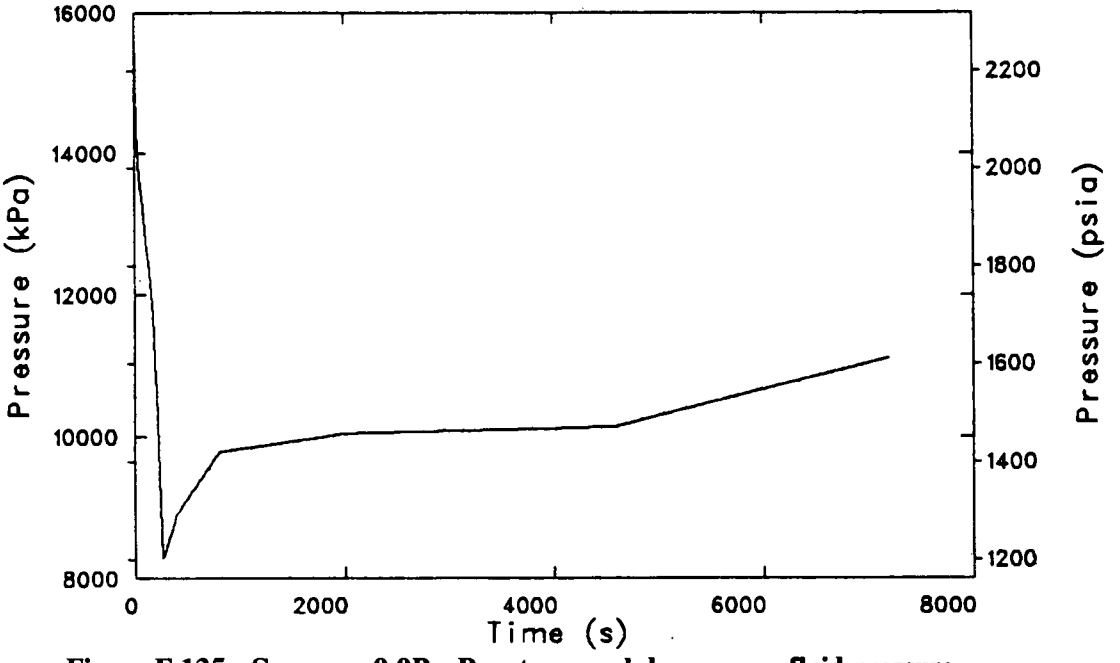

Figure F.135. Sequence 9.9B: Reactor vessel downcomer fluid pressure.

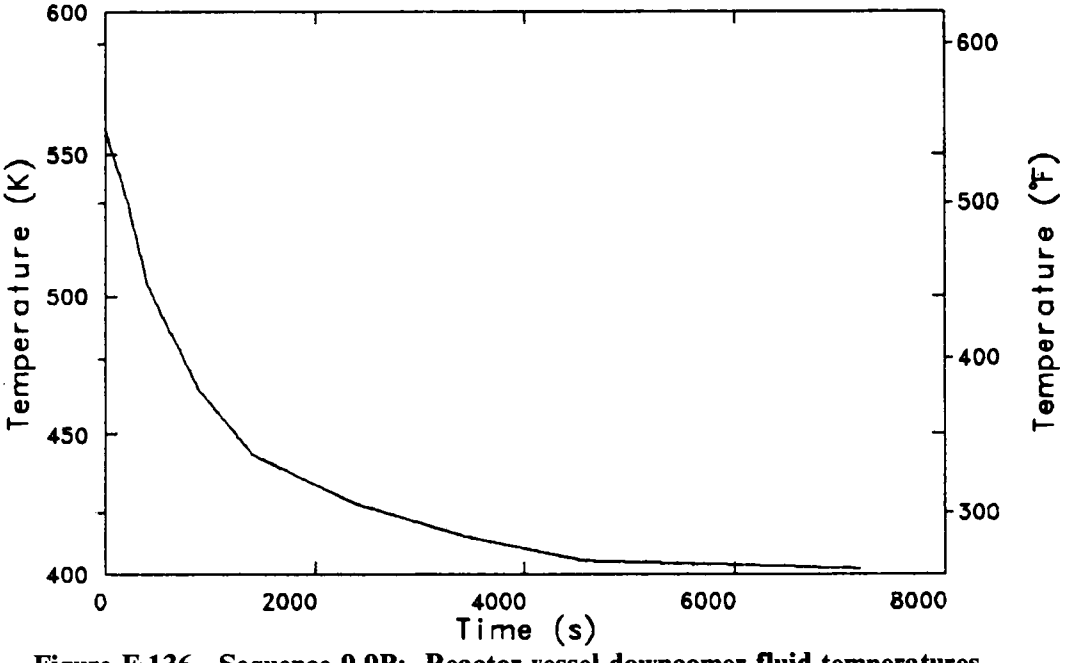

Figure F.136. Sequence 9.9B: Reactor vessel downcomer fluid temperatures.

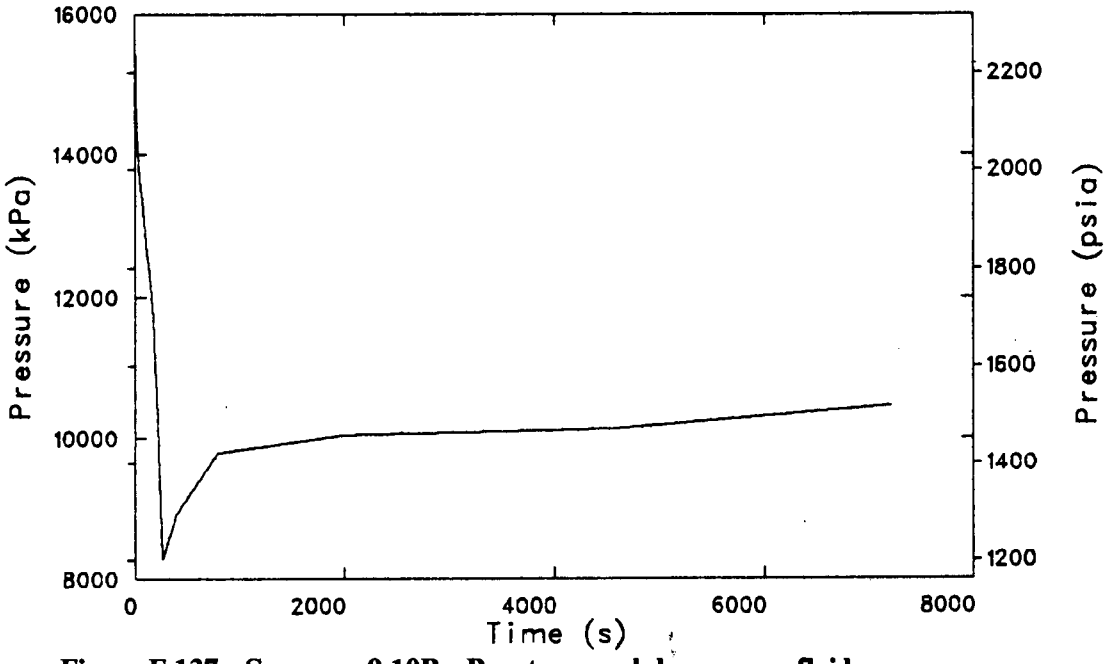

Figure F.137. Sequence 9.10B: Reactor vessel downcomer fluid pressure.

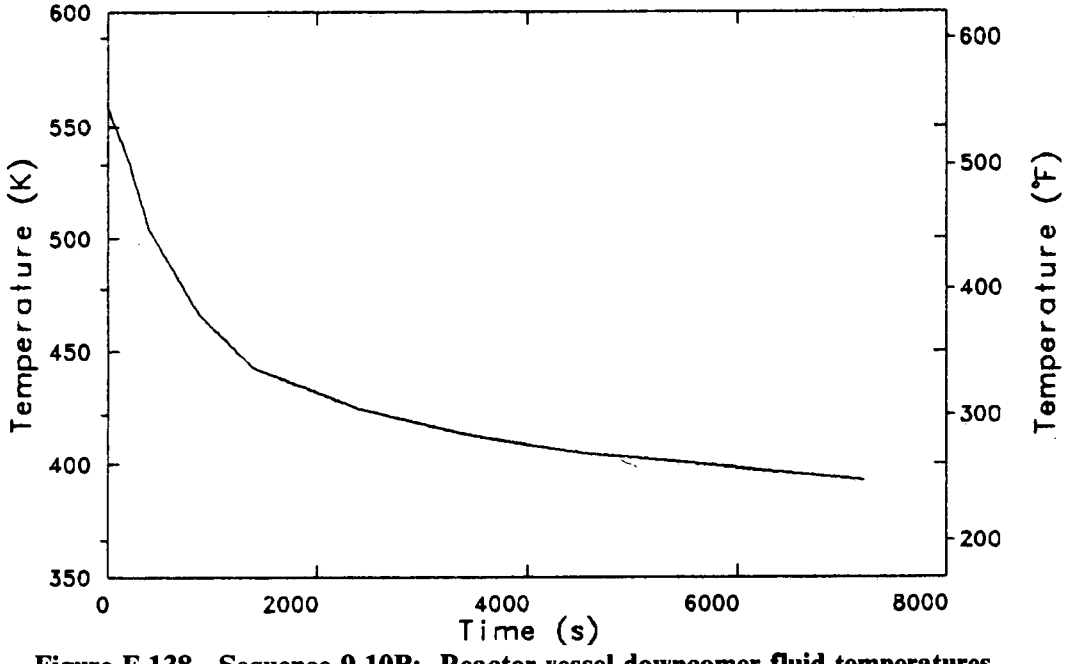

Figure F.138. Sequence 9.10B: Reactor vessel downcomer fluid temperatures.

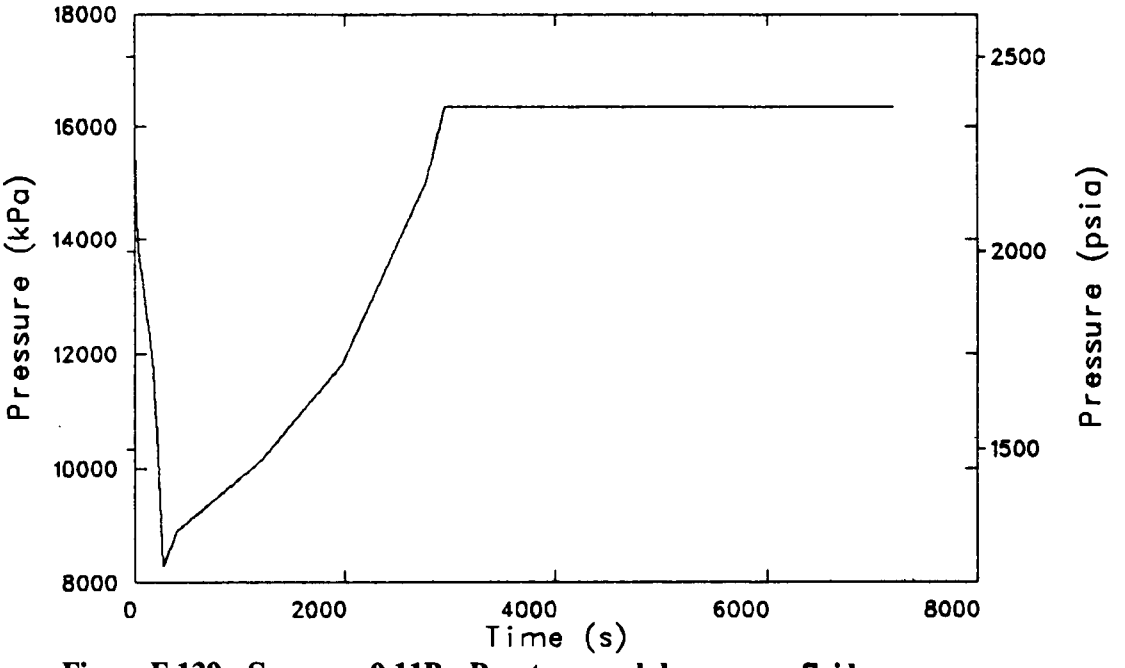

Figure F.139. Sequence 9.11B: Reactor vessel downcomer fluid pressure.

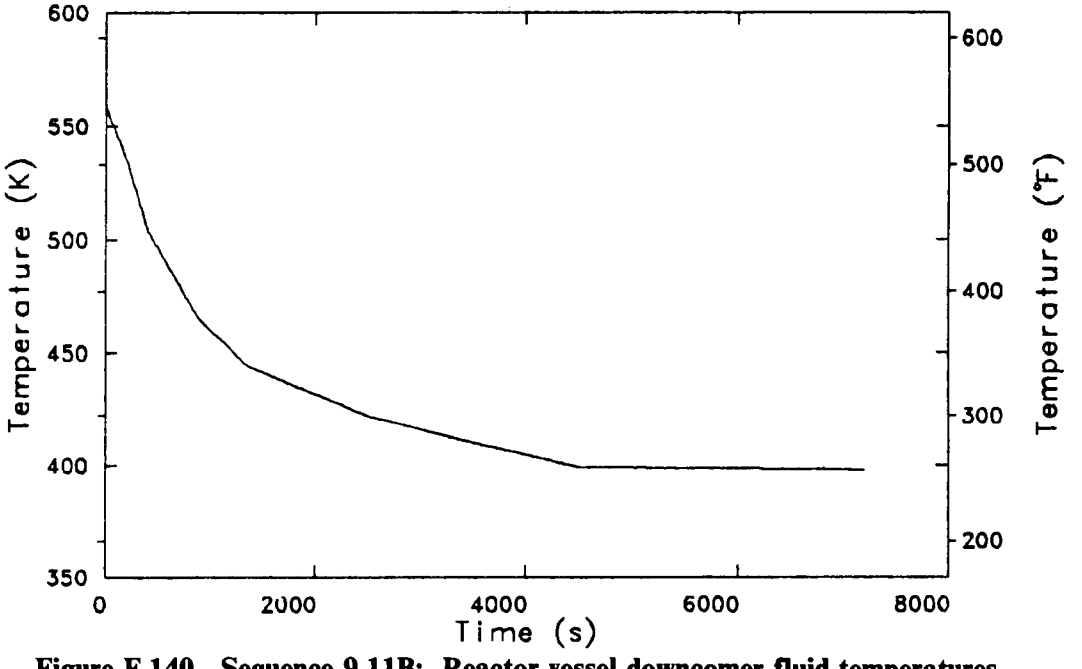

Figure F.140. Sequence 9.11B: Reactor vessel downcomer fluid temperatures.

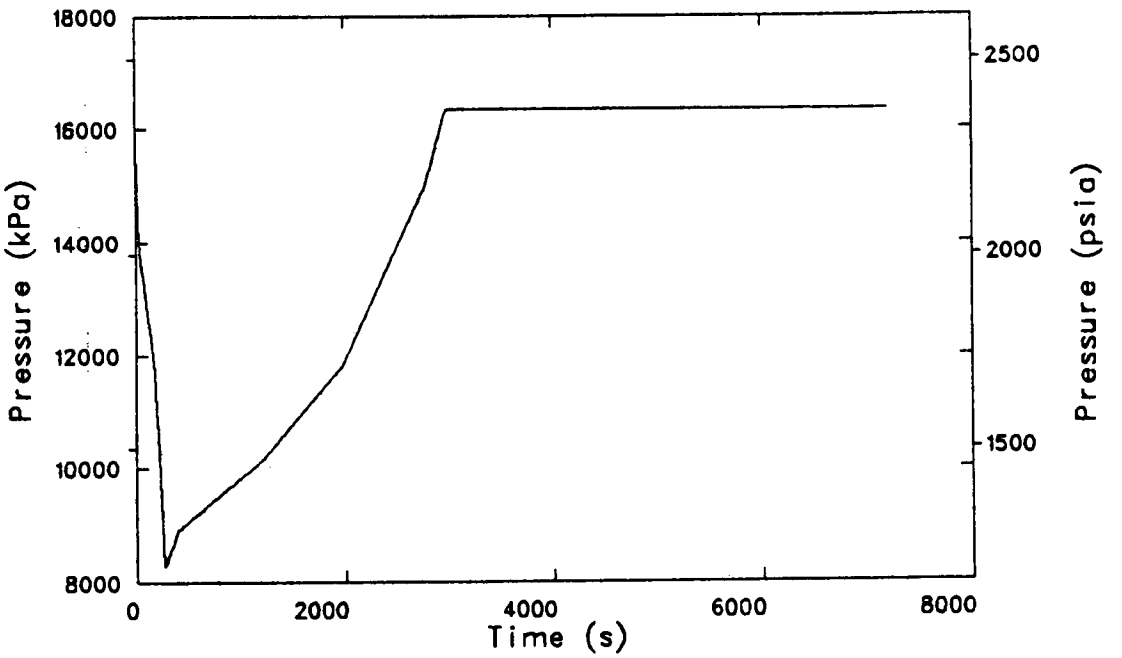

Figure F.141. Sequence 9.12B: Reactor vessel downcomer fluid pressure.

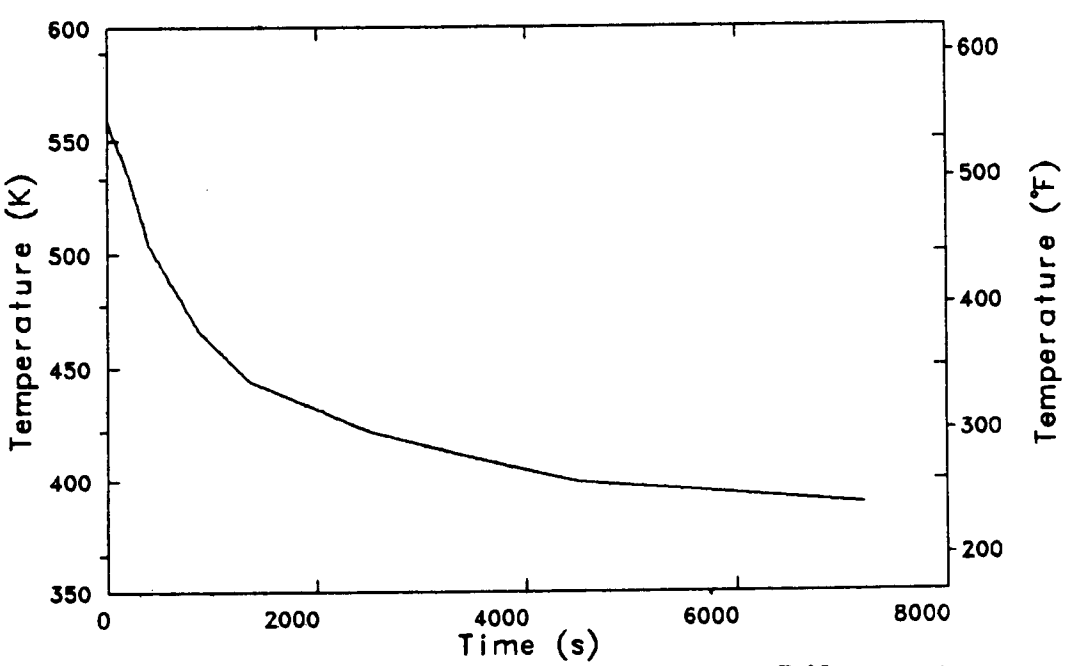

Figure F.142. Sequence 9.12B: Reactor vessel downcomer fluid temperatures.

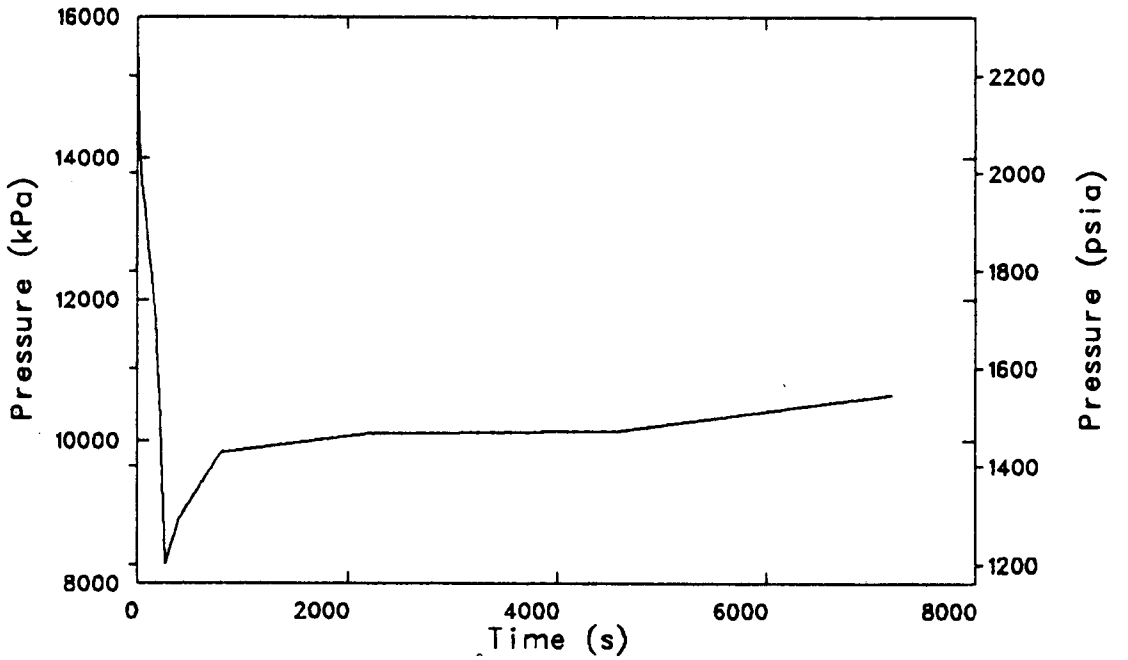

Figure F.143. Sequence 9.13B: Reactor vessel downcomer fluid pressure.

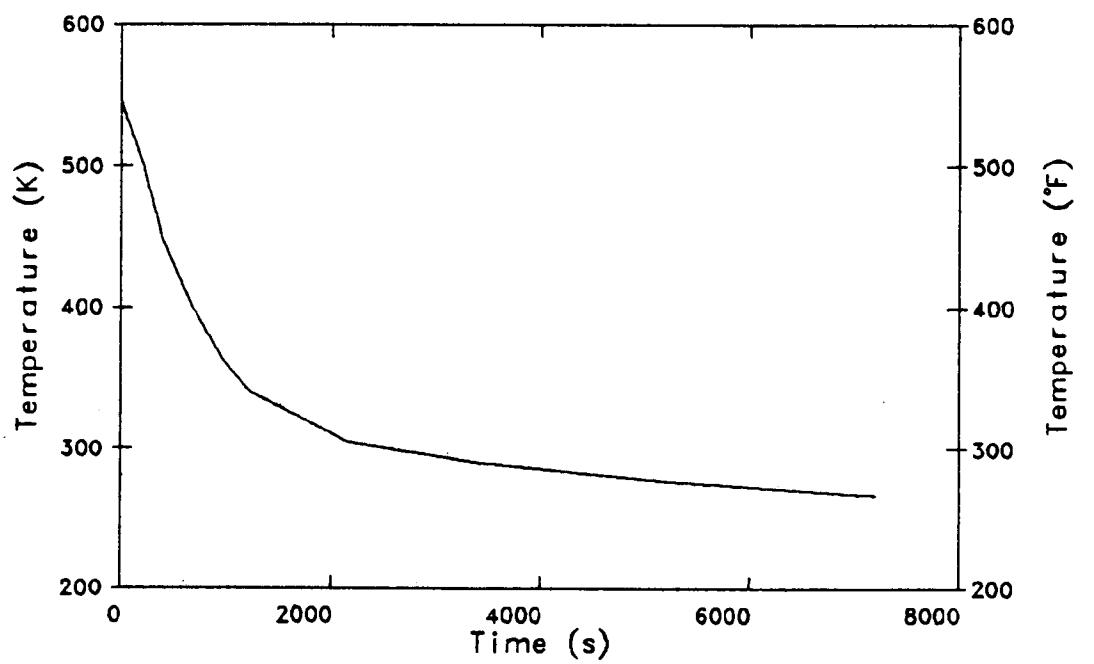

Figure F.144. Sequence 9.13B: Reactor vessel downcomer fluid temperatures.

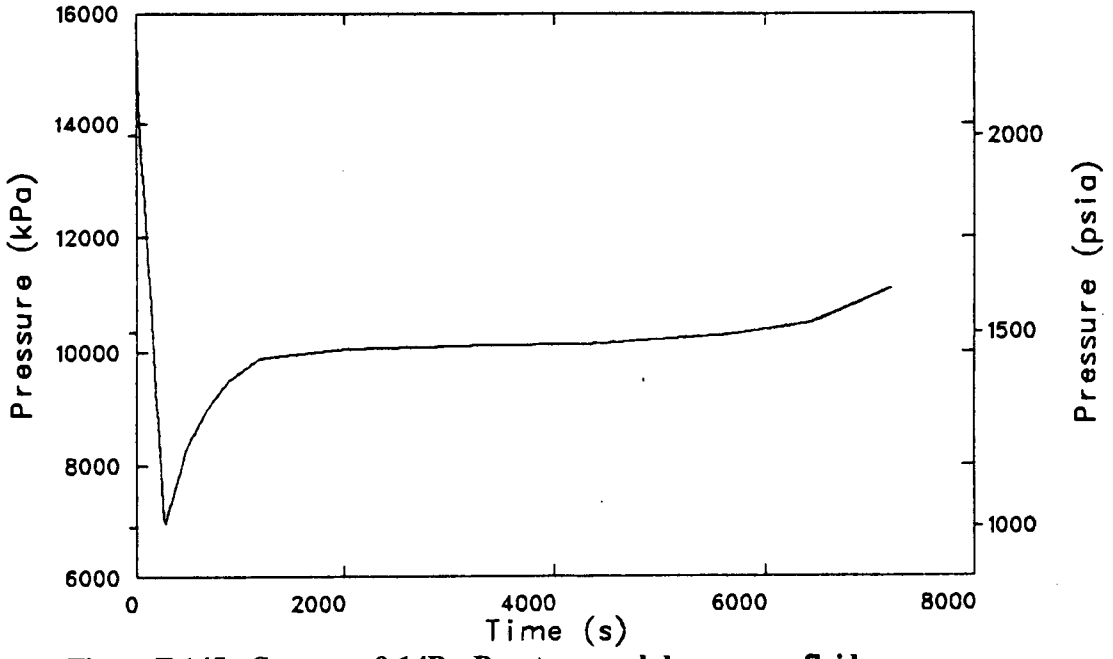

Figure F.145. Sequence 9.14B: Reactor vessel downcomer fluid pressure.

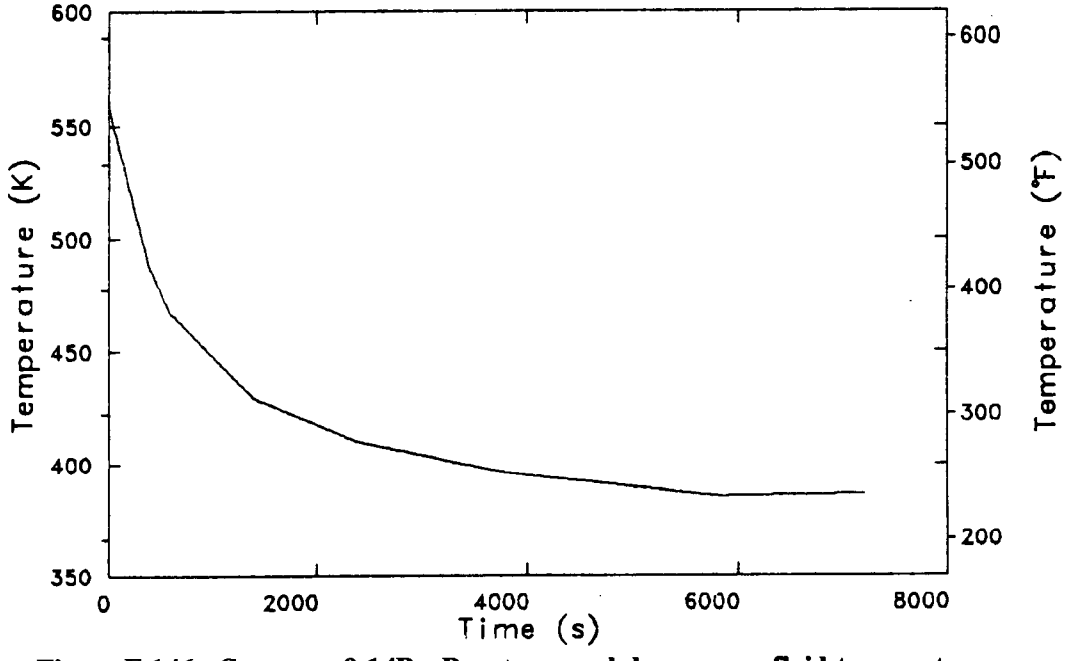

Figure F.146. Sequence 9.14B: Reactor vessel downcomer fluid temperatures.

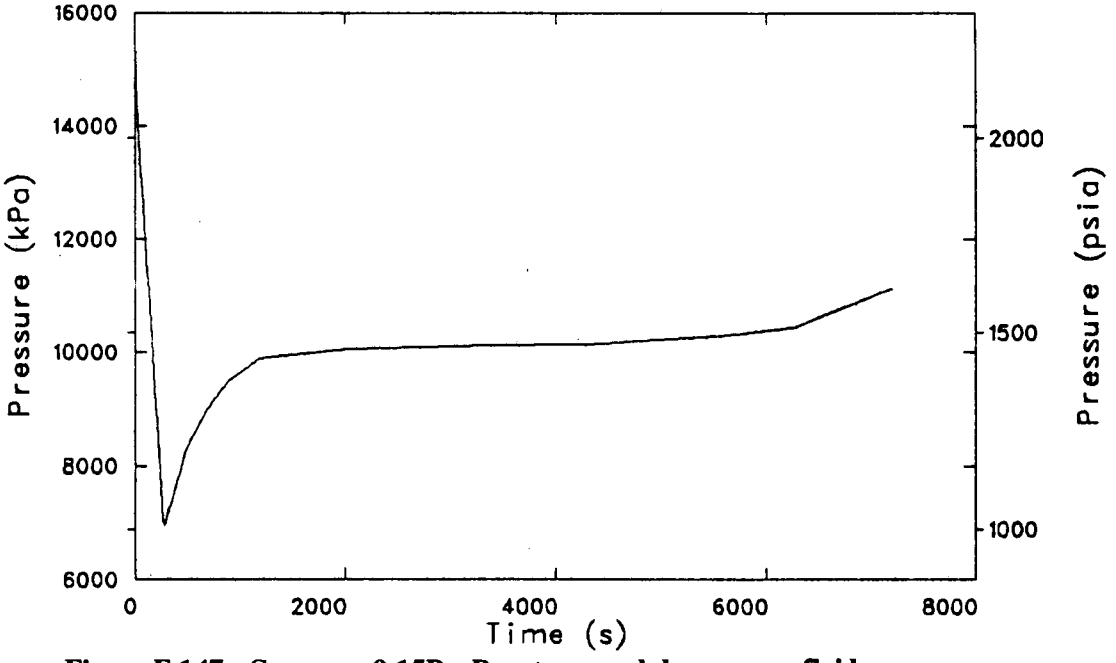

Figure F.147. Sequence 9.15B: Reactor vessel downcomer fluid pressure.

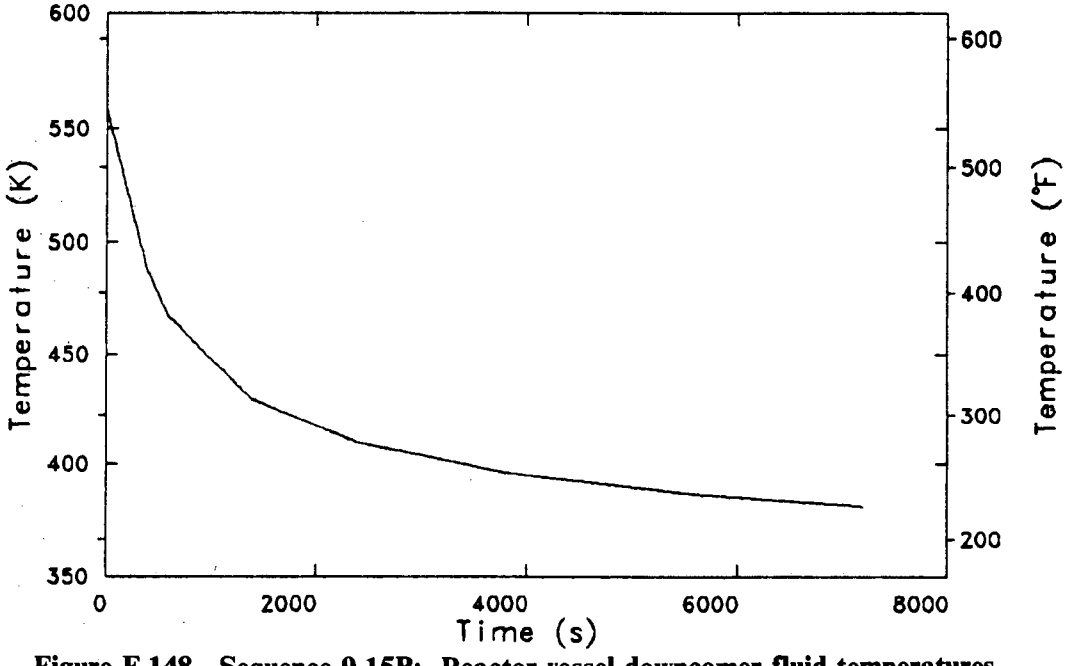

Figure F.148. Sequence 9.15B: Reactor vessel downcomer fluid temperatures.

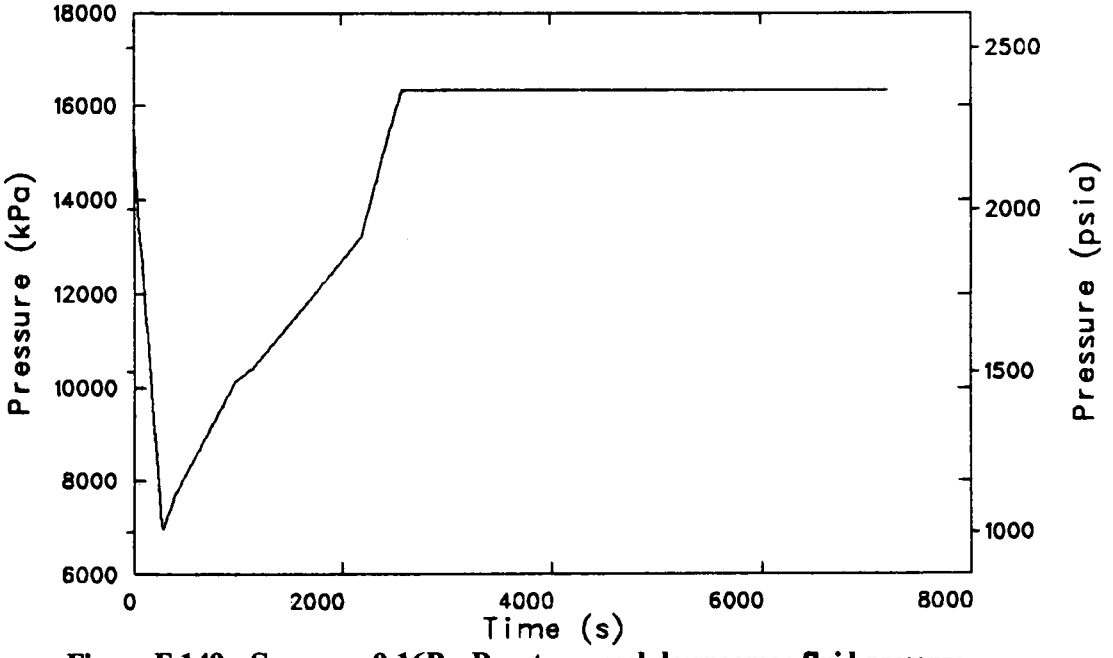

Figure F.149. Sequence 9.16B: Reactor vessel downcomer fluid pressure.

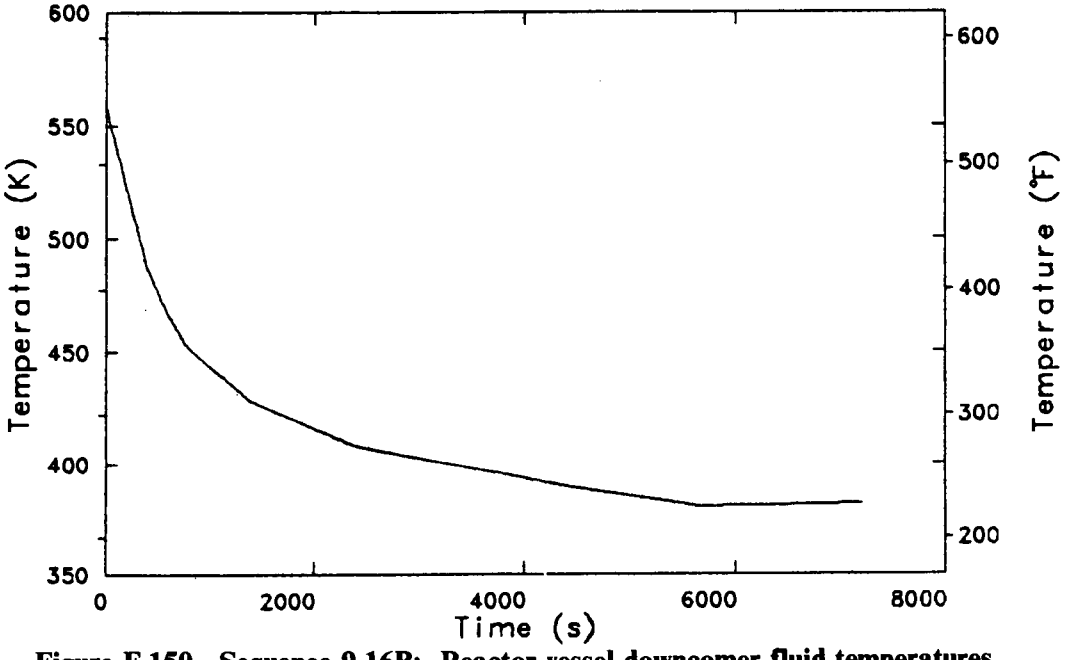

Figure F.150. Sequence 9.16B: Reactor vessel downcomer fluid temperatures.

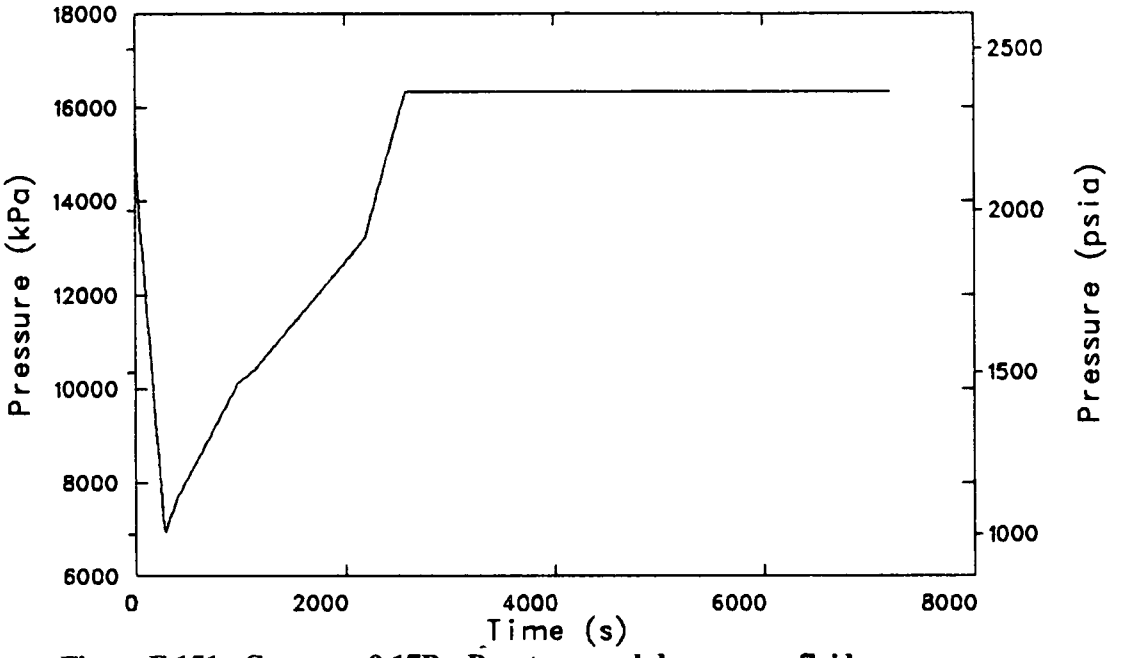

Figure F.151. Sequence 9.17B: Reactor vessel downcomer fluid pressure.

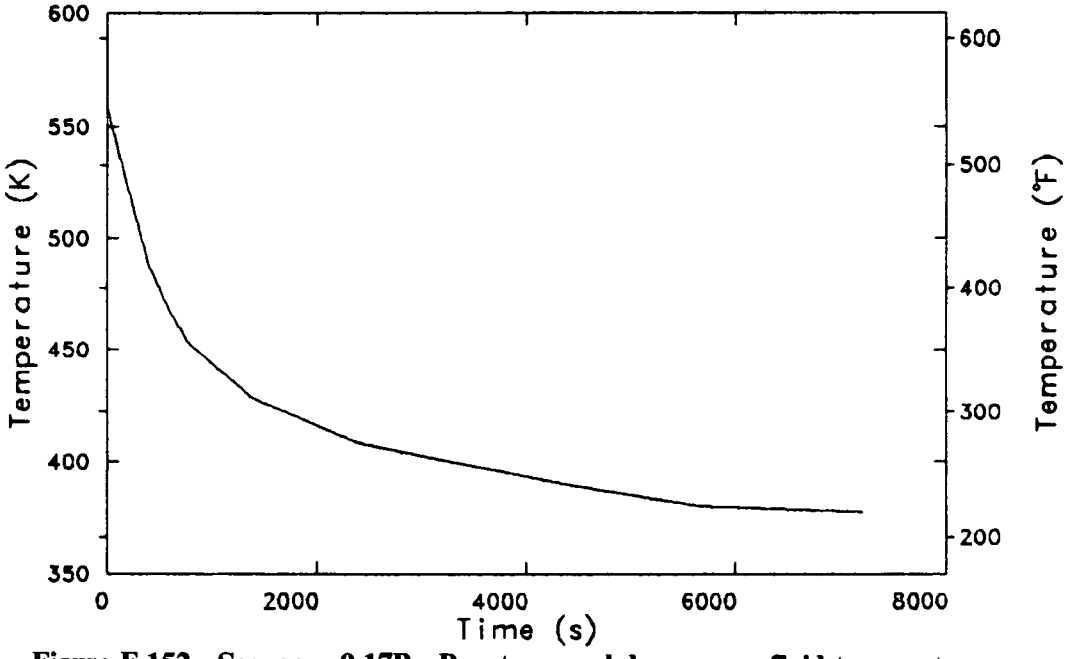

Figure F.152. Sequence 9.17B: Reactor vessel downcomer fluid temperatures.

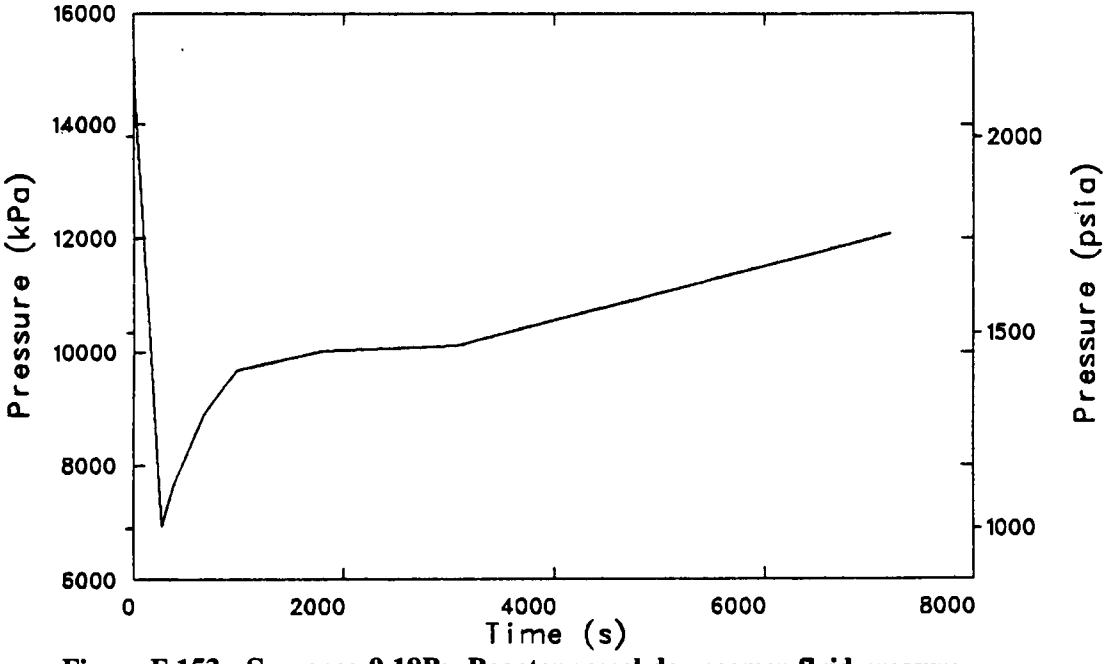

Figure F.153. Sequence 9.18B: Reactor vessel downcomer fluid pressure.

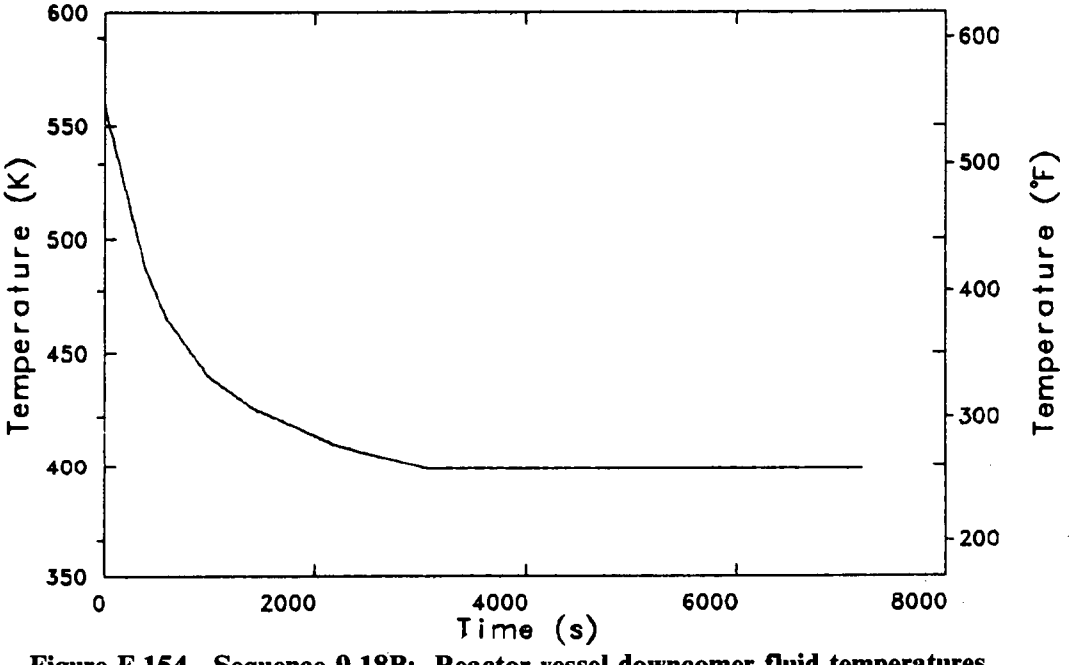

Figure F.154. Sequence 9.18B: Reactor vessel downcomer fluid temperatures.

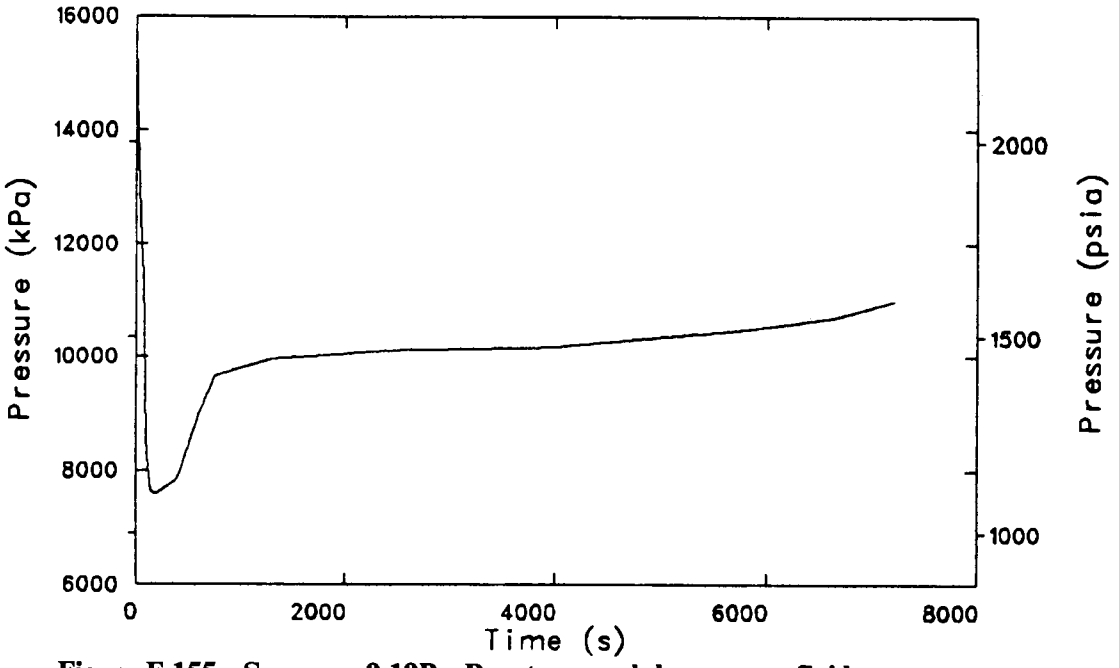

Figure F.155. Sequence 9.19B: Reactor vessel downcomer fluid pressure.

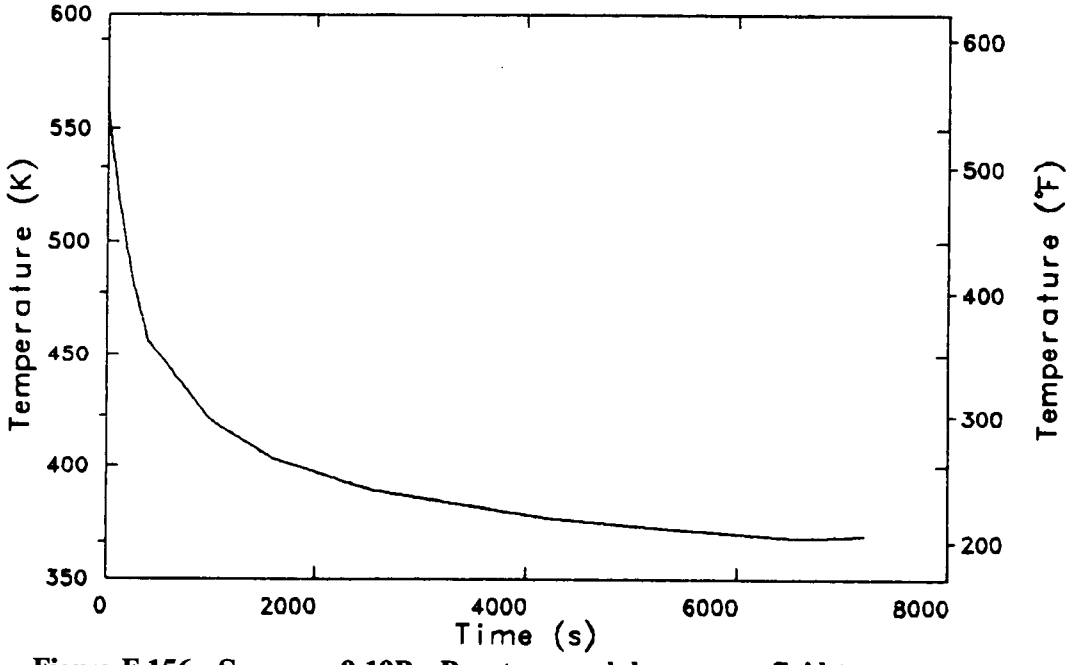

Figure F.156. Sequence 9.19B: Reactor vessel downcomer fluid temperatures.

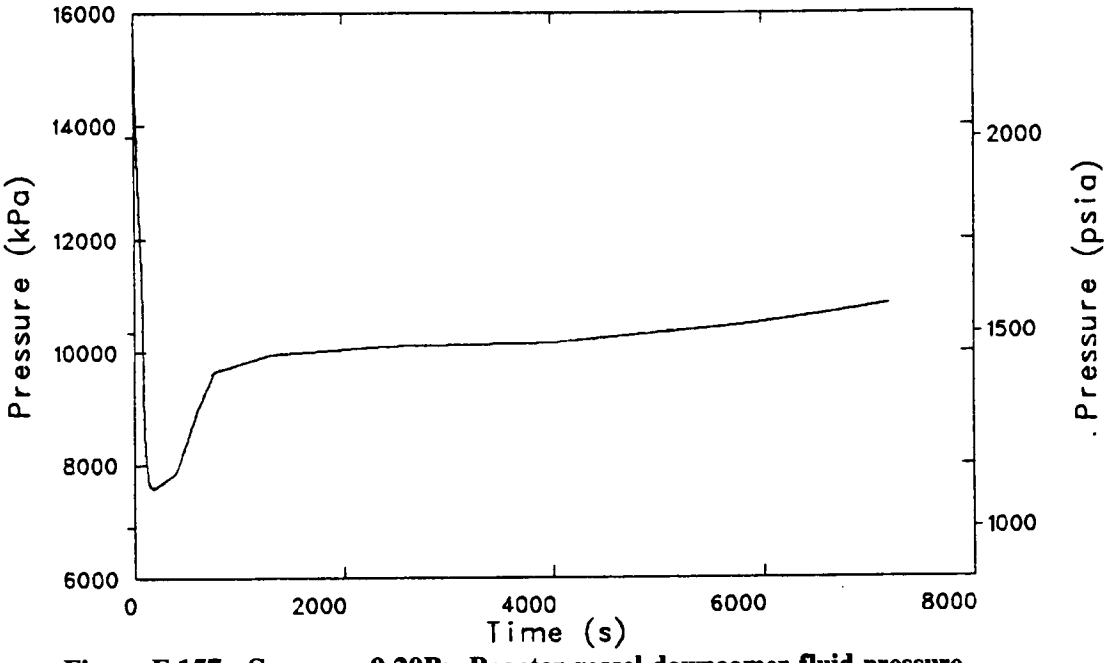

Figure F.157. Sequence 9.20B: Reactor vessel downcomer fluid pressure.

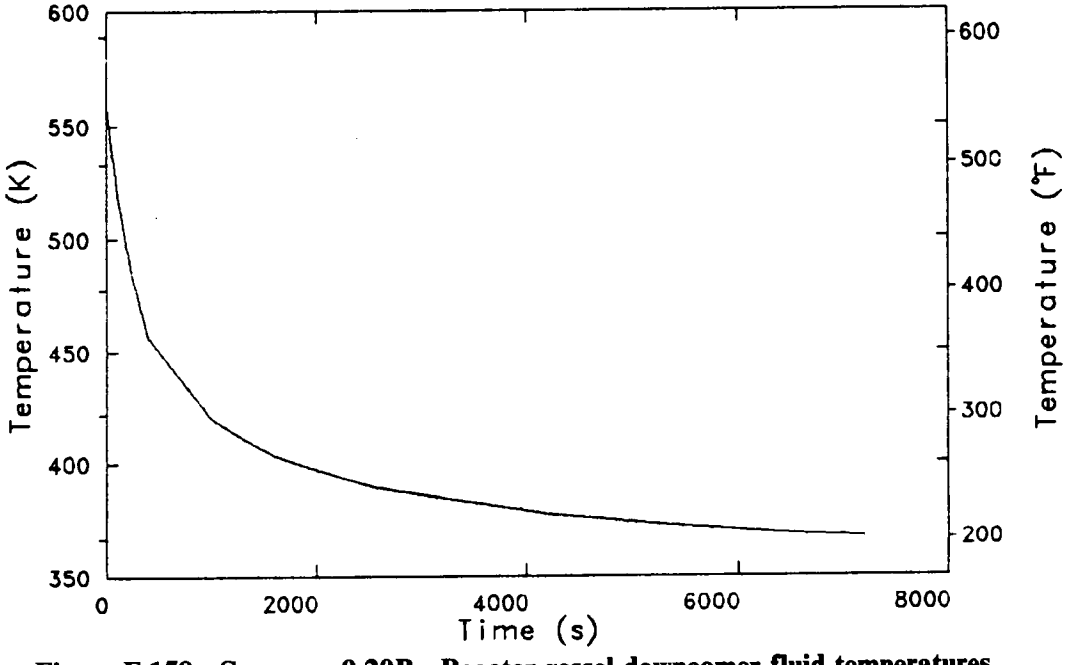

Figure F.158. Sequence 9.20B: Reactor vessel downcomer fluid temperatures.

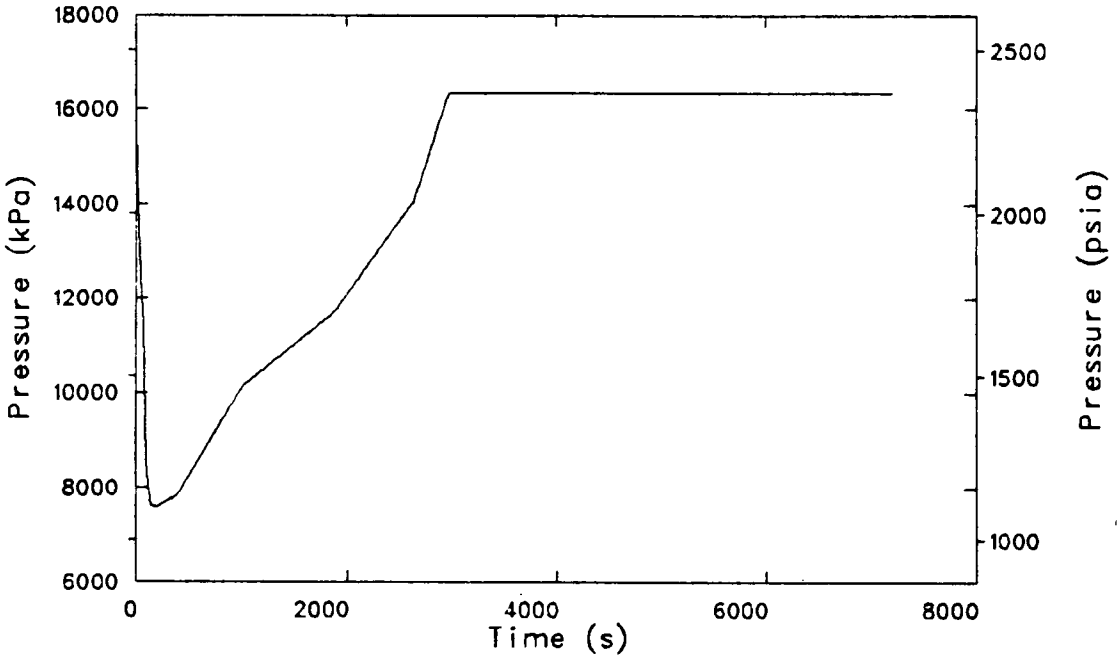

Figure F.159. Sequence 9.21B: Reactor vessel downcomer fluid pressure.

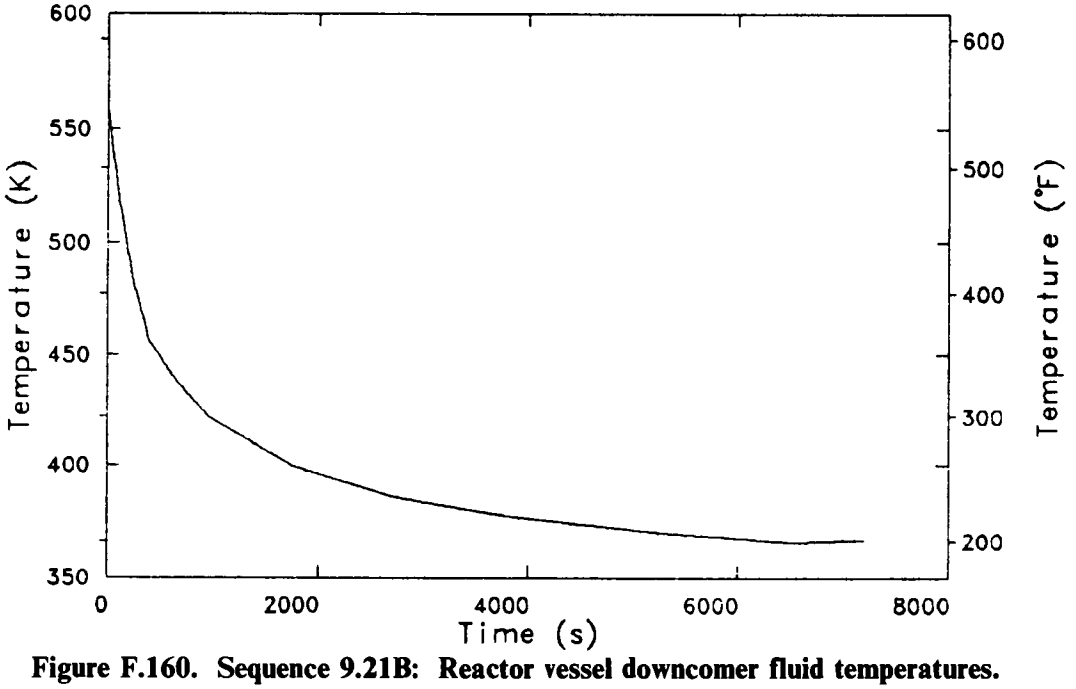

Figure F.160. Sequence 9.21B: Reactor vessel downcomer fluid temperatures.

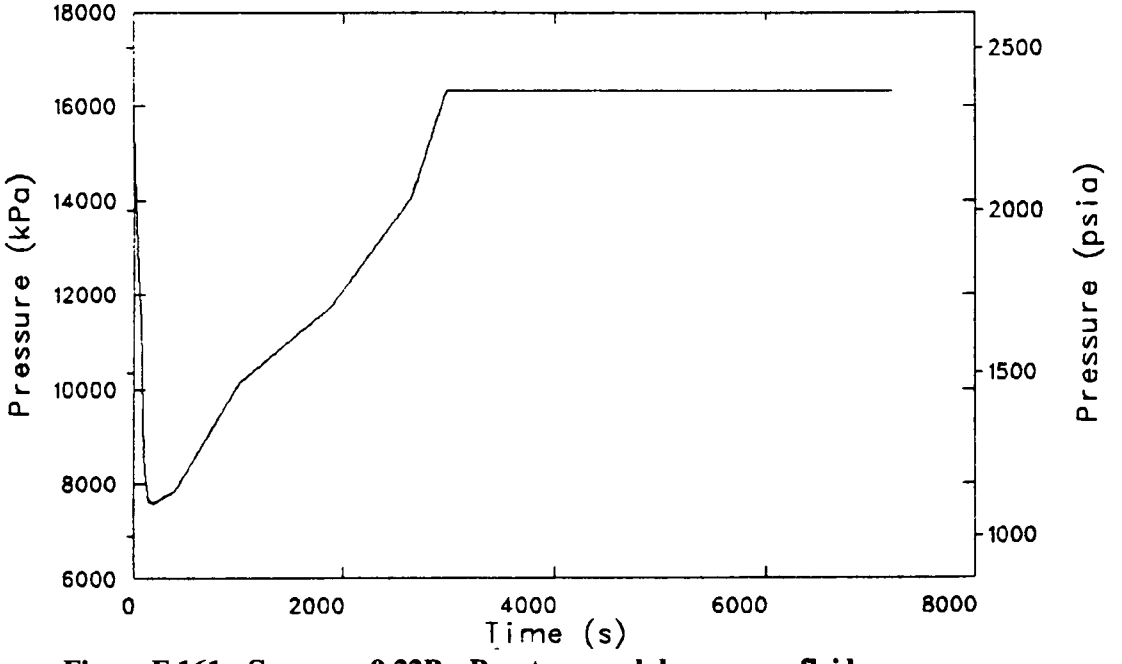

Figure F.161. Sequence 9.22B: Reactor vessel downcomer fluid pressure.

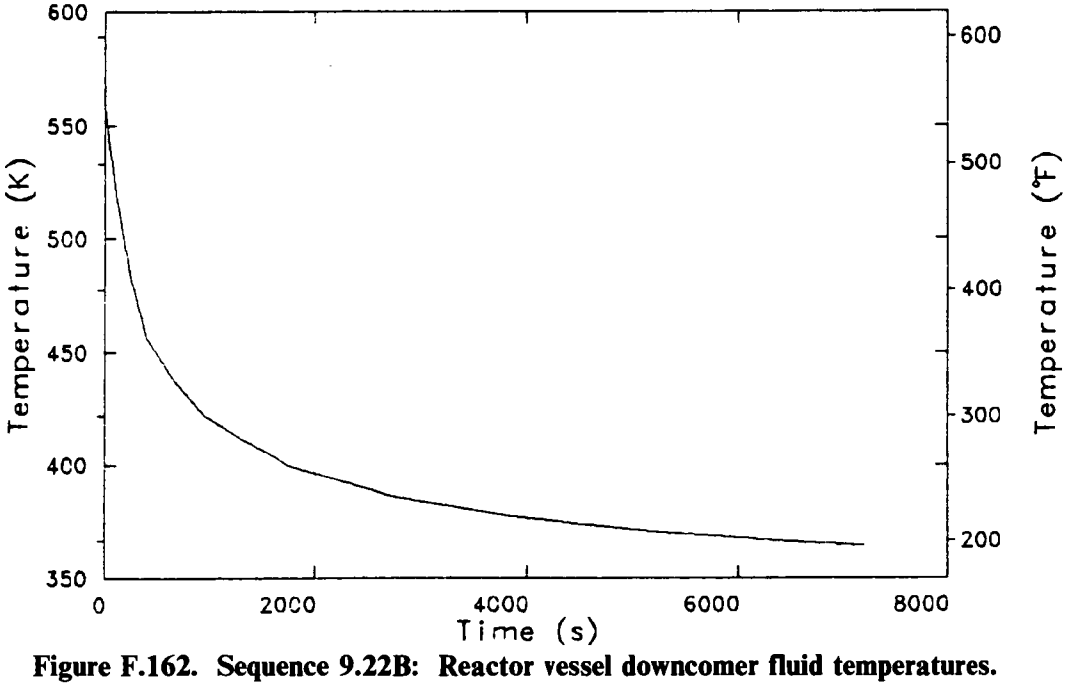

Figure F.162. Sequence 9.22B: Reactor vessel downcomer fluid temperatures.

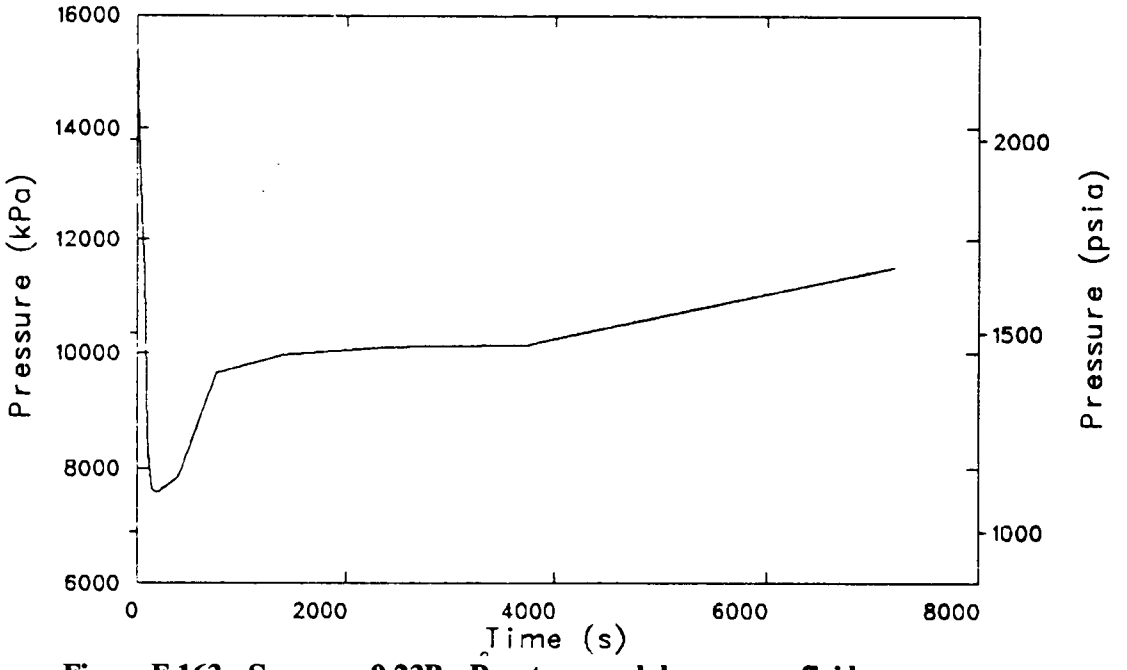

Figure F.163. Sequence 9.23B: Reactor vessel downcomer fluid pressure.

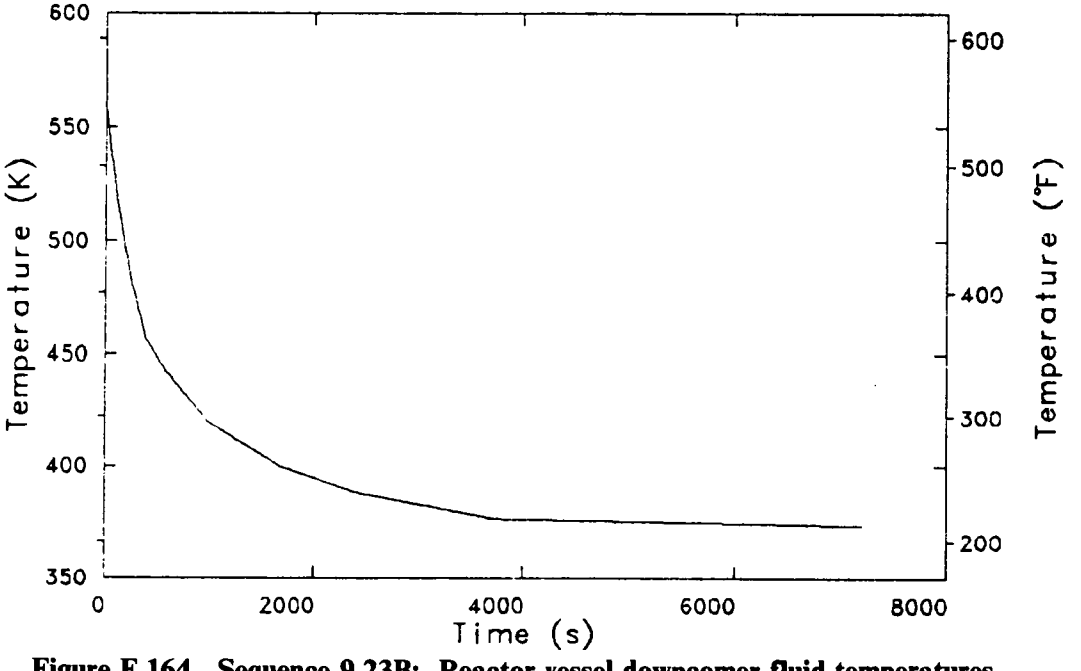

Figure F.164. Sequence 9.23B: Reactor vessel downcomer fluid temperatures.

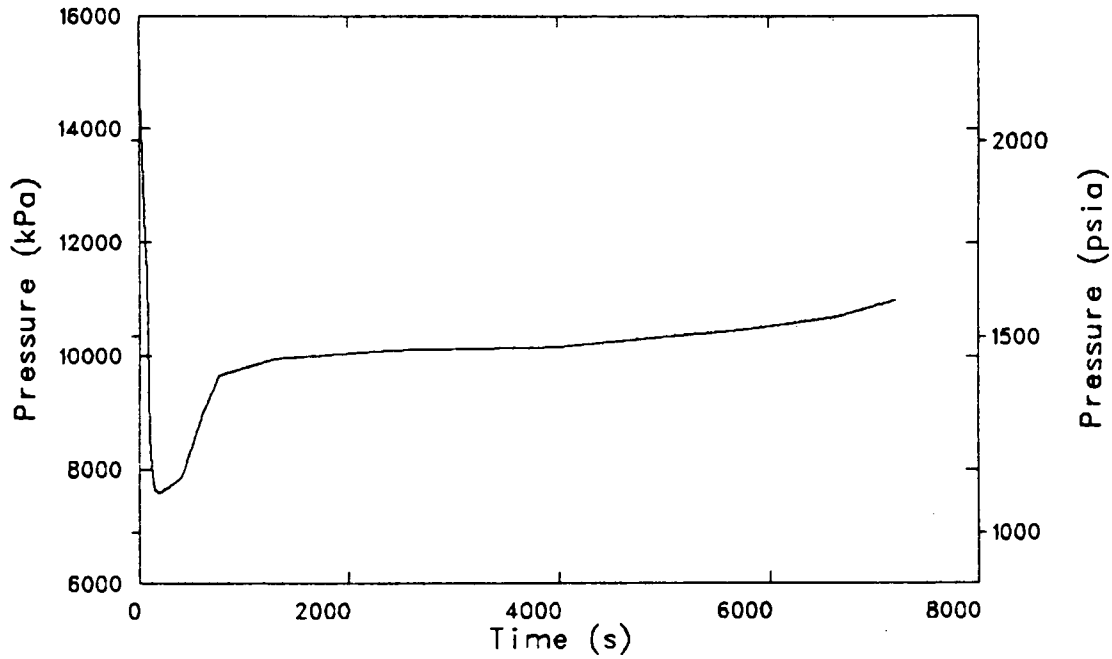

Figure F.165. Sequence 9.24: Reactor vessel downcomer fluid pressure.

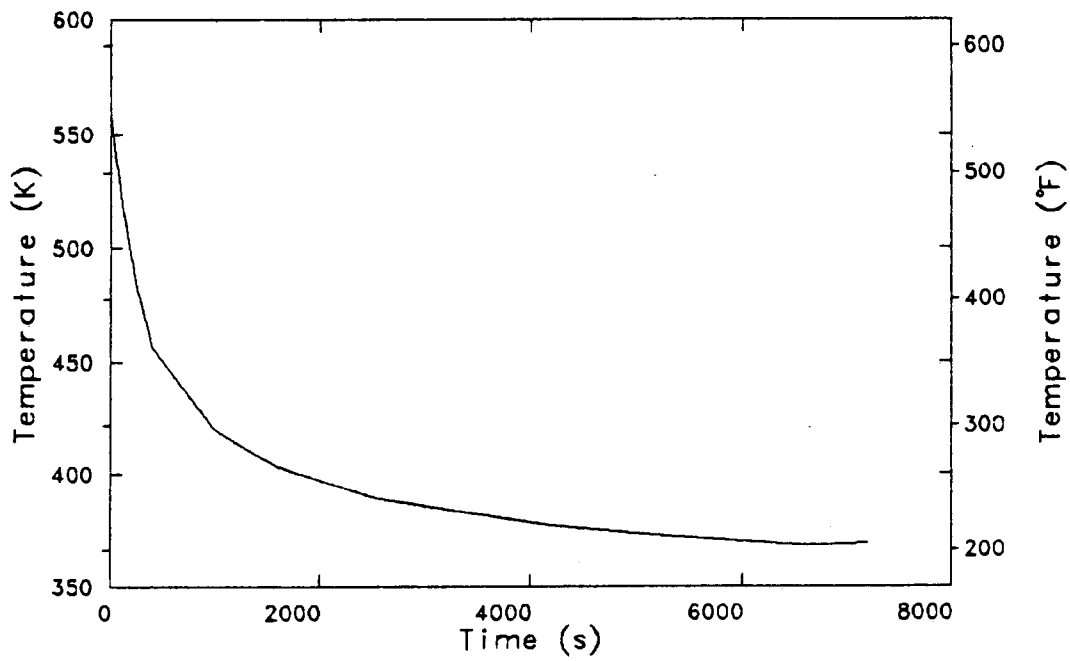

Figure F.166. Sequence 9.24: Reactor vessel downcomer fluid temperatures.

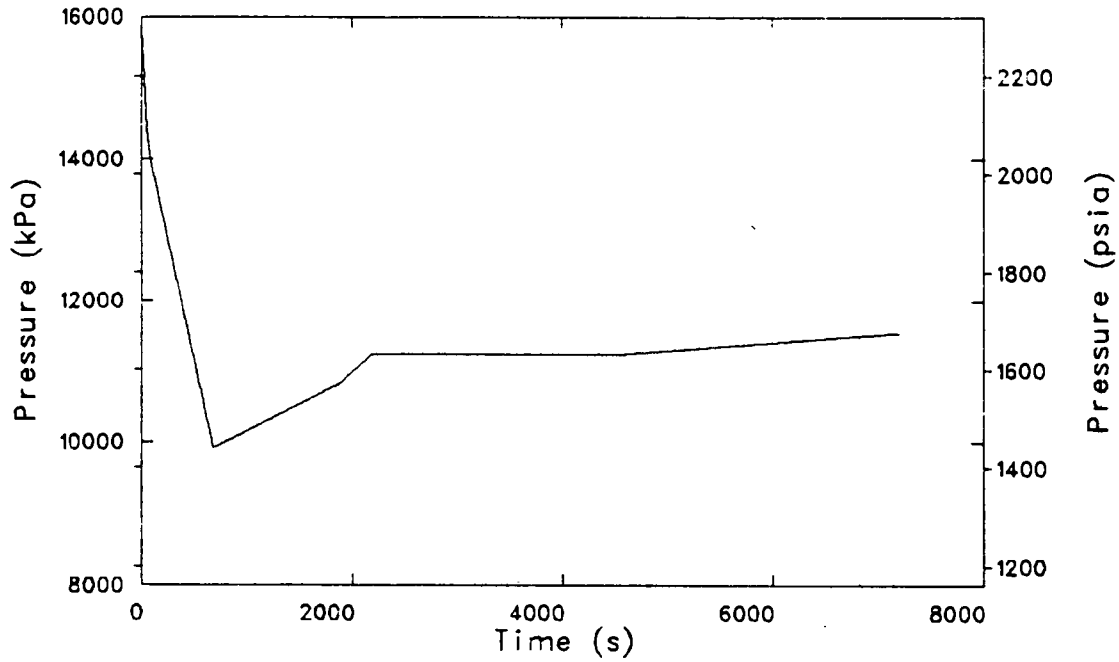

Figure F.167. Sequence 9.25: Reactor vessel downcomer fluid pressure.

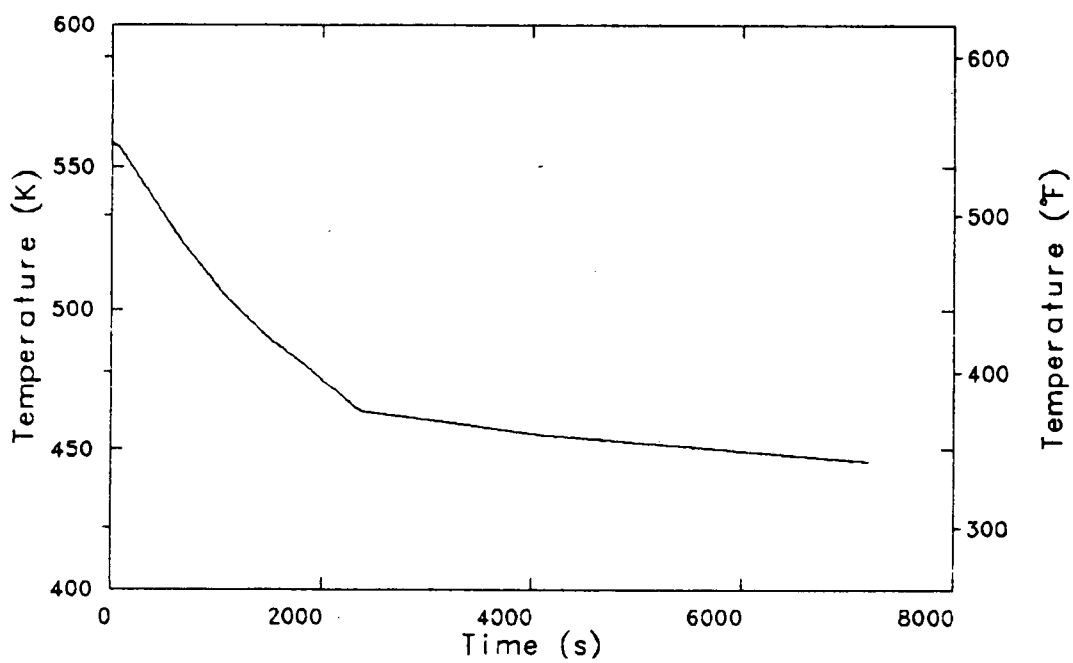

Figure F.168. Sequence 9.25: Reactor vessel downcomer fluid temperatures.

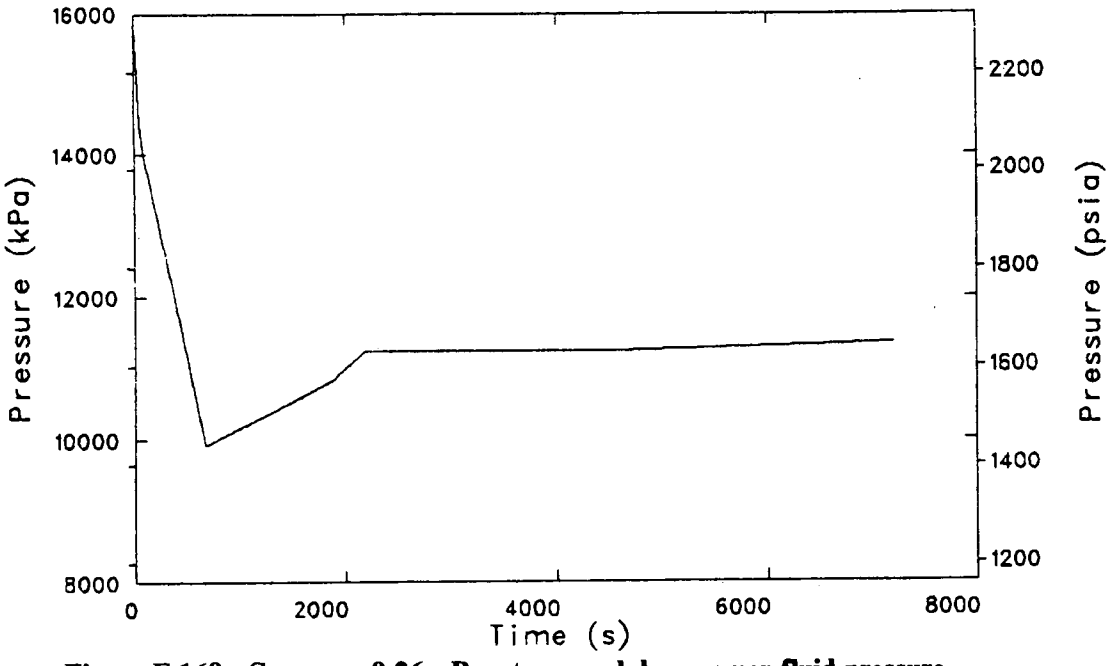

Figure F.169. Sequence 9.26: Reactor vessel downcomer fluid pressure.

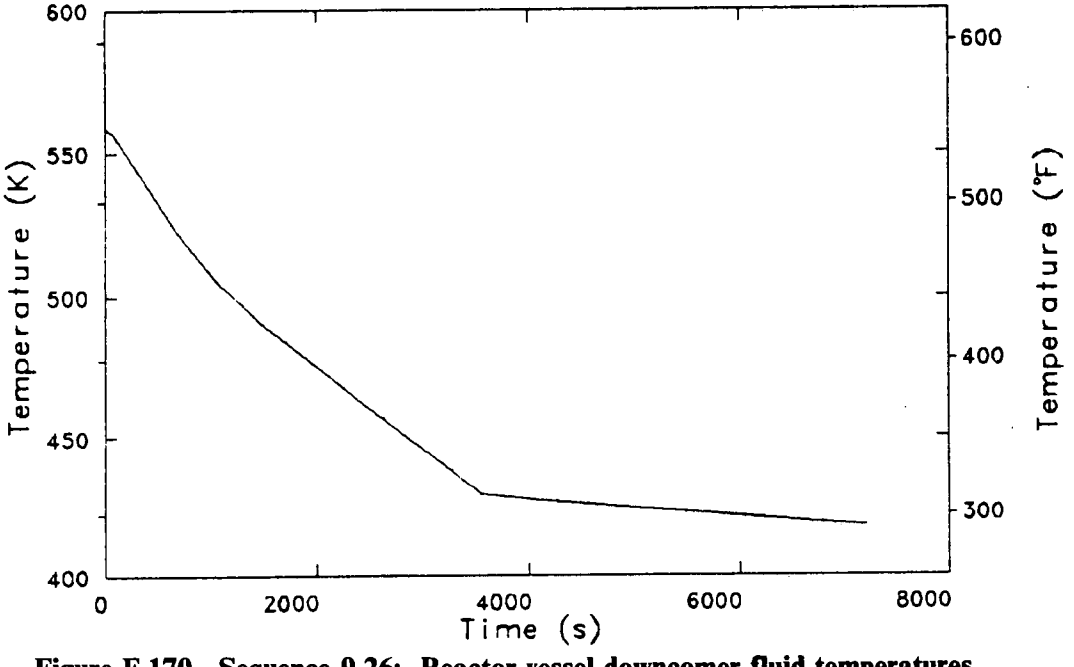

Figure F.170. Sequence 9.26: Reactor vessel downcomer fluid temperatures.

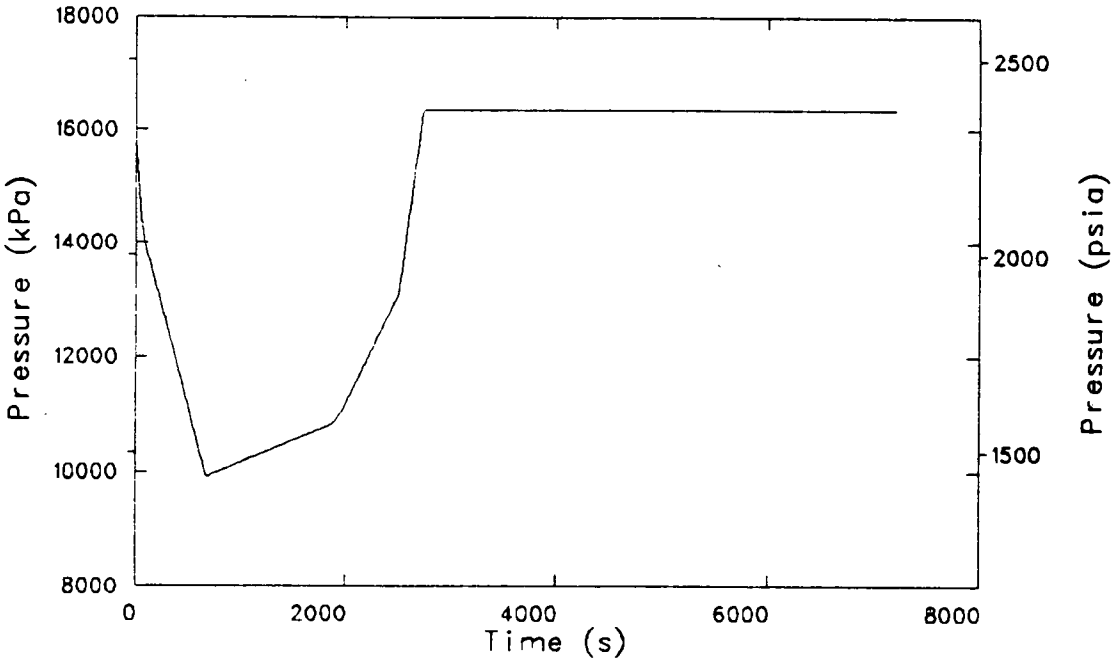

Figure F.171. Sequence 9.27: Reactor vessel downcomer fluid pressure.

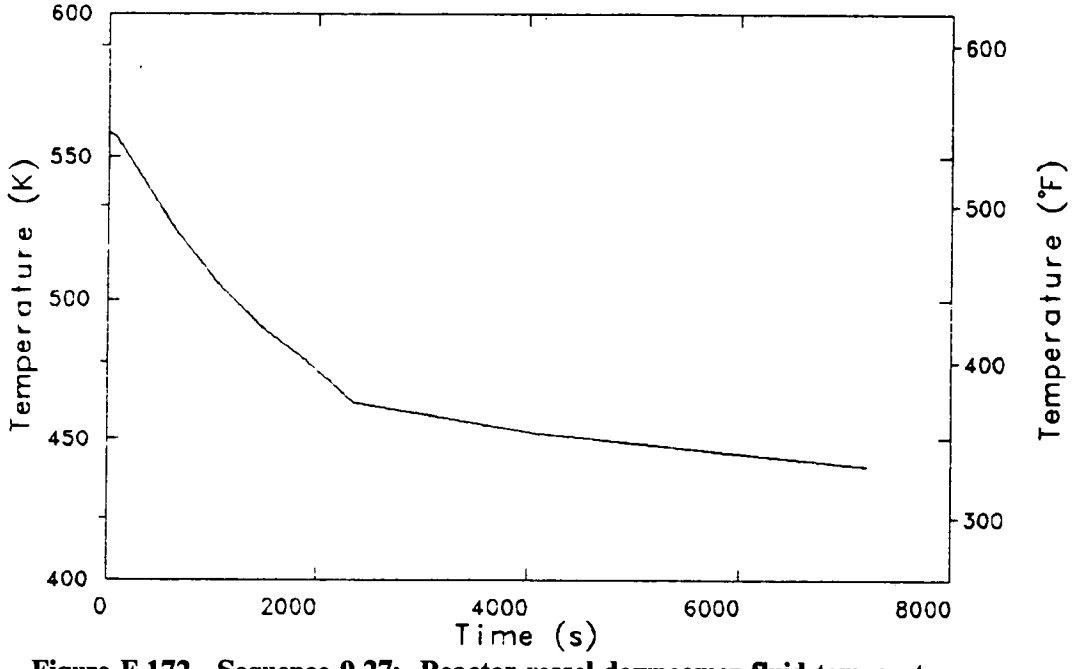

Figure F.172. Sequence 9.27: Reactor vessel downcomer fluid temperatures.

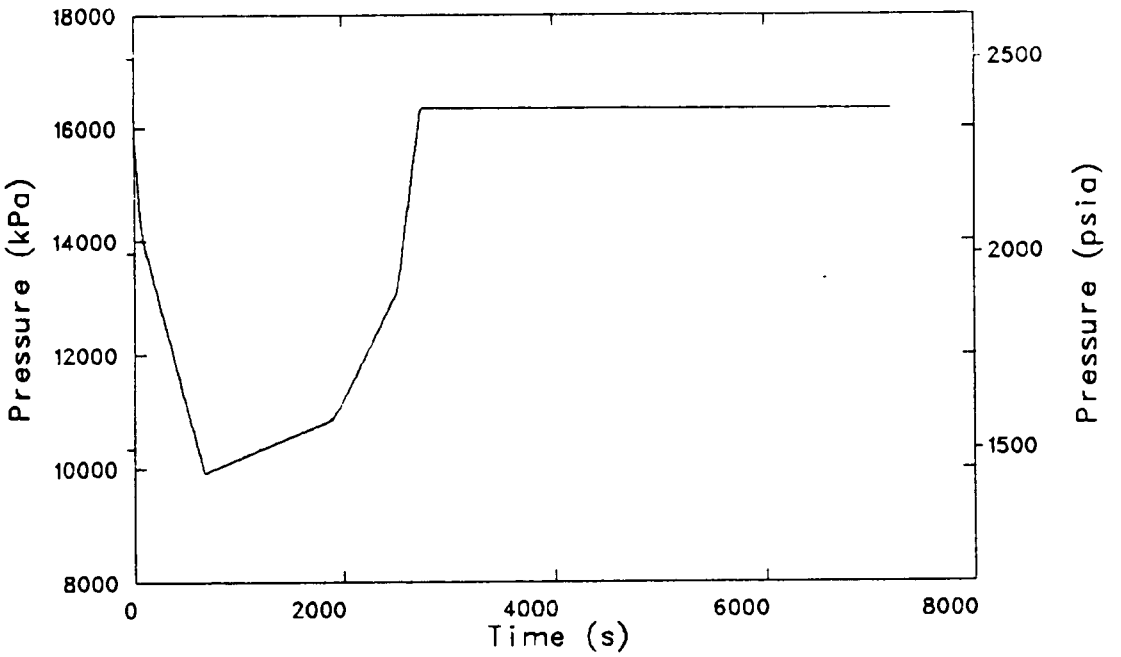

Figure F.173. Sequence 9.28: Reactor vessel downcomer fluid pressure.

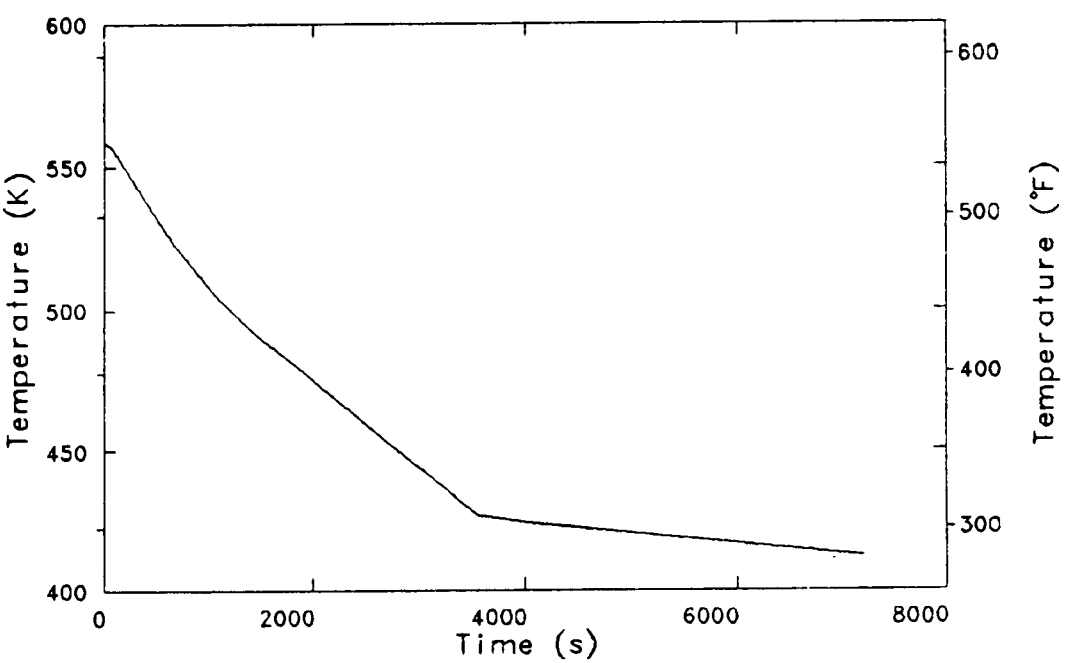

Figure F.174. Sequence 9.28: Reactor vessel downcomer fluid temperatures.

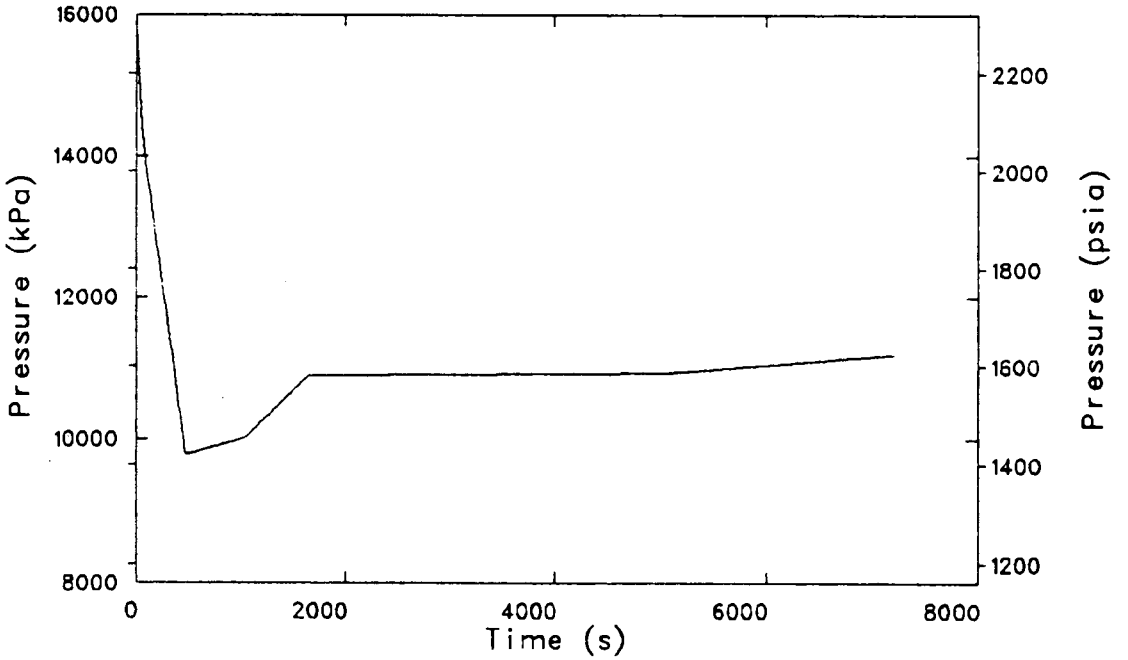

Figure F.175. Sequence 9.29: Reactor vessel downcomer fluid pressure.

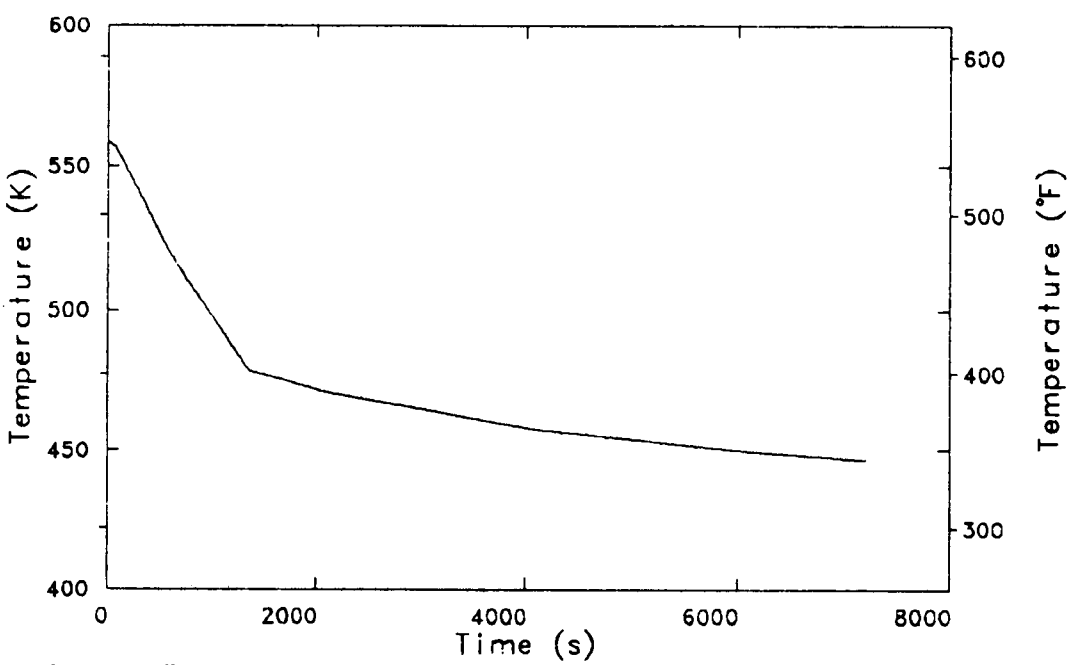

Figure F.176. Sequence 9.29: Reactor vessel downcomer fluid temperatures.

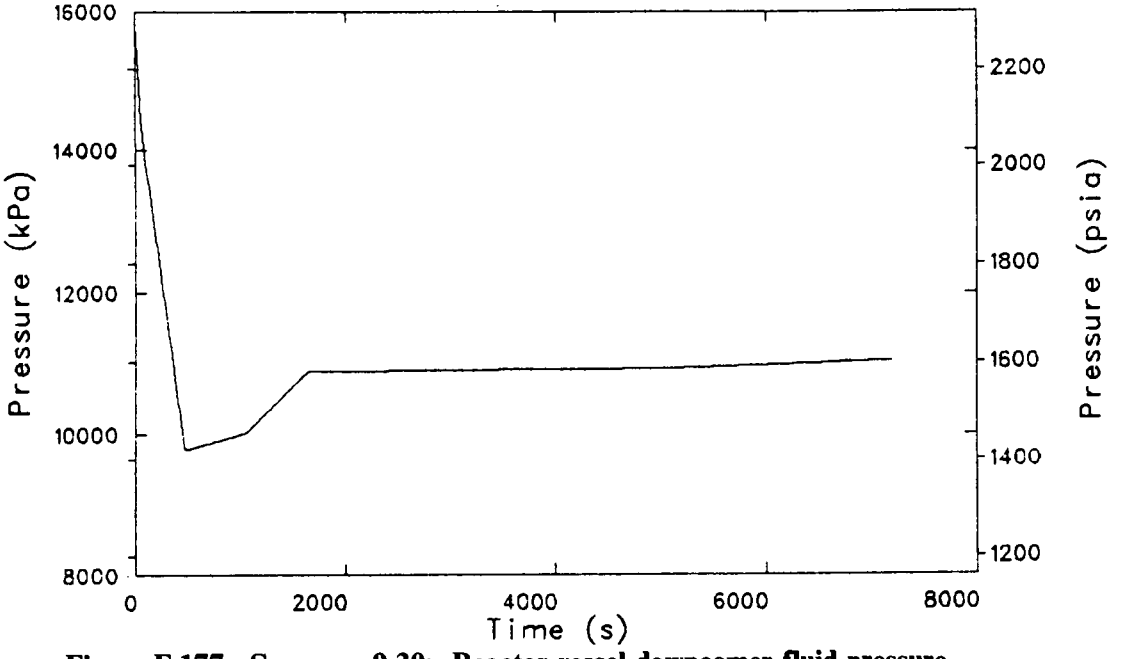

Figure F.177. Sequence 9.30: Reactor vessel downcomer fluid pressure.

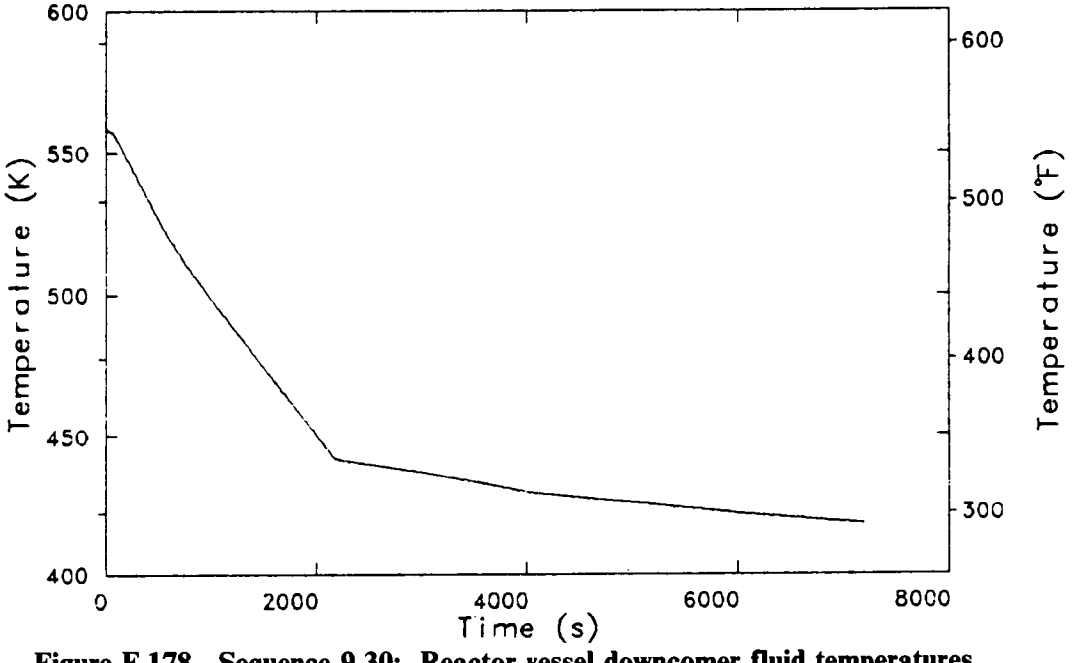

Figure F.178. Sequence 9.30: Reactor vessel downcomer fluid temperatures.

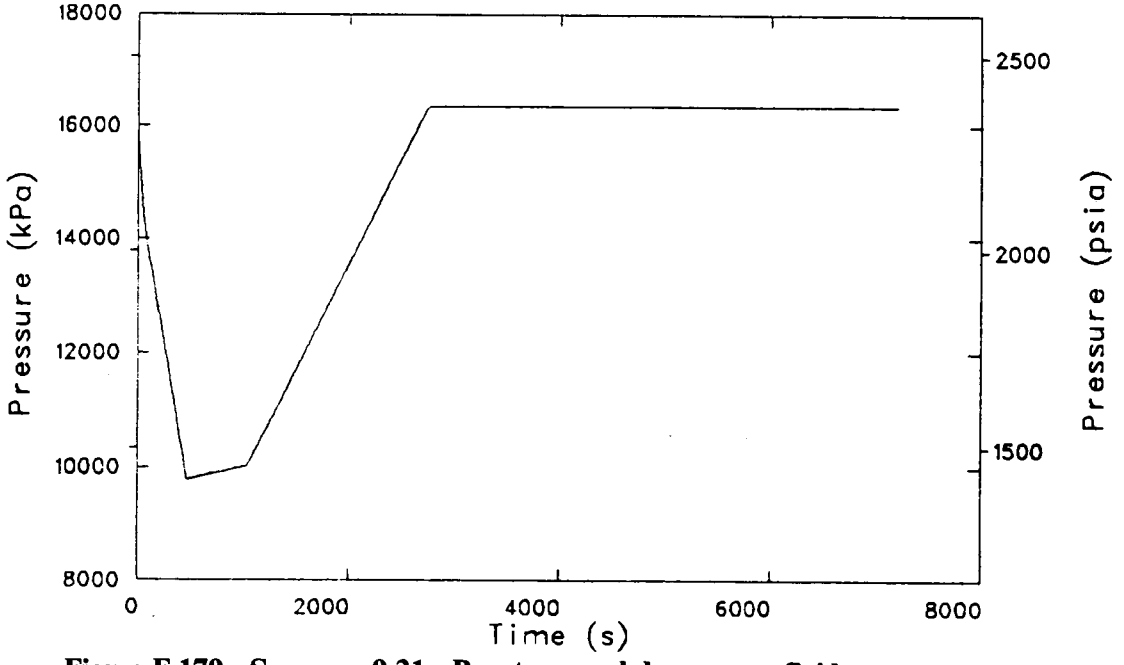

Figure F.179. Sequence 9.31: Reactor vessel downcomer fluid pressure.

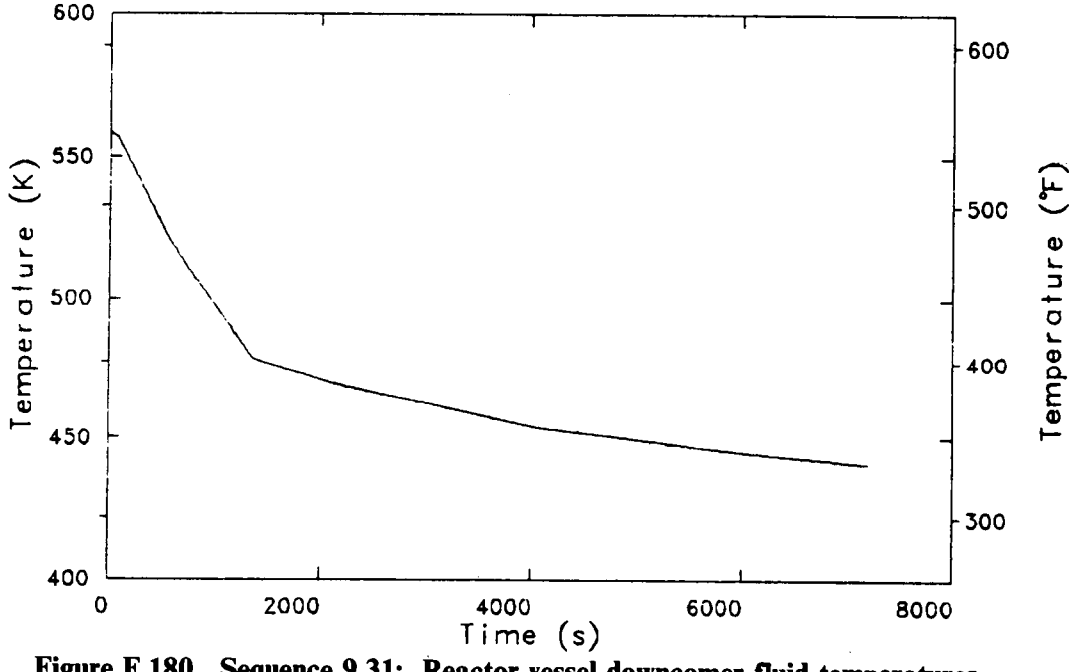

Figure F.180. Sequence 9.31: Reactor vessel downcomer fluid temperatures.

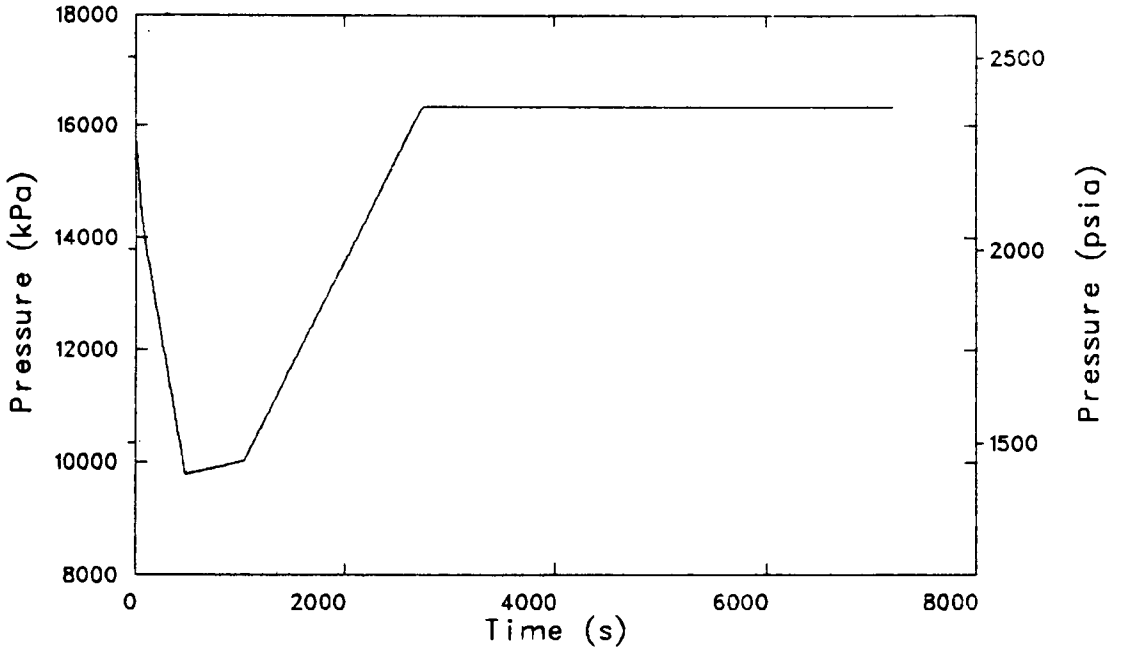

Figure F.181. Sequence 9.32: Reactor vessel downcomer fluid pressure.

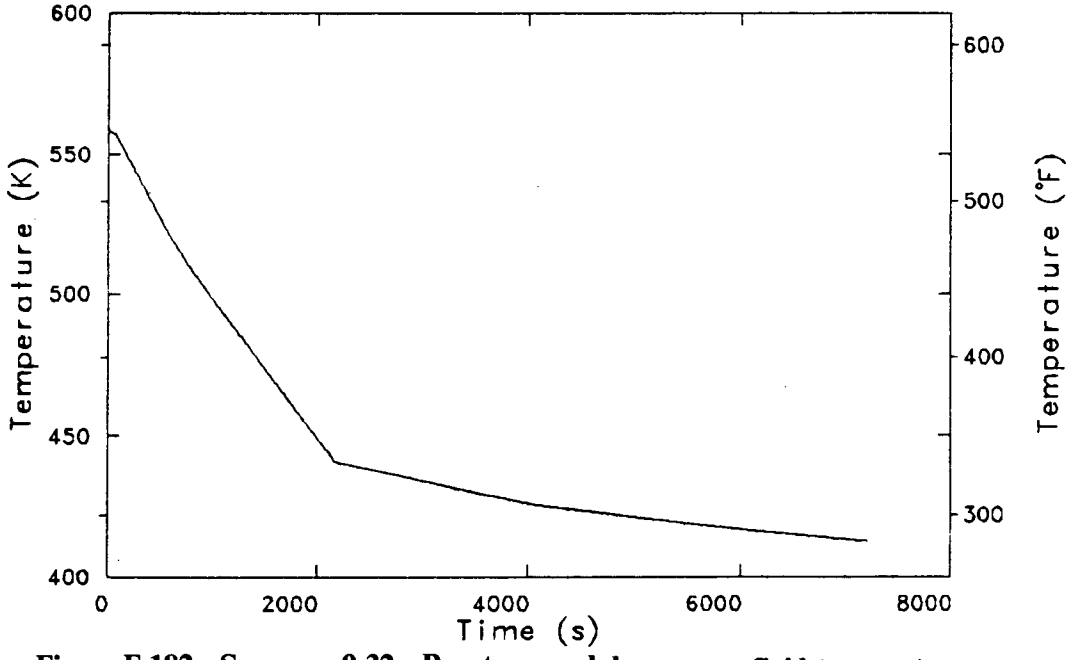

Figure F.182. Sequence 9.32: Reactor vessel downcomer fluid temperatures.

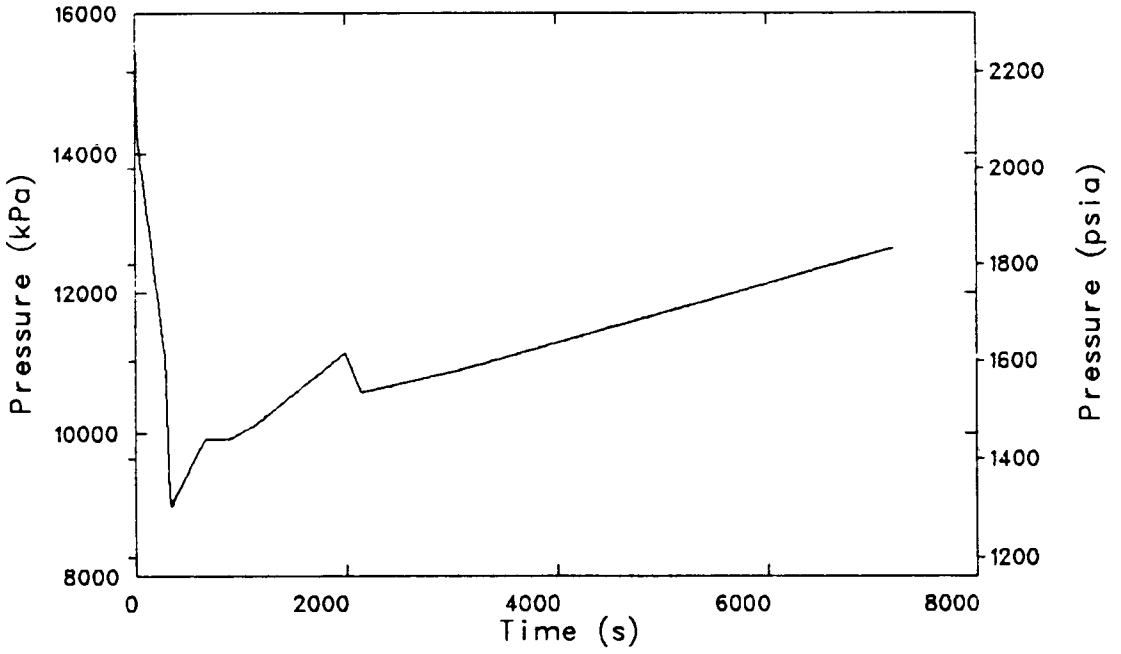

Figure F.183. Sequence 9.33: Reactor vessel downcomer fluid pressure.

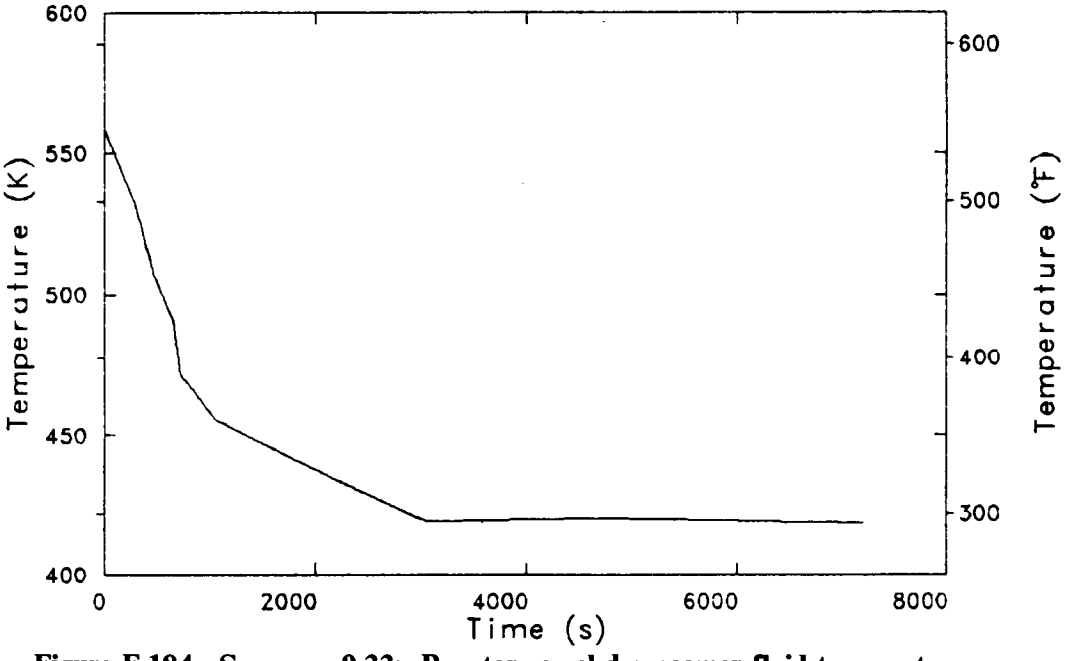

Figure F.184. Sequence 9.33: Reactor vessel downcomer fluid temperatures.

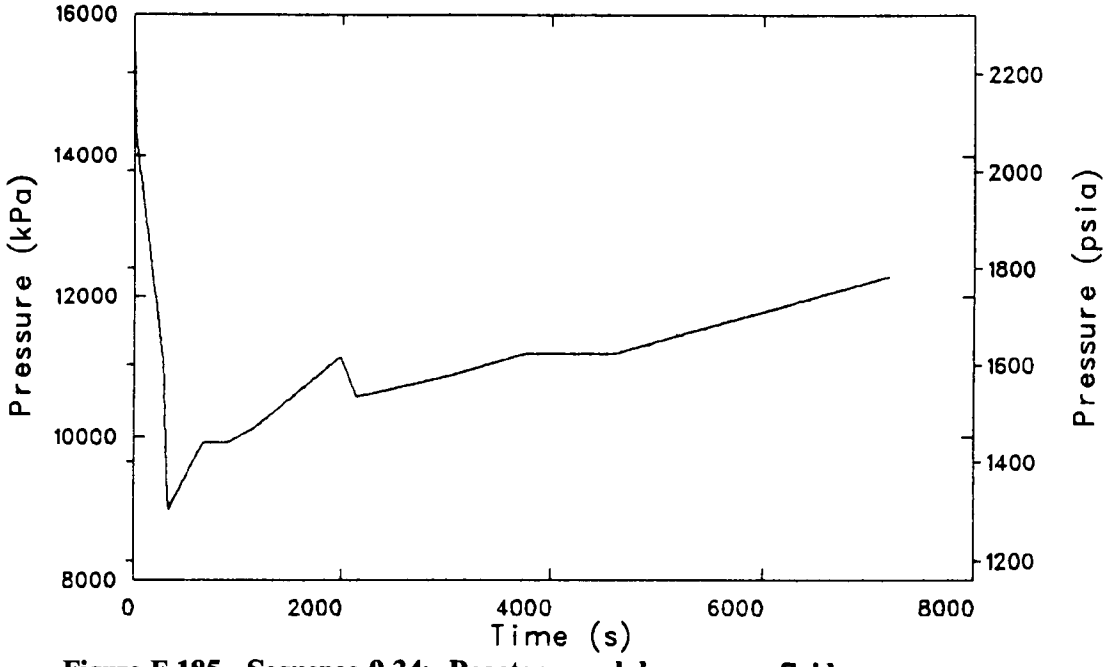

Figure F.185. Sequence 9.34: Reactor vessel downcomer fluid pressure.

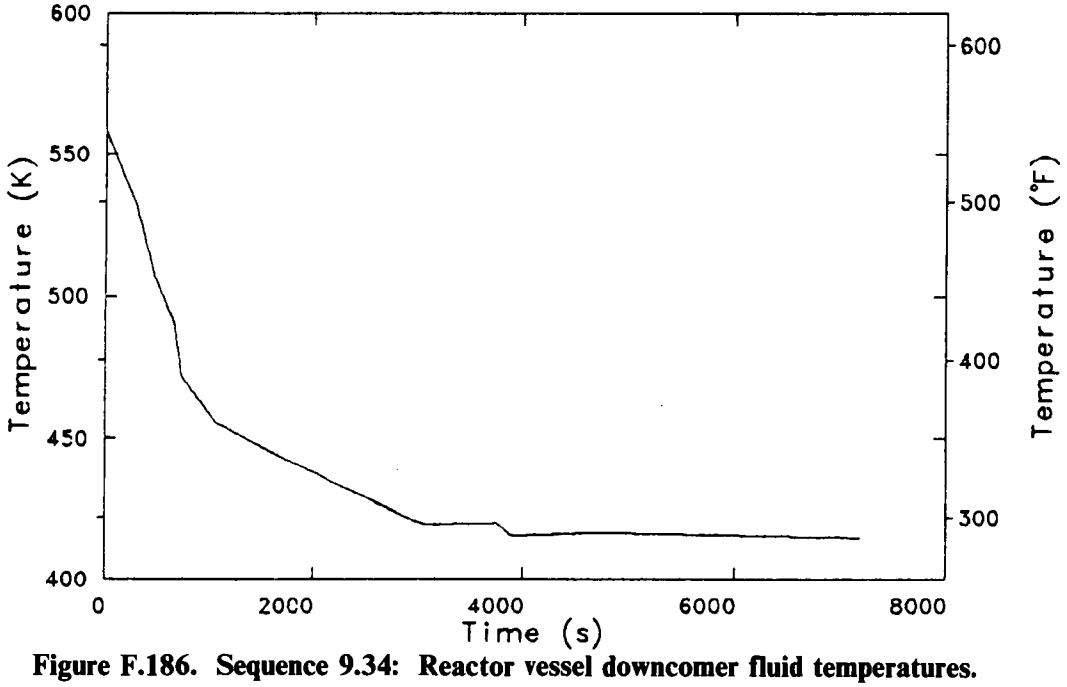

Figure F.186. Sequence 9.34: Reactor vessel downcomer fluid temperatures.

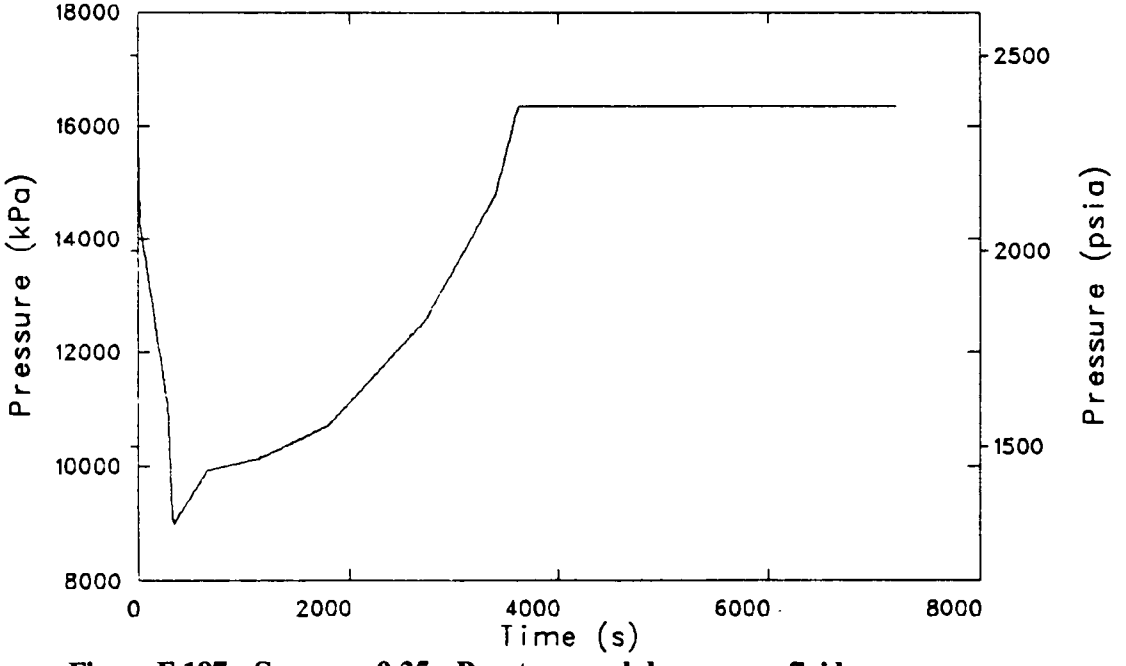

Figure F.187. Sequence 9.35: Reactor vessel downcomer fluid pressure.

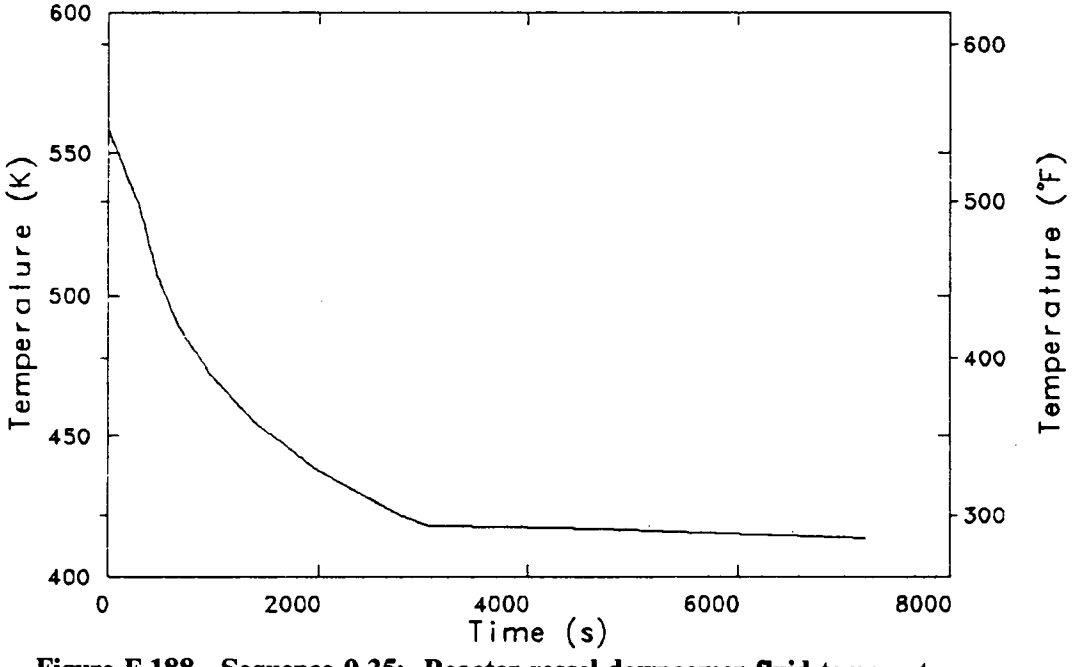

Figure F.188. Sequence 9.35: Reactor vessel downcomer fluid temperatures.

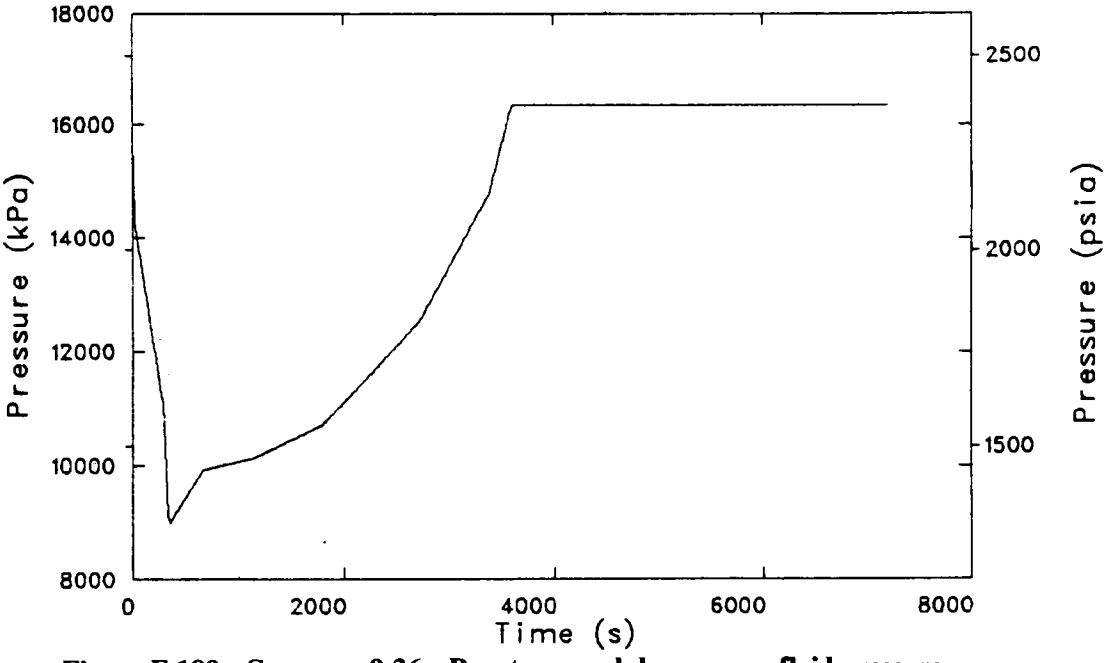

Figure F.189. Sequence 9.36: Reactor vessel downcomer fluid pressure.

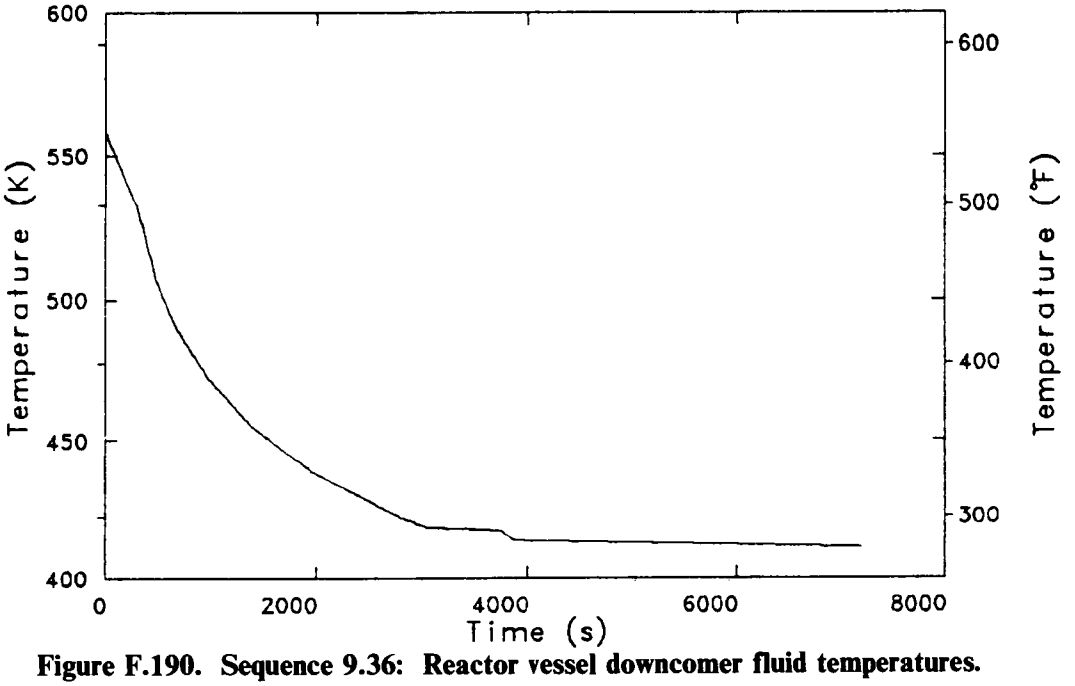

Figure F.190. Sequence 9.36: Reactor vessel downcomer fluid temperatures.

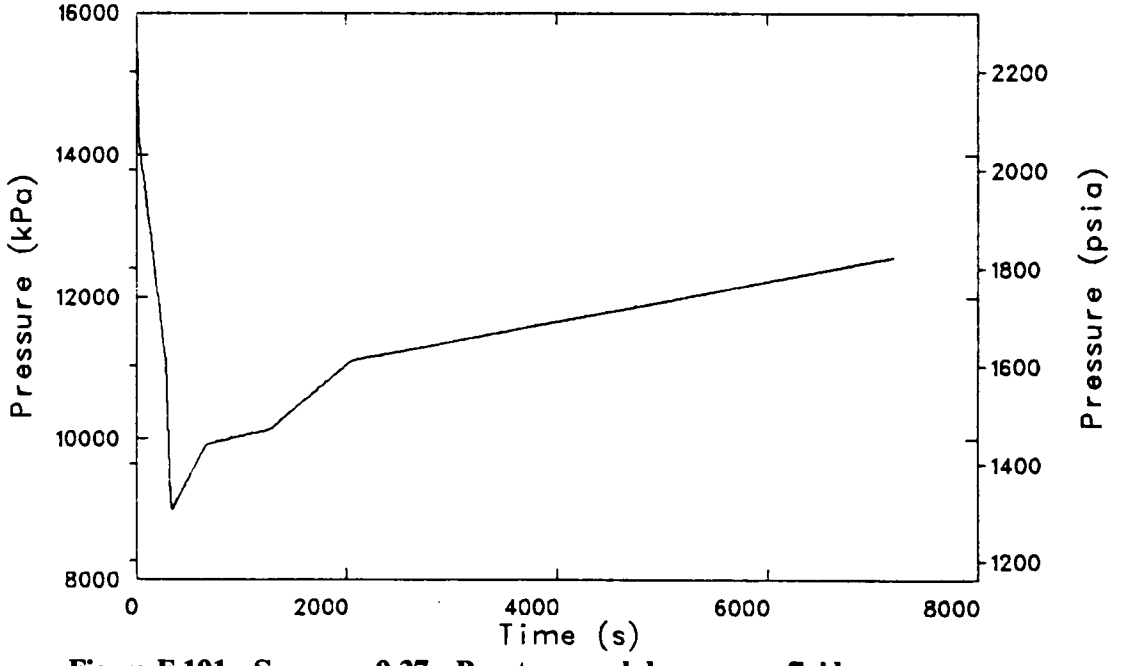

Figure F.191. Sequence 9.37: Reactor vessel downcomer fluid pressure.

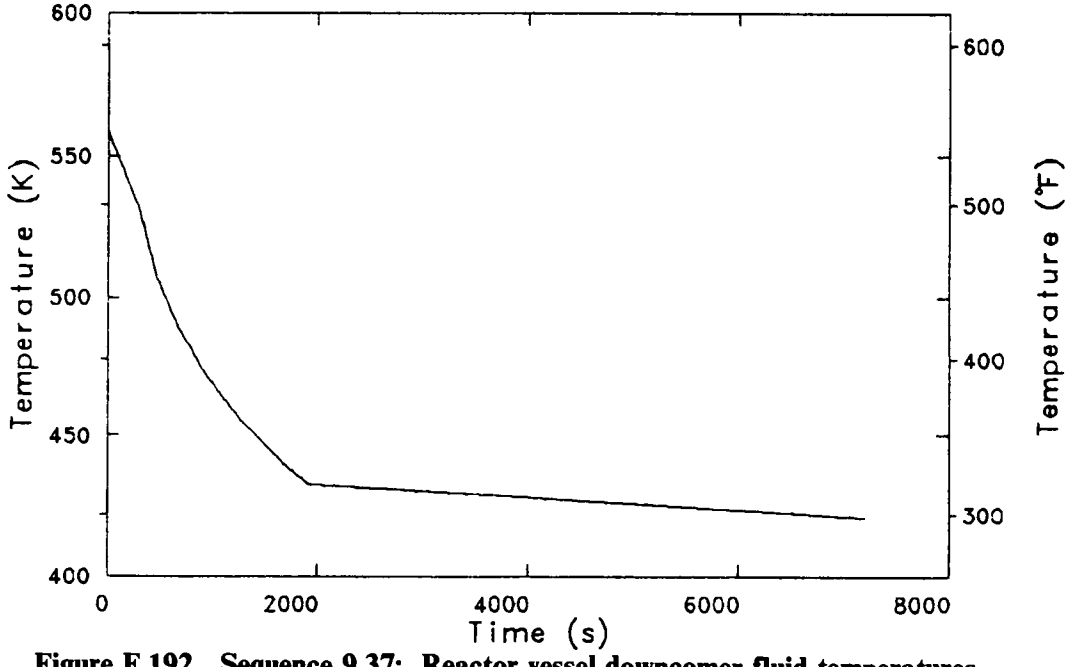

Figure F.192. Sequence 9.37: Reactor vessel downcomer fluid temperatures.

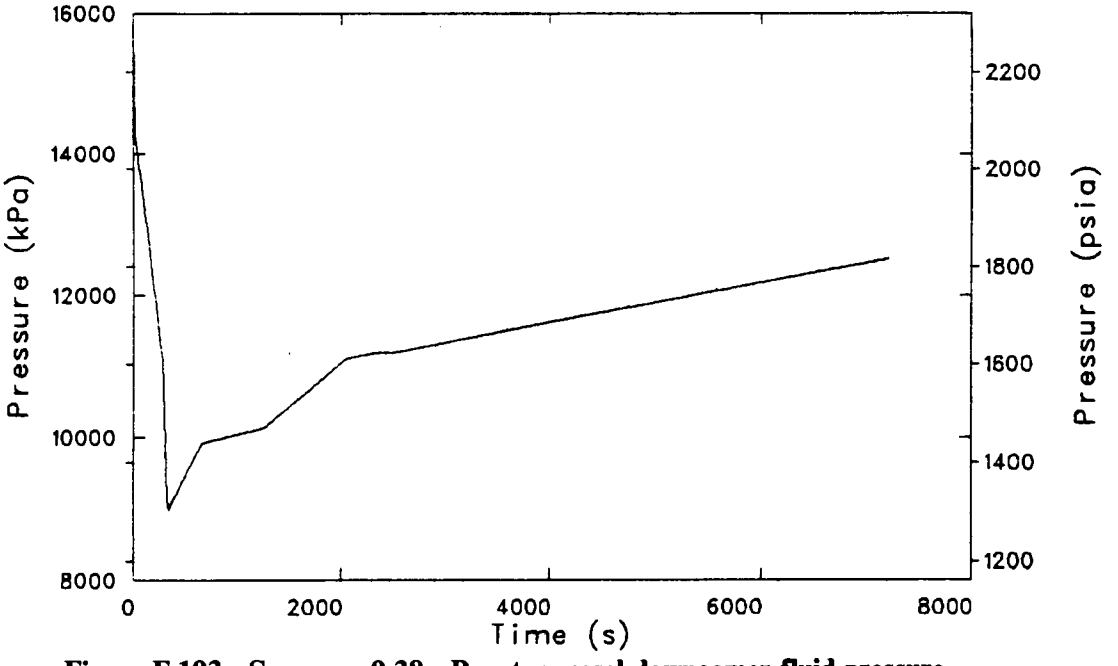

Figure F.193. Sequence 9.38: Reactor vessel downcomer fluid pressure.

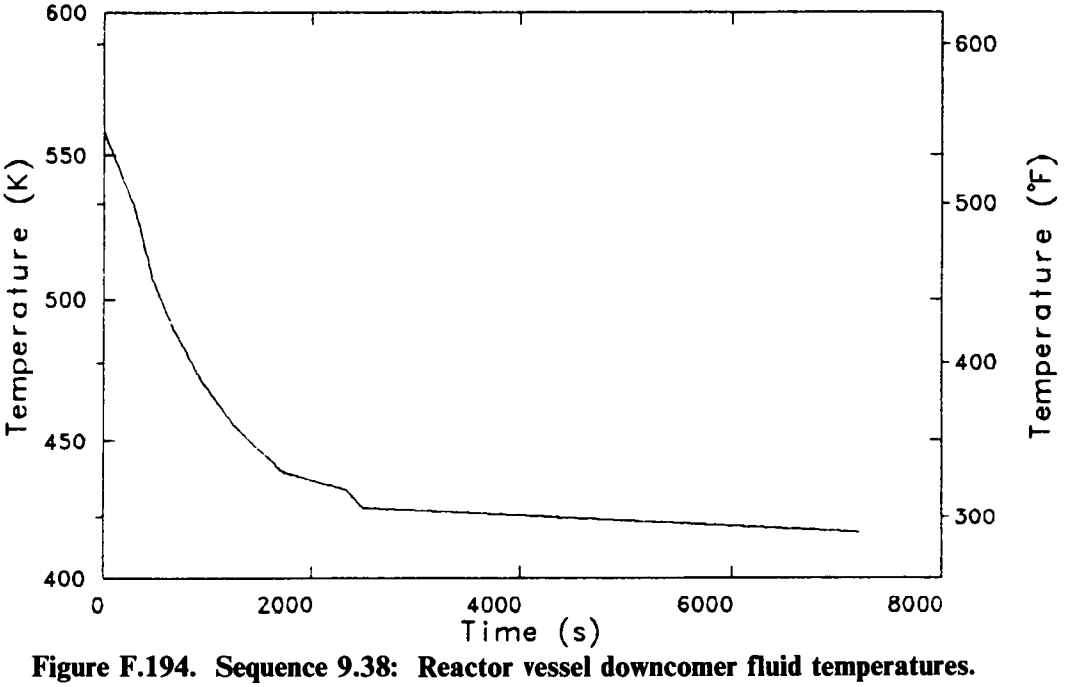

Figure F.194. Sequence 9.38: Reactor vessel downcomer fluid temperatures.

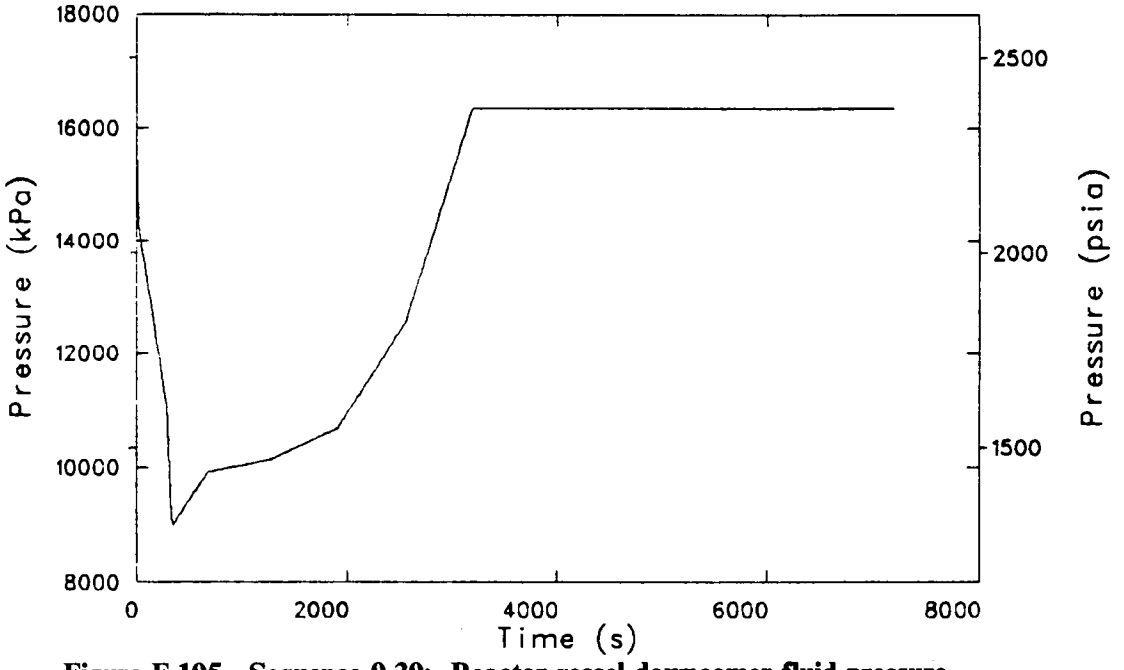

Figure F.195. Sequence 9.39: Reactor vessel downcomer fluid pressure.

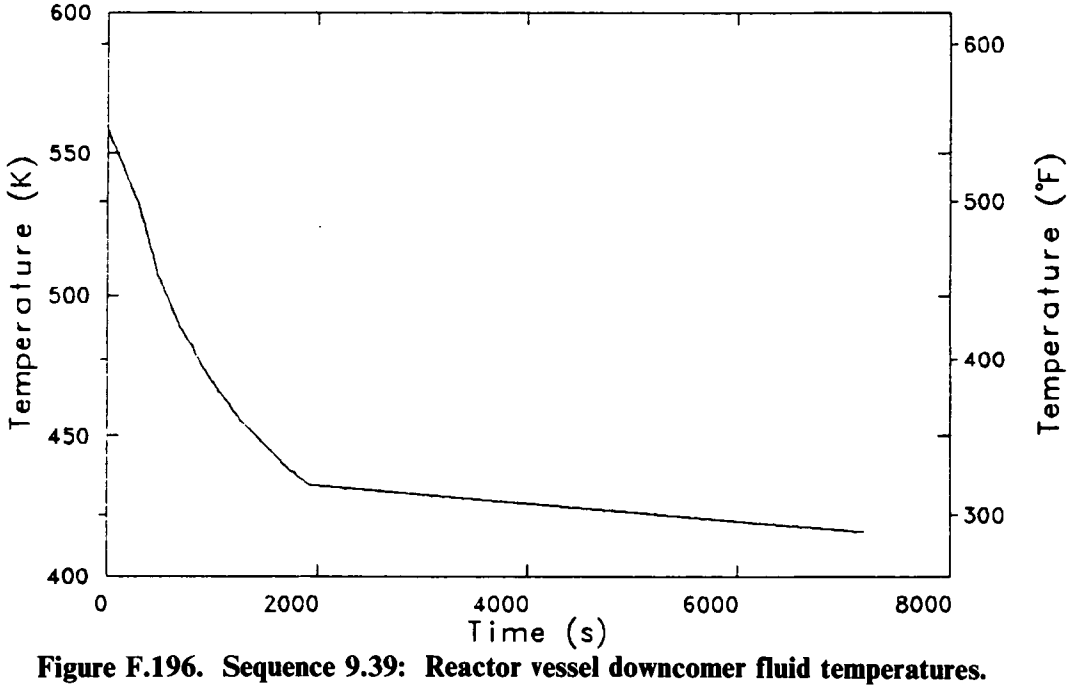

Figure F.196. Sequence 9.39: Reactor vessel downcomer fluid temperatures.

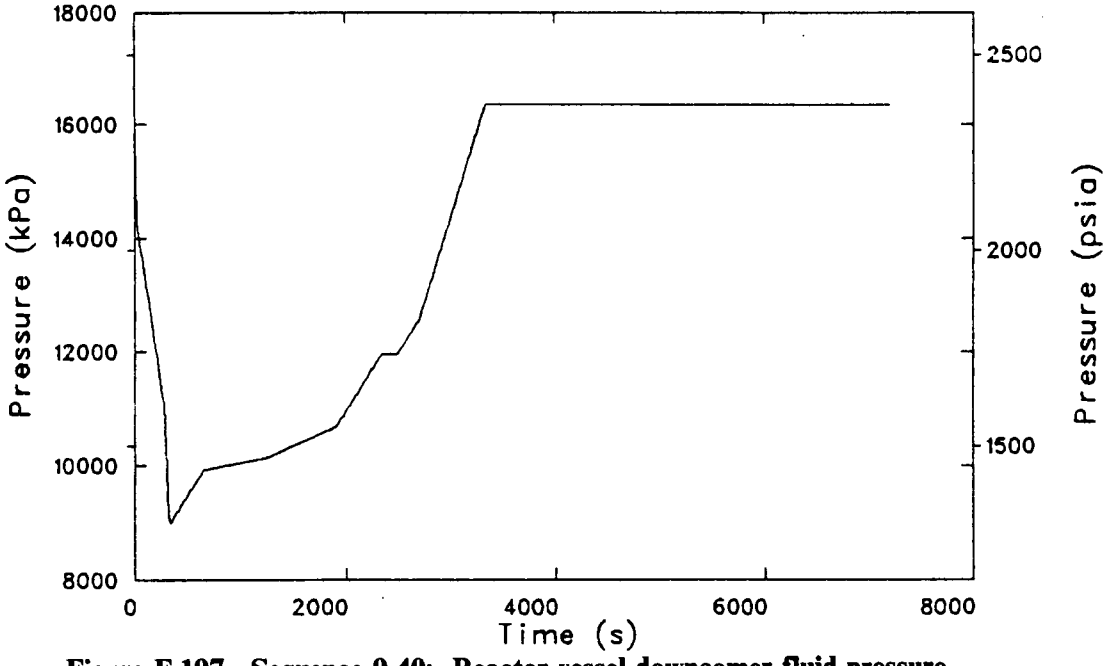

Figure F.197. Sequence 9.40: Reactor vessel downcomer fluid pressure.

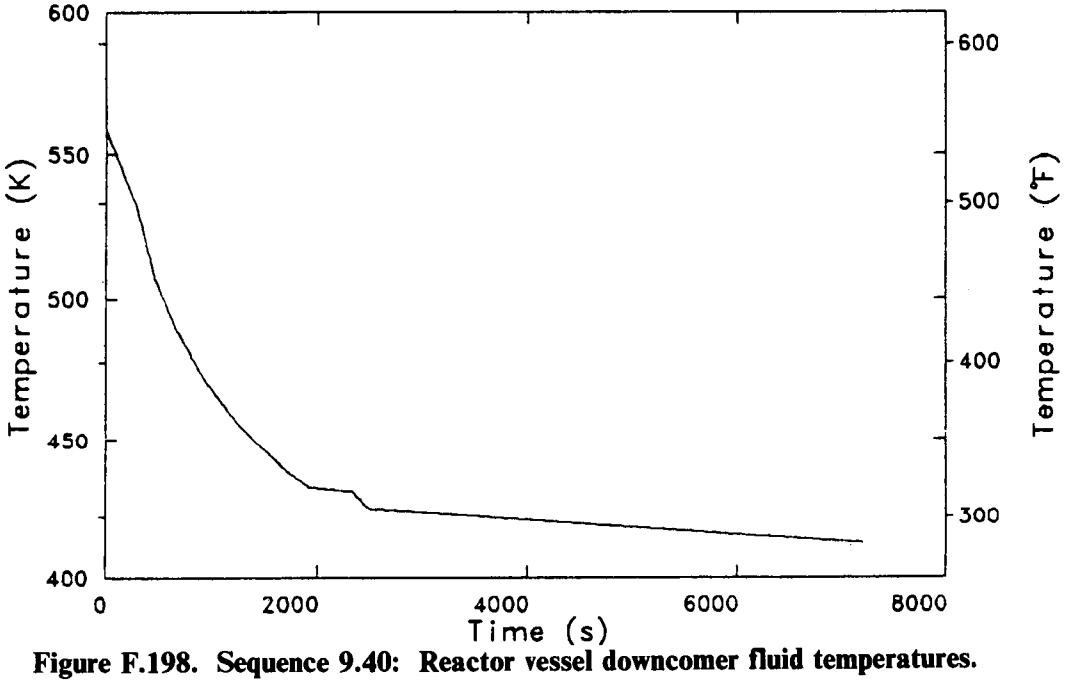

Figure F.198. Sequence 9.40: Reactor vessel downcomer fluid temperatures.

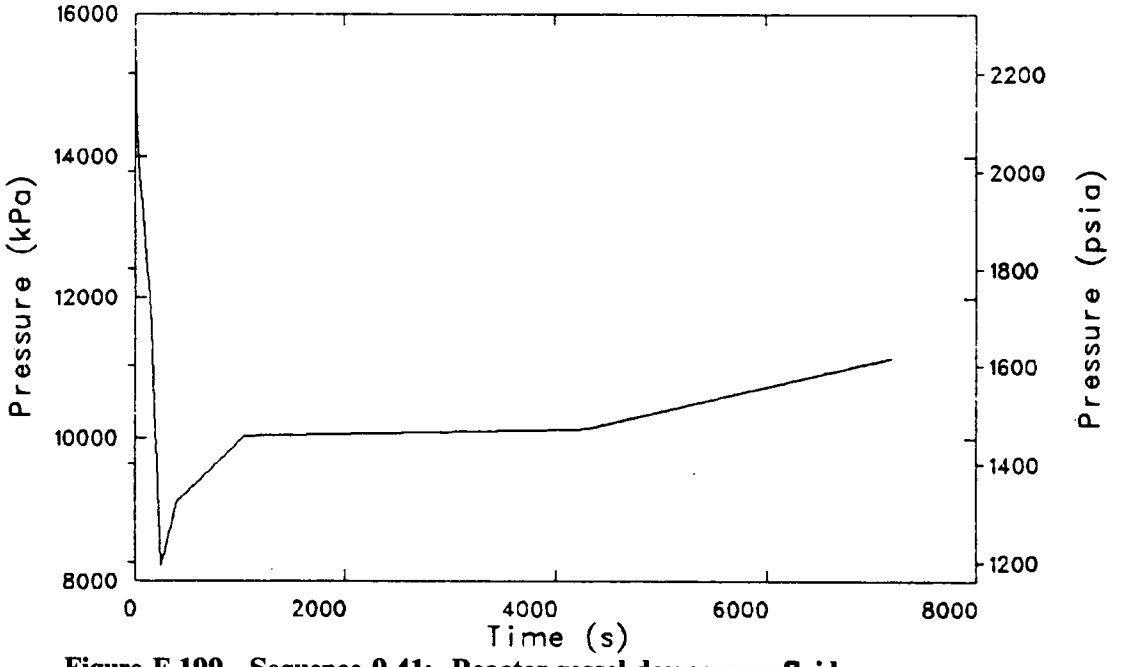

Figure F.199. Sequence 9.41: Reactor vessel downcomer fluid pressure.

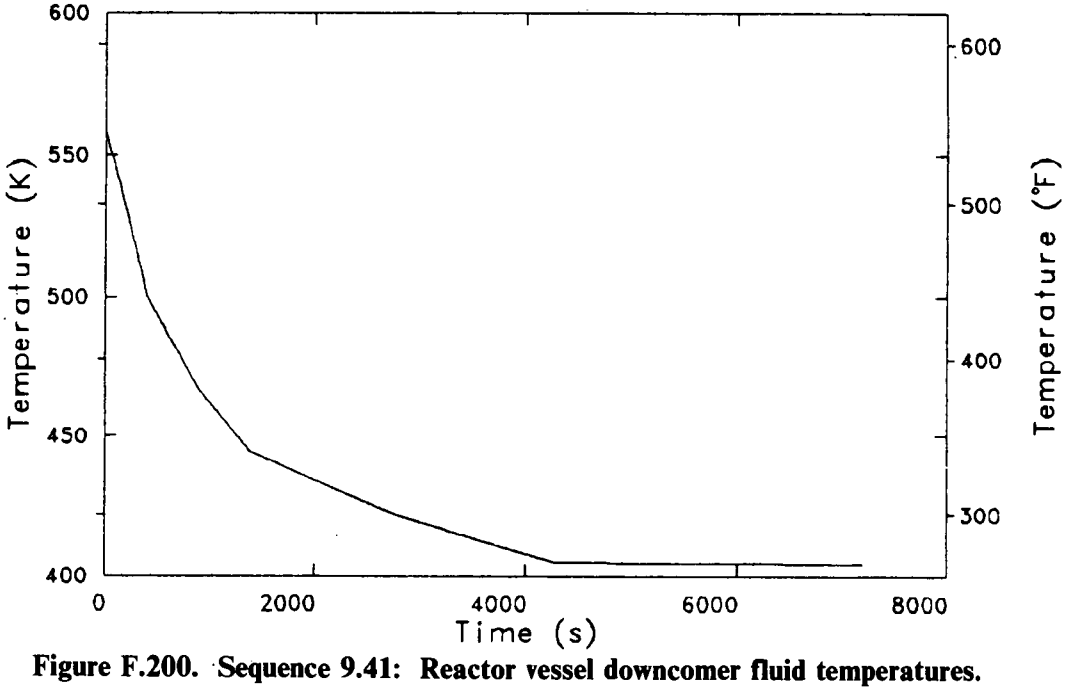

Figure F.200. Sequence 9.41: Reactor vessel downcomer fluid temperatures.

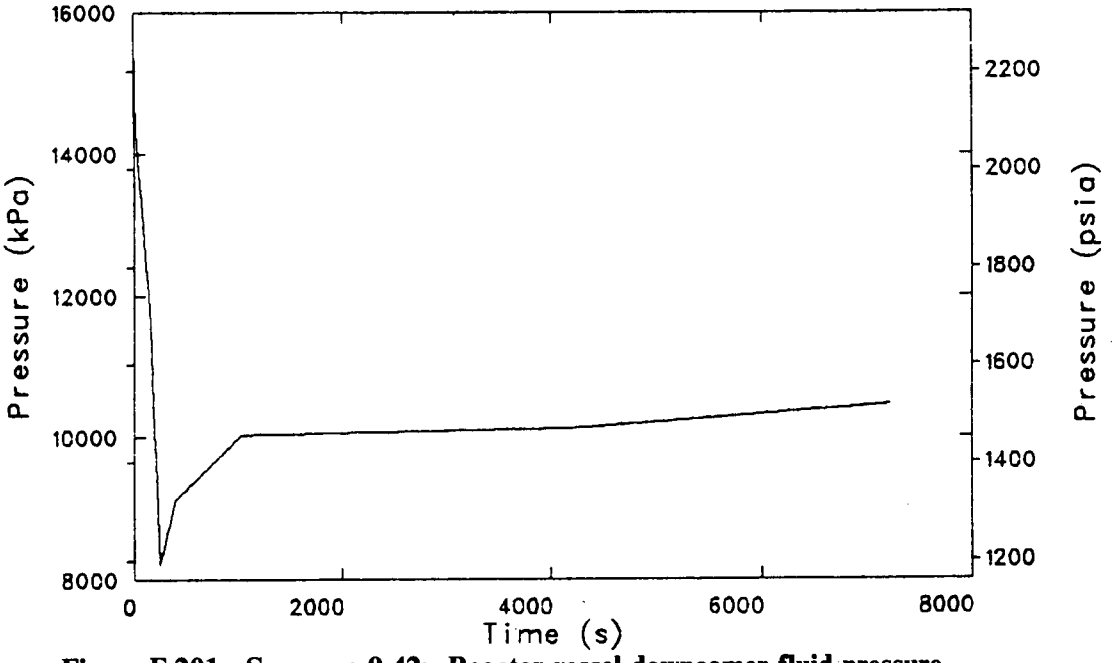

Figure F.201. Sequence 9.42: Reactor vessel downcomer fluid pressure.

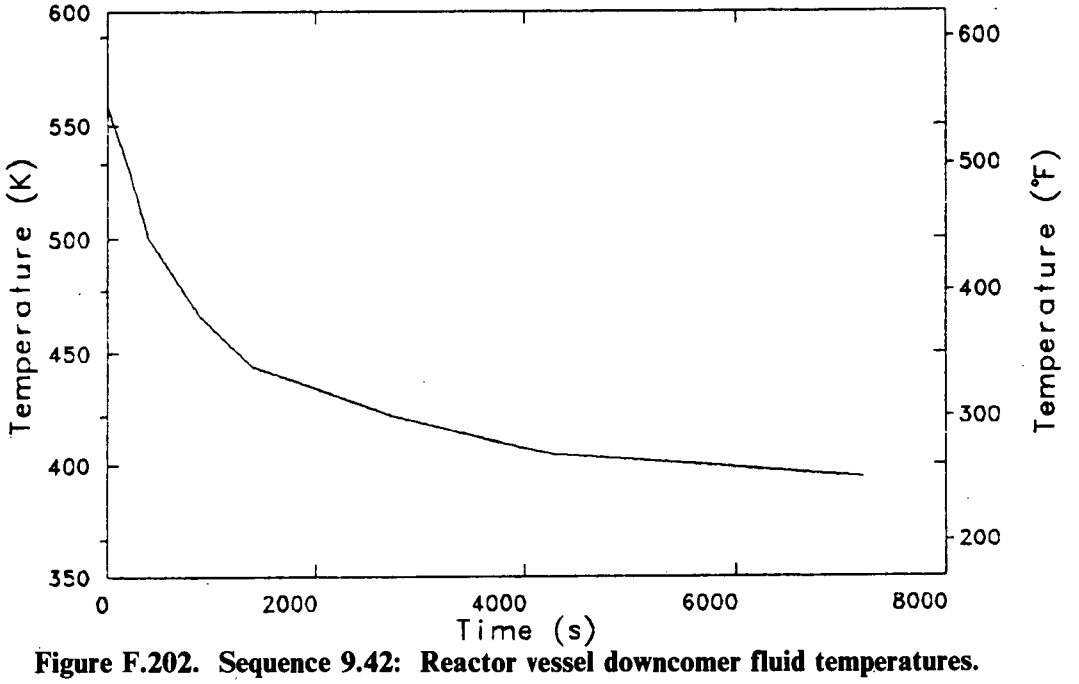

Figure F.202. Sequence 9.42: Reactor vessel downcomer fluid temperatures.

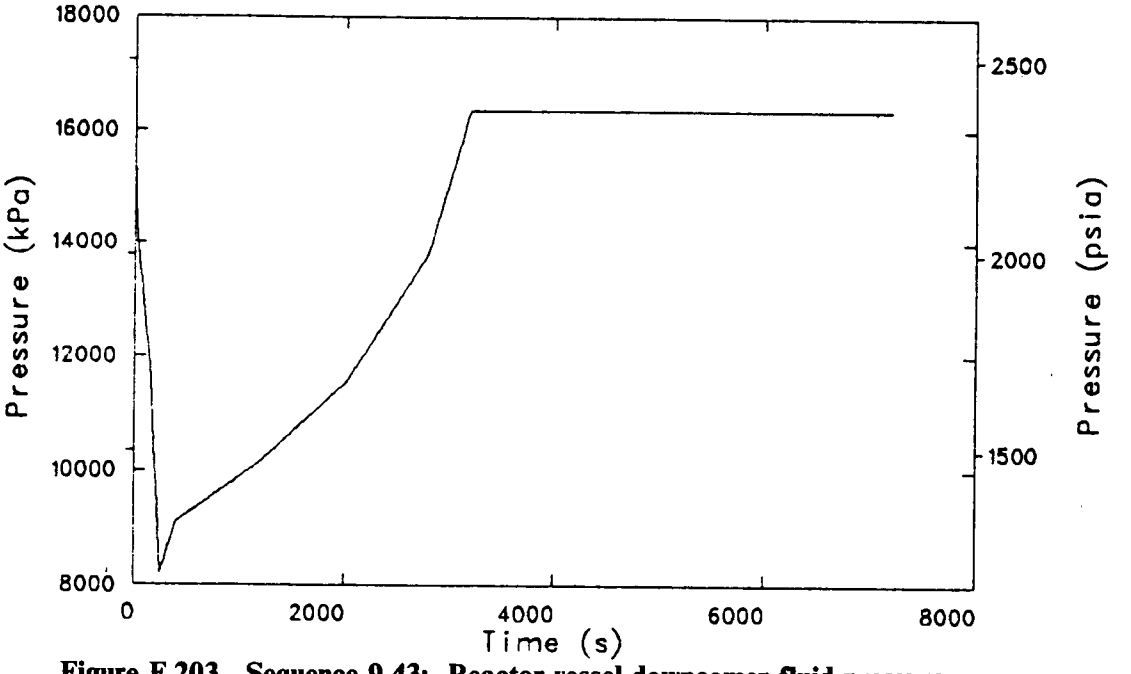

Figure F.203. Sequence 9.43: Reactor vessel downcomer fluid pressure.

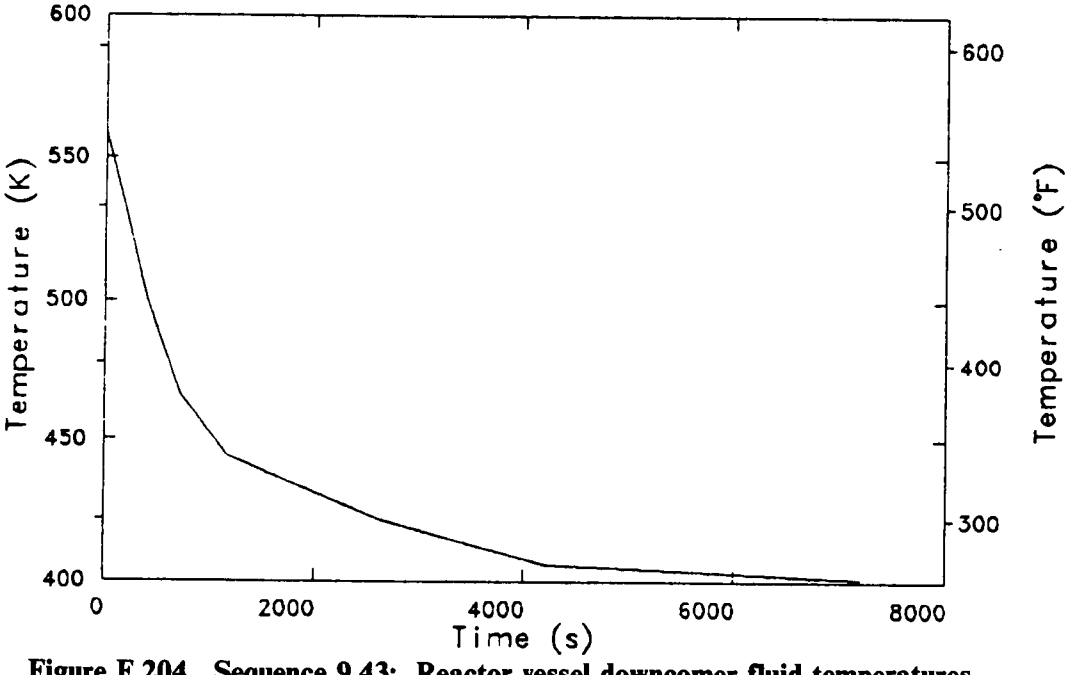

Figure F.204. Sequence 9.43: Reactor vessel downcomer fluid temperatures.

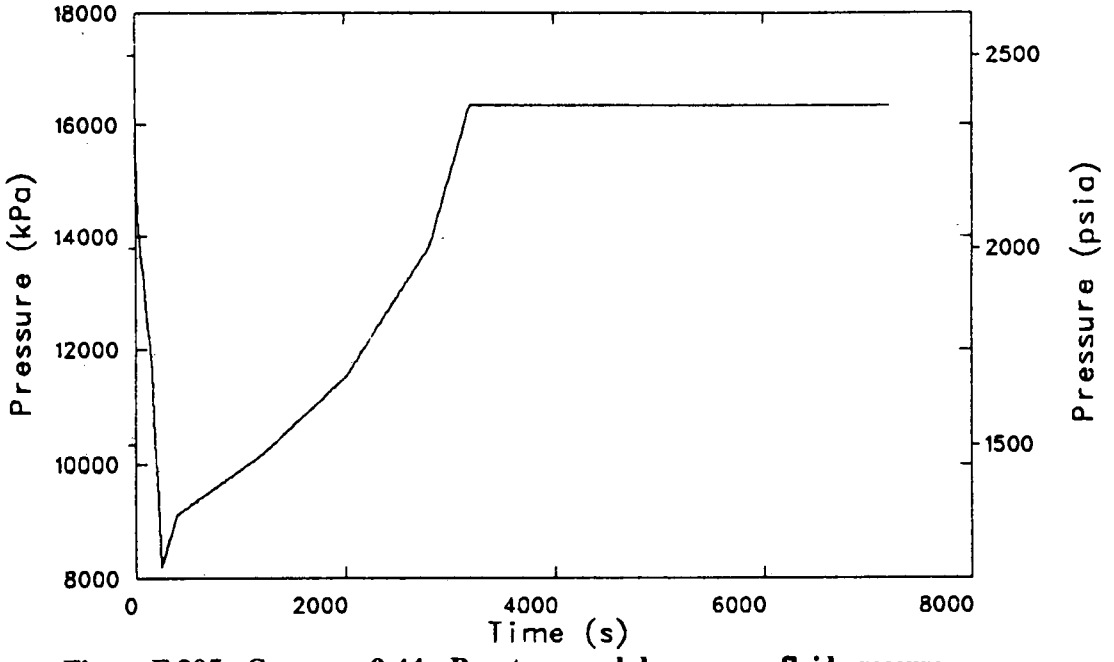

Figure F.205. Sequence 9.44: Reactor vessel downcomer fluid pressure.

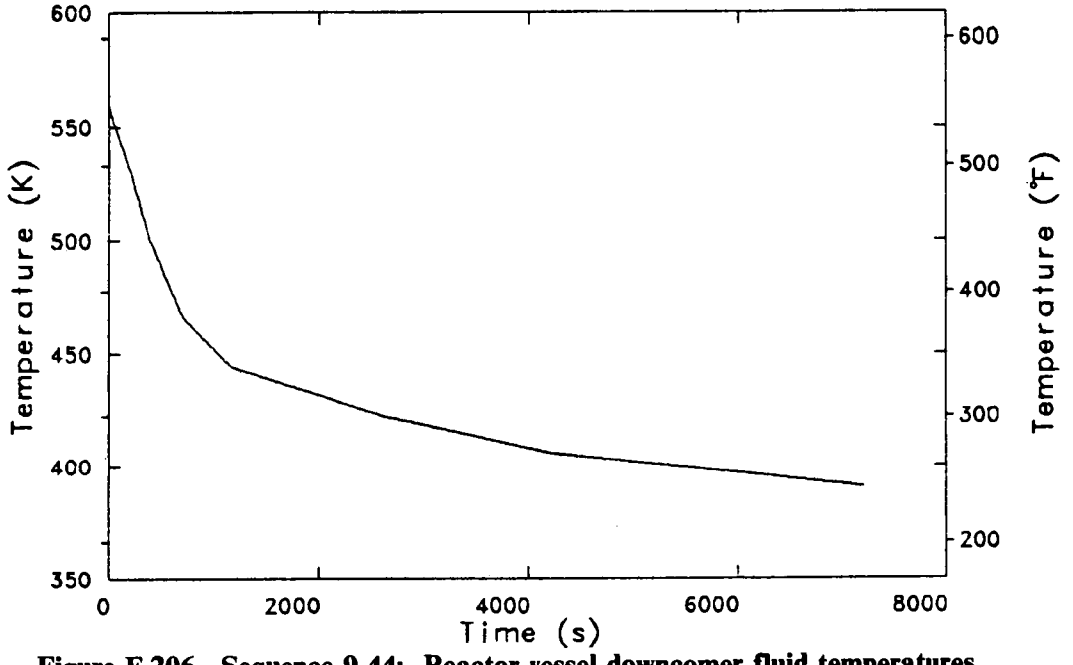

Figure F.206. Sequence 9.44: Reactor vessel downcomer fluid temperatures.

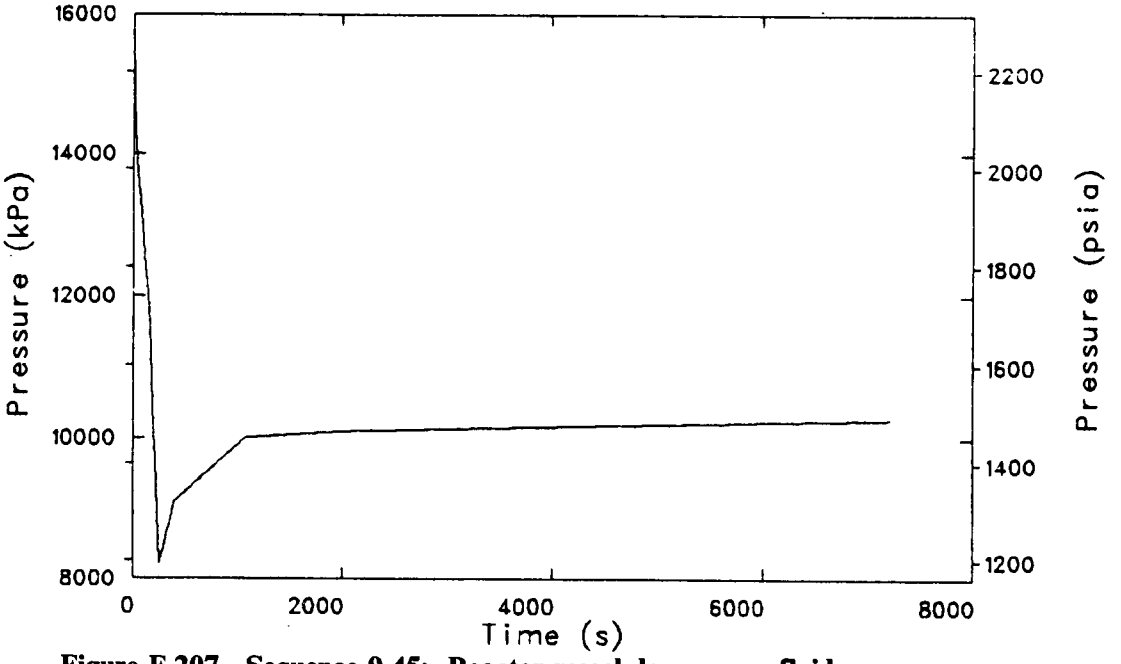

Figure F.207. Sequence 9.45: Reactor vessel downcomer fluid pressure.

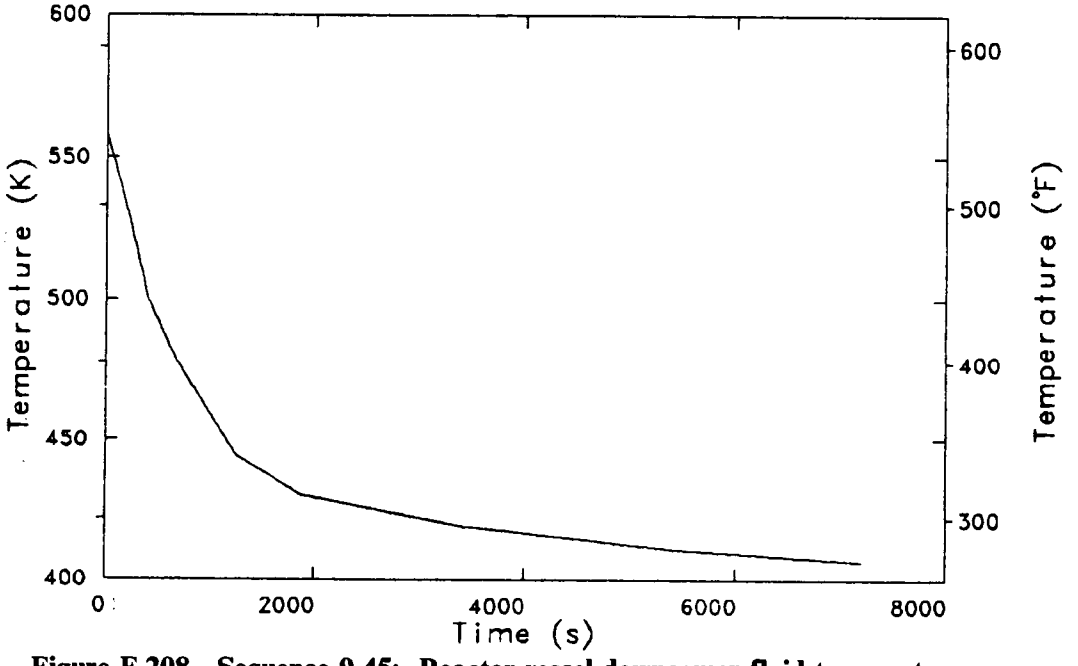

Figure F.208. Sequence 9.45: Reactor vessel downcomer fluid temperatures.

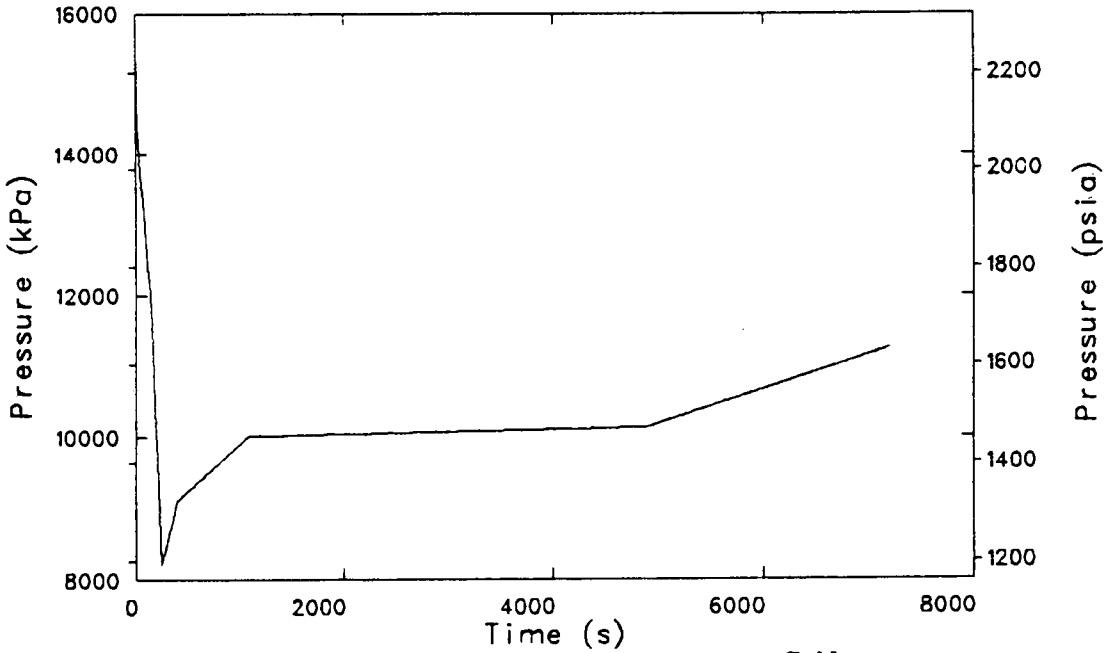

Figure F.209. Sequence 9.46: Reactor vessel downcomer fluid pressure.

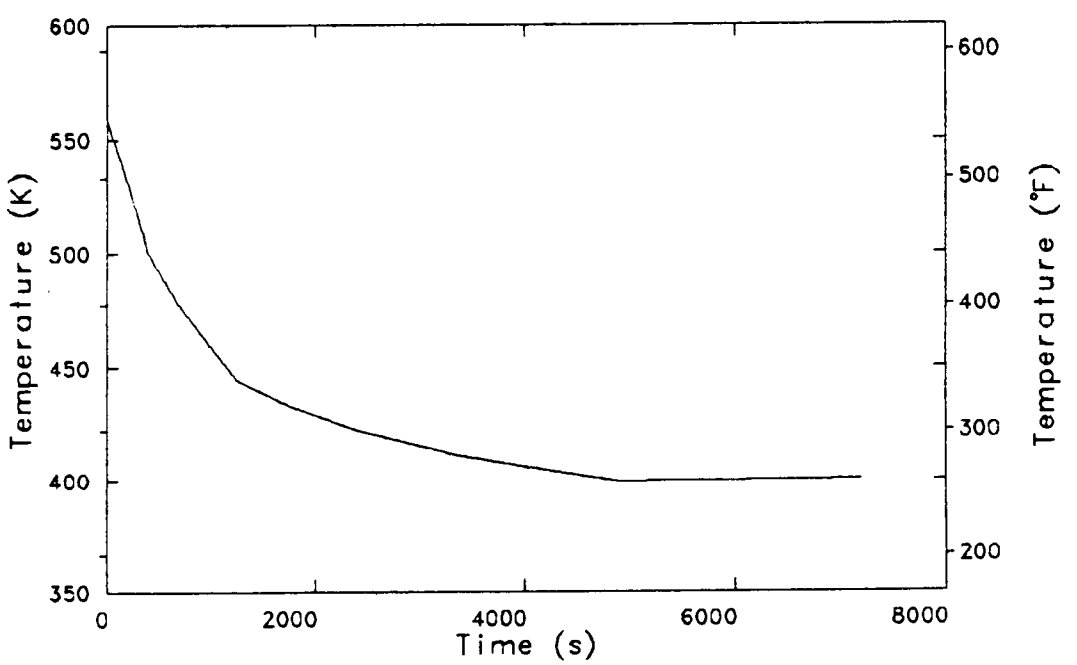

Figure F.210. Sequence 9.46: Reactor vessel downcomer fluid temperatures.

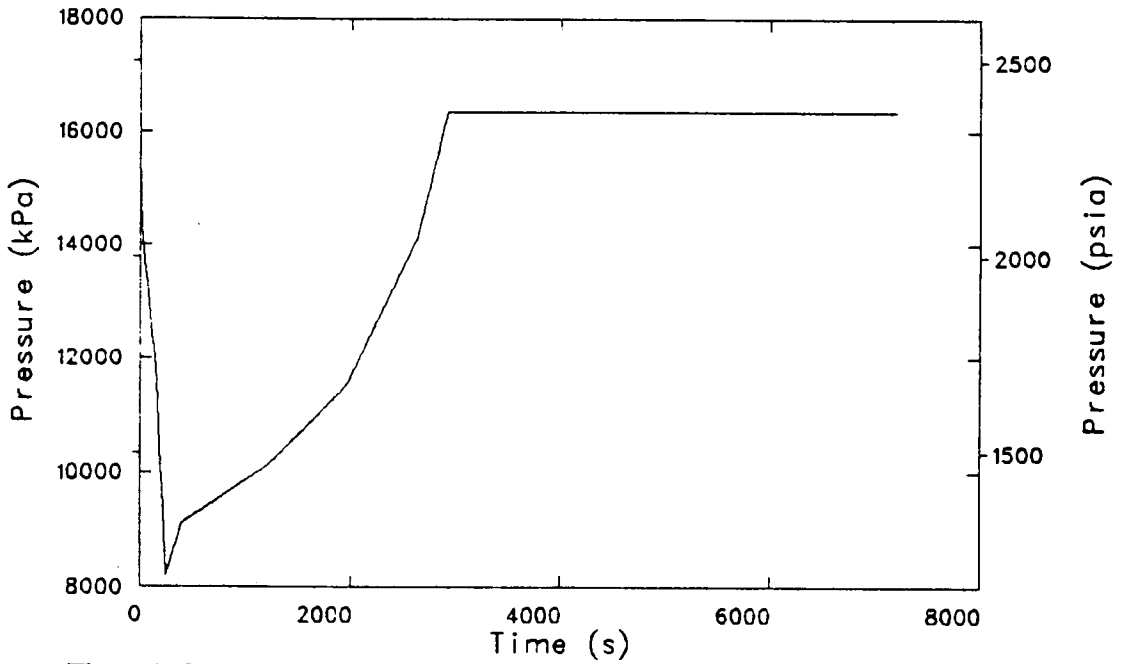

Figure F.211. Sequence 9.47: Reactor vessel downcomer fluid pressure.

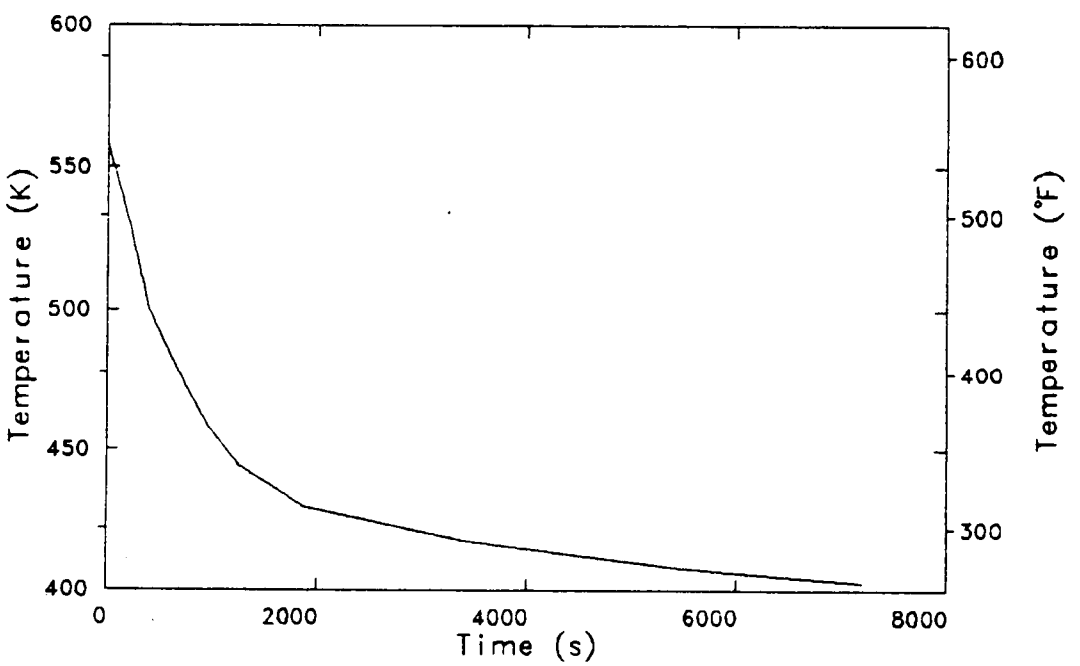

Figure F.212. Sequence 9.47: Reactor vessel downcomer fluid temperatures.

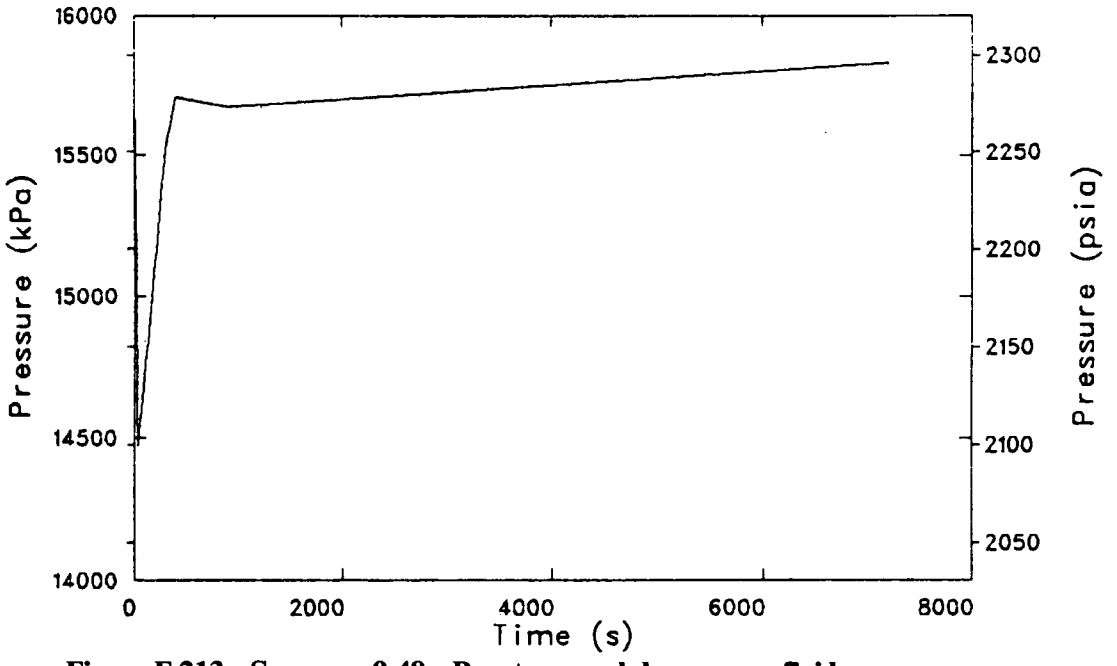

Figure F.213. Sequence 9.48: Reactor vessel downcomer fluid pressure.

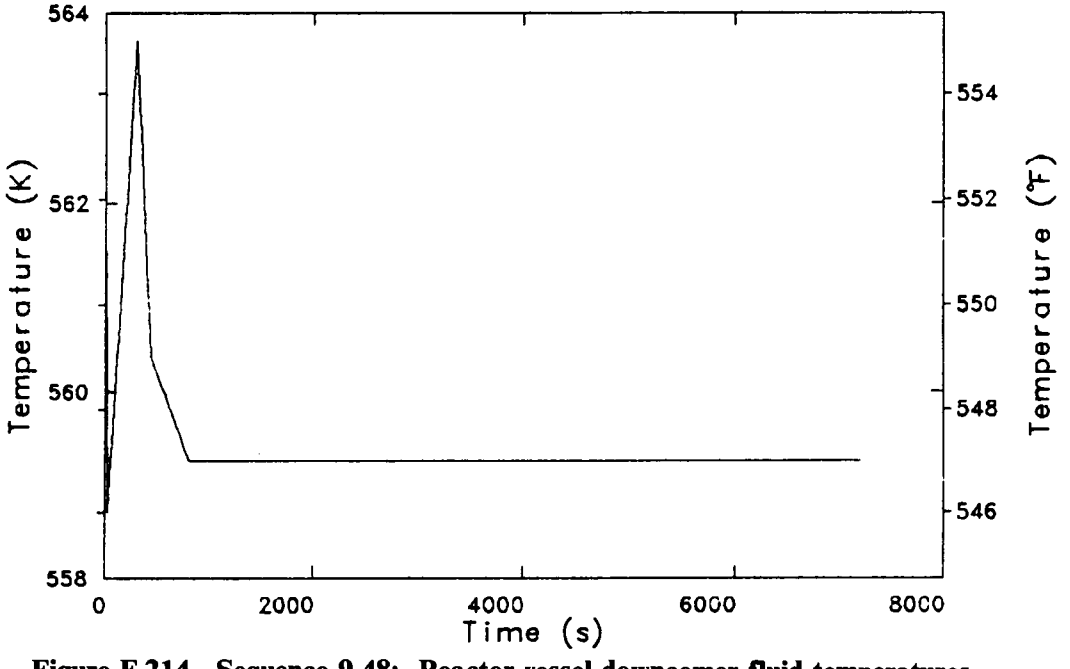

Figure F.214. Sequence 9.48: Reactor vessel downcomer fluid temperatures.

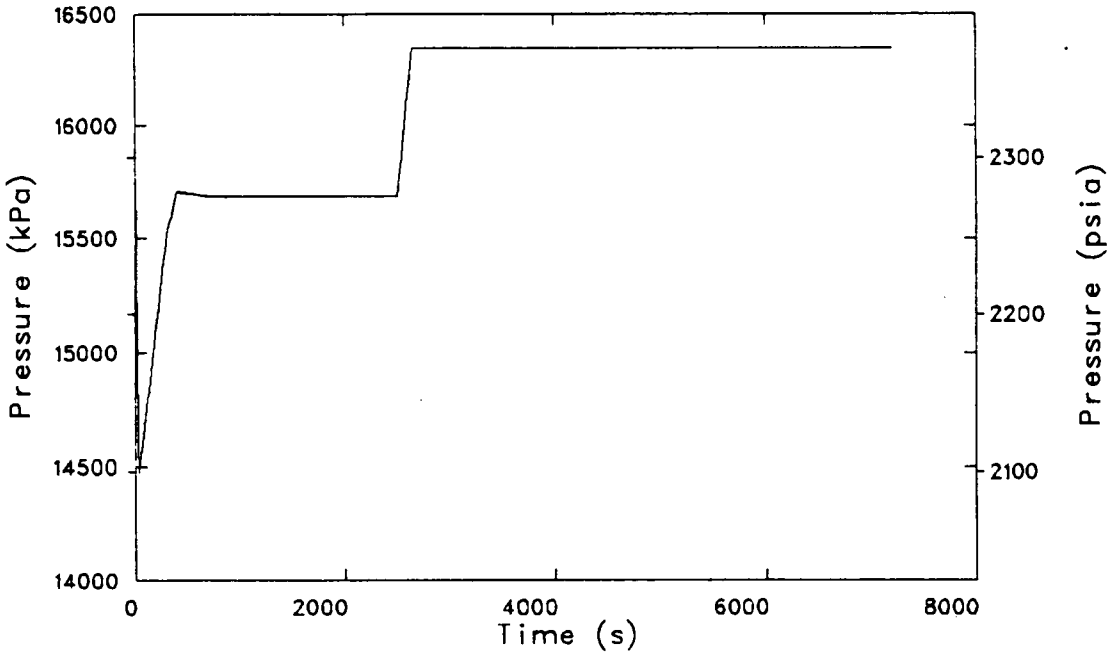

Figure F.215. Sequence 9.49: Reactor vessel downcomer fluid pressure.

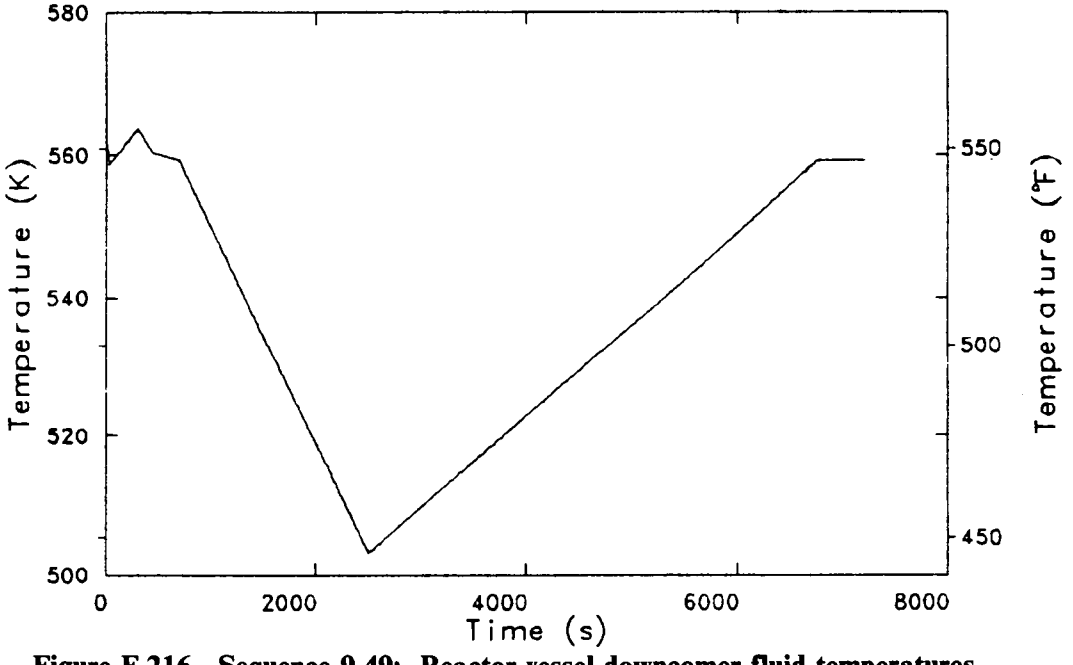

Figure F.216. Sequence 9.49: Reactor vessel downcomer fluid temperatures.

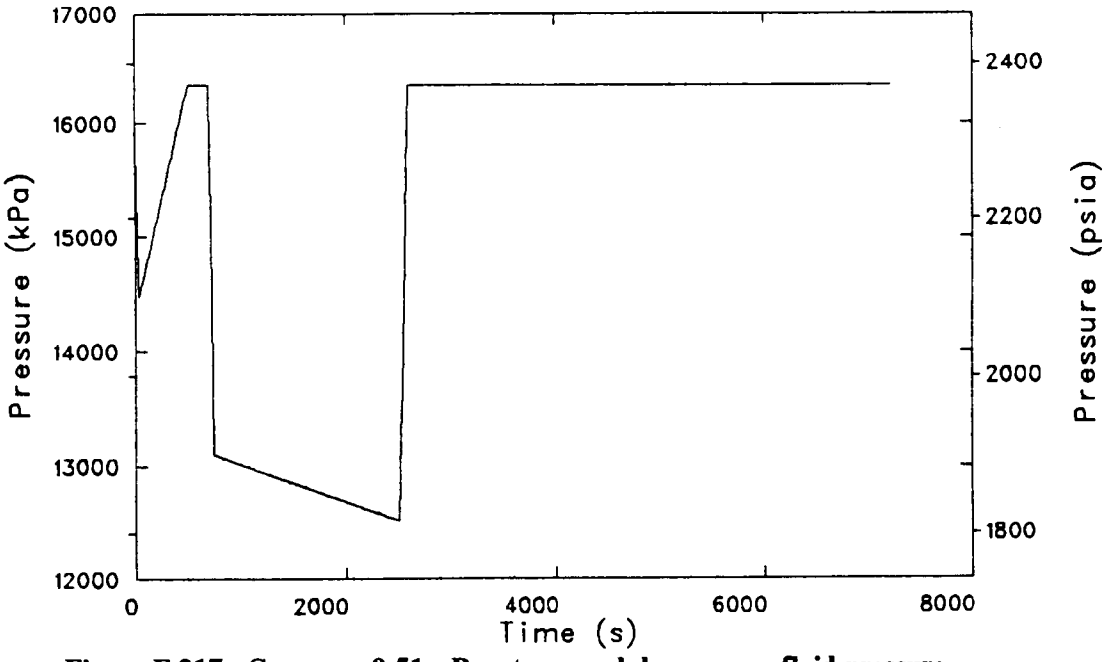

Figure F.217. Sequence 9.51: Reactor vessel downcomer fluid pressure.

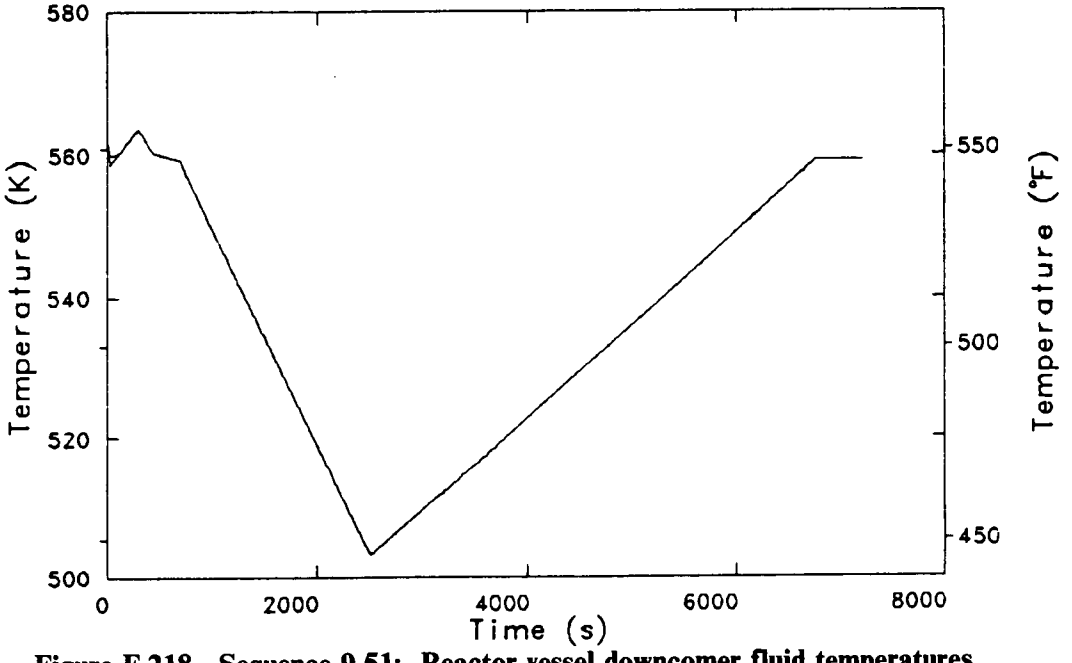

Figure F.218. Sequence 9.51: Reactor vessel downcomer fluid temperatures.

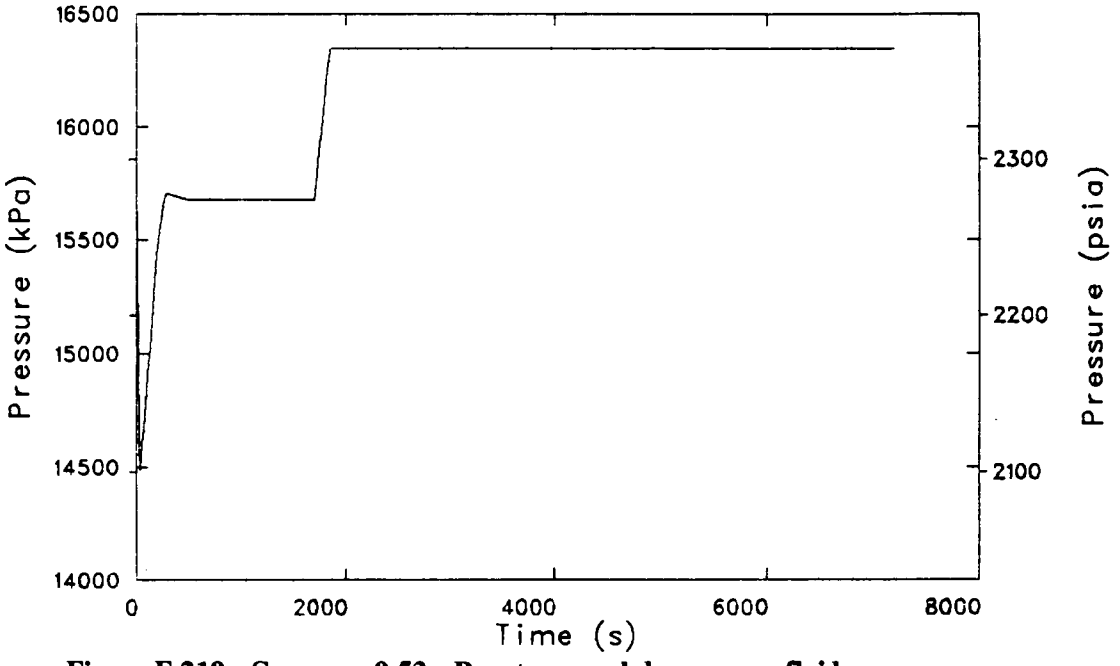

Figure F.219. Sequence 9.53: Reactor vessel downcomer fluid pressure.

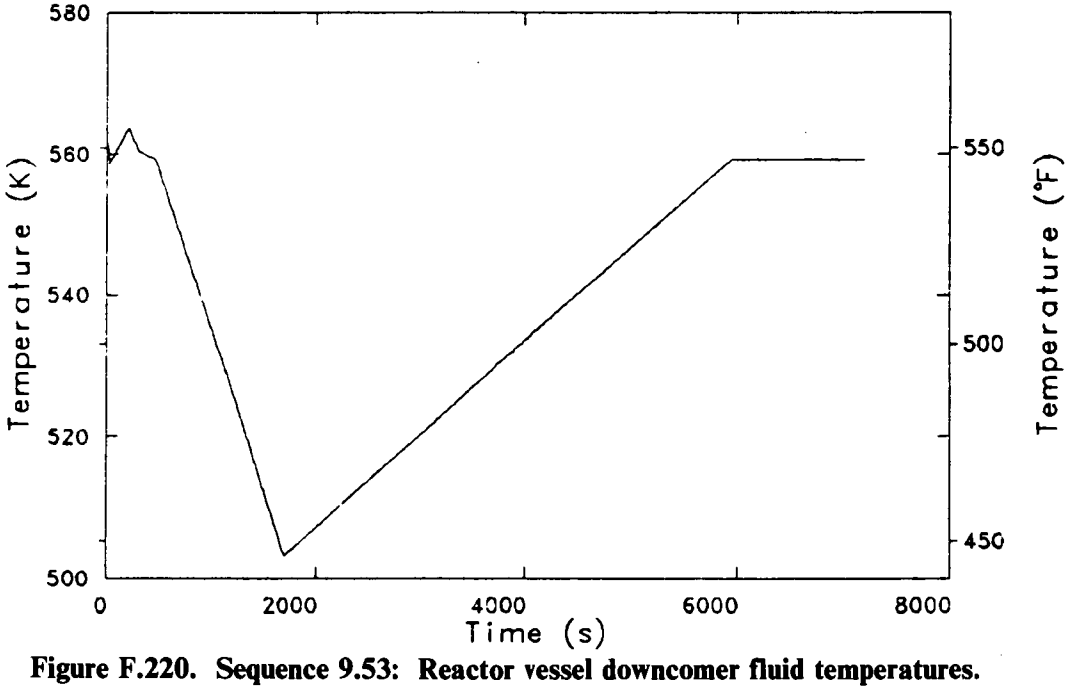

Figure F.220. Sequence 9.53: Reactor vessel downcomer fluid temperatures.

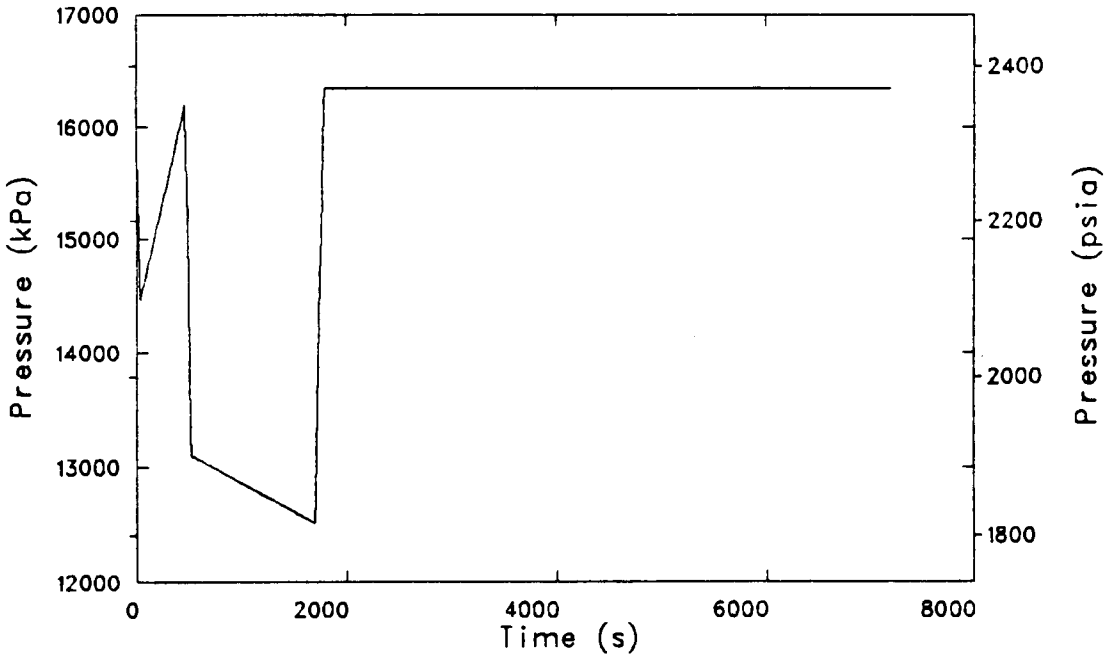

Figure F.221. Sequence 9.55: Reactor vessel downcomer fluid pressure.

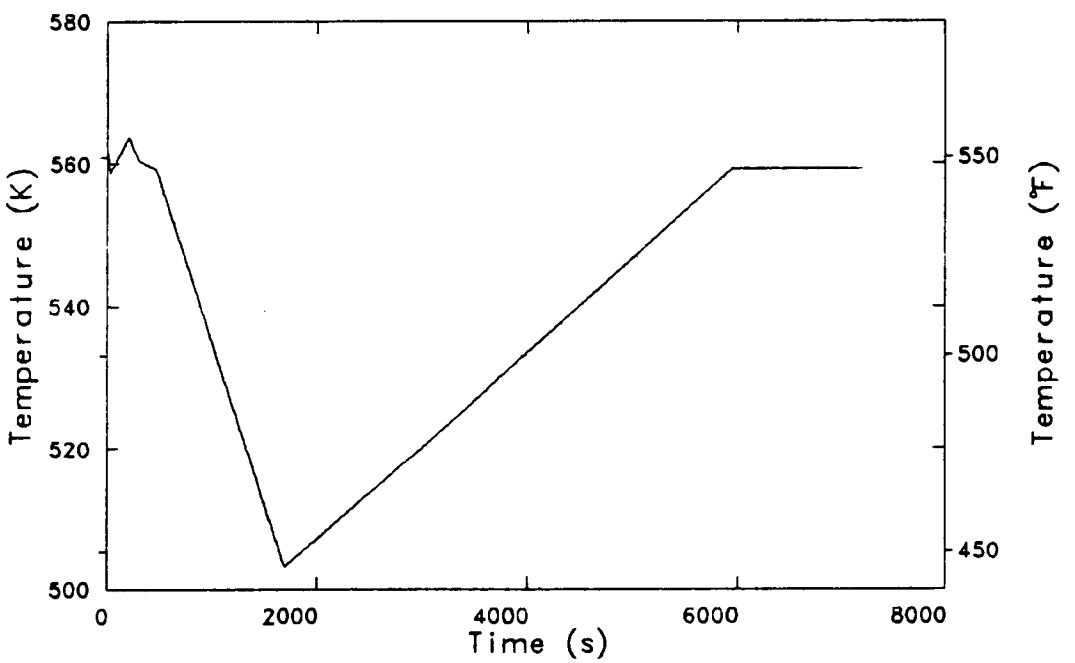

Figure F.222. Sequence 9.55: Reactor vessel downcomer fluid temperatures.

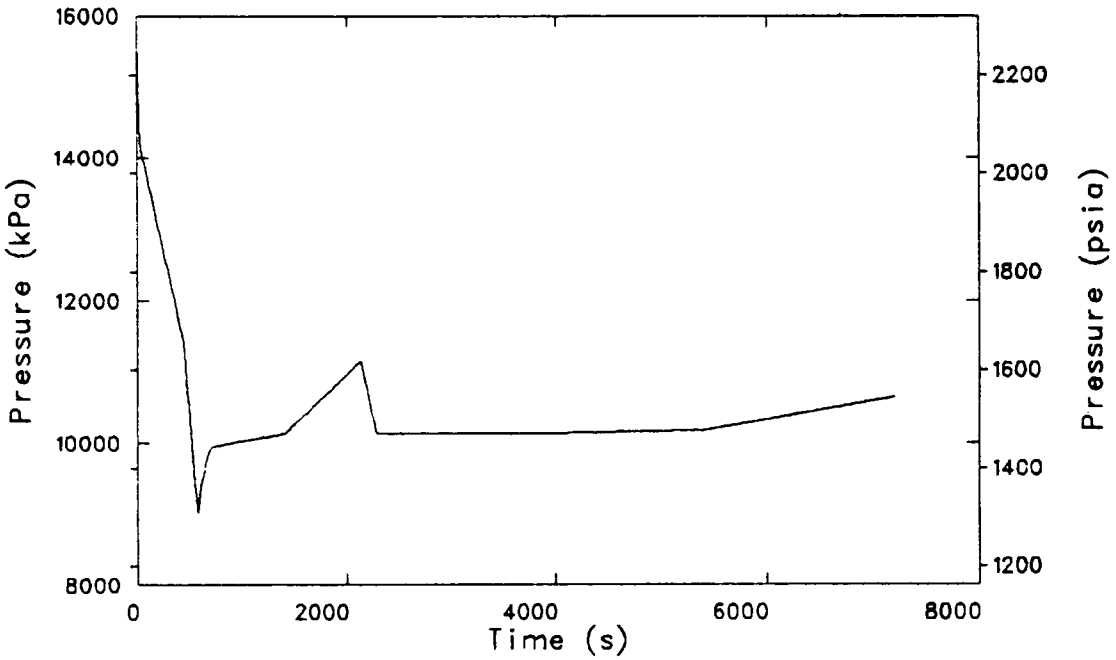

Figure F.223. Sequence 9.57: Reactor vessel downcomer fluid pressure.

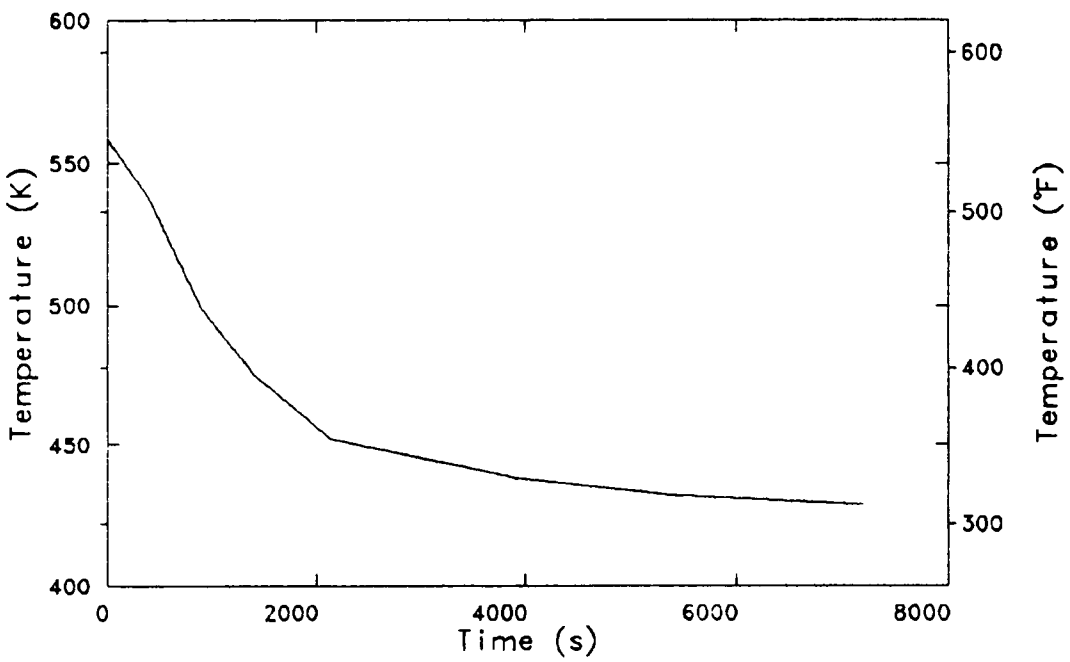

Figure F.224. Sequence 9.57: Reactor vessel downcomer fluid temperatures.

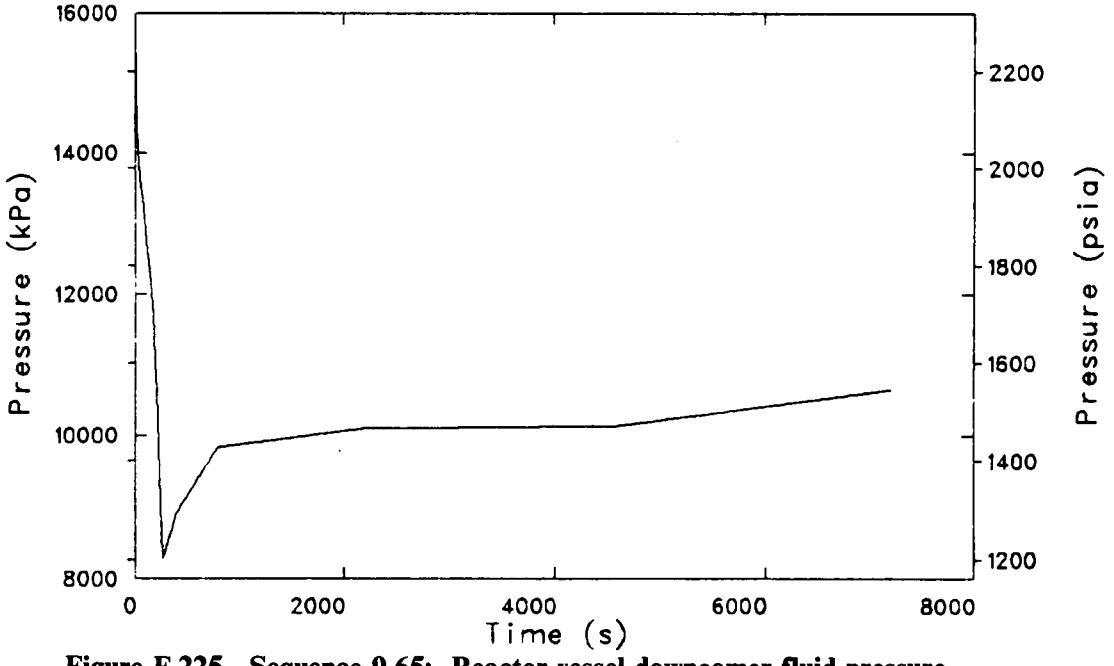

Figure F.225. Sequence 9.65: Reactor vessel downcomer fluid pressure.

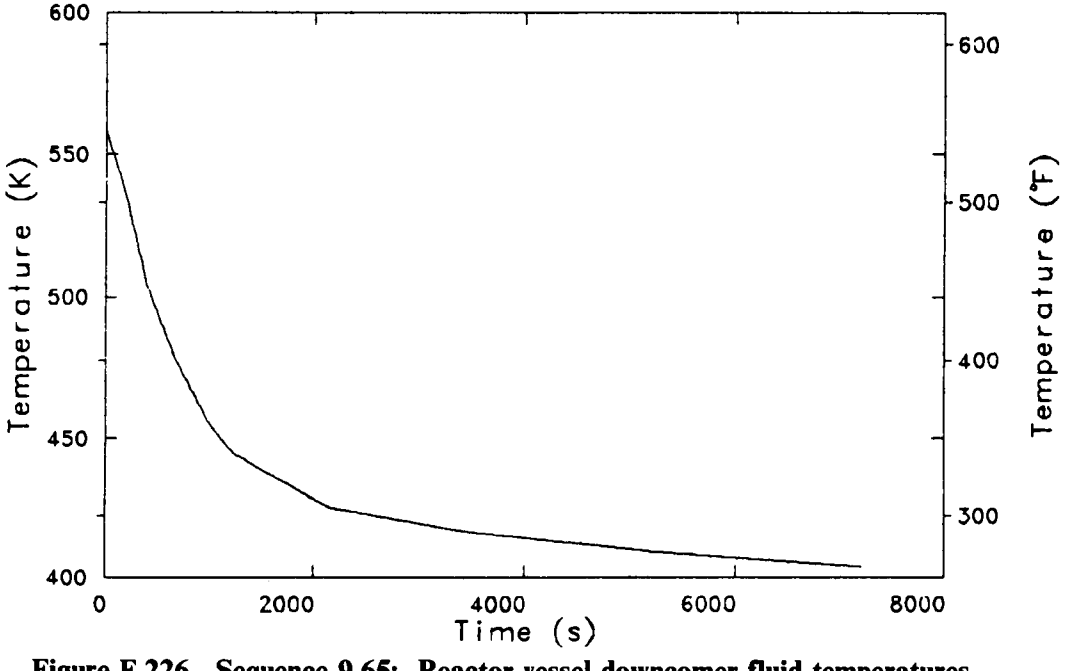

Figure F.226. Sequence 9.65: Reactor vessel downcomer fluid temperatures.

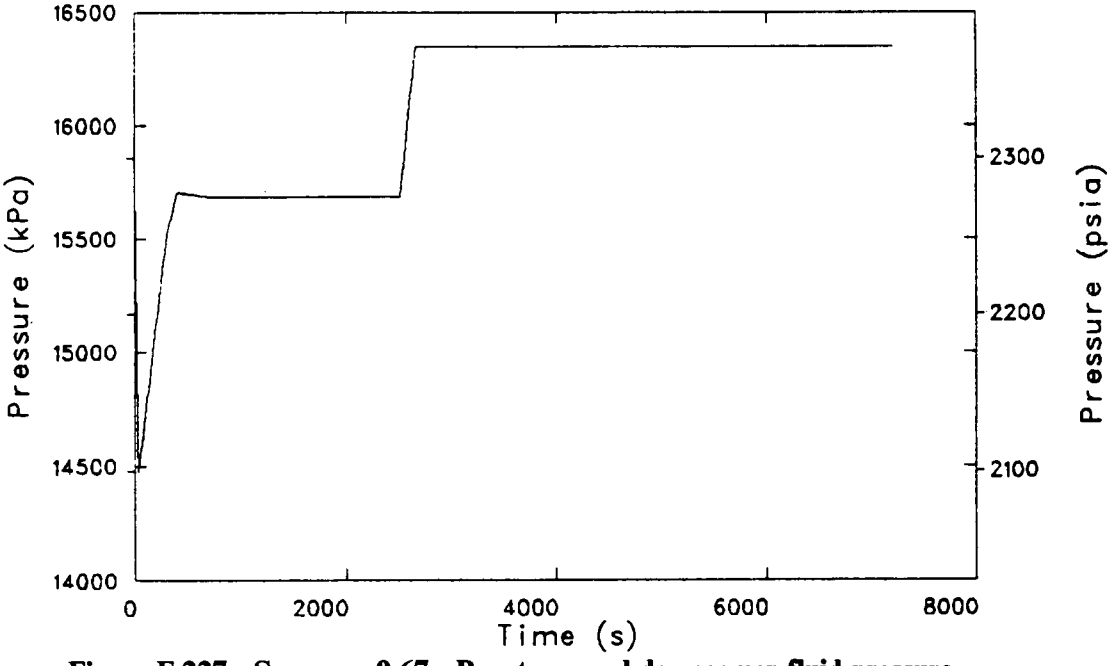

Figure F.227. Sequence 9.67: Reactor vessel downcomer fluid pressure.

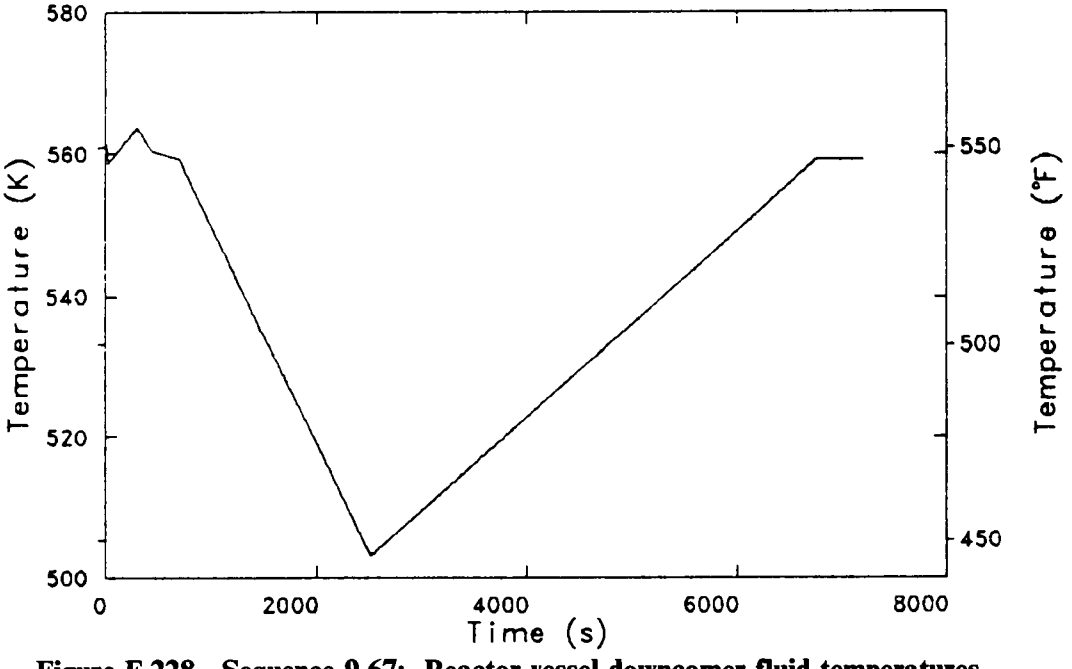

Figure F.228. Sequence 9.67: Reactor vessel downcomer fluid temperatures.

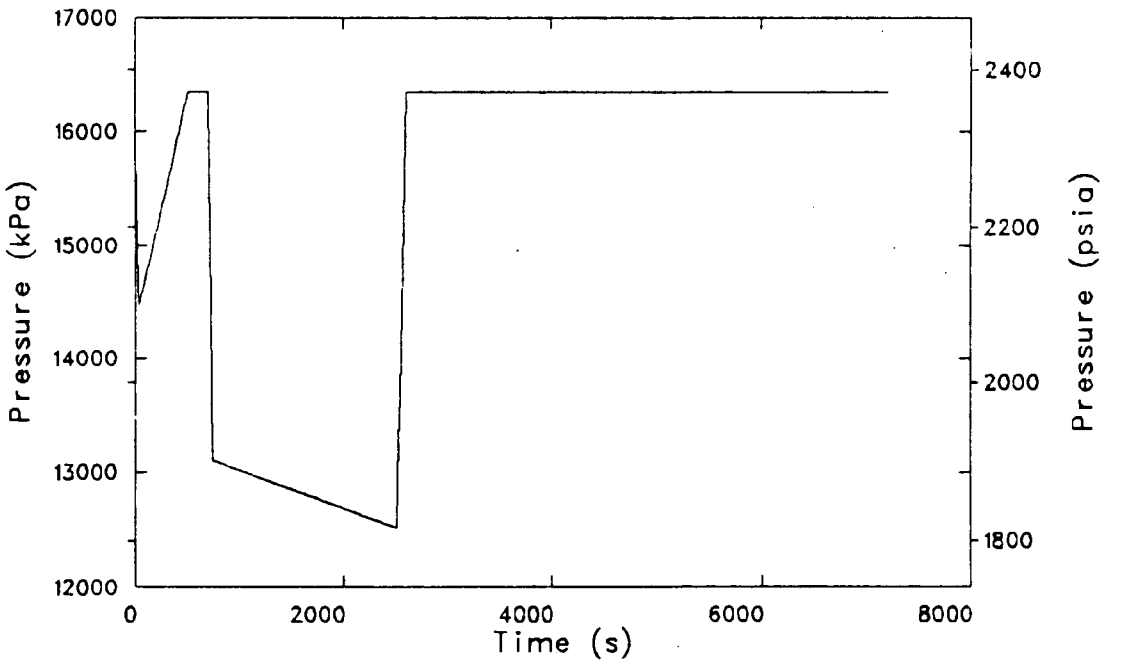

Figure F.229. Sequence 9.69: Reactor vessel downcomer fluid pressure.

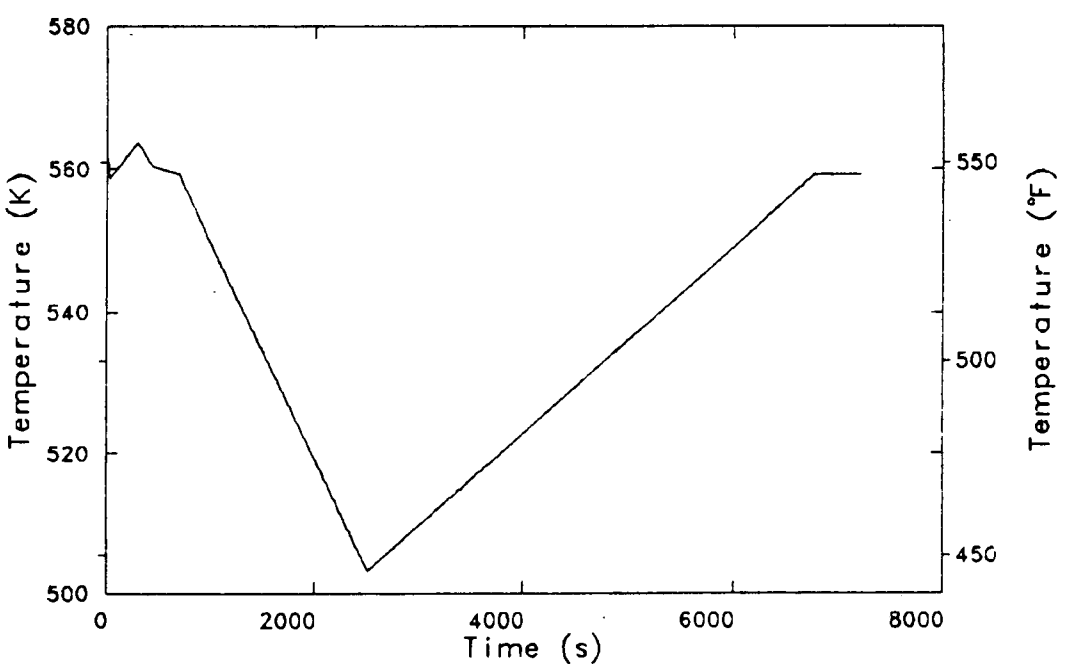

Figure F.230. Sequence 9.69: Reactor vessel downcomer fluid temperatures.

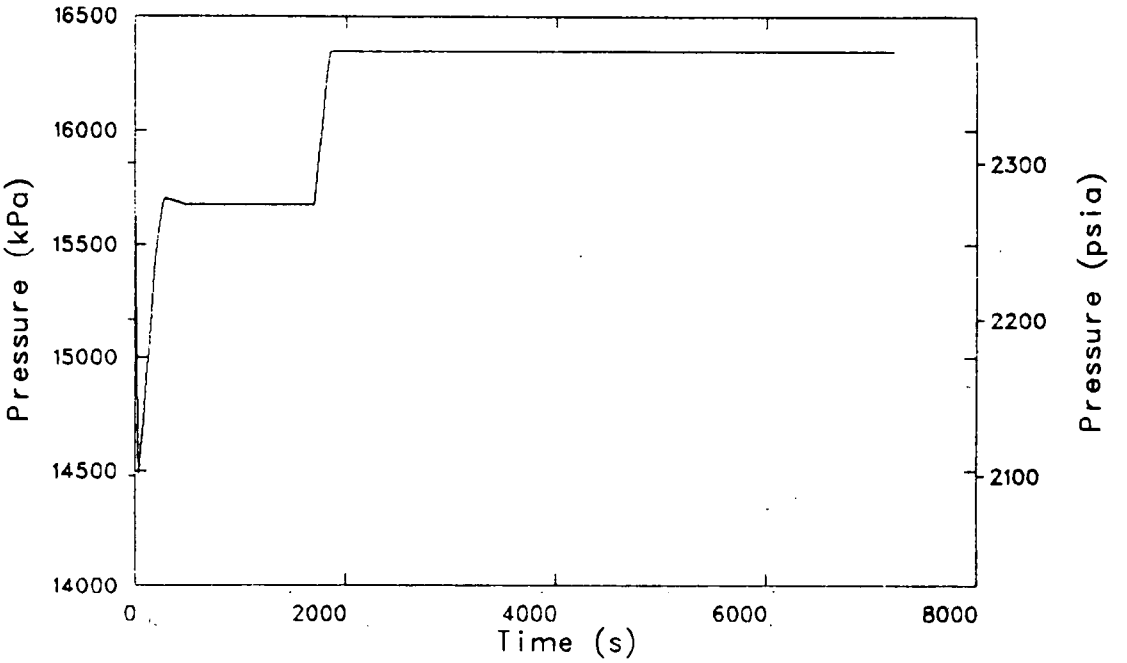

Figure F.231. Sequence 9.71: Reactor vessel downcomer fluid pressure.

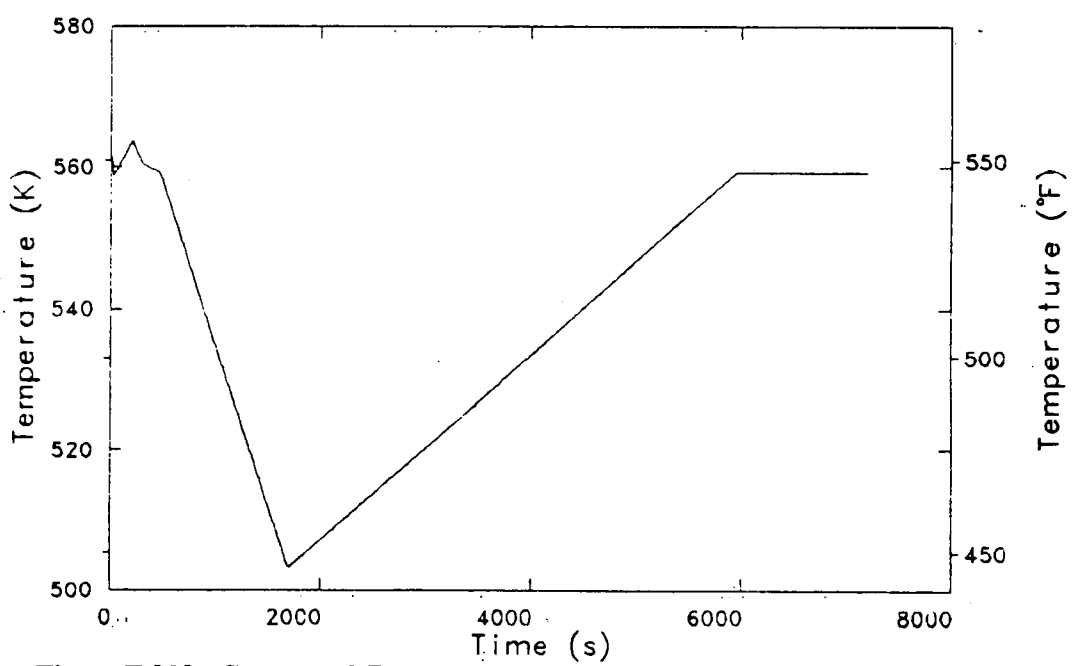

Figure F.232. Sequence 9.71: Reactor vessel downcomer fluid temperatures.

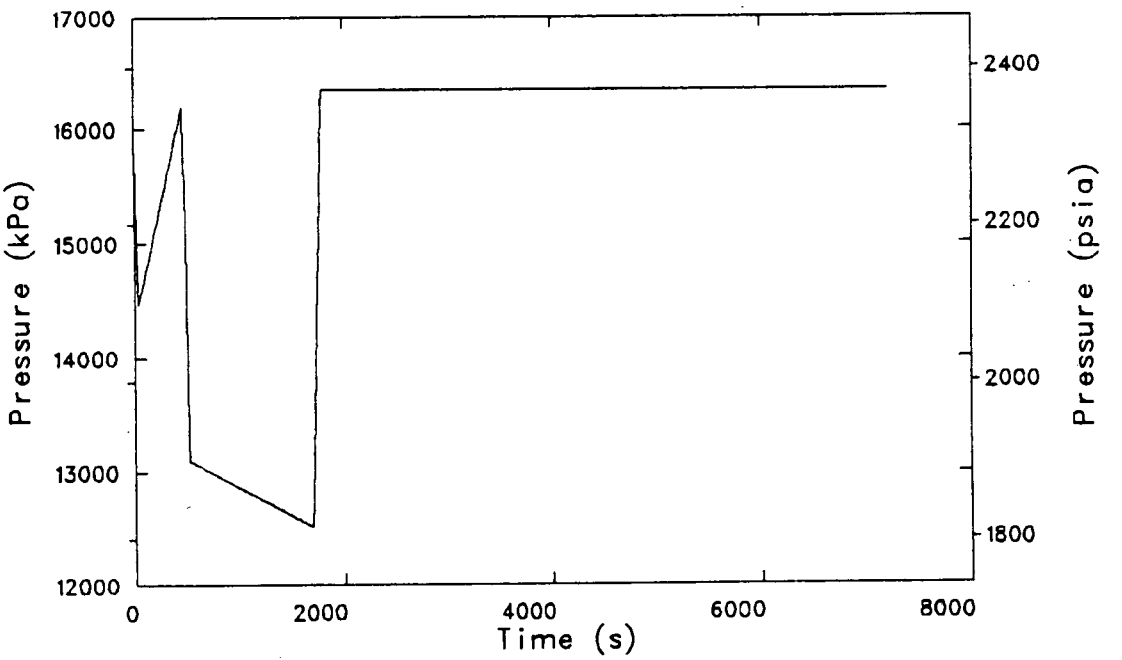

Figure F.233. Sequence 9.73: Reactor vessel downcomer fluid pressure.

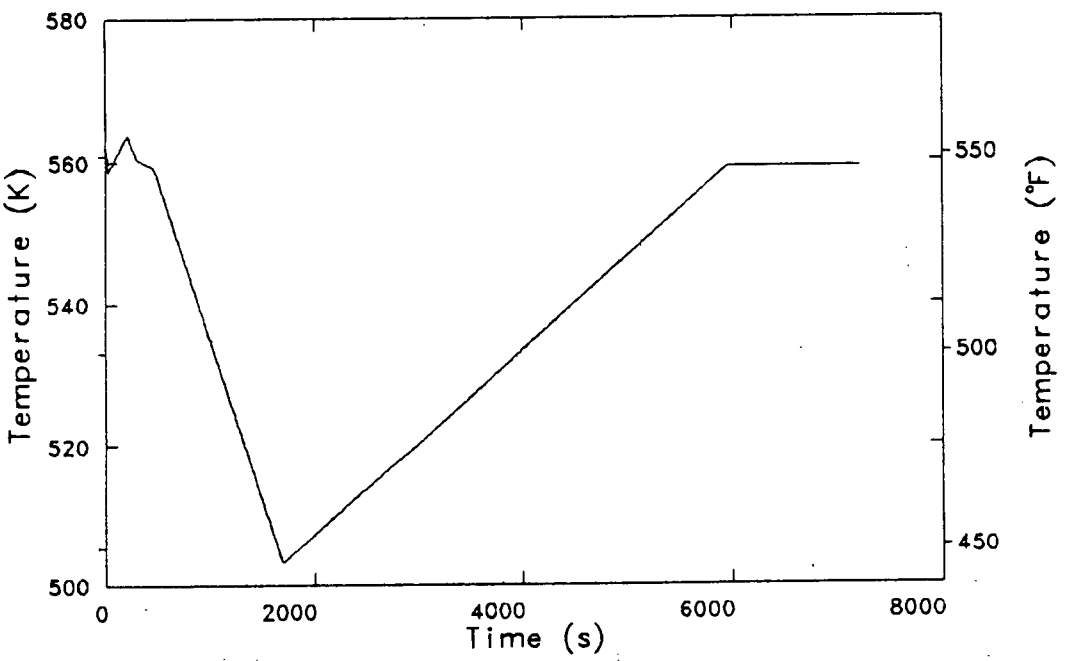

Figure F.234. Sequence 9.73: Reactor vessel downcomer fluid temperatures.

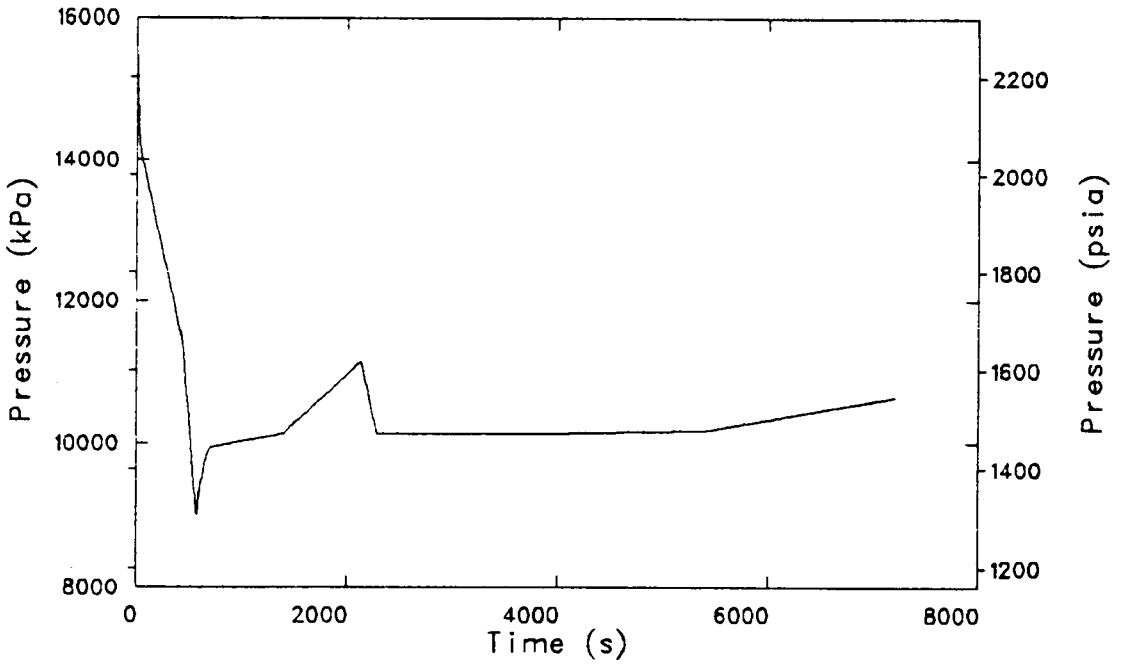

Figure F.235. Sequence 9.75: Reactor vessel downcomer fluid pressure.

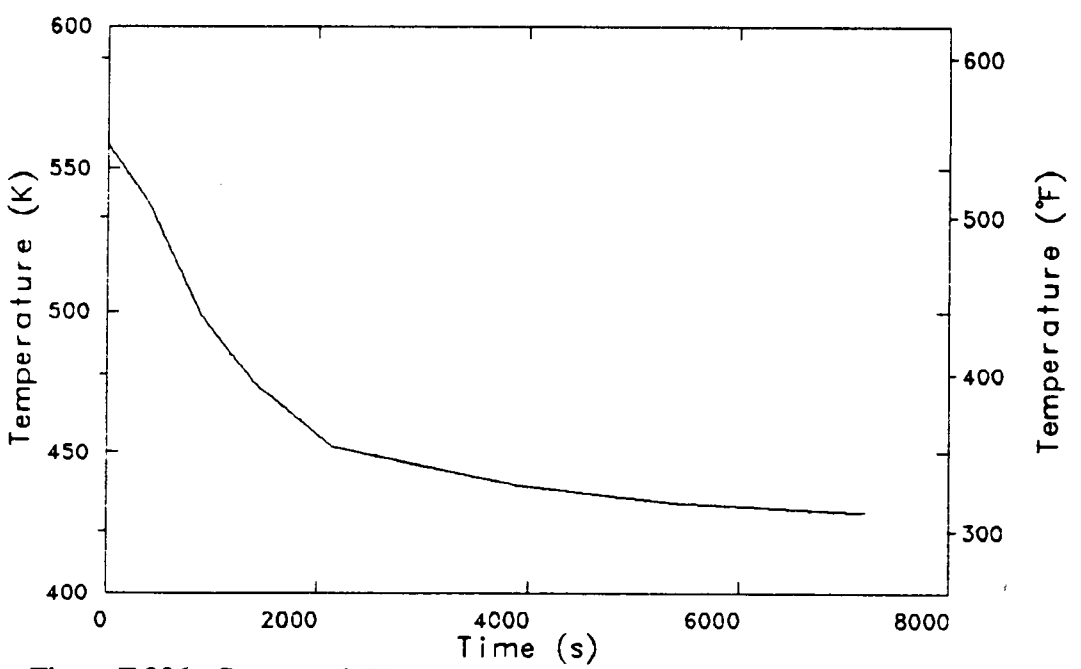

Figure F.236. Sequence 9.75: Reactor vessel downcomer fluid temperatures.

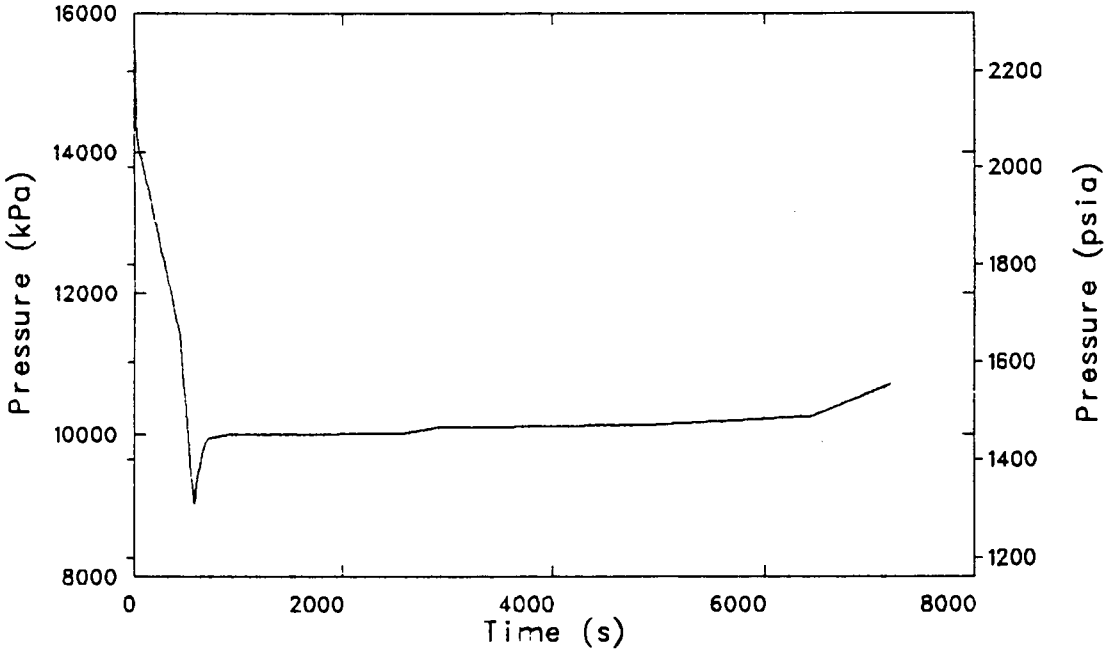

Figure F.237. Sequence 9.76: Reactor vessel downcomer fluid pressure.

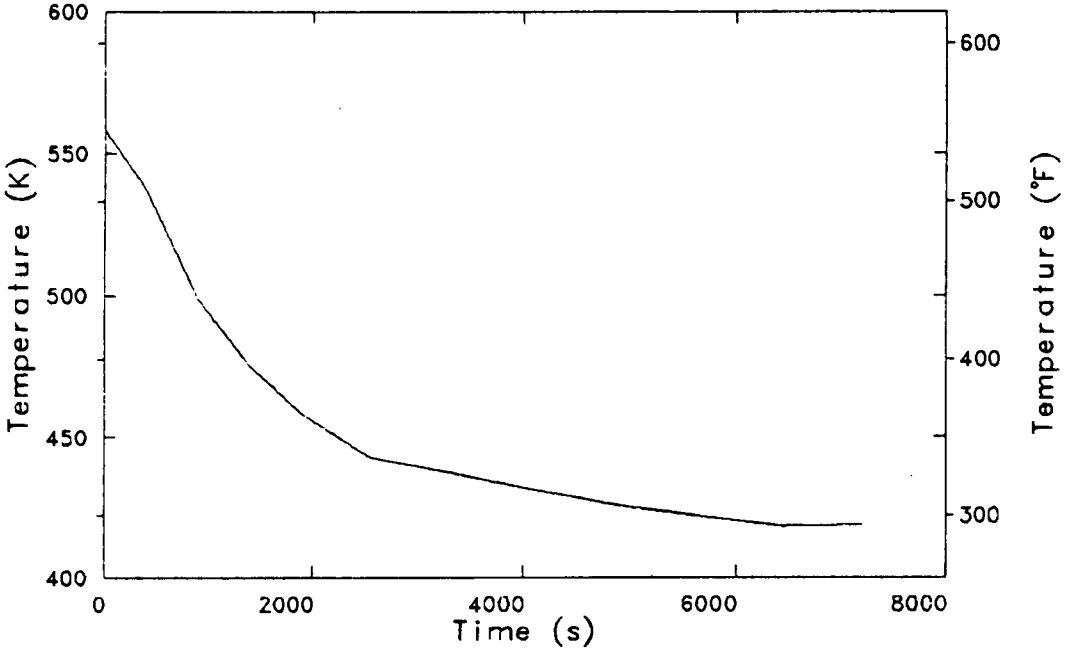

Figure F.238. Sequence 9.76: Reactor vessel downcomer fluid temperatures.

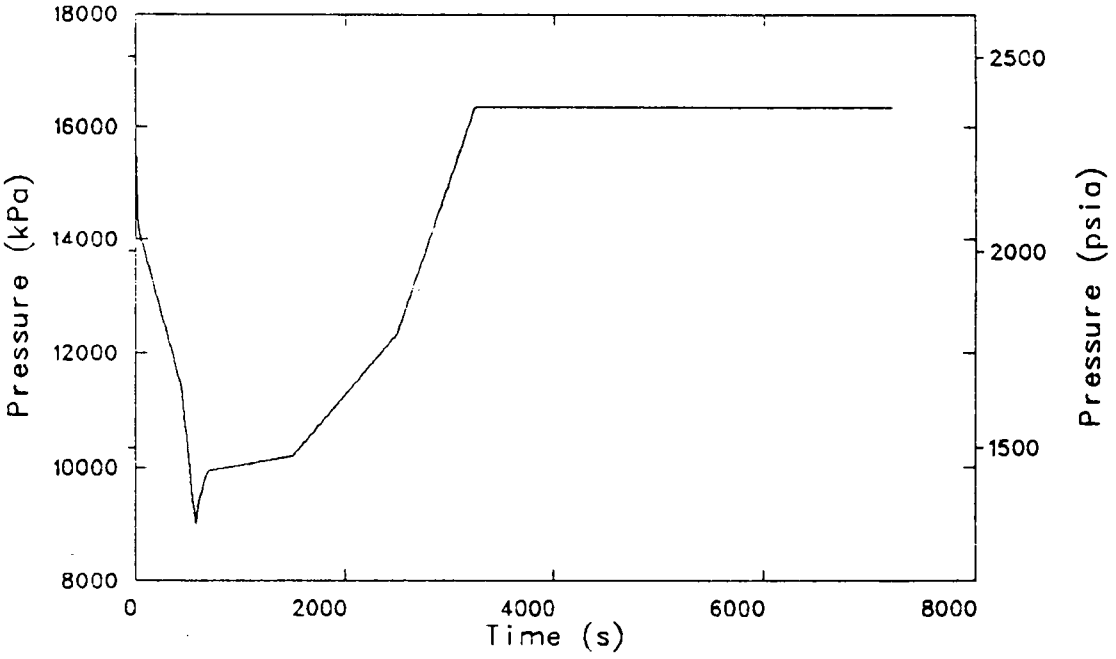

Figure F.239. Sequence 9.77: Reactor vessel downcomer fluid pressure.

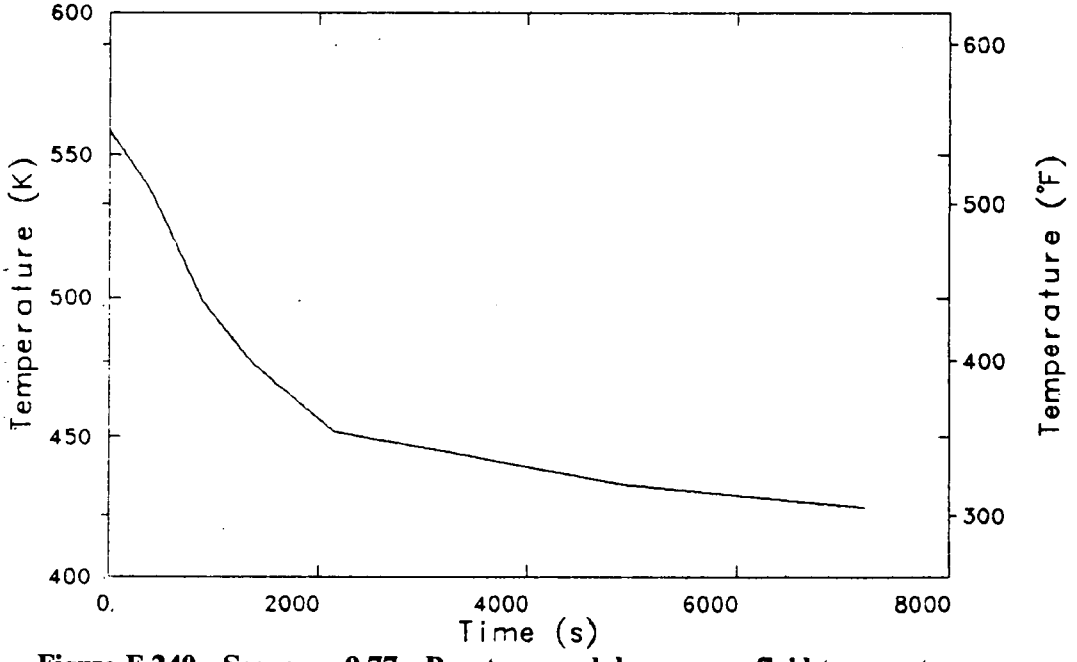

Figure F.240. Sequence 9.77: Reactor vessel downcomer fluid temperatures.

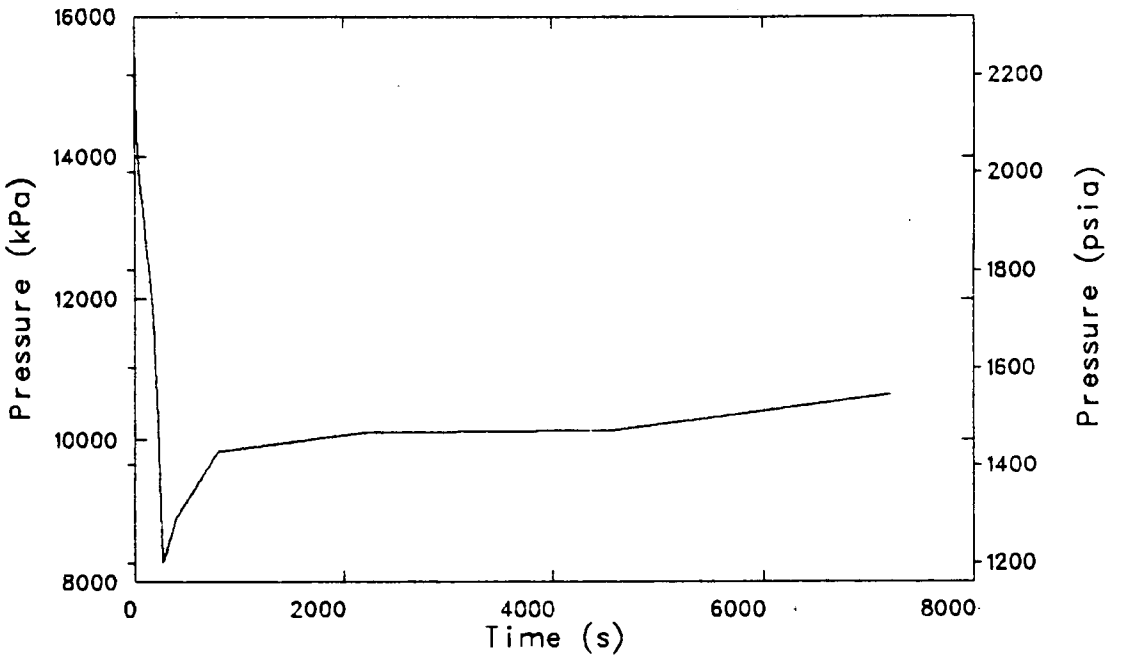

Figure F.241. Sequence 9.80: Reactor vessel downcomer fluid pressure.

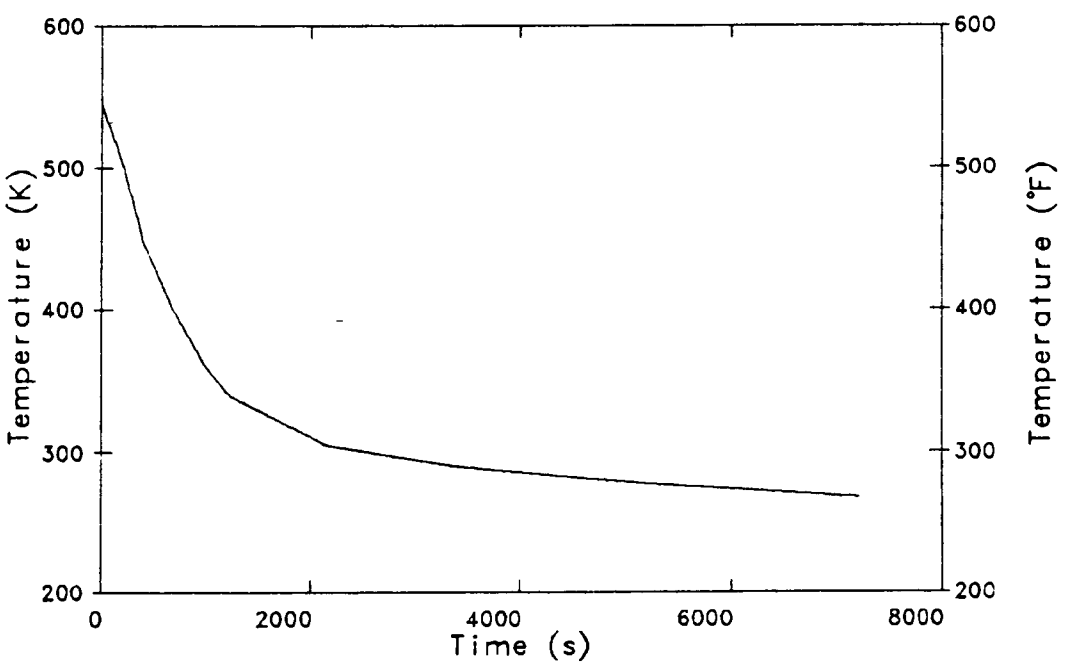

Figure F.242. Sequence 9.80: Reactor vessel downcomer fluid temperatures.

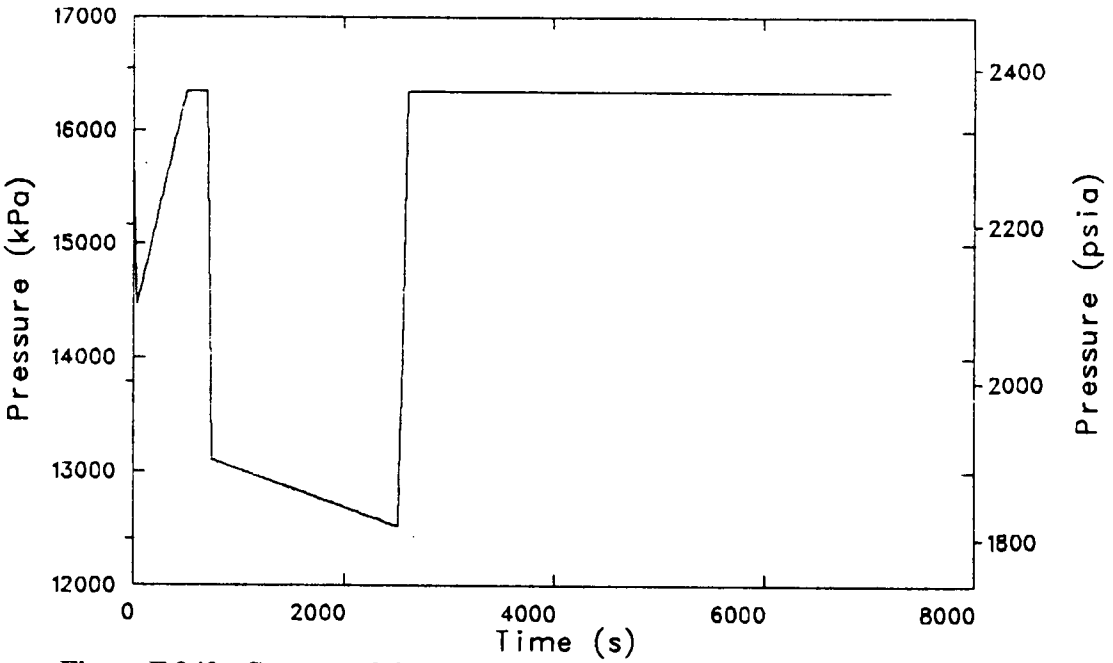

Figure F.243. Sequence 9.84: Reactor vessel downcomer fluid pressure.

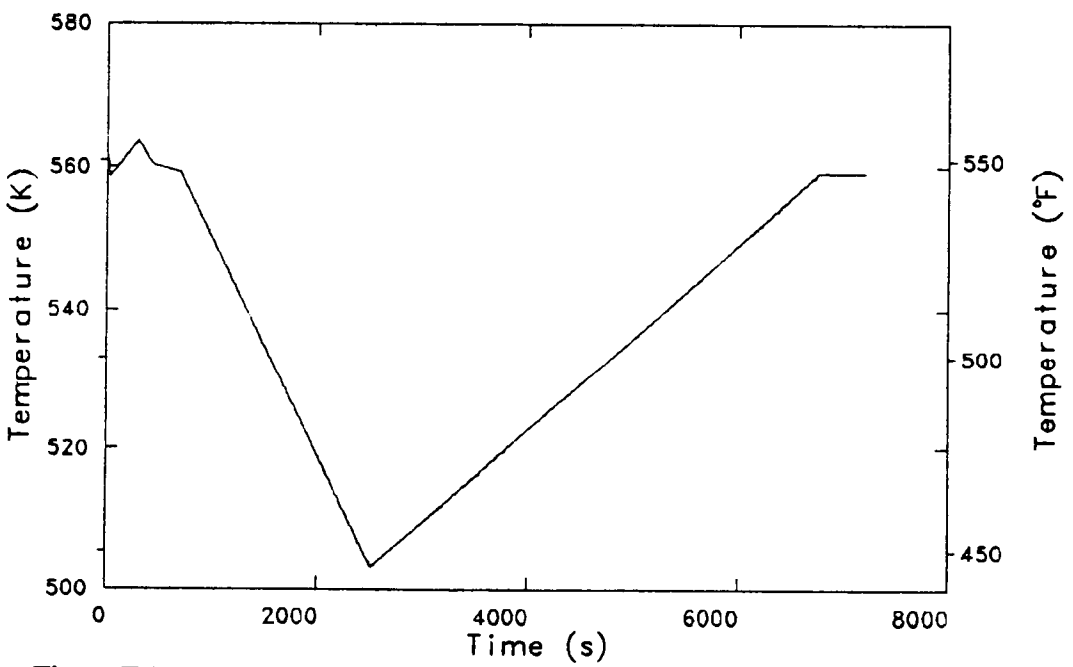

Figure F.244. Sequence 9.84: Reactor vessel downcomer fluid temperatures.

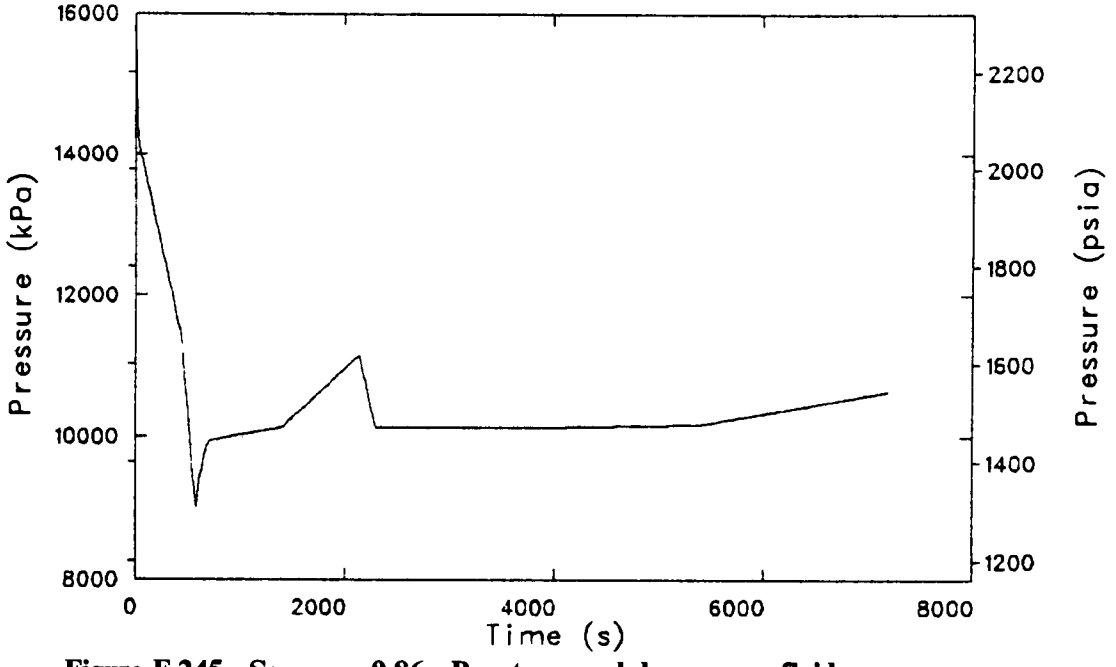

Figure F.245. Sequence 9.86: Reactor vessel downcomer fluid pressure.

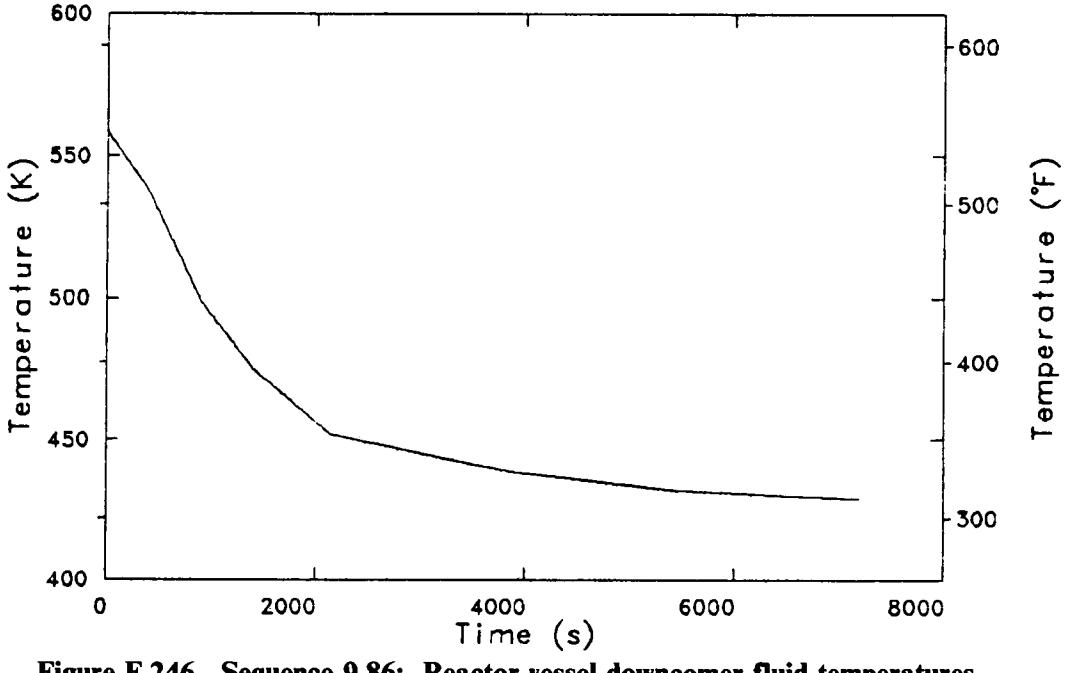

Figure F.246. Sequence 9.86: Reactor vessel downcomer fluid temperatures.

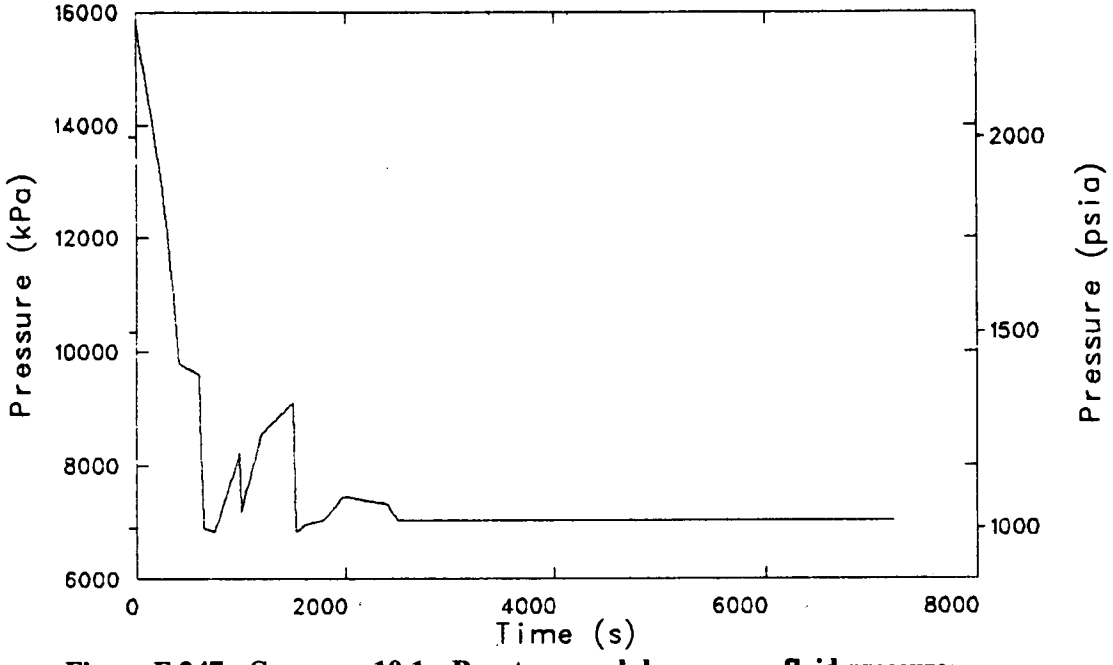

Figure F.247. Sequence 10.1: Reactor vessel downcomer fluid pressure.

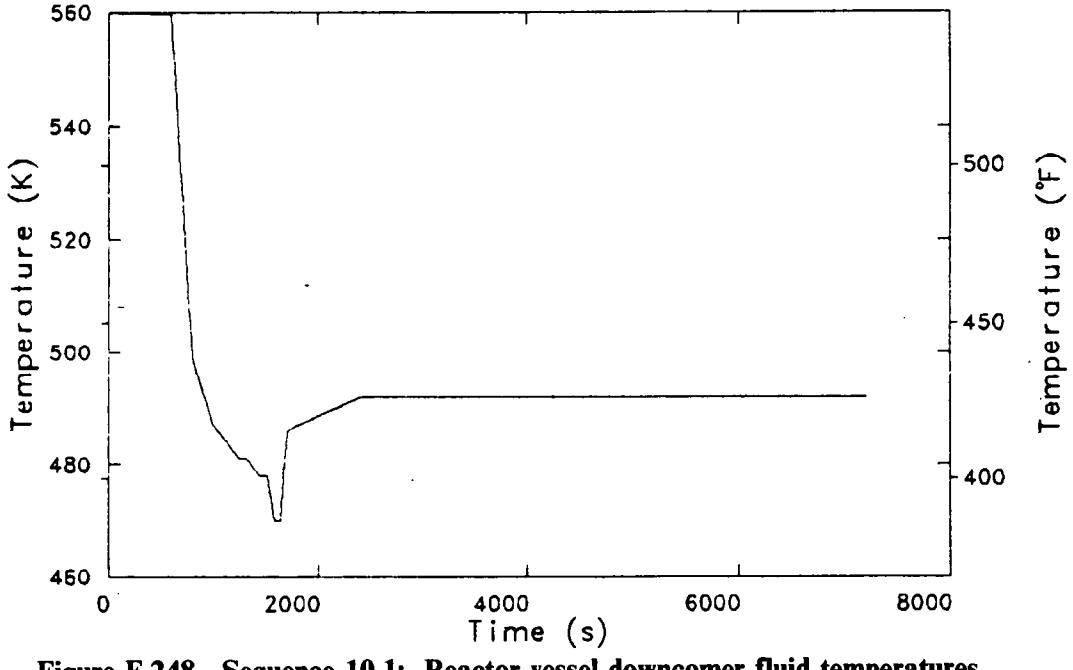

Figure F.248. Sequence 10.1: Reactor vessel downcomer fluid temperatures.

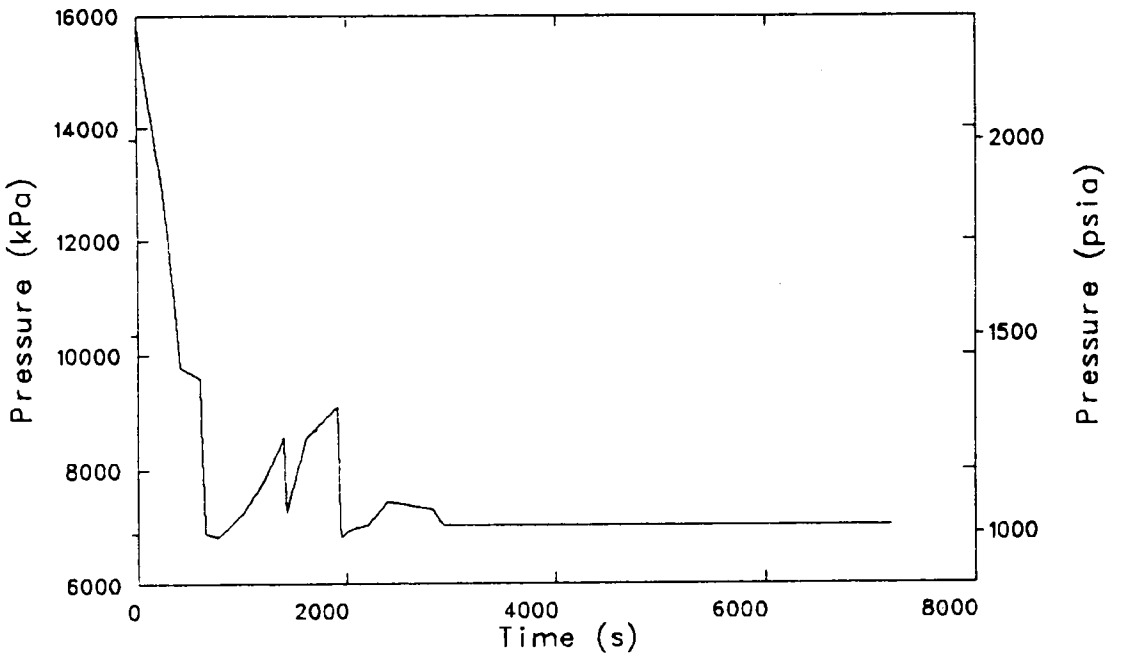

Figure F.249. Sequence 10.2: Reactor vessel downcomer fluid pressure.

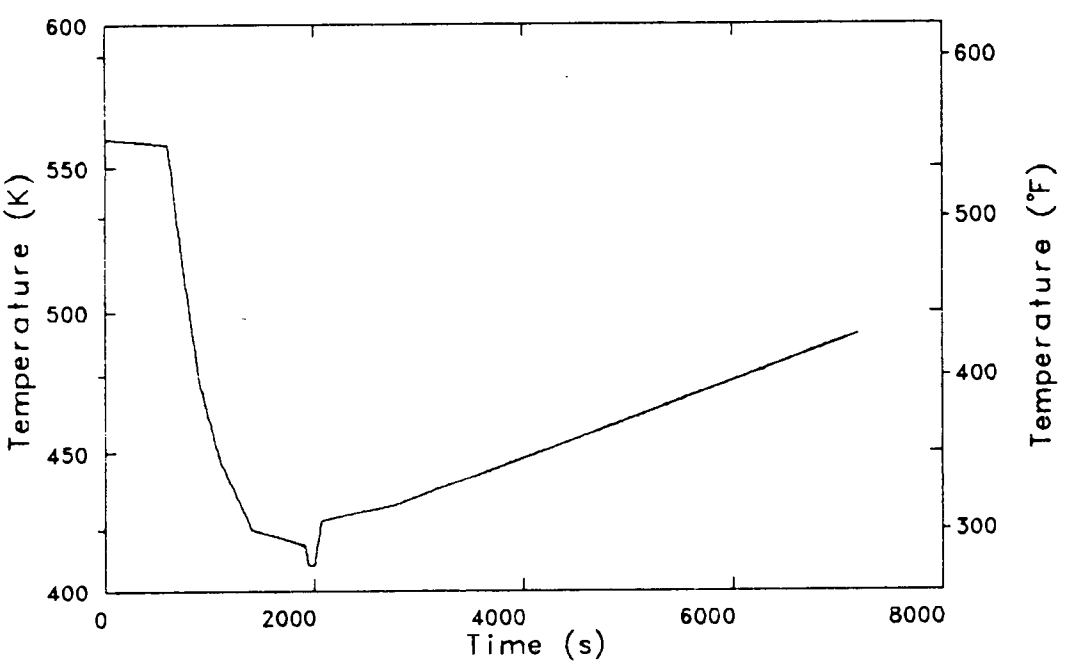

Figure F.250. Sequence 10.2: Reactor vessel downcomer fluid temperatures.

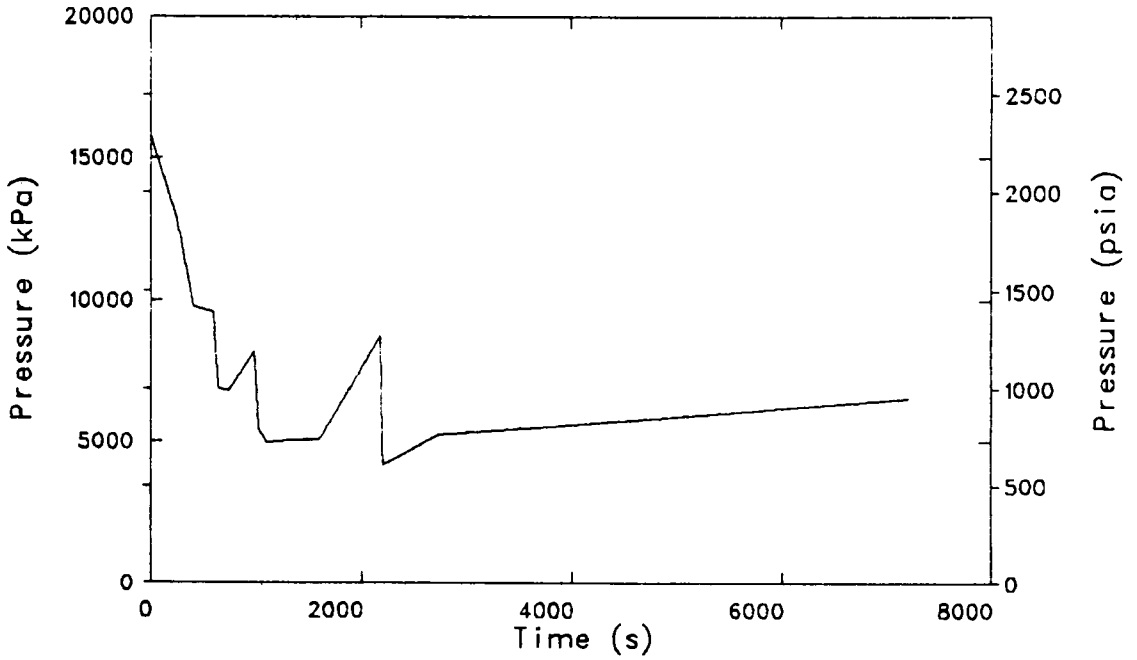

Figure F.251. Sequence 10.3: Reactor vessel downcomer fluid pressure.

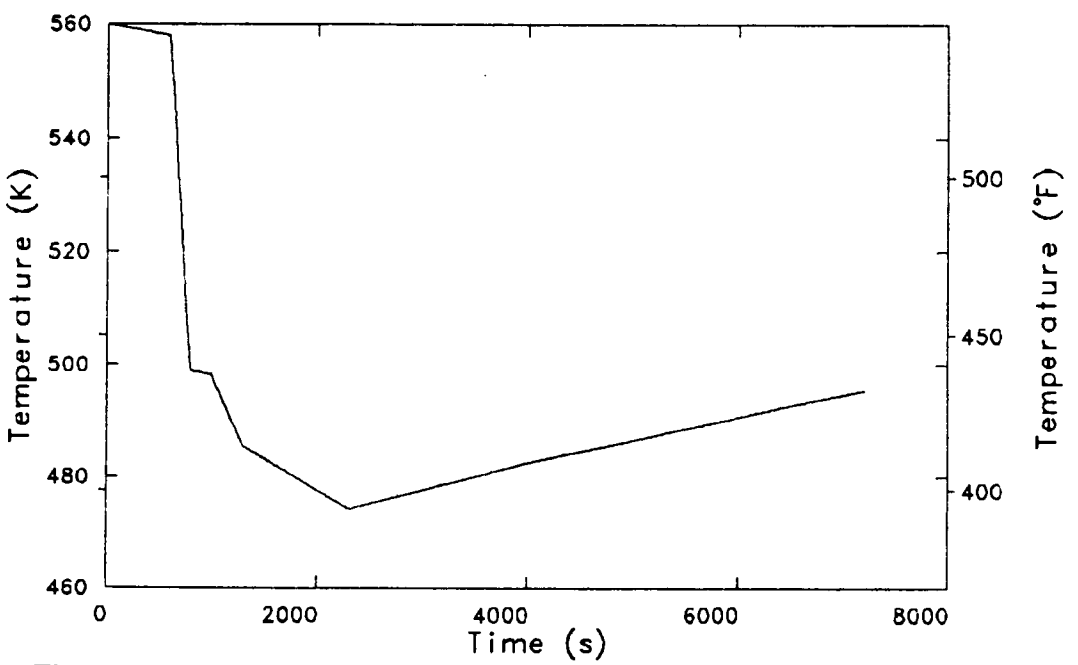

Figure F.252. Sequence 10.3: Reactor vessel downcomer fluid temperatures.

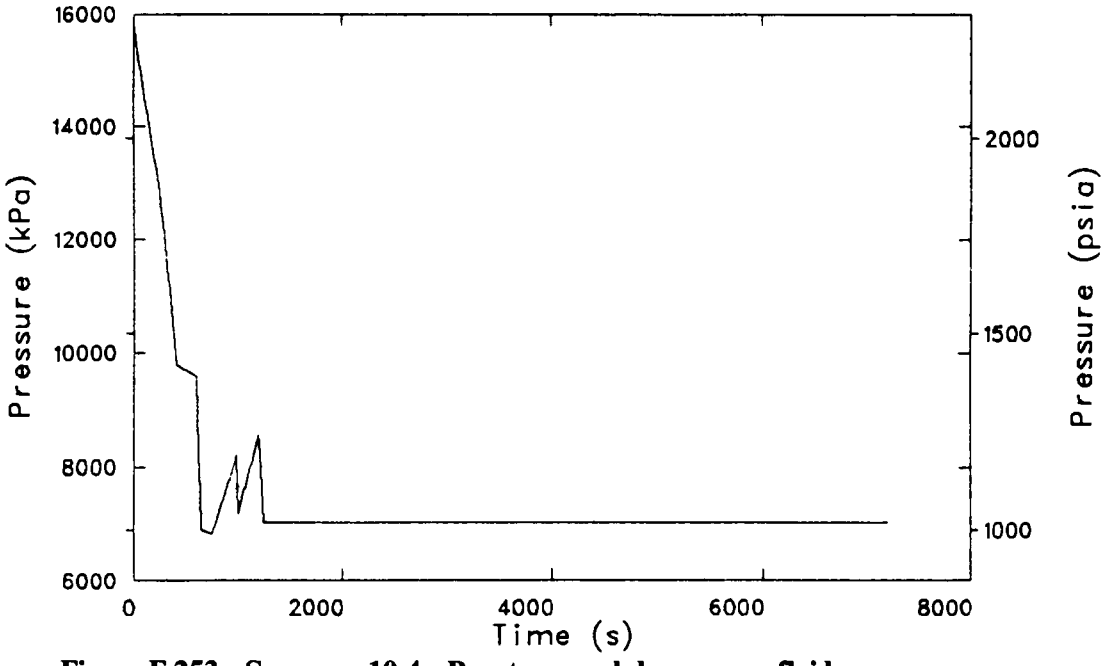

Figure F.253. Sequence 10.4: Reactor vessel downcomer fluid pressure.

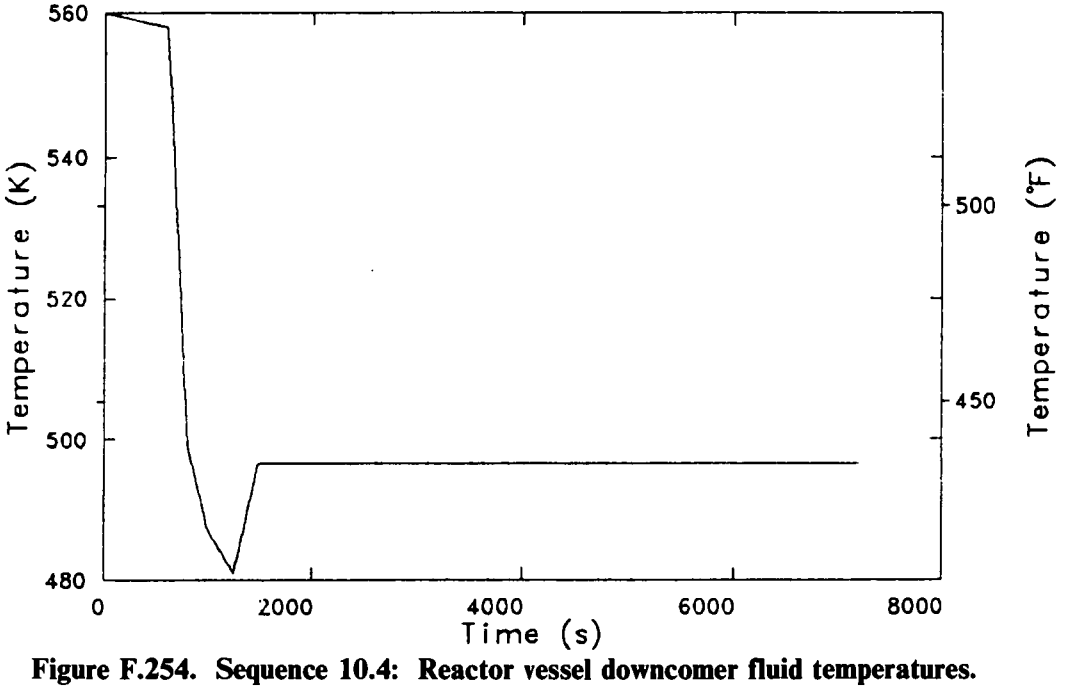

Figure F.254. Sequence 10.4: Reactor vessel downcomer fluid temperatures.

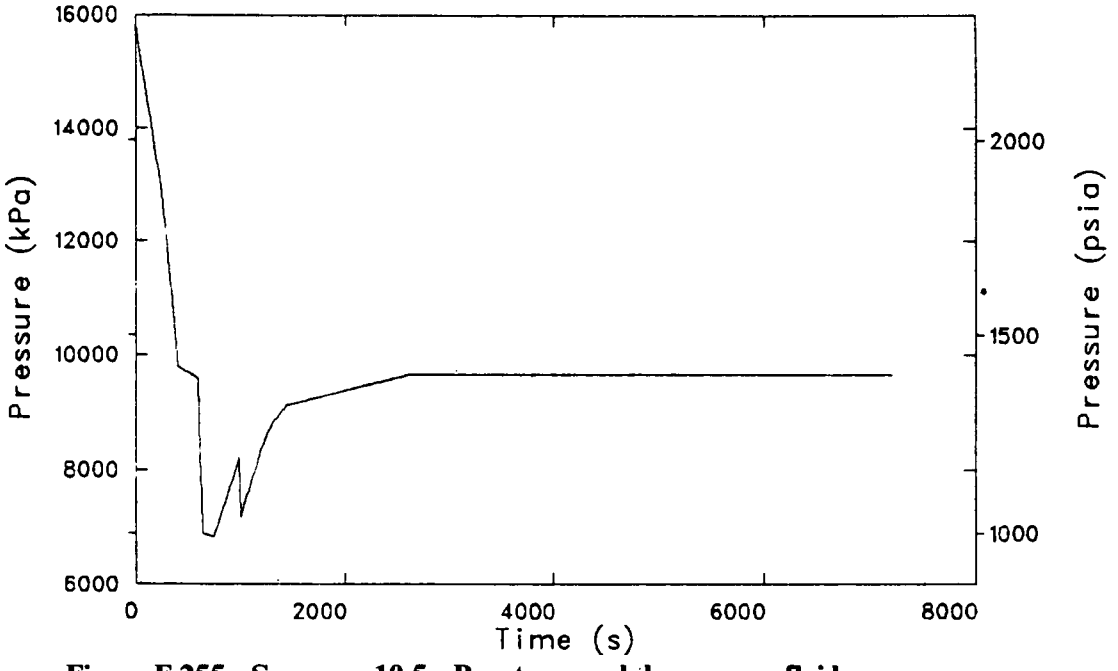

Figure F.255. Sequence 10.5: Reactor vessel downcomer fluid pressure.

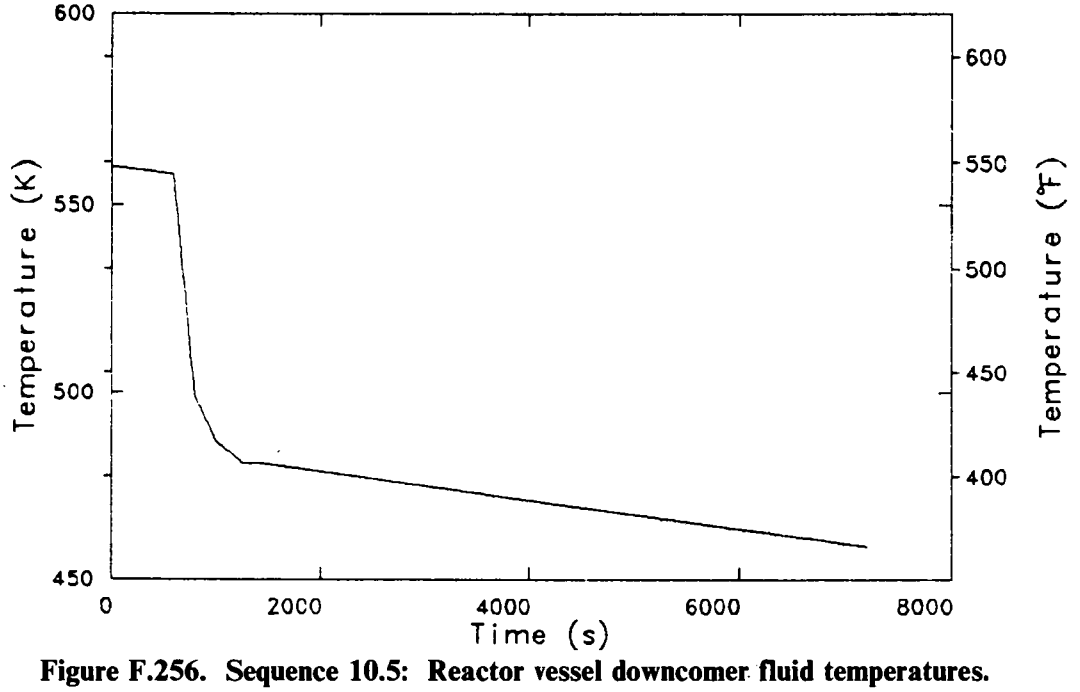

Figure F.256. Sequence 10.5: Reactor vessel downcomer fluid temperatures.

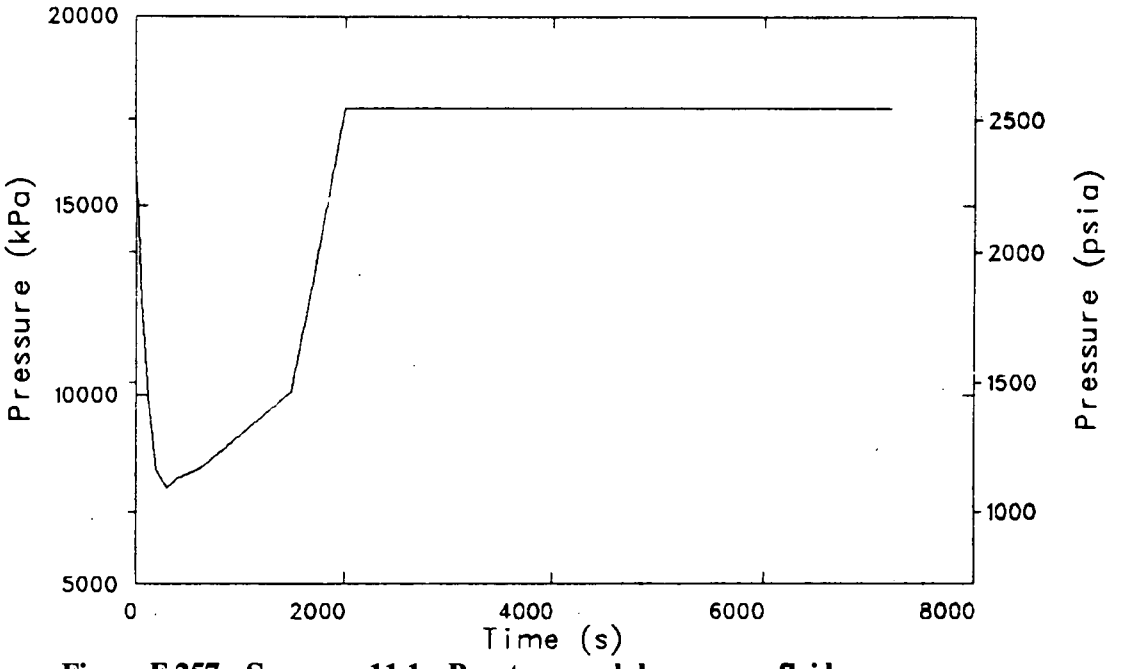

Figure F.257. Sequence 11.1: Reactor vessel downcomer fluid pressure.

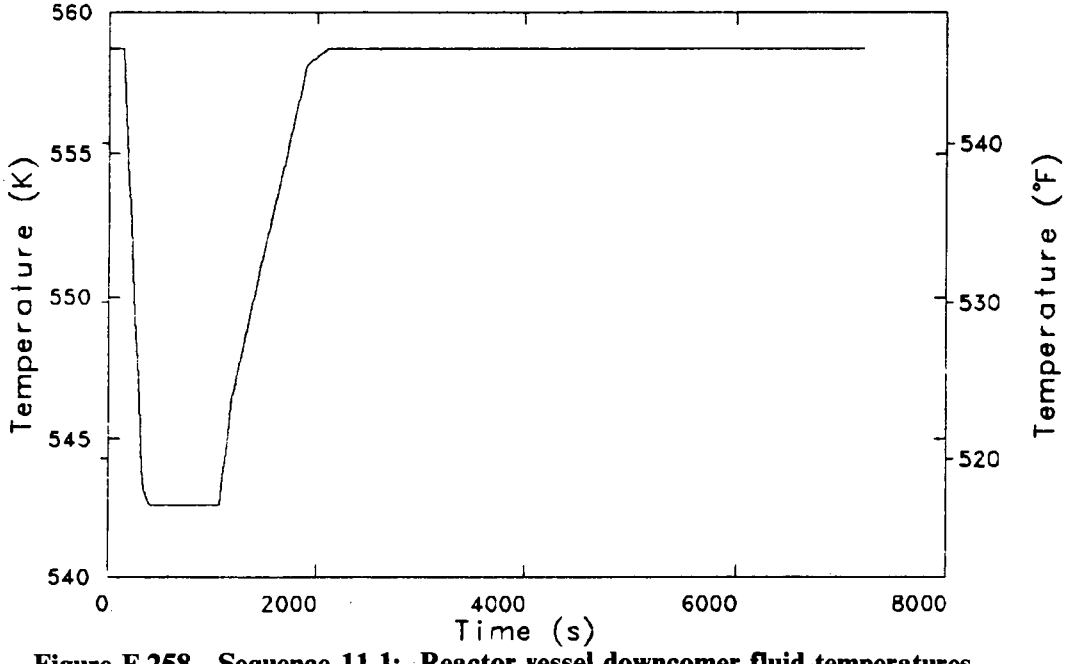

Figure F.258. Sequence 11.1: Reactor vessel downcomer fluid temperatures.

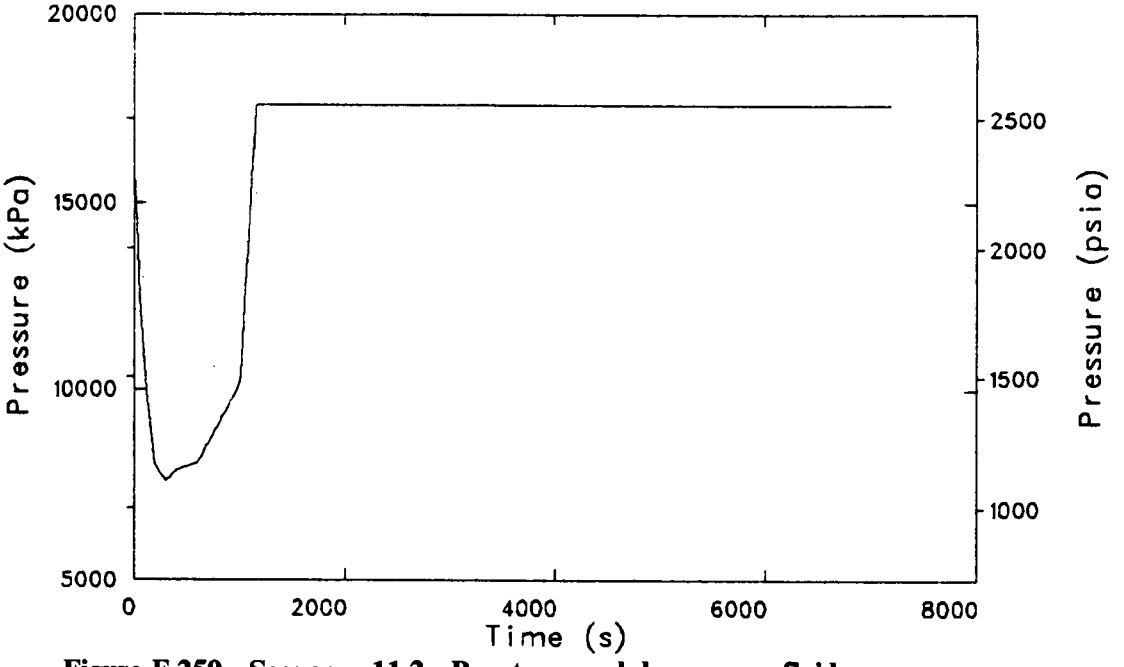

Figure F.259. Sequence 11.2: Reactor vessel downcomer fluid pressure.

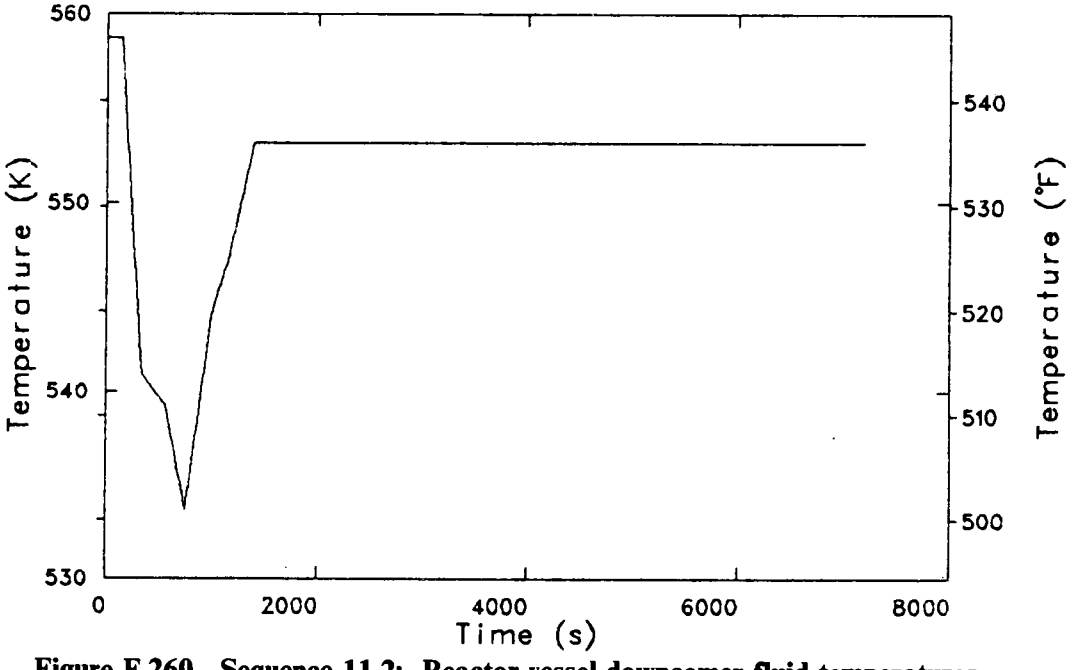

Figure F.260. Sequence 11.2: Reactor vessel downcomer fluid temperatures.

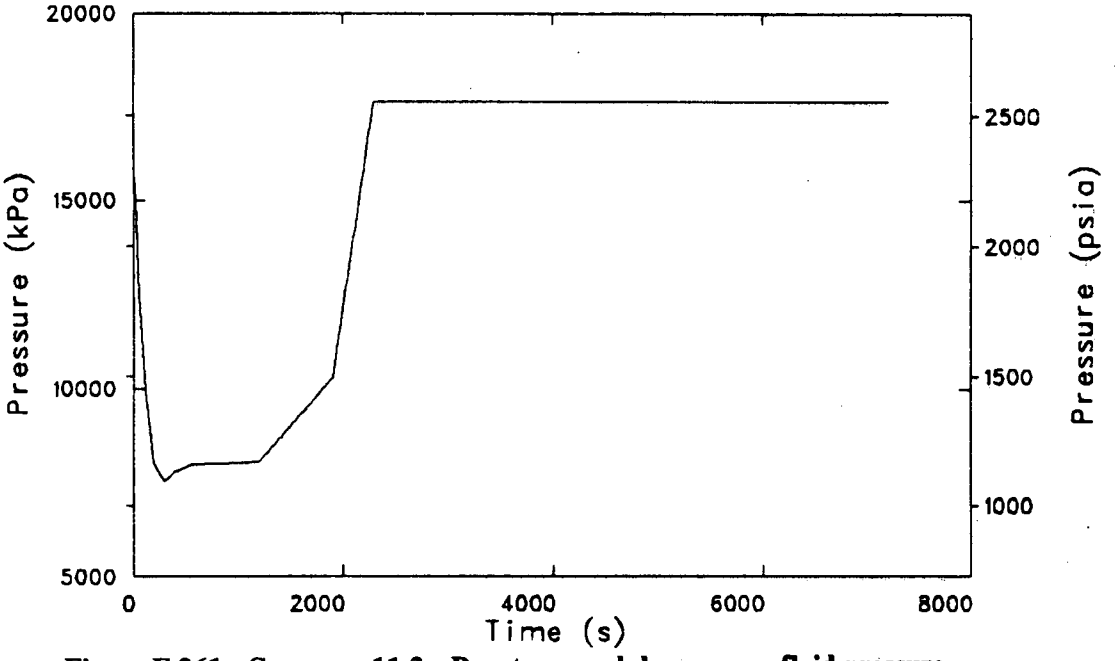

Figure F.261. Sequence 11.3: Reactor vessel downcomer fluid pressure.

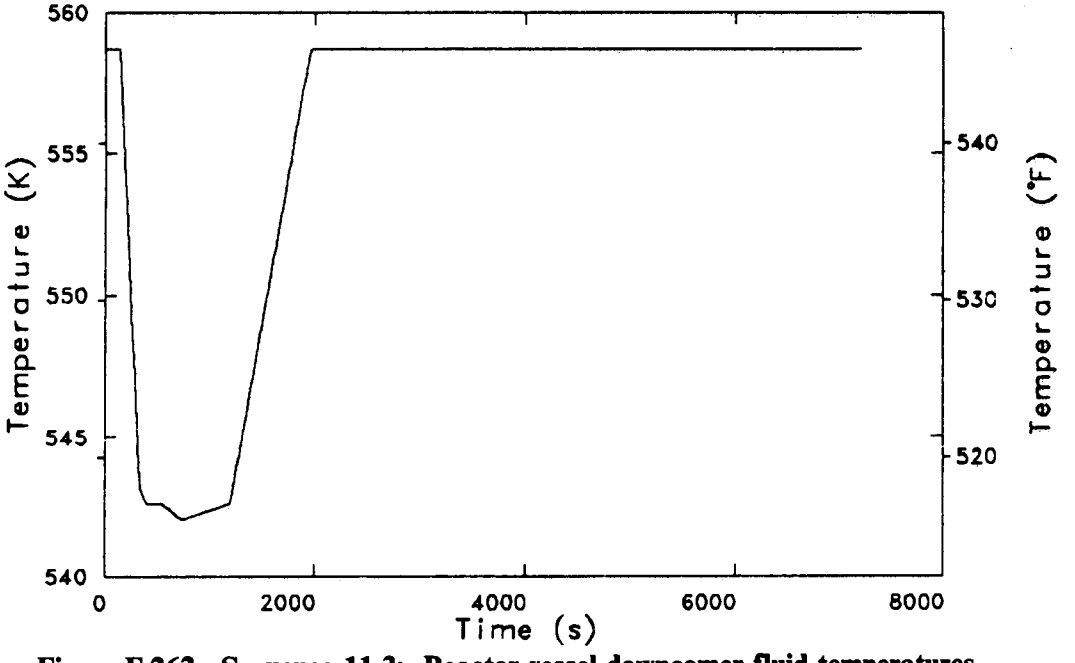

Figure F.262. Sequence 11.3: Reactor vessel downcomer fluid temperatures.

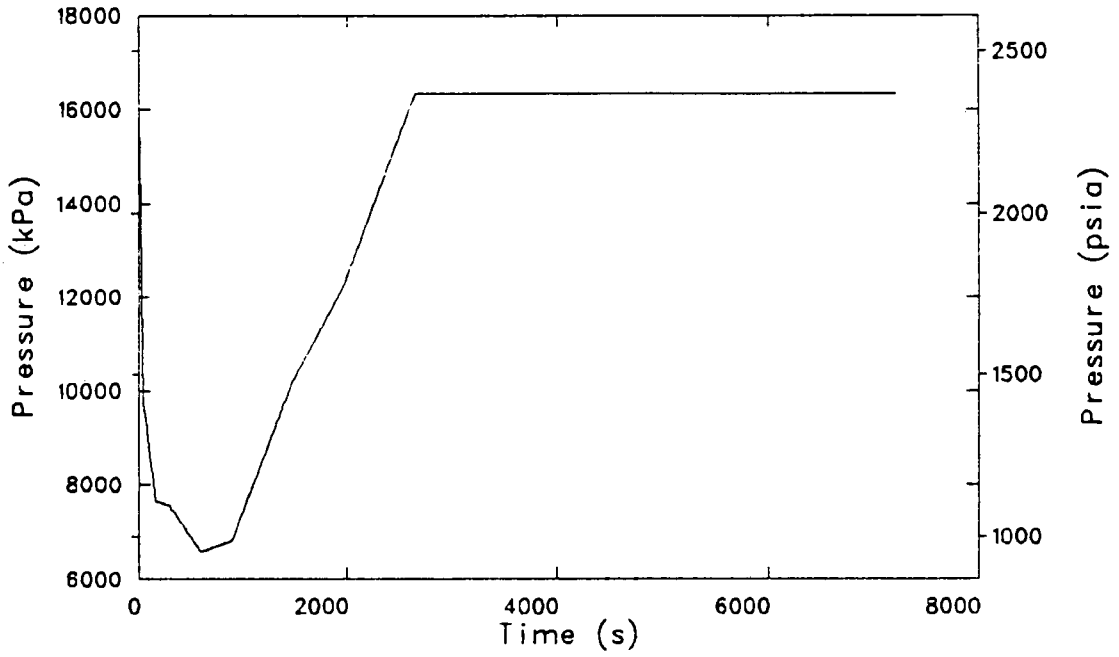

Figure F.263. Sequence 12.1: Reactor vessel downcomer fluid pressure.

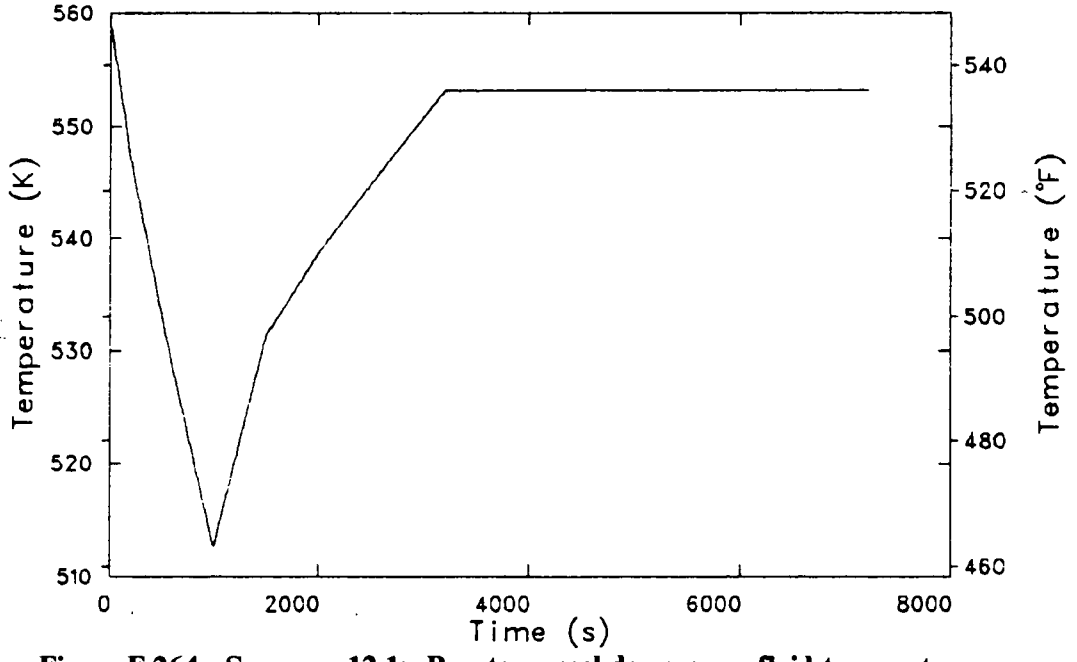

Figure F.264. Sequence 12.1: Reactor vessel downcomer fluid temperatures.

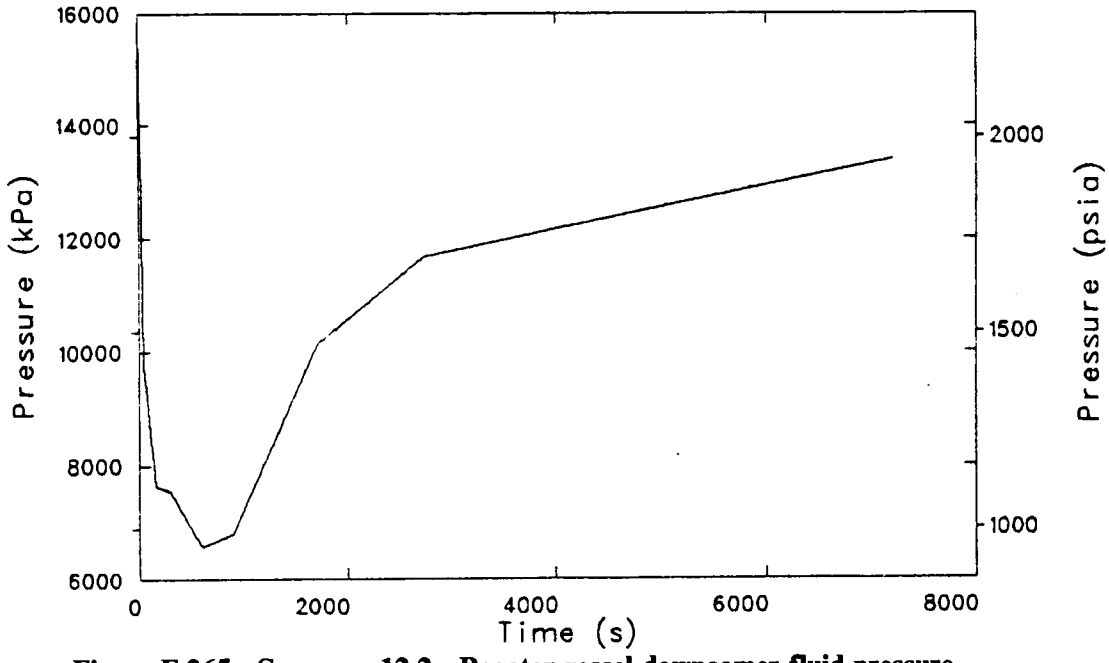

Figure F.265. Sequence 12.2: Reactor vessel downcomer fluid pressure.

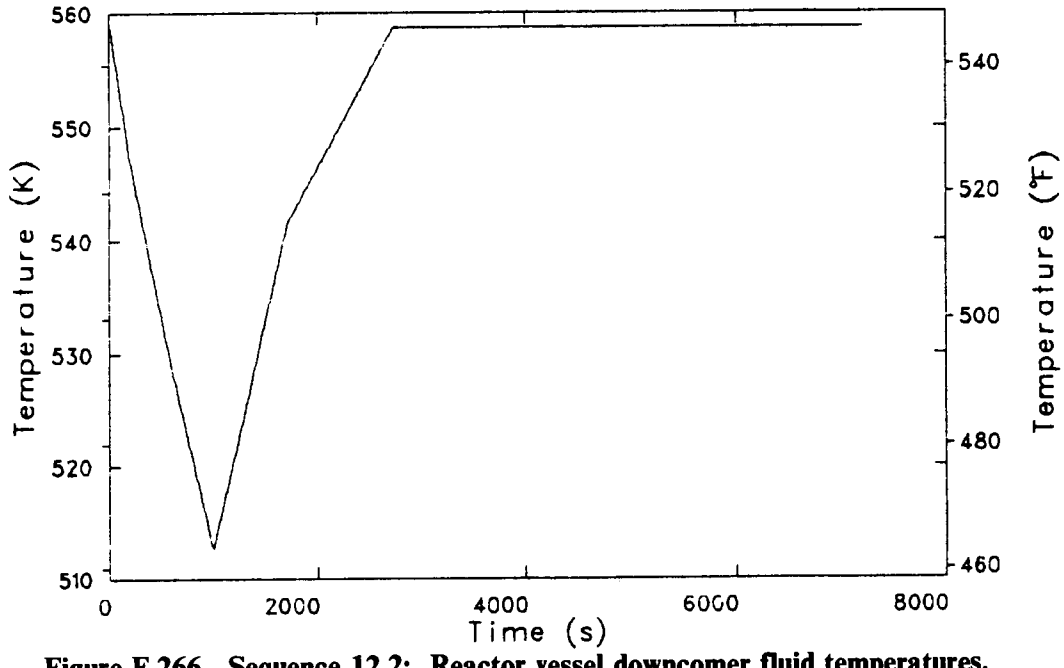

Figure F.266. Sequence 12.2: Reactor vessel downcomer fluid temperatures.

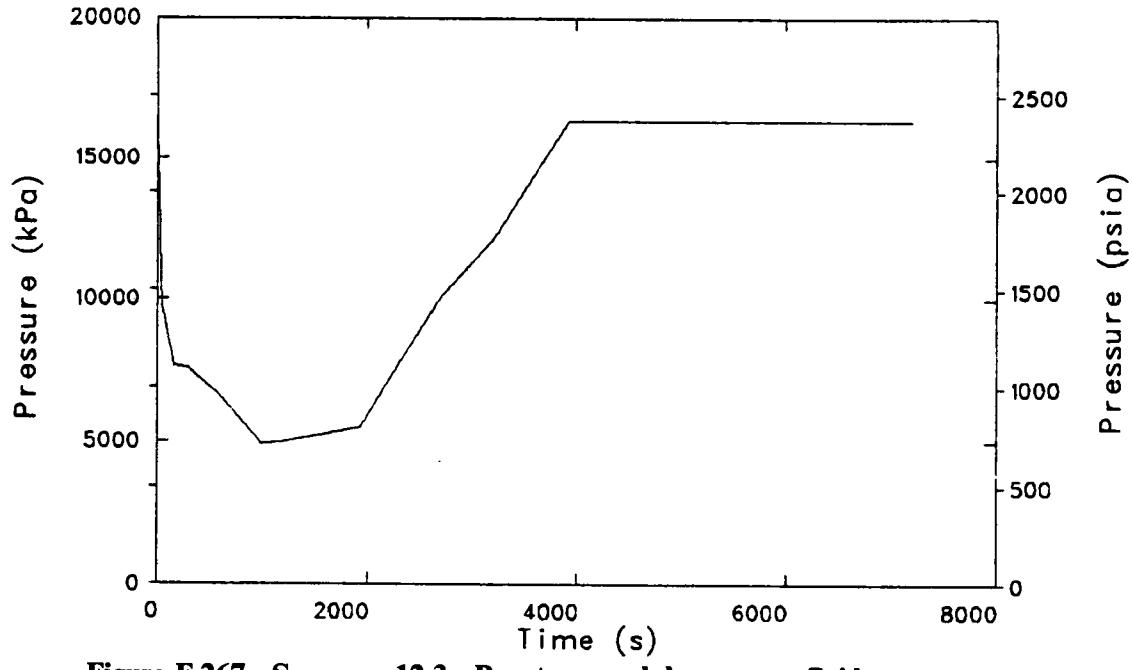

Figure F.267. Sequence 12.3: Reactor vessel downcomer fluid pressure.

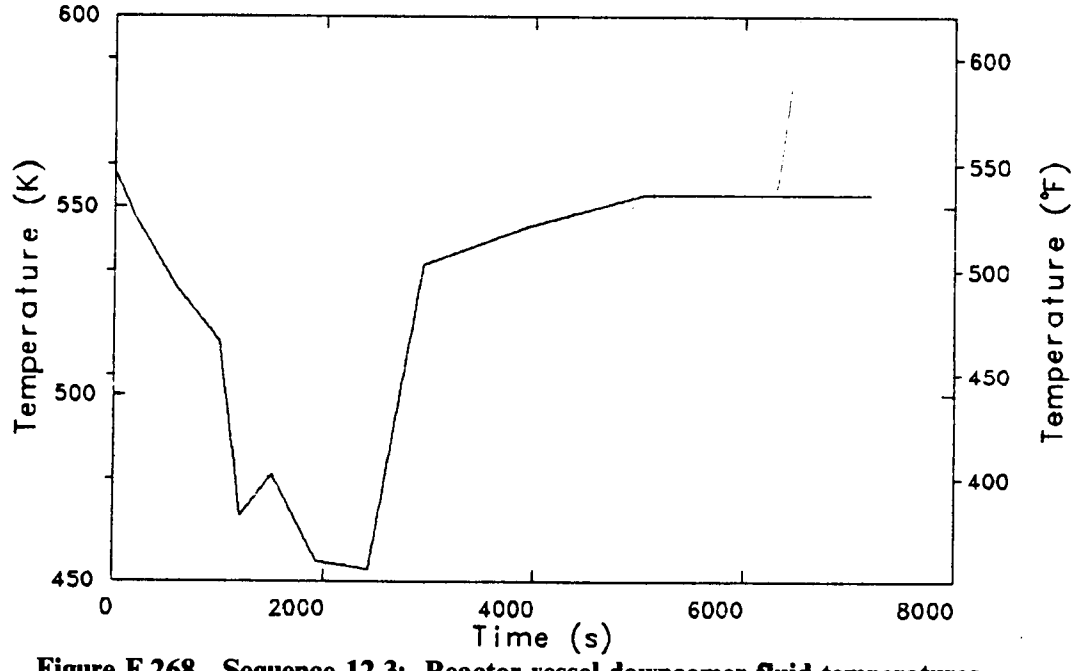

Figure F.268. Sequence 12.3: Reactor vessel downcomer fluid temperatures.

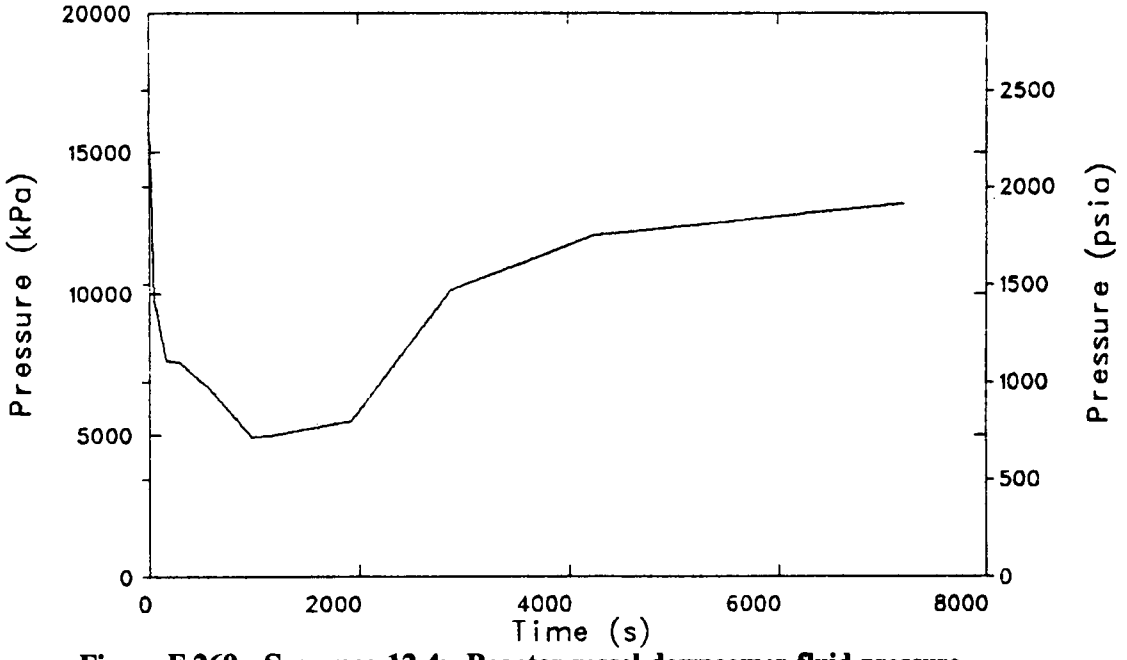

Figure F.269. Sequence 12.4: Reactor vessel downcomer fluid pressure.

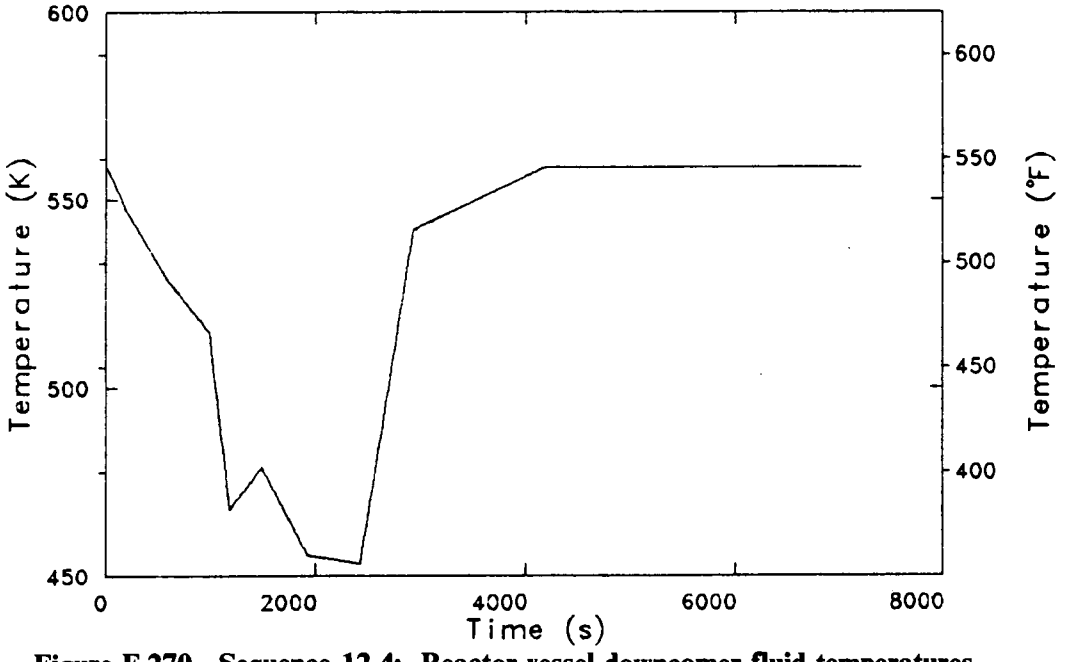

Figure F.270. Sequence 12.4: Reactor vessel downcomer fluid temperatures.

Reference

1. C. D. Fletcher, C. B. Davis, and D. M. Ogden, *Thermal-Hydraulic Analyses of Overcooling Sequences for the H. B. Robinson Unit 2 Pressurized Thermal Shock Study,* Idaho National Engineering Laboratory, NUREG/CR-3935, May, 1985.

Appendix G

THE USE OF *RTNDT* AND Δ*RTNDT* AS INDEPENDENT VARIABLES

R. D. Cheverton and D. G. Ball

Oak Ridge National Laboratory

APPENDIX G. THE USE OF *RTNDT* AND $\Delta RTNDT$ AS INDEPENDENT VARIABLES

For a study such as the one discussed in this report, it is convenient to use $RTNDT_s$ as an independent variable in the probabilistic fracture-mechanics analysis. This is because it allows one to apply the results to other reactor vessels, provided the transients analyzed are appropriate for the other vessels. However, since $RTNDT = RTNDT_0 + \Delta RTNDT$ and $\Delta RTNDT = f(F_0, \text{Cu}, \text{Ni})$, *RTNDT* is not actually an independent variable; that is, the actual independent variables are $RTNDT_0$, F_0, Cu and Ni and were used as such in two related studies.[1,2] As discussed in Sect. 5.3.1.7, for this particular study, values of $\bar{P}_j$ were obtained as a function of $\overline{RTNDTs}$, and in doing so both $RTNDT_0$ and $\Delta RTNDT_s$ were simulated, but only a single value of $\overline{RTNDT}_0$ was considered (0°F). This appendix discusses the derivation of the distribution function for $\Delta RTNDT$ and the error in using $\overline{RTNDT}_s$ as the independent variable.

The distribution function for $\overline{\Delta RTNDT}_s$ was obtained by performing a Monte Carlo analysis with Eq. (5.5), in which case F_0 and Cu were simulated and different values of $\bar{F}_0$, $\overline{\text{Cu}}$ and Ni were included. As in the two previous studies,[1,2] it was assumed that F_0 and Cu had normal distributions with $1\sigma = 0.3\ \bar{F}_0$ and 0.025 wt%, respectively. Based on this analysis, a normal distribution with $1\sigma = 0.14\ \overline{\Delta RTNDT}$ was selected for $\Delta RTNDT_s$.

The specific Monte Carlo cases calculated to obtain the typical distribution for $\Delta RTNDT$ are shown in Table G.1, and a typical histogram is presented in Figure G.1. It is apparent that (1) the distributions are essentially normal, although the tails are not well defined, (2) the sensitivity of σ to $\bar{F}_0$ and Ni is very small, and (3) the sensitivity to Cu is perhaps significant, although the extent to which it is significant depends on the sensitivity of $P(F|E)$ to the distribution function for $\Delta RTNDT$.

Table G.1. Monte Carlo–derived distributions for $\Delta RTNDT$

Input Parameters			σ	$\Delta RTNDT$ (°F)			
				2.5 Percentile		97.5 Percentile	
$\overline{\text{Cu}}$ (wt%)	Ni (wt%)	$\bar{F}_0$ (10^{19} n/cm^2)	(% of Mean)	Monte Carlo	Normal Approx.	Monte Carlo	Normal Approx.
0.2	1.0	2.0	16.1	127	125	243	243
0.3	1.0	2.0	12.5	212	212	349	353
0.2	0.2	2.0	16.4				
0.3	0.2	2.0	12.6				
0.15	1.0	2.0	20.2				
0.25	1.0	2.0	13.8				
0.35	1.0	2.0	11.6				
0.20	1.0	1.0	16.0				
0.20	1.0	4.0	16.1				

STATISTICS FOR OUTPUT VARIABLE DRTNDT

MINIMUM 44.47 MAXIMUM 231.87

MEAN 156.59 VARIANCE 383.0 STD. DEVIATION 19.57

PERCENTILES: 2.5% 118. 5.0% 124. 50.0% 157. 95.0% 188. 97.5% 194.

50000 POINT HISTOGRAM * = 77 POINTS

PROB	CUMP	DRTNDT (°C)		
0.0001	0.0	44.44	7	*
0.0001	0.0001	50.00	4	*
0.0002	0.0002	55.56	11	*
0.0002	0.0004	61.11	8	*
0.0002	0.0006	66.67	8	*
0.0002	0.0008	72.22	11	*
0.0004	0.0010	77.78	19	*
0.0005	0.0014	83.33	23	*
0.0011	0.0018	88.89	54	*
0.0015	0.0029	94.44	77	*
0.0027	0.0044	100.0	133	**
0.0052	0.0071	105.6	261	***
0.0096	0.0123	111.1	480	******
0.0182	0.0219	116.7	908	**********
0.0288	0.0401	122.2	1440	**********
0.0448	0.0689	127.8	2241	**********
0.0631	0.1137	133.3	3153	**********
0.0827	0.1768	138.9	4134	**********
0.1008	0.2594	144.4	5039	**********
0.1130	0.3602	150.0	5651	**********
0.1147	0.4732	155.6	5736	**********
0.1079	0.5880	161.1	5397	**********
0.0939	0.6959	166.7	4697	**********
0.0743	0.7898	172.2	3713	**********
0.0538	0.8641	177.8	2689	**********
0.0364	0.9179	183.3	1821	**********
0.0224	0.9543	188.9	1122	**********
0.0122	0.9767	194.4	611	********
0.0058	0.9890	200.0	292	****
0.0030	0.9948	205.6	151	**
0.0015	0.9978	211.1	75	*
0.0003	0.9993	216.7	17	*
0.0003	0.9997	222.2	14	*
0.0001	0.9999	227.8	3	*
	1.0000	233.3		

Figure G.1. $\Delta RTNDT_s$ **distribution from a Monte Carlo run for** $\mu(\mathrm{Cu}) = 0.3$, $\mu(F_0) = 2 \times 10^{19}$ **and Ni = 1.0.**

Rather than investigate this latter sensitivity directly, two sets of calculations were made to obtain $P(F|E)$ vs $\overline{Cu}$ for several HBR-2 postulated transients (8.6, 9.19B, 9.33, 9.41). For one set, $\overline{\Delta RTNDT_s}$ was used as an independent variable, and for the other set, F_0, Cu and Ni were used as independent variables. The results, shown in Figure G.2, indicate that the error in using $\overline{\Delta RTNDT_s}$ as an independent variable is (1) dependent on the transient, (2) positive for Cu > 0.25 and negative for Cu < 0.25 (the value of σ used for $\Delta RTNDT$ was based on Cu $\simeq$ 0.25), (3) larger for the less severe transients, and (4) substantial (factors of ~25 and 7) for the least severe dominant transient and the two extreme values of Cu considered (0.15 and 0.35, respectively).

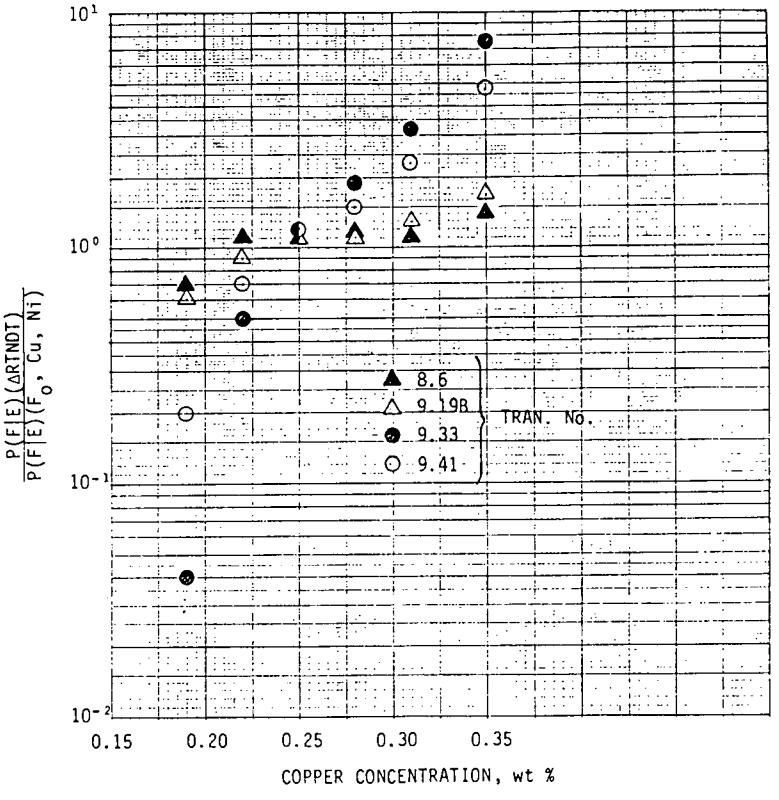

Figure G.2. Comparison of calculated values of $P(F|E)$ using $\Delta RTNDT_s$ as the independent variable and F_0, Cu and Ni as independent variables.

It is of interest to note that the error associated with using $\Delta RTNDT_s$ as an independent variable is not only the result of having to approximate the distribution function. This can be illustrated by calculating $P(F|E)$ for different combinations of F_0, Cu and Ni that result in the same value of $\overline{\Delta RTNDT_s}$. Table G.2 shows the results of a comparison analysis in which F_0 and Cu were simulated, two values of $\overline{Cu}$ were considered (0.2 and 0.35), and $\bar{F}_0$ and Ni were adjusted so that $\overline{\Delta RTNDT_s}$ was the same for both values of $\overline{Cu}$. As indicated, the lower value of Cu resulted in a higher value of $P(F|E)$, and the less severe the transient the greater the ratio.

Table G.2. Comparison of $P(F|E)$ values calculated using F_0, Cu and Ni as independent variables, considering two values of Cu but only one value of $\overline{\Delta RTNDT_s}$

HBR Transient	Minimum Coolant Temperature (°F)	Pressure at Time of Failure (ksi)	$P(F\|E)_1$[a] / $P(F\|E)_2$
8.6	201	1850	1.5
9.19B	203	1500	1.9
9.41	268	1500	6.7
9.33	294	1750	17

[a] $P(F|E)_1$: Cu = 0.20, Ni = 1.00, F_0 = 3.49E19, $\overline{RTNDT_0}$ = 0°F, $\overline{\Delta RTNDT_s}$ = 216°F.

$P(F|E)_2$: Cu = 0.35, Ni = 0.50, F_0 = 1.00E19, $\overline{RTNDT_0}$ = 0°F, $\overline{\Delta RTNDT_s}$ = 216°F.

The additional error introduced by variations in $\overline{RTNDT_0}$ when using $RTNDT$ as an independent variable was examined in a similar manner, that is, by comparing values of $P(F|E)$ corresponding to different values of $\overline{RTNDT_0}$. Three values of $\overline{RTNDT_0}$ were considerd (−56, 0, +56°F), and values of $P(F|E)$ corresponding to the two extremes were compared with that corresponding to 0°F, since $\overline{RTNDT_0}$ = 0°F was used to obtain the $\hat{P}_j$ vs $\overline{RTNDT_s}$ curves in this report (Appendix I). The results of the comparison, shown in Figure G.3, indicate that (1) the error is positive for $\overline{RTNDT_0}$ < 0°F and is negative for $\overline{RTNDT_0}$ > 0°F, (2) it increases with decreasing $RTNDT_s$ and is small for $\overline{RTNDT_s}$ > 200°F, and (3) the error is greater for the less severe transients.

Although it is convenient to use $RTNDT_s$ as an independent variable, it is apparent from the preceding discussion that the error in doing so can be substantial. Thus, one must use the $\hat{P}_j$ vs $\overline{RTNDT_s}$ curves in Appendix I with this understanding. For the most accurate results, $RTNDT_0$, F_0, Cu, and Ni should be used as independent variables in a detailed probabilistic fracture-mechanics analysis.

References

1. T. J. Burns *et al., Preliminary Development of an Integrated Approach to the Evaluation of Pressurized Thermal Shock Risk as Applied to the Oconee Unit 1 Nuclear Power Plant,* NUREG/CR-3770 (ORNL/TM-9176), November 1985.
2. D. L. Selby *et al., Pressurized Thermal Shock Evaluation of the Calvert Cliffs Unit 1 Nuclear Power Plant,* NUREG/CR-4022 (ORNL/TM-9408), September, 1985.

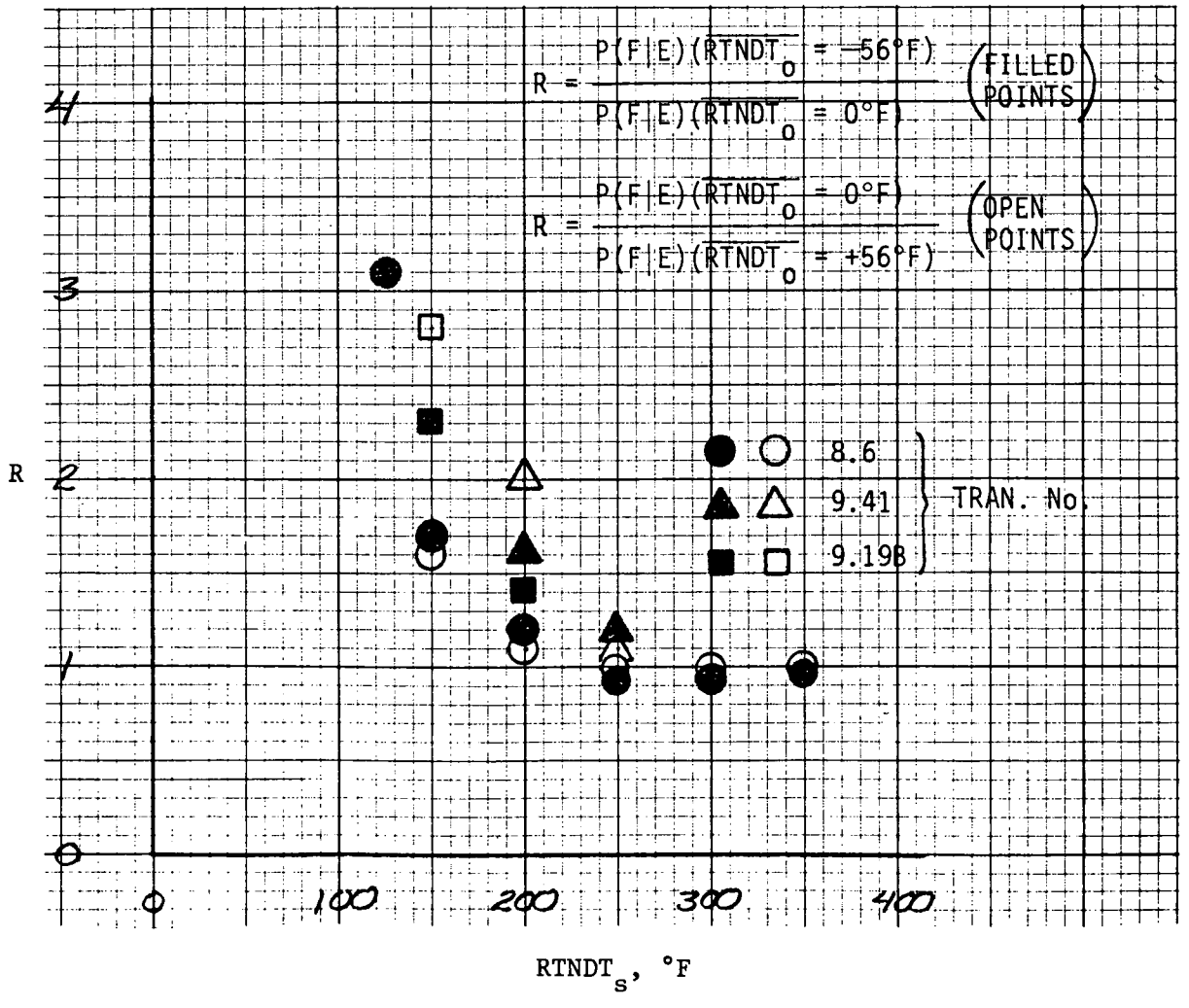

Figure G.3. Effect of $RTNDT_0$ on values of $P(F|E)$ calculated using $RTNDT_s$ as an independent variable.

Appendix H

IMPORTANCE SAMPLING METHODS IN THE OCA-P PROBABILISTIC FRACTURE-MECHANICS ANALYSIS

R. D. Cheverton and D. G. Ball

Oak Ridge National Laboratory

APPENDIX H. IMPORTANCE SAMPLING METHODS IN THE OCA-P PROBABILISTIC FRACTURE-MECHANICS ANALYSIS

To be able to calculate low probabilities of failure with acceptable accuracy and reasonable computer time, importance sampling was applied to three simulated parameters: crack depth, $\Delta RTNDT$, and $RTNDT$. For each of these parameters it was first demonstrated for a specific transient that a portion of the distribution function contributed little to the probability of failure. This portion was then omitted from a subsequent simulation, but was accounted for in the number of trials by multiplying N'_{vj} by a correction factor, as indicated by Eq. (5.14). For the crack-depth distribution, only the first flaw depth was not simulated, and the corresponding correction factor is given by

$$F_{1j} = \left[\int_{\Delta a_1}^{w} f(a)B(a)da\right]^{-1} = 3.24 \ . \tag{H.1}$$

The use of this acceleration method is indicated on the summary sheet in Appendix I by $IACCEL = 1$.

In the case of $\Delta RTNDT$ and $RTNDT$, a continuous sampling of the distribution can be replaced by a stratified sampling of the "positive" tail. For these studies, $\Delta RTNDT$ and $RTNDT$ were assumed to have normal distributions, and sampling was allowed to begin at 1.0 to 2.5 standard deviations above the mean, in increments of 0.25. Use of this method for $\Delta RTNDT$ is indicated on the summary sheet in Appendix I by $NDLRS = n$, where n indicates the start of sampling as given in Table H.1. The variable $NRTRS$ operates in a similar way for the $RTNDT$ distribution. The correction factors, F_{2j} and F_{3j}, corresponding to $\Delta RTNDT$ and $RTNDT$, are given in Table H.1 and are based on a normal (0, 1) distribution truncated at $\pm 3\sigma$.

The normal (0, 1) distribution, truncated at $\pm 3\sigma$, was used to establish a distribution for the strata between 1σ and 3σ for $\Delta RTNDT$ and $RTNDT_s$. A justification follows:

Table H.1. Details of importance sampling on $\Delta RTNDT_s$ and $RTNDT$ distributions

Identifying Number (*NDLRS* or *NRTRS*)	Start-of-Sampling Number of Standard Deviations Above Mean	Fraction of $N(0, 1)$ Distribution in Range: $x \rightarrow x + 0.25$	Fraction of Distribution Not Simulated[a]	Multiplicative Adjustment to the Number of Trials, F_{2j} and F_{3j}
1	1.0	0.0531	0.8422	6.3
2	1.25	0.0388	0.8954	9.6
3	1.50	0.0267	0.9343	15.2
4	1.75	0.0173	0.9611	25.7
5	2.00	0.0106	0.9784	46.4
6	2.25	0.0060	0.9891	91.7
7	2.50	0.0032	0.9951	204.1
8	2.75	0.0017	0.9983	588.2

[a]Assuming truncation at $\pm 3\sigma$.

Let $x \epsilon$ normal (μ,σ^2), $\mu - 3\sigma \leqslant x \leqslant \mu + 3\sigma$. Then the probability density function of x is given by

$$f(x) = \frac{c_1}{\sigma\sqrt{2\pi}} \exp\left[-\frac{(x-\mu)^2}{2\sigma}\right], \tag{H.2}$$

where c_1 is the constant that adjusts for the truncation at $\pm 3\sigma$. In the stratification process for this variable, a quantity of interest would be the fraction of the probability between $x = \mu + c_2\sigma$ and $x = \mu + c_3\sigma$, where c_2 and c_3 are constants. This fraction is given by

$$P(\mu + c_2\sigma \leqslant x \leqslant \mu + c_3\sigma) = \int_{\mu+c_2\sigma}^{\mu+c_3\sigma} \exp\left[-\frac{(x-\mu)^2}{2\sigma^2}\right] dx \ . \tag{H.3}$$

By changing variables $[y = (x - \mu)/\sigma, dy = dx/\sigma]$ Eq. (H.3) becomes

$$P(c_2 \leqslant y \leqslant c_3) = c_1 \int_{c_2}^{c_3} \frac{1}{\sqrt{2\pi}} \exp\left[-\frac{y^2}{2}\right] dy \ . \tag{H.4}$$

The integrand is the probability density function for a normal (0, 1) variable. Therefore, the above probability [Eq. (H.3)] is the same as that of a normal (0, 1) variable between c_2 and c_3. This yields the stratification process detailed in Table H.1.

Appendix I

COMPILATION OF RESULTS FOR HBR-HYPO PROBABILISTIC FRACTURE-MECHANICS ANALYSIS

R. D. Cheverton and D. G. Ball

Oak Ridge National Laboratory

APPENDIX I. COMPILATION OF RESULTS FOR HBR-HYPO PROBABILISTIC FRACTURE-MECHANICS ANALYSIS

Detailed results for the HBR-HYPO probabilistic fracture-mechanics analysis are included in this appendix so that a more thorough understanding of the effect of the various assumptions used in the fracture-mechanics model and of the different inputs to the fracture-mechanics analysis can be obtained. For instance, the duration of all postulated transients for this study was specified as two hours. As indicated by the summary sheets, in many cases the failures did not occur until late in the transient; thus, if the duration of the transient had been taken to be one hour instead of two hours, the $P(F|E)$ values would have been reduced substantially.

Sets of data are included in this appendix for most of the transients listed in Table 5.5.* Each set includes, in this order, (1) plots of primary-system pressure, downcomer coolant temperature and fluid-film heat-transfer coefficient vs time in the transient; (2) a summary sheet of digital output that includes $\hat{P}_j \int_0^w f(a)B(a)da$ [referred to in the data sets as "unadjusted $P(F|E)$"†] and histogram data for HBR-HYPO weld 2-273A on crack depths, times of failure, and values of $T-RTNDT$ at the crack tip corresponding to initiation and arrest events; (3) a plot of $\hat{P}_j \int_0^w f(a)B(a)da$ vs $\overline{RTNDT_s}$ for the (2-D, 2-D) flaw combination (axial flaws in the plate, and circumferential flaws) and the (2-D, 2-m) flaw combination (axial flaws in axial welds); (4) a plot of vessel wall temperature vs radial position in the wall (a/w) with time (t) as a parameter; (5) a plot of vessel wall temperature vs t with a/w as a parameter; (6) a plot of K_I vs t for 2-D flaws with a/w as a parameter; and (7) a set of critical-crack-depth curves for HBR-HYPO weld 2-273A corresponding to -2σ values for K_{Ic}, K_{Ia} and $RTNDT$, mean values of all other parameters, and an operating time of 32 EFPY.

The summary sheets include the error in the values of $P(F|E)$, based on a 95% confidence interval, and also the number of trials (number of vessels simulated), but the number of trials has not been corrected in those cases for which importance sampling was used. If importance sampling was used for one or more of the three affected parameters (crack depth, $\Delta RTNDT$, $RTNDT$), one or more of the corresponding quantities $IACCEL$, $NDLRS$, or $NRTRS$, respectively, will be greater than 0, as indicated near the bottom of the summary sheet. In the case of $NDLRS$ and $NRTRS$, the number given in the summary sheet (some multiple of σ) can be used to obtain the appropriate correction factor from Table H.1 for the number of trials.

*It should be noted that the dates given on the data sets have no reference to the HBR vessel and have no meaning other than computer case identification.

†For purposes of comparing the various transients, the value of n^*v in the summary sheets was always taken to be 1.0. Thus the adjusted value of $P(F|E)$ is the same as the unadjusted value. The actual adjusted values can be obtained by multiplying the unadjusted value by the appropriate weld volume (v), since the best estimate for n is 1.0.

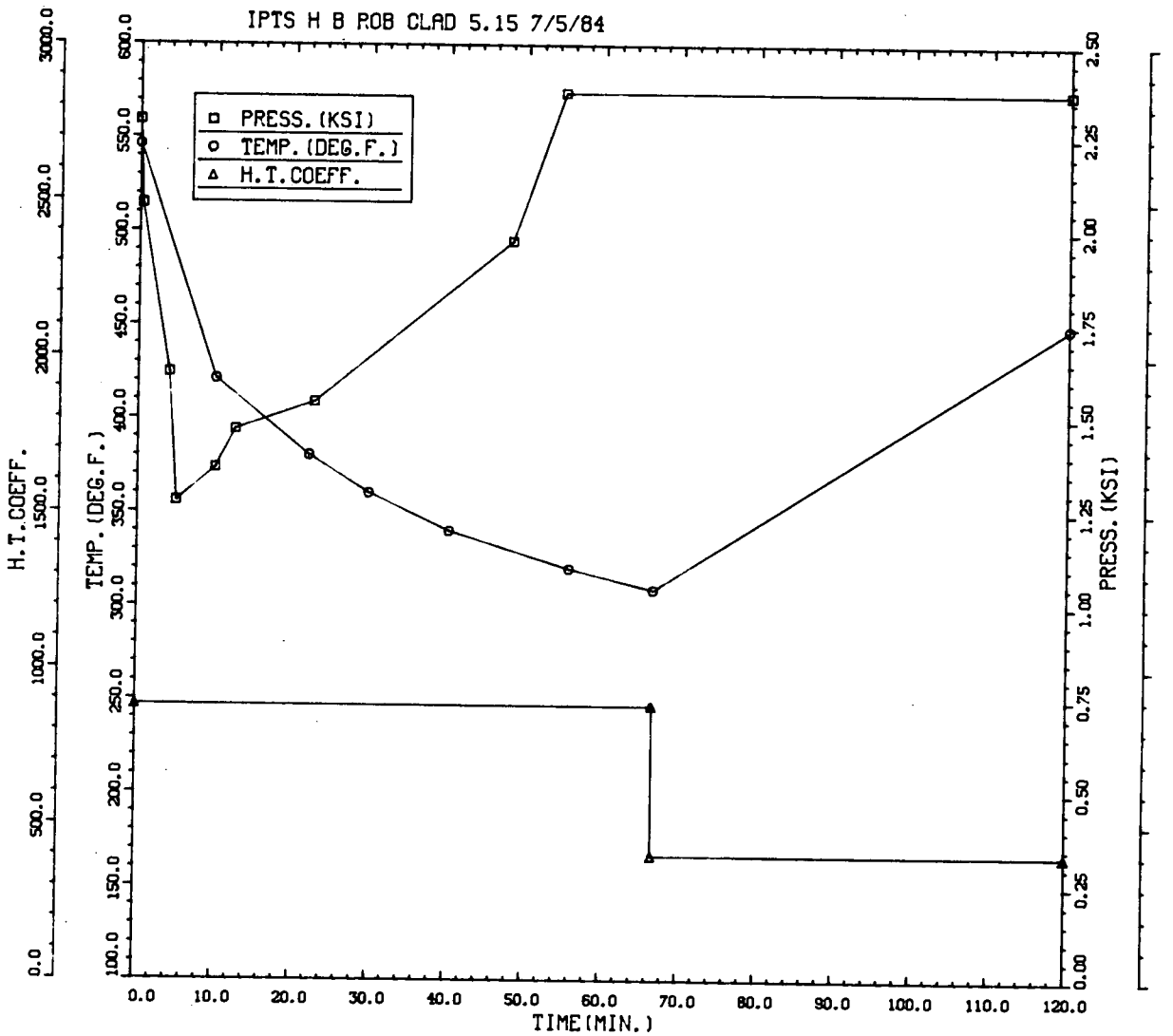

Figure I.1. Transient 5.15: Primary system pressure, downcomer coolant temperature, and fluid-film heat-transfer coefficient vs time in the transient.

Table I.1. Transient 5.15: Summary of digital output, including unadjusted $P(F|E)$ values and histogram data for crack depths, times of failure, and $T - RTNDT$ values at tip of crack corresponding to initiation and arrest events

```
IPTS H B ROB CLAD 5.15 7/5/84                    1. FLAWS/IN**3    DRTN(IS) =  211.2

          -------------UNADJUSTED--------------          ---ADJUSTED----
WELD      P(F/E)       95%CI     %ERR    P(INITIA)  N*V     P(F/E)     %ERR     NFAIL     NTRIALS

 1        1.65D-05   1.61D-06    9.77    1.97D-05  1.000   1.65D-05            401       110000

                                                   VESSEL  1.65D-05    9.77


DEPTHS FOR INITIAL INITIATION (IN)
                0.09  0.26  0.46  0.67  0.90  1.16  1.44  1.74  2.08
    NUMBER       0   190   175    71    33    11     1     0     0
    PERCENT     0.0  39.5  36.4  14.8   6.9   2.3   0.2   0.0   0.0


TIMES OF FAILURE(MINUTES)
                0.0  10.0  20.0  30.0  40.0  50.0  60.0  70.0  80.0  90.0 100.0 110.0 120.0
   PERCENT      0.0   0.0   0.0   0.0   1.5  45.4  53.1   0.0   0.0   0.0   0.0   0.0


 INITIATION T-RTNDT(DEG.F)
            -100.0 -75.0 -50.0 -25.0   0.0  25.0  50.0  75.0 100.0 125.0 150.0 175.0 200.0
   NUMBER        0     0     7   124   285    64     3     1     0     0     0     0
   PERCENT      0.0   0.0   1.4  25.6  58.9  13.2   0.6   0.2   0.0   0.0   0.0   0.0


 ARREST T-RTNDT(DEG.F)
             -50.0 -25.0   0.0  25.0  50.0  75.0 100.0 125.0 150.0 175.0 200.0 225.0 250.0
   NUMBER        0     0    10    11     0     0     0    32    30     0     0     0
   PERCENT      0.0   0.0  12.0  13.3   0.0   0.0   0.0  38.6  36.1   0.0   0.0   0.0


 # OF STD DEVS ABOVE MEAN DELTA RTNDT(FAILURES ONLY)
               1.00  1.25  1.50  1.75  2.00  2.25  2.50  2.75  3.00
   NUMBER        18    29    51    59    53    79    59    53
   PERCENT      4.5   7.2  12.7  14.7  13.2  19.7  14.7  13.2


 # OF STD DEVS ABOVE MEAN RTNDT(FAILURES ONLY)
               1.00  1.25  1.50  1.75  2.00  2.25  2.50  2.75  3.00
   NUMBER         7    20    44    47    68    76    83    56
   PERCENT      1.7   5.0  11.0  11.7  17.0  19.0  20.7  14.0


ICRKTP = 2   IACCEL = 1   NDLRS = 1   NRTRS = 1   DATE: 10/29/84   TIME: 22.17.19

CPU TIME:  3 MIN  0 SEC
```

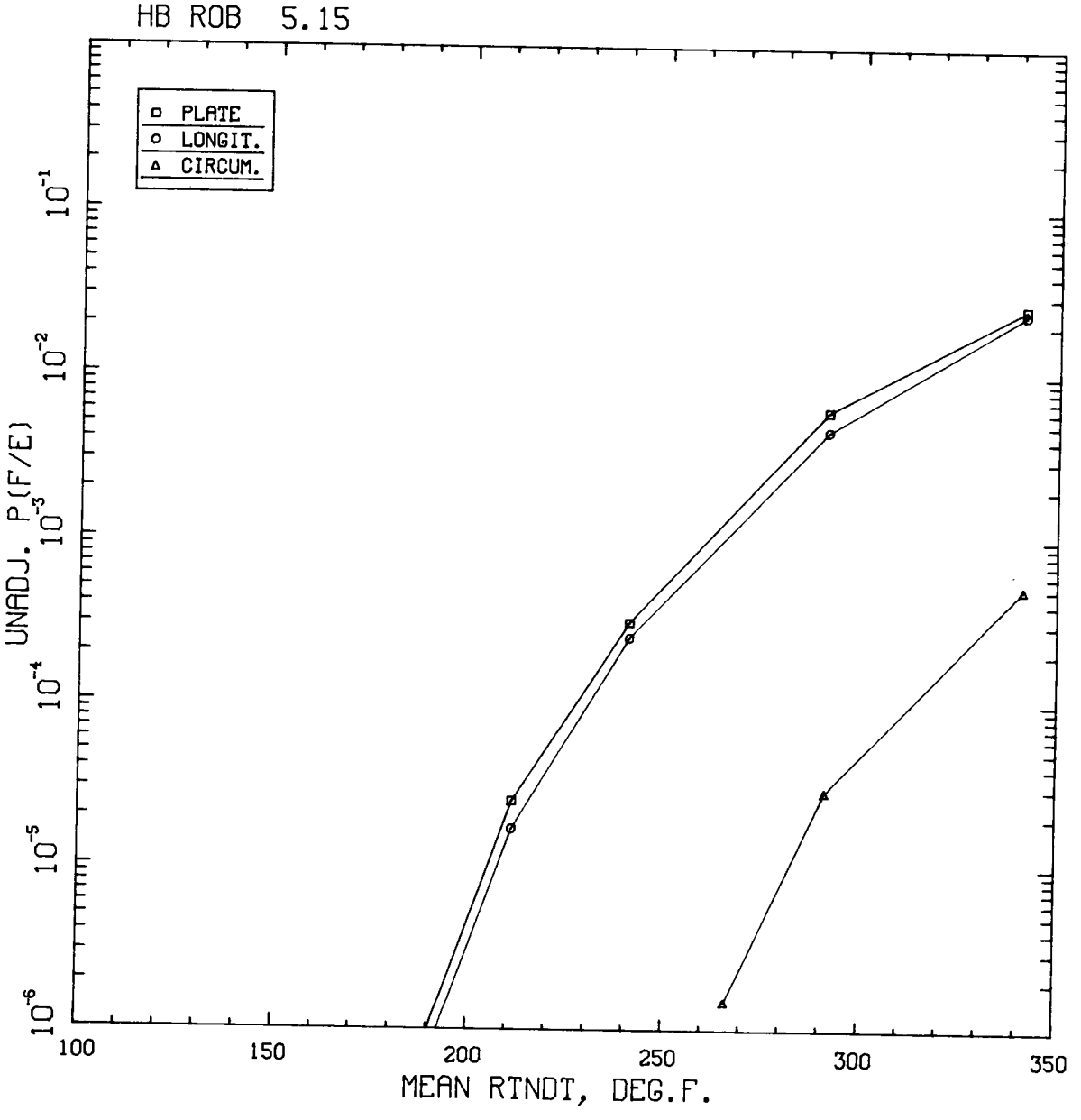

Figure I.2. Transient 5.15: $\hat{P}_j \int_0^w f(a)\, B(a)\, da$ vs $\overline{RTNDT_s}$ for (2-D, 2-D) and (2-D, 2m) flaw combinations.

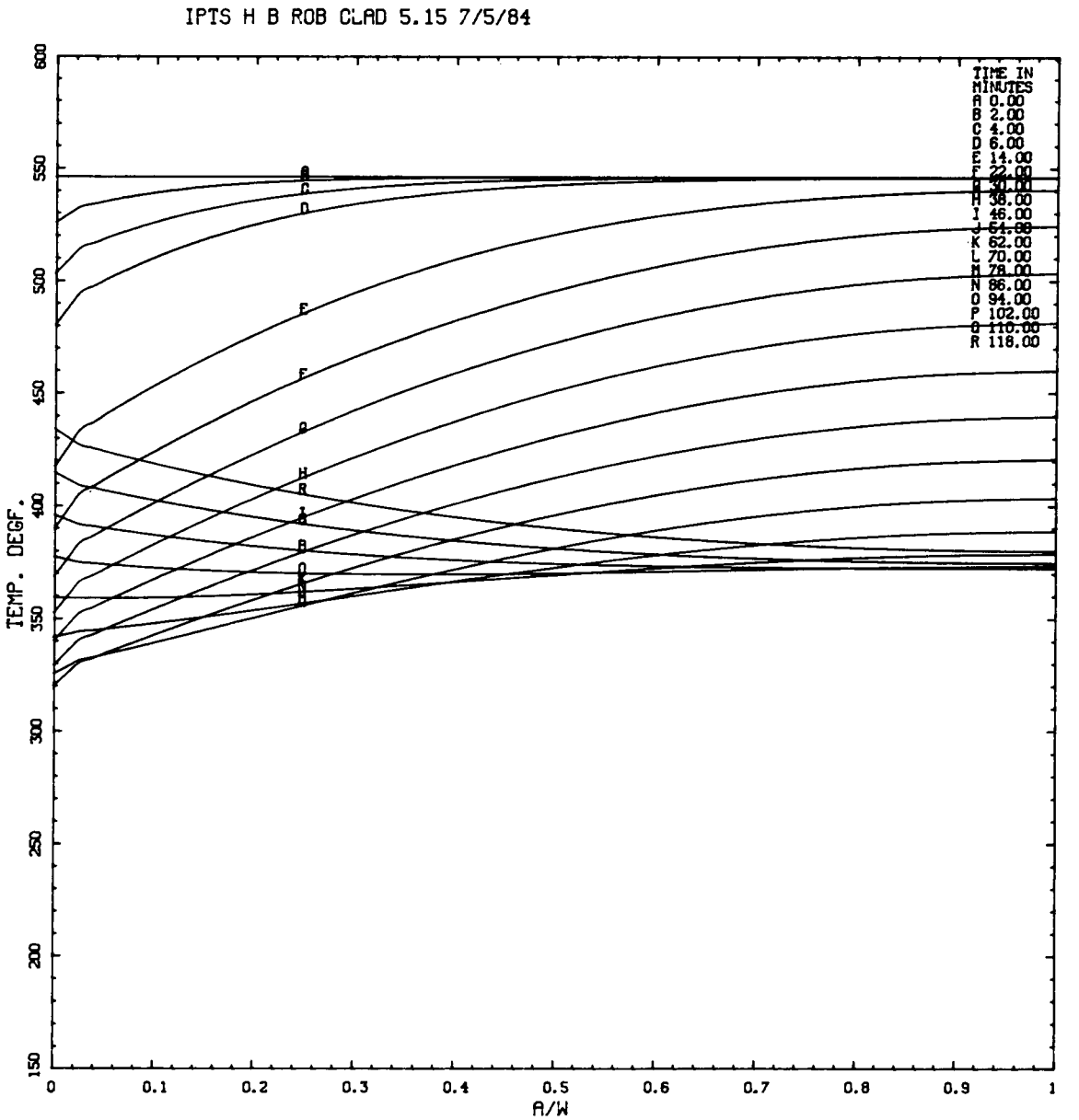

Figure I.3. Transient 5.15: Vessel wall temperature vs depth in wall (a/w) at various times (t) in transient.

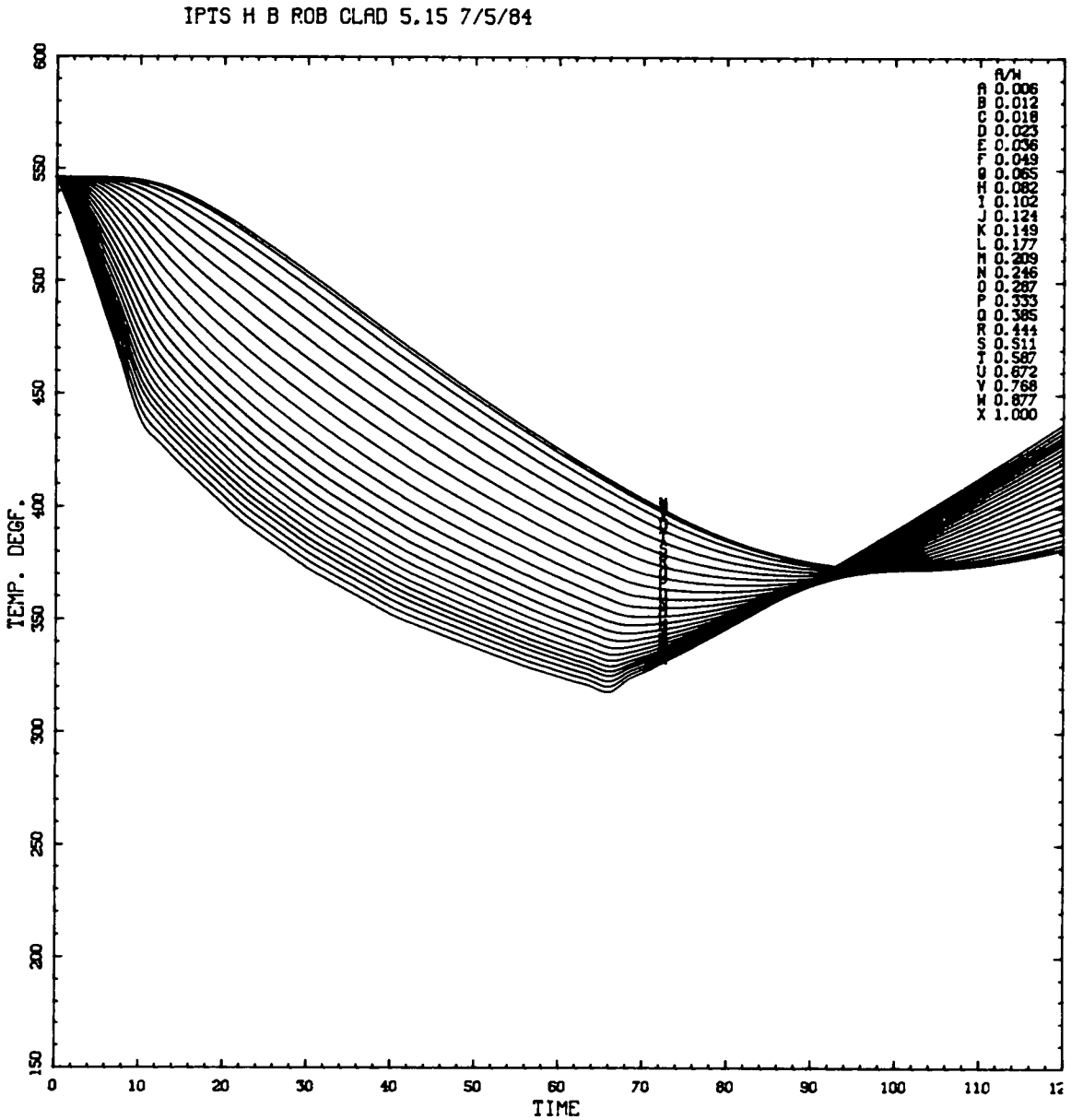

Figure I.4. Transient 5.15: Vessel wall temperature vs time (t) in transient at various depths in wall (a/w).

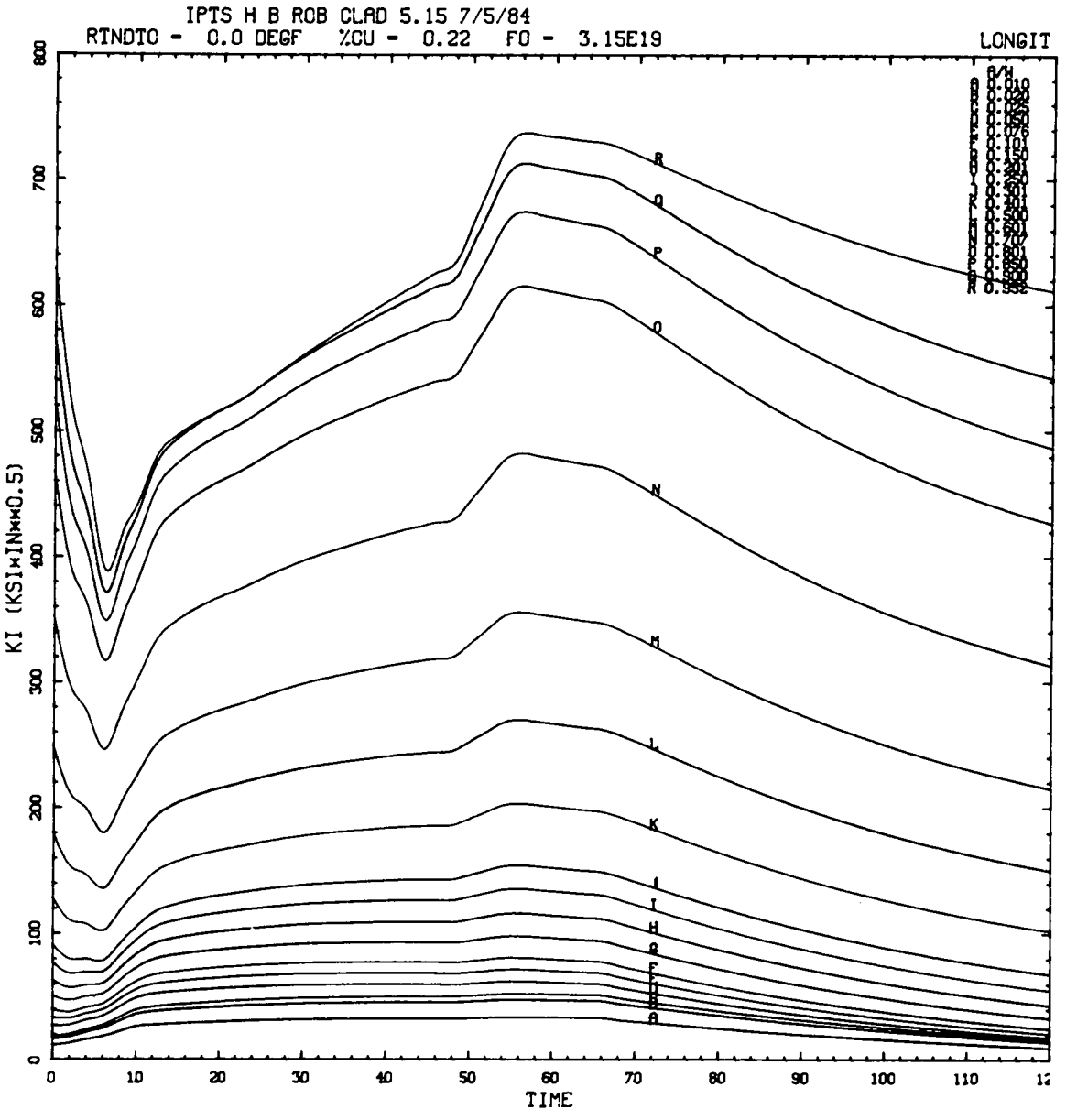

Figure I.5. Transient 5.15: K_I vs time (t) for various depths in wall (a/w).

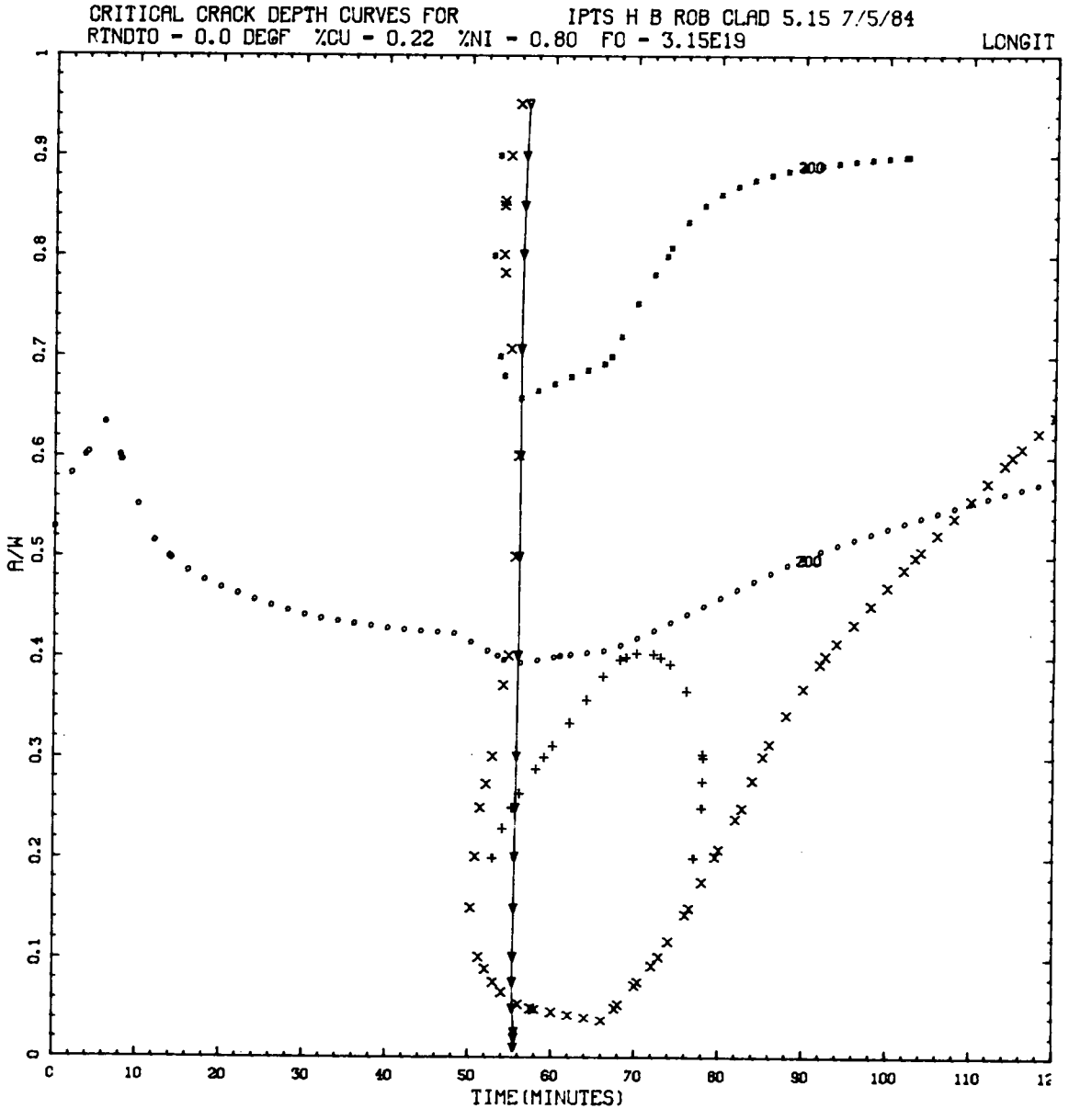

×, 2-D flaw, $K_I = K_{Ia}$
+, 2-m flaw, $K_I = K_{Ia}$
O, 2-D flaw, $K_I = 220$ MPa $\sqrt{m}$
■, 2-m flaw, $K_I = 220$ MPa $\sqrt{m}$
∇, WPS (warm prestressing)

Figure I.6. Transient 5.15: Critical-crack-depth curves for weld 2-273A based on -2σ values of K_{Ic}, K_{Ia}, and $\Delta RTNDT$, mean values of all other parameters, and 32-EFPY fluences.

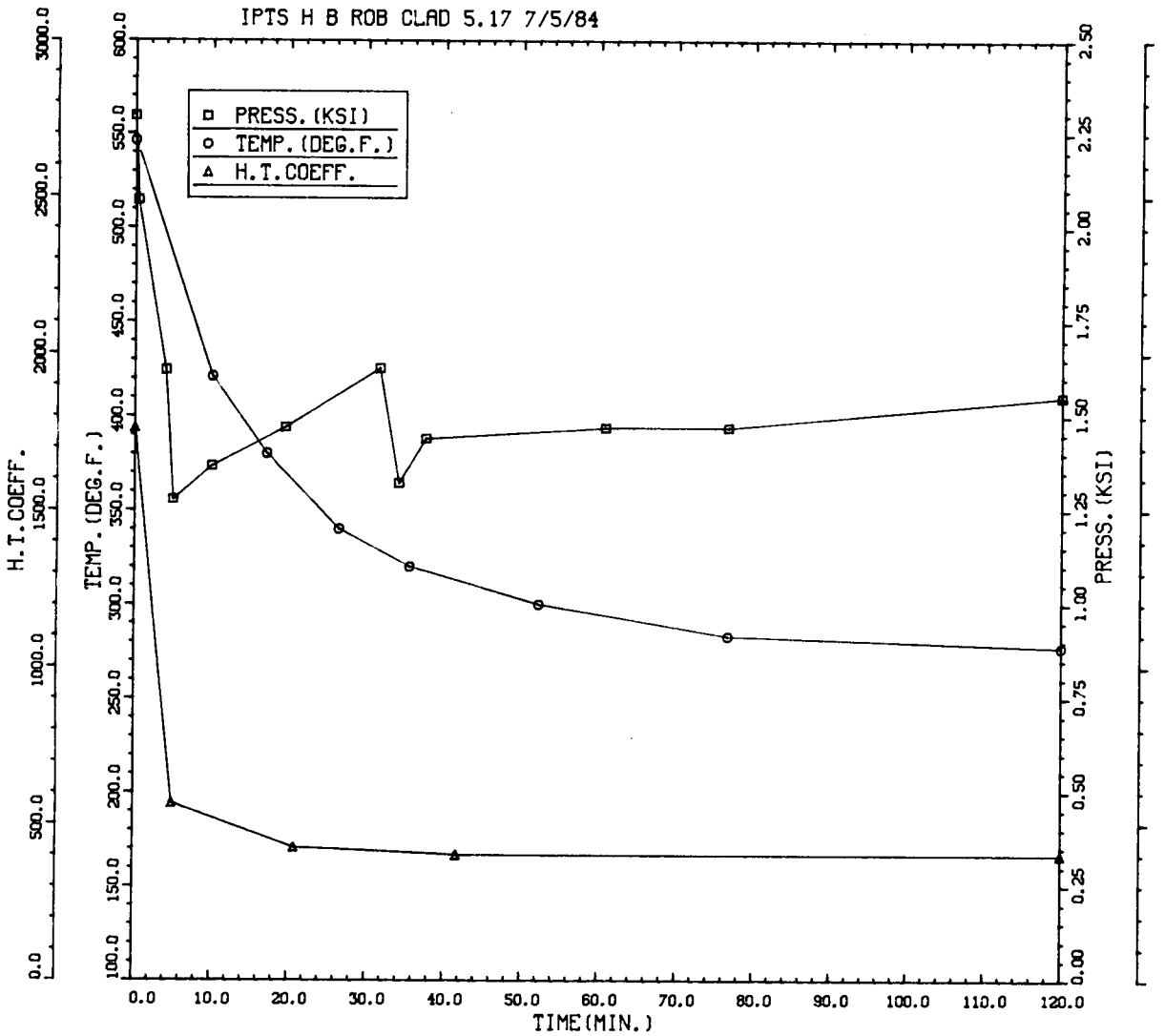

Figure I.7. Transient 5.17: Primary system pressure, downcomer coolant temperature, and fluid-film heat-transfer coefficient vs time in the transient.

Table I.2. Transient 5.17: Summary of digital output, including unadjusted $P(F|E)$ values and histogram data for crack depths, times of failure, and $T - RTNDT$ values at tip of crack corresponding to initiation and arrest events

IPTS H B ROB CLAD 5.17 7/5/84 1. FLAWS/IN**3 DRTN(IS) = 211.2

	----------UNADJUSTED----------					---ADJUSTED----			
WELD	P(F/E)	95%CI	%ERR	P(INITIA)	N*V	P(F/E)	%ERR	NFAIL	NTRIALS
1	4.05D-06	4.03D-07	9.94	9.29D-06	1.000	4.05D-06		388	190000
					VESSEL	4.05D-06	9.94		

DEPTHS FOR INITIAL INITIATION (IN)

	0.09	0.26	0.46	0.67	0.90	1.16	1.44	1.74	2.08
NUMBER	0	409	282	125	52	18	3	0	1
PERCENT	0.0	46.0	31.7	14.0	5.8	2.0	0.3	0.0	0.1

TIMES OF FAILURE(MINUTES)

	0.0	10.0	20.0	30.0	40.0	50.0	60.0	70.0	80.0	90.0	100.0	110.0	120.0
PERCENT	0.0	0.0	0.0	0.0	0.0	0.8	4.1	13.1	16.0	22.2	22.7	21.1	

INITIATION T-RTNDT(DEG.F)

	-100.0	-75.0	-50.0	-25.0	0.0	25.0	50.0	75.0	100.0	125.0	150.0	175.0	200.0
NUMBER	0	0	37	359	437	237	153	32	1	0	0	0	
PERCENT	0.0	0.0	2.9	28.6	34.8	18.9	12.2	2.5	0.1	0.0	0.0	0.0	

ARREST T-RTNDT(DEG.F)

	-50.0	-25.0	0.0	25.0	50.0	75.0	100.0	125.0	150.0	175.0	200.0	225.0	250.0
NUMBER	1	43	110	29	3	2	86	479	115	0	0	0	
PERCENT	0.1	5.0	12.7	3.3	0.3	0.2	9.9	55.2	13.2	0.0	0.0	0.0	

OF STD DEVS ABOVE MEAN DELTA RTNDT(FAILURES ONLY)

	1.00	1.25	1.50	1.75	2.00	2.25	2.50	2.75	3.00
NUMBER	0	18	28	58	64	52	81	87	
PERCENT	0.0	4.6	7.2	14.9	16.5	13.4	20.9	22.4	

OF STD DEVS ABOVE MEAN RTNDT(FAILURES ONLY)

	1.00	1.25	1.50	1.75	2.00	2.25	2.50	2.75	3.00
NUMBER	0	6	27	36	67	75	84	93	
PERCENT	0.0	1.5	7.0	9.3	17.3	19.3	21.6	24.0	

ICRKTP = 2 IACCEL = 1 NDLRS = 2 NRTRS = 2 DATE: 10/29/84 TIME: 22.26.18

CPU TIME: 5 MIN 6 SEC

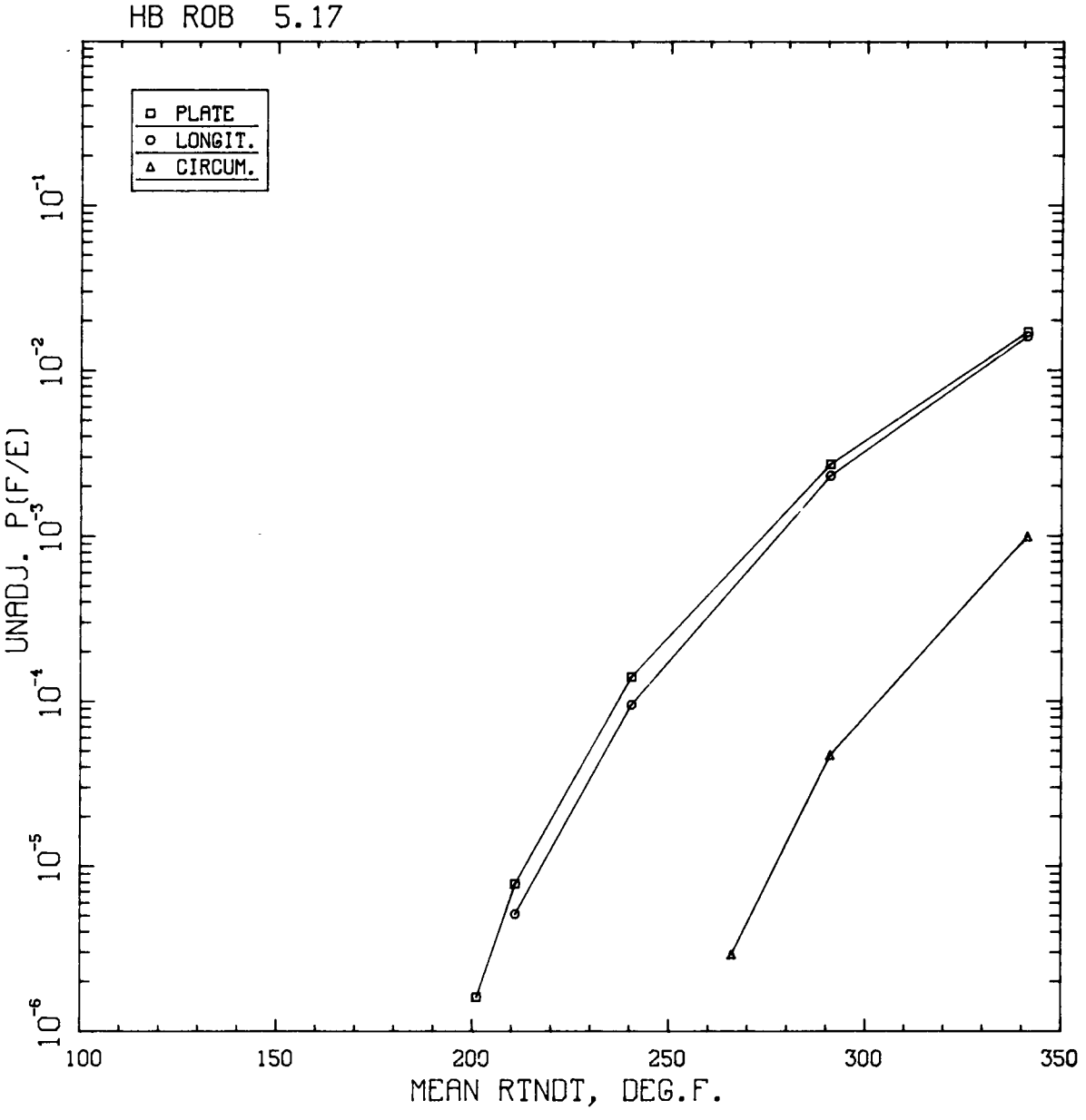

Figure I.8. Transient 5.17: $\hat{P}_j \int_0^w f(a)\, B(a)\, da$ vs $\overline{RTNDT_s}$ for (2-D, 2-D) and (2-D, 2m) flaw combinations.

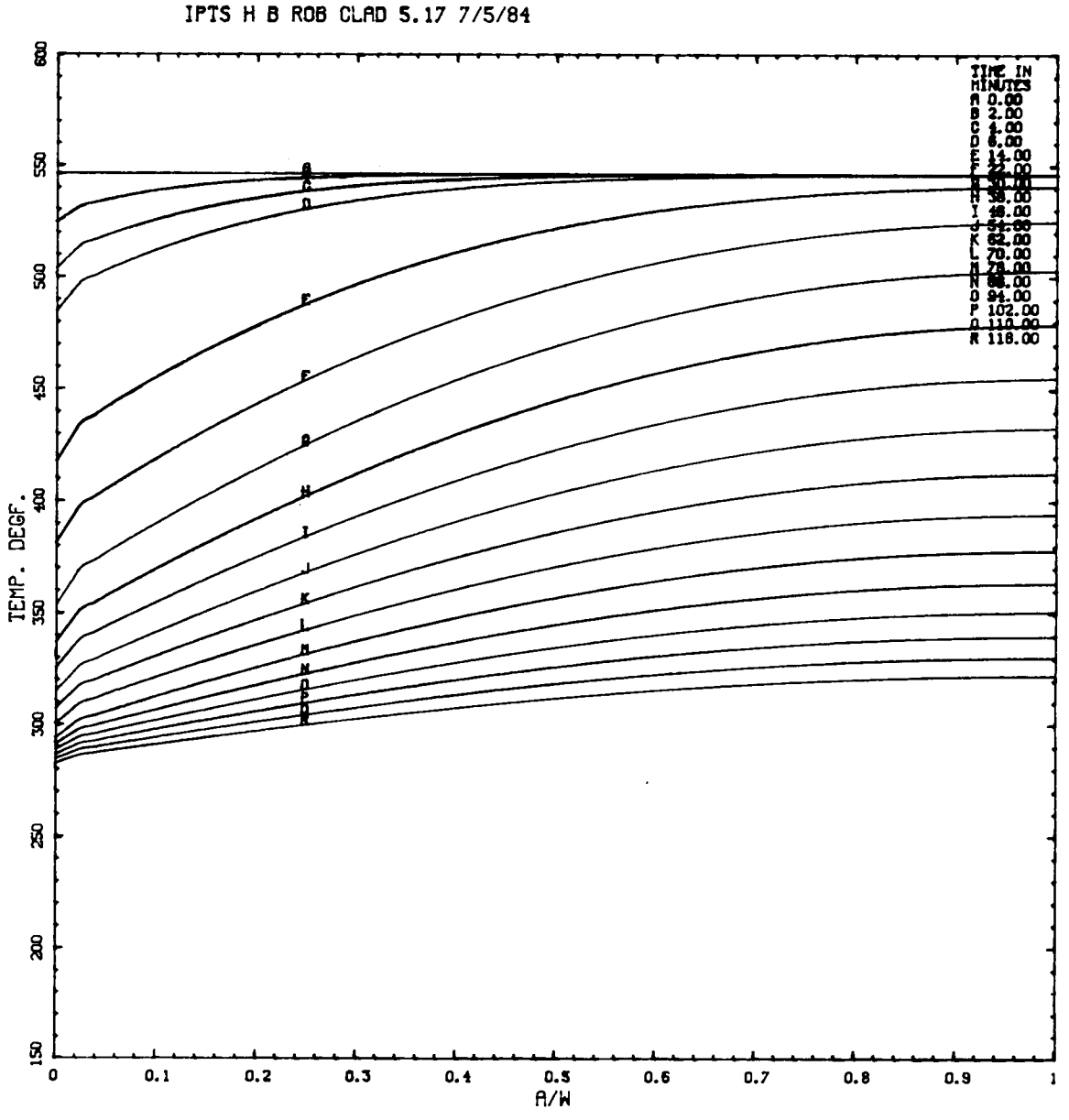

Figure I.9. Transient 5.17: Vessel wall temperature vs depth in wall (a/w) at various times (t) in transient.

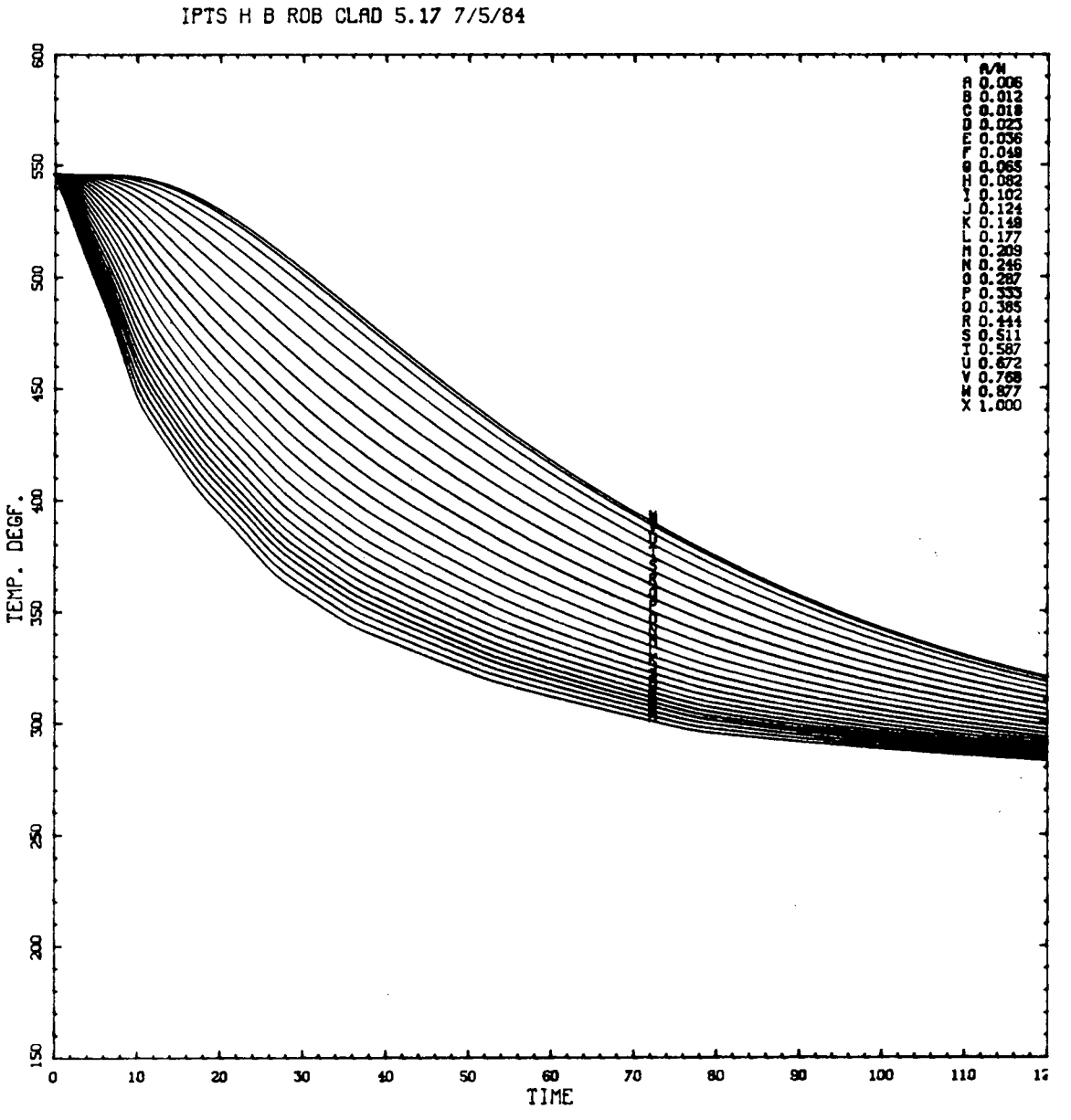

Figure I.10. Transient 5.17: Vessel wall temperature vs time (t) in transient at various depths in wall (a/w).

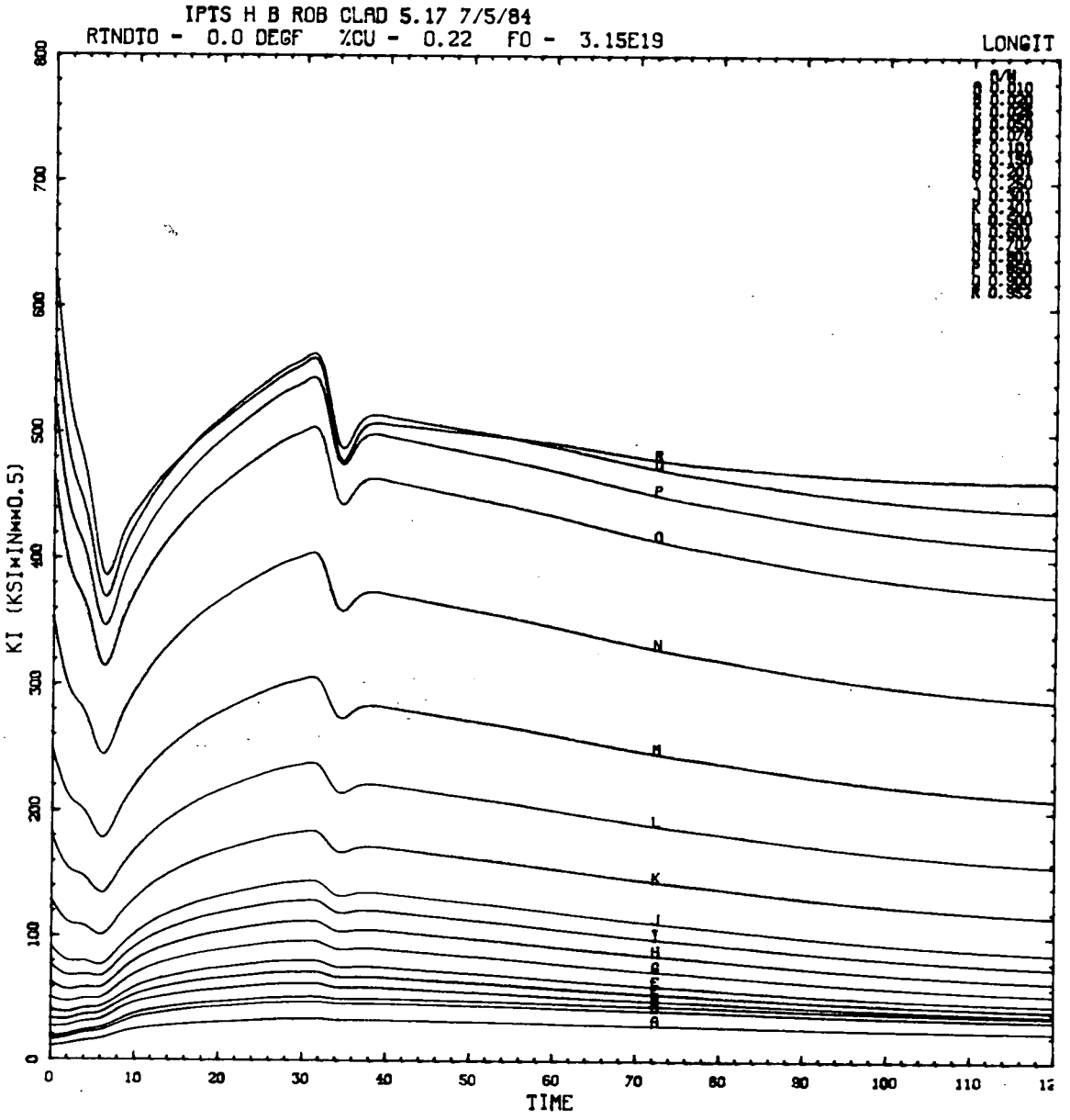

Figure I.11. Transient 5.17: K_I vs time (t) for various depths in wall (a/w).

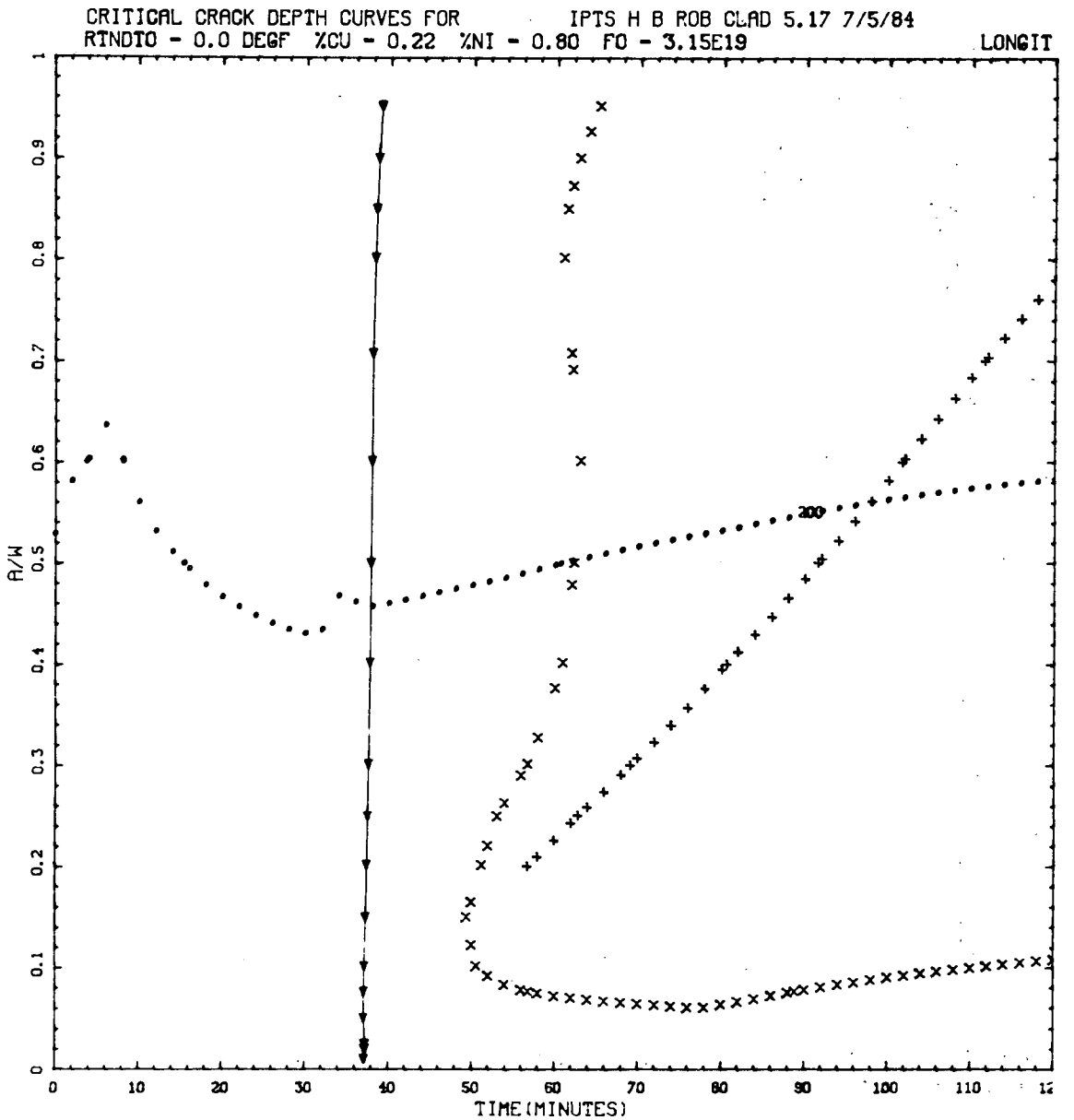

×, 2-D flaw, $K_I = K_{Ia}$
+, 2-m flaw, $K_I = K_{Ia}$
∇, WPS (warm prestressing)

Figure I.12. Transient 5.17: Critical-crack-depth curves for weld 2-273A based on -2σ values of K_{Ic}, K_{Ia}, and $\Delta RTNDT$, mean values of all other parameters, and 32-EFPY fluences.

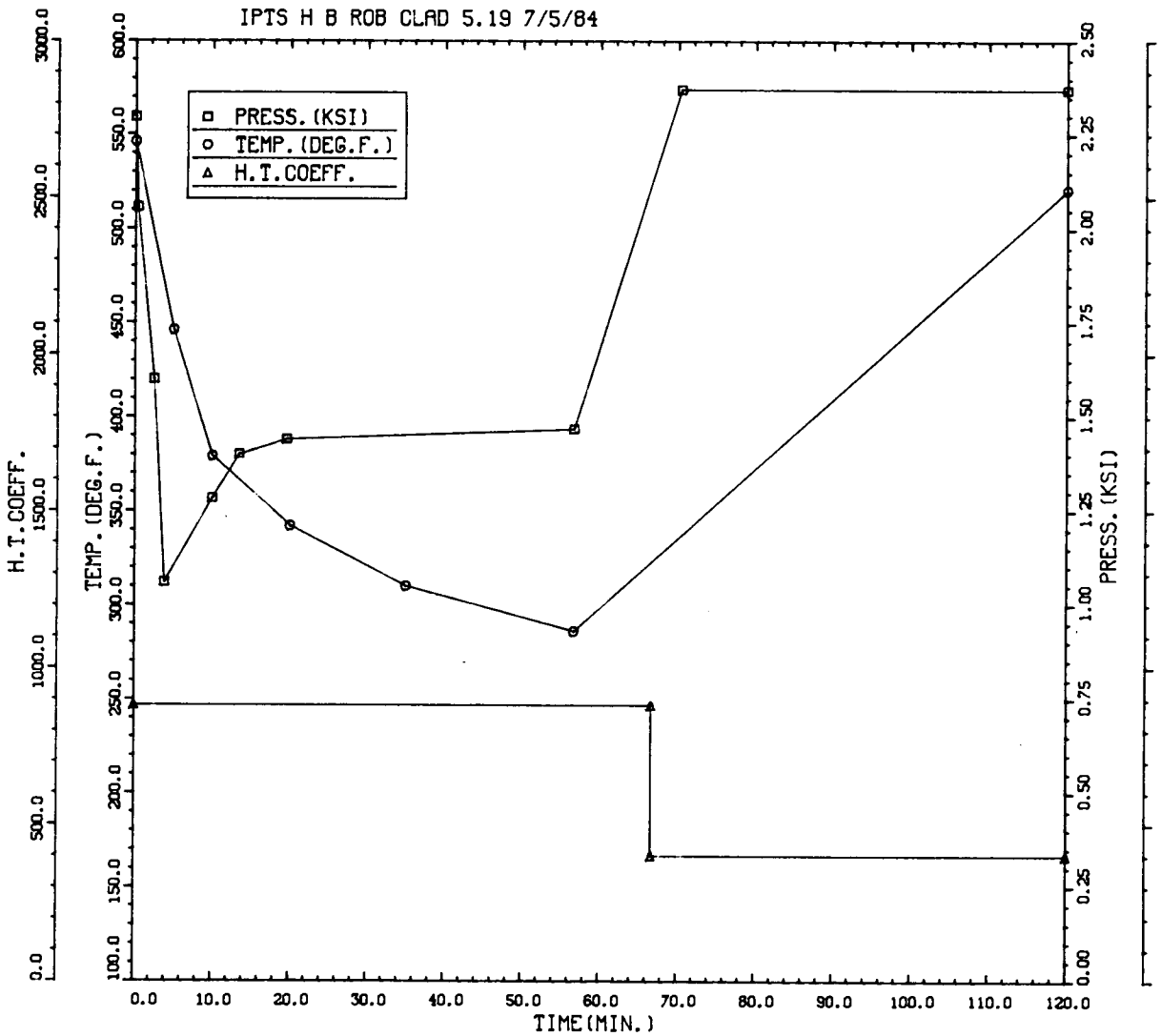

Figure I.13. Transient 5.19: Primary system pressure, downcomer coolant temperature, and fluid-film heat-transfer coefficient vs time in the transient.

Table I.3. Transient 5.19: Summary of digital output, including unadjusted $P(F|E)$ values and histogram data for crack depths, times of failure, and $T - RTNDT$ values at tip of crack corresponding to initiation and arrest events

```
        IPTS H B ROB CLAD 5.19 7/5/84                    1. FLAWS/IN**3    DRTN(IS) =  211.2

        -------------UNADJUSTED--------------            ---ADJUSTED----
WELD    P(F/E)      95%CI     %ERR   P(INITIA)  N*V      P(F/E)    %ERR    NFAIL    NTRIALS

 1      3.64D-06   3.72D-07  10.22   3.45D-05  1.000    3.64D-06            367     200000

                                              VESSEL    3.64D-06  10.22


DEPTHS FOR INITIAL INITIATION (IN)
              0.09  0.26  0.46  0.67  0.90  1.16  1.44  1.74  2.08
    NUMBER       0  1610  1172   460   173    51    13     1     1
    PERCENT    0.0  46.3  33.7  13.2   5.0   1.5   0.4   0.0   0.0


TIMES OF FAILURE(MINUTES)
              0.0  10.0  20.0  30.0  40.0  50.0  60.0  70.0  80.0  90.0 100.0 110.0 120.0
   PERCENT      0.0   0.0   0.0   0.0   1.1  30.5  56.9  11.4   0.0   0.0   0.0   0.0


 INITIATION T-RTNDT(DEG.F)
            -100.0 -75.0 -50.0 -25.0   0.0  25.0  50.0  75.0 100.0 125.0 150.0 175.0 200.0
   NUMBER         0     2   153  1236  1740   376   237    96    10     0     0     0
   PERCENT      0.0   0.1   4.0  32.1  45.2   9.8   6.2   2.5   0.3   0.0   0.0   0.0


 ARREST T-RTNDT(DEG.F)
             -50.0 -25.0   0.0  25.0  50.0  75.0 100.0 125.0 150.0 175.0 200.0 225.0 250.0
   NUMBER         0    17   133    80    11     7   232  2284   719     0     0     0
   PERCENT      0.0   0.5   3.8   2.3   0.3   0.2   6.7  65.6  20.6   0.0   0.0   0.0


 # OF STD DEVS ABOVE MEAN DELTA RTNDT(FAILURES ONLY)
              1.00  1.25  1.50  1.75  2.00  2.25  2.50  2.75  3.00
   NUMBER         0     9    22    44    65    56    85    86
   PERCENT      0.0   2.5   6.0  12.0  17.7  15.3  23.2  23.4


 # OF STD DEVS ABOVE MEAN RTNDT(FAILURES ONLY)
              1.00  1.25  1.50  1.75  2.00  2.25  2.50  2.75  3.00
   NUMBER         0     1     9    27    41    58   114   117
   PERCENT      0.0   0.3   2.5   7.4  11.2  15.8  31.1  31.9


ICRKTP = 2   IACCEL = 1   NDLRS = 2   NRTRS = 2   DATE: 10/29/84   TIME: 22.42.20

CPU TIME:  5 MIN 24 SEC
```

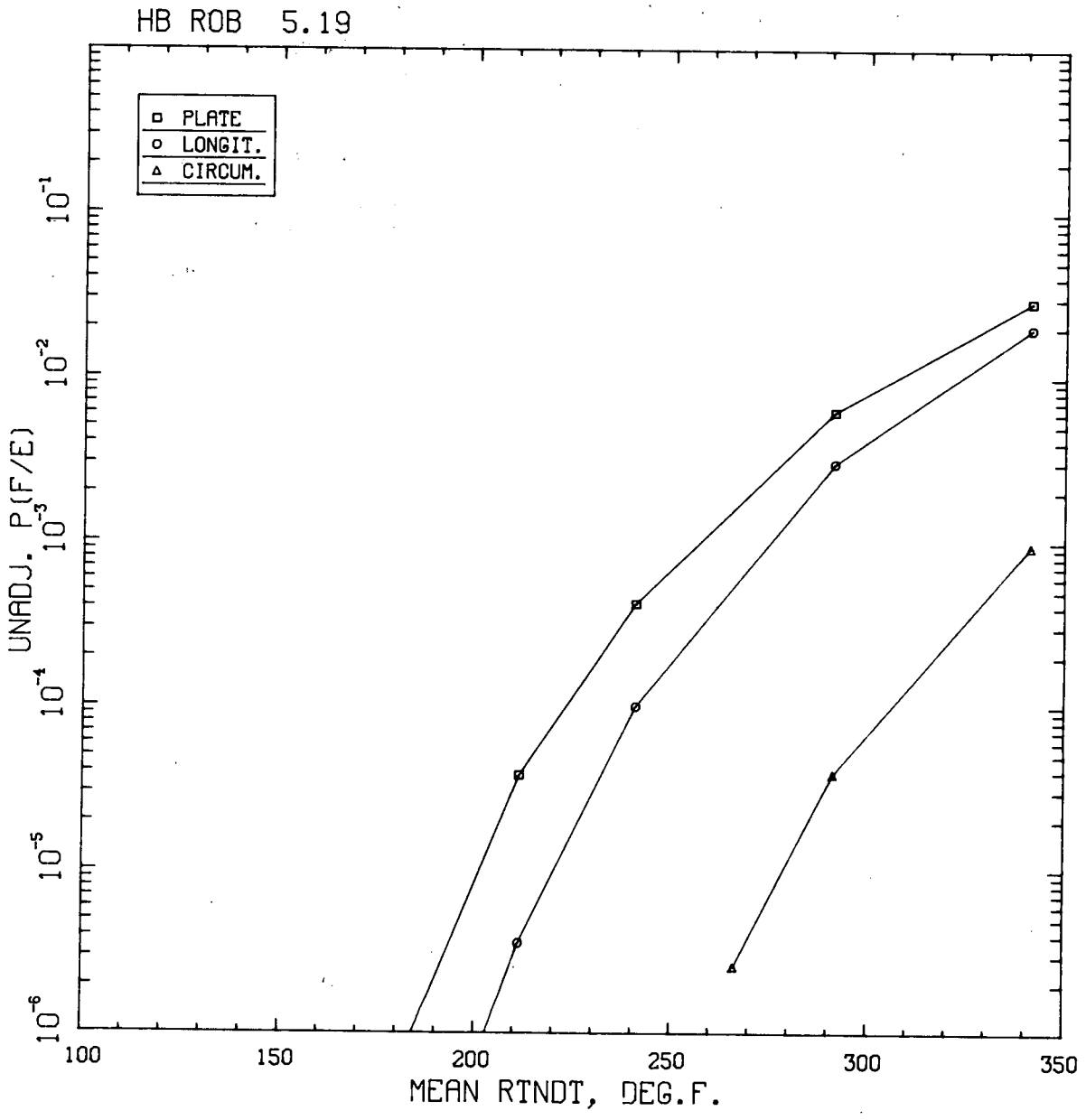

Figure I.14. Transient 5.19: $\hat{P}_j \int_0^w f(a)\, B(a)\, da$ **vs** $\overline{RTNDT_s}$ **for (2-D, 2-D) and (2-D, 2m) flaw combinations.**

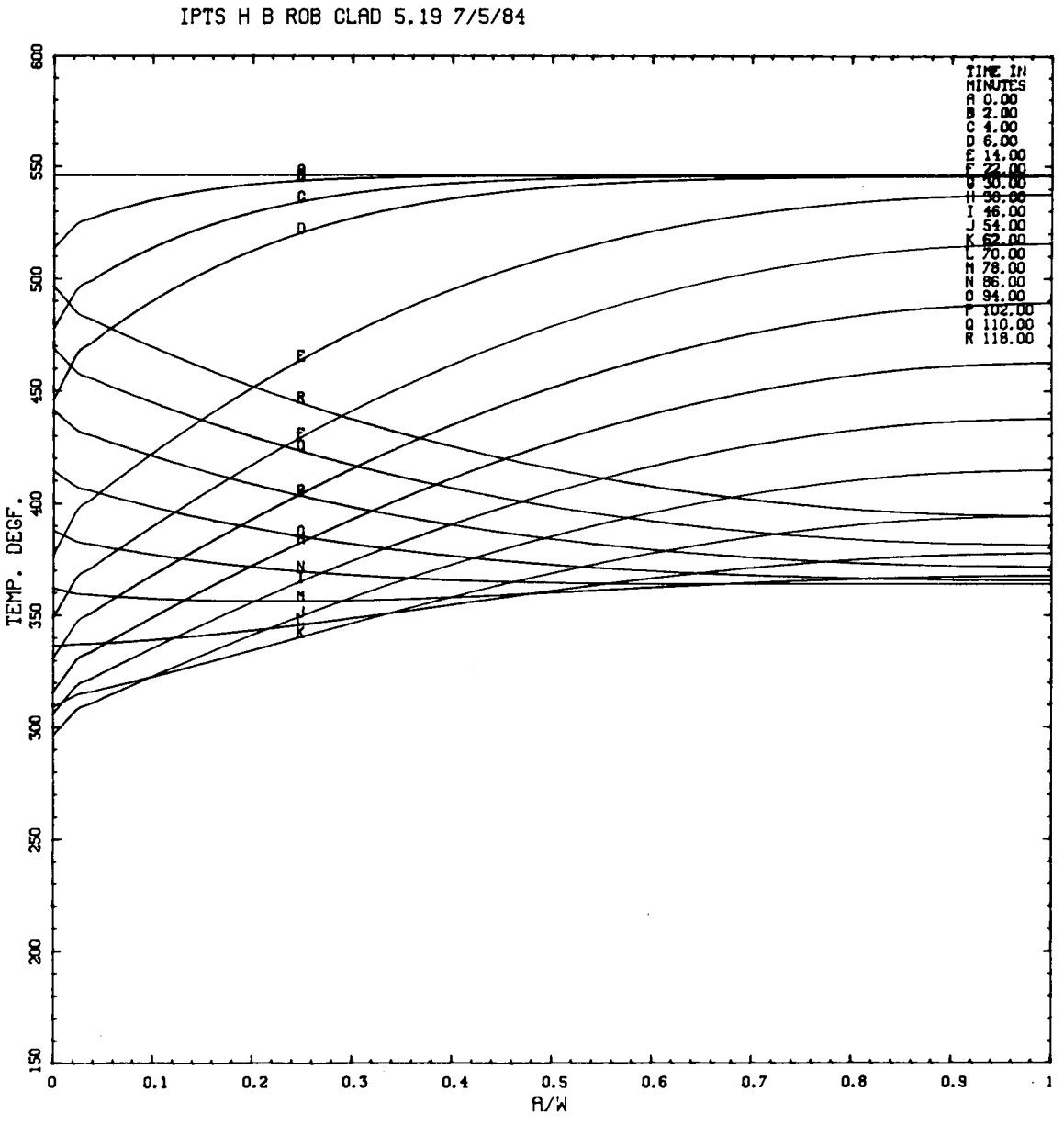

Figure I.15. Transient 5.19: Vessel wall temperature vs depth in wall (a/w) at various times (t) in transient.

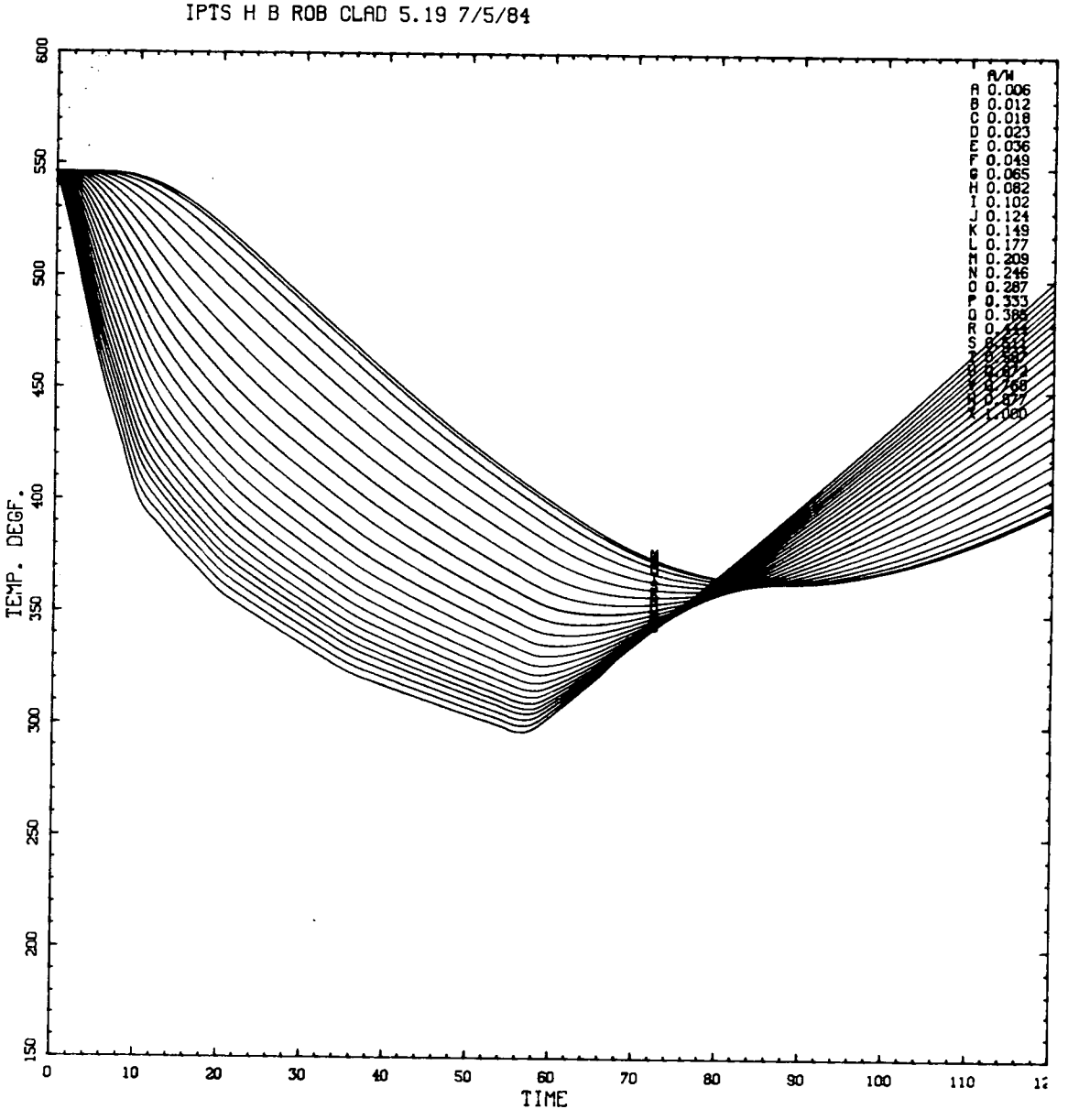

Figure I.16. Transient 5.19: Vessel wall temperature vs time (t) in transient at various depths in wall (a/w).

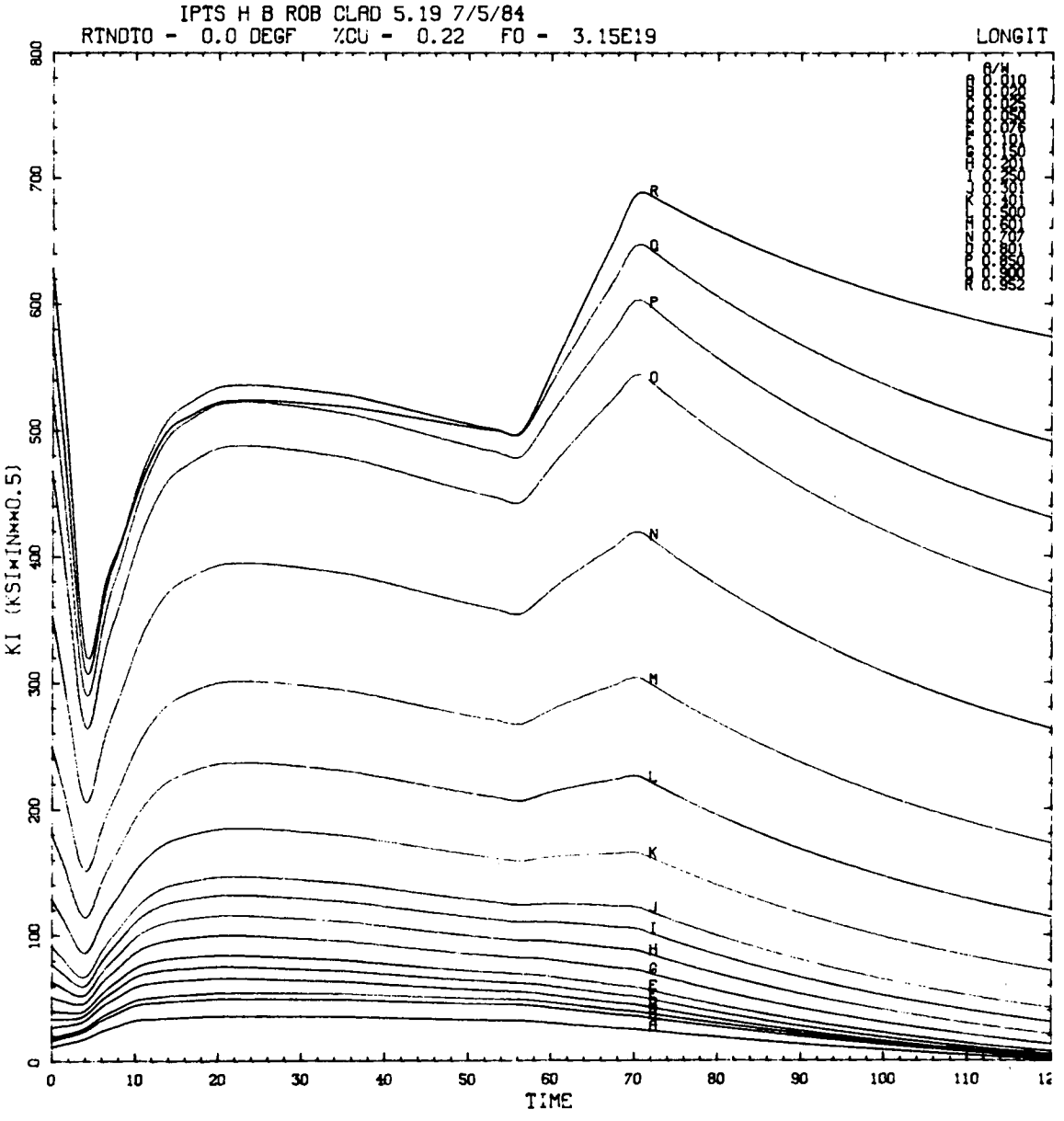

Figure I.17. Transient 5.19: K_I vs time (t) for various depths in wall (a/w).

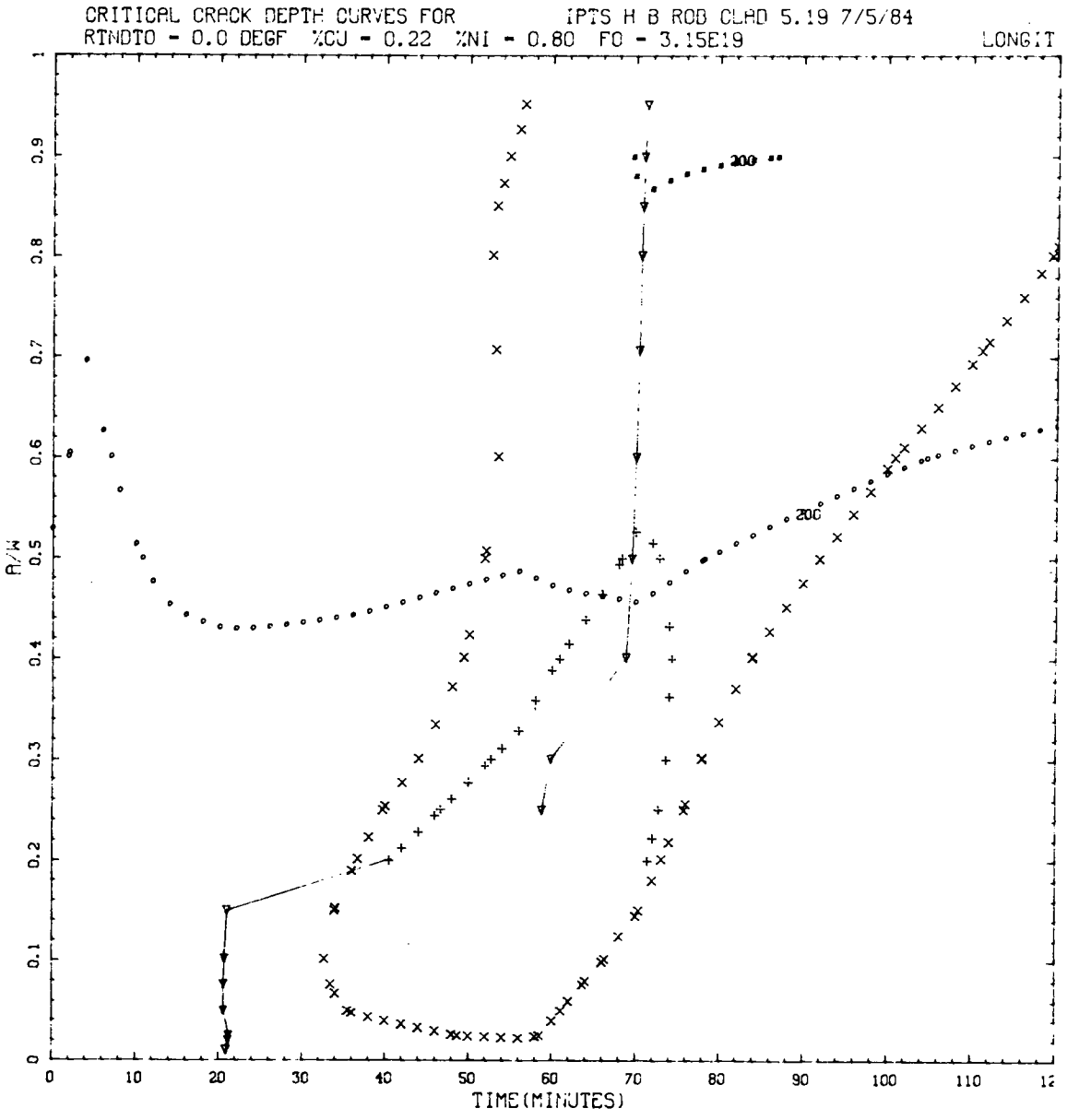

×, 2-D flaw, $K_I = K_{Ia}$
+, 2-m flaw, $K_I = K_{Ia}$
O, 2-D flaw, $K_I = 220$ MPa $\sqrt{m}$
■, 2-m flaw, $K_I = 220$ MPa $\sqrt{m}$
∇, WPS (warm prestressing)

Figure I.18. Transient 5.19: Critical-crack-depth curves for weld 2-273A based on -2σ values of K_{Ic}, K_{Ia}, and $\Delta RTNDT$, mean values of all other parameters, and 32-EFPY fluences.

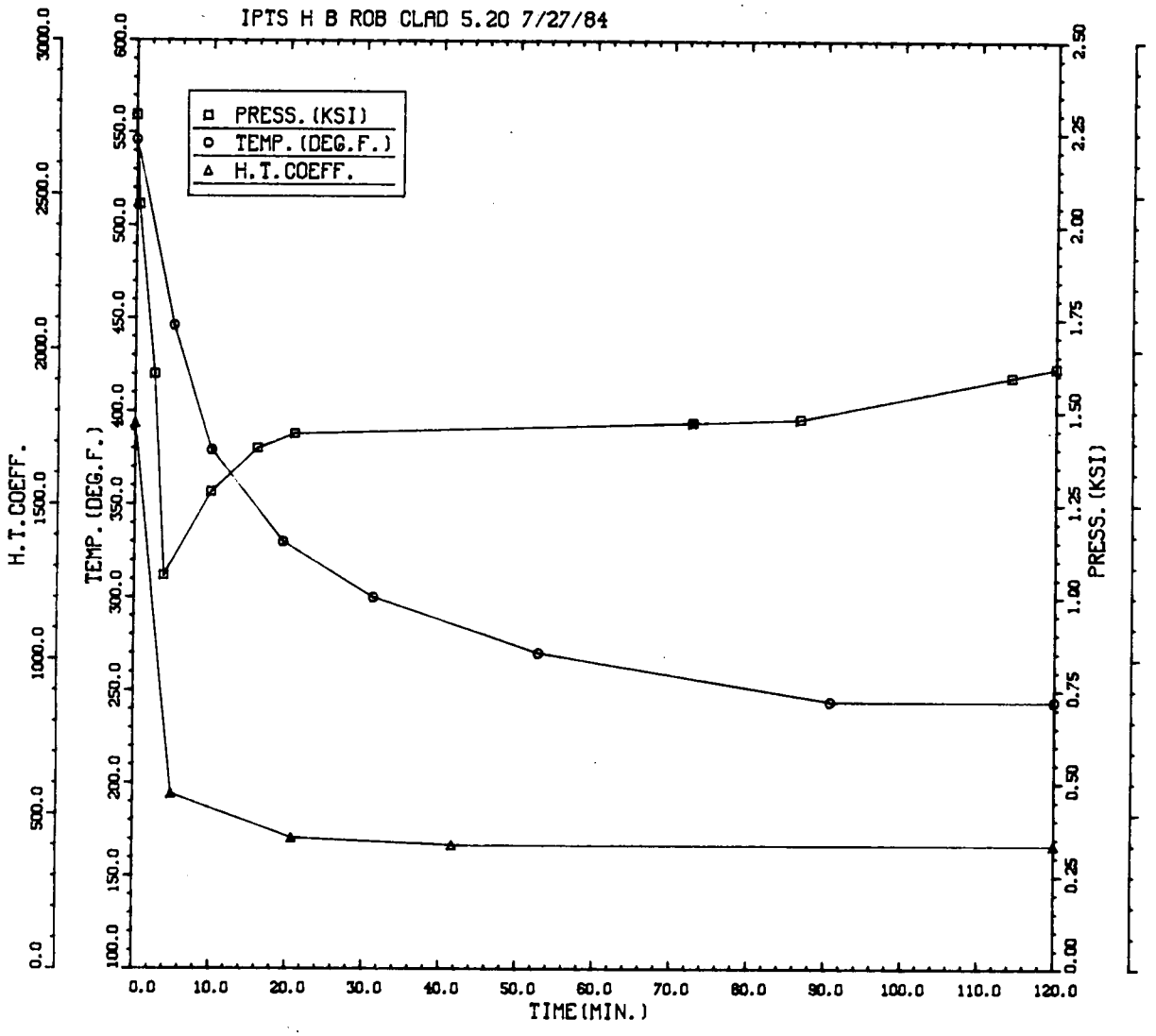

Figure I.19. Transient 5.20: Primary system pressure, downcomer coolant temperature, and fluid-film heat-transfer coefficient vs time in the transient.

Table I.4. Transient 5.20: Summary of digital output, including unadjusted $P(F|E)$ values and histogram data for crack depths, times of failure, and $T - RTNDT$ values at tip of crack corresponding to initiation and arrest events

IPTS H B ROB CLAD 5.20 7/27/84 1. FLAWS/IN**3 DRTN(IS) = 211.2

WELD	P(F/E)	95%CI	%ERR	P(INITIA)	N*V	P(F/E)	%ERR	NFAIL	NTRIALS
	----------UNADJUSTED----------					---ADJUSTED----			
1	1.43D-04	2.23D-05	15.59	2.14D-04	1.000	1.43D-04		158	200000
					VESSEL	1.43D-04	15.59		

DEPTHS FOR INITIAL INITIATION (IN)

	0.09	0.26	0.46	0.67	0.90	1.16	1.44	1.74	2.08
NUMBER	0	121	63	35	12	4	1	0	0
PERCENT	0.0	51.3	26.7	14.8	5.1	1.7	0.4	0.0	0.0

TIMES OF FAILURE(MINUTES)

	0.0	10.0	20.0	30.0	40.0	50.0	60.0	70.0	80.0	90.0	100.0	110.0	120.0
PERCENT	0.0	0.0	0.0	0.0	0.0	2.5	4.4	12.7	25.3	22.2	19.6	13.3	

INITIATION T-RTNDT(DEG.F)

	-100.0	-75.0	-50.0	-25.0	0.0	25.0	50.0	75.0	100.0	125.0	150.0	175.0	200.0
NUMBER	0	0	13	120	101	61	65	11	0	0	0	0	
PERCENT	0.0	0.0	3.5	32.3	27.2	16.4	17.5	3.0	0.0	0.0	0.0	0.0	

ARREST T-RTNDT(DEG.F)

	-50.0	-25.0	0.0	25.0	50.0	75.0	100.0	125.0	150.0	175.0	200.0	225.0	250.0
NUMBER	0	14	24	2	0	0	16	121	36	0	0	0	
PERCENT	0.0	6.6	11.3	0.9	0.0	0.0	7.5	56.8	16.9	0.0	0.0	0.0	

ICRKTP = 2 IACCEL = 1 NDLRS = 0 NRTRS = 0 DATE: 10/29/84 TIME: 22.42.23

CPU TIME: 5 MIN 29 SEC

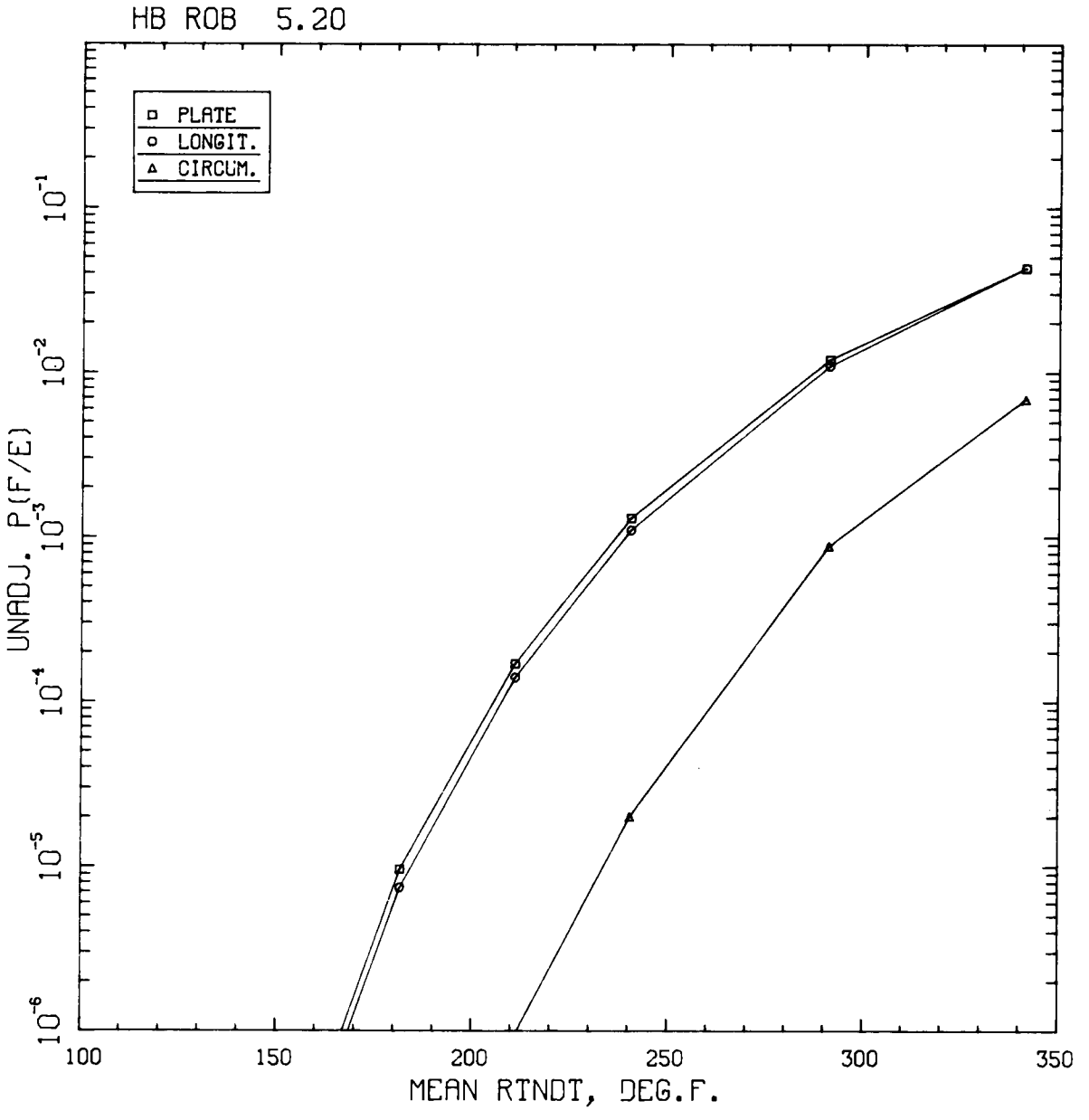

Figure I.20. Transient 5.20: $\hat{P}_j \int_0^w f(a)\, B(a)\, da$ vs $\overline{RTNDT_s}$ for (2-D, 2-D) and (2-D, 2m) flaw combinations.

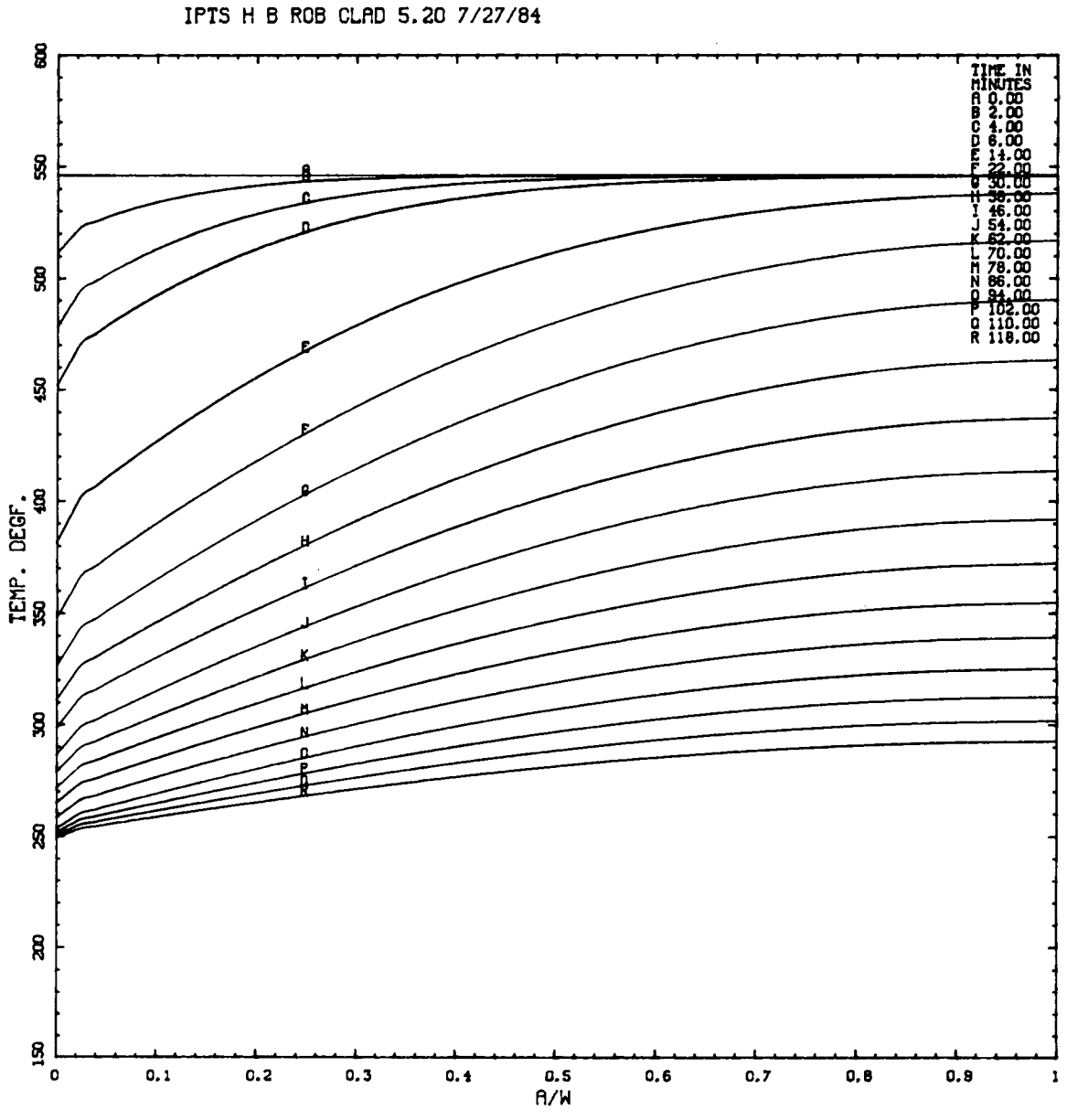

Figure I.21. Transient 5.20: Vessel wall temperature vs depth in wall (a/w) at various times (t) in transient.

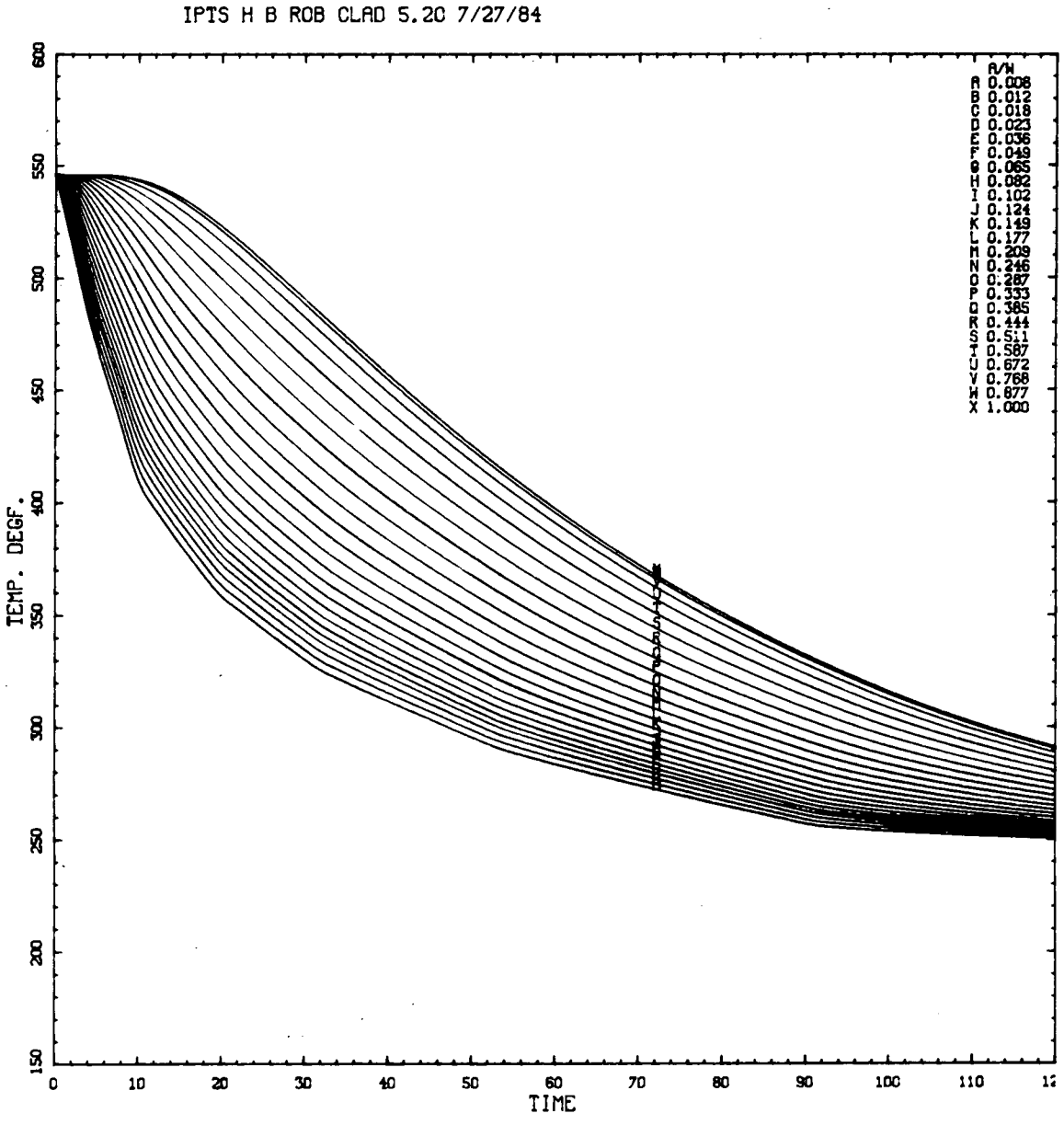

Figure I.22. Transient 5.20: Vessel wall temperature vs time (t) in transient at various depths in wall (a/w).

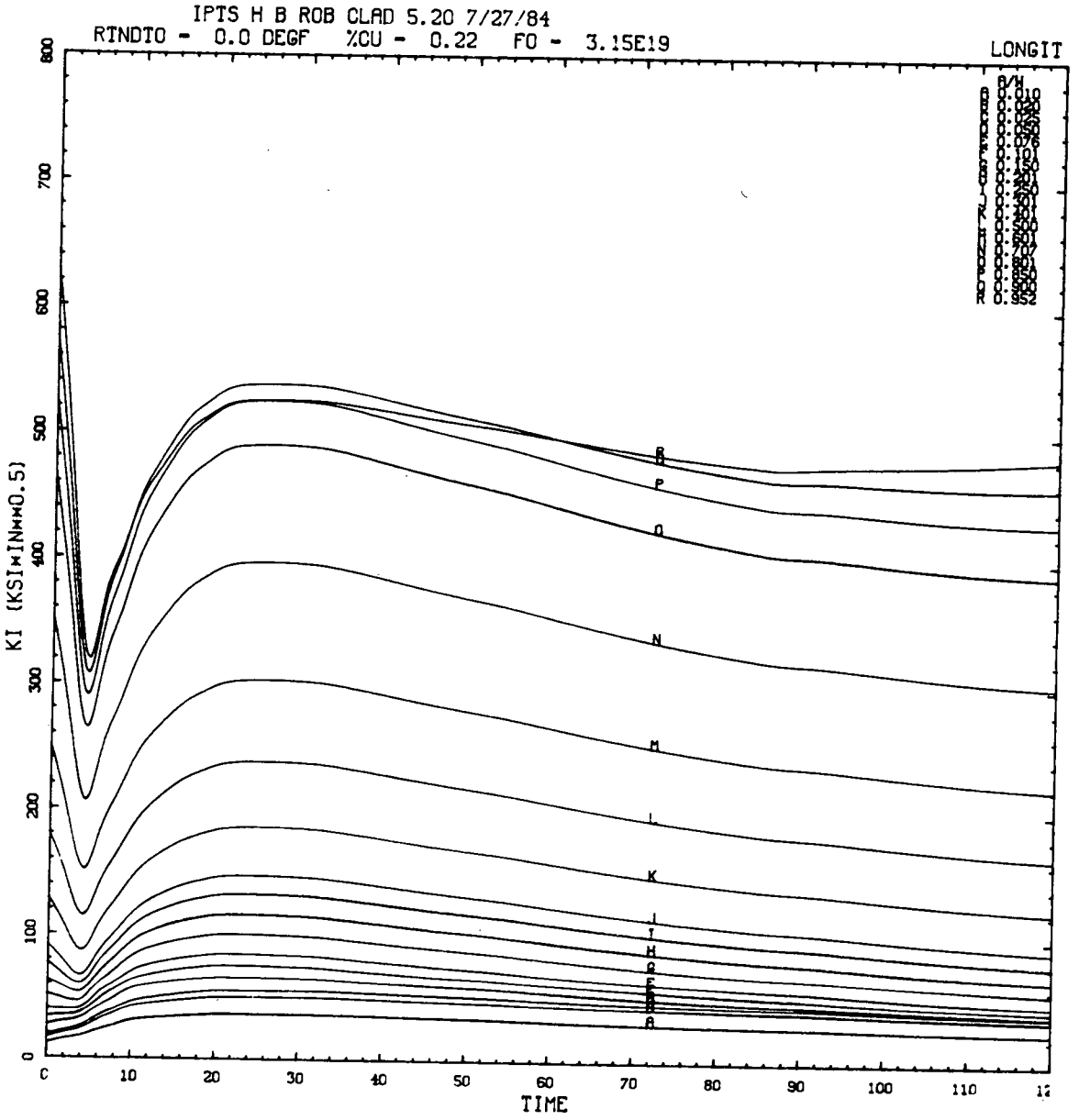

Figure I.23. Transient 5.20: K_I vs time (t) for various depths in wall (a/w).

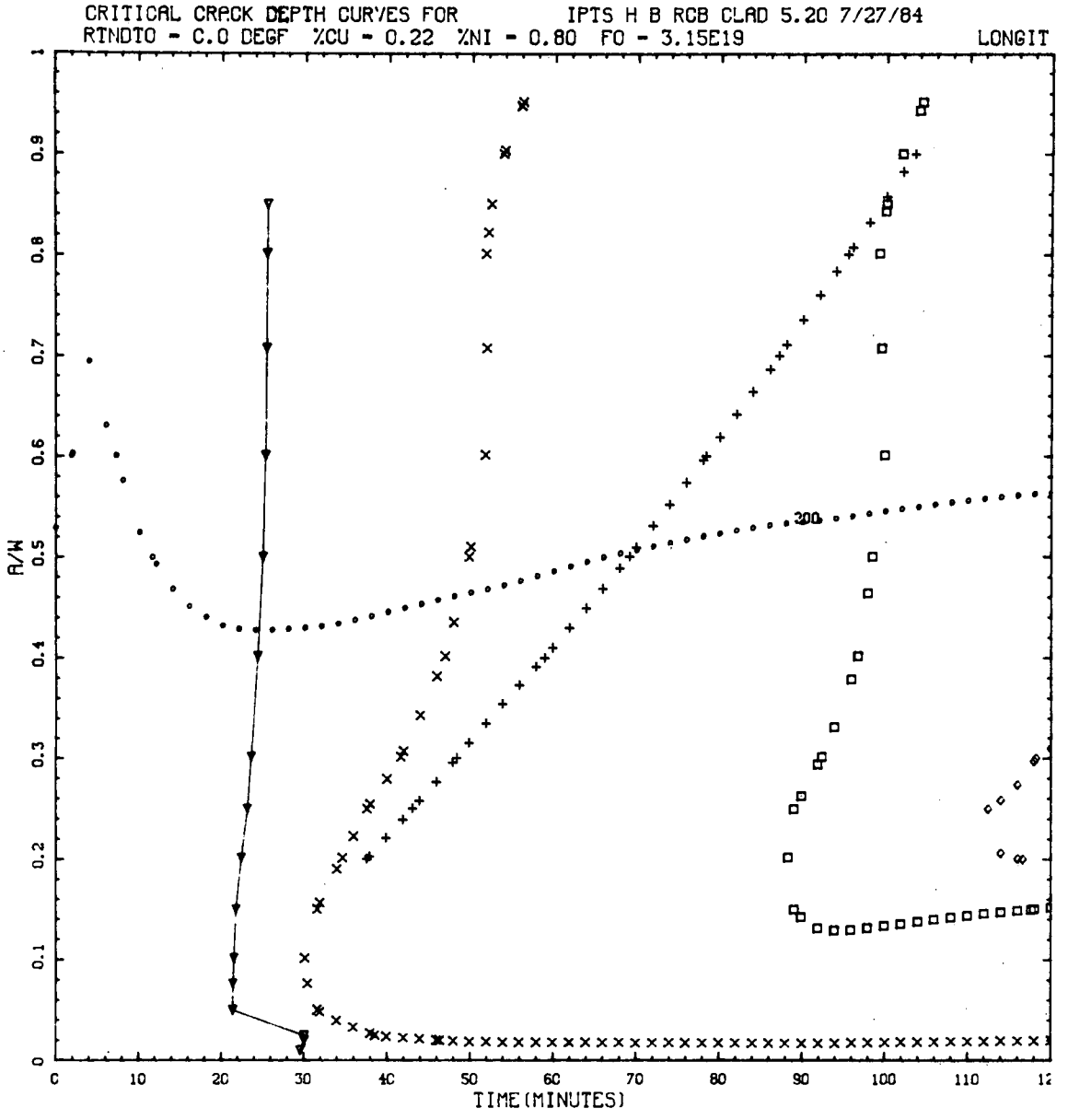

×, 2-D flaw, $K_I = K_{Ia}$
+, 2-m flaw, $K_I = K_{Ia}$
□, 2-D flaw, $K_I = K_{Ic}$
◊, 2-m flaw, $K_I = K_{Ic}$
O, 2-D flaw, $K_I = 220$ MPa $\sqrt{m}$
∇, WPS (warm prestressing)

Figure I.24. Transient 5.20: Critical-crack-depth curves for weld 2-273A based on -2σ values of K_{Ic}, K_{Ia}, and $\Delta RTNDT$, mean values of all other parameters, and 32-EFPY fluences.

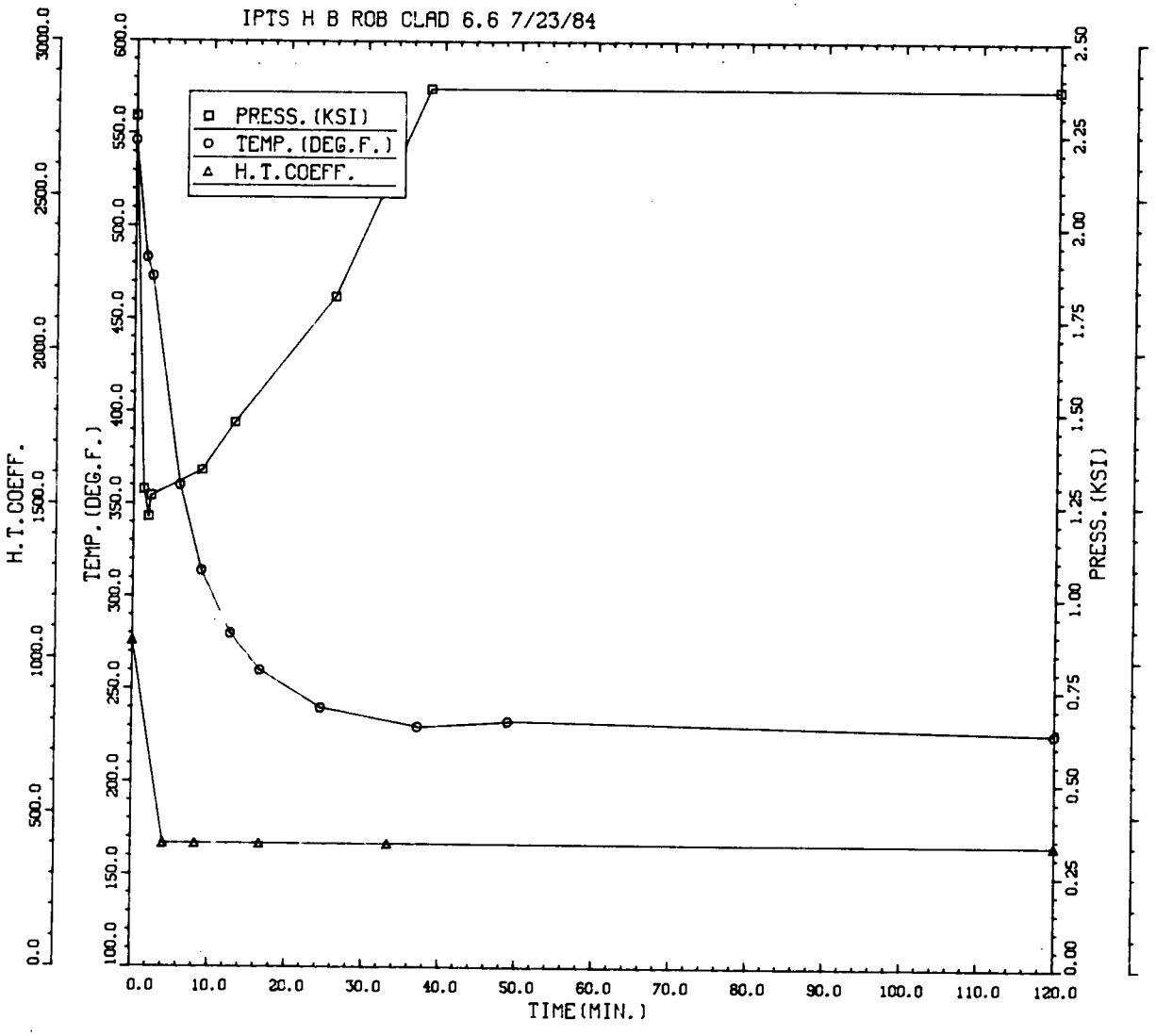

Figure I.25. Transient 6.6: Primary system pressure, downcomer coolant temperature, and fluid-film heat-transfer coefficient vs time in the transient.

Table I.5. Transient 6.6: Summary of digital output, including unadjusted $P(F|E)$ values and histogram data for crack depths, times of failure, and $T - RTNDT$ values at tip of crack corresponding to initiation and arrest events

IPTS H B ROB CLAD 6.6 7/23/84 1. FLAWS/IN**3 DRTN(IS) = 211.2

	----------UNADJUSTED----------					---ADJUSTED----			
WELD	P(F/E)	95%CI	%ERR	P(INITIA)	N*V	P(F/E)	%ERR	NFAIL	NTRIALS
1	8.83D-03	8.09D-04	9.16	9.08D-03	1.000	8.83D-03		451	30000
					VESSEL	8.83D-03	9.16		

DEPTHS FOR INITIAL INITIATION (IN)

	0.09	0.26	0.46	0.67	0.90	1.16	1.44	1.74	2.08
NUMBER	16	277	120	42	9	0	0	0	0
PERCENT	3.4	59.7	25.9	9.1	1.9	0.0	0.0	0.0	0.0

TIMES OF FAILURE(MINUTES)

	0.0	10.0	20.0	30.0	40.0	50.0	60.0	70.0	80.0	90.0	100.0	110.0	120.0
PERCENT	0.0	0.0	4.7	40.4	7.5	11.1	13.5	12.0	4.9	3.5	1.3	1.1	

INITIATION T-RTNDT(DEG.F)

	-100.0	-75.0	-50.0	-25.0	0.0	25.0	50.0	75.0	100.0	125.0	150.0	175.0	200.0
NUMBER	1	0	12	110	215	151	159	80	2	0	0	0	
PERCENT	0.1	0.0	1.6	15.1	29.5	20.7	21.8	11.0	0.3	0.0	0.0	0.0	

ARREST T-RTNDT(DEG.F)

	-50.0	-25.0	0.0	25.0	50.0	75.0	100.0	125.0	150.0	175.0	200.0	225.0	250.0
NUMBER	0	0	0	0	0	0	1	26	123	126	3	0	
PERCENT	0.0	0.0	0.0	0.0	0.0	0.0	0.4	9.3	44.1	45.2	1.1	0.0	

ICRKTP = 2 IACCEL = 0 NDLRS = 0 NRTRS = 0 DATE: 10/29/84 TIME: 23.26.22

CPU TIME: 0 MIN 57 SEC

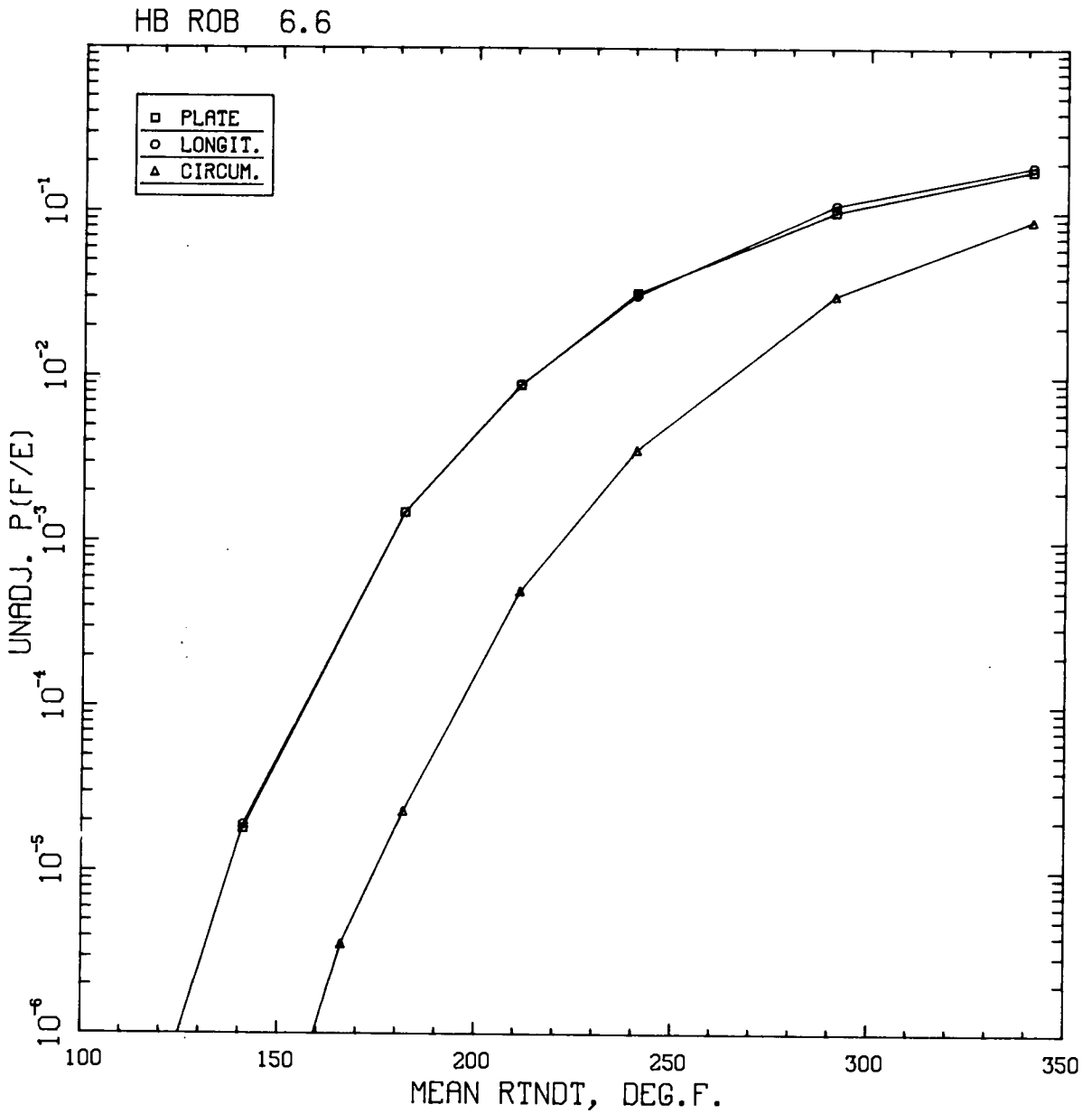

Figure I.26. Transient 6.6: $\hat{P}_j \int_0^w f(a)\, B(a)\, da$ vs $\overline{RTNDT_s}$ for (2-D, 2-D) and (2-D, 2m) flaw combinations.

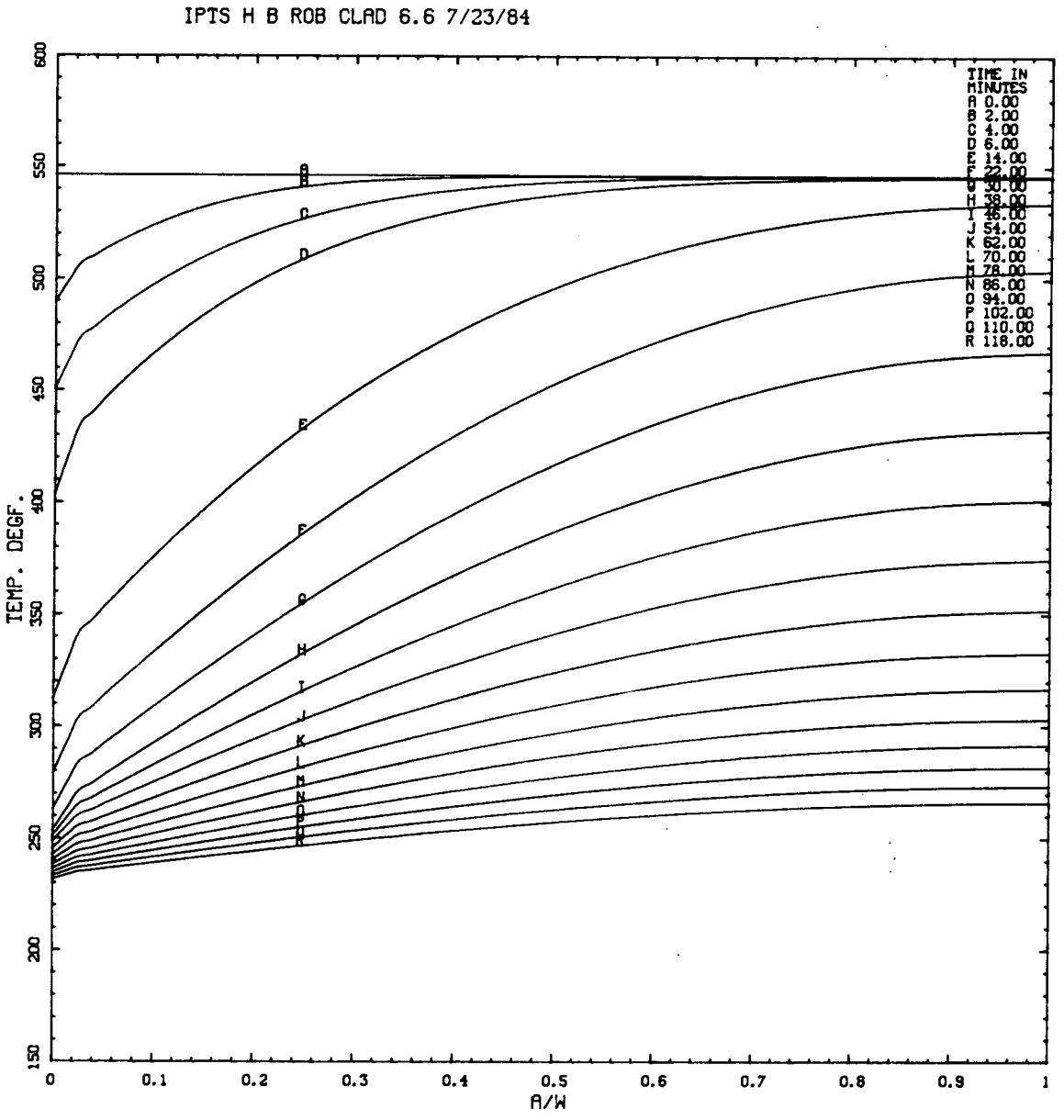

Figure I.27. Transient 6.6: Vessel wall temperature vs depth in wall (a/w) at various times (t) in transient.

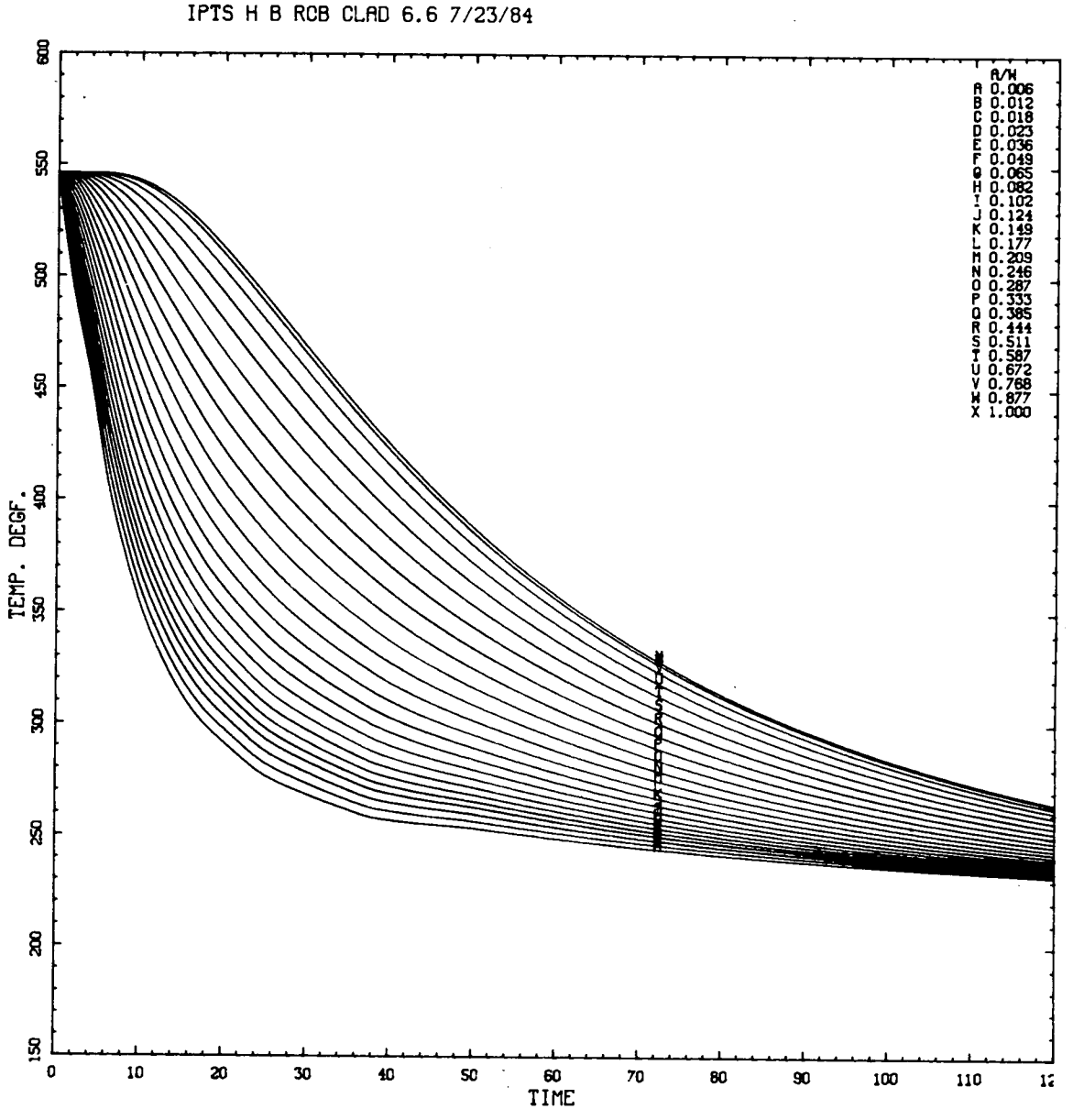

Figure I.28. Transient 6.6: Vessel wall temperature vs time (t) in transient at various depths in wall (a/w).

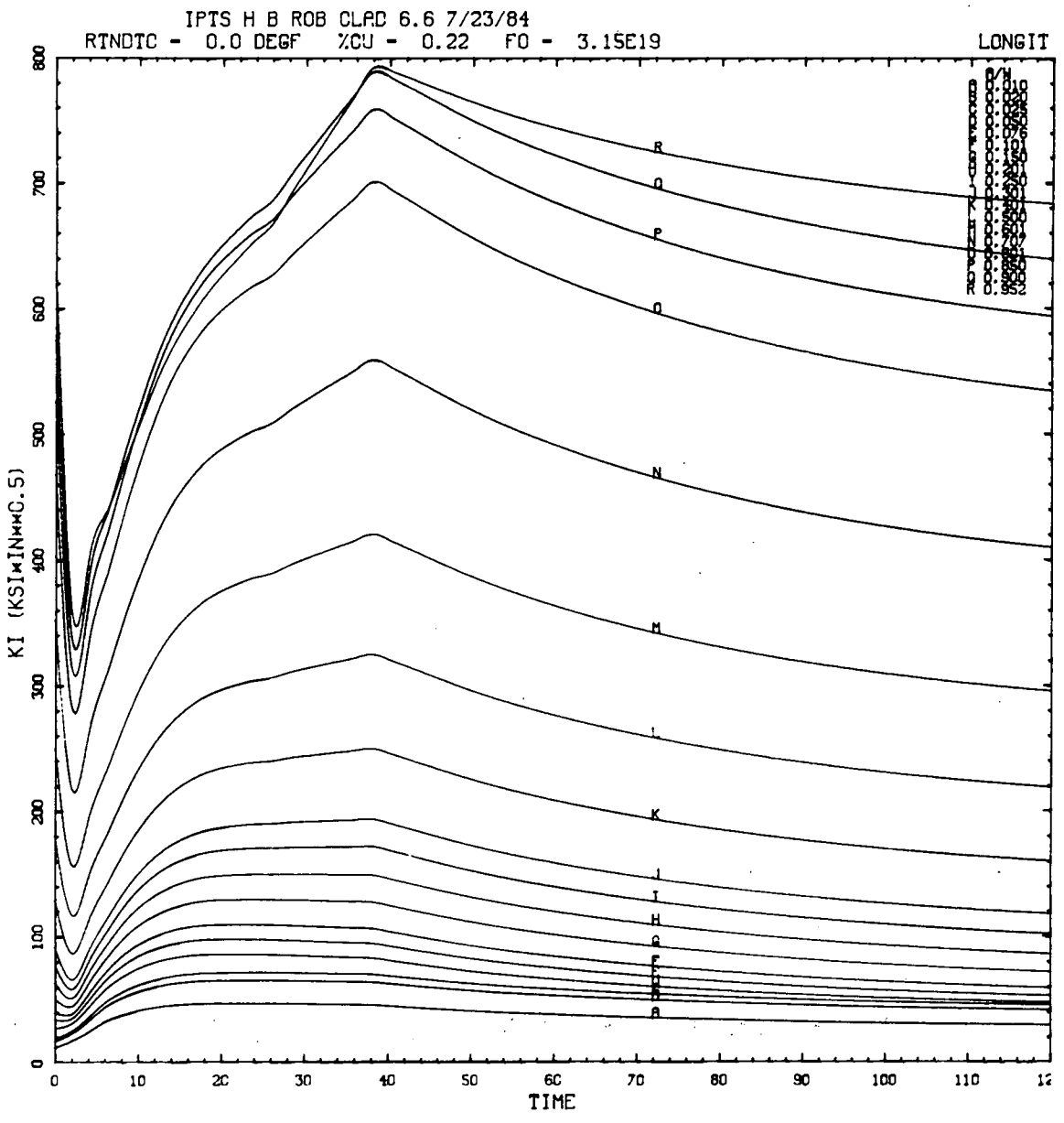

Figure I.29. Transient 6.6: K_I vs time (t) for various depths in wall (a/w).

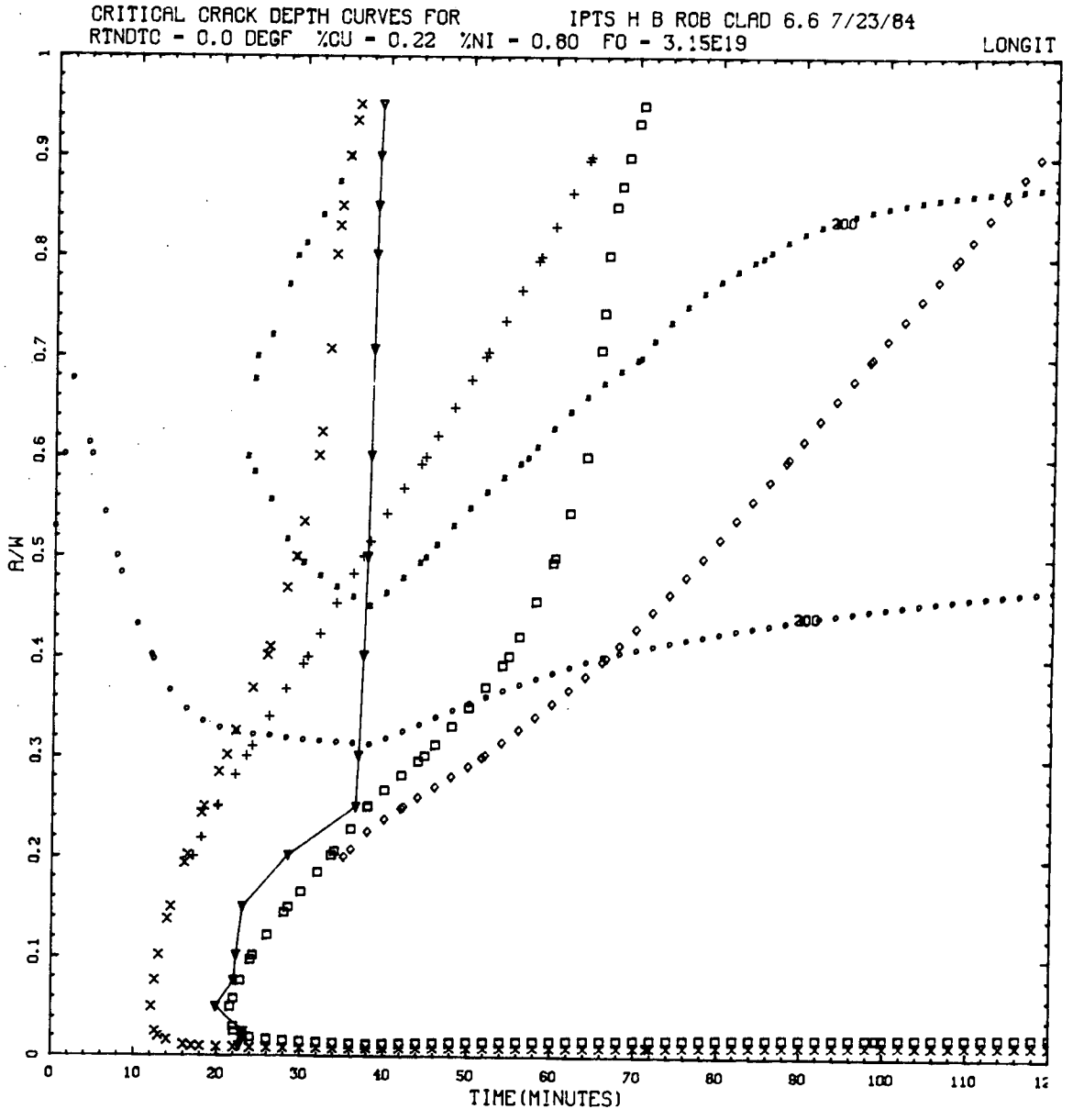

×, 2-D flaw, $K_I = K_{Ia}$
+, 2-m flaw, $K_I = K_{Ia}$
□, 2-D flaw, $K_I = K_{Ic}$
◊, 2-m flaw, $K_I = K_{Ic}$
○, 2-D flaw, K_I = 220 MPa $\sqrt{m}$
■, 2-m flaw, K_I = 220 MPa $\sqrt{m}$
∇, WPS (warm prestressing)

Figure I.30. Transient 6.6: Critical-crack-depth curves for weld 2-273A based on -2σ values of K_{Ic}, K_{Ia}, and $\Delta RTNDT$, mean values of all other parameters, and 32-EFPY fluences.

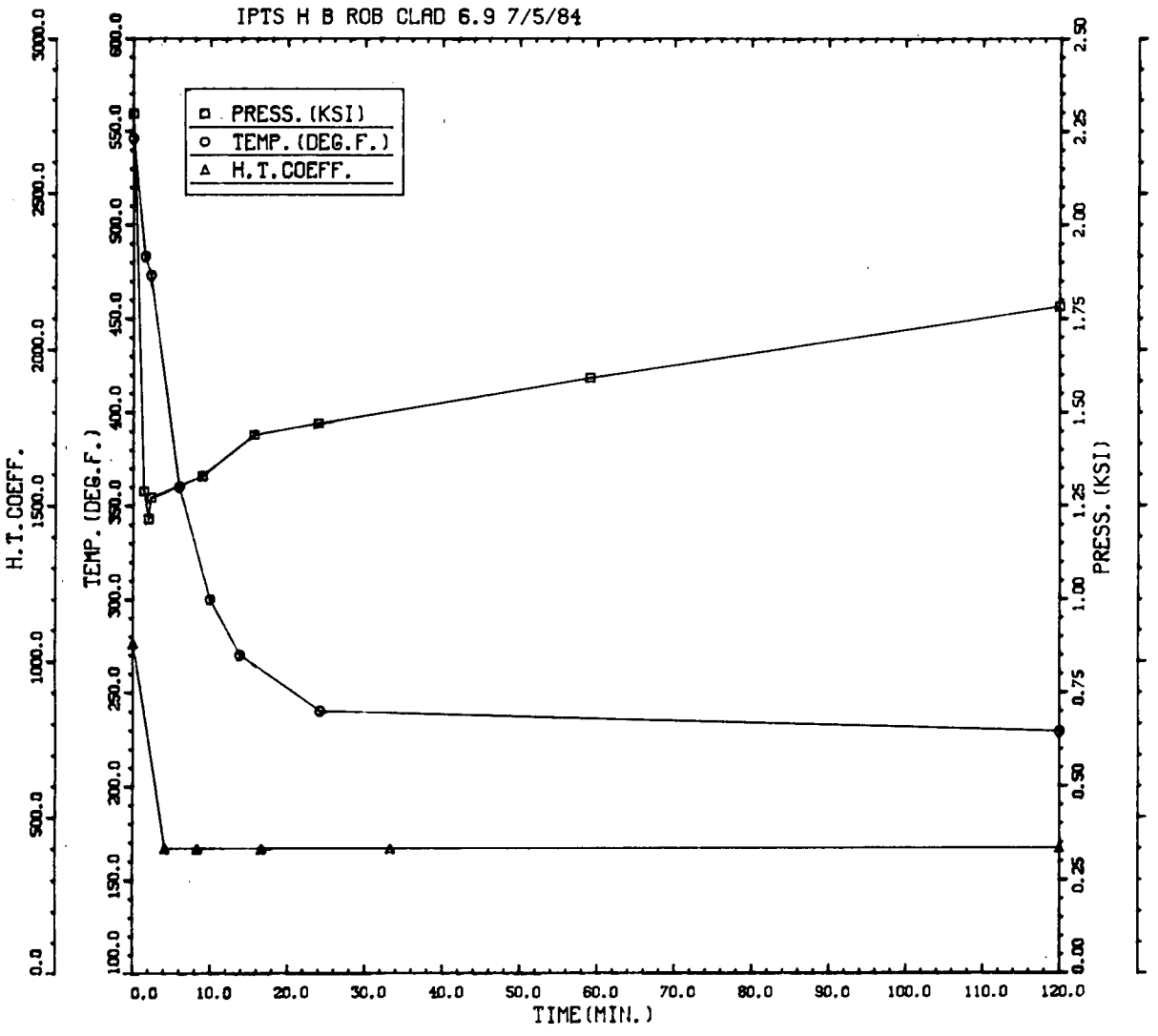

Figure I.31. Transient 6.9: Primary system pressure, downcomer coolant temperature, and fluid-film heat-transfer coefficient vs time in the transient.

Table I.6. Transient 6.9: Summary of digital output, including unadjusted $P(F|E)$ values and histogram data for crack depths, times of failure, and $T - RTNDT$ values at tip of crack corresponding to initiation and arrest events

IPTS H B ROB CLAD 6.9 7/5/84 1. FLAWS/IN**3 DRTN(IS) = 211.2

WELD	P(F/E)	95%CI	%ERR	P(INITIA)	N*V	P(F/E)	%ERR	NFAIL	NTRIALS
	----------UNADJUSTED----------					---ADJUSTED----			
1	2.68D-03	2.59D-04	9.65	3.27D-03	1.000	2.68D-03		411	90000
					VESSEL	2.68D-03	9.65		

DEPTHS FOR INITIAL INITIATION (IN)

	0.09	0.26	0.46	0.67	0.90	1.16	1.44	1.74	2.08
NUMBER	18	299	134	41	8	1	0	0	0
PERCENT	3.6	59.7	26.7	8.2	1.6	0.2	0.0	0.0	0.0

TIMES OF FAILURE(MINUTES)

	0.0	10.0	20.0	30.0	40.0	50.0	60.0	70.0	80.0	90.0	100.0	110.0	120.0
PERCENT	0.0	0.0	1.2	3.4	6.3	11.9	20.4	19.5	17.5	10.9	5.1	3.6	

INITIATION T-RTNDT(DEG.F)

	-100.0	-75.0	-50.0	-25.0	0.0	25.0	50.0	75.0	100.0	125.0	150.0	175.0	200.0
NUMBER	0	1	17	106	285	300	204	34	0	0	0	0	
PERCENT	0.0	0.1	1.8	11.2	30.1	31.7	21.5	3.6	0.0	0.0	0.0	0.0	

ARREST T-RTNDT(DEG.F)

	-50.0	-25.0	0.0	25.0	50.0	75.0	100.0	125.0	150.0	175.0	200.0	225.0	250.0
NUMBER	0	0	0	0	0	1	8	119	289	118	1	0	
PERCENT	0.0	0.0	0.0	0.0	0.0	0.2	1.5	22.2	53.9	22.0	0.2	0.0	

ICRKTP = 2 IACCEL = 0 NDLRS = 0 NRTRS = 0 DATE: 10/29/84 TIME: 23.33.58

CPU TIME: 2 MIN 32 SEC

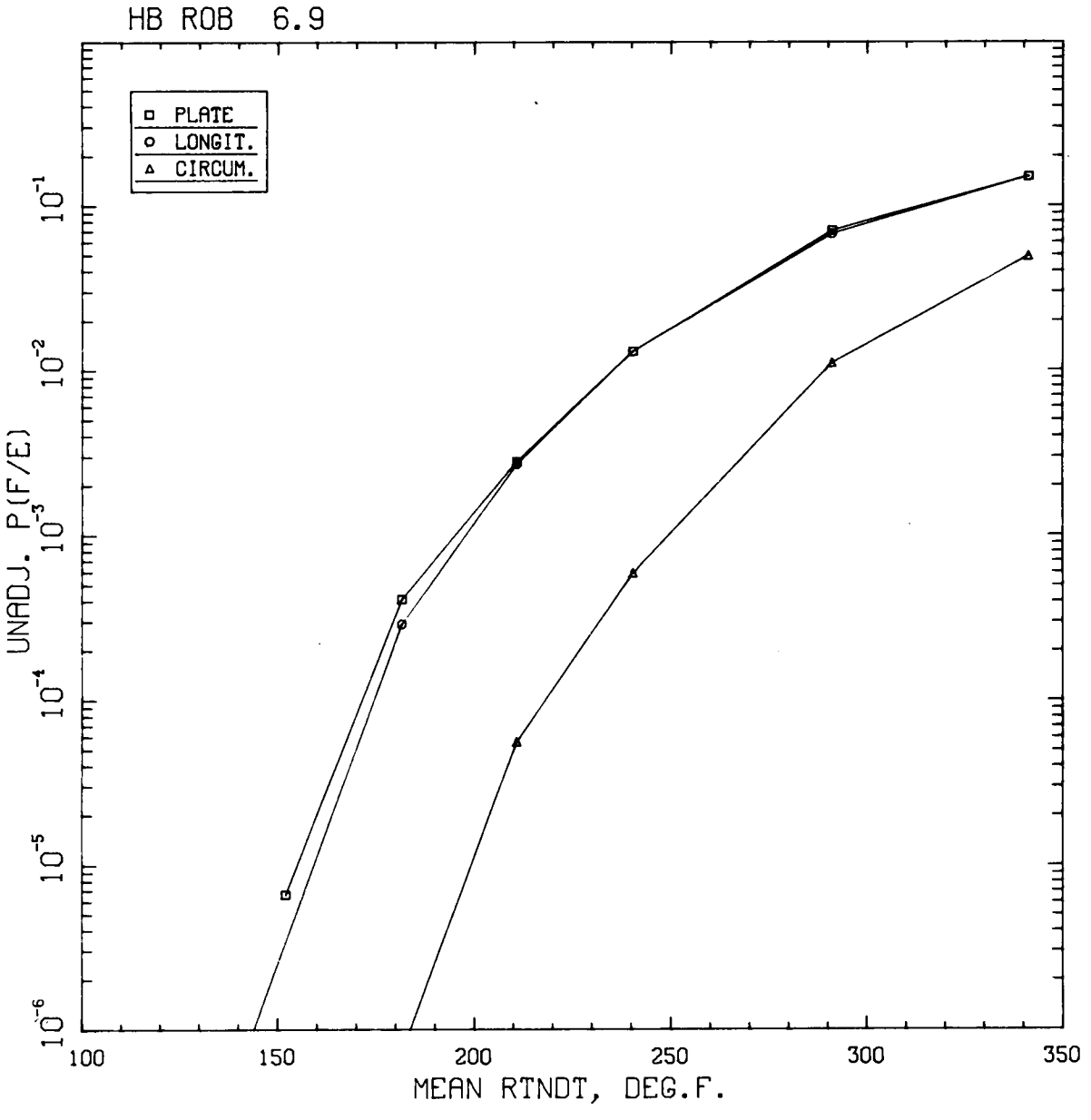

Figure I.32. Transient 6.9: $\hat{P}_j \int_0^w f(a)\, B(a)\, da$ vs $\overline{RTNDT_s}$ for (2-D, 2-D) and (2-D, 2m) flaw combinations.

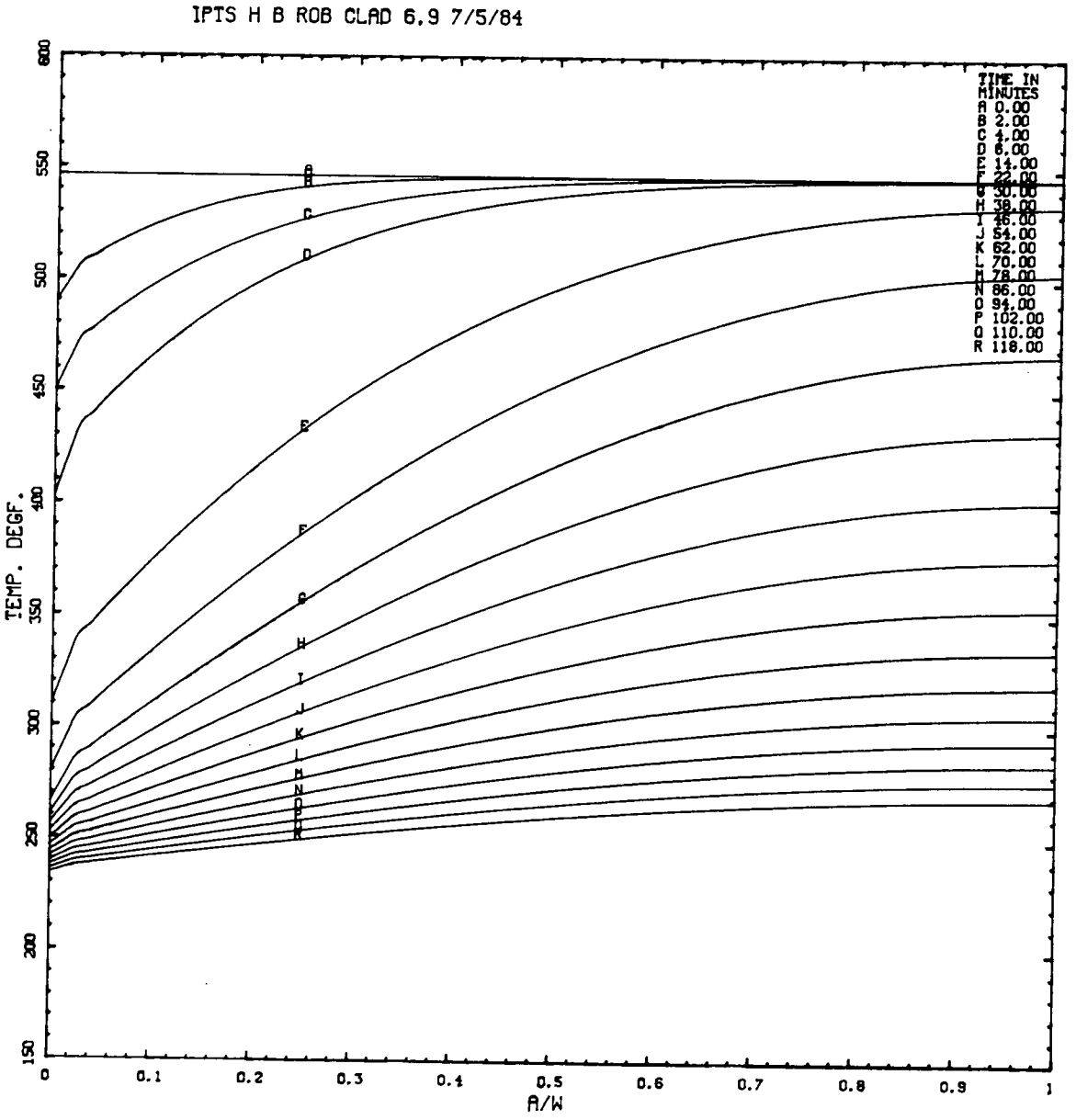

Figure I.33. Transient 6.9: Vessel wall temperature vs depth in wall (a/w) at various times (t) in transient.

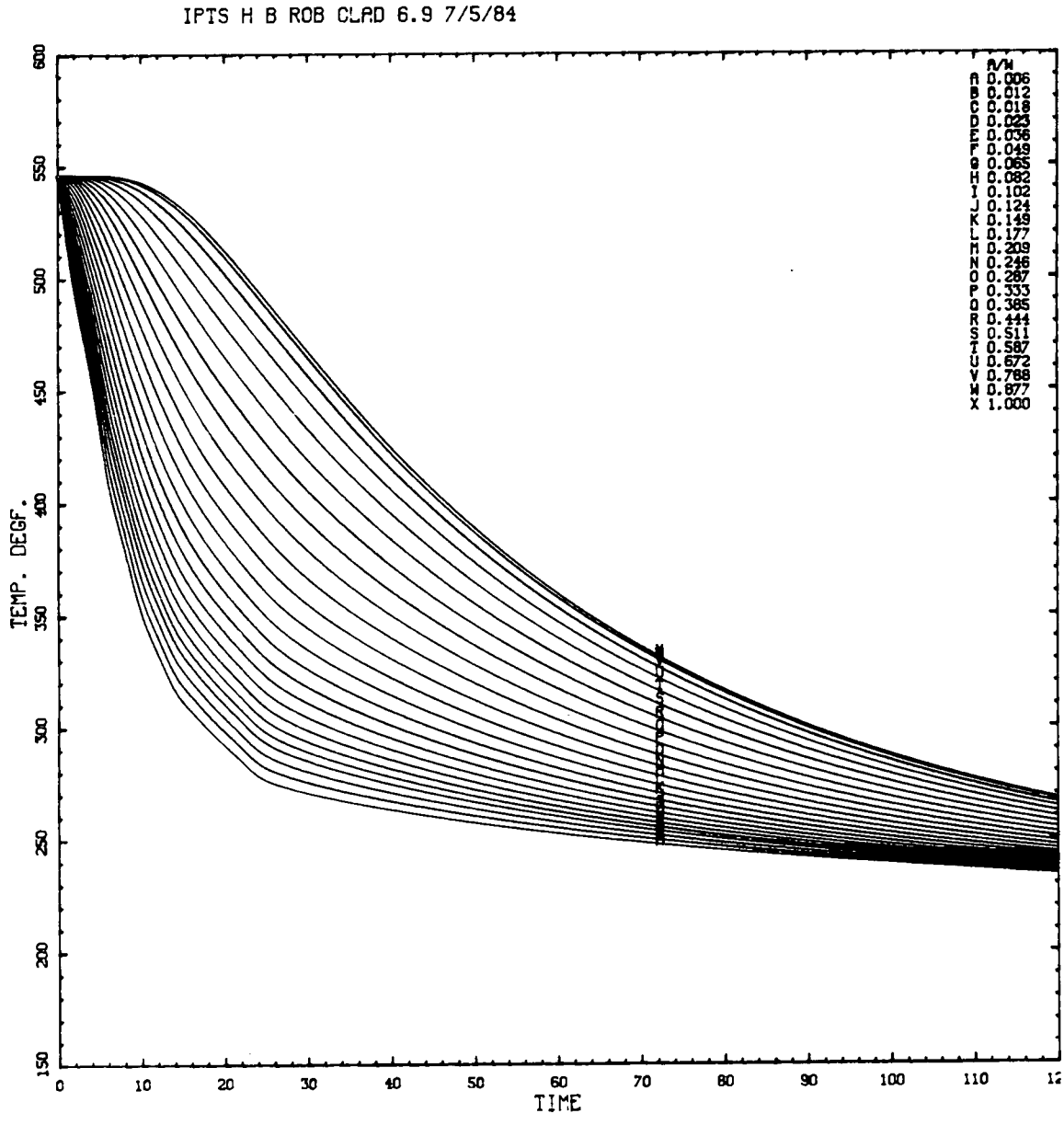

Figure I.34. Transient 6.9: Vessel wall temperature vs time (t) in transient at various depths in wall (a/w).

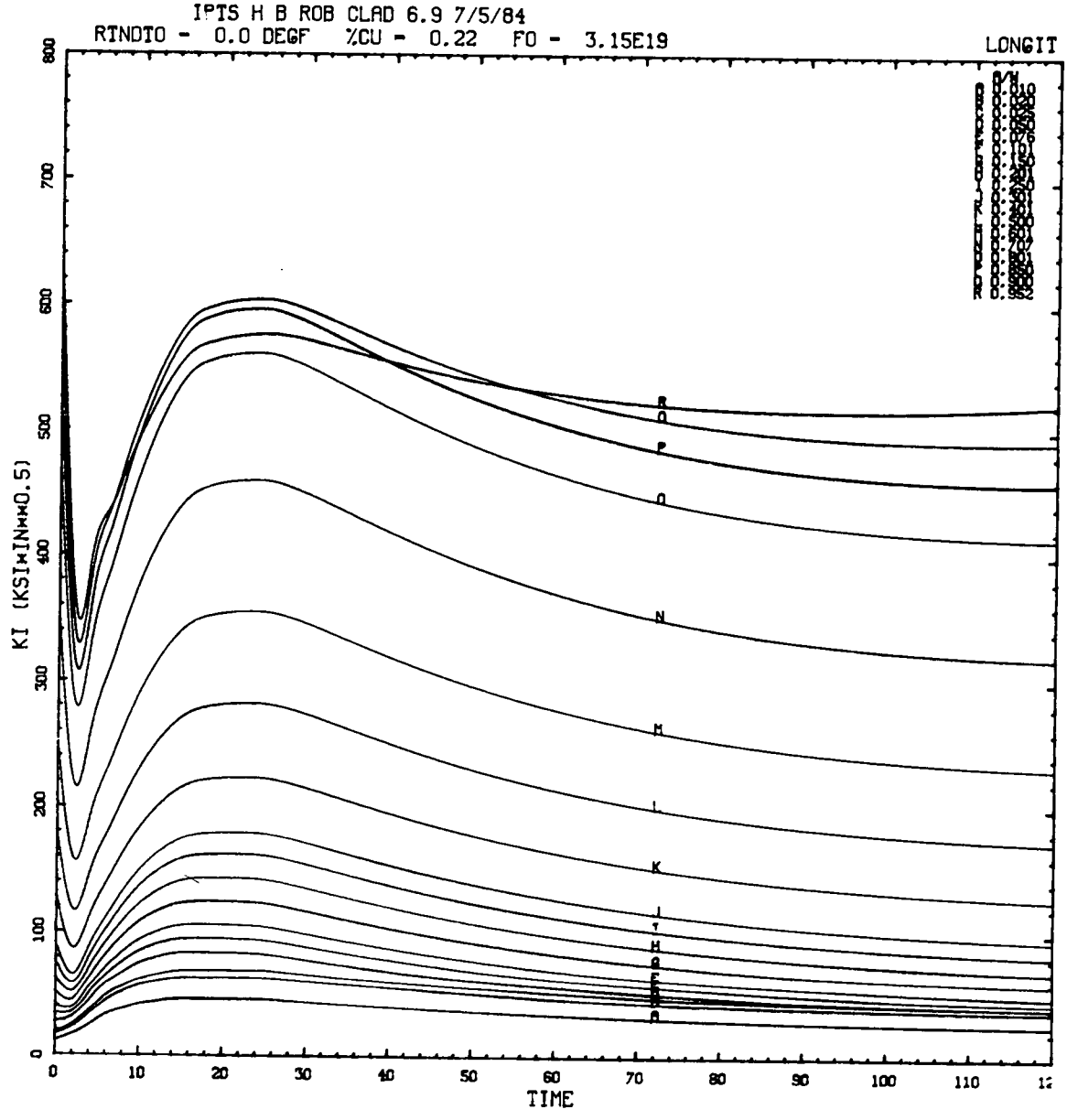

Figure I.35. Transient 6.9: K_I vs time (t) for various depths in wall (a/w).

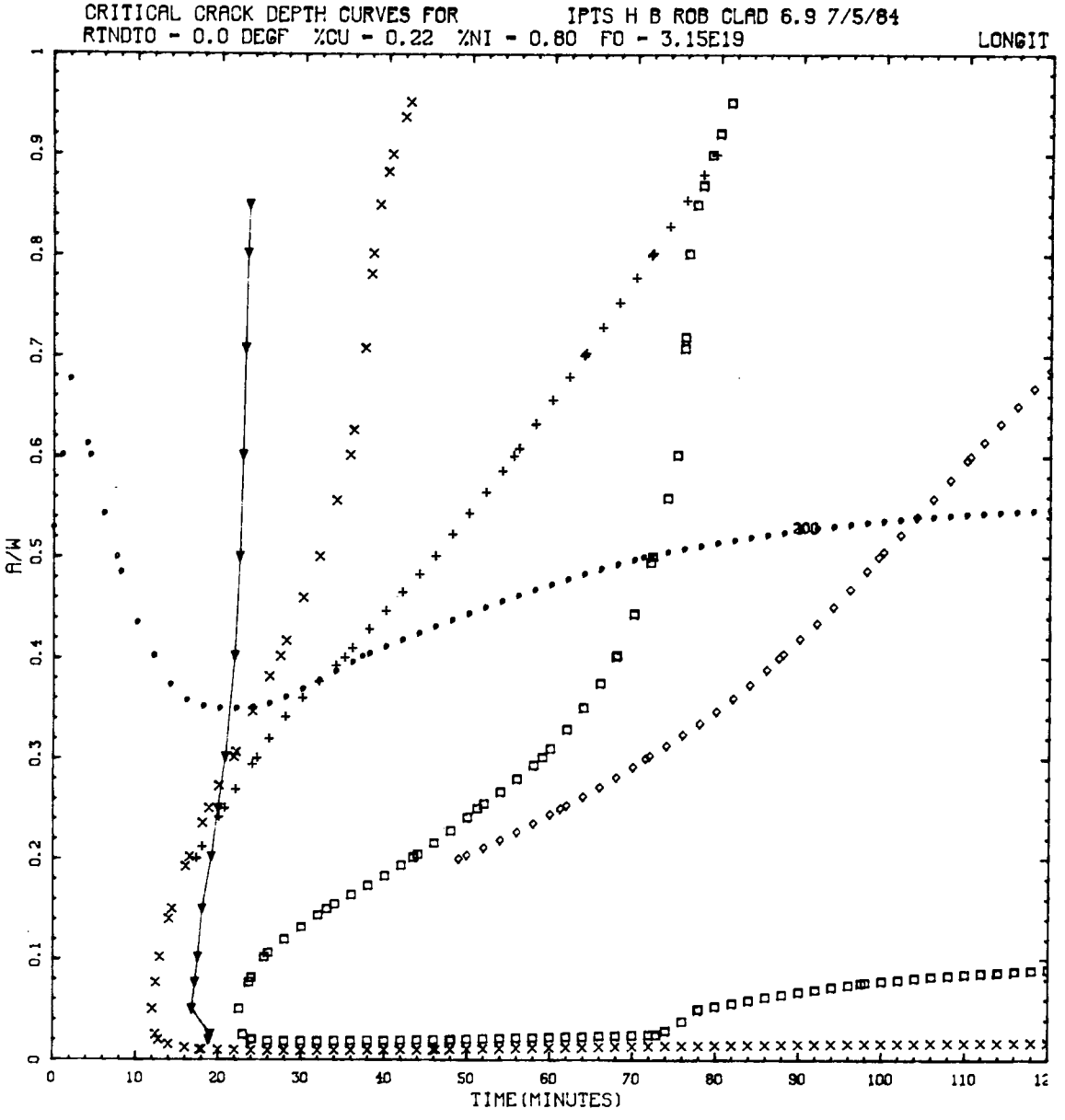

Figure I.36. Transient 6.9: Critical-crack-depth curves for weld 2-273A based on -2σ values of K_{Ic}, K_{Ia}, and $\Delta RTNDT$, mean values of all other parameters, and 32-EFPY fluences.

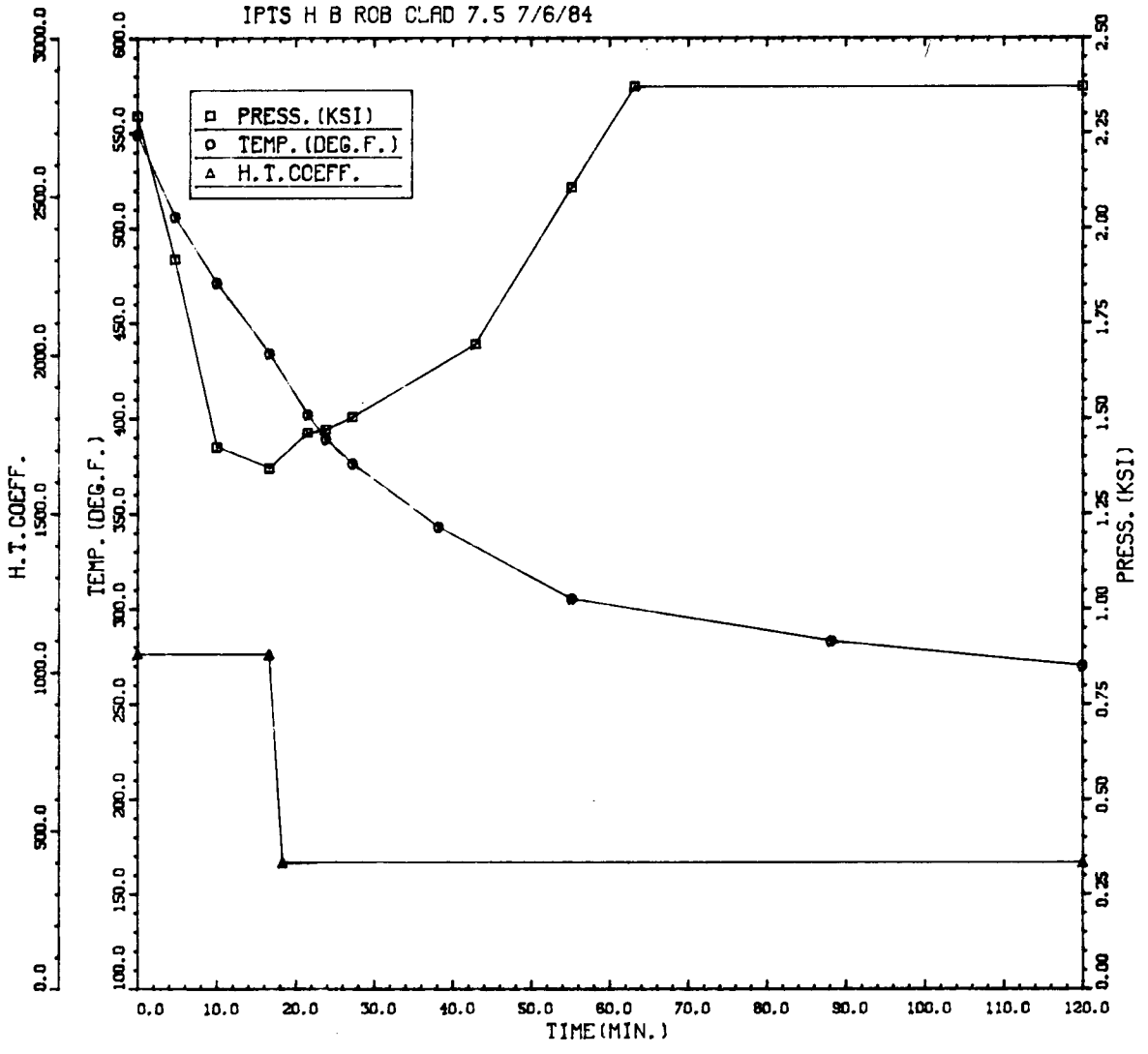

Figure I.37. Transient 7.5: Primary system pressure, downcomer coolant temperature, and fluid-film heat-transfer coefficient vs time in the transient.

Table I.7. Transient 7.5: Summary of digital output, including unadjusted $P(F|E)$ values and histogram data for crack depths, times of failure, and $T - RTNDT$ values at tip of crack corresponding to initiation and arrest events

IPTS H B ROB CLAD 7.5 7/6/84 1. FLAWS/IN**3 DRTN(IS) = 211.2

WELD	P(F/E)	95%CI	%ERR	P(INITIA)	N*V	P(F/E)	%ERR	NFAIL	NTRIALS
	----------UNADJUSTED----------					---ADJUSTED----			
1	1.21D-04	2.05D-05	16.99	1.29D-04	1.000	1.21D-04		133	200000
					VESSEL	1.21D-04	16.99		

DEPTHS FOR INITIAL INITIATION (IN)

	0.09	0.26	0.46	0.67	0.90	1.16	1.44	1.74	2.08
NUMBER	0	61	40	28	10	2	1	0	0
PERCENT	0.0	43.0	28.2	19.7	7.0	1.4	0.7	0.0	0.0

TIMES OF FAILURE(MINUTES)

	0.0	10.0	20.0	30.0	40.0	50.0	60.0	70.0	80.0	90.0	100.0	110.0	120.0
PERCENT	0.0	0.0	0.0	0.0	0.8	7.5	22.6	21.8	24.1	5.3	11.3	6.8	

INITIATION T-RTNDT(DEG.F)

	-100.0	-75.0	-50.0	-25.0	0.0	25.0	50.0	75.0	100.0	125.0	150.0	175.0	200.0
NUMBER	0	0	4	57	68	14	6	1	1	0	0	0	
PERCENT	0.0	0.0	2.6	37.7	45.0	9.3	4.0	0.7	0.7	0.0	0.0	0.0	

ARREST T-RTNDT(DEG.F)

	-50.0	-25.0	0.0	25.0	50.0	75.0	100.0	125.0	150.0	175.0	200.0	225.0	250.0
NUMBER	1	1	4	1	0	0	0	4	7	0	0	0	
PERCENT	5.6	5.6	22.2	5.6	0.0	0.0	0.0	22.2	38.9	0.0	0.0	0.0	

ICRKTP = 2 IACCEL = 1 NDLRS = 0 NRTRS = 0 DATE: 10/29/84 TIME: 23.36.12

CPU TIME: 5 MIN 28 SEC

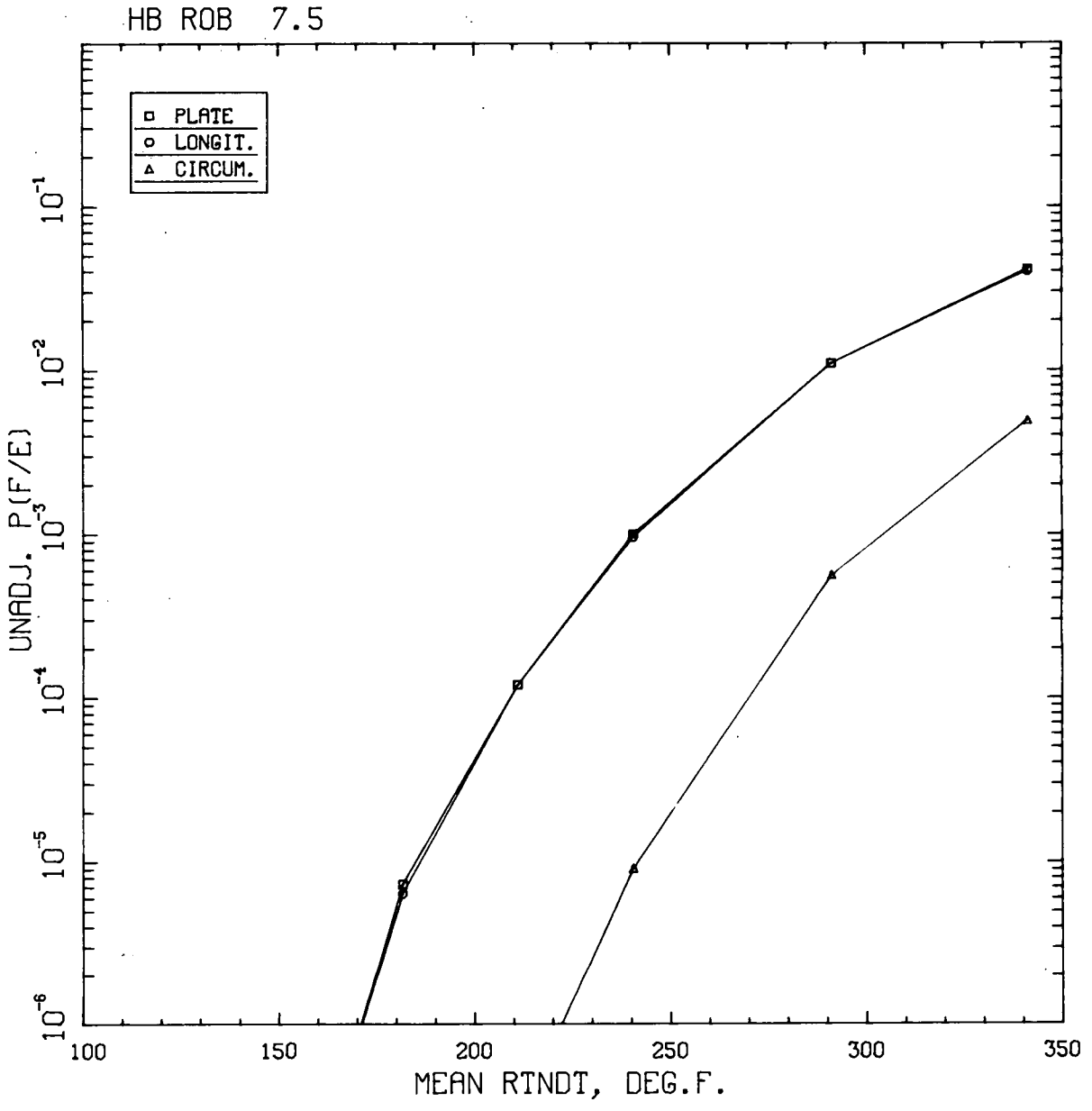

Figure I.38. Transient 7.5: $\hat{P}_j \int_0^w f(a)\, B(a)\, da$ vs $\overline{RTNDT_s}$ for (2-D, 2-D) and (2-D, 2m) flaw combinations.

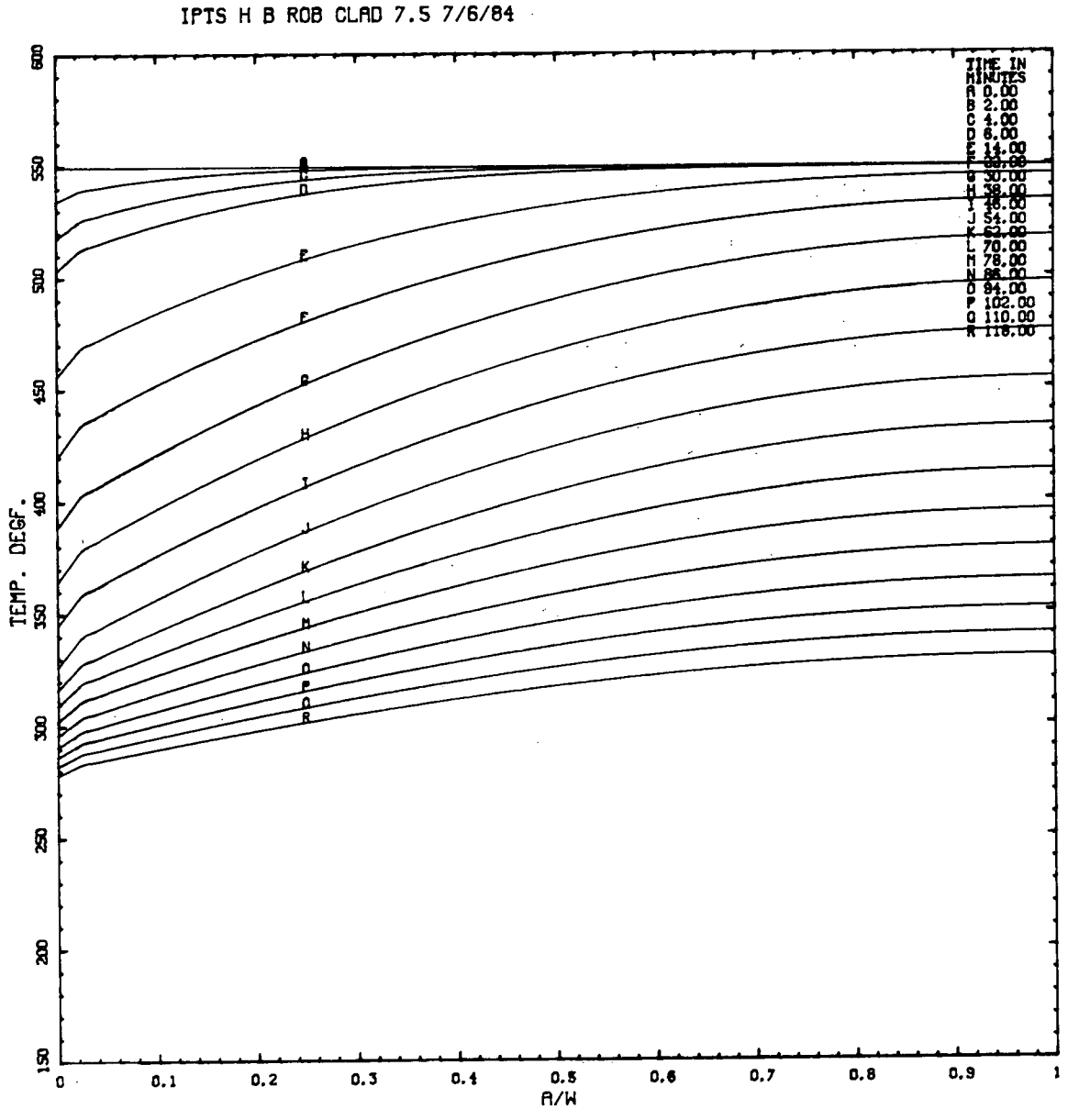

Figure I.39. Transient 7.5: Vessel wall temperature vs depth in wall (a/w) at various times (t) in transient.

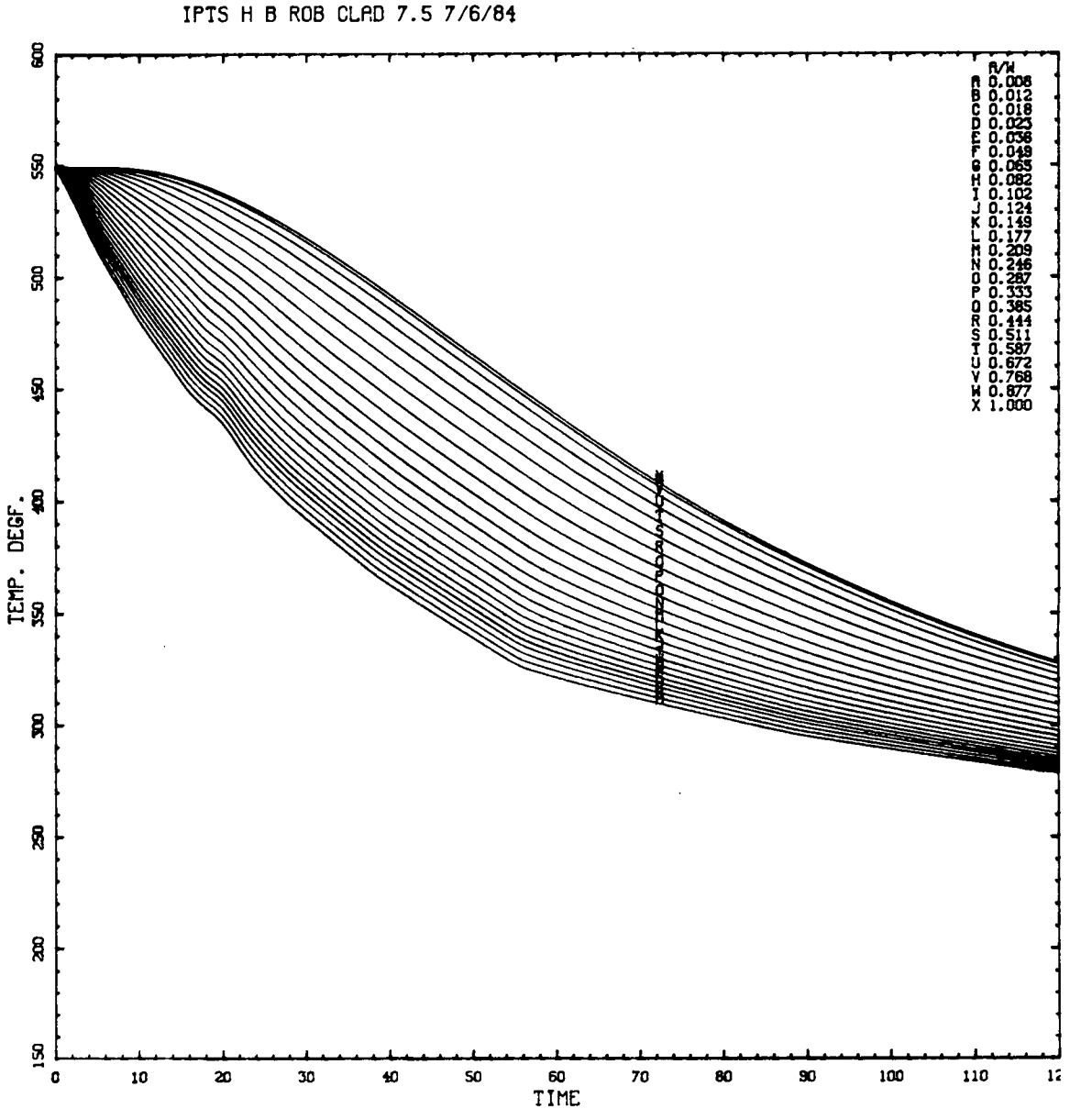

Figure I.40. Transient 7.5: Vessel wall temperature vs time (t) in transient at various depths in wall (a/w).

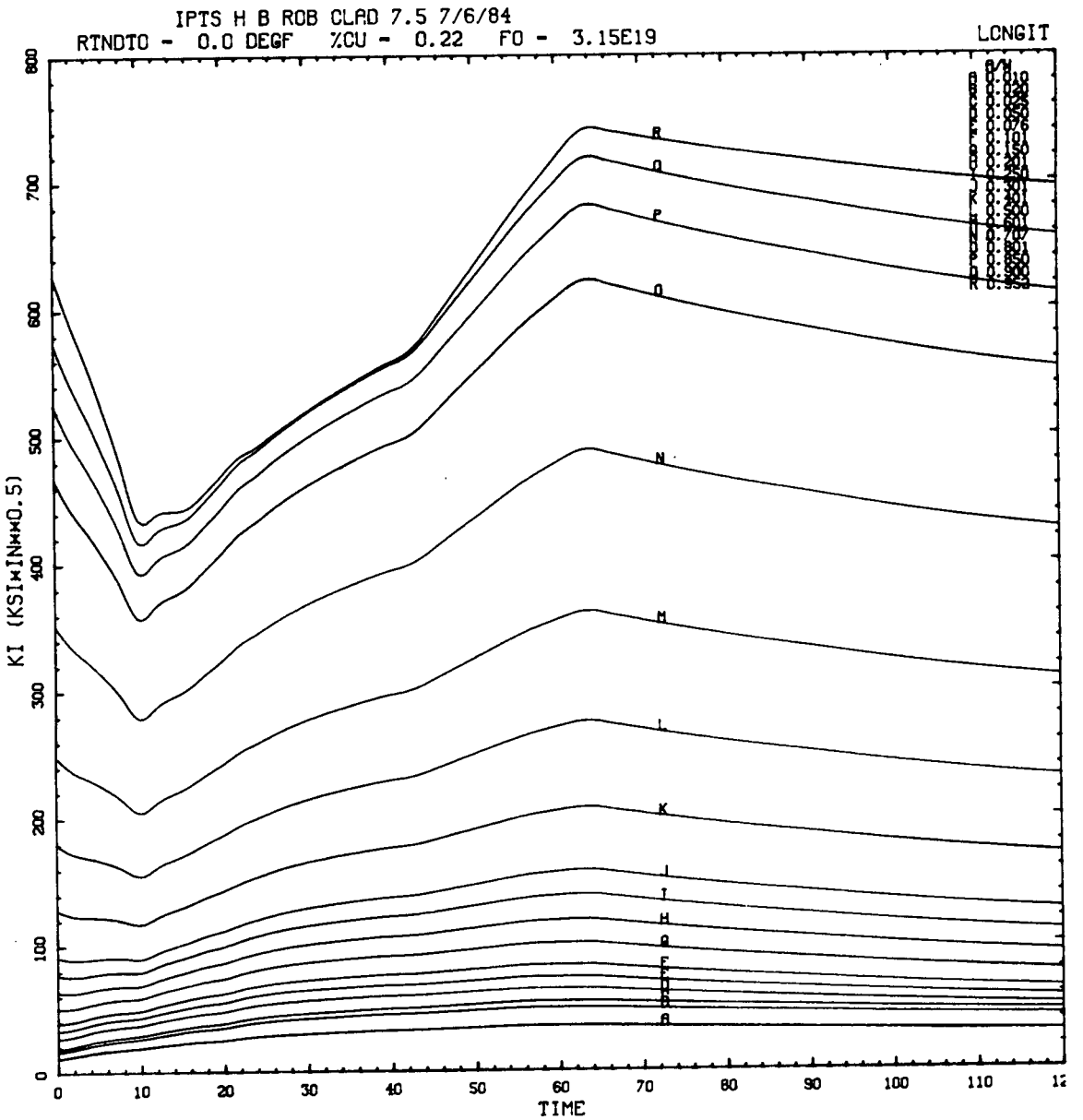

Figure I.41. Transient 7.5: K_I vs time (t) for various depths in wall (a/w).

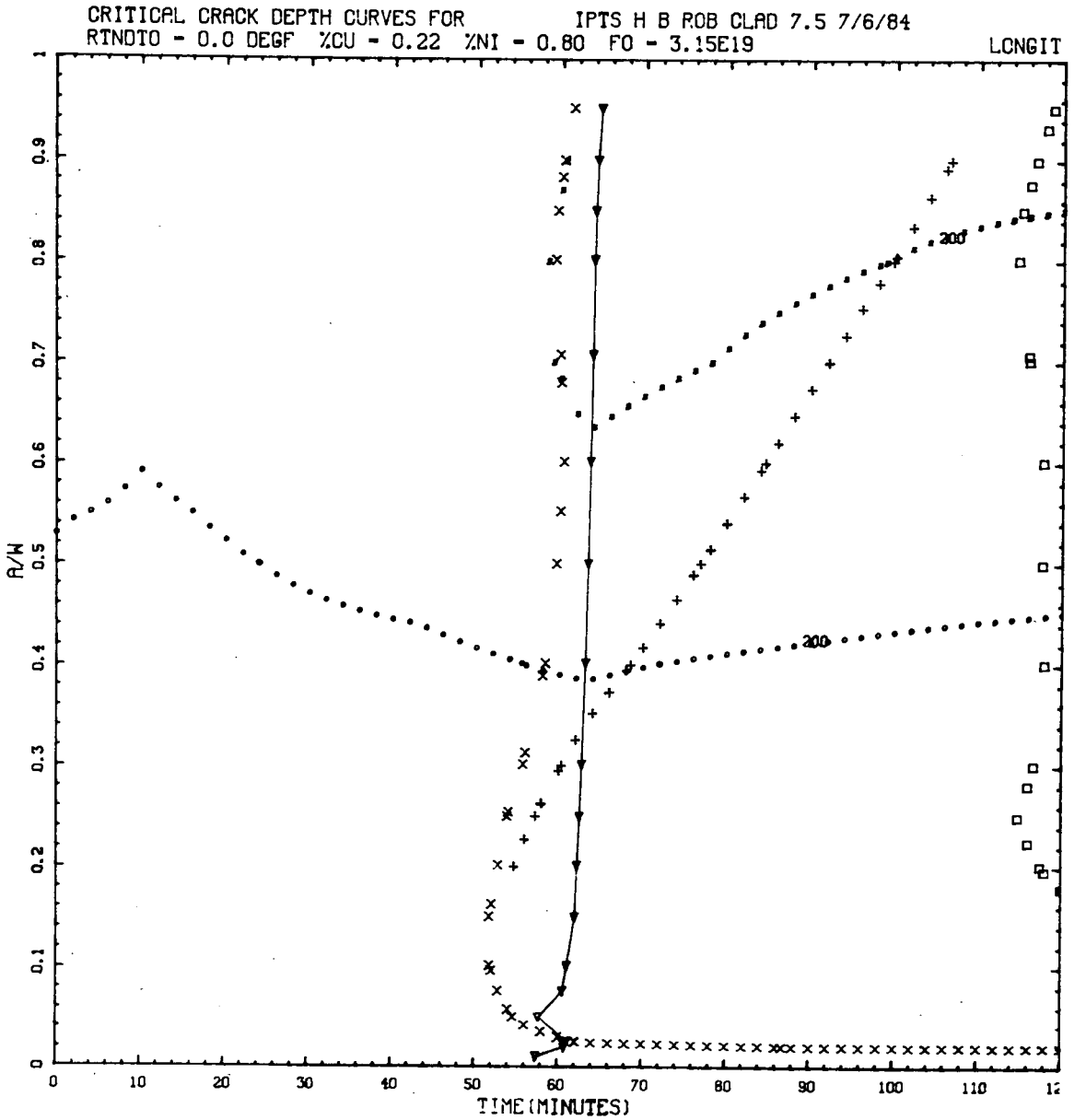

Figure I.42. Transient 7.5: Critical-crack-depth curves for weld 2-273A based on -2σ values of K_{Ic}, K_{Ia}, and $\Delta RTNDT$, mean values of all other parameters, and 32-EFPY fluences.

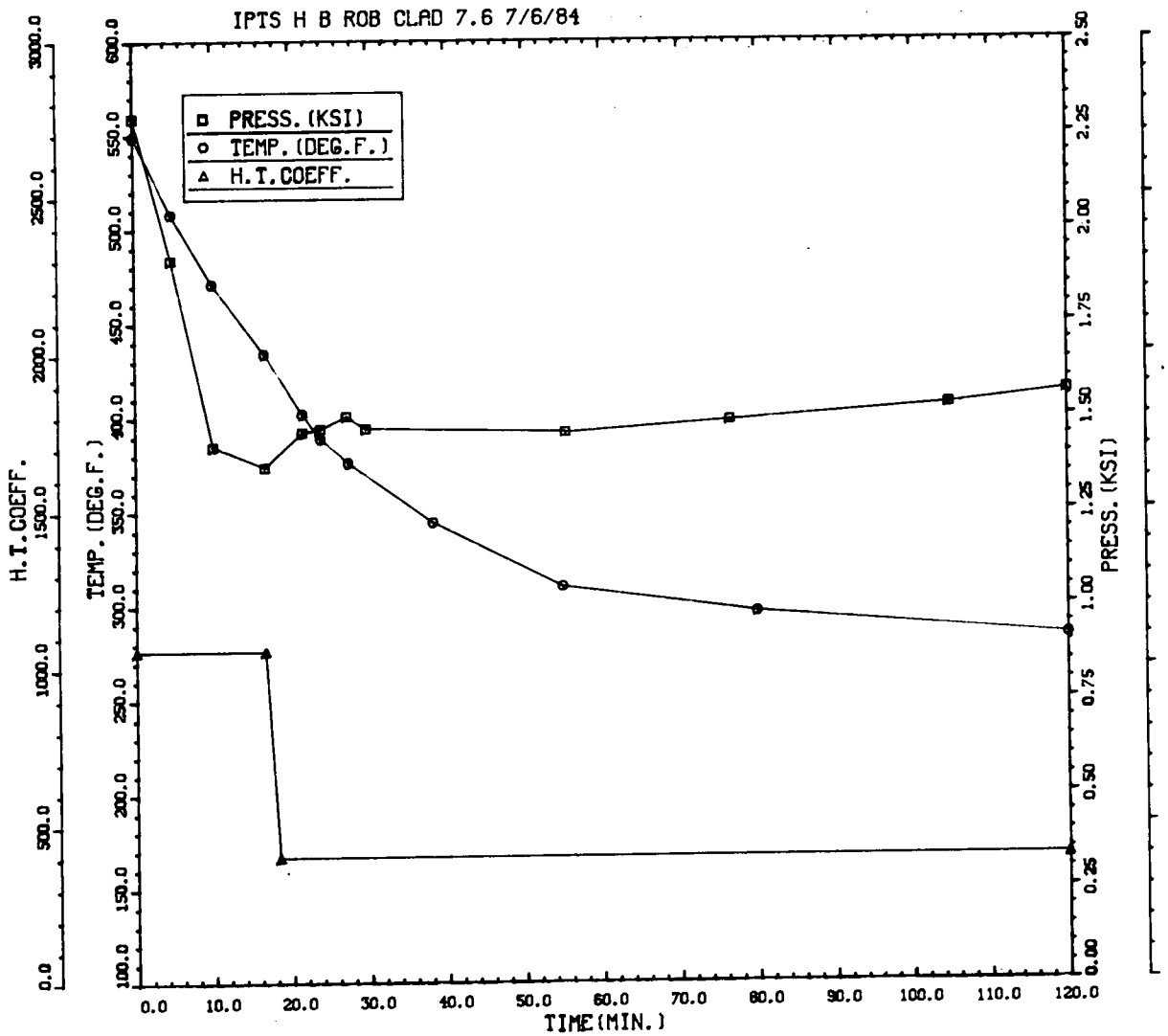

Figure I.43. Transient 7.6: Primary system pressure, downcomer coolant temperature, and fluid-film heat-transfer coefficient vs time in the transient.

Table I.8. Transient 7.6: Summary of digital output, including unadjusted $P(F|E)$ values and histogram data for crack depths, times of failure, and $T - RTNDT$ values at tip of crack corresponding to initiation and arrest events

IPTS H B ROB CLAD 7.6 7/6/84 1. FLAWS/IN**3 DRTN(IS) = 211.2

	UNADJUSTED					ADJUSTED			
WELD	P(F/E)	95%CI	%ERR	P(INITIA)	N*V	P(F/E)	%ERR	NFAIL	NTRIALS
1	1.10D-06	2.05D-07	18.60	2.97D-06	1.000	1.10D-06		111	200000
					VESSEL	1.10D-06	18.60		

DEPTHS FOR INITIAL INITIATION (IN)

	0.09	0.26	0.46	0.67	0.90	1.16	1.44	1.74	2.08
NUMBER	0	115	102	48	22	10	2	0	0
PERCENT	0.0	38.5	34.1	16.1	7.4	3.3	0.7	0.0	0.0

TIMES OF FAILURE(MINUTES)

	0.0	10.0	20.0	30.0	40.0	50.0	60.0	70.0	80.0	90.0	100.0	110.0	120.0
PERCENT	0.0	0.0	0.0	0.0	0.0	0.0	0.0	6.3	11.7	20.7	24.3	36.9	

INITIATION T-RTNDT(DEG.F)

	-100.0	-75.0	-50.0	-25.0	0.0	25.0	50.0	75.0	100.0	125.0	150.0	175.0	200.0
NUMBER	0	0	3	86	188	76	49	3	0	0	0	0	
PERCENT	0.0	0.0	0.7	21.2	46.4	18.8	12.1	0.7	0.0	0.0	0.0	0.0	

ARREST T-RTNDT(DEG.F)

	-50.0	-25.0	0.0	25.0	50.0	75.0	100.0	125.0	150.0	175.0	200.0	225.0	250.0
NUMBER	0	6	47	15	0	2	46	163	15	0	0	0	
PERCENT	0.0	2.0	16.0	5.1	0.0	0.7	15.6	55.4	5.1	0.0	0.0	0.0	

OF STD DEVS ABOVE MEAN DELTA RTNDT(FAILURES ONLY)

	1.00	1.25	1.50	1.75	2.00	2.25	2.50	2.75	3.00
NUMBER	0	4	2	17	15	17	24	32	
PERCENT	0.0	3.6	1.8	15.3	13.5	15.3	21.6	28.8	

OF STD DEVS ABOVE MEAN RTNDT(FAILURES ONLY)

	1.00	1.25	1.50	1.75	2.00	2.25	2.50	2.75	3.00
NUMBER	0	1	2	5	19	25	25	34	
PERCENT	0.0	0.9	1.8	4.5	17.1	22.5	22.5	30.6	

ICRKTP = 2 IACCEL = 1 NDLRS = 2 NRTRS = 2 DATE: 10/29/84 TIME: 23.49.59

CPU TIME: 5 MIN 20 SEC

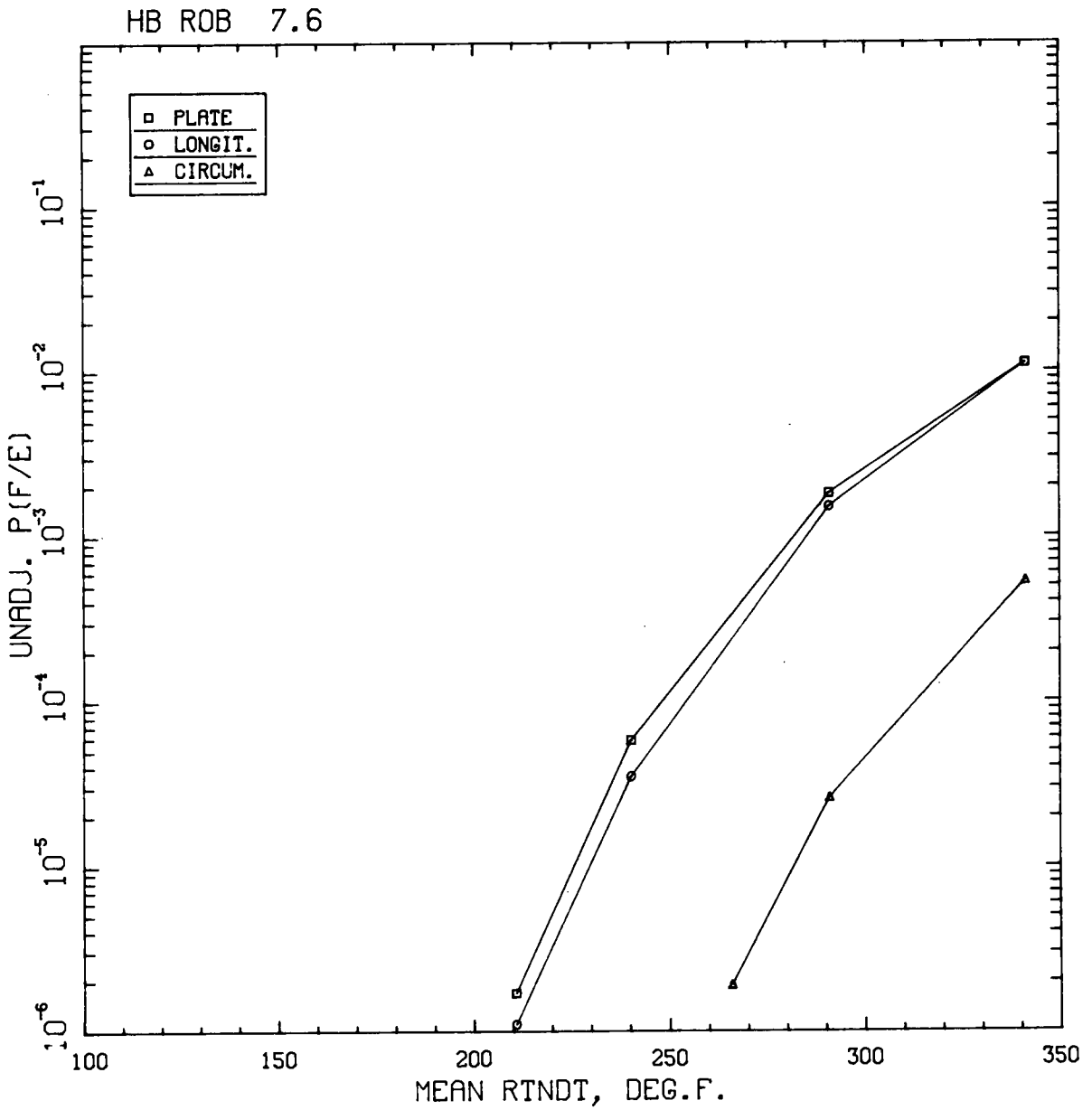

Figure I.44. Transient 7.6: $\hat{P}_j \int_0^w f(a)\, B(a)\, da$ vs $\overline{RTNDT}_s$ for (2-D, 2-D) and (2-D, 2m) flaw combinations.

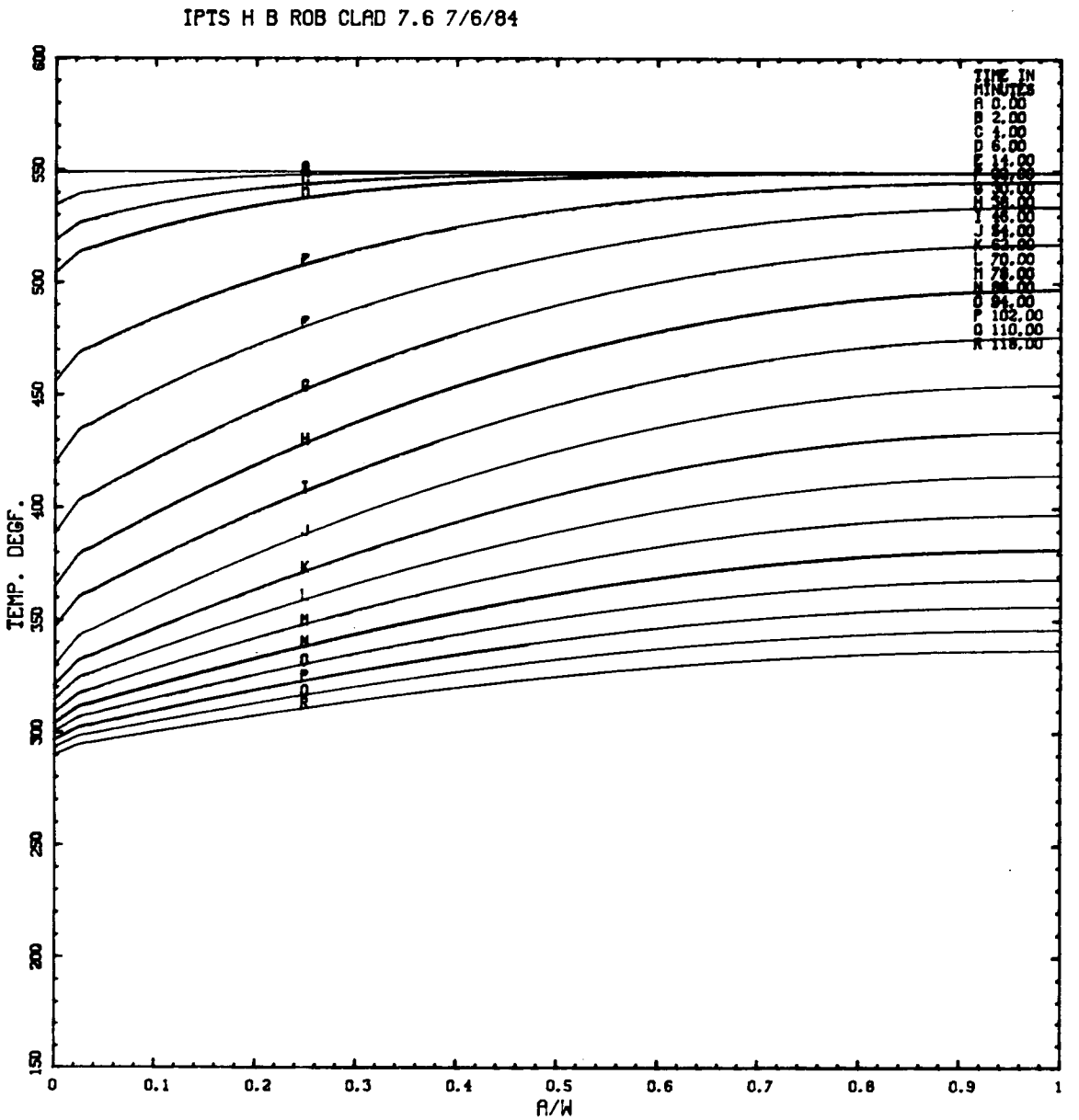

Figure I.45. Transient 7.6: Vessel wall temperature vs depth in wall (a/w) at various times (t) in transient.

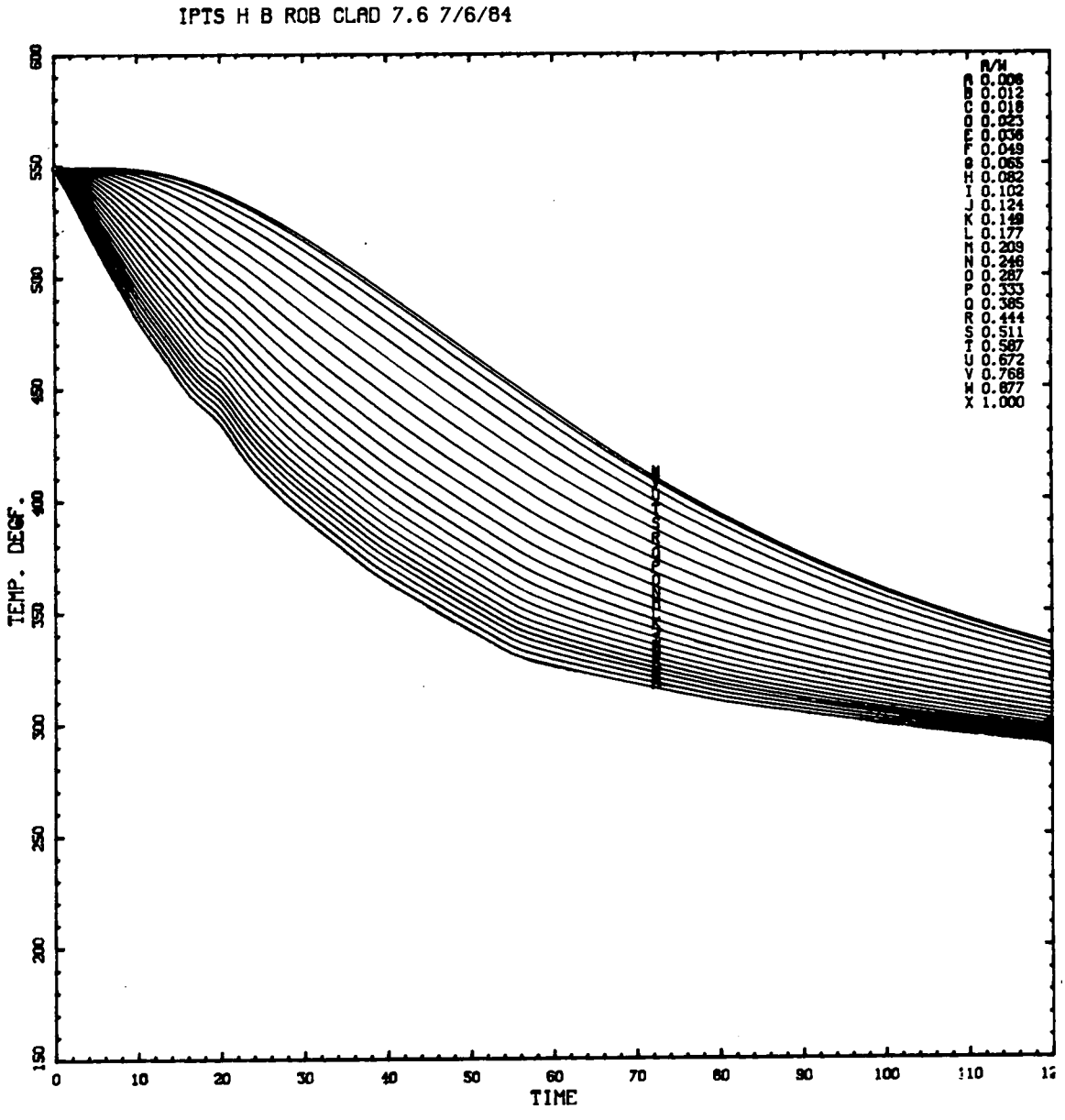

Figure I.46. Transient 7.6: Vessel wall temperature vs time (t) in transient at various depths in wall (a/w).

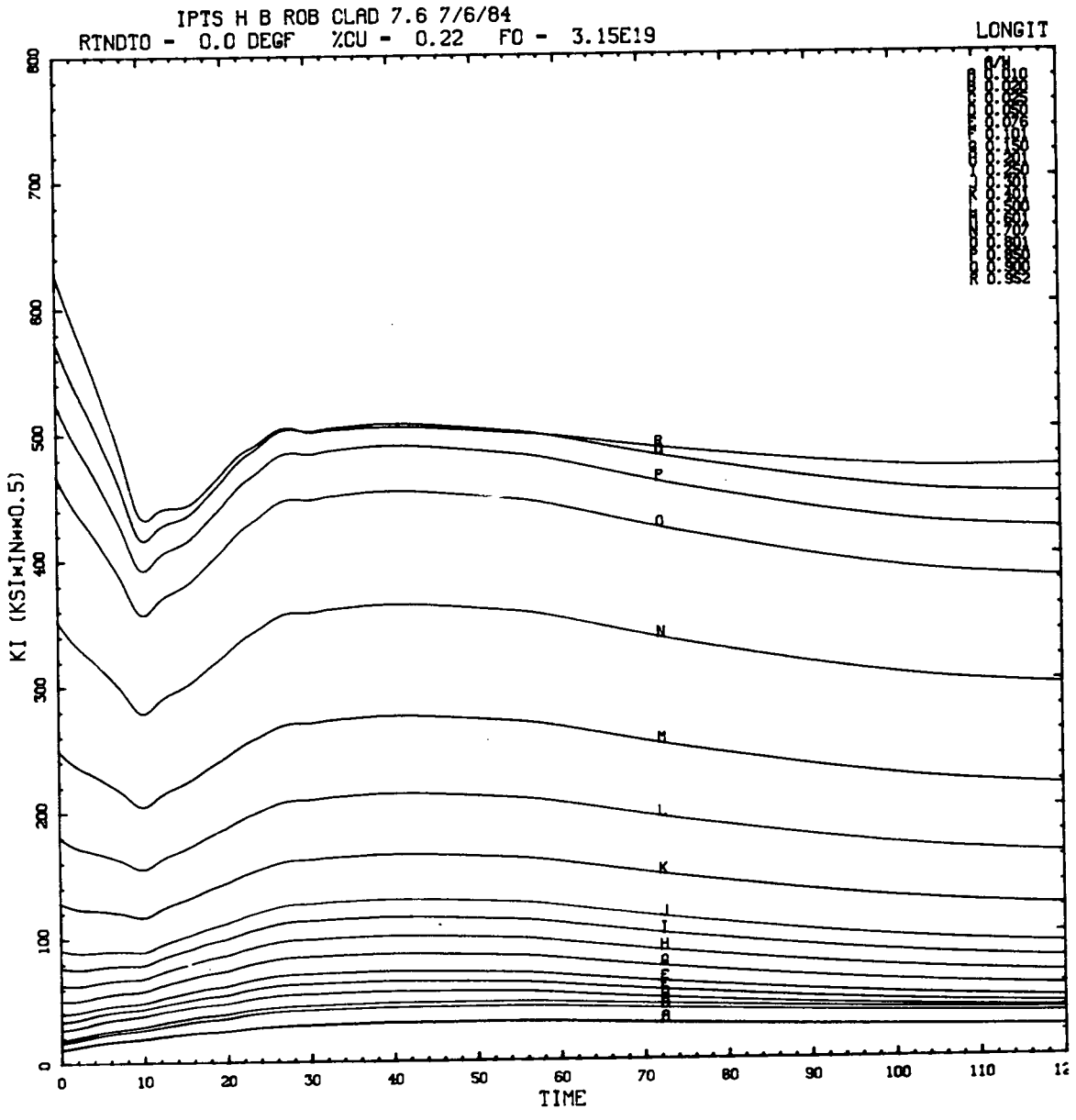

Figure I.47. Transient 7.6: K_I vs time (t) for various depths in wall (a/w).

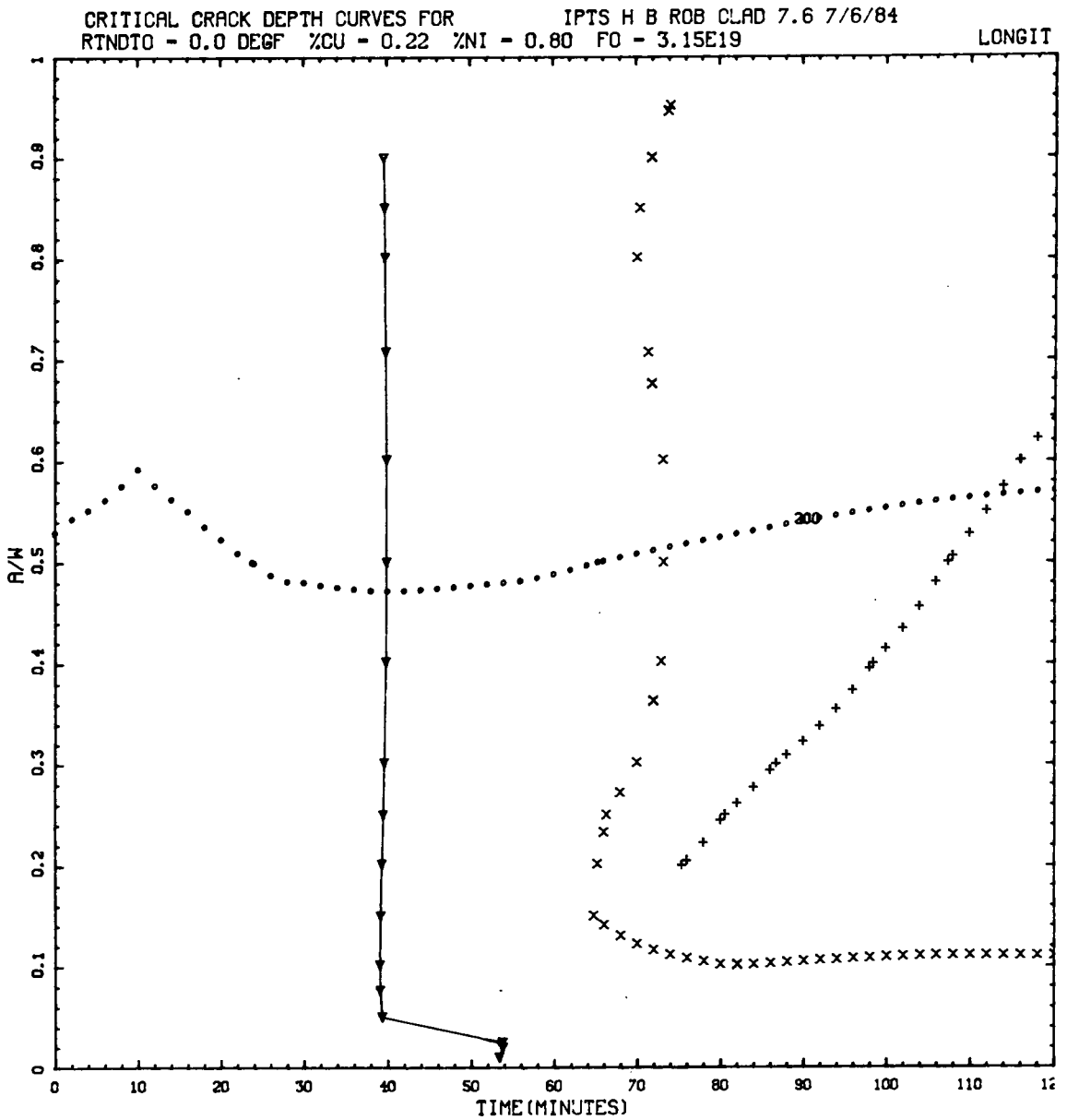

×, 2-D flaw, $K_I = K_{Ia}$
+, 2-m flaw, $K_I = K_{Ia}$
O, 2-D flaw, K_I = 220 MPa $\sqrt{m}$
∇, WPS (warm prestressing)

Figure I.48. Transient 7.6: Critical-crack-depth curves for weld 2-273A based on -2σ values of K_{Ic}, K_{Ia}, and $\Delta RTNDT$, mean values of all other parameters, and 32-EFPY fluences.

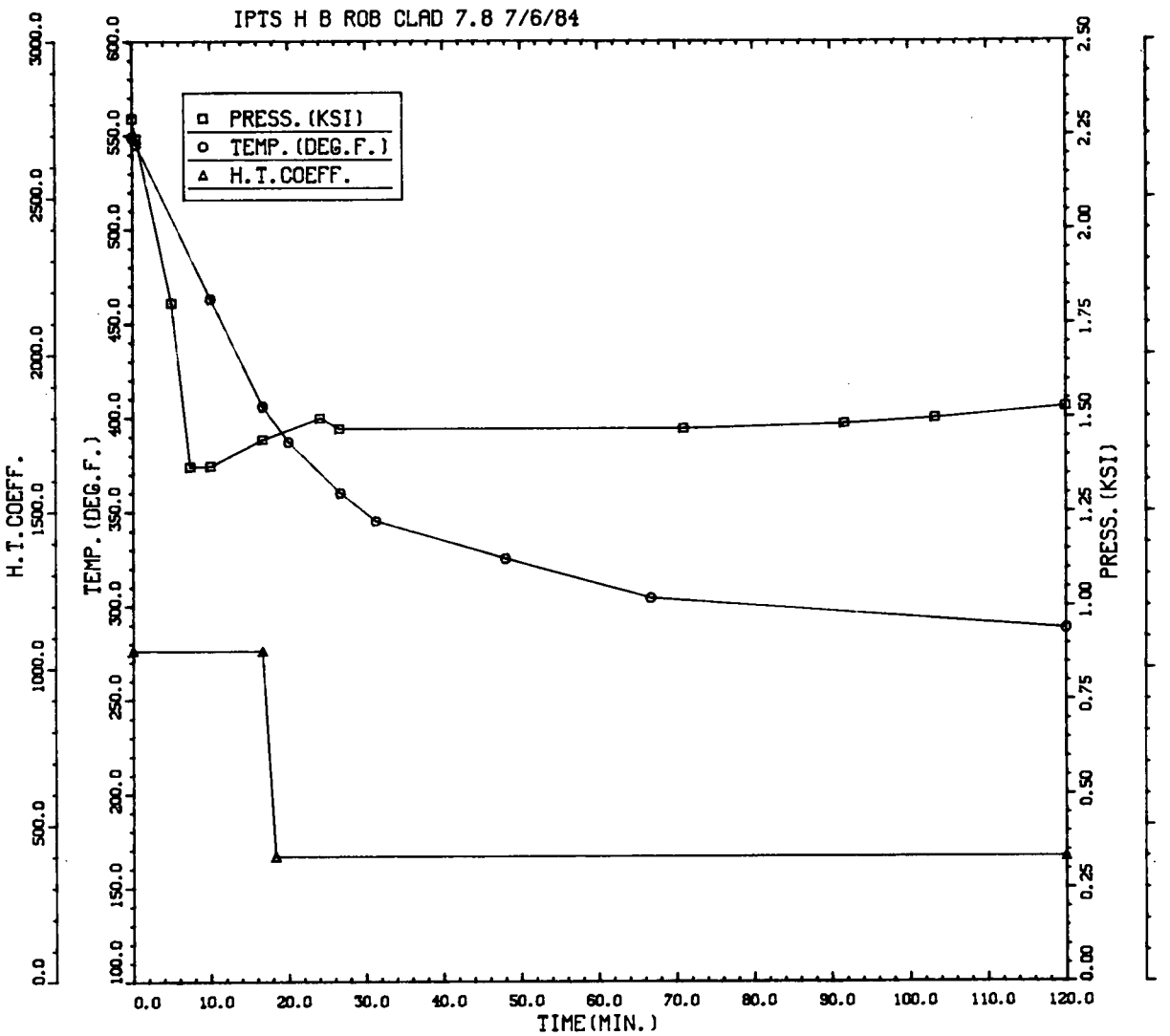

Figure I.49. Transient 7.8: Primary system pressure, downcomer coolant temperature, and fluid-film heat-transfer coefficient vs time in the transient.

Table I.9. Transient 7.8: Summary of digital output, including unadjusted $P(F|E)$ values and histogram data for crack depths, times of failure, and $T - RTNDT$ values at tip of crack corresponding to initiation and arrest events

```
IPTS H B ROB CLAD 7.8 7/6/84                    1. FLAWS/IN**3    DRTN(IS) =  211.2

            -------------UNADJUSTED--------------          ---ADJUSTED----
WELD    P(F/E)      95%CI     %ERR   P(INITIA)  N*V      P(F/E)    %ERR    NFAIL    NTRIALS

 1      4.76D-07   1.35D-07  28.29   1.78D-06  1.000    4.76D-07            48      200000

                                                VESSEL   4.76D-07  28.29


DEPTHS FOR INITIAL INITIATION (IN)
              0.09  0.26  0.46  0.67  0.90  1.16  1.44  1.74  2.08
   NUMBER      0    68    60    33    11     5     2     0     0
   PERCENT    0.0  38.0  33.5  18.4   6.1   2.8   1.1   0.0   0.0


TIMES OF FAILURE(MINUTES)
              0.0  10.0  20.0  30.0  40.0  50.0  60.0  70.0  80.0  90.0 100.0 110.0 120.0
  PERCENT     0.0   0.0   0.0   0.0   0.0   0.0   4.2   4.2   4.2  22.9  25.0  39.6


 INITIATION T-RTNDT(DEG.F)
            -100.0 -75.0 -50.0 -25.0   0.0  25.0  50.0  75.0 100.0 125.0 150.0 175.0 200.0
  NUMBER         0     0     4    76    86    26    28     4     0     0     0     0
  PERCENT      0.0   0.0   1.8  33.9  38.4  11.6  12.5   1.8   0.0   0.0   0.0   0.0


 ARREST T-RTNDT(DEG.F)
             -50.0 -25.0   0.0  25.0  50.0  75.0 100.0 125.0 150.0 175.0 200.0 225.0 250.0
  NUMBER         0     7    35     7     0     1    26    76    24     0     0     0
  PERCENT      0.0   4.0  19.9   4.0   0.0   0.6  14.8  43.2  13.6   0.0   0.0   0.0


 # OF STD DEVS ABOVE MEAN DELTA RTNDT(FAILURES ONLY)
              1.00  1.25  1.50  1.75  2.00  2.25  2.50  2.75  3.00
  NUMBER         0     1     1     1     8     8    13    16
  PERCENT      0.0   2.1   2.1   2.1  16.7  16.7  27.1  33.3


 # OF STD DEVS ABOVE MEAN RTNDT(FAILURES ONLY)
              1.00  1.25  1.50  1.75  2.00  2.25  2.50  2.75  3.00
  NUMBER         0     0     2     2     7    11     9    17
  PERCENT      0.0   0.0   4.2   4.2  14.6  22.9  18.8  35.4


ICRKTP = 2   IACCEL = 1   NDLRS = 2   NRTRS = 2   DATE: 10/29/84   TIME: 23.51.16

CPU TIME:  5 MIN 20 SEC
```

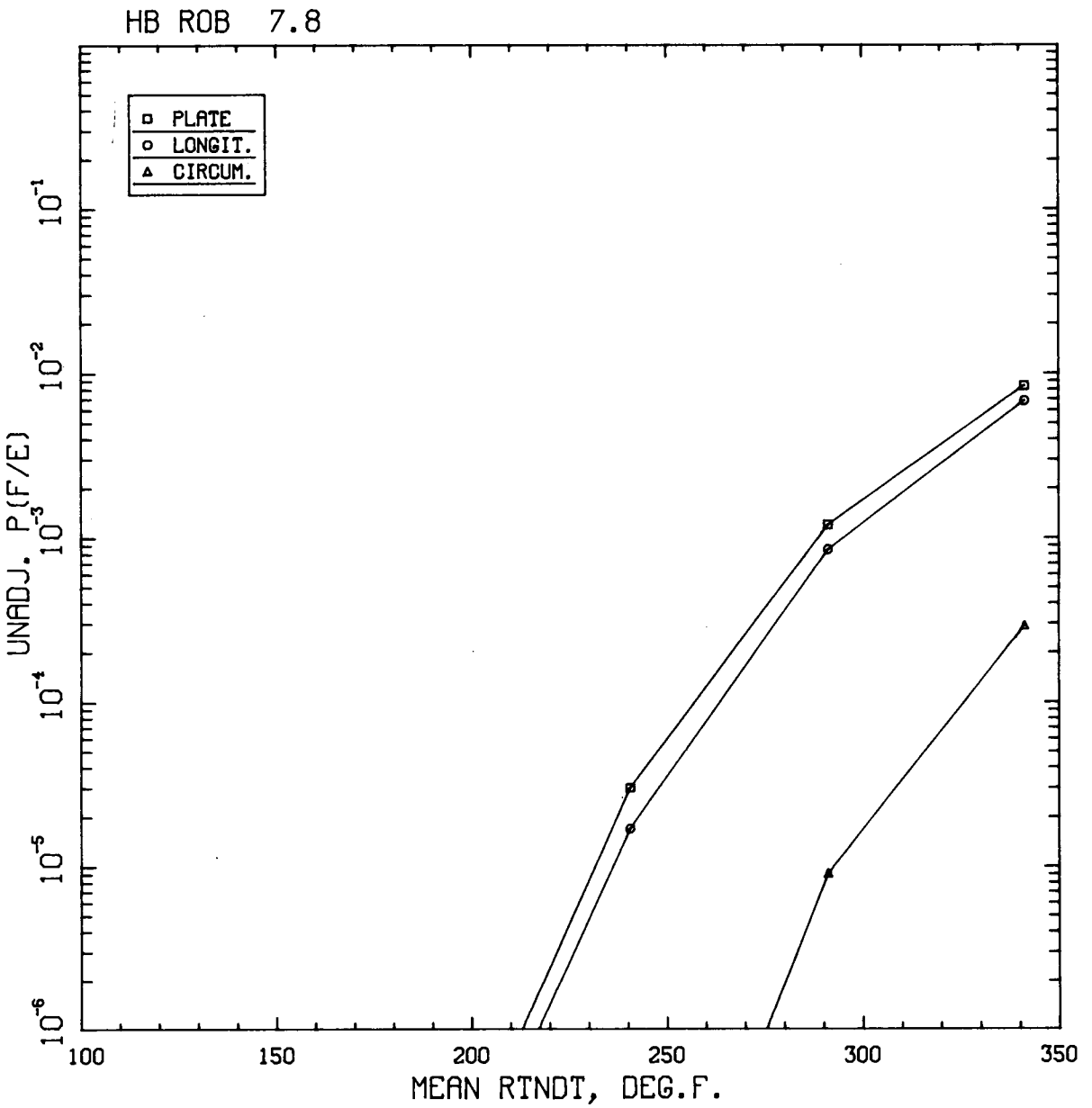

Figure I.50. Transient 7.8: $\hat{P}_j \int_0^w f(a)\, B(a)\, da$ vs $\overline{RTNDT_s}$ for (2-D, 2-D) and (2-D, 2m) flaw combinations.

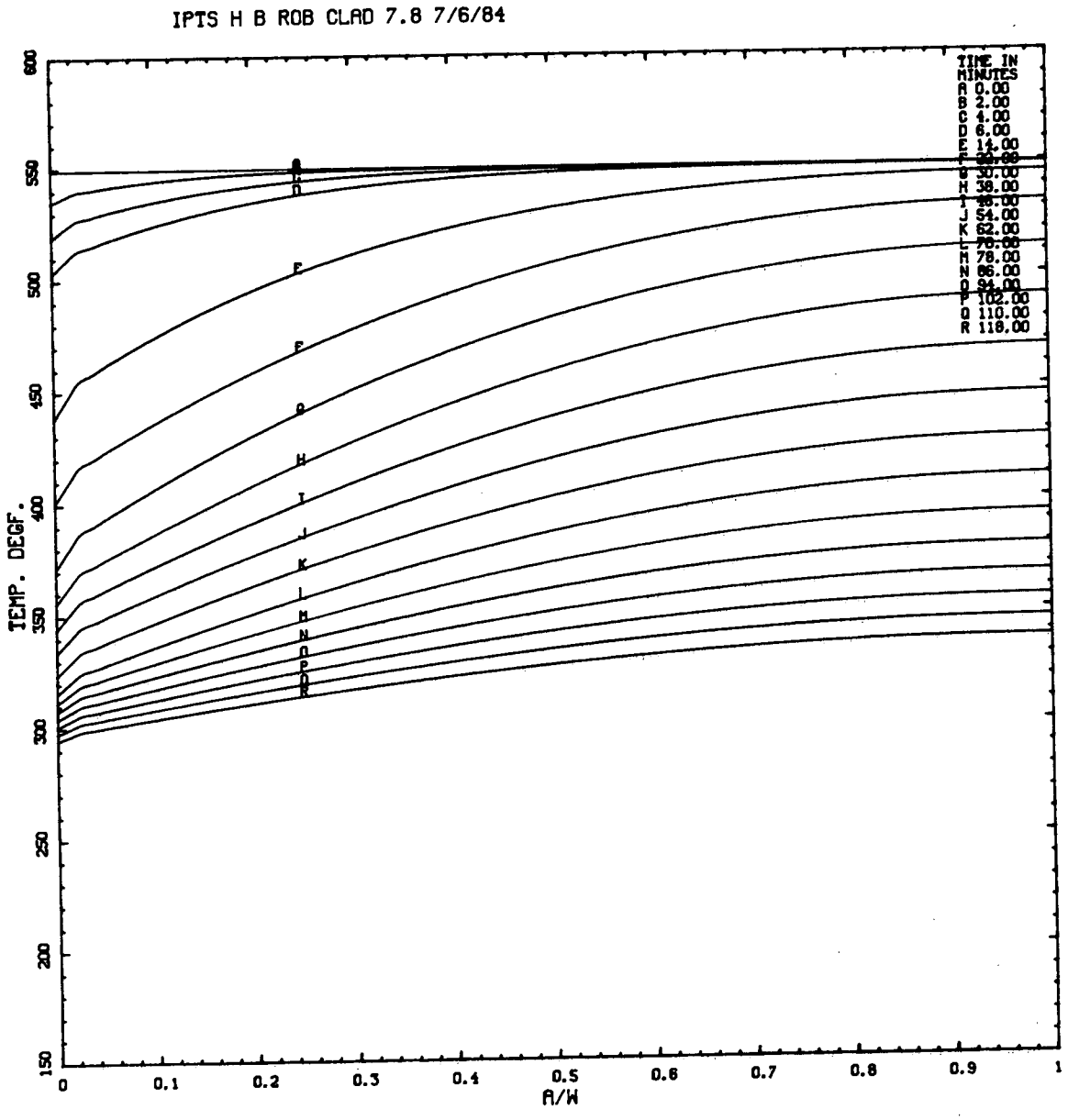

Figure I.51. Transient 7.8: Vessel wall temperature vs depth in wall (a/w) at various times (t) in transient.

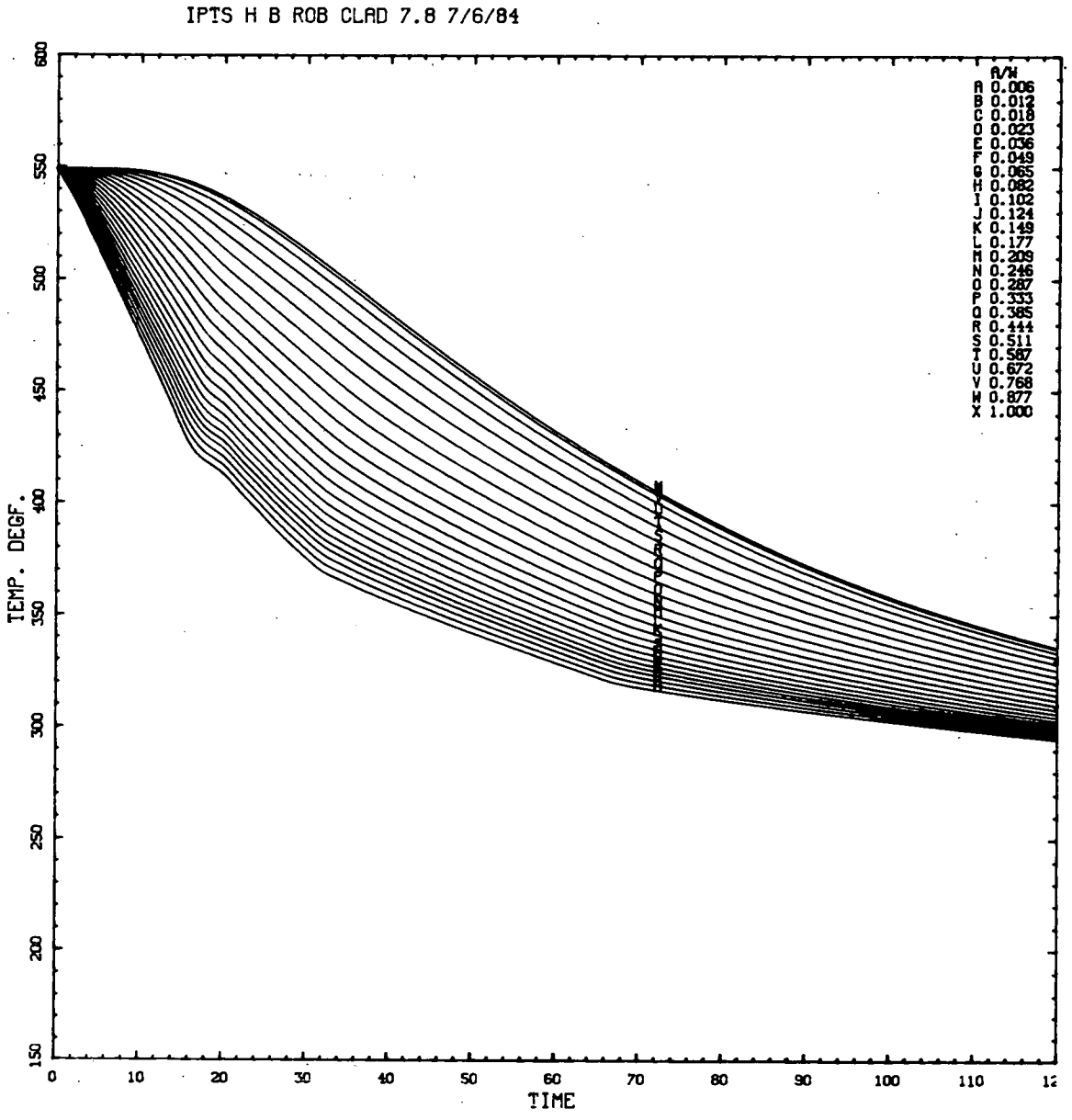

Figure I.52. Transient 7.8: Vessel wall temperature vs time (t) in transient at various depths in wall (a/w).

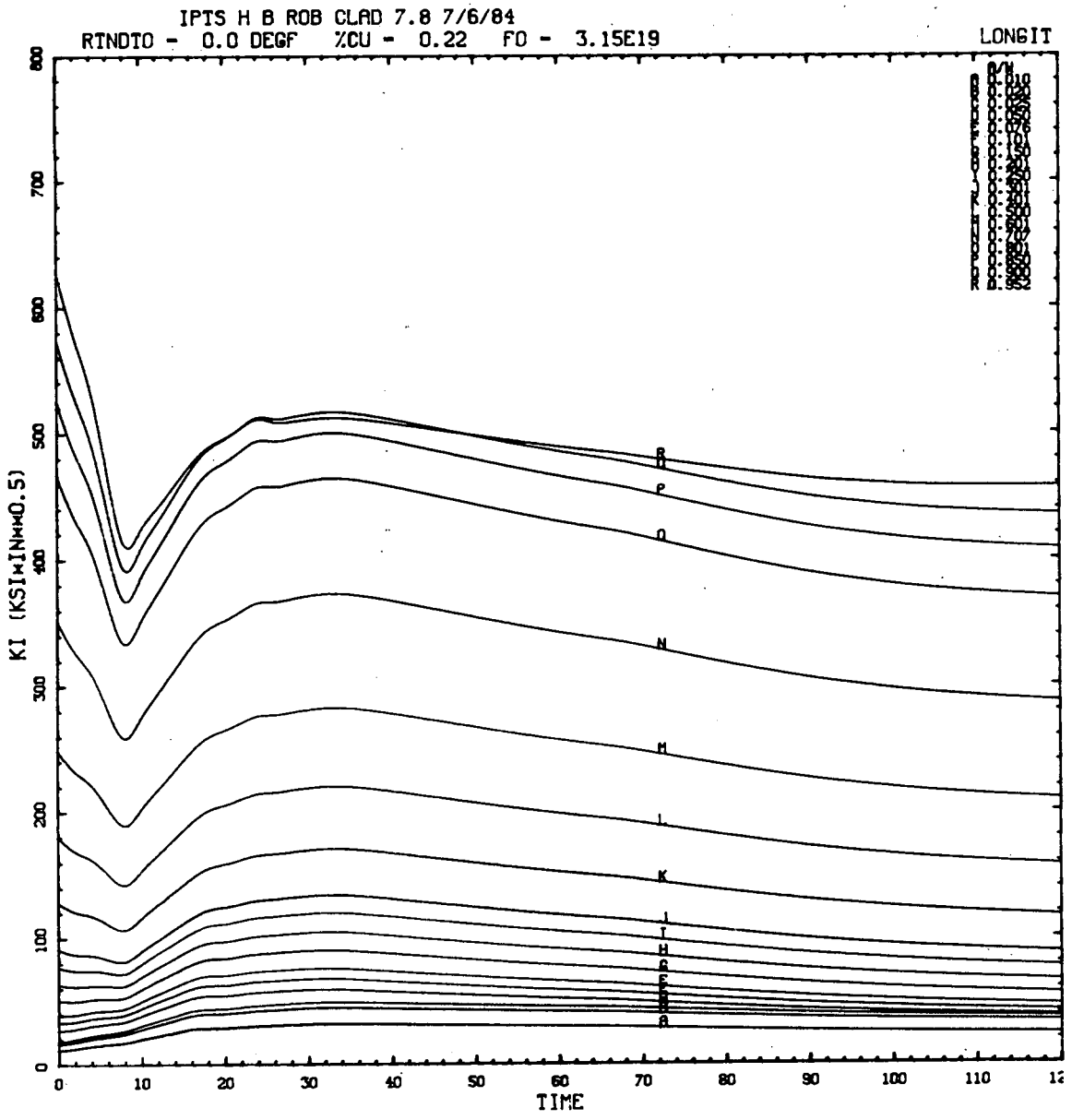

Figure I.53. Transient 7.8: K_I vs time (t) for various depths in wall (a/w).

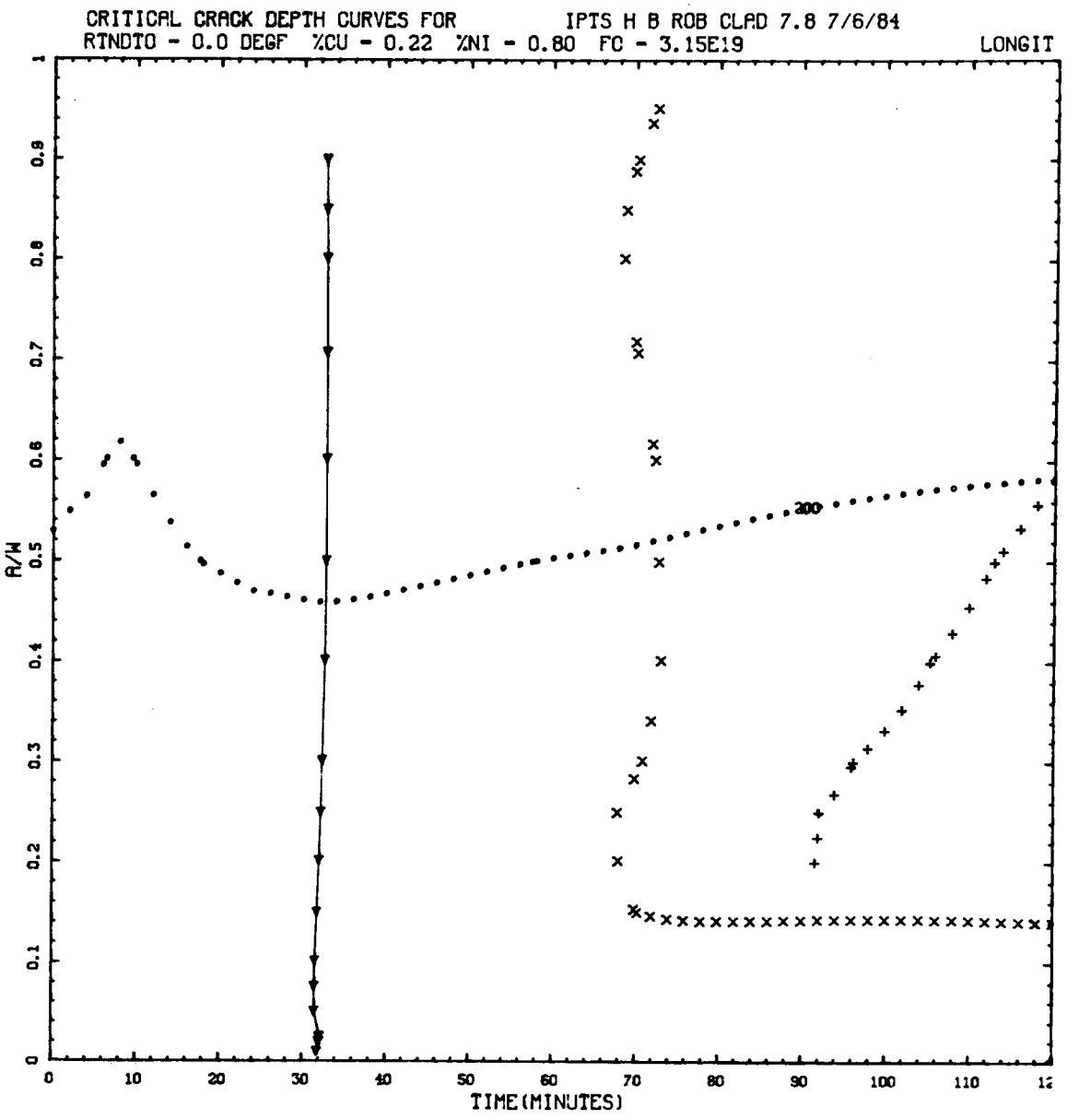

Figure I.54. Transient 7.8: Critical-crack-depth curves for weld 2-273A based on -2σ values of K_{Ic}, K_{Ia}, and $\Delta RTNDT$, mean values of all other parameters, and 32-EFPY fluences.

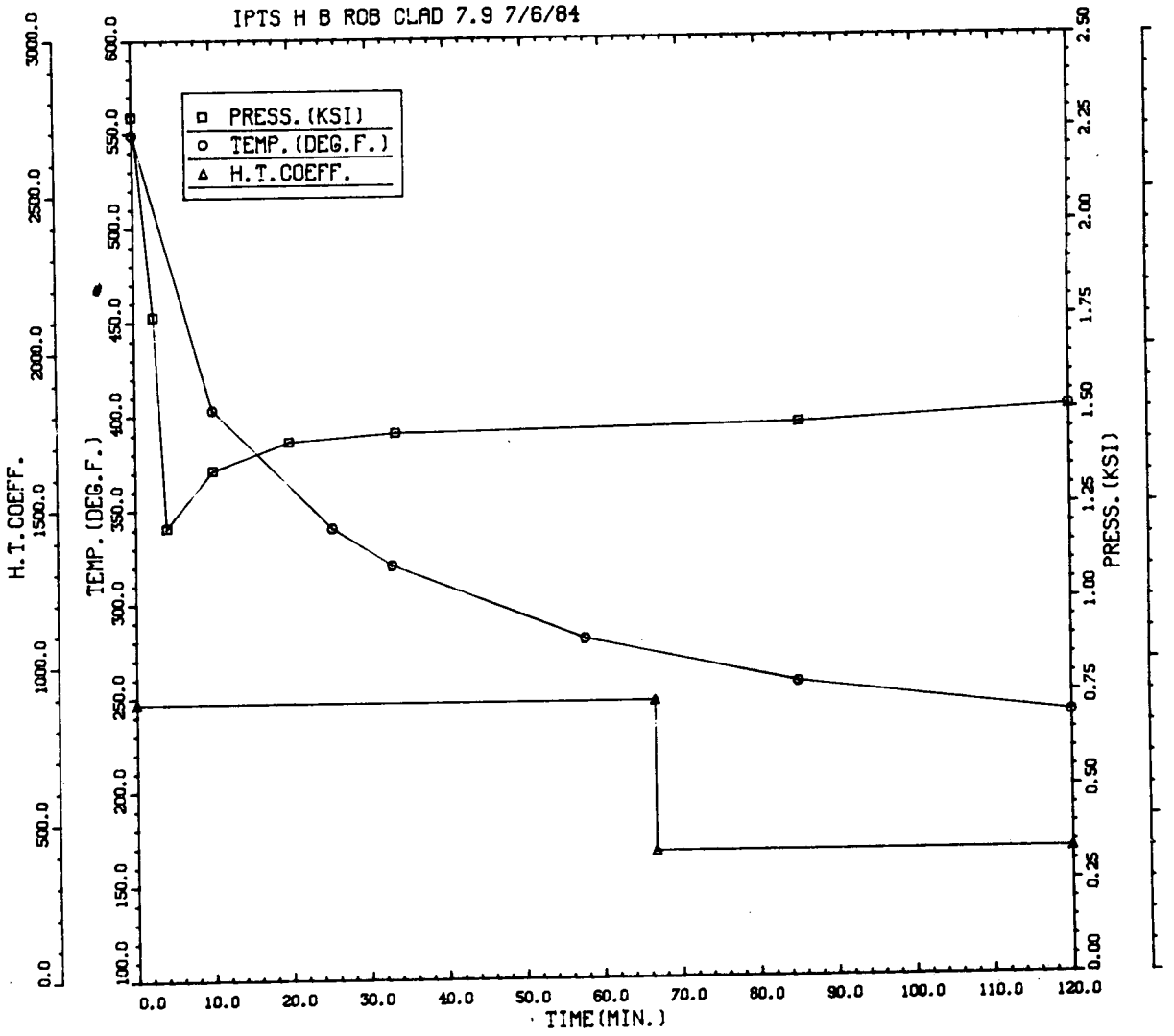

Figure I.55. Transient 7.9: Primary system pressure, downcomer coolant temperature, and fluid-film heat-transfer coefficient vs time in the transient.

Table I.10. Transient 7.9: Summary of digital output, including unadjusted $P(F|E)$ values and histogram data for crack depths, times of failure, and $T - RTNDT$ values at tip of crack corresponding to initiation and arrest events

IPTS H B ROB CLAD 7.9 7/6/84 1. FLAWS/IN**3 DRTN(IS) = 211.2

WELD	P(F/E)	UNADJUSTED 95%CI	%ERR	P(INITIA)	N*V	ADJUSTED P(F/E)	%ERR	NFAIL	NTRIALS
1	9.88D-05	1.86D-05	18.77	1.54D-04	1.000	9.88D-05		109	200000
					VESSEL	9.88D-05	18.77		

DEPTHS FOR INITIAL INITIATION (IN)

	0.09	0.26	0.46	0.67	0.90	1.16	1.44	1.74	2.08
NUMBER	0	88	45	27	7	3	0	0	0
PERCENT	0.0	51.8	26.5	15.9	4.1	1.8	0.0	0.0	0.0

TIMES OF FAILURE(MINUTES)

	0.0	10.0	20.0	30.0	40.0	50.0	60.0	70.0	80.0	90.0	100.0	110.0	120.0
PERCENT	0.0	0.0	0.0	0.0	0.0	6.4	2.8	1.8	15.6	24.8	25.7	22.9	

INITIATION T-RTNDT(DEG.F)

	-100.0	-75.0	-50.0	-25.0	0.0	25.0	50.0	75.0	100.0	125.0	150.0	175.0	200.0
NUMBER	0	0	13	78	74	50	43	8	0	0	0	0	
PERCENT	0.0	0.0	4.9	29.3	27.8	18.8	16.2	3.0	0.0	0.0	0.0	0.0	

ARREST T-RTNDT(DEG.F)

	-50.0	-25.0	0.0	25.0	50.0	75.0	100.0	125.0	150.0	175.0	200.0	225.0	250.0
NUMBER	0	14	8	2	0	1	9	99	24	0	0	0	
PERCENT	0.0	8.9	5.1	1.3	0.0	0.6	5.7	63.1	15.3	0.0	0.0	0.0	

ICRKTP = 2 IACCEL = 1 NDLRS = 0 NRTRS = 0 DATE: 10/30/84 TIME: 00.20.43

CPU TIME: 5 MIN 28 SEC

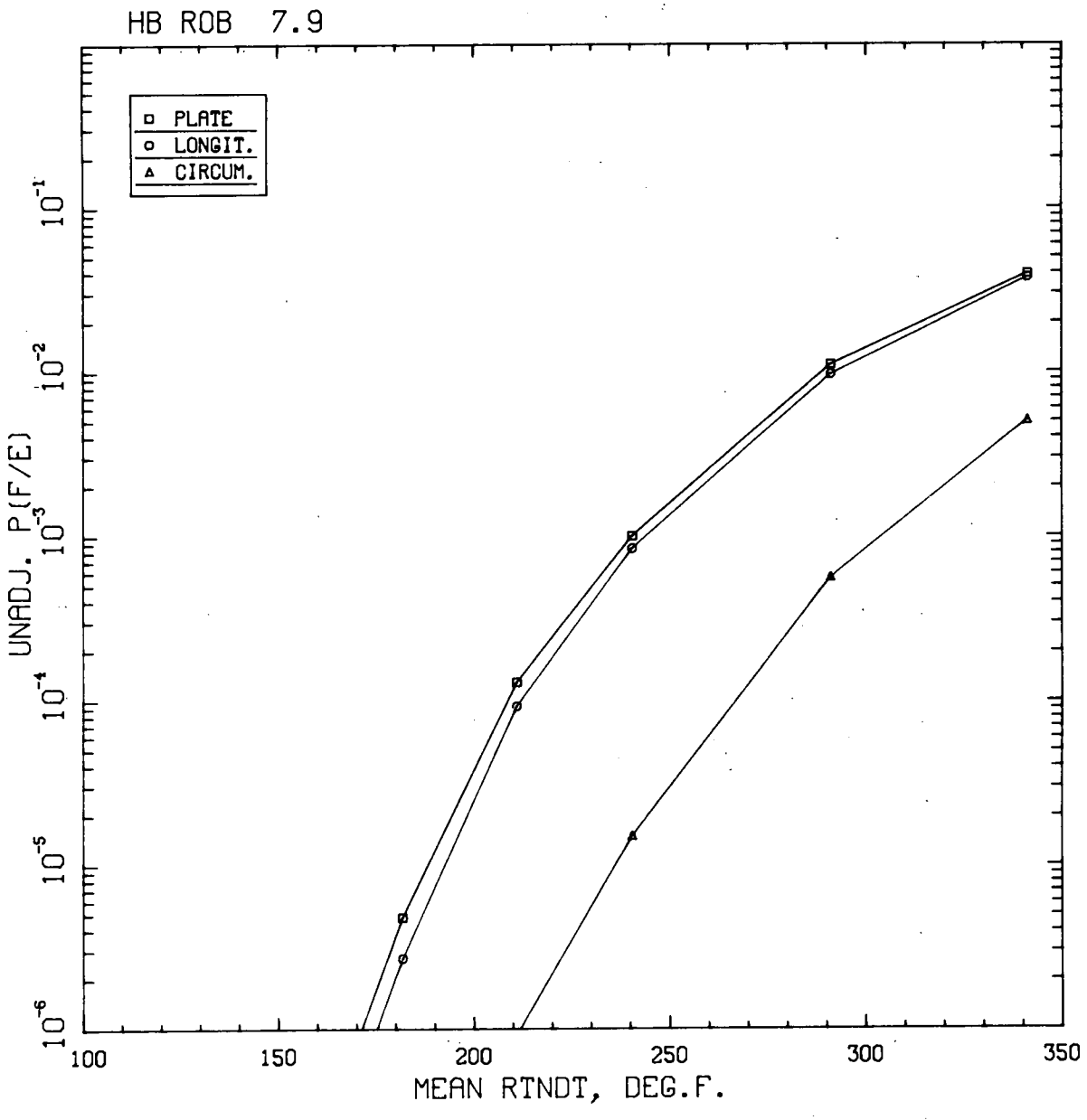

Figure I.56. Transient 7.9: $\hat{P}_j \int_0^w f(a)\, B(a)\, da$ vs $\overline{RTNDT_s}$ for (2-D, 2-D) and (2-D, 2m) flaw combinations.

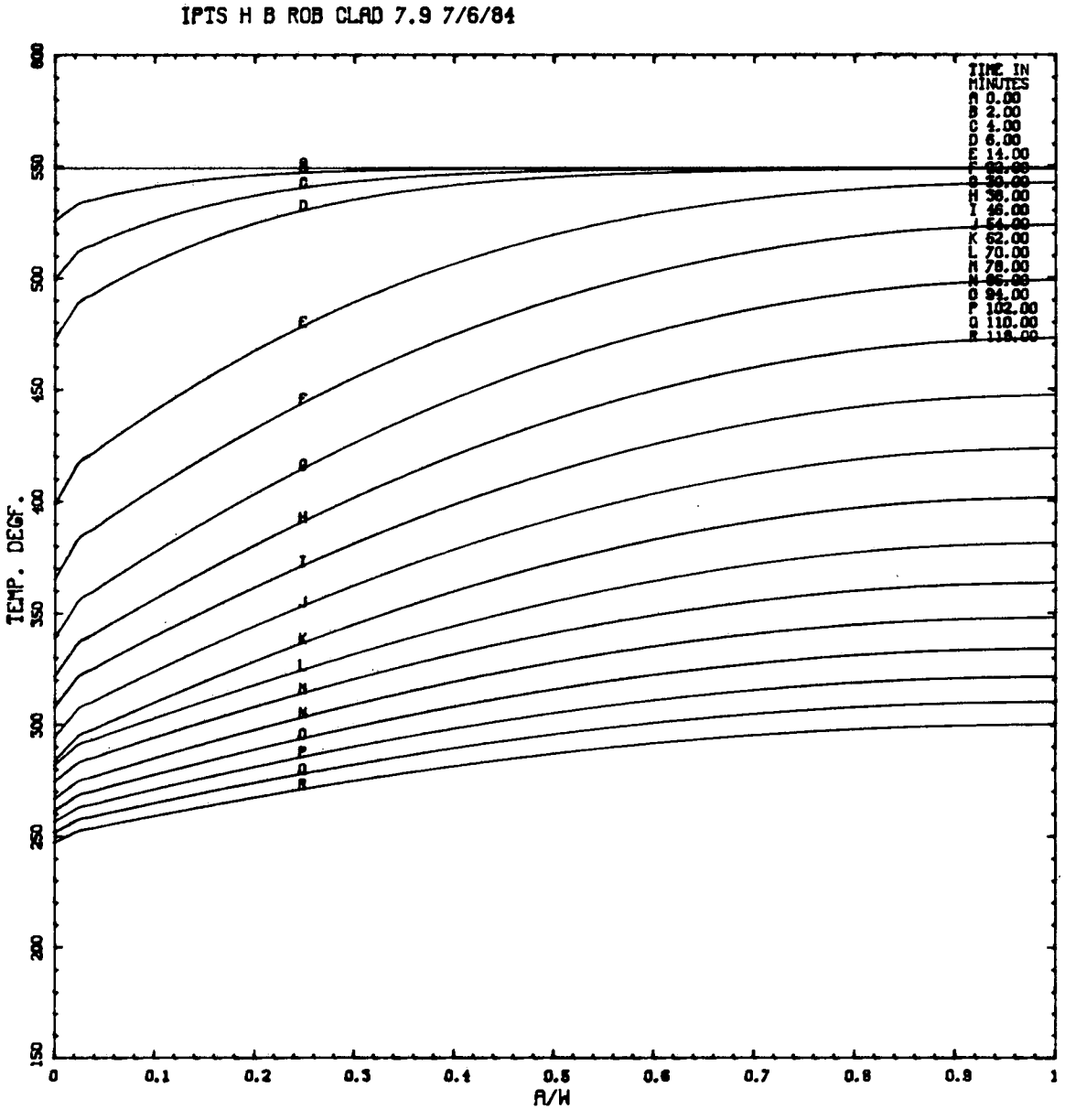

Figure I.57. Transient 7.9: Vessel wall temperature vs depth in wall (a/w) at various times (t) in transient.

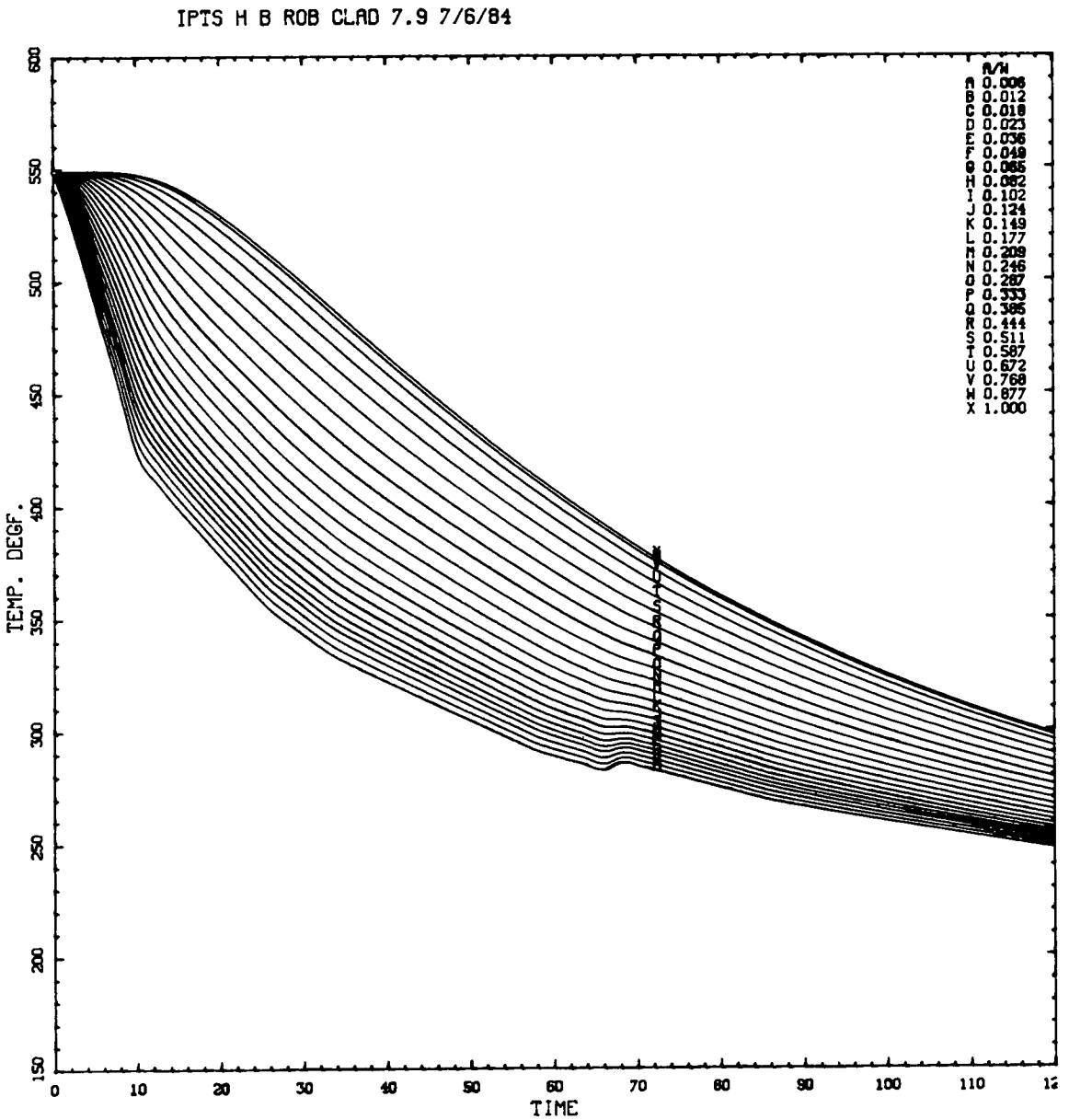

Figure I.58. Transient 7.9: Vessel wall temperature vs time (t) in transient at various depths in wall (a/w).

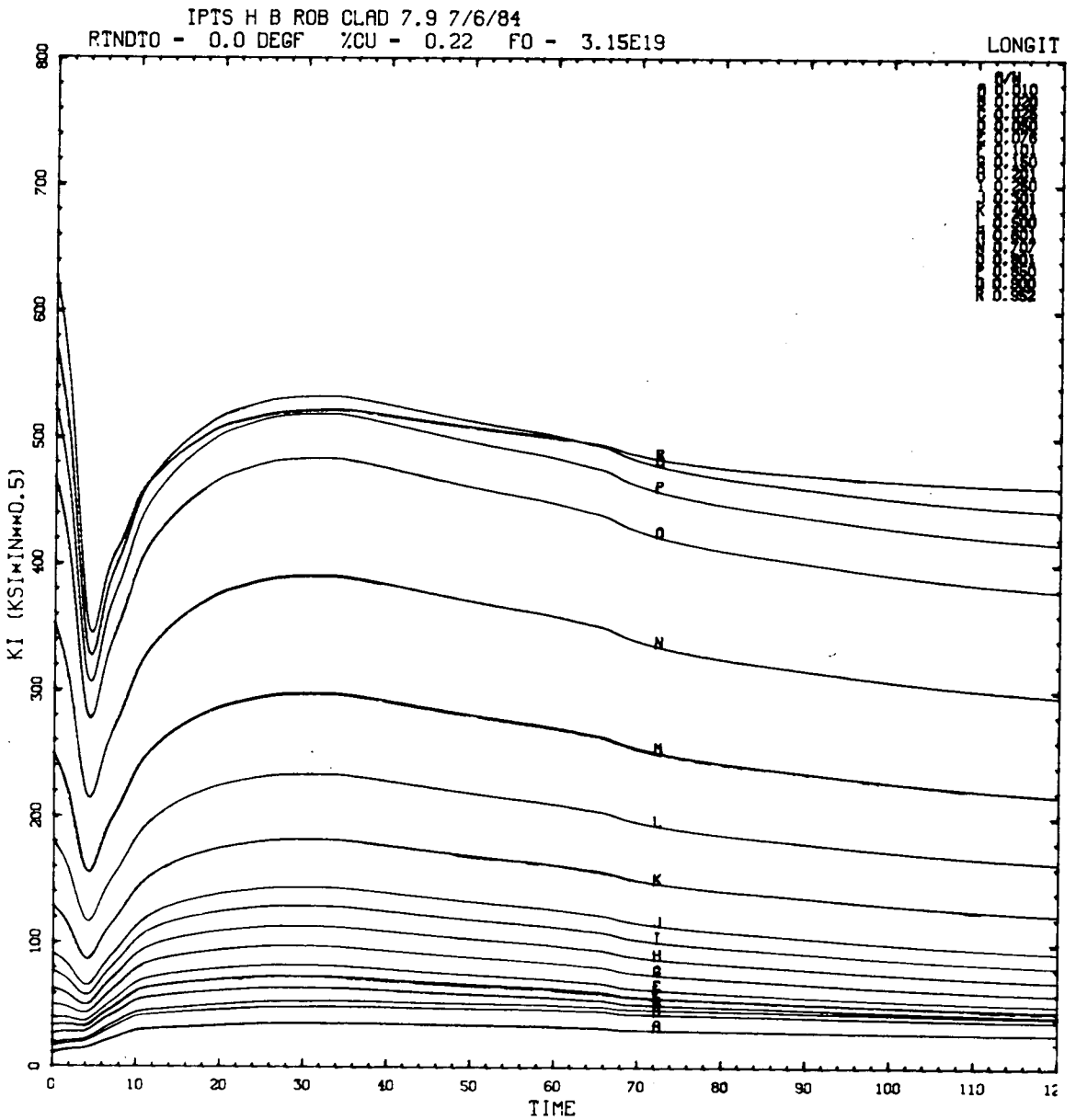

Figure I.59. Transient 7.9: K_I vs time (t) for various depths in wall (a/w).

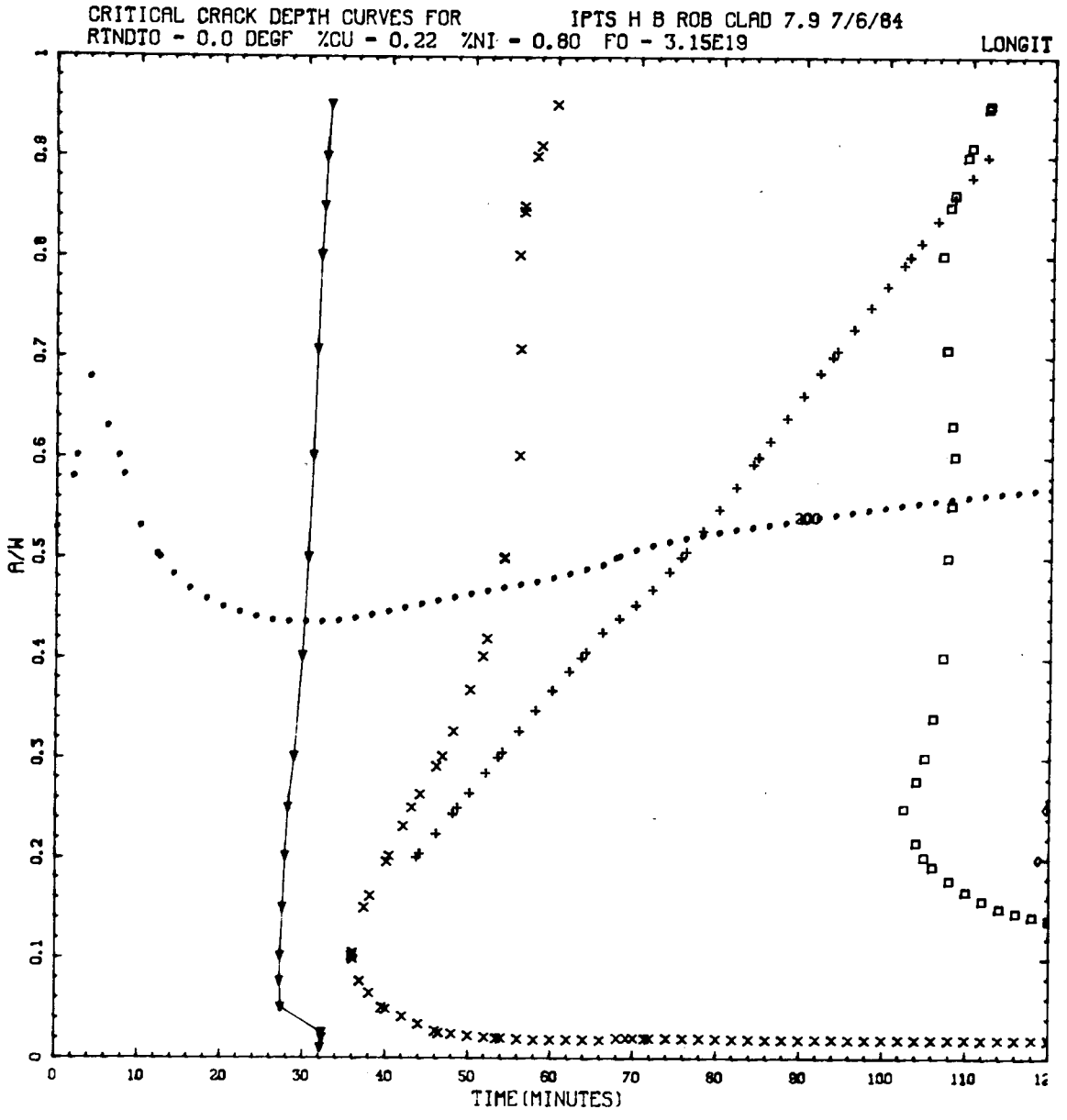

×, 2-D flaw, $K_I = K_{Ia}$
+, 2-m flaw, $K_I = K_{Ia}$
□, 2-D flaw, $K_I = K_{Ic}$
○, 2-D flaw, $K_I = 220$ MPa $\sqrt{m}$
∇, WPS (warm prestressing)

Figure I.60. Transient 7.9: Critical-crack-depth curves for weld 2-273A based on -2σ values of K_{Ic}, K_{Ia}, and $\Delta RTNDT$, mean values of all other parameters, and 32-EFPY fluences.

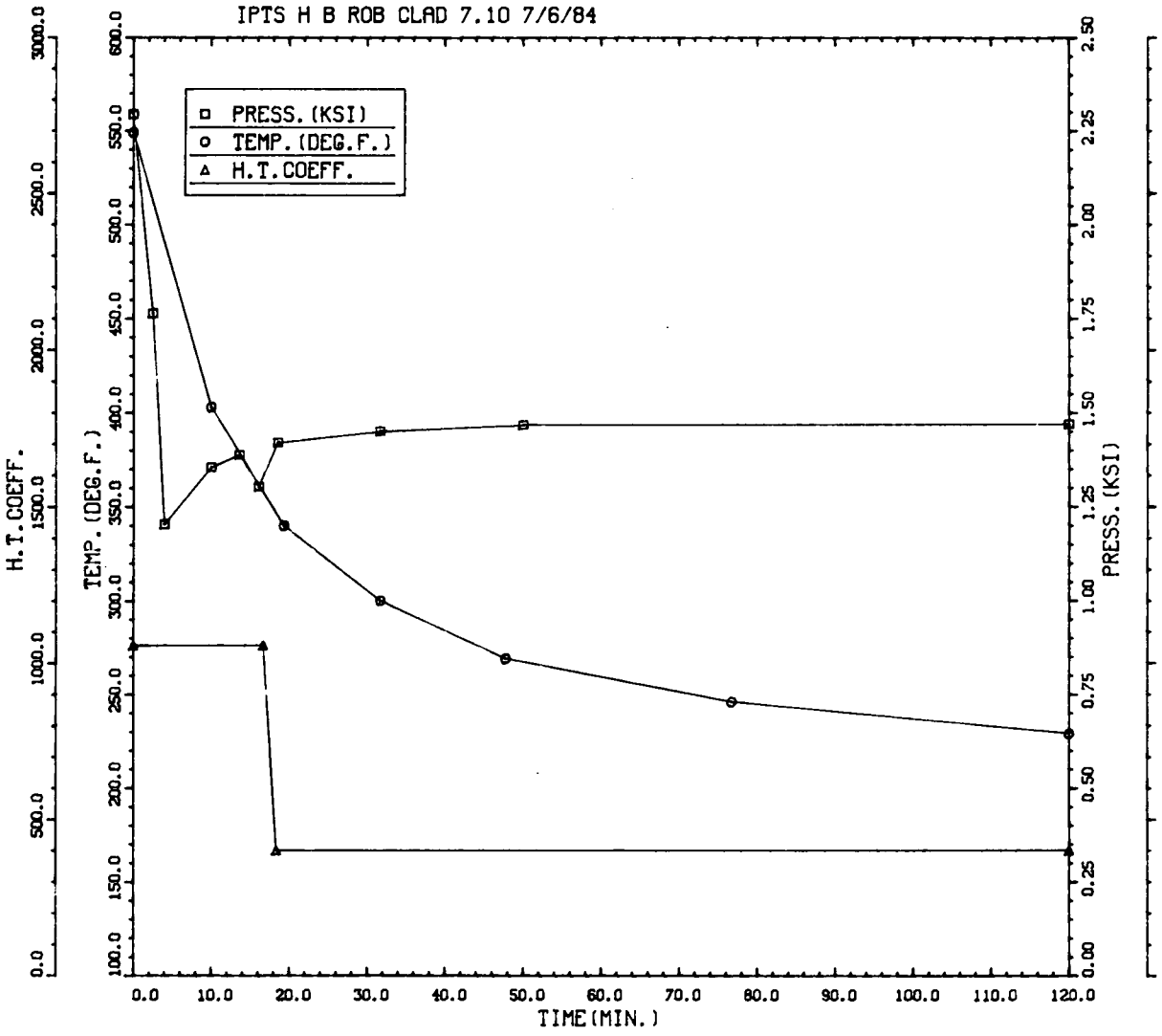

Figure I.61. Transient 7.10: Primary system pressure, downcomer coolant temperature, and fluid-film heat-transfer coefficient vs time in the transient.

Table I.11. Transient 7.10: Summary of digital output, including unadjusted $P(F|E)$ values and histogram data for crack depths, times of failure, and $T - RTNDT$ values at tip of crack corresponding to initiation and arrest events

IPTS H B ROB CLAD 7.10 7/6/84 1. FLAWS/IN**3 DRTN(IS) = 211.2

WELD	P(F/E) (UNADJUSTED)	95%CI	%ERR	P(INITIA)	N*V	P(F/E) (ADJUSTED)	%ERR	NFAIL	NTRIALS
1	2.61D-04	3.01D-05	11.54	3.90D-04	1.000	2.61D-04		288	200000
					VESSEL	2.61D-04	11.54		

DEPTHS FOR INITIAL INITIATION (IN)

	0.09	0.26	0.46	0.67	0.90	1.16	1.44	1.74	2.08
NUMBER	0	230	124	52	16	7	1	0	0
PERCENT	0.0	53.5	28.8	12.1	3.7	1.6	0.2	0.0	0.0

TIMES OF FAILURE(MINUTES)

	0.0	10.0	20.0	30.0	40.0	50.0	60.0	70.0	80.0	90.0	100.0	110.0	120.0
PERCENT	0.0	0.0	0.0	0.0	0.0	0.3	5.9	17.7	17.7	16.0	20.1	22.2	

INITIATION T-RTNDT(DEG.F)

	-100.0	-75.0	-50.0	-25.0	0.0	25.0	50.0	75.0	100.0	125.0	150.0	175.0	200.0
NUMBER	0	0	26	168	223	155	114	17	0	0	0	0	
PERCENT	0.0	0.0	3.7	23.9	31.7	22.0	16.2	2.4	0.0	0.0	0.0	0.0	

ARREST T-RTNDT(DEG.F)

	-50.0	-25.0	0.0	25.0	50.0	75.0	100.0	125.0	150.0	175.0	200.0	225.0	250.0
NUMBER	0	7	30	10	2	0	21	260	85	0	0	0	
PERCENT	0.0	1.7	7.2	2.4	0.5	0.0	5.1	62.7	20.5	0.0	0.0	0.0	

ICRKTP = 2 IACCEL = 1 NDLRS = 0 NRTRS = 0 DATE: 10/30/84 TIME: 00.16.07

CPU TIME: 5 MIN 28 SEC

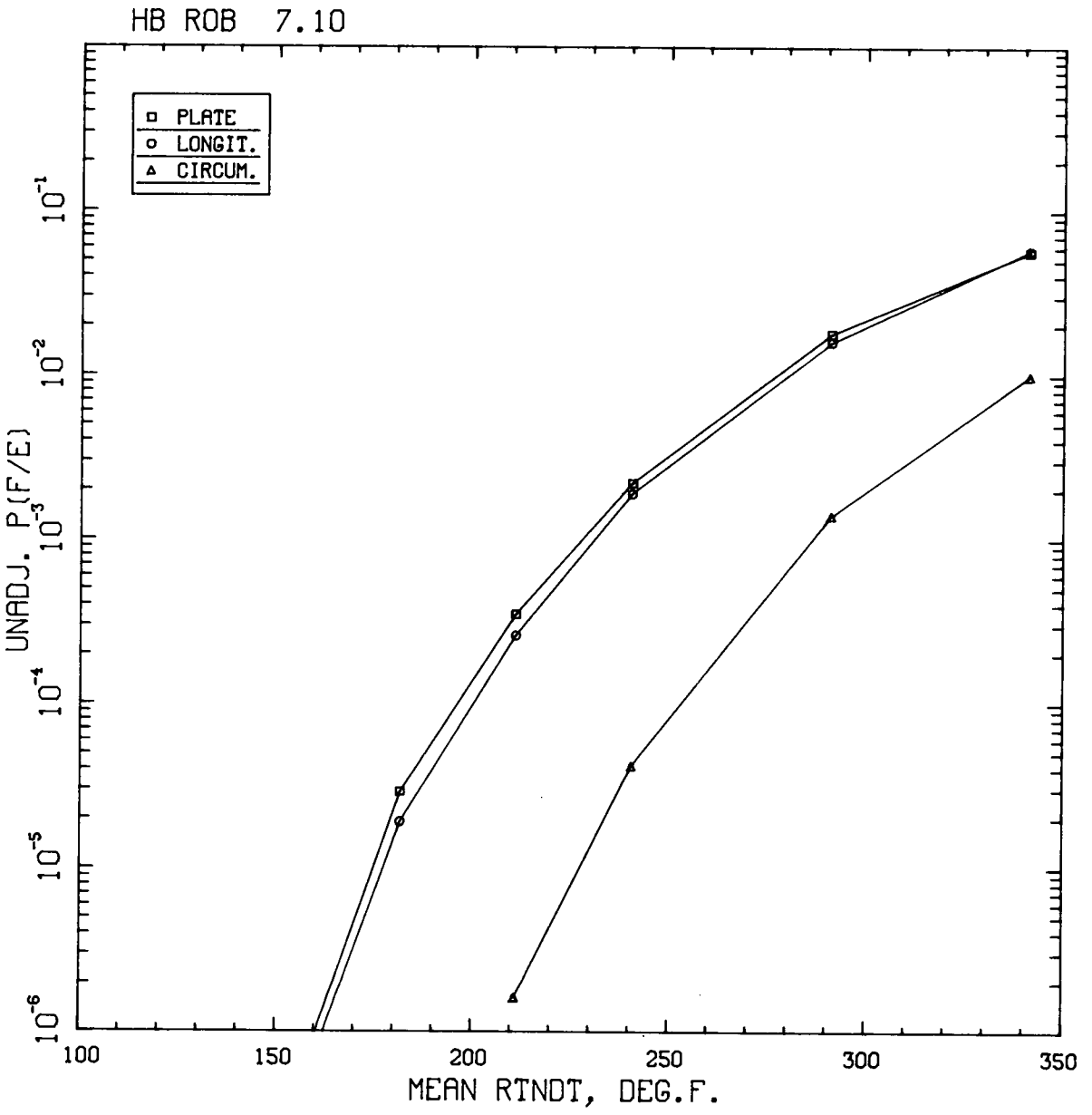

Figure I.62. Transient 7.10: $\hat{P}_j \int_0^w f(a)\, B(a)\, da$ **vs** $\overline{RTNDT_s}$ **for (2-D, 2-D) and (2-D, 2m) flaw combinations.**

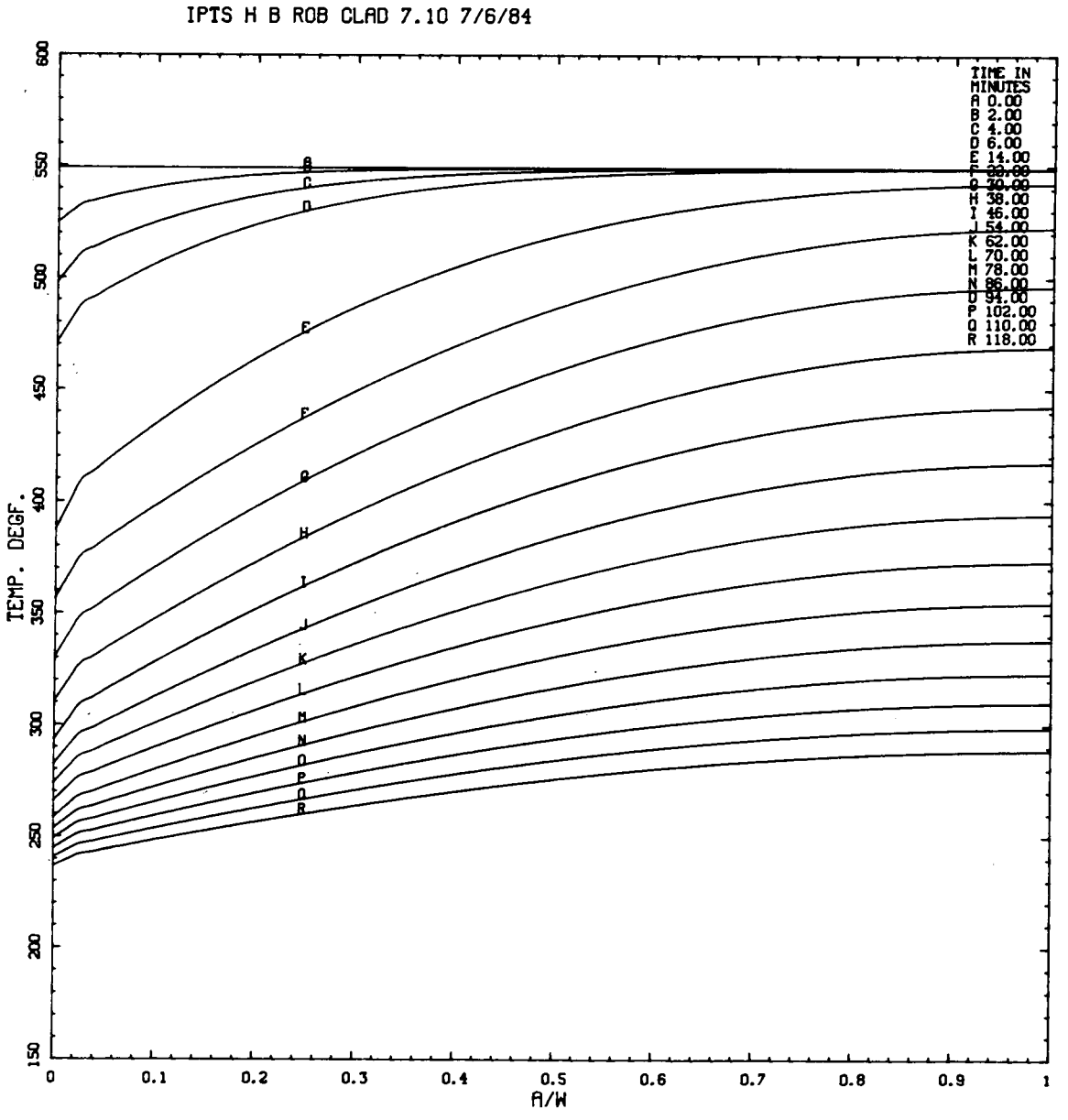

Figure I.63. Transient 7.10: Vessel wall temperature vs depth in wall (a/w) at various times (t) in transient.

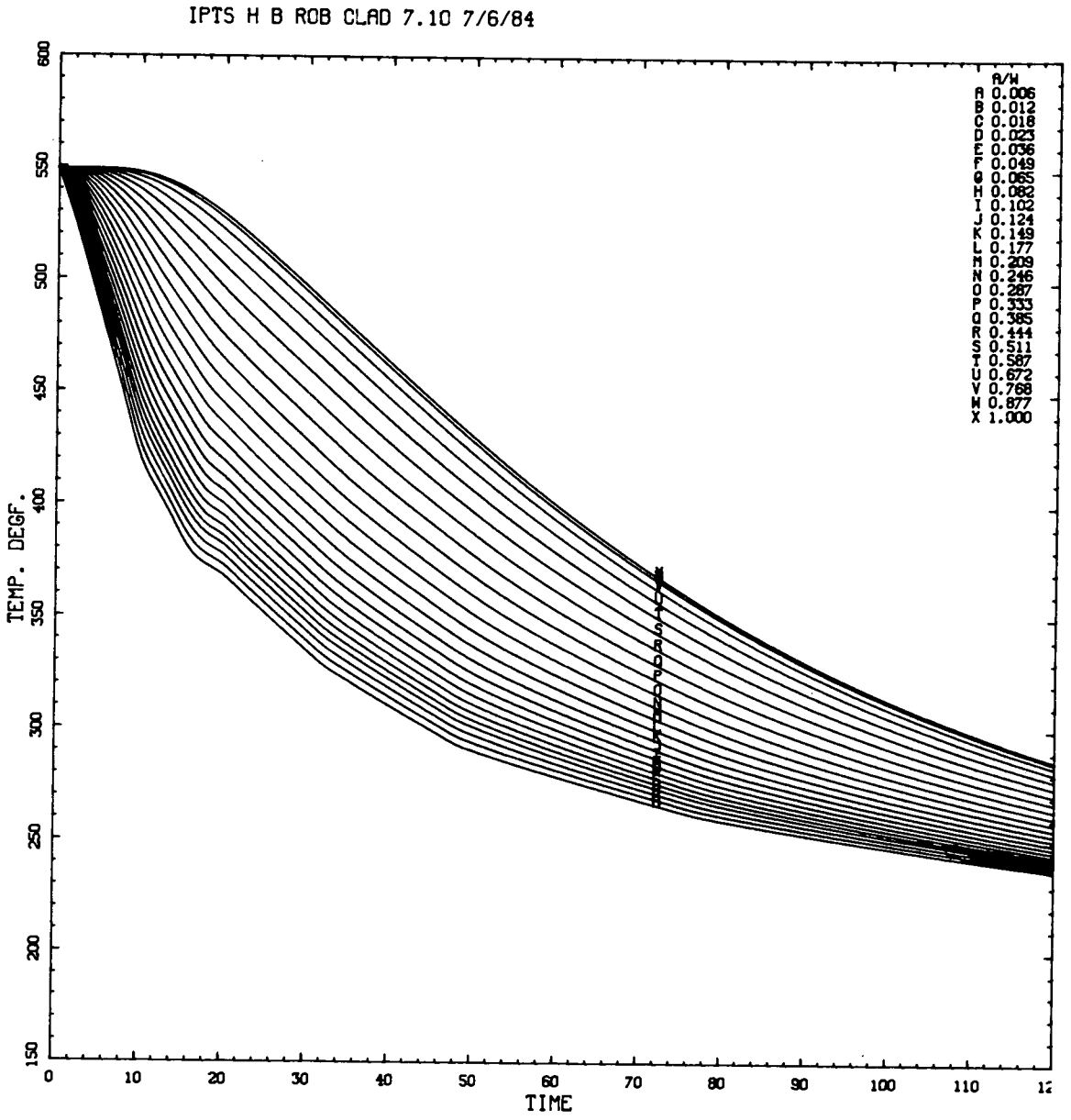

Figure I.64. Transient 7.10: Vessel wall temperature vs time (t) in transient at various depths in wall (a/w).

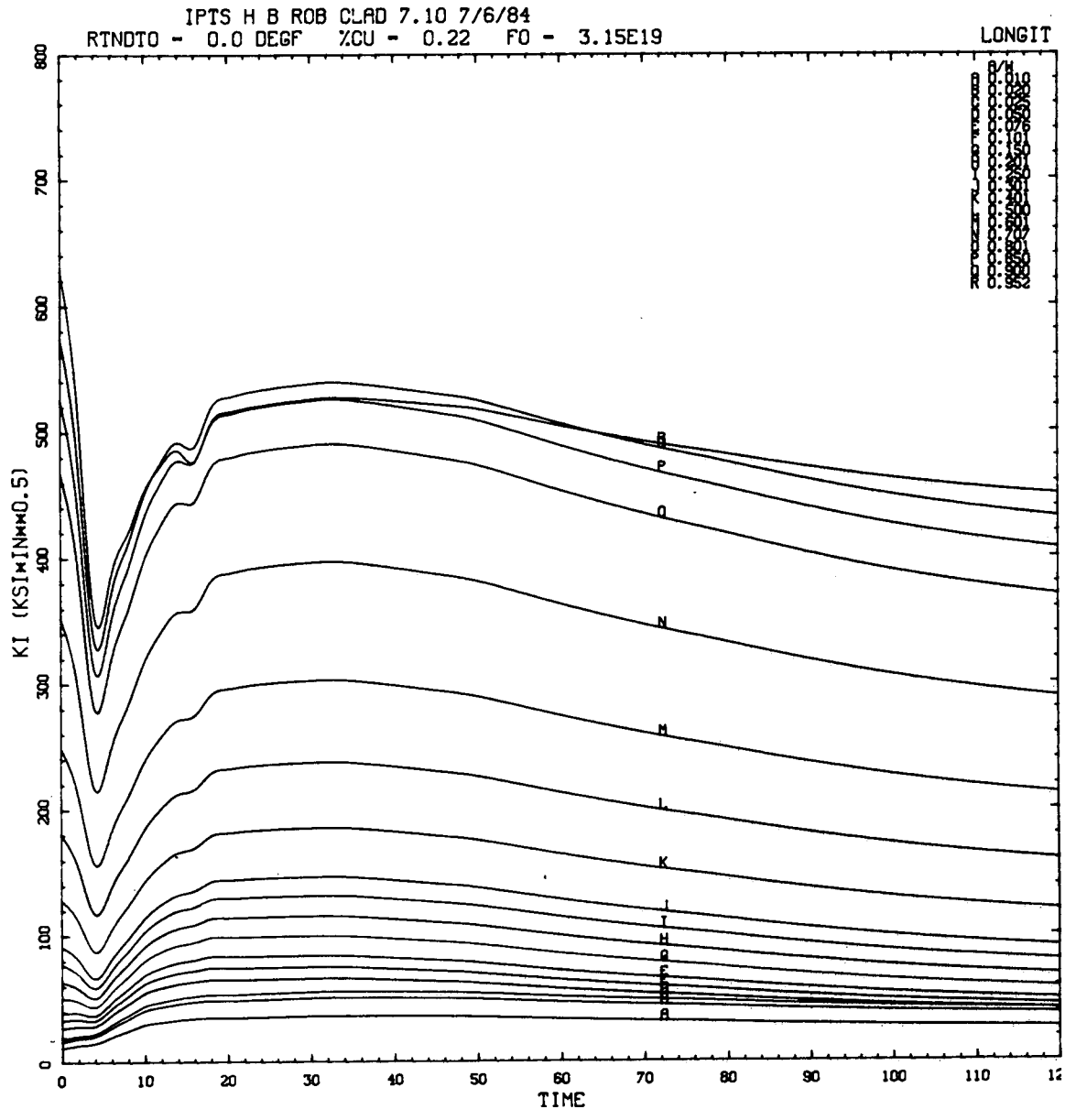

Figure I.65. Transient 7.10: K_I vs time (t) for various depths in wall (a/w).

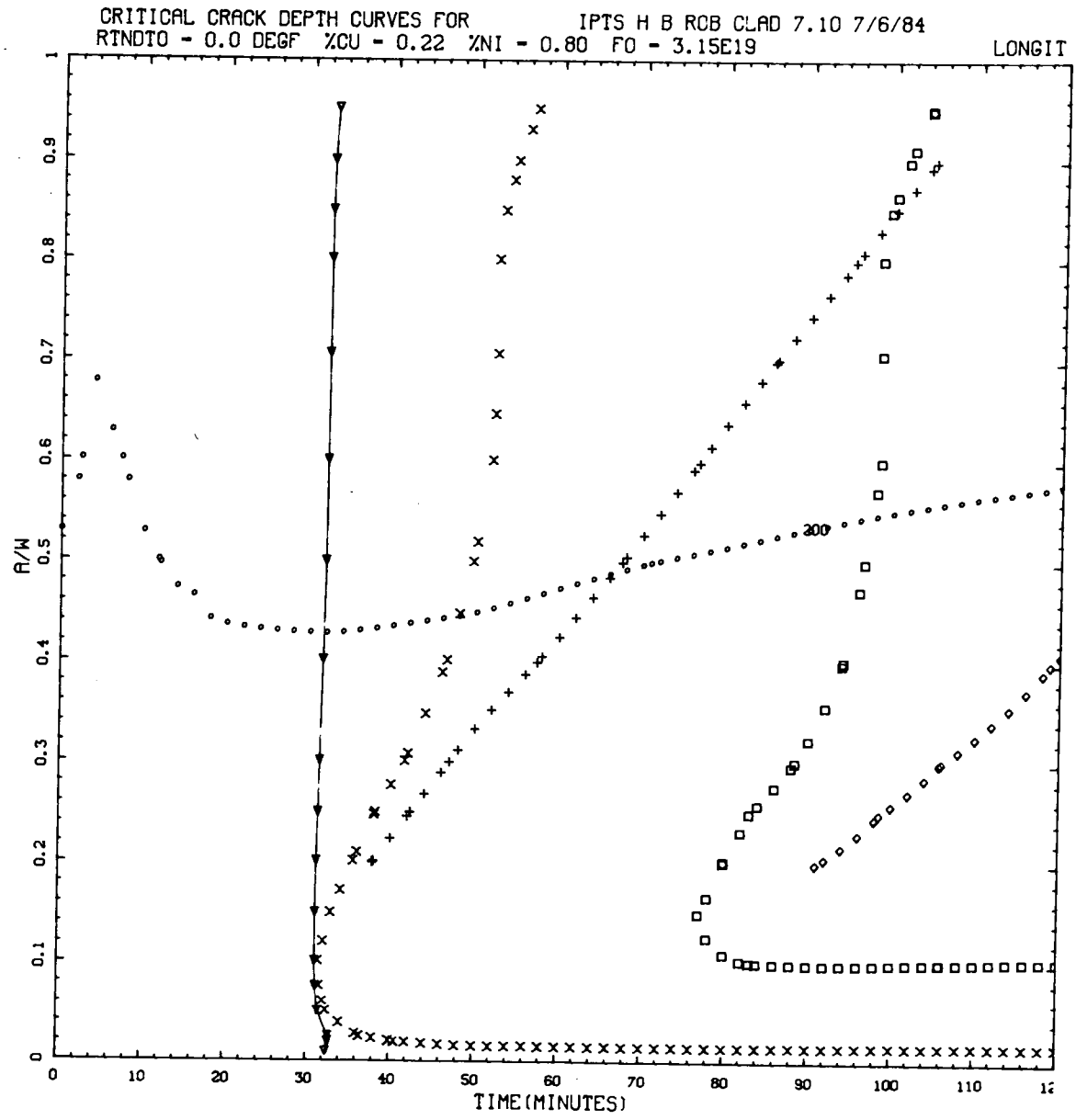

Figure I.66. Transient 7.10: Critical-crack-depth curves for weld 2-273A based on -2σ values of K_{Ic}, K_{Ia}, and $\Delta RTNDT$, mean values of all other parameters, and 32-EFPY fluences.

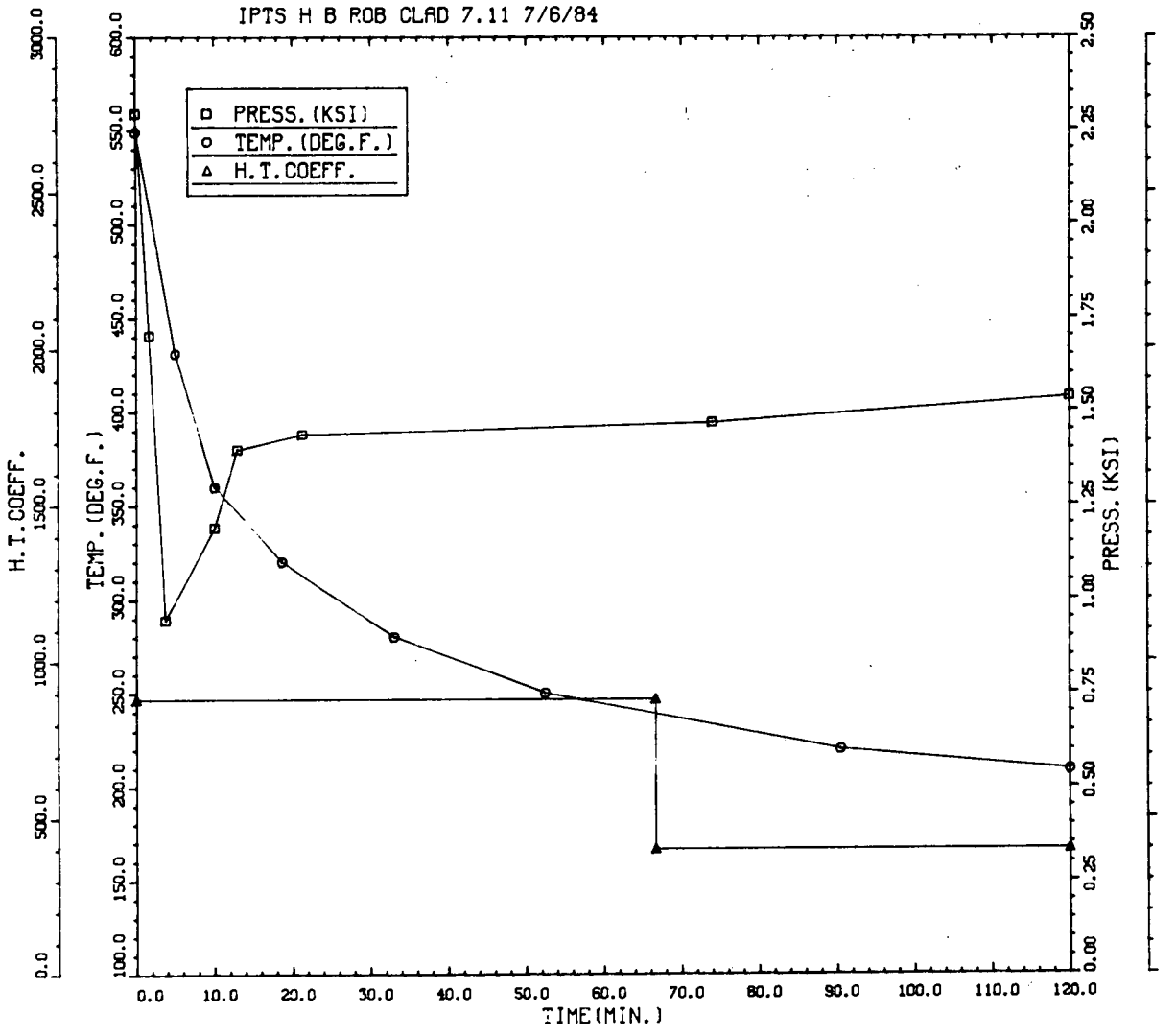

Figure I.67. Transient 7.11: Primary system pressure, downcomer coolant temperature, and fluid-film heat-transfer coefficient vs time in the transient.

Table I.12. Transient 7.11: Summary of digital output, including unadjusted $P(F|E)$ values and histogram data for crack depths, times of failure, and $T - RTNDT$ values at tip of crack corresponding to initiation and arrest events

IPTS H B ROB CLAD 7.11 7/6/84 1. FLAWS/IN**3 DRTN(IS) = 211.2

	UNADJUSTED					ADJUSTED			
WELD	P(F/E)	95%CI	%ERR	P(INITIA)	N*V	P(F/E)	%ERR	NFAIL	NTRIALS
1	1.52D-03	1.46D-04	9.63	1.81D-03	1.000	1.52D-03		413	160000
					VESSEL	1.52D-03	9.63		

DEPTHS FOR INITIAL INITIATION (IN)

	0.09	0.26	0.46	0.67	0.90	1.16	1.44	1.74	2.08
NUMBER	1	287	124	58	17	6	1	0	0
PERCENT	0.2	58.1	25.1	11.7	3.4	1.2	0.2	0.0	0.0

TIMES OF FAILURE(MINUTES)

	0.0	10.0	20.0	30.0	40.0	50.0	60.0	70.0	80.0	90.0	100.0	110.0	120.0
PERCENT	0.0	0.0	0.0	0.0	1.9	6.8	12.6	7.7	21.5	19.1	17.2	13.1	

INITIATION T-RTNDT(DEG.F)

	-100.0	-75.0	-50.0	-25.0	0.0	25.0	50.0	75.0	100.0	125.0	150.0	175.0	200.0
NUMBER	1	2	36	184	242	220	185	29	2	0	0	0	
PERCENT	0.1	0.2	4.0	20.4	26.9	24.4	20.5	3.2	0.2	0.0	0.0	0.0	

ARREST T-RTNDT(DEG.F)

	-50.0	-25.0	0.0	25.0	50.0	75.0	100.0	125.0	150.0	175.0	200.0	225.0	250.0
NUMBER	0	6	7	7	2	3	16	272	175	0	0	0	
PERCENT	0.0	1.2	1.4	1.4	0.4	0.6	3.3	55.7	35.9	0.0	0.0	0.0	

ICRKTP = 2 IACCEL = 0 NDLRS = 0 NRTRS = 0 DATE: 10/30/84 TIME: 00.29.03

CPU TIME: 4 MIN 25 SEC

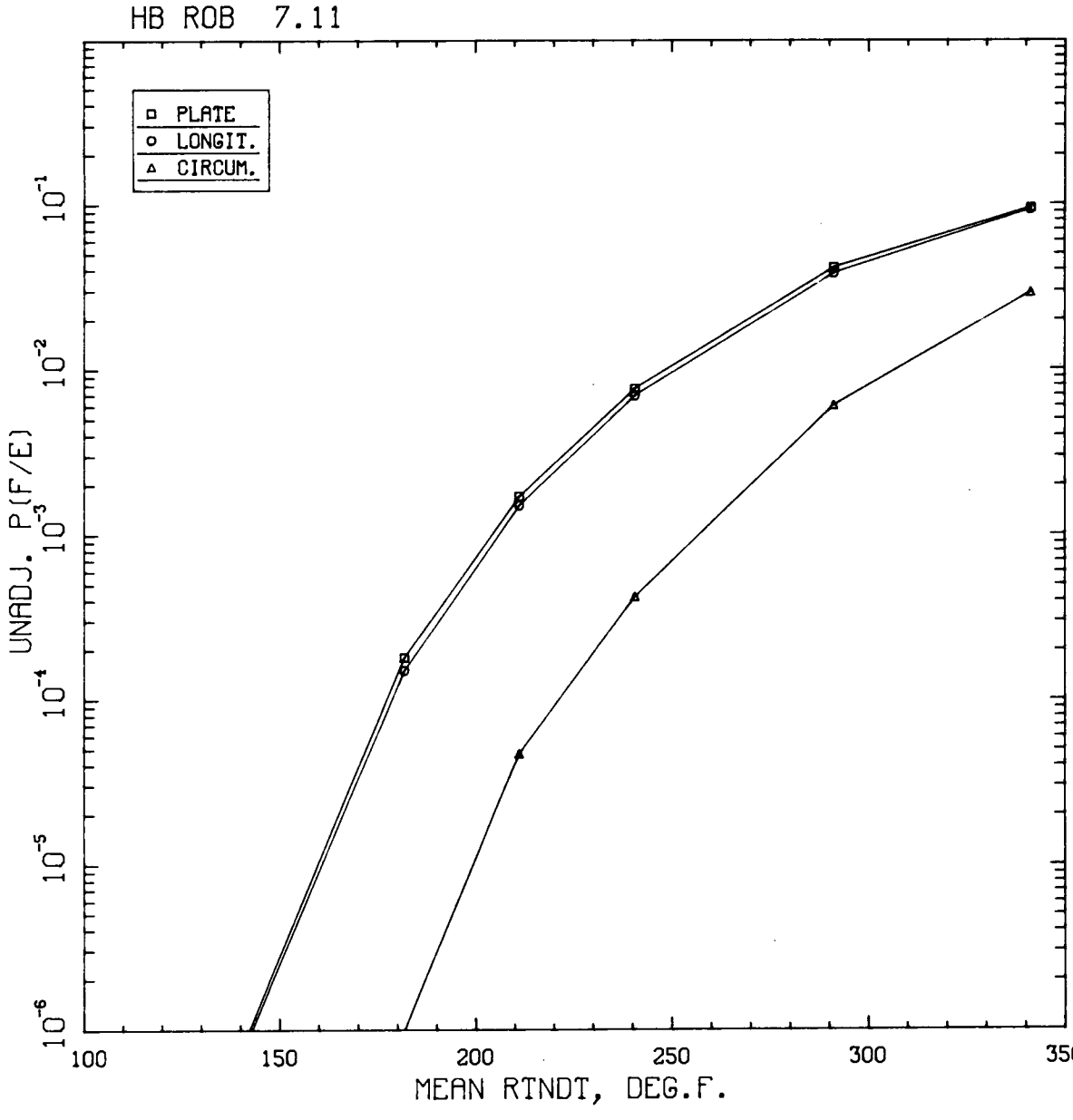

Figure I.68. Transient 7.11: $\hat{P}_j \int_0^w f(a)\, B(a)\, da$ vs $\overline{RTNDT_s}$ for (2-D, 2-D) and (2-D, 2m) flaw combinations.

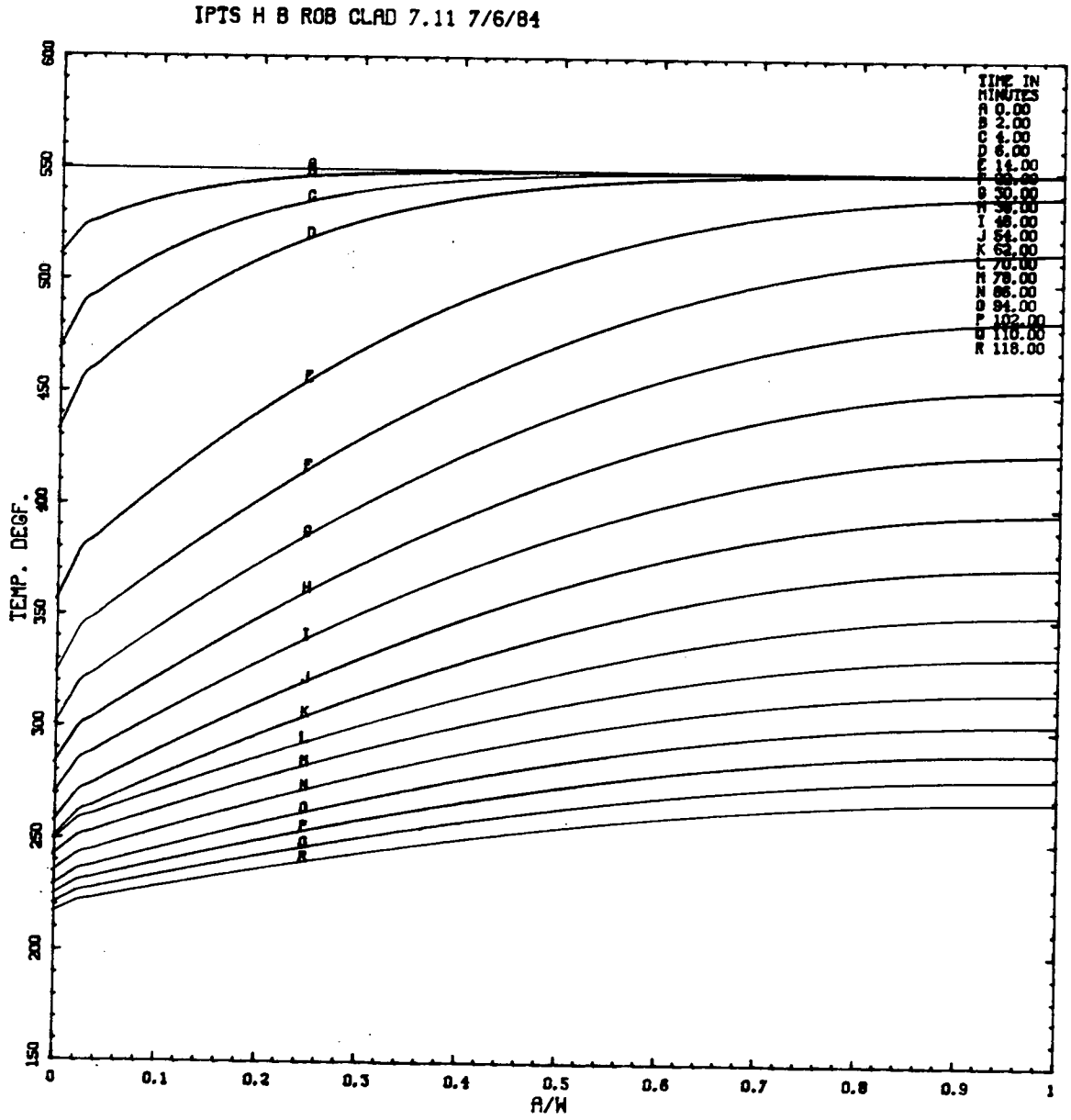

Figure I.69. Transient 7.11: Vessel wall temperature vs depth in wall (a/w) at various times (t) in transient.

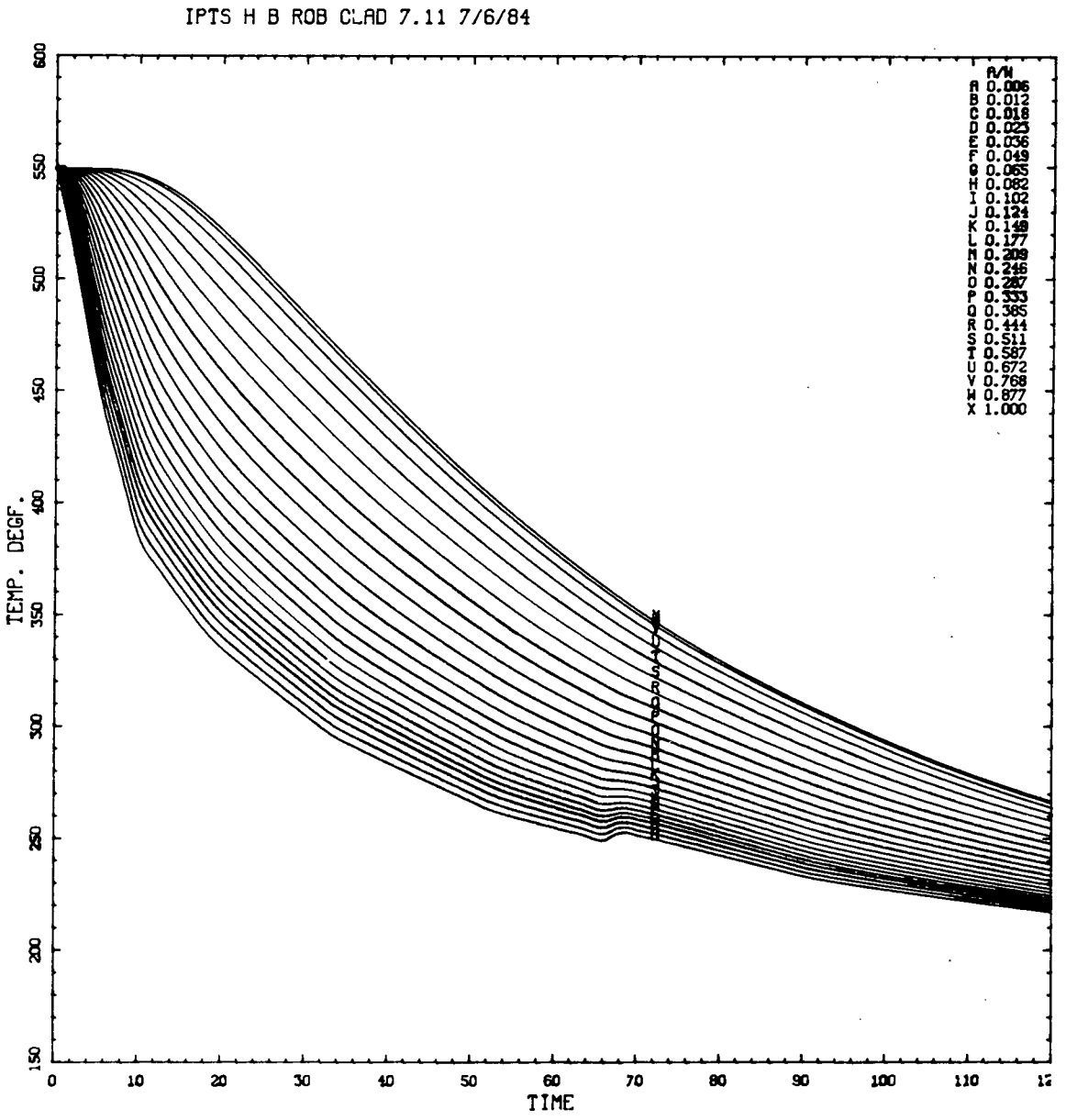

Figure I.70. Transient 7.11: Vessel wall temperature vs time (t) in transient at various depths in wall (a/w).

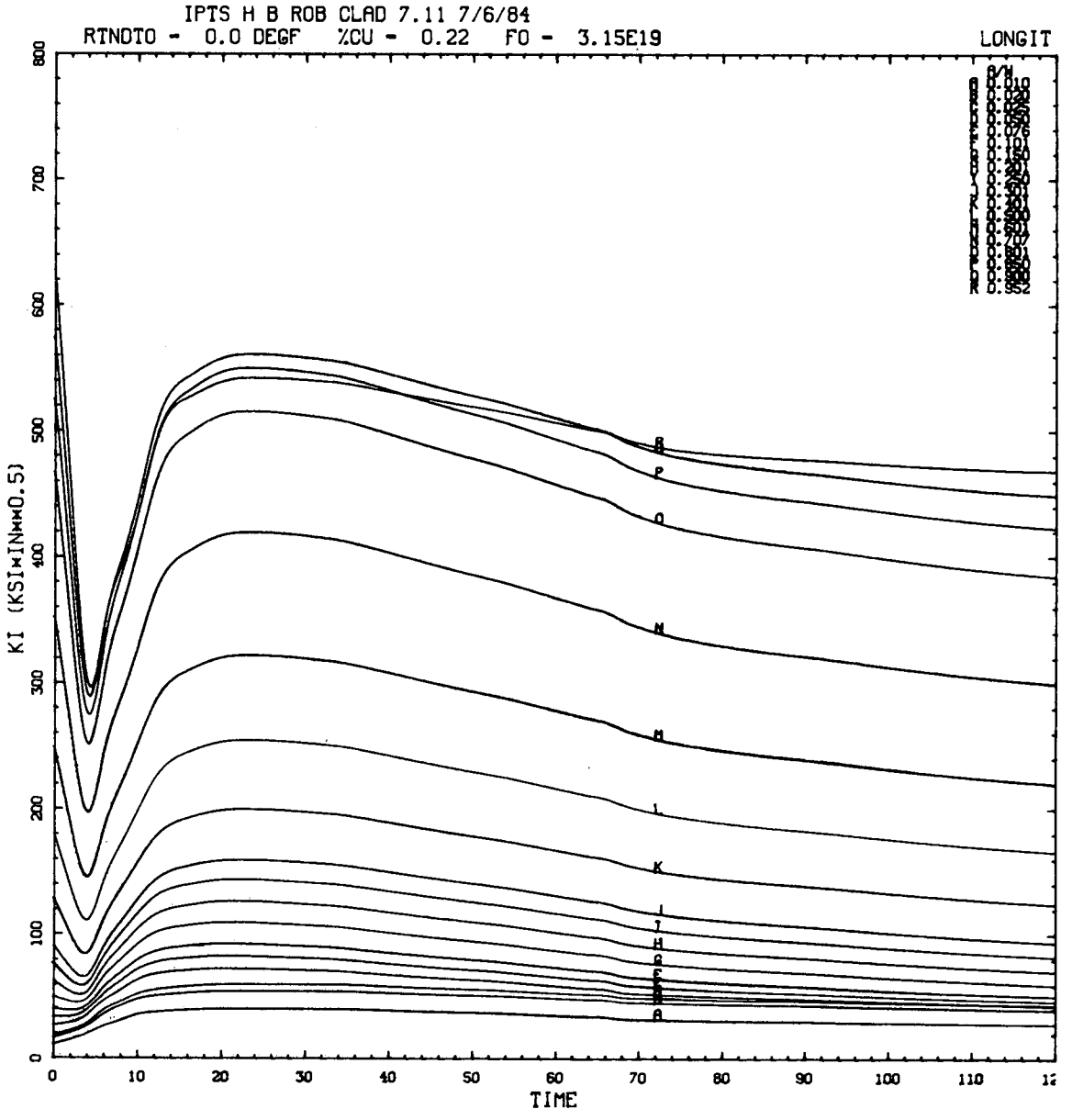

Figure I.71. Transient 7.11: K_I vs time (t) for various depths in wall (a/w).

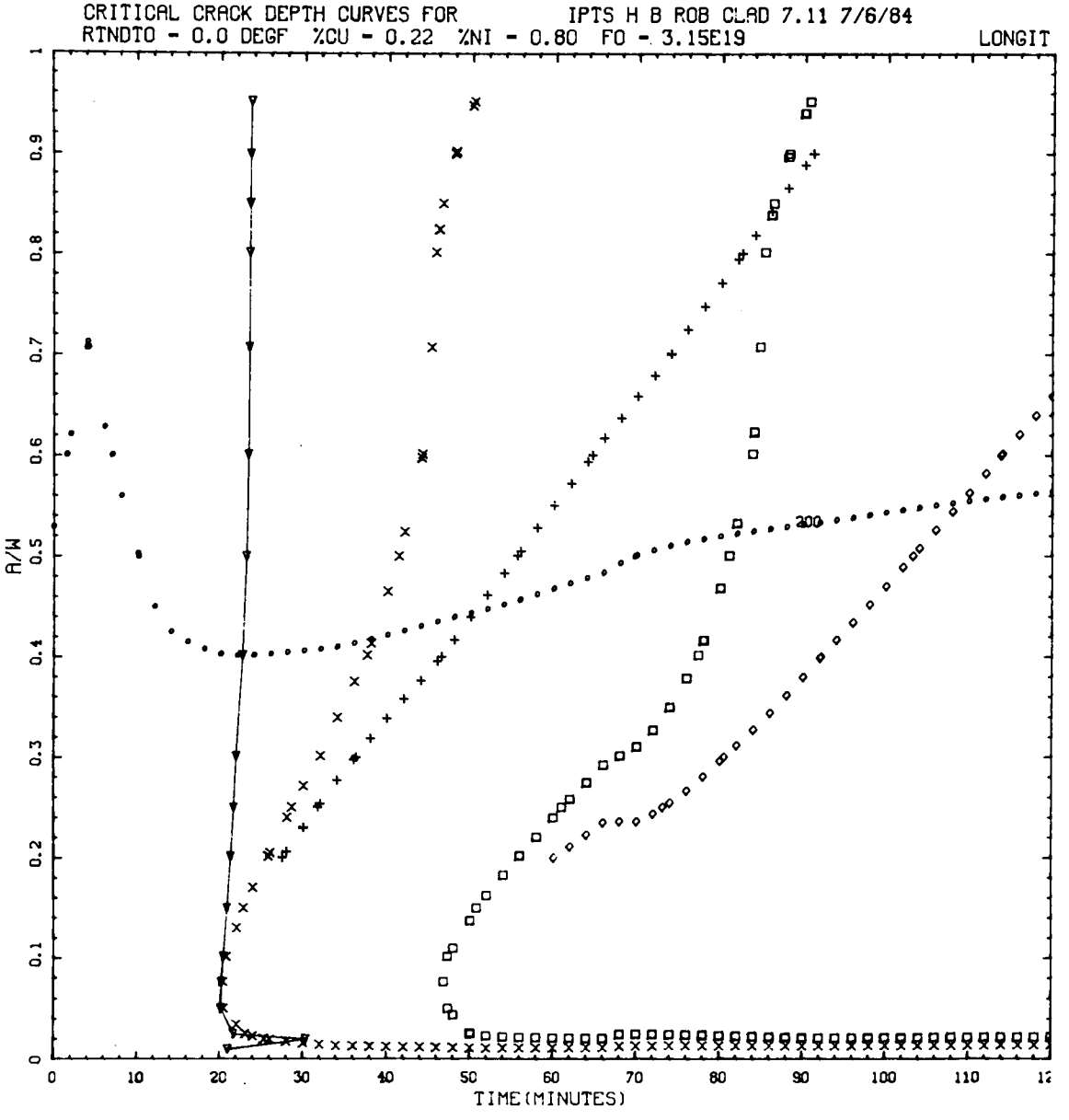

×, 2-D flaw, $K_I = K_{Ia}$
+, 2-m flaw, $K_I = K_{Ia}$
□, 2-D flaw, $K_I = K_{Ic}$
○, 2-D flaw, $K_I = 220$ MPa $\sqrt{m}$
∇, WPS (warm prestressing)

Figure I.72. Transient 7.11: Critical-crack-depth curves for weld 2-273A based on -2σ values of K_{Ic}, K_{Ia}, and $\Delta RTNDT$, mean values of all other parameters, and 32-EFPY fluences.

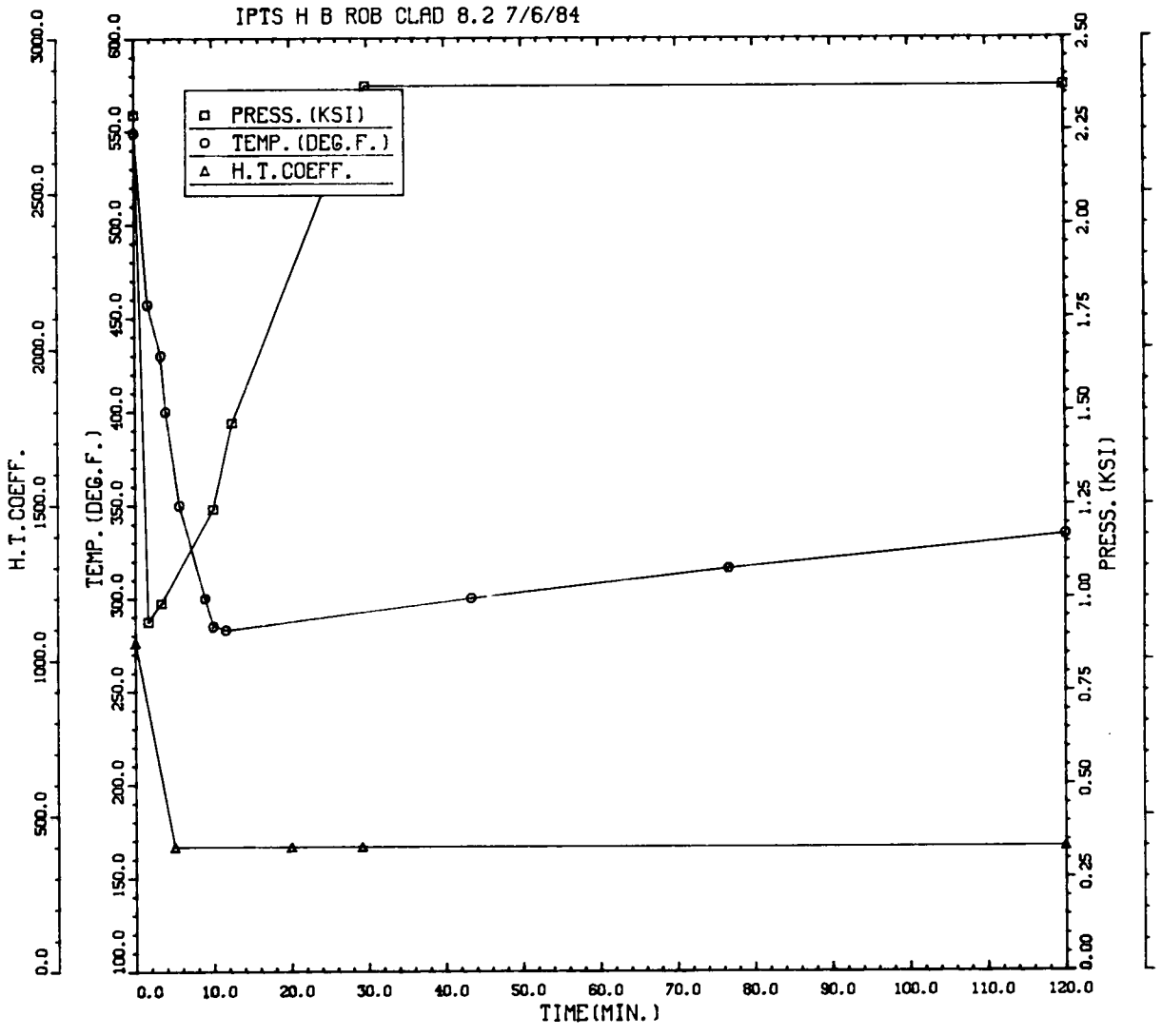

Figure I.73. Transient 8.2: Primary system pressure, downcomer coolant temperature, and fluid-film heat-transfer coefficient vs time in the transient.

Table I.13. Transient 8.2: Summary of digital output, including unadjusted $P(F|E)$ values and histogram data for crack depths, times of failure, and $T - RTNDT$ values at tip of crack corresponding to initiation and arrest events

```
        IPTS H B ROB CLAD 8.2 7/6/84                    1. FLAWS/IN**3    DRTN(IS) =  211.2

        -------------UNADJUSTED--------------           ---ADJUSTED----
WELD    P(F/E)      95%CI     %ERR   P(INITIA)  N*V      P(F/E)    %ERR    NFAIL    NTRIALS

 1      4.40D-05   4.35D-06   9.90   1.43D-04  1.000    4.40D-05           391      130000

                                                VESSEL   4.40D-05   9.90


DEPTHS FOR INITIAL INITIATION (IN)
              0.09  0.26  0.46  0.67  0.90  1.16  1.44  1.74  2.08
   NUMBER      12   670   408   132    43     7     0     0     0
   PERCENT    0.9  52.7  32.1  10.4   3.4   0.6   0.0   0.0   0.0


TIMES OF FAILURE(MINUTES)
              0.0  10.0  20.0  30.0  40.0  50.0  60.0  70.0  80.0  90.0 100.0 110.0 120.0
  PERCENT      0.0   0.0  22.0  22.0  18.9  19.9   7.4   5.6   2.0   2.0   0.0   0.0


 INITIATION T-RTNDT(DEG.F)
           -100.0 -75.0 -50.0 -25.0   0.0  25.0  50.0  75.0 100.0 125.0 150.0 175.0 200.0
  NUMBER        0     0     2   135   607   507   253   115    11     0     0     0
  PERCENT      0.0   0.0   0.1   8.3  37.2  31.1  15.5   7.1   0.7   0.0   0.0   0.0


 ARREST T-RTNDT(DEG.F)
            -50.0 -25.0   0.0  25.0  50.0  75.0 100.0 125.0 150.0 175.0 200.0 225.0 250.0
  NUMBER        0     0     0     0     0     6    27   327   587   291     1     0
  PERCENT      0.0   0.0   0.0   0.0   0.0   0.5   2.2  26.4  47.4  23.5   0.1   0.0


 # OF STD DEVS ABOVE MEAN DELTA RTNDT(FAILURES ONLY)
              1.00  1.25  1.50  1.75  2.00  2.25  2.50  2.75  3.00
  NUMBER        11    23    38    50    82    80    58    49
  PERCENT      2.8   5.9   9.7  12.8  21.0  20.5  14.8  12.5


 # OF STD DEVS ABOVE MEAN RTNDT(FAILURES ONLY)
              1.00  1.25  1.50  1.75  2.00  2.25  2.50  2.75  3.00
  NUMBER         1     4    29    39    54    89    94    81
  PERCENT      0.3   1.0   7.4  10.0  13.8  22.8  24.0  20.7


ICRKTP = 2   IACCEL = 0   NDLRS = 1   NRTRS = 1   DATE: 10/30/84   TIME: 00.20.53

CPU TIME:  3 MIN 31 SEC
```

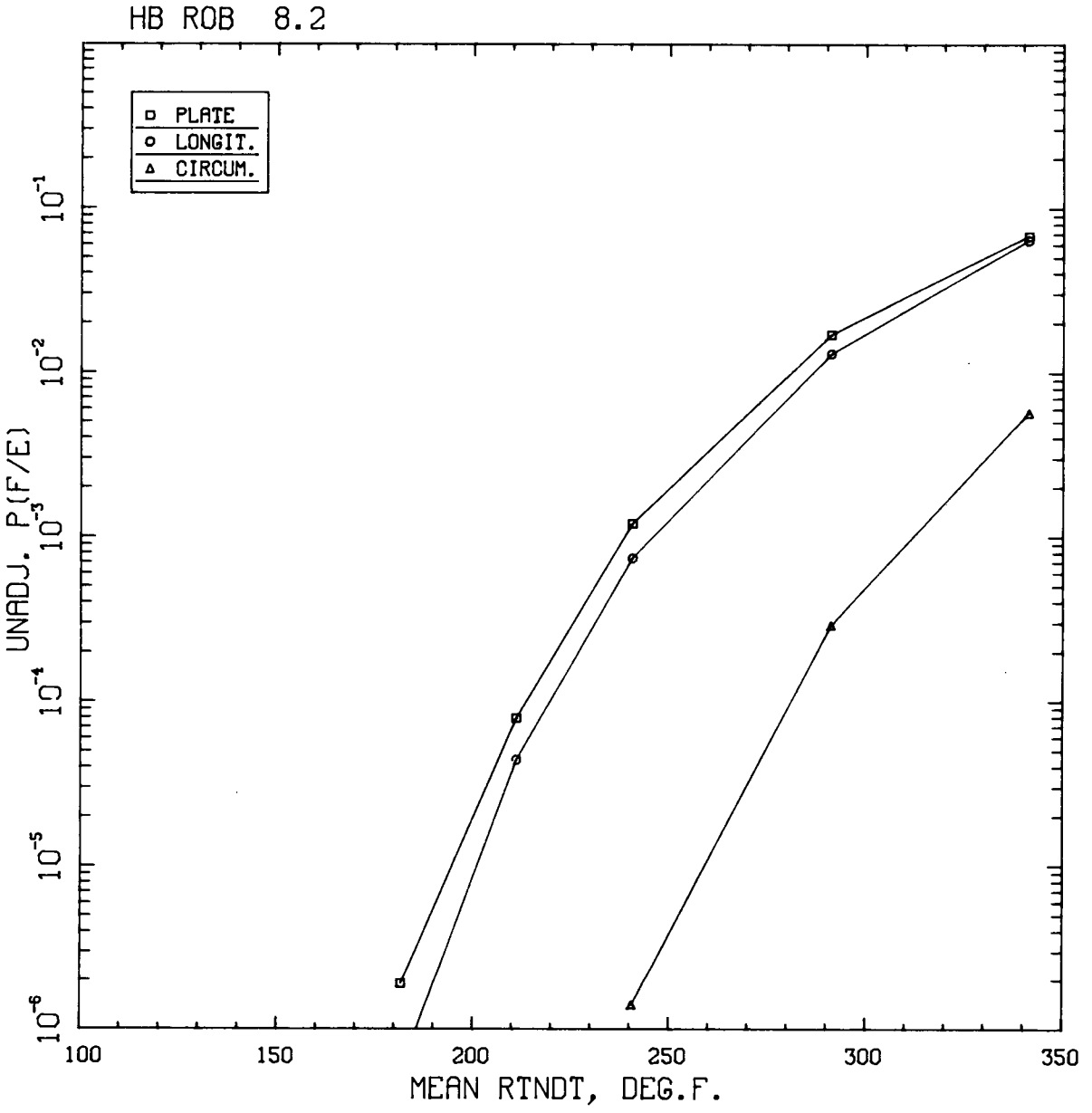

Figure I.74. Transient 8.2: $\hat{P}_j \int_0^w f(a)\, B(a)\, da$ vs $\overline{RTNDT_s}$ for (2-D, 2-D) and (2-D, 2m) flaw combinations.

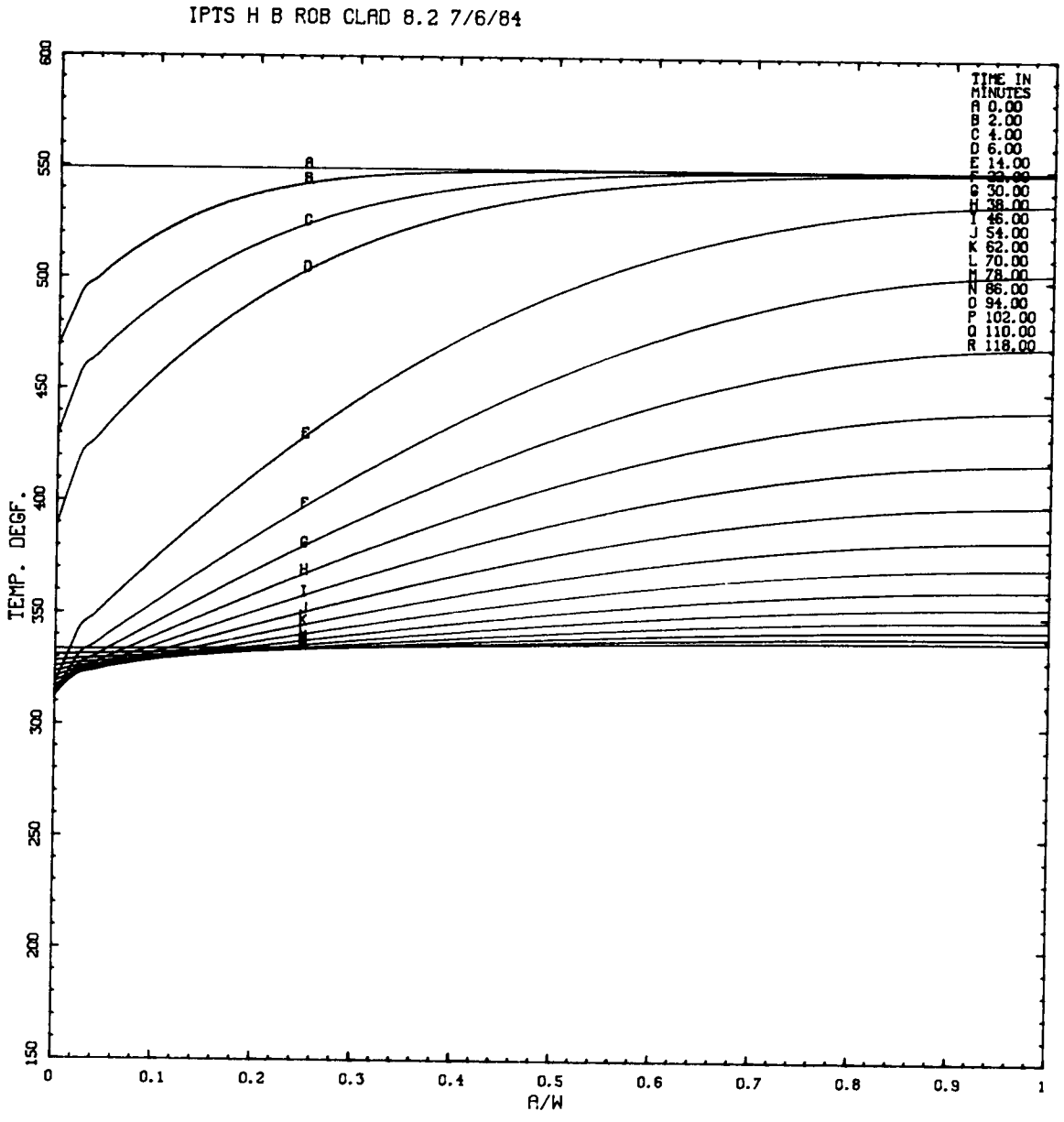

Figure I.75. Transient 8.2: Vessel wall temperature vs depth in wall (a/w) at various times (t) in transient.

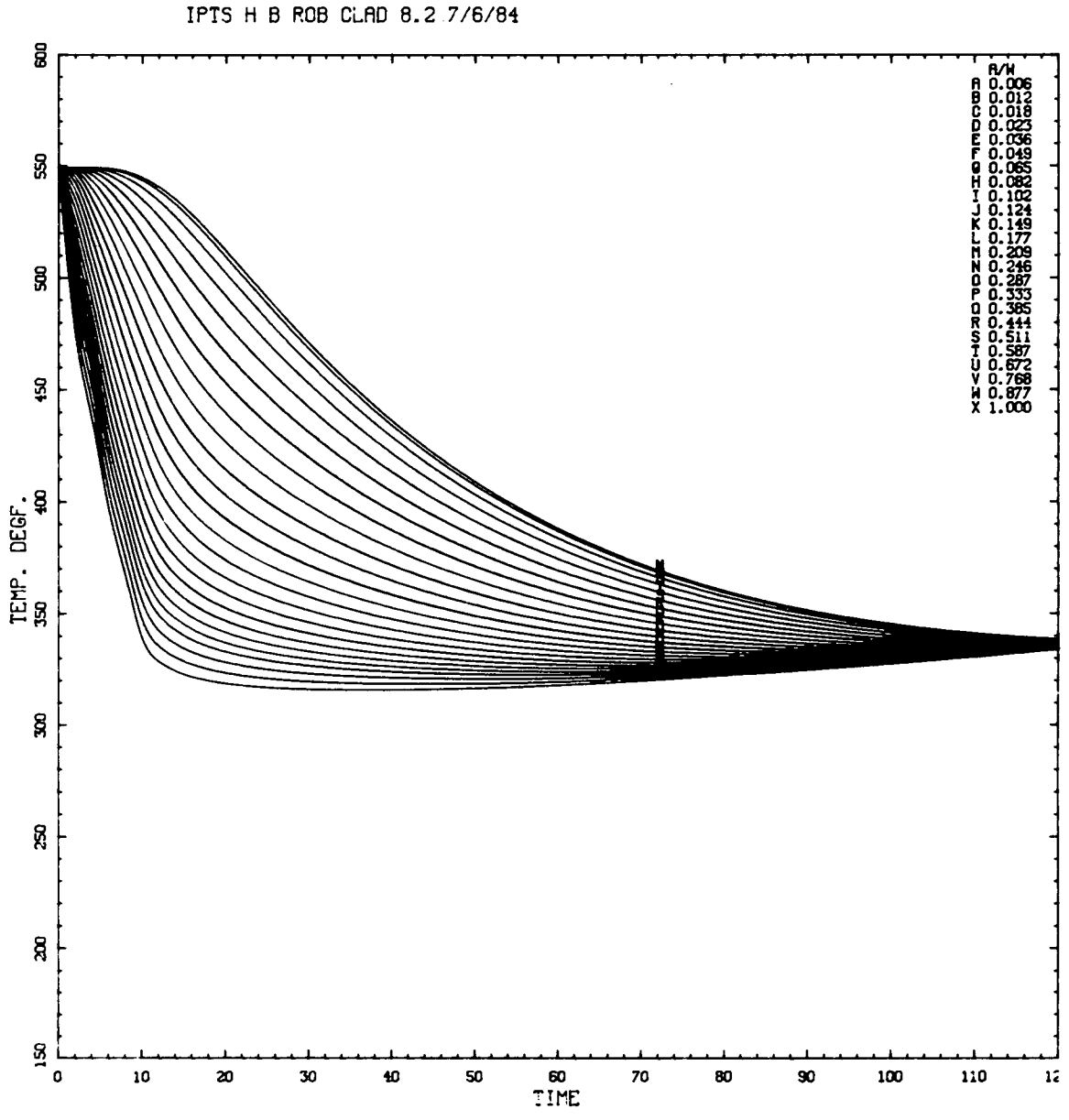

Figure I.76. Transient 8.2: Vessel wall temperature vs time (t) in transient at various depths in wall (a/w).

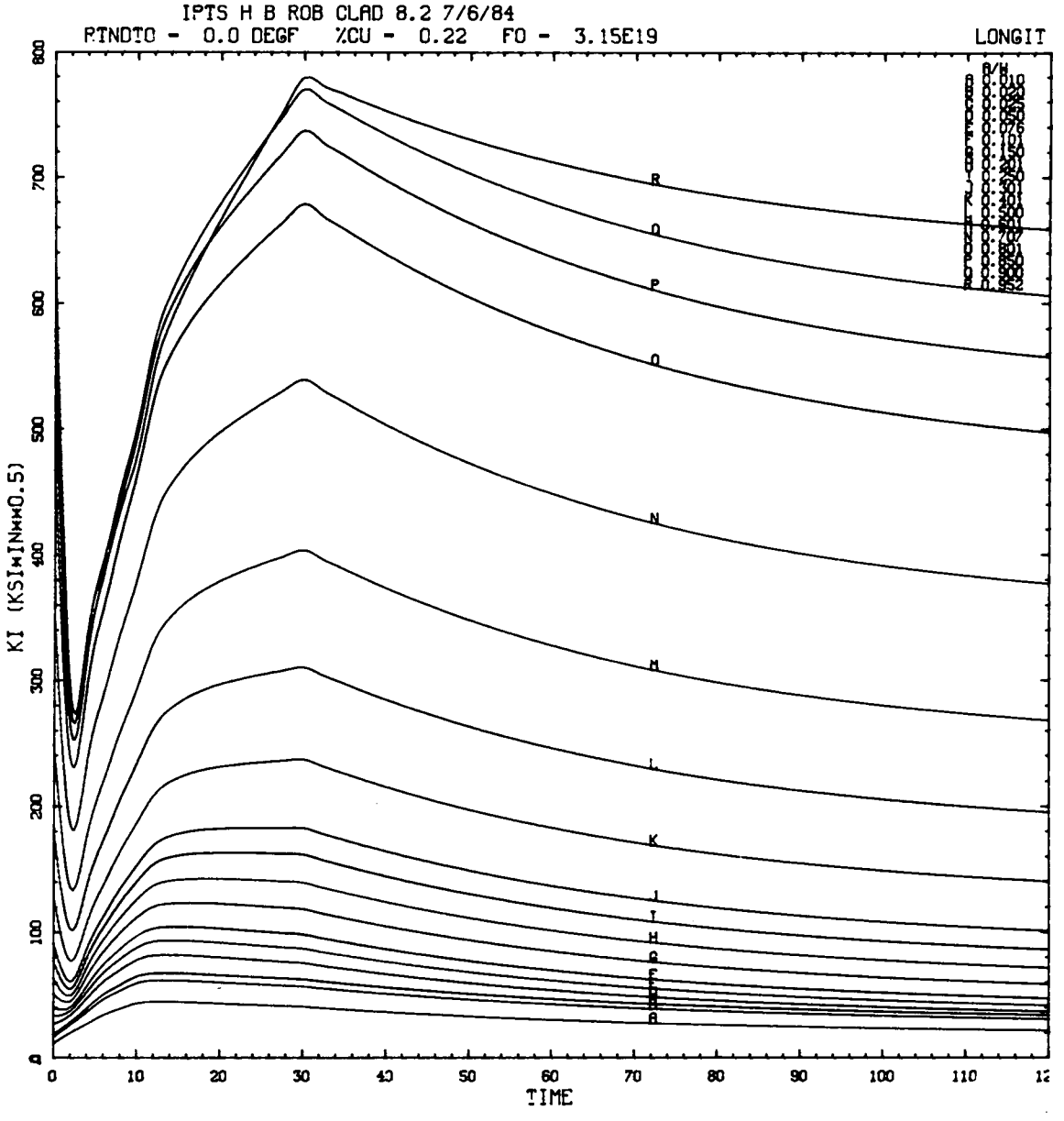

Figure I.77. Transient 8.2: K_I vs time (t) for various depths in wall (a/w).

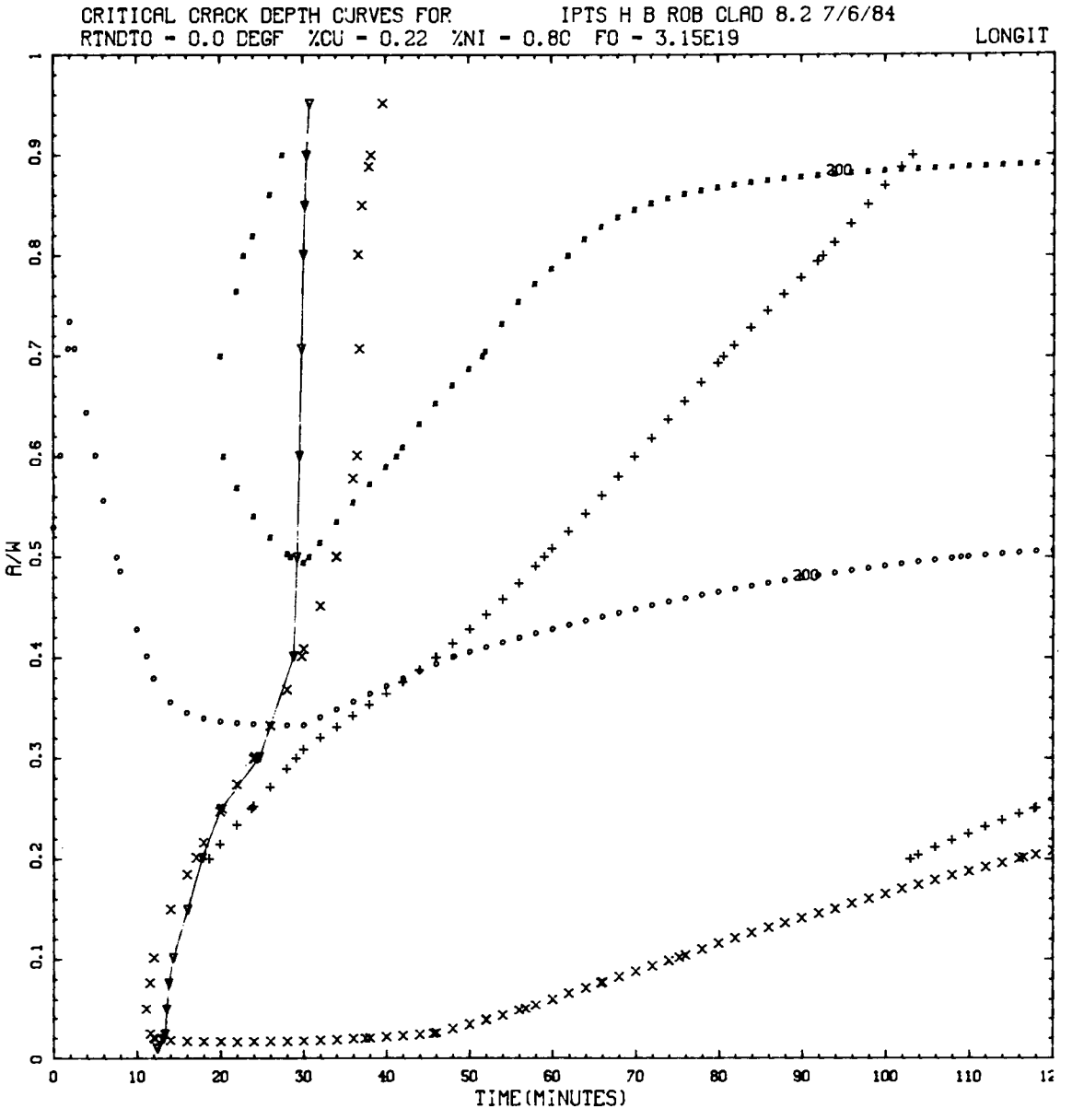

Figure I.78. Transient 8.2: Critical-crack-depth curves for weld 2-273A based on -2σ values of K_{Ic}, K_{Ia}, and $\Delta RTNDT$, mean values of all other parameters, and 32-EFPY fluences.

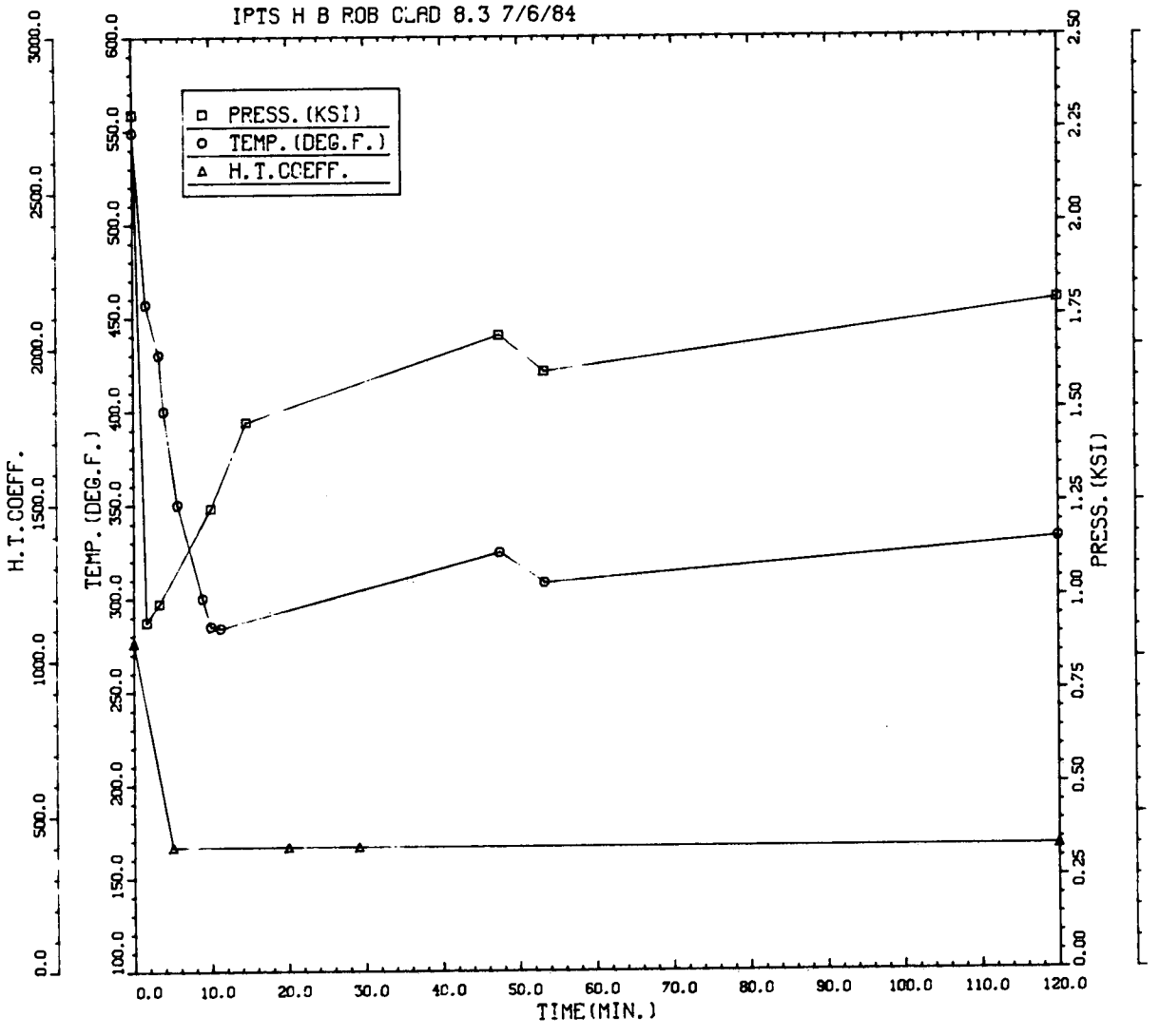

Figure I.79. Transient 8.3: Primary system pressure, downcomer coolant temperature, and fluid-film heat-transfer coefficient vs time in the transient.

Table I.14. Transient 8.3: Summary of digital output, including unadjusted $P(F|E)$ values and histogram data for crack depths, times of failure, and $T - RTNDT$ values at tip of crack corresponding to initiation and arrest events

IPTS H B ROB CLAD 8.3 7/6/84 1. FLAWS/IN**3 DRTN(IS) = 211.2

WELD	UNADJUSTED P(F/E)	95%CI	%ERR	P(INITIA)	N*V	ADJUSTED P(F/E)	%ERR	NFAIL	NTRIALS
1	3.89D-06	3.85D-07	9.89	4.95D-05	1.000	3.89D-06		392	200000
					VESSEL	3.89D-06	9.89		

DEPTHS FOR INITIAL INITIATION (IN)

	0.09	0.26	0.46	0.67	0.90	1.16	1.44	1.74	2.08
NUMBER	0	2827	1638	410	98	17	3	0	0
PERCENT	0.0	56.6	32.8	8.2	2.0	0.3	0.1	0.0	0.0

TIMES OF FAILURE(MINUTES)

	0.0	10.0	20.0	30.0	40.0	50.0	60.0	70.0	80.0	90.0	100.0	110.0	120.0
PERCENT	0.0	0.0	0.0	3.1	4.3	38.3	33.7	9.7	4.6	3.6	2.0	0.8	

INITIATION T-RTNDT(DEG.F)

	-100.0	-75.0	-50.0	-25.0	0.0	25.0	50.0	75.0	100.0	125.0	150.0	175.0	200.0
NUMBER	0	0	3	525	2478	2047	412	98	4	0	0	0	
PERCENT	0.0	0.0	0.1	9.4	44.5	36.8	7.4	1.8	0.1	0.0	0.0	0.0	

ARREST T-RTNDT(DEG.F)

	-50.0	-25.0	0.0	25.0	50.0	75.0	100.0	125.0	150.0	175.0	200.0	225.0	250.0
NUMBER	0	0	0	5	7	49	402	2369	2125	218	0	0	
PERCENT	0.0	0.0	0.0	0.1	0.1	0.9	7.8	45.8	41.1	4.2	0.0	0.0	

OF STD DEVS ABOVE MEAN DELTA RTNDT(FAILURES ONLY)

	1.00	1.25	1.50	1.75	2.00	2.25	2.50	2.75	3.00
NUMBER	0	7	15	29	54	71	108	108	
PERCENT	0.0	1.8	3.8	7.4	13.8	18.1	27.6	27.6	

OF STD DEVS ABOVE MEAN RTNDT(FAILURES ONLY)

	1.00	1.25	1.50	1.75	2.00	2.25	2.50	2.75	3.00
NUMBER	0	0	1	14	41	62	112	162	
PERCENT	0.0	0.0	0.3	3.6	10.5	15.8	28.6	41.3	

ICRKTP = 2 IACCEL = 1 NDLRS = 2 NRTRS = 2 DATE: 10/30/84 TIME: 00.33.12

CPU TIME: 5 MIN 23 SEC

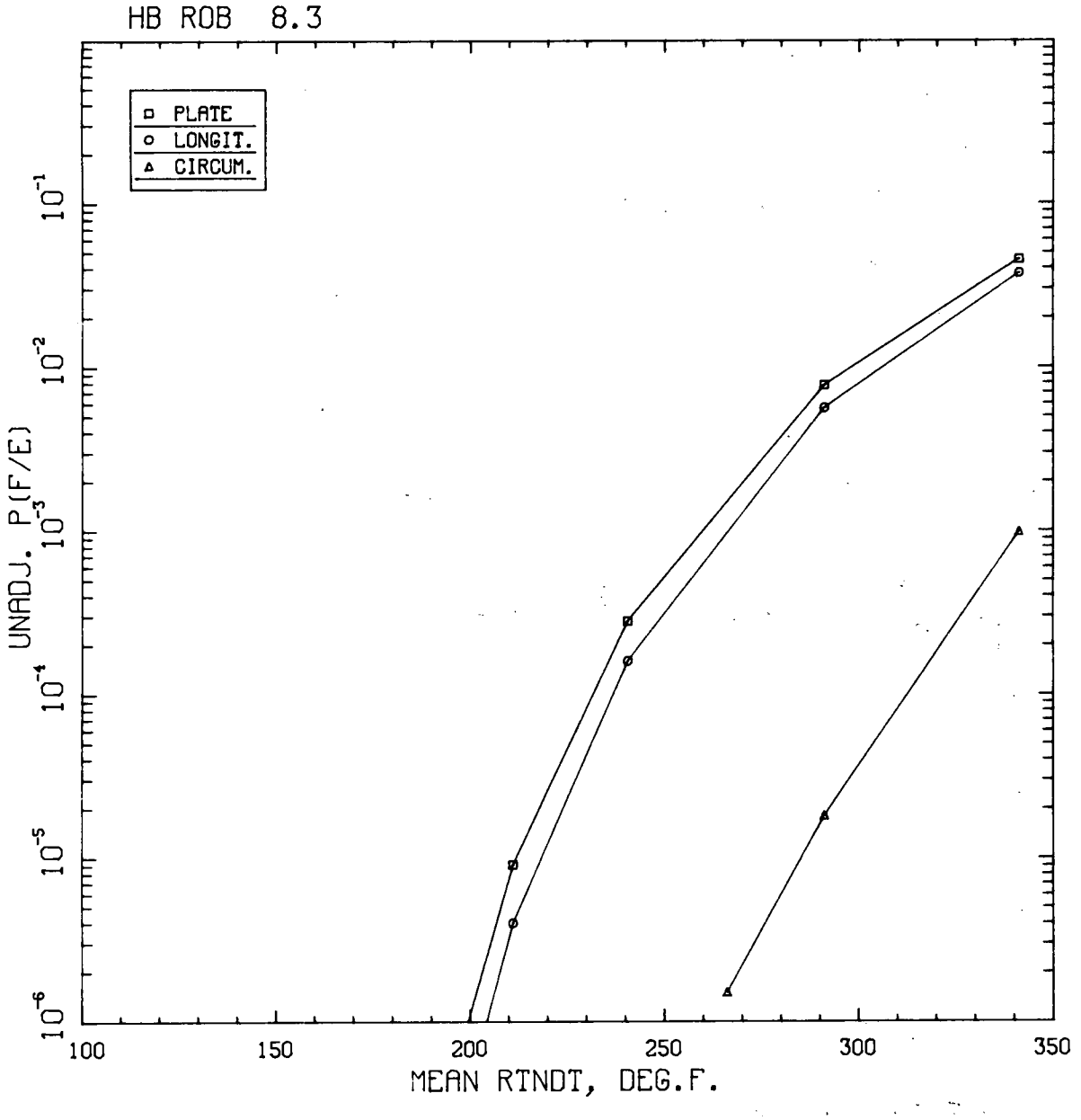

Figure I.80. Transient 8.3: $\hat{P}_j \int_0^w f(a)\, B(a)\, da$ vs $\overline{RTNDT_s}$ for (2-D, 2-D) and (2-D, 2m) flaw combinations.

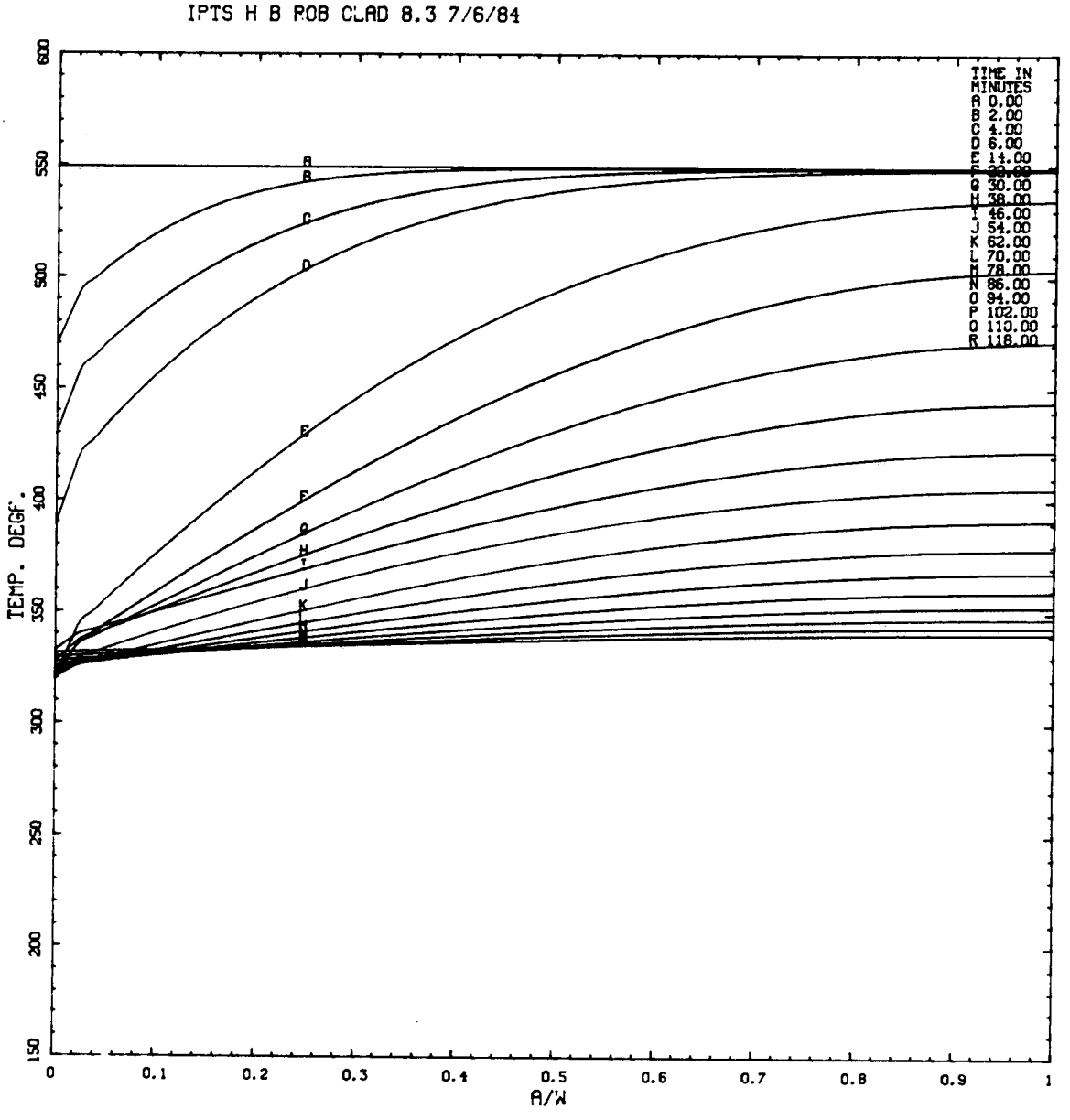

Figure I.81. Transient 8.3: Vessel wall temperature vs depth in wall (a/w) at various times (t) in transient.

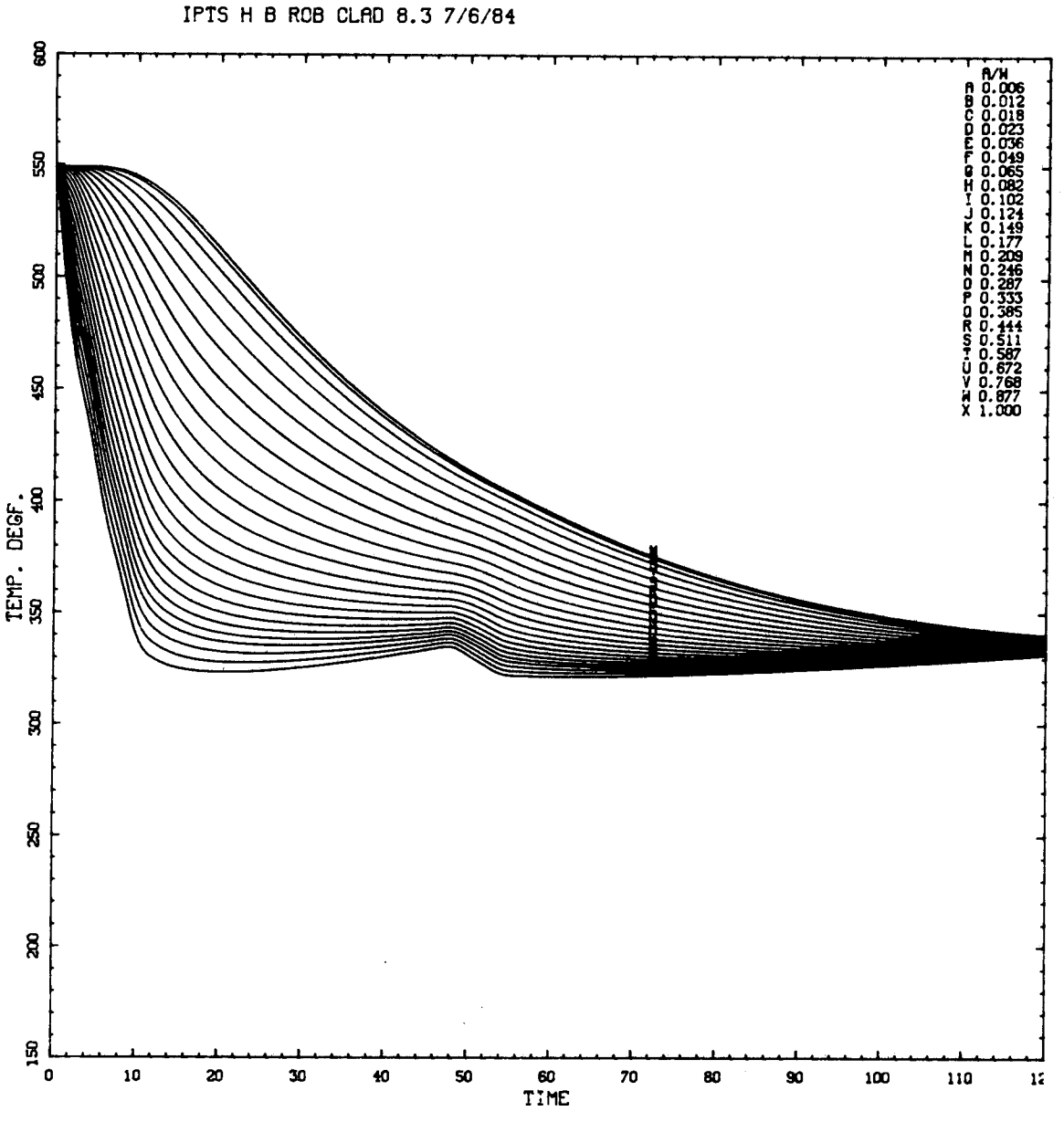

Figure I.82. Transient 8.3: Vessel wall temperature vs time (t) in transient at various depths in wall (a/w).

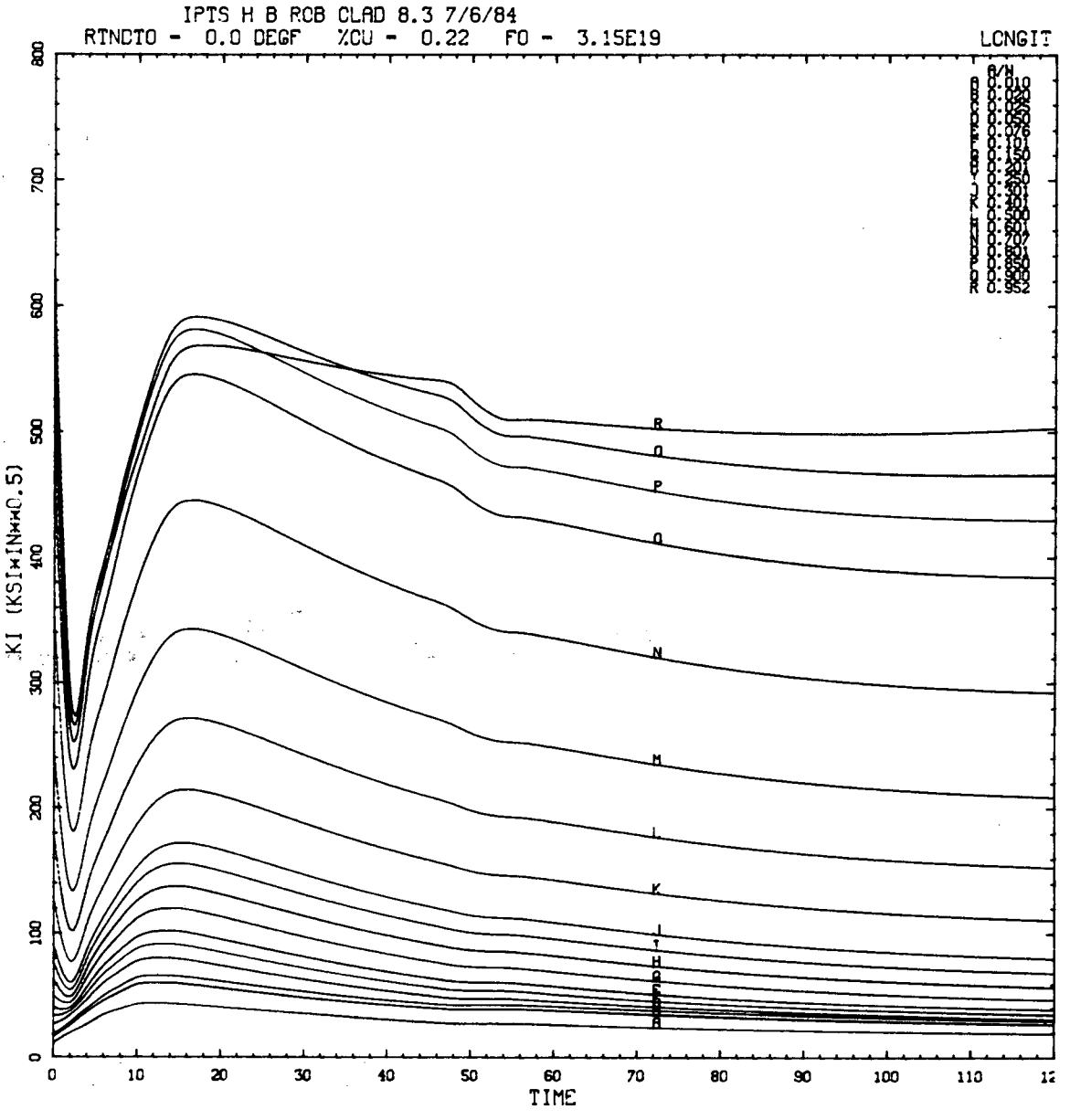

Figure I.83. Transient 8.3: K_I vs time (t) for various depths in wall (a/w).

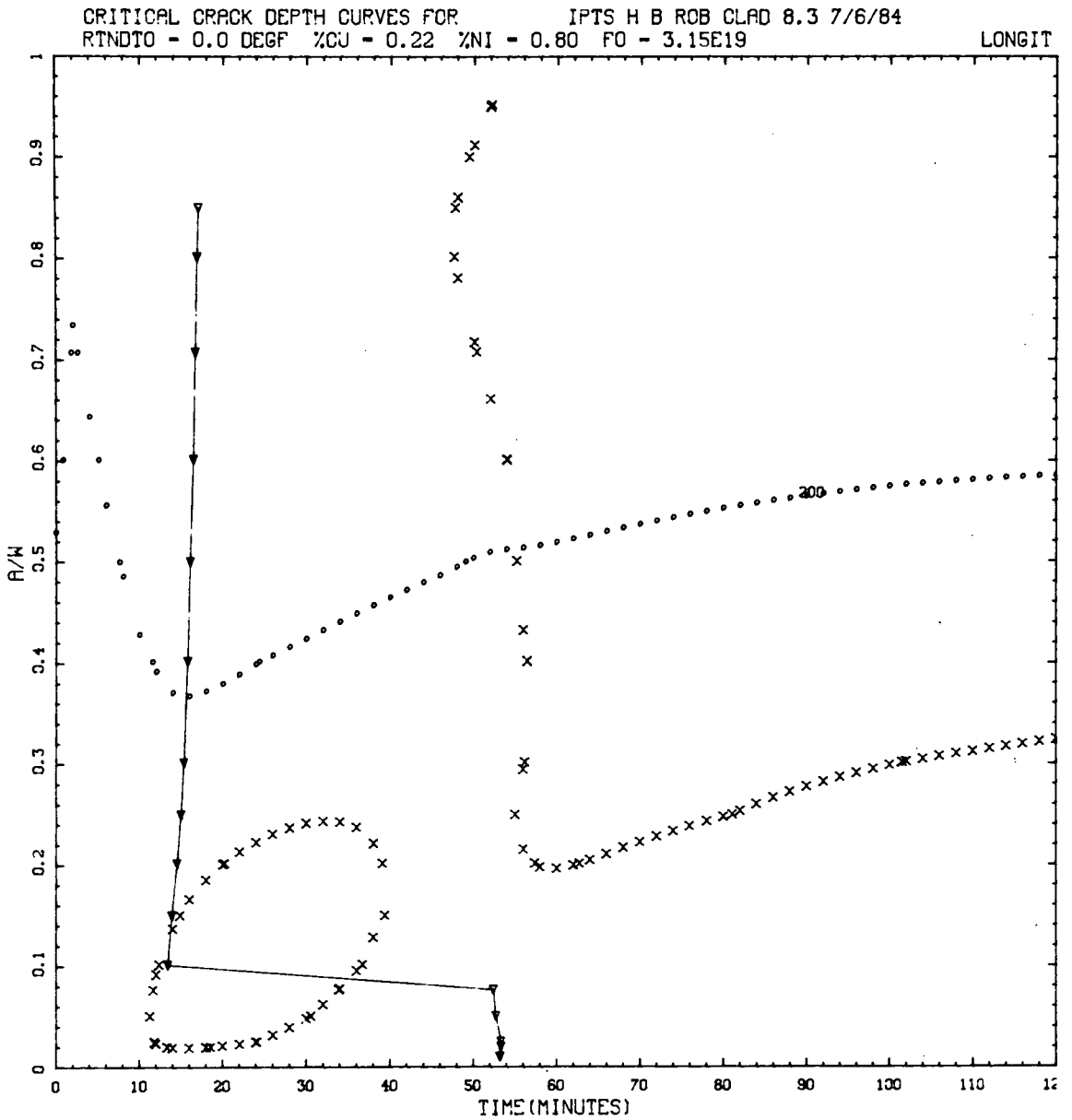

×, 2-D flaw, $K_I = K_{Ia}$
+, 2-m flaw, $K_I = K_{Ia}$
∇, WPS (warm prestressing)

Figure I.84. Transient 8.3: Critical-crack-depth curves for weld 2-273A based on -2σ values of K_{Ic}, K_{Ia}, and $\Delta RTNDT$, mean values of all other parameters, and 32-EFPY fluences.

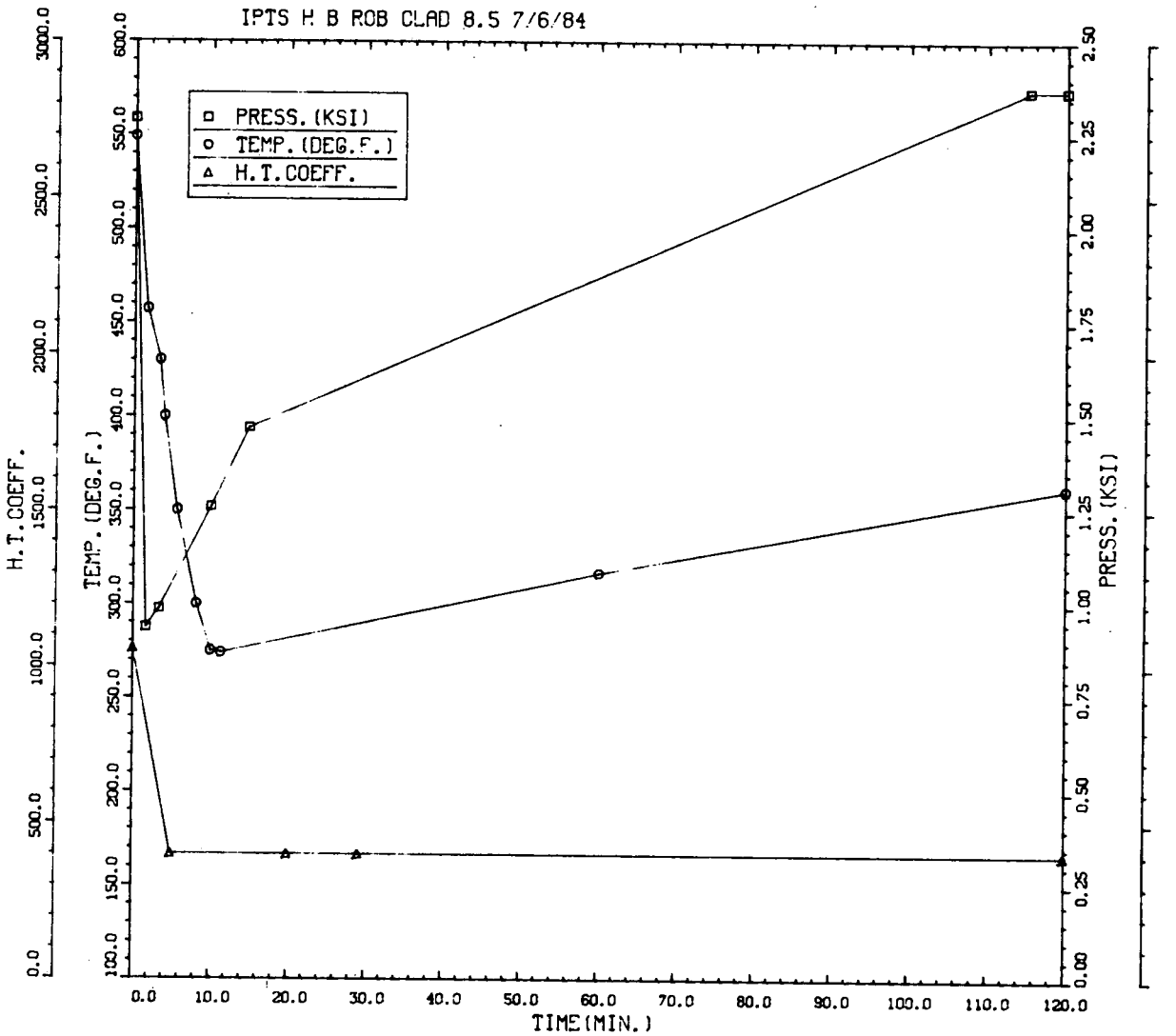

Figure I.85. Transient 8.5: Primary system pressure, downcomer coolant temperature, and fluid-film heat-transfer coefficient vs time in the transient.

Table I.15. Transient 8.5: Summary of digital output, including unadjusted $P(F|E)$ values and histogram data for crack depths, times of failure, and $T - RTNDT$ values at tip of crack corresponding to initiation and arrest events

IPTS H B ROB CLAD 8.5 7/6/84 1. FLAWS/IN**3 DRTN(IS) = 211.2

WELD	P(F/E)	95%CI	%ERR	P(INITIA)	N*V	P(F/E)	%ERR	NFAIL	NTRIALS
	UNADJUSTED					ADJUSTED			
1	8.47D-06	7.94D-07	9.37	1.03D-04	1.000	8.47D-06		433	40000
					VESSEL	8.47D-06	9.37		

DEPTHS FOR INITIAL INITIATION (IN)

	0.09	0.26	0.46	0.67	0.90	1.16	1.44	1.74	2.08
NUMBER	0	3187	1554	400	102	18	3	0	0
PERCENT	0.0	60.5	29.5	7.6	1.9	0.3	0.1	0.0	0.0

TIMES OF FAILURE(MINUTES)

	0.0	10.0	20.0	30.0	40.0	50.0	60.0	70.0	80.0	90.0	100.0	110.0	120.0
PERCENT	0.0	0.0	5.1	21.5	28.2	20.1	7.4	8.8	5.3	2.5	0.9	0.2	

INITIATION T-RTNDT(DEG.F)

	-100.0	-75.0	-50.0	-25.0	0.0	25.0	50.0	75.0	100.0	125.0	150.0	175.0	200.0
NUMBER	0	0	13	1105	2673	1475	536	250	6	0	0	0	
PERCENT	0.0	0.0	0.2	18.2	44.1	24.3	8.8	4.1	0.1	0.0	0.0	0.0	

ARREST T-RTNDT(DEG.F)

	-50.0	-25.0	0.0	25.0	50.0	75.0	100.0	125.0	150.0	175.0	200.0	225.0	250.0
NUMBER	0	0	0	0	3	23	304	2110	2774	411	0	0	
PERCENT	0.0	0.0	0.0	0.0	0.1	0.4	5.4	37.5	49.3	7.3	0.0	0.0	

OF STD DEVS ABOVE MEAN DELTA RTNDT(FAILURES ONLY)

	1.00	1.25	1.50	1.75	2.00	2.25	2.50	2.75	3.00
NUMBER	0	0	15	47	67	96	104	104	
PERCENT	0.0	0.0	3.5	10.9	15.5	22.2	24.0	24.0	

OF STD DEVS ABOVE MEAN RTNDT(FAILURES ONLY)

	1.00	1.25	1.50	1.75	2.00	2.25	2.50	2.75	3.00
NUMBER	0	0	3	22	47	79	141	141	
PERCENT	0.0	0.0	0.7	5.1	10.9	18.2	32.6	32.6	

ICRKTP = 2 IACCEL = 1 NDLRS = 3 NRTRS = 3 DATE: 10/30/84 TIME: 00.31.43

CPU TIME: 1 MIN 15 SEC

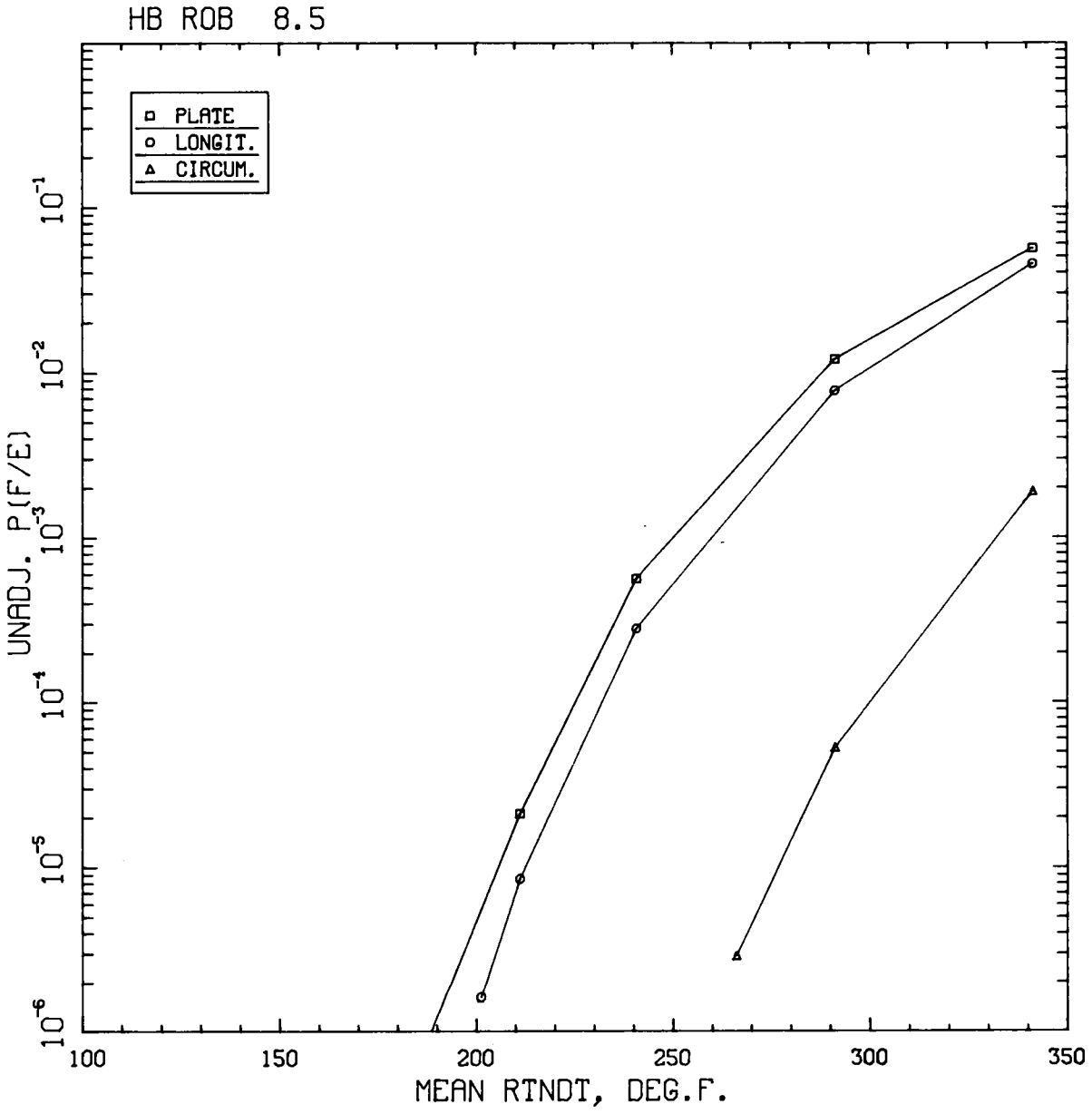

Figure I.86. Transient 8.5: $\hat{P}_j \int_0^w f(a)\, B(a)\, da$ vs $\overline{RTNDT_s}$ for (2-D, 2-D) and (2-D, 2m) flaw combinations.

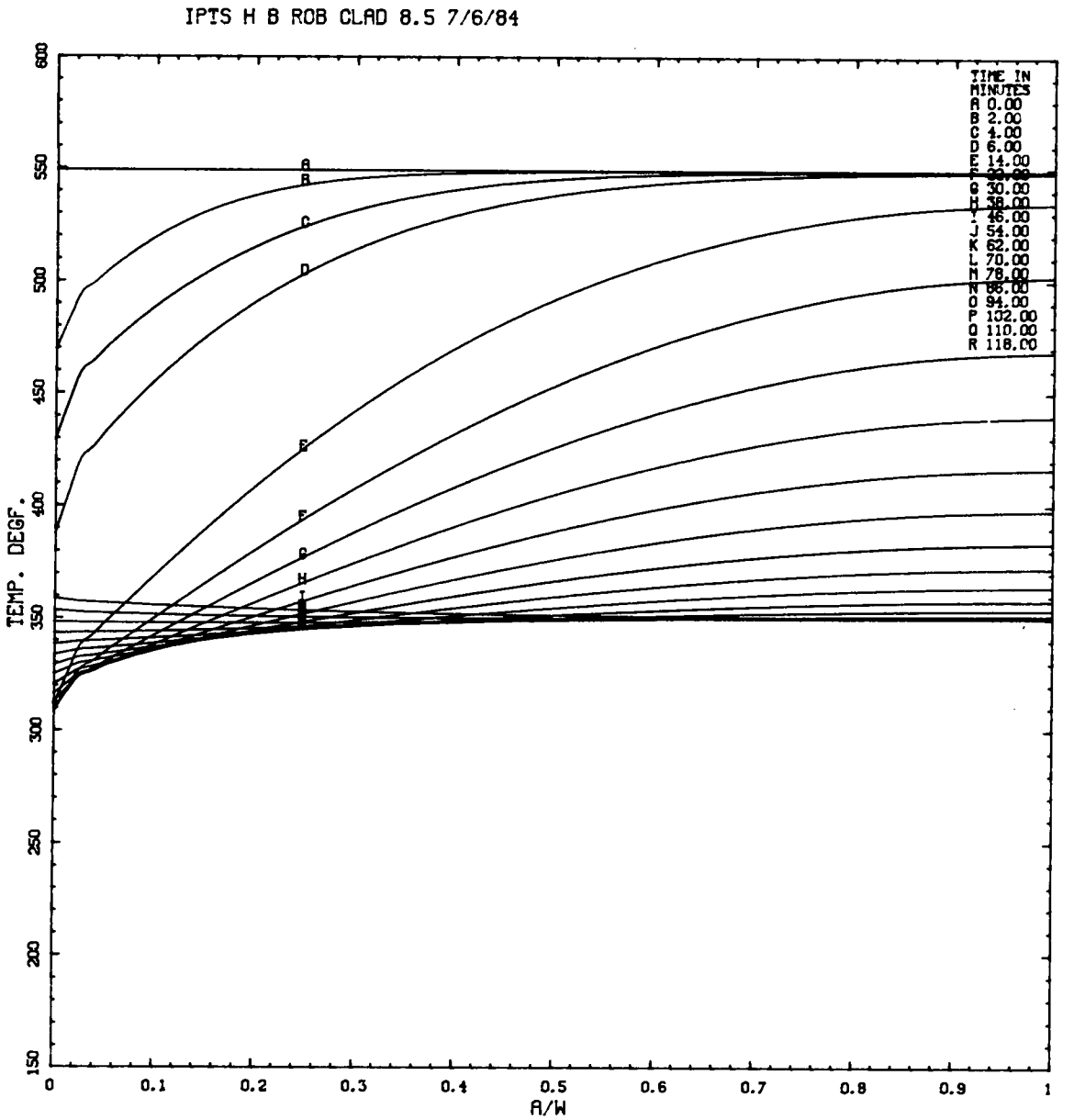

Figure I.87. Transient 8.5: Vessel wall temperature vs depth in wall (a/w) at various times (t) in transient.

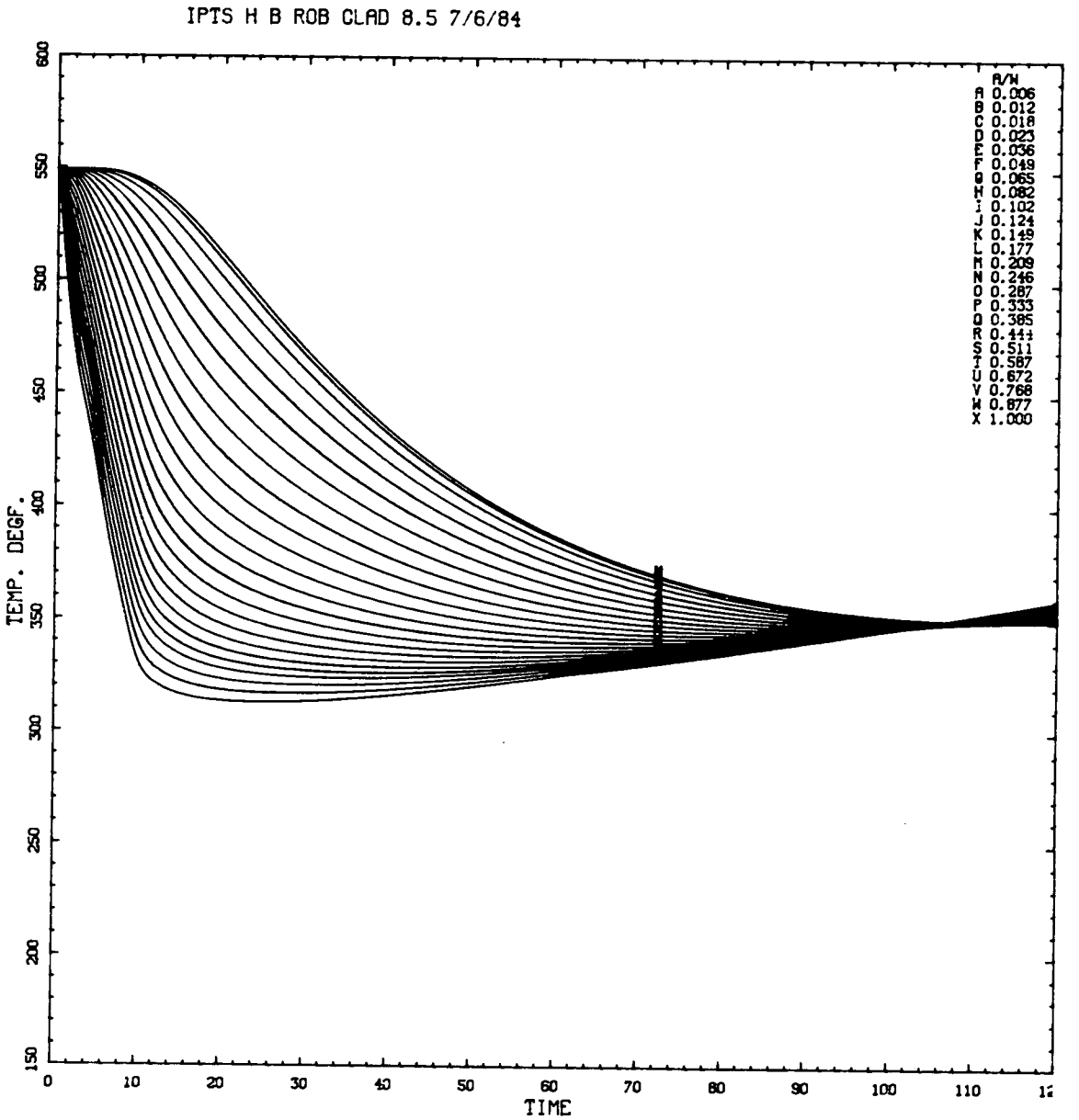

Figure I.88. Transient 8.5: Vessel wall temperature vs time (t) in transient at various depths in wall (a/w).

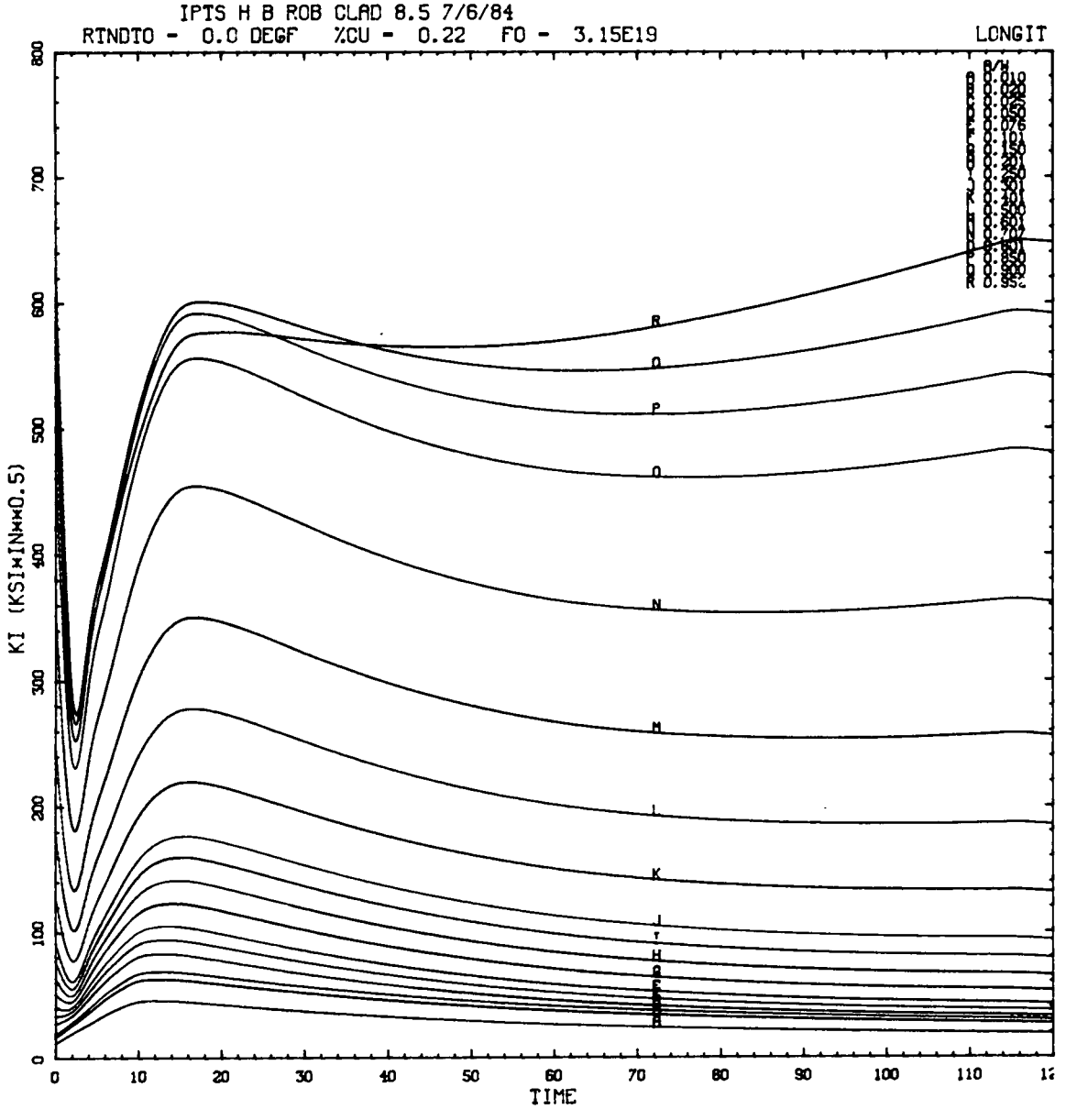

Figure I.89. Transient 8.5: K_I vs time (t) for various depths in wall (a/w).

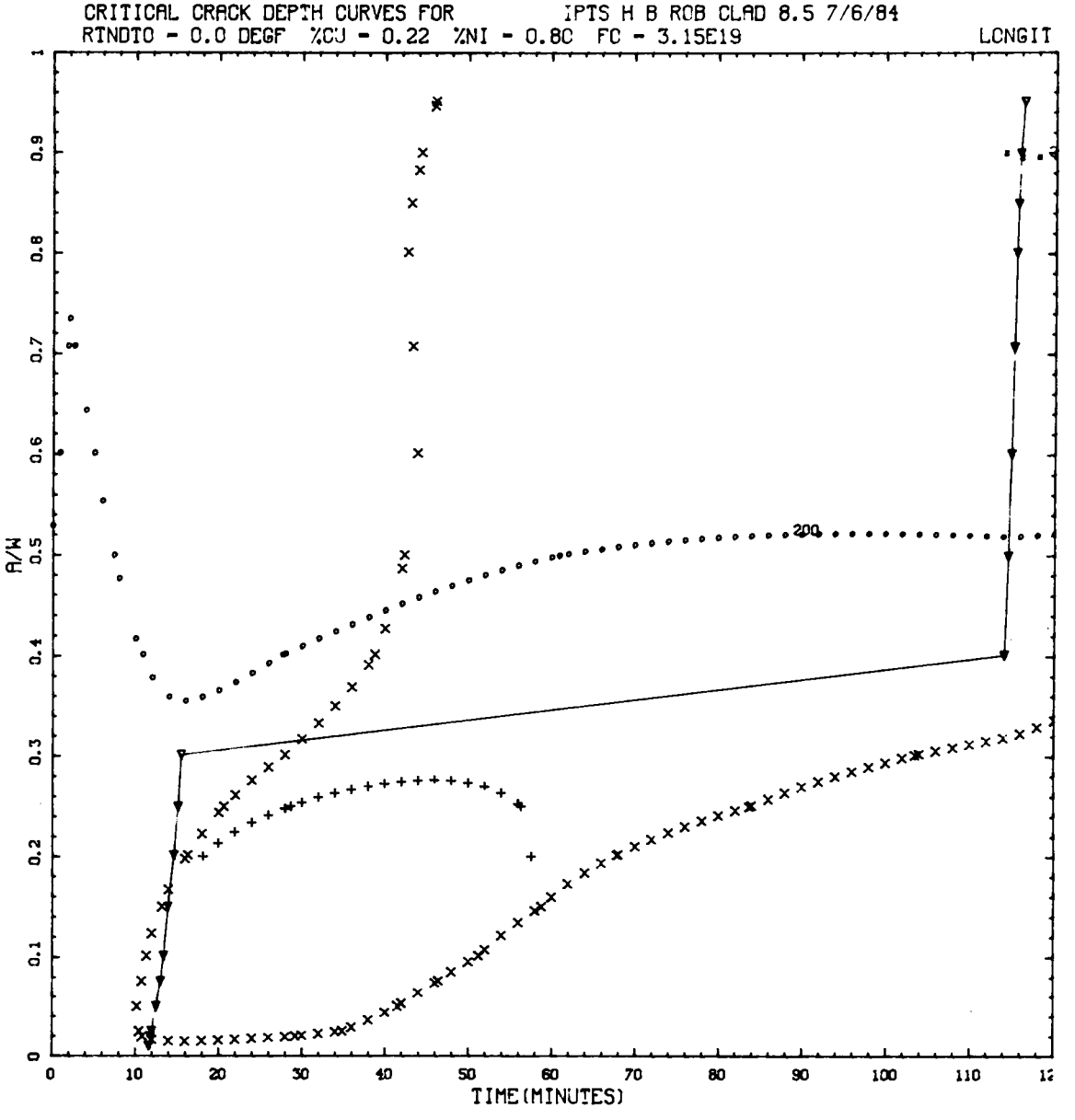

×, 2-D flaw, $K_I = K_{Ia}$
+, 2-m flaw, $K_I = K_{Ia}$
O, 2-D flaw, $K_I = 220$ MPa $\sqrt{m}$
■, 2-m flaw, $K_I = 220$ MPa $\sqrt{m}$
∇, WPS (warm prestressing)

Figure I.90. Transient 8.5: Critical-crack-depth curves for weld 2-273A based on -2σ values of K_{Ic}, K_{Ia}, and $\Delta RTNDT$, mean values of all other parameters, and 32-EFPY fluences.

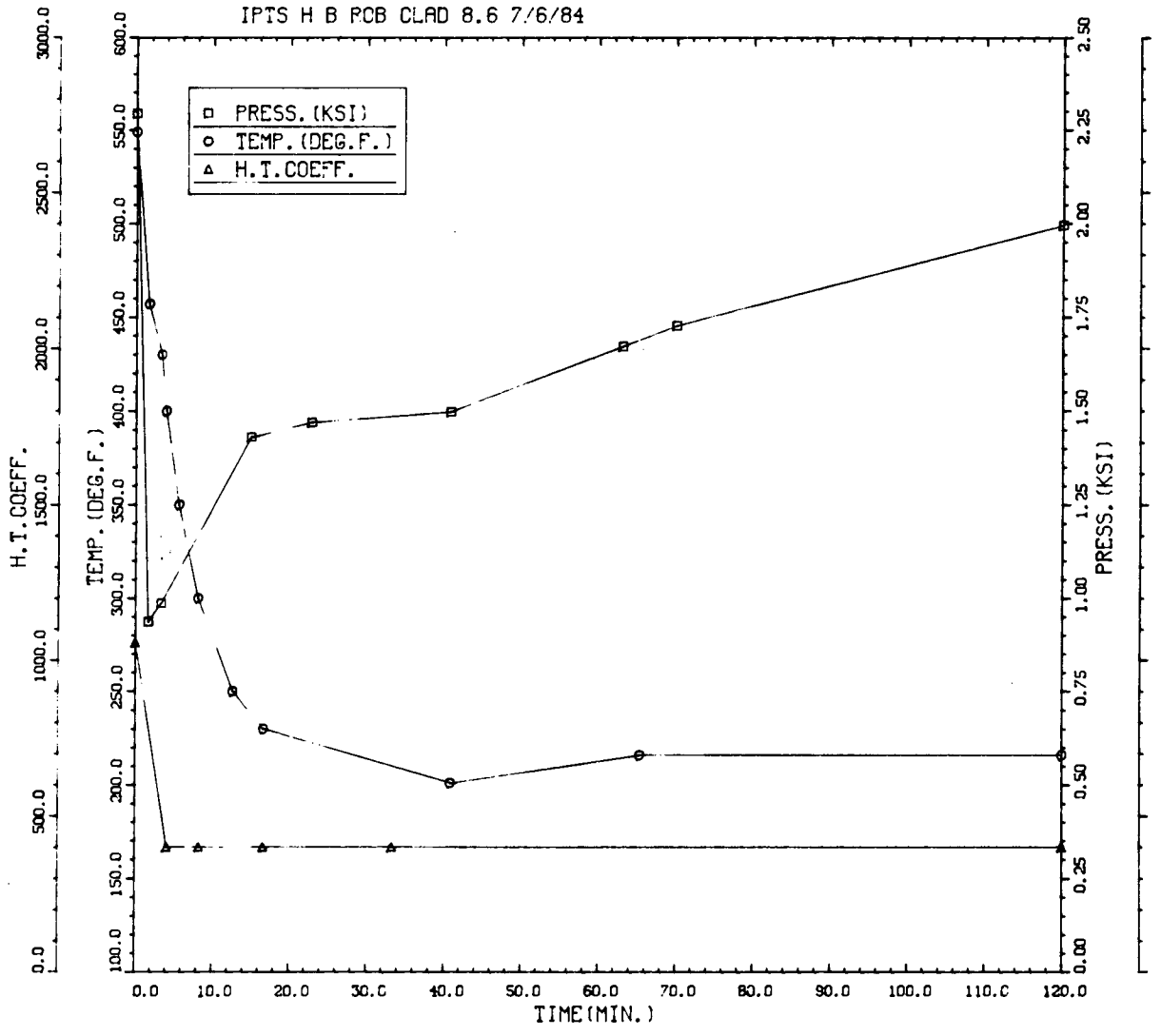

Figure I.91. Transient 8.6: Primary system pressure, downcomer coolant temperature, and fluid-film heat-transfer coefficient vs time in the transient.

Table I.16. Transient 8.6: Summary of digital output, including unadjusted $P(F|E)$ values and histogram data for crack depths, times of failure, and $T - RTNDT$ values at tip of crack corresponding to initiation and arrest events

IPTS H B ROB CLAD 8.6 7/6/84 1. FLAWS/IN**3 DRTN(IS) = 211.2

	UNADJUSTED					ADJUSTED			
WELD	P(F/E)	95%CI	%ERR	P(INITIA)	N*V	P(F/E)	%ERR	NFAIL	NTRIALS
1	1.56D-02	1.31D-03	8.40	1.87D-02	1.000	1.56D-02		530	20000
					VESSEL	1.56D-02	8.40		

DEPTHS FOR INITIAL INITIATION (IN)

	0.09	0.26	0.46	0.67	0.90	1.16	1.44	1.74	2.08
NUMBER	30	414	138	45	8	3	0	0	0
PERCENT	4.7	64.9	21.6	7.1	1.3	0.5	0.0	0.0	0.0

TIMES OF FAILURE(MINUTES)

	0.0	10.0	20.0	30.0	40.0	50.0	60.0	70.0	80.0	90.0	100.0	110.0	120.0
PERCENT	0.0	0.0	1.3	4.7	9.6	11.1	15.7	16.4	12.5	12.6	8.1	7.9	

INITIATION T-RTNDT(DEG.F)

	-100.0	-75.0	-50.0	-25.0	0.0	25.0	50.0	75.0	100.0	125.0	150.0	175.0	200.0
NUMBER	0	0	27	179	327	302	294	70	0	0	0	0	
PERCENT	0.0	0.0	2.3	14.9	27.3	25.2	24.5	5.8	0.0	0.0	0.0	0.0	

ARREST T-RTNDT(DEG.F)

	-50.0	-25.0	0.0	25.0	50.0	75.0	100.0	125.0	150.0	175.0	200.0	225.0	250.0
NUMBER	0	0	0	0	0	0	1	100	405	140	23	0	
PERCENT	0.0	0.0	0.0	0.0	0.0	0.0	0.1	14.9	60.5	20.9	3.4	0.0	

ICRKTP = 2 IACCEL = 0 NDLRS = 0 NRTRS = 0 DATE: 10/30/84 TIME: 00.43.21

CPU TIME: 0 MIN 41 SEC

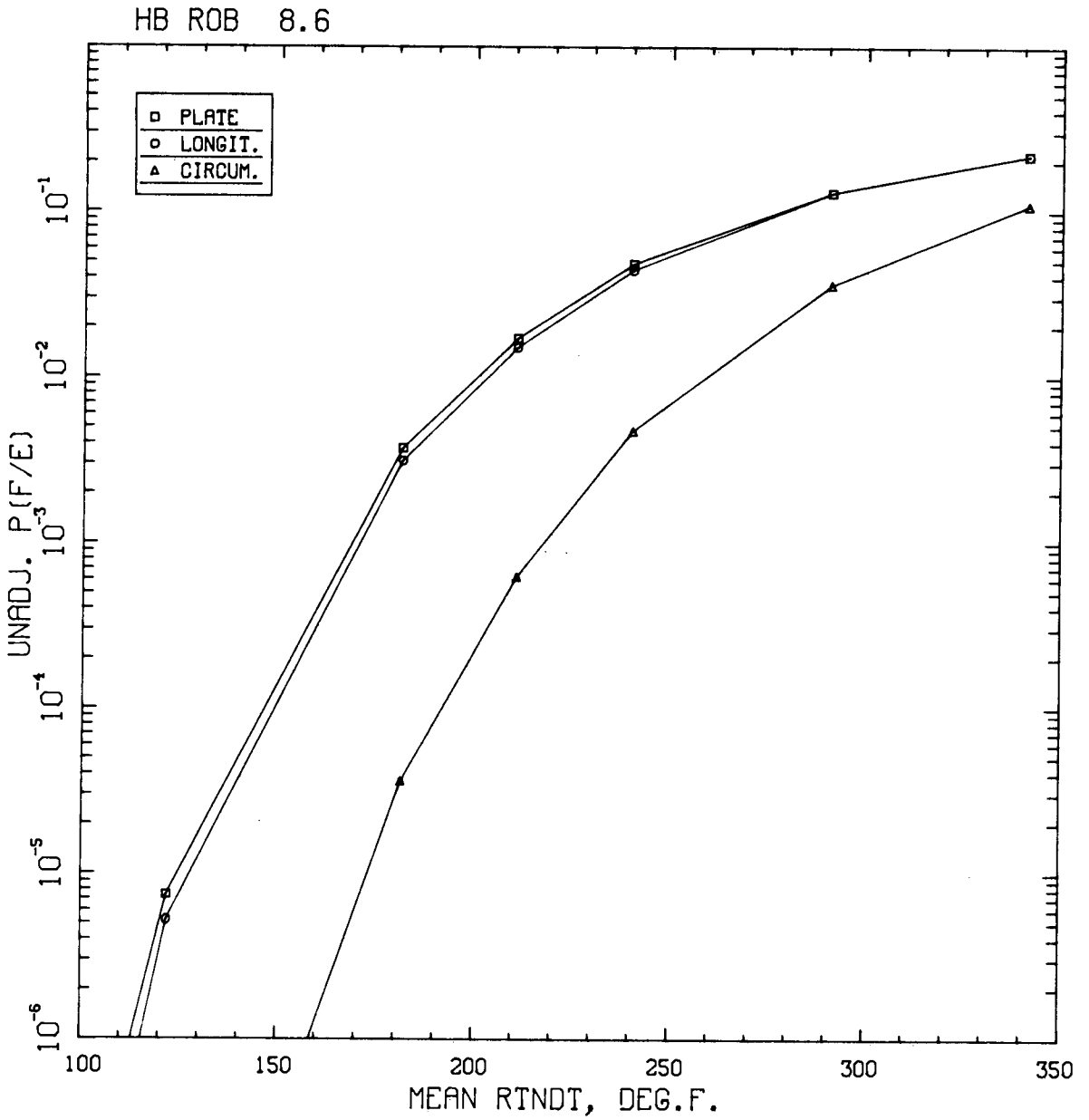

Figure I.92. Transient 8.6: $\hat{P}_j \int_0^w f(a)\, B(a)\, da$ vs $\overline{RTNDT}_s$ for (2-D, 2-D) and (2-D, 2m) flaw combinations.

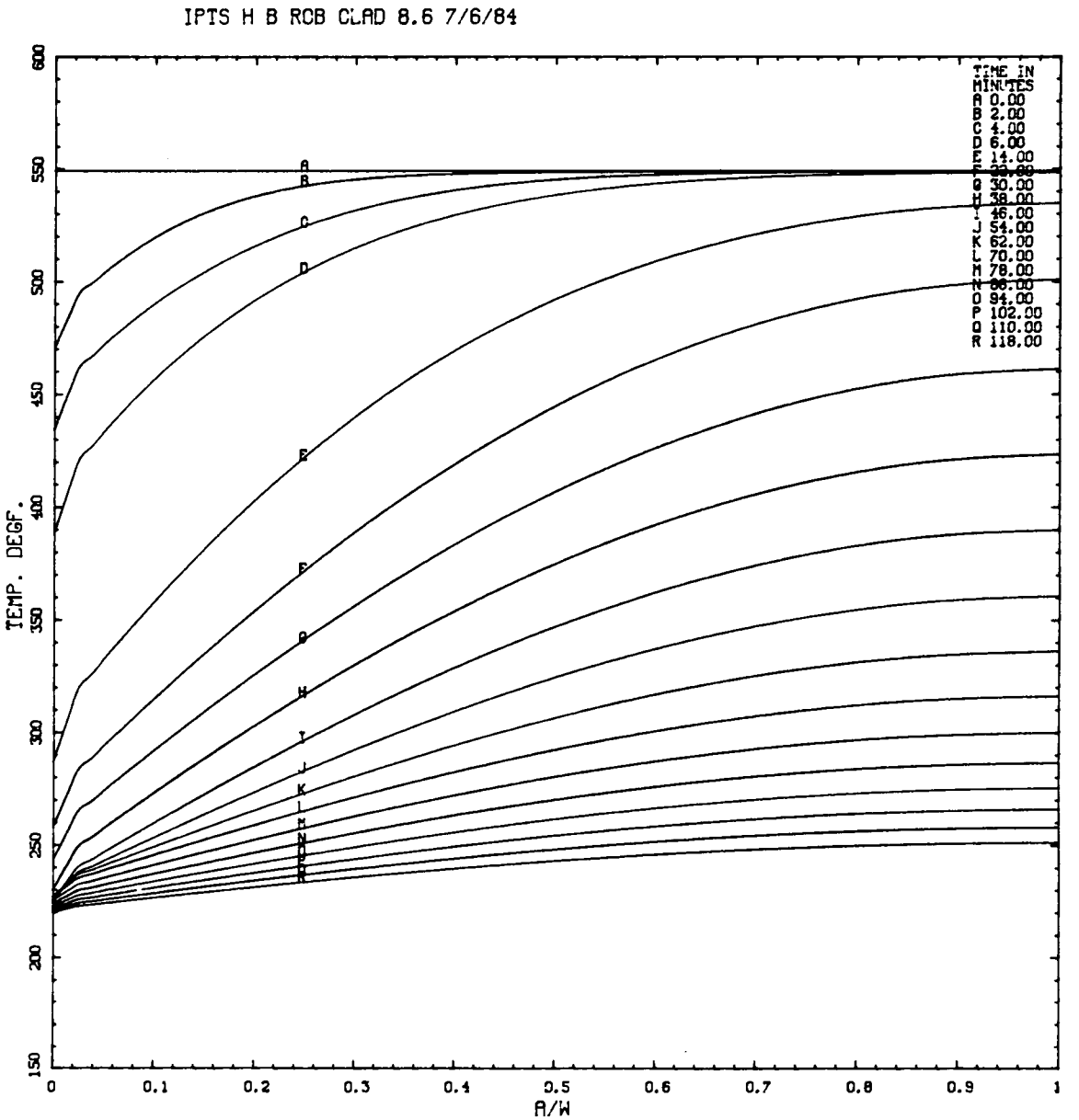

Figure I.93. Transient 8.6: Vessel wall temperature vs depth in wall (a/w) at various times (t) in transient.

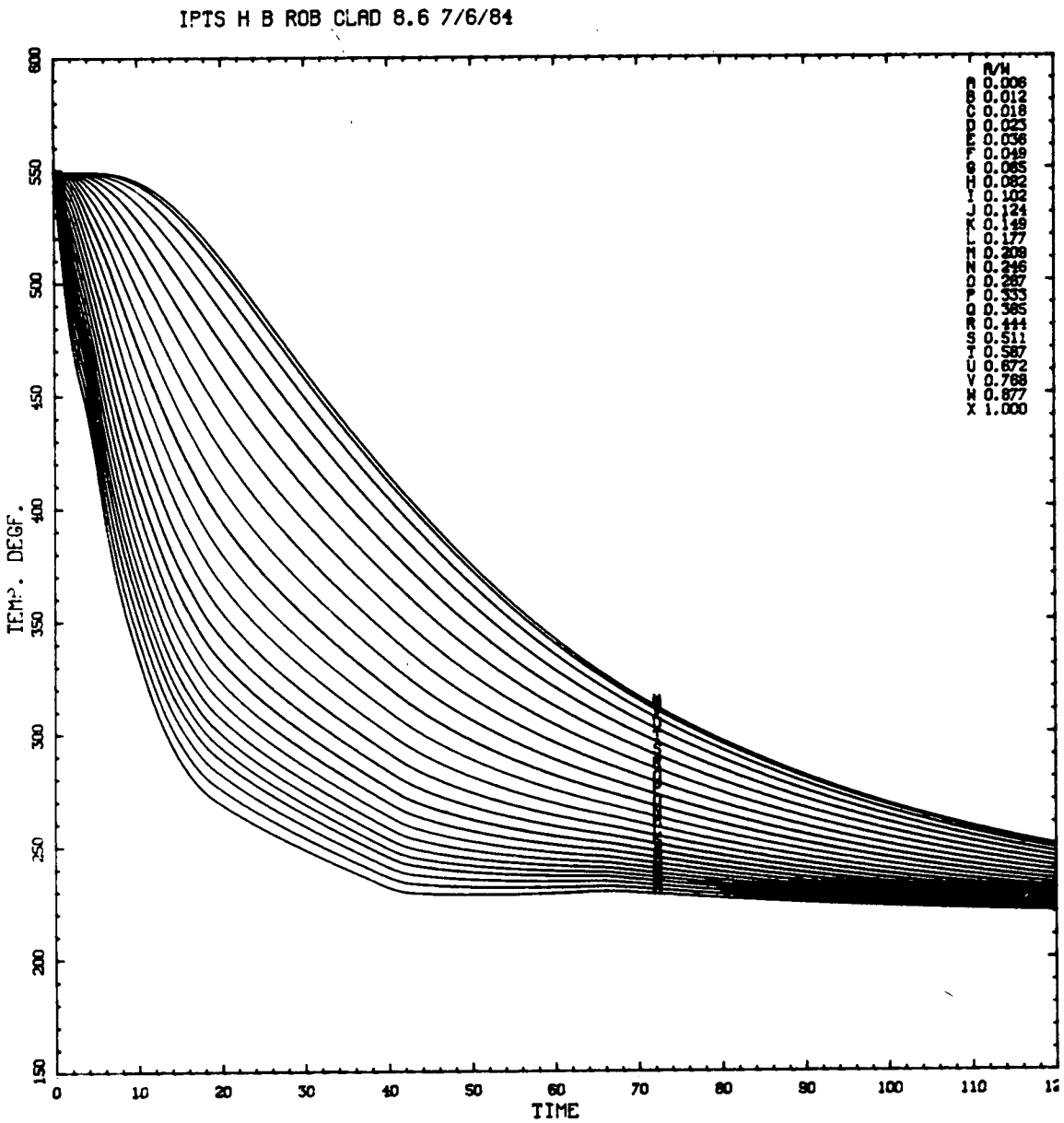

Figure I.94. Transient 8.6: Vessel wall temperature vs time (t) in transient at various depths in wall (a/w).

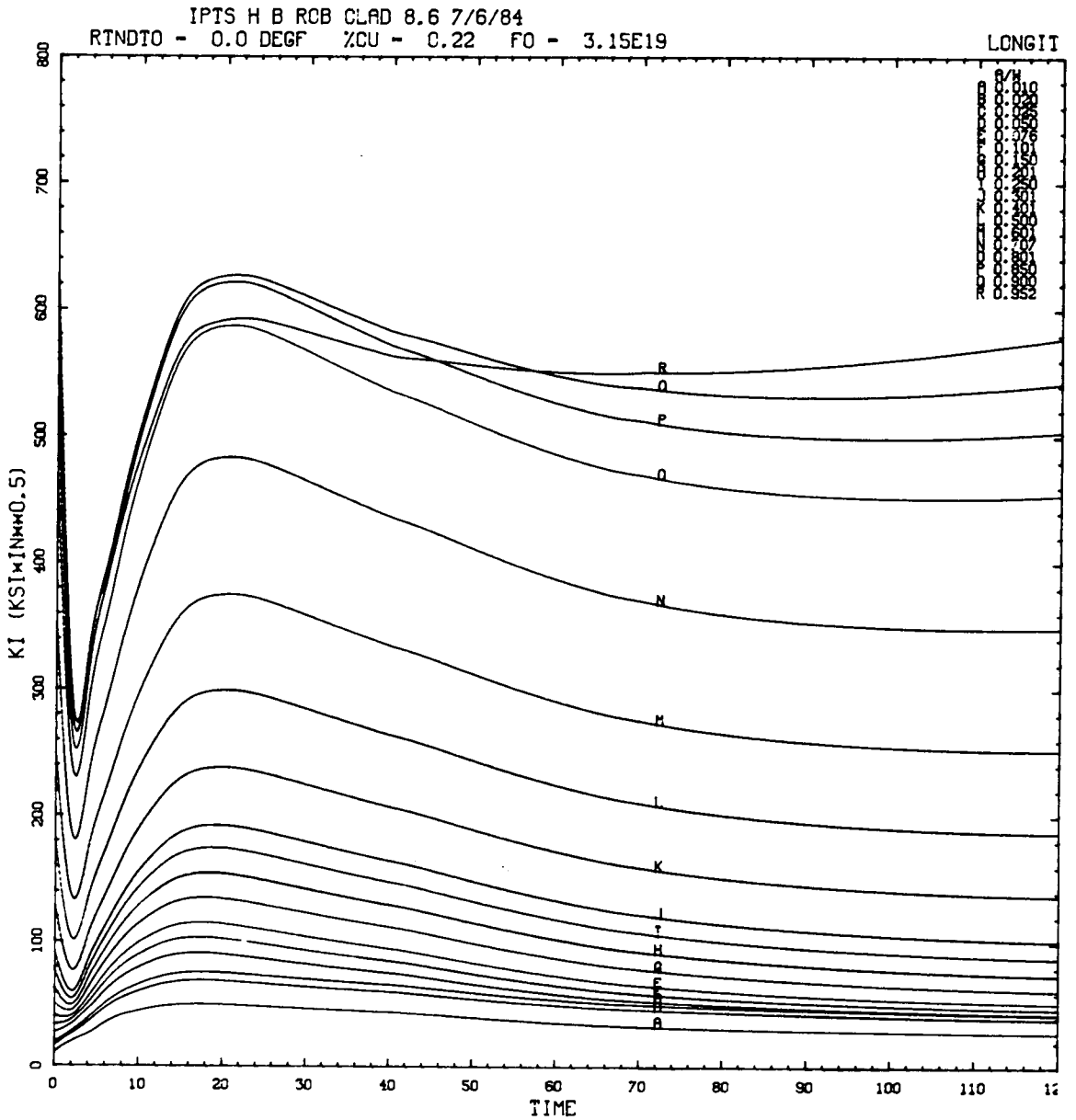

Figure I.95. Transient 8.6: K_I vs time (t) for various depths in wall (a/w).

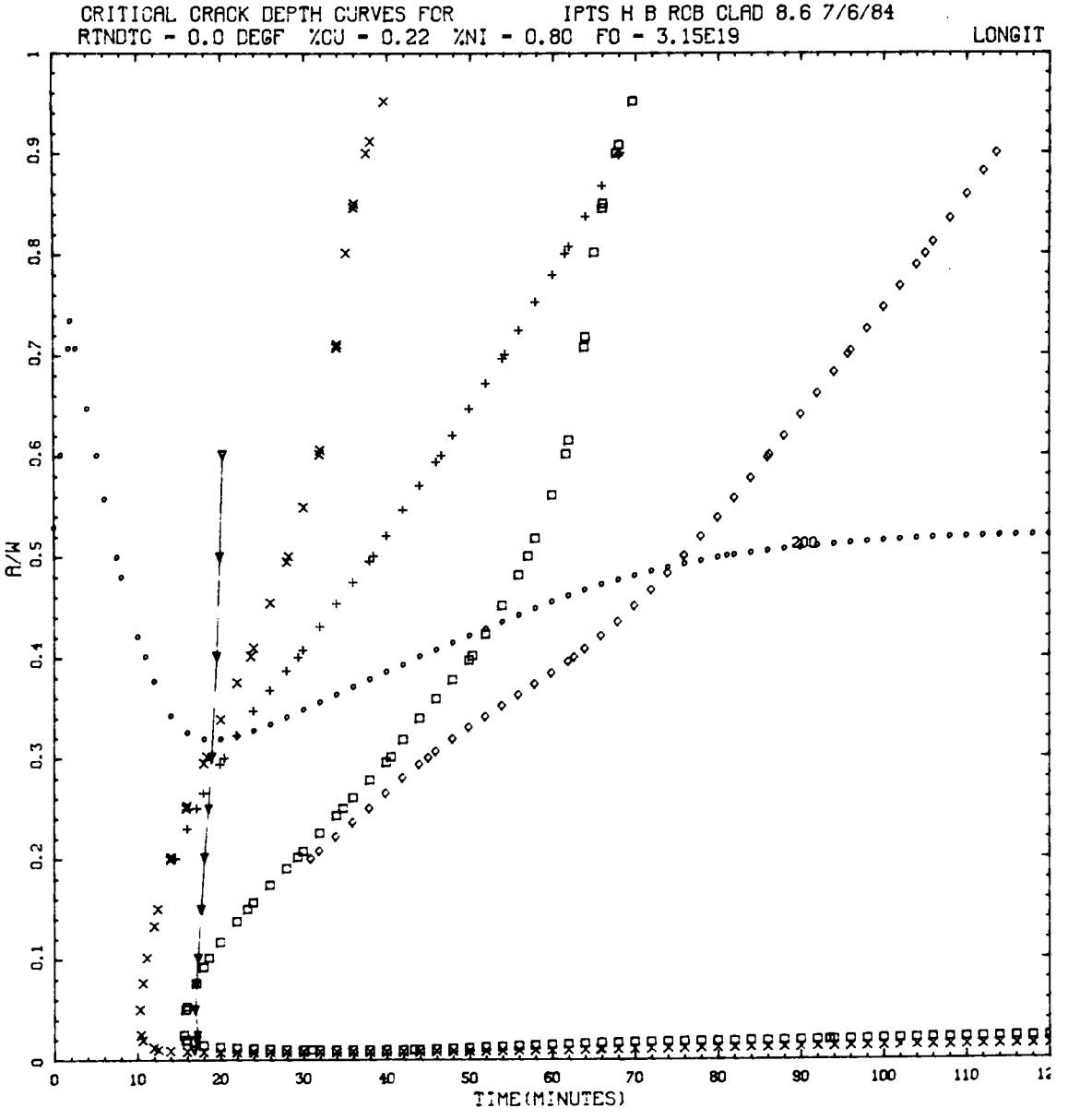

×, 2-D flaw, $K_I = K_{Ia}$
+, 2-m flaw, $K_I = K_{Ia}$
□, 2-D flaw, $K_I = K_{Ic}$
◊, 2-m flaw, $K_I = K_{Ic}$
O, 2-D flaw, $K_I = 220$ MPa $\sqrt{m}$
∇, WPS (warm prestressing)

Figure I.96. Transient 8.6: Critical-crack-depth curves for weld 2-273A based on -2σ values of K_{Ic}, K_{Ia}, and $\Delta RTNDT$, mean values of all other parameters, and 32-EFPY fluences.

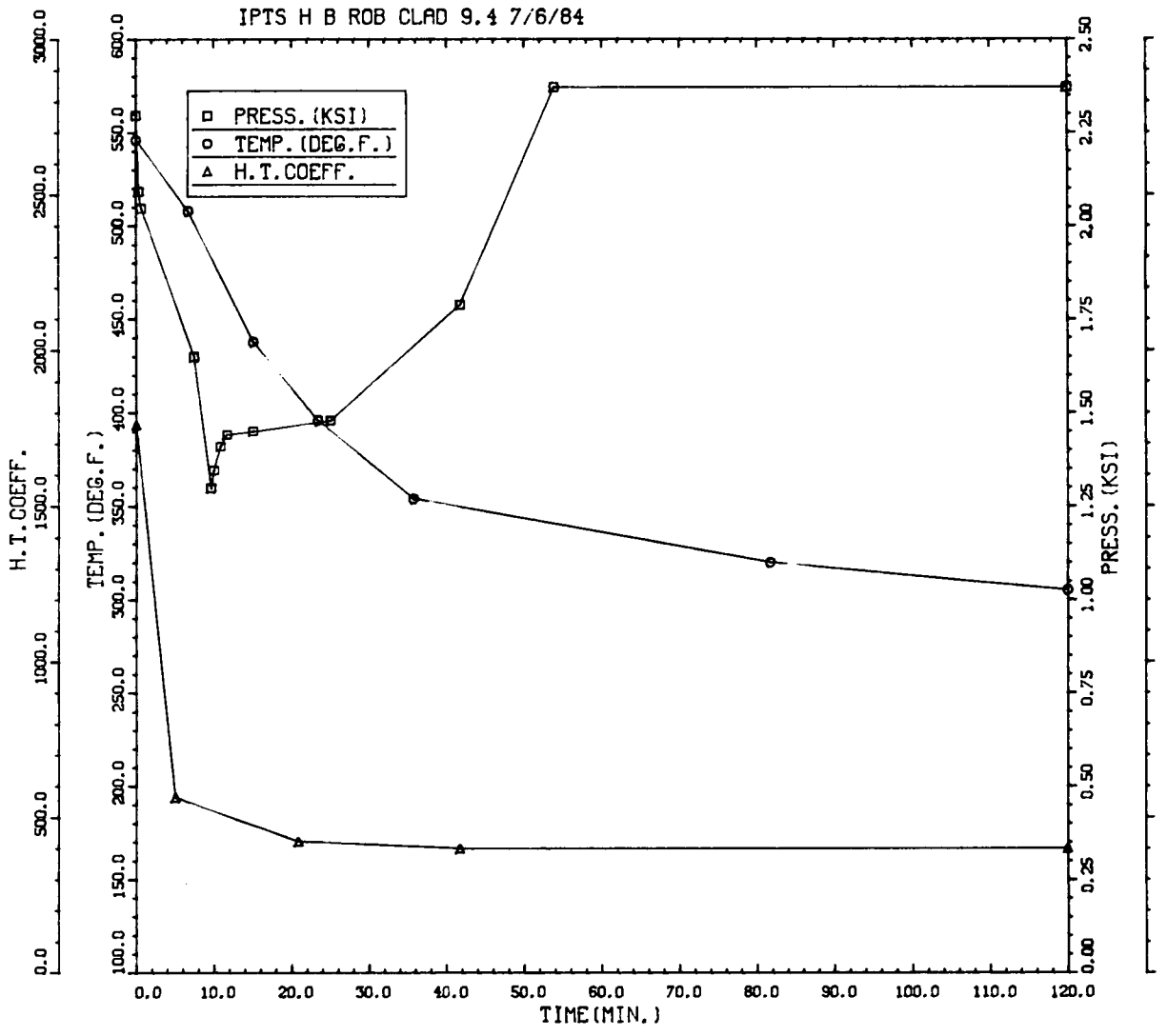

Figure I.97. Transient 9.4: Primary system pressure, downcomer coolant temperature, and fluid-film heat-transfer coefficient vs time in the transient.

Table I.17. Transient 9.4: Summary of digital output, including unadjusted $P(F|E)$ values and histogram data for crack depths, times of failure, and $T - RTNDT$ values at tip of crack corresponding to initiation and arrest events

```
IPTS H B ROB CLAD 9.4 7/6/84                    1. FLAWS/IN**3   DRTN(IS) =  211.2

            -------------UNADJUSTED--------------          ---ADJUSTED----
WELD    P(F/E)      95%CI     %ERR   P(INITIA)  N*V      P(F/E)    %ERR    NFAIL    NTRIALS

 1      3.05D-06   5.14D-07  16.86   3.54D-06  1.000    3.05D-06            135      200000

                                                VESSEL   3.05D-06  16.86


DEPTHS FOR INITIAL INITIATION (IN)
              0.09  0.26  0.46  0.67  0.90  1.16  1.44  1.74  2.08
   NUMBER       0    42    54    37    14     8     2     0     0
   PERCENT    0.0  26.8  34.4  23.6   8.9   5.1   1.3   0.0   0.0


TIMES OF FAILURE(MINUTES)
               0.0  10.0  20.0  30.0  40.0  50.0  60.0  70.0  80.0  90.0 100.0 110.0 120.0
  PERCENT      0.0   0.0   0.0   0.0   0.7   8.1   8.9  25.2  28.1   6.7   5.9  16.3


 INITIATION T-RTNDT(DEG.F)
            -100.0 -75.0 -50.0 -25.0   0.0  25.0  50.0  75.0 100.0 125.0 150.0 175.0 200.0
  NUMBER          0     0     3    36    92    25     6     2     0     0     0     0
  PERCENT       0.0   0.0   1.8  22.0  56.1  15.2   3.7   1.2   0.0   0.0   0.0   0.0


 ARREST T-RTNDT(DEG.F)
             -50.0 -25.0   0.0  25.0  50.0  75.0 100.0 125.0 150.0 175.0 200.0 225.0 250.0
  NUMBER          0     4    15     1     0     0     0     7     2     0     0     0
  PERCENT       0.0  13.8  51.7   3.4   0.0   0.0   0.0  24.1   6.9   0.0   0.0   0.0


 # OF STD DEVS ABOVE MEAN DELTA RTNDT(FAILURES ONLY)
              1.00  1.25  1.50  1.75  2.00  2.25  2.50  2.75  3.00
  NUMBER          5     6    13    24    18    23    18    28
  PERCENT       3.7   4.4   9.6  17.8  13.3  17.0  13.3  20.7


 # OF STD DEVS ABOVE MEAN RTNDT(FAILURES ONLY)
              1.00  1.25  1.50  1.75  2.00  2.25  2.50  2.75  3.00
  NUMBER          3     4     9    19    19    29    28    24
  PERCENT       2.2   3.0   6.7  14.1  14.1  21.5  20.7  17.8


ICRKTP = 2   IACCEL = 1   NDLRS = 1   NRTRS = 1   DATE: 10/31/84   TIME: 23.01.09

CPU TIME:  5 MIN 19 SEC
```

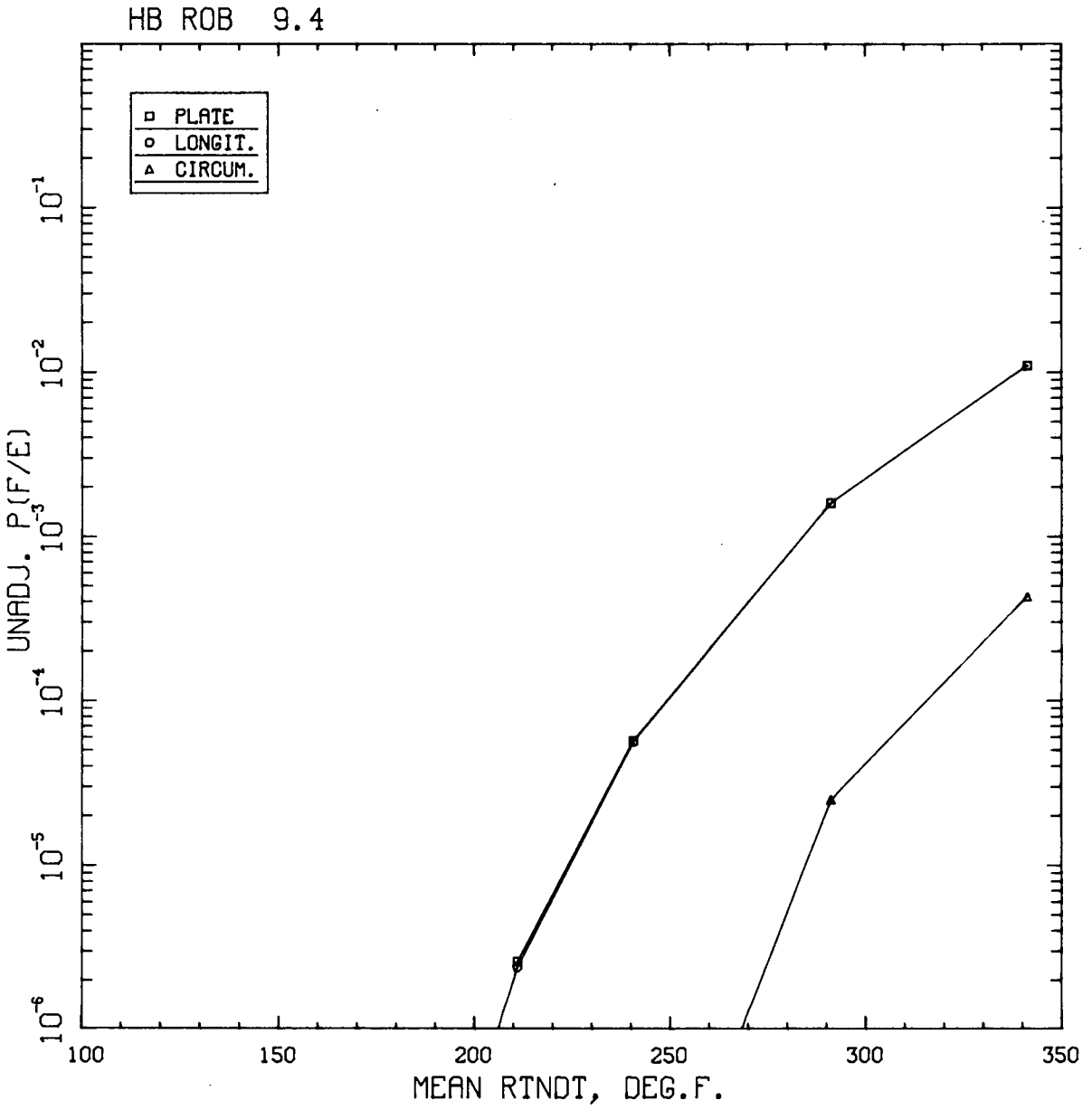

Figure I.98. Transient 9.4: $\hat{P}_j \int_0^w f(a)\, B(a)\, da$ vs $\overline{RTNDT_s}$ for (2-D, 2-D) and (2-D, 2m) flaw combinations.

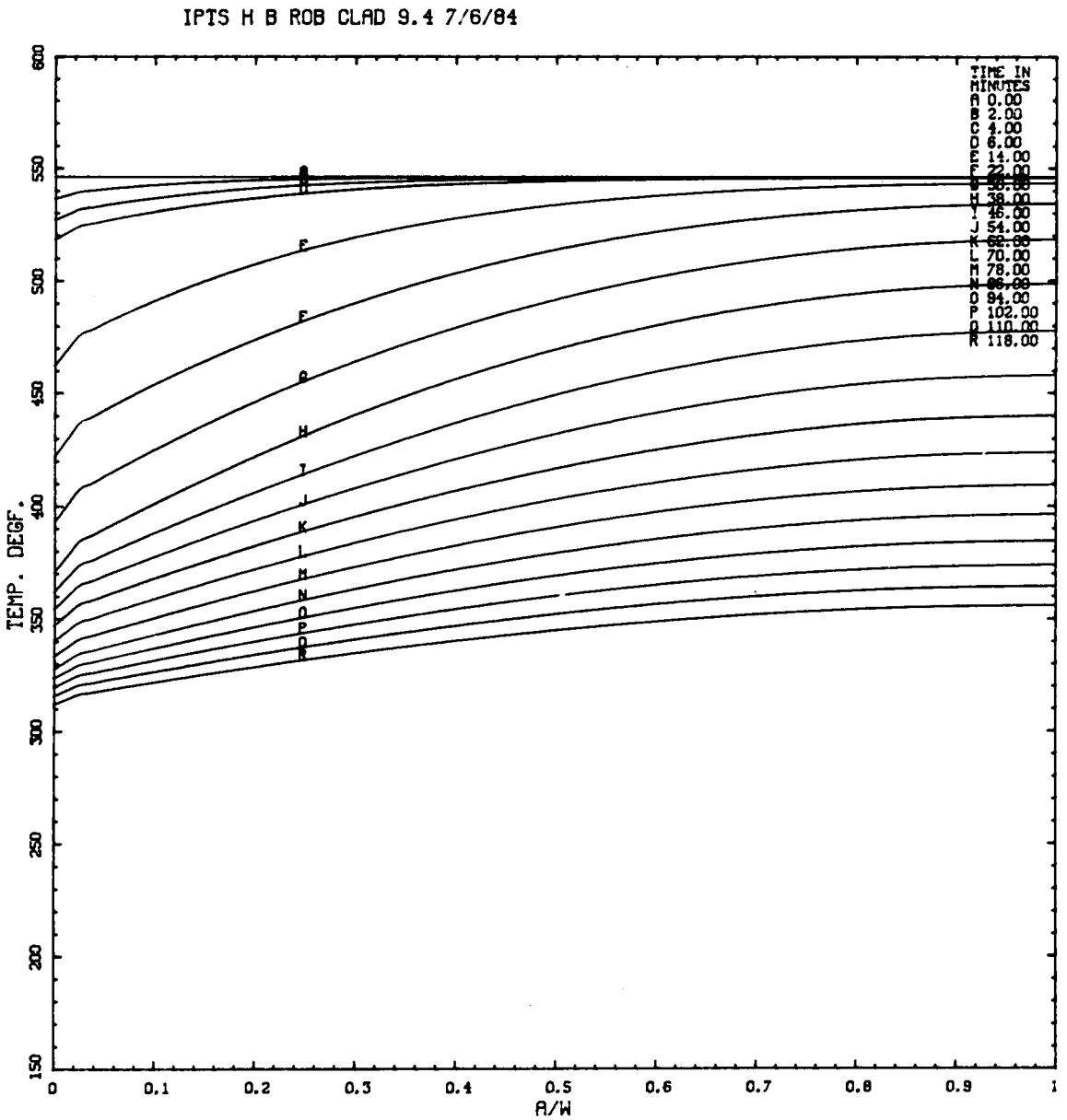

Figure I.99. Transient 9.4: Vessel wall temperature vs depth in wall (a/w) at various times (t) in transient.

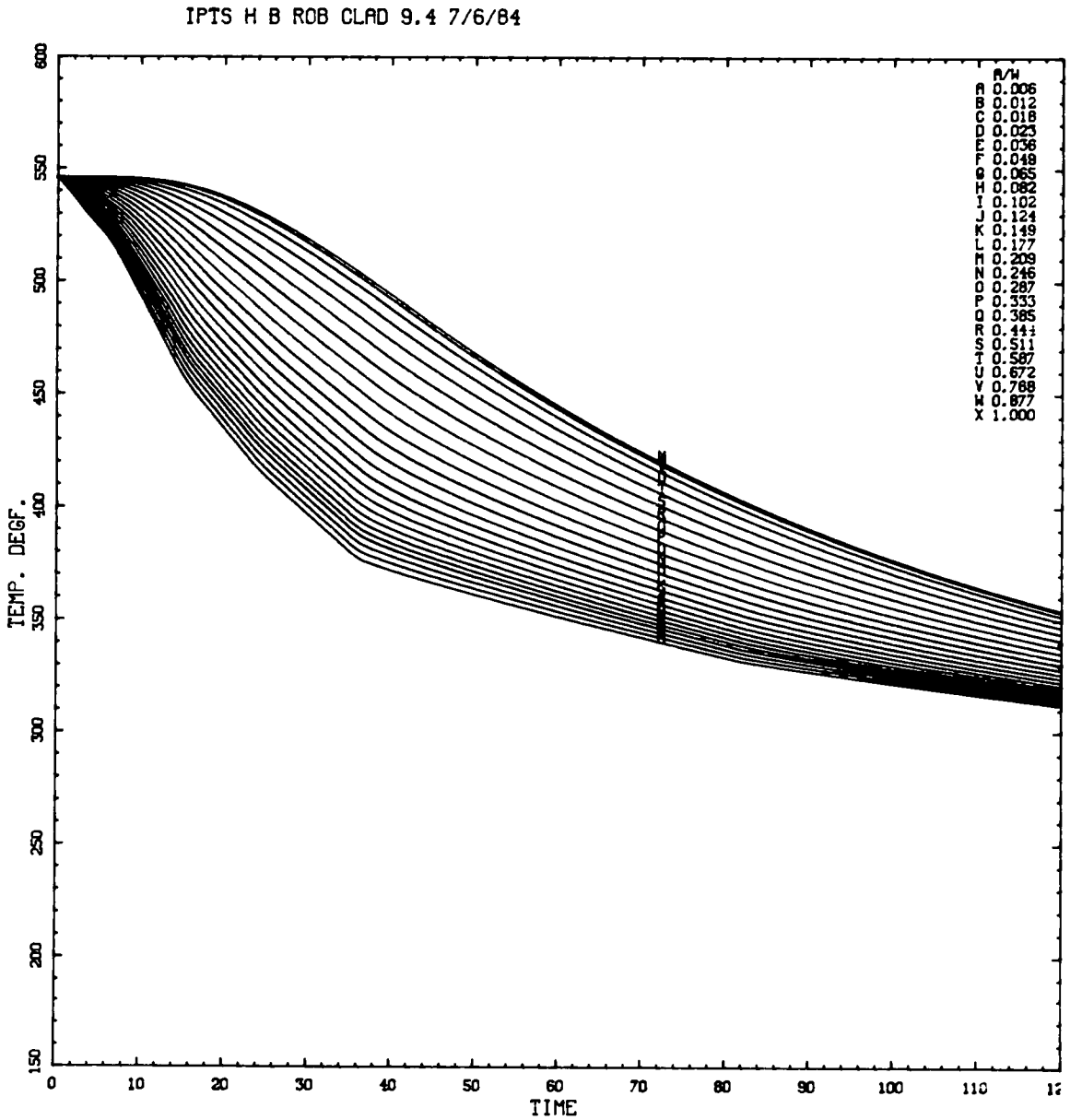

Figure I.100. Transient 9.4: Vessel wall temperature vs time (t) in transient at various depths in wall (a/w).

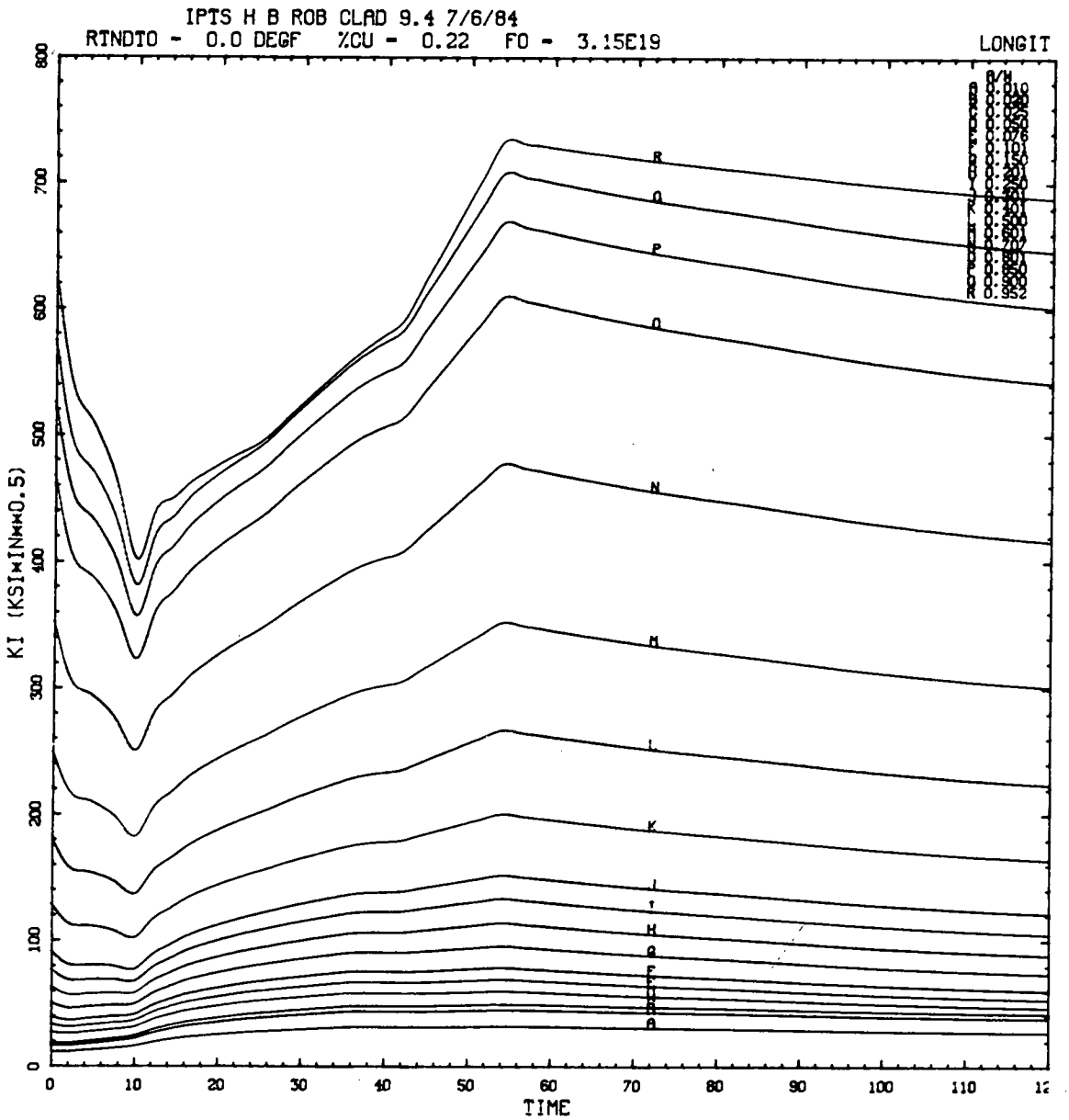

Figure I.101. Transient 9.4: K_I vs time (t) for various depths in wall (a/w).

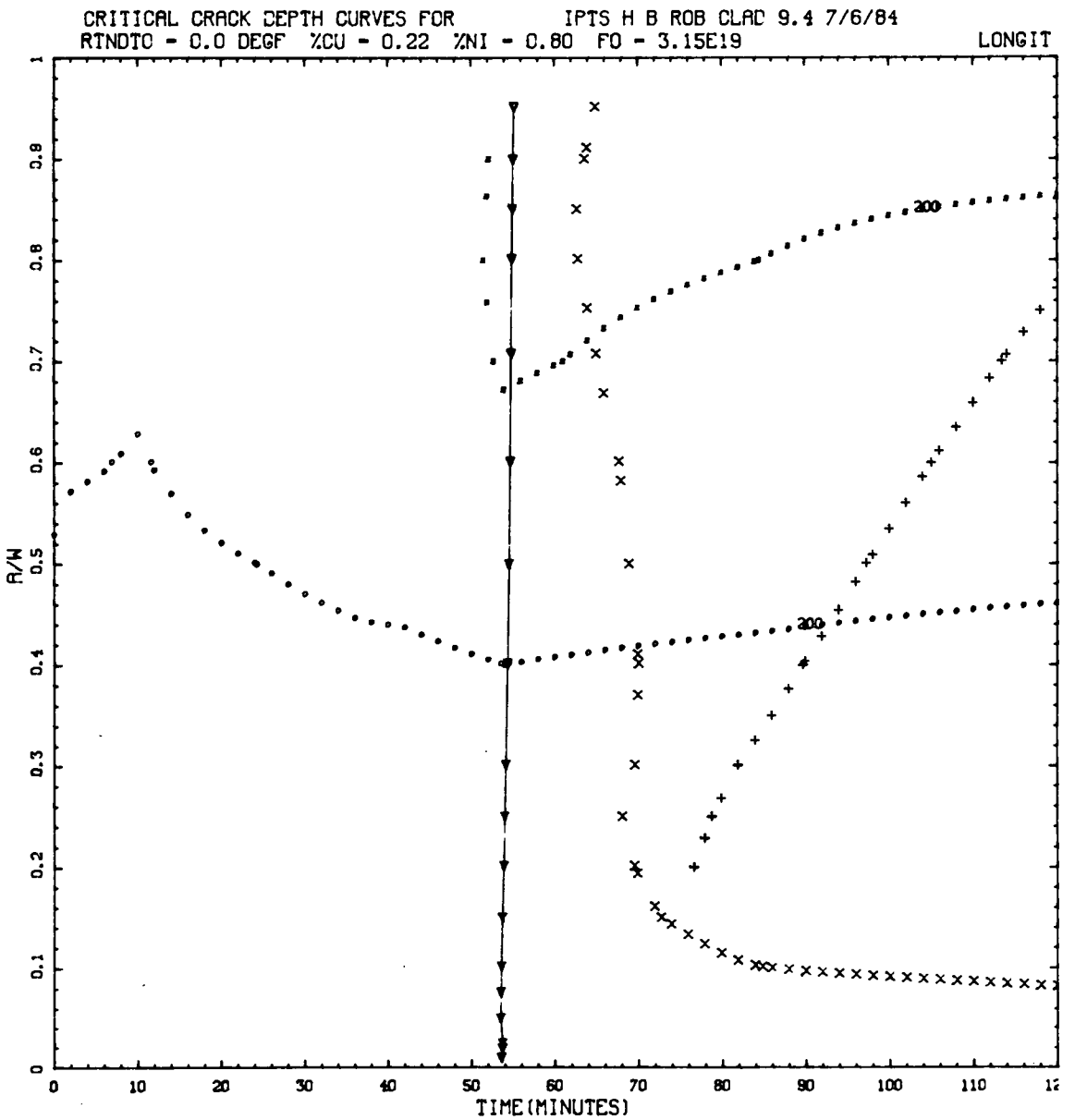

×, 2-D flaw, $K_I = K_{Ia}$
+, 2-m flaw, $K_I = K_{Ia}$
O, 2-D flaw, $K_I = 220$ MPa $\sqrt{m}$
■, 2-m flaw, $K_I = 220$ MPa $\sqrt{m}$
∇, WPS (warm prestressing)

Figure I.102. Transient 9.4: Critical-crack-depth curves for weld 2-273A based on -2σ values of K_{Ic}, K_{Ia}, and $\Delta RTNDT$, mean values of all other parameters, and 32-EFPY fluences.

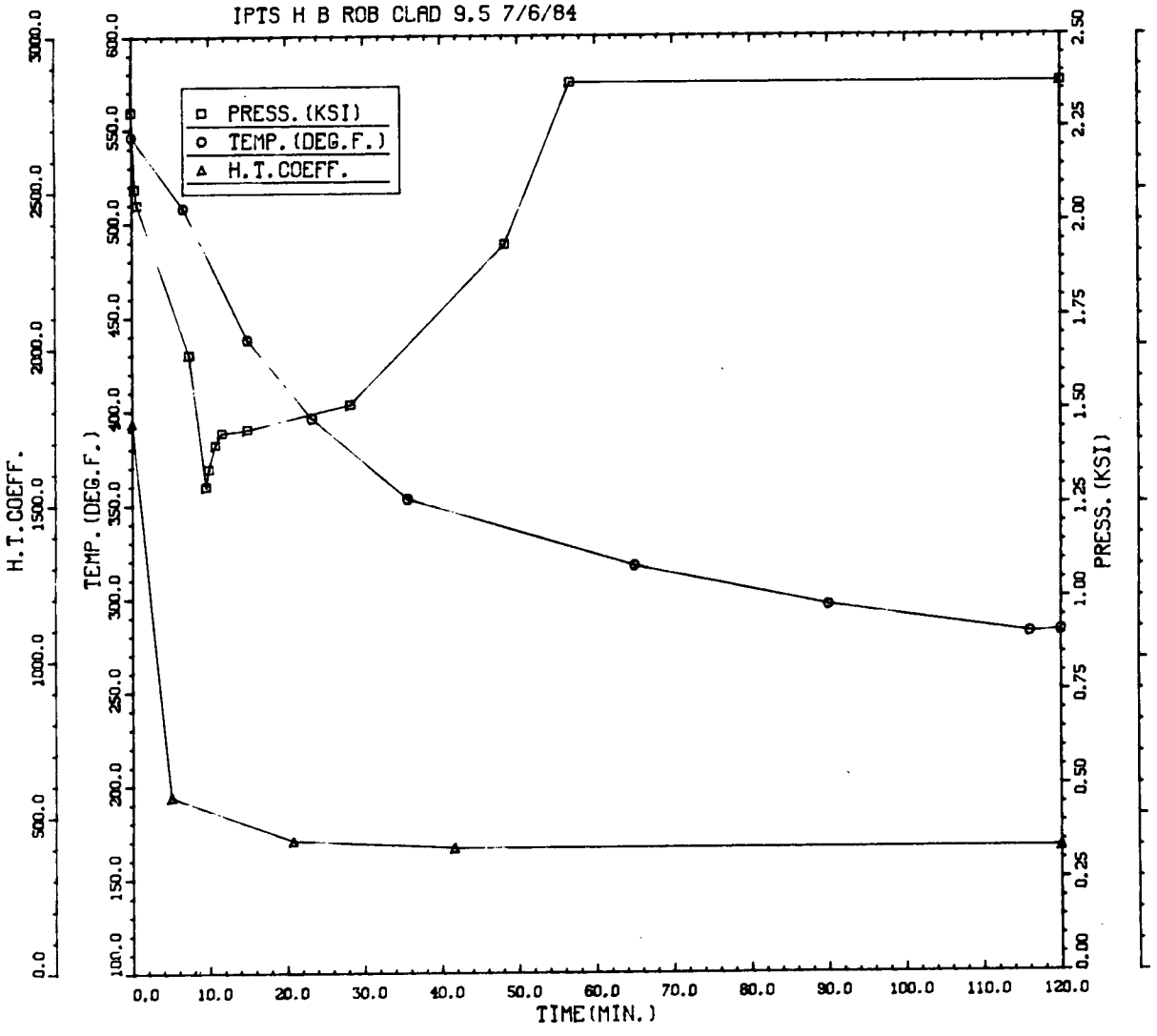

Figure I.103. Transient 9.5: Primary system pressure, downcomer coolant temperature, and fluid-film heat-transfer coefficient vs time in the transient.

Table I.18. Transient 9.5: Summary of digital output, including unadjusted $P(F|E)$ values and histogram data for crack depths, times of failure, and $T - RTNDT$ values at tip of crack corresponding to initiation and arrest events

```
IPTS H B ROB CLAD 9.5 7/6/84                          1. FLAWS/IN**3    DRTN(IS) =  211.2

            -------------UNADJUSTED--------------              ---ADJUSTED----
WELD    P(F/E)      95%CI     %ERR   P(INITIA)  N*V      P(F/E)    %ERR    NFAIL    NTRIALS

 1      4.72D-05   1.28D-05  27.18   5.35D-05  1.000    4.72D-05            52      200000

                                                VESSEL   4.72D-05  27.18


DEPTHS FOR INITIAL INITIATION (IN)
              0.09  0.26  0.46  0.67  0.90  1.16  1.44  1.74  2.08
   NUMBER       0    27    13    15     3     1     0     0     0
   PERCENT    0.0  45.8  22.0  25.4   5.1   1.7   0.0   0.0   0.0


TIMES OF FAILURE(MINUTES)
              0.0  10.0  20.0  30.0  40.0  50.0  60.0  70.0  80.0  90.0 100.0 110.0 120.0
  PERCENT       0.0   0.0   0.0   0.0   0.0   1.9   0.0   9.6  25.0  13.5  28.8  21.2


 INITIATION T-RTNDT(DEG.F)
           -100.0 -75.0 -50.0 -25.0   0.0  25.0  50.0  75.0 100.0 125.0 150.0 175.0 200.0
  NUMBER          0     1     3    29    23     3     2     0     0     0     0     0
  PERCENT       0.0   1.6   4.9  47.5  37.7   4.9   3.3   0.0   0.0   0.0   0.0   0.0


 ARREST T-RTNDT(DEG.F)
            -50.0 -25.0   0.0  25.0  50.0  75.0 100.0 125.0 150.0 175.0 200.0 225.0 250.0
  NUMBER        0     1     6     0     0     0     0     0     2     0     0     0
  PERCENT       0.0  11.1  66.7   0.0   0.0   0.0   0.0   0.0  22.2   0.0   0.0   0.0

ICRKTP = 2   IACCEL = 1   NDLRS = 0   NRTRS = 0   DATE: 10/30/84   TIME: 00.48.53

CPU TIME:  5 MIN 27 SEC
```

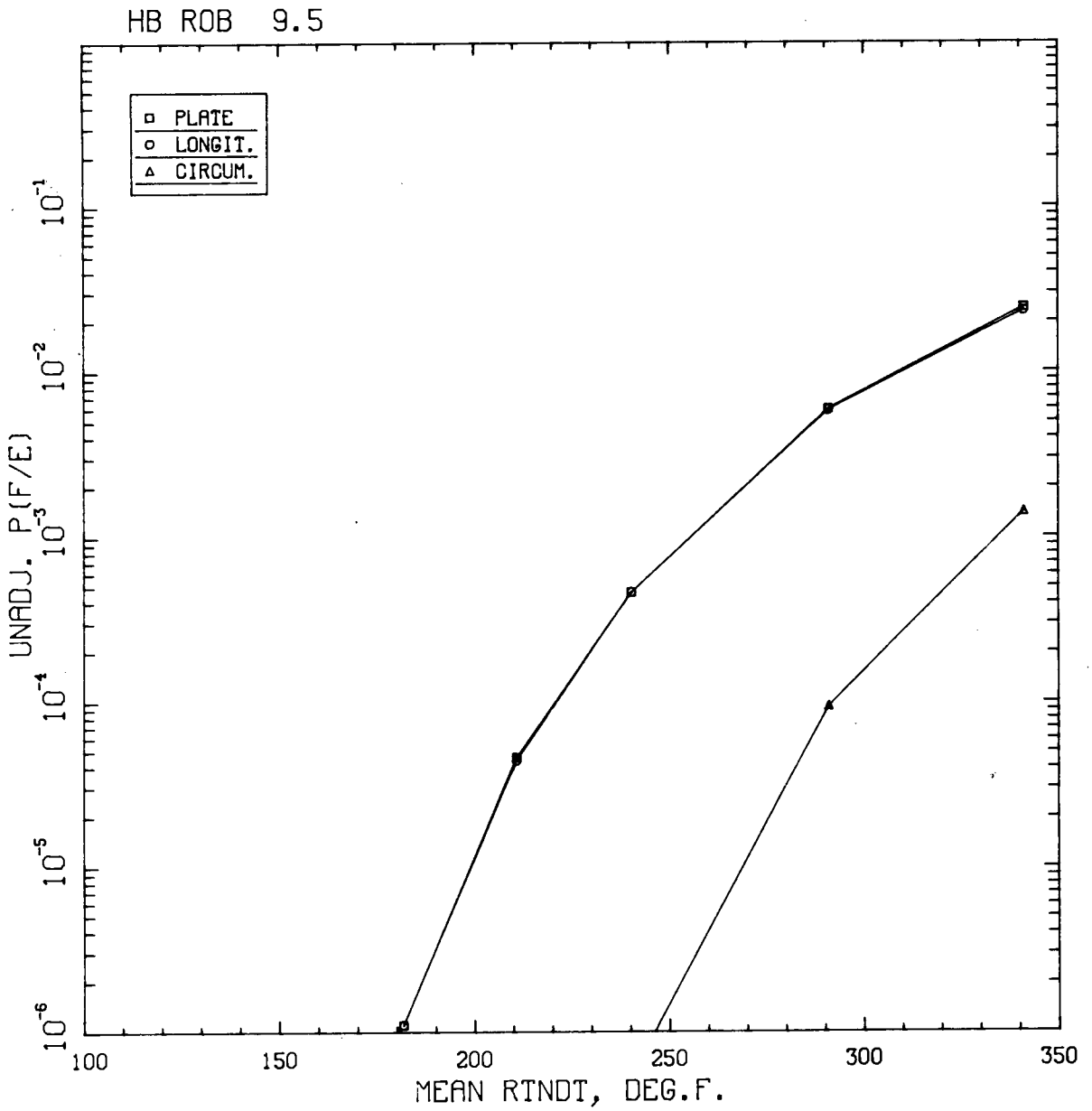

Figure I.104. Transient 9.5: $\hat{P}_j \int_0^w f(a)\, B(a)\, da$ vs $\overline{RTNDT_s}$ for (2-D, 2-D) and (2-D, 2m) flaw combinations.

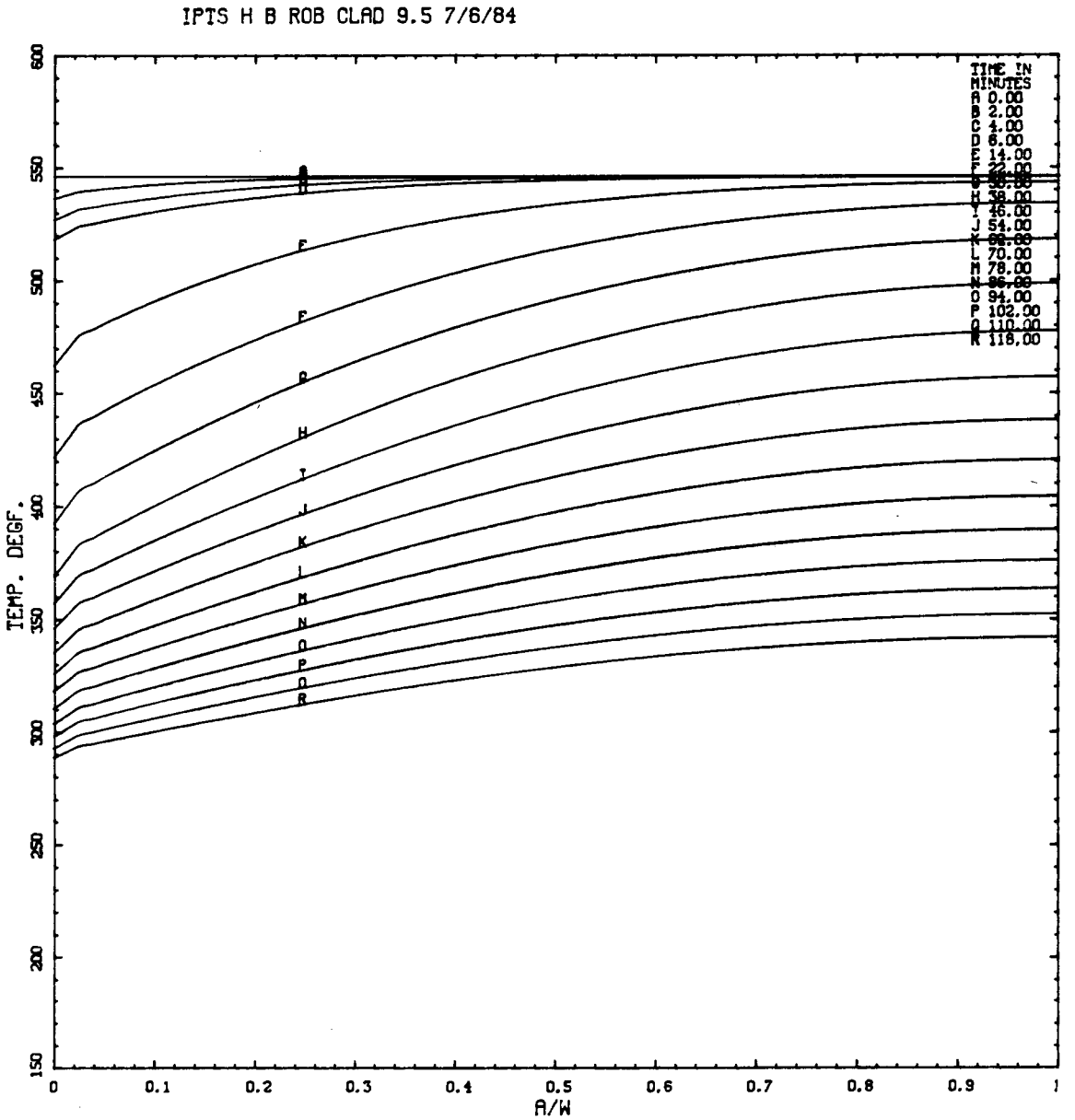

Figure I.105. Transient 9.5: Vessel wall temperature vs depth in wall (a/w) at various times (t) in transient.

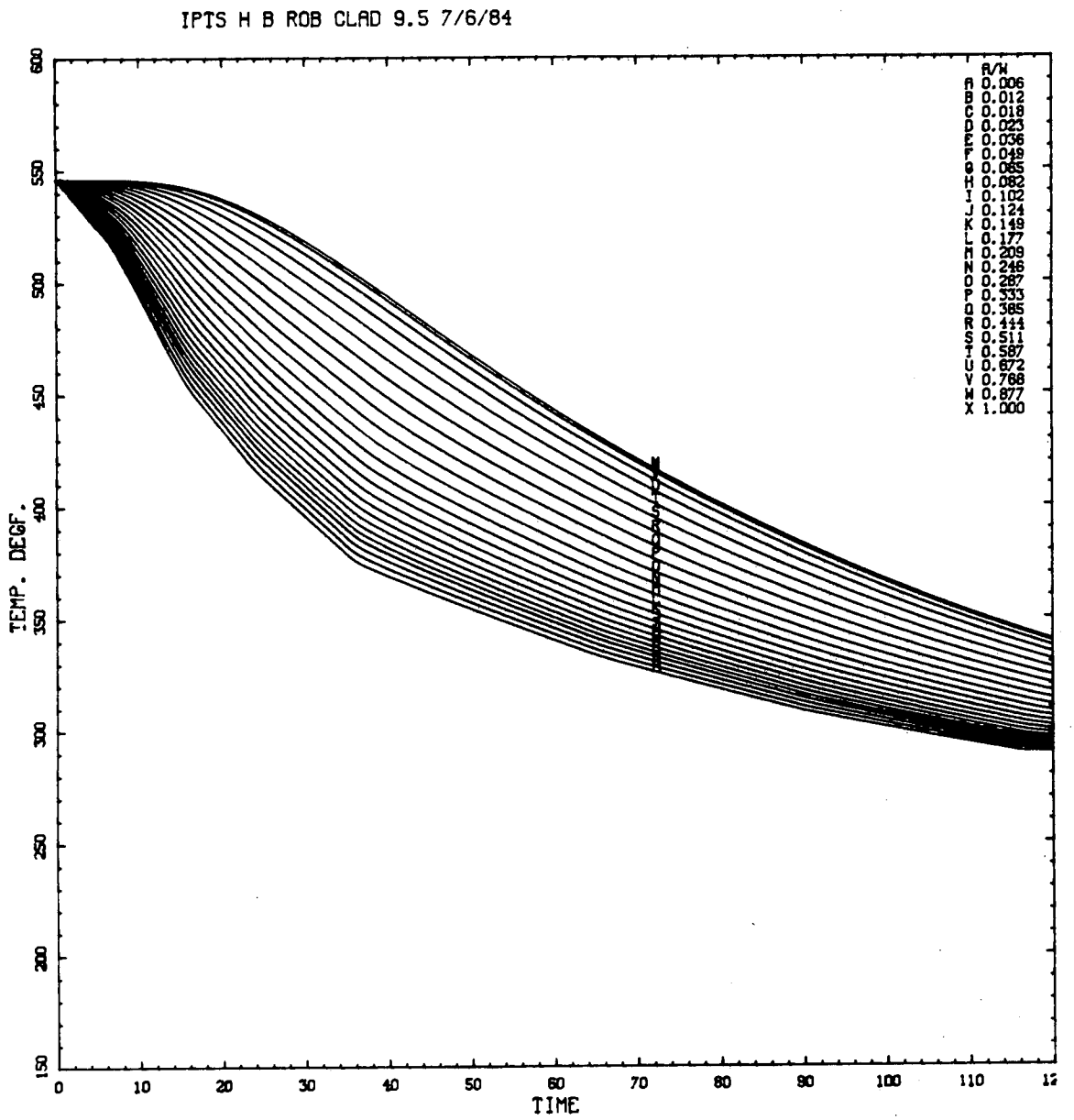

Figure I.106. Transient 9.5: Vessel wall temperature vs time (t) in transient at various depths in wall (a/w).

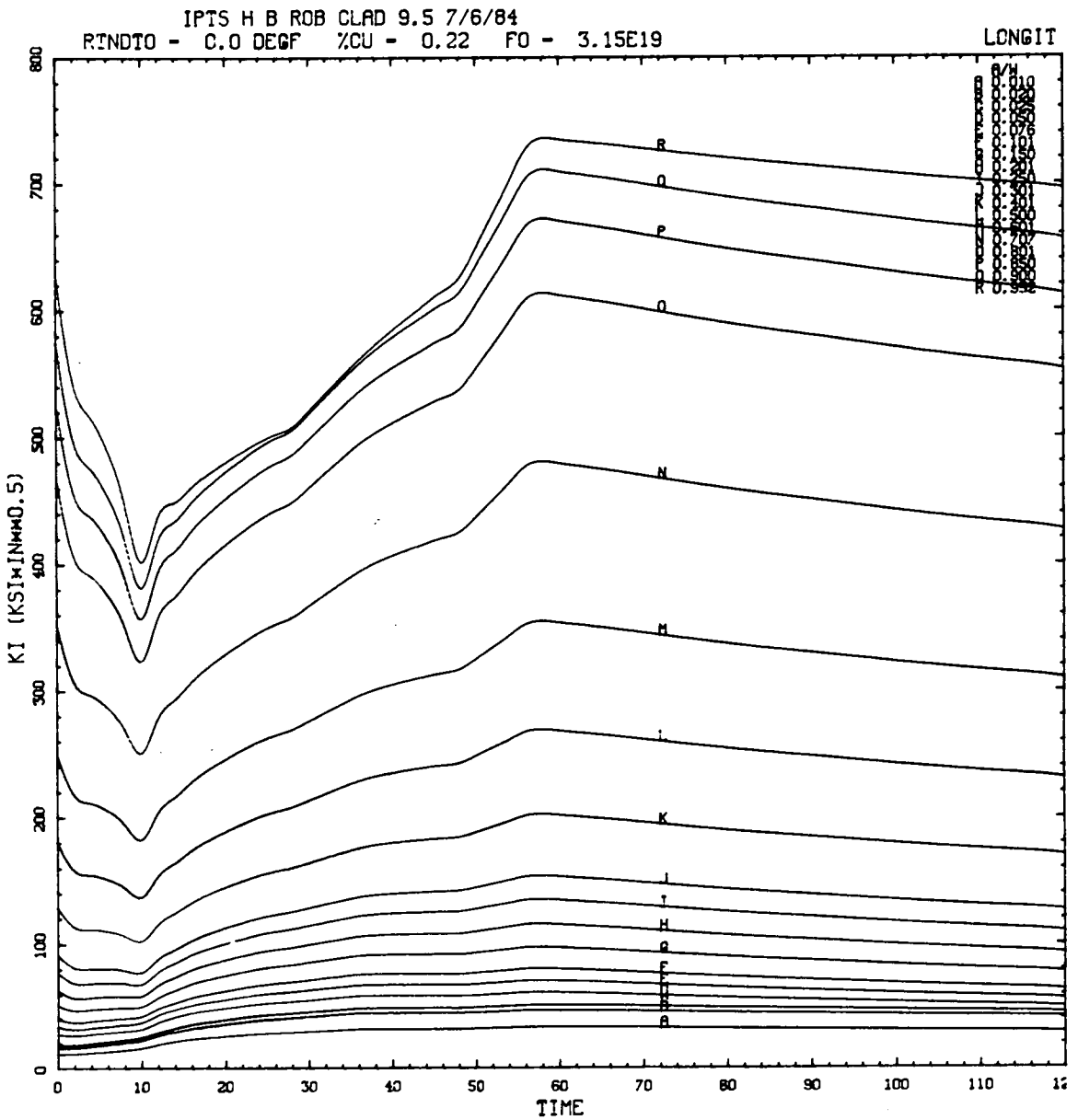

Figure I.107. Transient 9.5: K_I vs time (t) for various depths in wall (a/w).

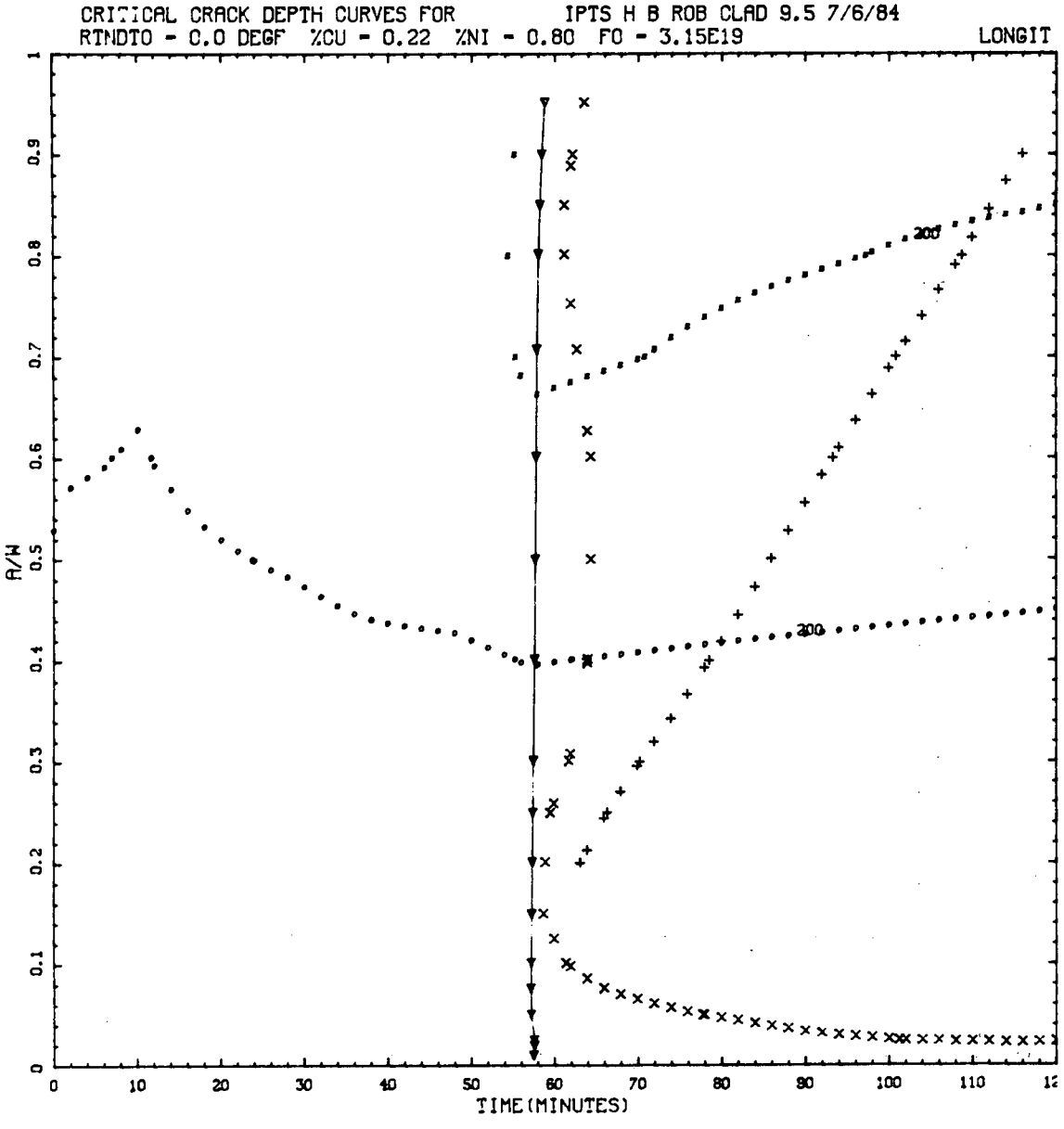

×, 2-D flaw, $K_I = K_{Ia}$
+, 2-m flaw, $K_I = K_{Ia}$
O, 2-D flaw, $K_I = 220$ MPa $\sqrt{m}$
■, 2-m flaw, $K_I = 220$ MPa $\sqrt{m}$
∇, WPS (warm prestressing)

Figure I.108. Transient 9.5: Critical-crack-depth curves for weld 2-273A based on -2σ values of K_{Ic}, K_{Ia}, and $\Delta RTNDT$, mean values of all other parameters, and 32-EFPY fluences.

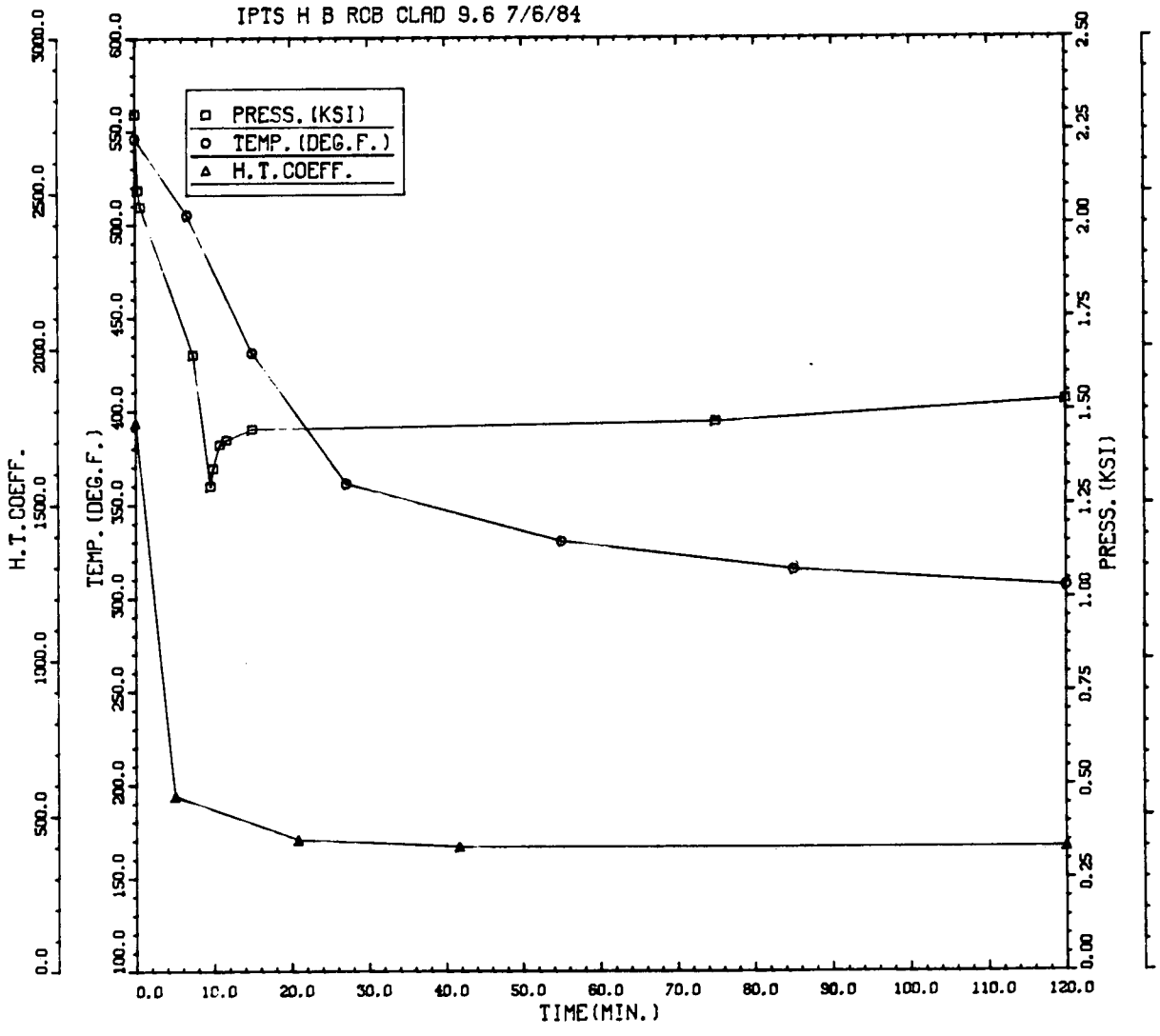

Figure I.109. Transient 9.6: Primary system pressure, downcomer coolant temperature, and fluid-film heat-transfer coefficient vs time in the transient.

Table I.19. Transient 9.6: Summary of digital output, including unadjusted $P(F|E)$ values and histogram data for crack depths, times of failure, and $T - RTNDT$ values at tip of crack corresponding to initiation and arrest events

IPTS H B ROB CLAD 9.6 7/6/84 1. FLAWS/IN**3 DRTN(IS) = 211.2

	UNADJUSTED					ADJUSTED			
WELD	P(F/E)	95%CI	%ERR	P(INITIA)	N*V	P(F/E)	%ERR	NFAIL	NTRIALS
1	1.57D-08	5.04D-09	32.22	8.08D-08	1.000	1.57D-08		37	200000
					VESSEL	1.57D-08	32.22		

DEPTHS FOR INITIAL INITIATION (IN)

	0.09	0.26	0.46	0.67	0.90	1.16	1.44	1.74	2.08
NUMBER	0	47	70	34	27	9	4	0	0
PERCENT	0.0	24.6	36.6	17.8	14.1	4.7	2.1	0.0	0.0

TIMES OF FAILURE(MINUTES)

	0.0	10.0	20.0	30.0	40.0	50.0	60.0	70.0	80.0	90.0	100.0	110.0	120.0
PERCENT	0.0	0.0	0.0	0.0	0.0	0.0	0.0	2.7	21.6	13.5	37.8	24.3	

INITIATION T-RTNDT(DEG.F)

	-100.0	-75.0	-50.0	-25.0	0.0	25.0	50.0	75.0	100.0	125.0	150.0	175.0	200.0
NUMBER	0	0	0	46	117	42	19	2	0	0	0	0	
PERCENT	0.0	0.0	0.0	20.4	51.8	18.6	8.4	0.9	0.0	0.0	0.0	0.0	

ARREST T-RTNDT(DEG.F)

	-50.0	-25.0	0.0	25.0	50.0	75.0	100.0	125.0	150.0	175.0	200.0	225.0	250.0
NUMBER	0	8	37	12	1	3	44	77	7	0	0	0	
PERCENT	0.0	4.2	19.6	6.3	0.5	1.6	23.3	40.7	3.7	0.0	0.0	0.0	

OF STD DEVS ABOVE MEAN DELTA RTNDT(FAILURES ONLY)

	1.00	1.25	1.50	1.75	2.00	2.25	2.50	2.75	3.00
NUMBER	0	0	0	0	2	3	12	20	
PERCENT	0.0	0.0	0.0	0.0	5.4	8.1	32.4	54.1	

OF STD DEVS ABOVE MEAN RTNDT(FAILURES ONLY)

	1.00	1.25	1.50	1.75	2.00	2.25	2.50	2.75	3.00
NUMBER	0	0	0	0	2	5	8	22	
PERCENT	0.0	0.0	0.0	0.0	5.4	13.5	21.6	59.5	

ICRKTP = 2 IACCEL = 1 NDLRS = 5 NRTRS = 5 DATE: 10/30/84 TIME: 00.52.43

CPU TIME: 5 MIN 18 SEC

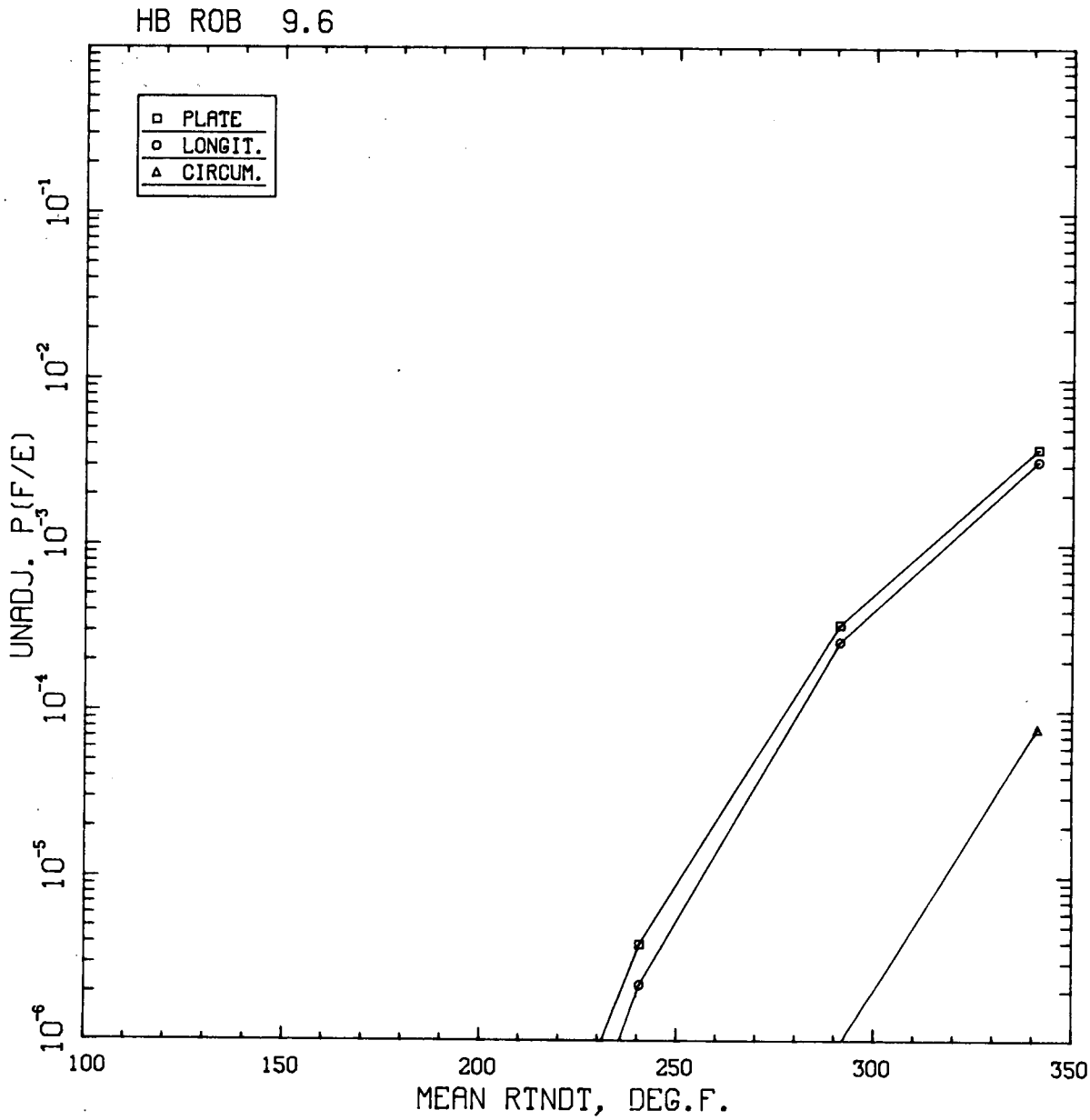

Figure I.110. Transient 9.6: $\hat{P}_j \int_0^w f(a)\, B(a)\, da$ vs $\overline{RTNDT_s}$ for (2-D, 2-D) and (2-D, 2m) flaw combinations.

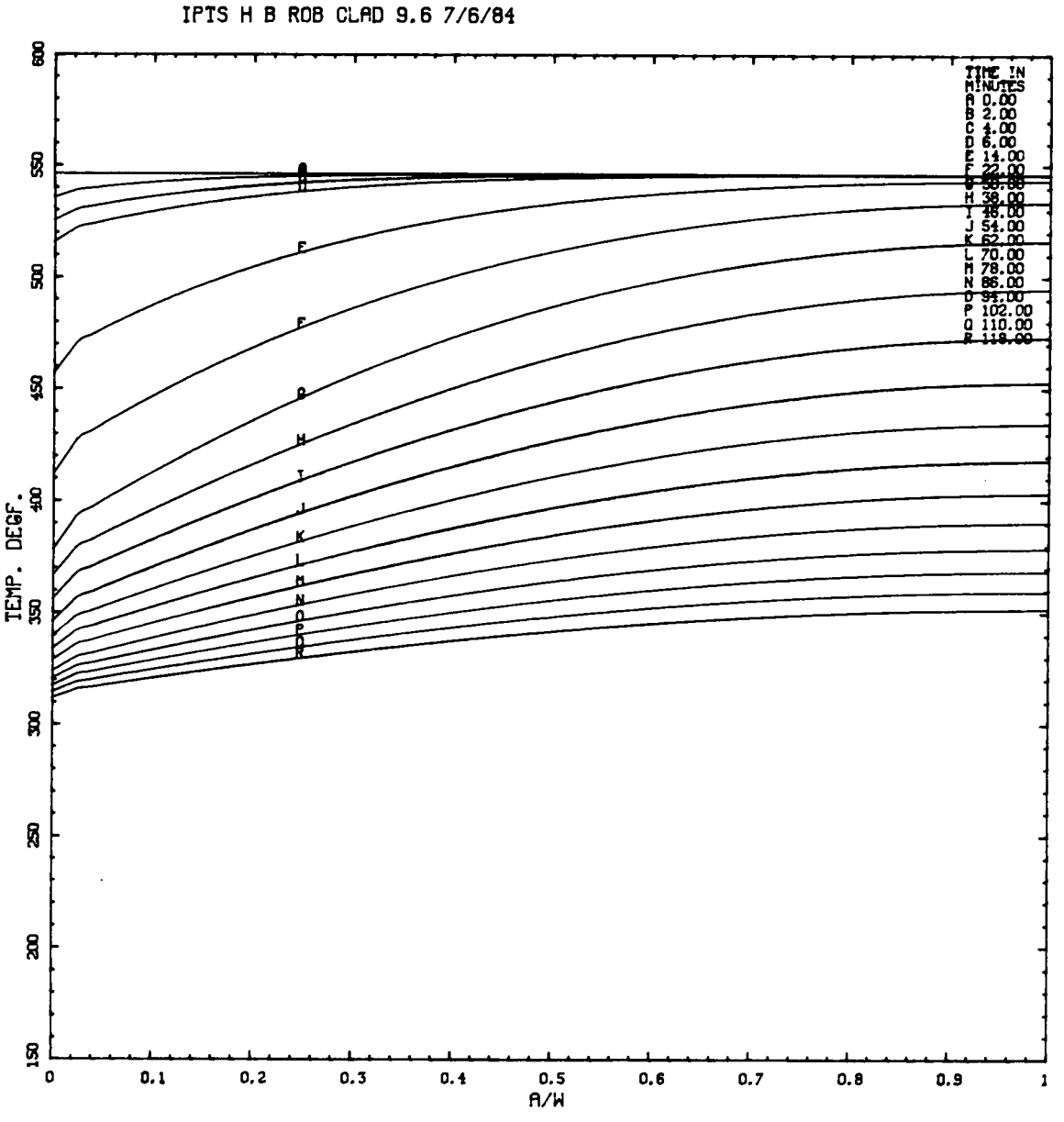

Figure I.111. Transient 9.6: Vessel wall temperature vs depth in wall (a/w) at various times (t) in transient.

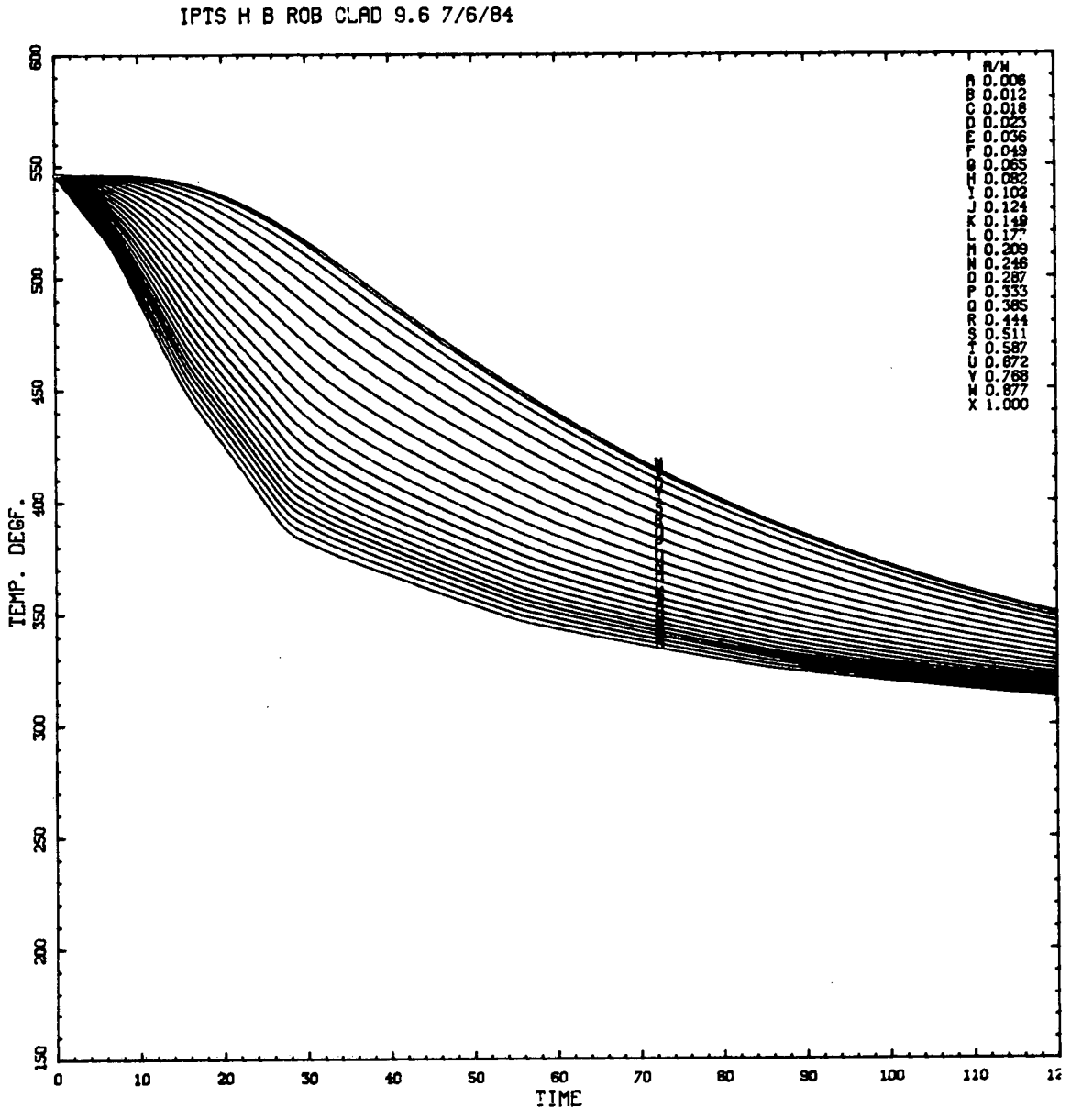

Figure I.112. Transient 9.6: Vessel wall temperature vs time (t) in transient at various depths in wall (a/w).

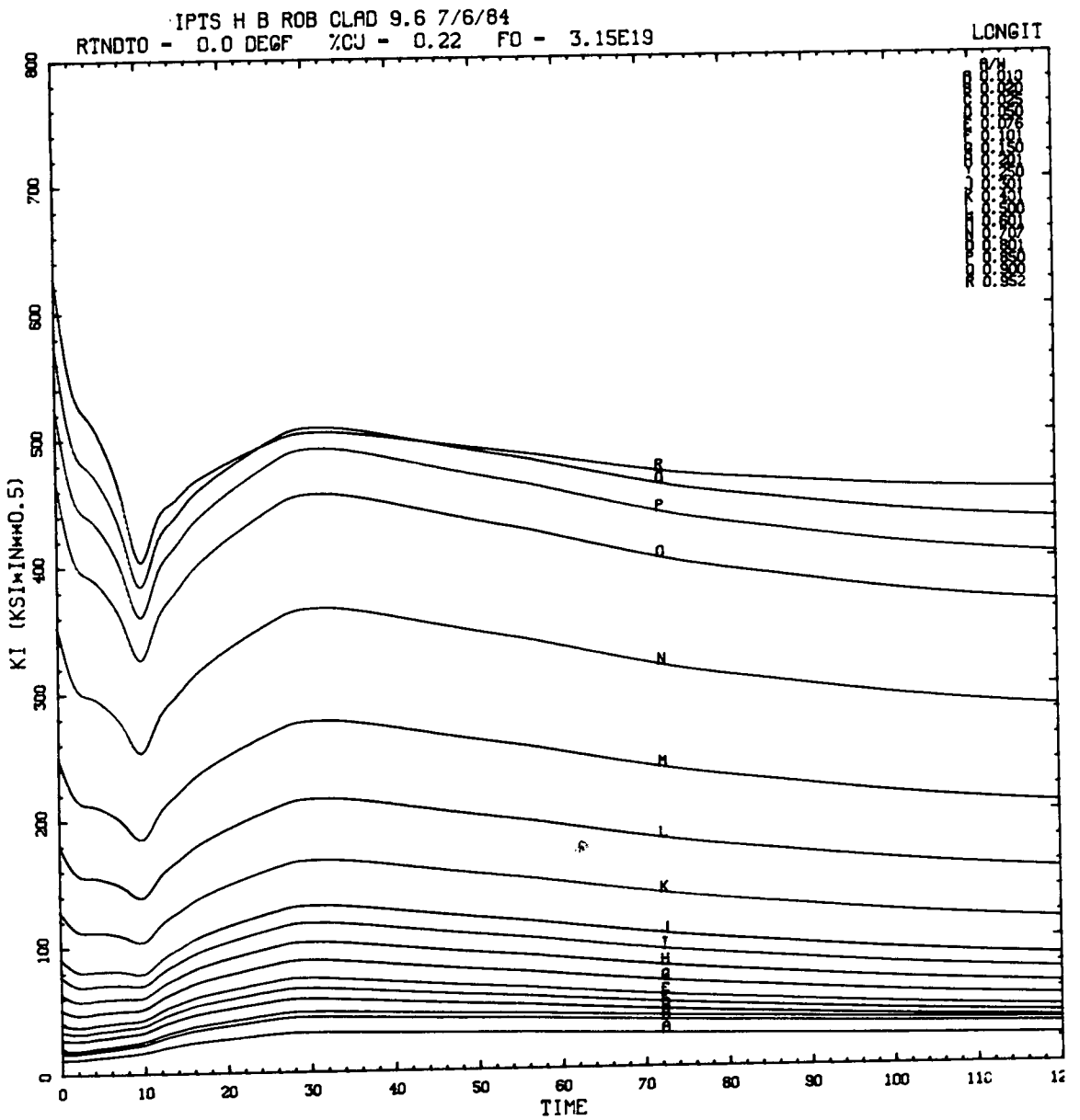

Figure I.113. Transient 9.6: K_I vs time (t) for various depths in wall (a/w).

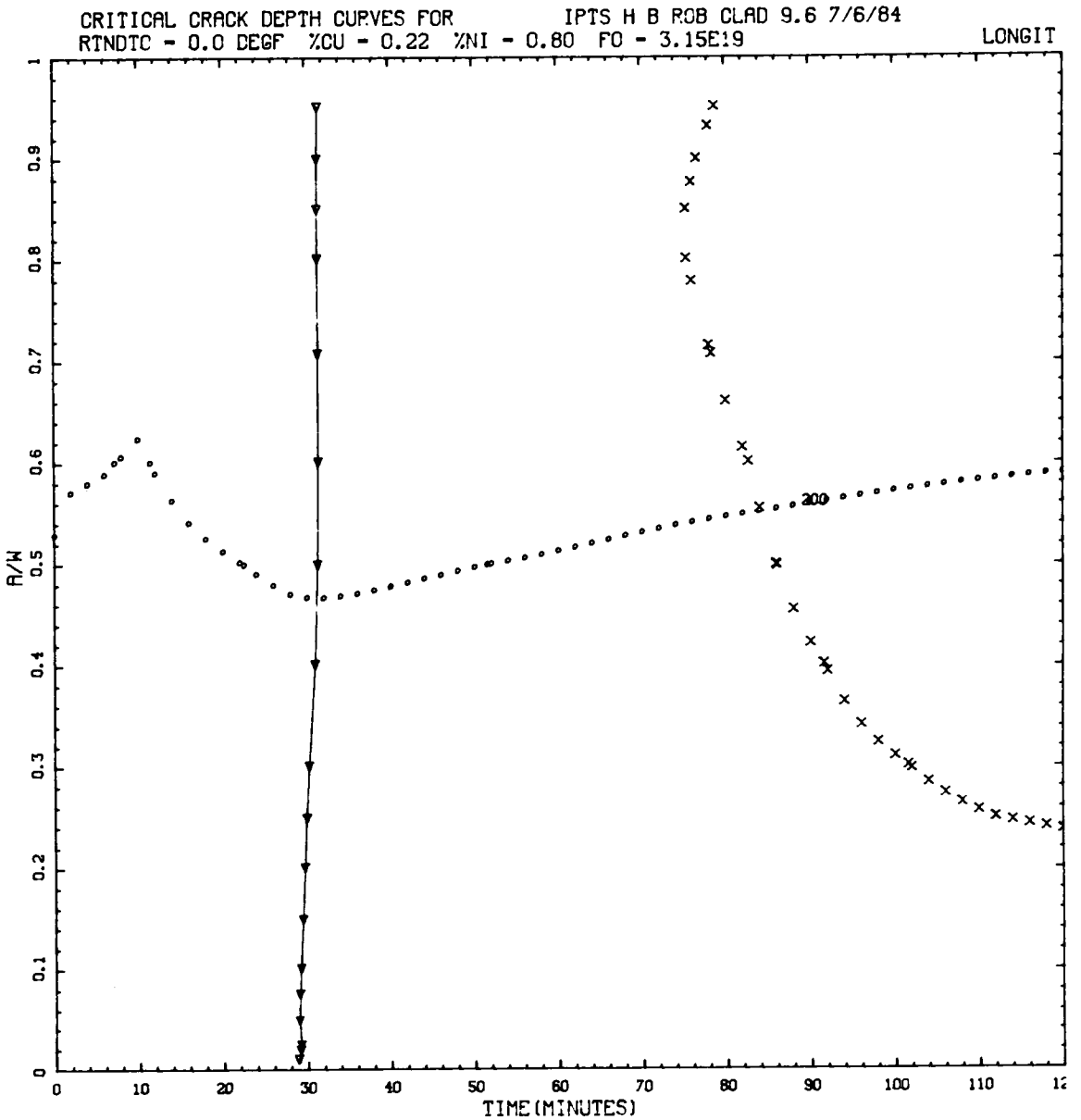

×, 2-D flaw, $K_I = K_{Ia}$
○, 2-D flaw, $K_I = 220$ MPa $\sqrt{m}$
▽, WPS (warm prestressing)

Figure I.114. Transient 9.6: Critical-crack-depth curves for weld 2-273A based on -2σ values of K_{Ic}, K_{Ia}, and $\Delta RTNDT$, mean values of all other parameters, and 32-EFPY fluences.

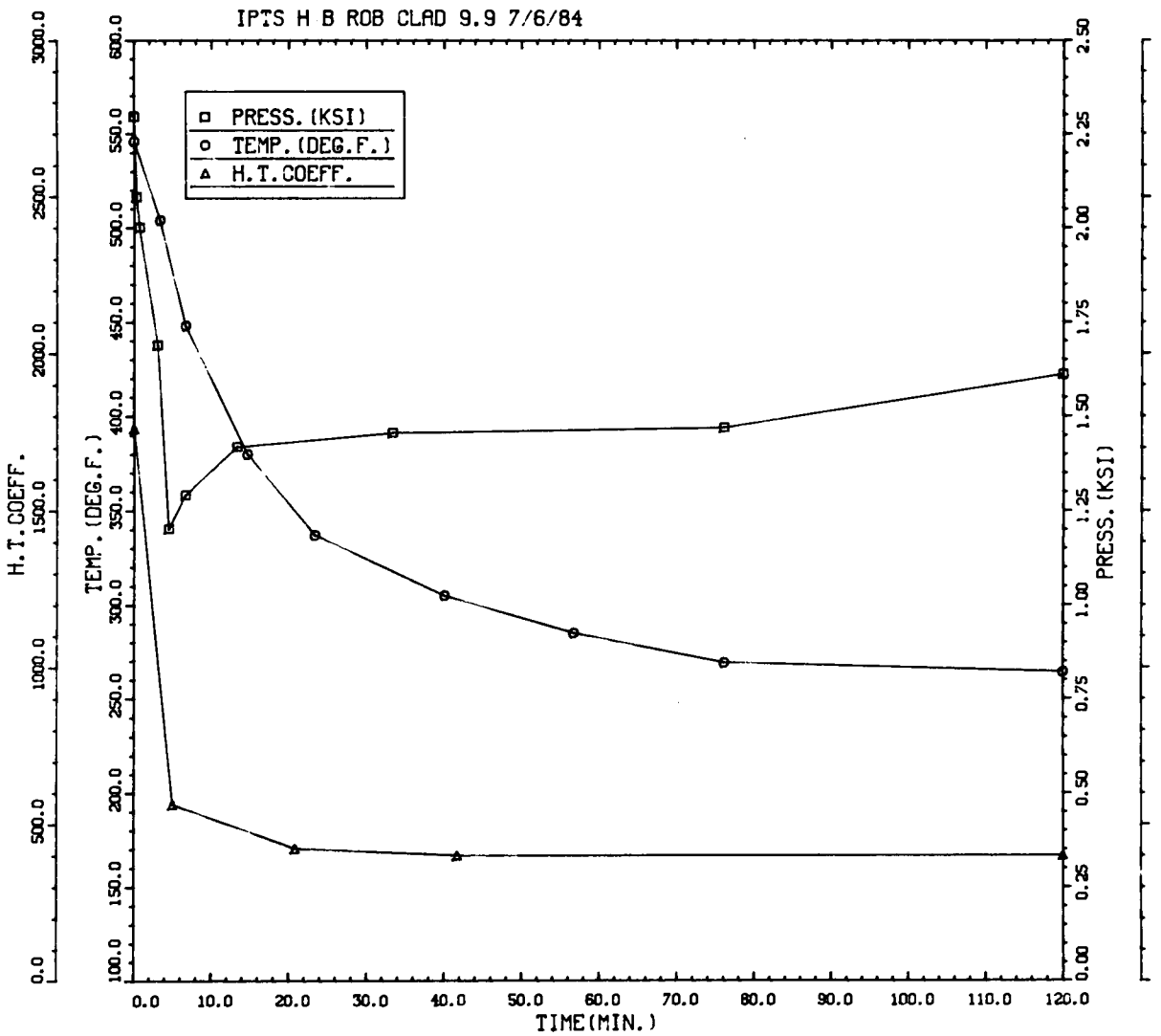

Figure I.115. Transient 9.9B: Primary system pressure, downcomer coolant temperature, and fluid-film heat-transfer coefficient vs time in the transient.

Table I.20. Transient 9.9B: Summary of digital output, including unadjusted $P(F|E)$ values and histogram data for crack depths, times of failure, and $T - RTNDT$ values at tip of crack corresponding to initiation and arrest events

IPTS H B ROB CLAD 9.9 7/6/84 1. FLAWS/IN**3 DRTN(IS) = 211.2

WELD	UNADJUSTED P(F/E)	95%CI	%ERR	P(INITIA)	N*V	ADJUSTED P(F/E)	%ERR	NFAIL	NTRIALS
1	2.45D-05	9.23D-06	37.72	4.90D-05	1.000	2.45D-05		27	200000
					VESSEL	2.45D-05	37.72		

DEPTHS FOR INITIAL INITIATION (IN)

	0.09	0.26	0.46	0.67	0.90	1.16	1.44	1.74	2.08
NUMBER	0	30	11	12	1	0	0	0	0
PERCENT	0.0	55.6	20.4	22.2	1.9	0.0	0.0	0.0	0.0

TIMES OF FAILURE(MINUTES)

	0.0	10.0	20.0	30.0	40.0	50.0	60.0	70.0	80.0	90.0	100.0	110.0	120.0
PERCENT	0.0	0.0	0.0	0.0	0.0	7.4	3.7	11.1	11.1	14.8	25.9	25.9	

INITIATION T-RTNDT(DEG.F)

	-100.0	-75.0	-50.0	-25.0	0.0	25.0	50.0	75.0	100.0	125.0	150.0	175.0	200.0
NUMBER	0	0	3	31	18	11	8	6	0	0	0	0	
PERCENT	0.0	0.0	3.9	40.3	23.4	14.3	10.4	7.8	0.0	0.0	0.0	0.0	

ARREST T-RTNDT(DEG.F)

	-50.0	-25.0	0.0	25.0	50.0	75.0	100.0	125.0	150.0	175.0	200.0	225.0	250.0
NUMBER	0	0	9	2	0	0	2	29	8	0	0	0	
PERCENT	0.0	0.0	18.0	4.0	0.0	0.0	4.0	58.0	16.0	0.0	0.0	0.0	

ICRKTP = 2 IACCEL = 1 NDLRS = 0 NRTRS = 0 DATE: 10/31/84 TIME: 22.13.06

CPU TIME: 5 MIN 29 SEC

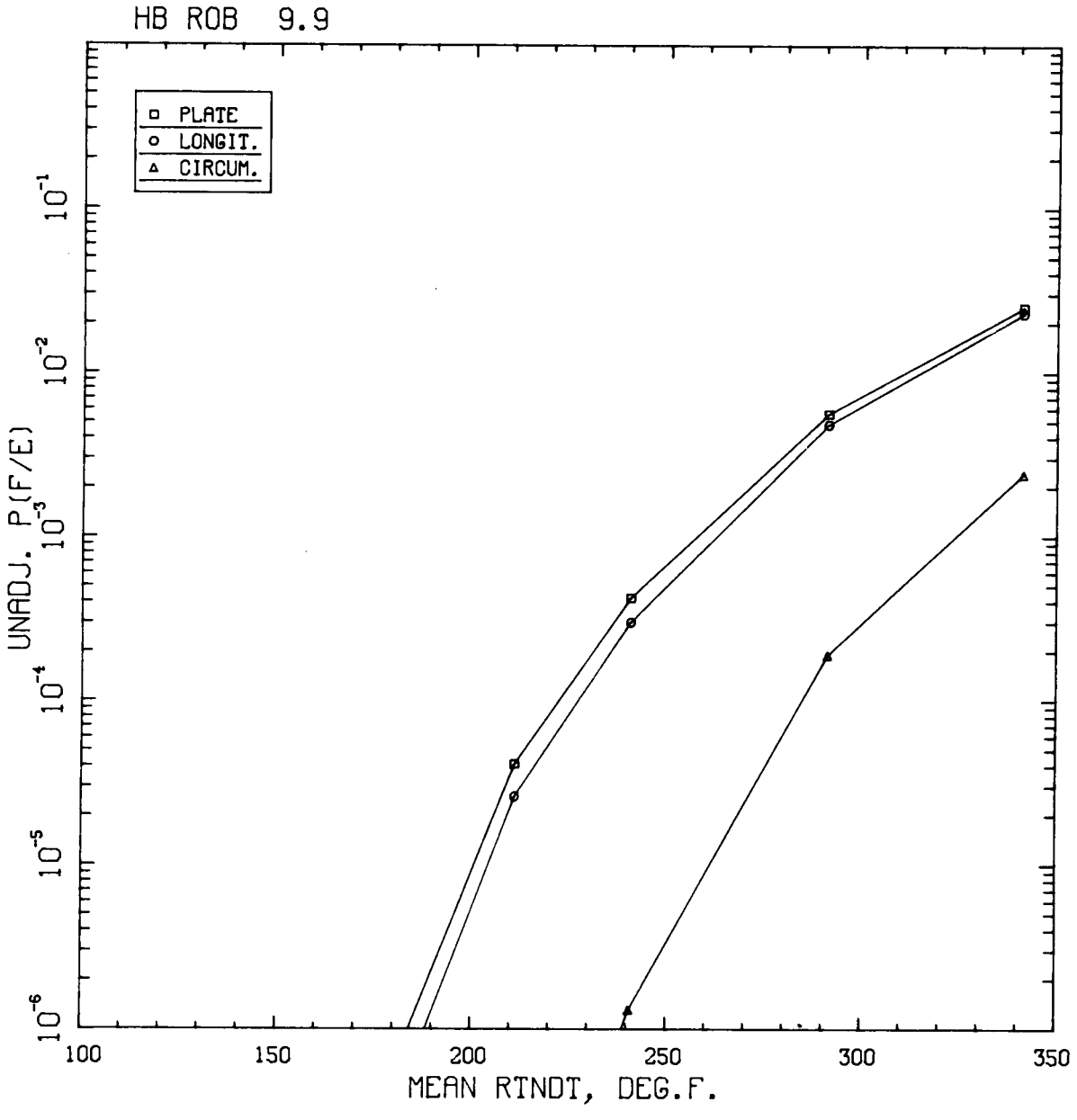

Figure I.116. Transient 9.9B: $\hat{P}_j \int_0^w f(a)\, B(a)\, da$ vs $\overline{RTNDT_s}$ for (2-D, 2-D) and (2-D, 2m) flaw combinations.

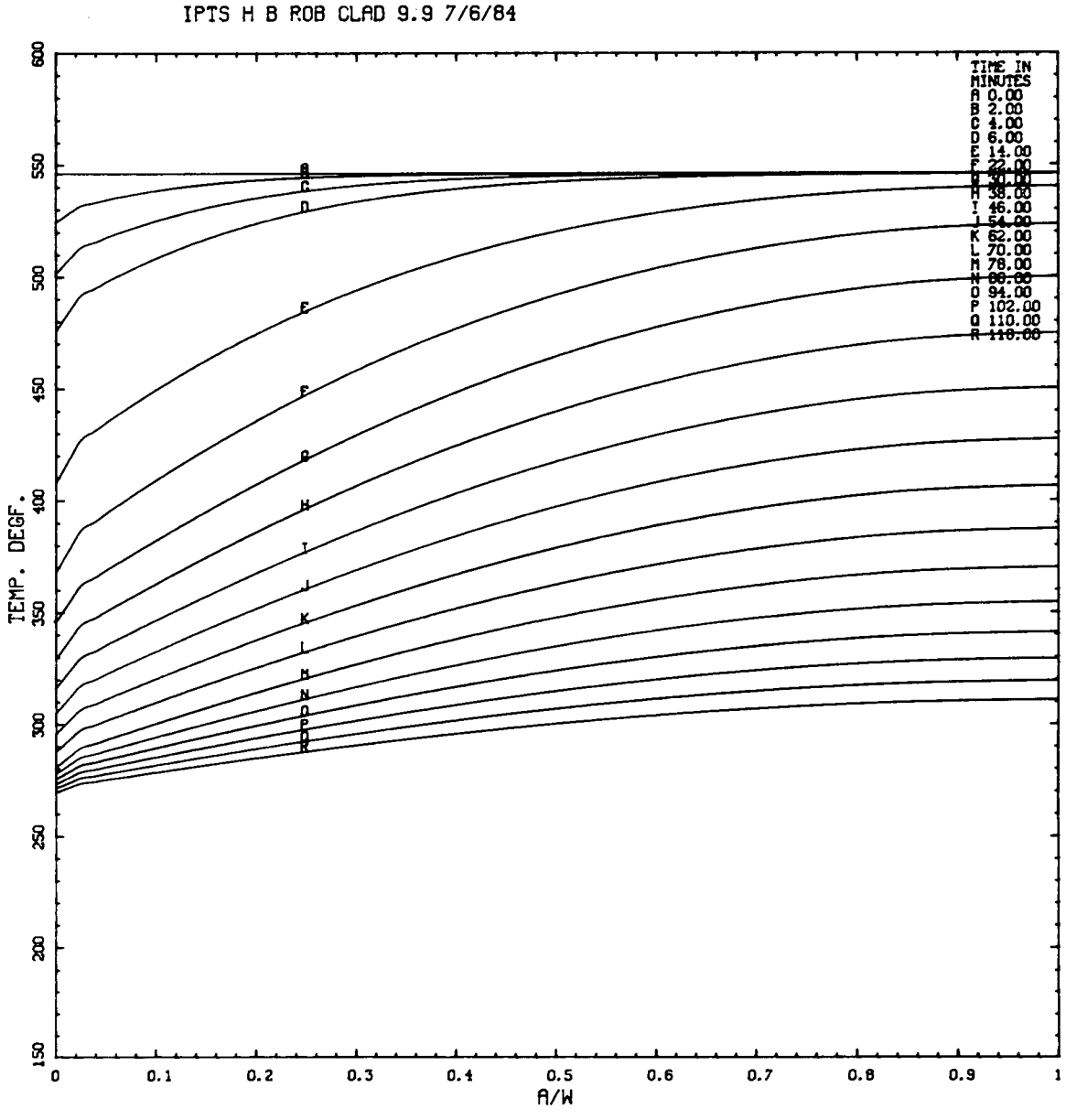

Figure I.117. Transient 9.9B: Vessel wall temperature vs depth in wall (a/w) at various times (t) in transient.

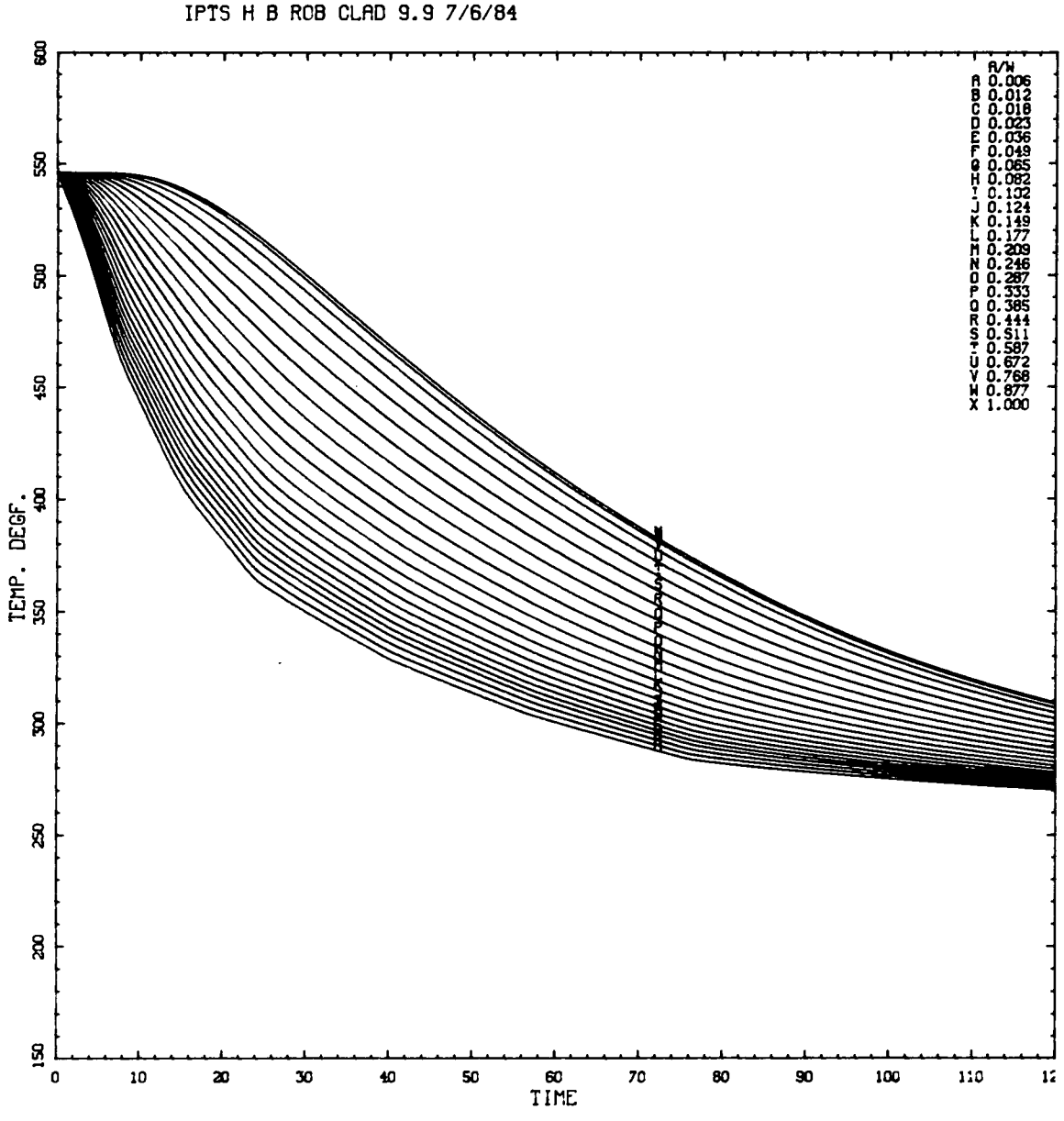

Figure I.118. Transient 9.9B: Vessel wall temperature vs time (t) in transient at various depths in wall (a/w).

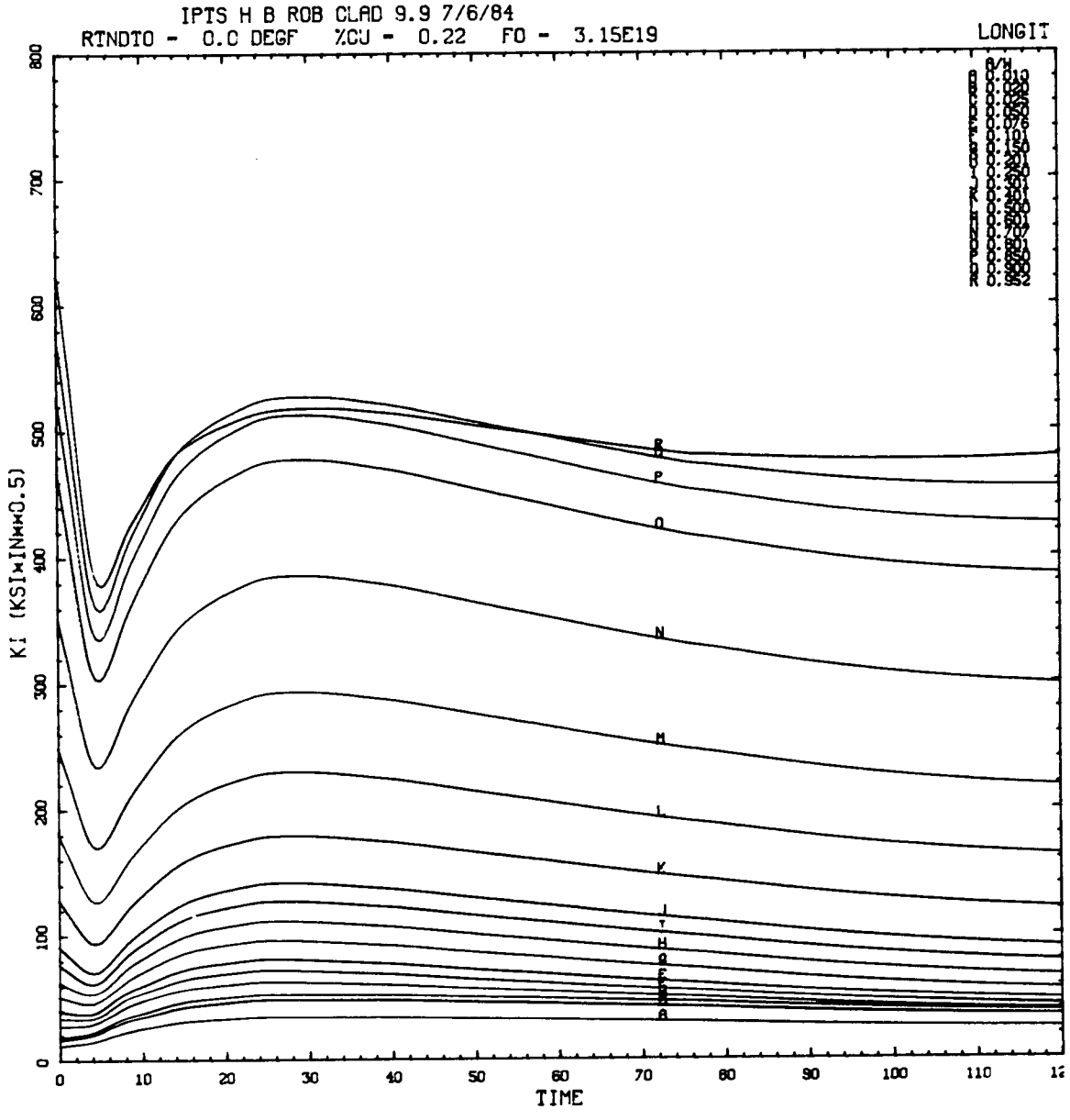

Figure I.119. Transient 9.9B: K_I vs time (t) for various depths in wall (a/w).

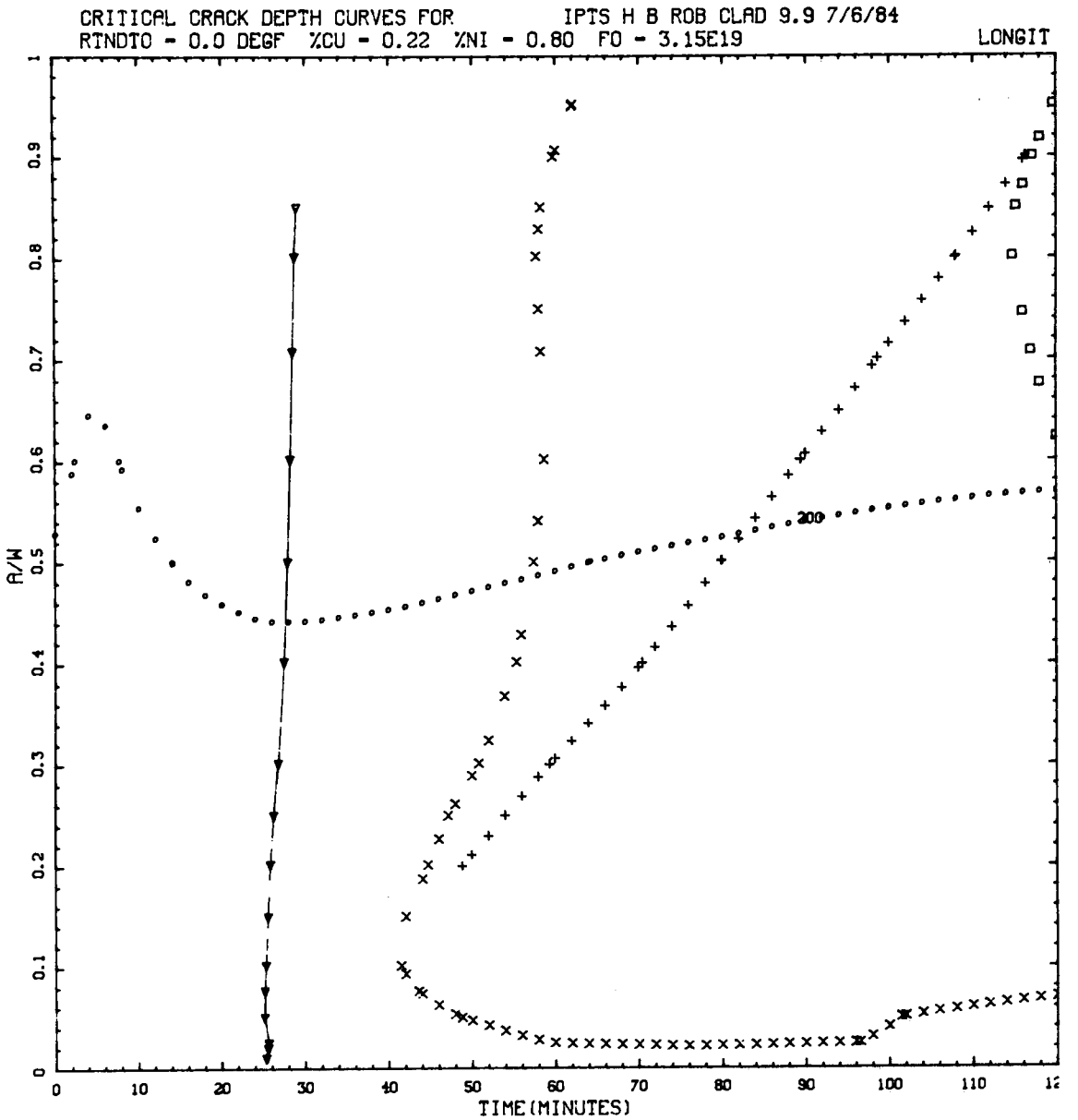

×, 2-D flaw, $K_I = K_{Ia}$
+, 2-m flaw, $K_I = K_{Ia}$
□, 2-D flaw, $K_I = K_{Ic}$
○, 2-D flaw, $K_I = 220$ MPa $\sqrt{m}$
∇, WPS (warm prestressing)

Figure I.120. Transient 9.9B: Critical-crack-depth curves for weld 2-273A based on -2σ values of K_{Ic}, K_{Ia}, and $\Delta RTNDT$, mean values of all other parameters, and 32-EFPY fluences.

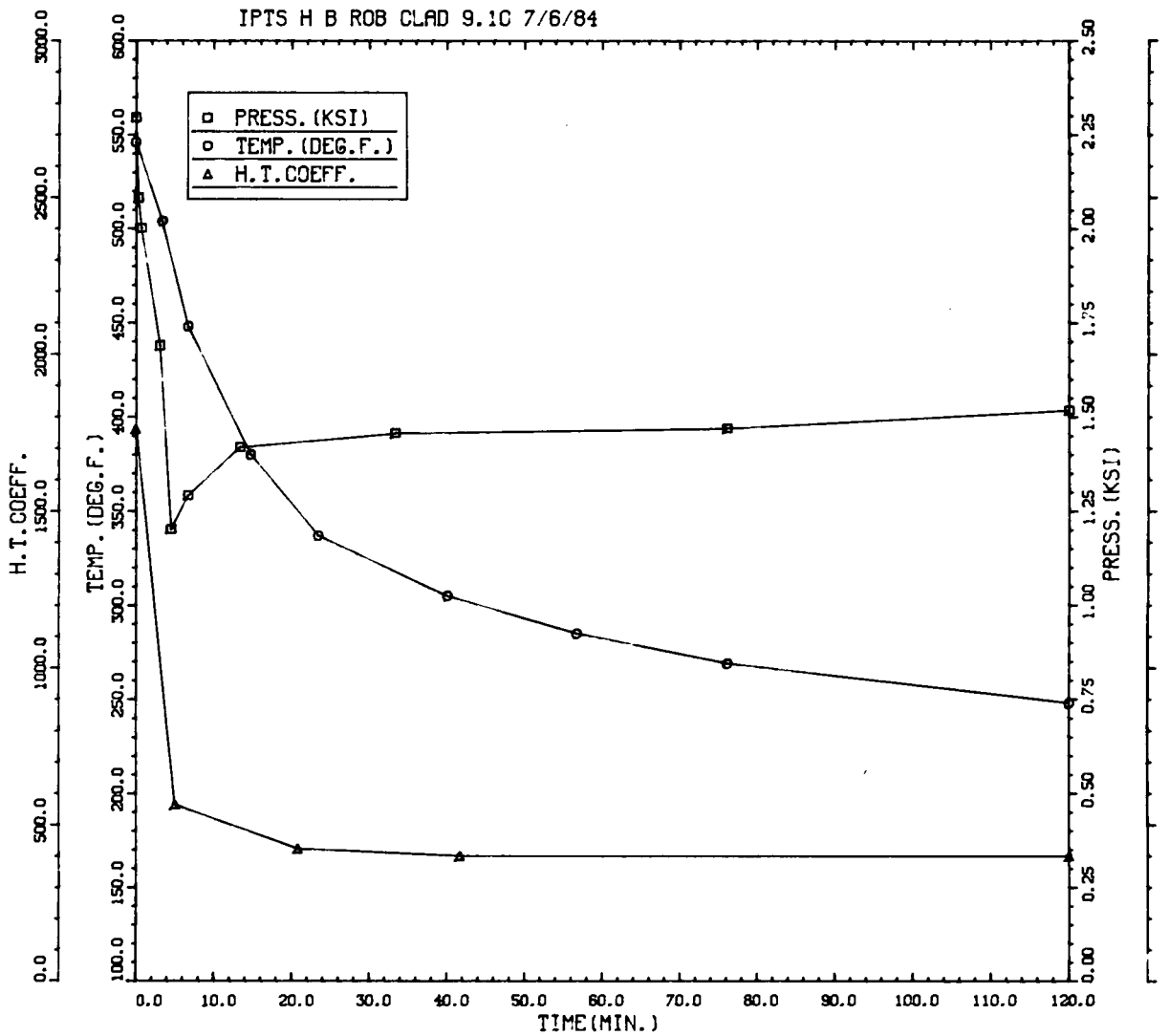

Figure I.121. Transient 9.10B: Primary system pressure, downcomer coolant temperature, and fluid-film heat-transfer coefficient vs time in the transient.

Table I.21. Transient 9.10B: Summary of digital output, including unadjusted $P(F|E)$ values and histogram data for crack depths, times of failure, and $T - RTNDT$ values at tip of crack corresponding to initiation and arrest events

IPTS H B ROB CLAD 9.10 7/6/84 1. FLAWS/IN**3 DRTN(IS) = 211.2

	UNADJUSTED					ADJUSTED			
WELD	P(F/E)	95%CI	%ERR	P(INITIA)	N*V	P(F/E)	%ERR	NFAIL	NTRIALS
1	2.81D-05	9.89D-06	35.20	5.35D-05	1.000	2.81D-05		31	200000
					VESSEL	2.81D-05	35.20		

DEPTHS FOR INITIAL INITIATION (IN)

	0.09	0.26	0.46	0.67	0.90	1.16	1.44	1.74	2.08
NUMBER	0	34	11	13	1	0	0	0	0
PERCENT	0.0	57.6	18.6	22.0	1.7	0.0	0.0	0.0	0.0

TIMES OF FAILURE(MINUTES)

	0.0	10.0	20.0	30.0	40.0	50.0	60.0	70.0	80.0	90.0	100.0	110.0	120.0
PERCENT	0.0	0.0	0.0	0.0	0.0	6.5	3.2	9.7	9.7	16.1	25.8	29.0	

INITIATION T-RTNDT(DEG.F)

	-100.0	-75.0	-50.0	-25.0	0.0	25.0	50.0	75.0	100.0	125.0	150.0	175.0	200.0
NUMBER	0	0	3	36	18	13	9	6	0	0	0	0	
PERCENT	0.0	0.0	3.5	42.4	21.2	15.3	10.6	7.1	0.0	0.0	0.0	0.0	

ARREST T-RTNDT(DEG.F)

	-50.0	-25.0	0.0	25.0	50.0	75.0	100.0	125.0	150.0	175.0	200.0	225.0	250.0
NUMBER	0	3	10	2	0	0	2	29	8	0	0	0	
PERCENT	0.0	5.6	18.5	3.7	0.0	0.0	3.7	53.7	14.8	0.0	0.0	0.0	

ICRKTP = 2 IACCEL = 1 NDLRS = 0 NRTRS = 0 DATE: 10/31/84 TIME: 22.39.48

CPU TIME: 5 MIN 27 SEC

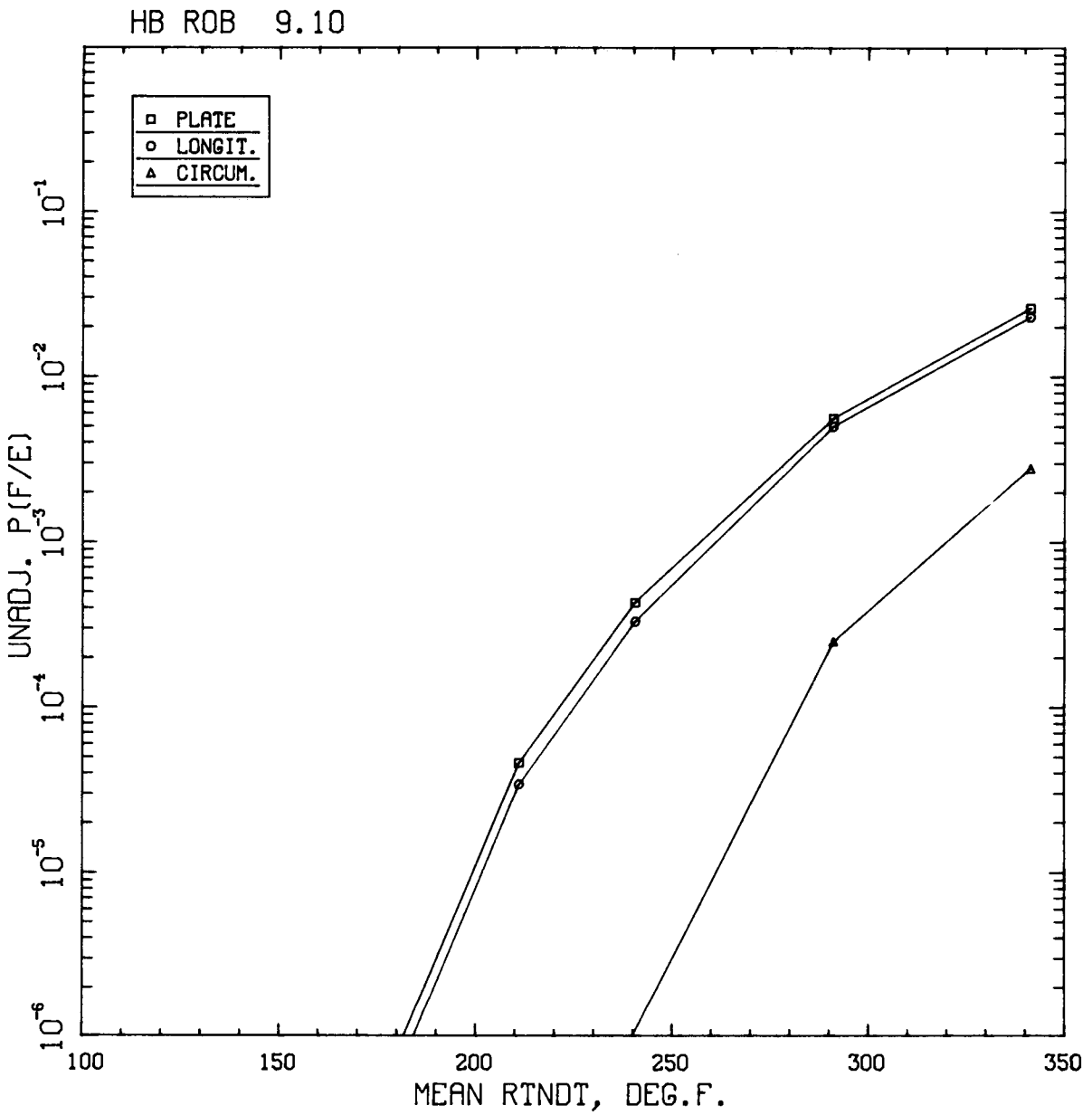

Figure I.122. Transient 9.10B: $\hat{P}_j \int_0^w f(a)\, B(a)\, da$ vs $\overline{RTNDT_s}$ for (2-D, 2-D) and (2-D, 2m) flaw combinations.

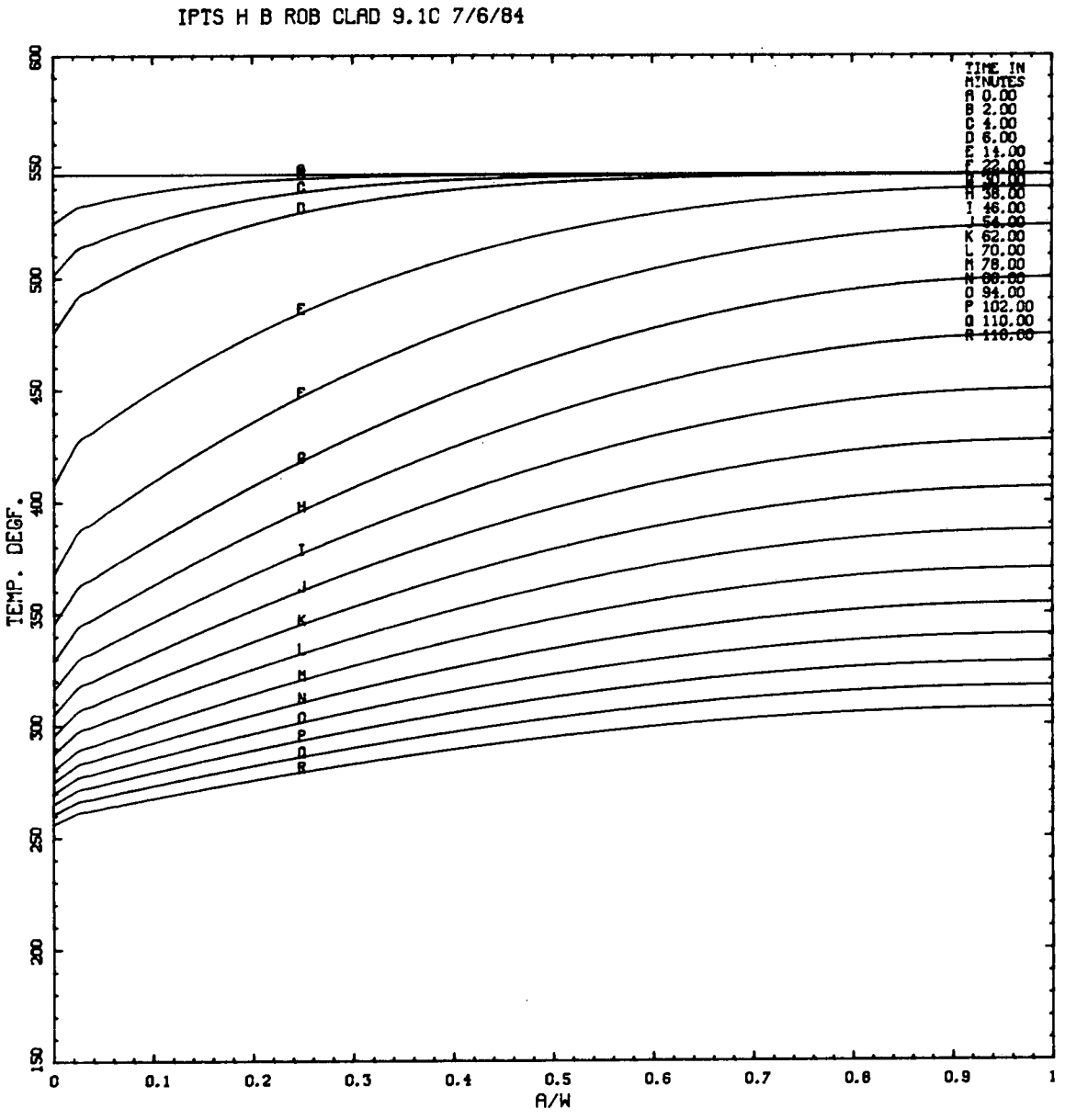

Figure I.123. Transient 9.10B: Vessel wall temperature vs depth in wall (a/w) at various times (t) in transient.

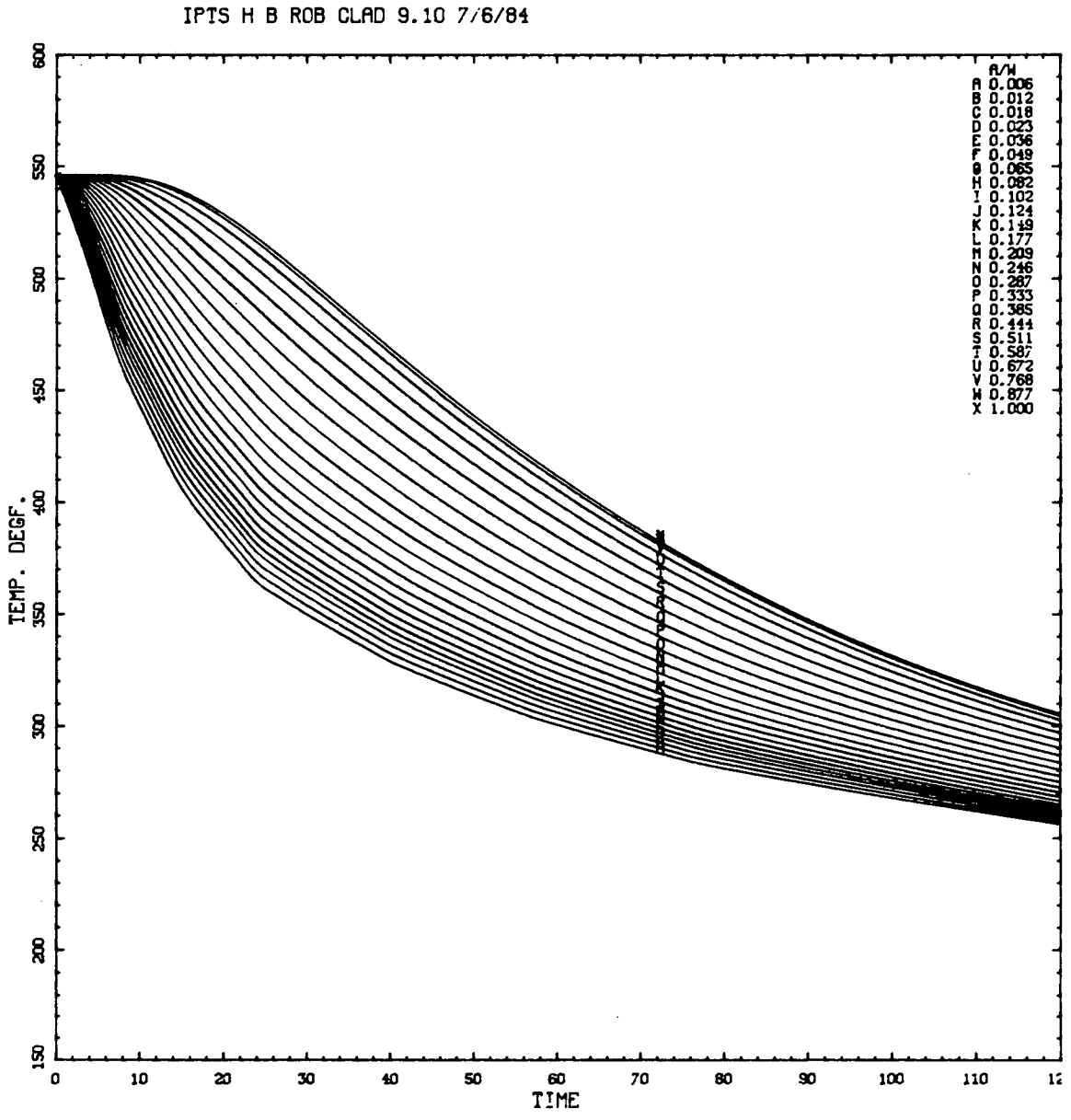

Figure I.124. Transient 9.10B: Vessel wall temperature vs time (t) in transient at various depths in wall (a/w).

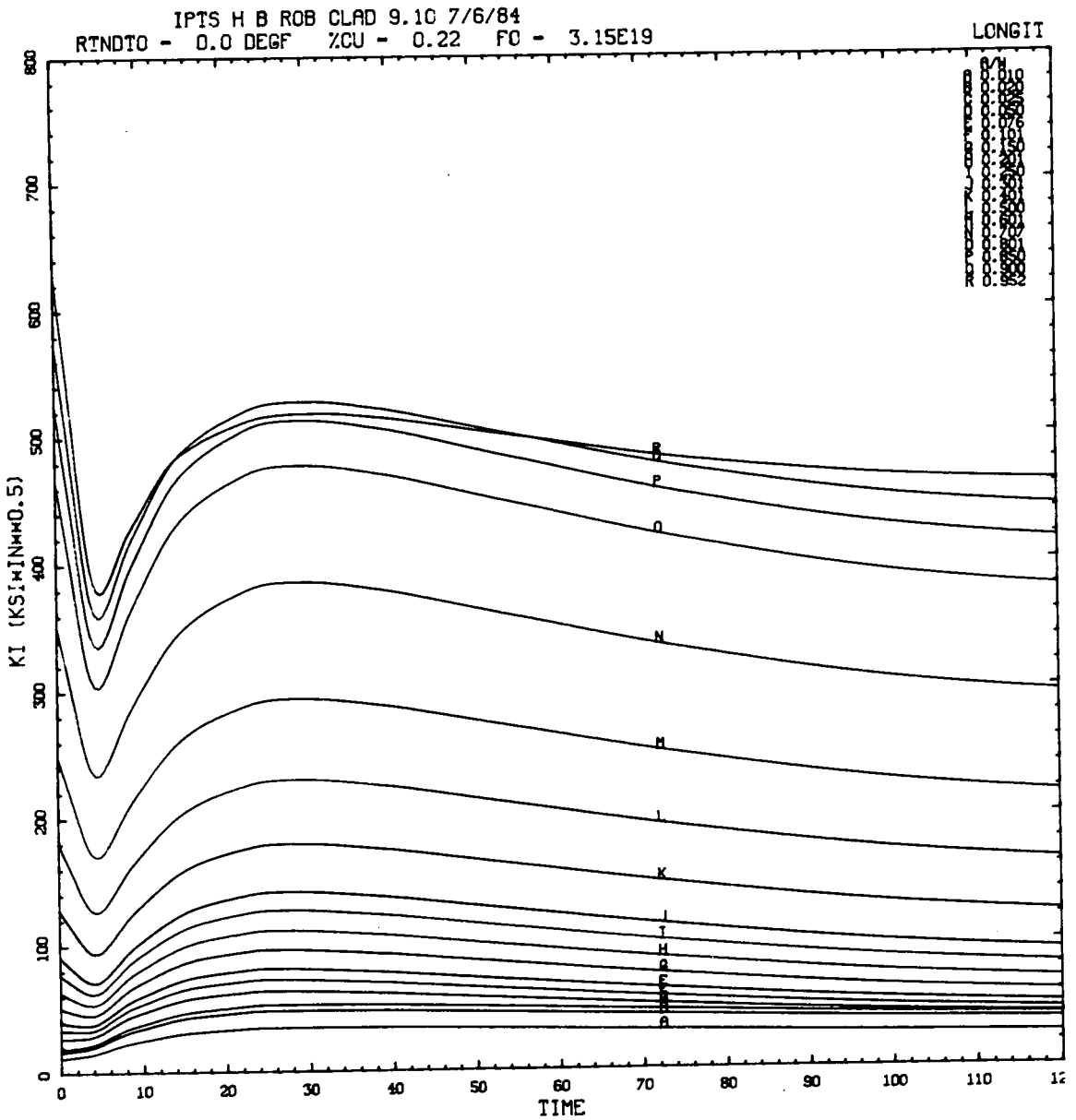

Figure I.125. Transient 9.10B: K_I vs time (t) for various depths in wall (a/w).

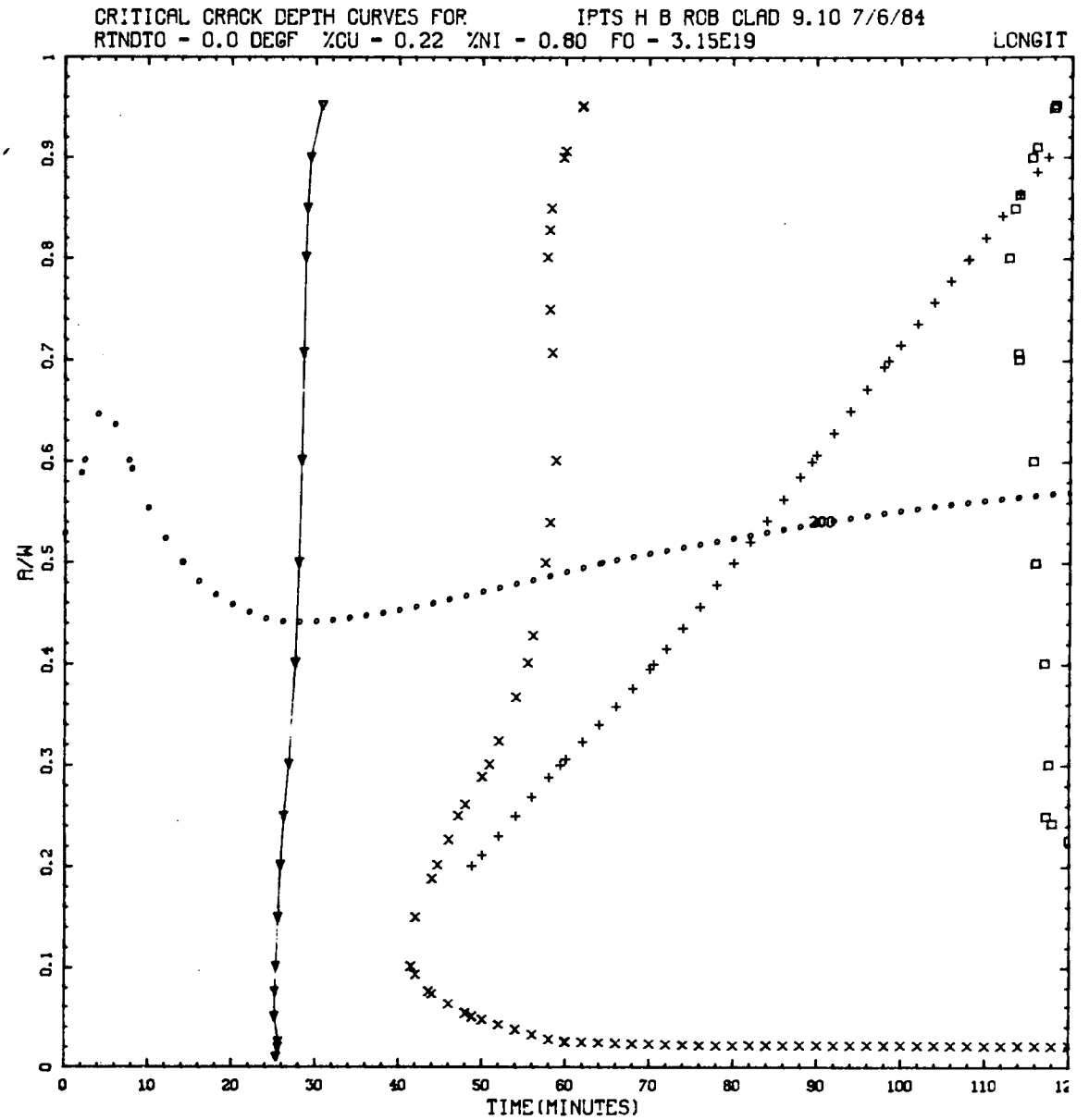

×, 2-D flaw, $K_I = K_{Ia}$
+, 2-m flaw, $K_I = K_{Ia}$
□, 2-D flaw, $K_I = K_{Ic}$
○, 2-D flaw, $K_I = 220$ MPa $\sqrt{m}$
∇, WPS (warm prestressing)

Figure I.126. Transient 9.10B: Critical-crack-depth curves for weld 2-273A based on -2σ values of K_{Ic}, K_{Ia}, and $\Delta RTNDT$, mean values of all other parameters, and 32-EFPY fluences.

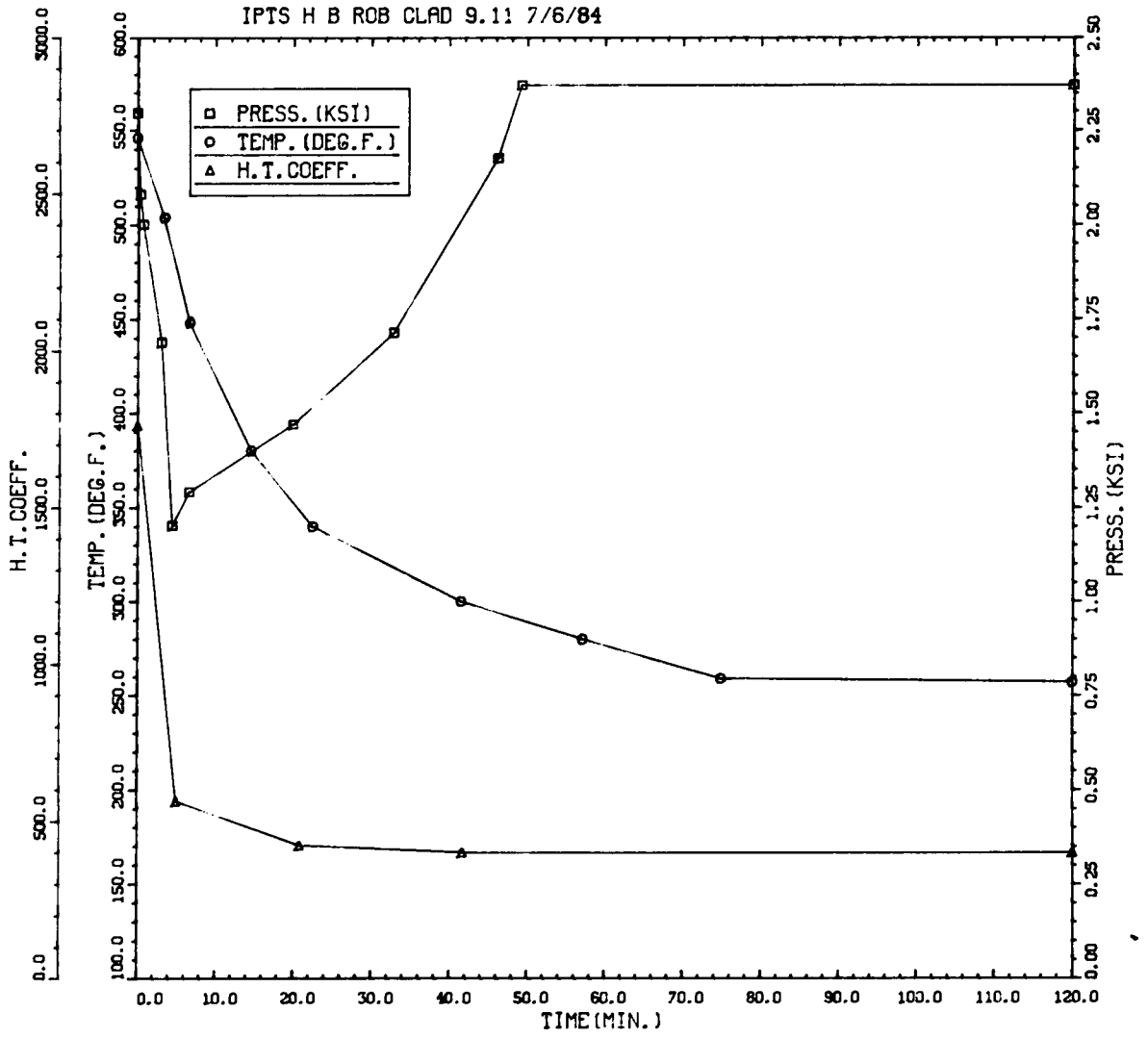

Figure I.127. Transient 9.11B: Primary system pressure, downcomer coolant temperature, and fluid-film heat-transfer coefficient vs time in the transient.

Table I.22. Transient 9.11B: Summary of digital output, including unadjusted $P(F|E)$ values and histogram data for crack depths, times of failure, and $T - RTNDT$ values at tip of crack corresponding to initiation and arrest events

IPTS H B ROB CLAD 9.11 7/6/84 1. FLAWS/IN**3 DRTN(IS) = 211.2

	UNADJUSTED					ADJUSTED			
WELD	P(F/E)	95%CI	%ERR	P(INITIA)	N*V	P(F/E)	%ERR	NFAIL	NTRIALS
1	7.88D-04	7.79D-05	9.89	8.24D-04	1.000	7.88D-04		391	90000
					VESSEL	7.88D-04	9.89		

DEPTHS FOR INITIAL INITIATION (IN)

	0.09	0.26	0.46	0.67	0.90	1.16	1.44	1.74	2.08
NUMBER	0	201	138	51	18	1	0	0	0
PERCENT	0.0	49.1	33.7	12.5	4.4	0.2	0.0	0.0	0.0

TIMES OF FAILURE(MINUTES)

	0.0	10.0	20.0	30.0	40.0	50.0	60.0	70.0	80.0	90.0	100.0	110.0	120.0
PERCENT	0.0	0.0	0.0	0.0	5.4	16.9	30.7	42.5	2.8	0.3	0.8	0.8	

INITIATION T-RTNDT(DEG.F)

	-100.0	-75.0	-50.0	-25.0	0.0	25.0	50.0	75.0	100.0	125.0	150.0	175.0	200.0
NUMBER	0	2	37	137	183	48	16	17	0	0	0	0	
PERCENT	0.0	0.5	8.4	31.1	41.6	10.9	3.6	3.9	0.0	0.0	0.0	0.0	

ARREST T-RTNDT(DEG.F)

	-50.0	-25.0	0.0	25.0	50.0	75.0	100.0	125.0	150.0	175.0	200.0	225.0	250.0
NUMBER	0	0	2	2	1	0	0	14	30	0	0	0	
PERCENT	0.0	0.0	4.1	4.1	2.0	0.0	0.0	28.6	61.2	0.0	0.0	0.0	

ICRKTP = 2 IACCEL = 1 NDLRS = 0 NRTRS = 0 DATE: 10/31/84 TIME: 01.21.48

CPU TIME: 2 MIN 34 SEC

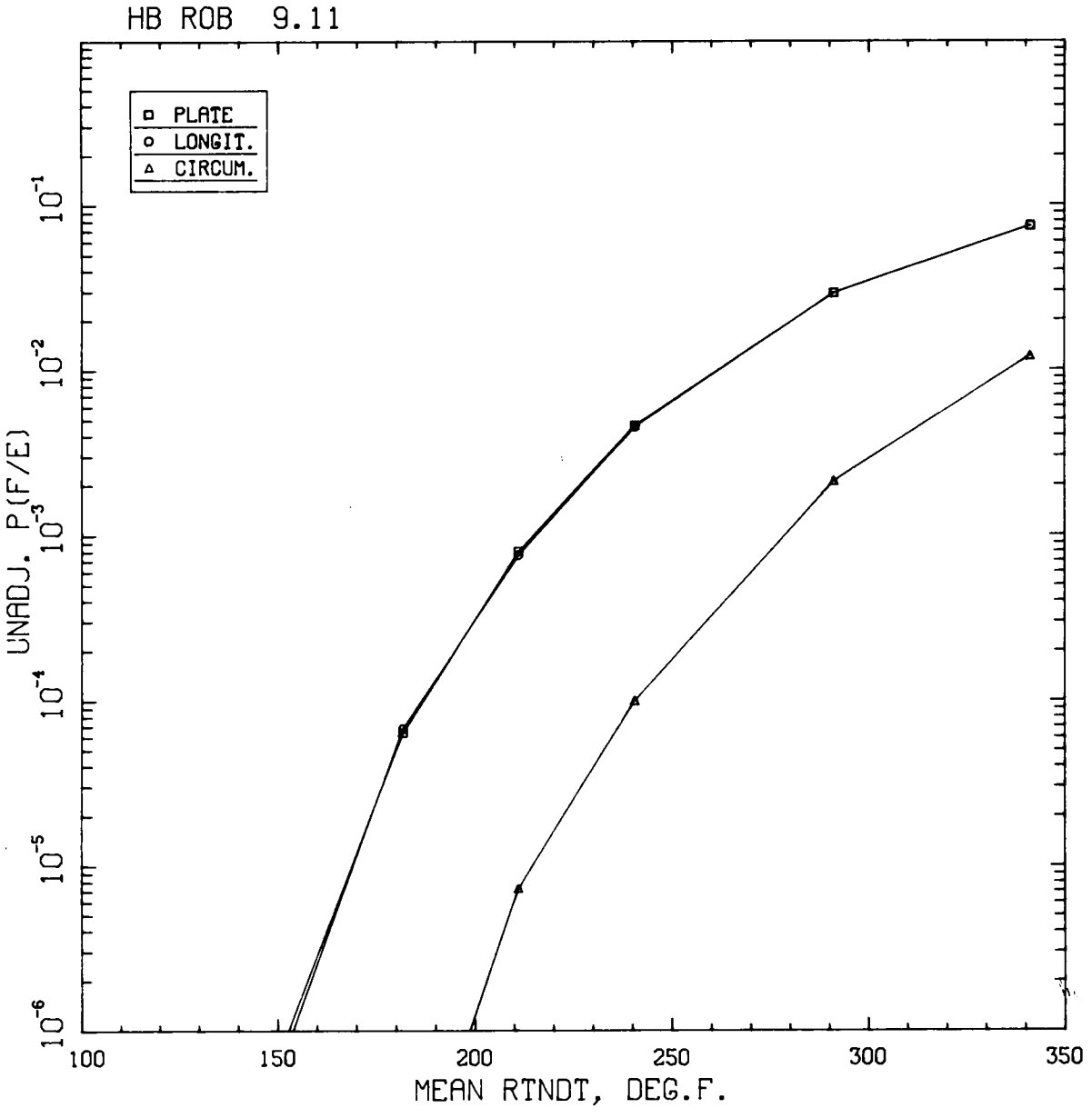

Figure I.128. Transient 9.11B: $\hat{P}_j \int_0^w f(a)\, B(a)\, da$ vs $\overline{RTNDT_s}$ for (2-D, 2-D) and (2-D, 2m) flaw combinations.

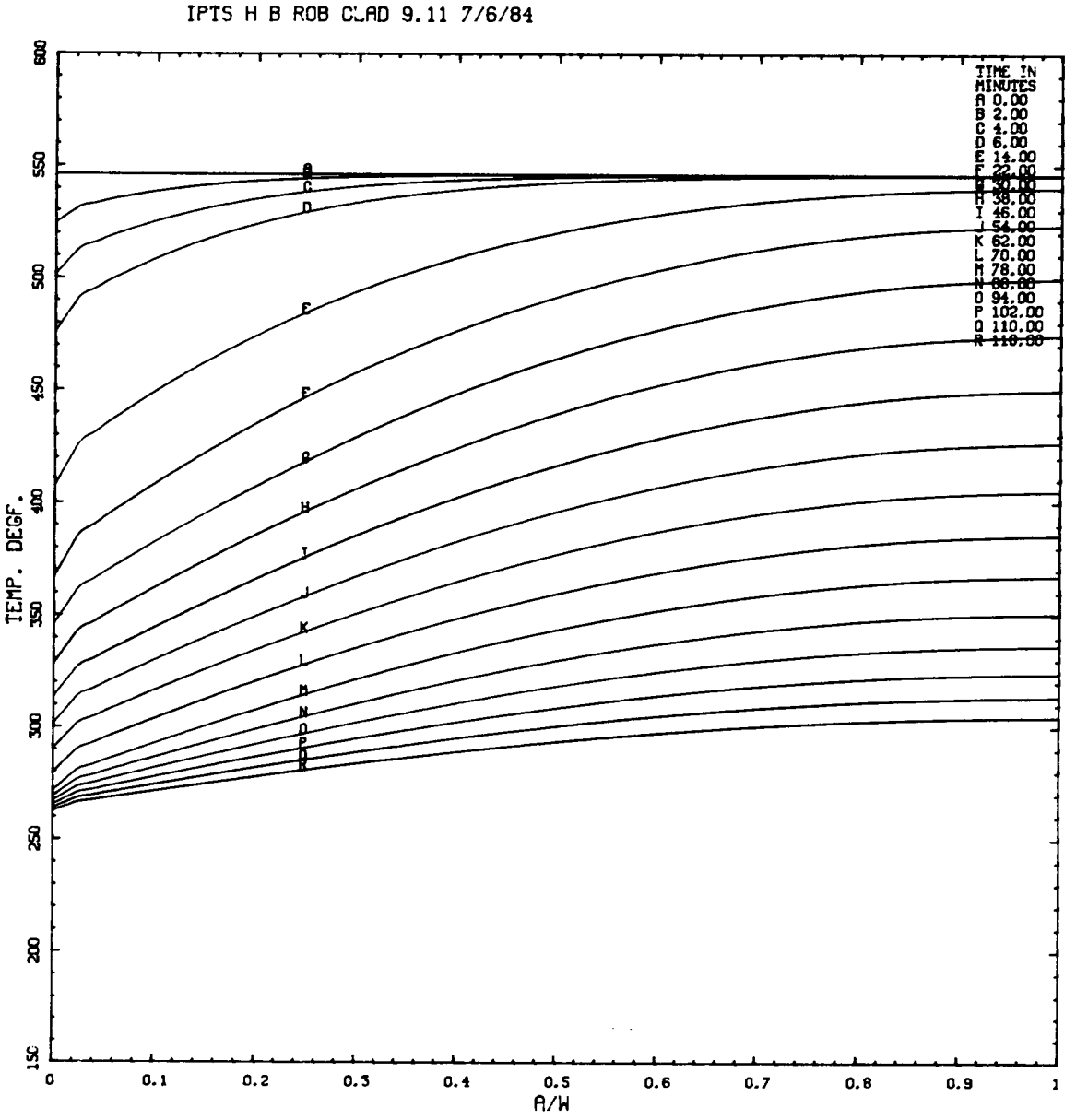

Figure I.129. Transient 9.11B: Vessel wall temperature vs depth in wall (a/w) at various times (t) in transient.

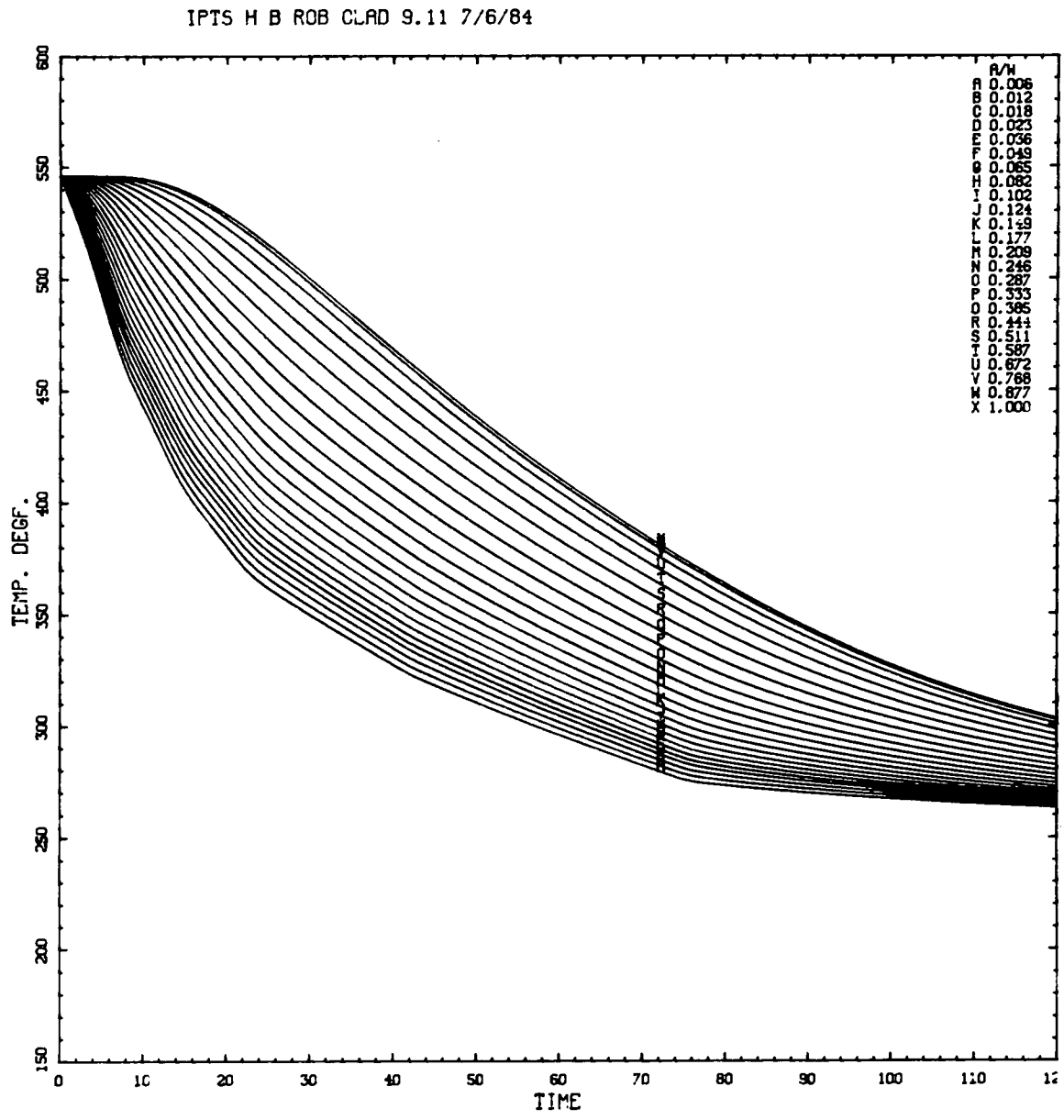

Figure I.130. Transient 9.11B: Vessel wall temperature vs time (t) in transient at various depths in wall (a/w).

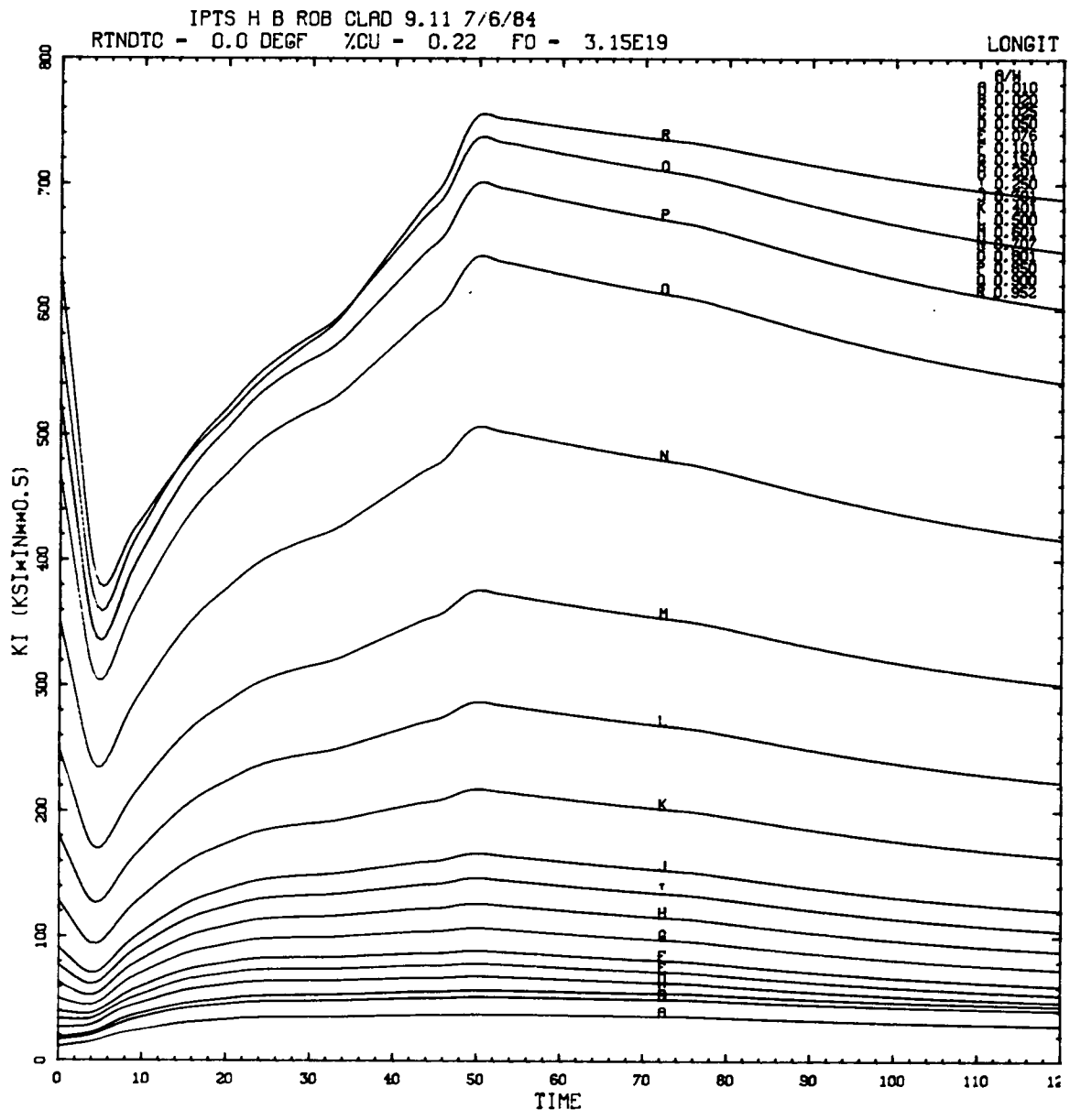

Figure I.131. Transient 9.11B: K_I vs time (t) for various depths in wall (a/w).

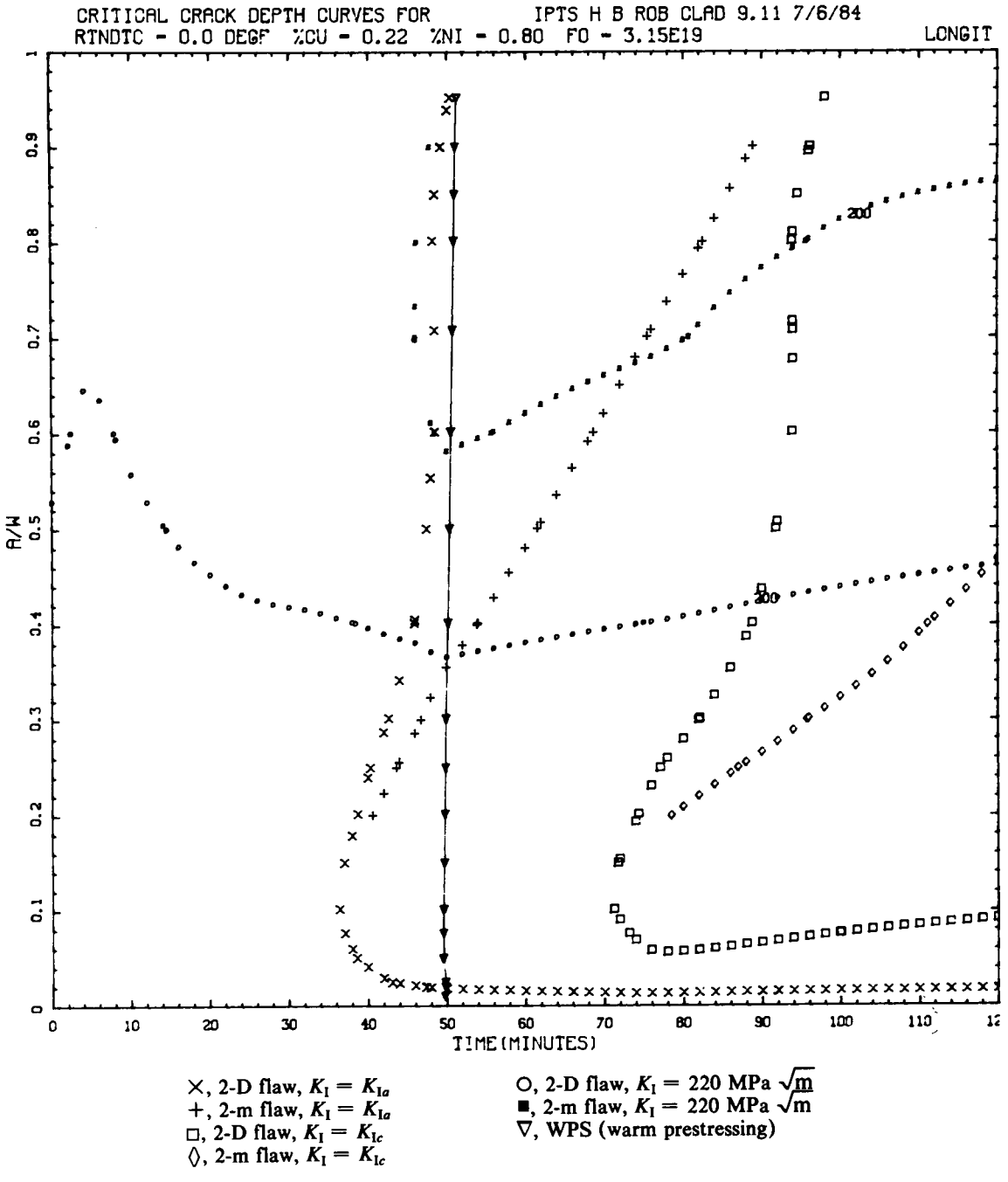

Figure I.132. Transient 9.11B: Critical-crack-depth curves for weld 2-273A based on -2σ values of K_{Ic}, K_{Ia}, and $\Delta RTNDT$, mean values of all other parameters, and 32-EFPY fluences.

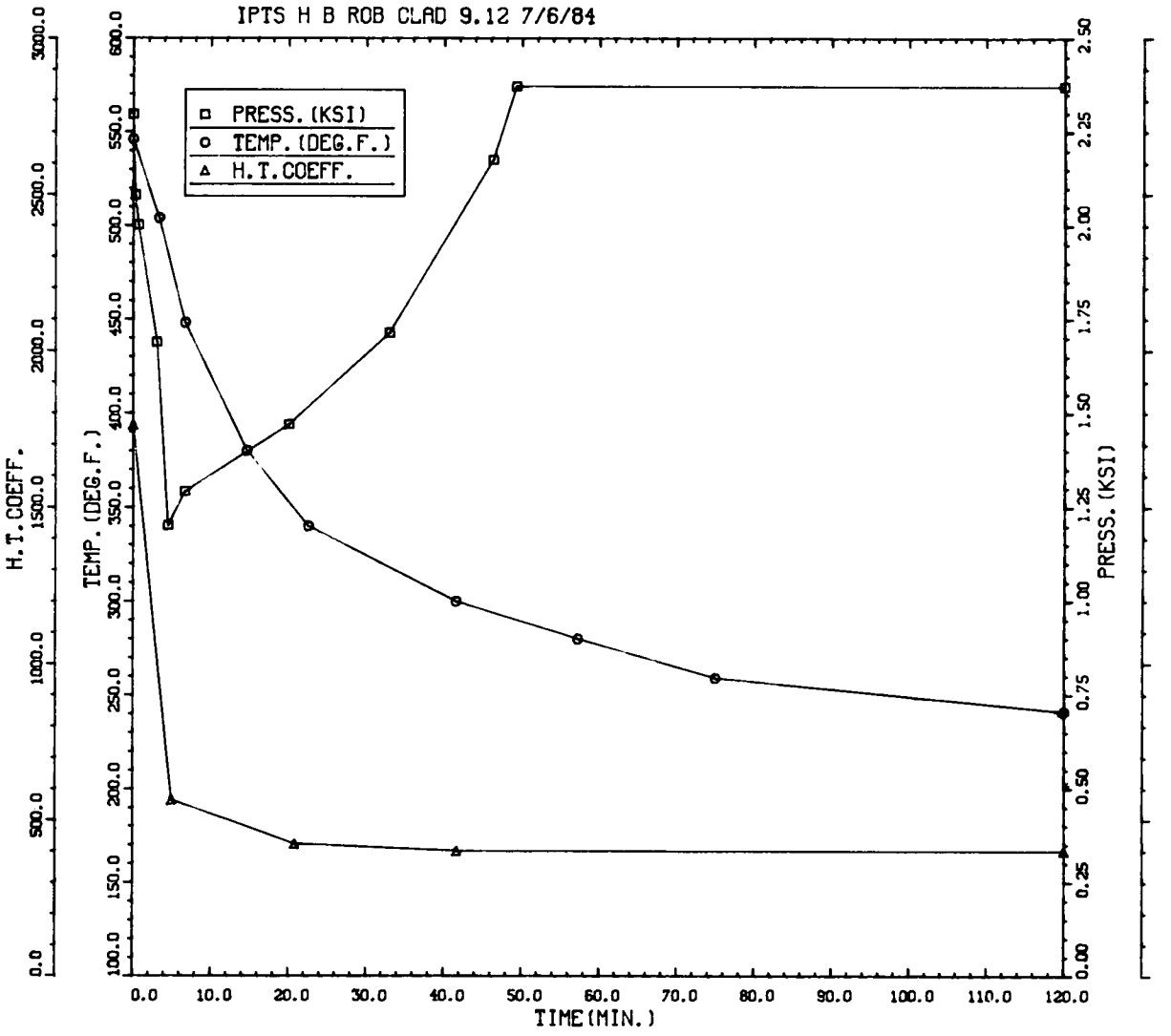

Figure I.133. Transient 9.12B: Primary system pressure, downcomer coolant temperature, and fluid-film heat-transfer coefficient vs time in the transient.

Table I.23. Transient 9.12B: Summary of digital output, including unadjusted $P(F|E)$ values and histogram data for crack depths, times of failure, and $T - RTNDT$ values at tip of crack corresponding to initiation and arrest events

IPTS H B ROB CLAD 9.12 7/6/84 1. FLAWS/IN**3 DRTN(IS) = 211.2

	----------UNADJUSTED----------					---ADJUSTED----			
ELD	P(F/E)	95%CI	%ERR	P(INITIA)	N*V	P(F/E)	%ERR	NFAIL	NTRIALS
1	9.92D-04	9.91D-05	9.99	1.04D-03	1.000	9.92D-04		383	70000
					VESSEL	9.92D-04	9.99		

DEPTHS FOR INITIAL INITIATION (IN)

	0.09	0.26	0.46	0.67	0.90	1.16	1.44	1.74	2.08
NUMBER	0	196	124	53	23	4	0	0	0
PERCENT	0.0	49.0	31.0	13.3	5.8	1.0	0.0	0.0	0.0

TIMES OF FAILURE(MINUTES)

	0.0	10.0	20.0	30.0	40.0	50.0	60.0	70.0	80.0	90.0	100.0	110.0	120.0
PERCENT	0.0	0.0	0.0	0.0	4.4	14.1	23.0	36.3	6.5	3.7	4.4	7.6	

INITIATION T-RTNDT(DEG.F)

	-100.0	-75.0	-50.0	-25.0	0.0	25.0	50.0	75.0	100.0	125.0	150.0	175.0	200.0
NUMBER	0	3	32	137	192	35	17	12	0	0	0	0	
PERCENT	0.0	0.7	7.5	32.0	44.9	8.2	4.0	2.8	0.0	0.0	0.0	0.0	

ARREST T-RTNDT(DEG.F)

	-50.0	-25.0	0.0	25.0	50.0	75.0	100.0	125.0	150.0	175.0	200.0	225.0	250.0
NUMBER	0	0	7	4	0	0	0	12	22	0	0	0	
PERCENT	0.0	0.0	15.6	8.9	0.0	0.0	0.0	26.7	48.9	0.0	0.0	0.0	

ICRKTP = 2 IACCEL = 1 NDLRS = 0 NRTRS = 0 DATE: 10/31/84 TIME: 01.22.53

CPU TIME: 2 MIN 2 SEC

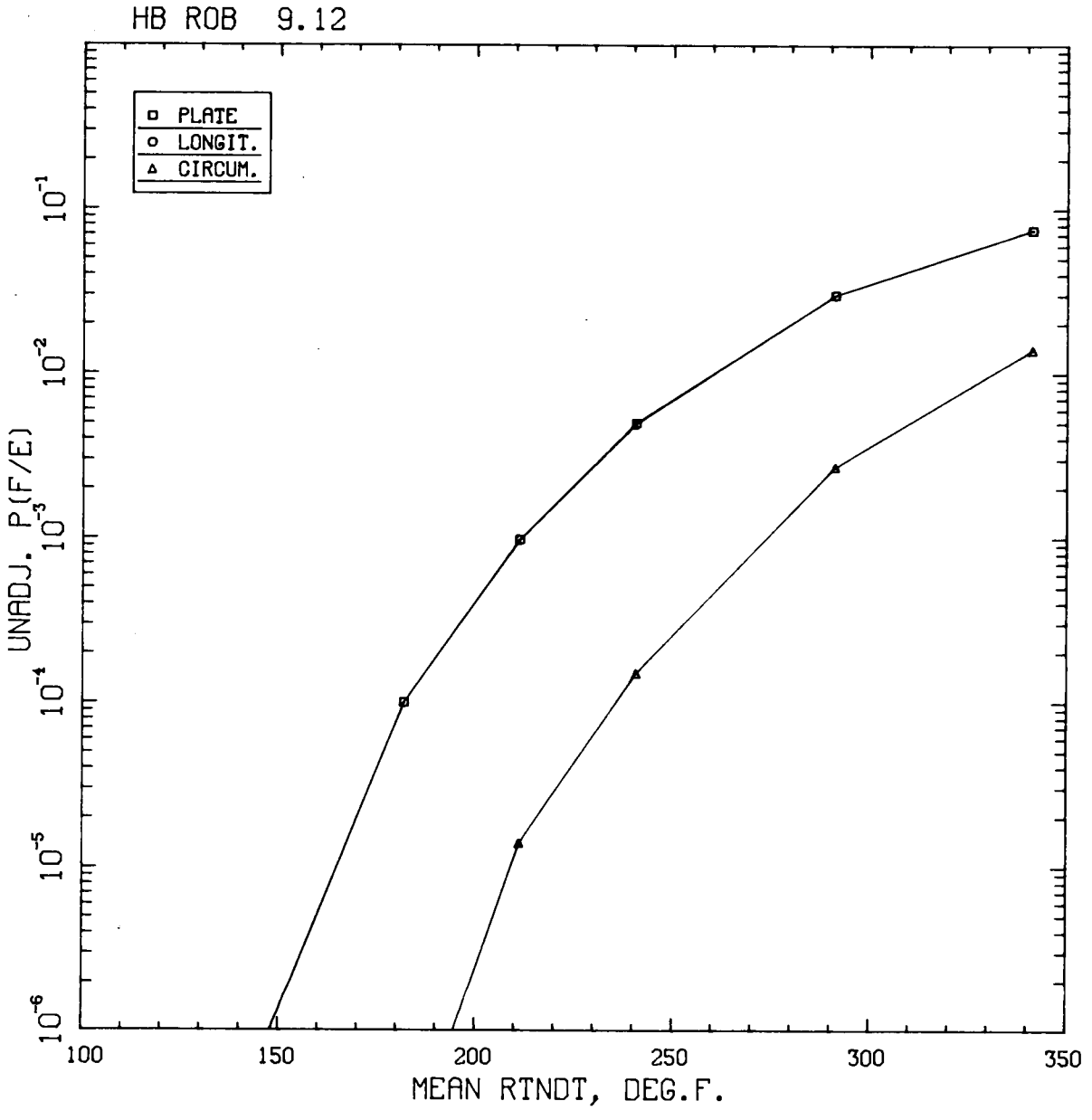

Figure I.134. Transient 9.12B: $\hat{P}_j \int_0^{\infty} f(a)\, B(a)\, da$ vs $\overline{RTNDT_s}$ for (2-D, 2-D) and (2-D, 2m) flaw combinations.

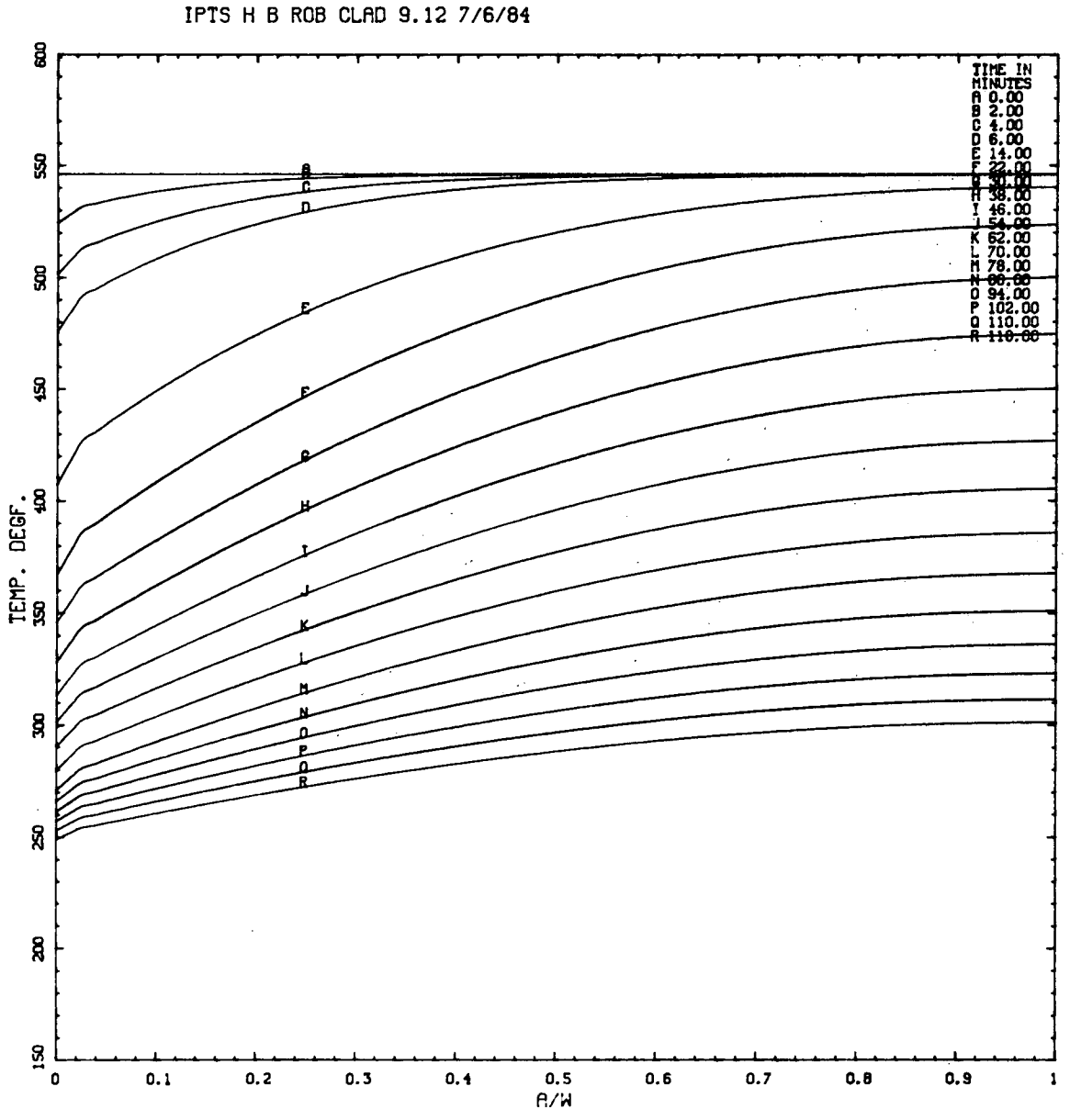

Figure I.135. Transient 9.12B: Vessel wall temperature vs depth in wall (a/w) at various times (t) in transient.

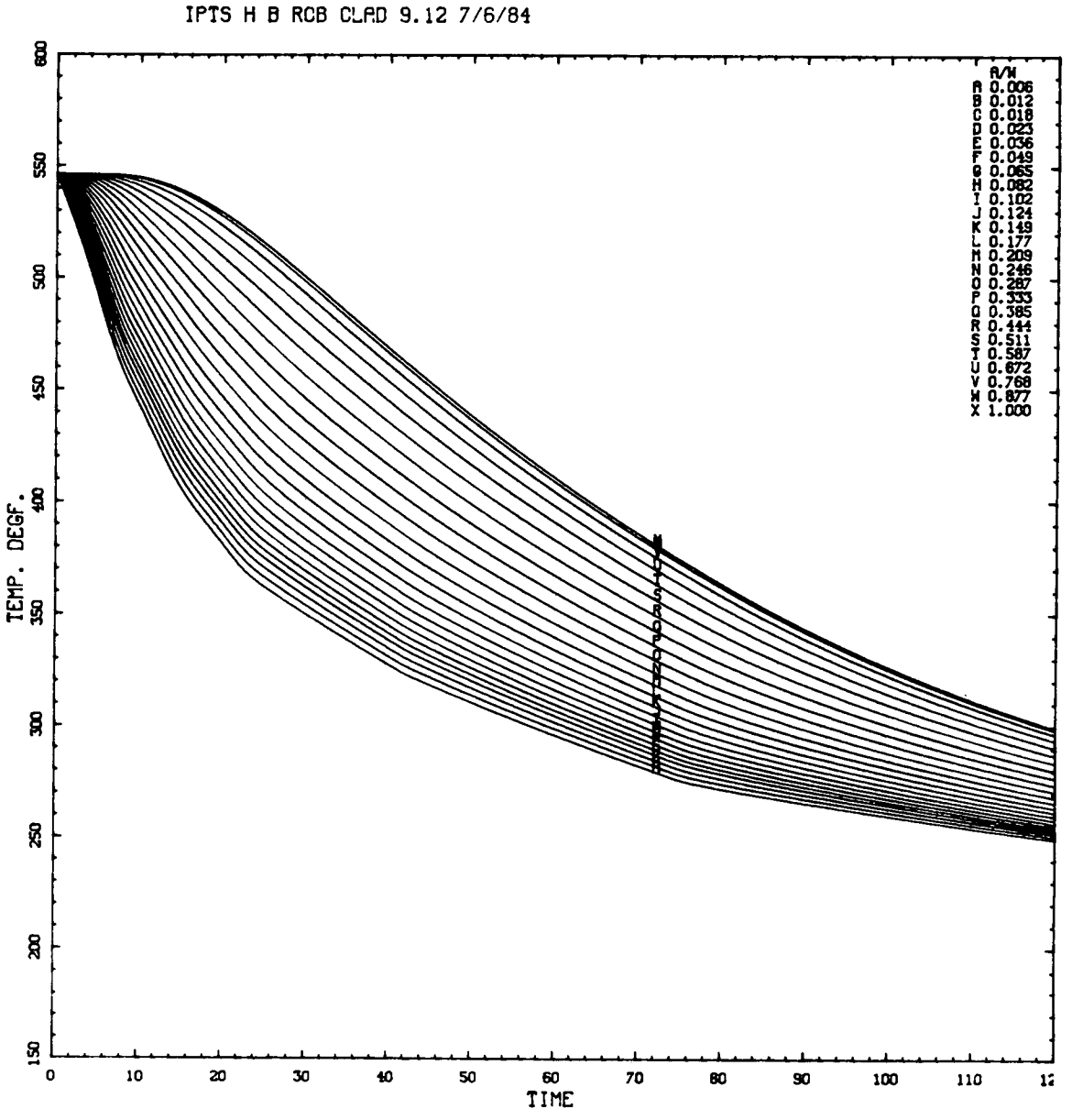

Figure I.136. Transient 9.12B: Vessel wall temperature vs time (t) in transient at various depths in wall (a/w).

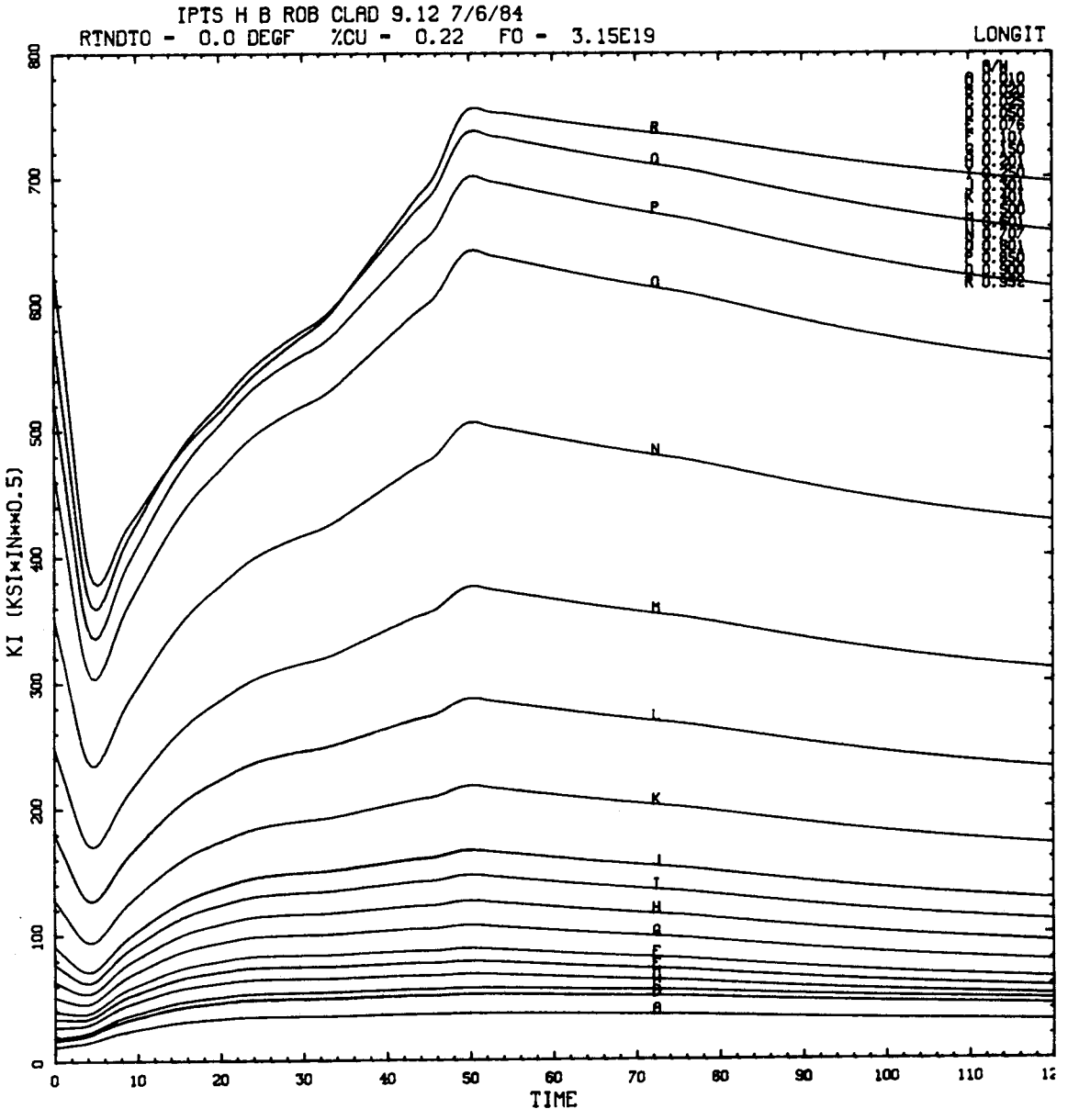

Figure I.137. Transient 9.12B: K_I vs time (t) for various depths in wall (a/w).

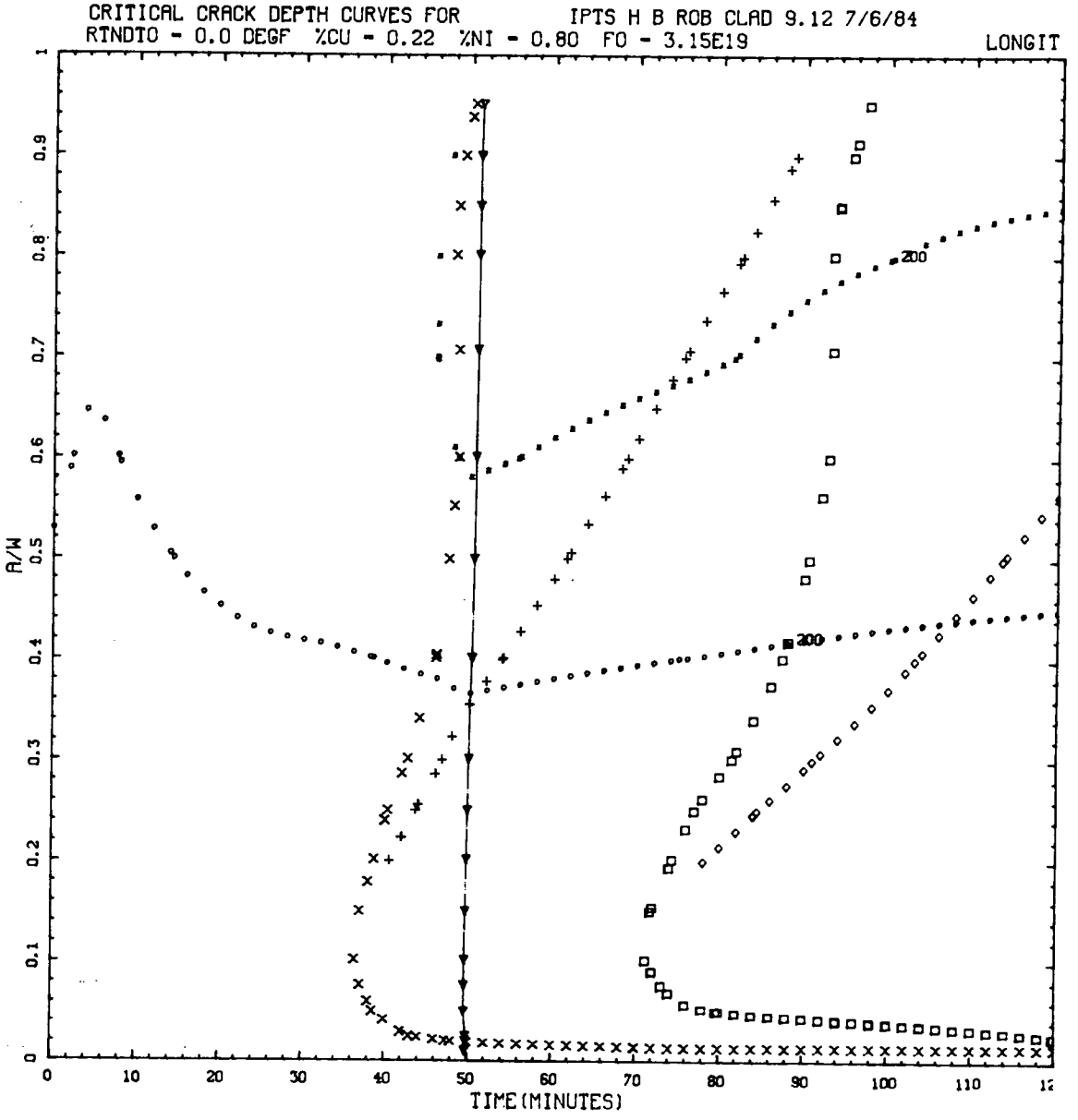

×, 2-D flaw, $K_I = K_{Ia}$
+, 2-m flaw, $K_I = K_{Ia}$
□, 2-D flaw, $K_I = K_{Ic}$
◊, 2-m flaw, $K_I = K_{Ic}$
○, 2-D flaw, $K_I = 220$ MPa $\sqrt{m}$
■, 2-m flaw, $K_I = 220$ MPa $\sqrt{m}$
∇, WPS (warm prestressing)

Figure I.138. Transient 9.12B: Critical-crack-depth curves for weld 2-273A based on -2σ values of K_{Ic}, K_{Ia}, and $\Delta RTNDT$, mean values of all other parameters, and 32-EFPY fluences.

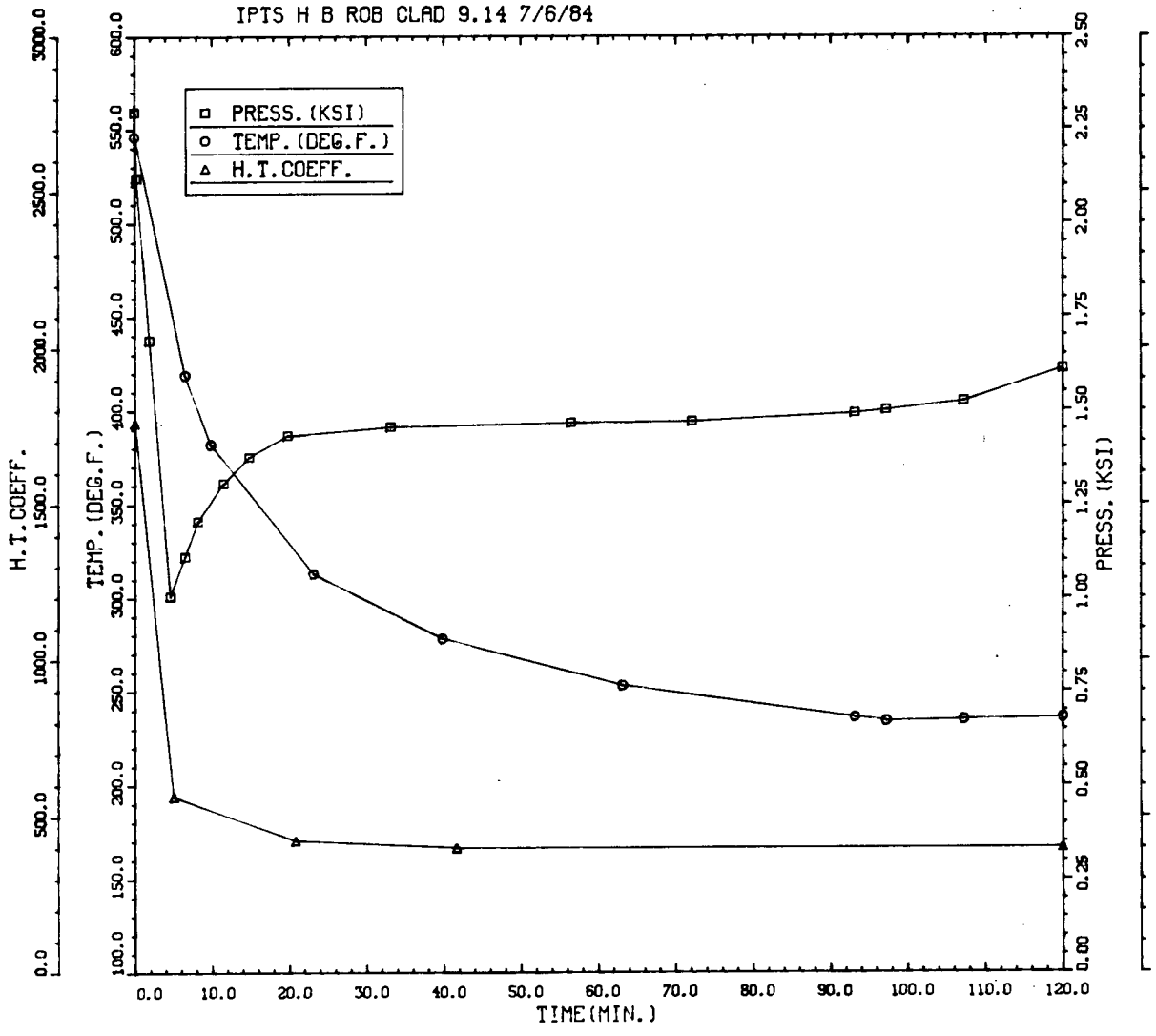

Figure I.139. Transient 9.14B: Primary system pressure, downcomer coolant temperature, and fluid-film heat-transfer coefficient vs time in the transient.

Table I.24. Transient 9.14B: Summary of digital output, including unadjusted $P(F|E)$, values and histogram data for crack depths, times of failure, and $T - RTNDT$ values at tip of crack corresponding to initiation and arrest events

IPTS H B ROB CLAD 9.14 7/6/84 1. FLAWS/IN**3 DRTN(IS) = 211

WELD	P(F/E)	95%CI	%ERR	P(INITIA)	N*V	P(F/E)	%ERR	NFAIL	NTRIA
	----------UNADJUSTED----------					---ADJUSTED----			
1	3.04D-04	3.25D-05	10.70	4.29D-04	1.000	3.04D-04		335	200000
					VESSEL	3.04D-04	10.70		

DEPTHS FOR INITIAL INITIATION (IN)

	0.09	0.26	0.46	0.67	0.90	1.16	1.44	1.74	2.08
NUMBER	0	255	129	59	21	8	1	0	0
PERCENT	0.0	53.9	27.3	12.5	4.4	1.7	0.2	0.0	0.0

TIMES OF FAILURE(MINUTES)

	0.0	10.0	20.0	30.0	40.0	50.0	60.0	70.0	80.0	90.0	100.0	110.0	120.
PERCENT	0.0	0.0	0.0	0.0	0.0	2.4	10.4	12.2	18.5	18.8	20.6	17.0	

INITIATION T-RTNDT(DEG.F)

	-100.0	-75.0	-50.0	-25.0	0.0	25.0	50.0	75.0	100.0	125.0	150.0	175.0	200.
NUMBER	0	0	37	194	224	148	151	26	0	0	0	0	
PERCENT	0.0	0.0	4.7	24.9	28.7	19.0	19.4	3.3	0.0	0.0	0.0	0.0	

ARREST T-RTNDT(DEG.F)

	-50.0	-25.0	0.0	25.0	50.0	75.0	100.0	125.0	150.0	175.0	200.0	225.0	25
NUMBER	0	8	38	11	1	0	17	261	109	0	0	0	
PERCENT	0.0	1.8	8.5	2.5	0.2	0.0	3.8	58.7	24.5	0.0	0.0	0.0	

ICRKTP = 2 IACCEL = 1 NDLRS = 0 NRTRS = 0 DATE: 10/31/84 TIME: 01.23.04

CPU TIME: 5 MIN 28 SEC

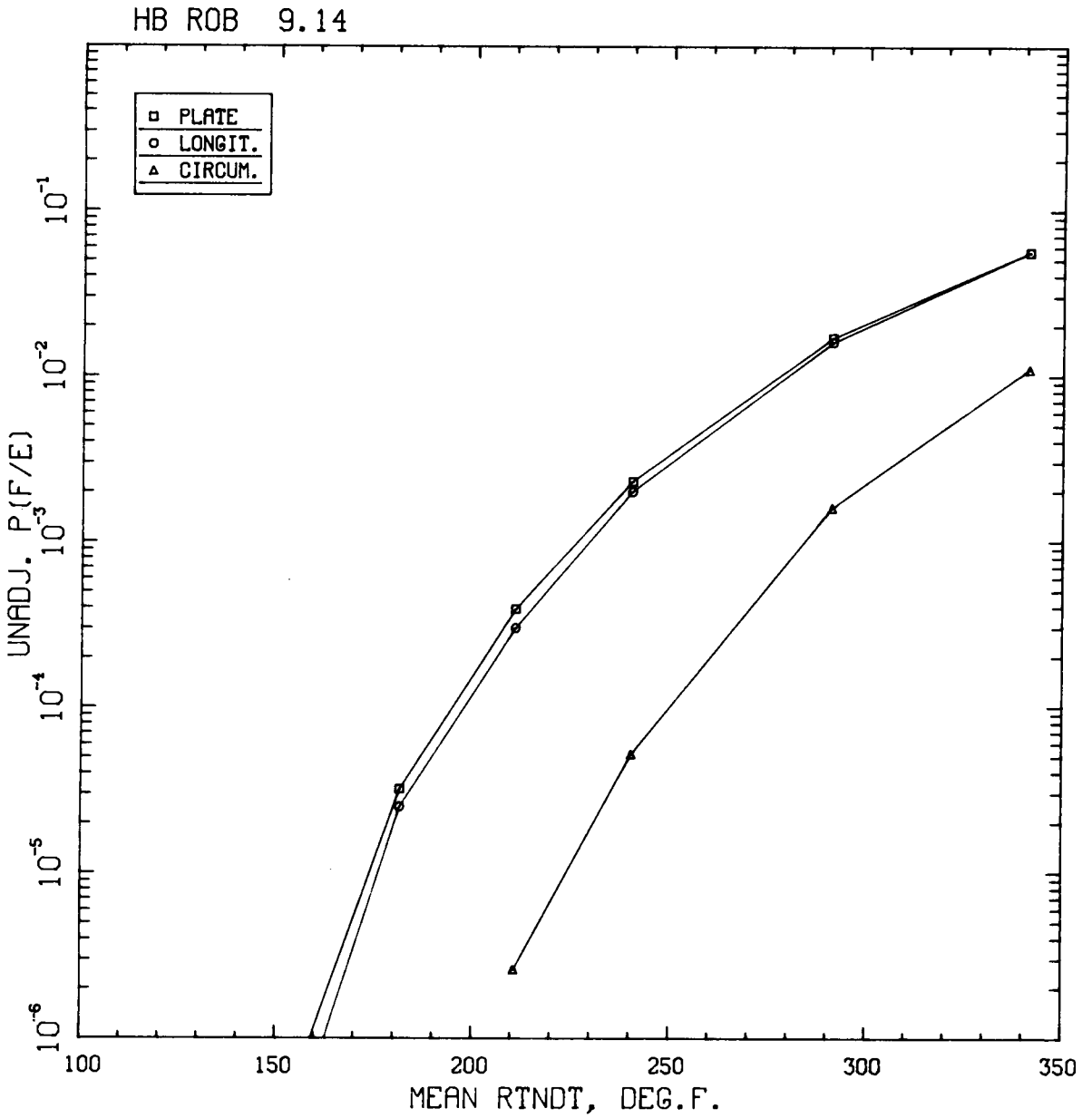

Figure I.140. Transient 9.14B: $\hat{P}_j \int_0^w f(a)\, B(a)\, da$ vs $\overline{RTNDT_s}$ for (2-D, 2-D) and (2-D, 2m) flaw combinations.

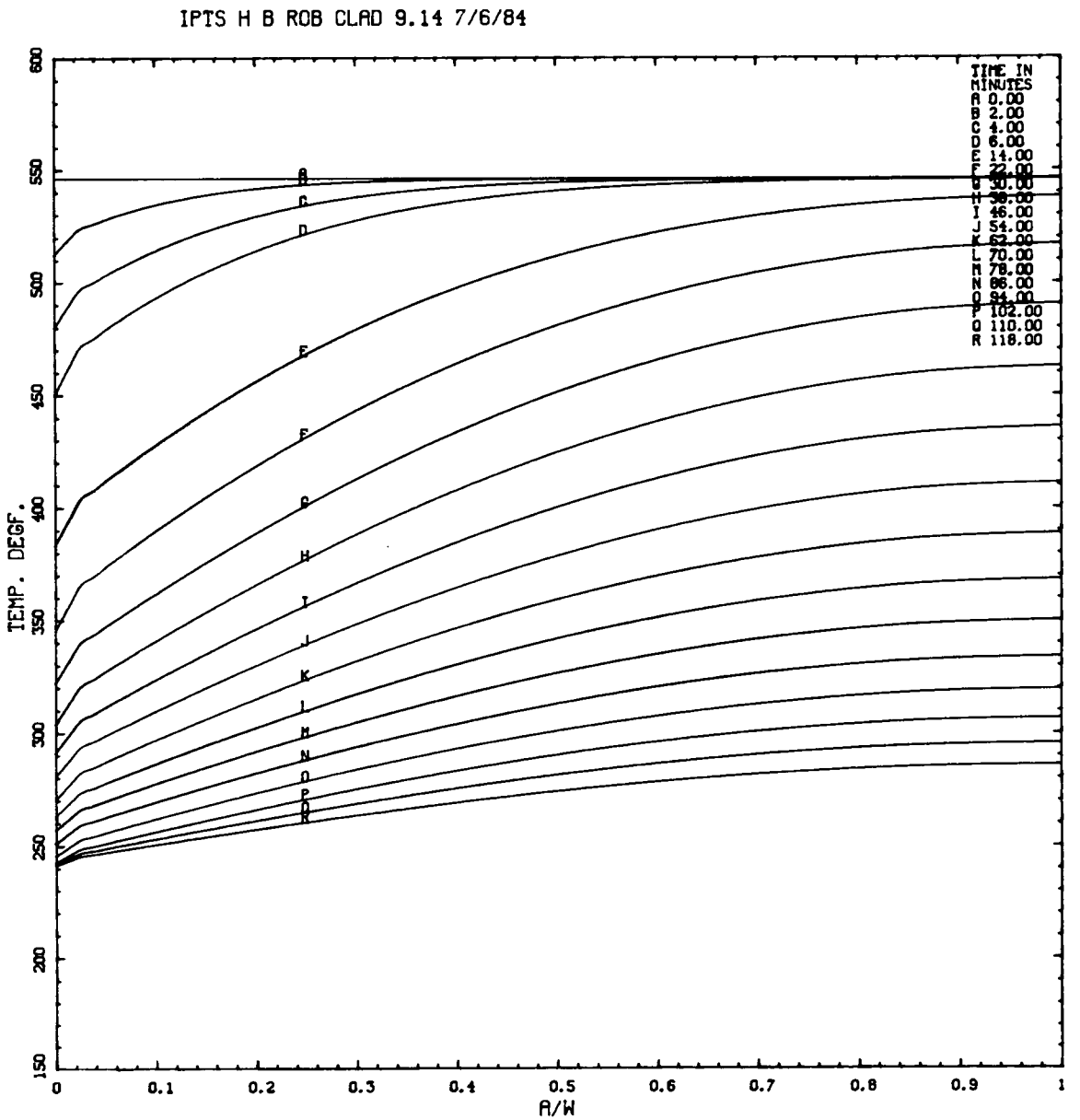

Figure I.141. Transient 9.14B: Vessel wall temperature vs depth in wall (a/w) at various times (t) in transient.

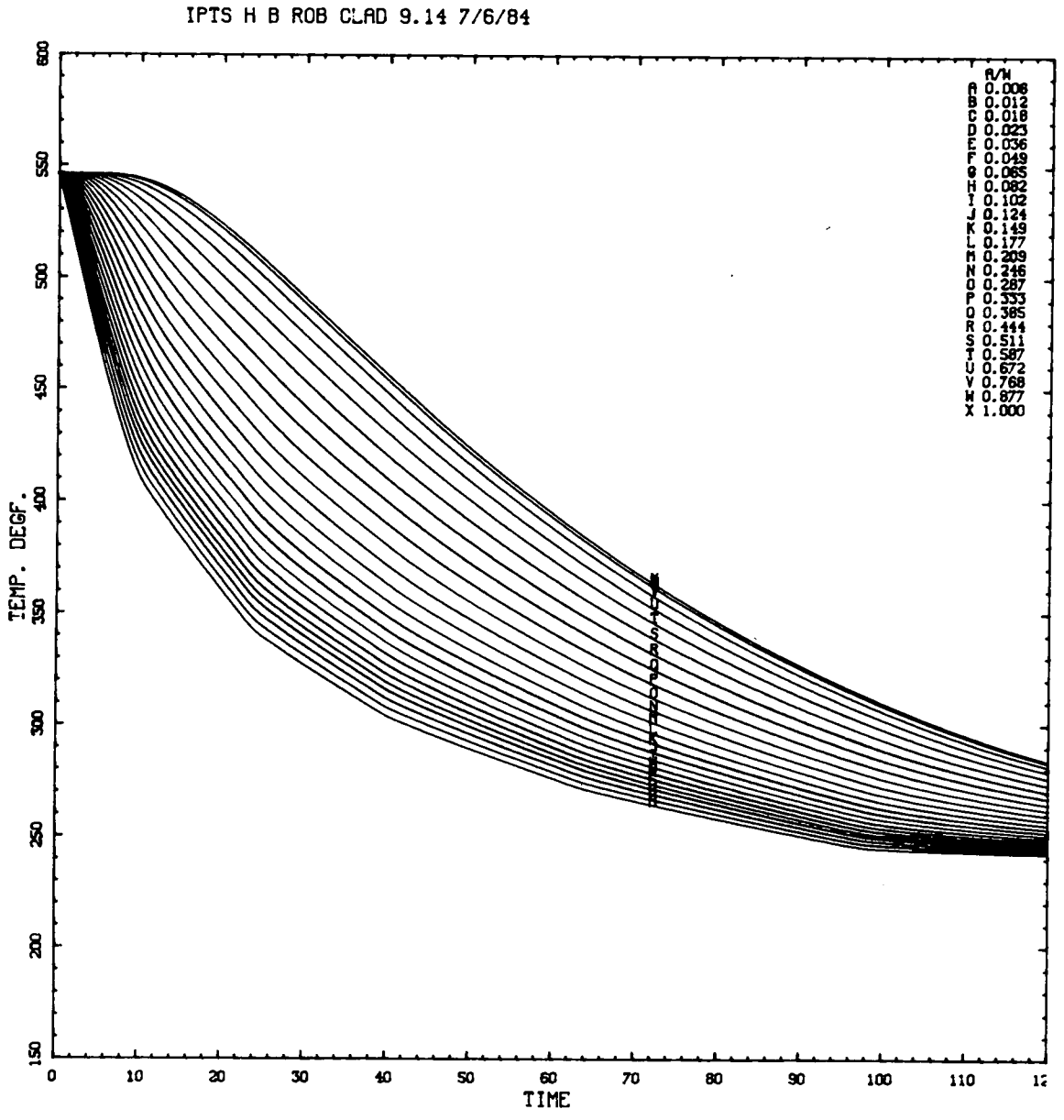

Figure I.142. Transient 9.14B: Vessel wall temperature vs time (t) in transient at various depths in wall (a/w).

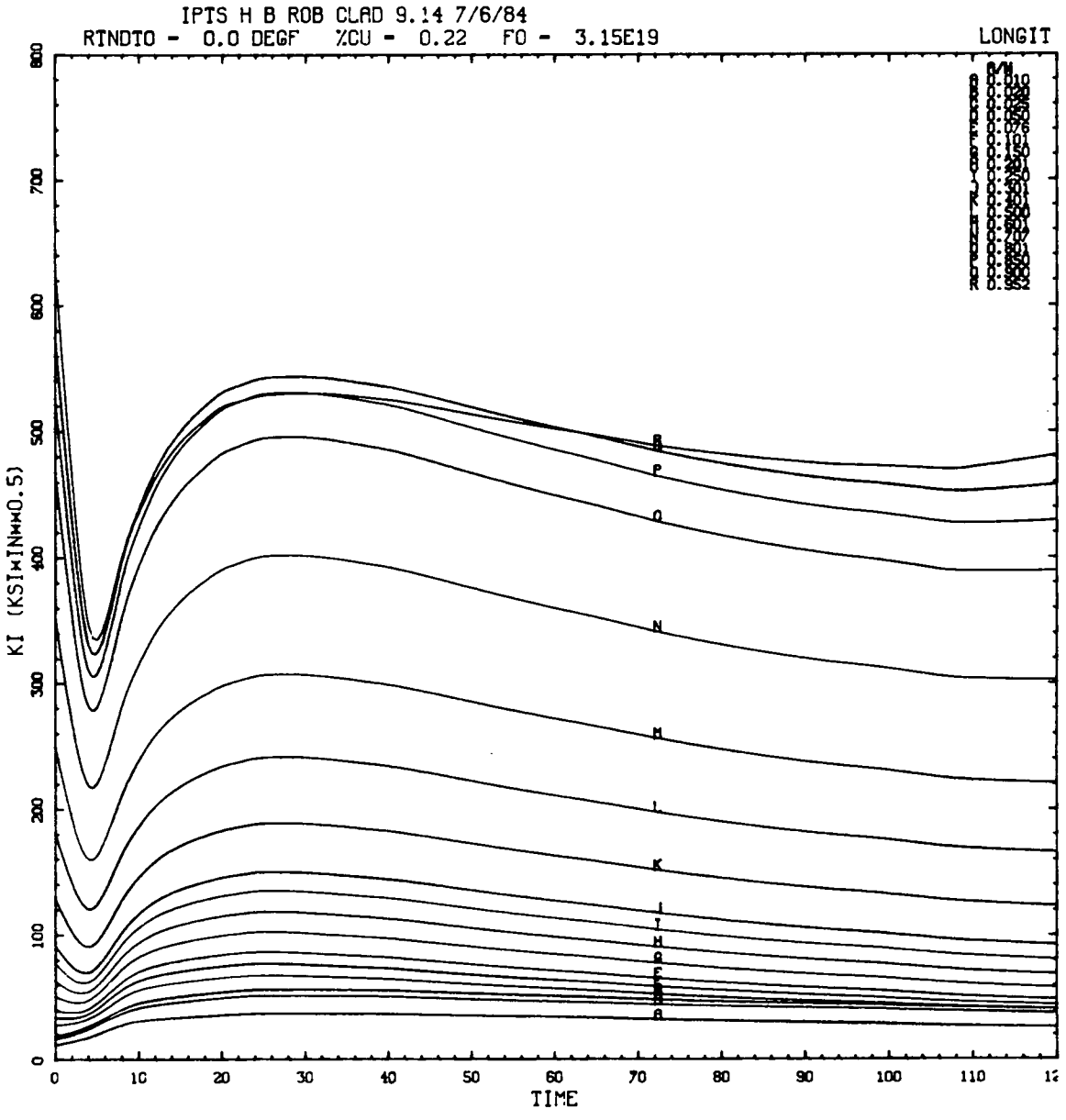

Figure I.143. Transient 9.14B: K_I vs time (t) for various depths in wall (a/w).

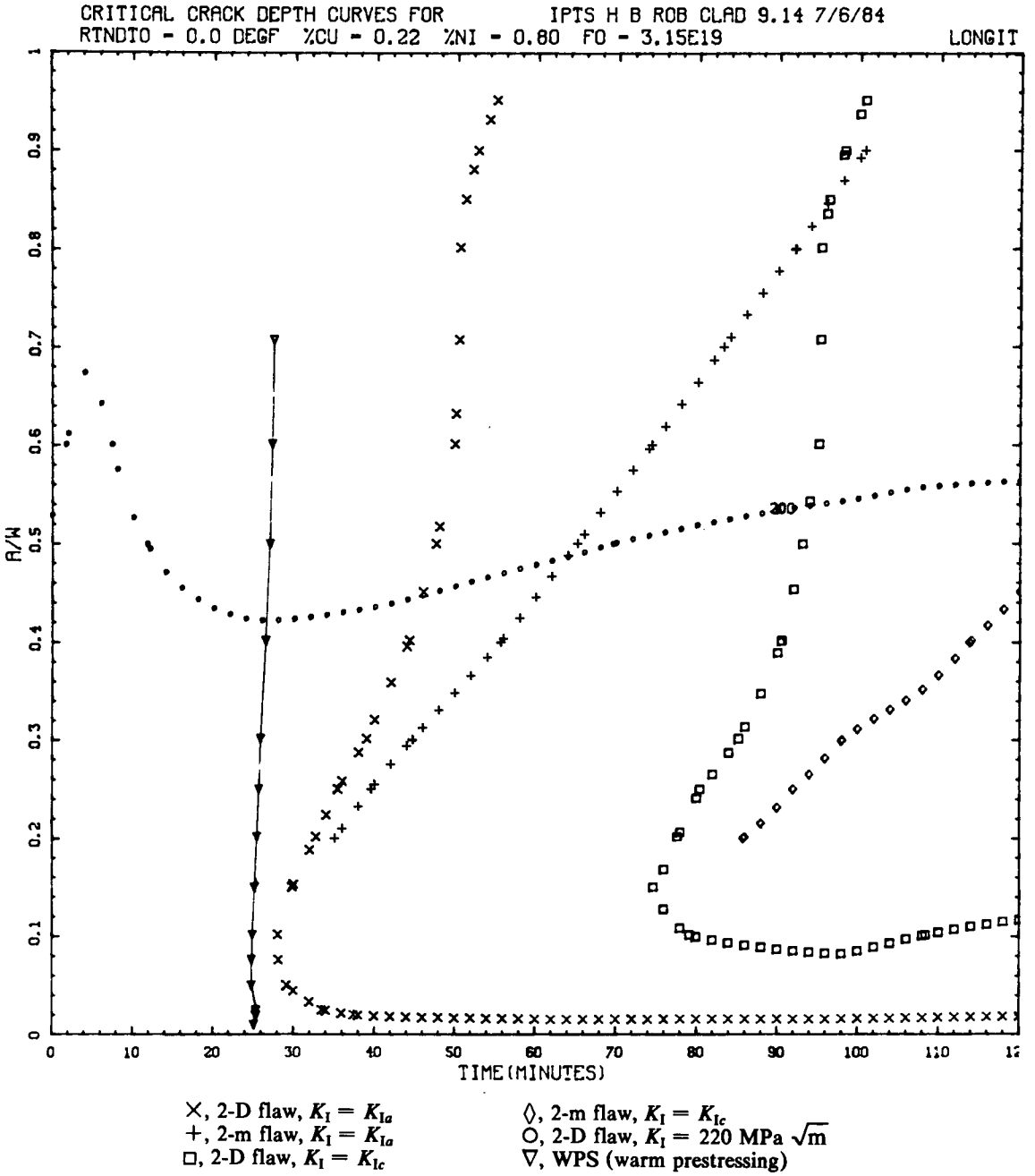

×, 2-D flaw, $K_I = K_{Ia}$
+, 2-m flaw, $K_I = K_{Ia}$
□, 2-D flaw, $K_I = K_{Ic}$
◊, 2-m flaw, $K_I = K_{Ic}$
O, 2-D flaw, $K_I = 220$ MPa $\sqrt{m}$
∇, WPS (warm prestressing)

Figure I.144. Transient 9.14B: Critical-crack-depth curves for weld 2-273A based on -2σ values of K_{Ic}, K_{Ia}, and $\Delta RTNDT$, mean values of all other parameters, and 32-EFPY fluences.

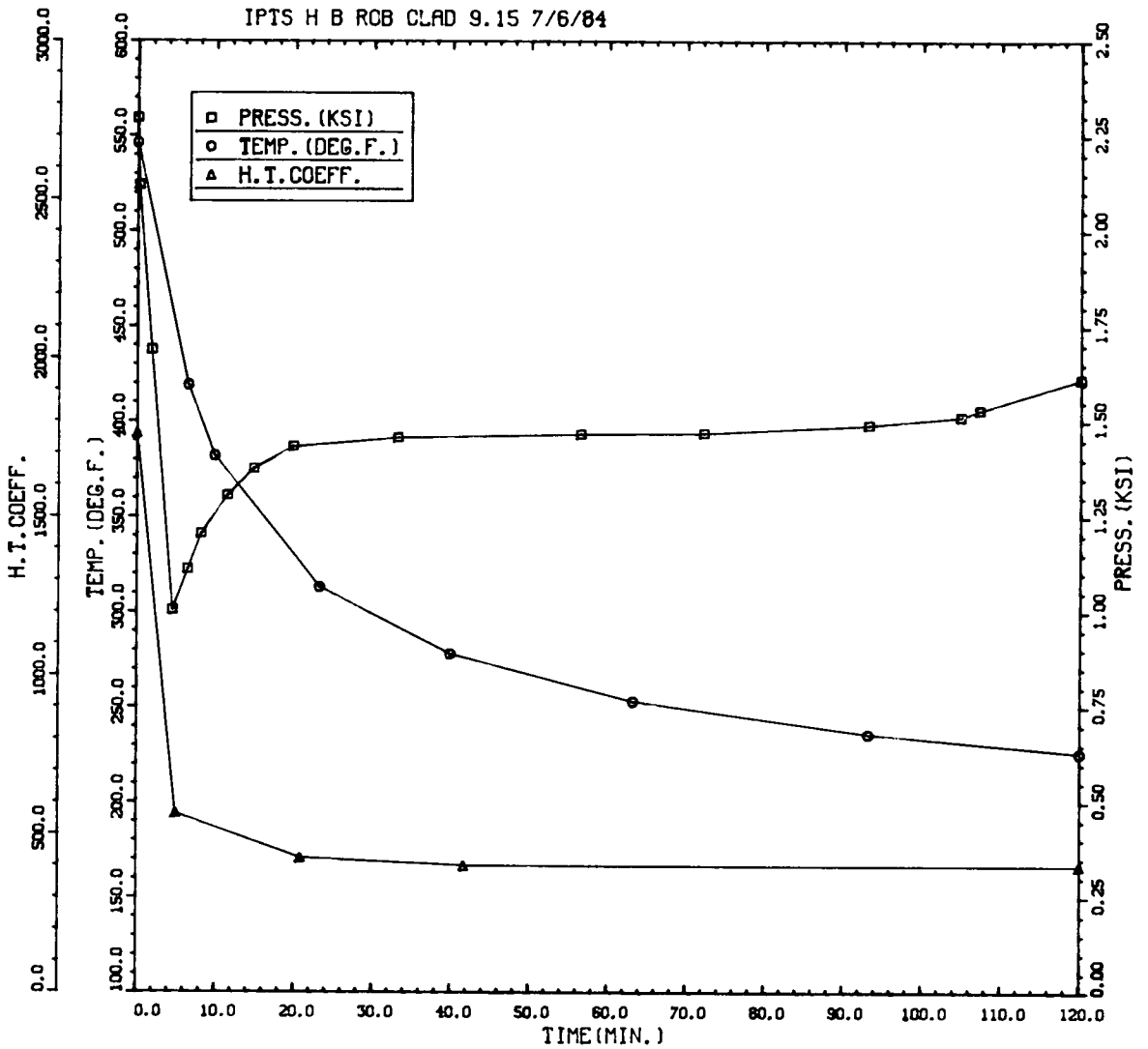

Figure I.145. Transient 9.15B: Primary system pressure, downcomer coolant temperature, and fluid-film heat-transfer coefficient vs time in the transient.

Table I.25. Transient 9.15B: Summary of digital output, including unadjusted $P(F|E)$ values and histogram data for crack depths, times of failure, and $T - RTNDT$ values at tip of crack corresponding to initiation and arrest events

IPTS H B ROB CLAD 9.15 7/6/84 1. FLAWS/IN**3 DRTN(IS) = 211.2

WELD	P(F/E) (UNADJUSTED)	95%CI	%ERR	P(INITIA)	N*V	P(F/E) (ADJUSTED)	%ERR	NFAIL	NTRIALS
1	3.26D-04	3.36D-05	10.34	4.49D-04	1.000	3.26D-04		359	200000
					VESSEL	3.26D-04	10.34		

DEPTHS FOR INITIAL INITIATION (IN)

	0.09	0.26	0.46	0.67	0.90	1.16	1.44	1.74	2.08
NUMBER	0	268	132	61	23	9	2	0	0
PERCENT	0.0	54.1	26.7	12.3	4.6	1.8	0.4	0.0	0.0

TIMES OF FAILURE(MINUTES)

	0.0	10.0	20.0	30.0	40.0	50.0	60.0	70.0	80.0	90.0	100.0	110.0	120.0
PERCENT	0.0	0.0	0.0	0.0	0.0	2.2	9.7	11.7	17.3	17.3	24.2	17.5	

INITIATION T-RTNDT(DEG.F)

	-100.0	-75.0	-50.0	-25.0	0.0	25.0	50.0	75.0	100.0	125.0	150.0	175.0	200.0
NUMBER	0	0	43	205	232	156	157	29	0	0	0	0	
PERCENT	0.0	0.0	5.2	24.9	28.2	19.0	19.1	3.5	0.0	0.0	0.0	0.0	

ARREST T-RTNDT(DEG.F)

	-50.0	-25.0	0.0	25.0	50.0	75.0	100.0	125.0	150.0	175.0	200.0	225.0	250.0
NUMBER	4	18	40	12	1	0	17	261	110	0	0	0	
PERCENT	0.9	3.9	8.6	2.6	0.2	0.0	3.7	56.4	23.8	0.0	0.0	0.0	

ICRKTP = 2 IACCEL = 1 NDLRS = 0 NRTRS = 0 DATE: 10/31/84 TIME: 01.31.03

CPU TIME: 5 MIN 29 SEC

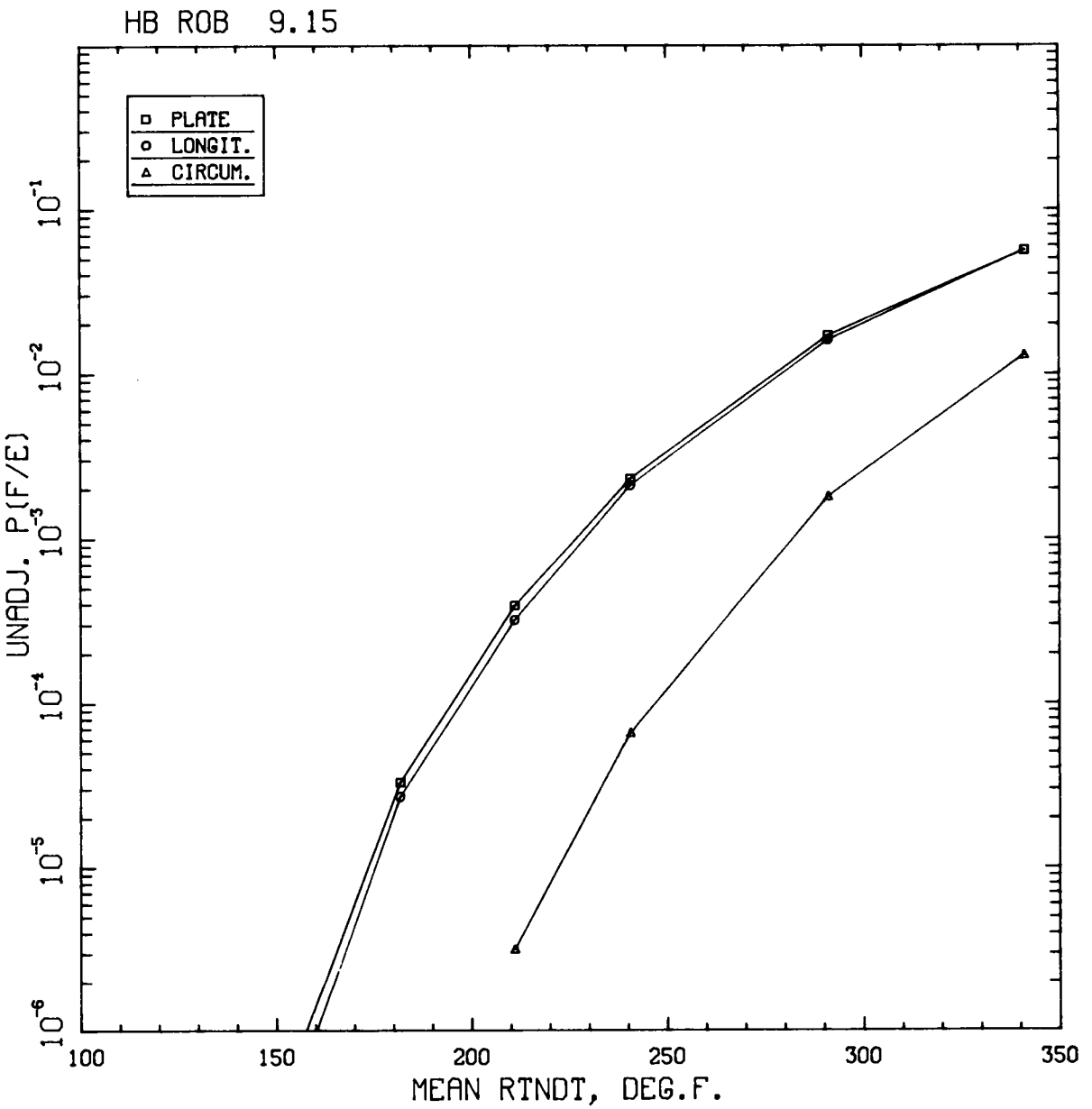

Figure I.146. Transient 9.15B: $\hat{P}_j \int_0^w f(a)\, B(a)\, da$ vs $\overline{RTNDT_s}$ for (2-D, 2-D) and (2-D, 2m) flaw combinations.

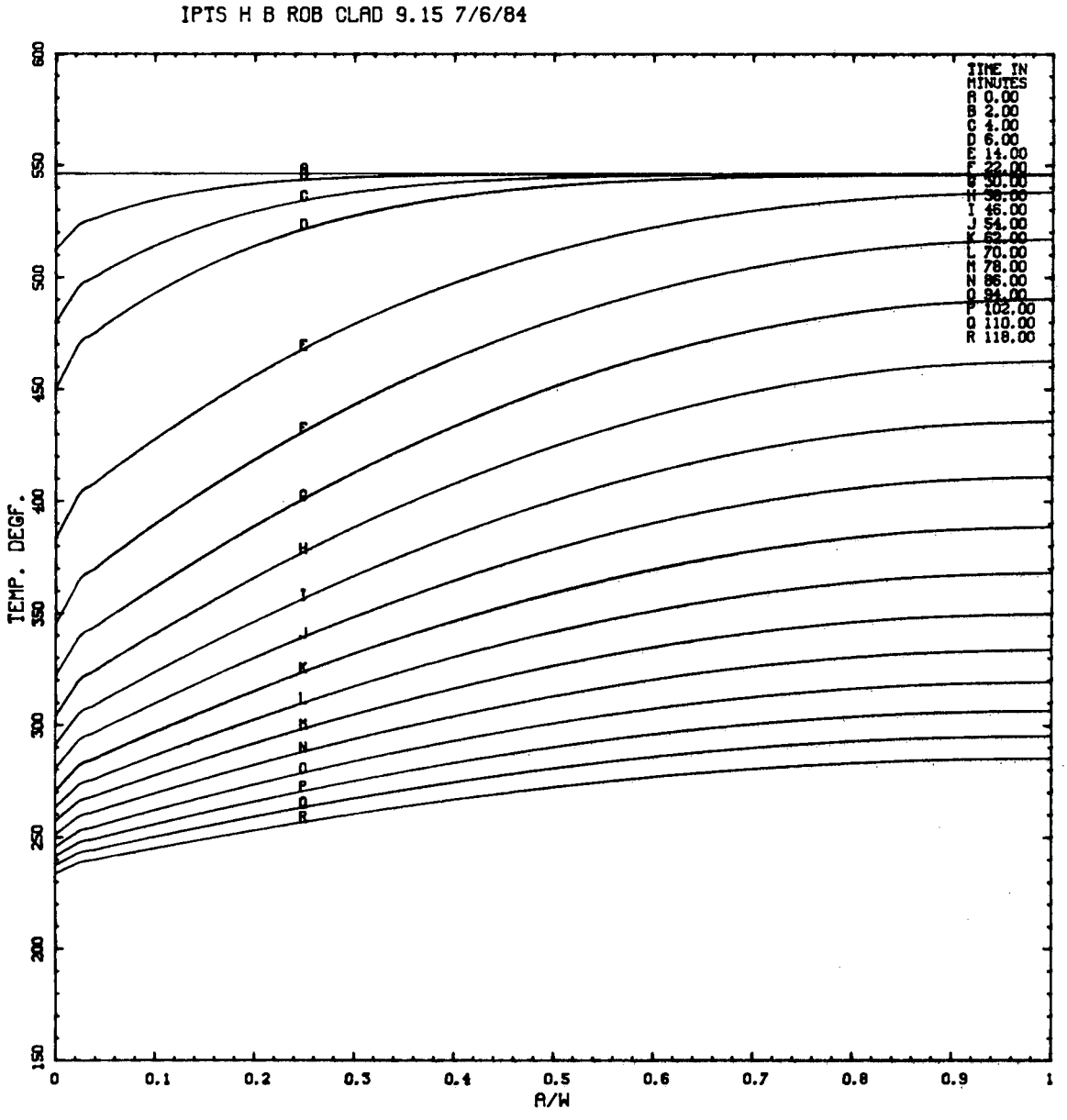

Figure I.147. Transient 9.15B: Vessel wall temperature vs depth in wall (a/w) at various times (t) in transient.

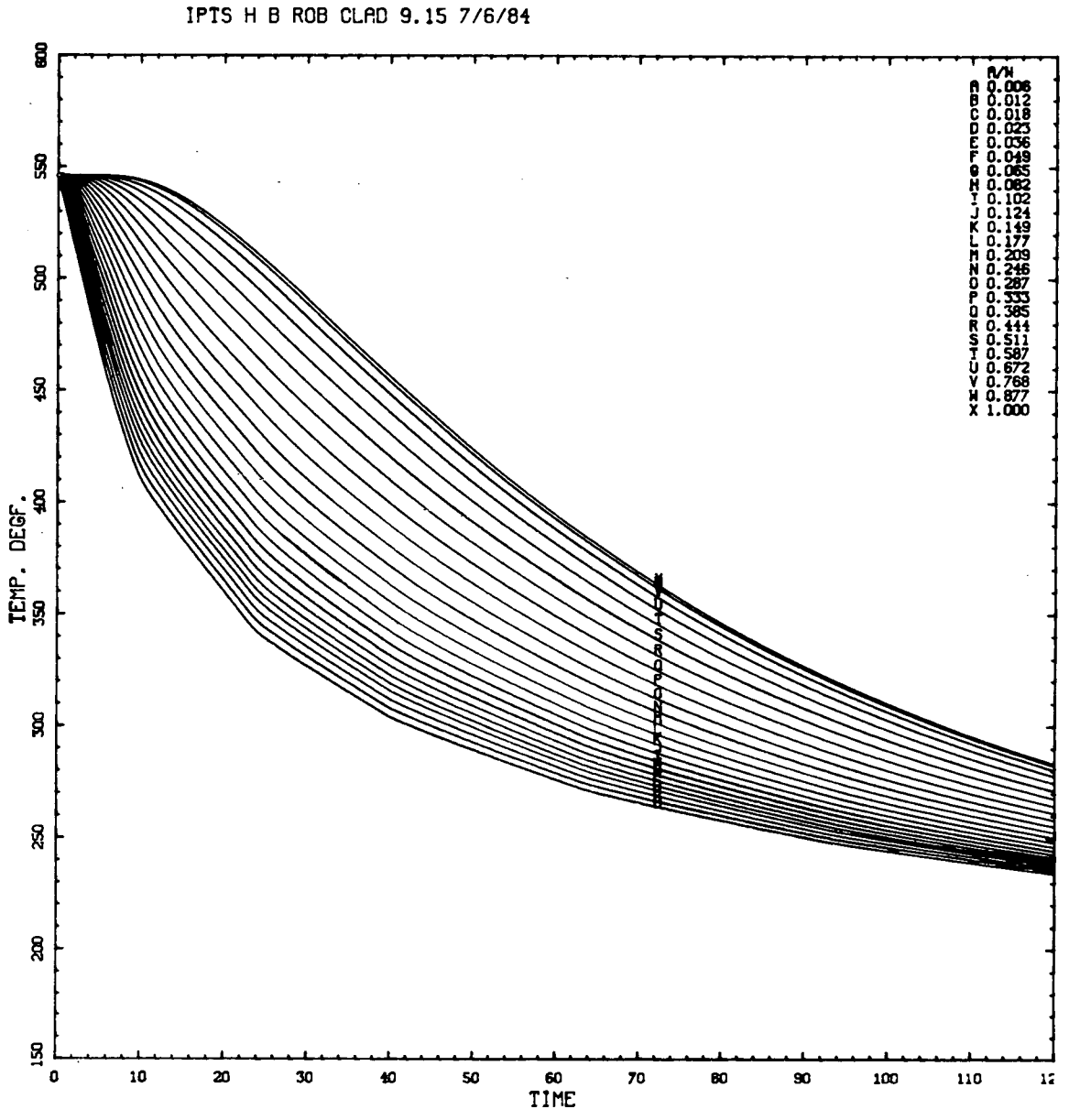

Figure I.148. Transient 9.15B: Vessel wall temperature vs time (t) in transient at various depths in wall (a/w).

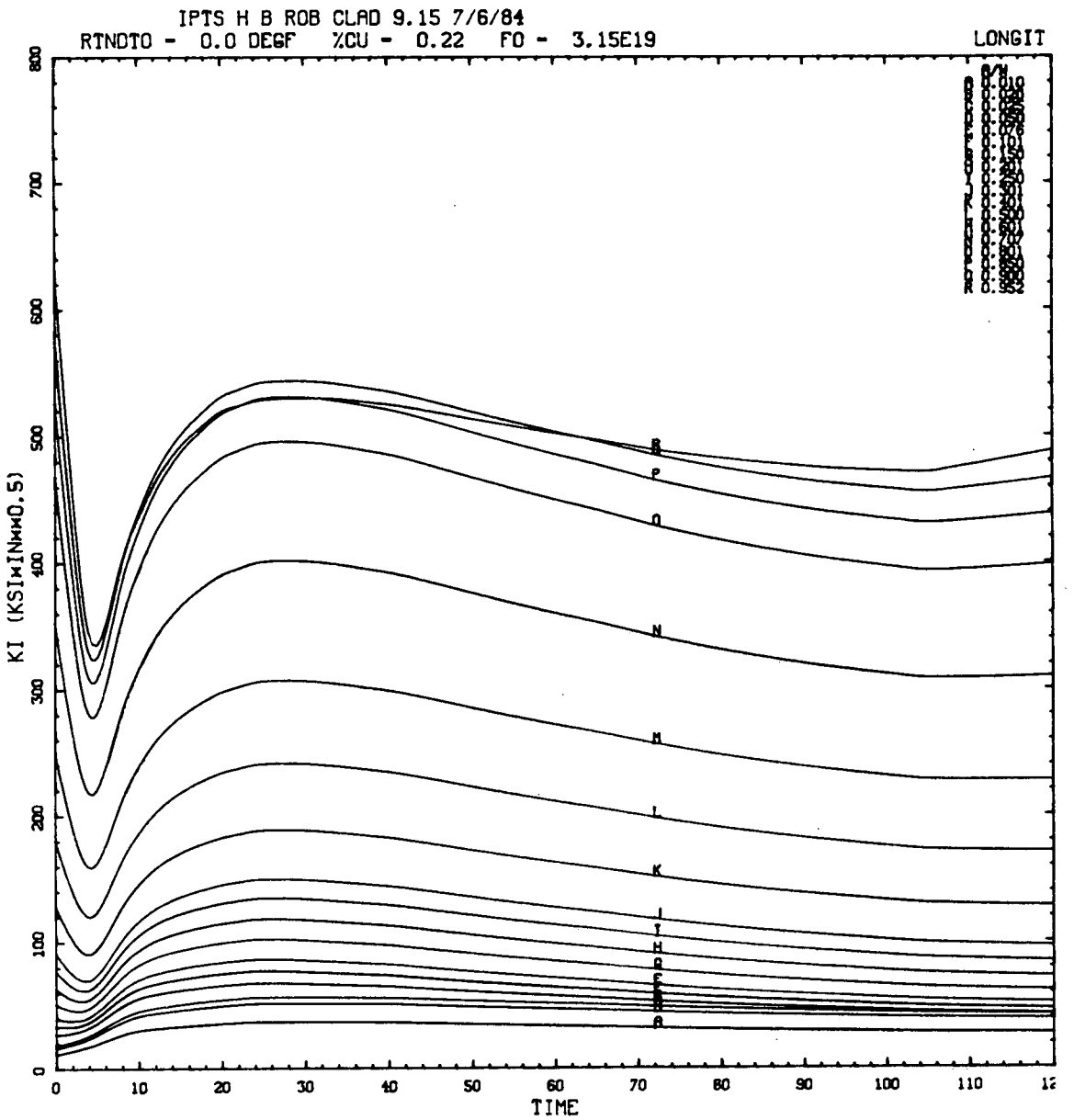

Figure I.149. Transient 9.15B: K_I vs time (t) for various depths in wall (a/w).

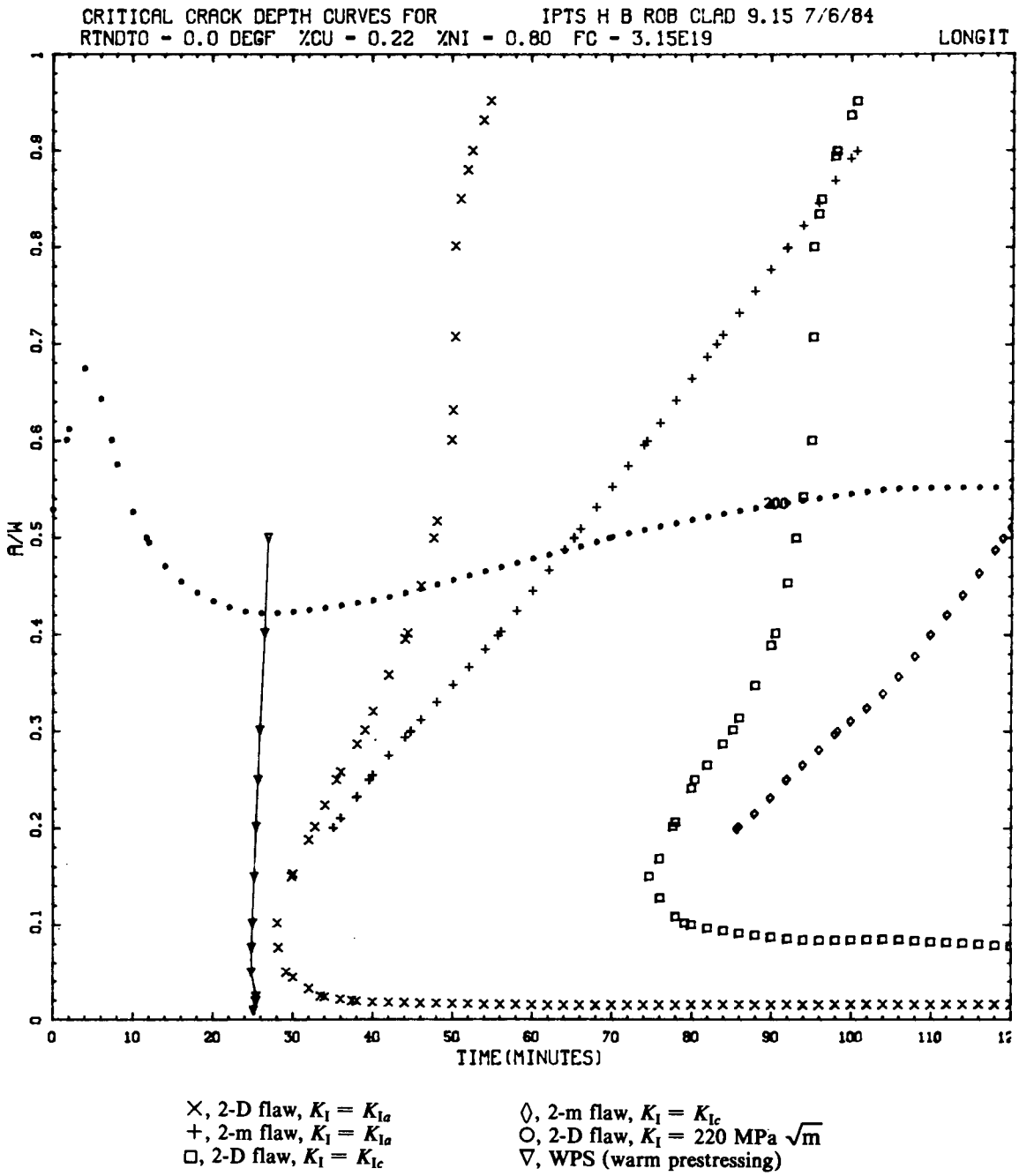

Figure I.150. Transient 9.15B: Critical-crack-depth curves for weld 2-273A based on -2σ values of K_{Ic}, K_{Ia}, and $\Delta RTNDT$, mean values of all other parameters, and 32-EFPY fluences.

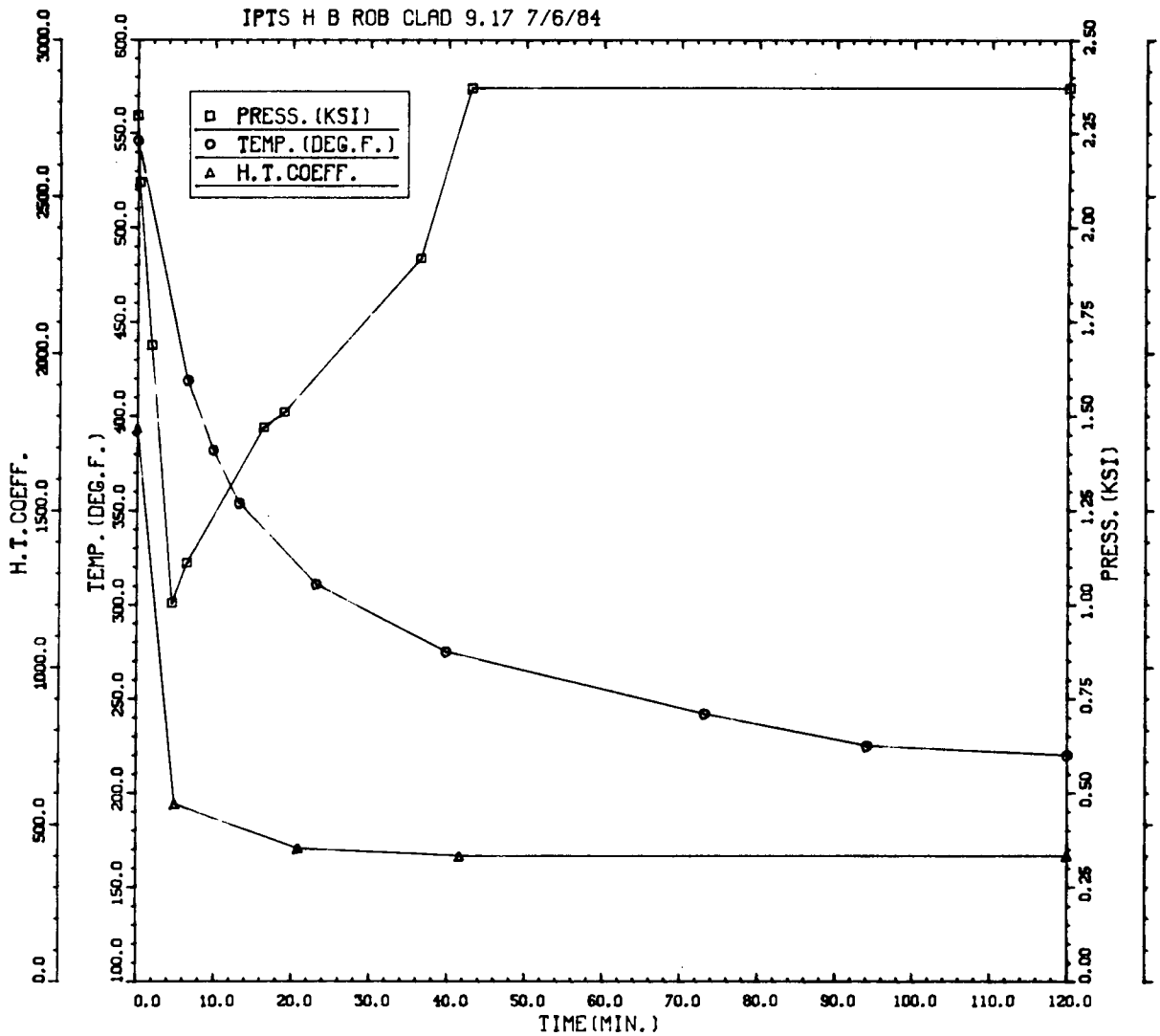

Figure I.151. Transient 9.17B: Primary system pressure, downcomer coolant temperature, and fluid-film heat-transfer coefficient vs time in the transient.

Table I.26. Transient 9.17B: Summary of digital output, including unadjusted $P(F|E)$ values and histogram data for crack depths, times of failure, and $T - RTNDT$ values at tip of crack corresponding to initiation and arrest events

IPTS H B ROB CLAD 9.17 7/6/84 1. FLAWS/IN**3 DRTN(IS) = 211.2

	----------UNADJUSTED----------					---ADJUSTED----			
WELD	P(F/E)	95%CI	%ERR	P(INITIA)	N*V	P(F/E)	%ERR	NFAIL	NTRIALS
1	4.15D-03	3.76D-04	9.05	4.26D-03	1.000	4.15D-03		458	20000
					VESSEL	4.15D-03	9.05		

DEPTHS FOR INITIAL INITIATION (IN)

	0.09	0.26	0.46	0.67	0.90	1.16	1.44	1.74	2.08
NUMBER	0	263	122	58	23	3	1	0	0
PERCENT	0.0	56.0	26.0	12.3	4.9	0.6	0.2	0.0	0.0

TIMES OF FAILURE(MINUTES)

	0.0	10.0	20.0	30.0	40.0	50.0	60.0	70.0	80.0	90.0	100.0	110.0	120.0
PERCENT	0.0	0.0	0.0	0.7	9.6	13.1	16.8	21.0	19.7	17.7	1.1	0.4	

INITIATION T-RTNDT(DEG.F)

	-100.0	-75.0	-50.0	-25.0	0.0	25.0	50.0	75.0	100.0	125.0	150.0	175.0	200.0
NUMBER	0	10	44	194	157	58	20	12	1	0	0	0	
PERCENT	0.0	2.0	8.7	38.3	33.0	11.5	4.0	2.4	0.2	0.0	0.0	0.0	

ARREST T-RTNDT(DEG.F)

	-50.0	-25.0	0.0	25.0	50.0	75.0	100.0	125.0	150.0	175.0	200.0	225.0	250.0
NUMBER	0	0	8	1	0	0	0	8	31	0	0	0	
PERCENT	0.0	0.0	16.7	2.1	0.0	0.0	0.0	16.7	64.6	0.0	0.0	0.0	

ICRKTP = 2 IACCEL = 1 NDLRS = 0 NRTRS = 0 DATE: 10/31/84 TIME: 01.34.53

CPU TIME: 0 MIN 41 SEC

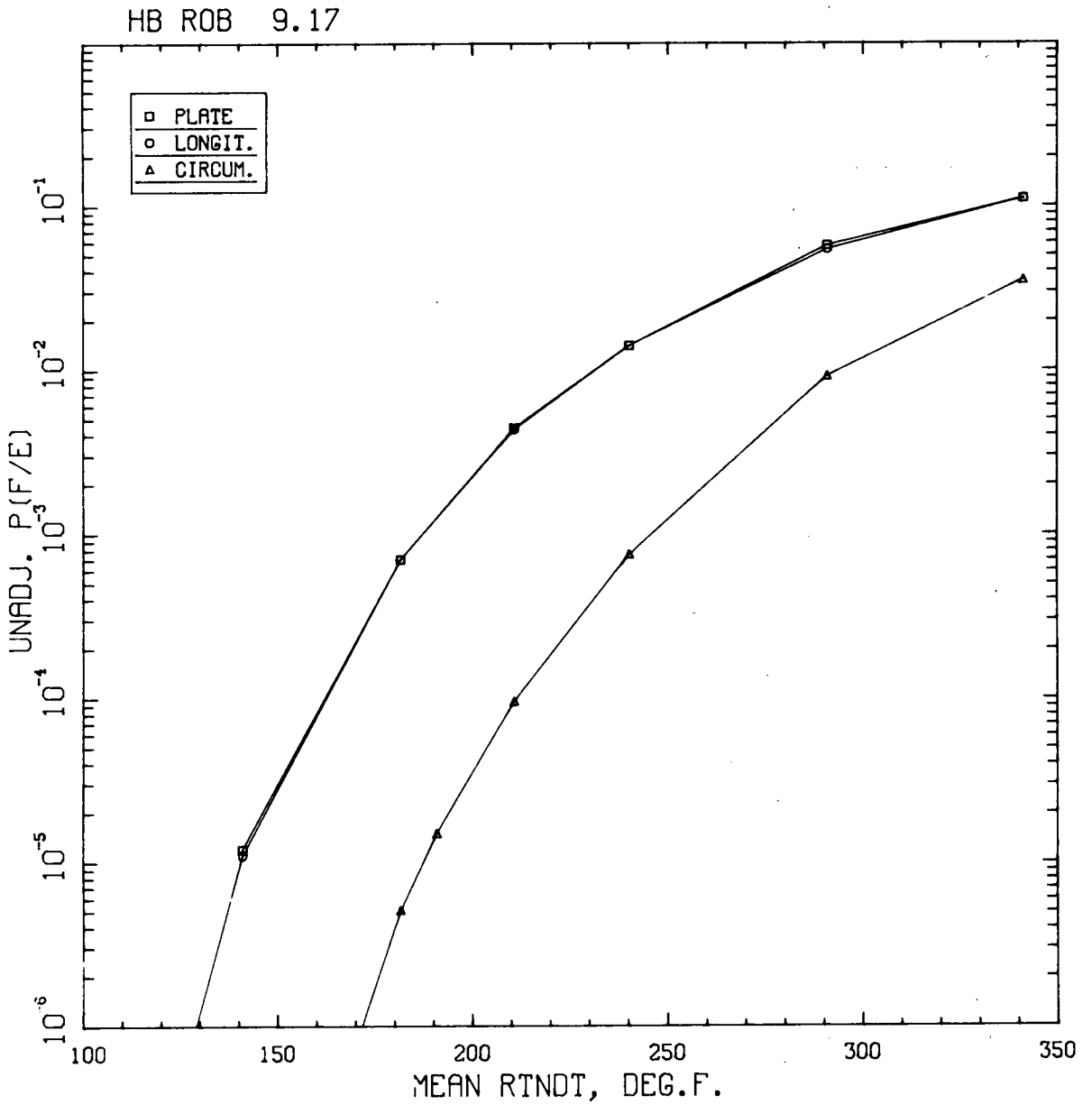

Figure I.152. Transient 9.17B: $\hat{P}_j \int_0^w f(a)\, B(a)\, da$ vs $\overline{RTNDT_s}$ for (2-D, 2-D) and (2-D, 2m) flaw combinations.

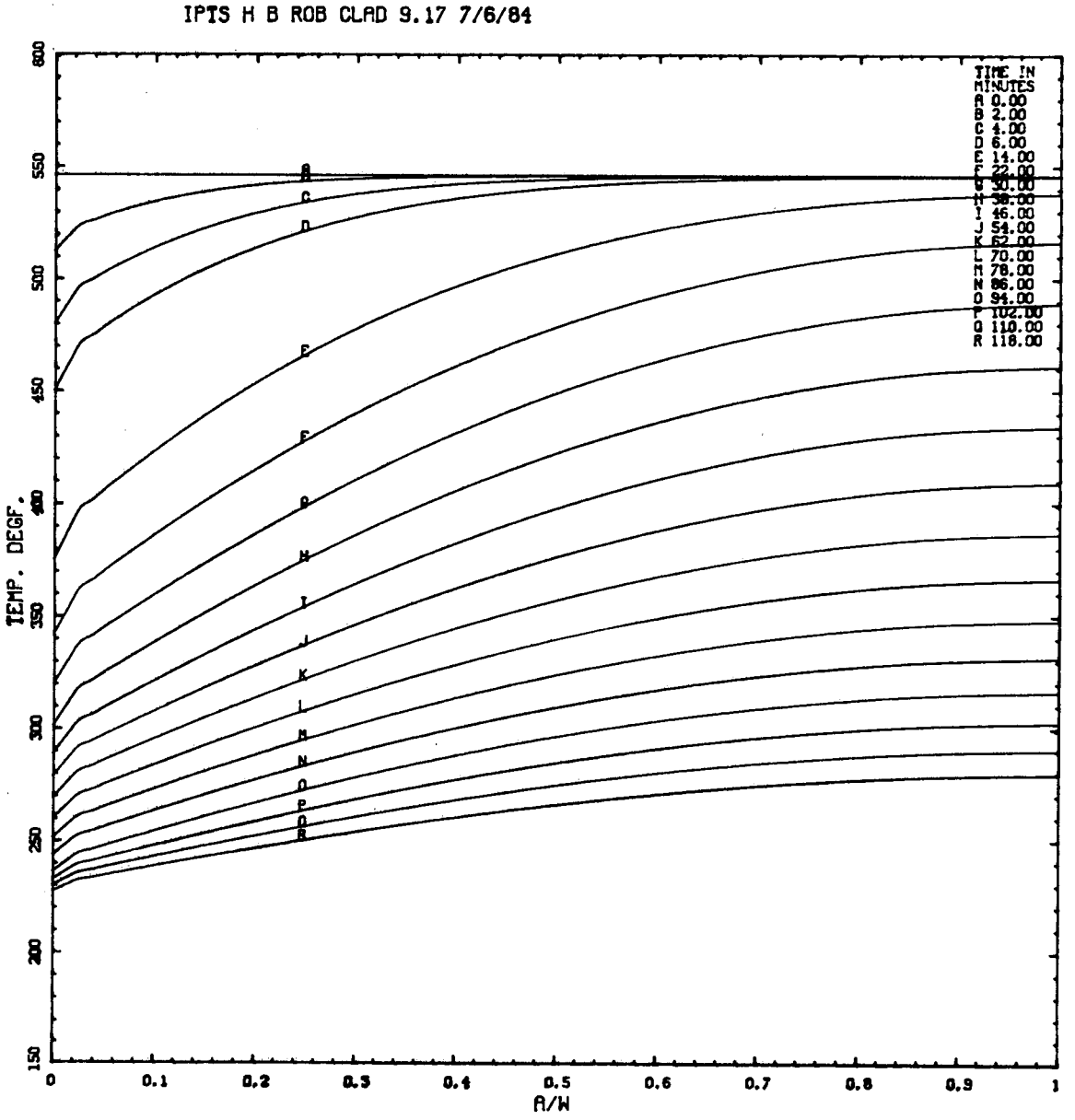

Figure I.153. Transient 9.17B: Vessel wall temperature vs depth in wall (a/w) at various times (t) in transient.

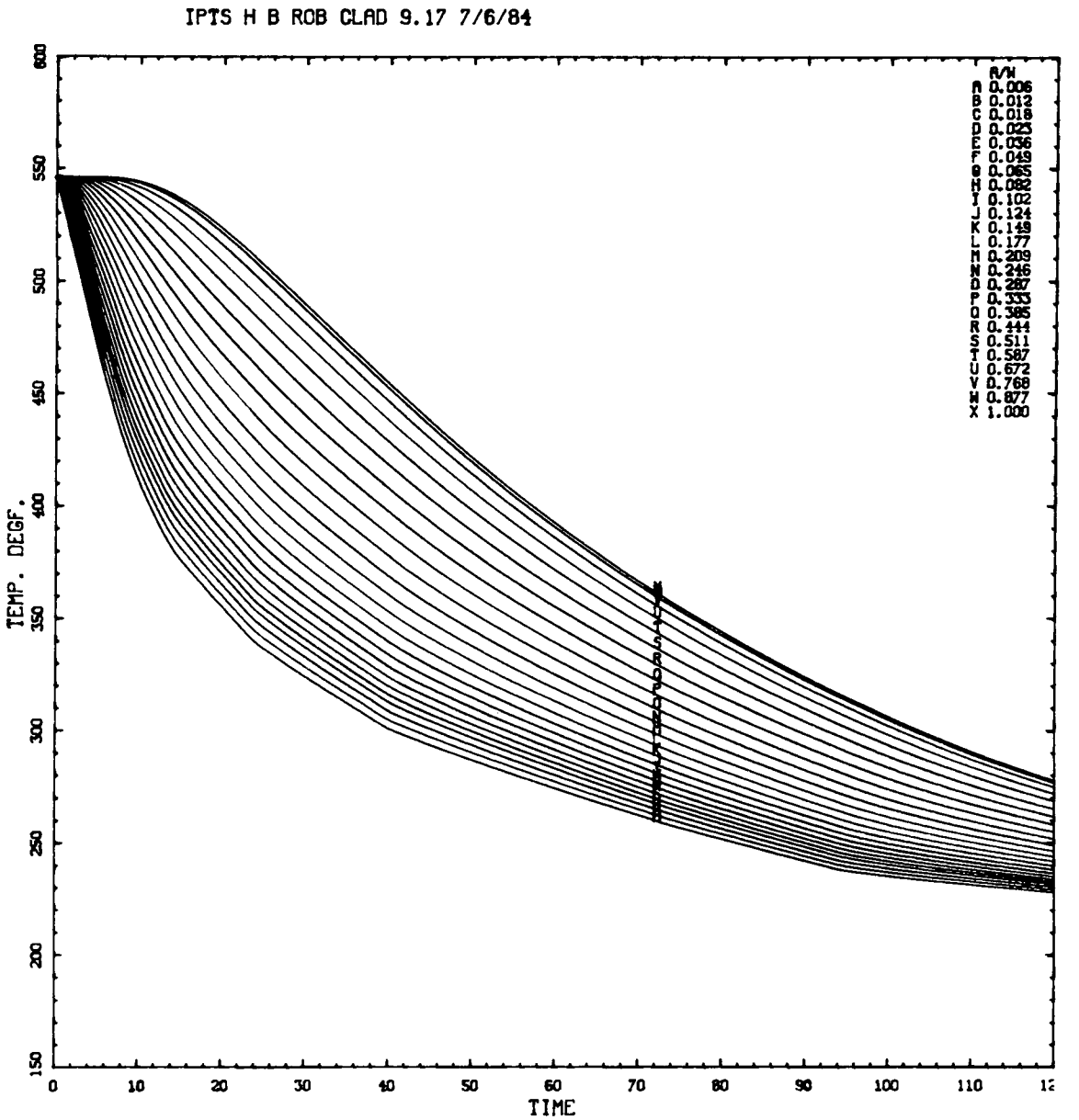

Figure I.154. Transient 9.17B: Vessel wall temperature vs time (t) in transient at various depths in wall (a/w).

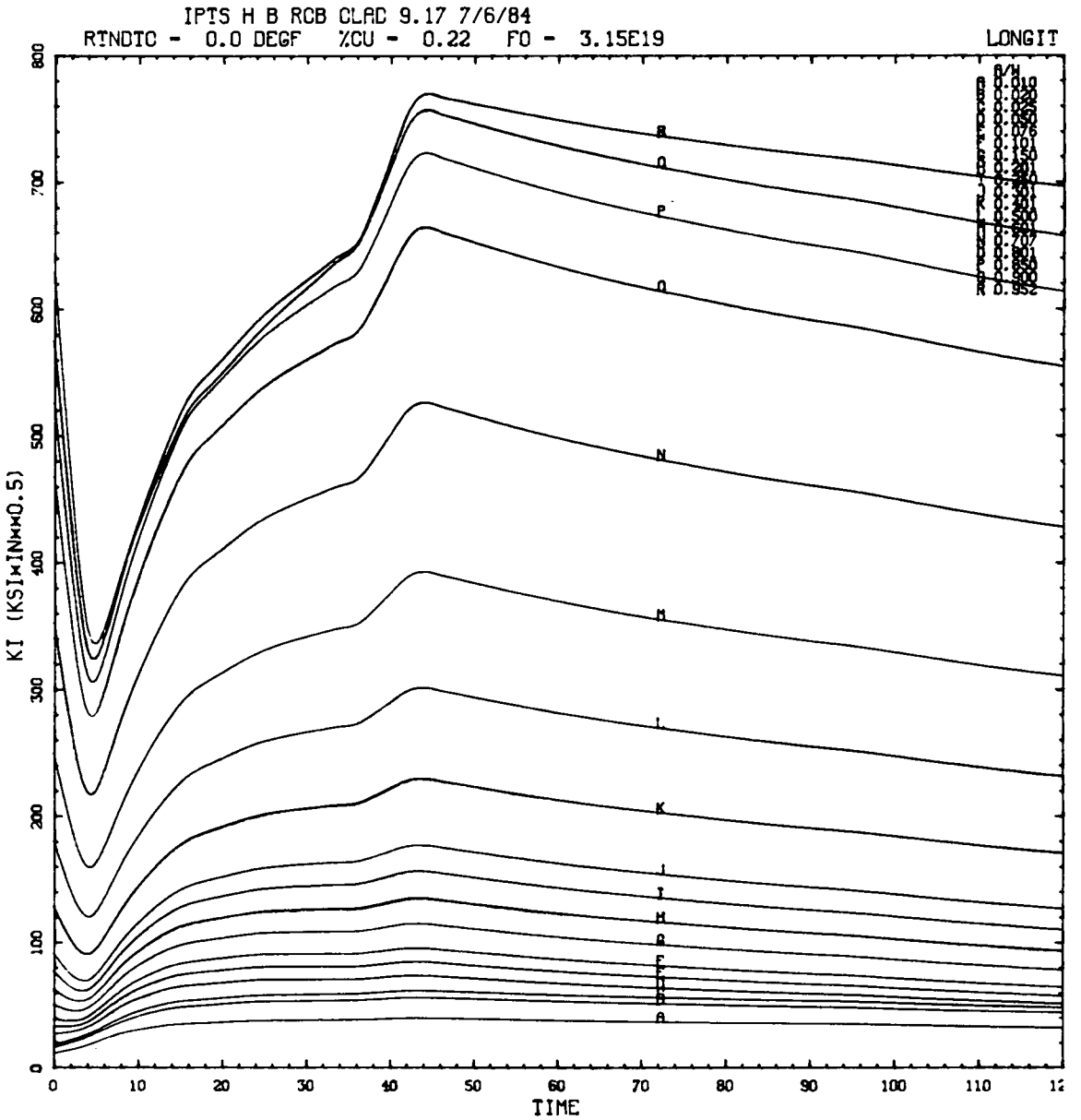

Figure I.155. Transient 9.17B: K_I vs time (t) for various depths in wall (a/w).

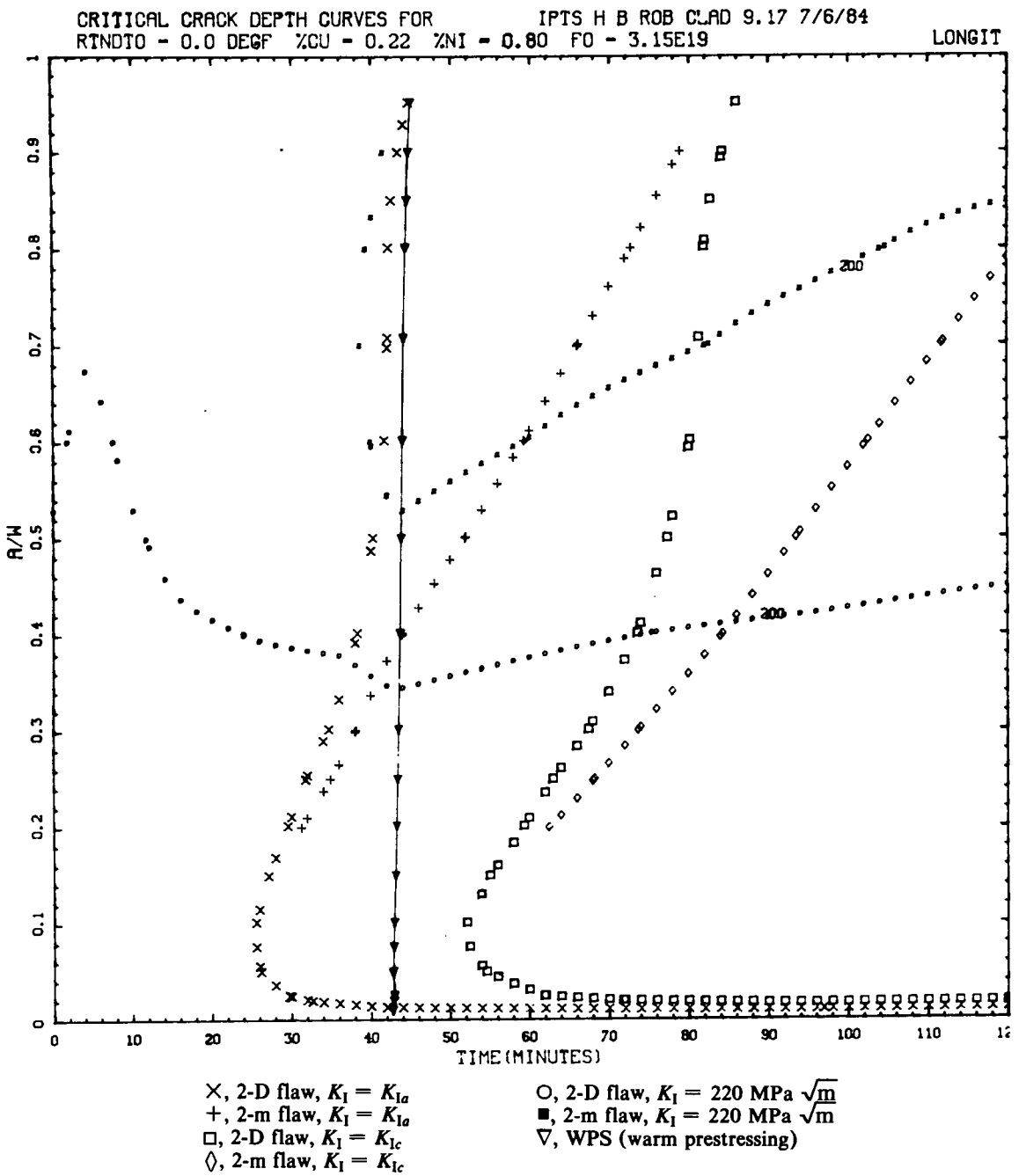

Figure I.156. Transient 9.17B: Critical-crack-depth curves for weld 2-273A based on -2σ values of K_{Ic}, K_{Ia}, and $\Delta RTNDT$, mean values of all other parameters, and 32-EFPY fluences.

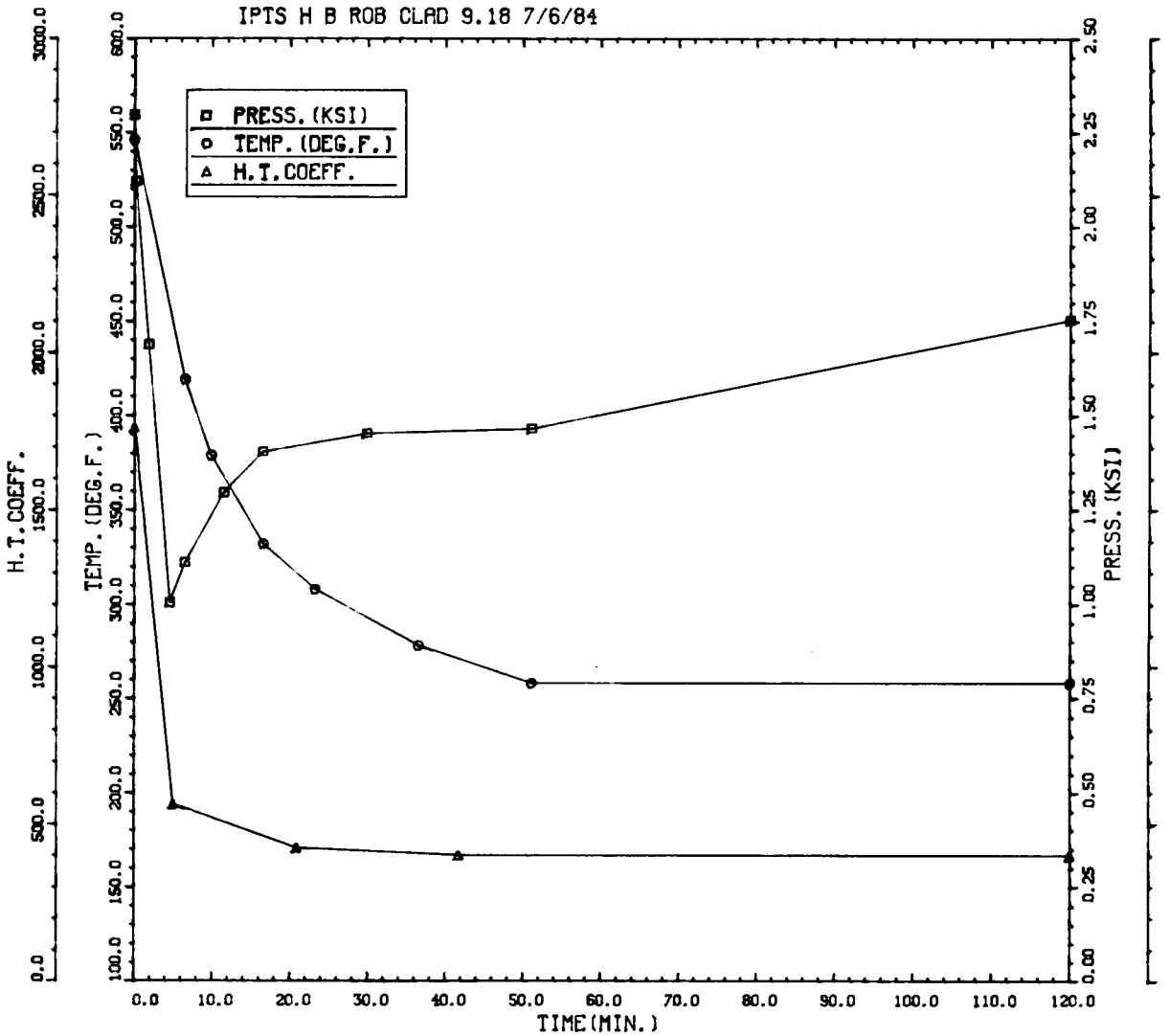

Figure I.157. Transient 9.18B: Primary system pressure, downcomer coolant temperature, and fluid-film heat-transfer coefficient vs time in the transient.

Table I.27. Transient 9.18B: Summary of digital output, including unadjusted $P(F|E)$ values and histogram data for crack depths, times of failure, and $T - RTNDT$ values at tip of crack corresponding to initiation and arrest events

IPTS H B ROB CLAD 9.18 7/6/84 1. FLAWS/IN**3 DRTN(IS) = 211.2

WELD	P(F/E) (UNADJUSTED)	95%CI	%ERR	P(INITIA)	N*V	P(F/E) (ADJUSTED)	%ERR	NFAIL	NTRIALS
1	2.48D-04	2.93D-05	11.85	3.82D-04	1.000	2.48D-04		273	200000
					VESSEL	2.48D-04	11.85		

DEPTHS FOR INITIAL INITIATION (IN)

	0.09	0.26	0.46	0.67	0.90	1.16	1.44	1.74	2.08
NUMBER	0	229	127	50	13	2	0	0	0
PERCENT	0.0	54.4	30.2	11.9	3.1	0.5	0.0	0.0	0.0

TIMES OF FAILURE(MINUTES)

	0.0	10.0	20.0	30.0	40.0	50.0	60.0	70.0	80.0	90.0	100.0	110.0	120.0
PERCENT	0.0	0.0	0.0	0.0	0.7	2.6	10.3	13.6	21.2	19.4	17.2	15.0	

INITIATION T-RTNDT(DEG.F)

	-100.0	-75.0	-50.0	-25.0	0.0	25.0	50.0	75.0	100.0	125.0	150.0	175.0	200.0
NUMBER	0	0	26	153	210	155	137	15	0	0	0	0	
PERCENT	0.0	0.0	3.7	22.0	30.2	22.3	19.7	2.2	0.0	0.0	0.0	0.0	

ARREST T-RTNDT(DEG.F)

	-50.0	-25.0	0.0	25.0	50.0	75.0	100.0	125.0	150.0	175.0	200.0	225.0	250.0
NUMBER	0	0	6	7	0	0	8	272	130	0	0	0	
PERCENT	0.0	0.0	1.4	1.7	0.0	0.0	1.9	64.3	30.7	0.0	0.0	0.0	

ICRKTP = 2 IACCEL = 1 NDLRS = 0 NRTRS = 0 DATE: 10/31/84 TIME: 01.41.07

CPU TIME: 5 MIN 29 SEC

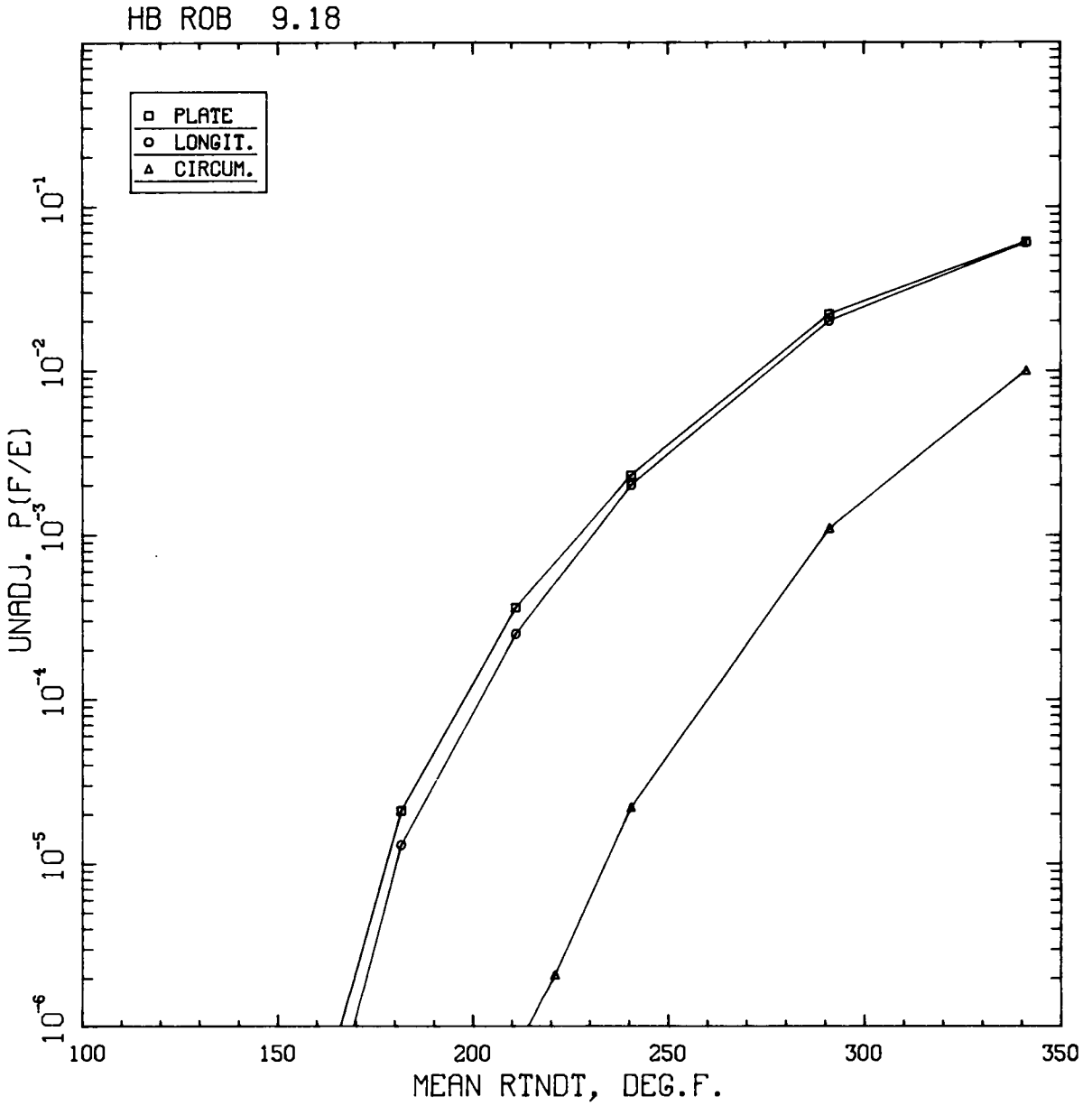

Figure I.158. Transient 9.18B: $\hat{P}_j \int_0^w f(a)\, B(a)\, da$ vs $\overline{RTNDT_s}$ for (2-D, 2-D) and (2-D, 2m) flaw combinations.

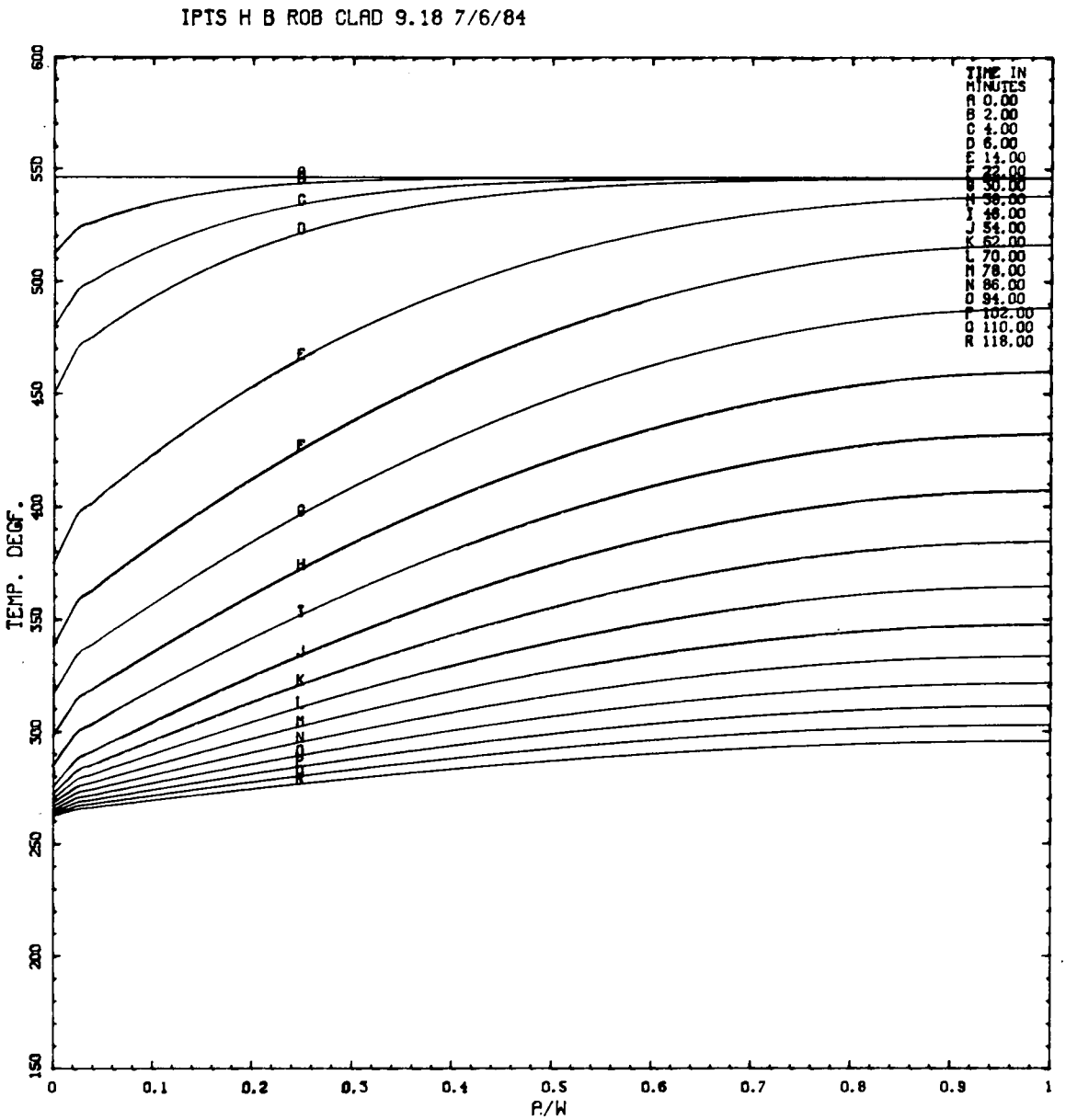

Figure I.159. Transient 9.18B: Vessel wall temperature vs depth in wall (a/w) at various times (t) in transient.

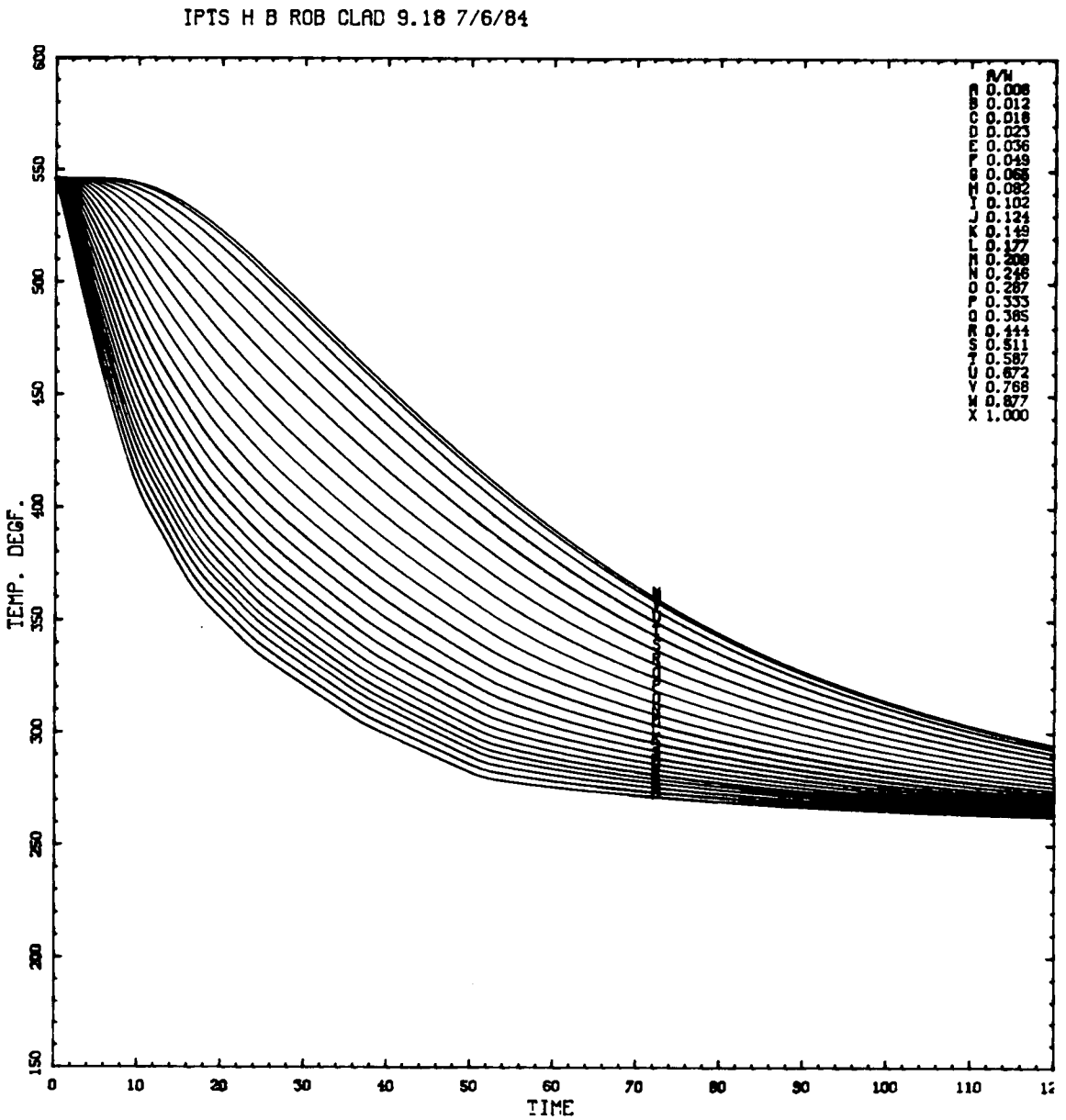

Figure I.160. Transient 9.18B: Vessel wall temperature vs time (t) in transient at various depths in wall (a/w).

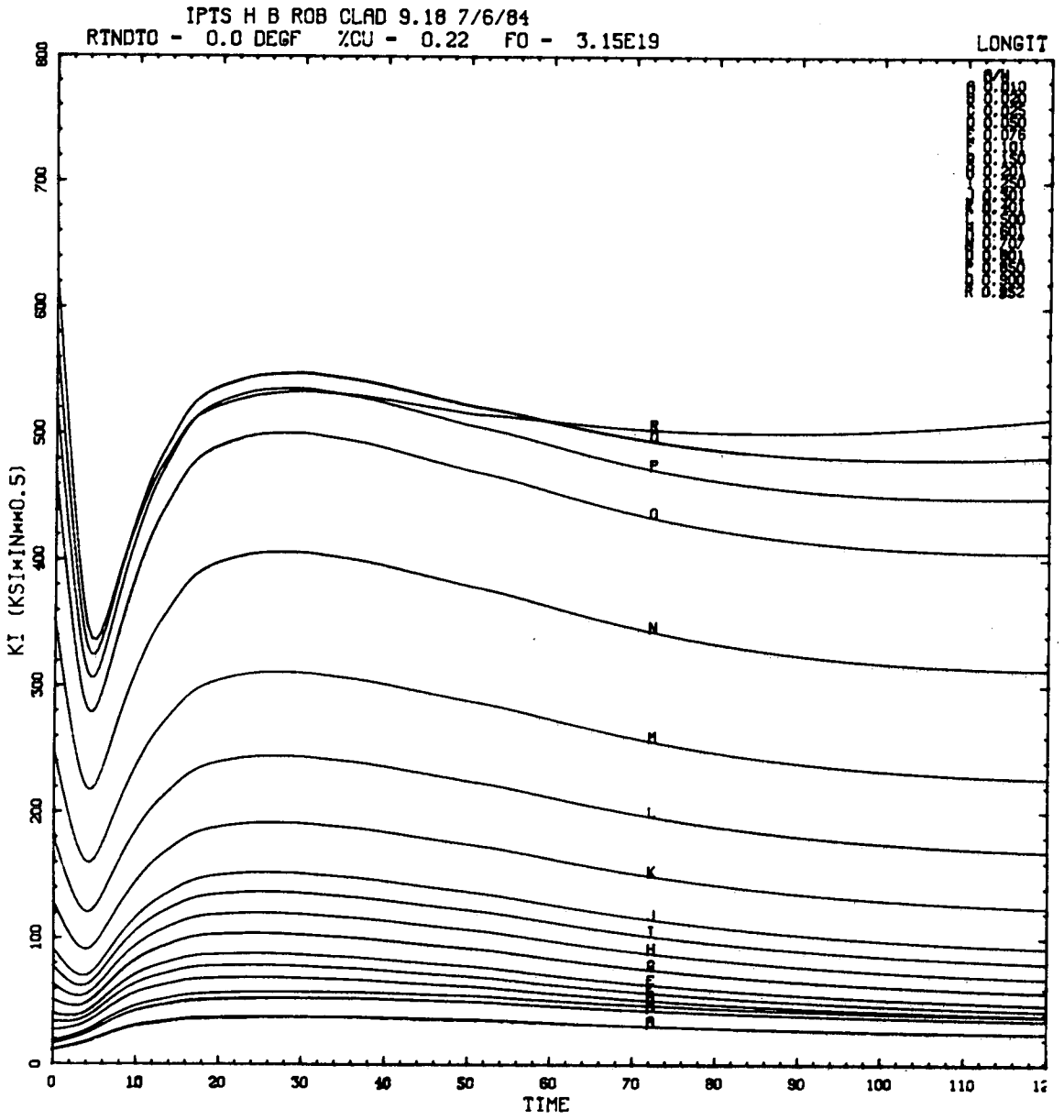

Figure I.161. Transient 9.18B: K_I vs time (t) for various depths in wall (a/w).

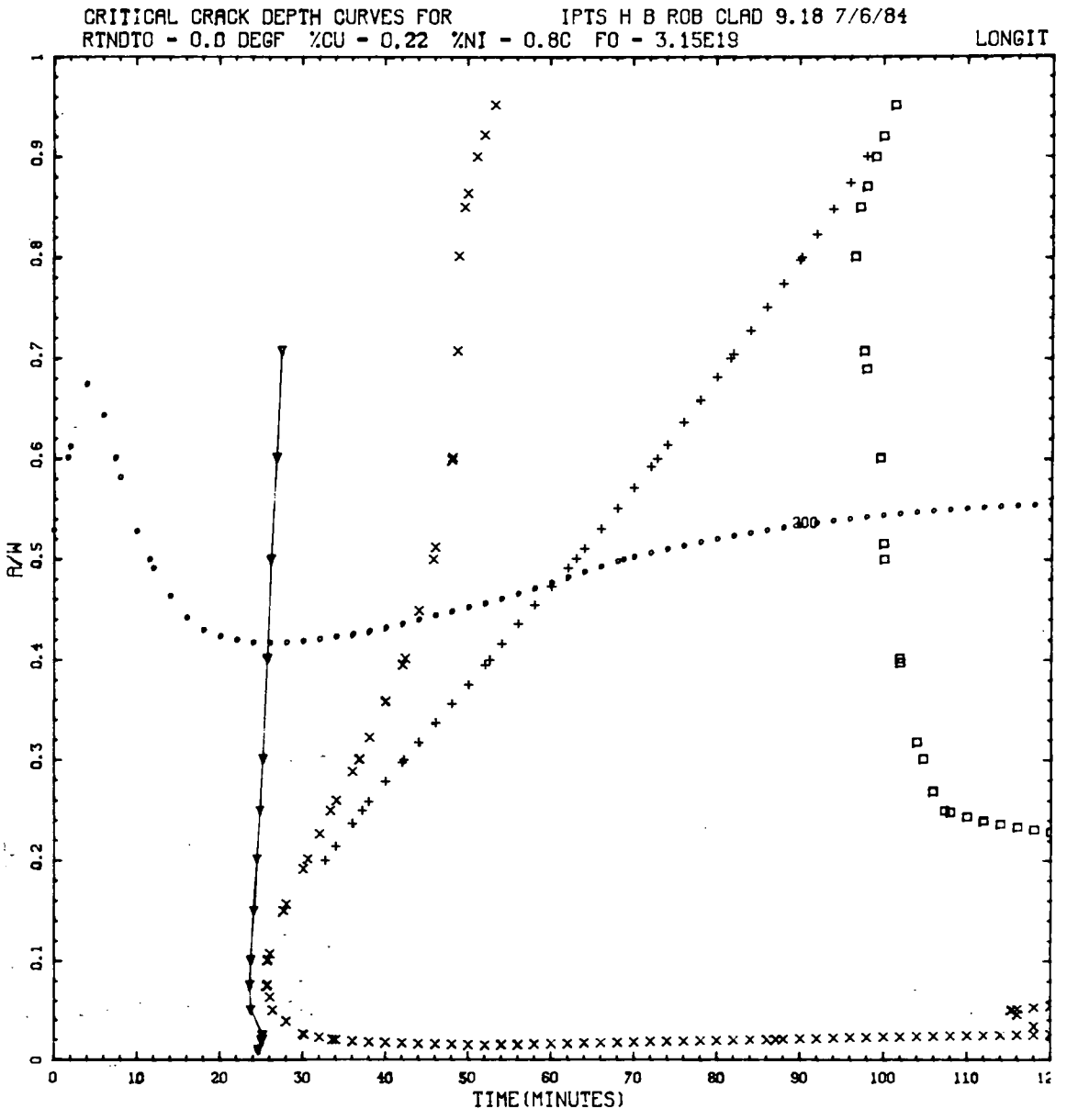

×, 2-D flaw, $K_I = K_{Ia}$
+, 2-m flaw, $K_I = K_{Ia}$
□, 2-D flaw, $K_I = K_{Ic}$
○, 2-D flaw, $K_I = 220$ MPa $\sqrt{m}$
∇, WPS (warm prestressing)

Figure I.162. Transient 9.18B: Critical-crack-depth curves for weld 2-273A based on -2σ values of K_{Ic}, K_{Ia}, and $\Delta RTNDT$, mean values of all other parameters, and 32-EFPY fluences.

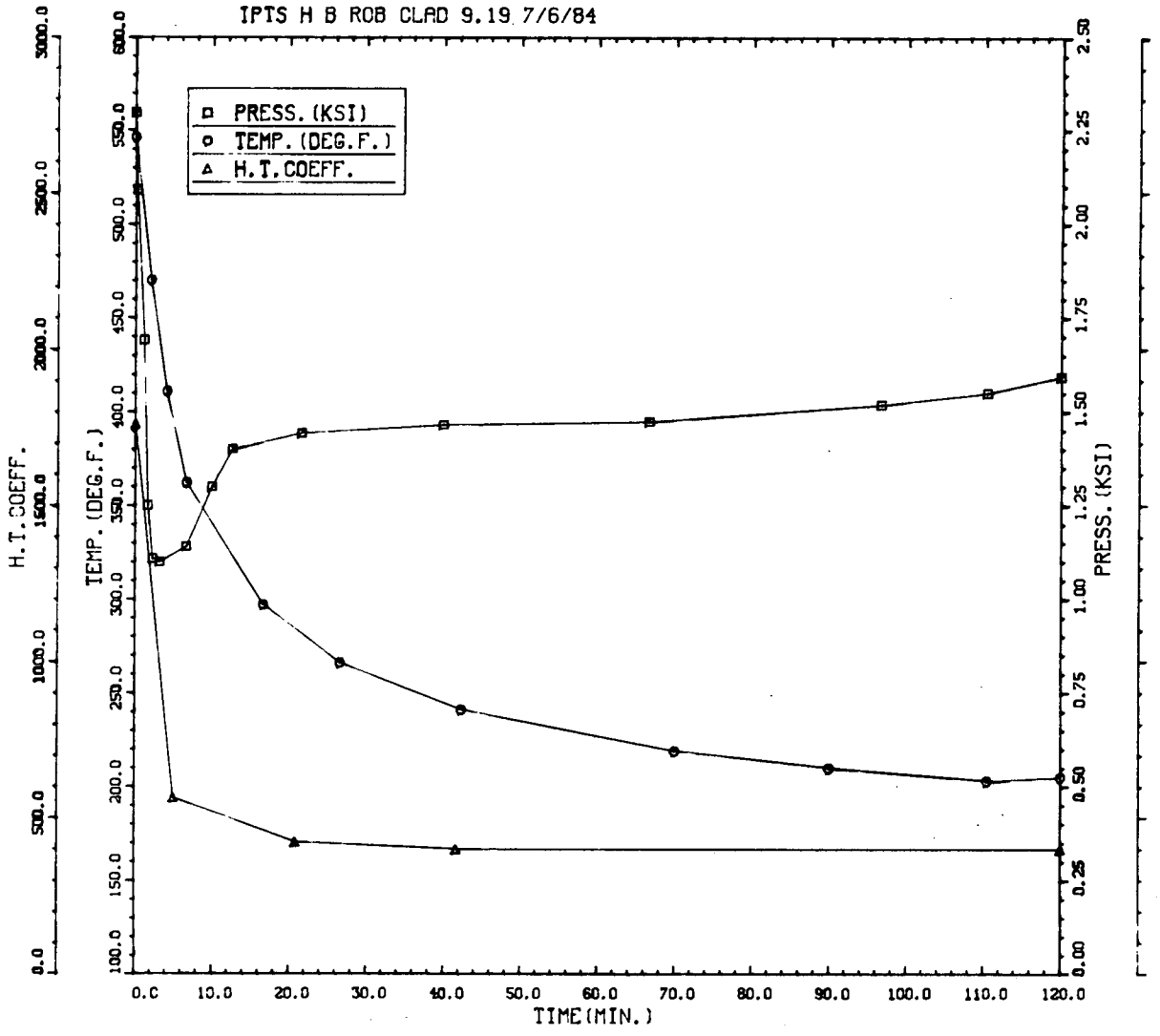

Figure I.163. Transient 9.19B: Primary system pressure, downcomer coolant temperature, and fluid-film heat-transfer coefficient vs time in the transient.

Table I.28. Transient 9.19B: Summary of digital output, including unadjusted $P(F|E)$ values and histogram data for crack depths, times of failure, and $T - RTNDT$ values at tip of crack corresponding to initiation and arrest events

IPTS H B ROB CLAD 9.19 7/6/84 1. FLAWS/IN**3 DRTN(IS) = 211.2

WELD	P(F/E)	95%CI	%ERR	P(INITIA)	N*V	P(F/E)	%ERR	NFAIL	NTRIALS
	----------UNADJUSTED----------					---ADJUSTED----			
1	2.37D-03	2.31D-04	9.73	2.79D-03	1.000	2.37D-03		404	100000
					VESSEL	2.37D-03	9.73		

DEPTHS FOR INITIAL INITIATION (IN)

	0.09	0.26	0.46	0.67	0.90	1.16	1.44	1.74	2.08
NUMBER	2	270	126	54	16	6	1	0	0
PERCENT	0.4	56.8	26.5	11.4	3.4	1.3	0.2	0.0	0.0

TIMES OF FAILURE(MINUTES)

	0.0	10.0	20.0	30.0	40.0	50.0	60.0	70.0	80.0	90.0	100.0	110.0	120.0
PERCENT	0.0	0.0	0.0	0.5	1.7	6.7	15.8	20.3	23.3	11.9	11.9	7.9	

INITIATION T-RTNDT(DEG.F)

	-100.0	-75.0	-50.0	-25.0	0.0	25.0	50.0	75.0	100.0	125.0	150.0	175.0	200.0
NUMBER	0	2	29	165	248	201	193	33	0	0	0	0	
PERCENT	0.0	0.2	3.3	18.9	28.5	23.1	22.2	3.8	0.0	0.0	0.0	0.0	

ARREST T-RTNDT(DEG.F)

	-50.0	-25.0	0.0	25.0	50.0	75.0	100.0	125.0	150.0	175.0	200.0	225.0	250.0
NUMBER	0	0	9	3	1	3	17	233	200	1	0	0	
PERCENT	0.0	0.0	1.9	0.6	0.2	0.6	3.6	49.9	42.8	0.2	0.0	0.0	

ICRKTP = 2 IACCEL = 0 NDLRS = 0 NRTRS = 0 DATE: 11/19/84 TIME: 22.48.58

CPU TIME: 2 MIN 50 SEC

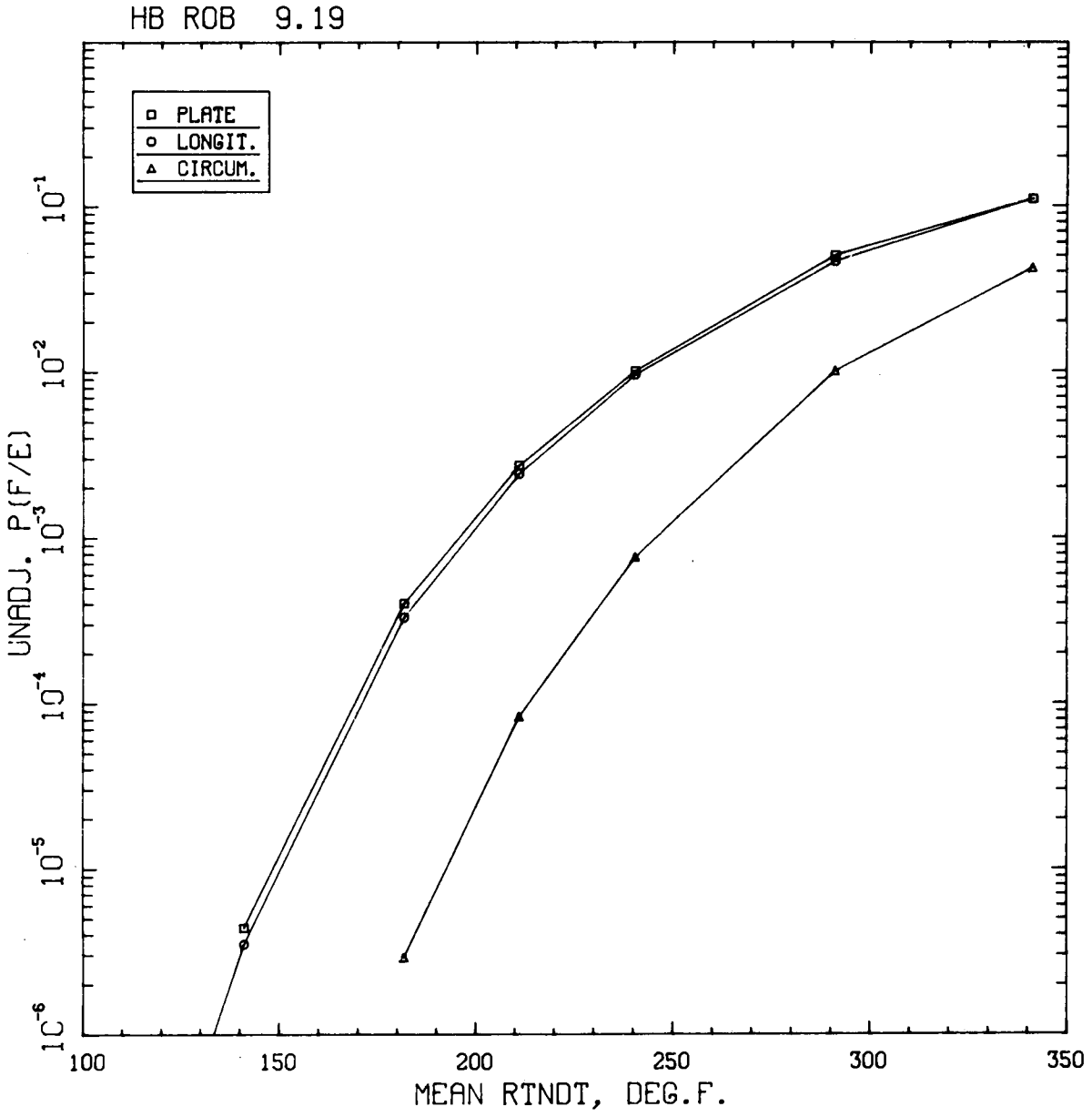

Figure I.164. Transient 9.19B: $\hat{P}_j \int_0^w f(a)\, B(a)\, da$ vs $\overline{RTNDT_s}$ for (2-D, 2-D) and (2-D, 2m) flaw combinations.

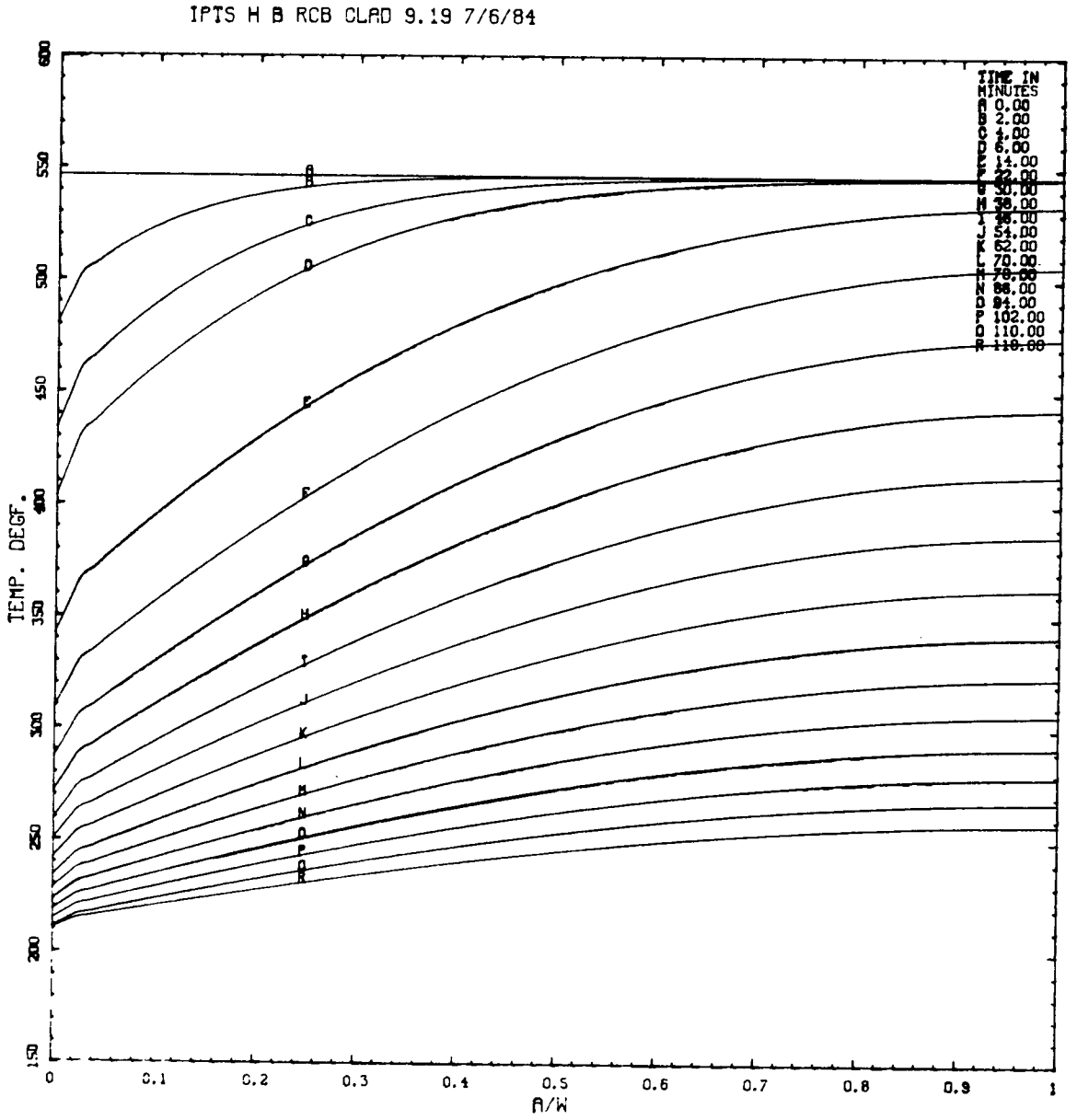

Figure I.165. Transient 9.19B: Vessel wall temperature vs depth in wall (a/w) at various times (t) in transient.

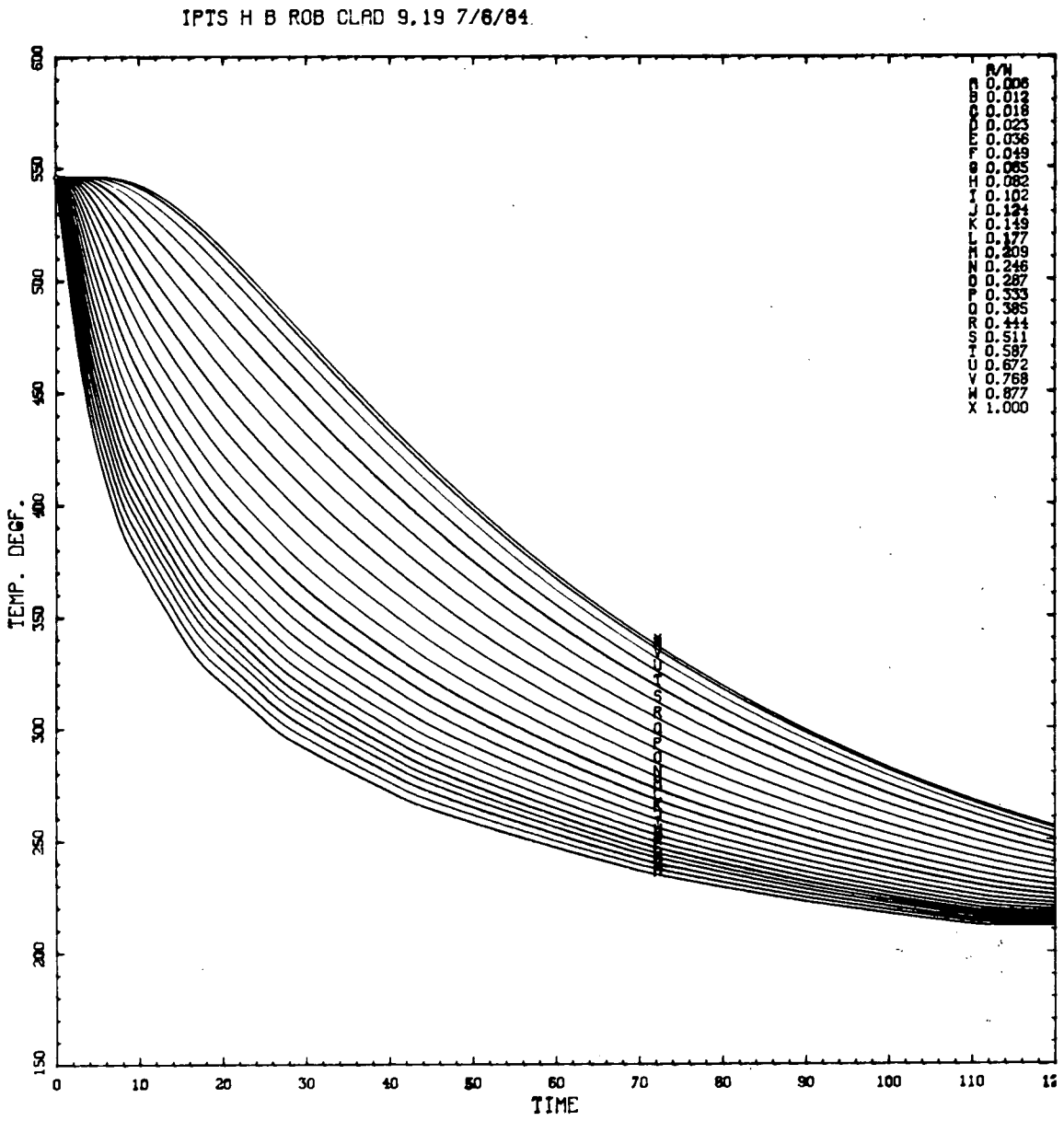

Figure I.166. Transient 9.19B: Vessel wall temperature vs time (t) in transient at various depths in wall (a/w).

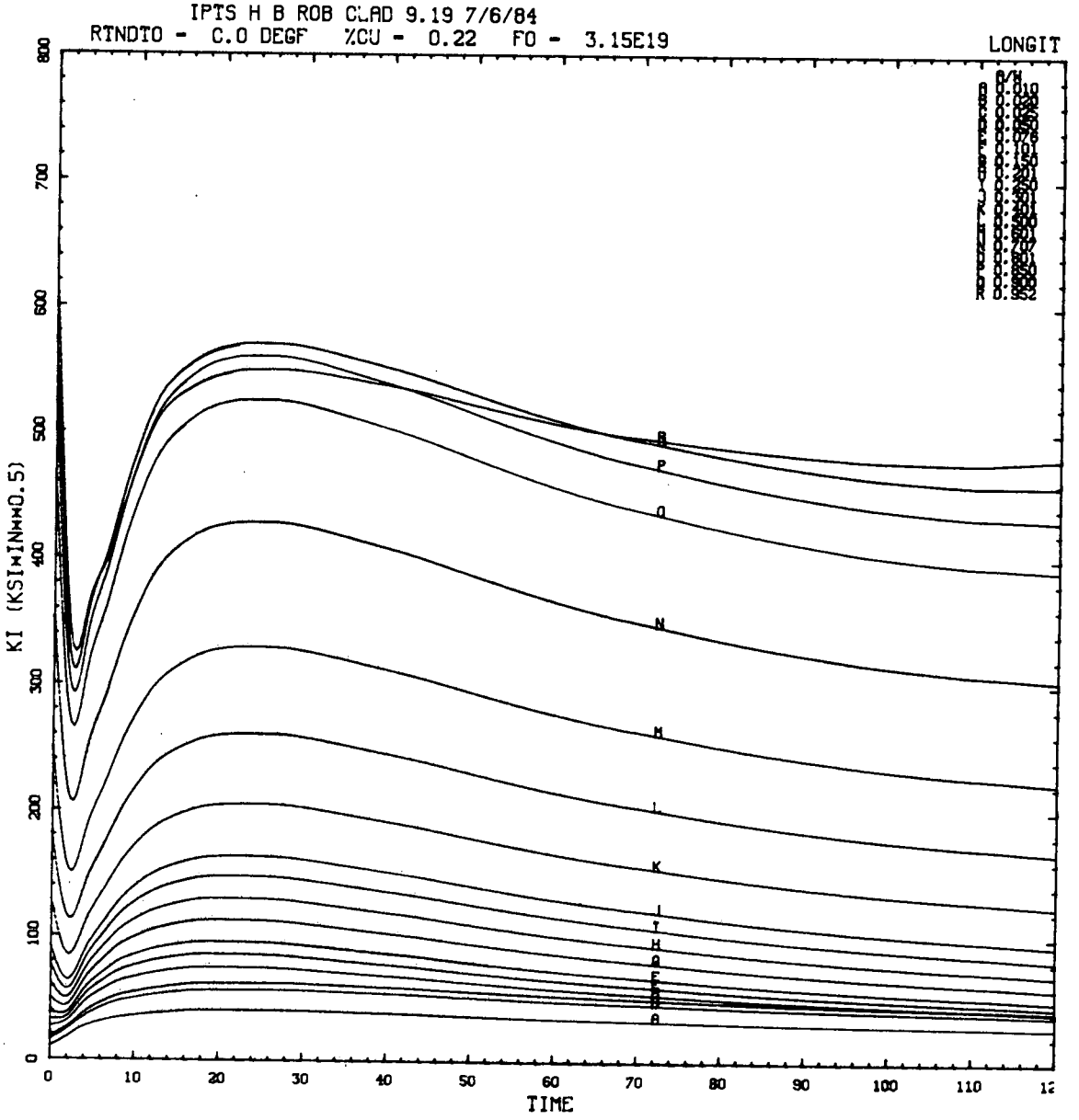

Figure I.167. Transient 9.19B: K_I vs time (t) for various depths in wall (a/w).

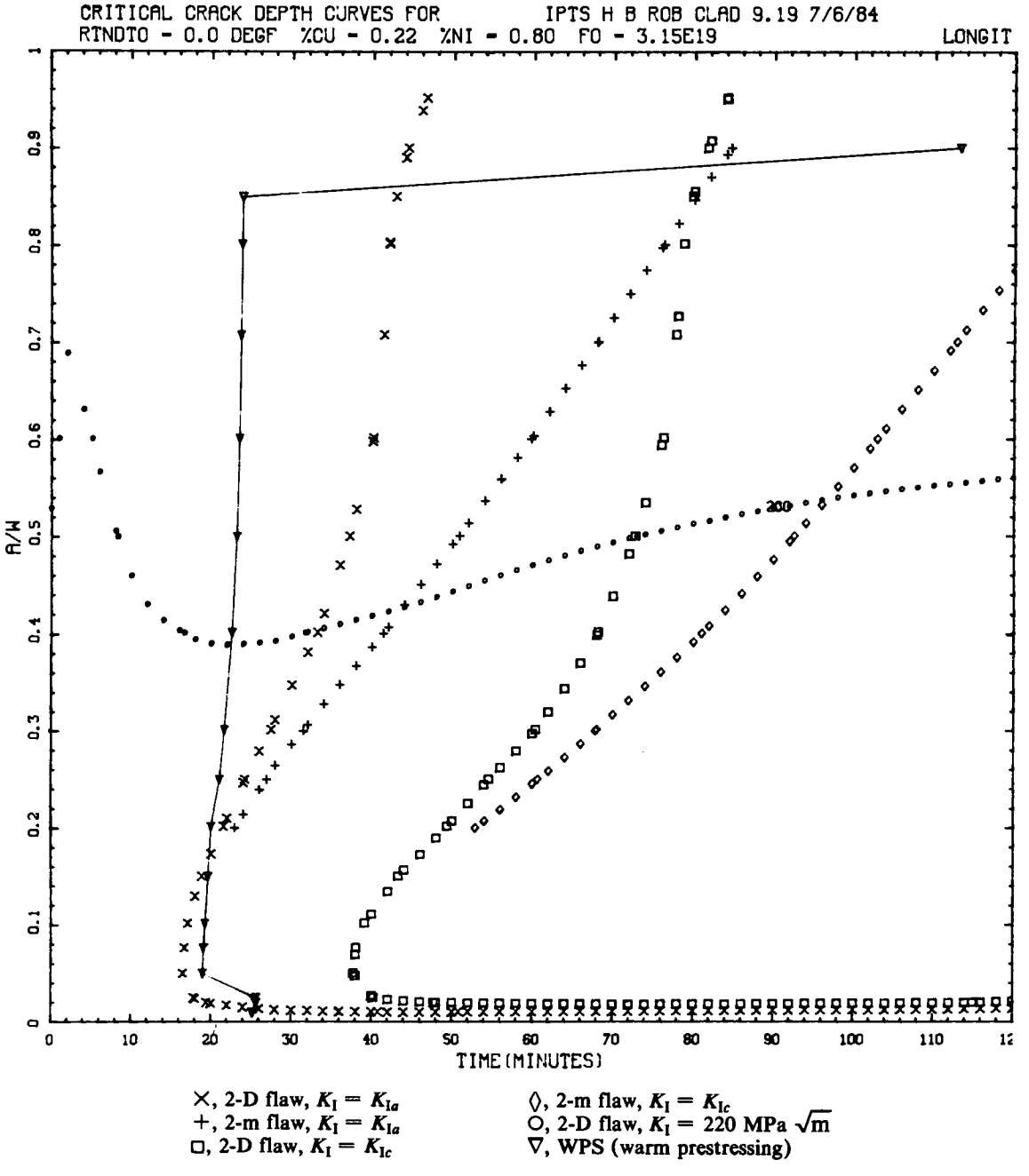

Figure I.168. Transient 9.19B: Critical-crack-depth curves for weld 2-273A based on -2σ values of K_{Ic}, K_{Ia}, and $\Delta RTNDT$, mean values of all other parameters, and 32-EFPY fluences.

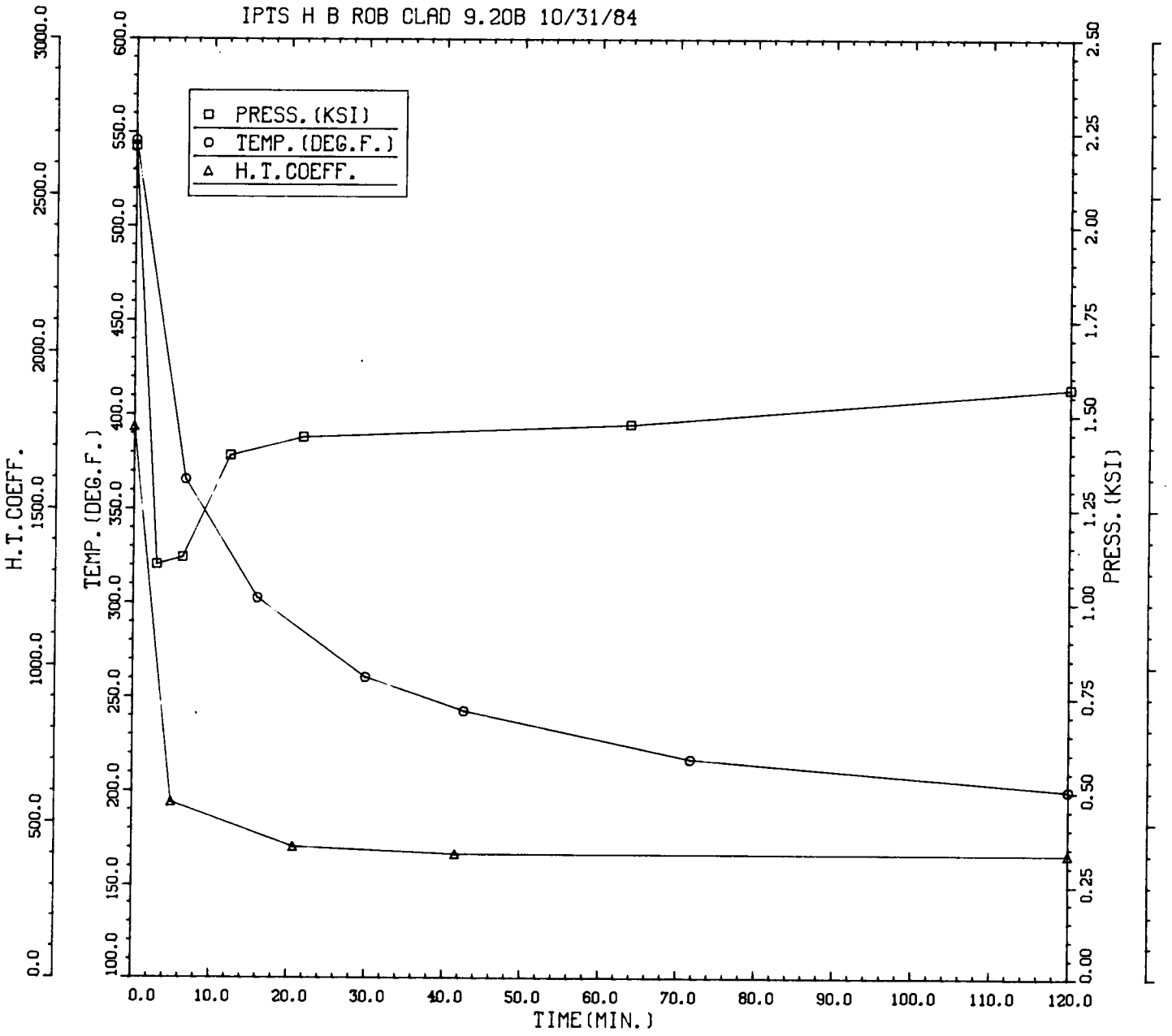

Figure I.169. Transient 9.20B: Primary system pressure, downcomer coolant temperature, and fluid-film heat-transfer coefficient vs time in the transient.

Table I.29. Transient 9.20B: Summary of digital output, including unadjusted $P(F|E)$ values and histogram data for crack depths, times of failure, and $T - RTNDT$ values at tip of crack corresponding to initiation and arrest events

```
IPTS H B ROB CLAD 9.20B 10/31/84                    1. FLAWS/IN**3    DRTN(IS) =  211.2

            -------------UNADJUSTED--------------              ---ADJUSTED----
WELD        P(F/E)      95%CI     %ERR    P(INITIA)  N*V       P(F/E)     %ERR     NFAIL     NTRIALS

 1          2.53D-03   2.51D-04   9.93    2.92D-03  1.000    2.53D-03                388       90000

                                                     VESSEL   2.53D-03    9.93


DEPTHS FOR INITIAL INITIATION (IN)
                 0.09  0.26  0.46  0.67  0.90  1.16  1.44  1.74  2.08
    NUMBER        0   251   116    58    18     4     1     0     0
    PERCENT     0.0  56.0  25.9  12.9   4.0   0.9   0.2   0.0   0.0


TIMES OF FAILURE(MINUTES)
                 0.0  10.0  20.0  30.0  40.0  50.0  60.0  70.0  80.0  90.0 100.0 110.0 120.0
   PERCENT       0.0   0.0   0.0   0.0   2.1   7.2  18.6  19.3  17.5  13.1  11.3  10.8


 INITIATION T-RTNDT(DEG.F)
              -100.0 -75.0 -50.0 -25.0   0.0  25.0  50.0  75.0 100.0 125.0 150.0 175.0 200.0
   NUMBER          0     1    29   169   224   173   177    30     0     0     0     0
   PERCENT       0.0   0.1   3.6  21.0  27.9  21.5  22.0   3.7   0.0   0.0   0.0   0.0


 ARREST T-RTNDT(DEG.F)
              -50.0 -25.0   0.0  25.0  50.0  75.0 100.0 125.0 150.0 175.0 200.0 225.0 250.0
   NUMBER          0     1     6     3     1     4    11   201   138     0     0     0
   PERCENT       0.0   0.2   1.4   0.7   0.2   1.0   2.7  48.4  45.3   0.0   0.0   0.0


ICRKTP = 2   IACCEL = 0   NDLRS = 0   NRTRS = 0   DATE: 11/19/84   TIME: 22.50.57

CPU TIME:  2 MIN 33 SEC
```

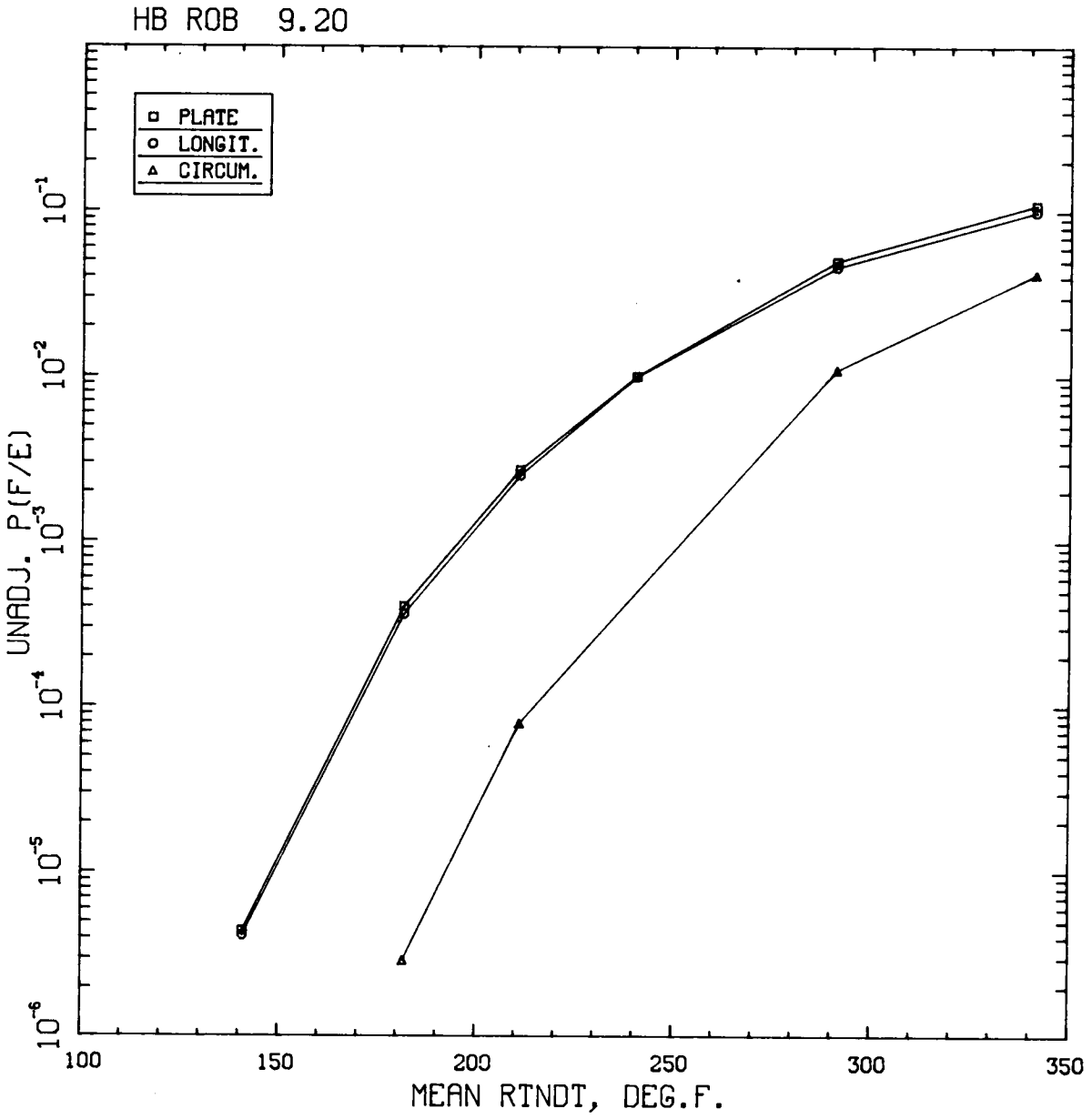

Figure I.170. Transient 9.20B: $\hat{P}_j \int_0^w f(a)\, B(a)\, da$ vs $\overline{RTNDT_s}$ for (2-D, 2-D) and (2-D, 2m) flaw combinations.

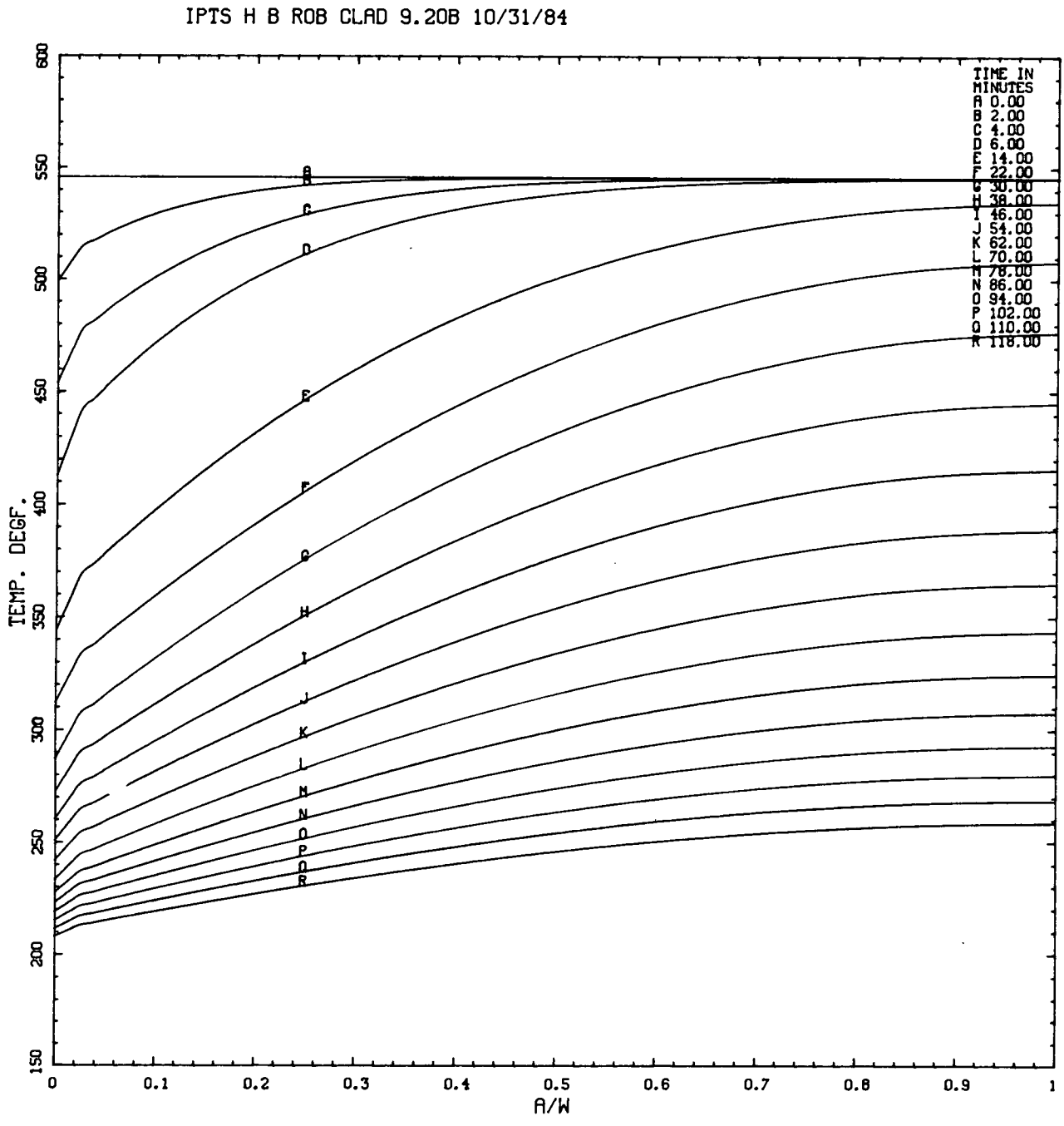

Figure I.171. Transient 9.20B: Vessel wall temperature vs depth in wall (a/w) at various times (t) in transient.

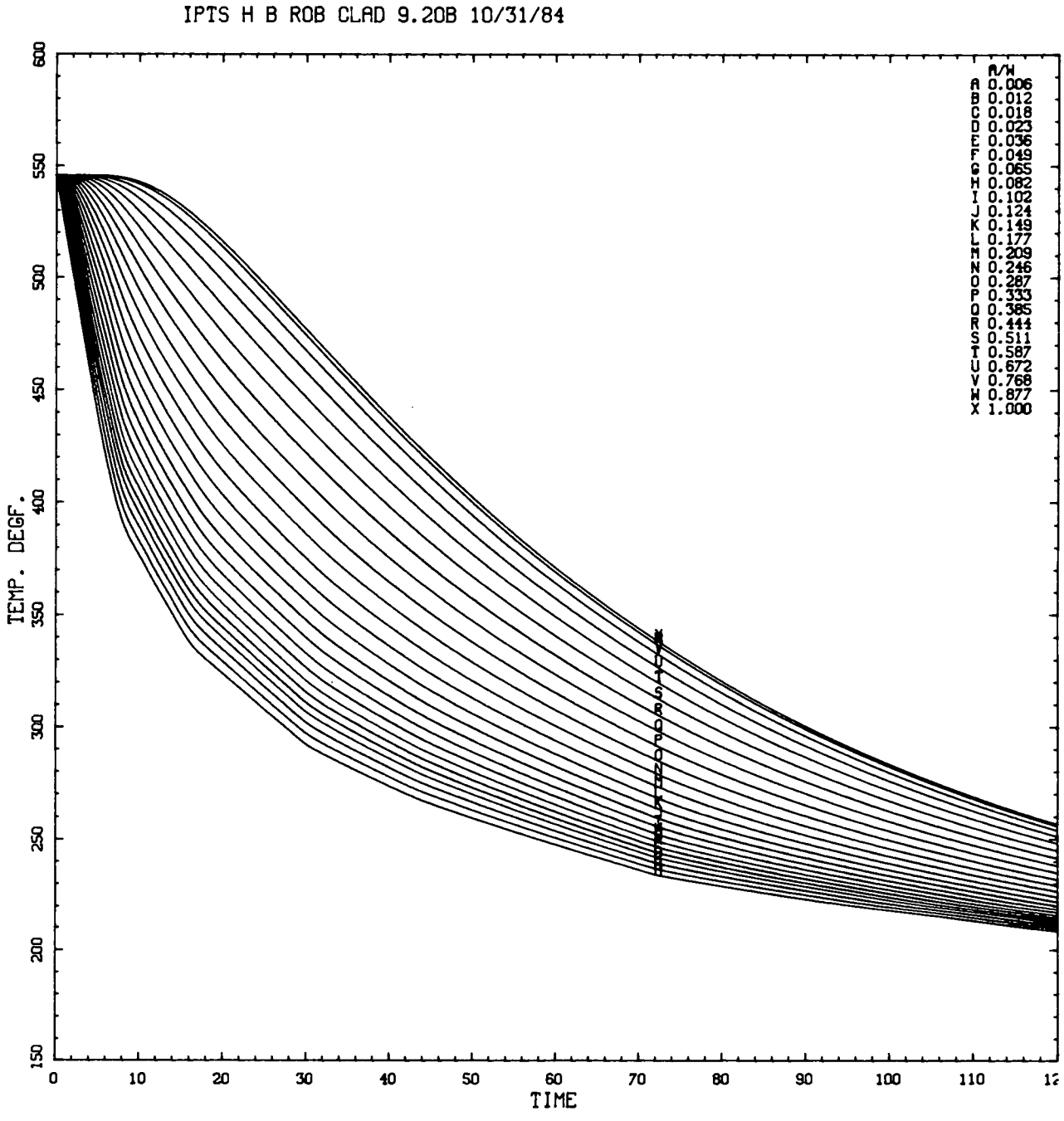

Figure I.172. Transient 9.20B: Vessel wall temperature vs time (t) in transient at various depths in wall (a/w).

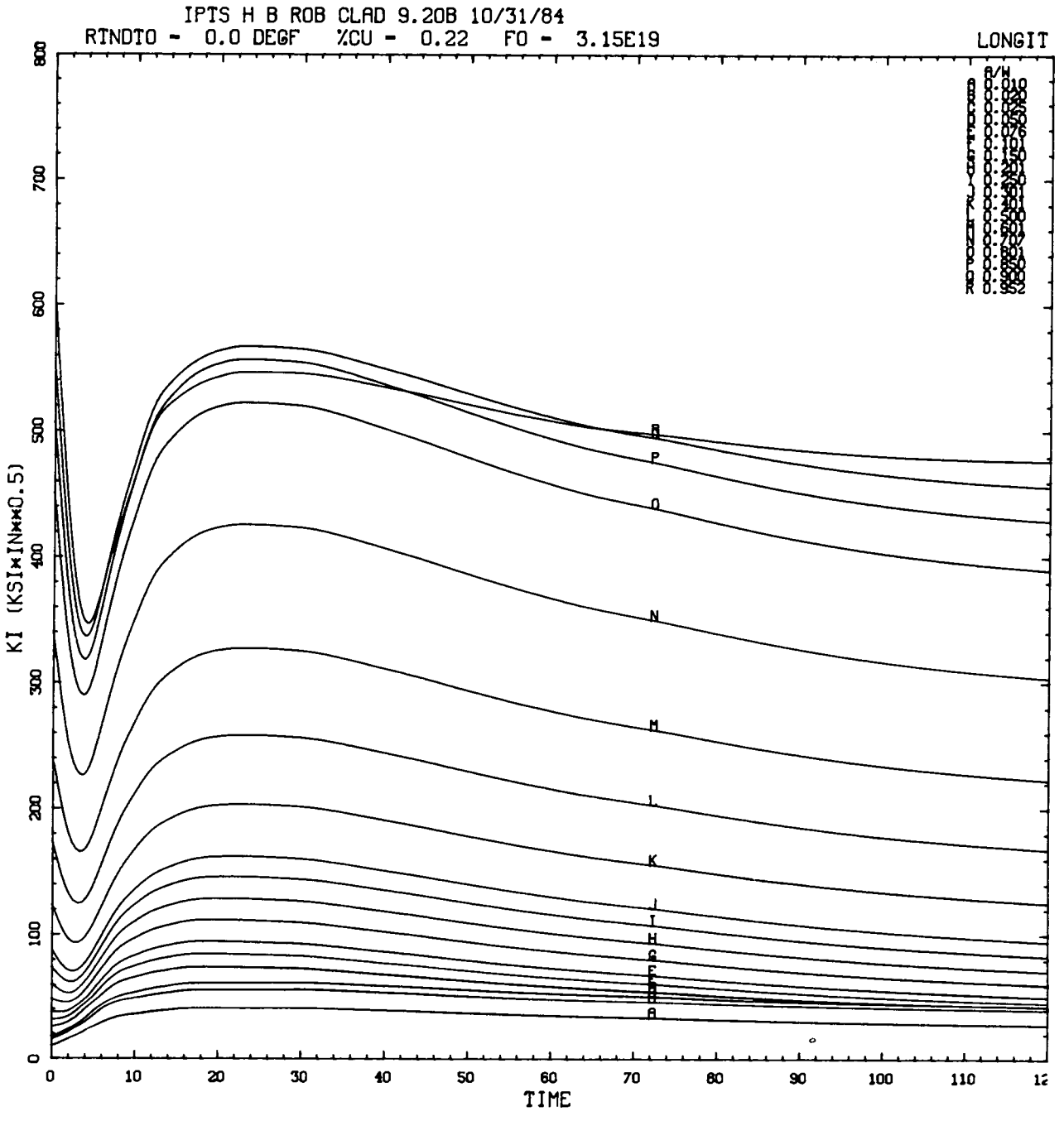

Figure I.173. Transient 9.20B: K_I vs time (t) for various depths in wall (a/w).

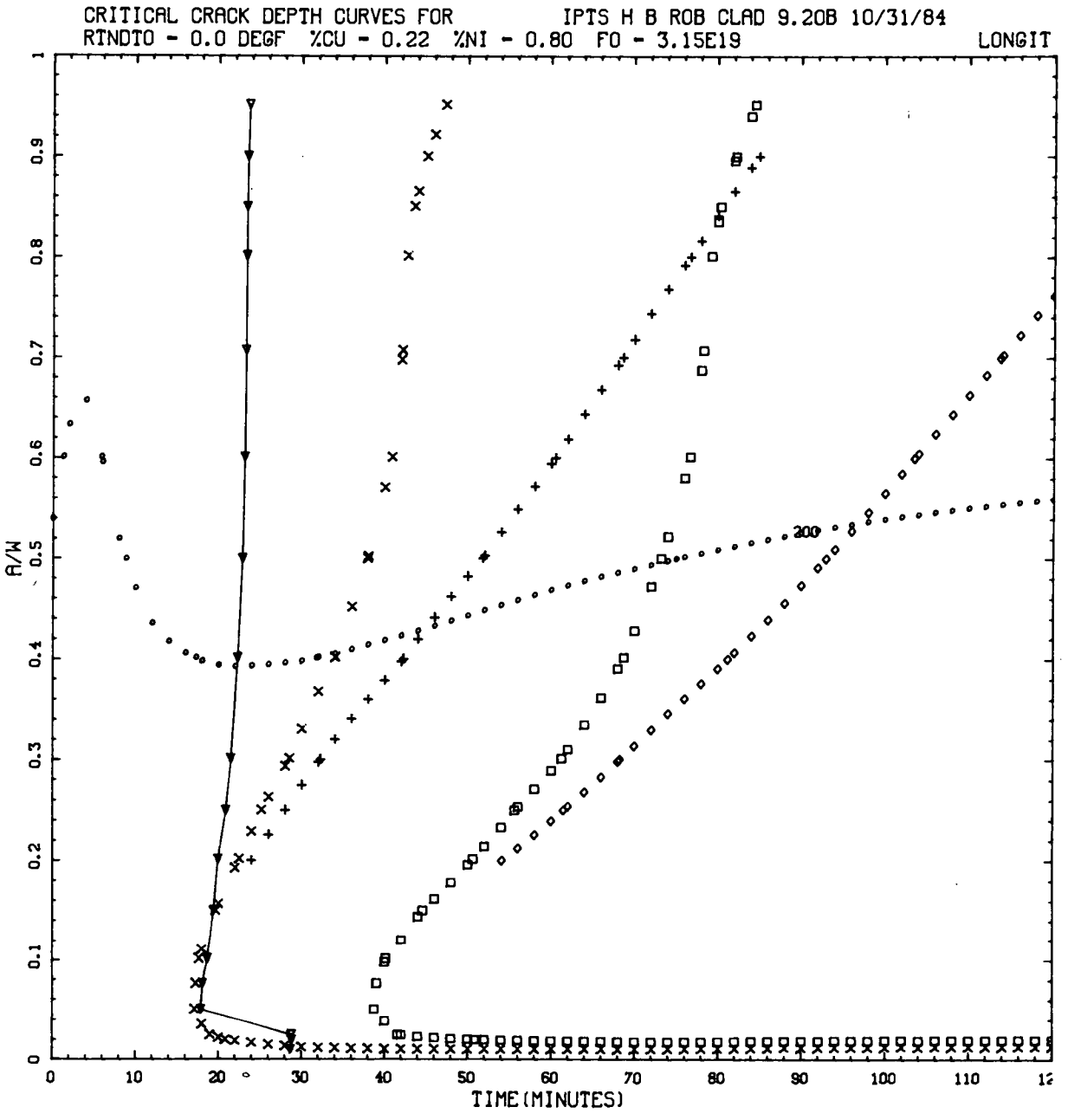

×, 2-D flaw, $K_I = K_{Ia}$
+, 2-m flaw, $K_I = K_{Ia}$
□, 2-D flaw, $K_I = K_{Ic}$
◊, 2-m flaw, $K_I = K_{Ic}$
O, 2-D flaw, $K_I = 220$ MPa $\sqrt{m}$
∇, WPS (warm prestressing)

Figure I.174. Transient 9.20B: Critical-crack-depth curves for weld 2-273A based on -2σ values of K_{Ic}, K_{Ia}, and $\Delta RTNDT$, mean values of all other parameters, and 32-EFPY fluences.

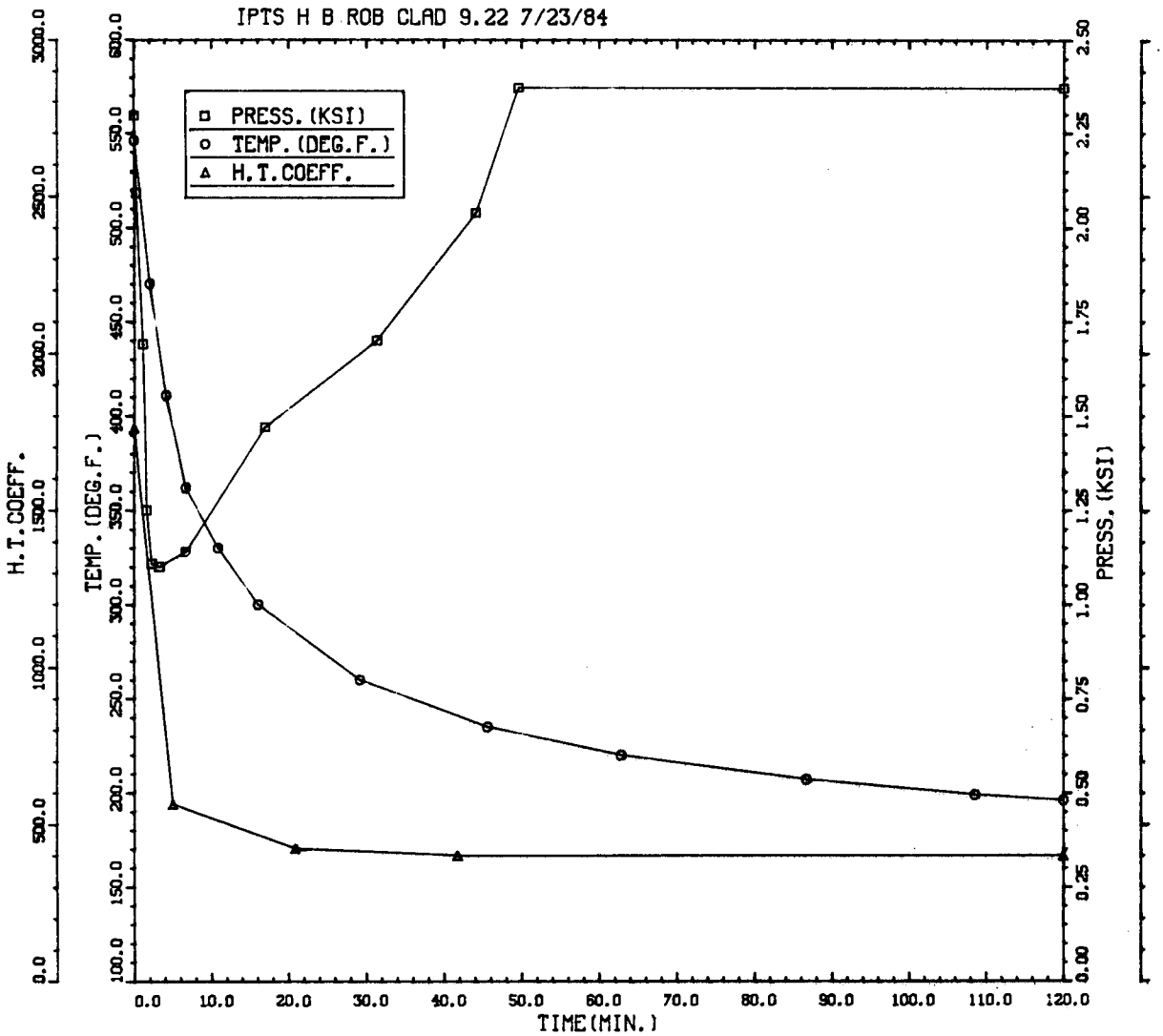

Figure I.175. Transient 9.22B: Primary system pressure, downcomer coolant temperature, and fluid-film heat-transfer coefficient vs time in the transient.

Table I.30. Transient 9.22B: Summary of digital output, including unadjusted $P(F|E)$ values and histogram data for crack depths, times of failure, and $T - RTNDT$ values at tip of crack corresponding to initiation and arrest events

IPTS H B ROB CLAD 9.22 7/23/84 1. FLAWS/IN**3 DRTN(IS) = 211.2

WELD	UNADJUSTED P(F/E)	95%CI	%ERR	P(INITIA)	N*V	ADJUSTED P(F/E)	%ERR	NFAIL	NTRIALS
1	1.20D-02	1.15D-03	9.58	1.22D-02	1.000	1.20D-02		410	20000
					VESSEL	1.20D-02	9.58		

DEPTHS FOR INITIAL INITIATION (IN)

	0.09	0.26	0.46	0.67	0.90	1.16	1.44	1.74	2.08
NUMBER	6	249	98	45	13	3	0	0	0
PERCENT	1.4	60.1	23.7	10.9	3.1	0.7	0.0	0.0	0.0

TIMES OF FAILURE(MINUTES)

	0.0	10.0	20.0	30.0	40.0	50.0	60.0	70.0	80.0	90.0	100.0	110.0	120.0
PERCENT	0.0	0.0	0.2	2.7	25.1	23.7	21.0	12.0	8.8	3.4	2.0	1.2	

INITIATION T-RTNDT(DEG.F)

	-100.0	-75.0	-50.0	-25.0	0.0	25.0	50.0	75.0	100.0	125.0	150.0	175.0	200.0
NUMBER	0	3	28	150	172	67	67	42	1	0	0	0	
PERCENT	0.0	0.6	5.3	28.3	32.5	12.6	12.6	7.9	0.2	0.0	0.0	0.0	

ARREST T-RTNDT(DEG.F)

	-50.0	-25.0	0.0	25.0	50.0	75.0	100.0	125.0	150.0	175.0	200.0	225.0	250.0
NUMBER	0	0	1	0	0	0	2	16	97	4	0	0	
PERCENT	0.0	0.0	0.8	0.0	0.0	0.0	1.7	13.3	80.8	3.3	0.0	0.0	

ICRKTP = 2 IACCEL = 0 NDLRS = 0 NRTRS = 0 DATE: 11/19/84 TIME: 22.50.26

CPU TIME: 0 MIN 41 SEC

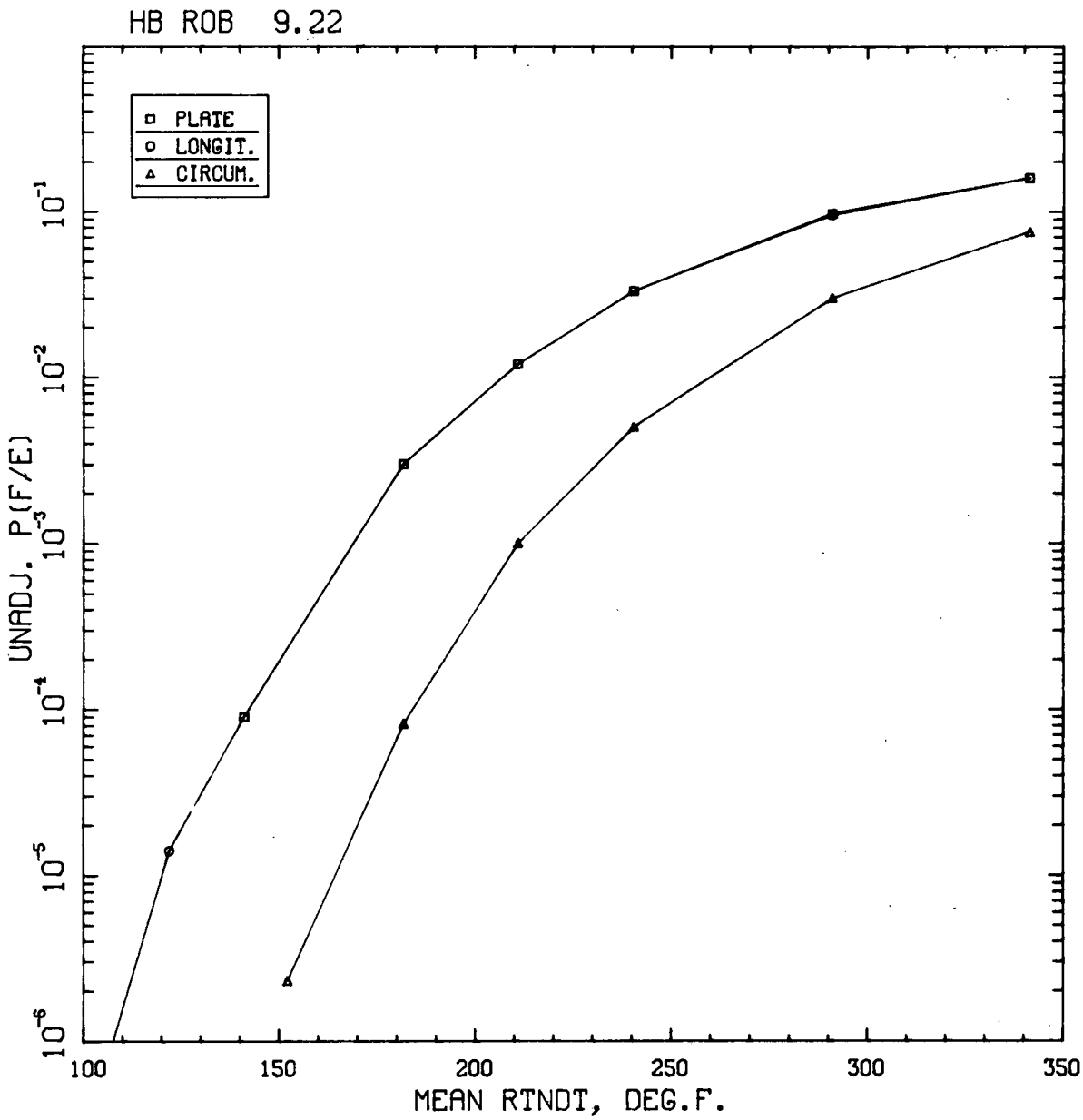

Figure I.176. Transient 9.22B: $\hat{P}_j \int_0^w f(a)\, B(a)\, da$ vs $\overline{RTNDT}$, for (2-D, 2-D) and (2-D, 2m) flaw combinations.

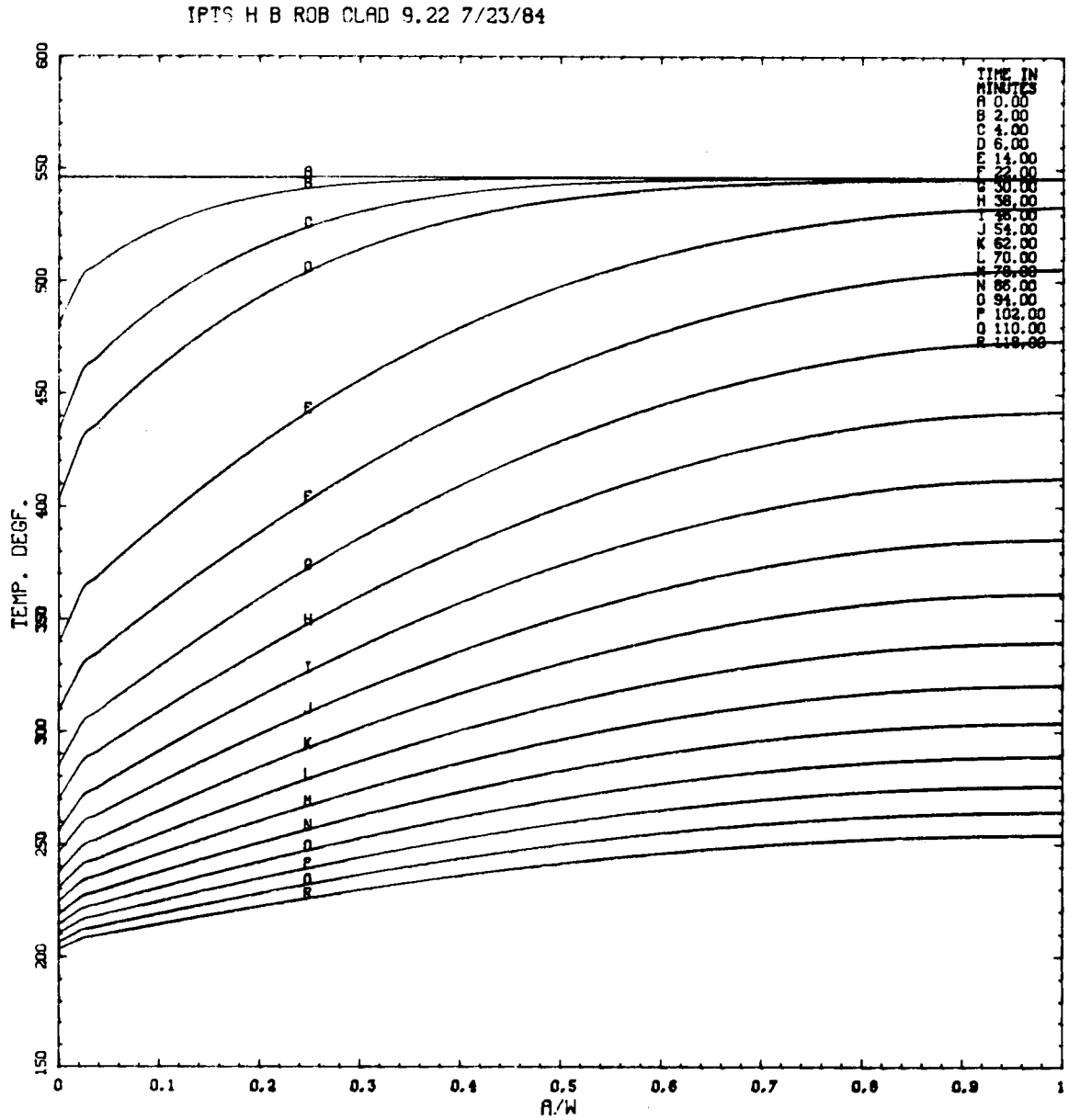

Figure I.177. Transient 9.22B: Vessel wall temperature vs depth in wall (a/w) at various times (t) in transient.

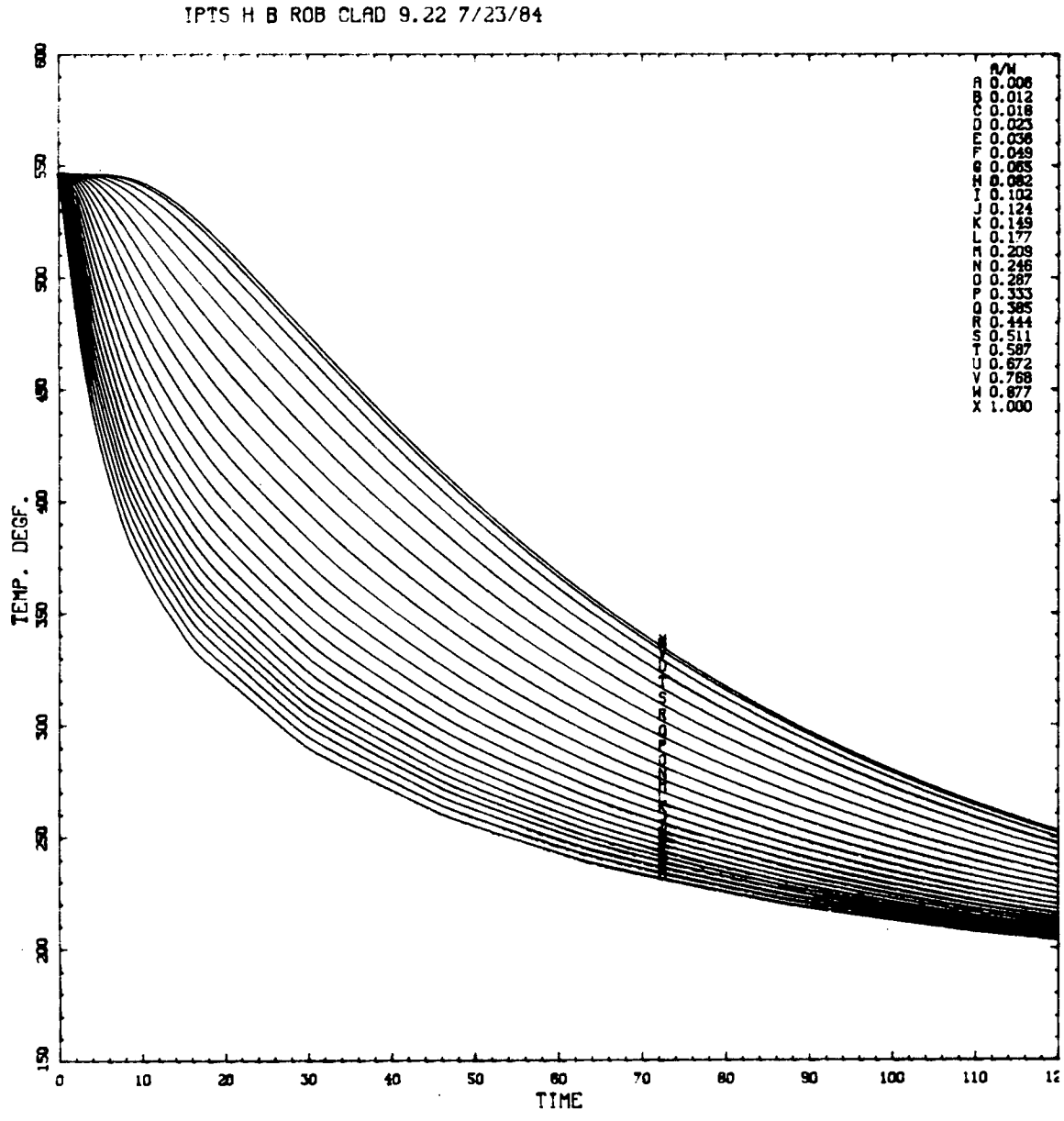

Figure I.178. Transient 9.22B: Vessel wall temperature vs time (t) in transient at various depths in wall (a/w).

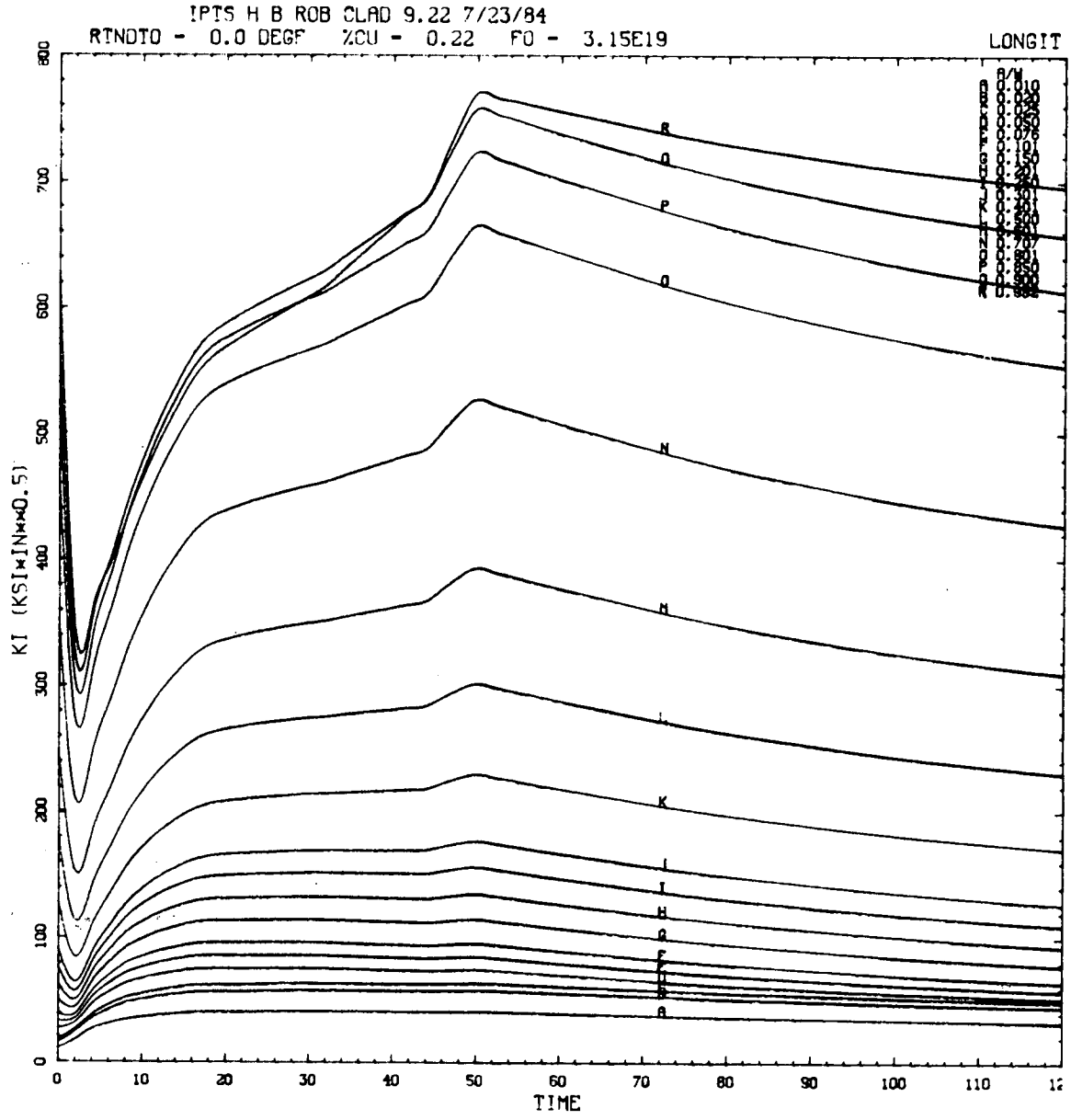

Figure I.179. Transient 9.22B: K_I vs time (t) for various depths in wall (a/w).

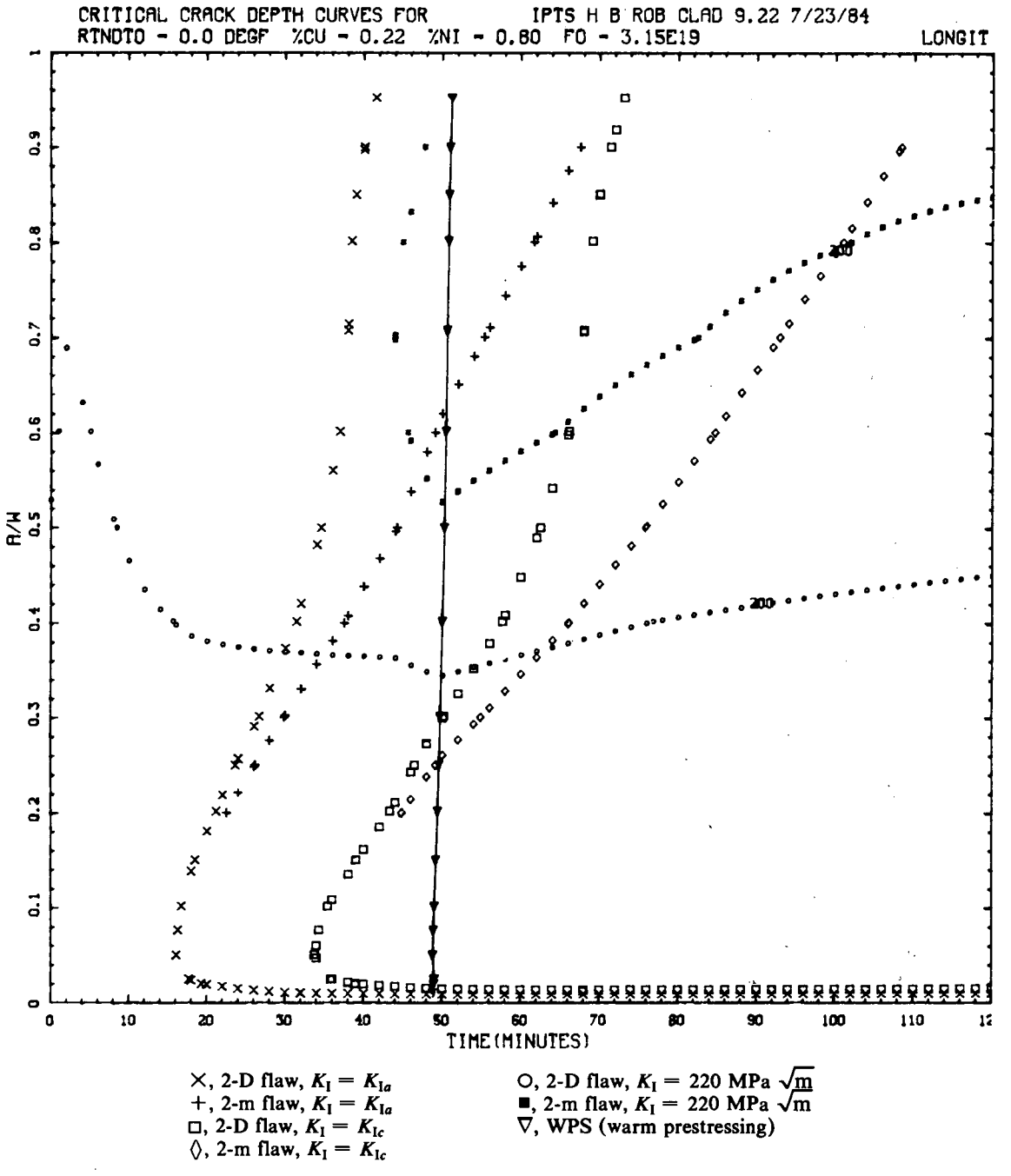

Figure I.180. Transient 9.22B: Critical-crack-depth curves for weld 2-273A based on -2σ values of K_{Ic}, K_{Ia}, and $\Delta RTNDT$, mean values of all other parameters, and 32-EFPY fluences.

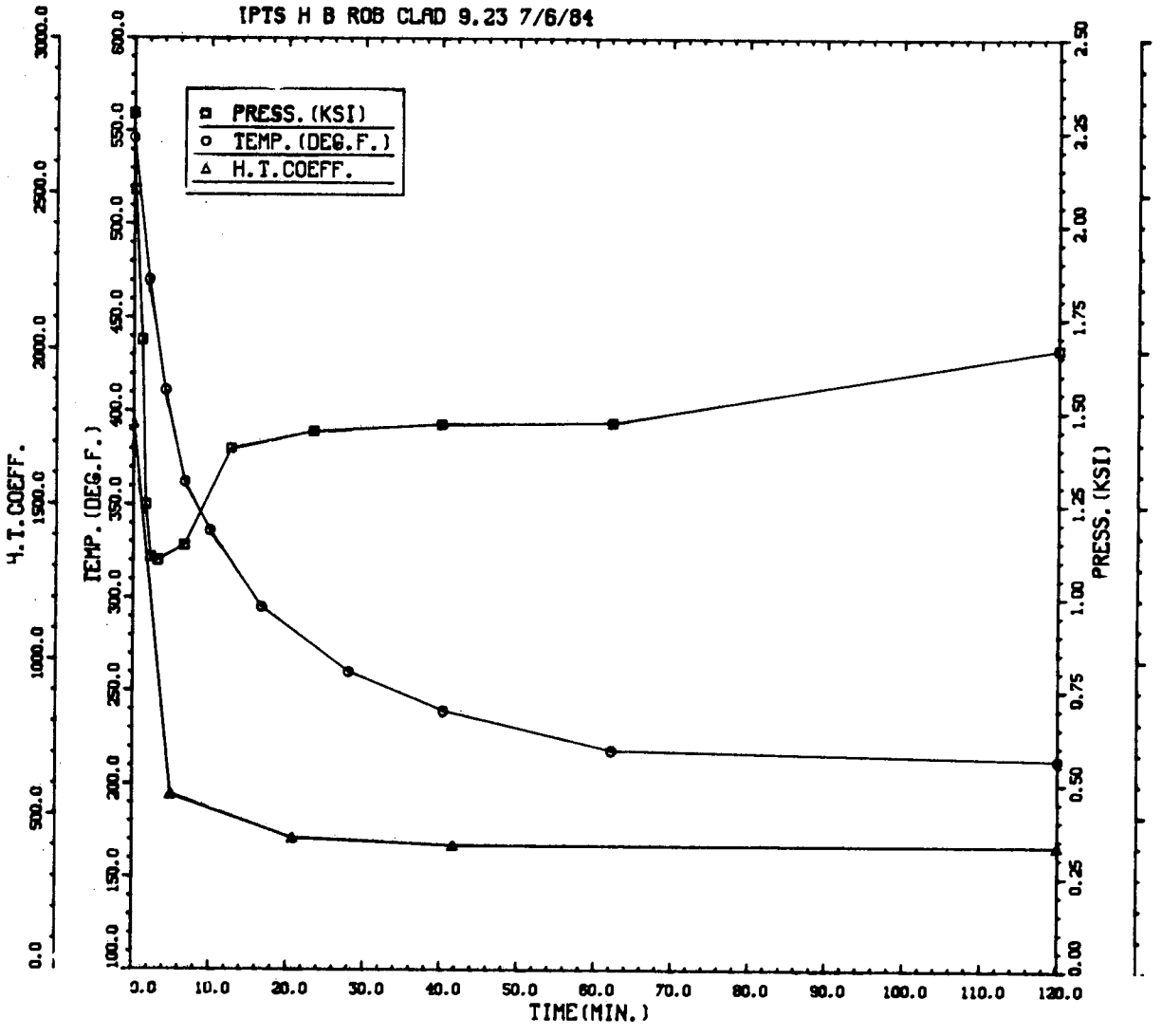

Figure I.181. Transient 9.23B: Primary system pressure, downcomer coolant temperature, and fluid-film heat-transfer coefficient vs time in the transient.

Table I.31. Transient 9.23B: Summary of digital output, including unadjusted $P(F|E)$ values and histogram data for crack depths, times of failure, and $T - RTNDT$ values at tip of crack corresponding to initiation and arrest events

IPTS H B ROB CLAD 9.23 7/6/84 1. FLAWS/IN**3 DRTN(IS) = 211.2

WELD	UNADJUSTED P(F/E)	95%CI	%ERR	P(INITIA)	N*V	ADJUSTED P(F/E)	%ERR	NFAIL	NTRIALS
1	3.22D-03	3.21D-04	9.97	3.86D-03	1.000	3.22D-03		384	70000
					VESSEL	3.22D-03	9.97		

DEPTHS FOR INITIAL INITIATION (IN)

	0.09	0.26	0.46	0.67	0.90	1.16	1.44	1.74	2.08
NUMBER	4	272	119	51	11	3	0	0	0
PERCENT	0.9	59.1	25.9	11.1	2.4	0.7	0.0	0.0	0.0

TIMES OF FAILURE(MINUTES)

	0.0	10.0	20.0	30.0	40.0	50.0	60.0	70.0	80.0	90.0	100.0	110.0	120.0
PERCENT	0.0	0.0	0.0	0.3	2.6	8.6	17.2	19.0	18.5	14.6	12.2	7.0	

INITIATION T-RTNDT(DEG.F)

	-100.0	-75.0	-50.0	-25.0	0.0	25.0	50.0	75.0	100.0	125.0	150.0	175.0	200.0
NUMBER	0	3	36	156	241	174	194	41	1	0	0	0	
PERCENT	0.0	0.4	4.3	18.4	28.5	20.6	22.9	4.8	0.1	0.0	0.0	0.0	

ARREST T-RTNDT(DEG.F)

	-50.0	-25.0	0.0	25.0	50.0	75.0	100.0	125.0	150.0	175.0	200.0	225.0	250.0
NUMBER	0	0	3	1	0	0	10	197	250	1	0	0	
PERCENT	0.0	0.0	0.6	0.2	0.0	0.0	2.2	42.6	54.1	0.2	0.0	0.0	

ICRKTP = 2 IACCEL = 0 NDLRS = 0 NRTRS = 0 DATE: 10/31/84 TIME: 01.46.46

CPU TIME: 2 MIN 1 SEC

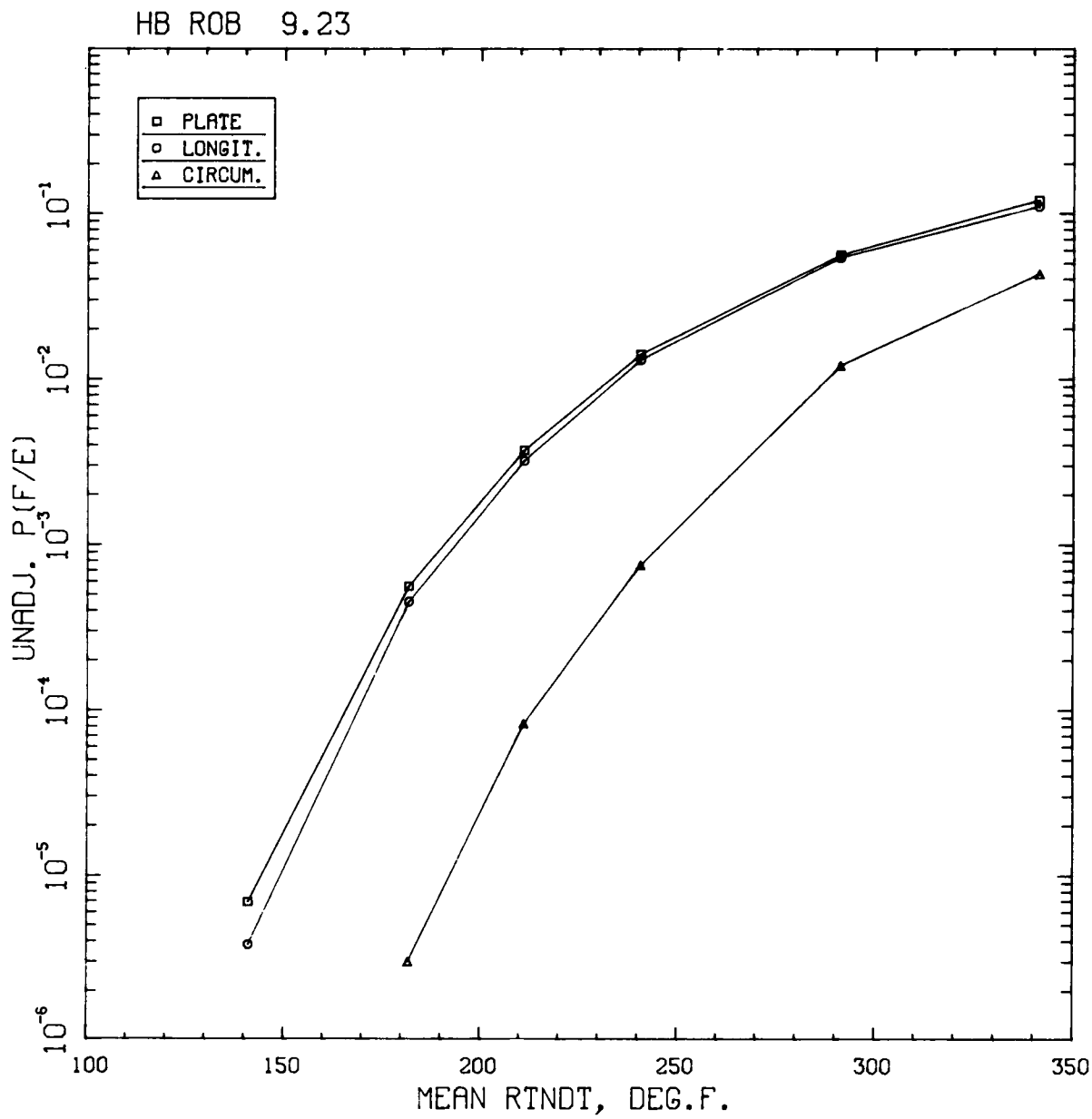

Figure I.182. Transient 9.23B: $\hat{P}_j \int_0^w f(a)\, B(a)\, da$ vs $\overline{RTNDT_s}$ for (2-D, 2-D) and (2-D, 2m) flaw combinations.

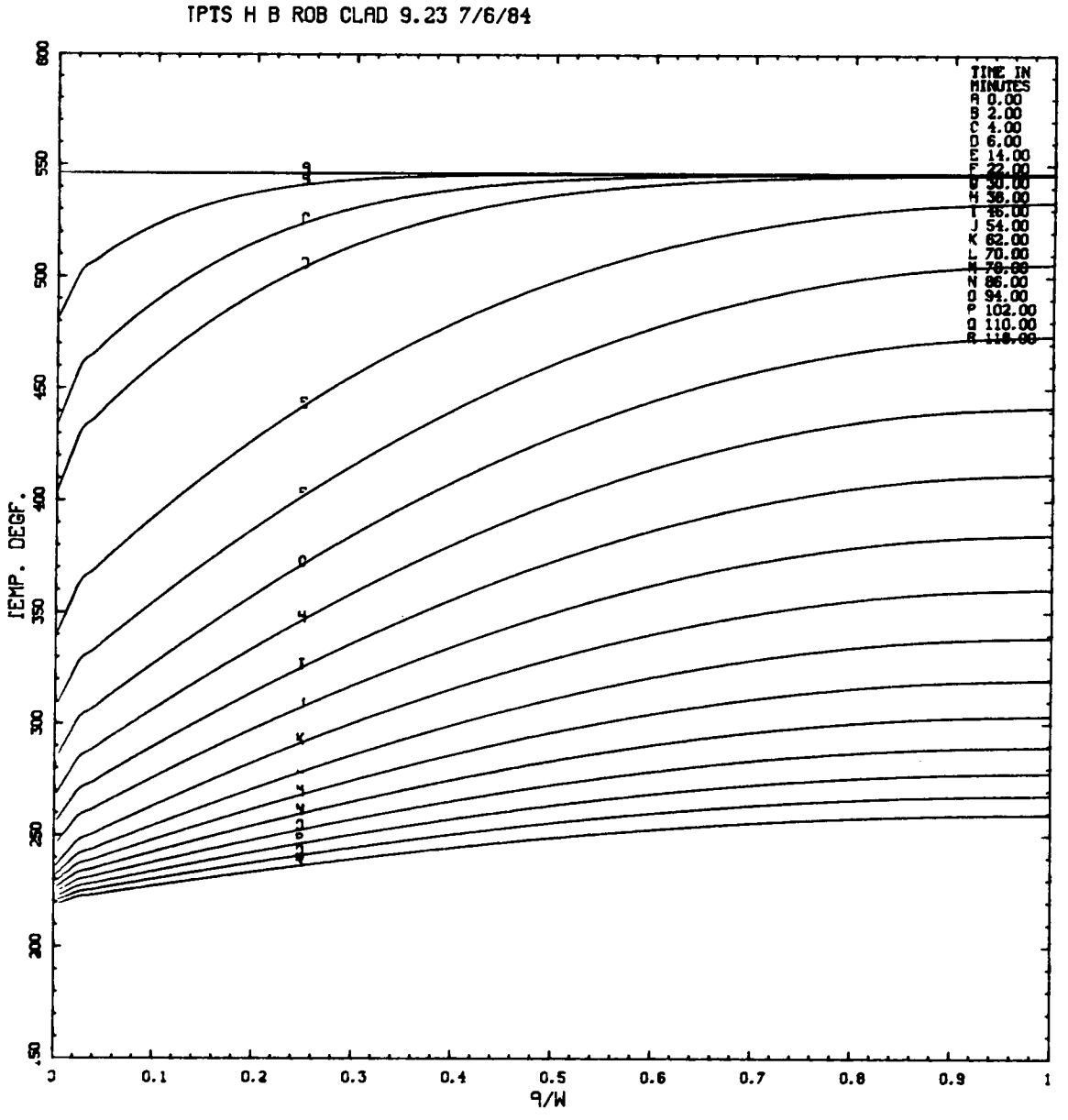

Figure I.183. Transient 9.23B: Vessel wall temperature vs depth in wall (a/w) at various times (t) in transient.

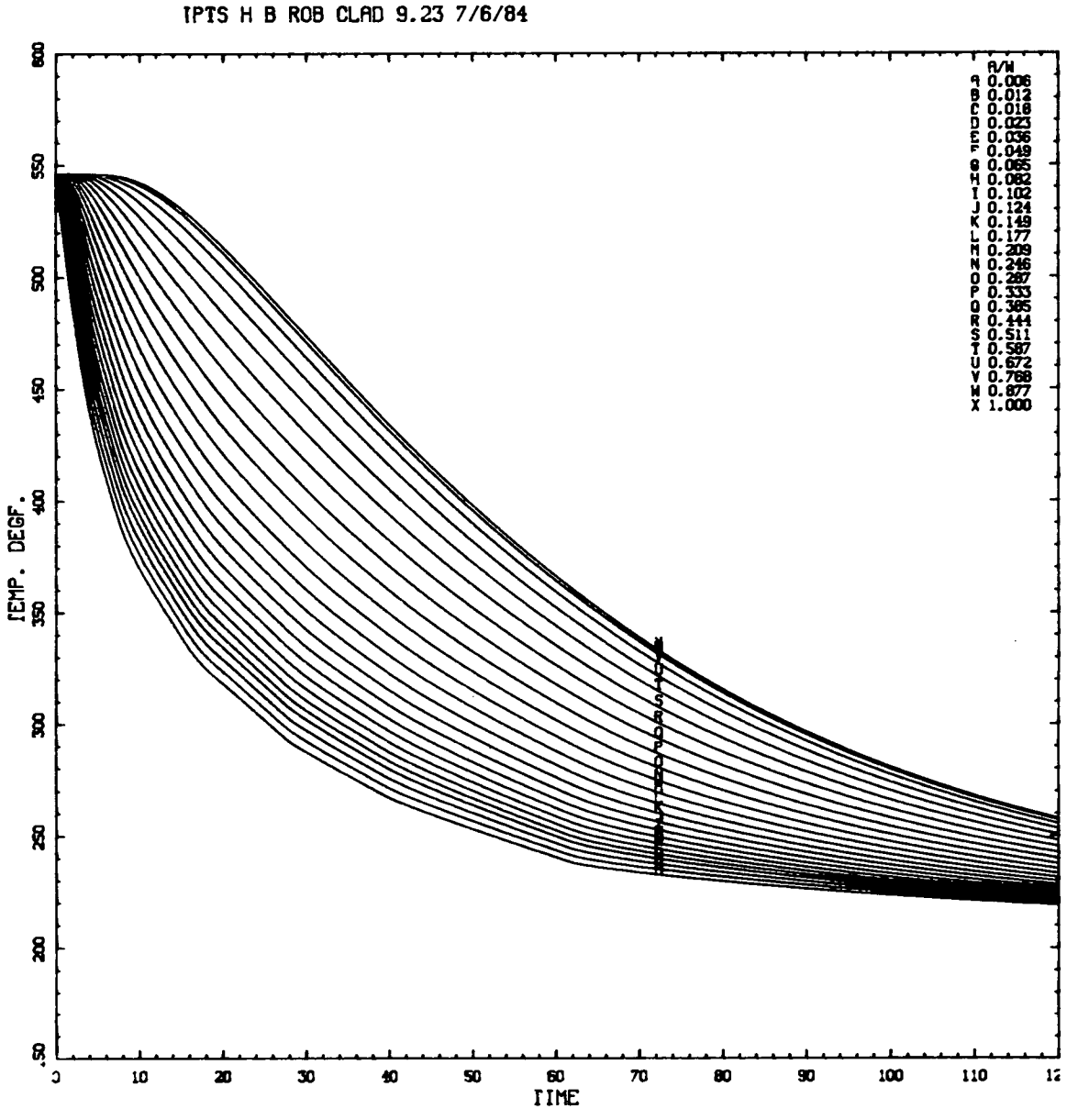

Figure I.184. Transient 9.23B: Vessel wall temperature vs time (t) in transient at various depths in wall (a/w).

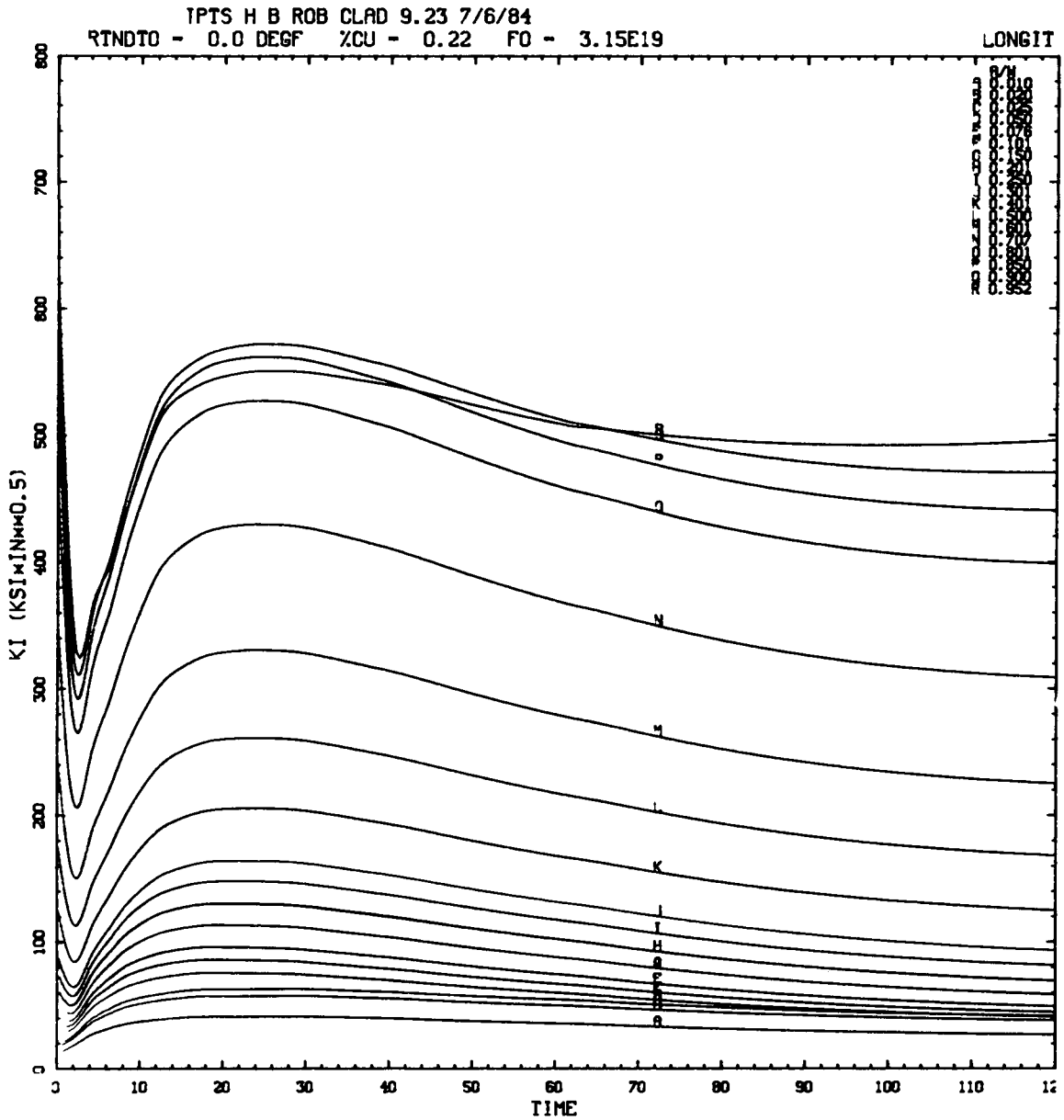

Figure I.185. Transient 9.23B: K_I vs time (t) for various depths in wall (a/w).

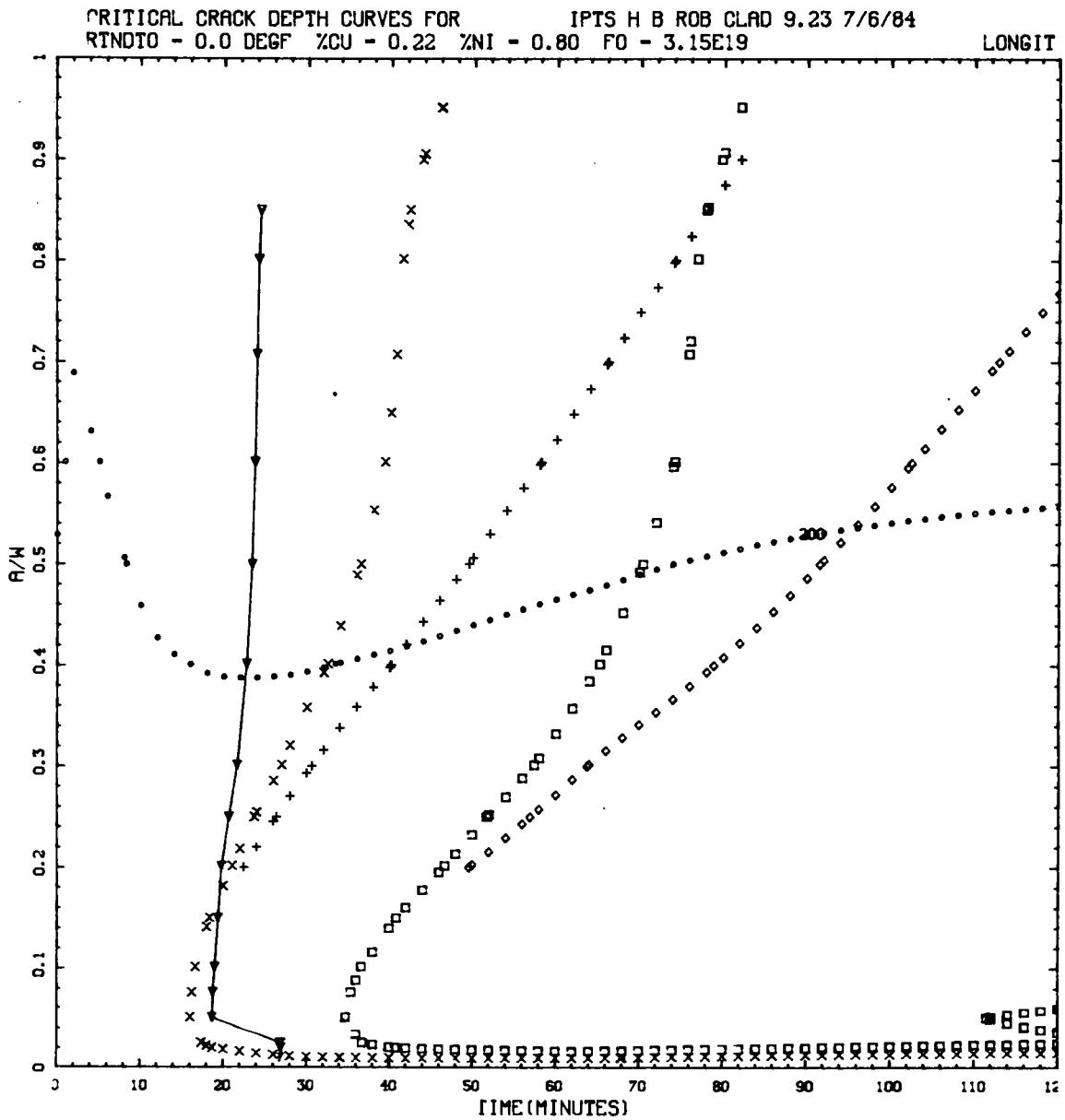

Figure I.186. Transient 9.23B: Critical-crack-depth curves for weld 2-273A based on -2σ values of K_{Ic}, K_{Ia}, and $\Delta RTNDT$, mean values of all other parameters, and 32-EFPY fluences.

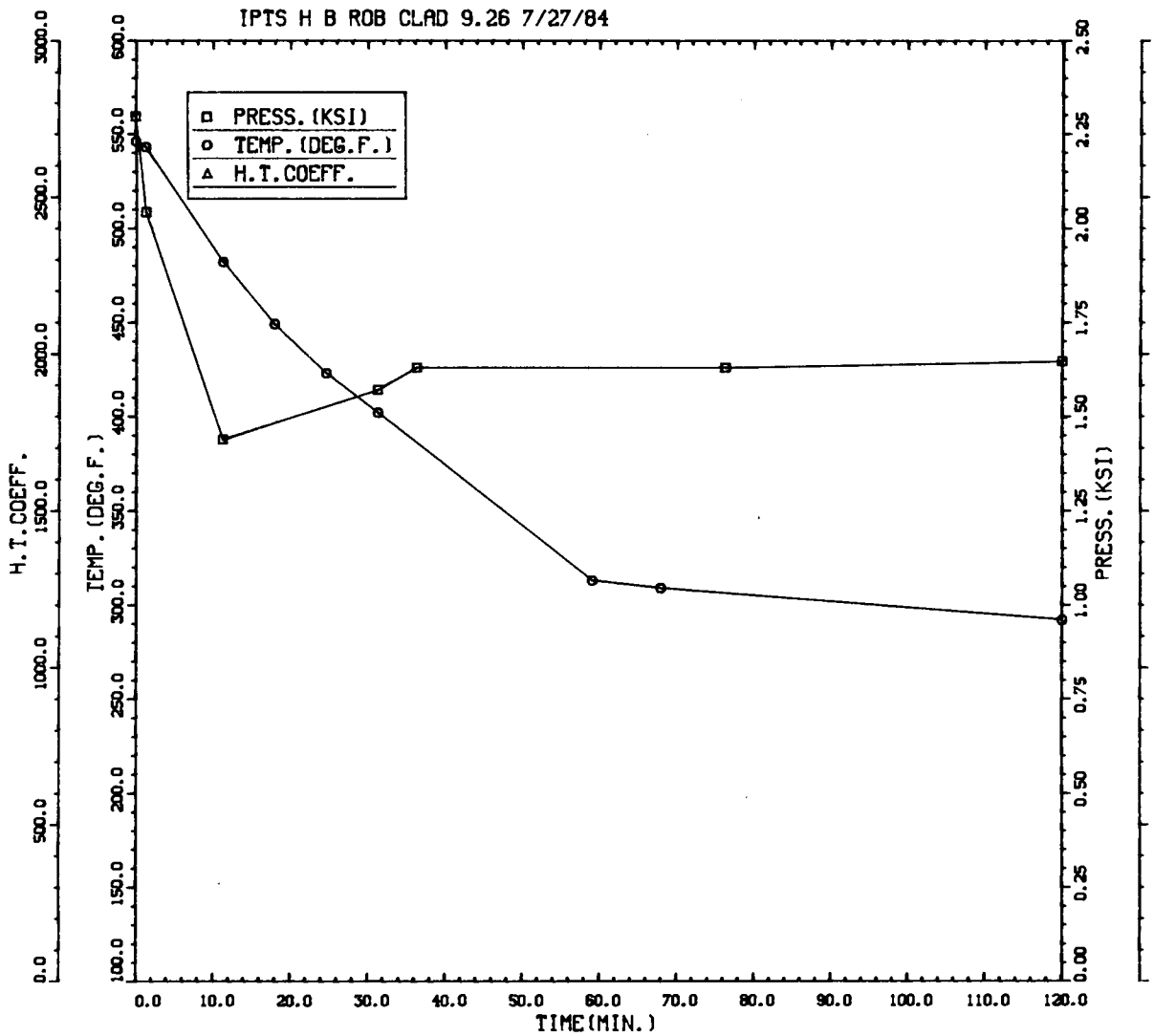

Figure I.187. Transient 9.26: Primary system pressure, downcomer coolant temperature, and fluid-film heat-transfer coefficient vs time in the transient.

Table I.32. Transient 9.26: Summary of digital output, including unadjusted $P(F|E)$ values and histogram data for crack depths, times of failure, and $T - RTNDT$ values at tip of crack corresponding to initiation and arrest events

IPTS H B ROB CLAD 9.26 7/27/84 1. FLAWS/IN**3 DRTN(IS) = 211.2

	----------UNADJUSTED----------					---ADJUSTED----			
WELD	P(F/E)	95%CI	%ERR	P(INITIA)	N*V	P(F/E)	%ERR	NFAIL	NTRIALS
1	5.49D-06	5.27D-07	9.61	1.66D-05	1.000	5.49D-06		415	150000
					VESSEL	5.49D-06	9.61		

DEPTHS FOR INITIAL INITIATION (IN)

	0.09	0.26	0.46	0.67	0.90	1.16	1.44	1.74	2.08
NUMBER	0	590	431	167	52	13	1	0	0
PERCENT	0.0	47.0	34.4	13.3	4.1	1.0	0.1	0.0	0.0

TIMES OF FAILURE(MINUTES)

	0.0	10.0	20.0	30.0	40.0	50.0	60.0	70.0	80.0	90.0	100.0	110.0	120.0
PERCENT	0.0	0.0	0.0	0.0	0.0	2.2	3.6	1.0	7.7	19.5	26.0	40.0	

INITIATION T-RTNDT(DEG.F)

	-100.0	-75.0	-50.0	-25.0	0.0	25.0	50.0	75.0	100.0	125.0	150.0	175.0	200.0
NUMBER	0	0	42	407	707	206	238	47	0	0	0	0	
PERCENT	0.0	0.0	2.6	24.7	42.9	12.5	14.5	2.9	0.0	0.0	0.0	0.0	

ARREST T-RTNDT(DEG.F)

	-50.0	-25.0	0.0	25.0	50.0	75.0	100.0	125.0	150.0	175.0	200.0	225.0	250.0
NUMBER	0	0	42	22	3	1	50	863	251	0	0	0	
PERCENT	0.0	0.0	3.4	1.8	0.2	0.1	4.1	70.0	20.4	0.0	0.0	0.0	

OF STD DEVS ABOVE MEAN DELTA RTNDT(FAILURES ONLY)

	1.00	1.25	1.50	1.75	2.00	2.25	2.50	2.75	3.00
NUMBER	0	17	21	51	63	64	108	91	
PERCENT	0.0	4.1	5.1	12.3	15.2	15.4	26.0	21.9	

OF STD DEVS ABOVE MEAN RTNDT(FAILURES ONLY)

	1.00	1.25	1.50	1.75	2.00	2.25	2.50	2.75	3.00
NUMBER	0	5	19	31	71	77	98	114	
PERCENT	0.0	1.2	4.6	7.5	17.1	18.6	23.6	27.5	

ICRKTP = 2 IACCEL = 1 NDLRS = 2 NRTRS = 2 DATE: 10/31/84 TIME: 01.49.38

CPU TIME: 4 MIN 5 SEC

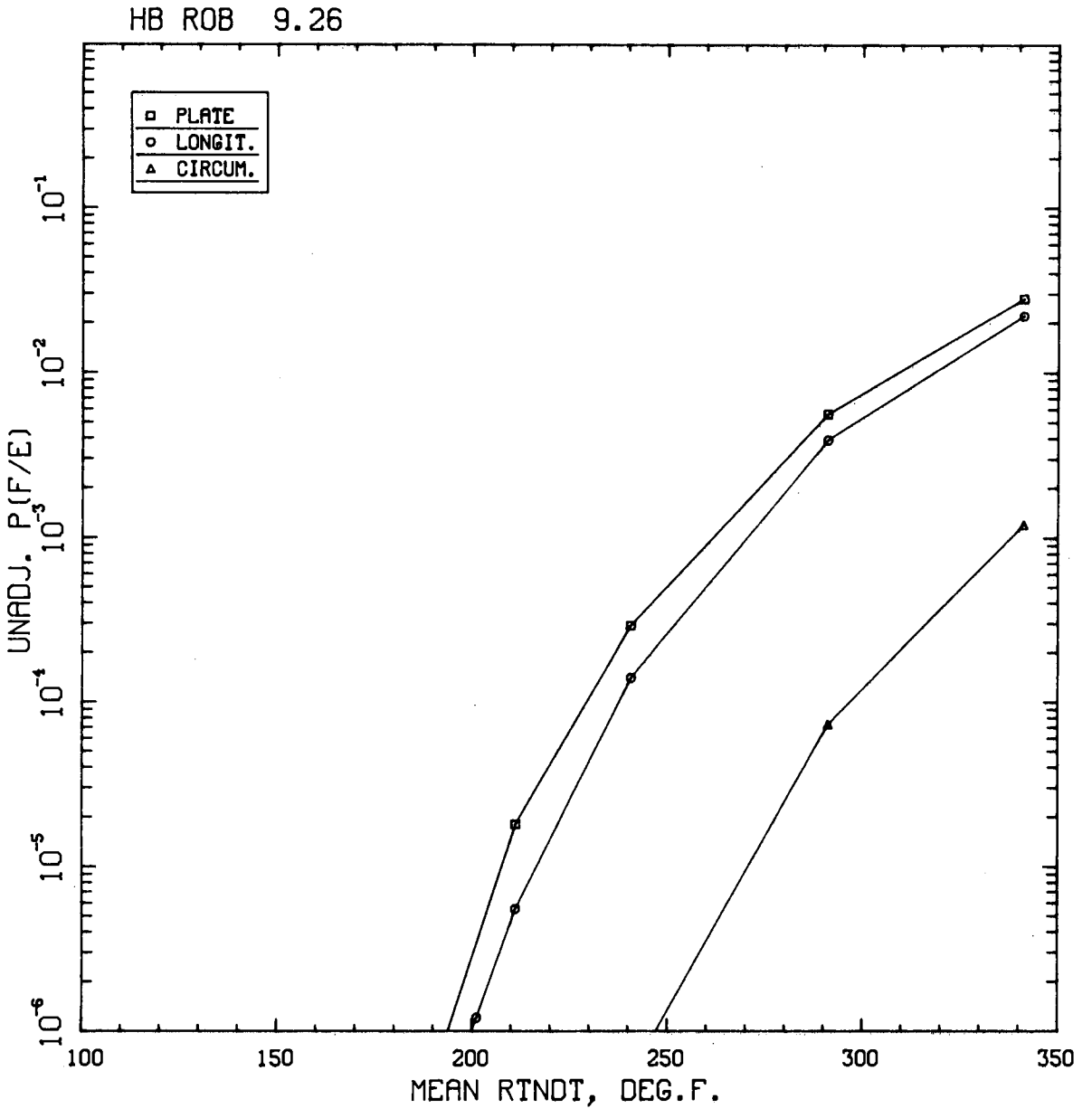

Figure I.188. Transient 9.26: $\hat{P}_j \int_0^w f(a)\, B(a)\, da$ vs $\overline{RTNDT}_s$ for (2-D, 2-D) and (2-D, 2m) flaw combinations.

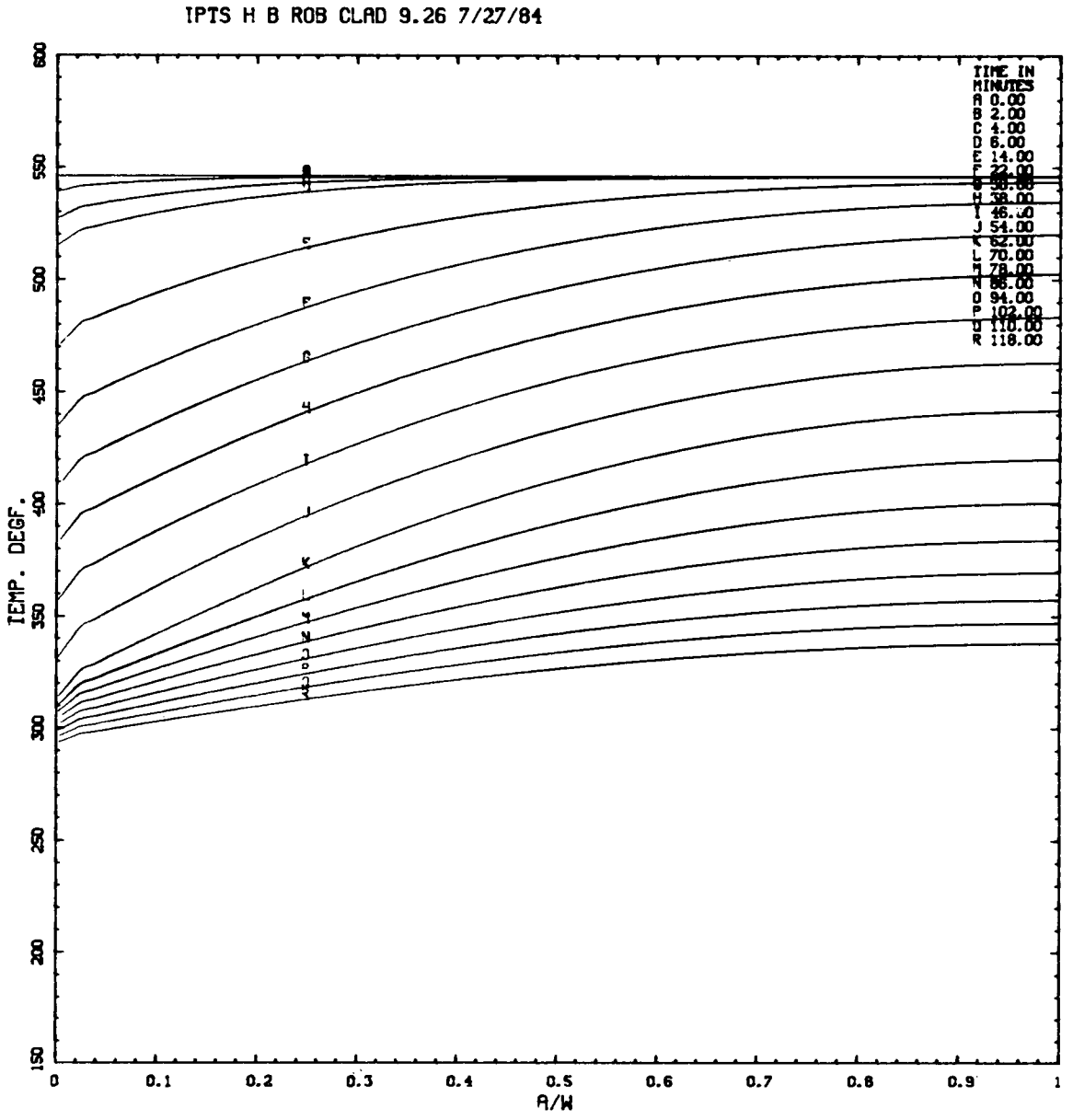

Figure I.189. Transient 9.26: Vessel wall temperature vs depth in wall (a/w) at various times (t) in transient.

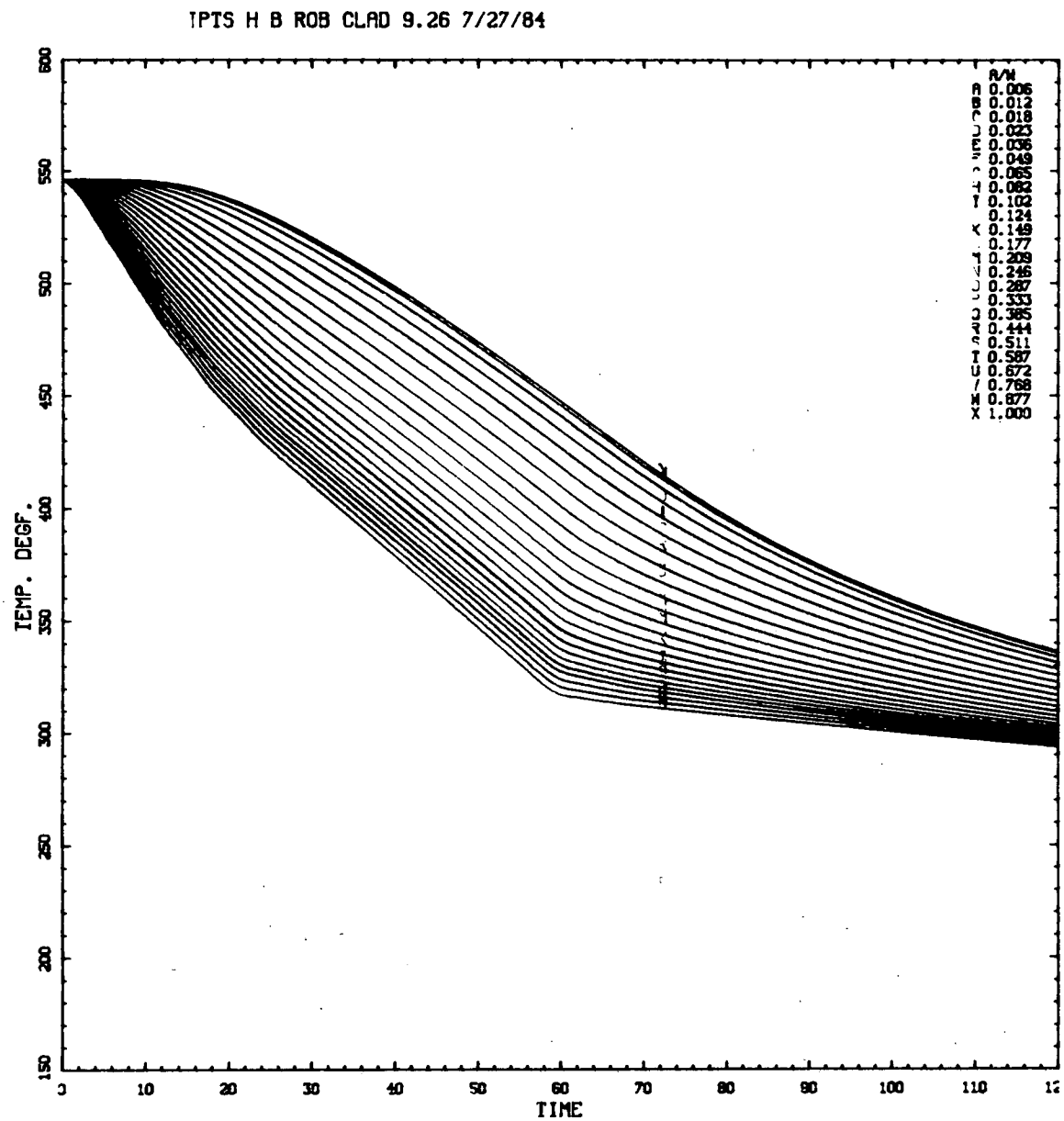

Figure I.190. Transient 9.26: Vessel wall temperature vs time (t) in transient at various depths in wall (a/w).

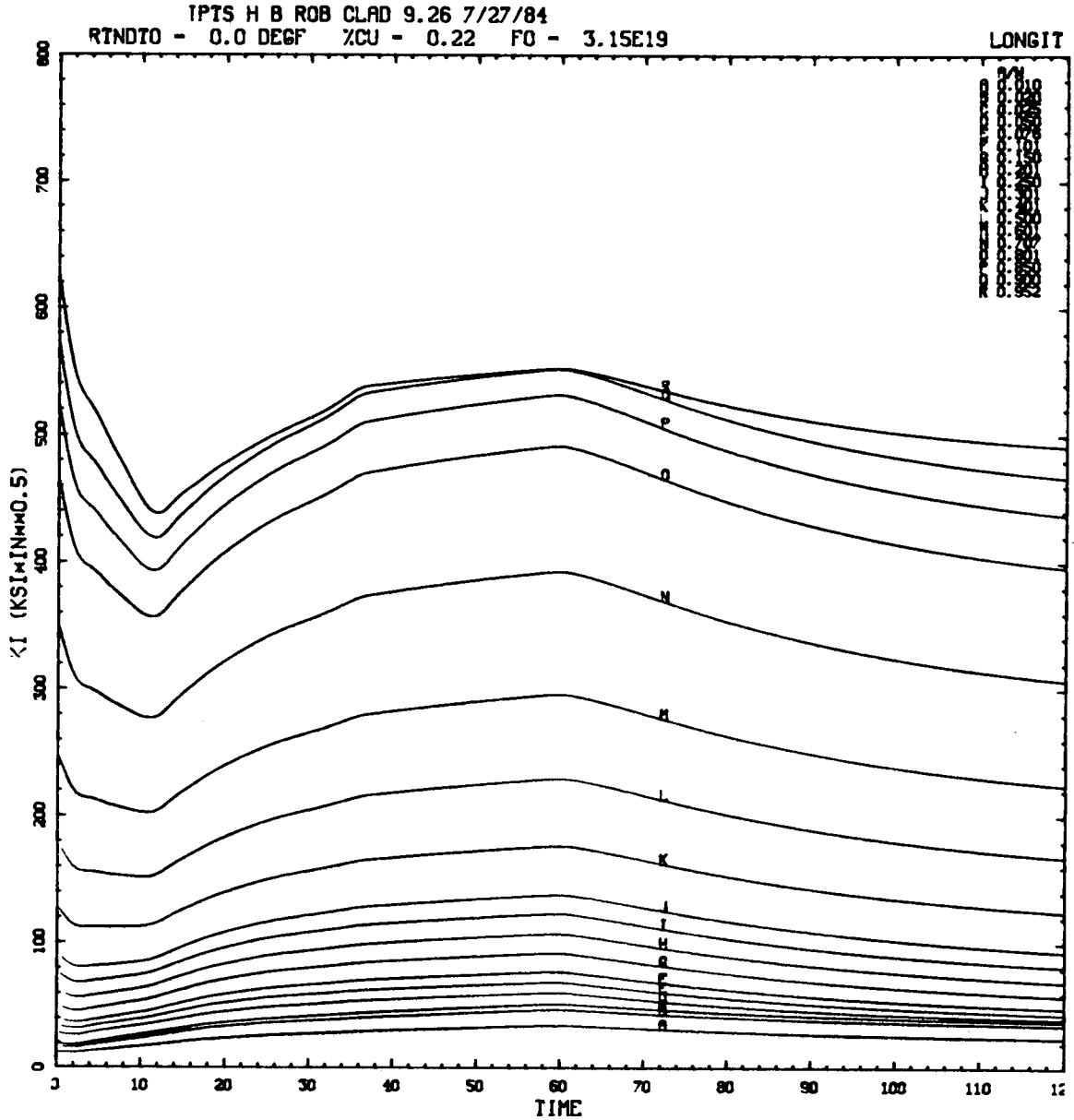

Figure I.191. Transient 9.26: K_I vs time (t) for various depths in wall (a/w).

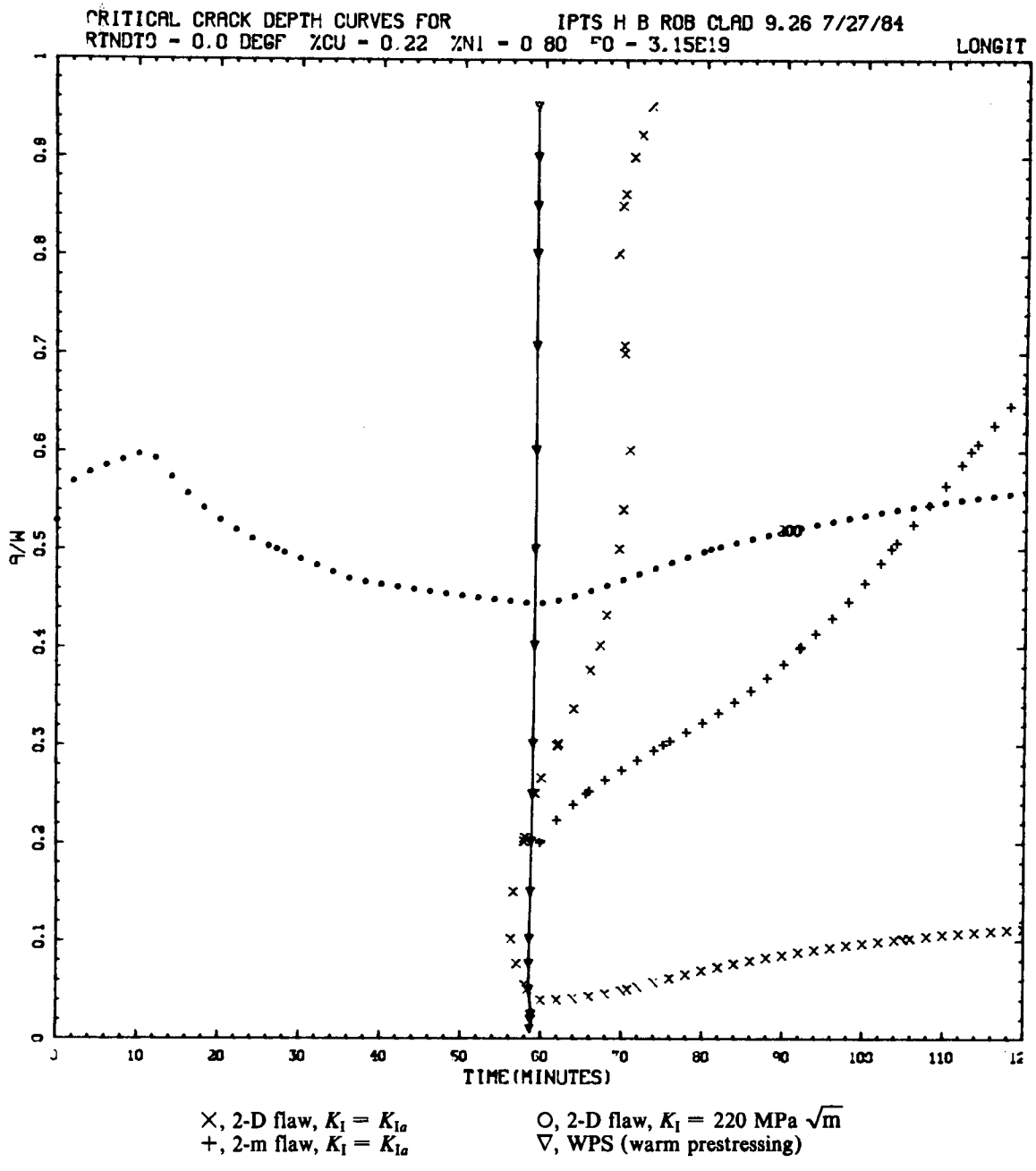

Figure I.192. Transient 9.26: Critical-crack-depth curves for weld 2-273A based on -2σ values of K_{Ic}, K_{Ia}, and $\Delta RTNDT$, mean values of all other parameters, and 32-EFPY fluences.

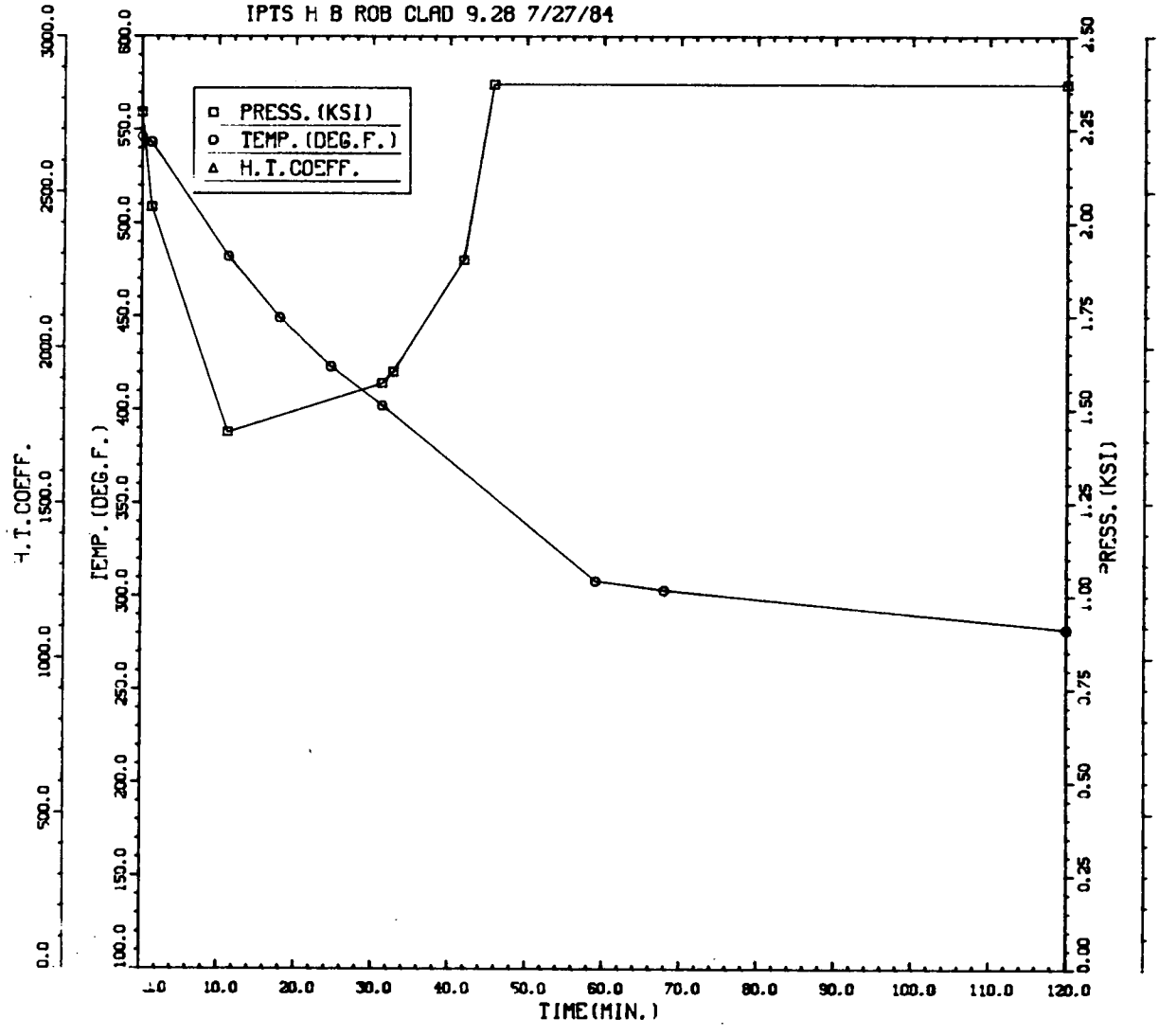

Figure I.193. Transient 9.28: Primary system pressure, downcomer coolant temperature, and fluid-film heat-transfer coefficient vs time in the transient.

Table I.33. Transient 9.28: Summary of digital output, including unadjusted $P(F|E)$ values and histogram data for crack depths, times of failure, and $T - RTNDT$ values at tip of crack corresponding to initiation and arrest events

IPTS H B ROB CLAD 9.28 7/27/84 1. FLAWS/IN**3 DRTN(IS) = 211.2

WELD	P(F/E) UNADJUSTED	95%CI	%ERR	P(INITIA)	N*V	P(F/E) ADJUSTED	%ERR	NFAIL	NTRIALS
1	1.26D-04	2.09D-05	16.62	1.47D-04	1.000	1.26D-04		139	200000
					VESSEL	1.26D-04	16.62		

DEPTHS FOR INITIAL INITIATION (IN)

	0.09	0.26	0.46	0.67	0.90	1.16	1.44	1.74	2.08
NUMBER	0	70	59	27	5	1	0	0	0
PERCENT	0.0	43.2	36.4	16.7	3.1	0.6	0.0	0.0	0.0

TIMES OF FAILURE(MINUTES)

	0.0	10.0	20.0	30.0	40.0	50.0	60.0	70.0	80.0	90.0	100.0	110.0	120.0
PERCENT	0.0	0.0	0.0	0.0	0.7	46.0	31.7	1.4	0.0	3.6	6.5	10.1	

INITIATION T-RTNDT(DEG.F)

	-100.0	-75.0	-50.0	-25.0	0.0	25.0	50.0	75.0	100.0	125.0	150.0	175.0	200.0
NUMBER	0	0	3	33	88	39	21	7	0	0	0	0	
PERCENT	0.0	0.0	1.6	17.3	46.1	20.4	11.0	3.7	0.0	0.0	0.0	0.0	

ARREST T-RTNDT(DEG.F)

	-50.0	-25.0	0.0	25.0	50.0	75.0	100.0	125.0	150.0	175.0	200.0	225.0	250.0
NUMBER	0	0	0	2	0	0	0	6	44	0	0	0	
PERCENT	0.0	0.0	0.0	3.8	0.0	0.0	0.0	11.5	84.6	0.0	0.0	0.0	

ICRKTP = 2 IACCEL = 1 NDLRS = 0 NRTRS = 0 DATE: 10/31/84 TIME: 01.51.02

CPU TIME: 5 MIN 28 SEC

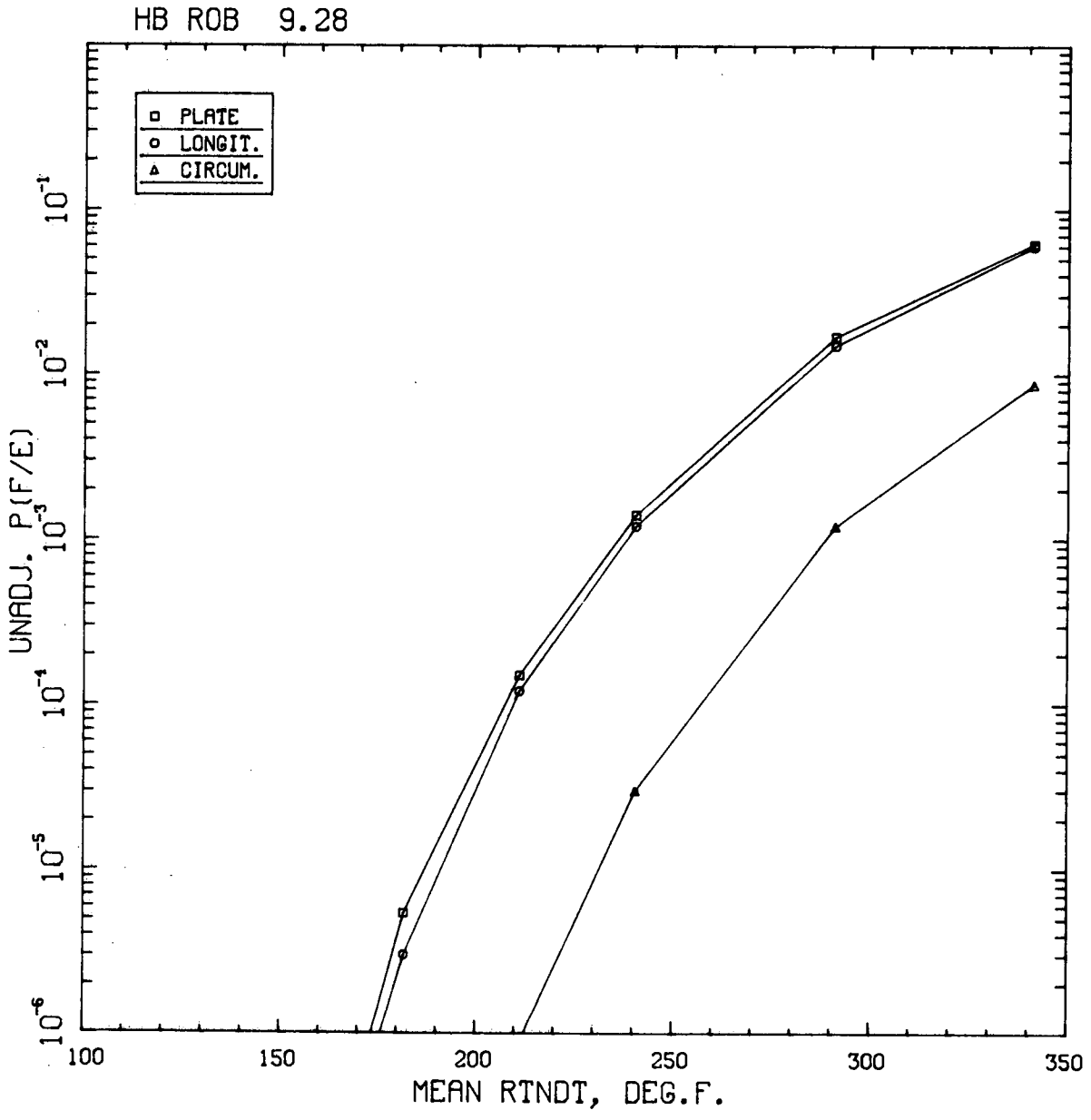

Figure I.194. Transient 9.28: $\hat{P}_j \int_0^w f(a)\, B(a)\, da$ **vs** $\overline{RTNDT_s}$ **for (2-D, 2-D) and (2-D, 2m) flaw combinations.**

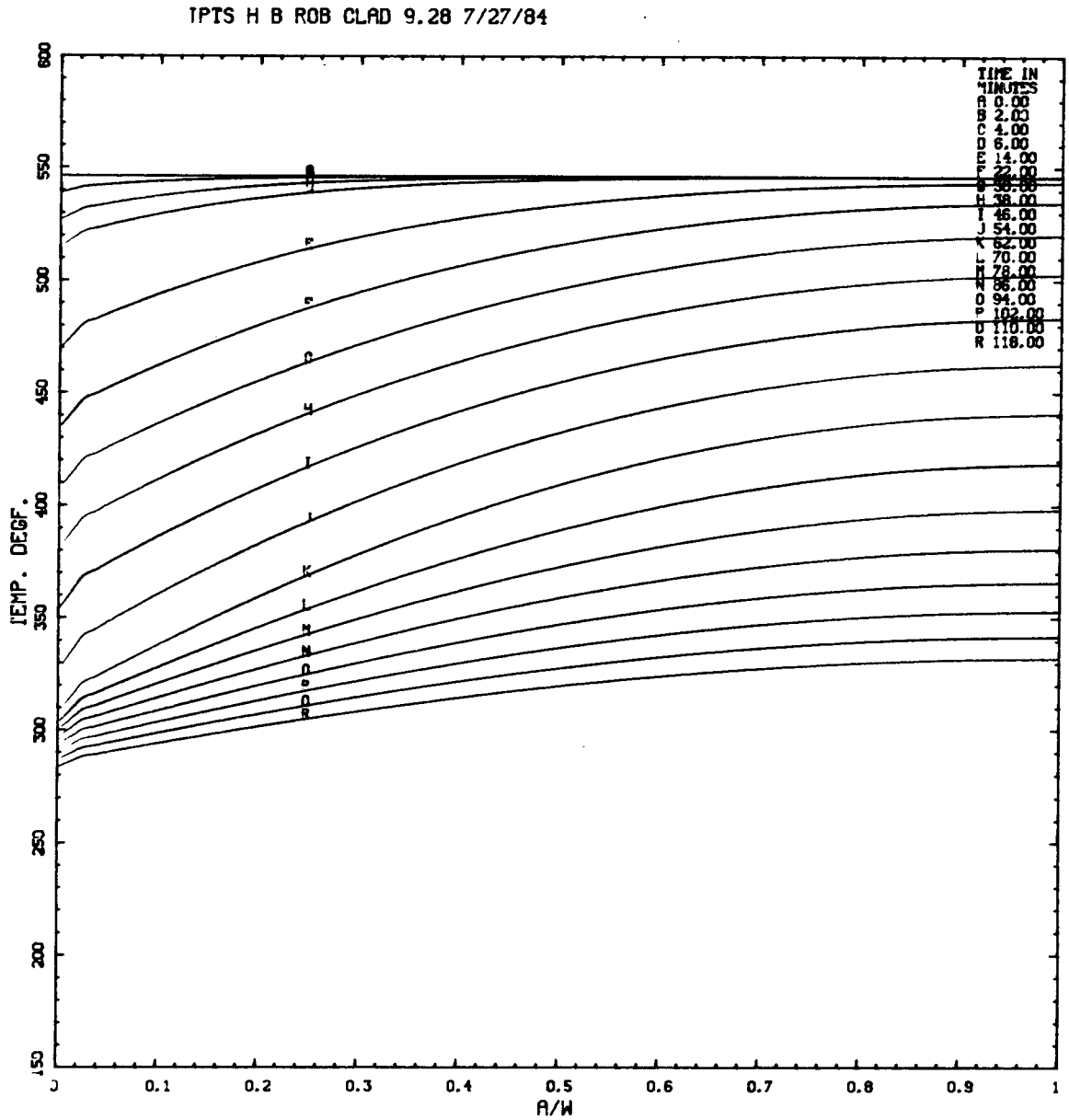

Figure I.195. Transient 9.28: Vessel wall temperature vs depth in wall (a/w) at various times (t) in transient.

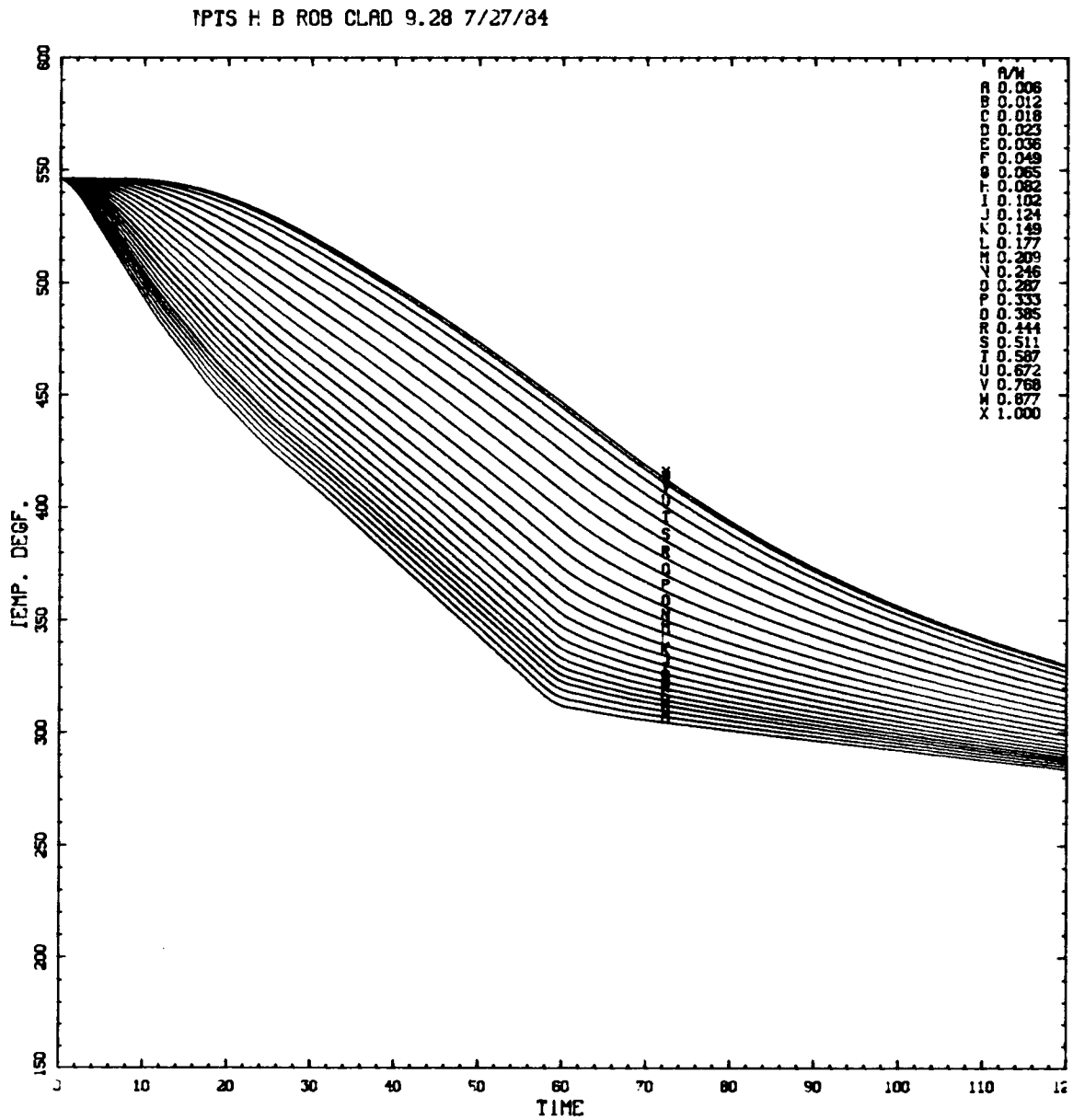

Figure I.196. Transient 9.28: Vessel wall temperature vs time (t) in transient at various depths in wall (a/w).

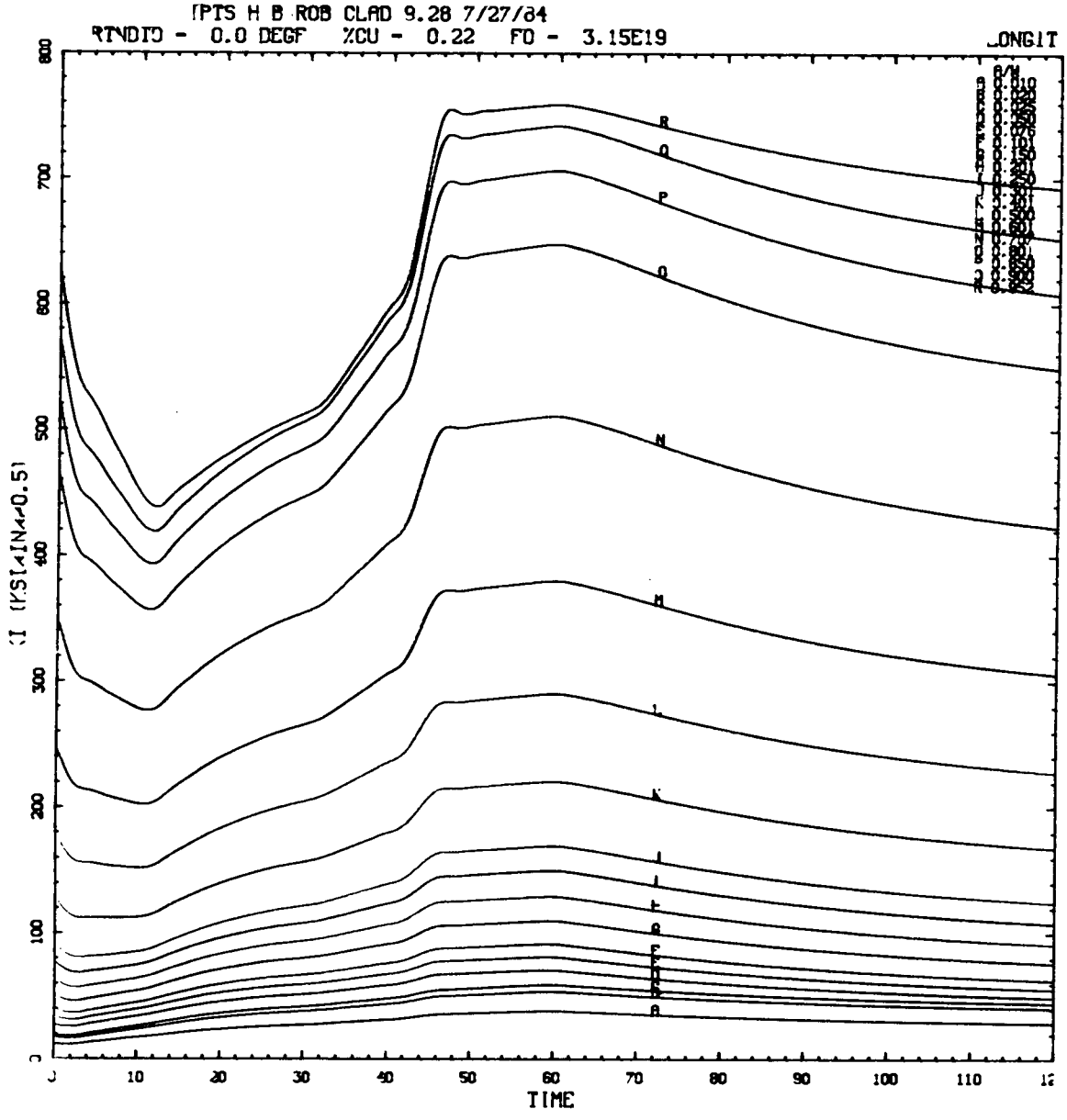

Figure I.197. Transient 9.28: K_I vs time (t) for various depths in wall (a/w).

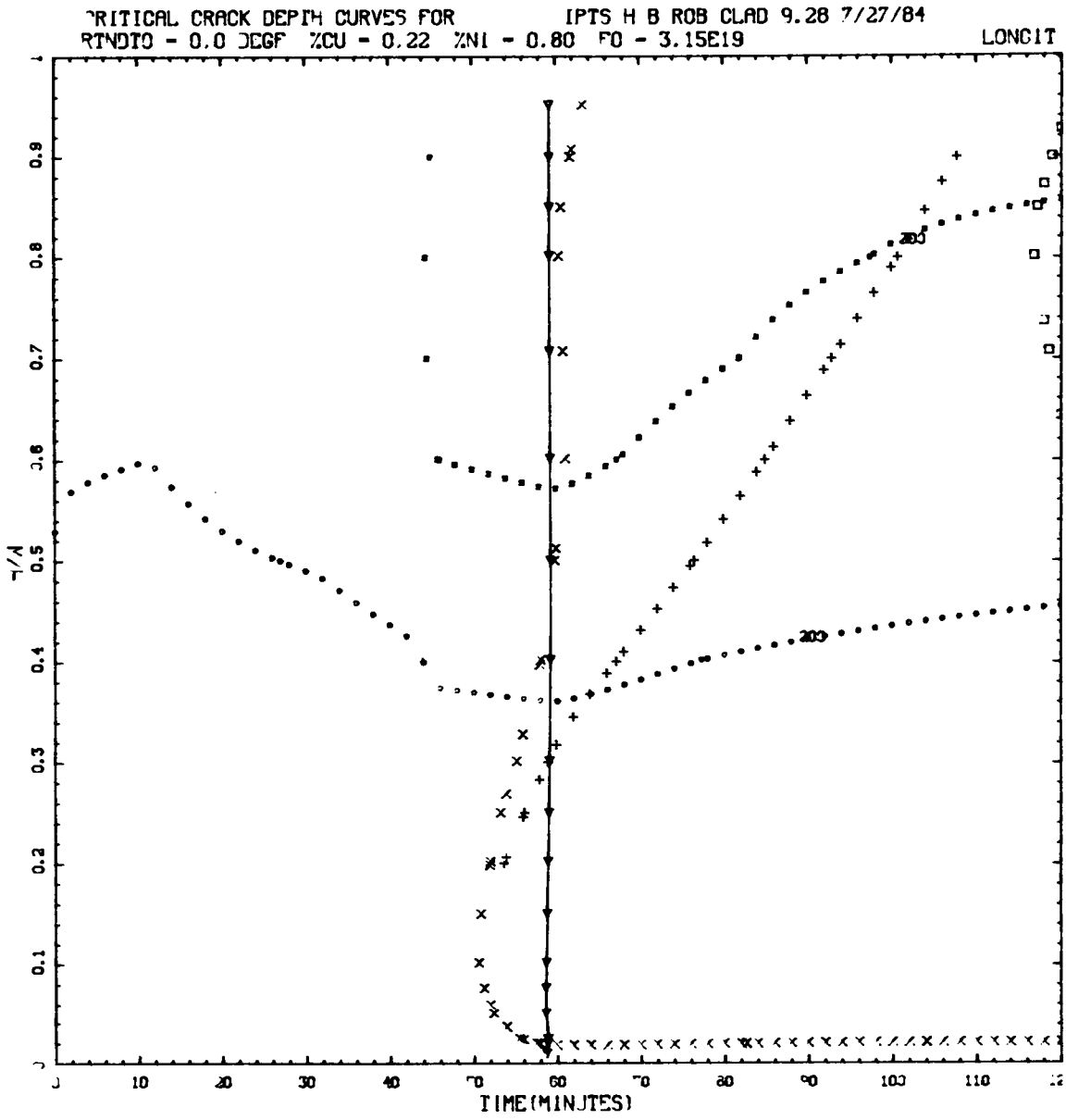

×, 2-D flaw, $K_I = K_{Ia}$
+, 2-m flaw, $K_I = K_{Ia}$
□, 2-D flaw, $K_I = K_{Ic}$
○, 2-D flaw, $K_I = 220$ MPa $\sqrt{m}$
■, 2-m flaw, $K_I = 220$ MPa $\sqrt{m}$
∇, WPS (warm prestressing)

Figure I.198. Transient 9.28: Critical-crack-depth curves for weld 2-273A based on -2σ values of K_{Ic}, K_{Ia}, and $\Delta RTNDT$, mean values of all other parameters, and 32-EFPY fluences.

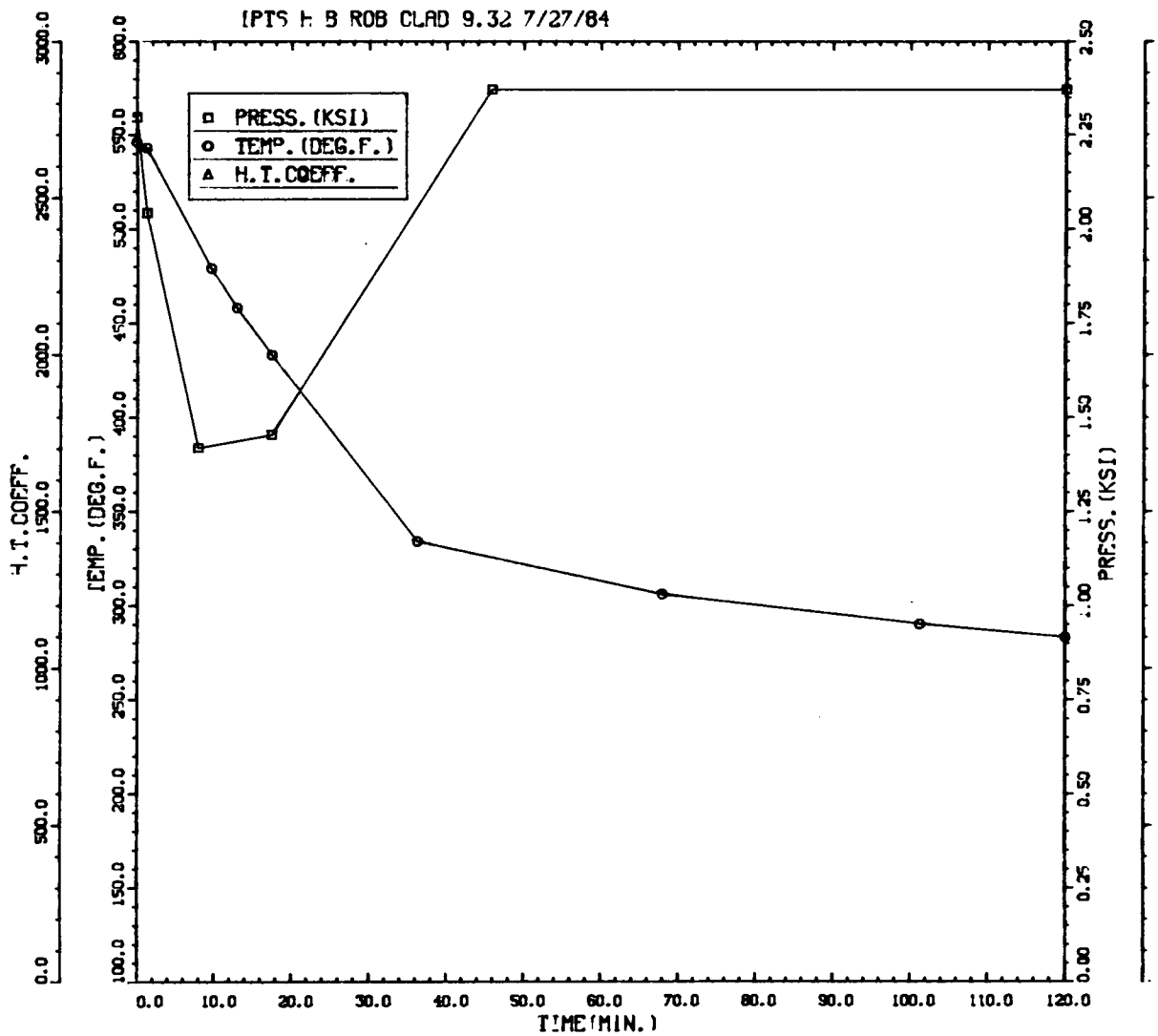

Figure I.199. Transient 9.32: Primary system pressure, downcomer coolant temperature, and fluid-film heat-transfer coefficient vs time in the transient.

Table I.34. Transient 9.32: Summary of digital output, including unadjusted $P(F|E)$ values and histogram data for crack depths, times of failure, and $T - RTNDT$ values at tip of crack corresponding to initiation and arrest events

IPTS H B ROB CLAD 9.32 7/27/84 1. FLAWS/IN**3 DRTN(IS) = 211.2

WELD	UNADJUSTED P(F/E)	95%CI	%ERR	P(INITIA)	N*V	ADJUSTED P(F/E)	%ERR	NFAIL	NTRIALS
1	6.44D-05	1.50D-05	23.26	6.89D-05	1.000	6.44D-05		71	200000
					VESSEL	6.44D-05	23.26		

DEPTHS FOR INITIAL INITIATION (IN)

	0.09	0.26	0.46	0.67	0.90	1.16	1.44	1.74	2.08
NUMBER	0	33	21	17	4	1	0	0	0
PERCENT	0.0	43.4	27.6	22.4	5.3	1.3	0.0	0.0	0.0

TIMES OF FAILURE(MINUTES)

	0.0	10.0	20.0	30.0	40.0	50.0	60.0	70.0	80.0	90.0	100.0	110.0	120.0
PERCENT	0.0	0.0	0.0	1.4	9.9	18.3	38.0	5.6	9.9	8.5	2.8	5.6	

INITIATION T-RTNDT(DEG.F)

	-100.0	-75.0	-50.0	-25.0	0.0	25.0	50.0	75.0	100.0	125.0	150.0	175.0	200.0
NUMBER	0	0	2	11	49	16	13	3	0	0	0	0	
PERCENT	0.0	0.0	2.1	11.7	52.1	17.0	13.8	3.2	0.0	0.0	0.0	0.0	

ARREST T-RTNDT(DEG.F)

	-50.0	-25.0	0.0	25.0	50.0	75.0	100.0	125.0	150.0	175.0	200.0	225.0	250.0
NUMBER	0	0	2	1	0	0	0	4	16	0	0	0	
PERCENT	0.0	0.0	8.7	4.3	0.0	0.0	0.0	17.4	69.6	0.0	0.0	0.0	

ICRKTP = 2 IACCEL = 1 NDLRS = 0 NRTRS = 0 DATE: 10/31/84 TIME: 02.02.00

CPU TIME: 5 MIN 28 SEC

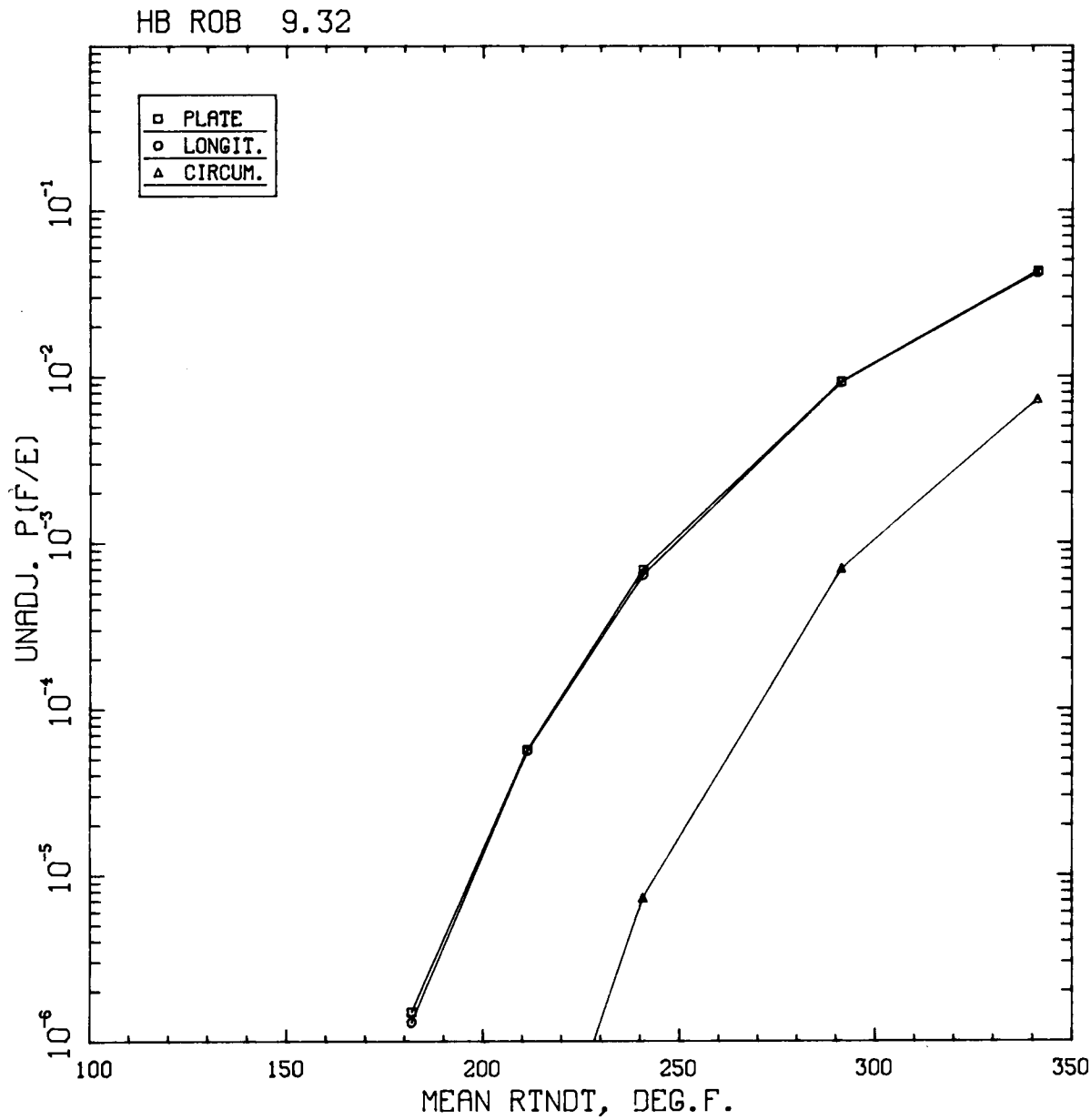

Figure I.200. Transient 9.32: $\hat{P}_j \int_0^w f(a)\, B(a)\, da$ vs $\overline{RTNDT}_s$ for (2-D, 2-D) and (2-D, 2m) flaw combinations.

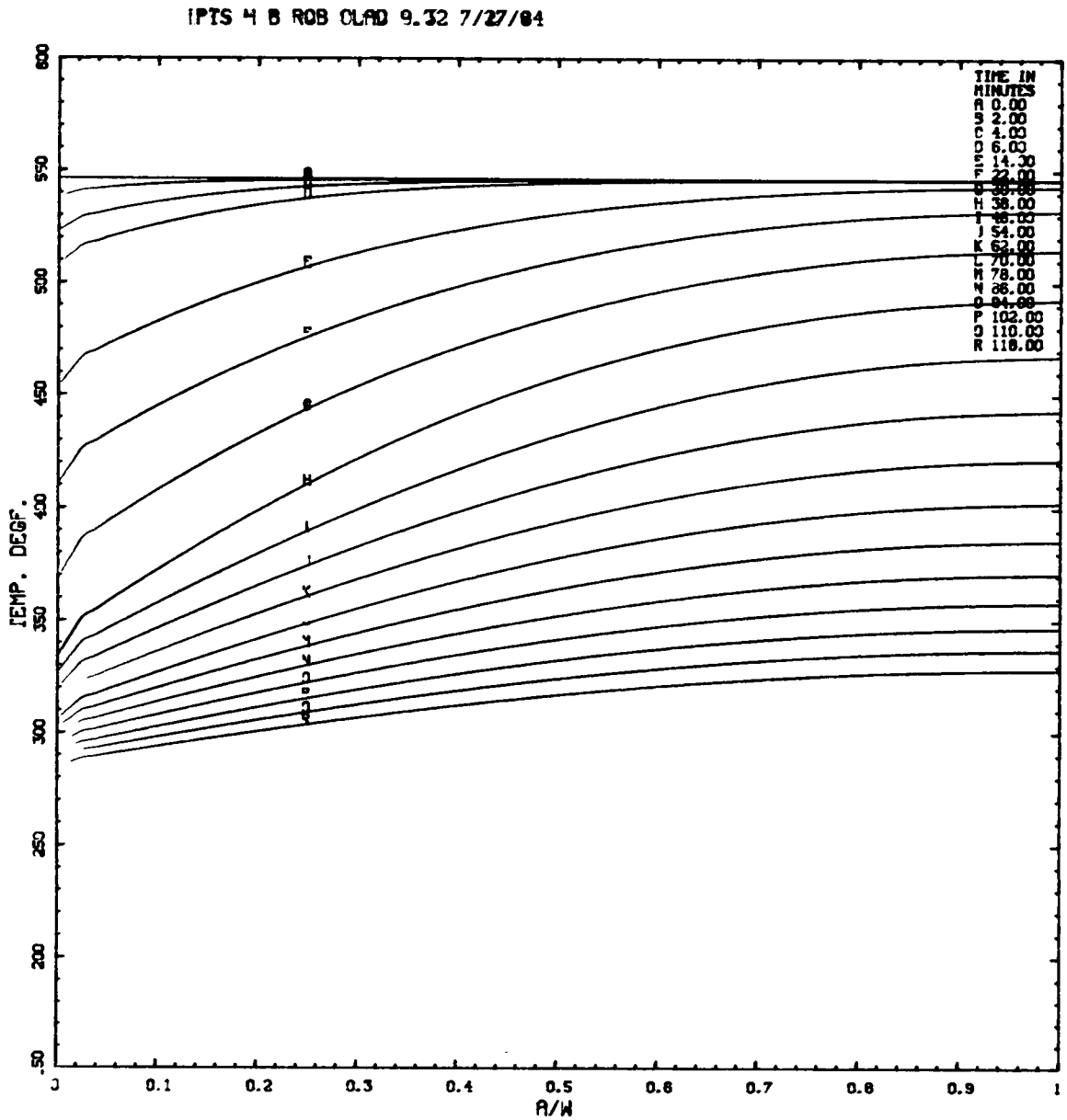

Figure I.201. Transient 9.32: Vessel wall temperature vs depth in wall (a/w) at various times (t) in transient.

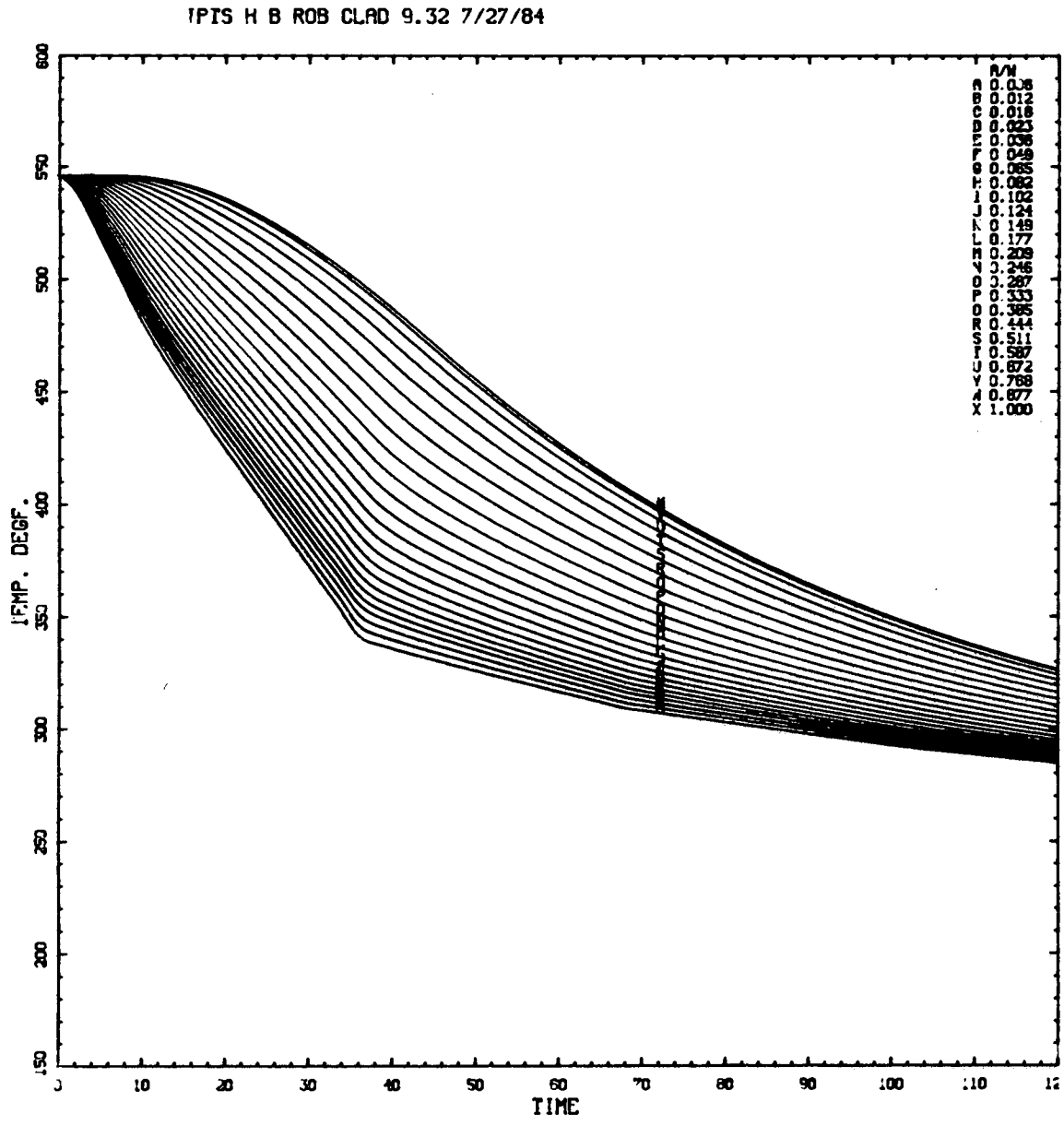

Figure I.202. Transient 9.32: Vessel wall temperature vs time (t) in transient at various depths in wall (a/w).

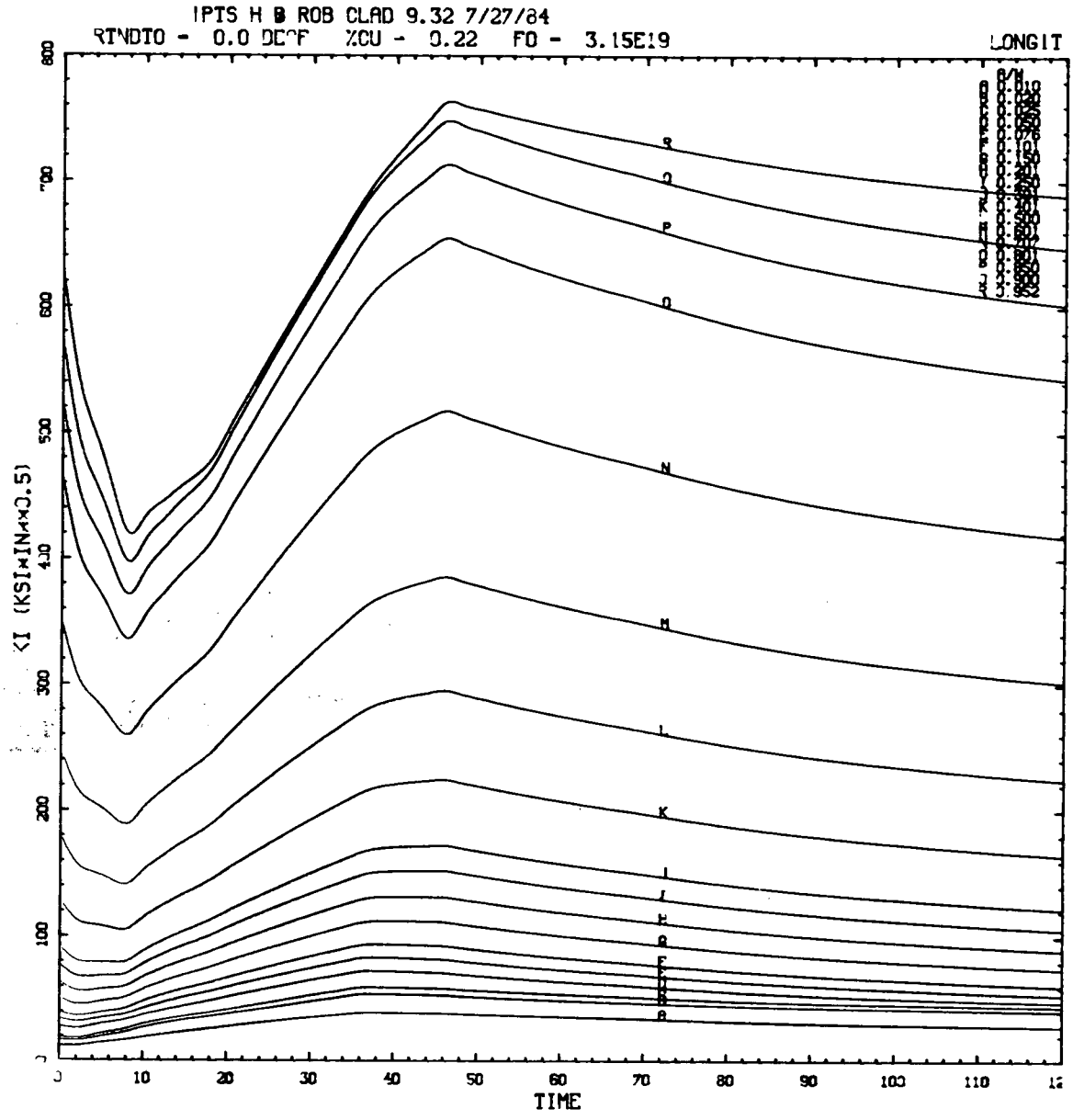

Figure I.203. Transient 9.32: K_I vs time (t) for various depths in wall (a/w).

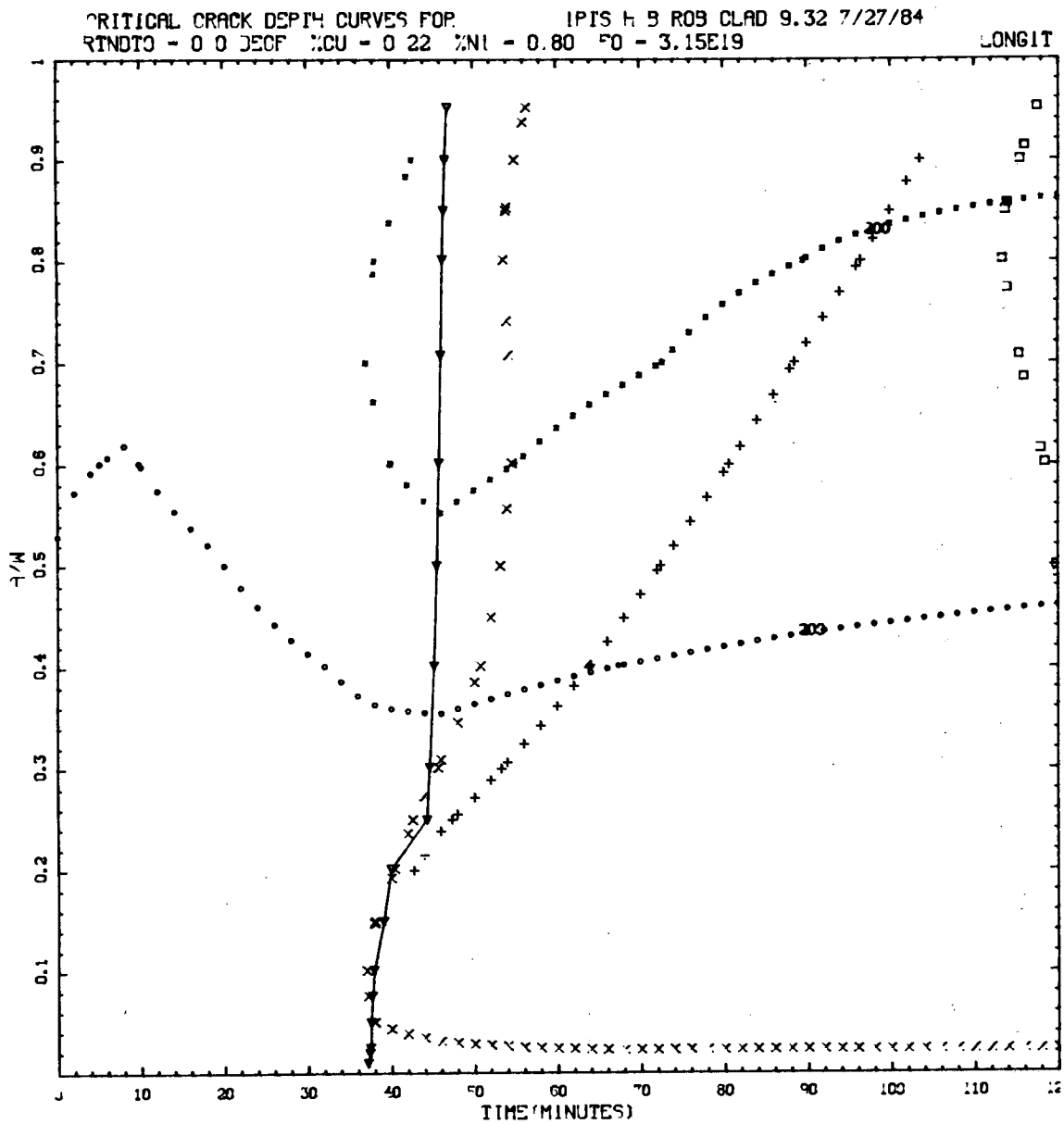

×, 2-D flaw, $K_I = K_{Ia}$
+, 2-m flaw, $K_I = K_{Ia}$
□, 2-D flaw, $K_I = K_{Ic}$
○, 2-D flaw, $K_I = 220$ MPa $\sqrt{m}$
■, 2-m flaw, $K_I = 220$ MPa $\sqrt{m}$
▽, WPS (warm prestressing)

Figure I.204. Transient 9.32: Critical-crack-depth curves for weld 2-273A based on -2σ values of K_{Ic}, K_{Ia}, and $\Delta RTNDT$, mean values of all other parameters, and 32-EFPY fluences.

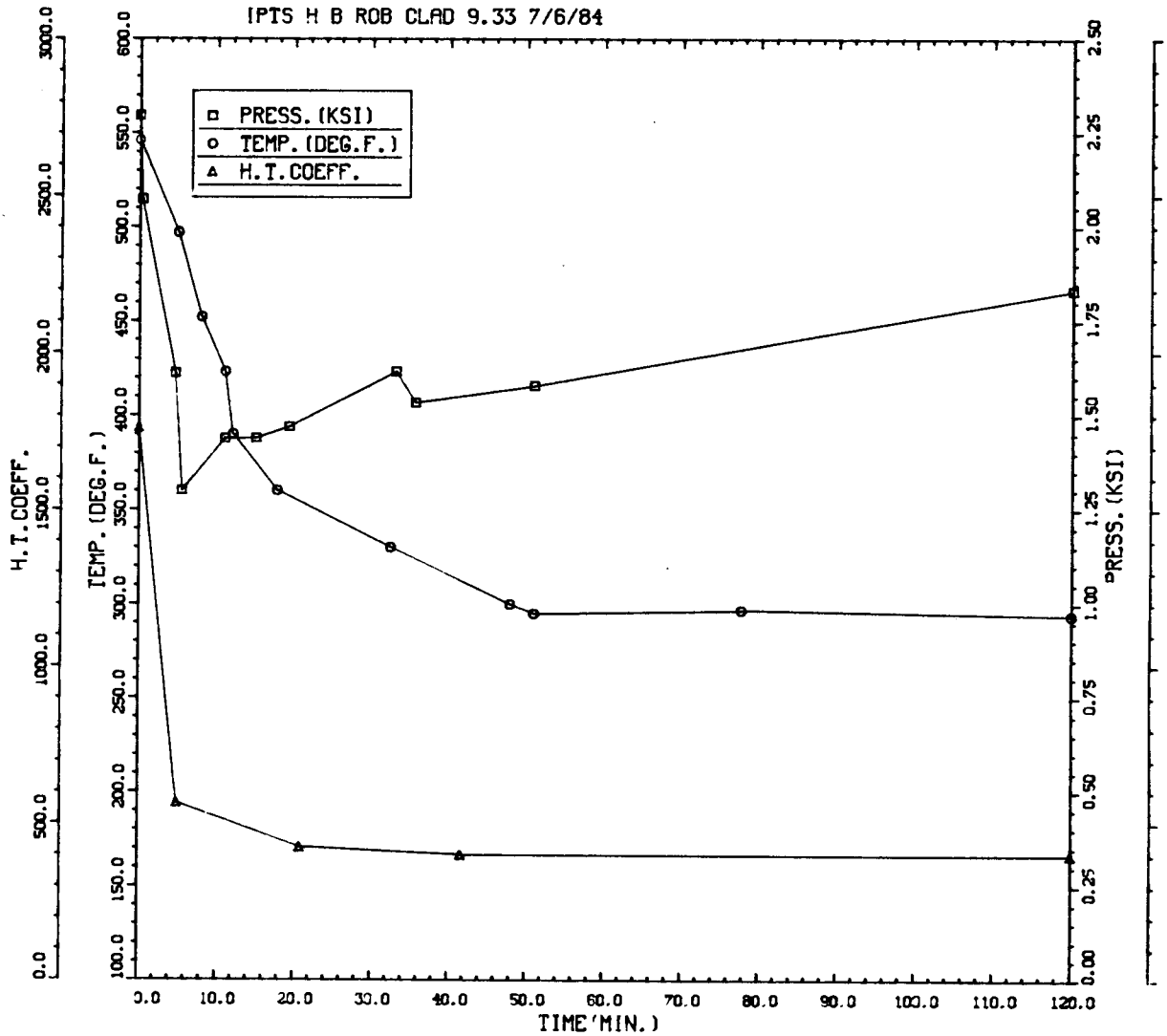

Figure I.205. Transient 9.33: Primary system pressure, downcomer coolant temperature, and fluid-film heat-transfer coefficient vs time in the transient.

Table I.35. Transient 9.33: Summary of digital output, including unadjusted $P(F|E)$ values and histogram data for crack depths, times of failure, and $T - RTNDT$ values at tip of crack corresponding to initiation and arrest events

```
IPTS H B ROB CLAD 9.33 7/6/84                    1. FLAWS/IN**3    DRTN(TS) =  211.2

            -------------UNADJUSTED--------------          ---ADJUSTED----
WELD        P(F/E)      95%CI     %ERR   P(INITIA)  N*V      P(F/E)    %ERR    NFAIL    NTRIALS

 1          6.64D-06   7.58D-07  11.42   1.40D-05  1.000   6.64D-06            294      200000

                                                   VESSEL   6.64D-06  11.42


DEPTHS FOR INITIAL INITIATION (IN)
                 0.09  0.26  0.46  0.67  0.90  1.16  1.44  1.74  2.08
    NUMBER        0   272   232    90    18     8     2     0     0
    PERCENT     0.0  43.7  37.3  14.5   2.9   1.3   0.3   0.0   0.0


TIMES OF FAILURE(MINUTES)
                 0.0  10.0  20.0  30.0  40.0  50.0  60.0  70.0  80.0  90.0 100.0 110.0 120.0
   PERCENT       0.0   0.0   0.0   0.0   1.0   1.4   1.7   6.5  13.9  22.4  25.5  27.6


 INITIATION T-RTNDT(DEG.F)
              -100.0 -75.0 -50.0 -25.0   0.0  25.0  50.0  75.0 100.0 125.0 150.0 175.0 200.0
   NUMBER          0     0    24   197   337   136   179    37     1     0     0     0
   PERCENT       0.0   0.0   2.6  21.6  37.0  14.9  19.6   4.1   0.1   0.0   0.0   0.0


 ARREST T-RTNDT(DEG.F)
              -50.0 -25.0   0.0  25.0  50.0  75.0 100.0 125.0 150.0 175.0 200.0 225.0 250.0
   NUMBER          0     2    34    22     2     0    18   429   110     0     0     0
   PERCENT       0.0   0.3   5.5   3.6   0.3   0.0   2.9  69.5  17.8   0.0   0.0   0.0


 # OF STD DEVS ABOVE MEAN DELTA RTNDT(FAILURES ONLY)
                 1.00  1.25  1.50  1.75  2.00  2.25  2.50  2.75  3.00
   NUMBER          3     9    24    31    43    49    73    62
   PERCENT       1.0   3.1   8.2  10.5  14.6  16.7  24.8  21.1


 # OF STD DEVS ABOVE MEAN RTNDT(FAILURES ONLY)
                 1.00  1.25  1.50  1.75  2.00  2.25  2.50  2.75  3.00
   NUMBER          2     4    15    35    49    56    67    66
   PERCENT       0.7   1.4   5.1  11.9  16.7  19.0  22.8  22.4


ICRKTP = 2   IACCEL = 1   NDLRS = 1   NRTRS = 1   DATE: 11/19/84   TIME: 22.51.11

CPU TIME:  5 MIN 22 SEC
```

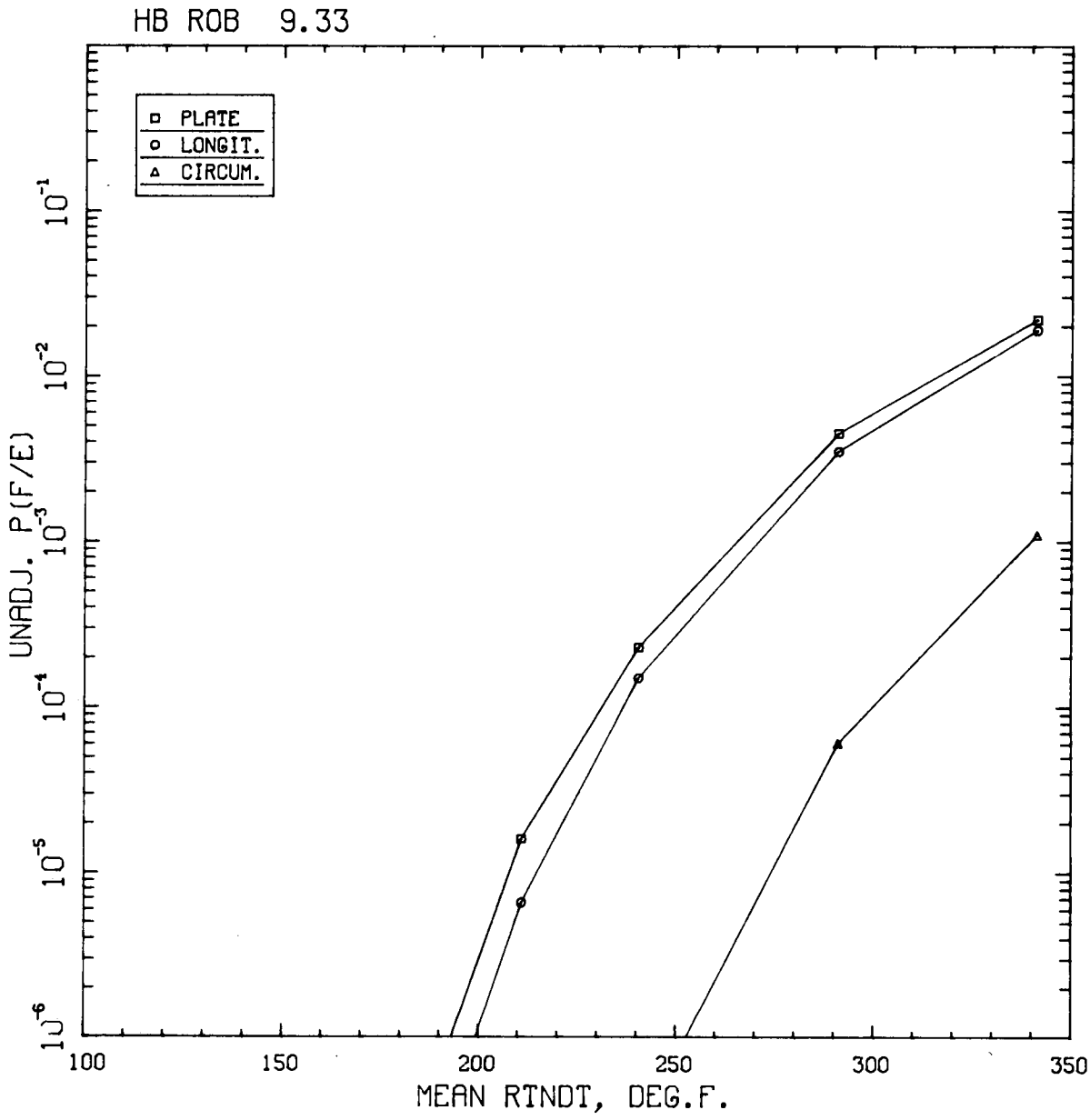

Figure I.206. Transient 9.33: $\hat{P}_j \int_0^w f(a)\, B(a)\, da$ vs $\overline{RTNDT_s}$ for (2-D, 2-D) and (2-D, 2m) flaw combinations.

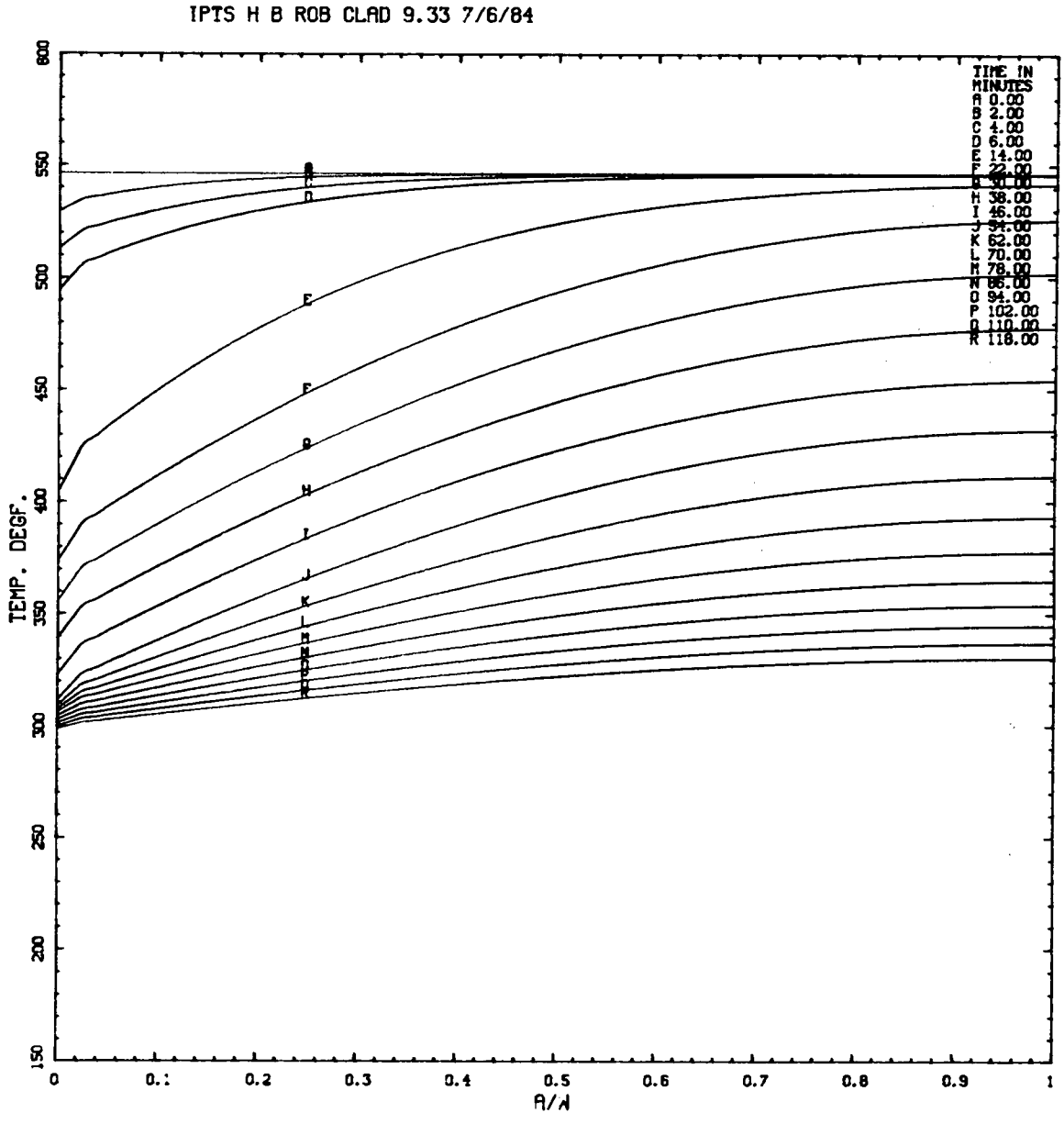

Figure I.207. Transient 9.33: Vessel wall temperature vs depth in wall (a/w) at various times (t) in transient.

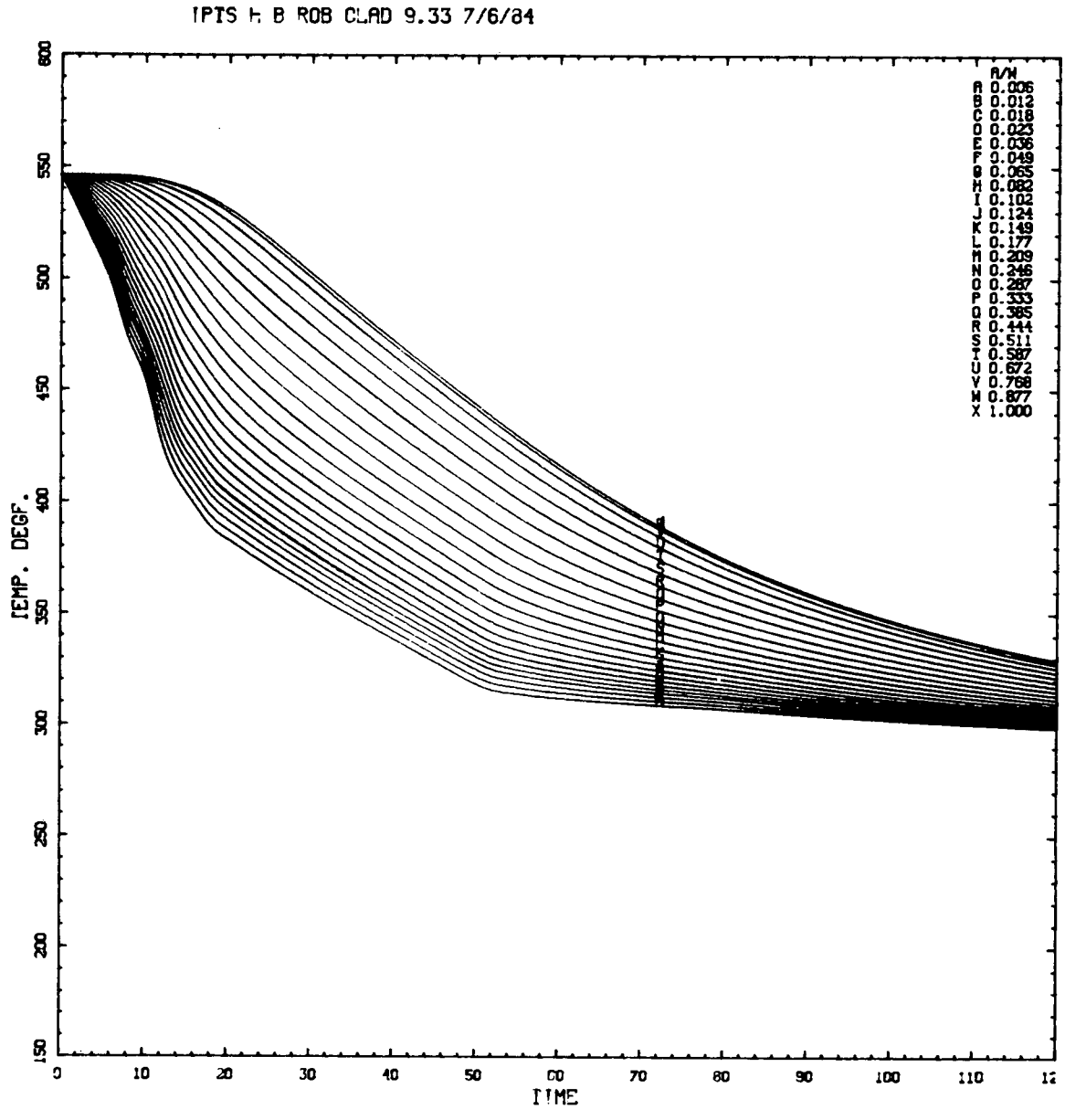

Figure I.208. Transient 9.33: Vessel wall temperature vs time (t) in transient at various depths in wall (a/w).

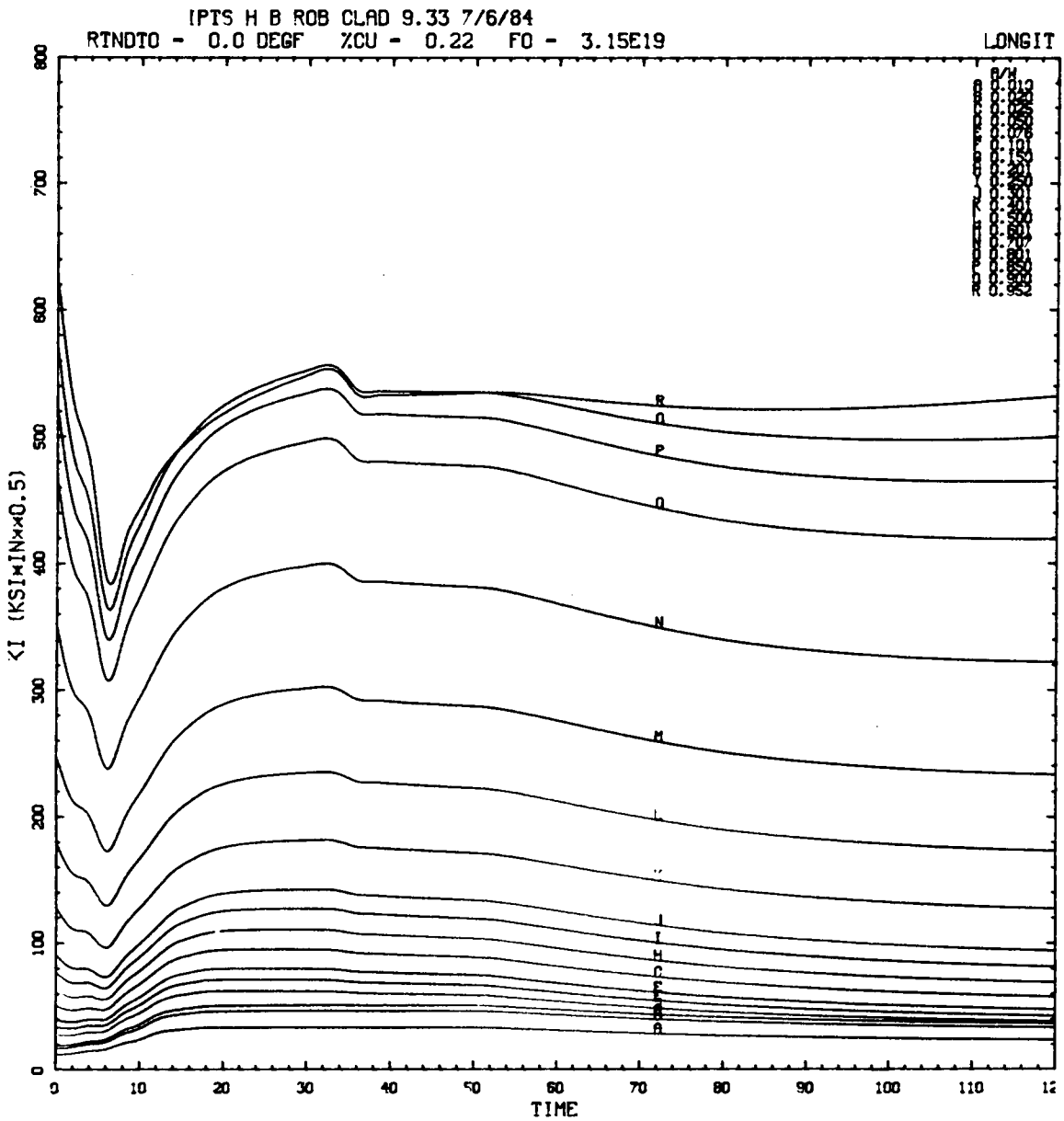

Figure I.209. Transient 9.33: K_I vs time (t) for various depths in wall (a/w).

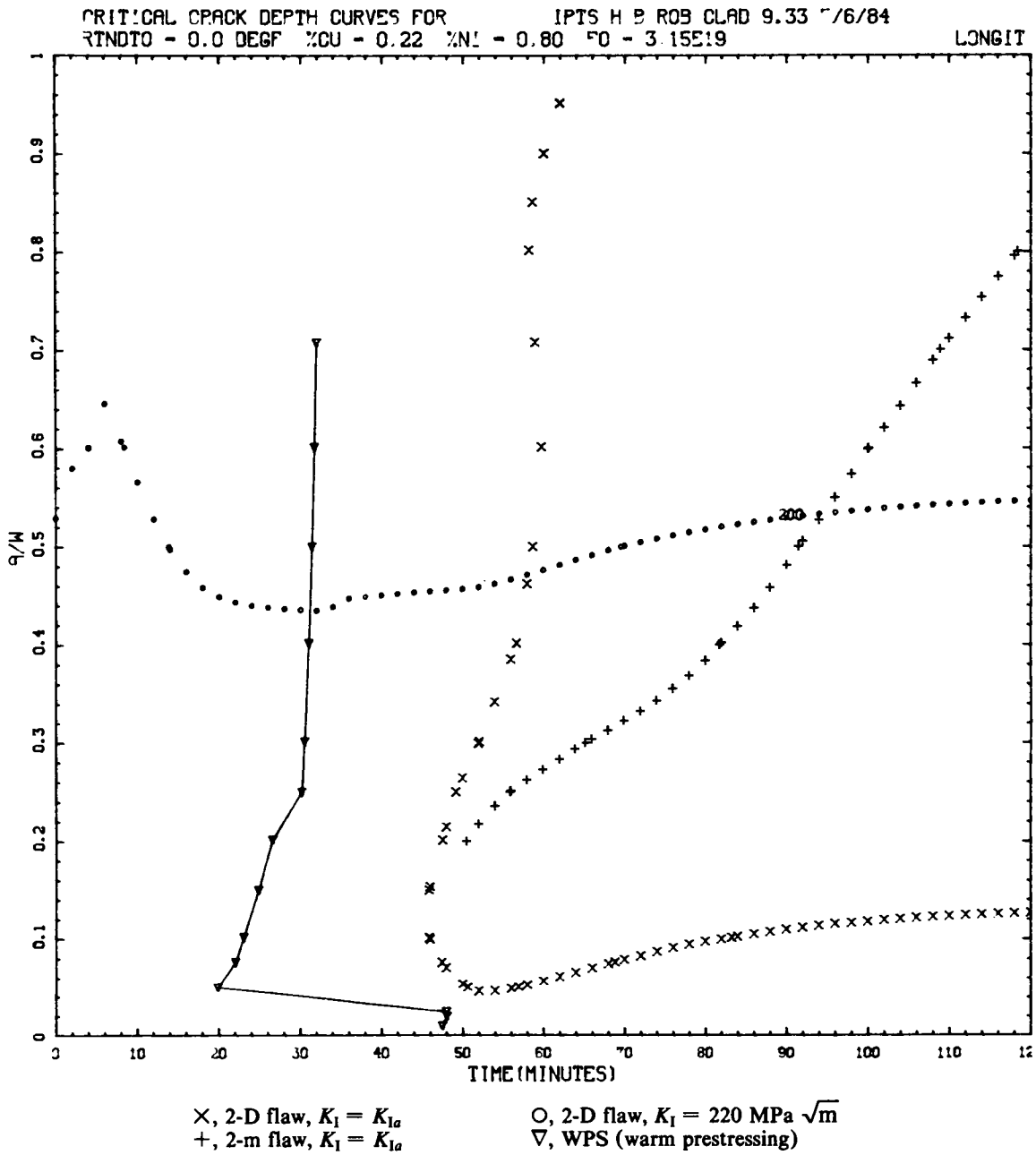

Figure I.210. Transient 9.33: Critical-crack-depth curves for weld 2-273A based on -2σ values of K_{Ic}, K_{Ia}, and $\Delta RTNDT$, mean values of all other parameters, and 32-EFPY fluences.

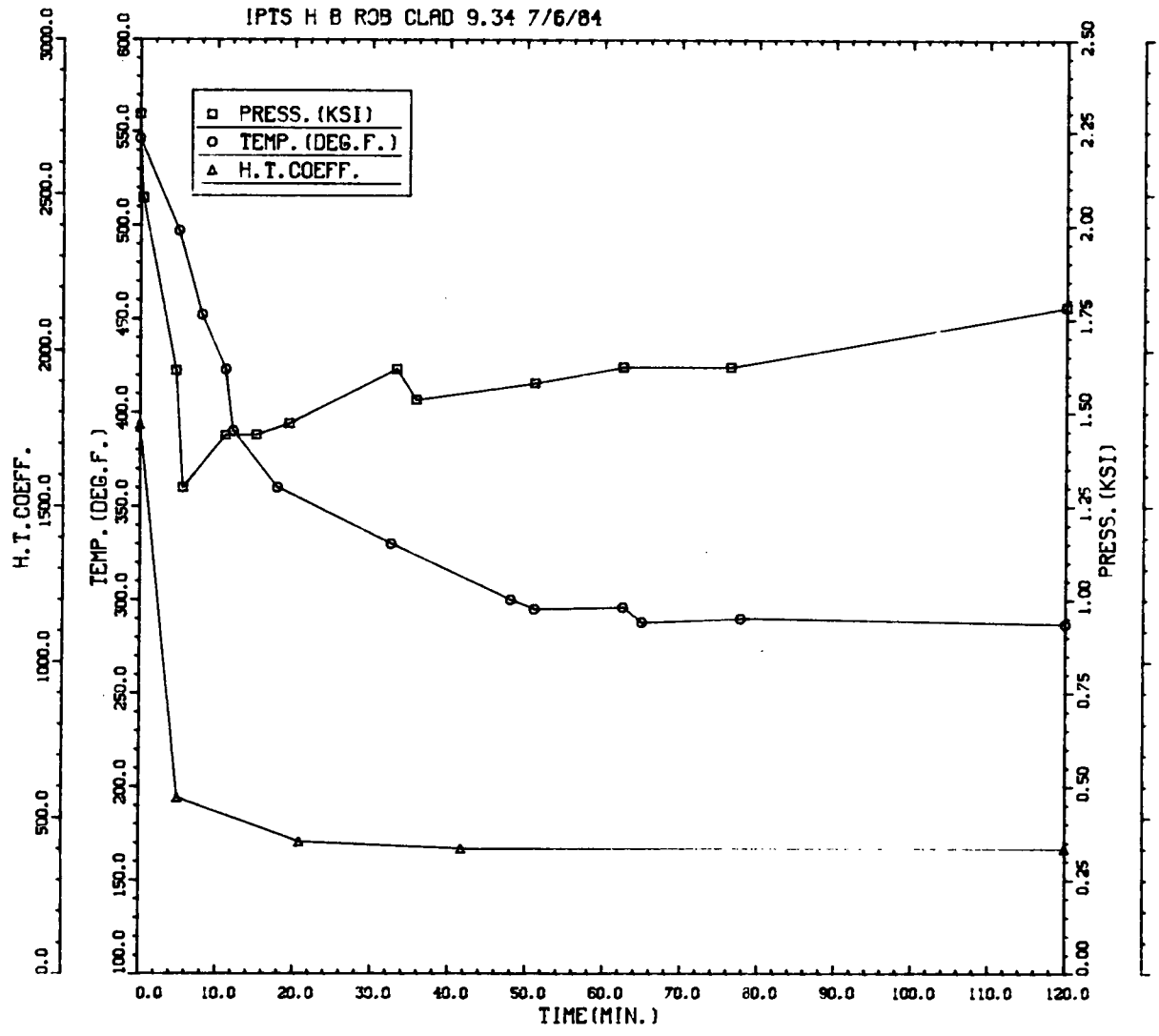

Figure I.211. Transient 9.34: Primary system pressure, downcomer coolant temperature, and fluid-film heat-transfer coefficient vs time in the transient.

Table I.36. Transient 9.34: Summary of digital output, including unadjusted $P(F|E)$ values and histogram data for crack depths, times of failure, and $T - RTNDT$ values at tip of crack corresponding to initiation and arrest events

```
IPTS H B ROB CLAD 9.34 7/6/84                    1. FLAWS/IN**3    DRTN(IS) =  211.2

            -------------UNADJUSTED--------------          ---ADJUSTED----
WELD        P(F/E)      95%CI     %ERR   P(INITIA)  N*V     P(F/E)    %ERR    NFAIL.   NTRIALS

 1          8.29D-06   8.47D-07  10.22   1.58D-05  1.000   8.29D-06            367      200000

                                                   VESSEL  8.29D-06  10.22


DEPTHS FOR INITIAL INITIATION (IN)
                0.09  0.26  0.46  0.67  0.90  1.16  1.44  1.74  2.08
   NUMBER        0    310   246    99    29    13     2     0     0
   PERCENT      0.0  44.3  35.2  14.2   4.1   1.9   0.3   0.0   0.0


TIMES OF FAILURE(MINUTES)
                0.0  10.0  20.0  30.0  40.0  50.0  60.0  70.0  80.0  90.0 100.0 110.0 120.0
  PERCENT       0.0   0.0   0.0   0.0   0.8   1.1   6.8   7.1  15.0  22.6  24.3  22.3


 INITIATION T-RTNDT(DEG.F)
              -100.0 -75.0 -50.0 -25.0   0.0  25.0  50.0  75.0 100.0 125.0 150.0 175.0 200.0
  NUMBER          0     0    24   235   378   173   187    45     2     0     0     0
  PERCENT       0.0   0.0   2.3  22.5  36.2  16.6  17.9   4.3   0.2   0.0   0.0   0.0


 ARREST T-RTNDT(DEG.F)
              -50.0 -25.0   0.0  25.0  50.0  75.0 100.0 125.0 150.0 175.0 200.0 225.0 250.0
  NUMBER          0     6    51    21     2     0    23   449   125     0     0     0
  PERCENT       0.0   0.9   7.5   3.1   0.3   0.0   3.4  66.3  18.5   0.0   0.0   0.0


 # OF STD DEVS ABOVE MEAN DELTA RTNDT(FAILURES ONLY)
                1.00  1.25  1.50  1.75  2.00  2.25  2.50  2.75  3.00
  NUMBER          6    16    30    50    53    58    82    72
  PERCENT       1.6   4.4   8.2  13.6  14.4  15.8  22.3  19.6


 # OF STD DEVS ABOVE MEAN RTNDT(FAILURES ONLY)
                1.00  1.25  1.50  1.75  2.00  2.25  2.50  2.75  3.00
  NUMBER          2     9    24    45    54    69    86    78
  PERCENT       0.5   2.5   6.5  12.3  14.7  18.8  23.4  21.3


ICRKTP = 2   IACCEL = 1   NDLRS = 1   NRTRS = 1   DATE: 10/31/84   TIME: 02.03.12

CPU TIME:  5 MIN 21 SEC
```

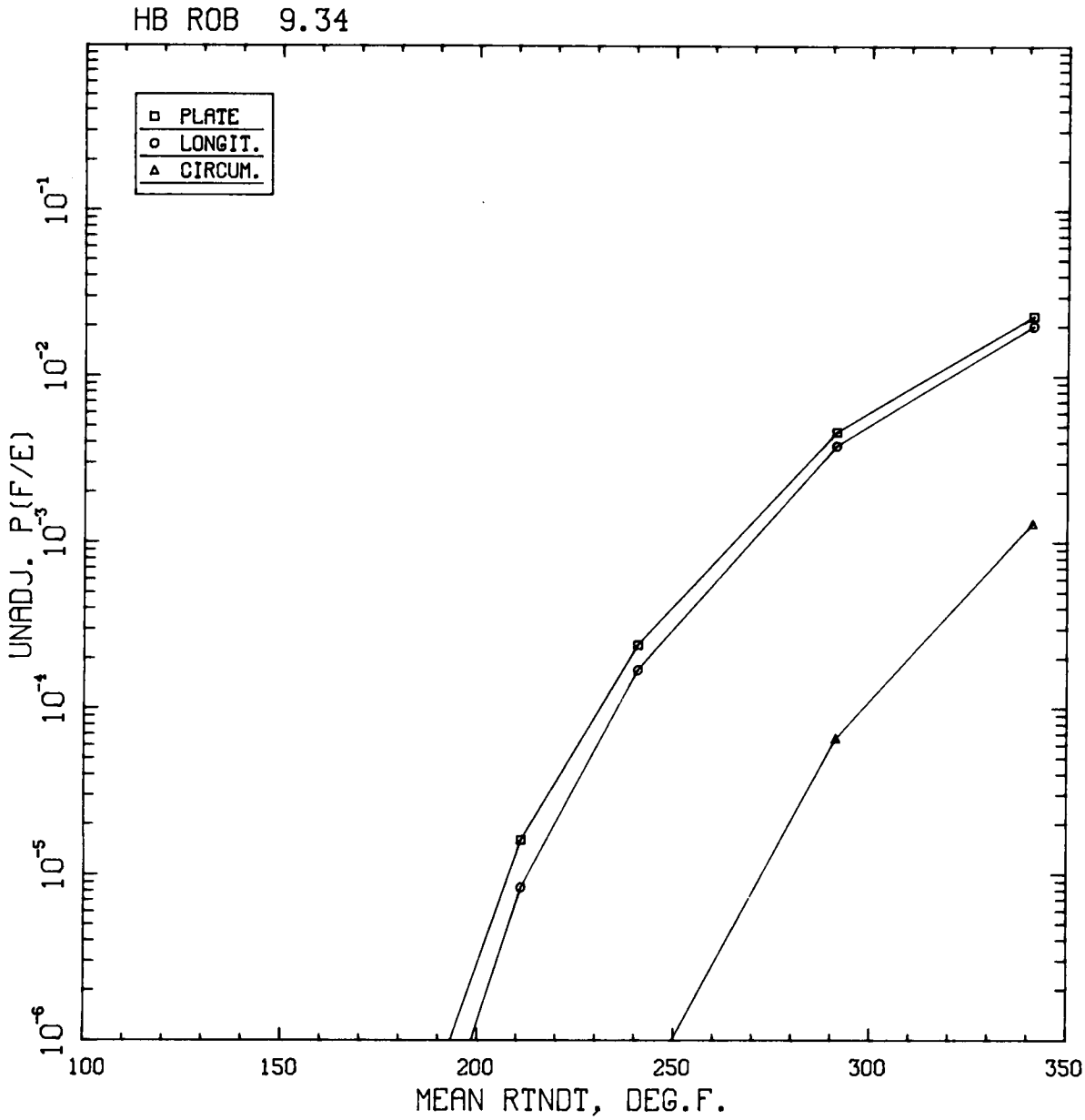

Figure I.212. Transient 9.34: $\hat{P}_j \int_0^w f(a)\, B(a)\, da$ vs $\overline{RTNDT_s}$ for (2-D, 2-D) and (2-D, 2m) flaw combinations.

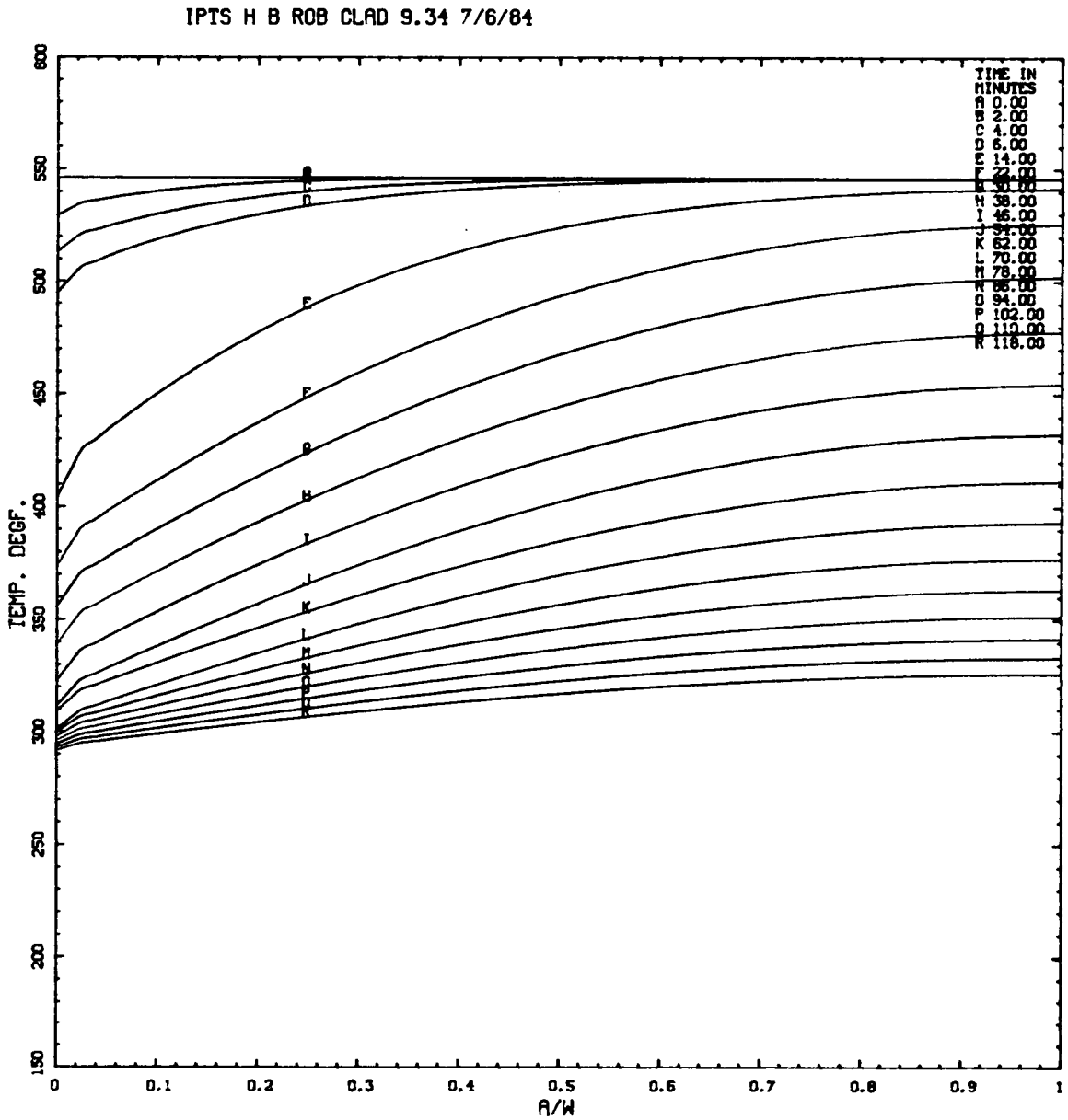

Figure I.213. Transient 9.34: Vessel wall temperature vs depth in wall (a/w) at various times (t) in transient.

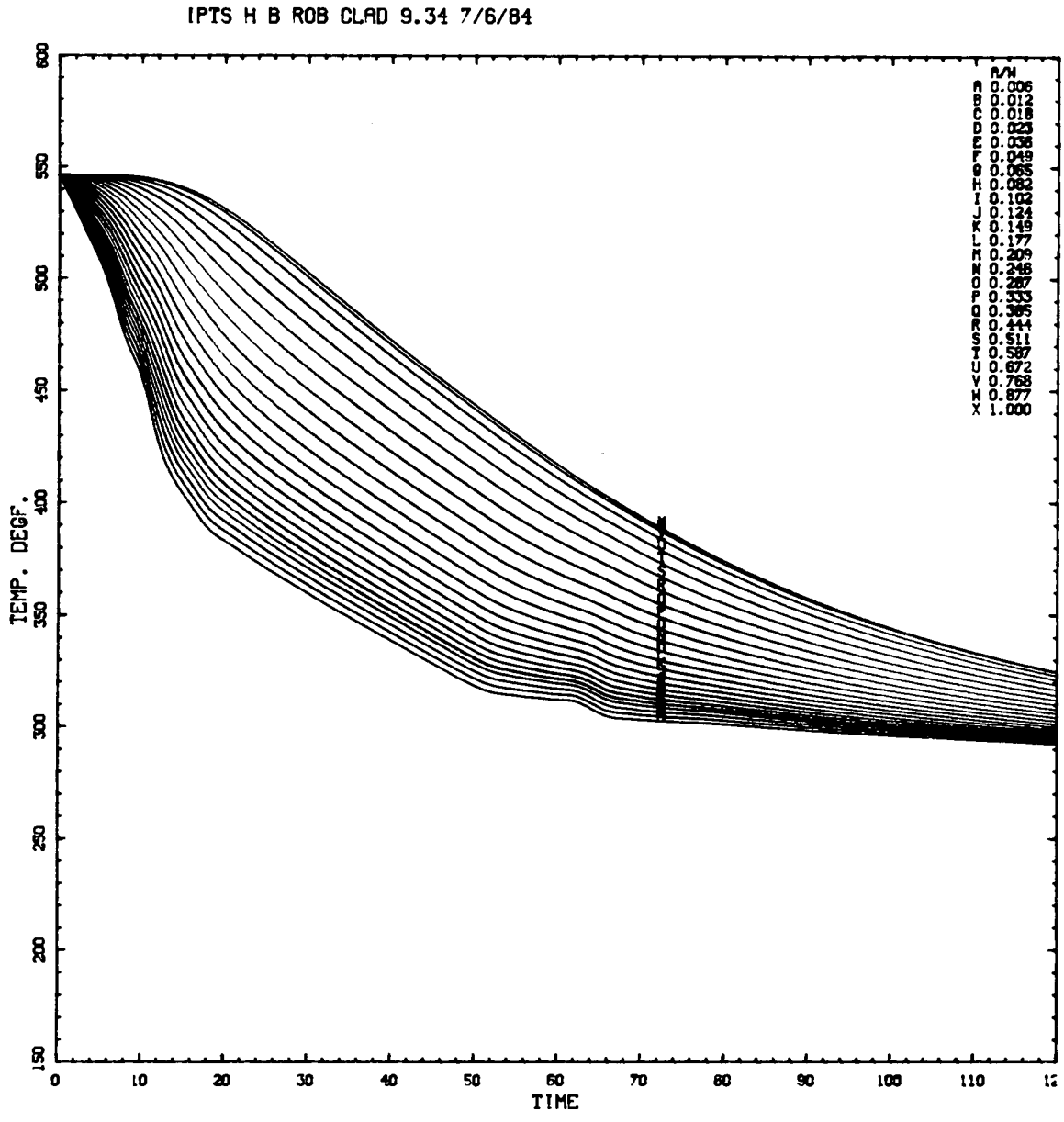

Figure I.214. Transient 9.34: Vessel wall temperature vs time (t) in transient at various depths in wall (a/w).

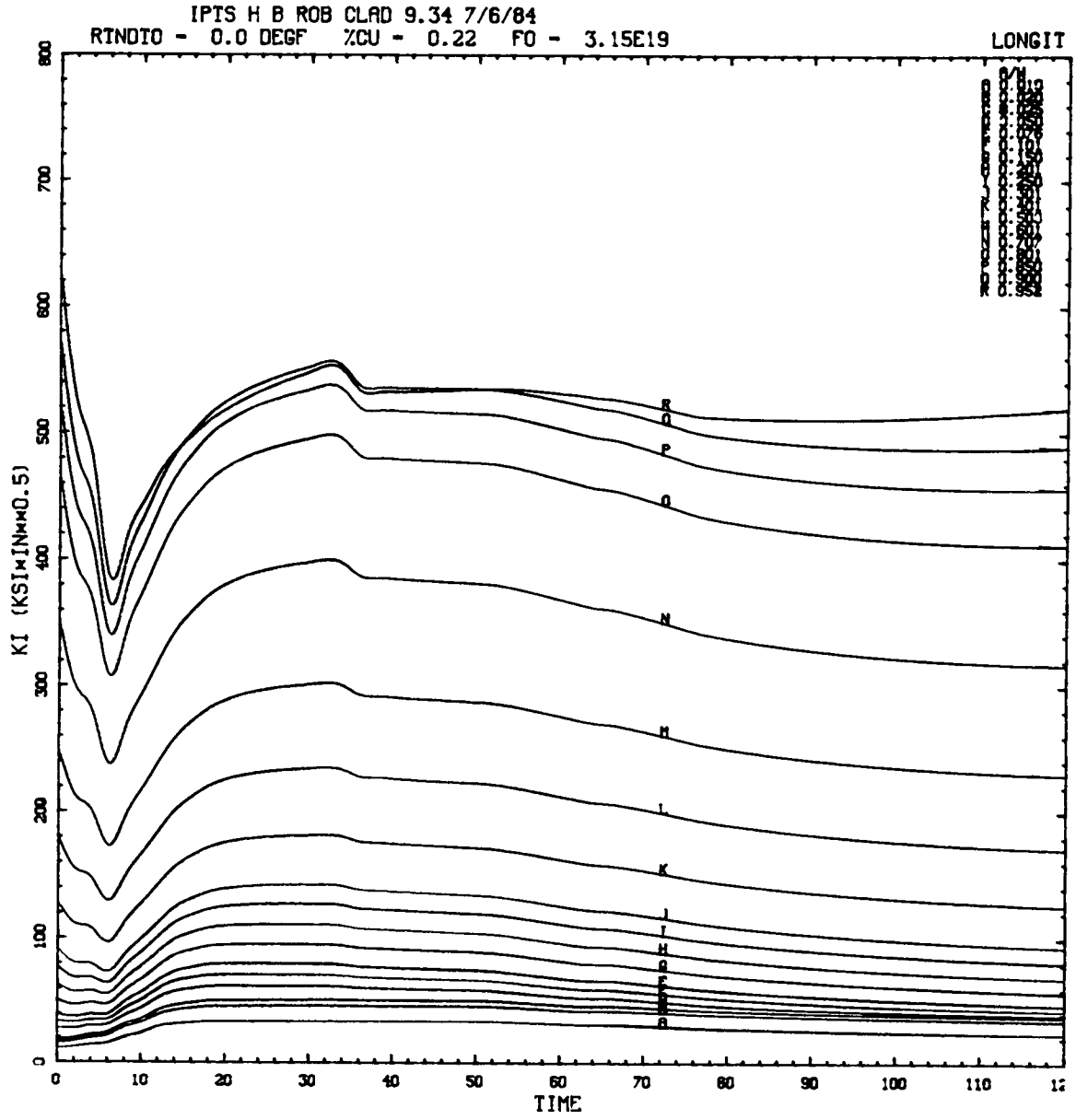

Figure I.215. Transient 9.34: K_I vs time (t) for various depths in wall (a/w).

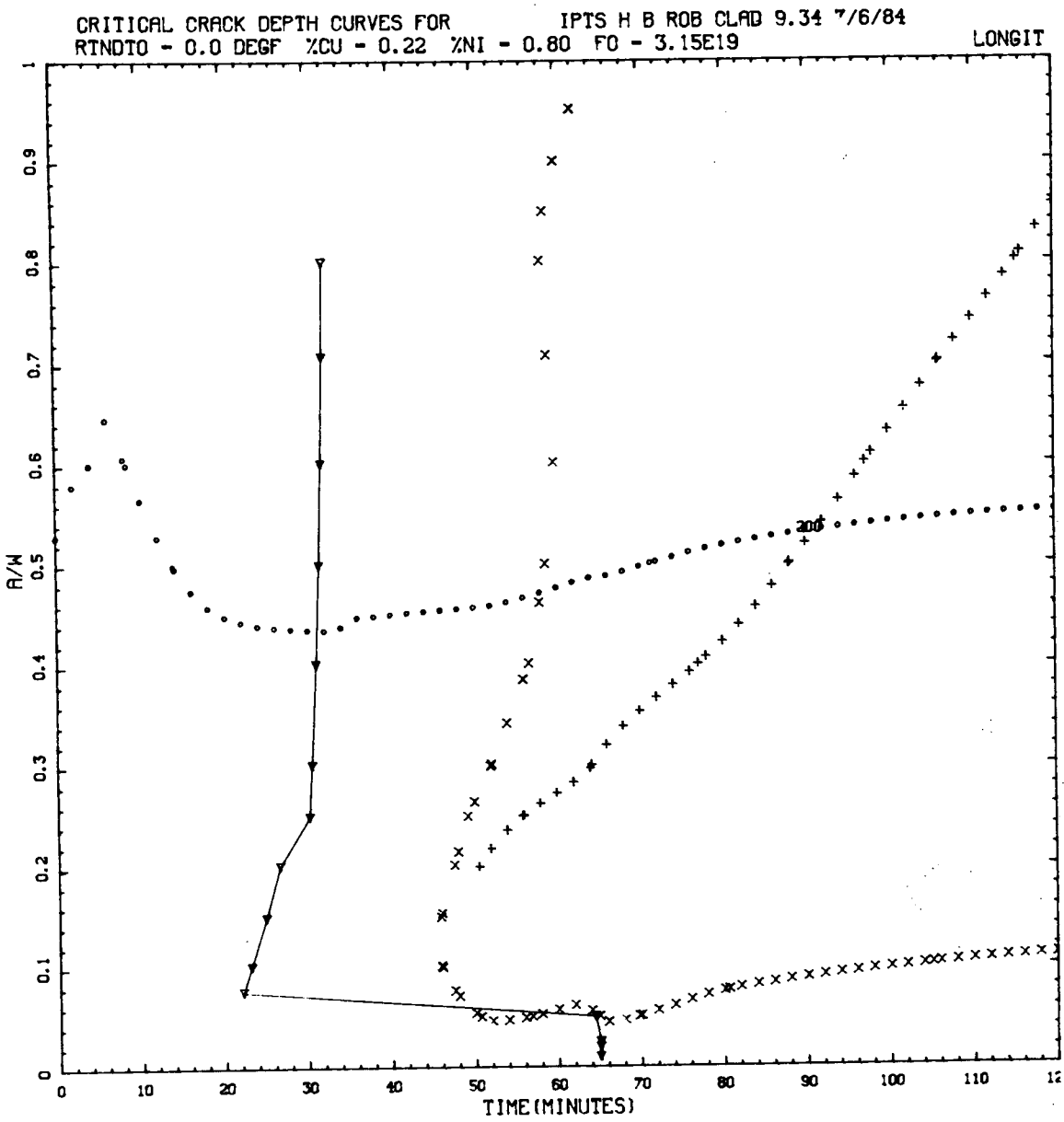

Figure I.216. Transient 9.34: Critical-crack-depth curves for weld 2-273A based on -2σ values of K_{Ic}, K_{Ia}, and $\Delta RTNDT$, mean values of all other parameters, and 32-EFPY fluences.

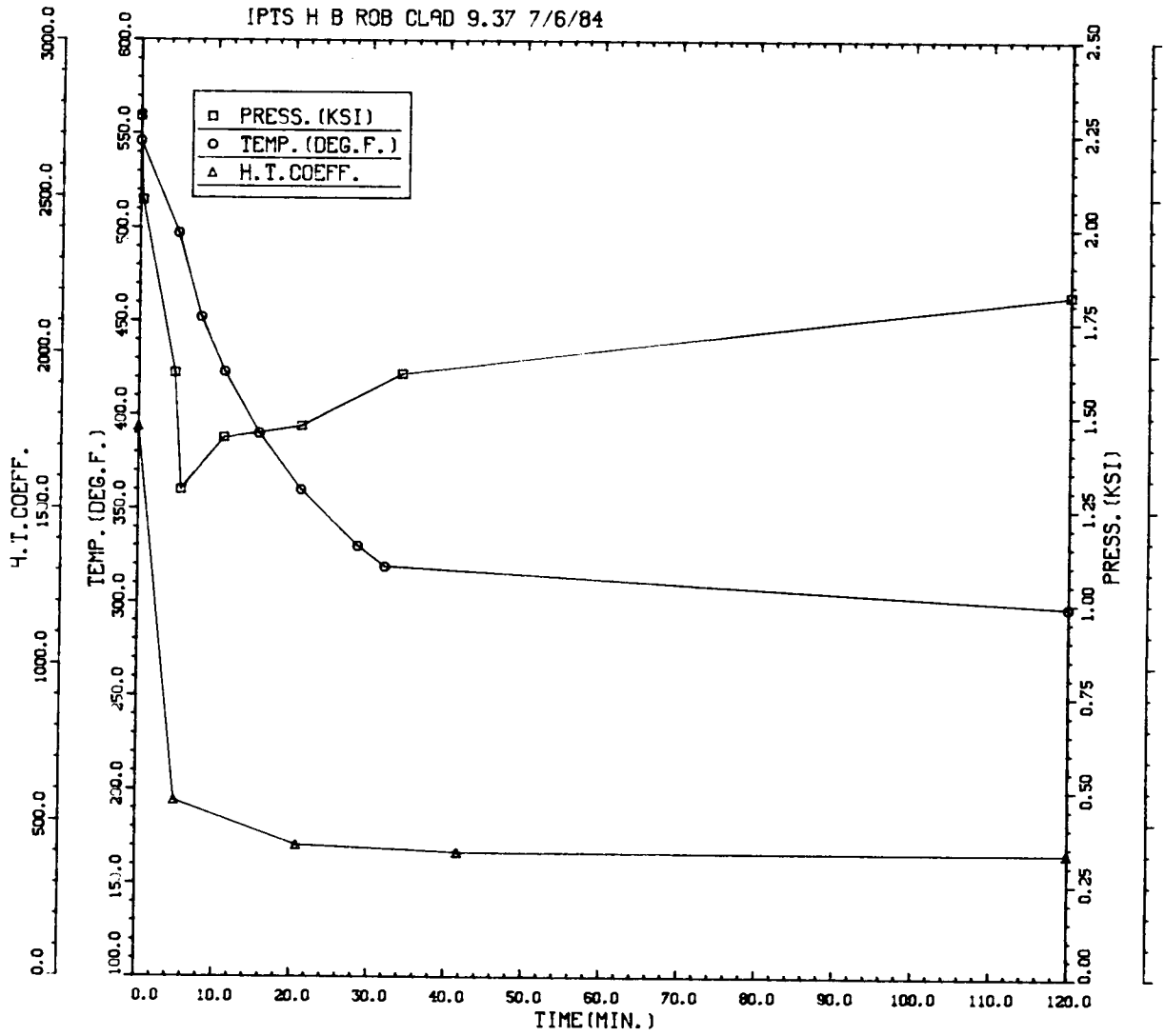

Figure I.217. Transient 9.37: Primary system pressure, downcomer coolant temperature, and fluid-film heat-transfer coefficient vs time in the transient.

Table I.37. Transient 9.37: Summary of digital output, including unadjusted $P(F|E)$ values and histogram data for crack depths, times of failure, and $T - RTNDT$ values at tip of crack corresponding to initiation and arrest events

```
IPTS H B ROB CLAD 9.37 7/6/84                    1. FLAWS/IN**3    DRTN(IS) =  211.2

            -------------UNADJUSTED--------------          ---ADJUSTED----
WELD        P(F/E)      95%CI     %ERR   P(INITIA)  N*V      P(F/E)    %ERR    NFAIL    NTRIALS

 1          1.30D-06   2.22D-07  17.12   2.05D-06  1.000    1.30D-06            131      200000

                                                   VESSEL   1.30D-06  17.12


DEPTHS FOR INITIAL INITIATION (IN)
                0.09  0.26  0.46  0.67  0.90  1.16  1.44  1.74  2.08
   NUMBER        0    76    76    38    10     5     2     0     0
   PERCENT      0.0  36.7  36.7  18.4   4.8   2.4   1.0   0.0   0.0


TIMES OF FAILURE(MINUTES)
                0.0  10.0  20.0  30.0  40.0  50.0  60.0  70.0  80.0  90.0 100.0 110.0 120.0
   PERCENT      0.0   0.0   0.0   0.0   0.0   0.0   4.6  10.7  16.0  26.0  17.6  25.2


 INITIATION T-RTNDT(DEG.F)
              -100.0 -75.0 -50.0 -25.0   0.0  25.0  50.0  75.0 100.0 125.0 150.0 175.0 200.0
   NUMBER        0     0     0    23   127   143    38     4     0     0     0     0     0
   PERCENT      0.0   0.0   0.0   6.9  37.9  42.7  11.3   1.2   0.0   0.0   0.0   0.0


 ARREST T-RTNDT(DEG.F)
               -50.0 -25.0   0.0  25.0  50.0  75.0 100.0 125.0 150.0 175.0 200.0 225.0 250.0
   NUMBER        0     0     0     8     1     2    12    89    92     0     0     0
   PERCENT      0.0   0.0   0.0   3.9   0.5   1.0   5.9  43.6  45.1   0.0   0.0   0.0


 # OF STD DEVS ABOVE MEAN DELTA RTNDT(FAILURES ONLY)
                1.00  1.25  1.50  1.75  2.00  2.25  2.50  2.75  3.00
   NUMBER        0     3     3    10    17    20    30    48
   PERCENT      0.0   2.3   2.3   7.6  13.0  15.3  22.9  36.6


 # OF STD DEVS ABOVE MEAN RTNDT(FAILURES ONLY)
                1.00  1.25  1.50  1.75  2.00  2.25  2.50  2.75  3.00
   NUMBER        0     0     3     6    20    31    31    40
   PERCENT      0.0   0.0   2.3   4.6  15.3  23.7  23.7  30.5


ICRKTP = 2   IACCEL = 1   NDLRS = 2   NRTRS = 2   DATE: 10/31/84   TIME: 22.48.44

CPU TIME:  5 MIN 19 SEC
```

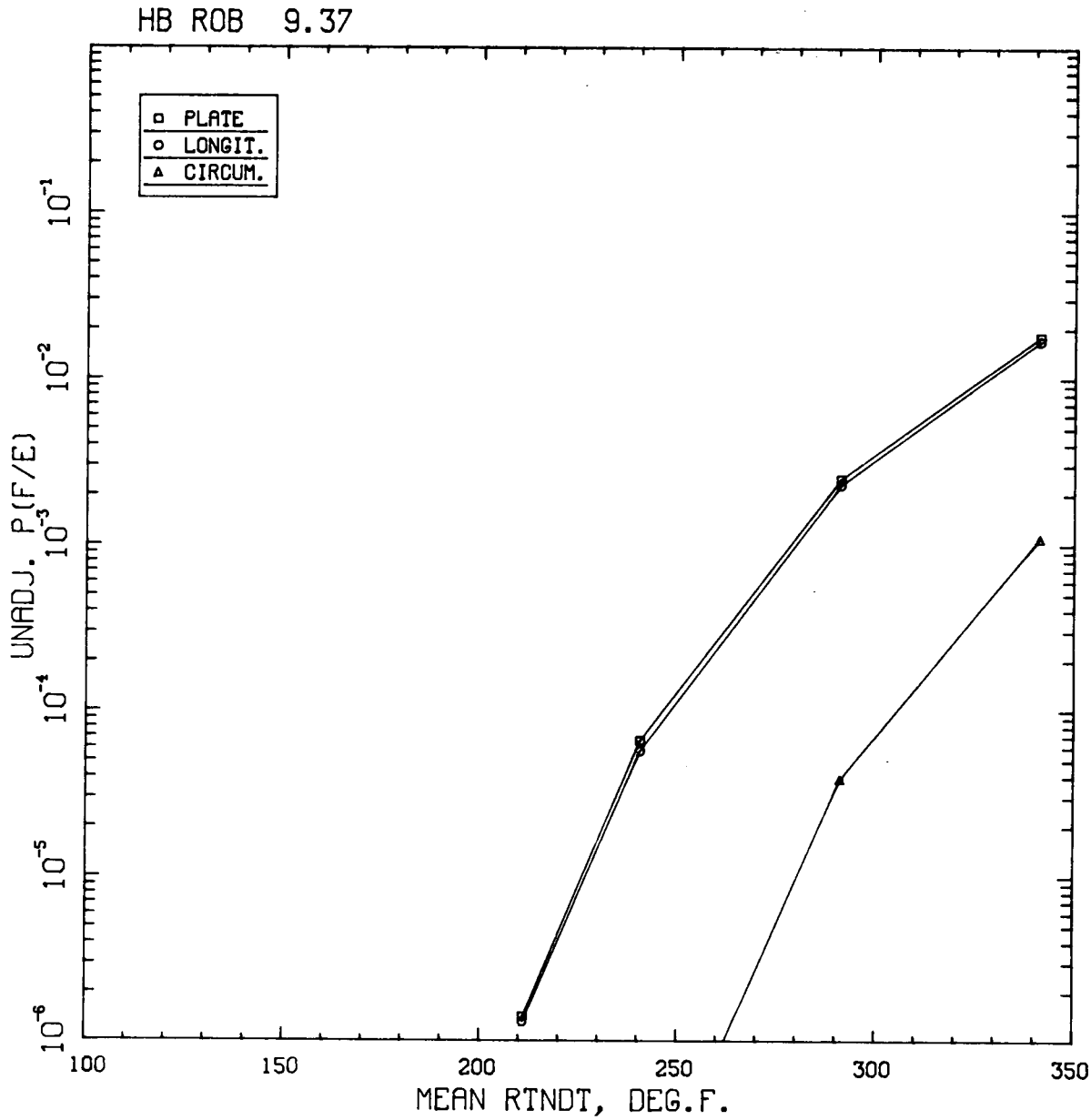

Figure I.218. Transient 9.37: $\hat{P}_j \int_0^w f(a)\, B(a)\, da$ **vs** $\overline{RTNDT_s}$ **for (2-D, 2-D) and (2-D, 2m) flaw combinations.**

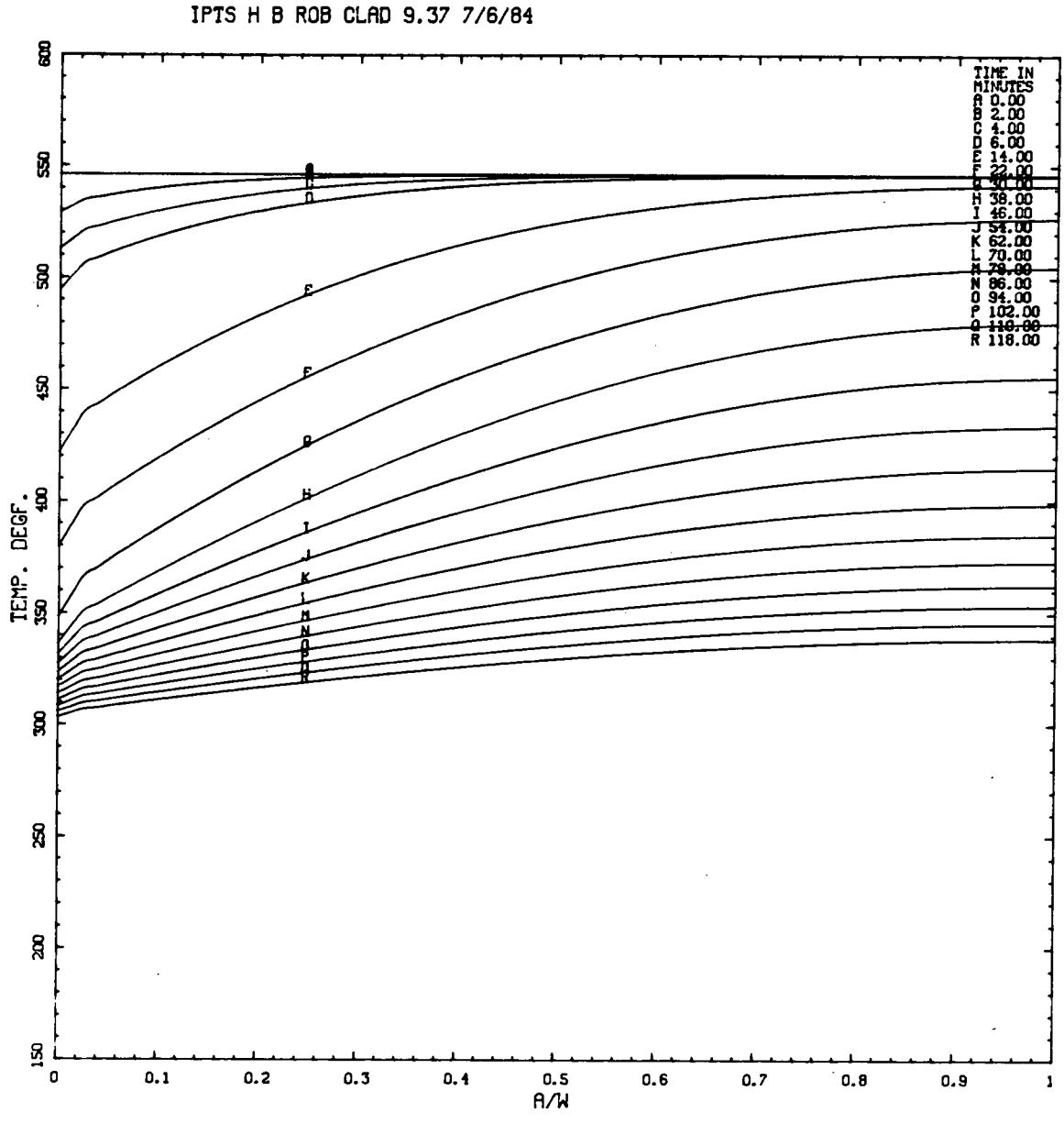

Figure I.219. Transient 9.37: Vessel wall temperature vs depth in wall (a/w) at various times (t) in transient.

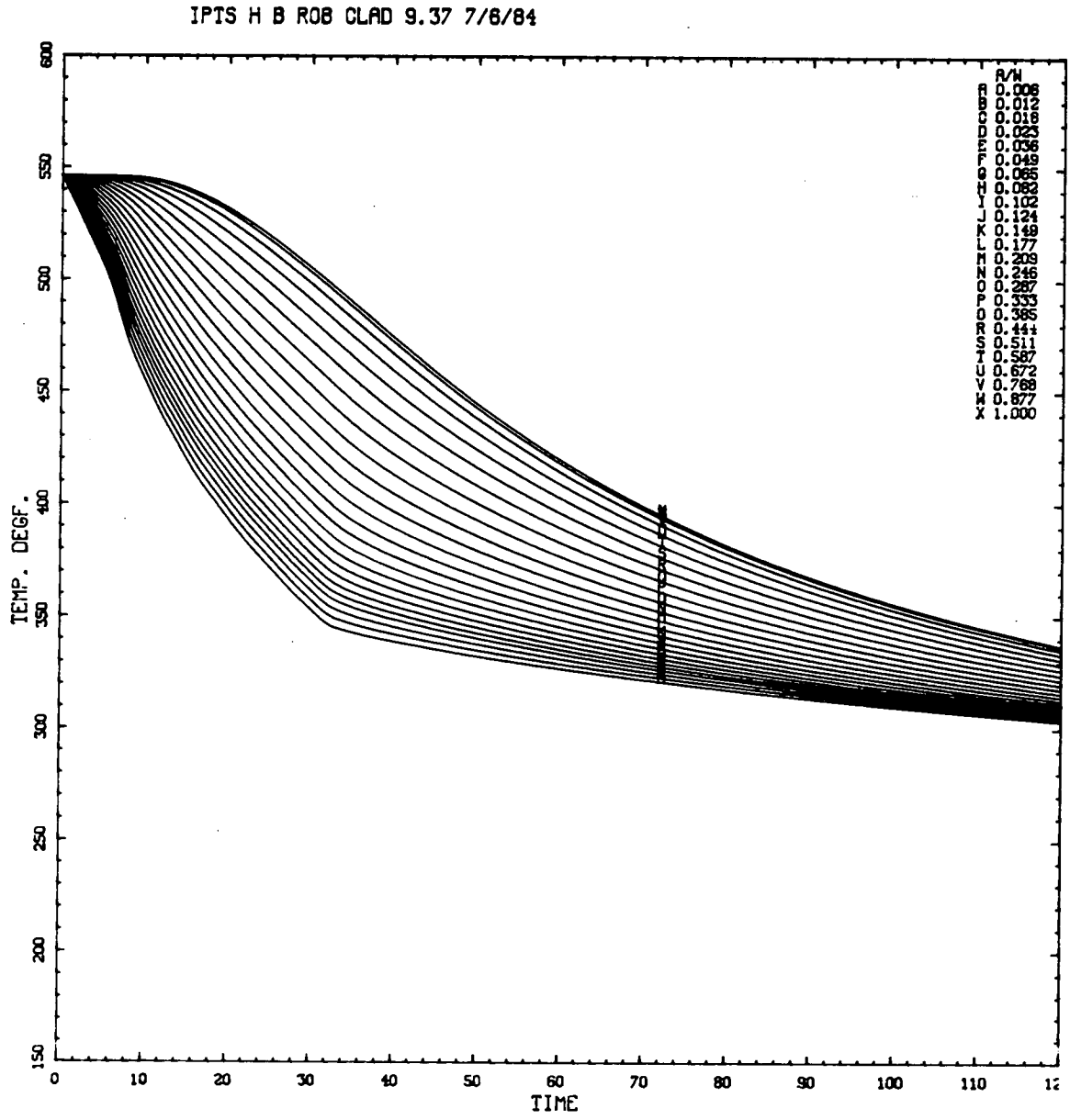

Figure I.220. Transient 9.37: Vessel wall temperature vs time (t) in transient at various depths in wall (a/w).

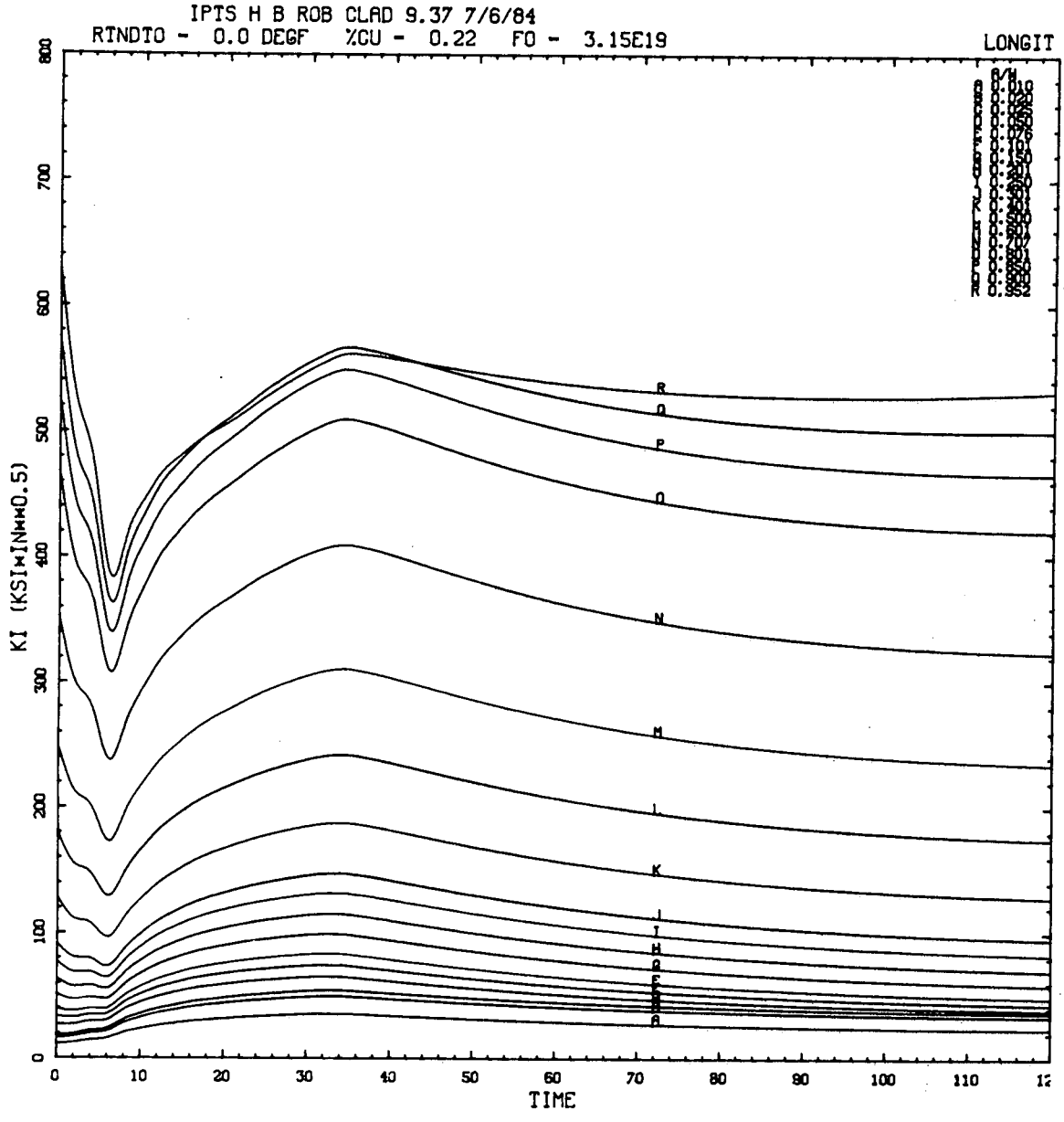

Figure I.221. Transient 9.37: K_I vs time (t) for various depths in wall (a/w).

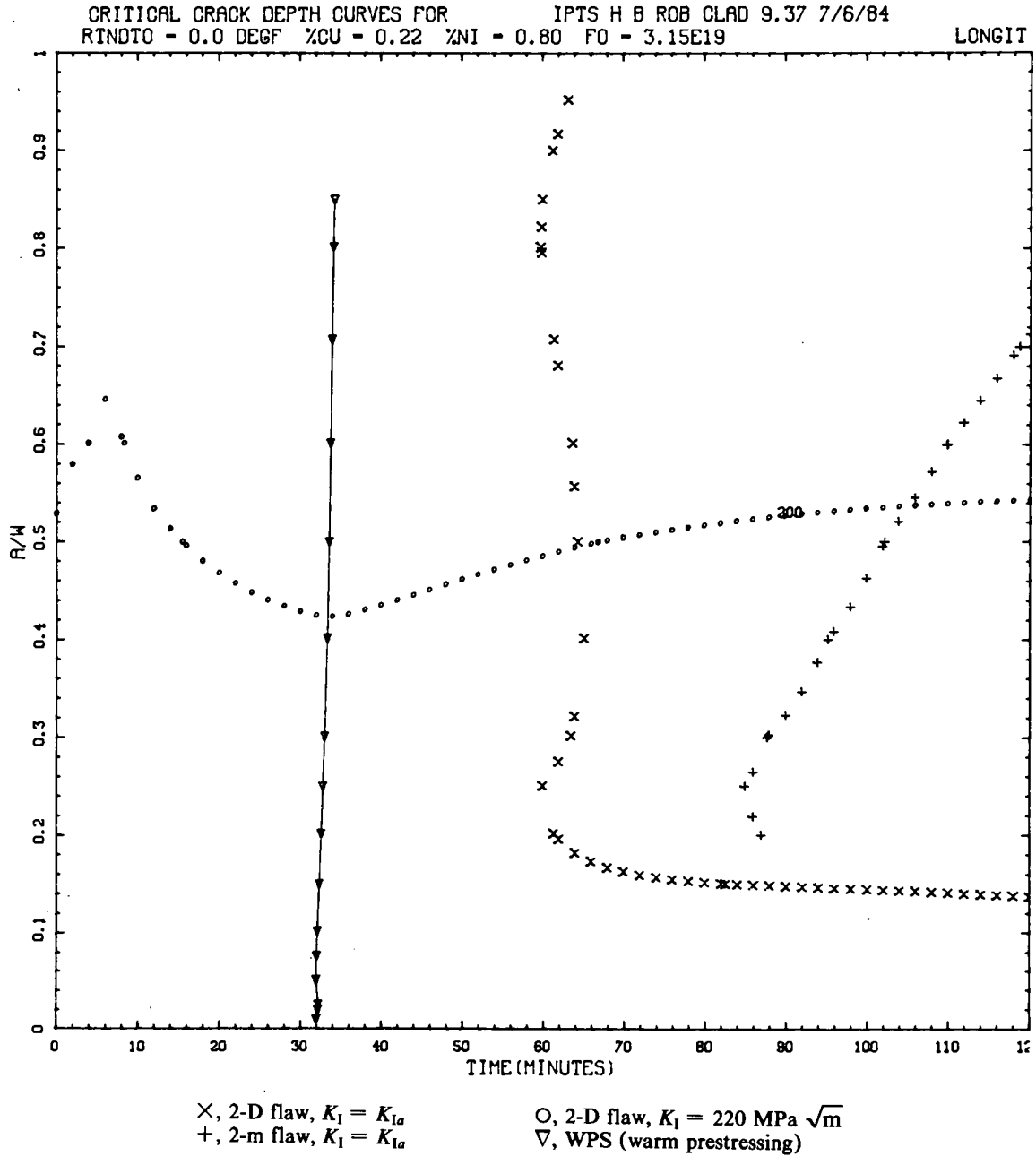

Figure I.222. Transient 9.37: Critical-crack-depth curves for weld 2-273A based on -2σ values of K_{Ic}, K_{Ia}, and $\Delta RTNDT$, mean values of all other parameters, and 32-EFPY fluences.

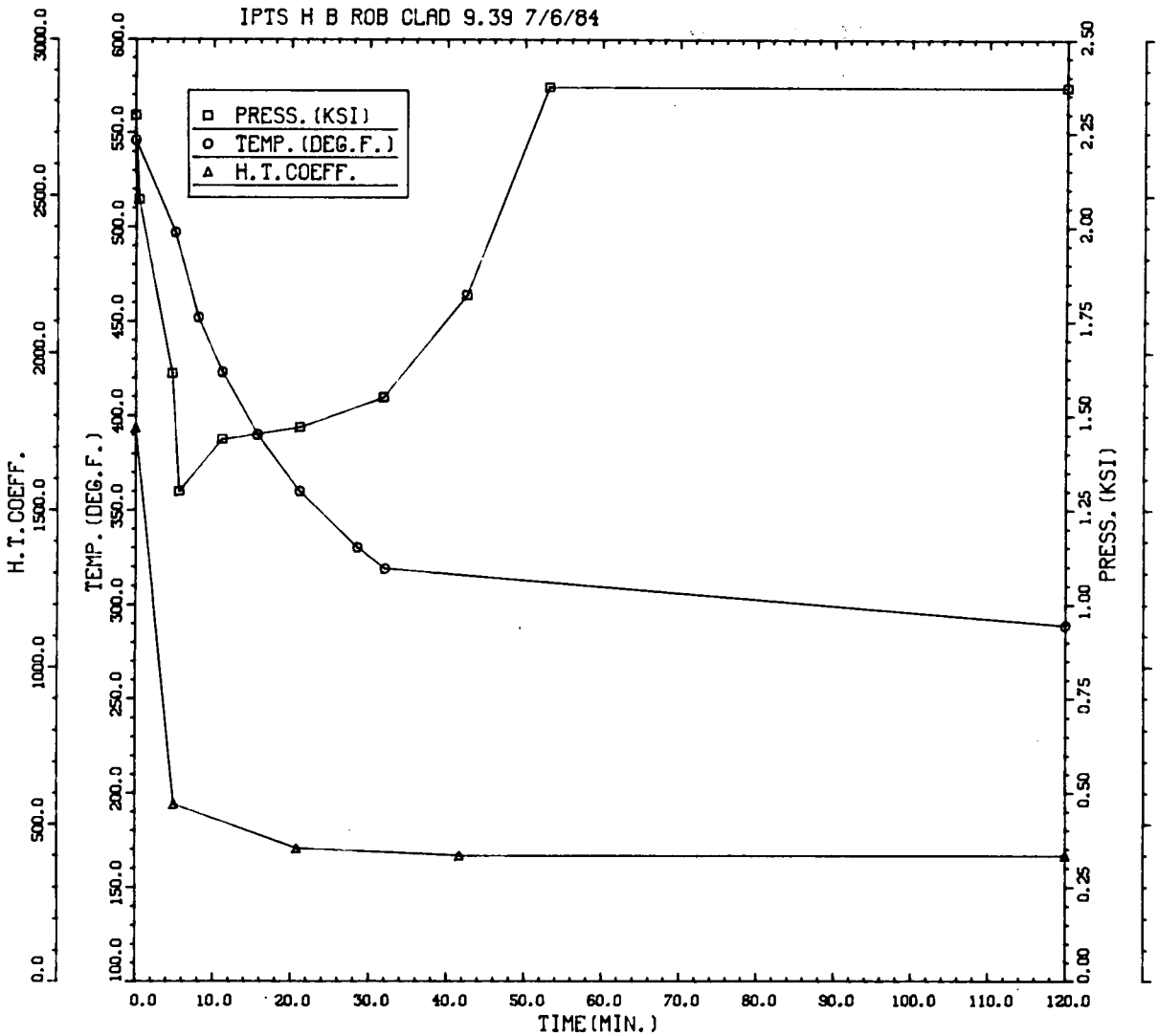

Figure I.223. Transient 9.39: Primary system pressure, downcomer coolant temperature, and fluid-film heat-transfer coefficient vs time in the transient.

Table I.38. Transient 9.39: Summary of digital output, including unadjusted $P(F|E)$ values and histogram data for crack depths, times of failure, and $T - RTNDT$ values at tip of crack corresponding to initiation and arrest events

IPTS H B ROB CLAD 9.39 7/6/84 1. FLAWS/IN**3 DRTN(IS) = 211

	UNADJUSTED					ADJUSTED			
WELD	P(F/E)	95%CI	%ERR	P(INITIA)	N*V	P(F/E)	%ERR	NFAIL	NTRIAL
1	1.32D-05	1.28D-06	9.68	1.51D-05	1.000	1.32D-05		409	140000
					VESSEL	1.32D-05	9.68		

DEPTHS FOR INITIAL INITIATION (IN)

	0.09	0.26	0.46	0.67	0.90	1.16	1.44	1.74	2.08
NUMBER	0	162	152	82	43	25	4	0	1
PERCENT	0.0	34.5	32.4	17.5	9.2	5.3	0.9	0.0	0.2

TIMES OF FAILURE(MINUTES)

	0.0	10.0	20.0	30.0	40.0	50.0	60.0	70.0	80.0	90.0	100.0	110.0	120.0
PERCENT	0.0	0.0	0.0	0.0	8.8	33.5	7.1	8.6	11.0	8.3	10.0	12.7	

INITIATION T-RTNDT(DEG.F)

	-100.0	-75.0	-50.0	-25.0	0.0	25.0	50.0	75.0	100.0	125.0	150.0	175.0	200.0
NUMBER	0	0	4	115	261	106	101	35	0	0	0	0	
PERCENT	0.0	0.0	0.6	18.5	42.0	17.0	16.2	5.6	0.0	0.0	0.0	0.0	

ARREST T-RTNDT(DEG.F)

	-50.0	-25.0	0.0	25.0	50.0	75.0	100.0	125.0	150.0	175.0	200.0	225.0	250.
NUMBER	0	14	16	10	0	0	1	85	87	0	0	0	
PERCENT	0.0	6.6	7.5	4.7	0.0	0.0	0.5	39.9	40.8	0.0	0.0	0.0	

OF STD DEVS ABOVE MEAN DELTA RTNDT(FAILURES ONLY)

	1.00	1.25	1.50	1.75	2.00	2.25	2.50	2.75	3.00
NUMBER	24	25	47	57	56	68	71	61	
PERCENT	5.9	6.1	11.5	13.9	13.7	16.6	17.4	14.9	

OF STD DEVS ABOVE MEAN RTNDT(FAILURES ONLY)

	1.00	1.25	1.50	1.75	2.00	2.25	2.50	2.75	3.00
NUMBER	8	29	45	54	61	76	75	61	
PERCENT	2.0	7.1	11.0	13.2	14.9	18.6	18.3	14.9	

ICRKTP = 2 IACCEL = 1 NDLRS = 1 NRTRS = 1 DATE: 11/03/84 TIME: 23.02.39

CPU TIME: 3 MIN 46 SEC

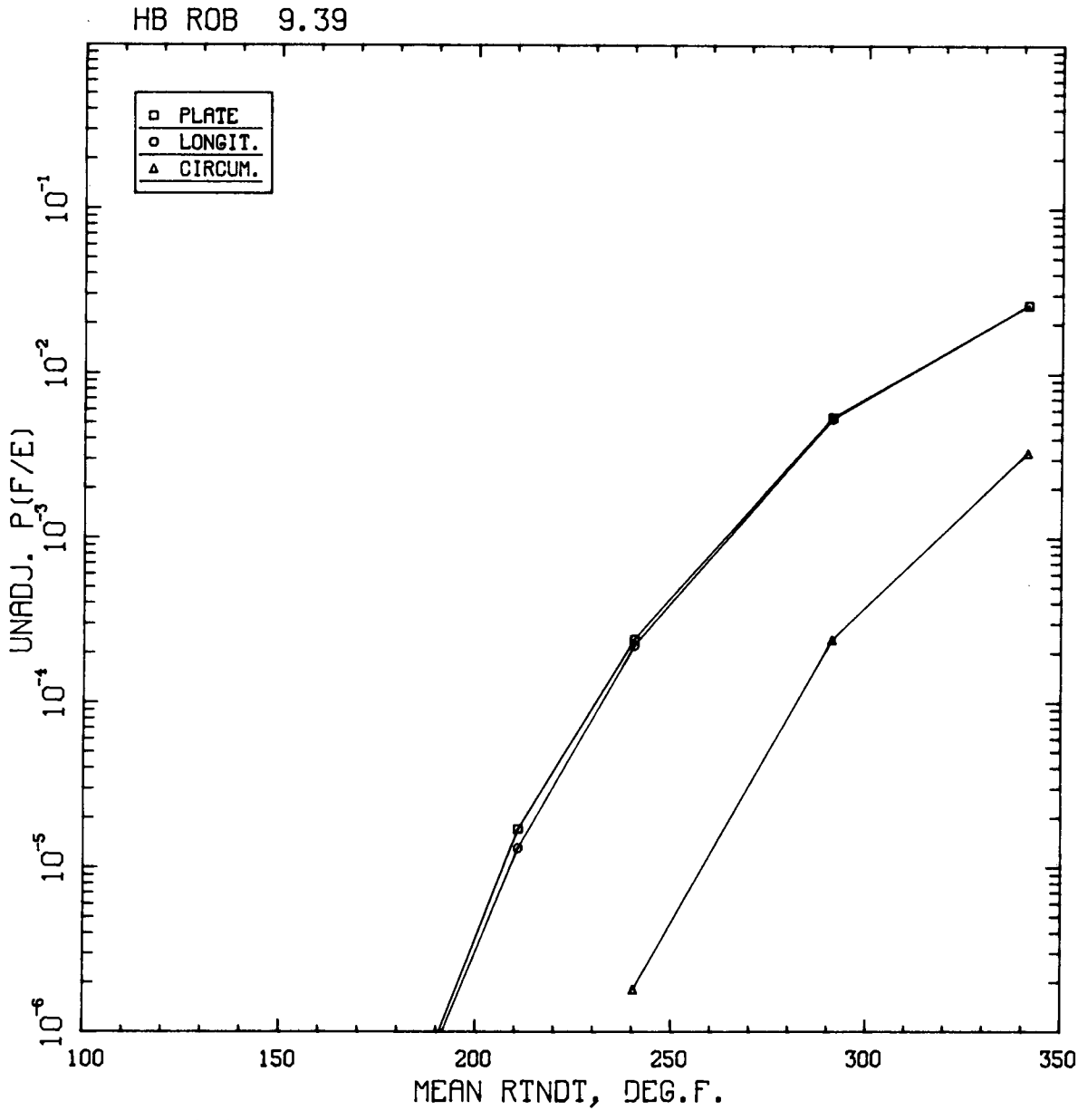

Figure I.224. Transient 9.39: $\hat{P}_j \int_0^w f(a)\, B(a)\, da$ vs $\overline{RTNDT_s}$ for (2-D, 2-D) and (2-D, 2m) flaw combinations.

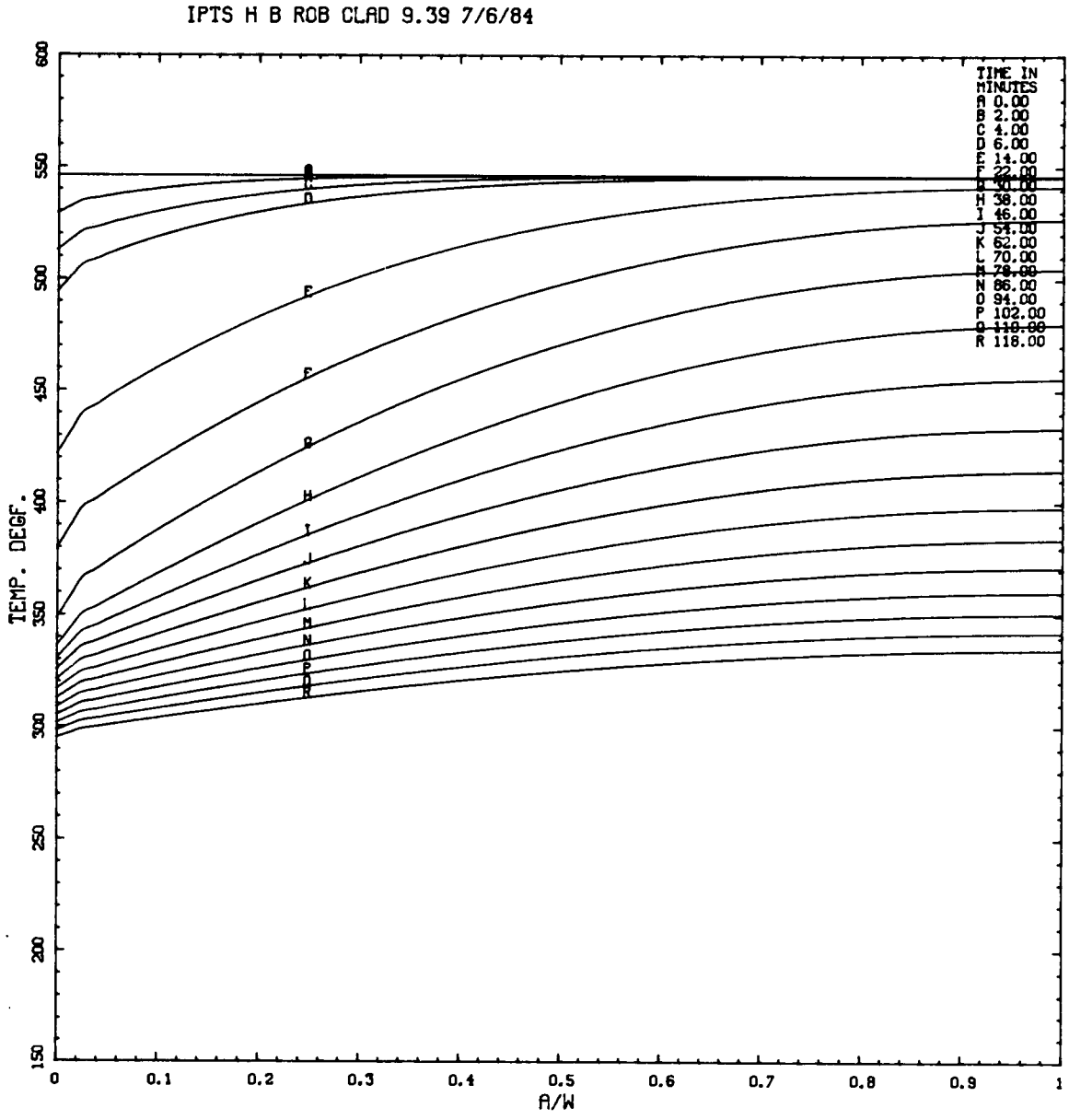

Figure I.225. Transient 9.39: Vessel wall temperature vs depth in wall (a/w) at various times (t) in transient.

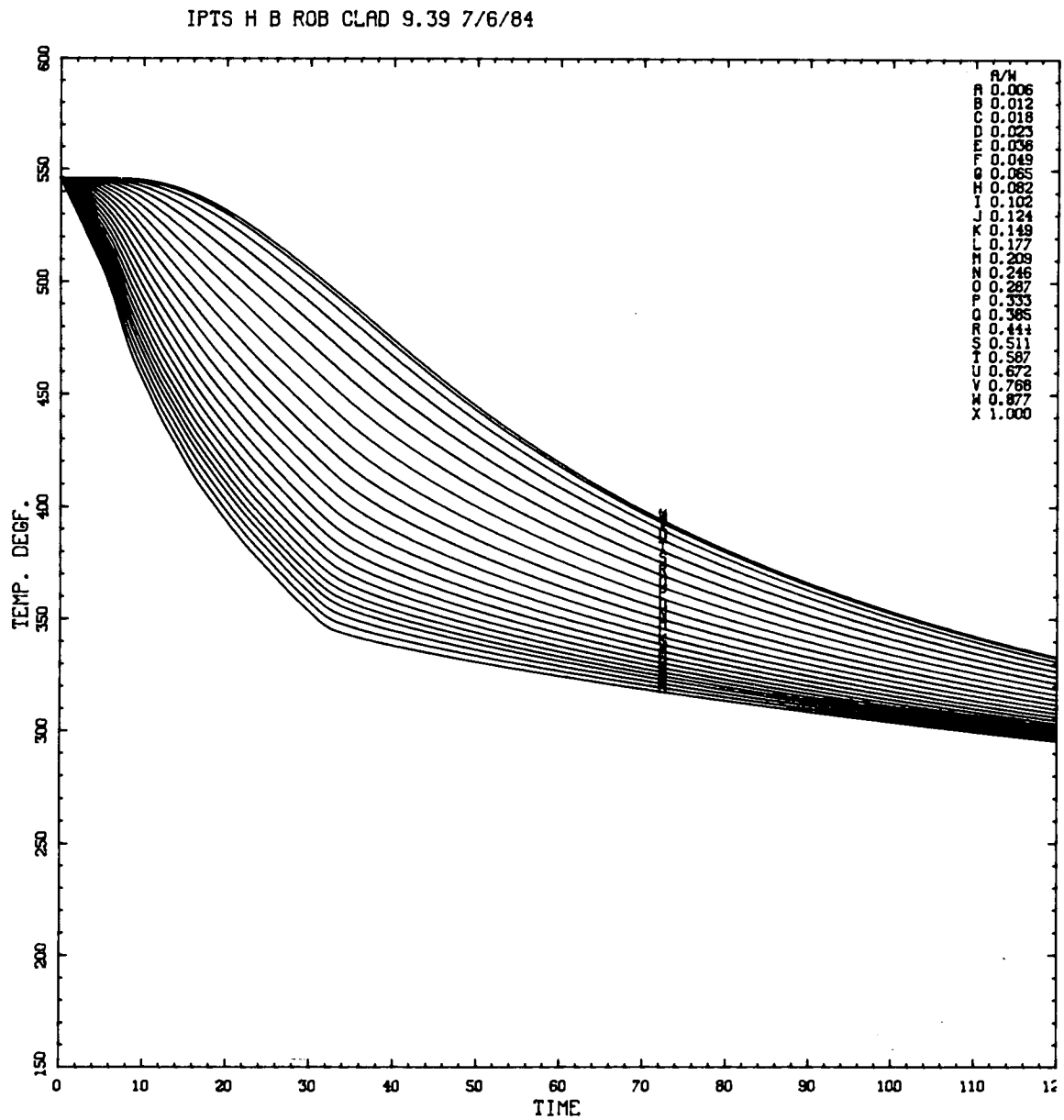

Figure I.226. Transient 9.39: Vessel wall temperature vs time (t) in transient at various depths in wall (a/w).

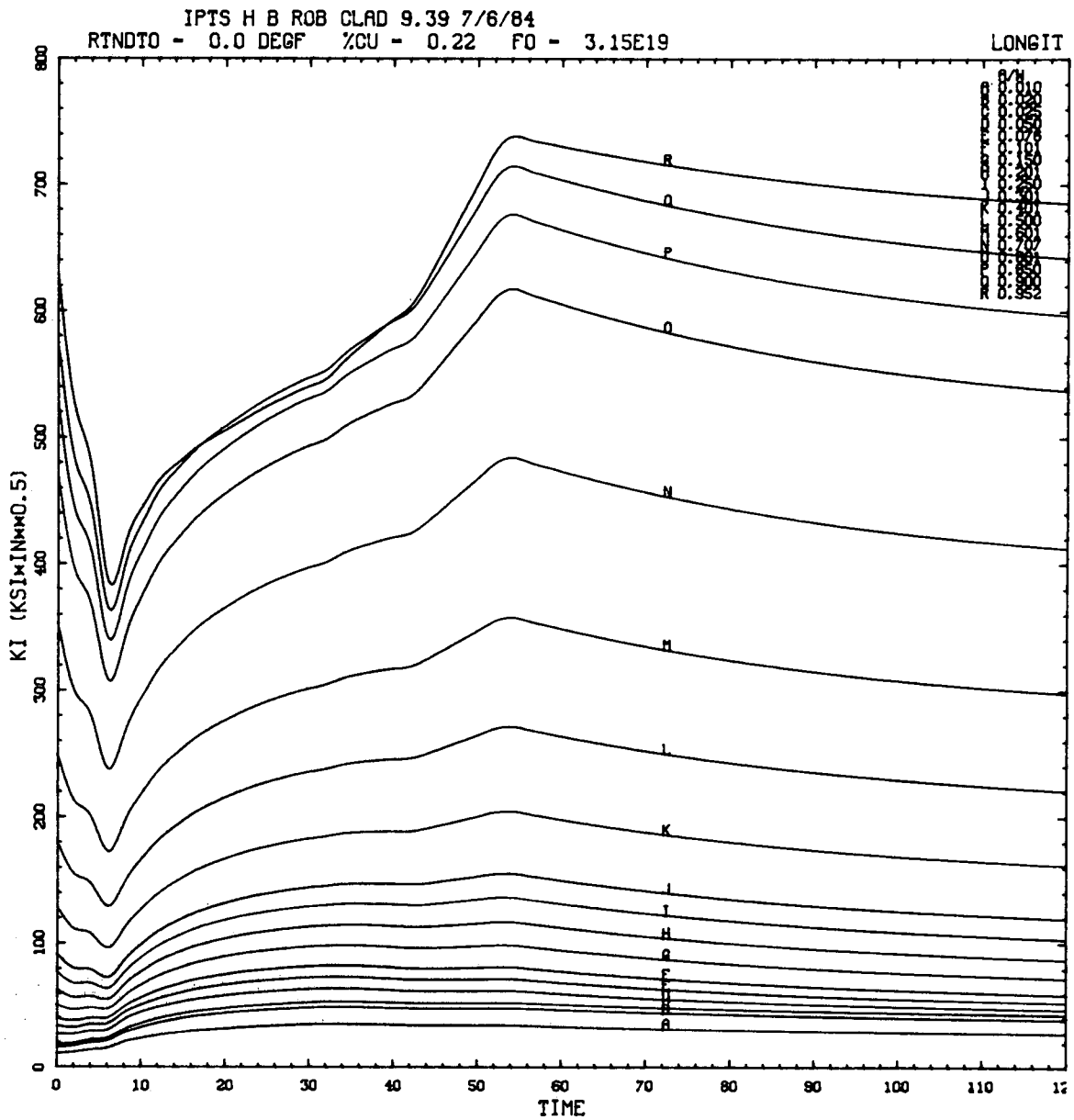

Figure I.227. Transient 9.39: K_I vs time (t) for various depths in wall (a/w).

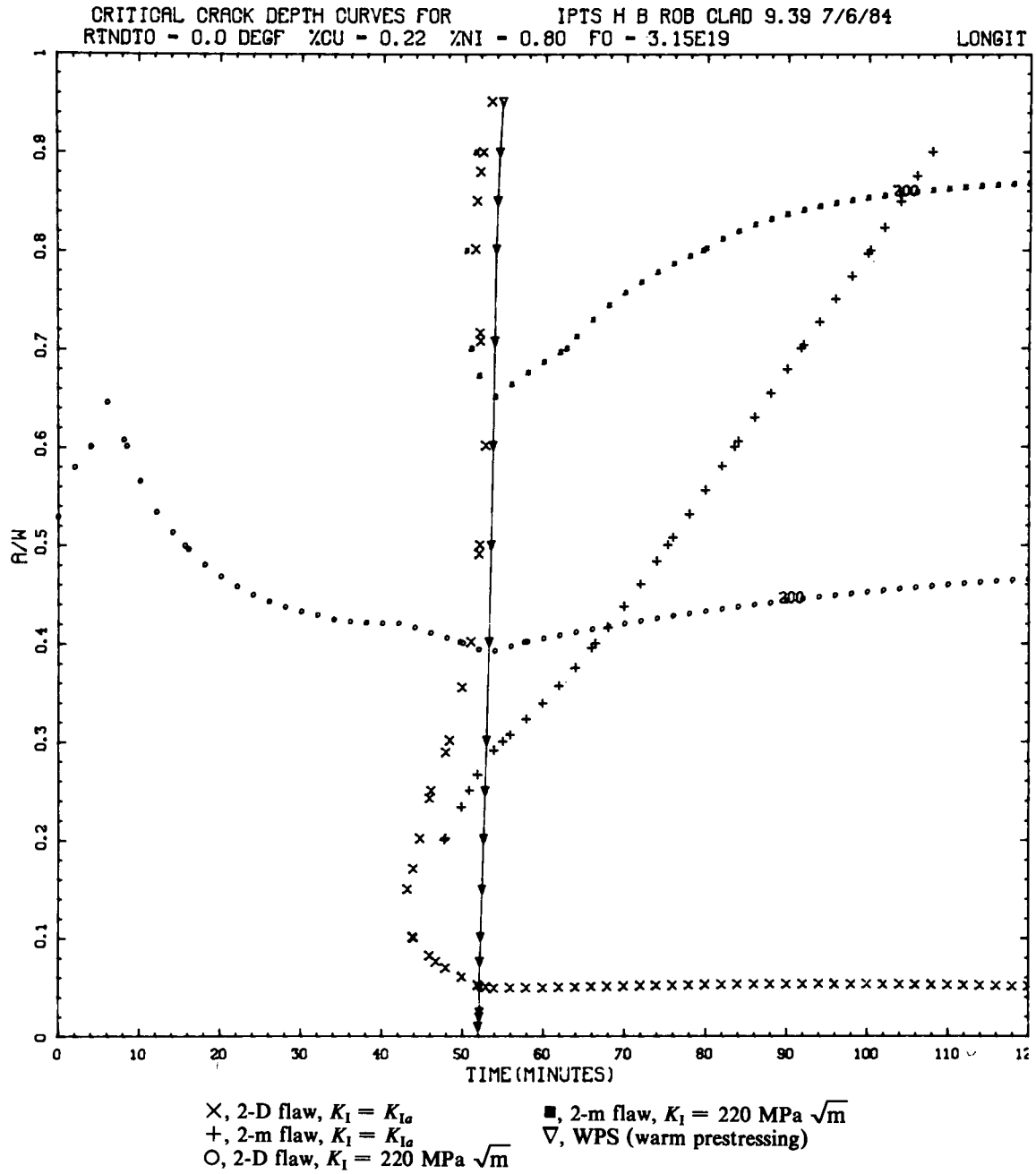

Figure I.228. Transient 9.39: Critical-crack-depth curves for weld 2-273A based on -2σ values of K_{Ic}, K_{Ia}, and $\Delta RTNDT$, mean values of all other parameters, and 32-EFPY fluences.

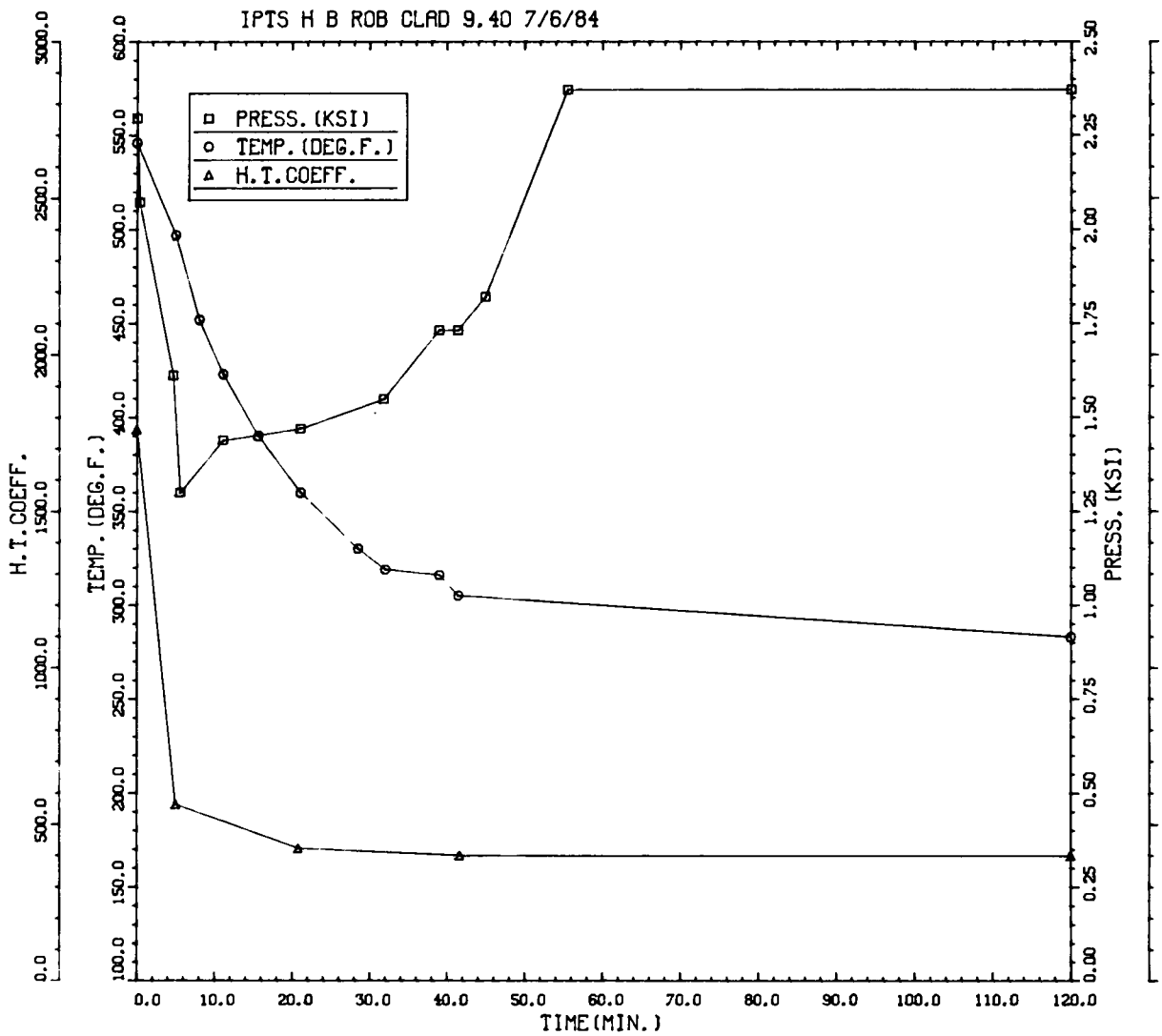

Figure I.229. Transient 9.40: Primary system pressure, downcomer coolant temperature, and fluid-film heat-transfer coefficient vs time in the transient.

Table I.39. Transient 9.40: Summary of digital output, including unadjusted $P(F|E)$ values and histogram data for crack depths, times of failure, and $T - RTNDT$ values at tip of crack corresponding to initiation and arrest events

IPTS H B ROB CLAD 9.40 7/6/84 1. FLAWS/IN**3 DRTN(IS) = 211.2

WELD	P(F/E) (UNADJUSTED)	95%CI	%ERR	P(INITIA)	N*V	P(F/E) (ADJUSTED)	%ERR	NFAIL	NTRIALS
1	2.99D-05	1.02D-05	34.12	3.45D-05	1.000	2.99D-05		33	200000
					VESSEL	2.99D-05	34.12		

DEPTHS FOR INITIAL INITIATION (IN)

	0.09	0.26	0.46	0.67	0.90	1.16	1.44	1.74	2.08
NUMBER	0	17	11	9	1	0	0	0	0
PERCENT	0.0	44.7	28.9	23.7	2.6	0.0	0.0	0.0	0.0

TIMES OF FAILURE(MINUTES)

	0.0	10.0	20.0	30.0	40.0	50.0	60.0	70.0	80.0	90.0	100.0	110.0	120.0
PERCENT	0.0	0.0	0.0	0.0	12.1	51.5	6.1	6.1	3.0	6.1	12.1	3.0	

INITIATION T-RTNDT(DEG.F)

	-100.0	-75.0	-50.0	-25.0	0.0	25.0	50.0	75.0	100.0	125.0	150.0	175.0	200.0
NUMBER	0	0	1	13	20	5	6	4	1	0	0	0	
PERCENT	0.0	0.0	2.0	26.0	40.0	10.0	12.0	8.0	2.0	0.0	0.0	0.0	

ARREST T-RTNDT(DEG.F)

	-50.0	-25.0	0.0	25.0	50.0	75.0	100.0	125.0	150.0	175.0	200.0	225.0	250.0
NUMBER	0	0	2	0	0	0	0	5	10	0	0	0	
PERCENT	0.0	0.0	11.8	0.0	0.0	0.0	0.0	29.4	58.8	0.0	0.0	0.0	

ICRKTP = 2 IACCEL = 1 NDLRS = 0 NRTRS = 0 DATE: 10/31/84 TIME: 02.21.00

CPU TIME: 5 MIN 30 SEC

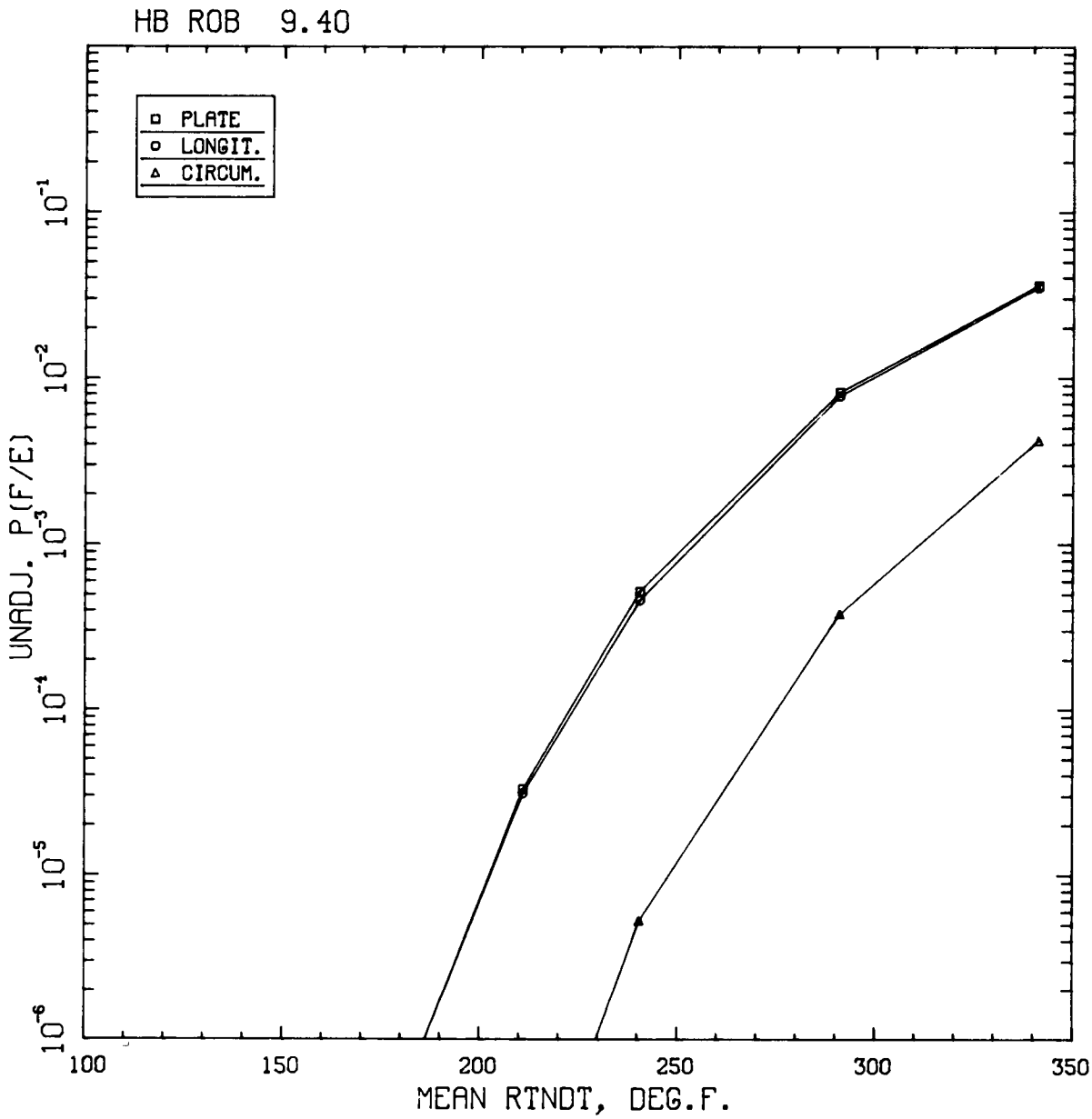

Figure I.230. Transient 9.40: $\hat{P}_j \int_0^w f(a)\, B(a)\, da$ vs $\overline{RTNDT_s}$ for (2-D, 2-D) and (2-D, 2m) flaw combinations.

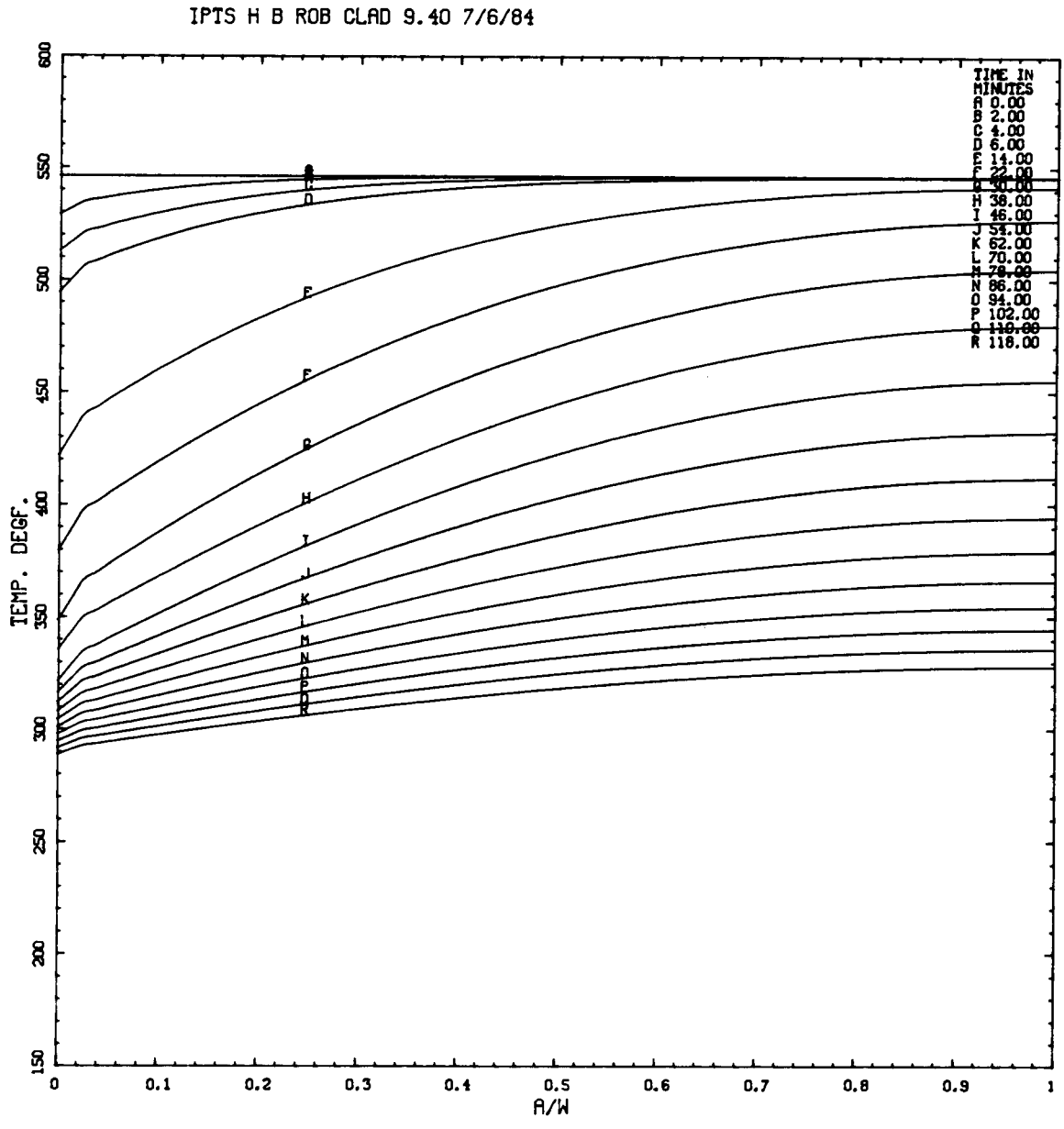

Figure I.231. Transient 9.40: Vessel wall temperature vs depth in wall (a/w) at various times (t) in transient.

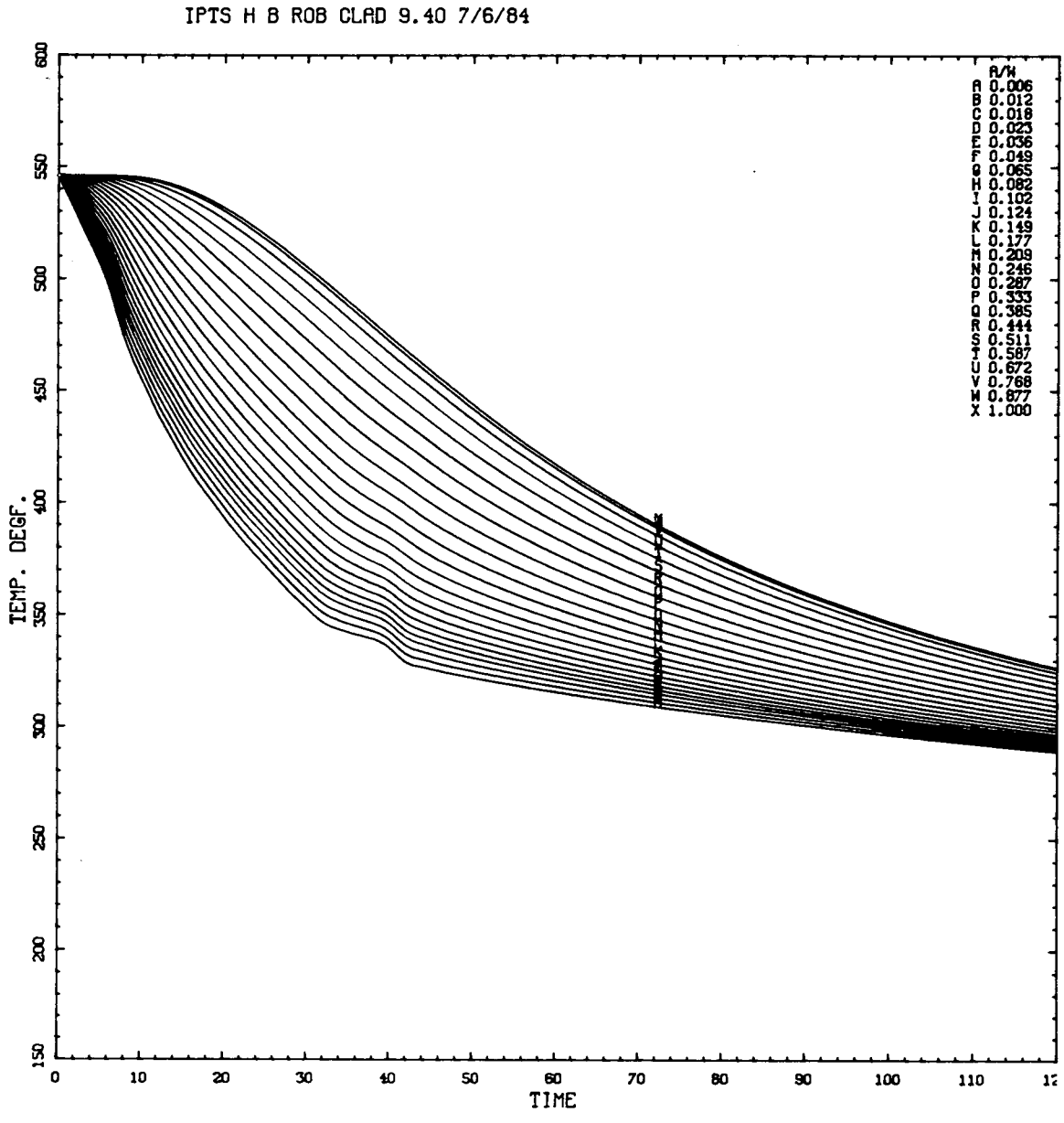

Figure I.232. Transient 9.40: Vessel wall temperature vs time (t) in transient at various depths in wall (a/w).

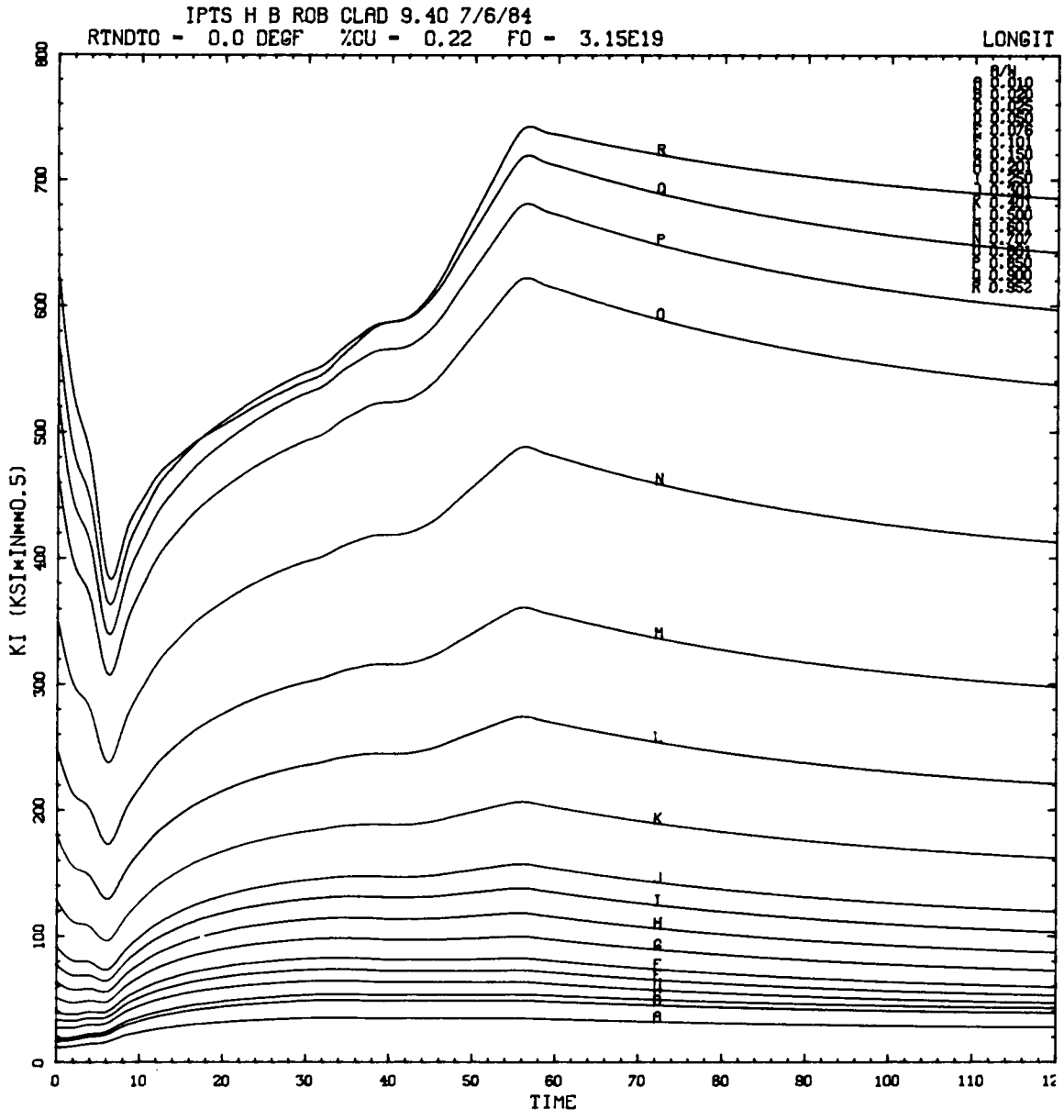

Figure I.233. Transient 9.40: K_I vs time (t) for various depths in wall (a/w).

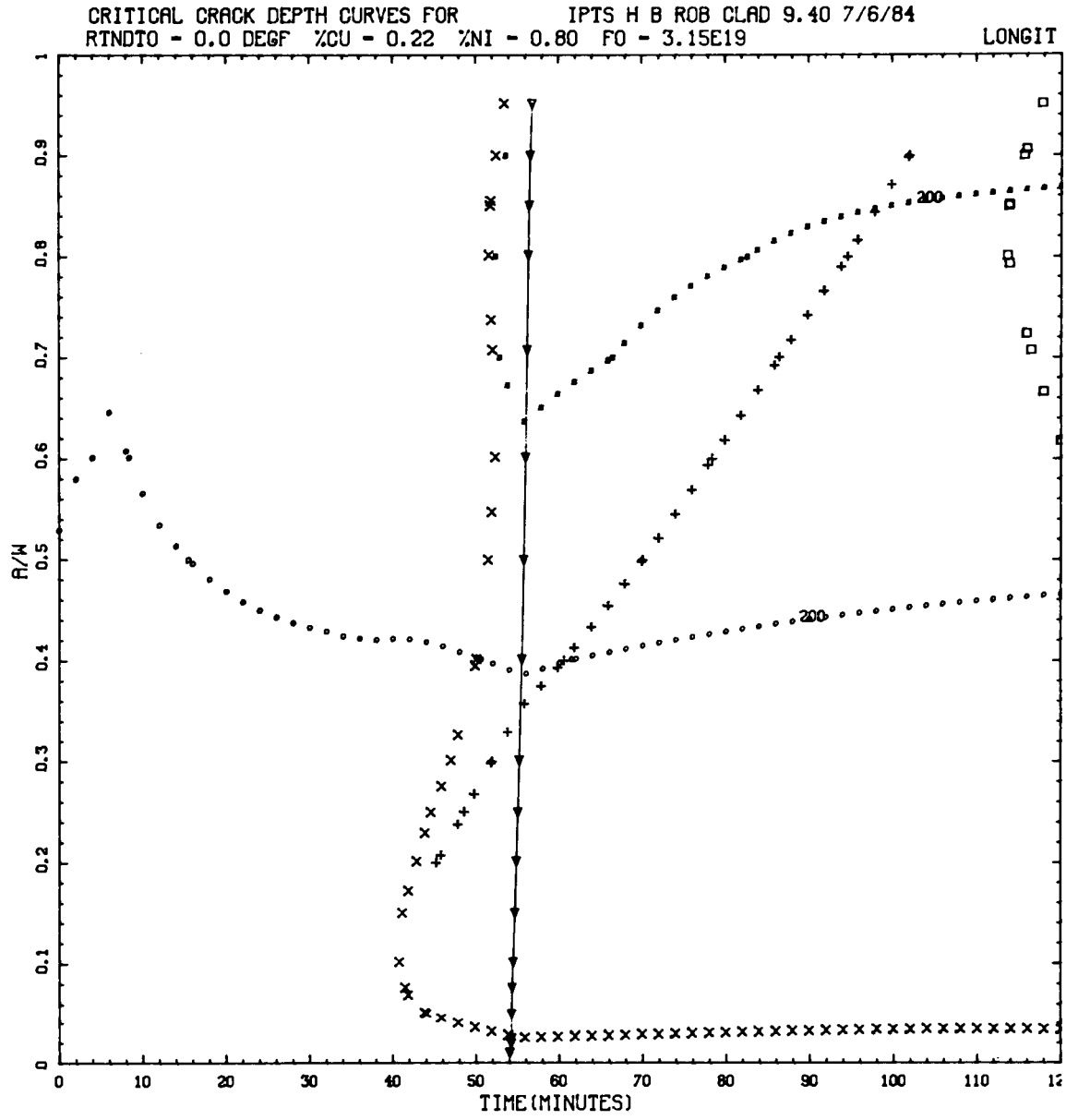

Figure I.234. Transient 9.40: Critical-crack-depth curves for weld 2-273A based on -2σ values of K_{Ic}, K_{Ia}, and $\Delta RTNDT$, mean values of all other parameters, and 32-EFPY fluences.

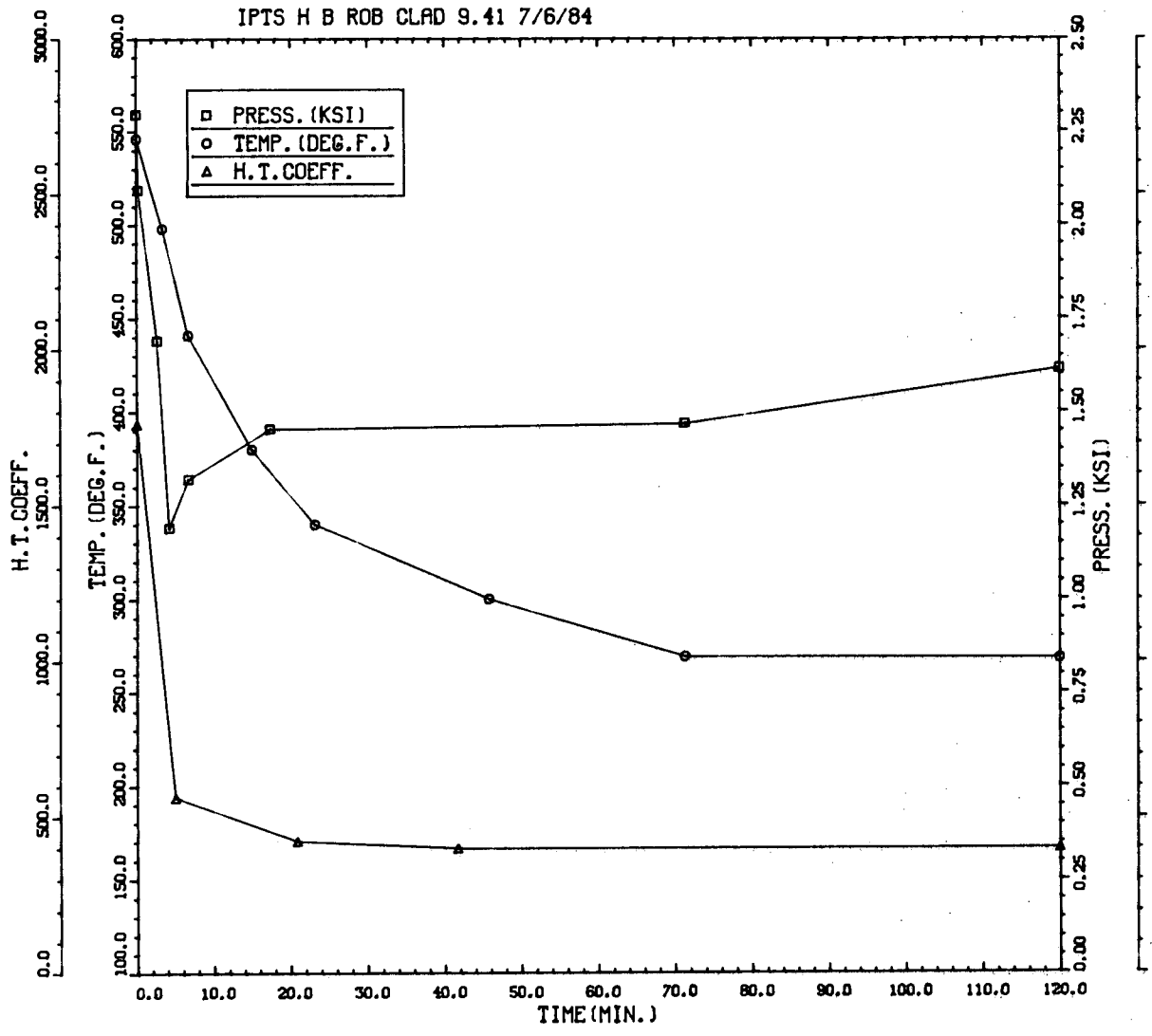

Figure I.235. Transient 9.41: Primary system pressure, downcomer coolant temperature, and fluid-film heat-transfer coefficient vs time in the transient.

Table I.40. Transient 9.41: Summary of digital output, including unadjusted $P(F|E)$ values and histogram data for crack depths, times of failure, and $T - RTNDT$ values at tip of crack corresponding to initiation and arrest events

IPTS H B ROB CLAD 9.41 7/6/84 1. FLAWS/IN**3 DRTN(IS) = 211.2

WELD	UNADJUSTED P(F/E)	95%CI	%ERR	P(INITIA)	N*V	ADJUSTED P(F/E)	%ERR	NFAIL	NTRIALS
1	2.72D-05	9.73D-06	35.78	6.35D-05	1.000	2.72D-05		30	200000
					VESSEL	2.72D-05	35.78		

DEPTHS FOR INITIAL INITIATION (IN)

	0.09	0.26	0.46	0.67	0.90	1.16	1.44	1.74	2.08
NUMBER	0	40	13	15	2	0	0	0	0
PERCENT	0.0	57.1	18.6	21.4	2.9	0.0	0.0	0.0	0.0

TIMES OF FAILURE(MINUTES)

	0.0	10.0	20.0	30.0	40.0	50.0	60.0	70.0	80.0	90.0	100.0	110.0	120.0
PERCENT	0.0	0.0	0.0	0.0	0.0	3.3	13.3	16.7	6.7	6.7	26.7	26.7	

INITIATION T-RTNDT(DEG.F)

	-100.0	-75.0	-50.0	-25.0	0.0	25.0	50.0	75.0	100.0	125.0	150.0	175.0	200.0
NUMBER	0	1	7	33	28	8	8	7	0	0	0	0	
PERCENT	0.0	1.1	7.6	35.9	30.4	8.7	8.7	7.6	0.0	0.0	0.0	0.0	

ARREST T-RTNDT(DEG.F)

	-50.0	-25.0	0.0	25.0	50.0	75.0	100.0	125.0	150.0	175.0	200.0	225.0	250.0
NUMBER	0	0	10	1	0	0	7	32	12	0	0	0	
PERCENT	0.0	0.0	16.1	1.6	0.0	0.0	11.3	51.6	19.4	0.0	0.0	0.0	

ICRKTP = 2 IACCEL = 1 NDLRS = 0 NRTRS = 0 DATE: 11/19/84 TIME: 23.00.33

CPU TIME: 5 MIN 30 SEC

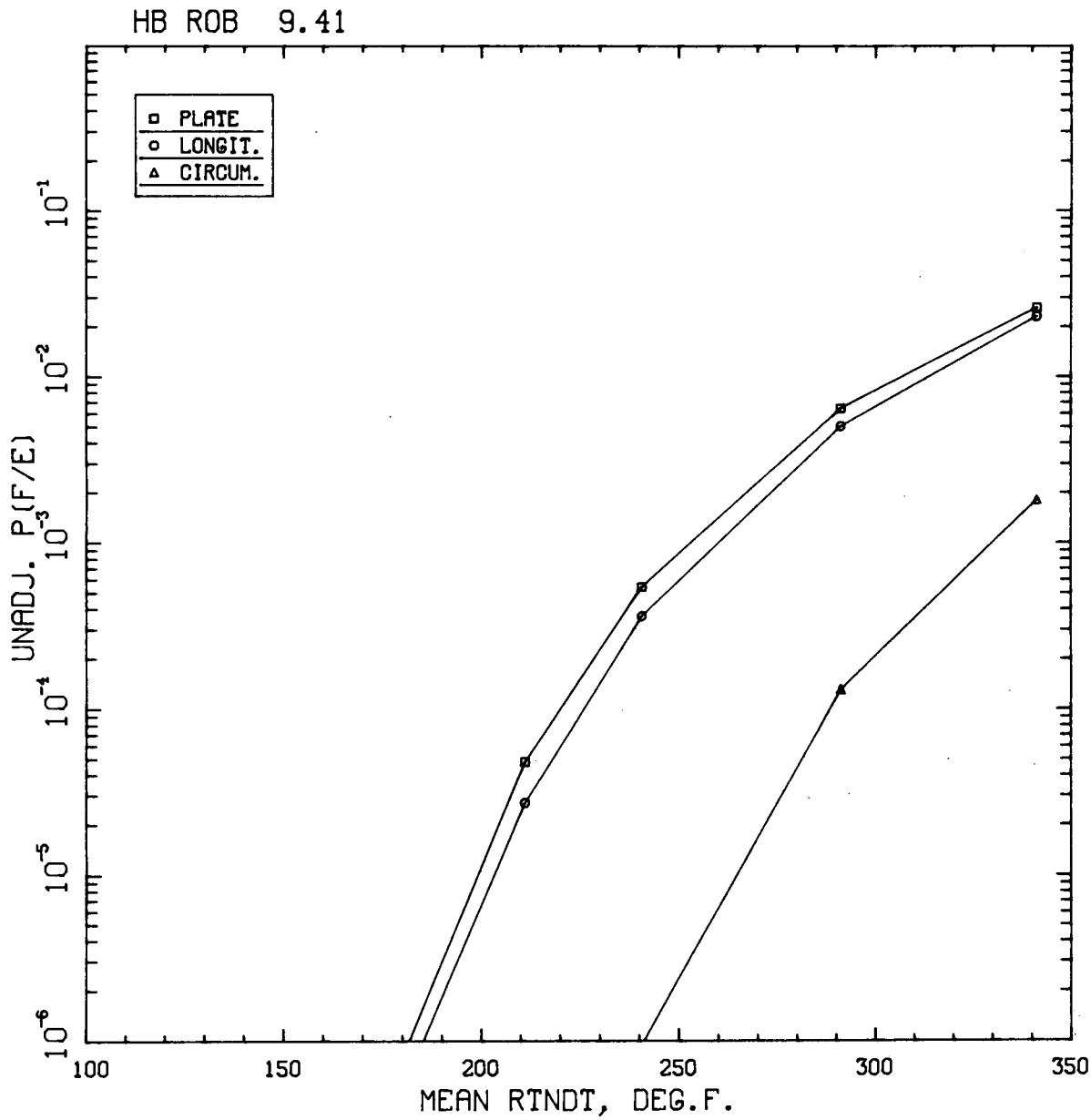

Figure I.236. Transient 9.41: $\hat{P}_j \int_0^w f(a)\, B(a)\, da$ vs $\overline{RTNDT_s}$ for (2-D, 2-D) and (2-D, 2m) flaw combinations.

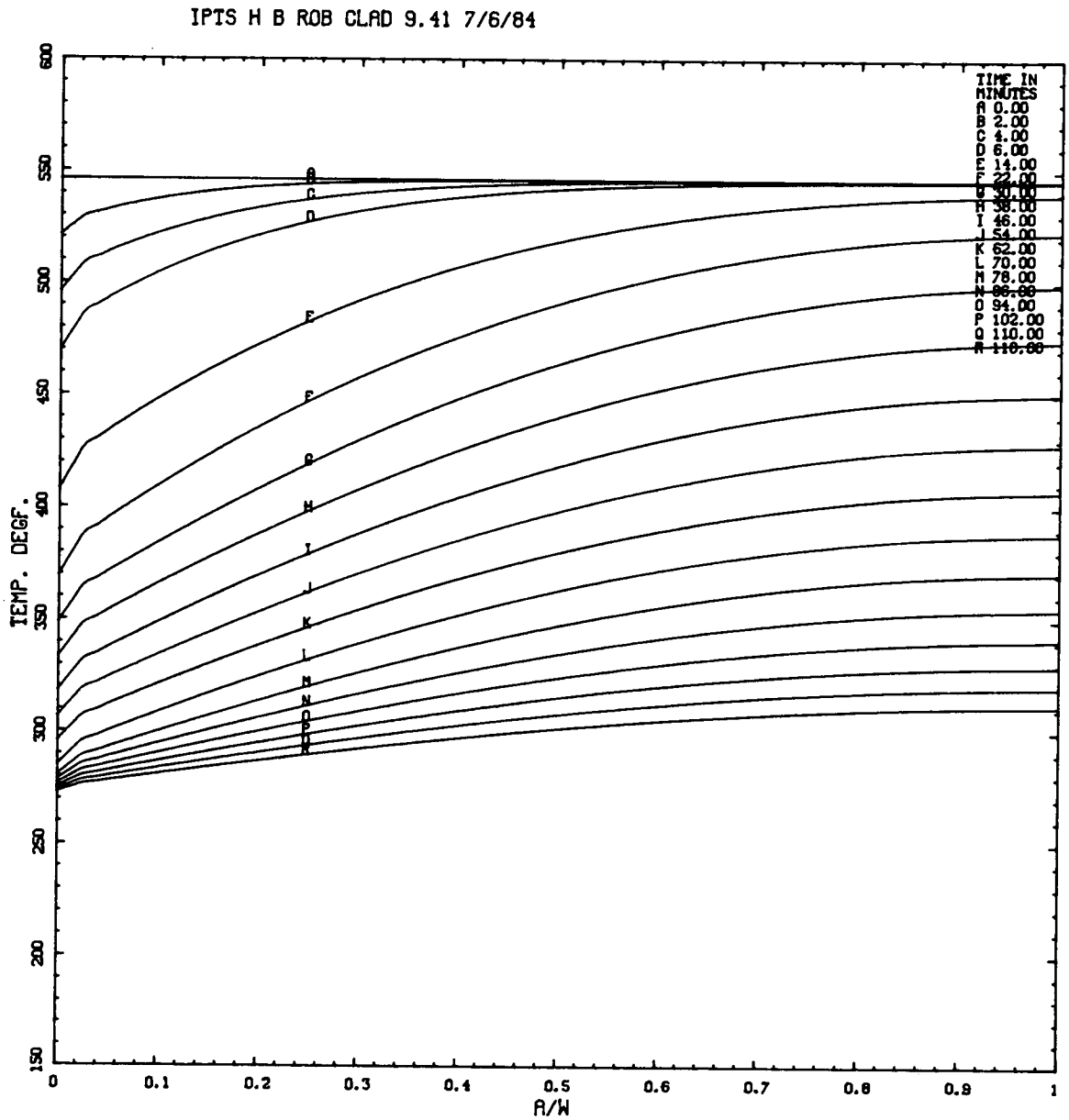

Figure I.237. Transient 9.41: Vessel wall temperature vs depth in wall (a/w) at various times (t) in transient.

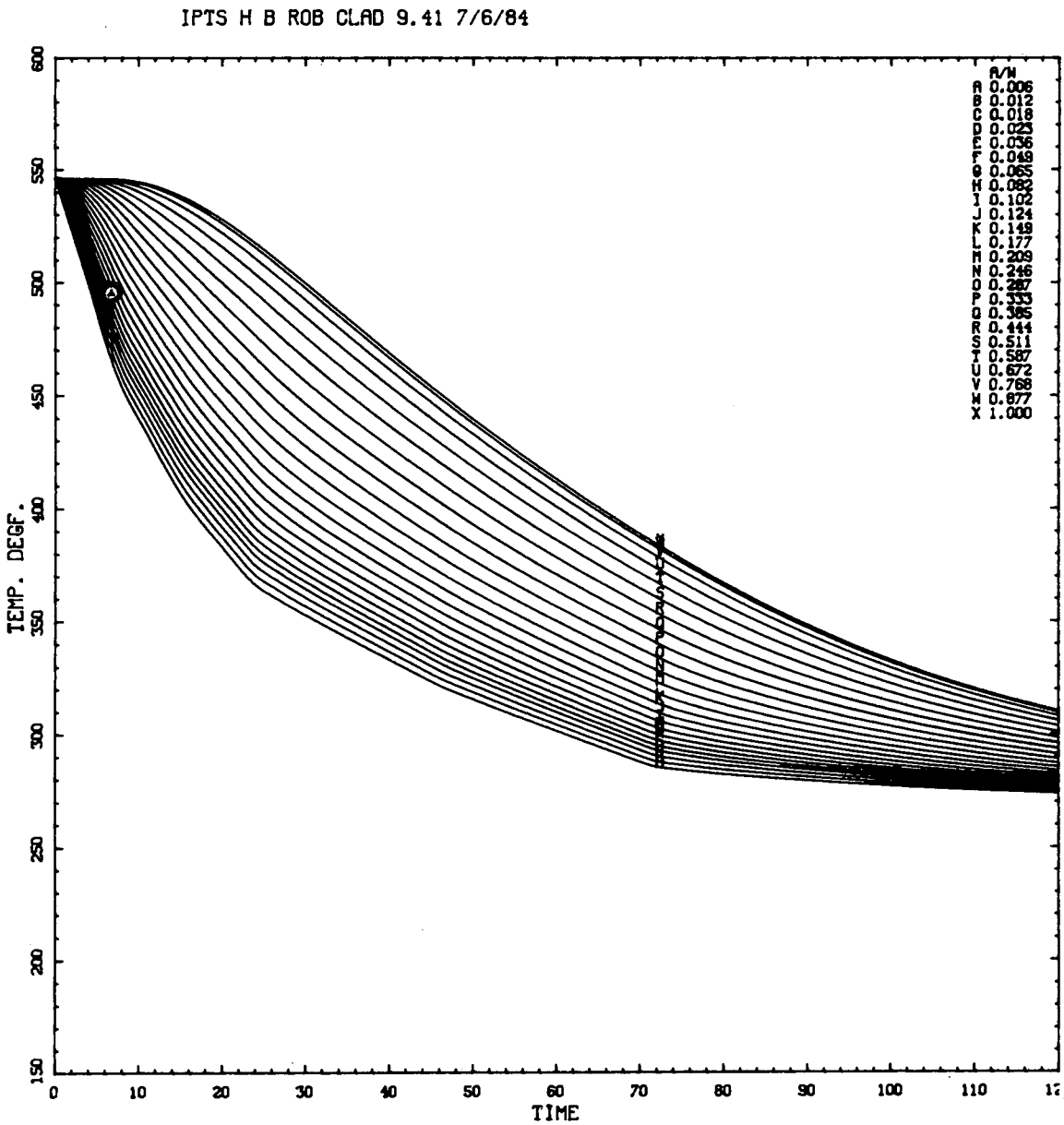

Figure I.238. Transient 9.41: Vessel wall temperature vs time (t) in transient at various depths in wall (a/w).

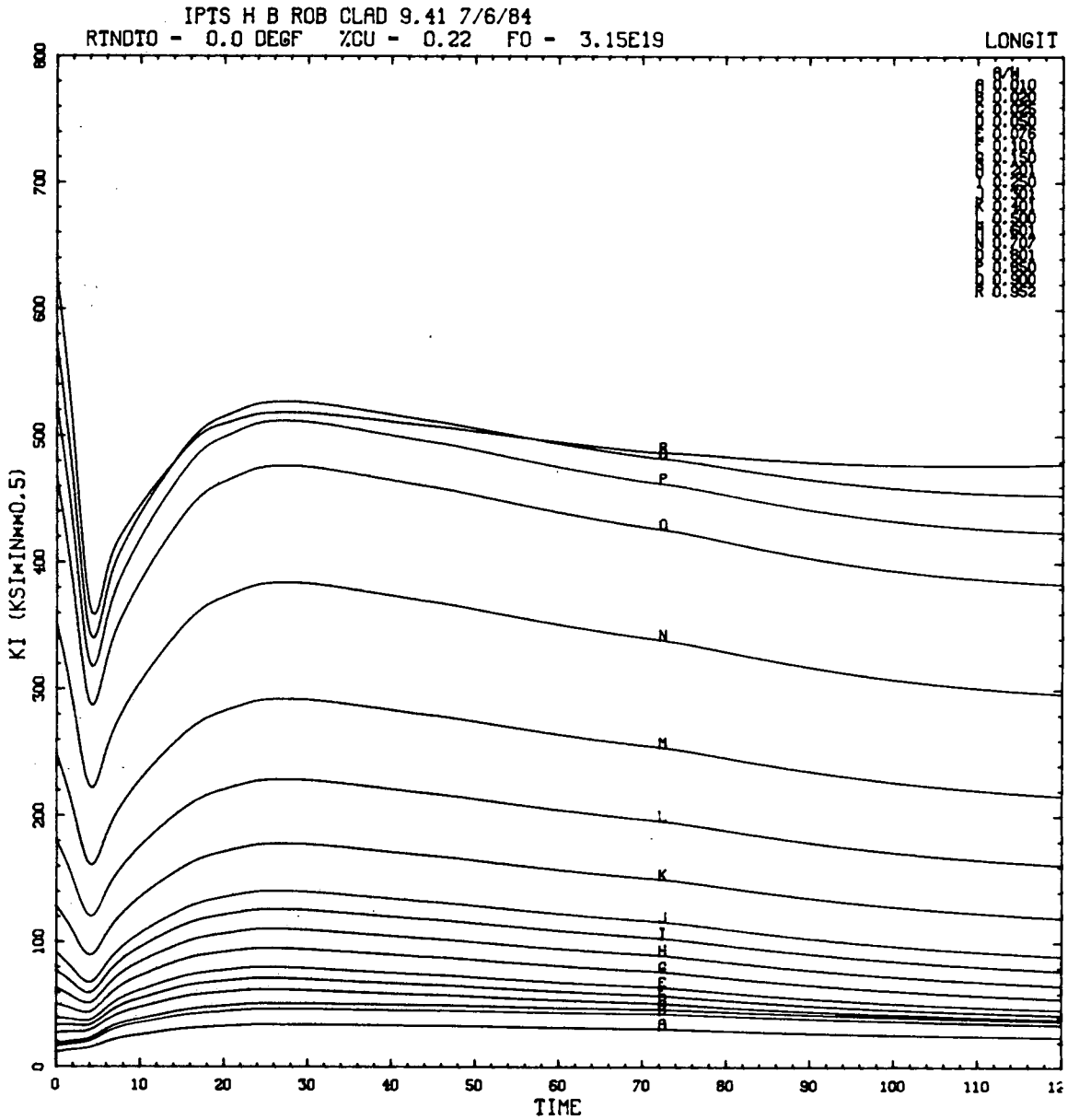

Figure I.239. Transient 9.41: K_I vs time (t) for various depths in wall (a/w).

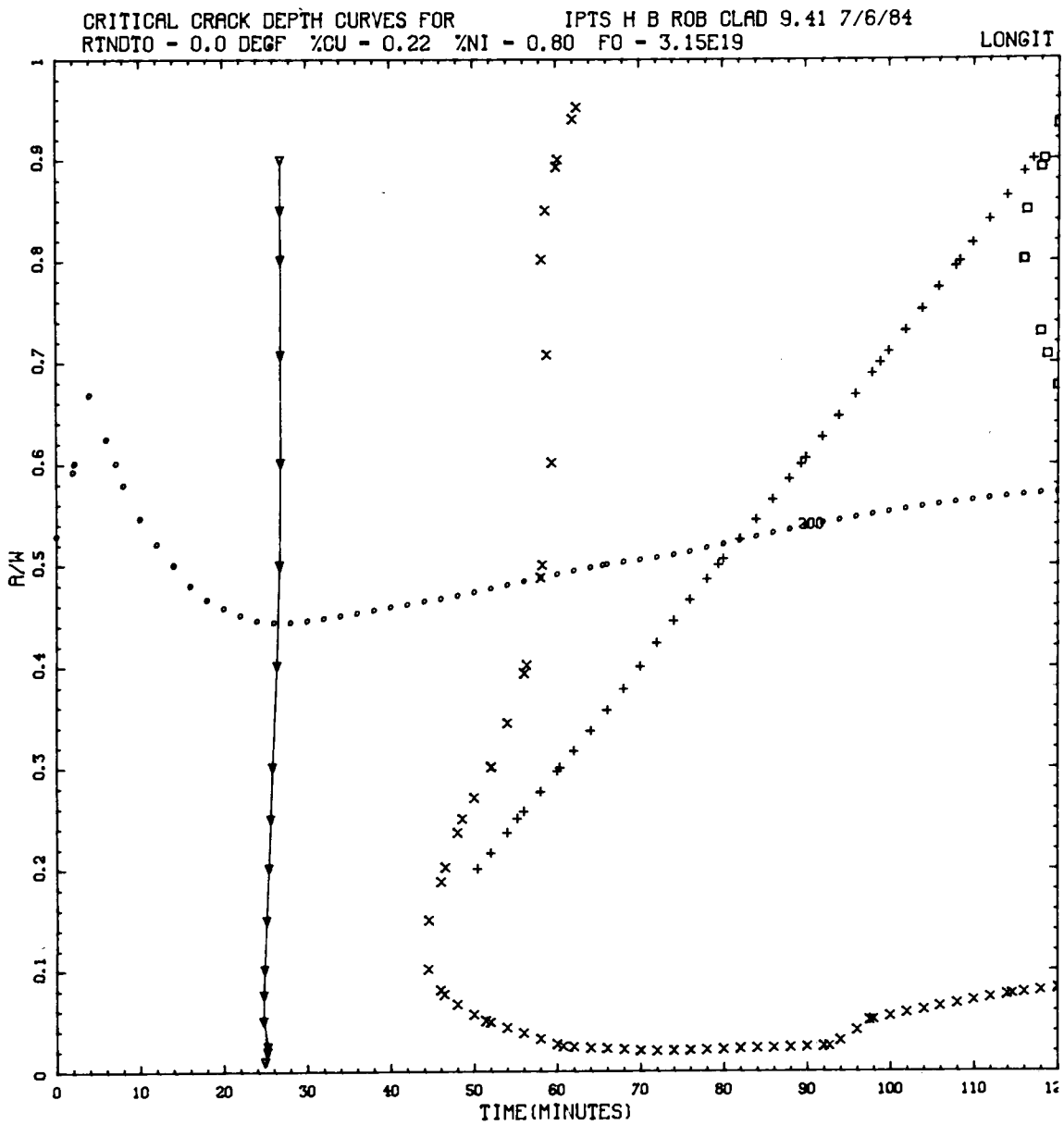

×, 2-D flaw, $K_I = K_{Ia}$
+, 2-m flaw, $K_I = K_{Ia}$
□, 2-D flaw, $K_I = K_{Ic}$
○, 2-D flaw, $K_I = 220$ MPa $\sqrt{m}$
∇, WPS (warm prestressing)

Figure I.240. Transient 9.41: Critical-crack-depth curves for weld 2-273A based on -2σ values of K_{Ic}, K_{Ia}, and $\Delta RTNDT$, mean values of all other parameters, and 32-EFPY fluences.

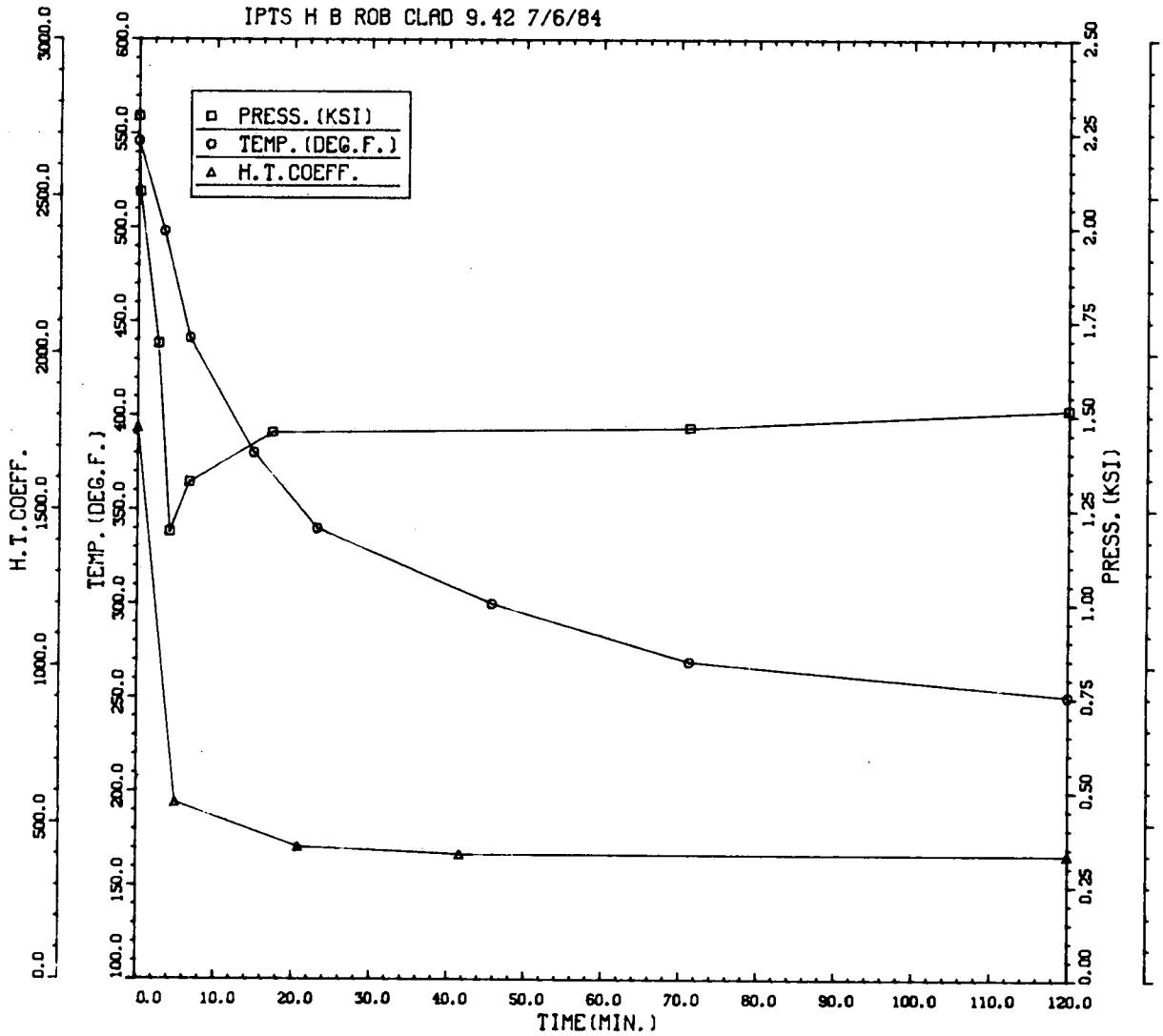

Figure I.241. Transient 9.42: Primary system pressure, downcomer coolant temperature, and fluid-film heat-transfer coefficient vs time in the transient.

Table I.41. Transient 9.42: Summary of digital output, including unadjusted $P(F|E)$ values and histogram data for crack depths, times of failure, and $T - RTNDT$ values at tip of crack corresponding to initiation and arrest events

IPTS H B ROB CLAD 9.42 7/6/84 1. FLAWS/IN**3 DRTN(IS) = 211.2

WELD	P(F/E)	95%CI	%ERR	P(INITIA)	N*V	P(F/E)	%ERR	NFAIL	NTRIALS
	----------UNADJUSTED----------					---ADJUSTED----			
1	3.26D-05	1.07D-05	32.66	6.62D-05	1.000	3.26D-05		36	200000
					VESSEL	3.26D-05	32.66		

DEPTHS FOR INITIAL INITIATION (IN)

	0.09	0.26	0.46	0.67	0.90	1.16	1.44	1.74	2.08
NUMBER	0	42	14	15	2	0	0	0	0
PERCENT	0.0	57.5	19.2	20.5	2.7	0.0	0.0	0.0	0.0

TIMES OF FAILURE(MINUTES)

	0.0	10.0	20.0	30.0	40.0	50.0	60.0	70.0	80.0	90.0	100.0	110.0	120.0
PERCENT	0.0	0.0	0.0	0.0	0.0	2.8	11.1	16.7	5.6	8.3	25.0	30.6	

INITIATION T-RTNDT(DEG.F)

	-100.0	-75.0	-50.0	-25.0	0.0	25.0	50.0	75.0	100.0	125.0	150.0	175.0	200.0
NUMBER	0	1	7	35	29	9	12	7	0	0	0	0	
PERCENT	0.0	1.0	7.0	35.0	29.0	9.0	12.0	7.0	0.0	0.0	0.0	0.0	

ARREST T-RTNDT(DEG.F)

	-50.0	-25.0	0.0	25.0	50.0	75.0	100.0	125.0	150.0	175.0	200.0	225.0	250.0
NUMBER	0	0	11	1	0	0	7	33	12	0	0	0	
PERCENT	0.0	0.0	17.2	1.6	0.0	0.0	10.9	51.6	18.8	0.0	0.0	0.0	

ICRKTP = 2 IACCEL = 1 NDLRS = 0 NRTRS = 0 DATE: 10/31/84 TIME: 02.26.21

CPU TIME: 5 MIN 28 SEC

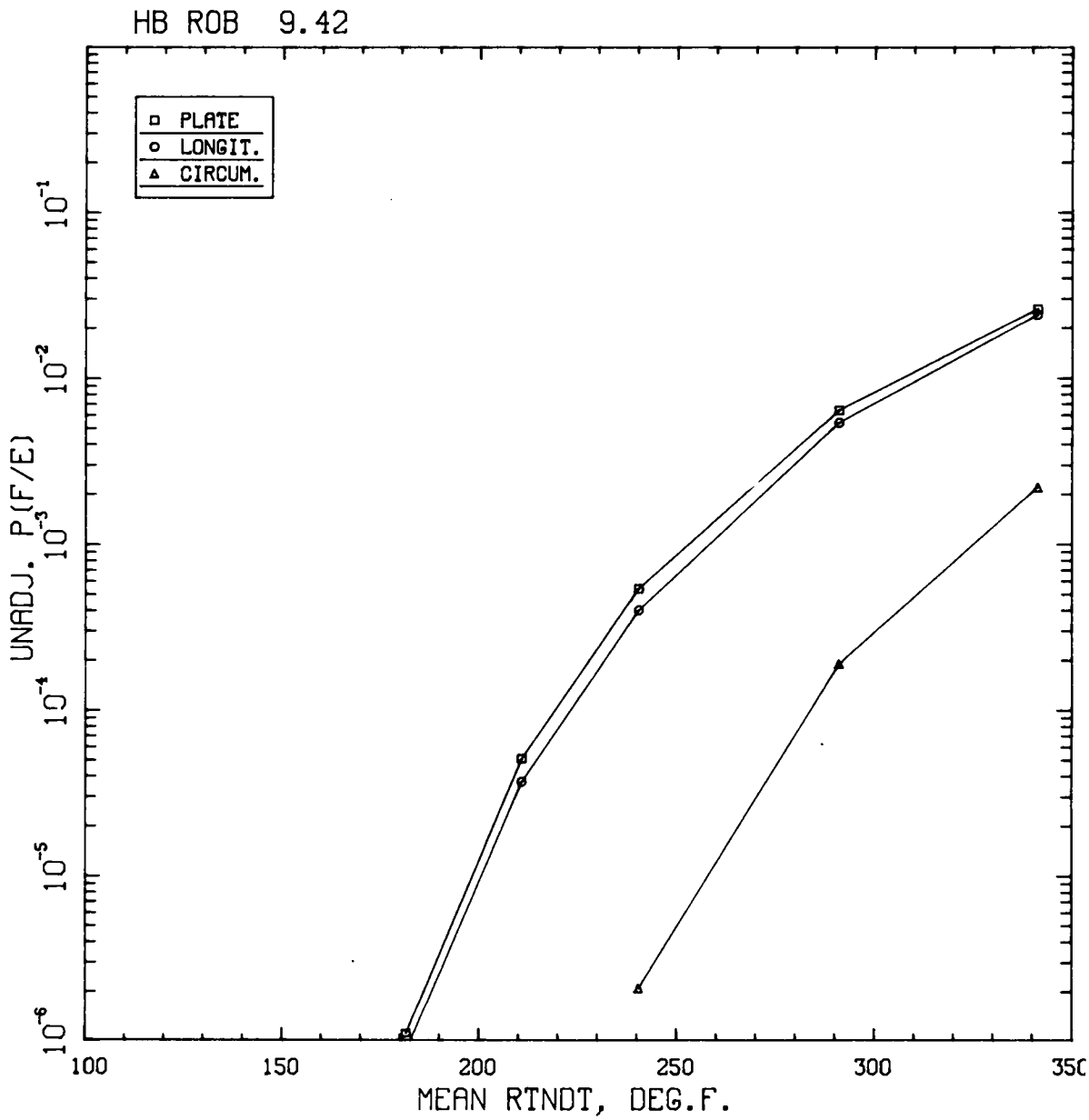

Figure I.242. Transient 9.42: $\hat{P}_j \int_0^w f(a)\, B(a)\, da$ vs $\overline{RTNDT_s}$ for (2-D, 2-D) and (2-D, 2m) flaw combinations.

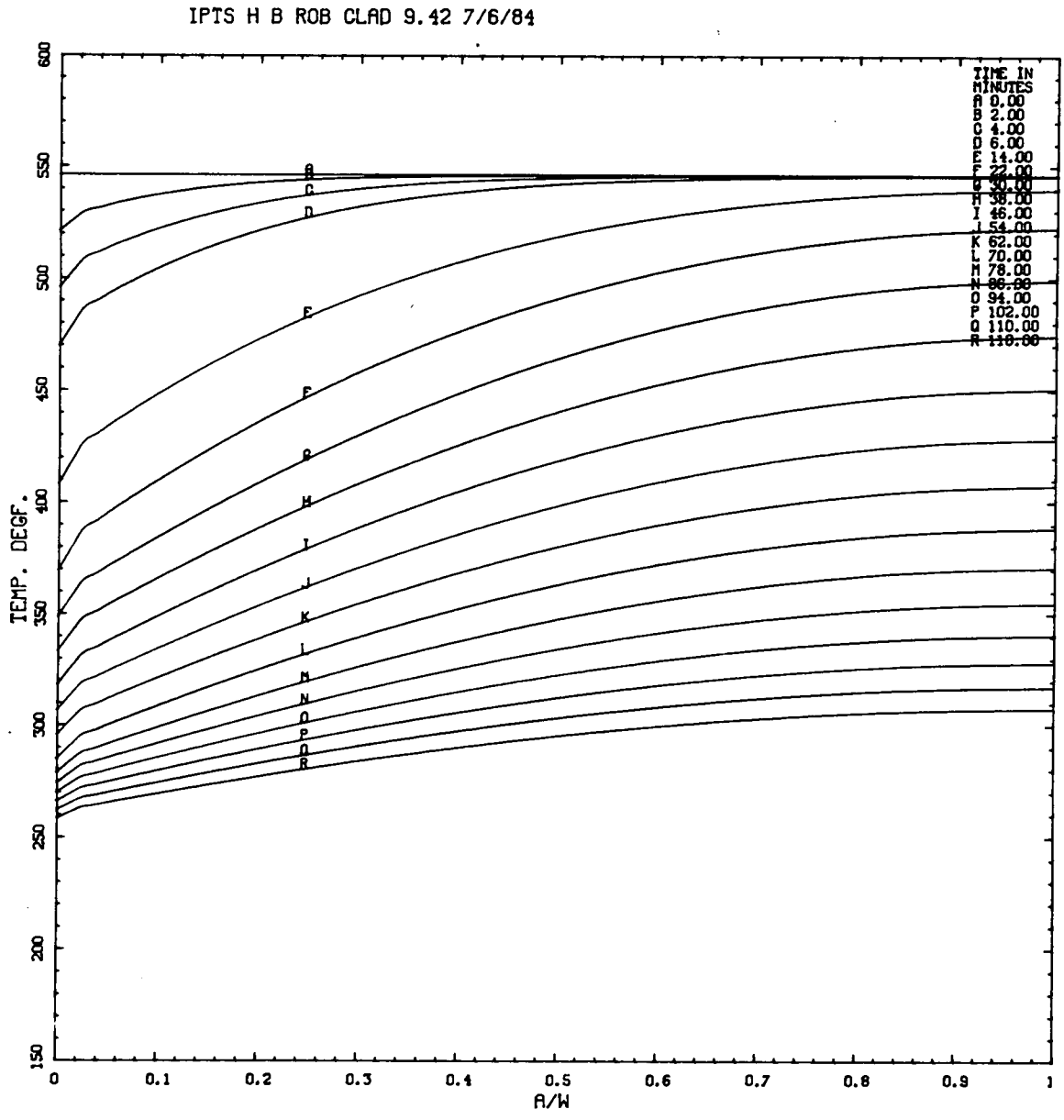

Figure I.243. Transient 9.42: Vessel wall temperature vs depth in wall (a/w) at various times (t) in transient.

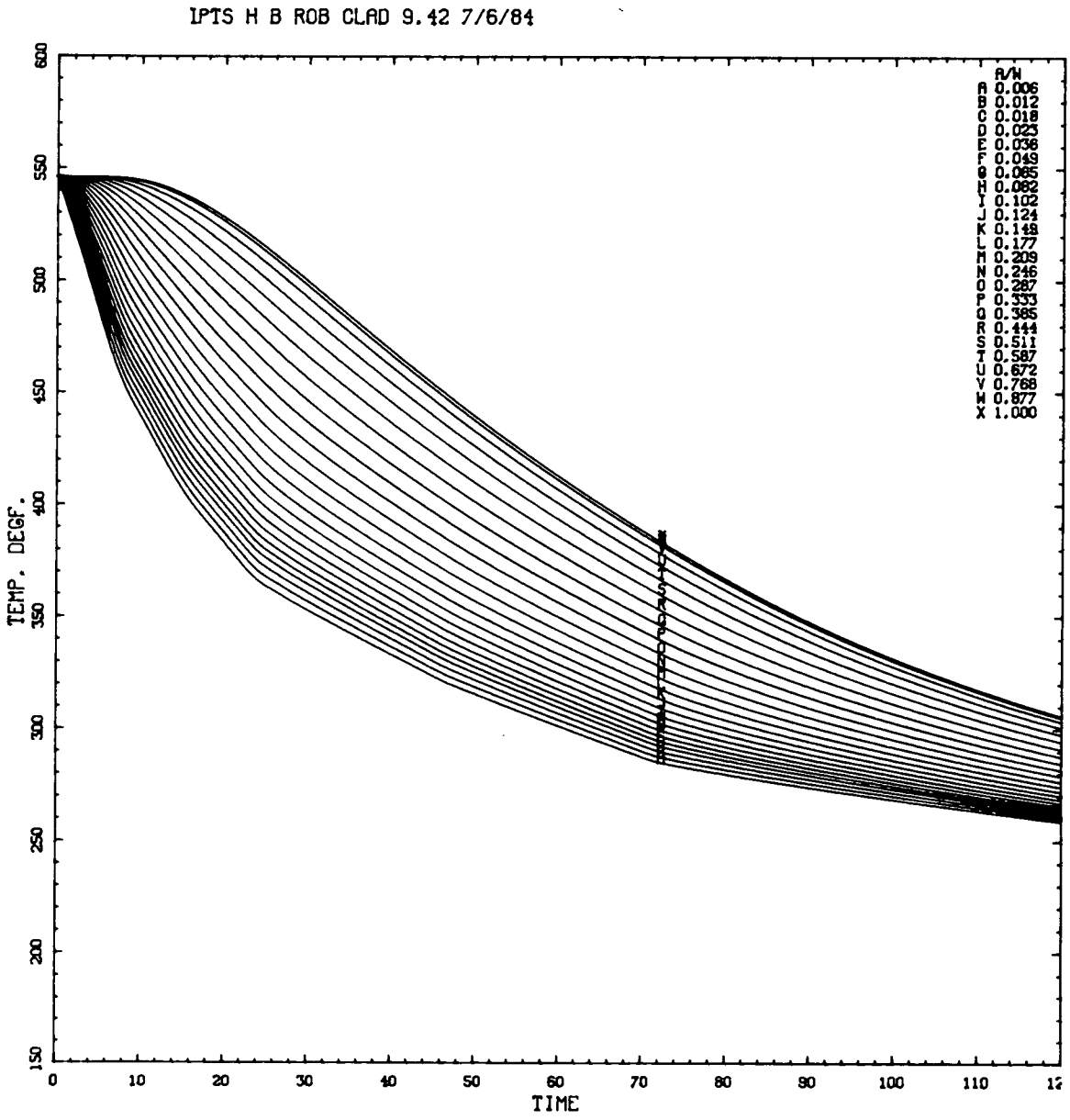

Figure I.244. Transient 9.42: Vessel wall temperature vs time (t) in transient at various depths in wall (a/w).

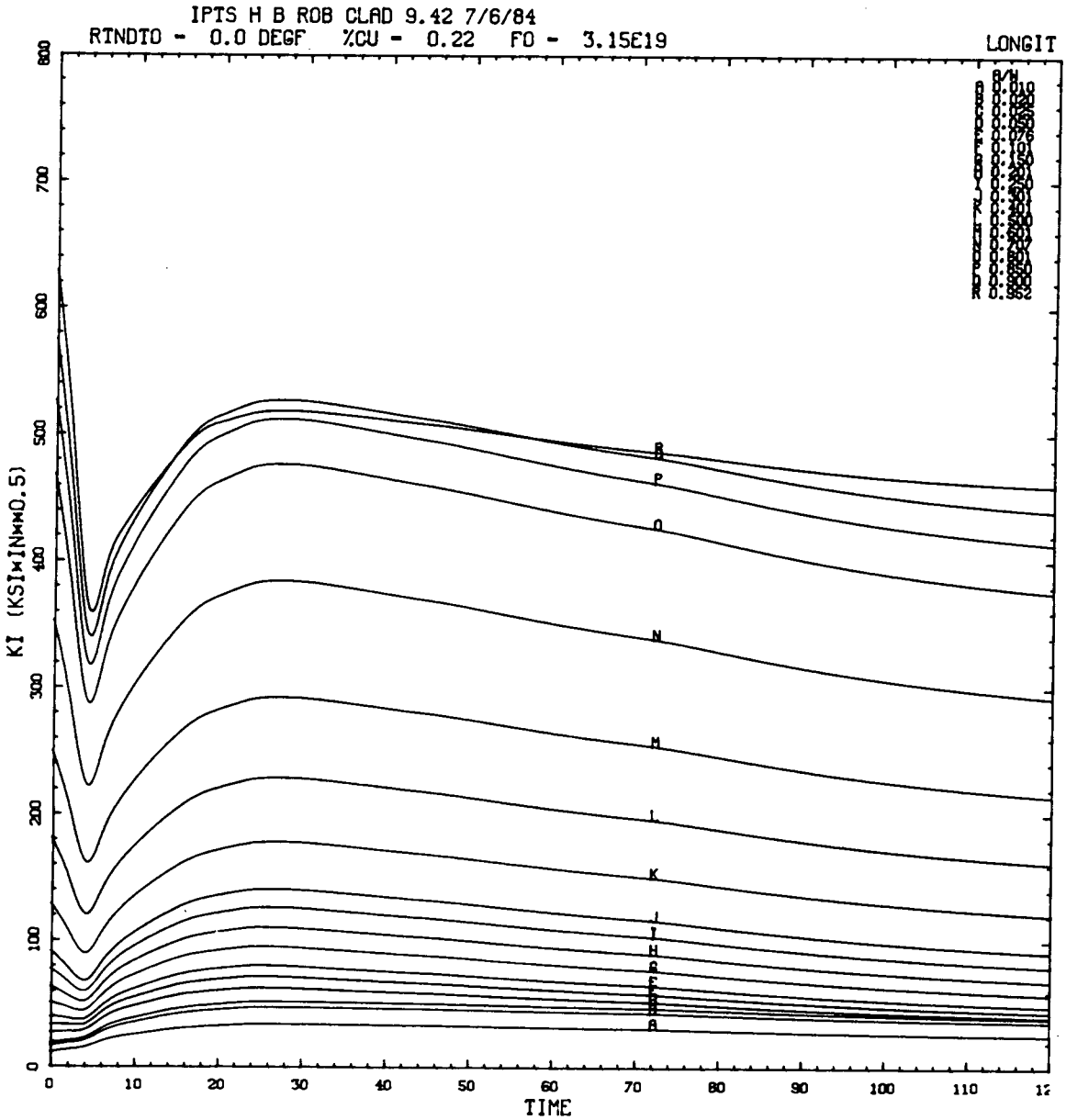

Figure I.245. Transient 9.42: K_I vs time (t) for various depths in wall (a/w).

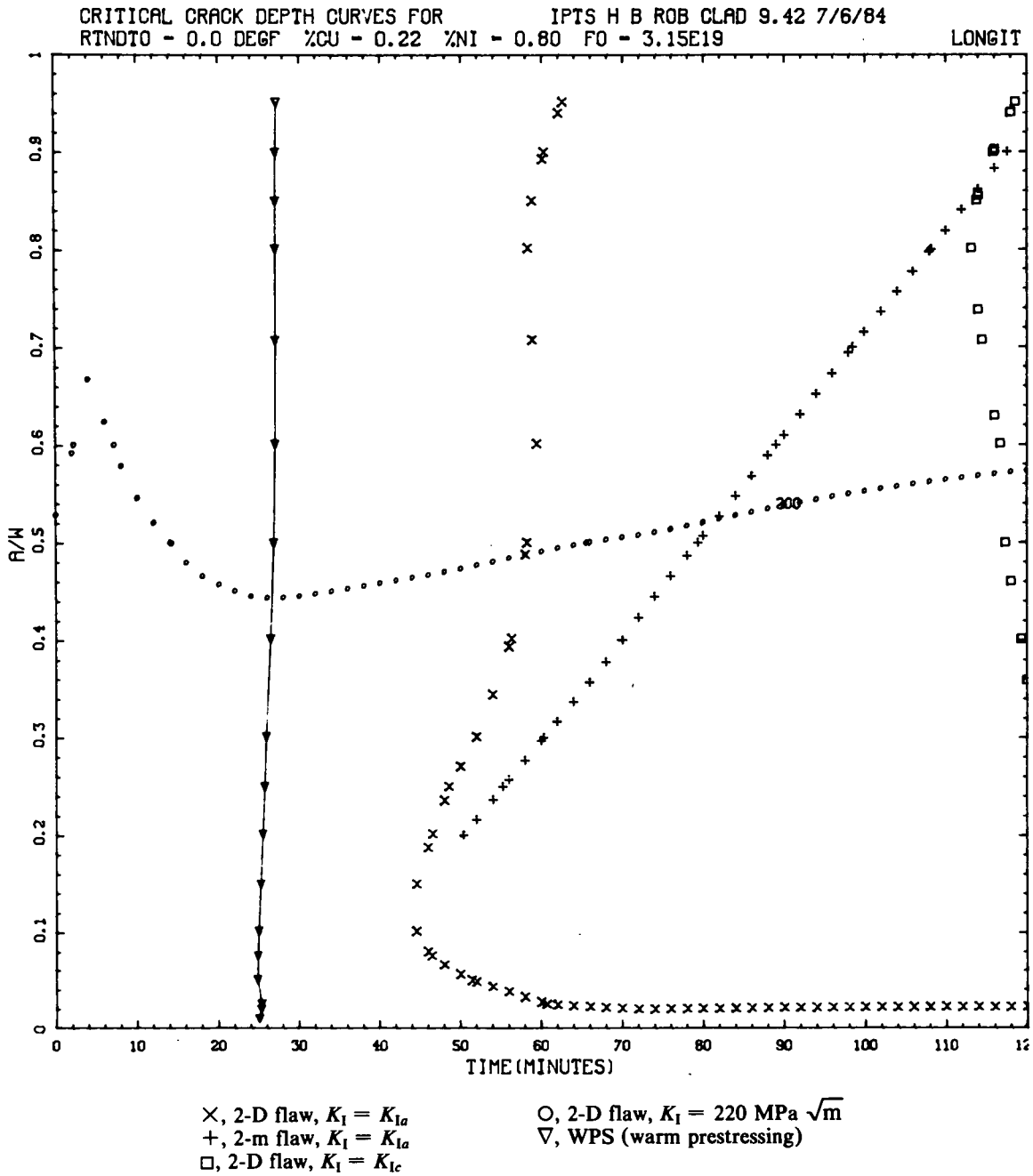

Figure I.246. Transient 9.42: Critical-crack-depth curves for weld 2-273A based on -2σ values of K_{Ic}, K_{Ia}, and $\Delta RTNDT$, mean values of all other parameters, and 32-EFPY fluences.

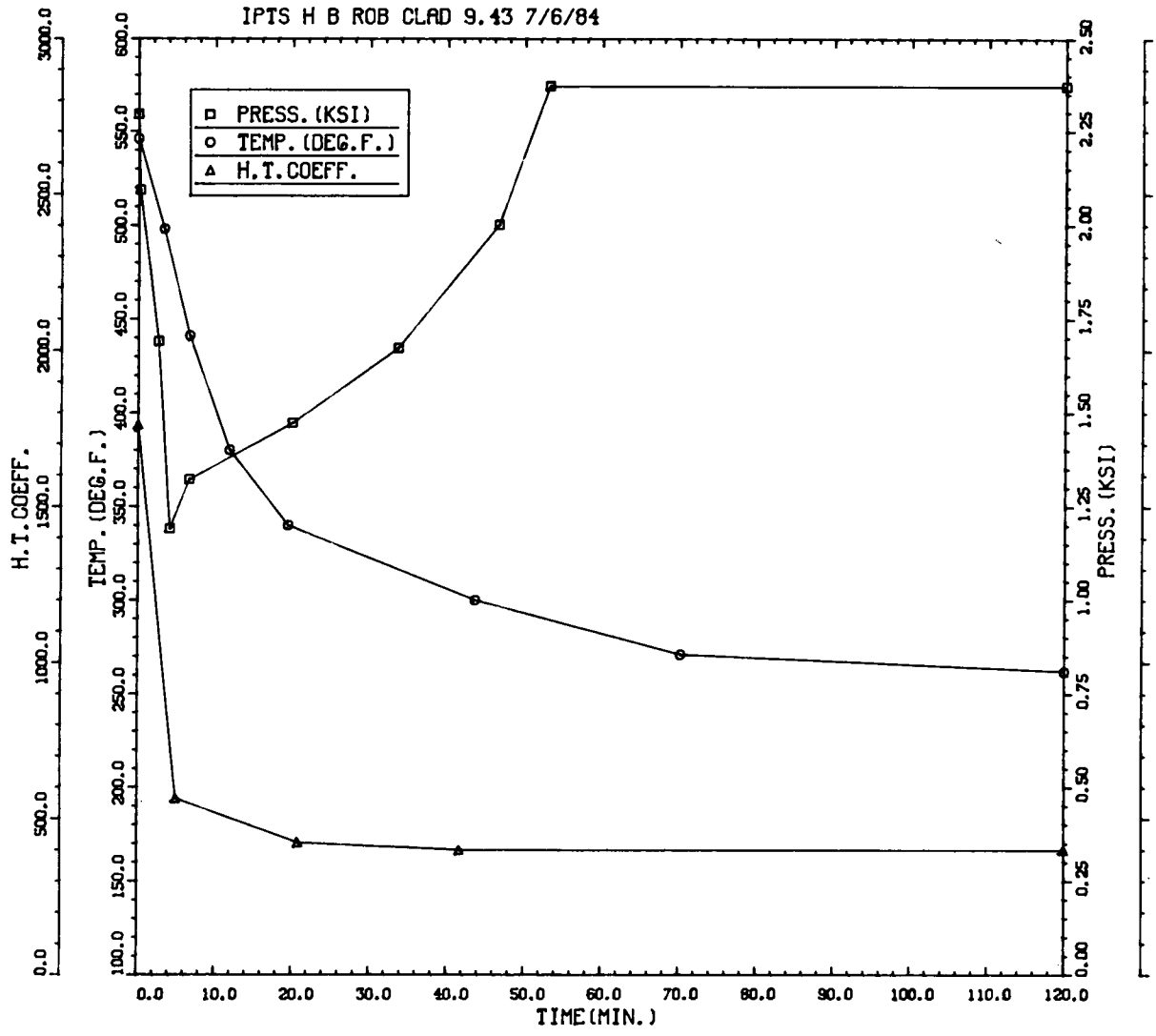

Figure I.247. Transient 9.43: Primary system pressure, downcomer coolant temperature, and fluid-film heat-transfer coefficient vs time in the transient.

Table I.42. Transient 9.43: Summary of digital output, including unadjusted $P(F|E)$ values and histogram data for crack depths, times of failure, and $T - RTNDT$ values at tip of crack corresponding to initiation and arrest events

IPTS H B ROB CLAD 9.43 7/6/84 1. FLAWS/IN**3 DRTN(IS) = 211.2

	----------UNADJUSTED----------					---ADJUSTED----			
WELD	P(F/E)	95%CI	%ERR	P(INITIA)	N*V	P(F/E)	%ERR	NFAIL	NTRIALS
1	3.37D-04	3.42D-05	10.15	3.55D-04	1.000	3.37D-04		372	200000
					VESSEL	3.37D-04	10.15		

DEPTHS FOR INITIAL INITIATION (IN)

	0.09	0.26	0.46	0.67	0.90	1.16	1.44	1.74	2.08
NUMBER	0	189	121	53	19	7	2	0	0
PERCENT	0.0	48.3	30.9	13.6	4.9	1.8	0.5	0.0	0.0

TIMES OF FAILURE(MINUTES)

	0.0	10.0	20.0	30.0	40.0	50.0	60.0	70.0	80.0	90.0	100.0	110.0	120.0
PERCENT	0.0	0.0	0.0	0.0	5.6	30.1	36.0	19.6	3.2	3.2	1.1	1.1	

INITIATION T-RTNDT(DEG.F)

	-100.0	-75.0	-50.0	-25.0	0.0	25.0	50.0	75.0	100.0	125.0	150.0	175.0	200.0
NUMBER	0	0	26	141	181	43	26	9	1	0	0	0	
PERCENT	0.0	0.0	6.1	33.0	42.4	10.1	6.1	2.1	0.2	0.0	0.0	0.0	

ARREST T-RTNDT(DEG.F)

	-50.0	-25.0	0.0	25.0	50.0	75.0	100.0	125.0	150.0	175.0	200.0	225.0	250.0
NUMBER	0	0	2	4	0	0	0	23	26	0	0	0	
PERCENT	0.0	0.0	3.6	7.3	0.0	0.0	0.0	41.8	47.3	0.0	0.0	0.0	

ICRKTP = 2 IACCEL = 1 NDLRS = 0 NRTRS = 0 DATE: 11/19/84 TIME: 22.50.52

CPU TIME: 5 MIN 31 SEC

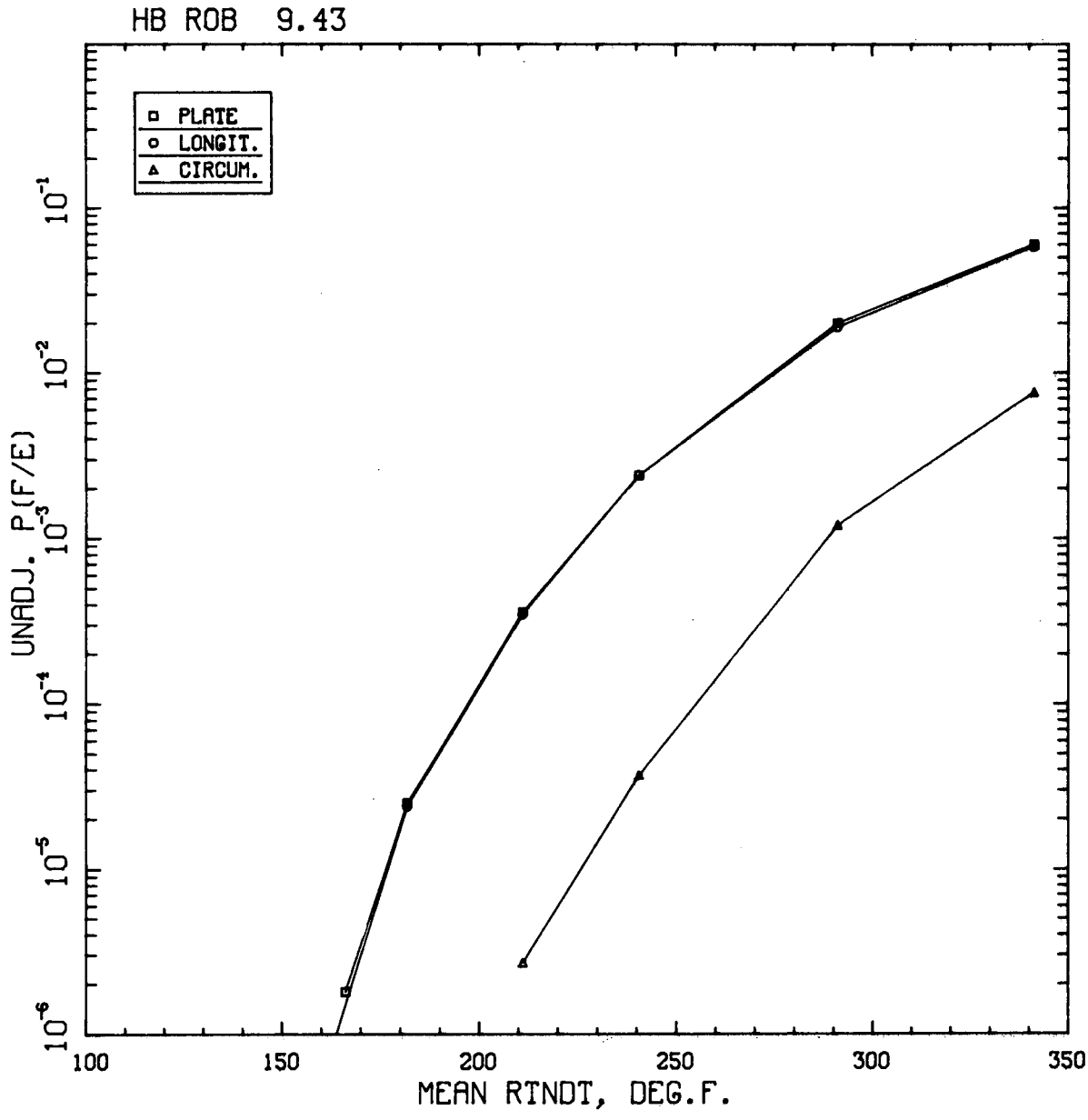

Figure I.248. Transient 9.43: $\hat{P}_j \int_0^w f(a)\, B(a)\, da$ vs $\overline{RTNDT}_s$ for (2-D, 2-D) and (2-D, 2m) flaw combinations.

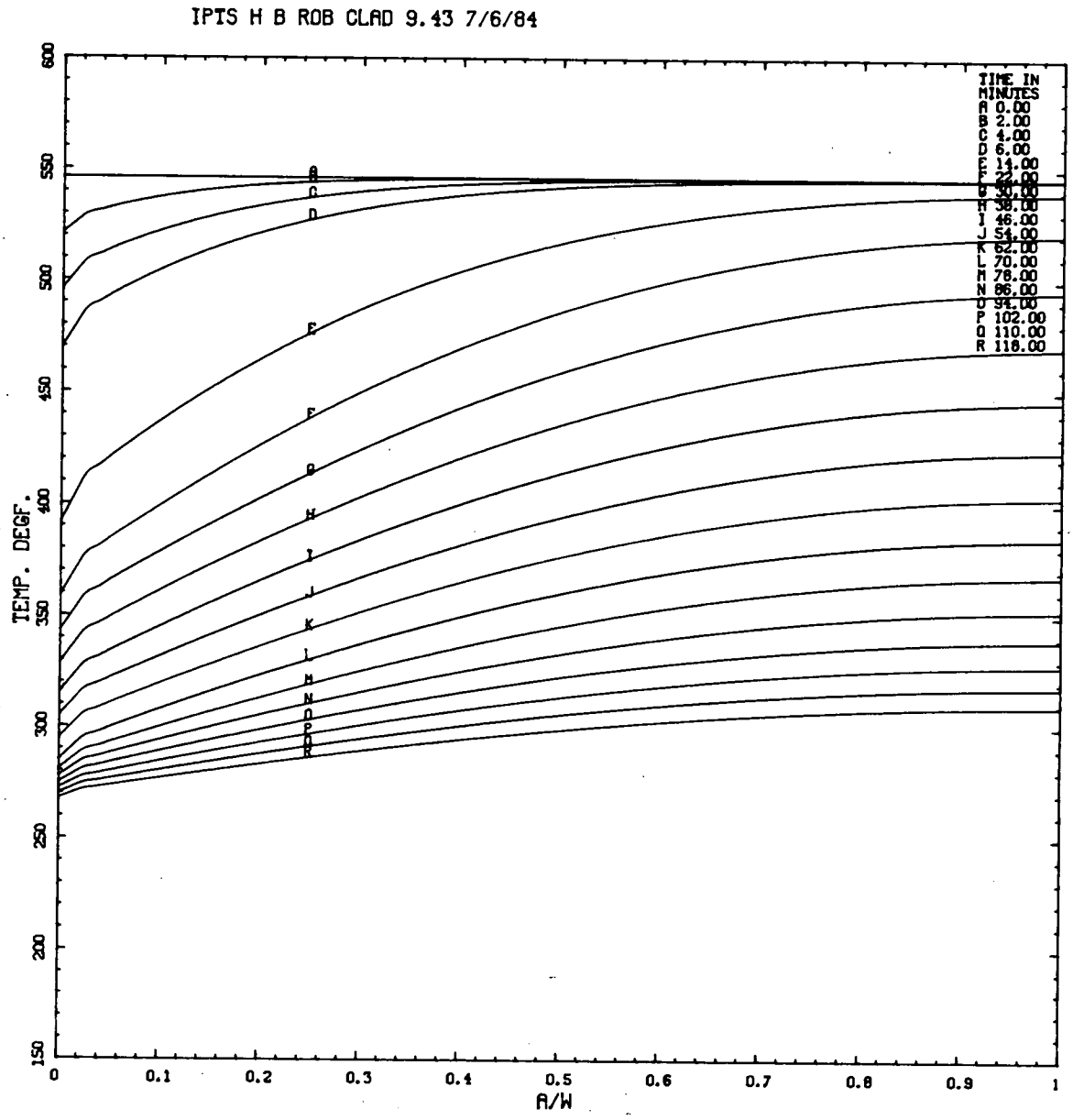

Figure I.249. Transient 9.43: Vessel wall temperature vs depth in wall (a/w) at various times (t) in transient.

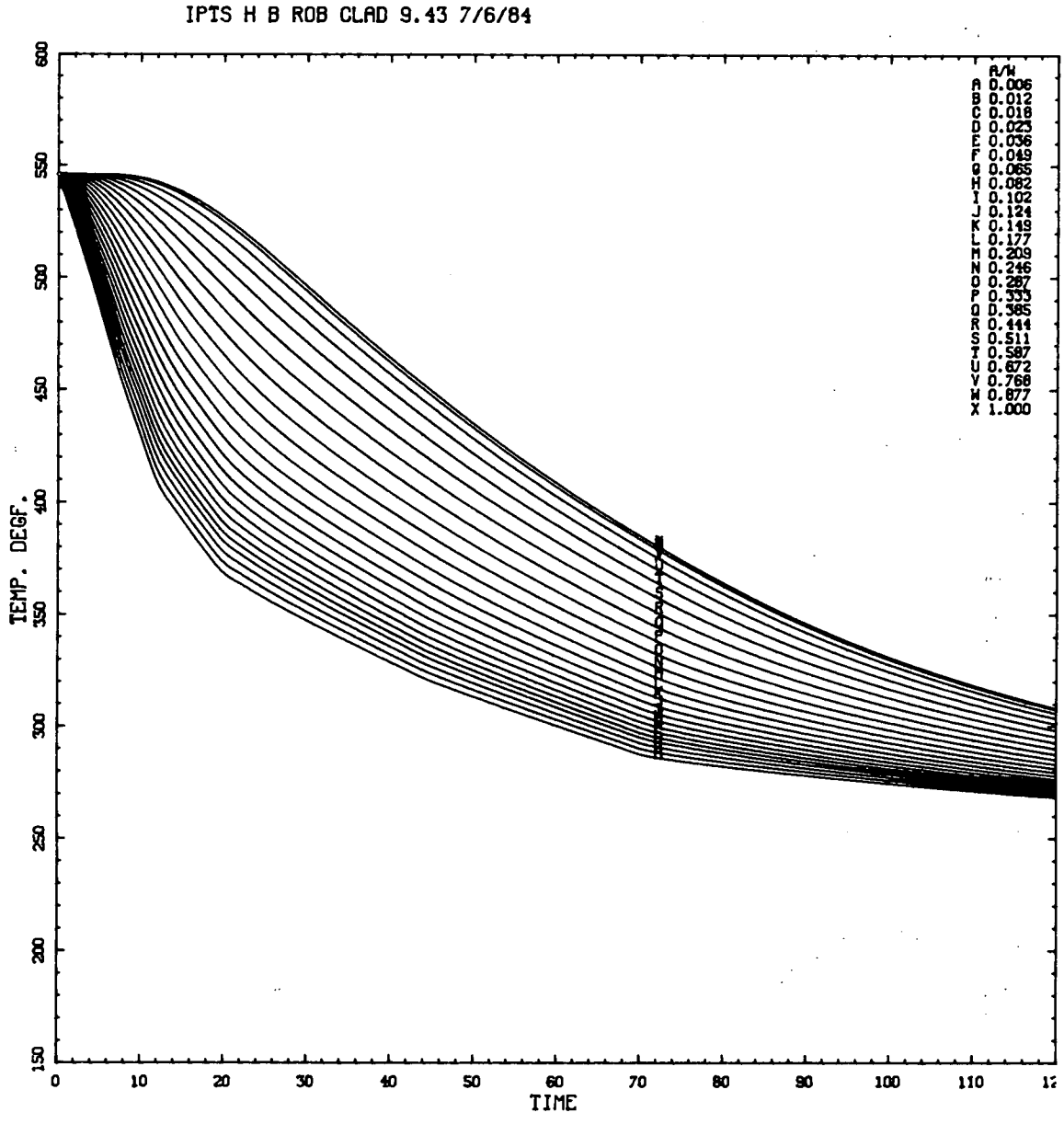

Figure I.250. Transient 9.43: Vessel wall temperature vs time (t) in transient at various depths in wall (a/w).

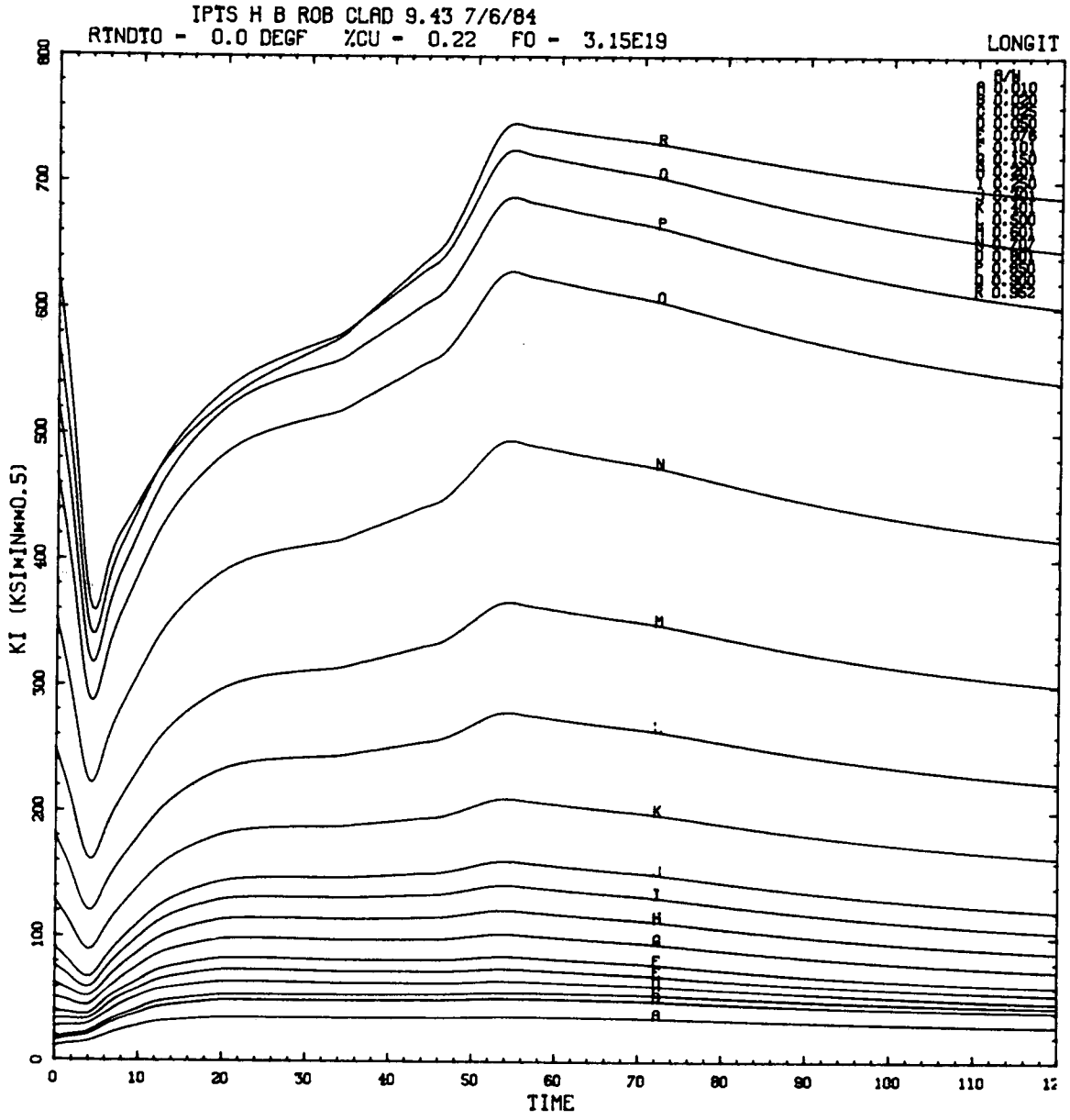

Figure I.251. Transient 9.43: K_I vs time (t) for various depths in wall (a/w).

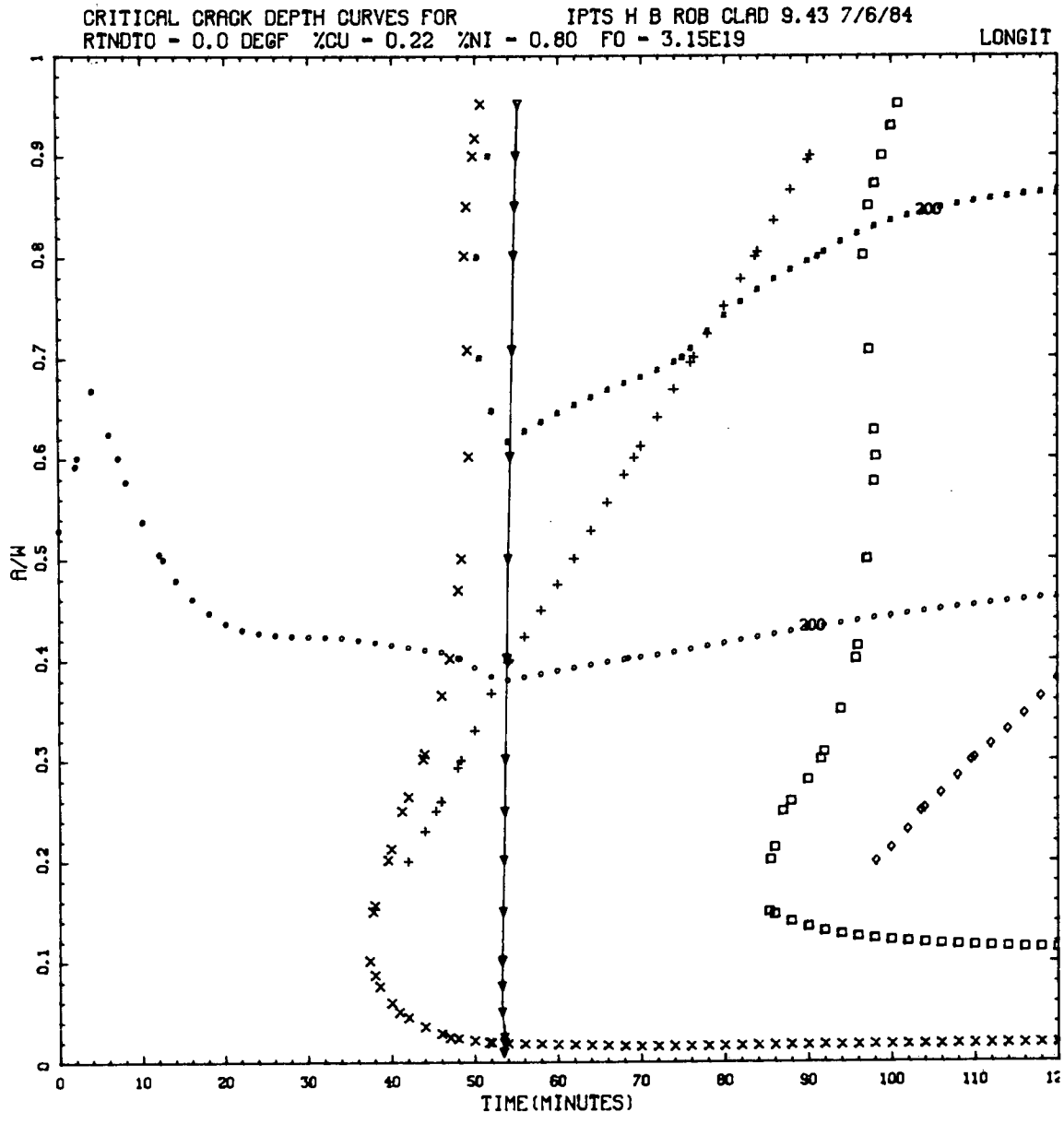

×, 2-D flaw, $K_I = K_{Ia}$
+, 2-m flaw, $K_I = K_{Ia}$
□, 2-D flaw, $K_I = K_{Ic}$
◊, 2-m flaw, $K_I = K_{Ic}$
O, 2-D flaw, $K_I = 220$ MPa $\sqrt{m}$
■, 2-m flaw, $K_I = 220$ MPa $\sqrt{m}$
∇, WPS (warm prestressing)

Figure I.252. Transient 9.43: Critical-crack-depth curves for weld 2-273A based on -2σ values of K_{Ic}, K_{Ia}, and $\Delta RTNDT$, mean values of all other parameters, and 32-EFPY fluences.

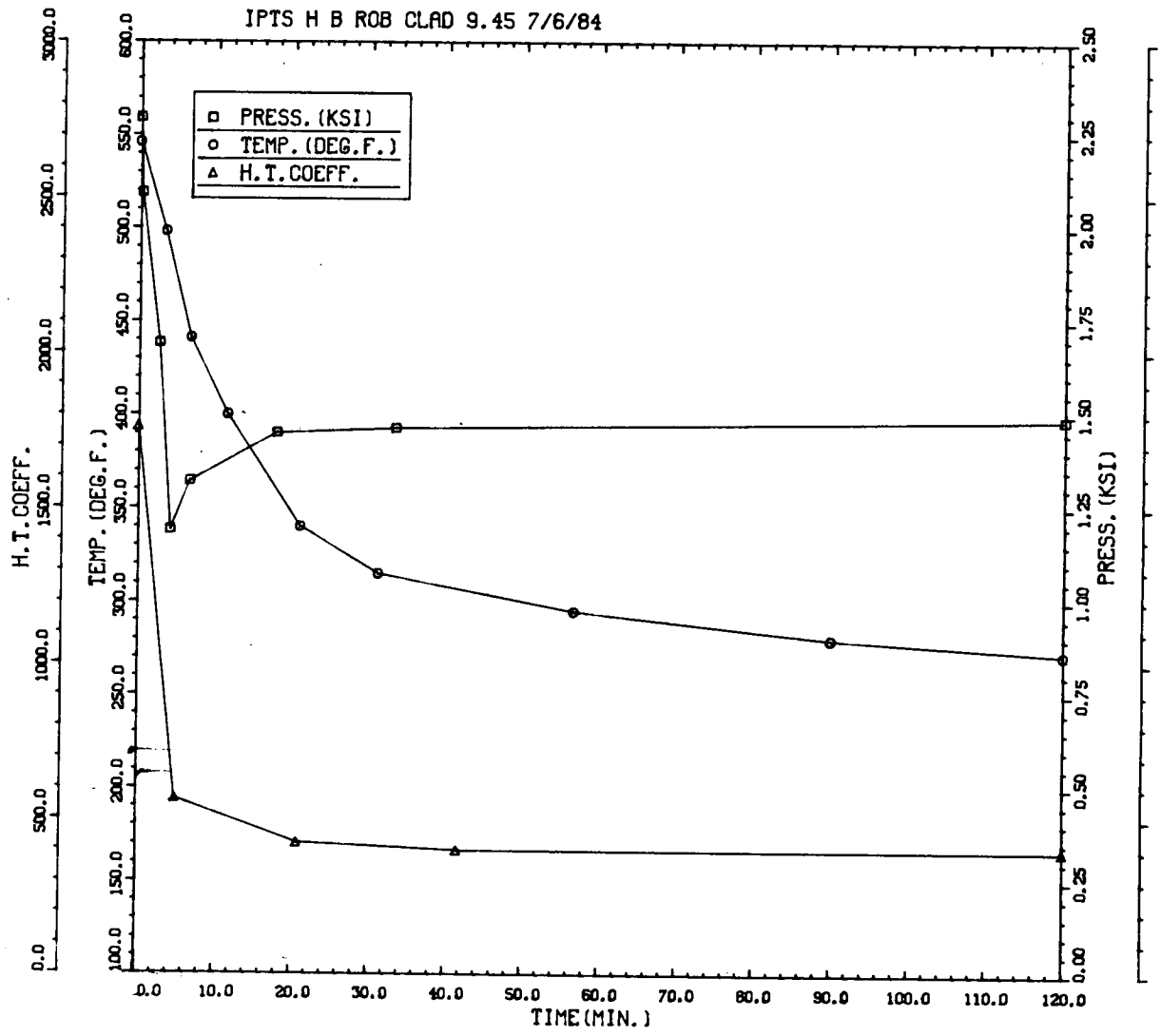

Figure I.253. Transient 9.45: Primary system pressure, downcomer coolant temperature, and fluid-film heat-transfer coefficient vs time in the transient.

Table I.43. Transient 9.45: Summary of digital output, including unadjusted $P(F|E)$ values and histogram data for crack depths, times of failure, and $T - RTNDT$ values at tip of crack corresponding to initiation and arrest events

IPTS H B ROB CLAD 9.45 7/6/84 1. FLAWS/IN**3 DRTN(IS) = 211.2

WELD	P(F/E) (UNADJUSTED)	95%CI (UNADJUSTED)	%ERR (UNADJUSTED)	P(INITIA) (UNADJUSTED)	N*V	P(F/E) (ADJUSTED)	%ERR (ADJUSTED)	NFAIL	NTRIALS
1	3.73D-06	5.68D-07	15.25	7.11D-06	1.000	3.73D-06		165	200000
					VESSEL	3.73D-06	15.25		

DEPTHS FOR INITIAL INITIATION (IN)

	0.09	0.26	0.46	0.67	0.90	1.16	1.44	1.74	2.08
NUMBER	0	126	107	55	17	8	2	0	0
PERCENT	0.0	40.0	34.0	17.5	5.4	2.5	0.6	0.0	0.0

TIMES OF FAILURE(MINUTES)

	0.0	10.0	20.0	30.0	40.0	50.0	60.0	70.0	80.0	90.0	100.0	110.0	120.0
PERCENT	0.0	0.0	0.0	0.0	0.0	0.6	7.9	18.2	18.8	20.6	18.8	15.2	

INITIATION T-RTNDT(DEG.F)

	-100.0	-75.0	-50.0	-25.0	0.0	25.0	50.0	75.0	100.0	125.0	150.0	175.0	200.0
NUMBER	0	0	1	63	207	142	65	7	0	0	0	0	
PERCENT	0.0	0.0	0.2	13.0	42.7	29.3	13.4	1.4	0.0	0.0	0.0	0.0	

ARREST T-RTNDT(DEG.F)

	-50.0	-25.0	0.0	25.0	50.0	75.0	100.0	125.0	150.0	175.0	200.0	225.0	250.0
NUMBER	0	4	30	13	3	1	22	190	57	0	0	0	
PERCENT	0.0	1.3	9.4	4.1	0.9	0.3	6.9	59.4	17.8	0.0	0.0	0.0	

OF STD DEVS ABOVE MEAN DELTA RTNDT(FAILURES ONLY)

	1.00	1.25	1.50	1.75	2.00	2.25	2.50	2.75	3.00
NUMBER	2	7	9	23	18	28	35	43	
PERCENT	1.2	4.2	5.5	13.9	10.9	17.0	21.2	26.1	

OF STD DEVS ABOVE MEAN RTNDT(FAILURES ONLY)

	1.00	1.25	1.50	1.75	2.00	2.25	2.50	2.75	3.00
NUMBER	2	6	7	21	21	30	40	38	
PERCENT	1.2	3.6	4.2	12.7	12.7	18.2	24.2	23.0	

ICRKTP = 2 IACCEL = 1 NDLRS = 1 NRTRS = 1 DATE: 10/31/84 TIME: 02.42.24

CPU TIME: 5 MIN 22 SEC

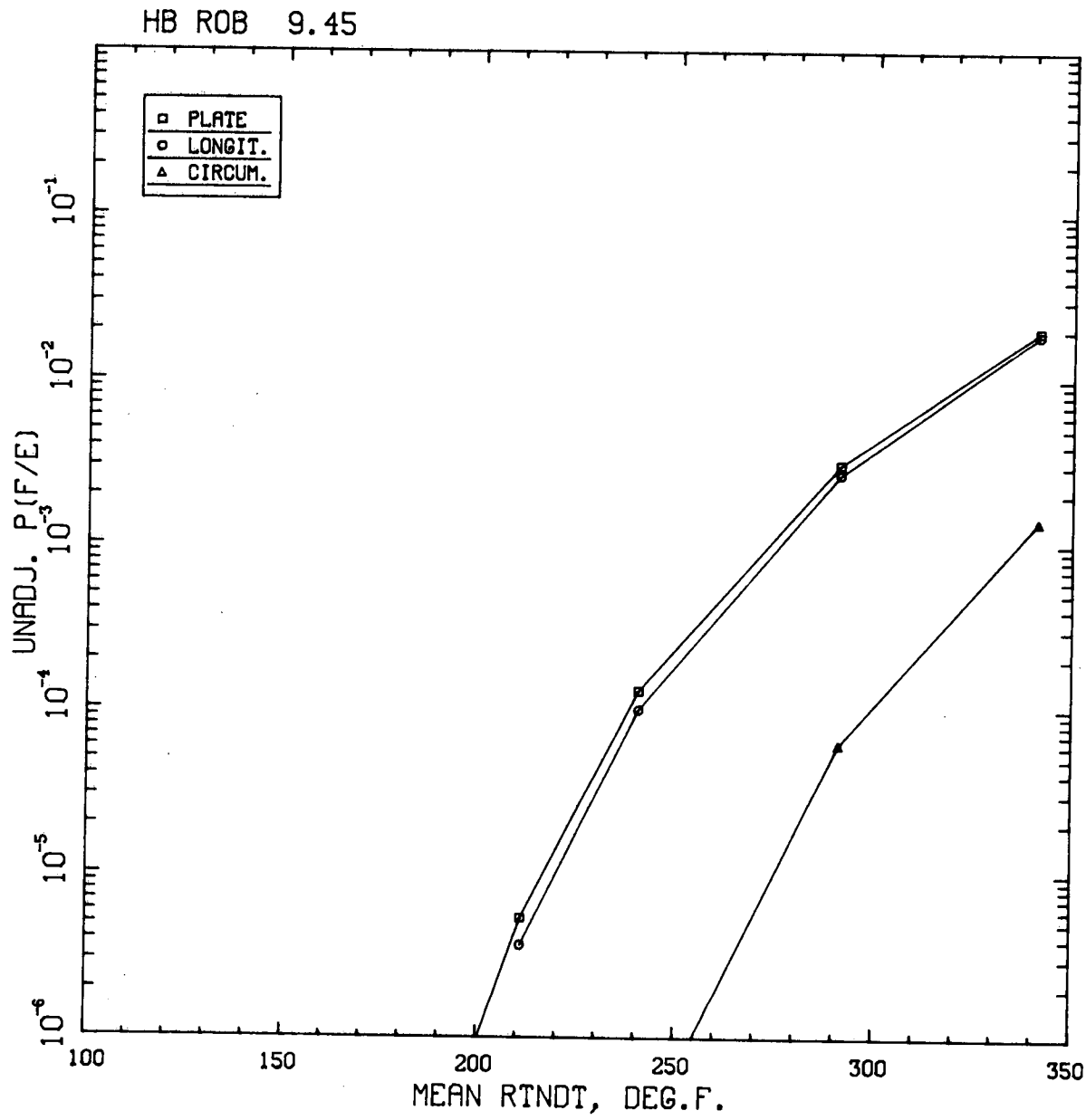

Figure I.254. Transient 9.45: $\hat{P}_j \int_0^w f(a)\, B(a)\, da$ vs $\overline{RTNDT_s}$ for (2-D, 2-D) and (2-D, 2m) flaw combinations.

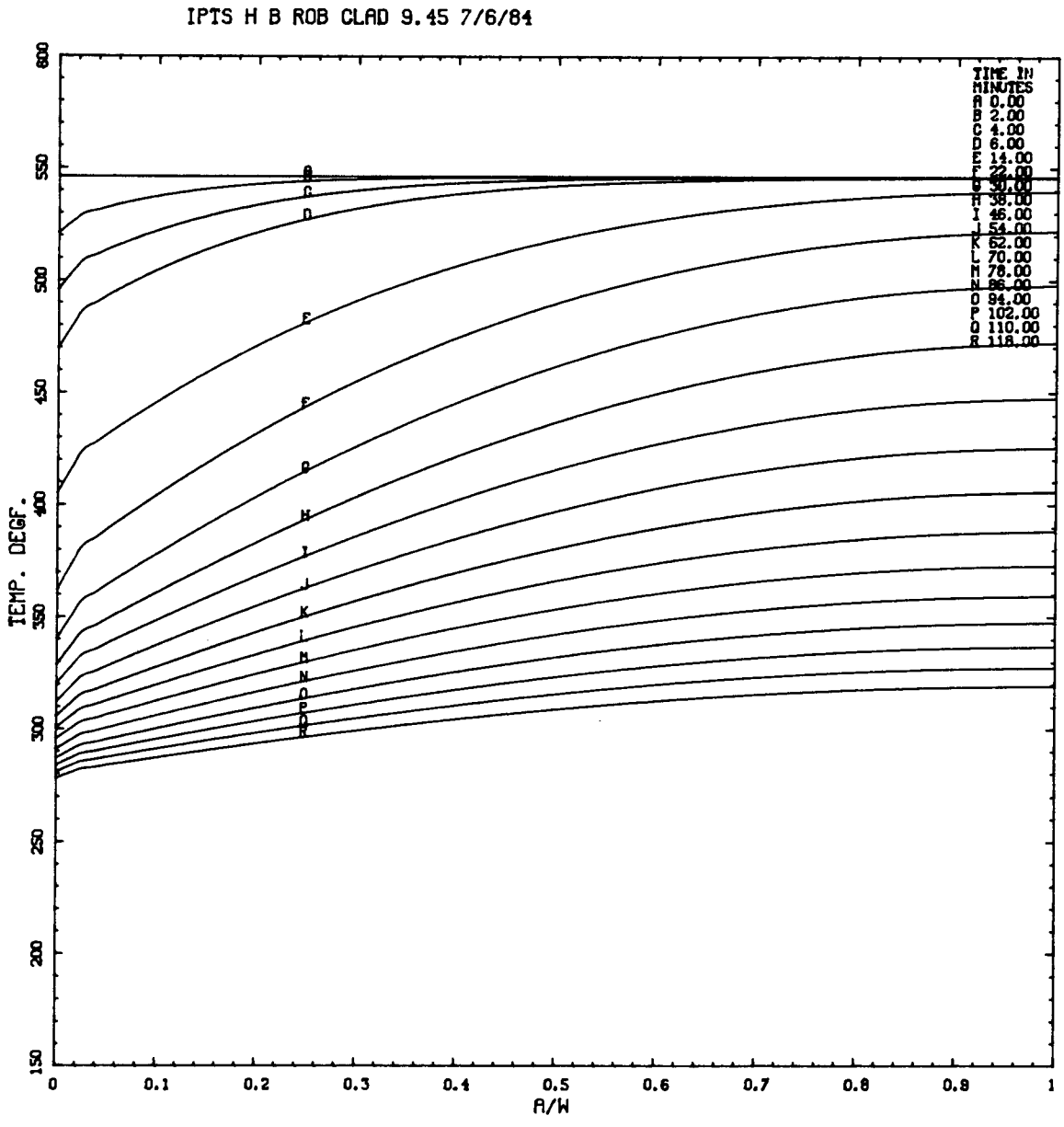

Figure I.255. Transient 9.45: Vessel wall temperature vs depth in wall (a/w) at various times (t) in transient.

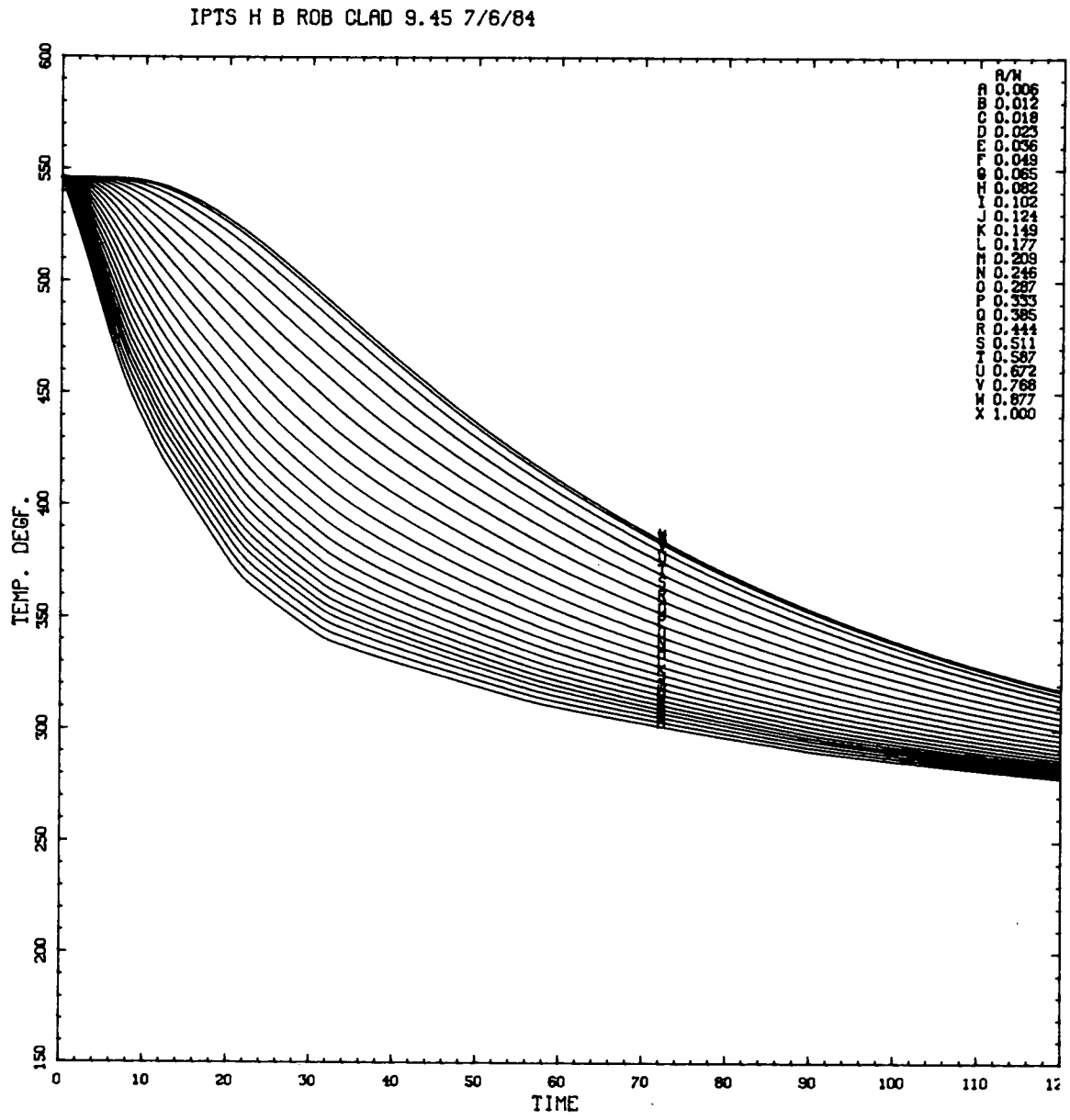

Figure I.256. Transient 9.45: Vessel wall temperature vs time (t) in transient at various depths in wall (a/w).

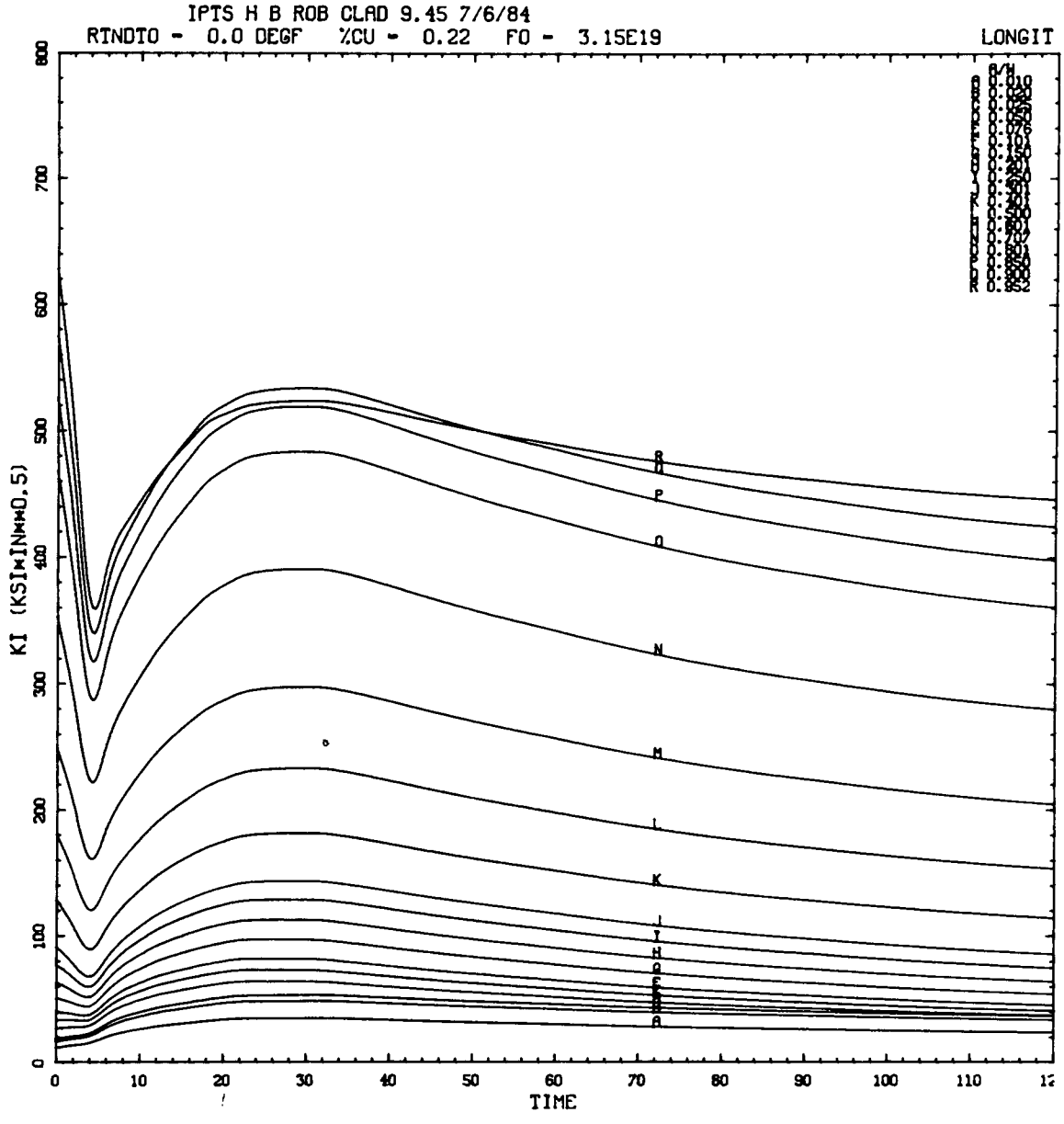

Figure I.257. Transient 9.45: K_I vs time (t) for various depths in wall (a/w).

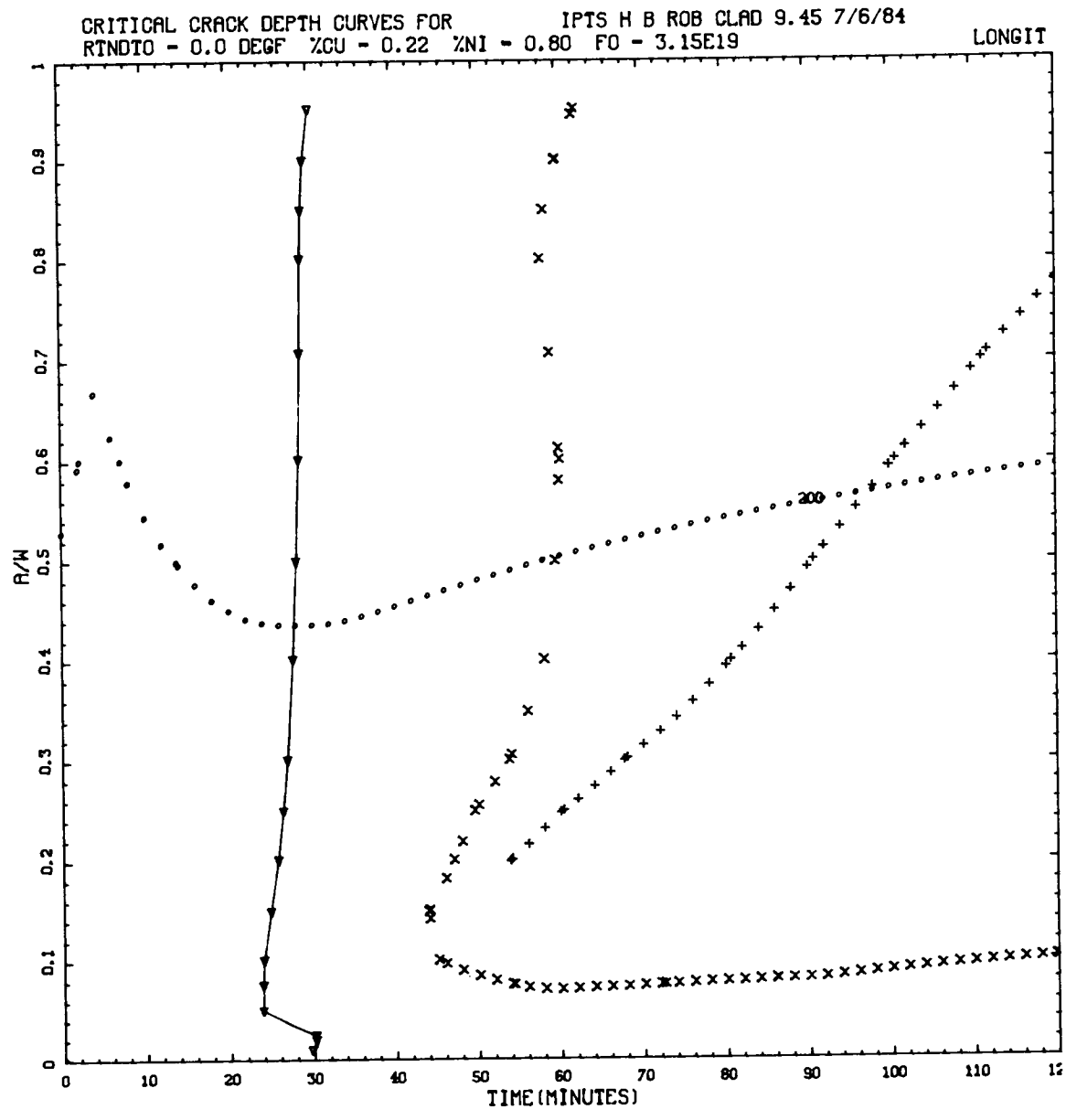

Figure I.258. Transient 9.45: Critical-crack-depth curves for weld 2-273A based on -2σ values of K_{Ic}, K_{Ia}, and $\Delta RTNDT$, mean values of all other parameters, and 32-EFPY fluences.

Appendix J

USEFUL RESULTS FOR THE LOG-NORMAL DISTRIBUTION

D. Bozarth and J. W. Minarick

Science Applications International Corporation

APPENDIX J. USEFUL RESULTS FOR THE LOG-NORMAL DISTRIBUTION

The log-normal distribution has been used extensively in the uncertainty analysis as the describing distribution for initiating events, event- tree branch probabilities, operator actions, and the initial flaw density. In most of these applications, the upper tail of the distribution is truncated either to restrict a probability to be in the range [0,1] or to place an upper bound on the number of initial flaws/m^3 in the vessel. When these bounds are placed on the distribution, the mean of the truncated distribution is shifted to the left from the theoretical mean. The technique for computing the mean of the truncated distribution is given in this appendix.

In addition, the mode of the log-normal distribution was used in deriving the parameters of the flaw density distribution. Since the mode of the log-normal is not given in most common texts, it is also derived herein.

J.1. Mean Value

If a random variable x is normally distributed, then the variable $y = e^x$ is said to be log-normally distributed. The parameters of the pdf of x, μ , and σ are the mean and standard deviation, respectively, of $x = (\ln y)$. By transformation of variables, the pdf (y) is

$$f(y) = \frac{1}{\sigma\sqrt{2\pi}\,y}\exp\left[-\frac{1}{2\sigma^2}(\ln y - \mu)^2\right] .$$

The mean of y is

$$E(y) = \int_0^\infty y f(y)\,dy = \frac{1}{\sigma\sqrt{2\pi}}\int_0^\infty \exp\left[-\frac{1}{2\sigma^2}(\ln y - \mu)^2\right]dy .$$

By letting $(\ln y - \mu)/\sigma = z$,

$$E(y) = \frac{e^\mu}{\sqrt{2\pi}}\int_{-\infty}^\infty \exp\left[-\frac{1}{2}z^2 + \sigma z\right]dz ,$$

which can be integrated by completing the square in the integrand:

$$E(y) = \frac{e^\mu}{\sqrt{2\pi}}\int_{-\infty}^\infty \exp\left[-\frac{1}{2}(z^2 - 2\sigma z + \sigma^2) + \frac{1}{2}\sigma^2\right]dz$$

$$= \frac{e^{\mu+\frac{\sigma^2}{2}}}{\sqrt{2\pi}}\int_{-\infty}^\infty \exp\left[-\frac{1}{2}(z - \sigma)^2\right]dz .$$

Next, by letting $z - \sigma = t$,

$$E(y) = \frac{e^{\mu+\frac{\sigma^2}{2}}}{\sqrt{2\pi}} \int_{-\infty}^{\infty} e^{-\frac{1}{2}t^2} dt \ ,$$

$$E(y) = e^{\mu+\frac{\sigma^2}{2}} \ . \tag{1}$$

Equation (1) is the theoretical mean of a log normal with parameters μ and σ. For a truncated distribution, everything is the same except the upper limit of integration changes. Equation (1) thus becomes

$$E(y) = \frac{e^{\mu+\frac{\sigma^2}{2}}}{\sqrt{2\pi}} \int_{-\infty}^{\frac{\ln y_m - \mu}{\sigma} - \sigma} e^{-\frac{1}{2}t^2} dt$$

$$= e^{\mu+\frac{\sigma^2}{2}} \left[N\left(0, \frac{\ln y_m - \mu}{\sigma} - \sigma\right)\right] \ . \tag{2}$$

Fortunately, the term in brackets above is tabulated as the standard normal distribution so that the truncated distribution mean is multiplied by a correction factor based on the length of the tail truncated. For example, for the flaw density distribution used in Chapter 7, the parameters of the distribution were $\mu = 2.9018$, $\sigma = 1.7035$, and the distribution was truncated at $y_m = 500\ \mathrm{m}^{-3}$. The mean of the distribution is:

$$E(y) = \exp\left[2.9035 + \left(\frac{1.7035}{2}\right)^2\right]$$

$$= \exp[4.35]$$

$$= 77.7 \ .$$

The correction factor for the mean of the truncated distribution is the area under the normal curve from $-\infty$ to $(\ln y_m - \mu)/\sigma - \sigma$. This is evaluated as

$$z = \frac{\ln y_m - \mu}{\sigma} - \sigma = \frac{\ln 500 - 2.9018}{1.7035} - 1.7035$$

$$= 0.24 \ .$$

From a table of standard normal distribution,

$$P(z \leqslant 0.24) = 0.60 \ .$$

Consequently, the truncated distribution mean is (0.60) (77.7) = 46.3 m^{-3}.

J.2. Derivation of the Mode of the Log-Normal Distribution

The mode is the most probable value of the random variable. Consequently, it is the value at which the pdf is maximized. To maximize $f(y)$, the fact that the logarithm is a single-valued transform is utilized and $\ln[f(y)]$ is maximized since a maximum in $\ln[f(y)]$ will occur at the same value of y as a maximum in $f(y)$. From the definition of $f(y)$,

$$d\frac{L(y)}{dy} = \ln[f(y)] \ ,$$

$$d\frac{L(y)}{dy} = -\frac{1}{y}\left[1 + \frac{1}{\sigma^2}\ln(y - \mu)\right] \ .$$

Setting this equal to zero and solving for y,

$$\frac{\ln y - \mu}{\sigma^2} = -1 \ .$$

Mode $(y) = e^{\mu - \sigma^2}$, which is the desired result.

Appendix K

RESPONSES TO UTILITY COMMENTS

D. L. Selby
Oak Ridge National Laboratory

APPENDIX K. RESPONSES TO UTILITY COMMENTS

The material presented in this report is part of an evaluation effort to provide information on the unresolved safety issue of pressurized thermal shock (PTS). Because PTS is an unresolved safety issue, NRC requires that a list of industry comments on the report and the changes which were made as a result of those comments be provided as an appendix to the report. The material presented in this appendix responds to that requirement. The comments are listed and discussed by chapter with comments on the appendices discussed along with the appropriate chapters. Only those comments considered to be pertinent to the PTS study are addressed; that is, comments simply pointing out grammatical or spelling errors are not included.

K.1. Chapter 1 Comments

No pertinent comments were made on Chapter 1.

K.2. Chapter 2 Comments

1. (*Section 2.7,3*). Each of the safety injection tanks can supply a minimum of 825 cubic feet of water rather than 775.

Response: We concur. The text was changed to reflect this correction. The change did not affect the analysis since the safety injection tanks were never involved in any of the transients.

2. (*Section 2.9.1.2*). The statement is mistakenly made that the station air compressor is normally not operating and must be manually started and valved in when needed to back up the instrument air compressors.

Response: We concur. The station air is normally running on its own header where air quality is not important, but can be manually valved into the instrument air system if necessary. The text has been corrected.

3. (*Section 2.9.1.4*). The service water system also provides heat removal to the emergency diesel generators.

Response: We concur. A change was made in the text to reflect this comment.

4. (*Section 2.9.3.1*). The text and tables of this section imply that loss of either DC Panel A or Panel B will result in failure of all steam dump valves in the closed position. In fact, only three steam dump valves will fail in the closed position if DC Panel A is lost. The other two will fail if Panel B is lost.

Response: We concur. Changes in the text were made to reflect this understanding.

K.3. Appendix A Comments

5. (*Section A.6*). CCW supplies oil cooler in charging pumps, not seal flow.

Response: We concur with this comment. However, the analysis assumes that the charging pumps will become unavailable on a loss of CCW. Thus, whether the unavailability is due to loss of seal flow or lube oil cooling, the analysis results will not be affected.

6. (*Section A.3.2*). Station air compressor is normally running and supplying its own header, but must be valved in when needed.

Response: This same comment was made with respect to Chapter 2. We agree with the comment and changes were made in the text to reflect this agreement. However, this does not impact the analysis since instrument air failures postulated included a pipe break in the 1A system and loss of service water to all compressors.

7. (*Table A.2*). Include BIT recirculation valves SI841 A&B, SI pump recirculation valves SI-856 A&B, SI pump discharge header cross-connect valves SI-878 A&B, RHR pump suction from containment sump valves SI-860 A&B and SI-861 A&B, RCS loop 2 to RHR pumps valves RHR-750 and RHR-751.

Response: These components were eliminated during the initial component screening phase. Response of these components to support system failures will not affect analysis results. The RHR recirculation mode is not expected to be important in PTS sequences.

8. (*Table A.3*). SWS provides oil cooler for feedwater pumps not seal water. Also SWS provides seal water for condensate pumps.

Response: With respect to the first point, feedwater pump dependency on SWS is still reflected in the analysis although the basis is incorrect. The text was changed to imply the correct reason for dependency.

9. (*Table A.3*). Include boric acid tank to charging pump and primary water blender in components requiring instrument air.

Response: Clarification has been provided by CP&L on the above items, but this information does not impact the analysis results. The boric acid tank and primary water blender were intentionally not selected as components for consideration.

10. (*Table A.3*). The majority of the valves listed under components requiring electric power are air-operated not motor-operated.

Response: The valves were noted as air-operated valves in the text but with power supplies to actuate the solenoids. Thus electric power is required.

11. (*Section A.4.3.12*). Clarification provided on CCW pumps which do not specifically actuate on an SI signal. In addition, comments provided concerning "plant will not be

operating if diesel generators are not available," and "one SI pump is on the tie bus, remaining bus would have two pumps operable."

Response: Information acknowledged. The bus failure modes addressed in the analysis assumed failure of the diesel generators on demand. The new information does not impact the analysis results.

12. (*Table A.6*). Loss of 4KV bus 2 will also result in loss of all but one SI pump. Also loss of 4KV bus 3 will result in loss of two of three charging pumps.

Response: Information acknowledged. Changes were made in the table to reflect this information. The revised information does not impact analysis results.

13. (*Table A.6*). Why is there a delayed turbine trip due to eventual EH system depressurization on loss of power to EH system components and actuation control?

Response: The EH system is assumed to maintain closing pressure on the turbine stop, intercept, reheat, and governor valves. If the EH pumps or control power fail, the EH system cannot respond to a signal to start the pumps to maintain pressure. If power to EH control fails, depressurization cannot be detected or corrected.

14. (*Table A.6*). Why do the steam PORVs fail closed on loss of 480V bus E2 if load reject signal PM-477 exists.

Response: See text Section A.4.3.4. Steam Dump Controller T-408 is powered by 480V bus E2. If the load reject signal exists, PORV control has been switched to T_{avg} control under T-408. The steam PORVs have been assumed to remain closed on loss of control power. If this is incorrect and the steam PORVs can fail open on loss of control power, the interaction analysis could be impacted.

15. (*Table A.6*). RCPs and pressurizer heaters can be locally tripped if control power is lost.

Response: The clarification is acknowledged, but the analysis results are not affected by this information.

K.4. Chapter 3 Comments

16. (*Section 3.3.2.1*). The flow restrictor on the new steam generators is in the nozzle; therefore, a break upstream of this restrictor would be impossible.

Response: We agree. The original statement was made with respect to the flow restrictor in the pipe and did not consider the flow restrictor in the nozzle as it should have since the nozzle restrictor is the controlling oriface. Reference to breaks upstream of the flow restrictor were removed from the text.

17. (*Section 3.2.2*). The text states that failure to trip RCPs on SI signal is a violation of emergency procedures. This is not correct as the procedures at the time of the present

study required RCP trip on RCS pressure less than 1300 psi, not SI actuation. Also for a number of events the resultant RCP trip may not be reached as the set point was chosen to discriminate between LOCAs and other more probable events, and the RCP trip is itself a major factor as regards PTS severity. The writeup should be corrected.

Response: Reference to pump trip on SI actuation was incorrect. The text was changed to indicate RCP trip on RCS pressure less than 1300 psi. It should be noted that in the thermal-hydraulic analysis the RCP trip was made when the pressure dropped below 1300 psi.

18. (*Section 3.3.2.1*). The text could amplify on the effect of core decay heat. Specifically low core decay heat, consistent with hot shutdown, also includes increased steam generator inventory which was considered in T/H analysis.

Response: In this section we are only concerned with determining the core decay heat levels which should be associated with the full power and hot 0% power conditions. The importance of the hot 0% power condition due to water inventory is presented and discussed in Section 2.4.1. It was not deemed necessary to repeat that discussion in Section 3.3.2.1.

19. (*Section 3.5.1*). The reactor trip as initiator does not appear to lead to stuck pressurizer PORVs, to a frequency greater than 1E-7/Rx.YR. On the other hand Appendix B data would suggest a higher probability. Although specifically stuck PORVs were considered as an initiator, this would appear to be a limitation that should be discussed.

Response: The pressurizer PORVs do not open on every reactor trip. In order to lift the PORVs on this plant, it was determined that additional failures (e.g., charging system fails to run back) were necessary. This substantially decreases the demand for the PORVs to lift and thus decreases the opportunity for failure to close. In addition the pressurizer PORV failure to close probability of 1.2E-3 used in the analysis includes the failure of the operator to recognize the failed PORV and close the block valve. This operator failure probability was included since it was demonstrated that a prolonged PORV failure was necessary to be considered an overcooling event. These factors contributed to a relatively low frequency for PORV failures following a reactor trip. However, there were three sequences involving PORV failure following a reactor trip which had frequencies greater than 1E-7: sequences 180, 2685, and 5553 on the reactor trip tree shown in Figure 3.5 of the report. These sequences were assigned to the residual sequence 9.97 to simplify the analysis. Finally, the highest potential for PORV failure following reactor trip is when a feed-and-bleed situation develops. In this case there are repeated demands on the lifting and closing of the valve which greatly increases the probability of an eventual failure to close. This type of event was examined but not specifically analyzed since it led to a small-break LOCA with a lower frequency than the initiating-event frequency used in the analysis of the small-break LOCA.

20. (*Table 3.16*). The Table 3.16 should clarify the frequencies (e.g., it implies both scenario 10.1 and 10.4 have 5E-3/yr) and the table may be used independent of the text.

Response: A footnote was added to this table to explain the use of the frequency values for these two sequences.

K.5. Appendix B Comments

21. (*Table B.1*). The steam-side PORVs do not automatically open on trips greater than 70% power; however, it has been indicated by the operators at HBR-2 that the steam-side PORVs do occasionally open as a result of trips from high power conditions.

Response: This information was noted in the text. However, a footnote was also added to explain that the assumption of opening on each reactor trip does not introduce a conservatism since if the number of openings were less, the failure/demand would be higher and the number of failures/RY would still be the same value.

22. (*Table B.1*). With respect to the air-operated valve failure probabilities (given a set of three valves in a system and the first valve is failed) the reference NUREG/CR-2770 information does not seem correct for valves failing to close. The NUREG was not reviewed; however, it seems likely the probability of the second valve failing and both remaining valves failing is biased by loss of instrument air at the valves. However, in this case the failure is in the closed position, which would not be appropriate for use in the failure to close branch points.

Response: The data taken from the NUREG is based on a composite of failure to open, failure to close, and failure to operate. Based on a review of the data, it is our belief that the coupling is not strongly associated with loss of instrument air. The couplings appear to be most strongly associated with maintenance and inspection/testing practices. With this in mind, it is our opinion that coupling factors used for the air-operated valves are not overly conservative.

K.6. Appendix C Comments

No pertinent comments on Appendix C were received.

K.7. Appendix D Comments

23. (*Section D.3.5*). Provide some explanation as to why the operators would not close the MSIVs in the case of a single steam dump valve failure to close.

Response: The text was revised to make it clear that it was our opinion that the MSIVs would not be closed for this sequence because there would not be a perception on the part of the operator for a need to close the MSIVs.

K.8. Chapter 4 Comments

24. (*Section 4.4.1.7*). The total stagnation case should be further discussed. Also it may be more appropriately included in another section (e.g., where uncertainties are addressed).

Response: The section on total stagnation was expanded in Appendix E and reference to this appendix was made in the text. There is a good argument for including the discussion

of total stagnation in Chapter 7 rather than in Chapter 4. However, after consideration we chose to leave the discussion in Chapter 4. This decision was made because we wanted to emphasize the point that an evaluation of the mixing phenomenon under various stagnation conditions may be an important part of the thermal-hydraulic analysis.

K.9. Appendix E Comments

No pertinent comments on Appendix E were received.

K.10. Appendix F Comments

25. (*Figures F.1 - F.270*). Include a note on these figures that "The scenarios simulated contain significant conservatisms in operator actions, equipment failures, or both." This note was included on the figures in the INEL report, NUREG 3977.

Response: The note above was included on the INEL figures because the full-scale calculations could be construed as being representative of a class of transients and the reader may not be aware of the actual sequence of events used in arriving at the final thermal-hydraulic traces. In Appendix F, the thermal-hydraulic traces refer only to a number which corresponds to a specific sequence. This refers the reader to the appropriate sequence of events and thus to the equipment or operator failures assumed in the sequence. Therefore, we do not think that it is appropriate to add the note to these figures since it would detract from their significance. It should also be pointed out that for similar reasons the note was not included on the thermal-hydraulic traces included in the INEL report that describes the evaluation of the individual sequences.

K.11. Chapter 5 Comments

26. (*Section 5.5.2*). The sensitivity studies (in particular temperature) are not consistent with the temperature uncertainty(s) identified by INEL. Presumably the same is true for pressure and heat transfer coefficients--but this is not clear from the text. Specifically the INEL report identifies an uncertainty in temperature (as a function of the downcomer fluid temperature). The result is an uncertainty that is a minimum at the highest and lowest temperatures and a maximum at an intermediate temperature. It is requested these be repeated, or at a minimum selected transients be repeated and the differences discussed/generalized.

Response: The purpose of the sensitivity analysis is to illustrate the impact on TWC probability of perturbations in individual parameters. This is not an uncertainty analysis and therefore the perturbations used in the sensitivity analysis are not necessarily one-sigma values. For convenience, some of the perturbations are one-sigma values and are identified as such. For others, such as temperature, pressure, and heat transfer coefficient, the perturbations used in the sensitivity analysis are not one-sigma values and were not intended to be interpreted as such. A sentence was added in the text to clearly point out that, unless specifically stated, perturbations are not one-sigma values.

K.12. Appendix G Comments

No pertinent comments on Appendix G were received.

K.13. Appendix H Comments

No pertinent comments on Appendix H were received.

K.14. Appendix I Comments

No pertinent comments on Appendix I were received.

K.15. Chapter 6 Comments

No pertinent comments on Chapter 6 were received.

K.16. Chapter 7 Comments

27. (*Section 7.3.3*). The methodology employed to obtain TWC probability from conditional probability utilizes conditional probabilities for a single flaw per region times the number of flaws per region. The approach does not appear to be correct as used in Chapter 7, as the increased flaw density assumed leads to about sixteen flaws per weld--using 500 flaws per cubic meter. Although the PTS report does not allow definitive estimates of the fraction of flaws that can lead to TWC it appears that those in the range of order of magnitude 0.2 to 0.6 inches deep are the "capable flaws" and these represent about 35% of all flaws, given Equation 5.11. This suggests that assuming a flaw density greater than about 1/0.35, or on the order of three flaws per region, will lead to multiple counting of flaws, and indicates the HBR-HYPO results in Chapter 7 may be about a factor of five too large.

Response: The above comment, although somewhat of an oversimplification of the problem, does point out an area of deficiency in the treatment of multiple flaws per region. There does appear to be instances where multiple counting of flaw failures per Monte Carlo trial may have occurred. In the uncertainty analysis, failures of flaws within a given size group were always considered to be independent of the failure of any other flaw size group. Under this assumption, the conditional failure probability would continue to increase (although not necessarily linearly) with flaw density until the probability of having a flaw in each flaw depth group approaches one. Since the fracture-mechanics calculations indicate that there are both dependent and independent failures, the approach used in the analysis will lead to a double counting effect. Examination of the data indicates that the factor of five indicated in the comment may be a reasonable estimate of the conservatism in the upper range of the uncertainty distribution.

K.17. Appendix J Comments

No pertinent comments on Appendix J were received.

K.18. Chapter 8 Comments

28. (*Section 8.2.3*). The statement that substantial increase in PTS risk could result in many cases does not appear consistent with the observation that most transients reached essentially the asymptotic value, particularly for the more severe transients. Thus additional justification would be appropriate.

Response: The comment made in Chapter 8 was meant to imply that the PTS risk for many specific sequences would substantially increase if a longer analysis period were allowed. It was not meant to imply anything about the effect of analysis time increase on the integrated PTS risk. A sentence was added in the text to make this point clear. Although it is true that the more severe thermal-hydraulic transients reached an asymptotic value prior to the two-hour analysis period and longer analysis periods would have little effect on these transients, it must be remembered that a great majority of the transients considered, including the two highest PTS risk events, would not be classified as extremely severe thermal-hydraulic events. In the case of the two highest PTS risk events, over 50% of the failure probability in the two-hour period occurs in the last 20 minutes of the analysis. This implies that the asymptotic value of the failure distribution for these sequences may not have been reached within the two-hour analysis period. It should be noted, however, that extended analysis times should not be considered simply because the asymptotic value of the failure distribution has not been reached. Extended analysis times should be considered only when the asymptotic value of the failure distribution has not been reached and there is some evidence that the cooldown transient could be allowed to continue unabated beyond a two-hour time frame.

29. (*Section 8.3*). It is our understanding that external flooding has been recently analyzed and is not a severe event.

Response: Preliminary studies performed at the time this report was published indicated that flooding of the external reactor vessel was not an important PTS concern for HBR Unit 2. A footnote which makes this point was added to the text in Chapter 8 of the report.

30. (*Section 8.3*). Item number 5 indicates that the two-hour transient time should be investigated. The two-hour transient time is very conservative since most of the transients are based on minimal or no mitigating operator action. When operator actions are included, temperature decay rates are reduced, final transient temperatures are increased and transient severity is significantly reduced.

Response: The statement as presented in Section 8.3 is simply pointing out the importance of the analysis time. Both shorter and longer time periods are suggested for potential investigations. As pointed out in the above comment, there are many events for which operator actions not considered in this analysis could greatly reduce the TWC potential of the event. In these cases shorter analysis periods may be very appropriate. However, one must also consider the event where there is little that the operator can do or there are conflicting objectives for the operator such as making sure the core is cooled but not overcooling the vessel. In these cases there may be a need for analysis beyond the two-hour period.

NUREG/CR-4183
Volume 2
ORNL/TM-9567/V2
Distribution Category RG

INTERNAL DISTRIBUTION

1. L. S. Abbott
2. D. G. Ball
3. S. Ball
4. B. R. Bass
5. T. J. Burns
6. D. G. Cacuci
7. R. D. Cheverton
8. J. S. Crowell
9. D. M. Eissenberg
10. G. F. Flanagan
11. F. C. Maienschein
12. A. P. Malinauskas
13. F. R. Mynatt
14. R. T. Santoro
15. D. L. Selby
16. H. T. Trammell
17. J. D. White
18. G. D. Whitman
19. A. Zucker
20. P. W. Dickson, Jr. (Consultant)
21. G. H. Golub (Consultant)
22. D. Steiner (Consultant)
23. Central Research Library
24. Y-12 Document Ref. Section
25. Laboratory Records ORNL, RC
26. ORNL Patent Office

27–29. EP&MD Reports Office

EXTERNAL DISTRIBUTION

30. Office of the Assistant Manager for Energy Research and Development, DOE-ORO, Oak Ridge, TN 37830.
31. B. Chexal, Electric Power Research Institute, 3412 Hillview Ave., P.O. Box 10412, Palo Alto, CA 94303.
32. S. Rosen, Institute of Nuclear Power Operations, 1820 Water Place, Atlanta, GA 30339.
33. S. M. Mirsky, Baltimore Gas & Electric Company, P.O. Box 1475, Baltimore, MD 21203.
34. J. Phillips, Corporate Nuclear Safety, Carolina Power and Light Co., Fayettville Street Mall, Raleigh, NC 27602
35. C. D. Fletcher, EG&G Idaho, Inc., P.O. Box 1625, Idaho Falls, ID 83415.
36. C. B. Davis, EG&G Idaho, Inc., P.O. Box 1625, Idaho Falls, ID 83415.
37. L. Pedersen, Pacific Northwest Laboratory, Battelle Bldg., Richland, WA 99352.
38. B. Boyack, Los Alamos National Laboratory, P.O. Box 1663, Los Alamos, MN 87545.
39. P. Saha, Brookhaven National Laboratory, Upton, NY 11973.
40. T. G. Theofanous, University of California, Department of Nuclear and Chemical Engineering, Santa Barbara, CA 93106.

41–42. R. Oliver, Corporate Nuclear Safety, Carolina Power and Light Co., Fayettville Street Mall, Raleigh, NC 27602.

43. P. Guill, Duke Power Company, P.O. Box 33189, Charlotte, NC 28242.
44. D. Peck, Combustion Engineering Inc., 1000 Prospect Hill Rd., Windsor, CT 06095.
45. J. W. Minarick, Science Applications International Corporation, Jackson Plaza Tower, 800 Oak Ridge Turnpike, Oak Ridge, TN 37830.

U.S. Nuclear Regulatory Commission, Washington, D.C. 20555:

46. C. E. Johnson
47. G. Requa
48. J. N. Reyes
49. M. Vagins
50. R. H. Woods

51–52. Technical Information Center

53–302. Given distribution as shown in NRC Category RG, Systems and Reliability Reports.

NOTICE

When you no longer need this report, please return it to D. L. Selby, Engineering Physics and Mathematics Division, Bldg. 6025, MS 18W, Oak Ridge National Laboratory, P. O. Box X, Oak Ridge, Tennessee 37831. Thank you.

NRC FORM 335 (2-84) NRCM 1102, 3201, 3202

U.S. NUCLEAR REGULATORY COMMISSION

BIBLIOGRAPHIC DATA SHEET

SEE INSTRUCTIONS ON THE REVERSE

1. REPORT NUMBER (Assigned by TIDC, add Vol. No., if any)
NUREG/CR-4183
Volume 2
ORNL/TM-9567/V2

2. TITLE AND SUBTITLE
Pressurized Thermal Shock Evaluation of the H. B. Robinson Unit 2 Nuclear Power Plant

3. LEAVE BLANK

4. DATE REPORT COMPLETED

MONTH	YEAR
March	1985

5. AUTHOR(S) D. G. Ball, R. D. Cheverton, G. F. Flanagan, D. L. Selby, P. N. Austin, D. P. Bozarth, D. E. Korns, C. L. Mason, A. F. McBride, J. W. Minarick, L. B. LaMonica, R. Olson, G. L. Zigler, C. B. Davis, C. D. Fletcher, D. M. Ogden, P. Gherson, K. Iyer, H. P. Nourbakhsh, T. G. Theofanous, P. Humphreys, L. D. Phillips, and D. Embrey

6. DATE REPORT ISSUED

MONTH	YEAR
September	1985

7. PERFORMING ORGANIZATION NAME AND MAILING ADDRESS (Include Zip Code)
Oak Ridge National Laboratory
P. O. Box X
Oak Ridge, TN 37830

8. PROJECT/TASK/WORK UNIT NUMBER

9. FIN OR GRANT NUMBER
B0468

10. SPONSORING ORGANIZATION NAME AND MAILING ADDRESS (Include Zip Code)
Division of Risk Analysis and Operations,
Office of Nuclear Regulatory Research,
U.S. Nuclear Regulatory Commission,
Washington, DC 20555

11a. TYPE OF REPORT
Final

b. PERIOD COVERED (Inclusive dates)
3/1/84 - 9/1/85

12. SUPPLEMENTARY NOTES

13. ABSTRACT (200 words or less)

An evaluation of the risk of pressurized thermal shock (PTS) resulting in a through-the-wall crack in a reactor pressure vessel was performed for the H. B. Robinson Unit 2 nuclear power plant. The information presented in this report covers one of three plant-specific studies performed for NRC. The other two studies, for Oconee Unit 1 and Calvert Cliffs Unit 1, are documented in NUREG/CR-3770 and NUREG/CR-4022, respectively. The specific objectives of the H. B. Robinson study were (1) to further refine the methodology for evaluating the risk of PTS, (2) to provide a best estimate of the frequency of a through-the-wall crack for the H. B. Robinson Unit 2 vessel, (3) to determine the dominant PTS sequences for the unit, and (4) to evaluate the effectiveness of potential corrective measures. The examination of tens of thousands of transients indicated that PTS was not an important core melt initiator for H. B. Robinson Unit 2. The dominant risk sequences were determined to be failure of steam relief valves to close on multiple steam lines.

14. DOCUMENT ANALYSIS – a. KEYWORDS/DESCRIPTORS
Overcooling, PTS, Risk, PRA, Uncertainties, H. B. Robinson, Westinghouse, Probabilistic, Fracture-mechanics

b. IDENTIFIERS/OPEN-ENDED TERMS
RELAP5, OCA-P, REMIX

15. AVAILABILITY STATEMENT
Unlimited

16. SECURITY CLASSIFICATION
(This page) Unclassified
(This report) Unclassified

17. NUMBER OF PAGES
627

18. PRICE